PEGASOS Refinement Project

Volume 5
SP3 - Site Response Characterization -

Evaluation Summaries and Hazard Input Documents

by

Philippe L.A. Renault, Norman A. Abrahamson & SP3 Experts

Olten, 20. December 2013
Rev.1: 18. August 2014

Dedicated to the memory of Jost A. Studer

This report is dedicated to the memory of our friend and colleague Dr. Jost A. Studer. Jost Studer contributed significantly to the PEGASOS and PEGASOS Refinement Project in the last decade and passed away on 8. January 2013 on his way to work.

Contents

Part I

Development of soil models

Chapter 1

Introduction

The geotechnical and geophysical investigations at the nuclear power plant (NPP) sites form the basis for the definition of the soil/rock profiles for the site-response calculations. The investigations required at each site are specified in appendix B [Renault et al. 2008] of the project plan [swissnuclear 2011] and is consitent with international standards as IAEA [2004]. The derived structural models for the site-response calculation should be valid for the geological structures in the approximate neighborhood of security-relevant structures like the reactor building or the emergency building. However, it is generally not possible to perform seismic measurements in their direct vicinity. The evaluation of the relevant sites has therefore to be obtained by inter- or extrapolation, taking into account all measurements at possibly similar structures in the direct vicinity. This results in different possible structural models. For all sites, an extensive documentation was prepared by the nuclear power plants and their contractors. Various models are proposed in the reports, taking into consideration the geological and geotechnical data, along with the geophysical and laboratory measurements.

1.1 Structure of the Report

Description of the Site Investigations and Initial Results

The first part of the report describes the site investigations and collected data. The initial proposed soil models and modifications of the models are presented for each site in the chapters 3 to 6. The soil models developed in these chapters are based on the common assessment of the SP3 experts and were developed in order to have a common basis with candidate models.

Evaluation Summaries of the SP3 Experts

Part II to V of the report include the individual evaluation summaries of the SP3 experts. Those represent revised version compared to the original PEGASOS summaries. For a discussion and description of the 2D/3D effects and models, which were not re-assessed in the framework of the PRP, the reader is referred to the PEGASOS Final Report, Volume 6. The following chapters contain the expert's assessments:

Part II - Chapter 1, Part III - Chapter 1, Part IV - Chapter 1, Part V - Chapter 1.

Hazard Input Documents for SP3

The Hazard Input Documents (HID) are developed to include all of the elements of each expert's assessments of importance to the hazard calculations. Although the HIDs provide the information required for the hazard calculations, they do not include any technical explanation or justification for the models or parameters that comprise the models. Those explanations are given in the Evaluation Summaries. The following chapters include the final HID for each of the SP3 models:

Part II - Chapter 2, Part III - Chapter 2, Part IV - Chapter 2, Part V - Chapter 2.

Chapter 2

Site Investigation and Initial Soil Models

2.1 Site Investigations

After the PEGASOS project, the SP3 experts and Swiss plants saw potential for a reduction of the epistemic uncertainty of the hazard through a more realistic quantification of the uncertainty in the site-specific soil properties by performing measurements at the NPP sites. Thus, according to the project plan [swissnuclear 2011] the NPPs were charged to perform new site investigations in order to collect more data, with the aim to better constrain the uncertainties. Between 2008-2009, the Swiss NPPs have collected new site-specific geotechnical data on soil profiles and the non-linear soil properties, based on the project specific site investigation specification PMT-TB-1010 [Renault et al. 2008]. Different measurement techniques (reflexion and refraction seismic, multichannel analysis of surface waves, ambient vibration array and V/H measurements, logging, up-/downhole and crosshole seismics) have been used in the framework of the new campaign, which also enabled an estimation of the range of their applicability and a quantification of the associated uncertainties.

Responsibility for the contracting and execution of most of the SP3 tasks lied with the individual NPPs, as the data collection for the site response characterization required access to the facility sites. However, the SP3 Experts were in charge to make the final review and accept the collected and interpreted site investigation data before the data were used for the site response calculation. The site specific reports of the site investigation are documented in Interoil [2009c]; AMEC [2009b]; NOK [2009a, b] (TP3-GTC-1001, TP3-GTC-1002, TP3-GTC-1003 and TP3-GTC-1004). Additional data for the sites were evaluated according to SP3 Experts requests on WS2a/SP3 (22. October 2009) and WS2b/SP3 (19. November 2009) and are documented in Interoil [2009a]; AMEC [2009a]; Interoil [2009b]; AXPO [2010a, b] (TP3-GTC-1006 to TP3-GTC-1010).

The comparison of the results of the different techniques revealed—at the surprise of all involved experts—that for the case of the Swiss NPPs the uncertainty for the soil models increased, as the evaluation of the data lead to significantly different interpretations of the soil models.

Based on the gained insight of the field measurements, site response calculations have been conducted using the new model parameters for the soil profiles and non-linear properties. The same three methods as used in the PEGASOS SP3 logic trees (1-D equivalent linear time domain method, 1-D equivalent linear Random Vibration Theory (RVT) method, and 1-D truly non-linear time domain method) have been evaluated with the new soil data, based on the project specific site investigation specification [Renault and Abrahamson 2010]. For each computation method benchmark and cross-check computations have been performed. Again, the NPPs were responsible for the site response calculations. Once all site response calculation results [KKG-KKN 2010; AMEC 2010a; AXPO 2010c; AMEC 2010b; KKG 2010; AXPO 2010d] (TP3-SUP-1011 to TP3-SUP-1016) were quality assured and made available to the project in 2010, they were included into a homogeneous database [Hölker 2013a] (RDZ-ASW-1003).

After re-evaluation of κ by SP2 in 2012 new values were defined and lead to the need of a revision of the RVT input spectra. In order to be fully consistent, the re-analysis of the site response by the equivalent linear (EQL) methods (SHAKE and RVT) was performed with the new target κ_0 values. The time histories used for SHAKE were adjusted in frequency content to be consistent with the spectral shape of the RVT input spectra. This was not the case for the first site amplification runs performed in 2010 which resulted in different spectral shapes between the SHAKE and RVT input response spectra. The results of the re-evaluation at the beginning of 2013 are documented in AMEC [2013]; AXPO [2013]; KKG [2013] (TP3-SUP-1086, TP3-SUP-1090, TP3-SUP-1090). The new results were included in the SP3 database as a new dataset and used by the SP3 experts for their final evaluation.

A positive observation from the site response calculations was e.g., that non-linear time domain computations for the same site and input data were performed by two independent contractors with two different constitutive models. Surprisingly, the site amplification results were in very good agreement to each other, which may be due to the vast amount of collected high quality data for this project or the excellent modeling skills of the contractors. The initial benchmark of the RVT contractors revealed something unexpected to the experts. For the same boundary conditions the site amplification functions resulting from computations with different software packages and contractors lead to notable different results. In the framework of the PRP a couple of investigations have been performed to understand these discrepancies, but couldn't be resolved to the full satisfaction of the project management team. Similar conclusions have also been drawn from other authors [Graizer 2011; Kottke and Rathje 2013]. As the RVT approach to site response analysis has become very popular in recent years, because it is much less labor intensive since it does not require choosing and scaling time series, these differences should be further assessed in the future.

In the end, it needs to be pointed out that the final soil profiles and material properties were developed on a consensus basis among the SP3 experts in order to have a common starting point. The weights and all other model parameters, as well as use of the available site amplification factors were developed individually.

2.2 Variability in the Velocity Profiles

2.2.1 V_S-profiles

After evaluation and comparison of the different candidate shear-wave velocity profiles per site, the SP3 experts agreed to set a common range of uncertainty for all NPP sites. For the RVT the variability was defined by:

- 25% variation on the V_S-profile (with $\mu/1.25$ and $\mu \cdot 1.25$; assuming a log-normal distribution).
- The defined upper and lower bound of the material models are assumed correspond to two standard deviations.

In total 250 V_S-profiles were randomized per site in order to serve as candidates for the site amplification RVT computation (see TP3-SUP-1006). If the realizations were outside of the bounds specified by the SP3 experts, alternative realizations were used. In total 50 feasible realizations have been retained and used (TP3-SUP-1008).

2.2.2 V_P-profiles

The variability of the V_P-profile has been defined as follows: In the soil above the ground water table: 25%, in the soil below the water table: 10% and in the rock: 25%. The depths of the water table below the surface is summarized for all sites in Table I-2.1

Site	Depth [m]
Beznau	5
E-Beznau	5
Gösgen	6.5
Leibstadt	26
Mühleberg	4

Table I-2.1: Depth of water table below the surface.

Those base V_P-profile have been modified with (see chapter 5.1 of the specification PMT-TB-1014 [Renault and Abrahamson 2010]):

$$V_P = \sqrt{V_{P,elastic}^2 - \frac{4}{3}(V_{S,elastic}^2 - V_S^2)} \tag{I-2.1}$$

where $V_{S,elastic}$ and $V_{P,elastic}$ are the velocity profiles defined in the technical notes for each site. V_S is the shear wave velocity profile calculated at the end of the EQL or RVT analysis. This is equivalent to assume that the bulk modulus of the soil is strain independent. Those modified V_P-profiles were then used as input for the equivalent linear analyses (EQL) and random vibration theory (RVT) runs.

2.3 General Procedure for the Determination of the P-wave Velocity Profiles

The PRP procedure foresees only the selection of one P-wave velocity profile. The V_P-profile was derived by taking the preferred model and applying a V_P/V_S velocity factor of 2.5 in the sediment layer above the water table and $\sqrt{3}$ in the rock; this is equivalent to assuming a Poisson's ratio of 0.4 in the sediments and of 0.25 in the rock. This applies to all sites except Leibstadt. Below the water table additional constraints have to be taken into account to reflect the presence of water filling the voids: the wave velocity shall be higher than 1500 m/s if the water is perfectly de-aired. The theoretical P-wave velocity is given by:

$$V_P = \sqrt{\frac{K^S + \frac{4}{3}G^S + \frac{K_f}{\varphi}}{\rho_S(1-\varphi) + \rho_f\varphi}} \tag{I-2.2}$$

where:

- K^S and G^S are the soil bulk and shear modulus
- φ the soil porosity
- K_f the bulk modulus of water
- ρ_S ρ_f the soil specific gravity and the water mass density

The soil shear modulus is computed from the shear wave velocity with

$$V_S = \sqrt{\frac{G^S}{\rho_S(1-\varphi)}}. \tag{I-2.3}$$

The preceding formulas also apply to the soil above the water table provided K_f and ρ_f are set equal to zero.

The P-wave velocity profile was calculated with the following procedure:

- G^S is computed from the shear wave velocity;
- φ is computed with the laboratory data for the soil specific gravity ρ_S and soil total mass density ρ and a water mass density $\rho_f = 1$ t/m^3 ; then: $\rho = (1-\varphi)\rho_S + \varphi\rho_f$
- Poisson's ratio for the soil below the water table is kept equal to 0.4 as above the water table; then $K^S = 4.92\ G^S$;
- K^f is first assumed equal to 2250 MPa (value applicable for perfectly de-aired water) and V_P calculated with the formula above;
- Results are compared to the data and K_f is possibly modified close to the water table surface (1000 MPa $< K_f <$ 2250 MPa) to reflect the possible lack of soil saturation in that zone and to better fit the measured data. At large depths, totally de-aired water may be assumed (K_f = 2250 MPa) and values as high as 2250 MPa may be considered.

2.4 Generic Logic Tree for SP3

The basic logic tree behind all individual SP3 expert specific logic trees is illustrated in Figure I-2.1. Conceptually, it consists of three main logic tree levels and the interpolation of amplification factors. Level 1 is representing here the evaluation method. In a simplified way, the weight for the NL method can be set to 0% at PGA<0.3 g and to 80% at PGA>1g. Inbetween there is a linear interpolation. The sum of the weights of SHAKE and RVT corresponds to (1 – weight of NL). The relative weights of the EQL methods are: SHAKE 50%, RVTbc 25% and RVTrand 25%. Level 2 is dealing with the soil profiles. In case of the NL branch only the profile P1 (or P6) is applied. Level 3 is treating the material model. In case of NL and RVTrand only the best estimate material model is usually used. For SHAKE and RVTbc the material models M1, M2, M3 have weights of 25%, 50% and 25%.

Amplification factors are interpolated linearly for each spectral frequency between the available PGA values, or extrapolated as constant value. Depending on the expert, they can conceptually also have an aleatory variability "logic tree", but practically it is zero. Furthermore, there is a maximum ground motion logic tree defined by the SP3 experts.

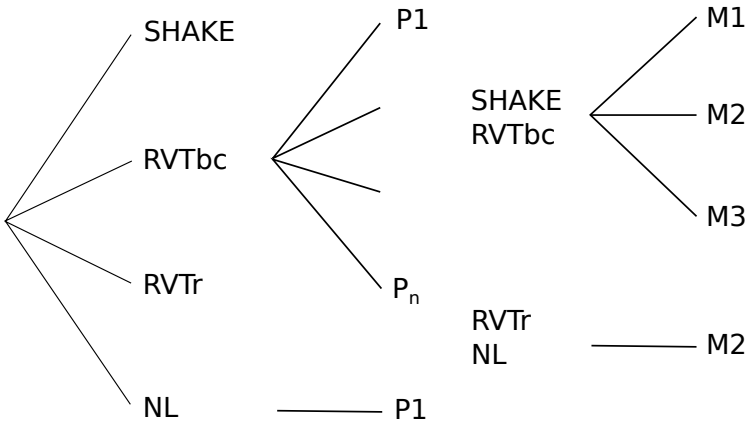

Figure I-2.1: Basic logic tree structure for SP3.

Chapter 3

Proposed Velocity Profiles for KKB-EKKB Sites

This chapter explains the rationale behind the proposed three velocity profiles for the Beznau site. It also takes into account all the information released in the file "TP3-GTC-1009 Additional-Site-Invest-Data-KKB-EKKB", in particular the documents "TN-290.05-3 - Profile NOK postWS.pdf" and "Beznau-DC-V_S-comparisons" .

3.1 Initially Proposed Velocity Profiles and Comments

3.1.1 Original Proposal, September 2009 (KKB213D0016-Rev.0)

One major difference with the previous PEGASOS velocity profiles was a reduction of the impedance contrast at the base of Opalinus Clay (higher velocities in Opalinus Clay, and lower in top Lias). The proposed models were based primarily on cross-hole data, with large correction factors to account for anisotropy, especially in the Opalinus Clay unit. The "reference" model was proposed to MK1. Model MK2 was a modification with a 10% reduction in gravel and Opalinus Clay, and a simplified profile underneath. The third model (PM) assumed smaller anisotropy values, and more homogeneous units, except in the top lias units which exhibit a pronounced low velocity zone: the Schilfsandstein unit was assumed to have a low velocity because of high porosity; the larger velocity jump however is at the base of the gravel layer (see Fig. I-3.1).

The models proposed for EKKB (see Fig. I-3.2) were simply adapted from the KKB models taking into account:

- the larger thickness of gravel layer (22 m instead of 9 m),
- the slightly smaller depth of the top Lias (56 m instead of 64 m),
- the slightly smaller depth of the reference homogeneous bedrock - Top Gipskeuper (122 m instead of 129 m).

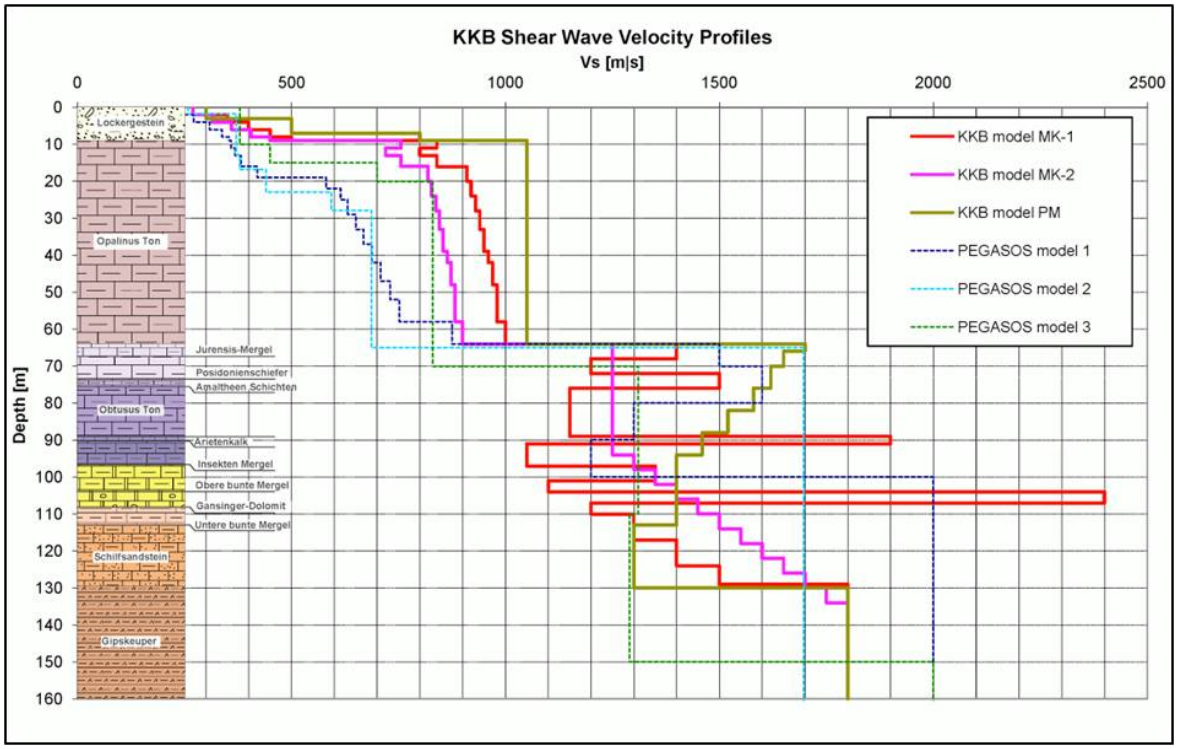

Figure I-3.1: KKB Models proposed by the NOK experts in comparison to the original Pegasos1 velocity profiles.

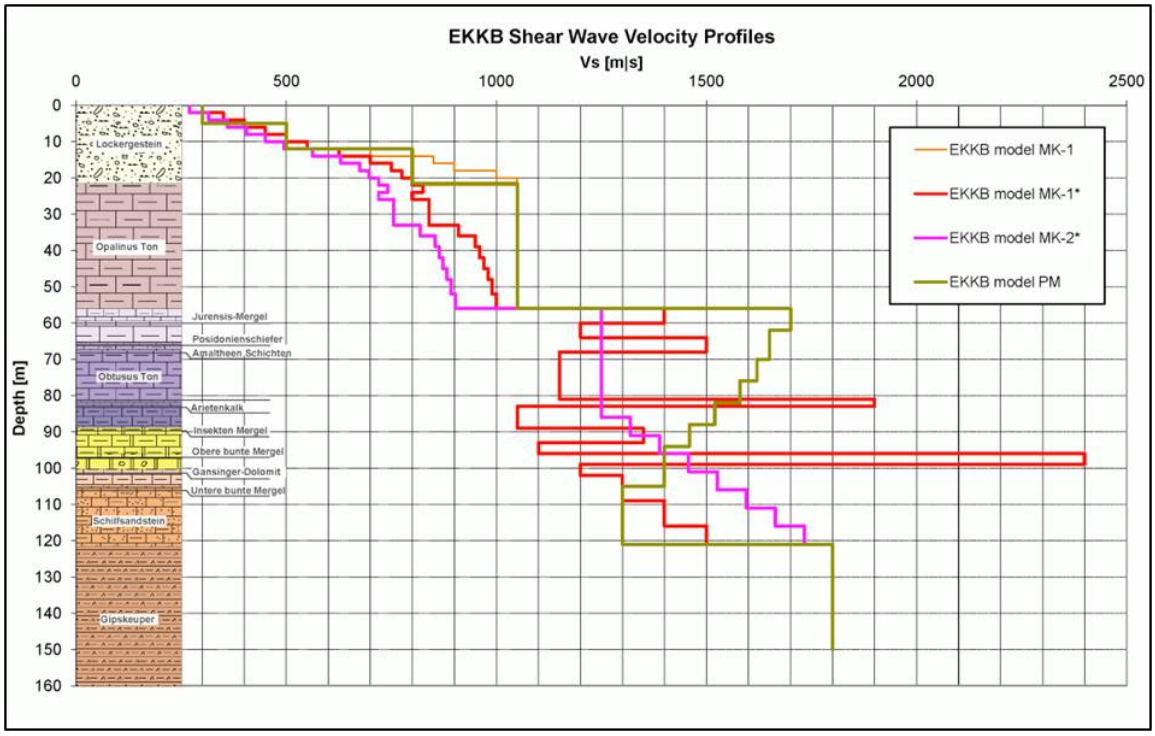

Figure I-3.2: EKKB Models proposed by the NOK experts in comparison to the original Pegasos1 velocity profiles.

3.1.2 Comments from the Workshop WS2b/SP3 (November 2009)

The major comments on these propositions and "to do list" were summarized in the summary presentation by N. Abrahamson (TFI-RF-1149).

- KKB and EKKB should be assigned different velocity profiles, as the thickness of the Opalinus Clay unit is highly variable, and even though the fundamental frequency is constant around 2.5 - 3 Hz, over the whole area.
- It was asked also to check the proposed profiles through the associated dispersion curves
- Rock (including opalinus clay)
  - It was agreed to assign the bedrock a velocity of 1800 m/s at a depth of 130 m.
  - KKB / MK1 model was thought acceptable while MK2 deep gradient should be reduced to reach 1500 m/s at 130 m depth, in order to be consistent with measured Swiss data.
  - The PM model did not look consistent with the available data and was thus dropped;
  - The issue of the velocity in the upper part of the Opalinus Clay was raised, and the need was underlined to look for additional constraints (possibly from MASW) and to develop a third model with a special focus on this issue
- Gravel layer
  - it was decided to adjust the MK1 model with increasing V_S at shallow depths to be more consistent with cross-hole and ambient vibration data.
  - KKB: 400 m/s to 500 m/s at 9 m depth
  - EKKB: from 500 m/s at 9 m to 600 m/s at 22 m

The velocity profiles proposed by the utilities give a major weight to borehole data. The main rationale behind the proposition of modifications or new profiles thus lies in the due accounting of dispersion curve data. They were thus checked by comparing the corresponding dispersion curves with the measured ones, from both MASW and AMV techniques.

3.2 Modifications and Proposed Velocity Profiles for KKB-Beznau

The work of the SP3 expert group has thus been to assign a balanced weight to all sources of information, i.e., both surface wave and body wave techniques. This was done by adapting the MK1 and MK2 models (slightly modified according to the conclusions of 19. November 2009), based primarily on Swiss data, and proposing a third model based primarily on dispersion curve data – especially for the shallow and intermediate parts. The adaptations of MK1* and MK2* models were driven by the observation that the corresponding Rayleigh wave velocities were too fast at intermediate to high frequencies, and by the introduction of some weathering at the top of the Opalinus Clay to correct this. The modifications / adaptations were done basically on a trail and error basis.

(*Note : There is an error in Figure I-3.1 of "TN-290.05-3 - Profile NOK postWS" : MK1 and MK2 are inverted : MK1 should be the blue velocity profile, i.e. the fastest one.*)

3.2.1 Model B1 : "Simple WOC" (WOC = Weathered Opalinus Clay)

The base model is the modified MK2 model of early January 2010 (cf. Figures I-3.3 and I-3.4).

- The bedrock does not take into account the short wavelength vertical heterogeneities associated with thin layering (modified as asked on 19.-20. November 2009).
- The main further modification concerns the top 15 m of Opalinus Clay: the velocity has been significantly reduced between 9 and 24 m depth, with now a rather regular increase from 500 m/s to to 700 m/s at 20 m depth: there is no longer any low velocity zones in the Top Opalinus Clay.

The new dispersion curves are consistent both with the AMV dispersion curves at intermediate frequencies (because of the weathered top Opalinus Clay) and the high frequency low MASW velocities (low surface velocities in gravel). The modifications are indicated in Figure I-3.4 with a comparison of January MK2 model (light blue, KKB WS simple) and the new model (thick blue, simple WOC = 100120 Simple)

3.2.2 Model B2 : "Complex WOC"

The base model is the modified MK1 model of early January, with the "complex" velocity profile in the Lias units, following the cross-hole data. The further modifications consist in reducing the velocity down to a depth of 26 m, i.e., in the gravel layer (9m thick) and in the upper part of Opalinus Clay

- Gravel layer : the velocity has been significantly reduced (gradient from 270 to 450 m/s, instead of 400 to 500 m/s) in order to match the MASW measurements
- Top Opalinus Clay (9 - 26 m): the large velocity jump between gravel and OC was replaced by an almost linear velocity gradient, without any velocity jump. Once again, the rationale behind these modifications is a better matching of measured dispersion curves at intermediate (AMV) and high (MASW) frequencies. The modifications are indicated in Figure I-3.5 with a comparison of the January 2010 MK1 model (light green, KKB WS complex) and the new model (thick green, complex WOC = 100120 Complex)

3.2.3 Model B3 : AMV

This model is indeed the simplest one as it is essentially derived from the inversion of dispersion curves, which do not allow the resolution of thin layers. The base model was the model proposed by SED on the basis of array recordings of ambient vibrations, with some simple extrapolation at large depth on the basis of borehole data, and some reduction in the upper part of Opalinus Clay to better fit the MASW results (originally not taken into account in the inversion.

The comparison of dispersion curves in Figure I-3.4 shows that the three different profiles provide the following ranking :

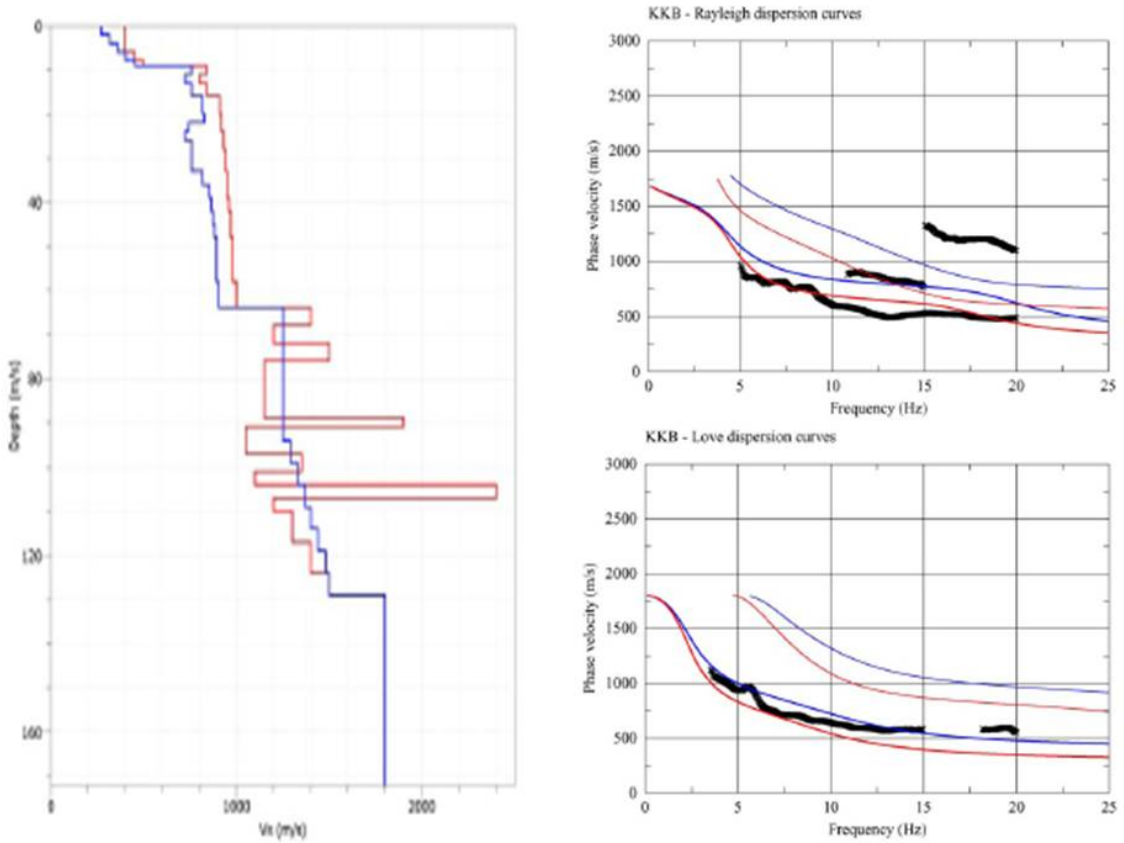

Figure I-3.3: KKB : Modified MK1 and MK2 models (January 2010): velocity profiles and dispersion curves (Rayleigh and Love waves). MK1 is blue on right and red on left. (From TN-290.05-3 - Profile NOK postWS).

"Low" frequency 5-10 Hz	Intermediate frequency 10-15 Hz	High frequency f > 15 Hz
AMV < Simple < Complex	AMV < Simple < Complex	Complex = Simple < AMV

3.3 Proposed Velocity Profiles for EKKB-Beznau

The proposed profiles for EKKB are directly adapted from the KKB profiles with due accounting for the changes in the thicknesses of gravel and Opalinus Clay layers, and the total depth over Gipskeuper unit. They are displayed in Figures I-3.5 and I-3.6.

3.3.1 Model EB1 : "Simple WOC" (WOC = Weathered Opalinus Clay)

The only change with respect to the KKB corresponding profiles are the following:

- Depth range 9 - 22 m (gravel instead of OC) : almost linear gradient from 450 m/s to 600 m/s,
- Depth range 52 - 64 m : changes in the depth of the OC / Lias interface (56 m instead of 64 m),

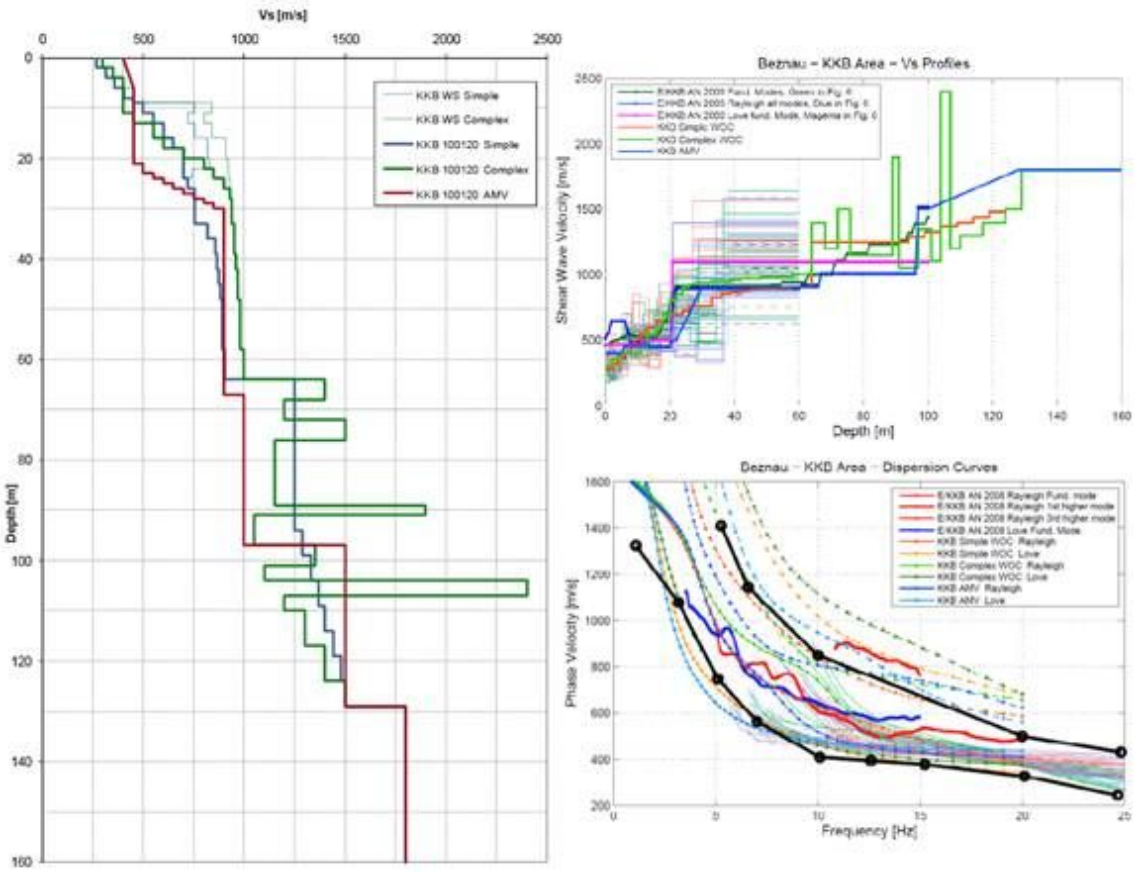

Figure I-3.4: KKB: Comparison of dispersion curves for the 3 final models with the DC measurements. (From TP3-TN-1068 Soil-Models-Beznau).

- Depth 86 - 121 m : the light gradient has been moved upward by 8 m to match the Top Gipskeuper depth of 121 m instead of 129 m.

3.3.2 Model EB2 : "Complex WOC"

The changes with respect to the KKB are very similar to those performed for the "simple WOC" model; however, the base model was the EKKB unmodified MK2 model, so that the velocity profile within the Opalinus Clay is slightly different (slightly lower indeed at equivalent depths):

- Depth range 9 - 22 m (gravel instead of OC) : almost linear gradient from 500 m/s to 600 m/s,
- depth range 22 - 56 m : slight changes in the OC velocity,
- Depth 56 - 121 m : the complex profile has been moved upward by 8 m to match the Top Gipskeuper depth of 121 m instead of 129 m.

3.3.3 Model EB3 : AMV

The changes with respect to the KKB AMV B3 profile are:

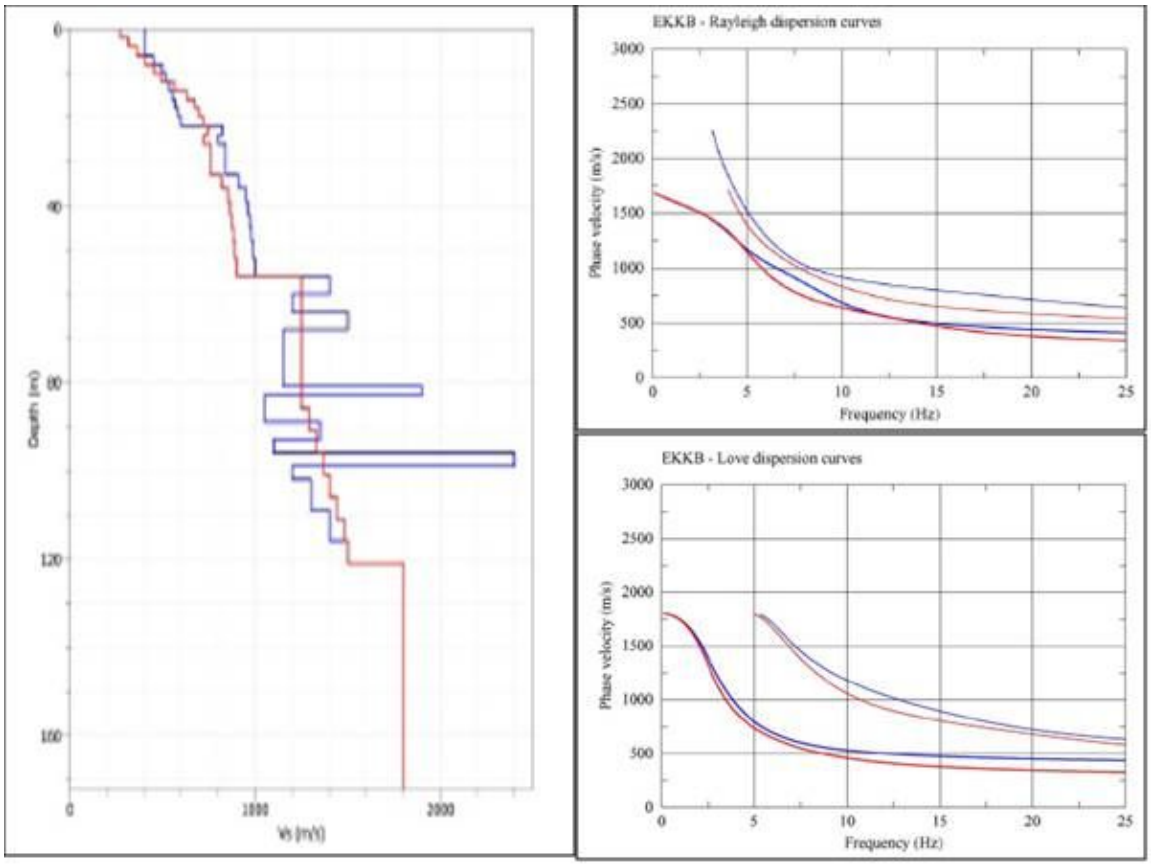

Figure I-3.5: EKKB: Modified MK1 (blue) and MK2 (red) models (January 2010): velocity profiles and dispersion curves (Rayleigh and Love waves). (From TN-290.05-3 - Profile NOK postWS).

- a slightly lower velocities in the top 6 m of the gravel layer,
- a much thinner weathered part at the top of Opalinus Clay (only a 10 m thickness is needed to reach the velocity of 900 m/s, instead of 31 m for B3),
- the thickness of the two homogeneous layers below Opalinus Clay and above Gipskeuper have been changed to 40 m for the layer with $V_S = 1000$ m/s (instead of 30 m), and to 24 m for the layer with $V_S = 1500$ m/s (instead of 32 m).

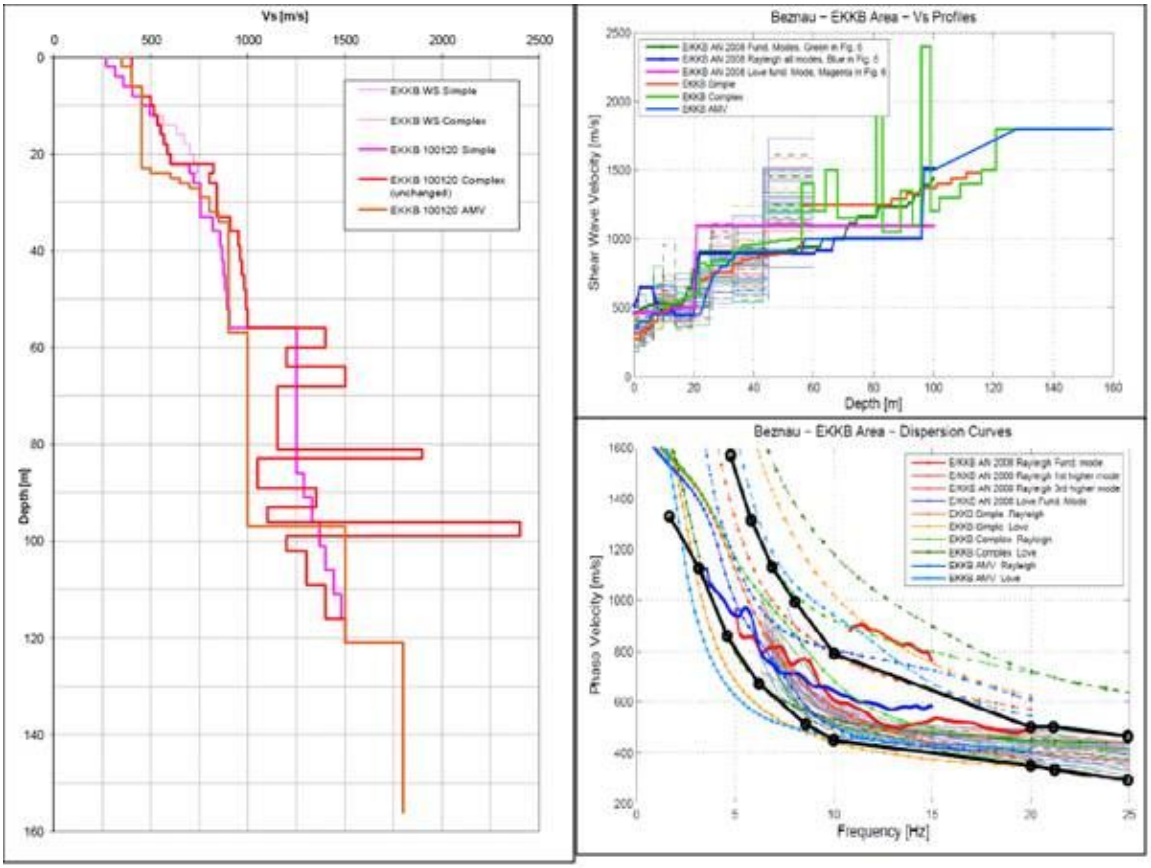

Figure I-3.6: EKKB: Comparison of dispersion curves for the 3 final models with the DC measurements. (From TP3-TN-1069).

3.3.4 Review of Model P3 for Opalinus Clay

In the meeting of 5. March 2010, SP3 experts discussed the model P3 mainly with respect to the appropriateness of the V_S profile for the Opalinus Clay layer. The utilities considered the shear wave velocities of model P3 too low. Based on the information forwarded by AXPO (AXPO Report KKB 213 D0020: Projekt SOBE-BEL, Comments to PRP-SP3 Expert Models and Expert Request from SP3-Working Meeting of 5. March 2010, Part 2: Reactor Building, Results of Settlement Measurements) providing the settlement of the reactor building during and after construction (10 mm under a vertical pressure of 0.55 MPa). The experts made some back-calculations to compute the shear modulus of the Opalinus Clay.

The assumptions are as follows:

- Foundation radius of the structure : 18.9 m
- Dead load at the end of construction : 556 MN
- Settlement at the end of construction : 10 mm

As a matter of fact the settlement was almost reached 1 year before the end of construction and did not change at least for the following 5 years. One notices that starting in 1982 (13 years after the end of construction) there is dramatic change and that the settlements are now doubled.

Nevertheless, taking the value at the end of construction the shear modulus of the Opalinus Clay that can be back-figured from the measurements is equal to:

$$F = K \cdot w = [4G \cdot r/(1-\nu)]w \rightarrow G = 556 \cdot 0.6/4/18.9/0.01 = 450\,\text{MPa} \qquad \text{(I-3.1)}$$

It is assumed to have a homogeneous half space, since the Opalinus layer at EKKB is 34 m thick. This assumption is approximately correct for a static calculation (no wave propagation). For KKB the thickness of the Opalinus layer is even larger: 71 m. Furthermore a Poisson's ratio of 0.4 is taken, since there seems to be any consolidation taking place after construction; a drained behavior is therefore more representative of the actual behavior. The corresponding shear wave velocity would be $V_s = \sqrt{(G/\rho)} = \sqrt{(450/2.4E-3)} = 430$ m/s.

If we compute the induced axial strain it is smaller than $\varepsilon = w/H = 0.01/34 = 3 \cdot E-4$ and the shear strain is smaller than $(1+\nu)\varepsilon = 4 \cdot E-4$. This is a rather small value.

From the discussions during the meeting the Opalinus Clay is almost linear but we can conservatively assume that the "elastic" shear modulus would be of the order of 40% higher than the value computed above; this would give an elastic shear wave velocity of 510 m/s. Even if we multiply the back-calculated shear modulus by a factor of 2, the elastic shear wave velocity would not exceed 610 m/s. These values turn out to be very surprisingly close to those assigned to profile P3 (at least for the best estimate values (450 m/s to 900 m/s).

It is proposed to keep the shear wave profiles in the Opalinus Clay, or to shift the P3 V_S-profile assuming that the best estimate profile presently considered is in fact the lower bound and to define the best estimate and the upper bound by multiplying those values by 1.25 and 1.56. This is a small change from what was anticipated in the meeting, but from the SP3 Experts notes the NPP Beznau representative mentioned a few mm of settlement for a vertical stress

of 1.8 MPA. The measurements give 10 mm for 0.55 MPA (quite a difference). This proposal has to be discussed and to be decided with AXPO and the SP3 experts on 5. March.

3.3.5 Discussion on the V_S-profiles

Two experts were not satisfied with the low shear wave velocities in the soil layer and the team had extensive discussions on this topic and tried to find alternatives with higher V_S in the soil part which also satisfies the eigenfrequency and dispersion curve criteria. No alternative was found which satisfies all criteria (eigenfrequency, dispersion curves, higher shear wave in the soil and in the rock acceptable shear wave values). Finally the shear wave velocities in the soil layer were accepted (in spite the deficit to be rather low in the soil layer) because the criteria eigenfrequency, dispersion curve, rock velocities are satisfied. Overall the velocities cover an acceptable range and the individual experts will assign weights to the individual profiles.

3.4 V_P-profile for Beznau

For Beznau the referenced model for the shear-wave velocity profile is P1; the parameters take the values $\rho_S = 2.675$ t/m^3, $\rho = 2.2$ t/m^3 below the water table and $\rho_f = 1.0$ t/m^3, then $\varphi = 0.28$. The water bulk-modulus was set equal to 1400 MPa. The final computed V_P is depicted in Figure I-3.7 together with the measured data.

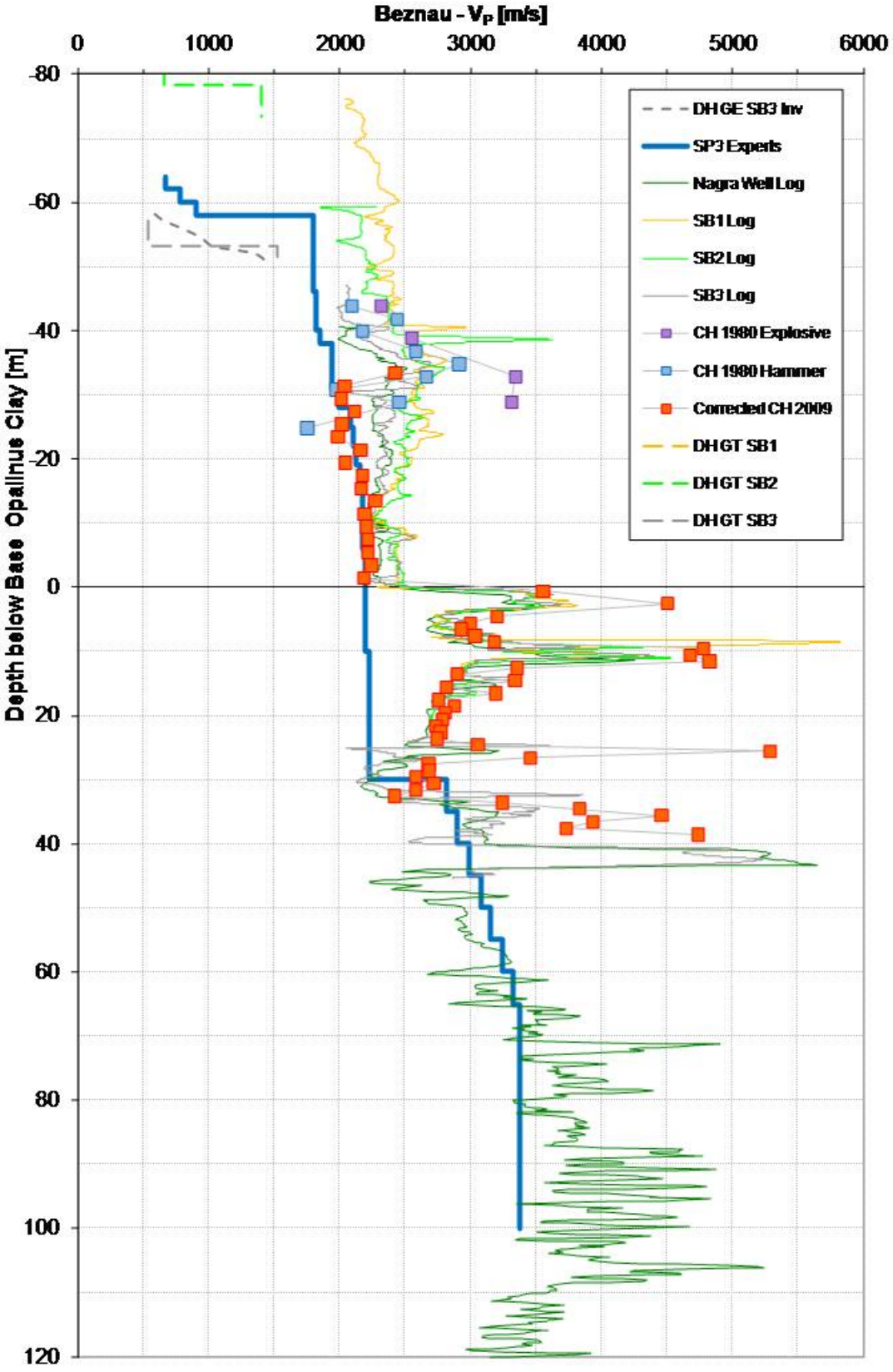

Figure I-3.7: V_S-model and measurements for Beznau (KKB).

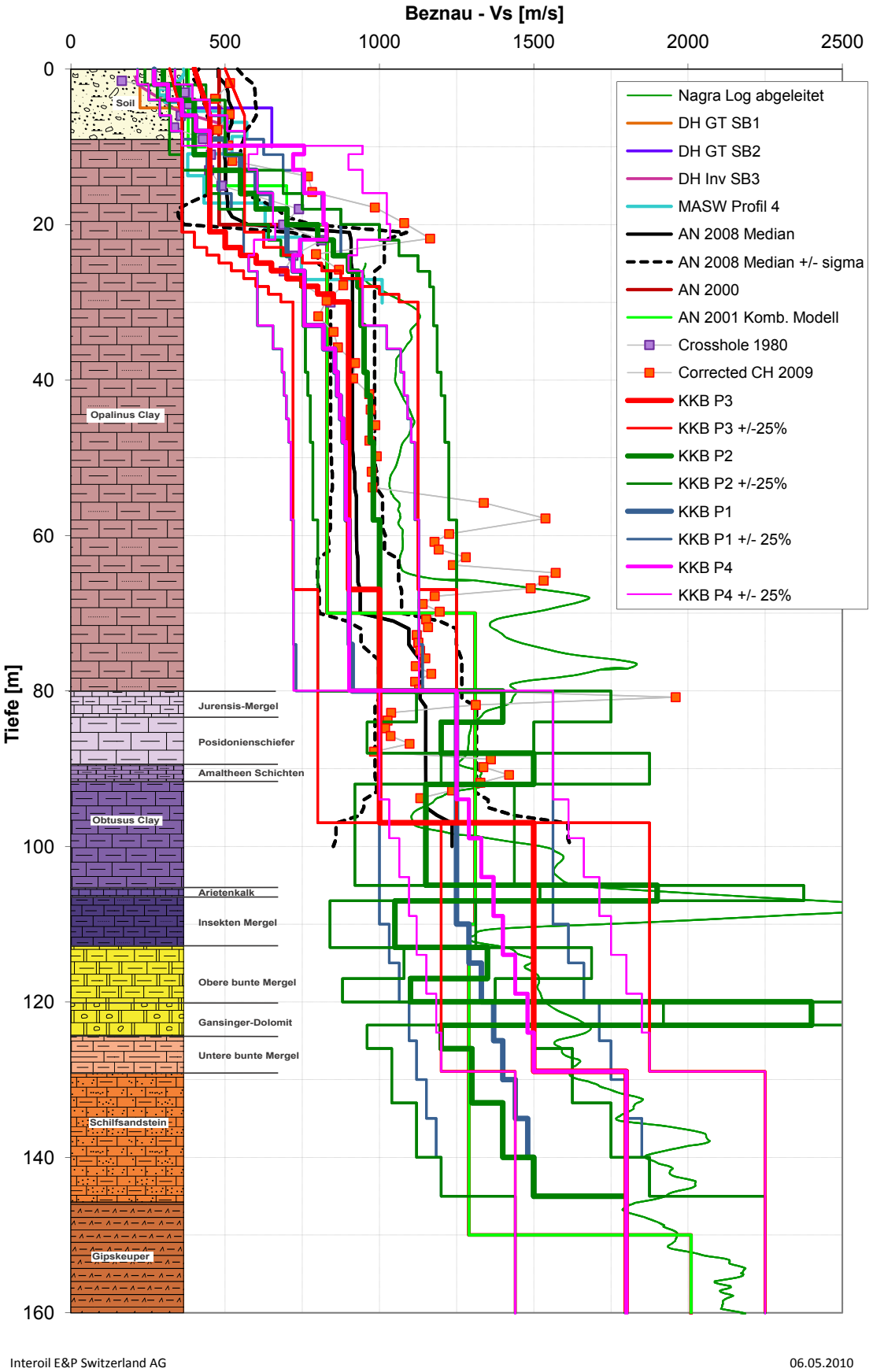

Figure I-3.8: V_S-profiles representative for the whole KKB area.

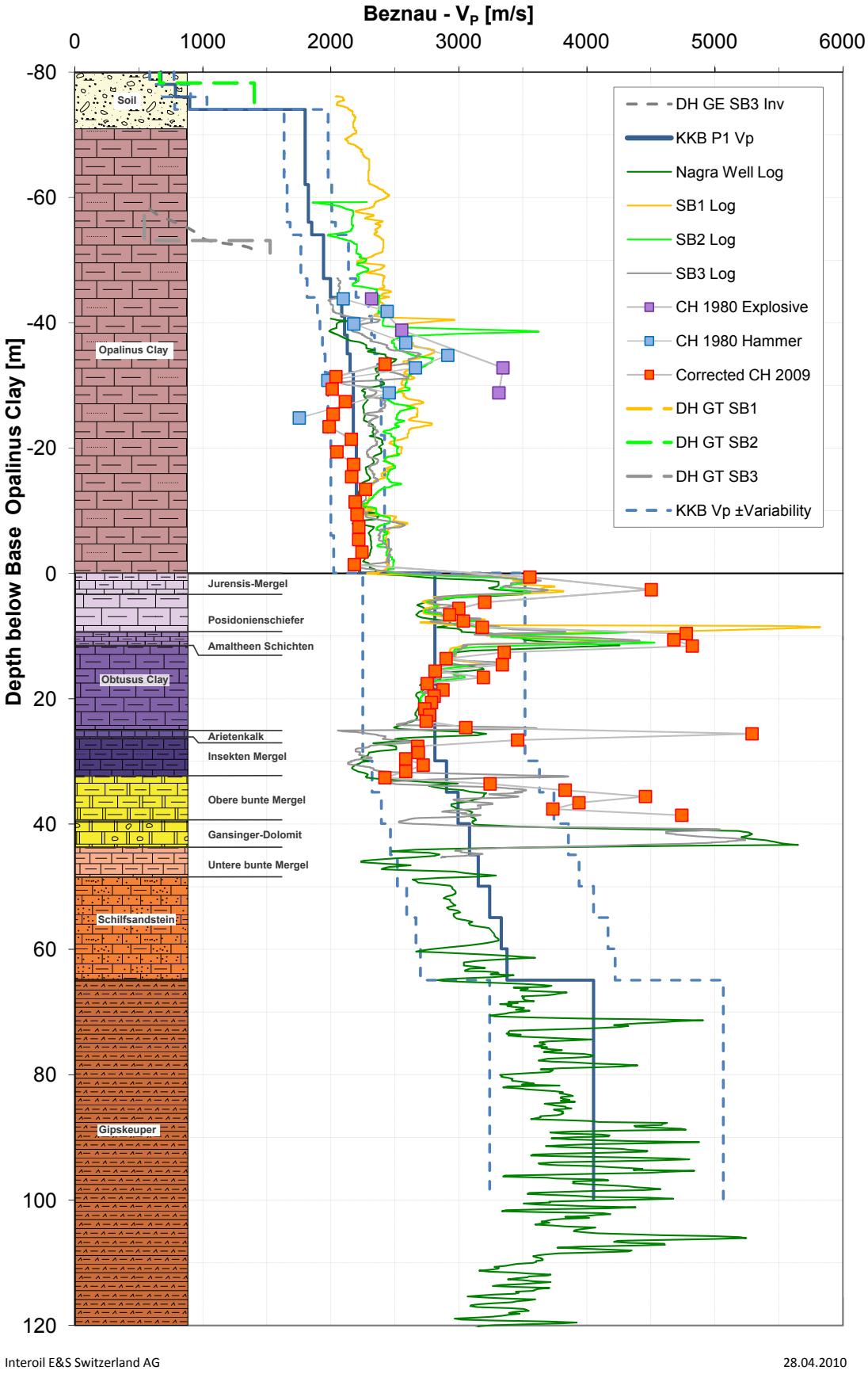

Figure I-3.9: V_P-profiles representative for the whole KKB area.

3.5 Material Models

3.5.1 General Comment

The selected models are based on first priority on tests results and on the results published by Rollins et al. [1998] and Menq [2003]. Menq's curve takes into account a dependence of G/G_{max} on the confining stress while Rollins' curve does not. Furthermore, Menq's curve corresponds to a weaker material compared to Rollins.

Accordingly, examination of the G/G_{max} curves shows that Menq's mean curve coincide with the lower bound of the tests data and Rollins mean to the upper bound. The mean curve is defined as the average between the lower bound and the upper bound curves.

As lower bound for the damping, Rollins mean damping curve was used, while Menq's mean curve was used for the upper bound. From the observations and from also theory, a stiffer material exhibits lower material damping and a softer material, higher material damping.

Those curves have been modified to a small extent to better fit the observed data.

3.5.2 Model for the Beznau Site

For KKB, due to the limited thickness of the soil layer only one set of curves is provided for this site. In the large strain range, the data fit very well the mean curve while the resonant column tests better fit the upper bound curve.

For the damping ratio, the measured values at high strains are too high compared to literature values and the scatter is very large. Even the original Seed's curve and the original data used for the PEGASOS project show lower damping than the new tests results. Therefore the damping curves were fitted to the measured values in the low strain range and damping reflects the nearly nonlinear behavior of stiff rock extrapolated to commonly encountered values in the large strain range. The proposed shear modulus and damping reflects the nearly nonlinear behavior of stiff rock material.

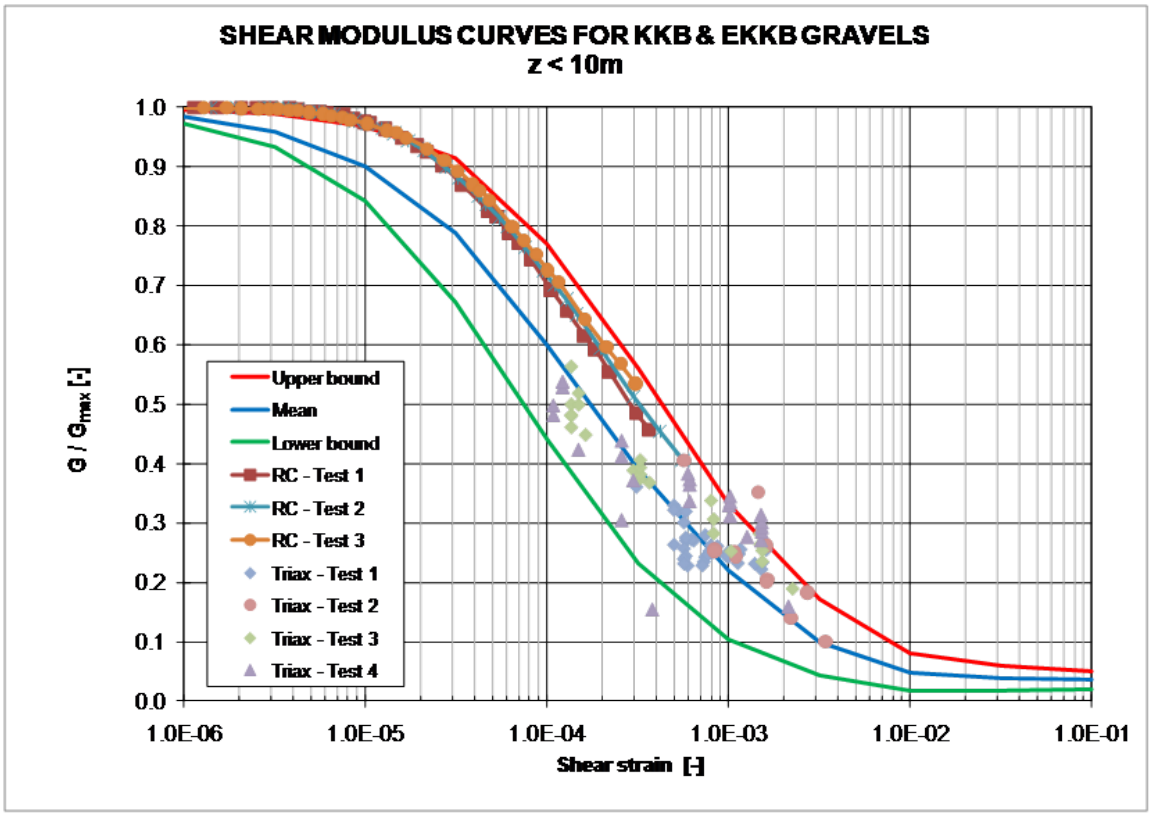

Figure I-3.10: Shear Modulus for $0 < z < 10$ m at KKB.

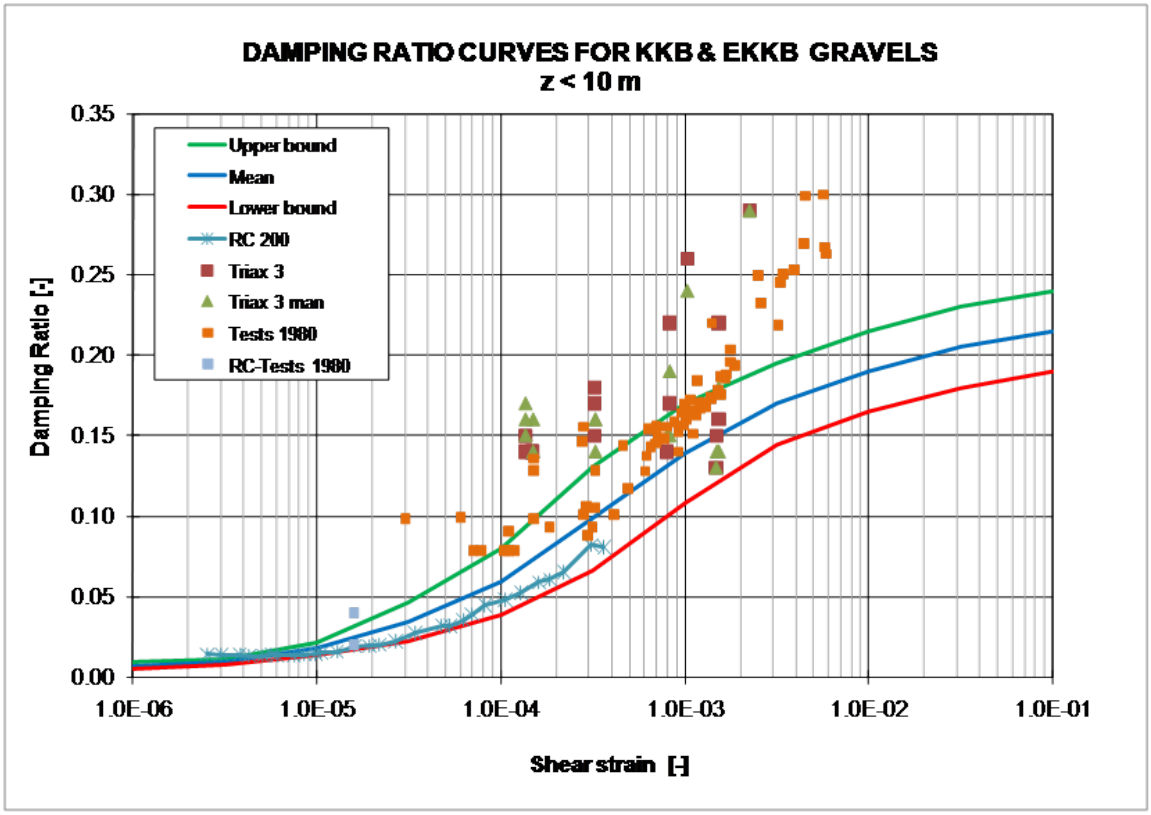

Figure I-3.11: Damping Ratio for $0 < z < 10$ m at KKB.

3.6 Supporting Figures for Beznau

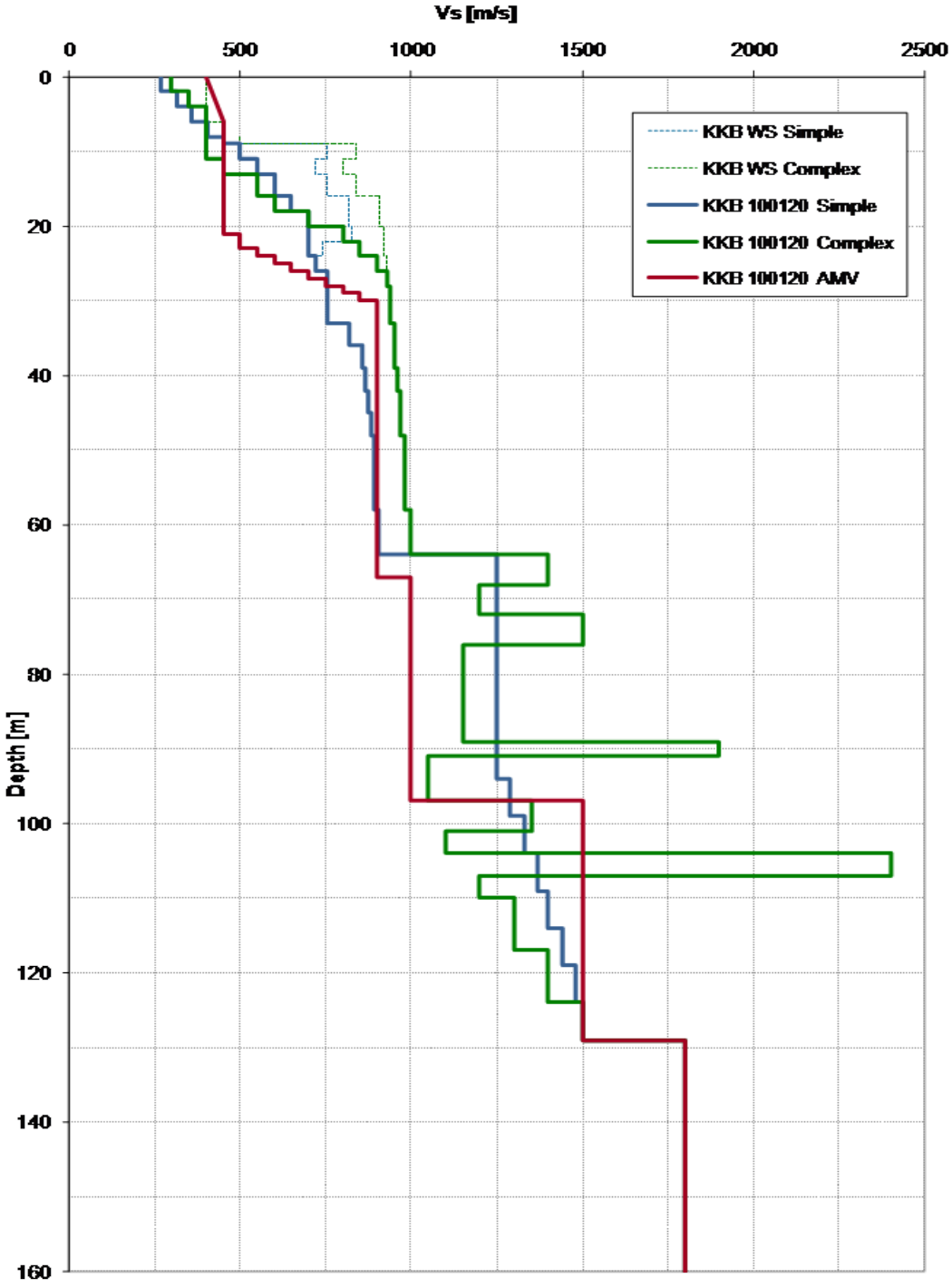

Figure I-3.12: V_S-profiles evaluated by the experts during previous meetings (KKB).

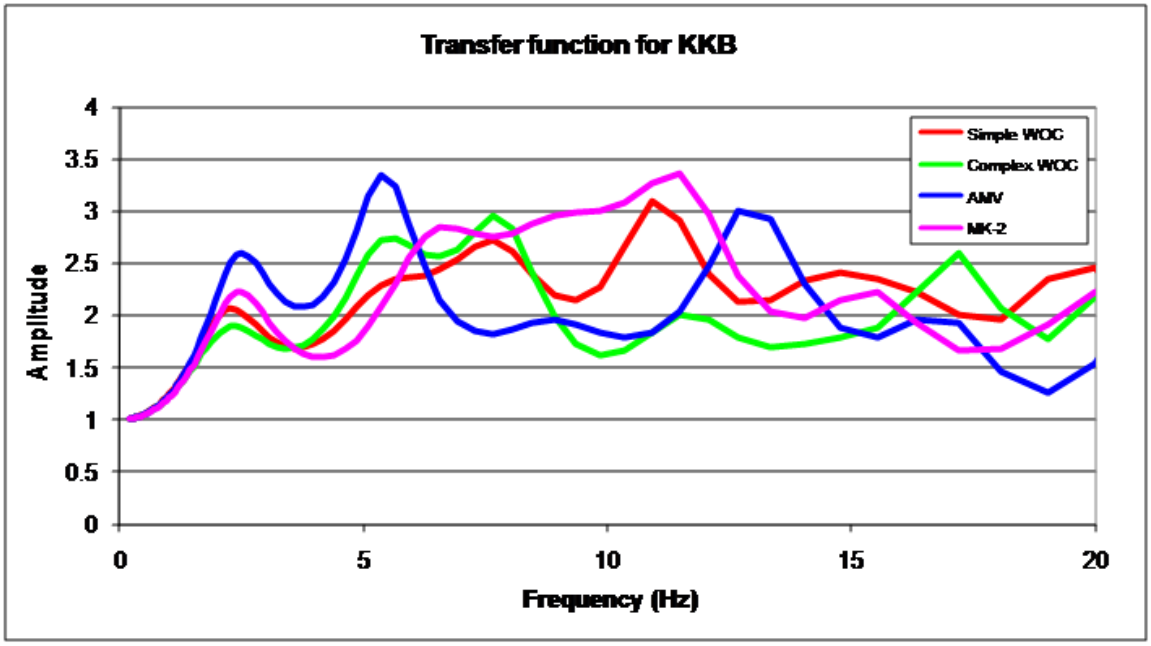

Figure I-3.13: Transfer functions for proposed soil profiles (KKB).

Table I-3.1: Fundamental frequencies, Beznau site.

Profile	Frequency
P1 (Simple WOC)	2.27 Hz
P2 (Complex WOC)	2.51 Hz
P3 (AMV)	2.51 Hz
P4 (MK-2)	2.51 Hz

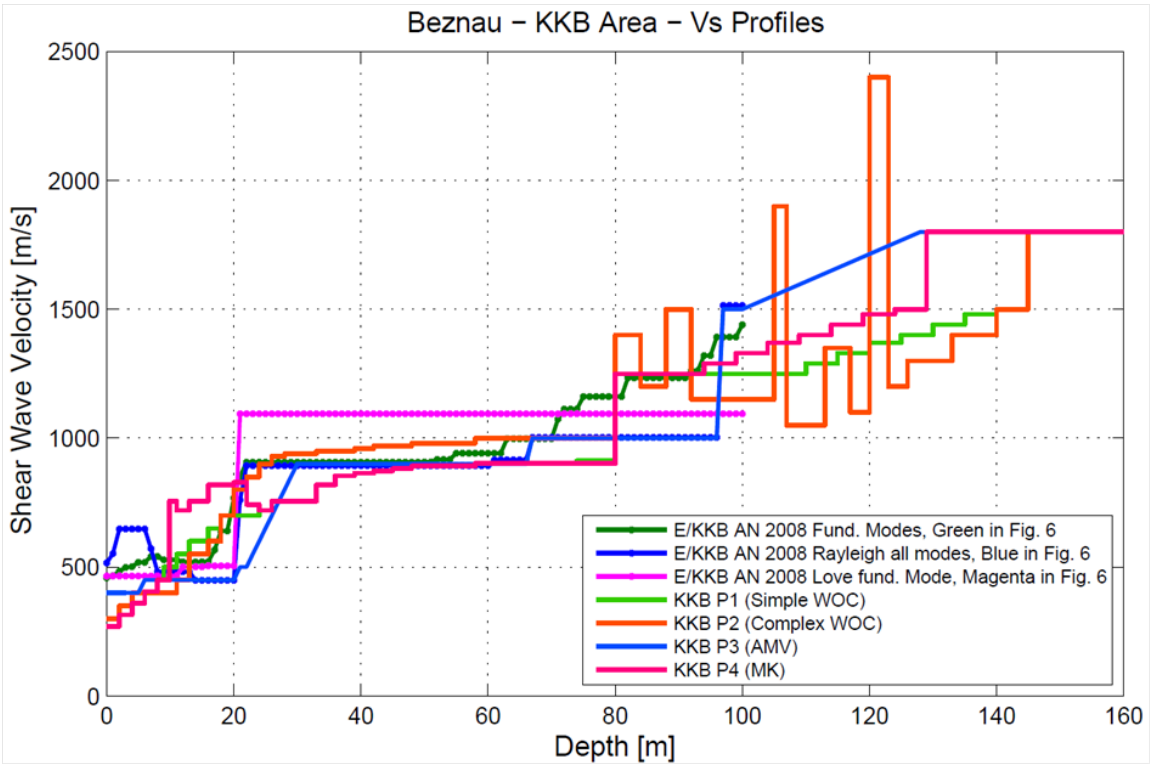

Figure I-3.14: V_S-Profiles (KKB).

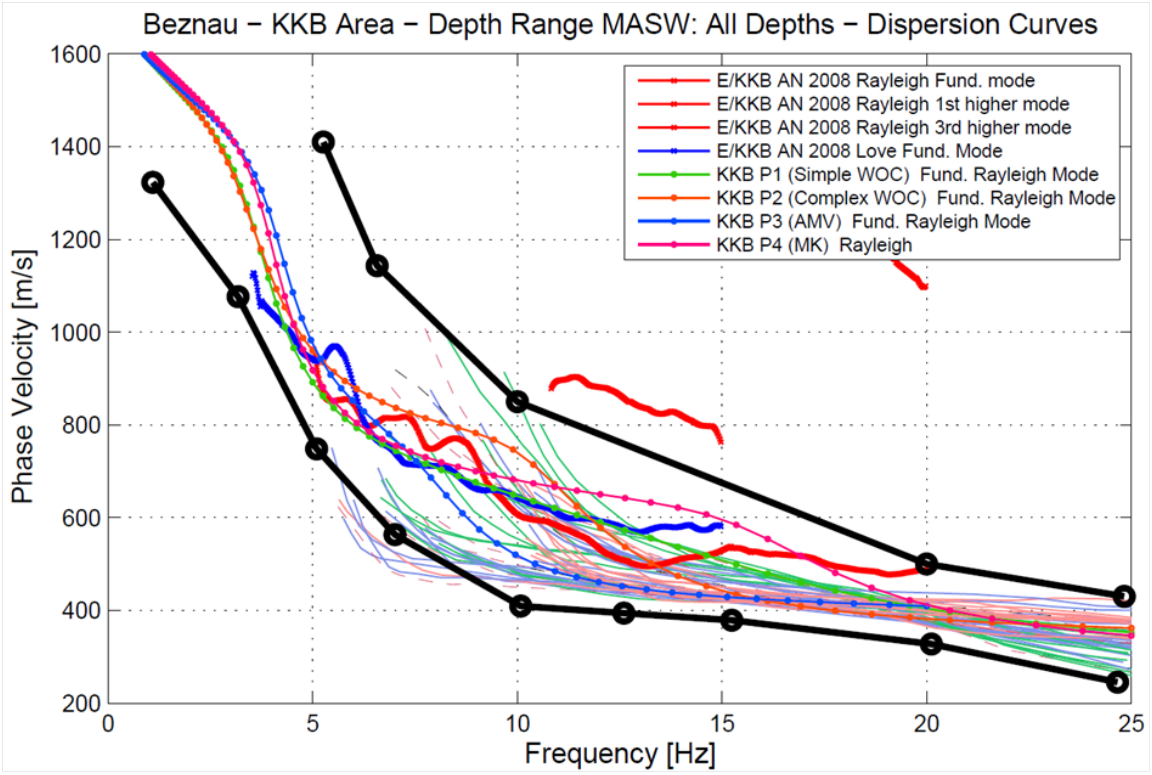

Figure I-3.15: Dispersion curves and bounds (KKB).

3.7 Comparison of PEGASOS vs. PRP Profiles and Material Models

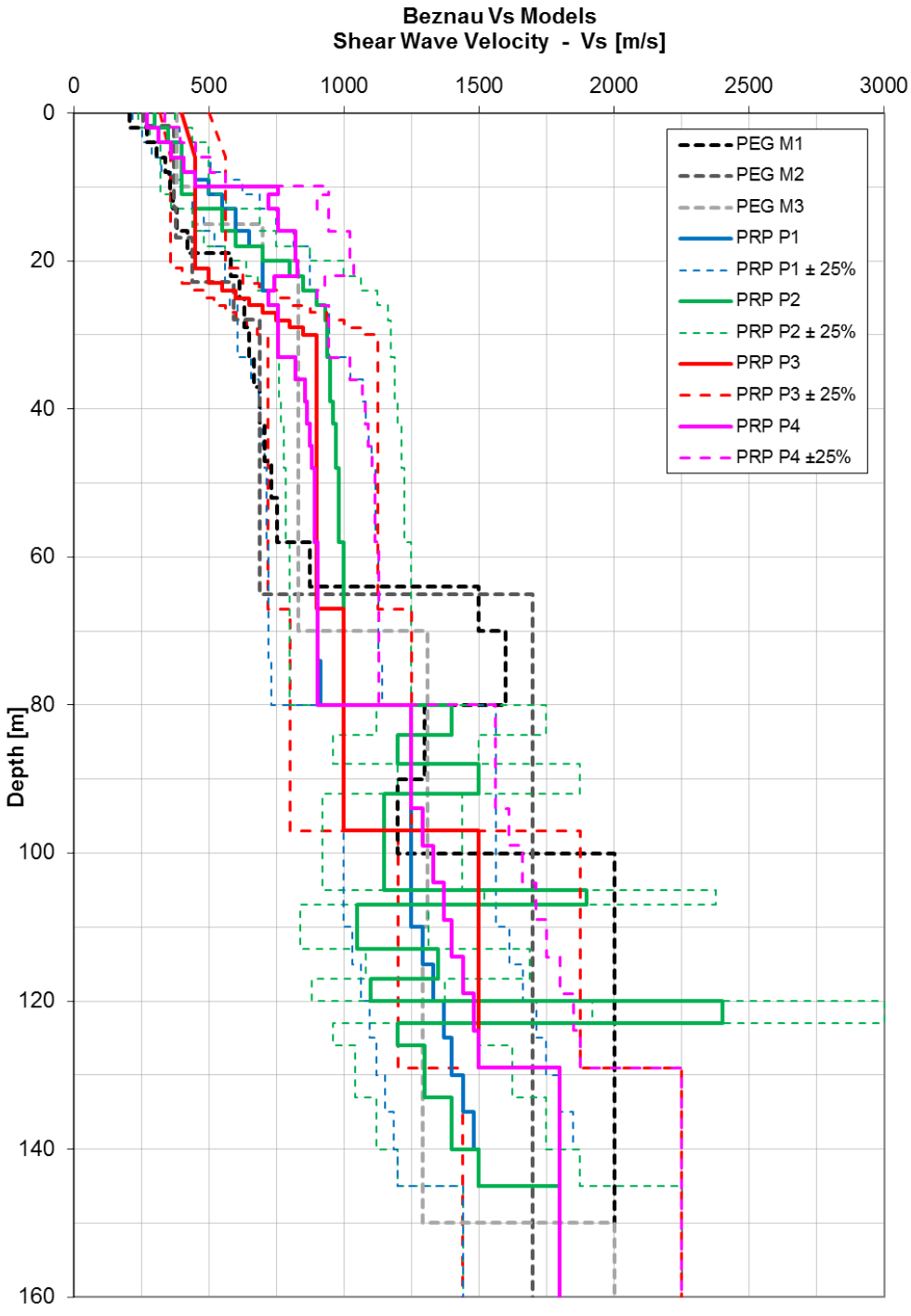

Figure I-3.16: Comparison of PEGASOS and PRP V_S-models for Beznau.

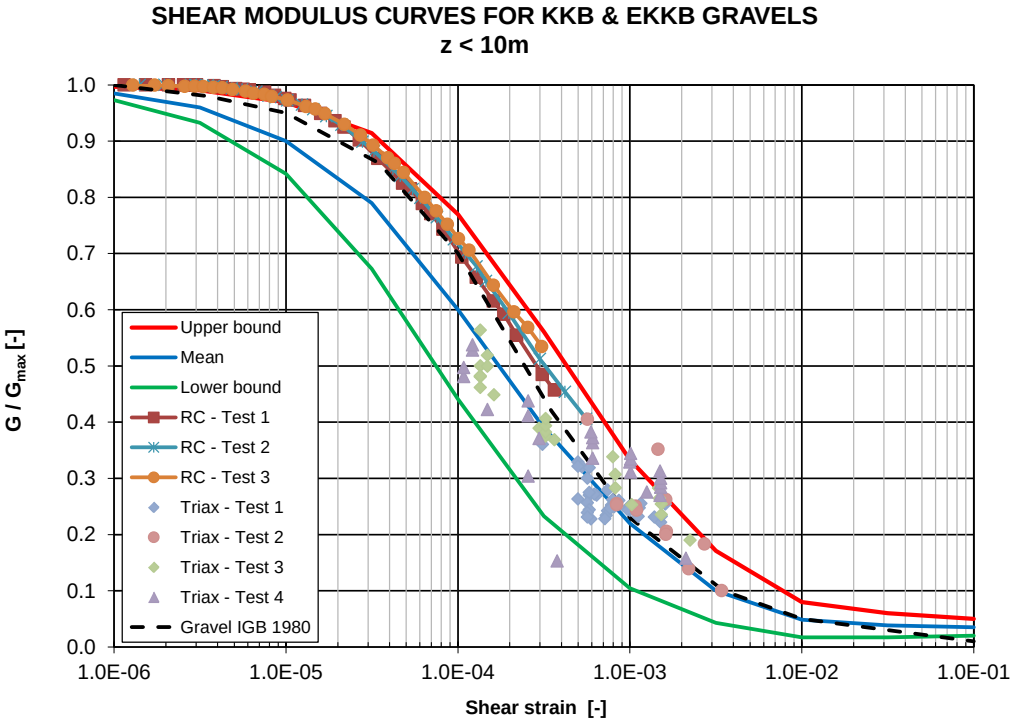

Figure I-3.17: Beznau - Shear modulus curves for KKB and EKKB for gravel, $z < 10$ m.

3.8 V_P-profile for E-Beznau

For E-Beznau the referenced model for the S-wave velocity profile is P1; the parameters take the values $\rho_S = 2.675$ t/m^3, $\rho = 2.2$ t/m^3 below the water table and $\rho_f = 1.0$ t/m^3, then $\varphi = 0.28$. The water bulk modulus was set equal to 1500 MPa between 6 m and 12 m depth and to 1800 MPa below in the soil layer. The final computed V_P-profile is depicted in the following figure with the measured data.

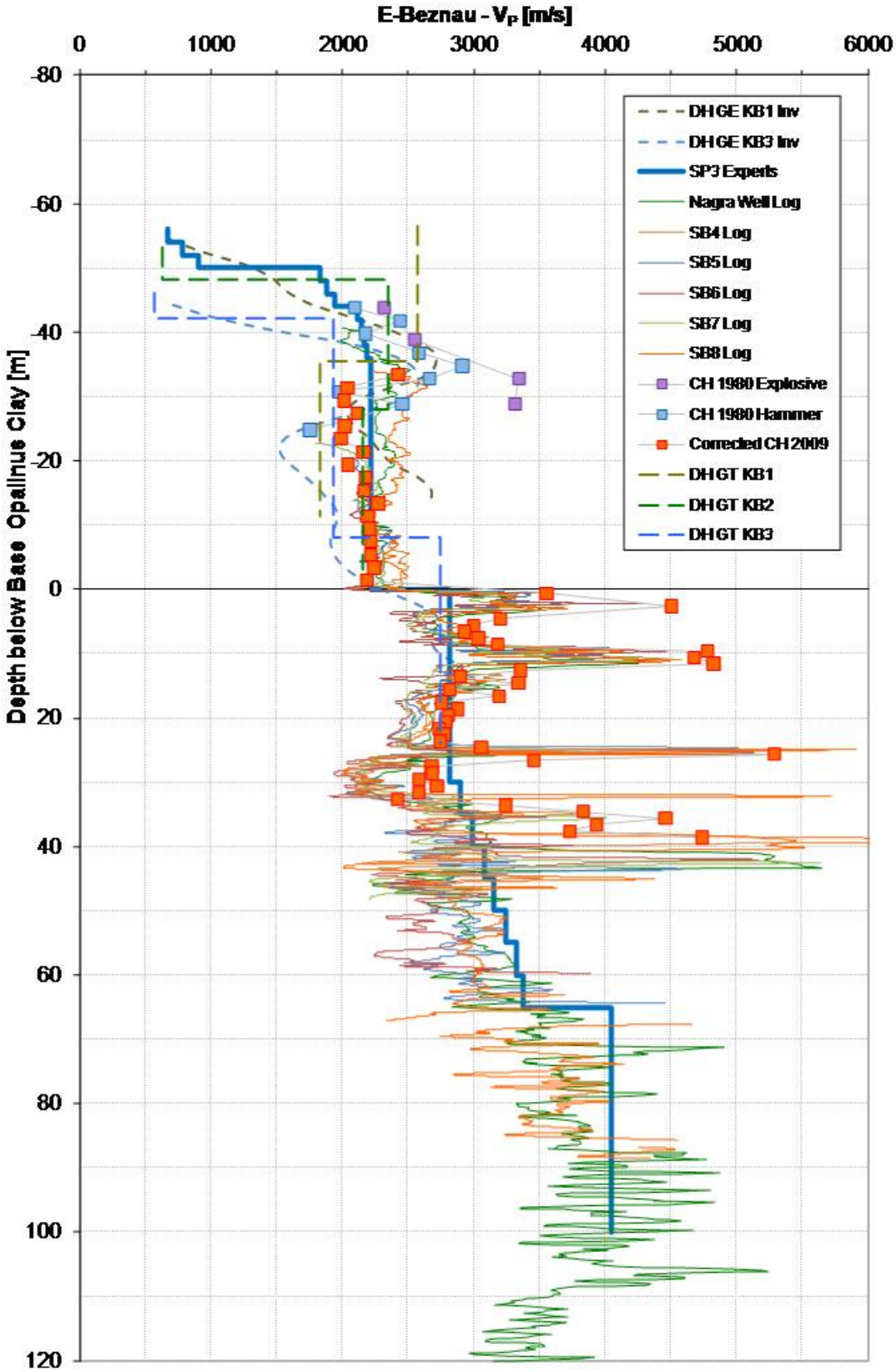

Figure I-3.18: V_P-model and measurements for E-Beznau (EKKB).

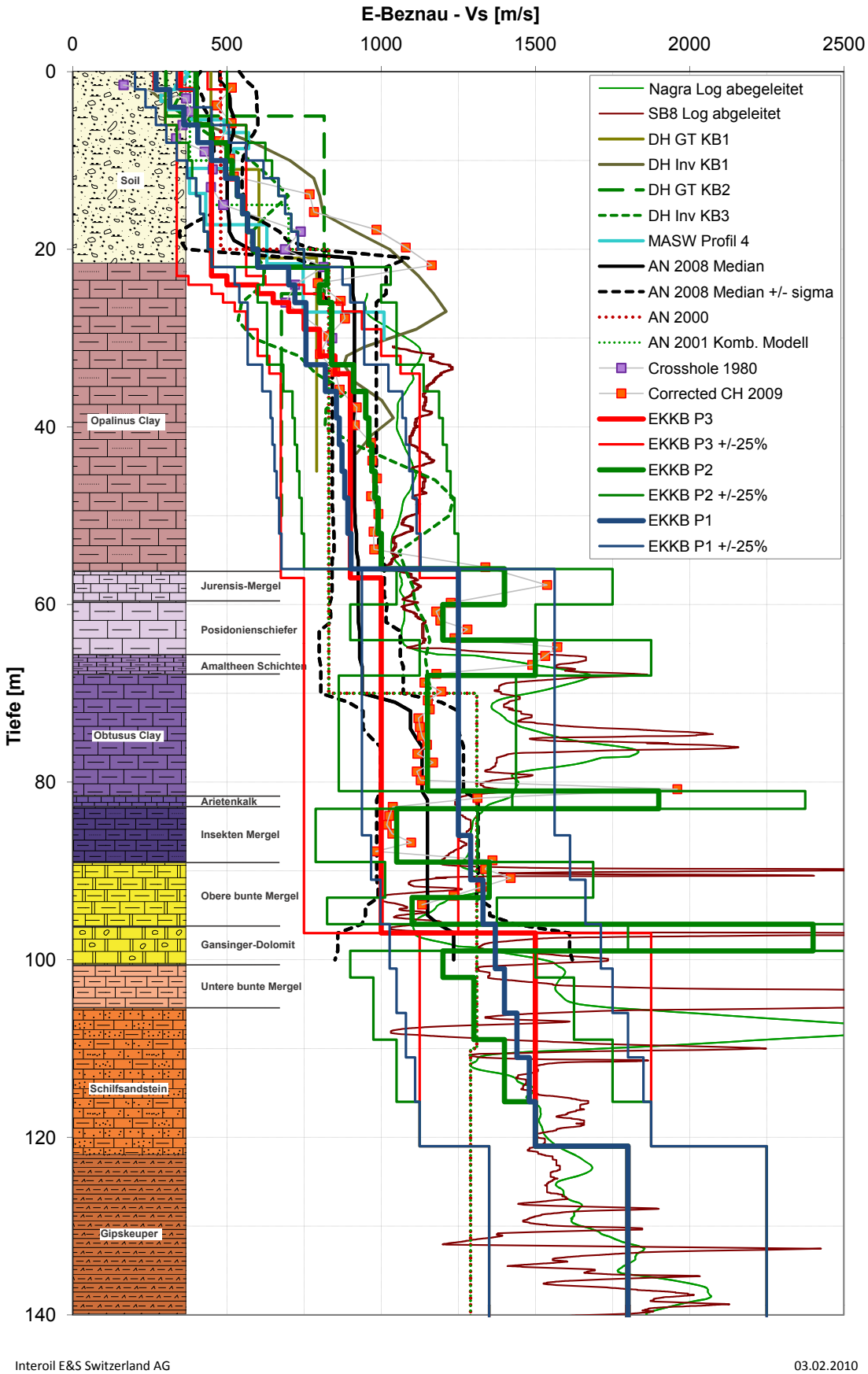

Figure I-3.19: V_S-profiles representative for the whole EKKB area.

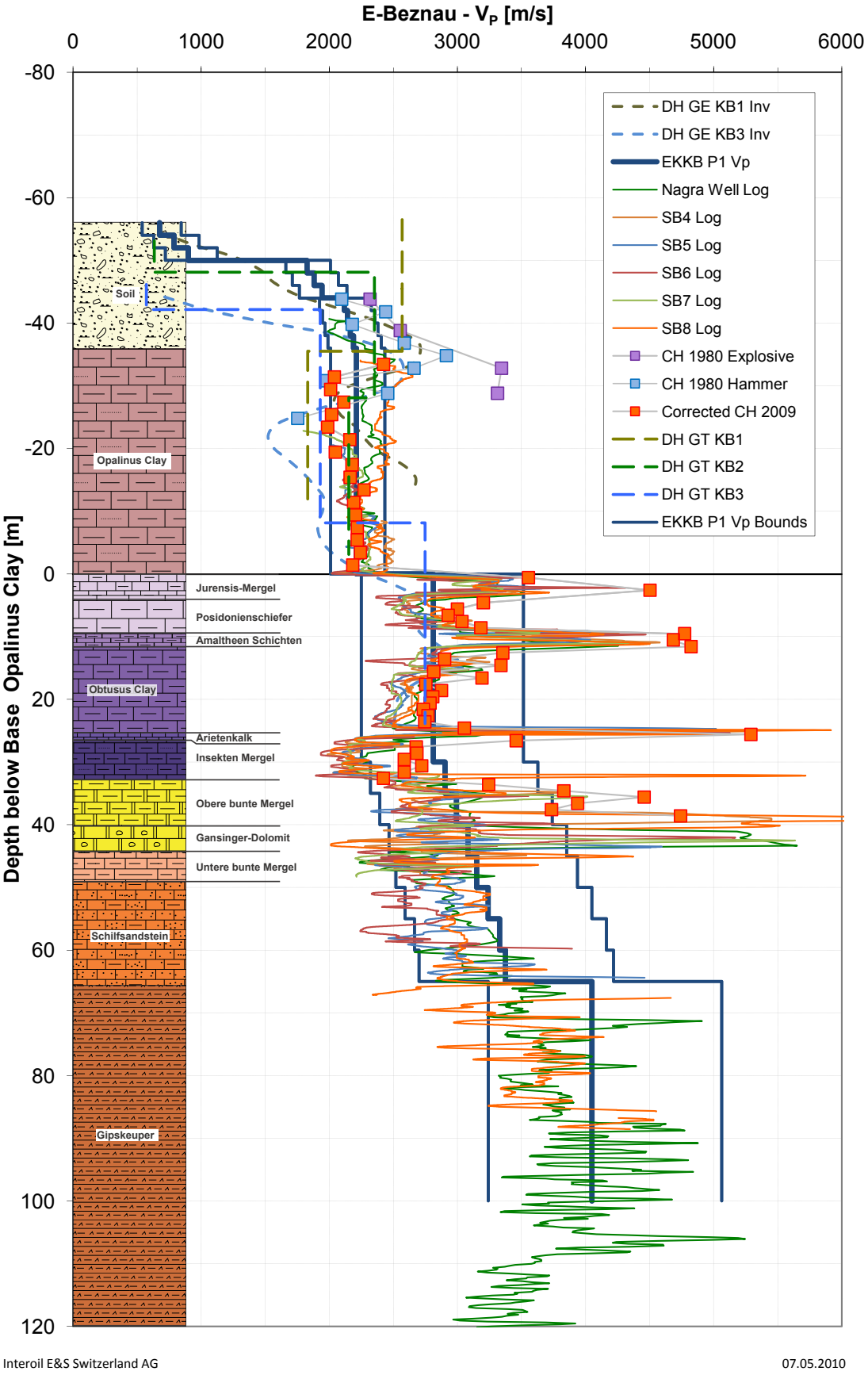

Figure I-3.20: V_P-Profiles representative for the whole EKKB area.

3.9 Material Model for the E-Beznau Site

For EKKB, due to the thickness of the soil layer, two different sets of curves are introduced corresponding to two different confining pressures; the first set corresponds to the top 10 m and the second one to the bottom part (10 to 21 m). The lower bound curve for G/G_{max} for the lower layer was corrected for confining pressure according to Menq's equation which leads to a slightly stiffer material. The upper bound curve, which comes from Rollins, does not depend on the confining pressure and is therefore kept unchanged with respect to KKB. The same corrections apply to the damping curves, but the corrections are small. The proposed shear modulus and damping reflects the nearly nonlinear behavior of stiff rock material.

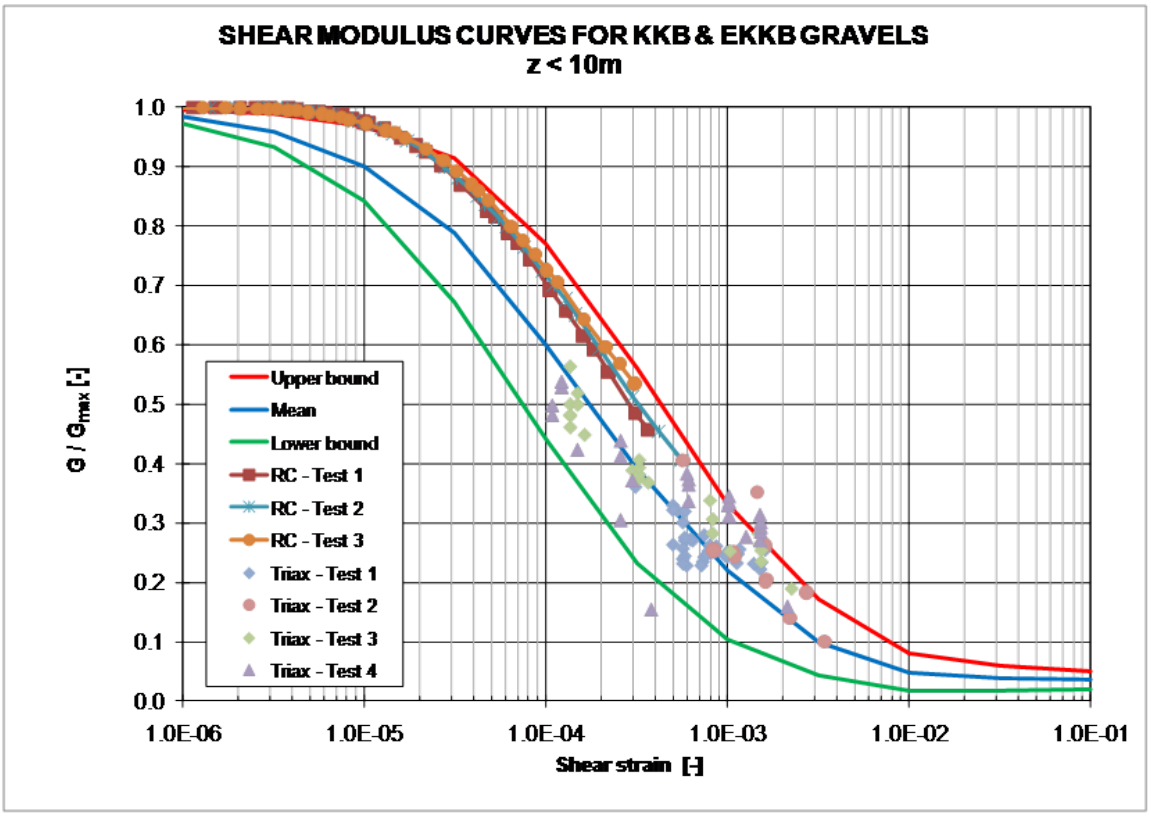

Figure I-3.21: Shear Modulus for 0 < z < 10 m (EKKB).

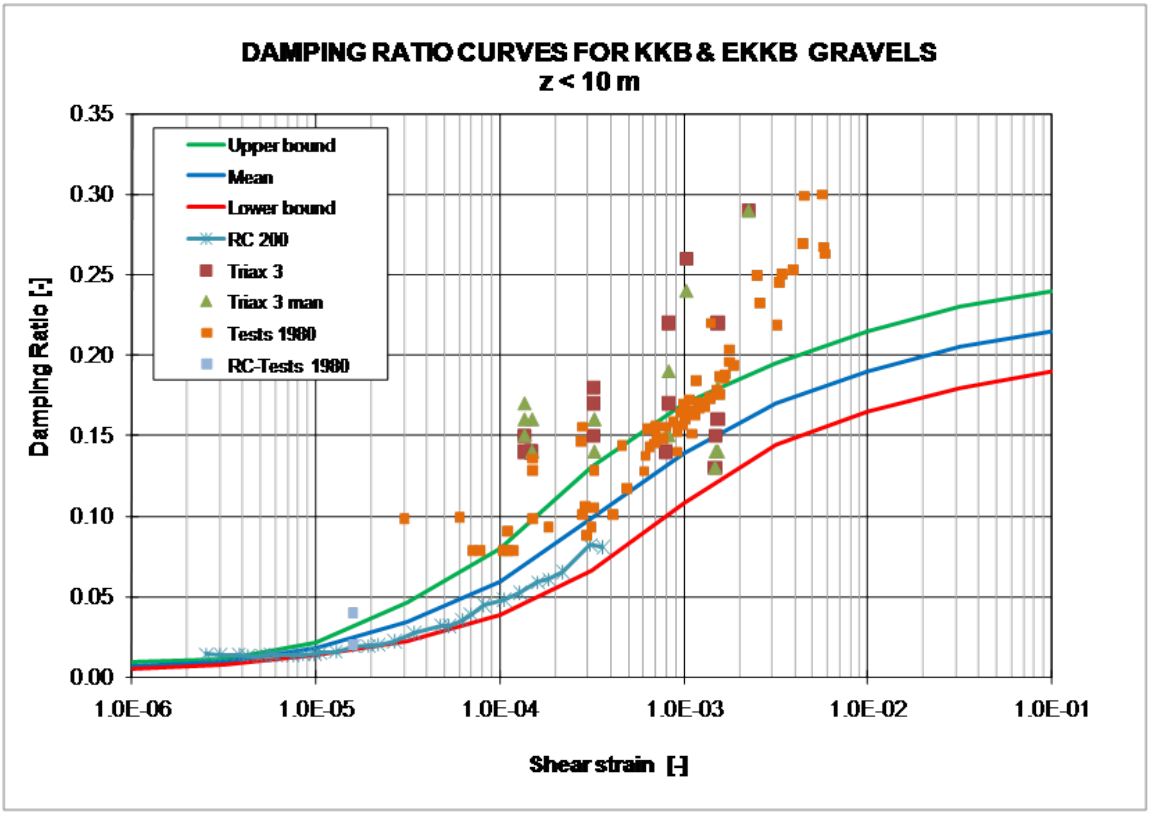

Figure I-3.22: Damping Ratio for 0 < z < 10 m (EKKB).

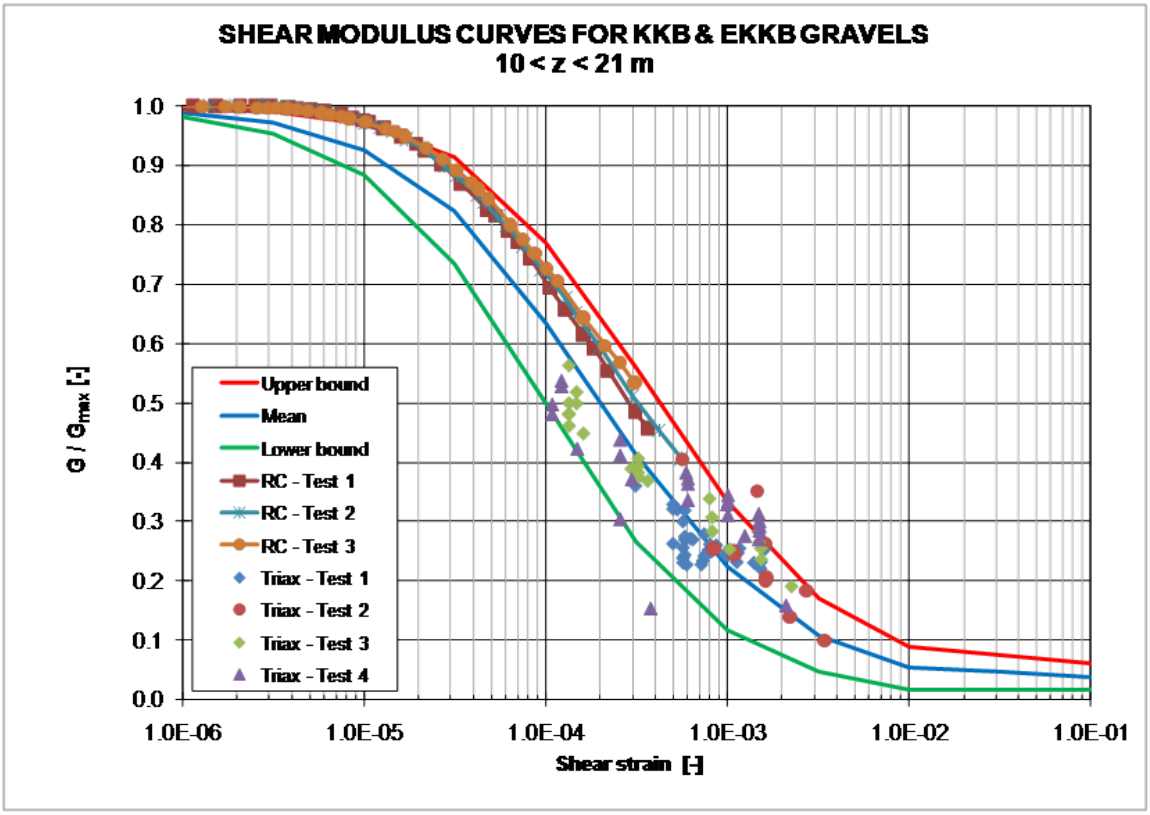

Figure I-3.23: Shear Modulus for 10 < z < 21 m (EKKB).

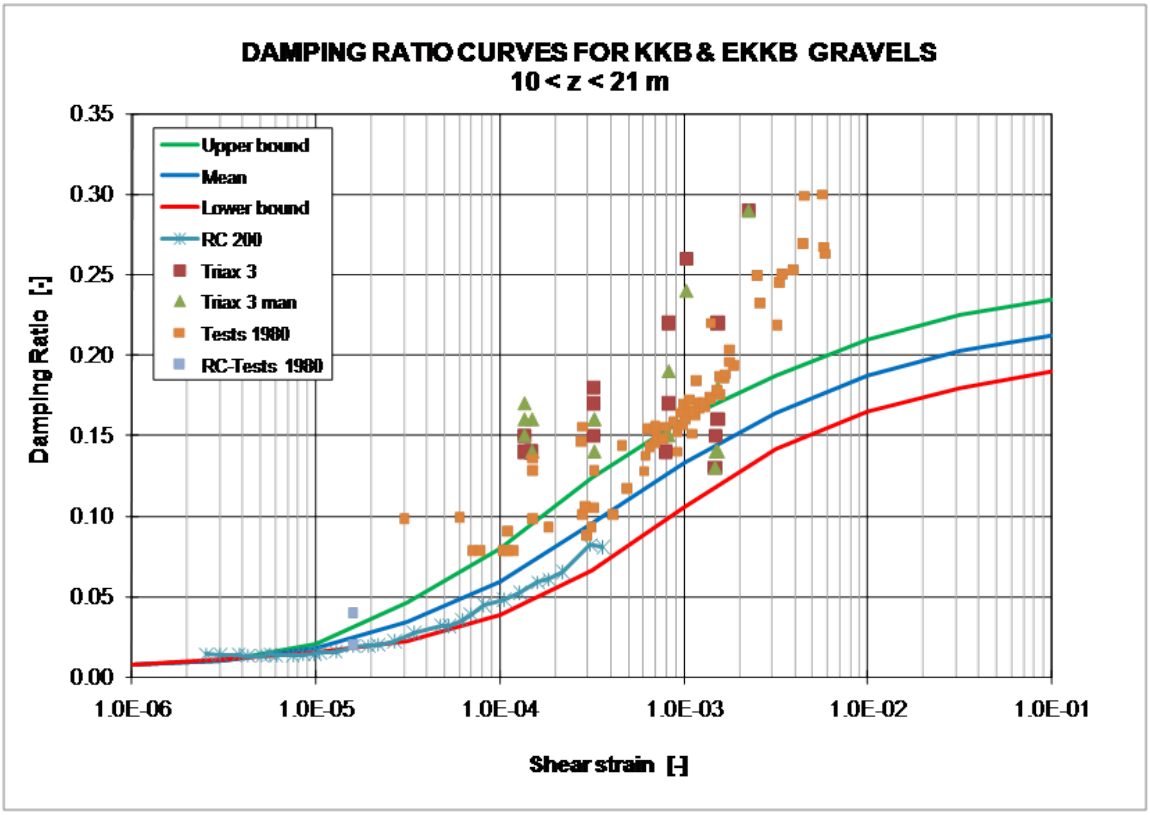

Figure I-3.24: Damping Ratio for 10 < z < 21 m (EKKB).

3.10 Supporting Figures for E-Beznau

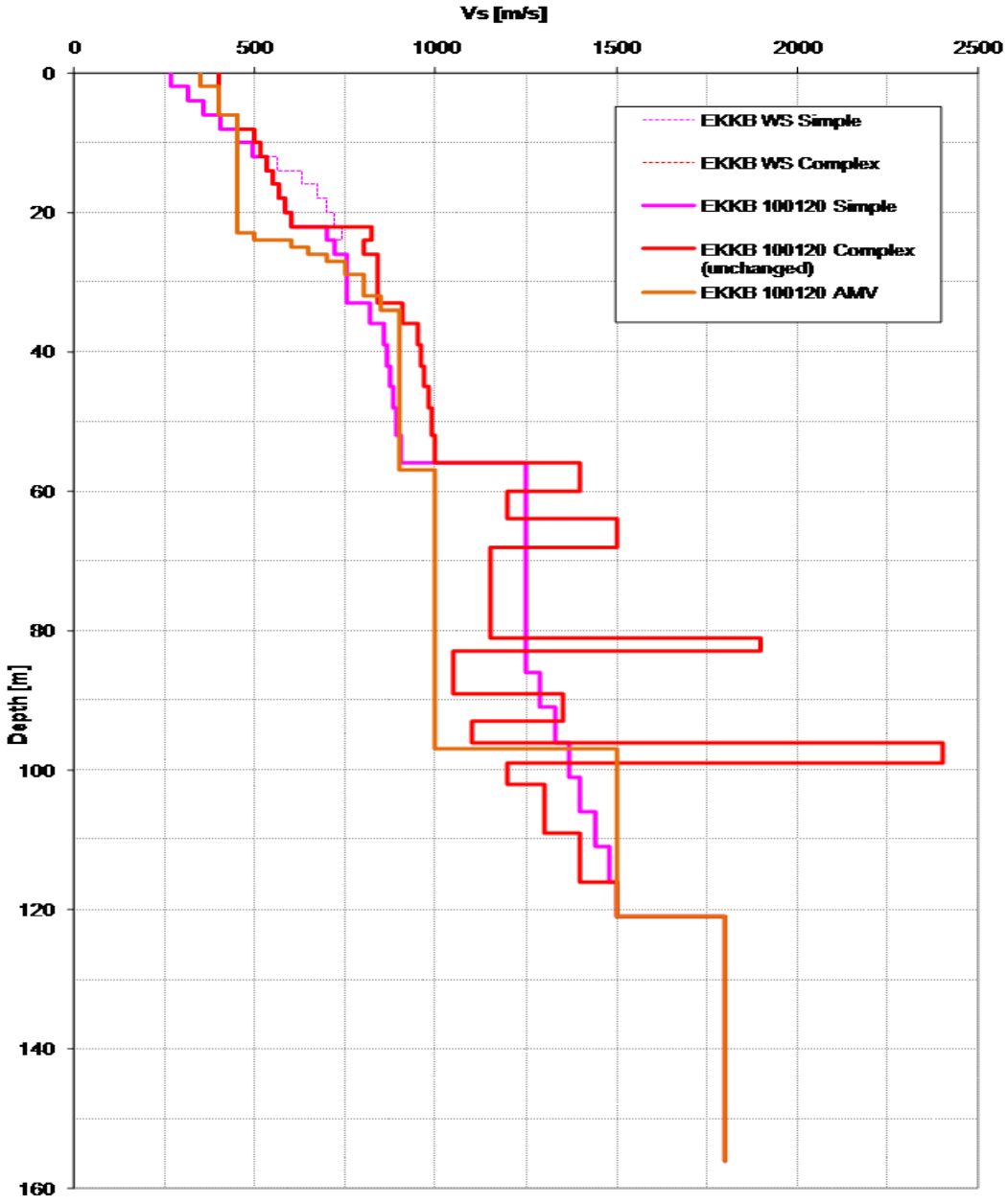

Figure I-3.25: V_S-profiles evaluated by the experts during previous meetings (EKKB).

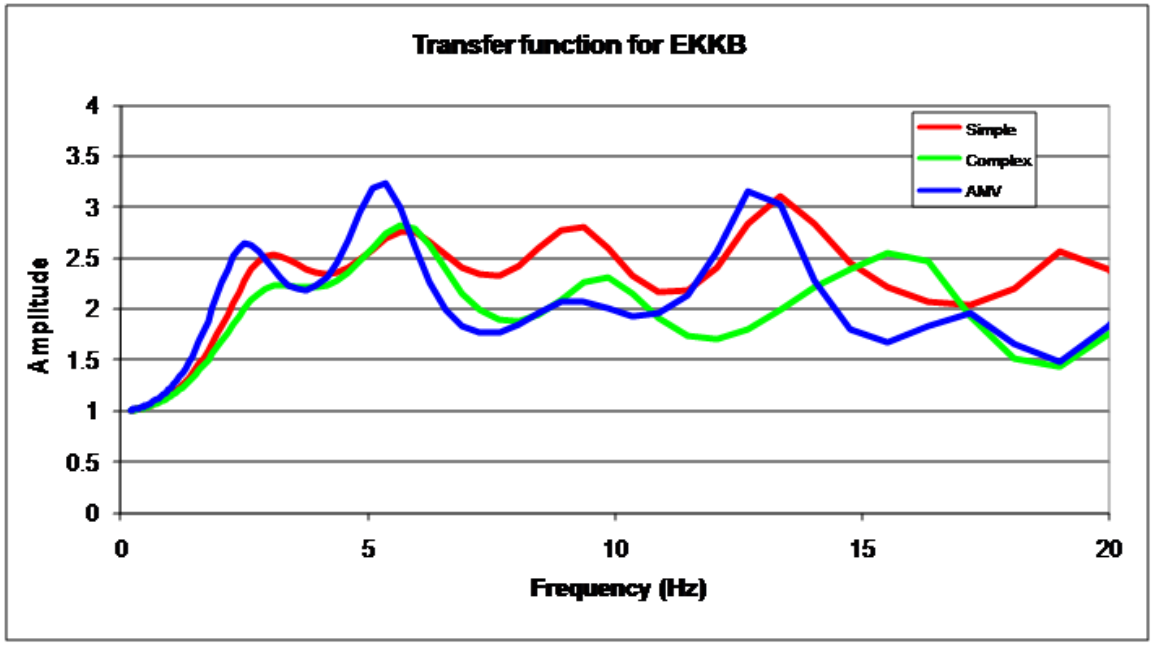

Figure I-3.26: Transfer functions for proposed soil profiles (EKKB).

Table I-3.2: Fundamental frequencies, E-Beznau site.

Profile	Frequency
P1 (Simple WOC)	3.08 Hz
P2 (Complex WOC)	3.24 Hz
P3 (AMV)	2.51 Hz

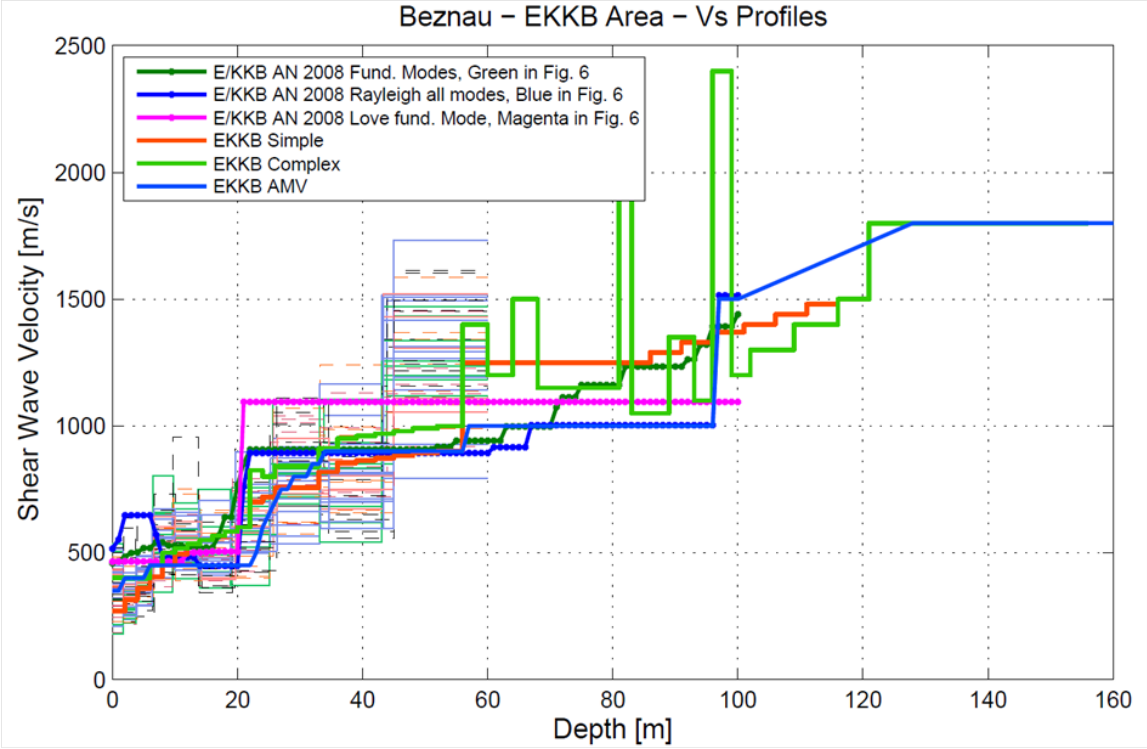

Figure I-3.27: V_S-Profiles (EKKB).

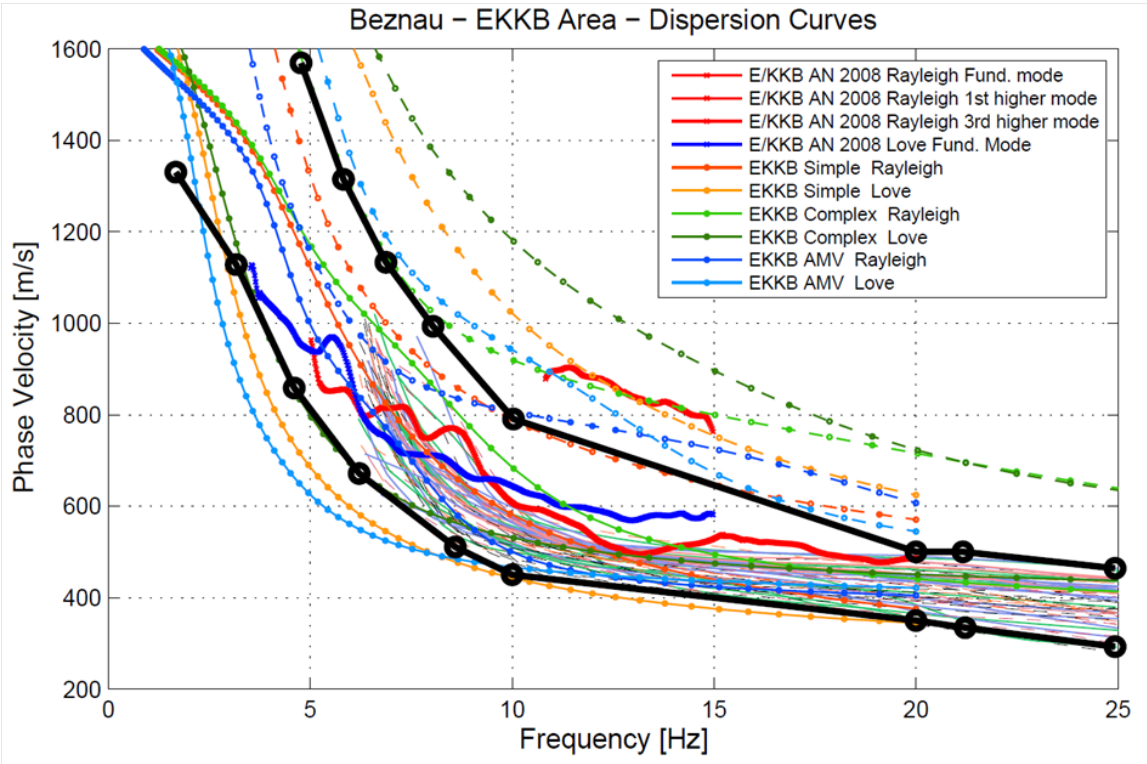

Figure I-3.28: Dispersion curves and bounds (EKKB).

3.11 Comparison of PEGASOS vs. PRP Profiles and Material Models

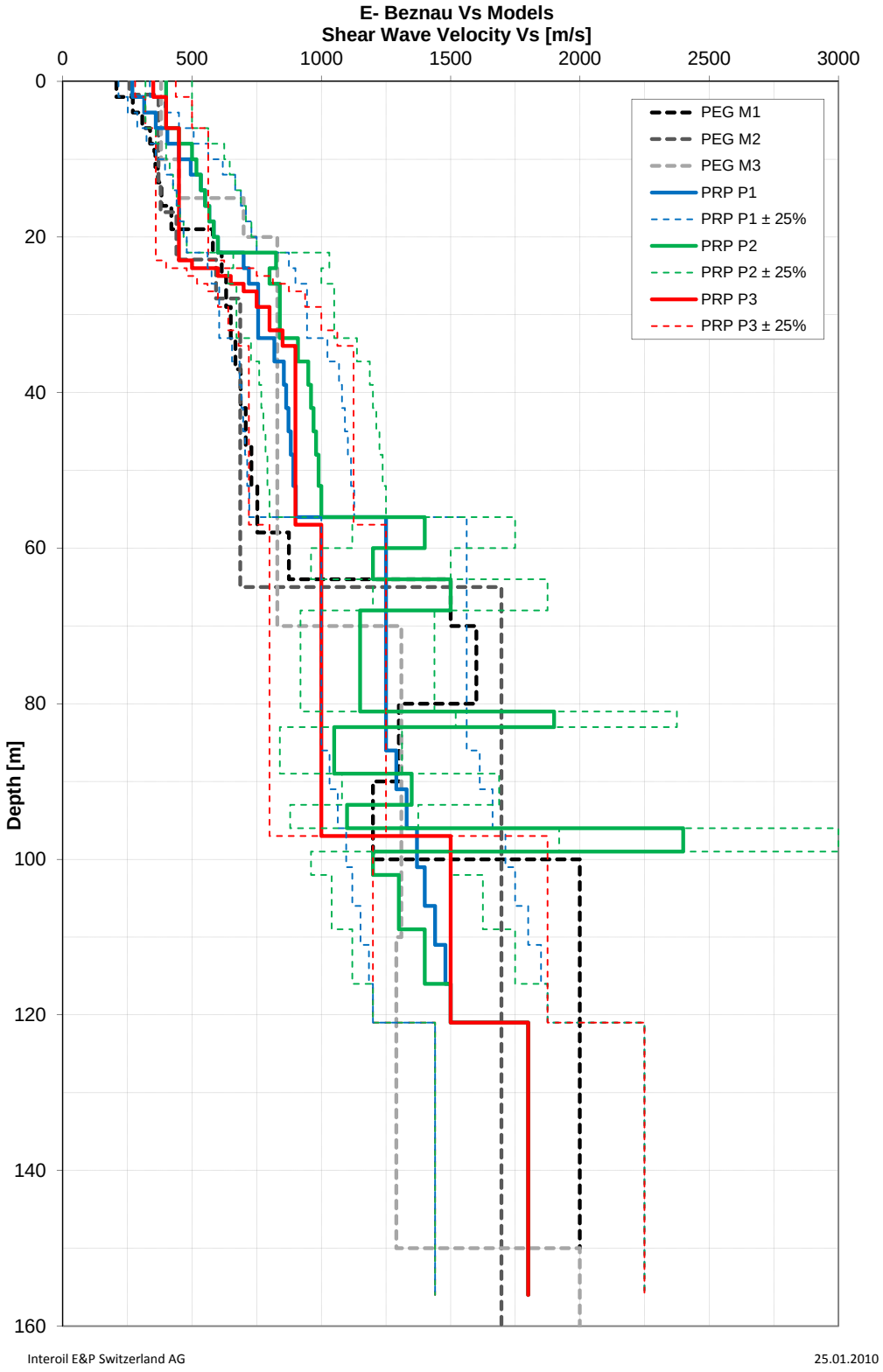

Figure I-3.29: Comparison of PEGASOS and PRP V_S-models for E-Beznau.

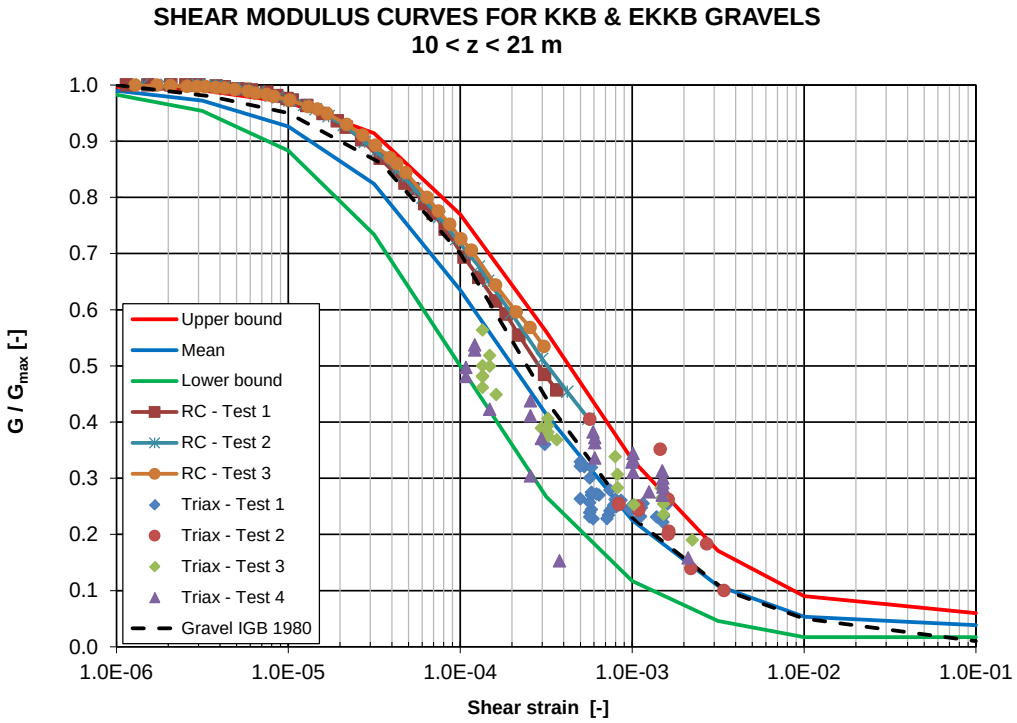

Figure I-3.30: E-Beznau - Shear modulus curves for gravel, $10 < z < 22$ m.

Chapter 4

Proposed Velocity Profiles for KKG-KKN Sites

4.1 General Comments

The main goal of this chapter is to describe how SP3 experts extended the model space in order to cover the Center, Body and Range of possible models for the site-response calculation. The SP3 expert assessment included all geophysical measurements, even if in some cases the uncertainties of the measurements were high (e.g., for some downhole measurements). Measurements were excluded in cases where the area was outside the area of interest (e.g. for some MASW results) or when dispersion curves were questionable. The experts took into account high-frequency measures of wave velocity (sonic, cross-hole) and low frequency measures (e.g. surface wave methods), in addition to the effect of anisotropy as identified at some sites from borehole information.

The Center, Body and Range issue might lead to an increase in the number of soil/rock models originally proposed by KKG-KKN experts. The defined models need to be within the bounds specified for the fundamental frequency of resonance, f_0, and for the dispersion curve of the Rayleigh wave fundamental mode. The frequency f_0 is defined from the range of measured values from H/V spectral ratios, plus an additional uncertainty in the upper and lower frequency band. The fundamental frequencies of resonance of the proposed models were tested using 1D soil response analysis. The range of dispersion curves allowed is defined by a validation process of the dispersion curves obtained from ambient vibration array measurements and MASW measurements. Also in this case the permitted range is slightly increased by the SP3 experts.

Parameters defining the non-linear behavior are based on first priority on tests results and on the experimental data published by Rollins et al. [1998] and Menq [2003]. Menq's curves take into account a dependence of G/G_{max} on the confining stress while Rollins' curves do not. Furthermore, Menq's curve corresponds to a weaker material compared to Rollins.

Accordingly, examination of the G/G_{max} curves shows that Menq's mean curve coincide with the lower bound of the tests data and Rollins mean to the upper bound. The mean curve is defined as the average between the lower bound and the upper bound curves.

For damping, Rollins mean damping curve was used for the lower bound, while Menq's mean curve was used for the upper bound. From the observations and also from theory, a stiffer material exhibits lower material damping and a softer material, higher material damping. Those curves have been modified to a small extent to better fit the observed data.

The purpose here is therefore to define the models for the one-dimensional site response analyses to be carried out, such that soil amplification can be calculated at the locations of the Swiss Nuclear Power Plants. The intention of the SP3 experts was to keep the number of models as low as possible in order to reduce the computational effort for the site-response calculations. The specifications on 1D site response calculations for NPP sites are defined in Renault and Abrahamson [2010] (PMT-TB-1014). The specifications cover three methodologies for the site response analyses: equivalent linear frequency domain analysis (EQL) using e.g. SHAKE, equivalent linear Random Vibration analysis (RVT) and full non-linear time domain analysis (NL). The SHAKE runs will not use any soil randomization procedure. Models therefore have to cover the range, and upper and lower bounds of possible models. RVT uses soil randomization in order to cover possible models with layering not resolved by the proposed models and covering the range of possible models. The soil randomization allows for variations of up to 25% on the V_S-profile, assuming log-normal distribution in each soil layer, whereas the 25% correspond to two standard deviations. The resulting V_S-profiles however need to be checked to be within the bounds specified for the fundamental frequency of resonance f_0 and the dispersion curve of the Rayleigh wave fundamental mode defined for each site. The model's $f_0$in the soil-randomization process should be estimated using a simplified version of the Rayleigh procedure after Dobry et al. [1976]. The check is made before starting the RVT computation. For the non-linear computation only the best estimate profile, and the upper and lower bound profiles are used.

4.2 Velocity Profiles for KKG and KKN Sites

In the following the rationale behind the proposed velocity profiles for the NPP Gösgen site (KKG) and ATEL site (KKN) will be explained. It takes into account the extensive documentation prepared by Interoil E&P Switzerland and different contractors, and the discussions held during the workshops on 22. October 2009, 20. January, 2. February and 5. March 2010, as well as the background documents distributed before and after these workshops.

4.2.1 Initially Proposed Velocity Profiles and Comments

Original Proposal, June 2009 (TP3-GTC-1001)

Initial models were proposed in report IO09-TA0618_Main_Report_June2009.pdf and appendices (IO09-TA0618_Appendices_June2009.pdf), taking into consideration the geological and geotechnical data, and the geophysical and laboratory measurements in an expert elicitation process. Measurements include boring, logging, MASW, uphole seismic, downhole seismic, crosshole seismic investigations, including a deviation survey, deformability tests, standard penetration tests, and ambient vibration array and single station measurements. The installation of permanent seismometers at one borehole site will provide ground motion recordings during future earthquakes.

The Quaternary section (soil layer) consists of well graded, highly compacted gravel. Embedded within this are some lenses made out of silty sand, their lateral extension depends on the thickness and may cover a radius of up to 25 m. Silt material was not observed. For the site amplification, it was proposed that soil is assumed to consist of gravel only. The rock intervals of the cored wells encountered the following formations: Crenularis and Geissberg Members, which differ only in color, and the Effingen Member. For the KKG site and the KKN site, the same reference rock shear wave velocity of 2000 m/s was proposed in the initial models. This value was later modified by SP3 experts. Finally it is proposed that there is no spatial distribution of the geotechnical parameters that could be recognized for the Gösgen area. Therefore, the NPP experts concluded that it is meaningful to describe both sites, the KKG site and the KKN site, by a common set of non-linear parameter distributions for the Gösgen area.

Linear shear wave velocity profiles were assumed for the rock layers (Crenularis/Geissberg Member and Effingen Member). The velocities were estimated mostly from sonic log and crosshole measurements. A quadratic functional form of the profile was selected for the soil layer. The top soil layer of the KKN site was regarded to be slightly stiffer than that at the KKG site even if it was not possible to identify such a trend in the measurements. The thickness of the harder part of the bedrock – the Crenularis/Geissberg Member – was assessed to be slightly higher at KKN. Site amplification factors for the two-layer models for both sites are very similar with somewhat higher variability for the KKN site (see Fig. I-4.1 and I-4.2).

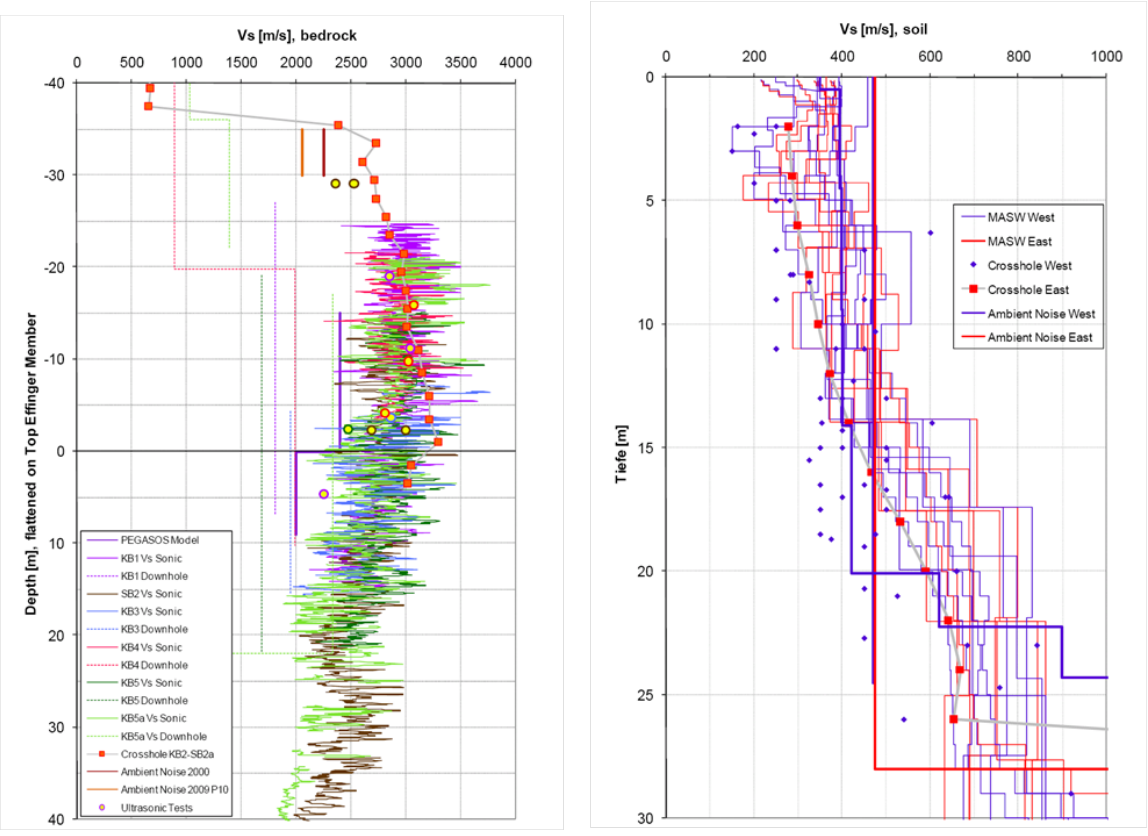

Figure I-4.1: Measured V_S-profiles in rock and soil, taken from the main report IO09-TA0618_Main_Report_June2009.pdf (Fig.15 and Fig.14).

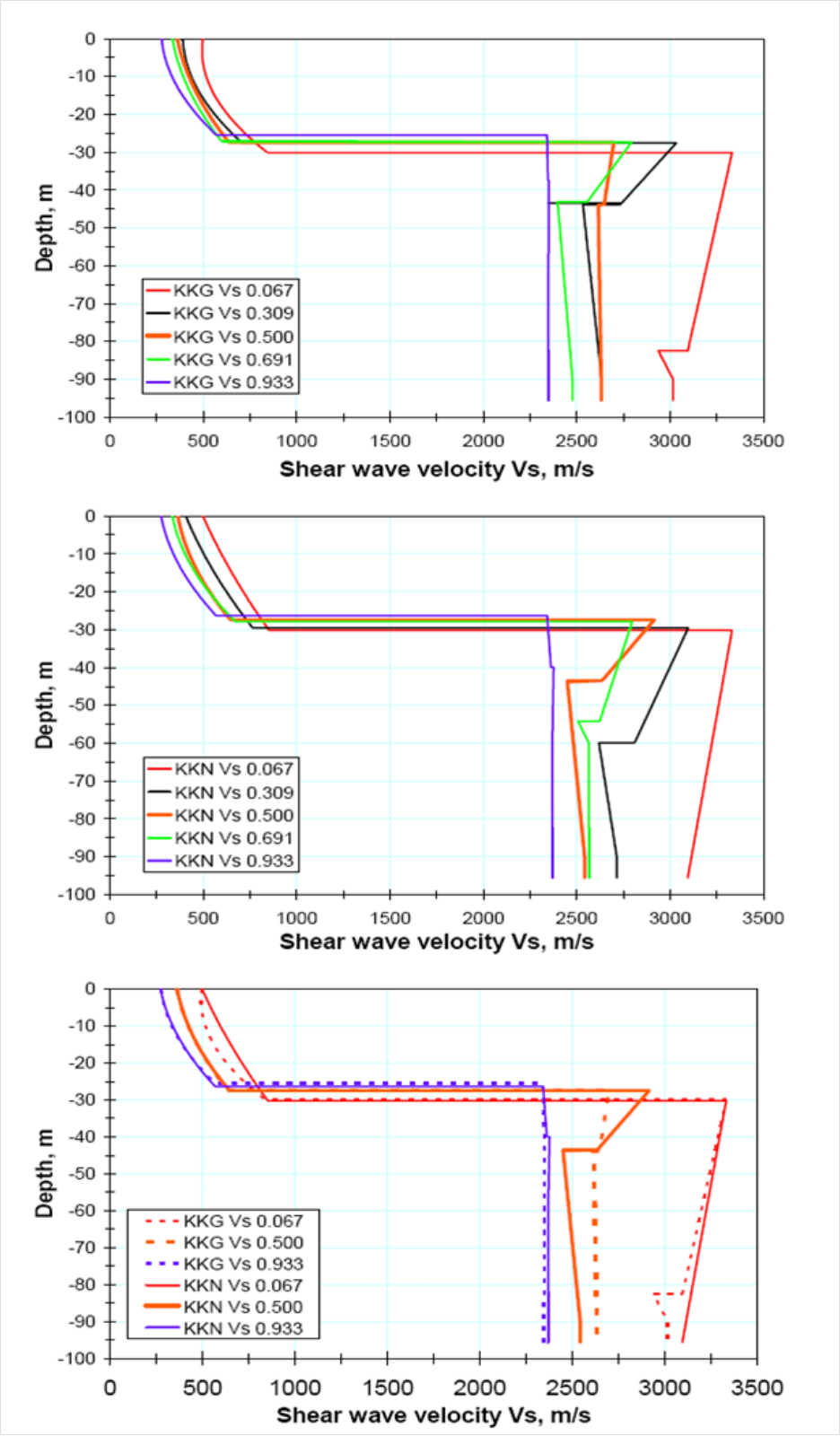

Figure I-4.2: Proposed V_S-profiles at sites KKG and KKN (Fig. 28 of main report IO09-TA0618_Main_Report_June2009.pdf). Shear wave velocity profiles corresponding to the fractiles of the Johnson system of distributions and to the median for a) the KKG site, b) the KKN site, and c) in comparison of the two sites.

Comments from the Workshop WS2a/SP3 (October 2009), Additional Data and Following Workshops

The SP3 experts acknowledged the overall impressive set of new, high quality data, which provides a rather consistent view of the site underground structure at Gösgen. The main open issues and question that needed to be addressed were the following:

1. Despite the fact that apparently all other surveys indicate a rather identical underground structure over the area, the H/V signatures significantly differ from one site to another (while all of them do exhibit a peak around 4 - 5 Hz, but with different amplitudes).
2. H/V measurements indicate that there is variability of the bedrock down to larger depth (H/V peak is at about 0.6 Hz).
3. H/V curves in the areas with Karst and weathered rock are not explained by the proposed models. The Karst layer/ weathered rock is not represented in the proposed model.
4. In the bedrock, wave speeds seem to depend on the wavelength. Results from down-hole measurements should not be discarded.
5. If the reference rock shear velocity is chosen to be 2000 m/s, all the velocity profiles should have the same value at larger depths. The connection between the proposed models and the reference velocity is not given.
6. The polynomial form of the velocity model for the soil is unrealistic for a homogeneous geological unit.
7. The laboratory tests for the liquefaction assessment of the quaternary layer have been performed without stress reversal, and cannot represent the in-situ situation.
8. The G/G_{max} curves for the gravel layer (Fig. 29a) with a lower threshold for strains larger than $5 \cdot 10^{-4}$ is certainly not possible.
9. The damping curves versus strain are very low and are not supported by the laboratory data.

In order to answer these questions a number of additional data were requested, that are summarized in the summary presentation TFI-RF-1120. Several documents were prepared as a consequence of the SP3 meeting in October 2009, including:

- The additional data requested by SP3 experts [Interoil 2009c] (TP3-GTC-1008).
- Comment on KKG - Gösgen shear wave velocity profile by A. Pecker, including non-linear properties (TP3-TN-1062, see Section 4.3) (see Fig. I-4.13).
- Comment on KKG - Gösgen shear wave velocity profile by J.Studer (see Section 4.3.4).
- A technical note on soil liquefaction (TP3-TN-1055, see Section 9.1).
- An alternative rock profile based on measured dispersion curves and H/V peak at 0.6 Hz (TP3-TN-1061, see Section 4.4).

During the meetings on 20. January and 2. February 2010, a draft proposal for the profiles was prepared. During the feedback workshop with representatives of the NPPs on5. March 2010, it was decided to include a rock model based on velocity data of NAGRA [1992] (the V_P-profile of Schafisheim - Checkshot corrected sonic-log - can be found there). Moreover in order to prevent double counting of damping in the SP2 model and in the deep rock profiles proposed by SP3 experts, it was decided to not account for damping in rock and to use a linear elastic model.

4.3 Soil Velocity Profile Gösgen Site

4.3.1 Data

The geophysical data used for the derivation of the shear wave velocity profile through the alluvium layer are taken from Interoil [2009c]. In accordance with the expert elicitation, the following assumptions have been retained:

- No distinction is made between both sites and all data are merged together.
- The most reliable data for the determination of the shear wave velocity profile consist of thecross hole tests (1972 and 2009), the 2009 ambient noise vibration measurements, the MASW profiles (KB0 @ 08KKG-P3, KB1 @ 08KKG-P2, KB/SB2 @ 08KKG-P3, KB/SB2 @ 08KKGP4,KB3 @ 08KKG-P4, KB3 @ 08KKG-P5, KB4 @ 08KKG-P2, KB4 @ 08KKG-P5, KB5 @ 08KKG-P5, Stat. 506 @ 08KKG-P4, Anatolian RS1 to RS5). Only those data are used in the following.
- The depth to the bottom of the alluvium layer has been fixed at 27.5 m, which means that all data below that depth are not considered in the analysis.

In the data processing, the 2009 ambient noise vibration measurements are not taken into consideration because they are almost constant throughout depth in the soil layer and therefore do not permit any gradient to be determined. Only the "Preferred Model P" in Fäh et al. (2003), has been included in the data. For the MASW measurements, which are interpreted in the original report with step like variations, the constant value in a given sublayer is attributed to the point at mid-depth of the sublayer.

With those restrictions the data used for the evaluations are plotted in Figure I-4.3. It is worth noting that the non intrusive tests (ambient noise, MASW) exhibit a different trend with depth than the cross hole tests. The former ones seem to indicate a change in the velocity gradient around 15 m depth, while the latter ones exhibit a smooth variation with depth. However, it is likely that the surface wave tests are less reliable than the cross hole tests at depths greater than 15 - 20 m; likewise,the cross hole tests are probably less accurate close to the ground surface.

4.3.2 Interpretation

The raw data presented in Figure I-4.3 have been fitted to an equation of the type:

$$V_S(z) = V_0 \left(\frac{z+d}{H+d} \right)^p \tag{I-4.1}$$

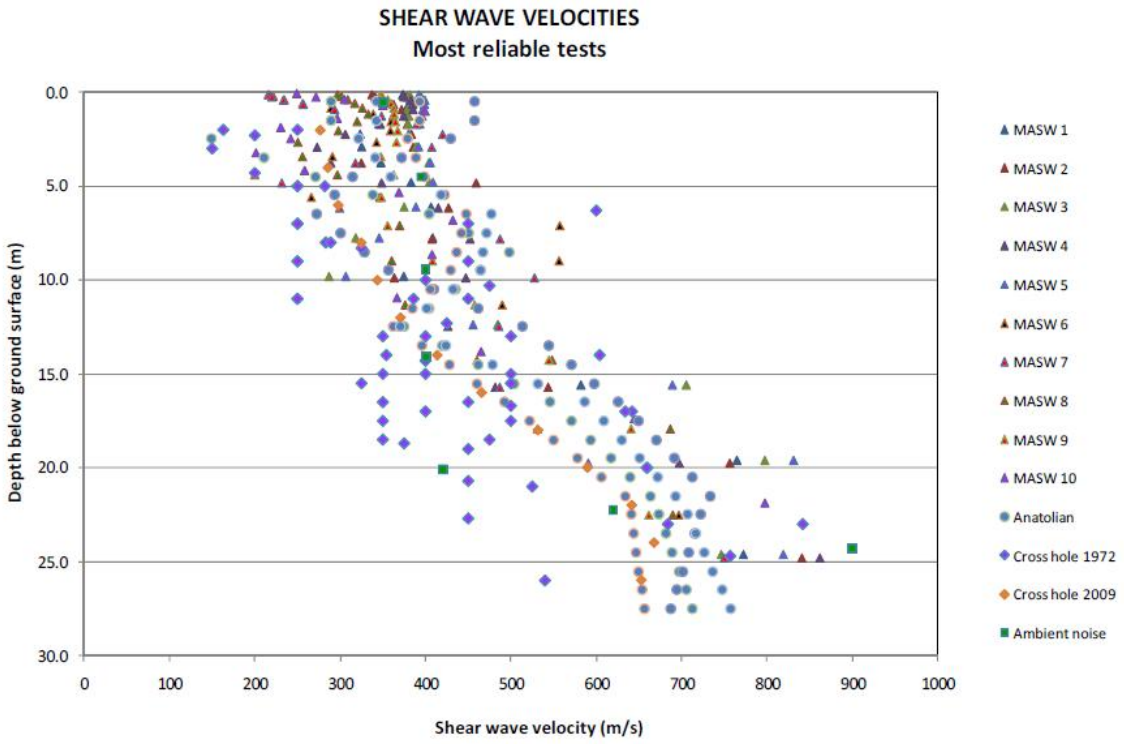

Figure I-4.3: Data used for the analysis at the Gösgen site.

where V_0, d and p are numerical parameters to be determined by the regression analysis. H is the total depth of the soil layer, taken equal to 27.5 m. In order to get meaningful and physically acceptable results the following constraints have been imposed on the parameters:

$$0 \leq d, \qquad 0 \leq p \leq 1$$

Different sets of values have been used for the regression analysis:

- All data between 0 and 27.5 m in a single set;
- MASW and Anatolian measurements between 0 and 27.5 m in a single set;
- Cross-hole tests between 0 and 27.5 m in a single set.

In addition for each category defined above, except for the cross-holes that do not exhibit the same trend, the data have been also split into two subsets: 0 to 15 m and 15 m to 27.5 m. The results of the regression are given in Table I-4.1 and presented in Figure I-4.4.

The results call for the following comments:

- When, in a given set, the data from 0 to 27.5 m are used, the shear wave velocity exhibits a linear increase with depth ($p = 1.0$);
- When two subsets are used, the top 15 m still exhibit a linear variation with depth while the bottom 12.5 m show a milder rate of increase ($p < 1.0$);
- The MASW fit is very close to the best fit through all data, probably because the number of measurements is large compared to the few cross-hole measurements;

Table I-4.1: Results of the regression analyses.

	Depth [m]	V_0 [m/s]	d	p
All data	0-27.5	719	18.2	1
	0-15	561	35.8	1
	15-27.5	680	0	0.67
MASW & Anatolian	0-27.5	765	16.9	1
	0-15	539	20	0.51
	15-27.5	780	0	0.58
Cross holes	0-27.5	695	3.6	0.98

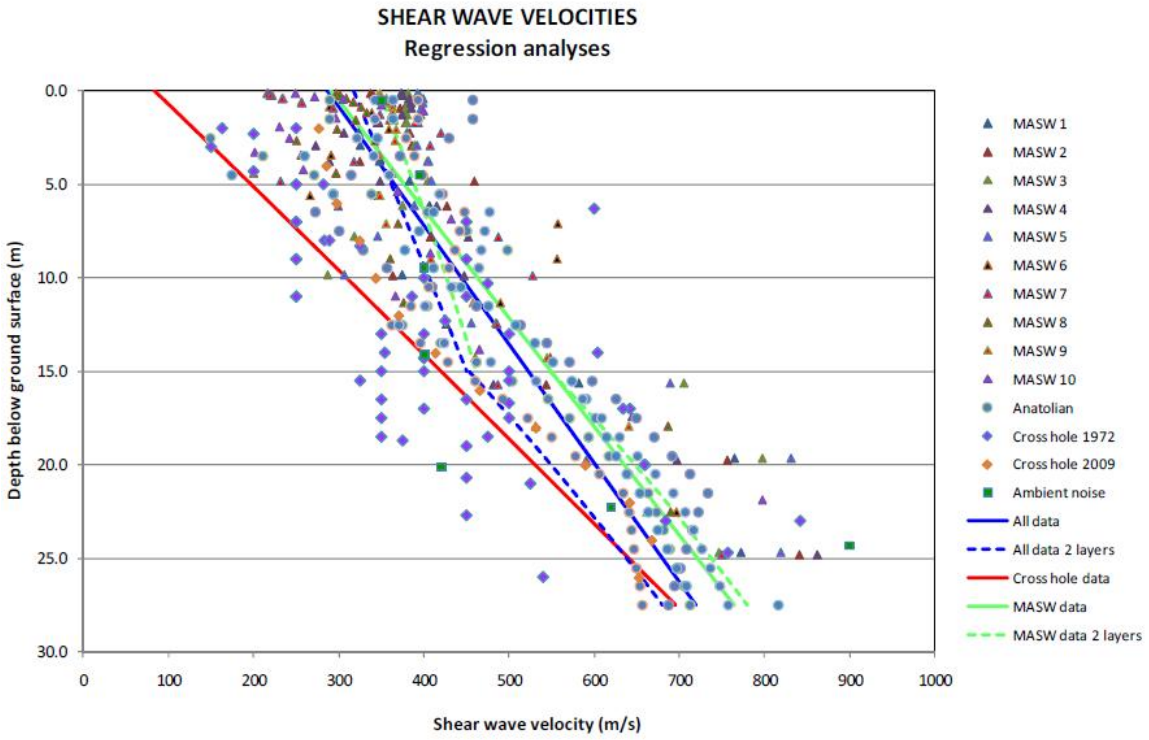

Figure I-4.4: Adjusted shear wave velocity profiles for Gösgen.

- With all the data divided into two subsets, the regression analysis exhibits a velocity jump at 15 m depth (like for the MASW tests); since there is no geological evidence for this jump, the lower part of the curve has been adjusted to give a continuous velocity profile at 15 m depth (the parameter V_0 given in Table I-4.1 corresponds to this adjustment).

4.3.3 Proposed Shear Wave Velocity Profiles

For the site response analysis it is proposed to consider the three following profiles:

- The preferred profile is the one labeled "all data" in Figure I-4.4 (blue solid line) which is based on all good quality available data.

- The first alternative profile is the one labeled "cross-hole" in Figure I-4.4 (red solid line), which probably reflects a lower bound profile and a more accurate estimate below 15 m;
- The second alternative stems from the visual inspection of the data which indicates a slight different behavior above and below 15 m depth. The corresponding curve is labeled "all data 2 layers" in Figure I-4.4 (blue dashed line).

The associated parameters to use with Equation I-4.1 are listed in Table I-4.2.

Table I-4.2: Parameters defining the design velocity profiles (see equation I-4.1).

	Depth [m]	V_0 [m/s]	d	p
Preferred profile	0-27.5	720	18.2	1
First alternative	0-27.5	695	3.6	0.98
Second alternative	0-15	565	35.8	1
	15-27.5	680	0	0.67

4.3.4 Important Remarks

1. The design profiles defined above are only based on a visual inspection, some physical reasoning and curve fitting through the data. No geological or geotechnical evidences support one rather than the other. The final choice shall be guided by comparison of the dispersion curves produced by these profiles (in combination with the rock velocity profiles) with the experimental dispersion curves.
2. The laboratory data (resonant column tests or bender tests) would indicate a less strong dependence of the shear wave velocity on the confining pressure (or depth). On the basis of document 2008_1_003_rqust, recently provided by Fachgebiet Geotechnik (Renormalisation of the G/G_{max} data), the power exponent in Equation I-4.1 would be of the order of 0.25 to 0.30. However a plot of V_S versus depth assuming this mild (usual for cohesionless materials) dependence would not fit at all the data. Since the laboratory tests were performed on reconstituted samples, it may occur that grain bonding or cementation are lost and the tests consequently yield much smaller values for the shear wave velocity. Therefore, priority is given to the field values for the determination of the velocity profile.

Shear Wave Velocity Profile

Shear wave velocity data from KKG - Gösgen site are taken for regression analysis. The data of MASW measurements, Anatolian measurements, cross-hole measurements from 1972 and cross-hole measurements from 2009 are analyzed separately by linear regression. The linear functions are then combined with weighing factors to a final weighted linear trend function.

Follow weights for individual measurements are applied:

The results of the regression of shear wave velocity profile data are shown in Figure I-4.5. For comparison, the profile proposed by A. Pecker is added to the figure.

Table I-4.3: Applied weights for the individuals measurements.

Method	Weighting
MASW measurements	35%
Anatolian measurements	20%
Cross-hole measurements from 1979	10%
Cross-hole measurements from 2009	35%

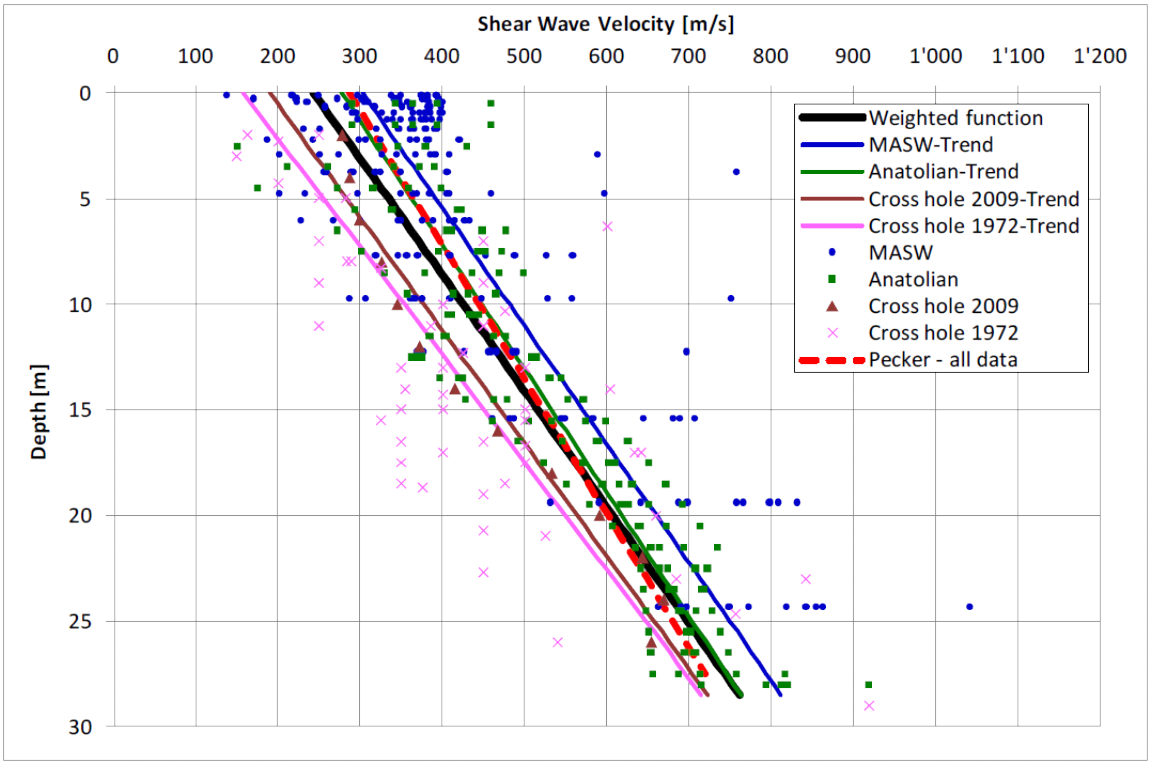

Figure I-4.5: Regression of shear wave velocity profile data for Gösgen.

4.3.5 Non-linear Properties

In the document IO09-TA0618 "Site Investigation for KKG & ATEL", the NPP experts recommended variations of the G/G_{max} and damping curves versus shear strain which were not accepted by the SP3 experts; the main reason was the lower threshold set on the G/G_{max} curve beyond 10^{-4}. Published results for non-linear properties of gravel materials have been examined: they are coming from Seed,Rollins et al. [1998] and Menq [2003]. The results are depicted in Figure I-4.6 and Figure I-4.7.

- The curves proposed by Rollins *et al* are established from 15 different investigations with confining pressures ranging from 30 to 490 kPa, coefficient of uniformity included between 7 and 1.2 and 76 and a range of mean grain size (D_{50}) between 0.5 mm and 24 mm. The red curve is the best fit through all the data

- Menq provides an explicit equation relating G/G_{max} to the confining pressure, D_{50} and coefficient of uniformity. The curves plotted in Figure I-4.6 and Figure I-4.7 are established for the following set of coefficients: $D_{50} = 10$ mm, $C_u = 5$ (upper G/G_{max}

curve) and 20 and a confining pressure of 150 kPa corresponding approximately to the confining pressure at a depth of 7 m in the soil profile. Although the D_{50} corresponds to the measured value on the Gösgen gravel, the actual measured coefficient of uniformity is much larger than the assumed value, of the order of 90. However use of such a large coefficient would yield a curve with a much rapid decrease of G versus the shear strain. This would not be consistent with the experimental data plotted in the document 2008_1_003_rqust.

Comparing those data with those presented in the document 2008_1_003_rqust, it turns out that quite a fair agreement is reached between the best fit curve from Rollins et al. [1998] and the lower bound curve from the same authors, which nicely coincides with Menq's curve for C_u=20. Since Menq's curve is the only one that allows for stress dependence of G/G_{max} it is suggested to use Menq's equation with D_{50}=10 mm, C_u=5 to 20 to define a range of acceptable curves. It is also interesting to note that using Menq's formula with $C_u = 20$ and a void ratio of 0.29 (a reasonable value for such material at this density) one would predict an elastic shear modulus of 340 MPa under a confining pressure of 0.15 MPa; this value compares very well with the mean shear wave velocity measured at 7 m depth (confining pressure of 0.15 MPa):

$$V_S = \sqrt{\frac{G_{max}}{\rho}} = \sqrt{\frac{340}{2.210^{-3}}} \approx 400\text{m/s}. \tag{I-4.2}$$

The damping curves predicted by Menq also agree fairly well with other published results and could equally be used. The upper curve is associated with C_u=20 and the lower one with C_u=5.

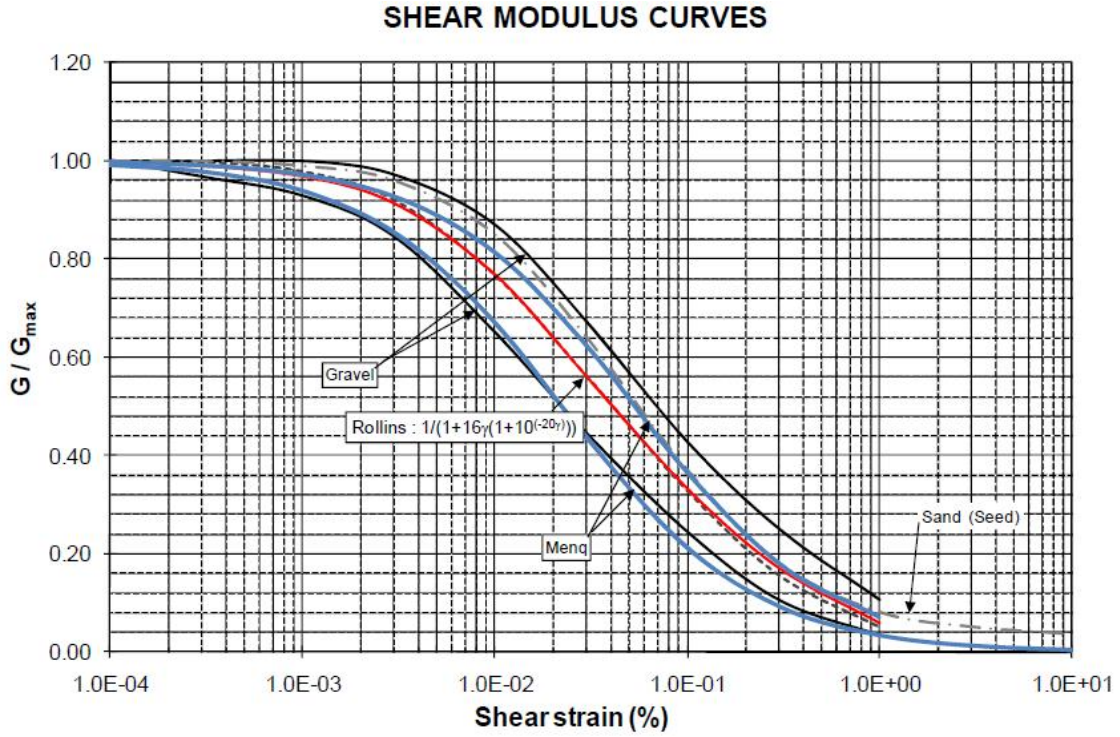

Figure I-4.6: Shear modulus versus shear strain for gravels.

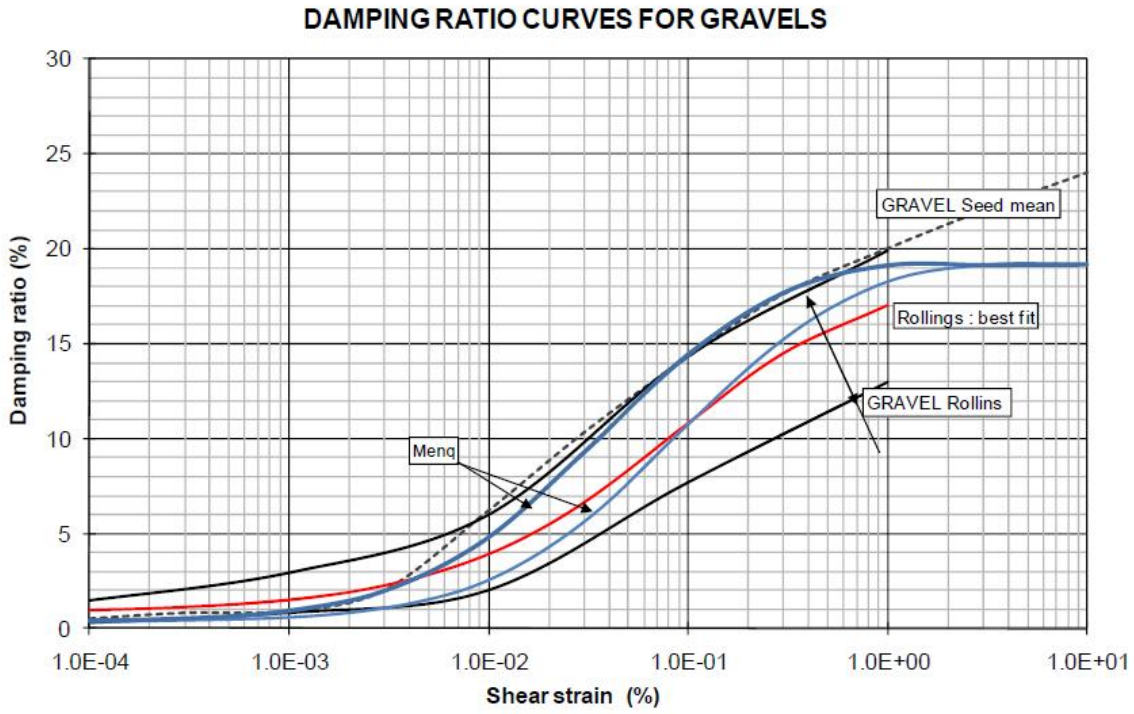

Figure I-4.7: Damping ratio versus shear strain for gravels.

4.4 Alternative Rock Models for Gösgen, SP3 Working Meeting in January 2010

Results from down-hole measurements show that shear-wave velocity in rock might be considerably below 2000 m/s for Gösgen. The difference between down-hole and crosshole measurements cannot be explained so far. From cross-hole measurements we might propose a rock S-wave reference velocity of about 2500 m/s at shallow depth below the sedimentary cover (see Interoil report Fig. 28). In the following the derivation of alternative rock models for site Gösgen is summarized. H/V measurements and down-hole measurements indicate that there is variability of the bedrock down to larger depth. The areas with karst and weathered rock (reduced V_S) can be identified through the reduced amplitude of the H/V peak at 4 - 5 Hz. It is interesting that at these sites an additional peak appears. In the southern part, this peak is at about 0.6 Hz. At HV03 close to KKG there might be a peak at 1 Hz. It seems as if the reduced bedrock quality at the surface is related to changes in the deeper parts. Such deeper structural features might be also identified from hybrid seismic from a series of reflections in the Kalkmergel (Effinger layer). These reflectors are visible in the sonic log in borehole SB2 and are related to the variation of the clay content. Additional H/V measurements on a denser grid and in areas of identified Karst layers were requested, but not performed so far. We can assign the 0.6 Hz peak to the fundamental frequency of resonance f_0 of the entire structure down to about 660 m depths, which would then result in V_S values below 2000 m/s over thick layers in the rock. An inversion of the ambient vibration dispersion curve measured by Resonance was applied to develop alternative models, assuming that the H/V peak at 0.6 Hz is related to f_0 or to the peak in the ellipticity of the fundamental mode Rayleigh wave.

- The ellipticity function is forced to explain the H/V amplitude (green models without depth constrain; blue models with the constrain that at a depth of 660 m the S-wave velocity is between 2900 and 3100 m/s)
  - Requires a velocity inversion (Fig. I-4.8)
  - Explains the H/V peak at 0.6 Hz (Fig. I-4.9)
  - Does not explain the measured dispersion curve in the frequency band 4.5 - 5.5 Hz (Quality of the dispersion curve in this band is not known) (Fig. I-4.10)
  - Results in an amplification peak at 0.6 Hz (Fig. I-4.11) that might also explain the observed H/V peak.
- The ellipticity function has a weak peak close to the H/V peak (red, magenta)
  - Does not explain the H/V peak amplitude at 0.6 Hz (Fig. I-4.9)
  - Can explain the observed dispersion curve (better for structures in magenta) (Fig. I-4.10)
  - Results in an amplification at 0.8 - 1.0 Hz (Fig. I-4.11)

Adding a layer of high velocity to three inverted models (see Fig. I-4.12) does not change the amplification behavior (Compare black curves with colored curves in Figure I-4.11). However, the amplitude of the ellipticity close to f_0 is reduced by introducing such a high-velocity layer.

The selected models in Figure I-4.12 reach 2500 m/s shear-wave velocity between 220 and 580 m depth.

4.4.1 Conclusion

In order to account for the uncertainties in the measured shear-wave velocities, several models for the rock are proposed that explain some of the observed features. No model explains all observations. For this reason several rock profiles need to be defined for the Gösgen site so that the range of possible rock models is covered. A model with 2500 m/s S-wave velocity close to the surface should also be included (not shown in Figures I-4.8 to I-4.12).

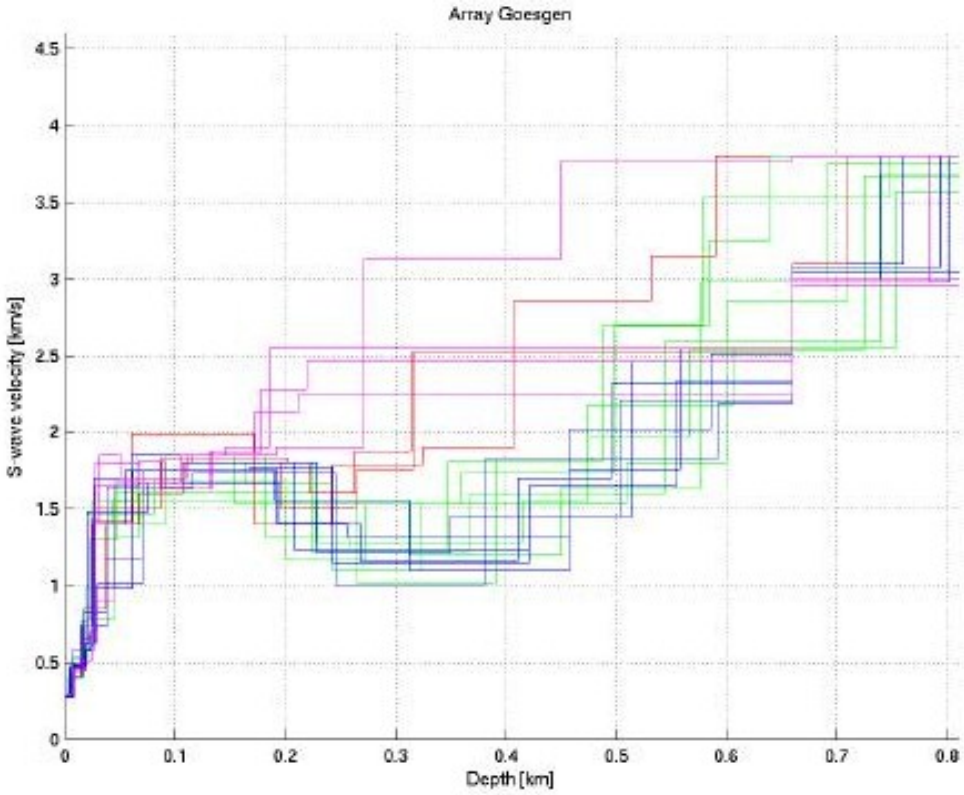

Figure I-4.8: Inverted structural models using different constrains.

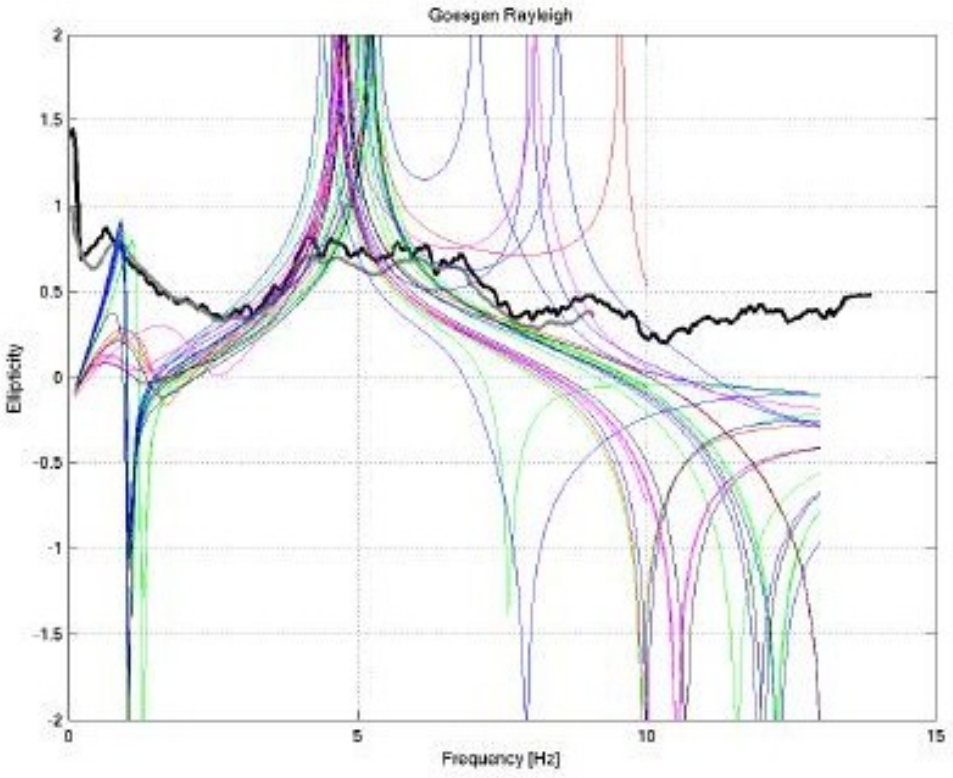

Figure I-4.9: Ellipticity of the fundamental mode Rayleigh wave of the inverted structural models compared to the H/V spectral ratio observed at the central station of the array.

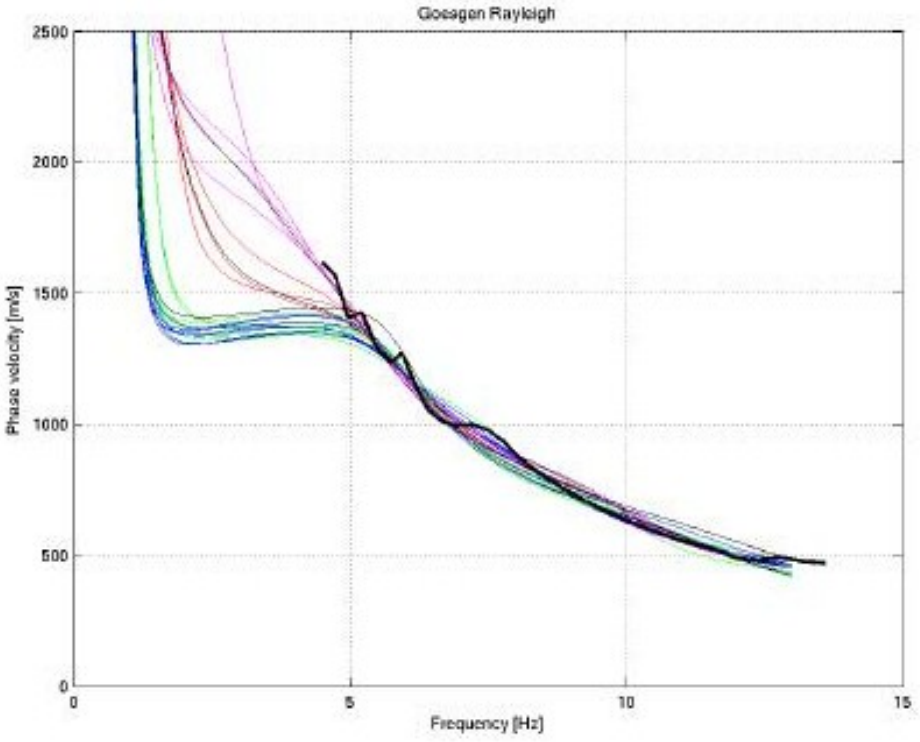

Figure I-4.10: Phase velocity curve of the inverted structural models compared to the observed dispersion curve in the array.

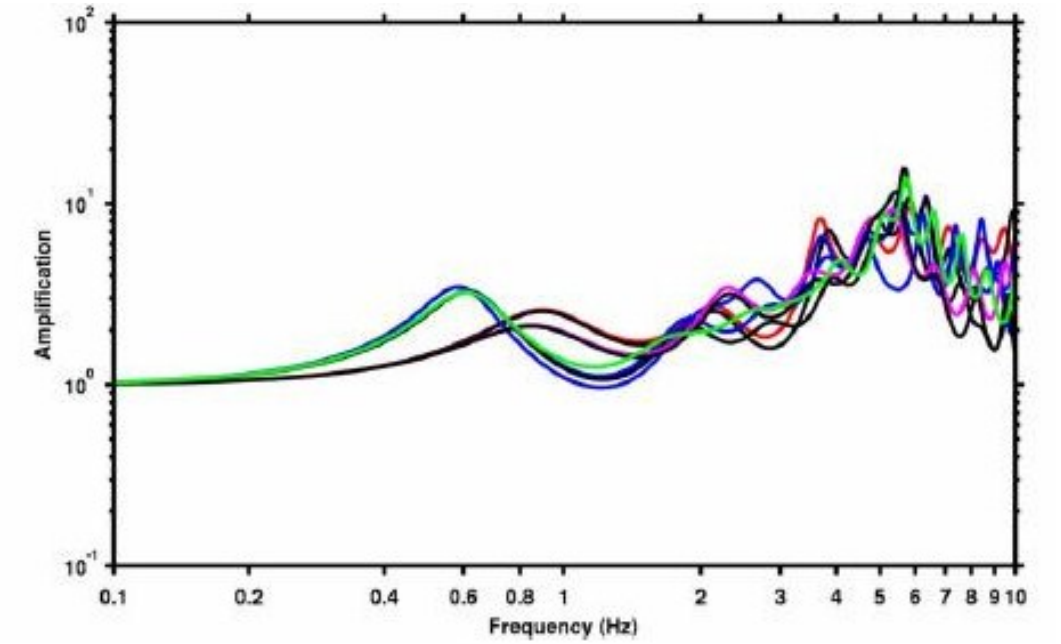

Figure I-4.11: Amplification expressed in the frequency domain (Fourier spectral amplification) for a selection of models. The selected models are shown in Figure I-4.12. The black curves refer to models for which a high velocity layer has been added close to the surface. The reference for the amplification is a rock with V_S=3800 m/s. If the V_S reference is selected as 2500 m/s, the amplitudes have to be multiplied by a factor 0.75; if the V_S reference is 2000 m/s the factor is 0.65.

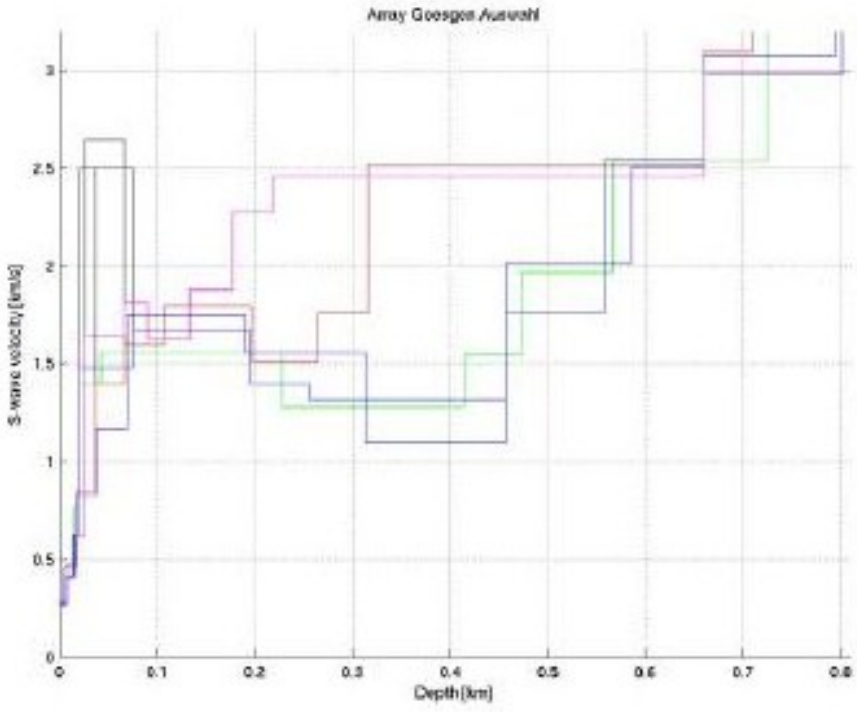

Figure I-4.12: Selected structural models for which amplification has been computed (see Figure I-4.11). The black parts are added to inverted models in order to test their small influence on the amplification.

Table I-4.4: Numerical values for the models in Figure I-4.12.

Thickness [km]	S-velocity [km/s]
Nr. 7 (green)	
0.0079890	0.2712100
0.0070306	0.4111200
0.0050387	0.7658600
0.0229150	1.4006000
0.1848800	1.5623000
0.1870500	1.2804000
0.0576630	1.5516000
0.0941610	1.9656000
0.1587400	2.5394000
0.2947400	3.6668000
-	3.8000000
Nr. 12 (red)	
0.0079998	0.2700000
0.0090013	0.4876000
0.0199980	0.8497500
0.0299990	1.4000000
0.0400890	1.6001000
0.0887660	1.7993000
0.0686630	1.5091000
0.0515890	1.7625000
0.3439000	2.5250000
0.0500120	3.0991000
-	3.8000000
Nr. 14 (blue)	
0.0079800	0.2799600
0.0066541	0.4081100
0.0060938	0.6250100
0.0548840	2.5000000
0.1197800	1.6736000
0.0607650	1.3992000
0.2018800	1.3221000
0.0996330	1.7646000
0.1023300	2.5491000
0.1424300	2.9819000
-	3.8000000
Nr. 17 (blue)	
0.0051605	0.2705400

Continuation on the next page ...

Table I-4.4 – Continuation of previous page

Thickness [km]	S-velocity [km/s]
0.0121590	0.4578600
0.0202590	0.8246300
0.0324870	1.1737000
0.1203800	1.7455000
0.1227500	1.5592000
0.1449400	1.1000000
0.1274100	2.0250000
0.0744620	2.5143000
0.1349900	3.0817000
-	3.8000000
Nr. 21 (magenta)	
0.0058129	0.2900000
0.0101870	0.4112500
0.0107810	0.6255700
0.0400630	1.6531000
0.0233620	1.8055000
0.0433840	1.6322000
0.0445900	1.8755000
0.0412760	2.2835000
0.4405400	2.4614000
0.1630700	2.9983000
-	3.8000000
Nr. 12X modified Nr.12 (black)	
0.0079998	0.2700000
0.0090013	0.4876000
0.0199980	0.8497500
0.0299990	2.5000000
0.0400890	1.6001000
0.0887660	1.7993000
0.0686630	1.5091000
0.0515890	1.7625000
0.3439000	2.5250000
0.0500120	3.0991000
-	3.8000000
Nr. 14X modified Nr.14 (black)	
0.0079800	0.2799600
0.0066541	0.4081100
0.0060938	0.6250100
0.0548840	2.5000000

Continuation on the next page ...

Table I-4.4 – Continuation of previous page

Thickness [km]	S-velocity [km/s]
0.1197800	1.6736000
0.0607650	1.3992000
0.2018800	1.3221000
0.0996330	1.7646000
0.1023300	2.5491000
0.1424300	2.9819000
-	3.8000000
Nr. 21X modified Nr.21 (black)	
0.0058129	0.2900000
0.0101870	0.4112500
0.0107810	0.6255700
0.0400630	2.6531000
0.0233620	1.8055000
0.0433840	1.6322000
0.0445900	1.8755000
0.0412760	2.2835000
0.4405400	2.4614000
0.1630700	2.9983000
-	3.8000000

4.5 Modifications and Proposed Velocity Profiles

The selection of soil profiles are based on the original material in Interoil [2009c] (TP3-GTC-1001), the additional data requested and provided by SP3 experts in Interoil [2009b] (TP3-GTC-1008), the assessment in TP3-TN-1062 (see Section 4.3), the alternative rock profiles proposed in TP3-TN-1061 (see Section 4.4) and the quality-checked dispersion curves from MASW and ambient vibration array analysis (see Figure I-4.14). The bounds for the eigenfrequency of the soil layer are defined from H/V observations and f_0 values are in the range 3.5 - 6.5 Hz. The bounds for the permitted dispersion curves are also shown in Figure I-4.14 as black lines. The density for the sediment layers above the ground water table is 2.0 g/cm^3 and for the layers below the ground water Table 2.2 g/cm^3.

In order to account for the uncertainties in the measured S-wave velocities in rock, several models for the rock are proposed that explain some of the observed features. No model explains all observations. For this reason several rock profiles need to be defined so that the range of possible rock models is covered. The models that explain the H/V peak at 0.6 Hz and the dispersion curves from ambient-vibration observations are models A2 and B1 in Figure I-4.15, which are characterized by a velocity inversion at greater depth. Model A2 takes into account the low average S-waves in rock obtained from downhole measurements at different borehole sites, whereas B1 considers the measurements from cross-hole and sonic logs in the uppermost rock layer. Both models consider an average soil-velocity profile with a total thickness of 28.5 meters. The rock reference velocity is newly defined as 2500 m/s, which is reached at a depth of 558 m.

Additional models with high S-wave rock velocity are included (models D1, DCmax and DCmin), as originally proposed by NPP experts. These rock models were derived mostly from cross-hole measurements and the sonic logs. Three models are proposed. Model D1 is based on measurements performed by NAGRA [2001]. In the soil layer an average soil-velocity profile is taken with a total thickness of 27.5 meters. The rock reference velocity of 2500 m/s is reached at a depth of 80 m.

Models DCmax and DCmin are selected to cover the range of measured velocities in the soil layer, as defined by the measured dispersion curves. The rock layer is chosen assuming a constant velocity in the uppermost layer that corresponds to the rock reference velocity of 2500 m/s and is reached at a depth of 27.5 m.

All profiles are representative of the whole area of the KKG/KKN site as proposed by NPP experts in their original report. The transfer functions for proposed soil/rock profiles are given in Figure I-4.17, reflecting the variability in the fundamental frequency of the soil and the observed low-frequency peak in H/V at 0.6 Hz, as well as the variability of the amplitude of the observed H/V peak in the range 3.5-6.5 Hz.

For the non-linear calculation only one of the velocity models is chosen which corresponds to the best estimate of the proposed soil profiles. The SP3 experts agreed on the soil profile proposed in model B1. Because non-linear computations are restricted in model size and can hardly treat models of a depth of 500 - 600 m, a new model was defined (model B1*) that combines the soil profile from model B1 with the constant-velocity rock model in models DCmin and DCmax.

The procedure foresees only the selection of one P-wave velocity profile from which two additional profiles are derived using the modeling results from S-wave propagation. The V_P-profile was derived by taking the best estimate (model B1*) and applying a V_P/V_S velocity factor of 2.5 in the sediment layer and $\sqrt{3.0}$ in the rock. The constraint of the water table (at 6.5 m) restricts V_P such that the velocity needs to be larger than 1600 m/s. Furthermore, the V_P measurements were used to define the V_P gradient as shown in Figure I-4.27. The soil randomization allows for variations of up to 15% on the V_P-profile, except of the soils below the ground water table where the variation is up to 10%.

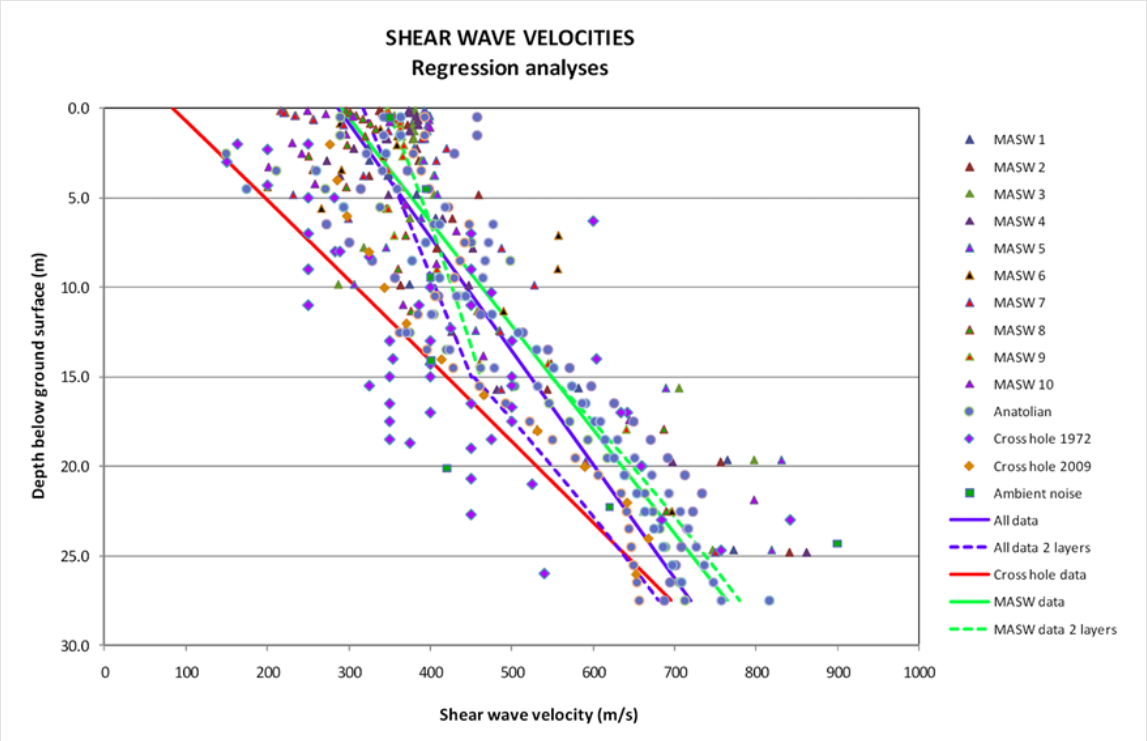

Figure I-4.13: Adjusted shear wave velocity profiles for soils from the technical note TP3-TN-1062.

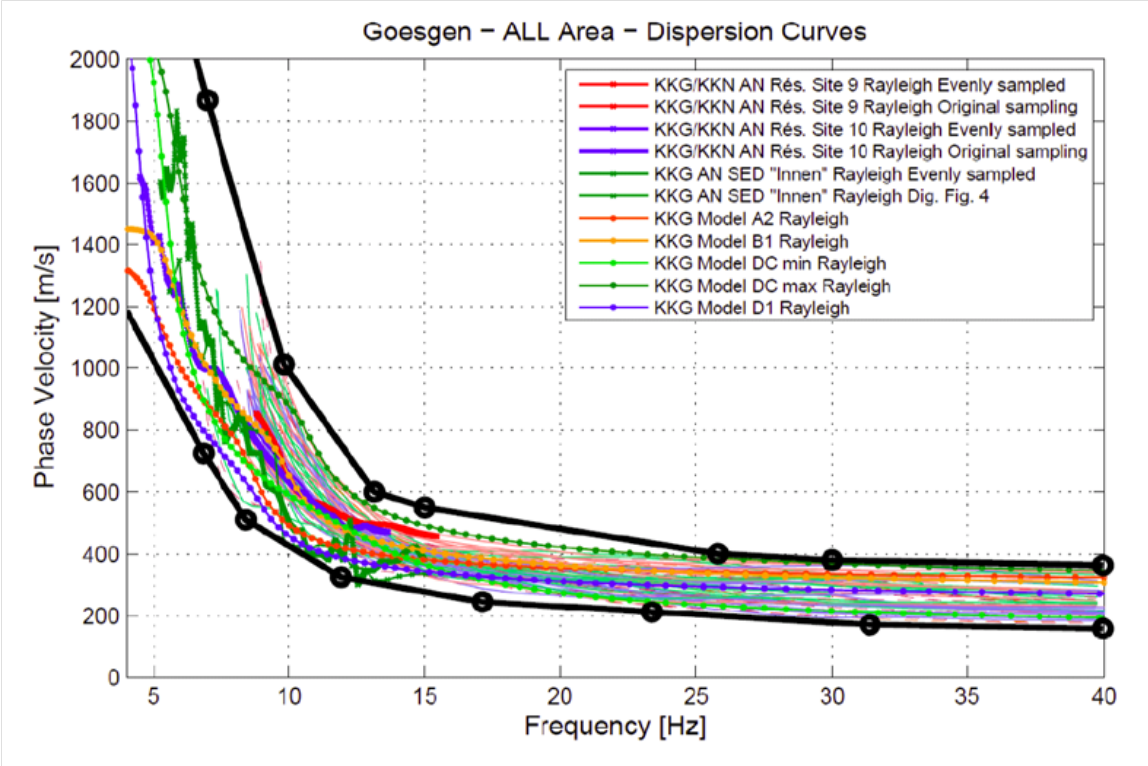

Figure I-4.14: Measured dispersions curves from MASW (thin lines) and ambient vibration array measurements (thick lines), compared to the dispersion curves of the SP3 expert models (lines with dots). The thick black lines define the bounds of allowed dispersion curves.

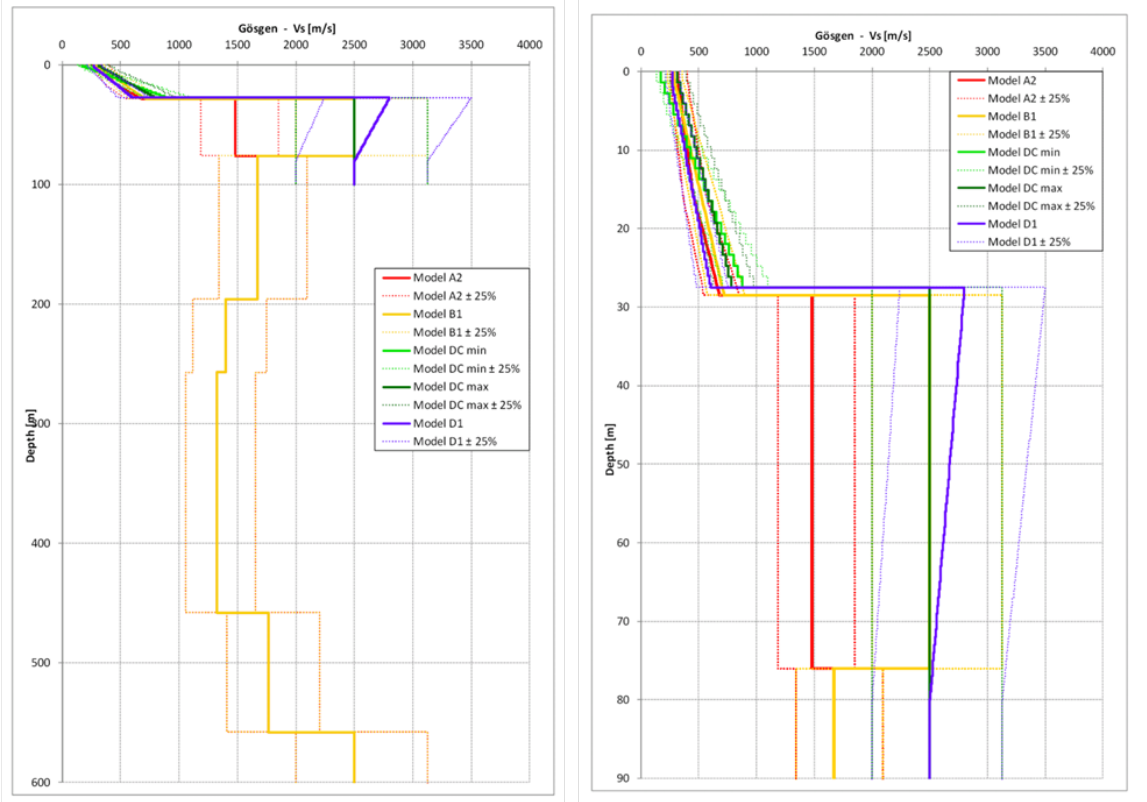

Figure I-4.15: Proposed velocity profiles representative for the whole area of the KKG/KKN site indicating also the two standard deviations for the soil randomization when using RVT ±25%).

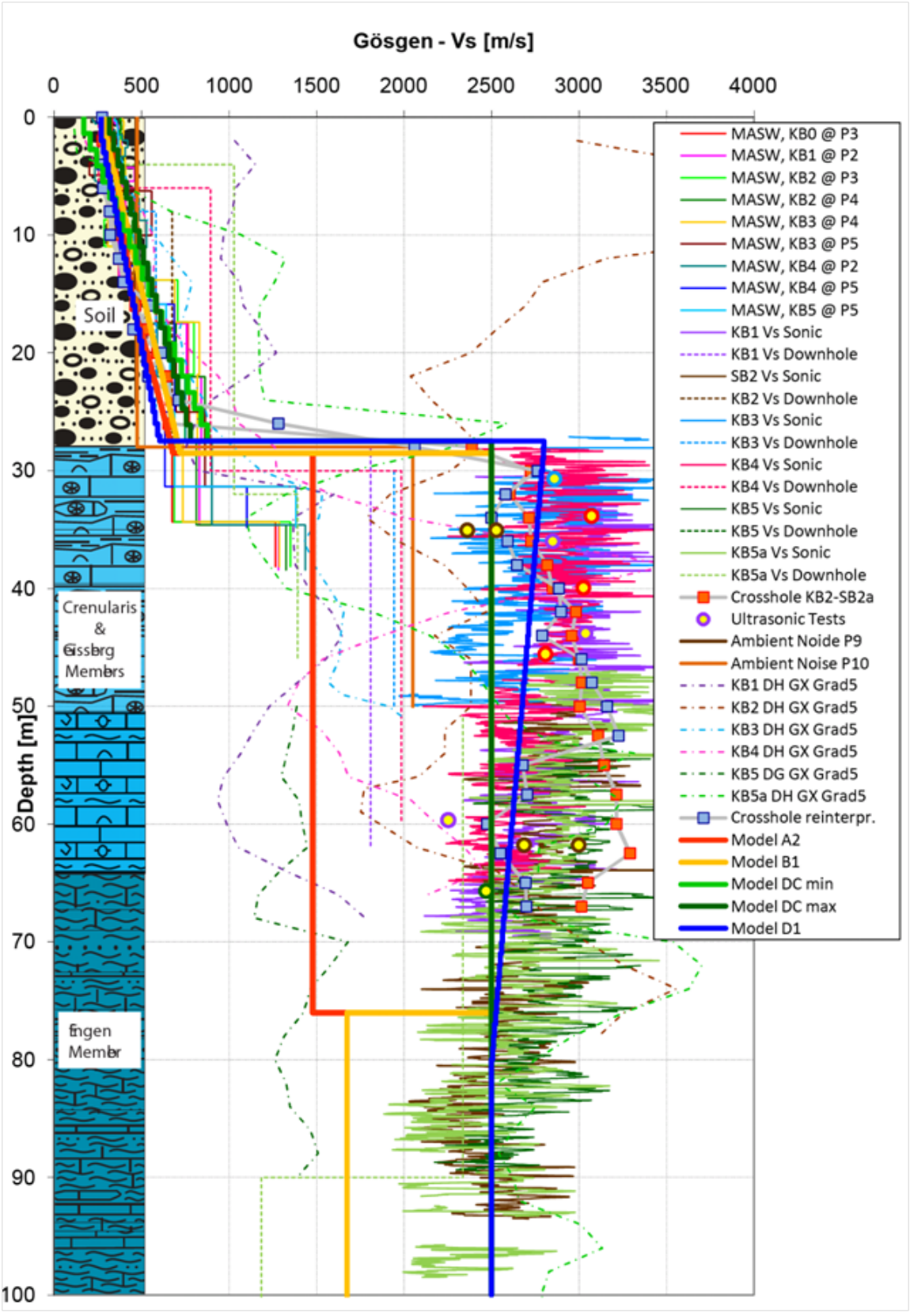

Figure I-4.16: Comparison between proposed V_S-models and measurement results.(KKG).

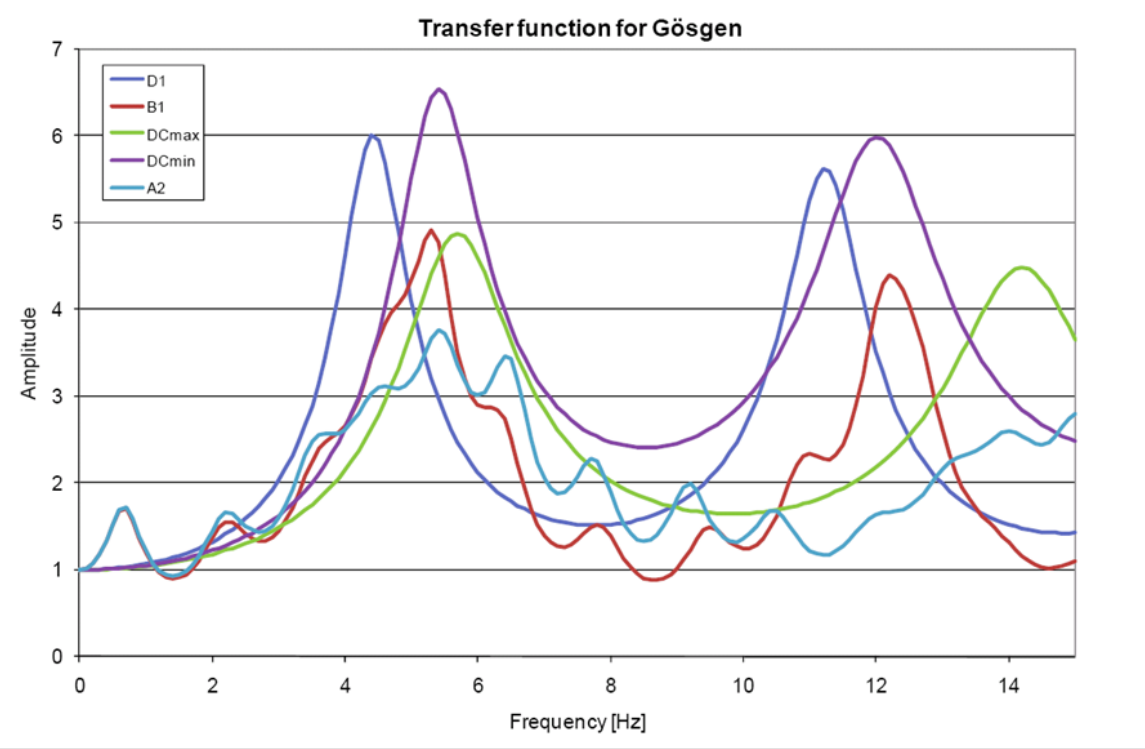

Figure I-4.17: Transfer functions for proposed soil/rock profiles (Ver. 04.02.2010)(KKG).

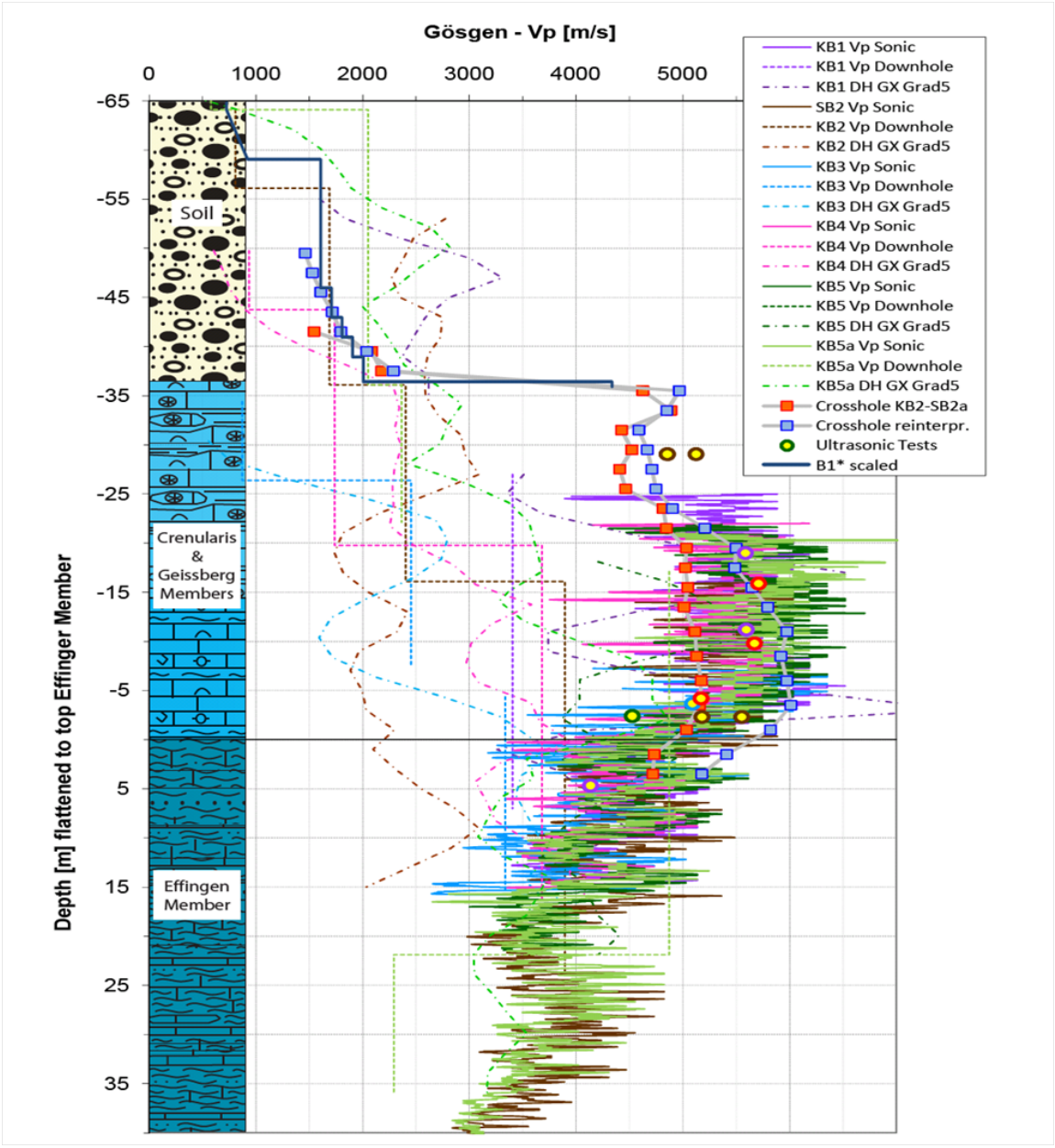

Figure I-4.18: Comparison between the proposed V_P-model and measurement results.(KKG).

4.5.1 V_P-profile for Gösgen

For Gösgen the referenced model for the S-wave velocity profile is B1*; the parameters take the values $\rho_S = 2.675$ t/m^3, $\rho = 2.2$ t/m^3 below the water table and $\rho_f = 1.0$ t/m^3, then $\varphi = 0.28$. The water bulk modulus was set equal to 1000 MPa at the water table surface and to 2250 MPa at 12 m depth and kept constant below. The final computed V_P is depicted in the following figure with the measured data.

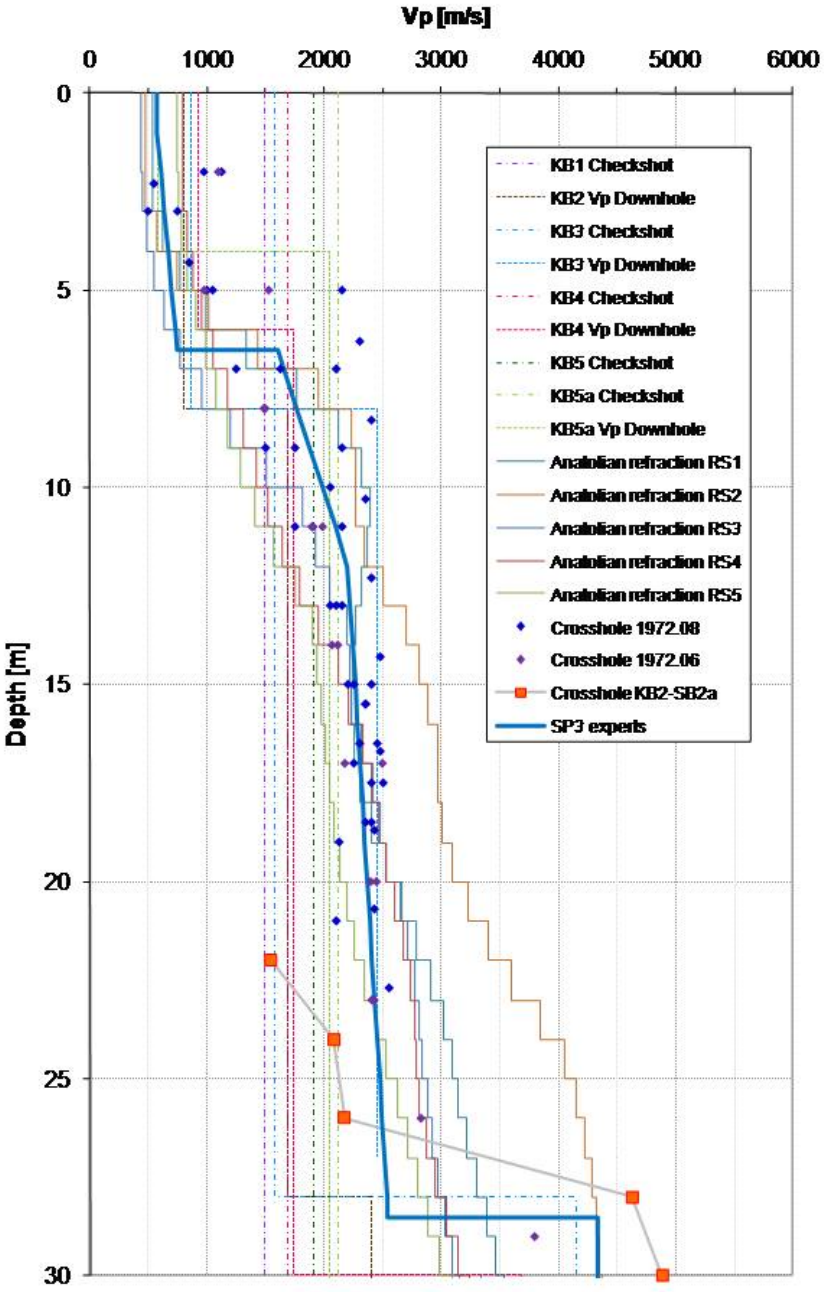

Figure I-4.19: V_P model and measurements Gösgen (KKG and KKN).

4.6 Material models

4.6.1 General Comment

The selected models are based on first priority on tests results and on the results published by Rollins et al. [1998] and Menq [2003]. Menq's curve takes into account a dependence of G/G_{max} on the confining stress while Rollins' curve does not. Furthermore, Menq's curve corresponds to a weaker material compared to Rollins.

Accordingly, examination of the G/G_{max} curves shows that Menq's mean curve coincide with the lower bound of the tests data and Rollins mean to the upper bound. The mean curve is defined as the average between the lower bound and the upper bound curves.

As lower bound for the damping, Rollins mean damping curve was used, while Menq's mean curve was used for the upper bound. From the observations and from also theory, a stiffer material exhibits lower material damping and a softer material, higher material damping. Those curves have been modified to a small extent to better fit the observed data.

4.6.2 Model for the Gösgen Site

Due to the thickness of the soil layer, two different sets of curves are introduced corresponding to two different confining pressures; the first set corresponds to the top 10 m and the second one to the bottom part (10 to 28.5 m). The lower bound curve for G/G_{max} for the lower layer was corrected for confining pressure according to Menq's equation which leads to a slightly stiffer material. The upper bound curve, which comes from Rollins, does not depend on the confining pressure and is therefore kept unchanged regardless of the depth. The same corrections apply to the damping curves, but the corrections are small.

The G/G_{max} curves fit well the data with the exception of few values which are not believed reliable. Based on the G/G_{max} curves, the damping curves were derived from Menq's and Rollins' equations. They fit the data in the low strain range but are higher than the data in the large strain range. However, the very small damping ratios measured at large strains are not thought reliable.

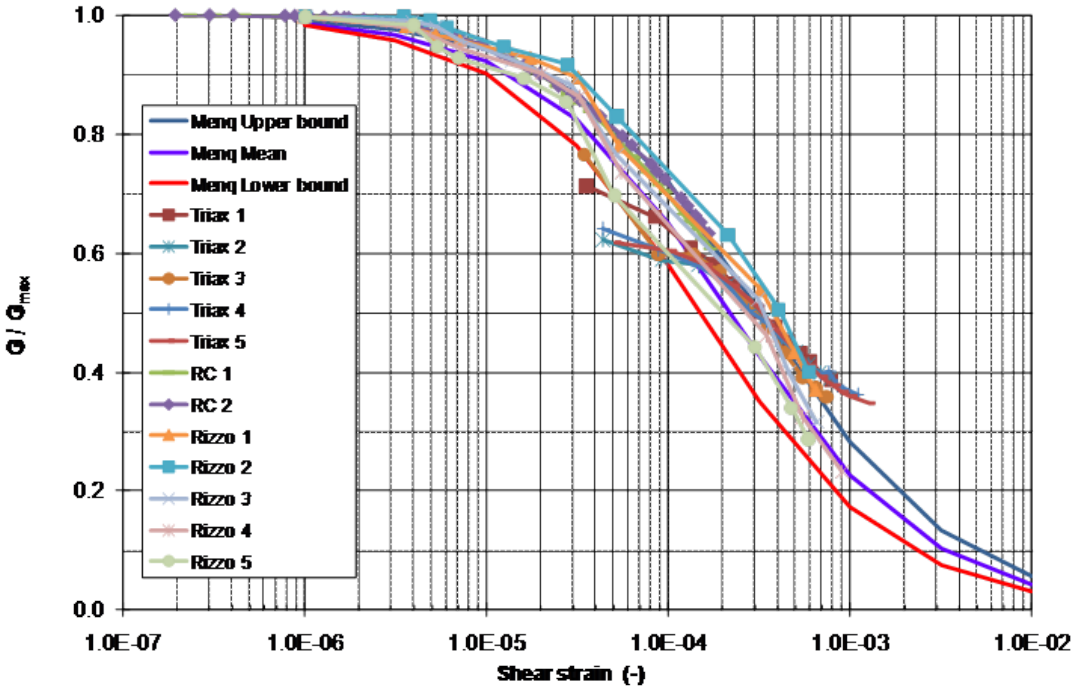

Figure I-4.20: Shear modulus curves for z < 10 m (KKG).

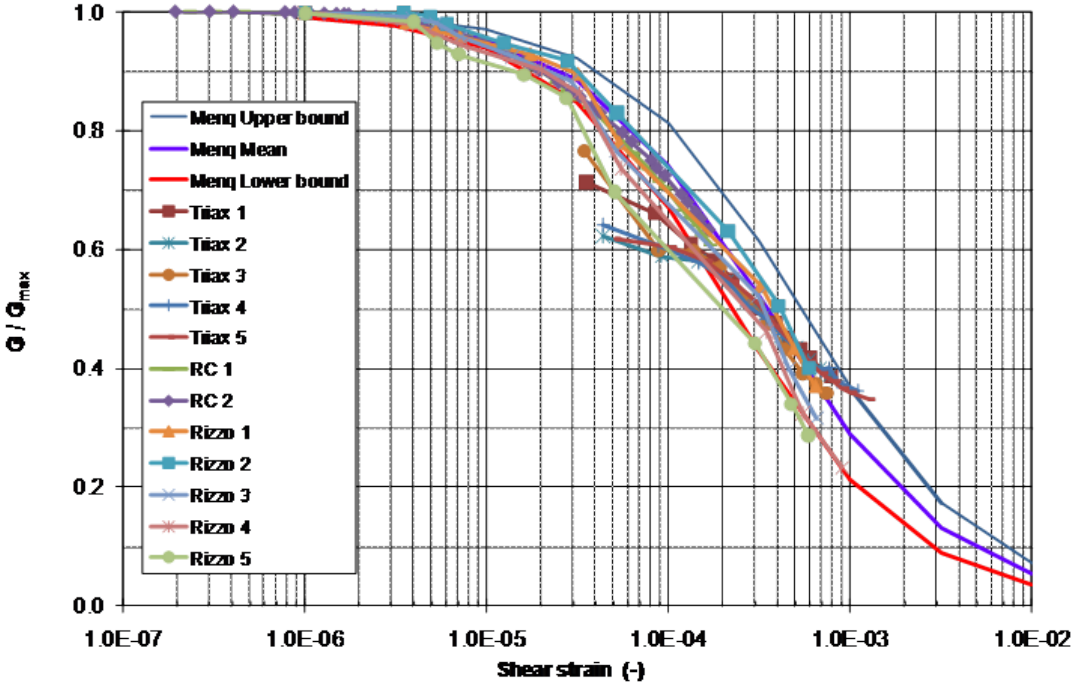

Figure I-4.21: Shear modulus curves for 10 < z < 27.5 m (KKG).

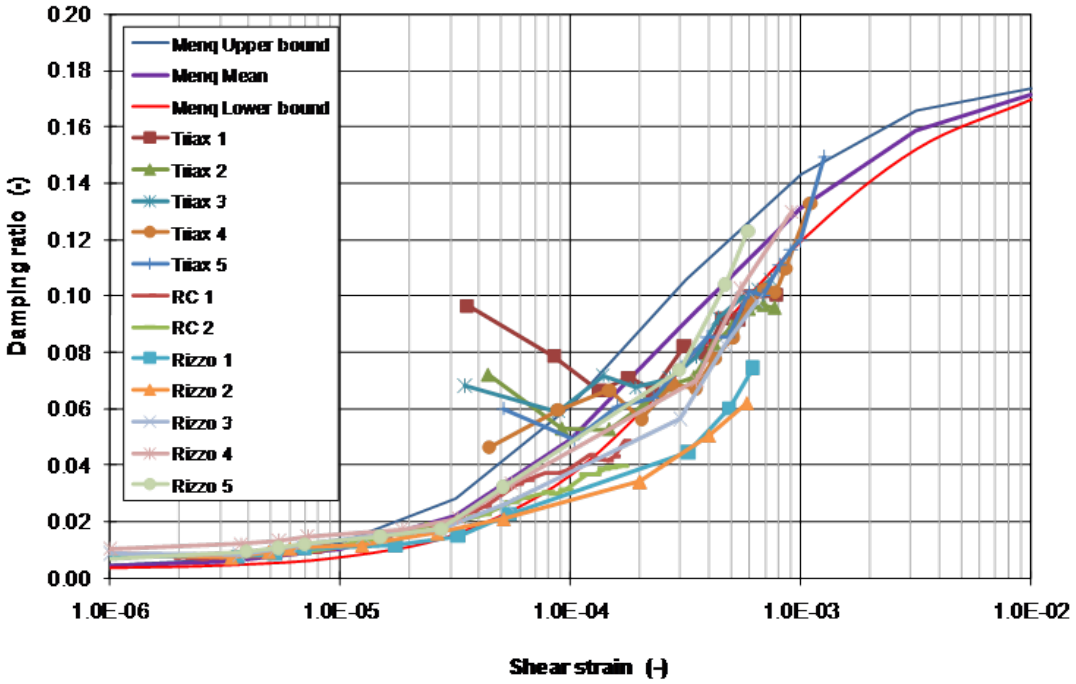

Figure I-4.22: Damping ratio curves for z < 10 m (KKG).

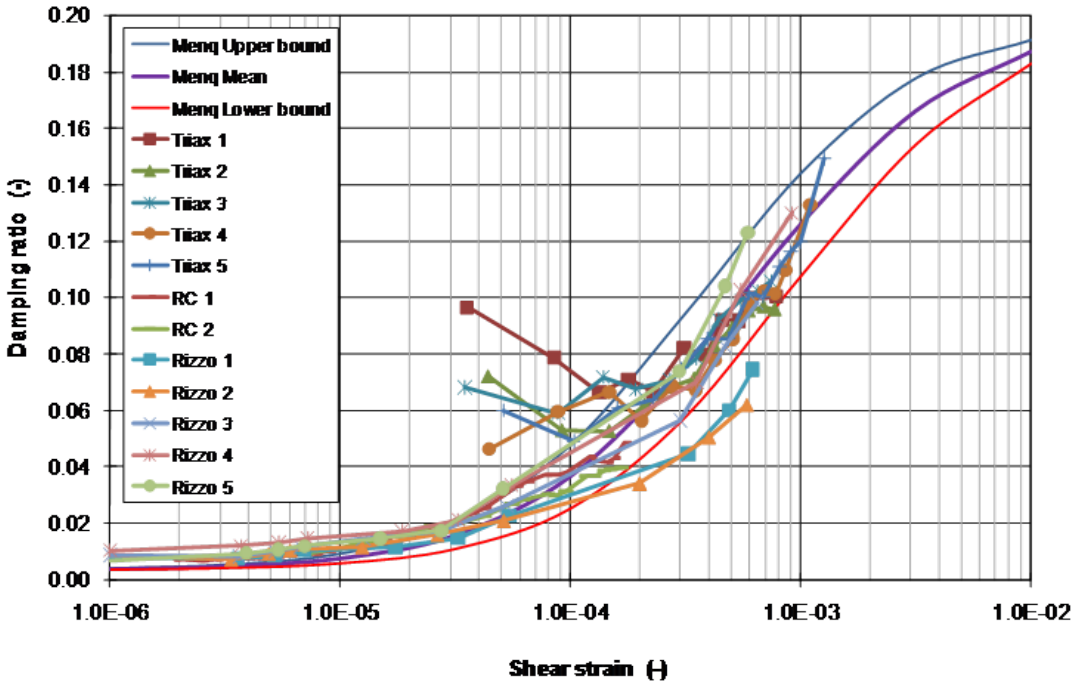

Figure I-4.23: Damping ratio curves for 10 < z < 27.5 m (KKG).

4.7 Comparison of Data and Experts Models in Gösgen (EXT-TN-1095)

Unlike the site of Leibstadt which is a single-plant site and unlike the Beznau island whose two sites are treated separately by the SP3 experts, Mühleberg and Gösgen are two-plant sites treated as one by the experts. However, unlike Mühleberg where below the sub-horizontal base Quaternary the Molasse can be considered as a more or less homogeneous, laterally continuous medium, the geology below the Gösgen area changes rapidly. Figure I-4.24 shows that the Quaternary soil shows a trend towards higher thicknesses when moving to the south and that the Malm sediments (Crenularis, Geissberg and Effingen Members) plunge to the south.

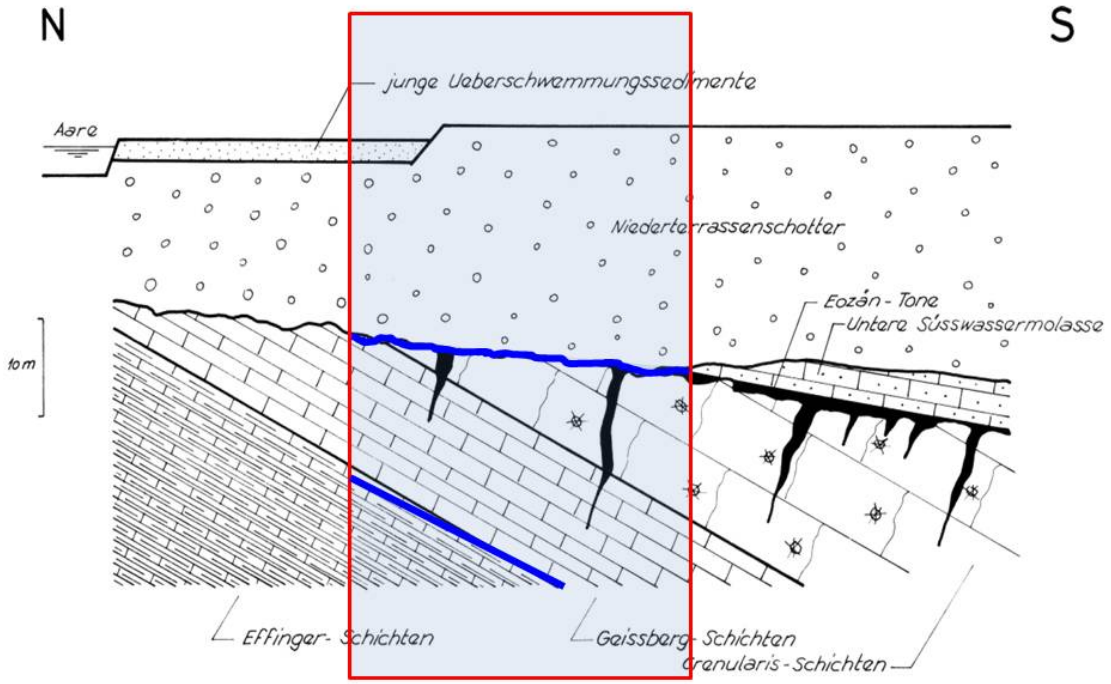

Figure I-4.24: N-S Cross-section through the Gösgen Site. The area covered by the site investigations is framed in red. The two geological interfaces with associated velocity contrast are marked in blue: (a) the Base Quaternary (or top bedrock resp. top Crenularis Member) and (b) the Top Effingen Member (or base Crenularis-Geissberg Members).

The different depths of the interfaces associated with velocity contrasts make the comparison of datasets acquired at different locations in the investigation area difficult. Variations caused by different lithologies are masked if absolute depths are used. To mitigate the problem a flattening was used in some figures whereby the depths are referred to a main geological contrast rather than to topography.

When developing their common model for the KKG and the KKN sites the experts relied on

different datasets acquired at locations with different subsoil conditions. As an example, the crosshole survey was performed between wells KB2 and SB2, located south of the sites, where a larger thickness of the Crenularis-Geissberg members is encountered. In the figures presenting the comparison between experts' models and measured datasets, a first stratigraphic column is therefore shown (on the left hand side) pertaining to the subsoil condition at the sites while a second column is shown (on the right hand side) showing the conditions at the KB2/SB2 location. Datasets and models are flattened to the top Effingen member which allows the velocity contrast between this member and the shallower members to be seen. In essence, one stratigraphic column would be necessary per investigation location.

4.8 Supporting Figures for Gösgen

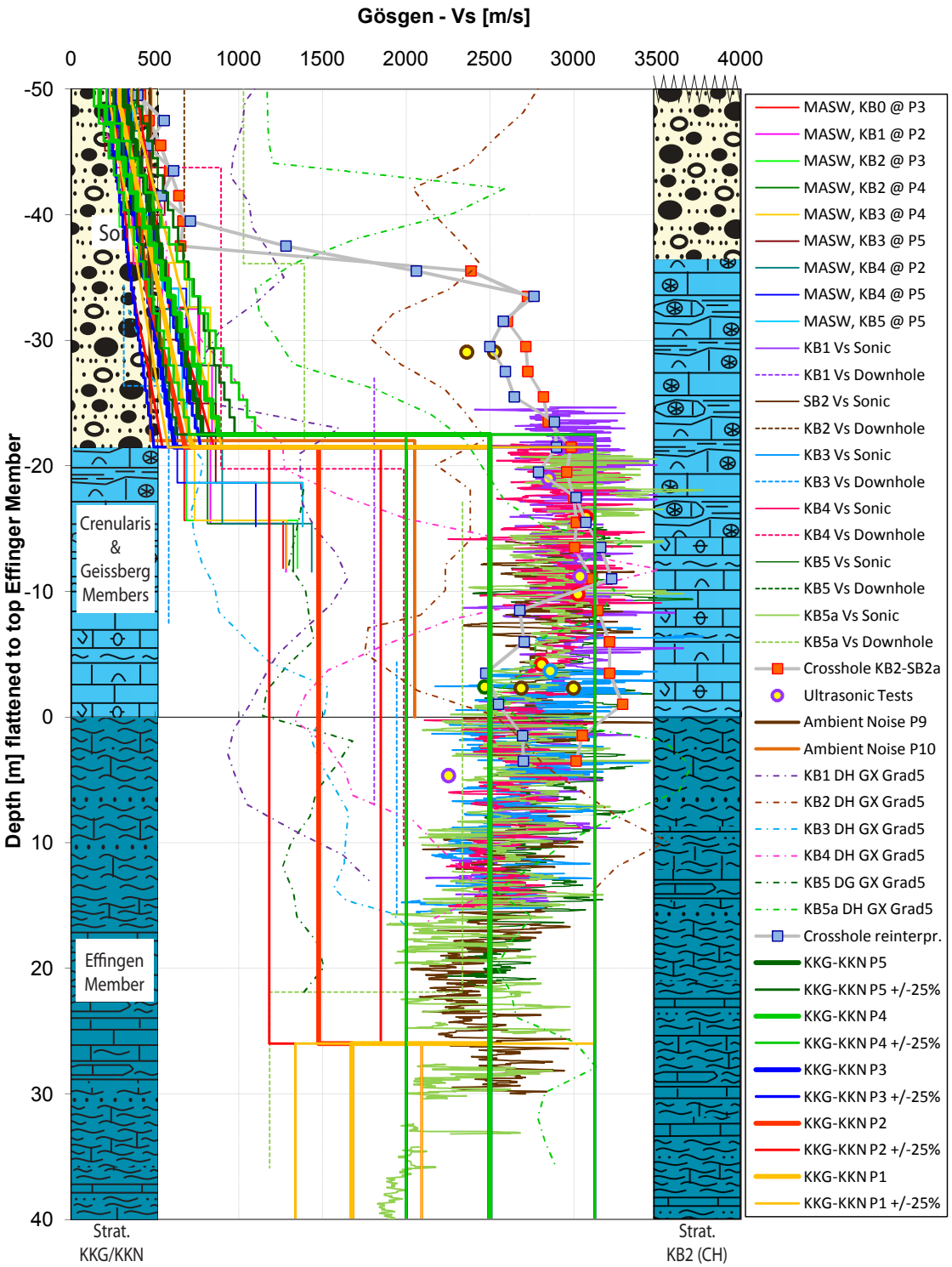

Figure I-4.25: V_S-profiles representative for the whole KKG-KKN area compared to data - shallow.

Table I-4.5: Fundamental frequencies, Gösgen site.

Profile	Frequency
P1 (B1)	5.3 Hz
P2 (A2)	5.4 Hz
P3 (D1 modif)	4.4 Hz
P4 (DCmin)	5.4 Hz
P5 (DCmax)	5.7 Hz

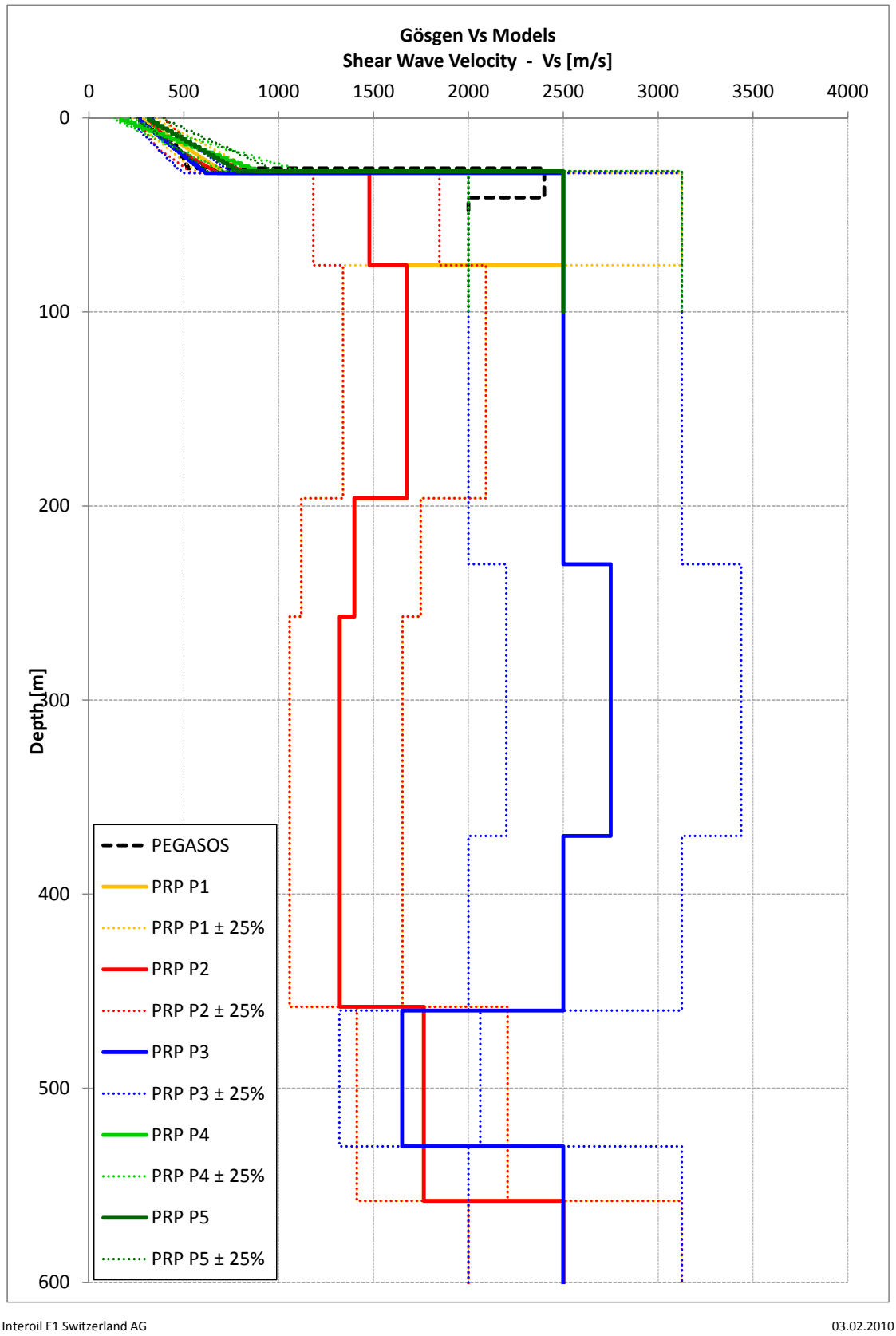

Figure I-4.26: V_S-profiles representative for the whole KKG-KKN area comparred to data - deep.

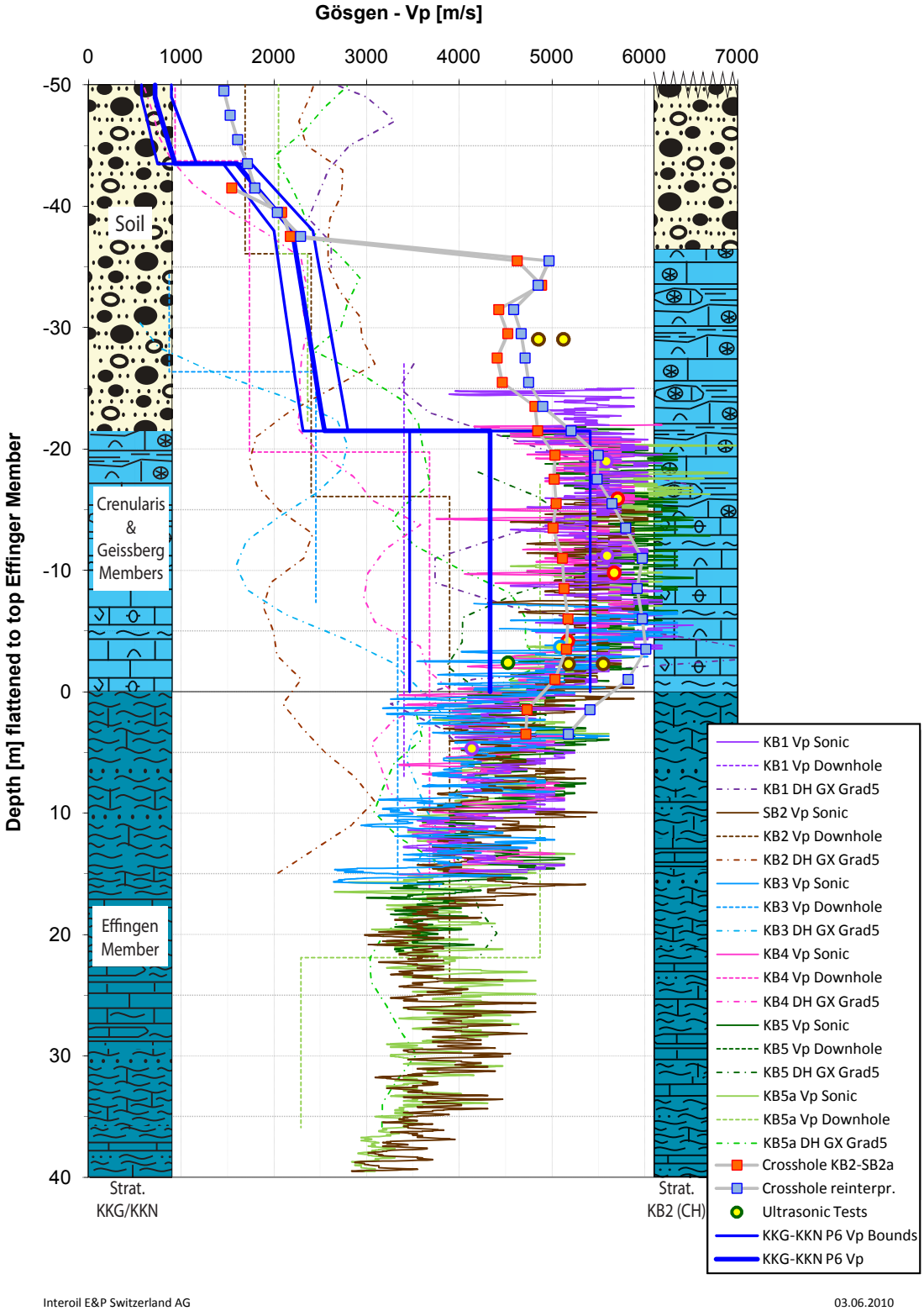

Figure I-4.27: V_P-profiles representative for the whole KKG-KKN area compared to data.

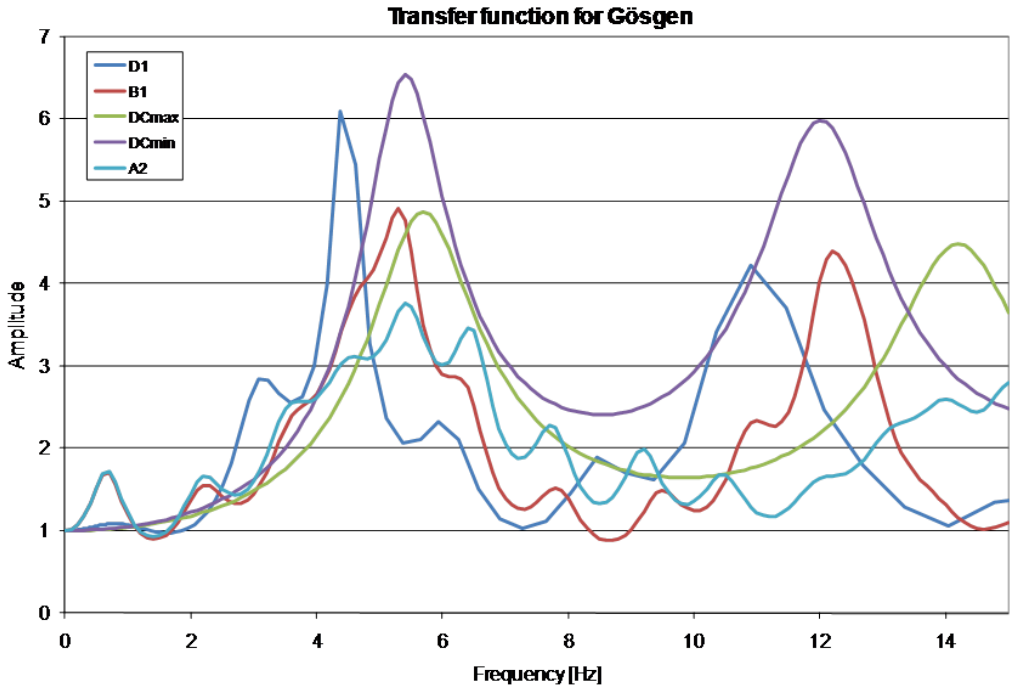

Figure I-4.28: Transfer functions for proposed soil profiles (KKG).

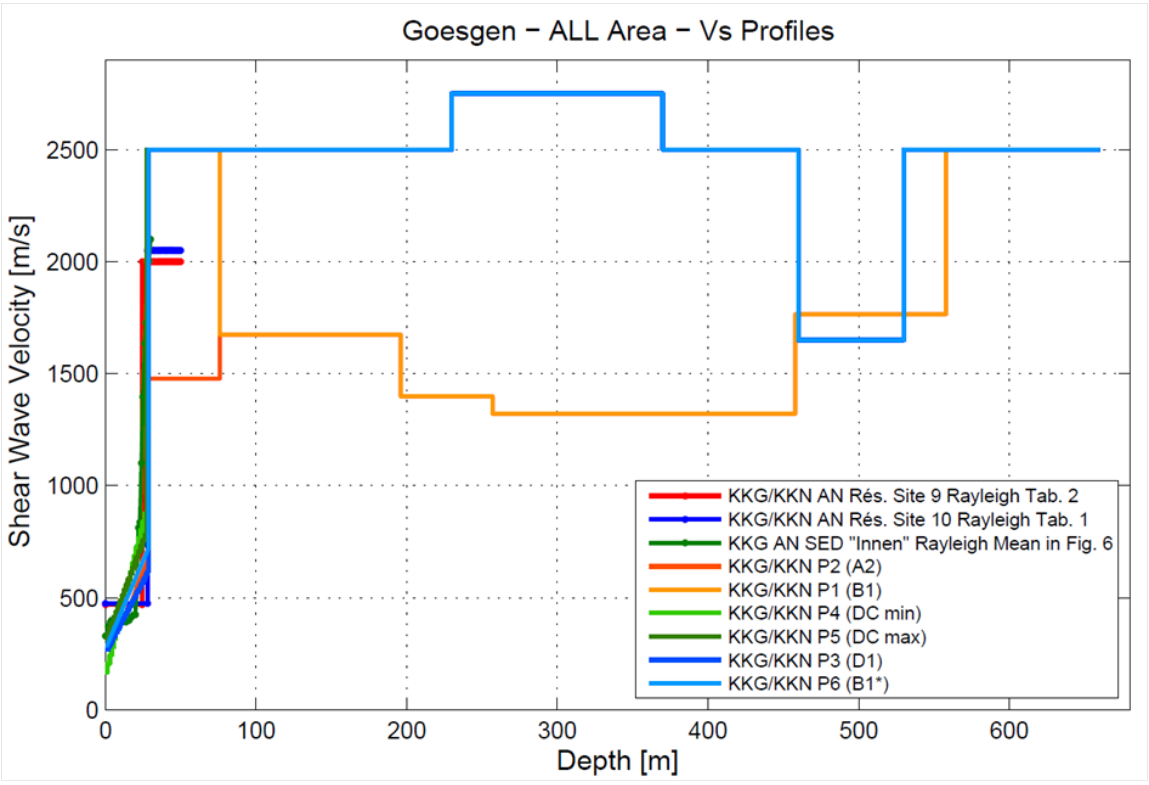

Figure I-4.29: V_S-Profiles (KKG).

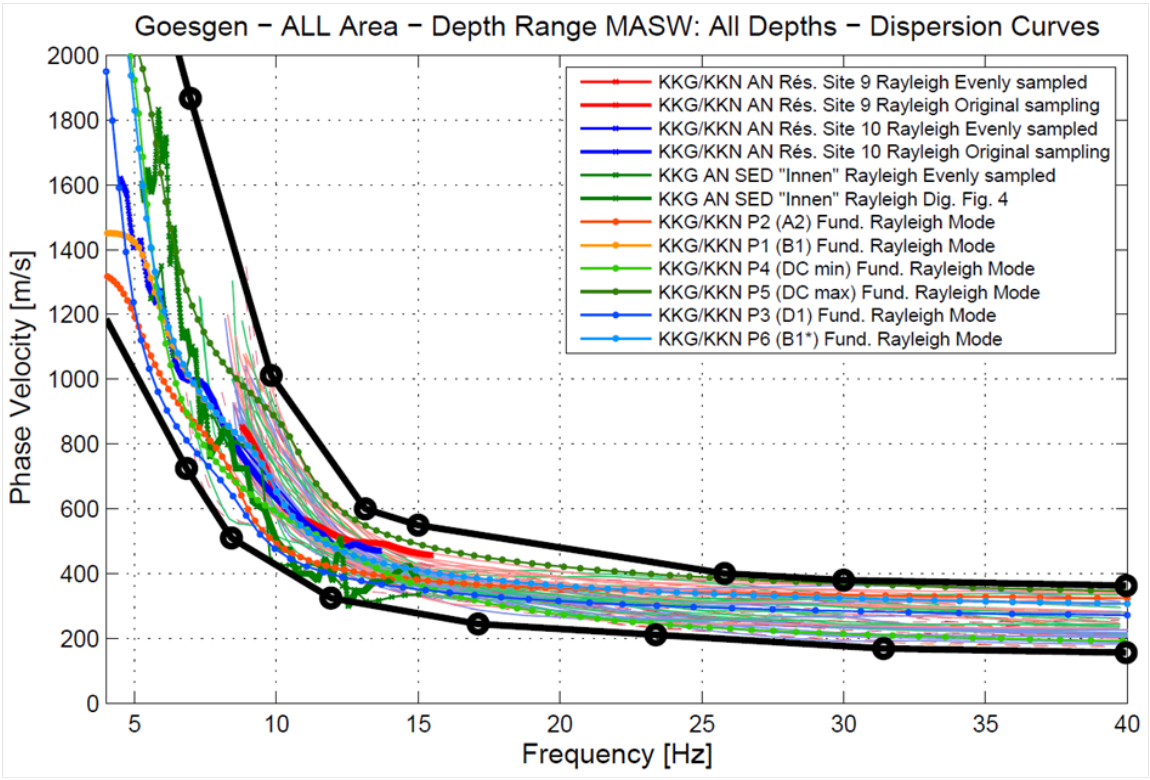

Figure I-4.30: Dispersion curves and bounds (KKG).

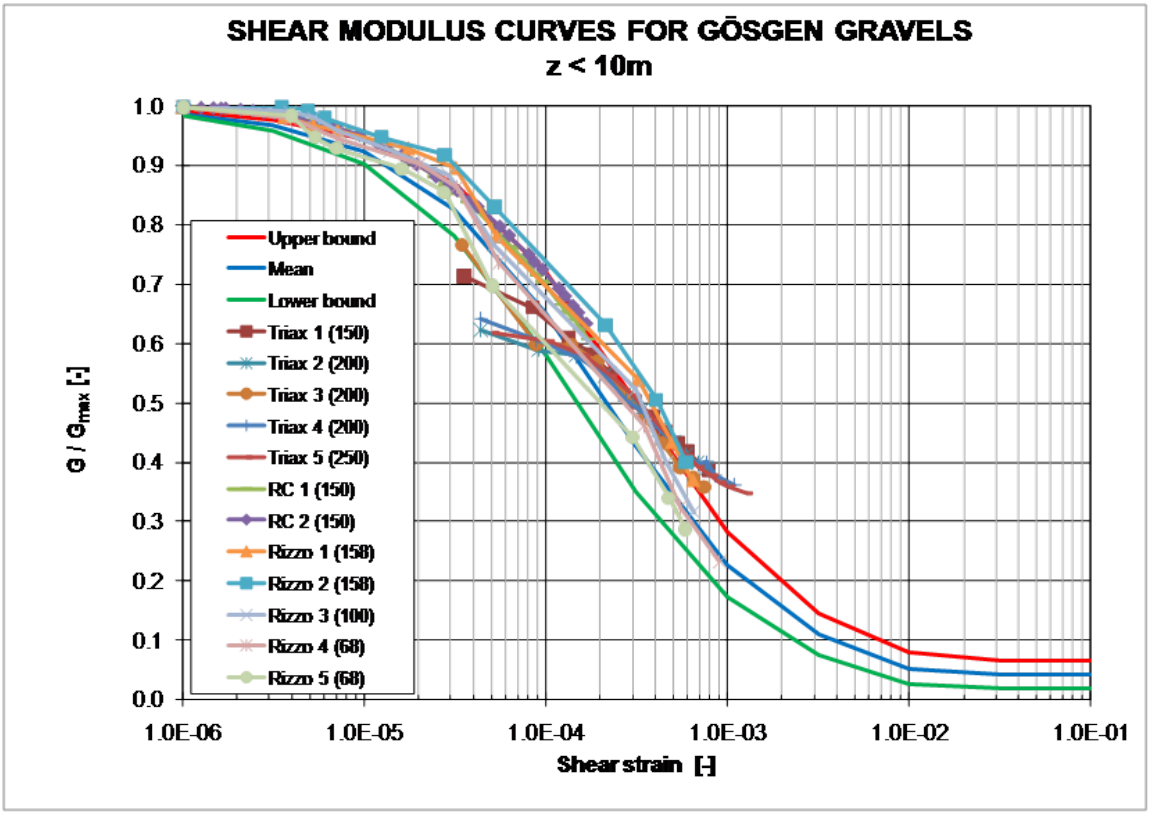

Figure I-4.31: Shear Modulus for 0 < z < 10 m (KKG).

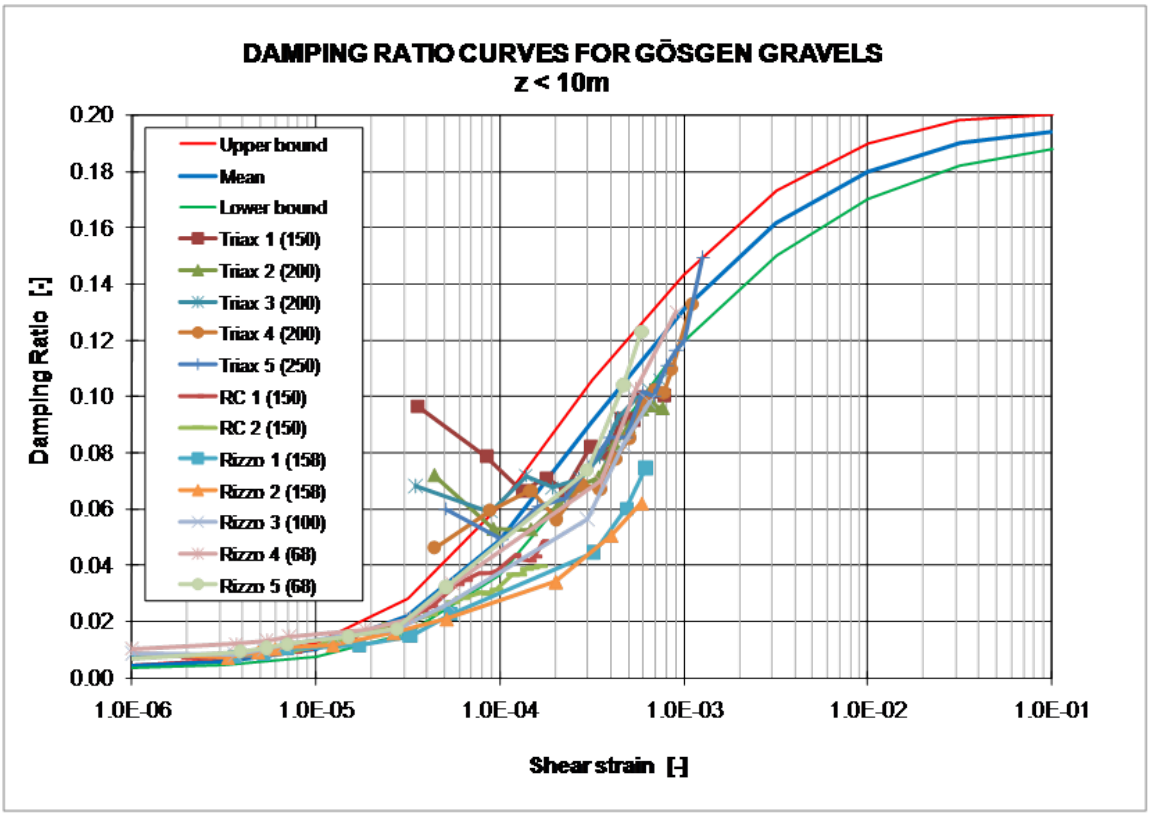

Figure I-4.32: Damping Ratio for 0 < z < 10 m (KKG).

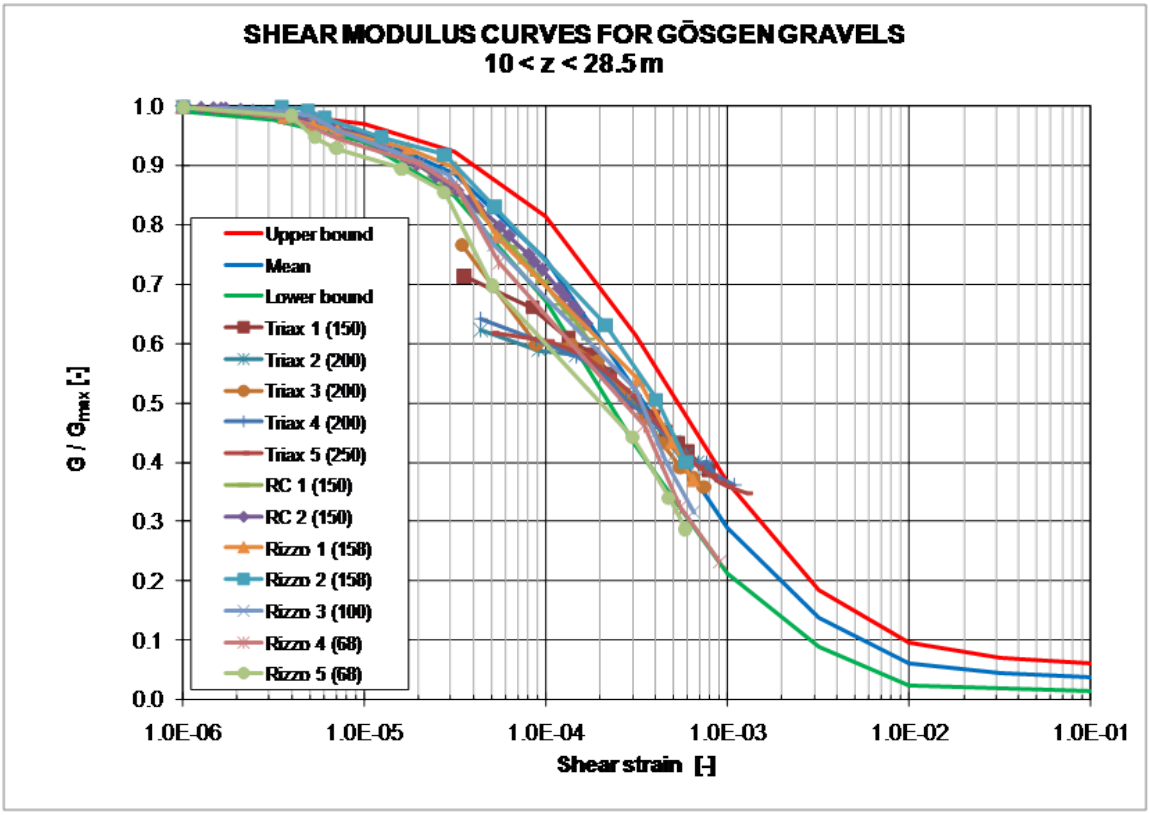

Figure I-4.33: Shear Modulus for 10 < z < 28.5 m (KKG).

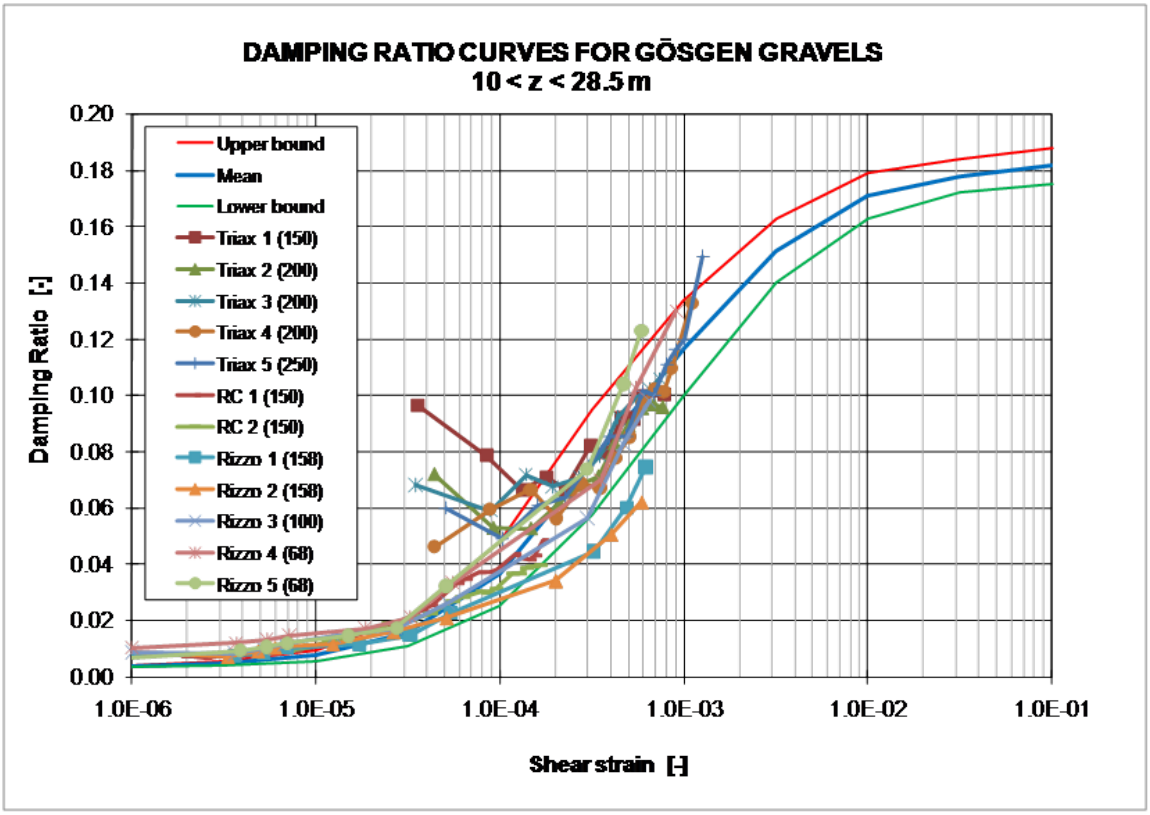

Figure I-4.34: Damping Ratio for 10 < z < 28.5 m (KKG).

4.9 Comparison of PEGASOS vs. PRP Profiles and Material Models

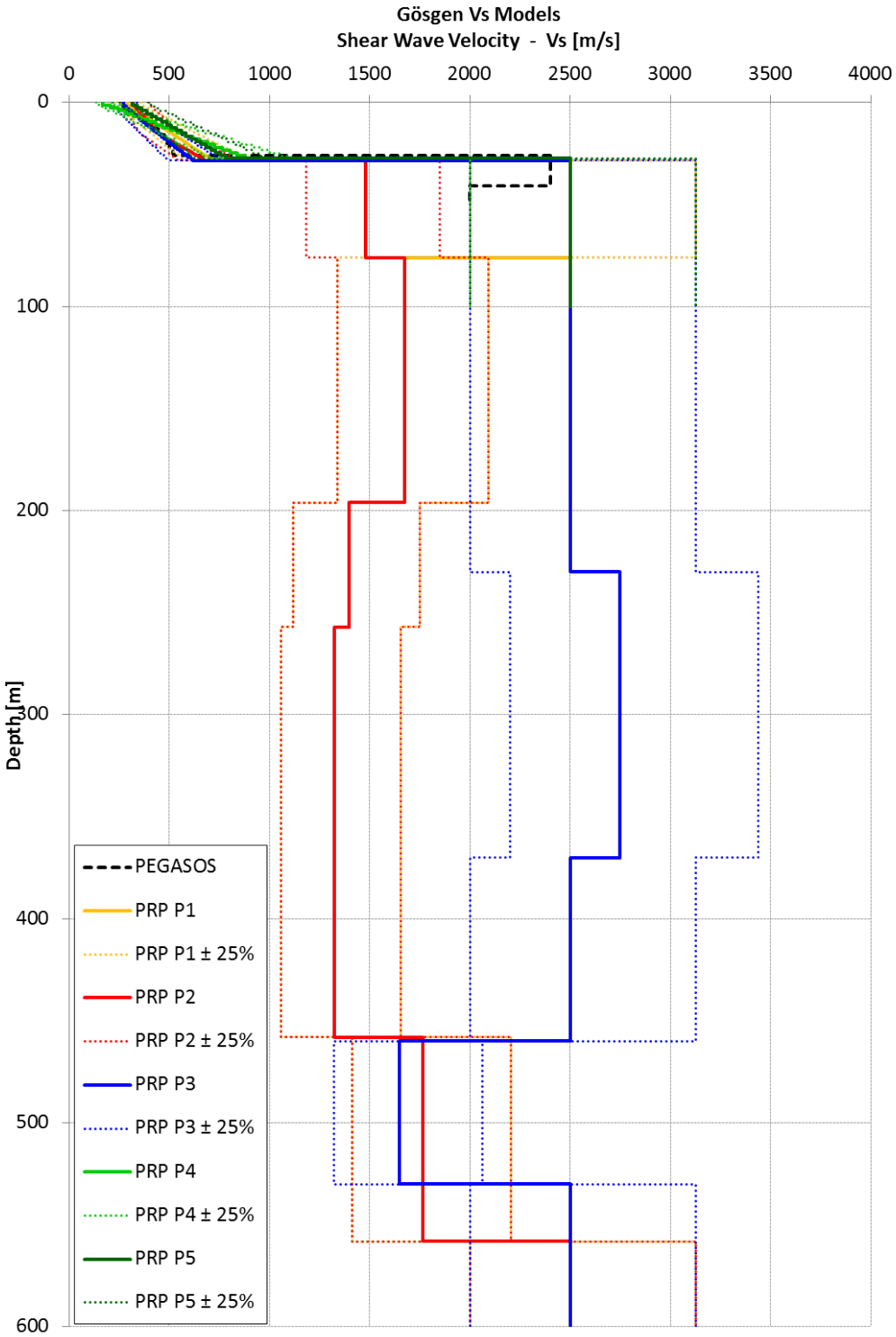

Figure I-4.35: Comparison of PEGASOS and PRP V_S-models for Gösgen.

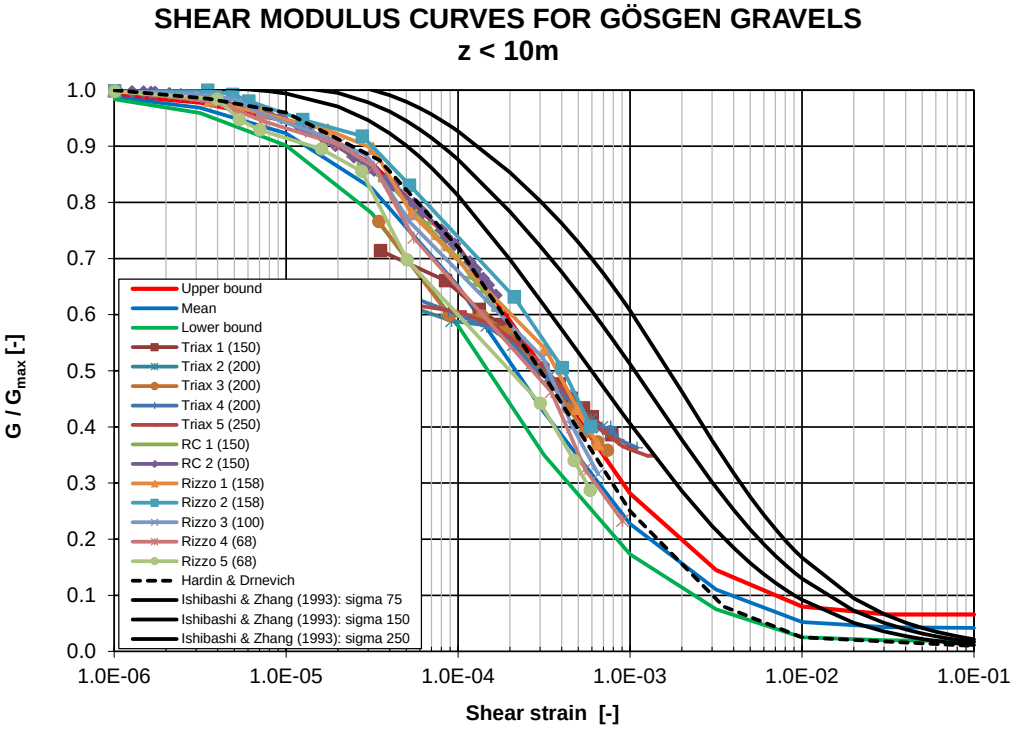

Figure I-4.36: Gösgen - Shear modulus curves for gravel, $z < 10$ m.

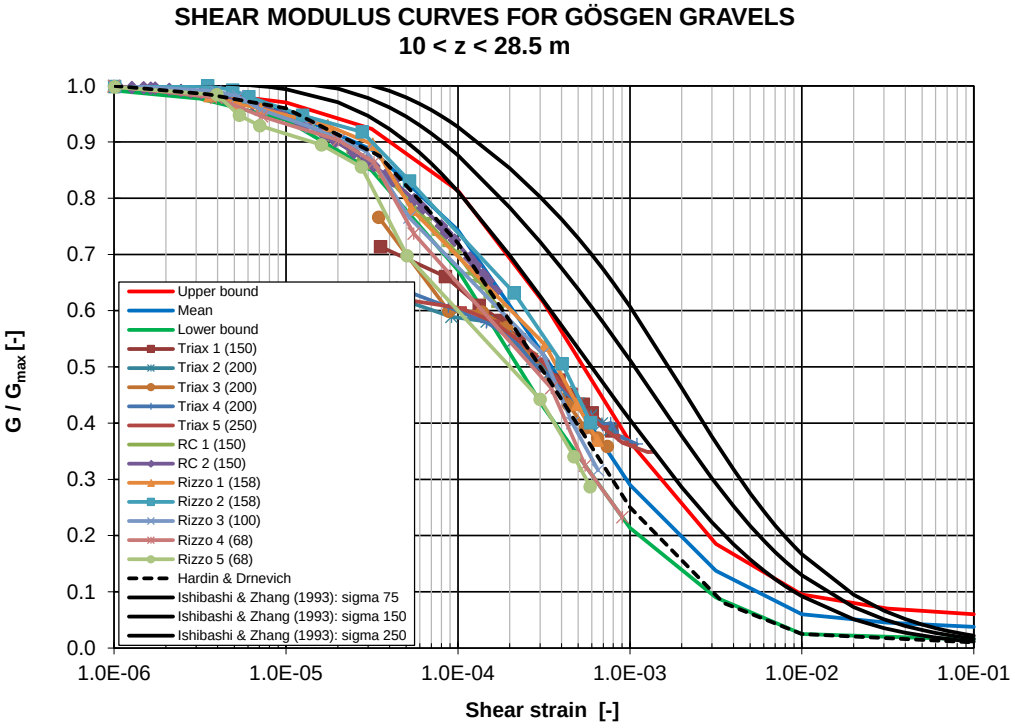

Figure I-4.37: Gösgen - Shear modulus curves, gravel, $10 < z < 28.5$ m.

Chapter 5

Proposed Velocity Profiles for KKL Site

This chapter explains the rationale behind the proposed three velocity profiles for the Leibstadt site. It takes into account the discussions held during the workshops on 19. November 2009, and 19. January 2010, as well as the background documents distributed before and after these two meetings.

5.1 Initally Proposed Velocity Profiles and Comments

5.1.1 Original Proposal, September 2009 ("TB-213-KG09003")

Various models were proposed, with different weights assigned to the non-invasive (surface wave) and invasive (borehole) data, with correction factors to account for anisotropy. All models however rely on cross-hole data for the rock units (i.e., non-gravel units: Wellenmergel, Wellendolomit, Röt and Buntsandstein). They are displayed in Figure I-5.1.

5.1.2 Comments from the Workshop WS2b/SP3 (November 2009)

The major comments on these propositions and "to do list" were summarized in the summary presentation by N. Abrahamson (TFI-RF-1149). Besides the agreement to assign the deep Crystalline rock a velocity of 2200 m/s, the discussion led to the proposal of three additional / alternative models, with however the same profile beyond 40 m depth (i.e., basically cross-hole data, corrected for anisotropy), to take into account the following elements:

- The existance of the low velocity zone (20 m depth) seen in gravels from cross-hole was questioned and thus, "MKi" models were modified to exhibit smooth gradient with a shear-wave velocity in the gravel regularly increasing with depth, with or without a significant jump at 30 m depth to account for a "cemented" layer at the bottom of the gravel layer.

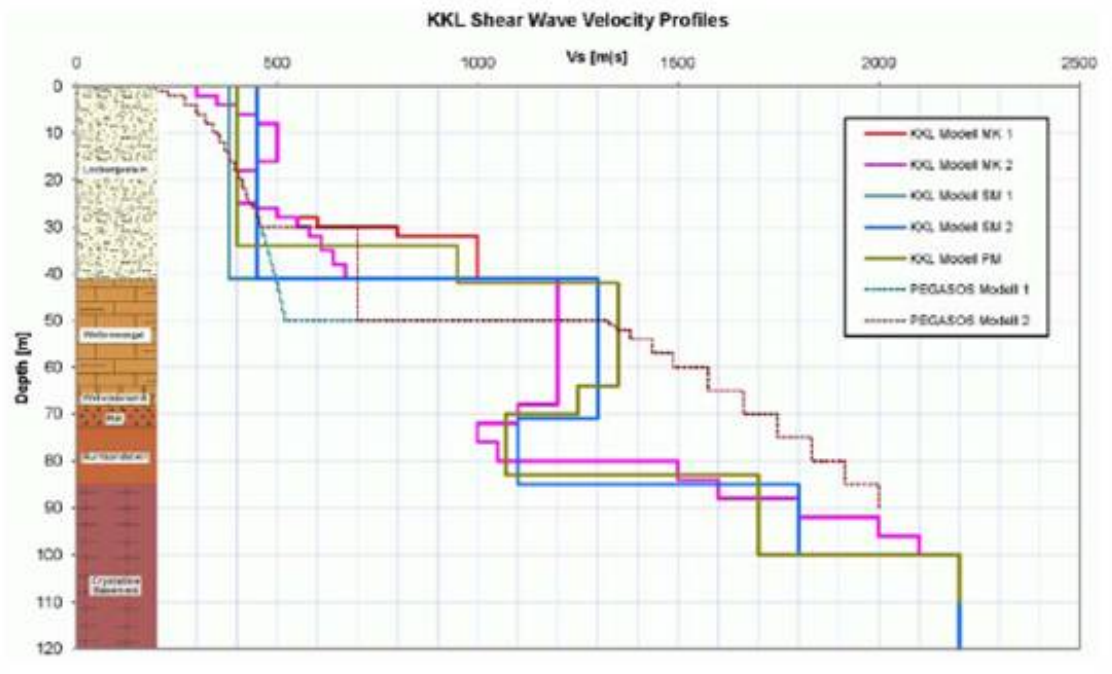

Figure I-5.1: Velocity profiles proposed in September 2009 by the NOK experts, and comparison with the original PEGASOS velocity models (from "TB-213-KG09003").

- It was also decided to have a model based on the ambient vibration data (model named "DF") associated with larger velocities within the gravel layer, and also a more pronounced gradient – especially at depth.
- These models had however to be checked through a comparison of the corresponding dispersion curves with the measured ones.

These three additional models are displayed in Figure I-5.2 with comparison to the original PEGASOS profiles, and the corresponding dispersion curves in Figure I-5.3.

Another issue was related with the amount of anisotropy in the bedrock (below 41 m depth), which was found slightly larger than accounted for in the original velocity profiles. It was thus decided to check the actual values and, possibly, to apply a slightly larger reduction factor to cross-hole data.

5.1.3 Modifications and Proposed Velocity Profiles

The three velocity profiles proposed by the SP3 expert group were derived from the following main considerations:

- try as much as possible to assign a balanced weight to all sources of information, i.e., both surface wave and body wave techniques; and
- try to constrain the three profiles to be representative of the variability of the measured dispersion curves at intermediate and high frequencies, while keeping track of the borehole information.

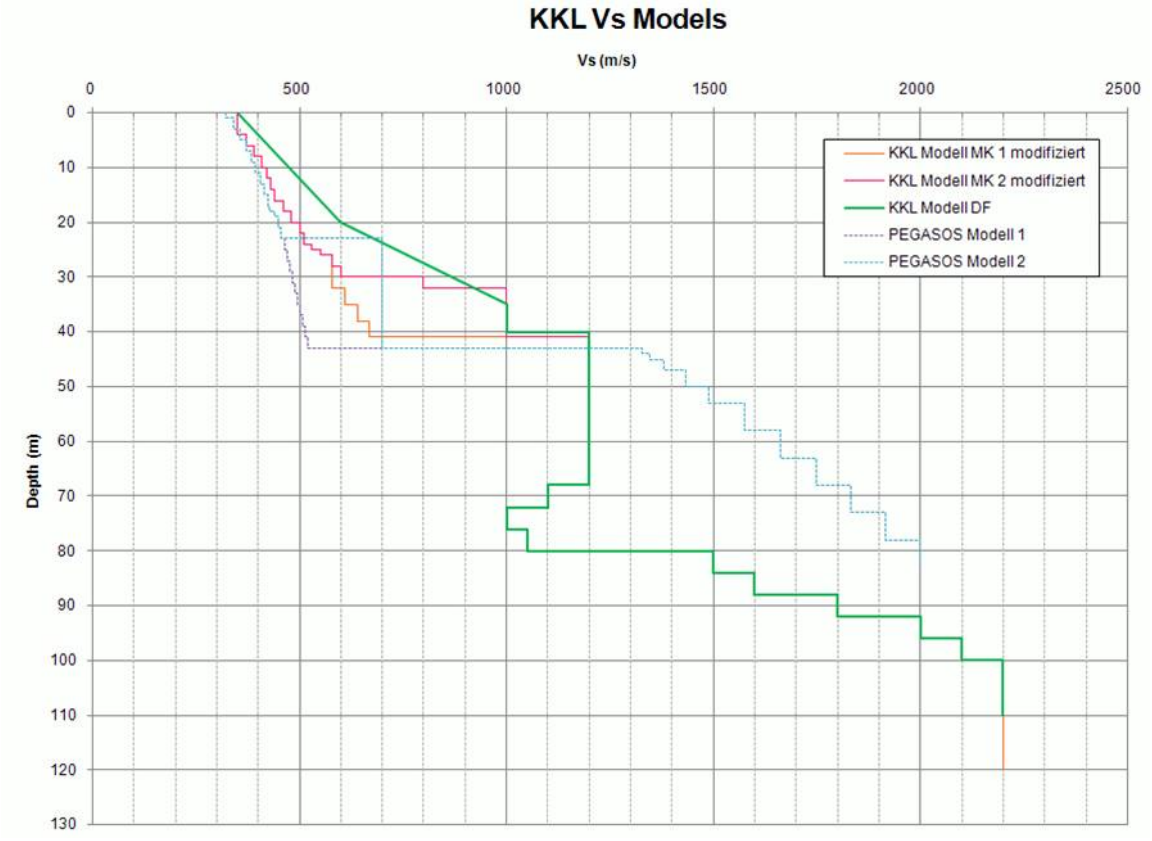

Figure I-5.2: Modified velocity profiles as done during the 19. November 2009 workshop (from document "KKL_V_Models-Data-100104").

The new models proposed after the November workshop (MK1 modified, MK2 modified and DF), were compared with the available measured DCs, as provided in Figure I-5.4, and were found, especially at high frequency to all underestimate the Rayleigh wave phase velocity derived from MASW measurements. Therefore, new models were tried during the 19. January 2010 working meeting, on the basis of those proposed in September (MK1, MK2), and the simple one derived from the inversion of ambient vibrations array measurements. New anisotropy reduction factors were also accounted for. The resulting three final models and the associated dispersion curves are displayed in Figures I-5.5 and I-5.6. Figure I-5.5 also includes the other velocity profiles considered, just for comparison and keeping due track of the whole work that has been done.

Model L1 : "DF-20100119"

It is by far the simplest one and is based on the inversion of the DC curves obtained from ambient vibration measurements (AMV); the original proposal by SED (D. Fäh) has been slightly modified (slight velocity increase) at shallow depth to match the high-frequency DC derived from MASW measurements, and to match the fundamental frequency band as well.

Model L2 : "MK2-Crosshole-Anisotropy"

Is is the most complex one and is based mainly on the cross-hole data, with some corrections however. It is thus very close to the original "MK1" proposal, with two changes:

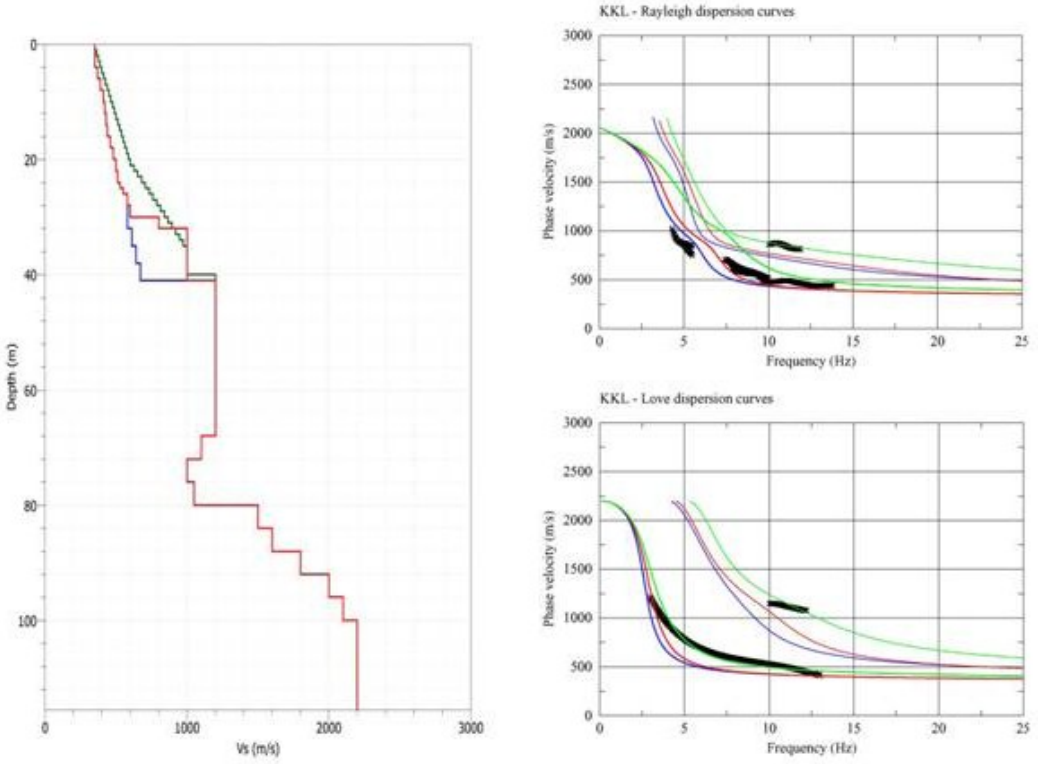

Figure I-5.3: Proposed velocity profiles and associated dispersion curves (Rayleigh and Love), as of 7. January 2010 (document "TN-290.05-3 - Profile NOK postWS" within "TP3-GTC-1010 Additional-Site-Invest-Data_KKL"). Green = DF, Blue = MK1, Red = MK2.

- The very shallow velocity (top 4 m) has been assigned a 400 m/s value as MASW dispersion curves do display high frequency (15 - 25 Hz) Rayleigh wave velocities larger than this value.
- The correction for anisotropy of cross-hole data has been slightly increased with respect the ratios taken into account in the document "TB-213-KG09003" (9. September) in the Wellenmergel, Wellendolomit and Buntsandstein units (according to anisotropy values reported in the document "KKL_Ratios_Anisotropy_100104").

Model L3 : "MK-2-20100119"

The last one is a "hybrid" one taking into account surface wave (AMV, MASW) and body wave (cross-hole, downhole) measurements. The basic idea was to use cross-hole data in the bedrock (i.e., from top Wellenmergel at 41 m depth, which cannot be sampled with much details with surface wave techniques), and to use surface wave data for the gravel layer.

- The bedrock model is the same as in the original "MKi" models proposed in September 2009 (i.e., with original anisotropy correction factors, document TB-213-KG09003)
- The surface gravel model is mainly adapted from the L1 model, with some velocity reduction at depth in the "cemented" part. The original will was to avoid the gradient increase in the deeper part of the gravel layer, in order to account for a "non-cemented"

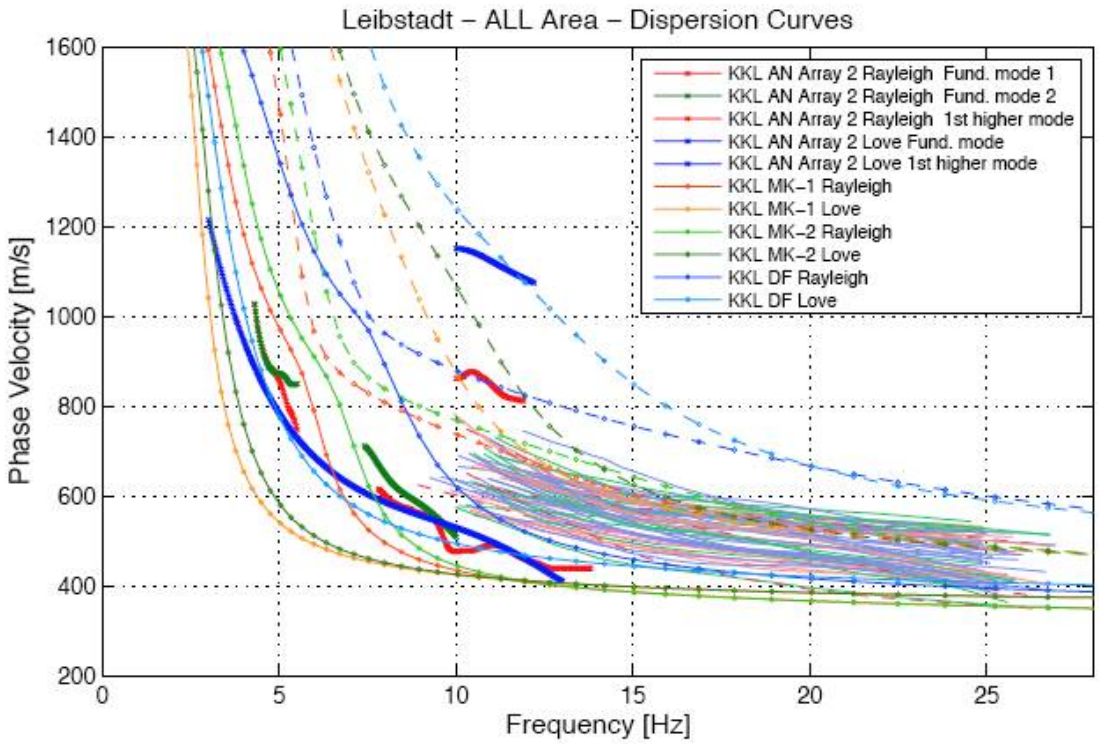

Figure I-5.4: Comparison of proposed profiles (early January 2010) with the available measured dispersion curves (document "kkl_DCs" within "TP3-GTC-1010 Additional-Site-Invest-Data_KKL").

gravel as in the original PEGASOS studies. However, there was no way to fulfill this will given the measured dispersion curves and fundamental frequencies.

5.1.4 Concluding Comments

The first two proposed models are based primarily on AMV and MASW data (L1="DF"), cross-hole data (L2= "MK2-Crosshole-Anisotropy", respectively; the third one is hybrid.

These models exhibit higher shallow velocities in the gravel and slightly reduced velocities in the non-crystalline rock, with respect to the previous ones: this is directly related with the improved match with DC at intermediate and high frequencies.

Finally, all three models consider large shear-wave velocities for the deep gravel (beyond 30 m): all attempts to have reduced velocity to mimic the absence of any cemented layer did not provide acceptable match with observed dispersion curves.

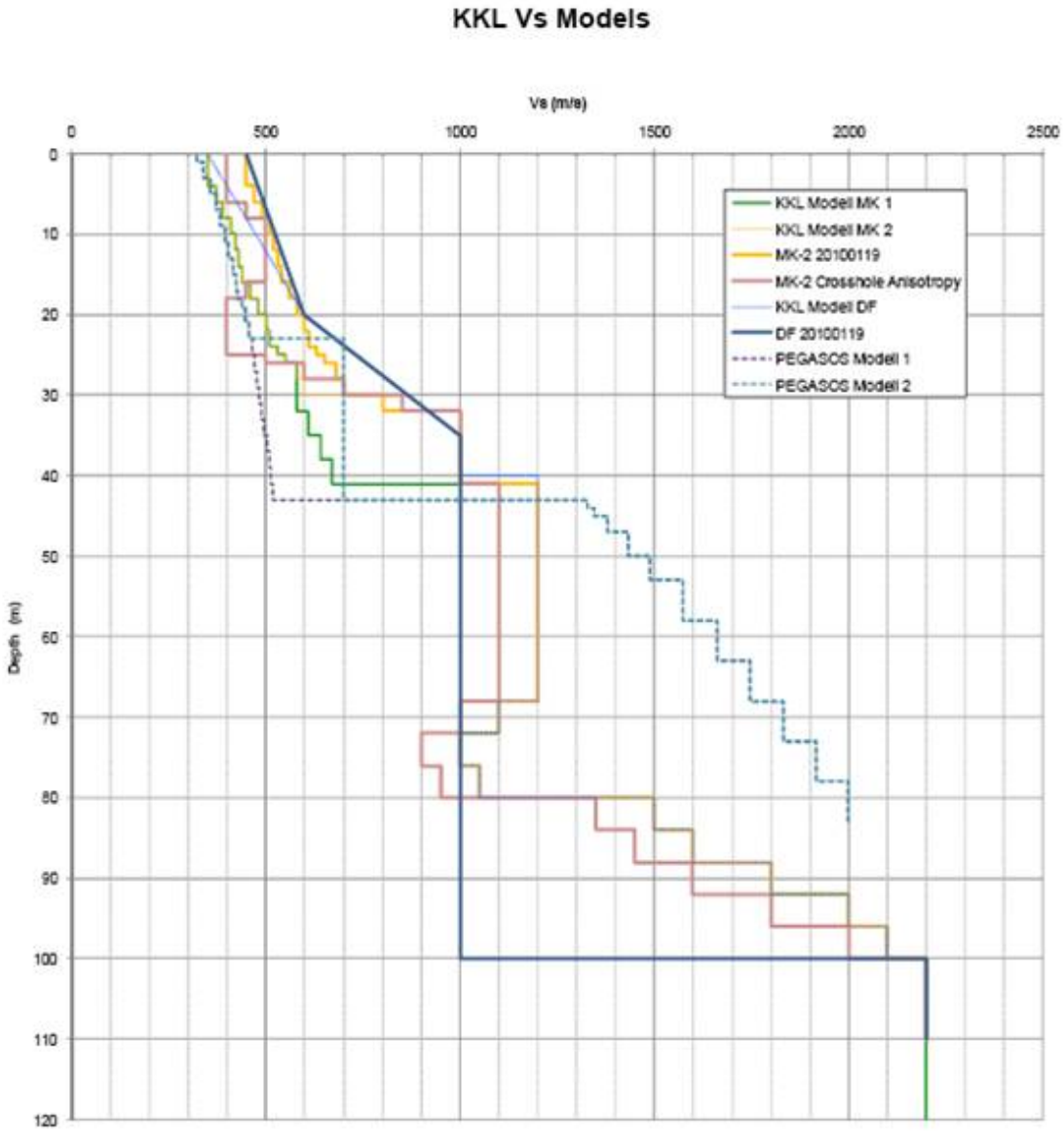

Figure I-5.5: Comparison of all the velocity profiles considered from November 2009 to January 2010 (from document " PRP_Soil_Models_Leibstadt", January 30, 2010).

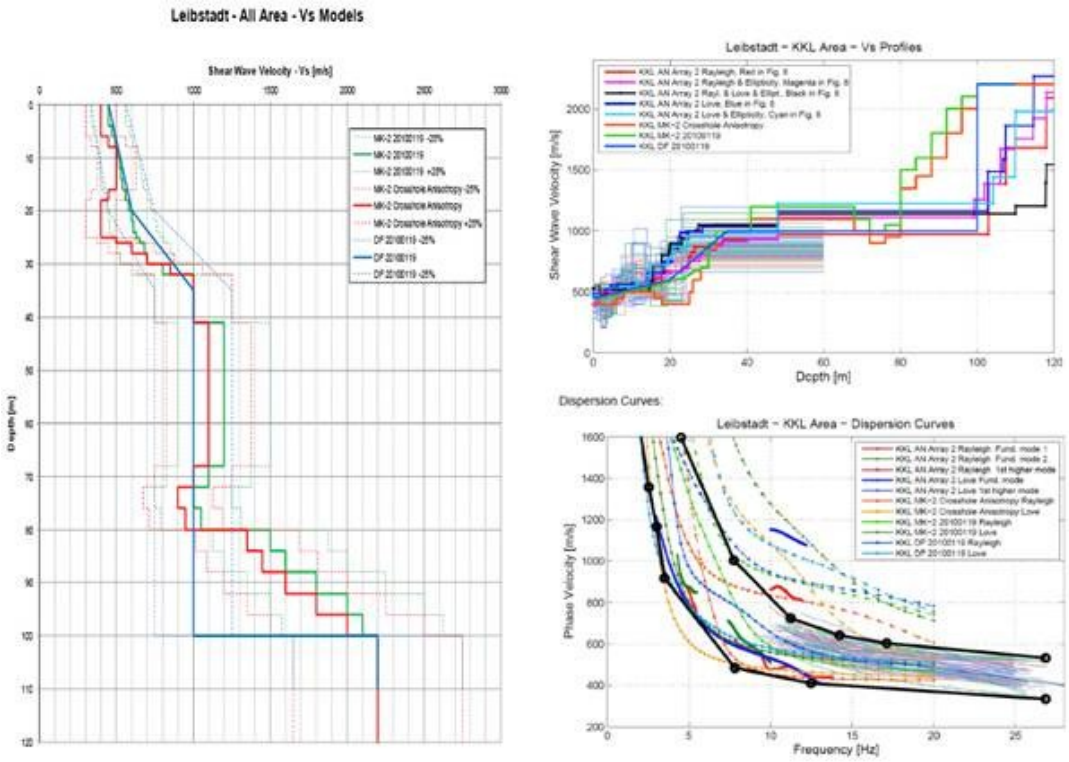

Figure I-5.6: Finally proposed velocity profiles and associated dispersion curves (Rayleigh and Love), as of January 20, 2010 (document "PRP_Soil_Models_Leibstadt", January 30, 2010).

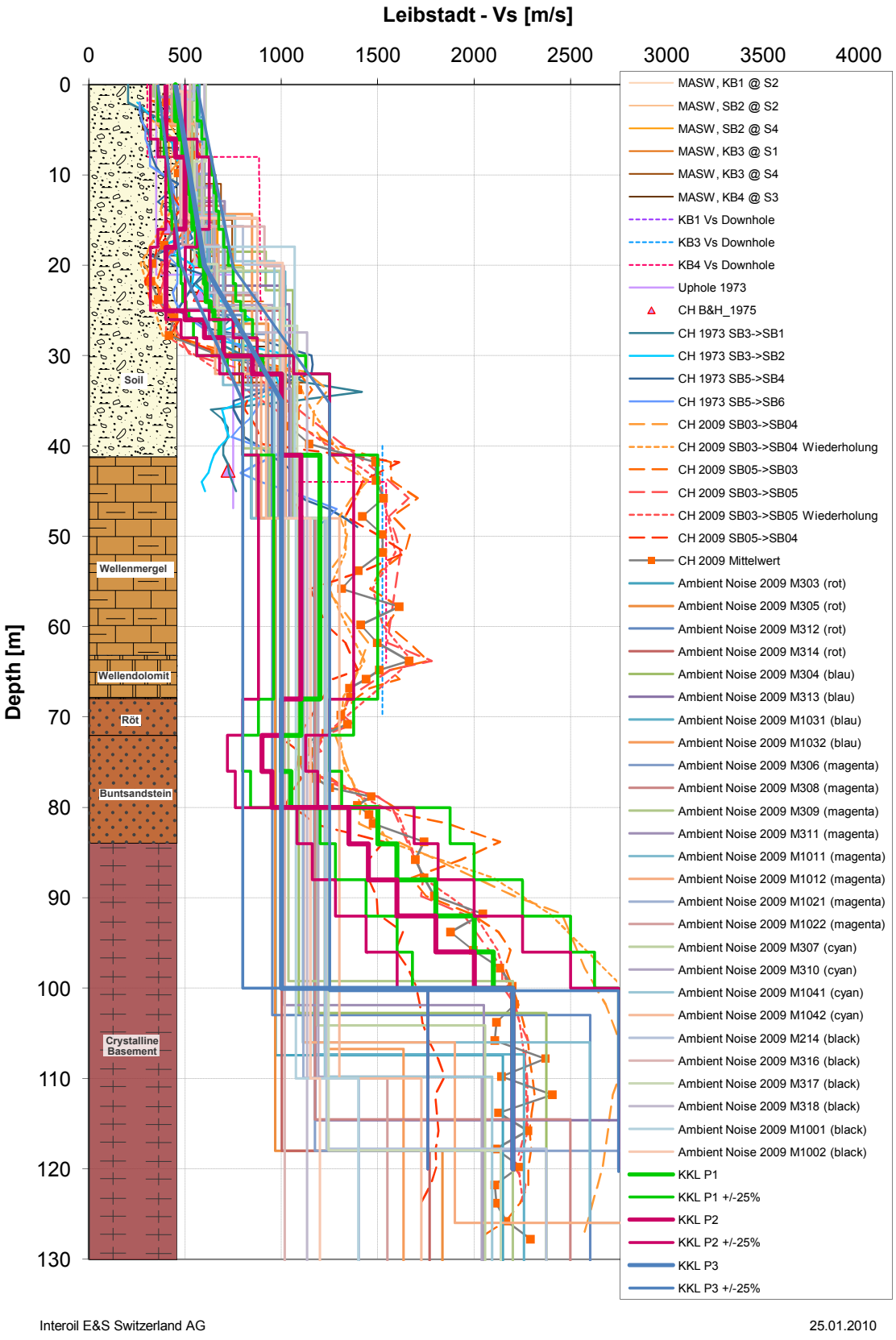

Figure I-5.7: V_S-profiles representative for the whole KKL area.

5.2 V_P-profile for Leibstadt

For this site, originally the V_P profile was derived from the model of D. Fäh for V_S (DF modified). At the meeting on 2. February 2010 it was decided to modify the proposed profile "DF modified": the new profile is steeper between 0 - 20 m and constant = 1000 m/s between 40 - 100 m. This resulted in an edge between 80 - 100 m for the V_P profile. Thus, it was decided to introduce a gradient between 80 - 100 m with V_P going from 2200 - 4000 m/s and then a jump to 4840 m/s. Therefore the ratio of V_P/V_S is no longer is equal to 2.2 for this site.

In the soil part the originally calculated V_P curve was moved to the left in order to better fit the experimental data because it was pointed out that the V_P profile was biased towards the upper side of the curves. This resulted in a proposition to have two gradients: 0 - 15 m with 800 - 1100 m/s and 15 - 26 m with 1100 - 1600 m/s.

Below the water table, the same procedure as for the other sites was used with a ratio K^S/G^S equal to 3.24 (Poisson's ratio of 0.36, corresponding to the value above the water table) and the parameters $\rho_S = 2.65$ t/m^3, $\rho = 2.2$ t/m^3 and $\rho_f = 1.0$ t/m^3, then $\varphi = 0.275$. The water bulk modulus was set equal to 1000 MPa at the water table surface (26 m) and to 1500 MPa at 34 m depth and kept constant below. The final computed V_P is depicted in the Figure I-5.8 with the measured data.

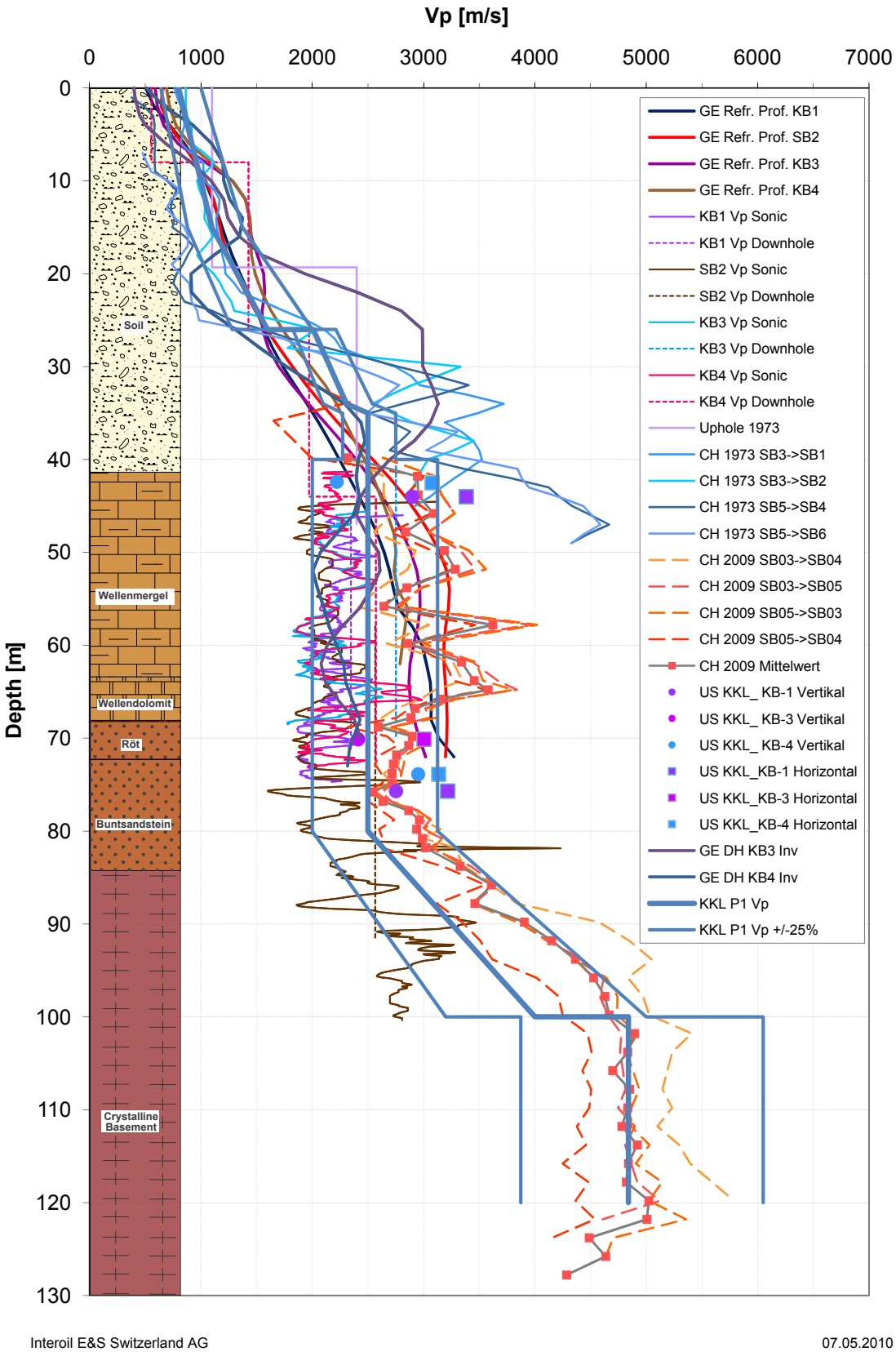

Figure I-5.8: V_P-profiles representative for the whole KKL area.

5.3 Material Models

5.3.1 General Comment

The selected models are based on first priority on tests results and on the results published by Rollins et al. [1998] and Menq [2003]. Menq's curve takes into account a dependence of $G/G-max$ on the confining stress while Rollins' curve does not. Furthermore, Menq's curve corresponds to a weaker material compared to Rollins.

Accordingly, examination of the $G/G-max$ curves shows that Menq's mean curve coincide with the lower bound of the tests data and Rollins mean to the upper bound. The mean curve is defined as the average between the lower bound and the upper bound curves.

As lower bound for the damping, Rollins mean damping curve was used, while Menq's mean curve was used for the upper bound. From the observations and from also theory, a stiffer material exhibits lower material damping and a softer material, higher material damping.

Those curves have been modified to a small extent to better fit the observed data.

5.3.2 Model for the Leibstadt Site

For Leibstadt, due to the thickness of the soil layer, two different sets of curves are introduced. The first set corresponds to the top 10 m which is associated with an uncemented soil stratum. The second set corresponds to the bottom part which includes some cemented lenses.

For the upper layer the same procedure as for the other sites is used and is mainly based on the GSD2 data (Dresden) while for the lower layer the curves are mainly selected to fit the data of material GSD5 (ETH). This last layer is a stiffer material compared to the top layer and has the largest range of values to fit the tests results, which may reflect its partial cementation.

For the damping curves, in the upper layer the same procedure as for the other sites was used; in the bottom layer the damping curves were adjusted to yield a smaller damping at low strain levels (stiffer materials) and the same damping as the upper layer at large strains, when the cementation is broken.

The proposed shear modulus and damping reflects the nearly nonlinear behavior of stiff rock material.

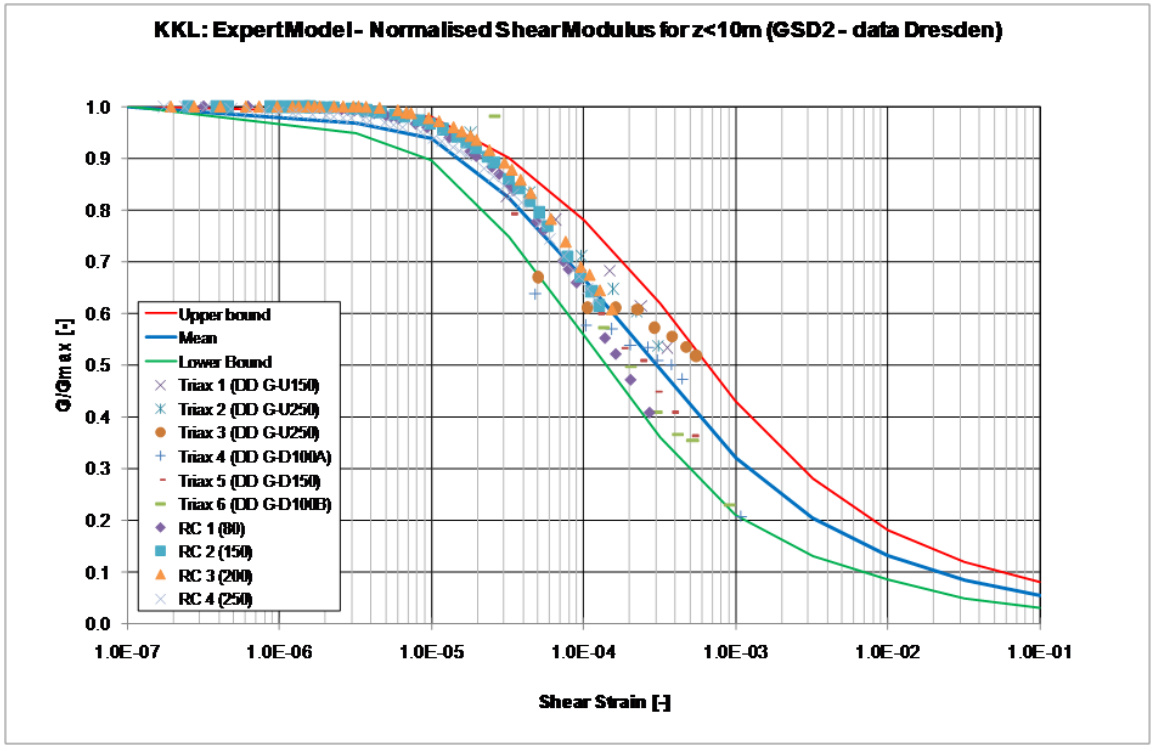

Figure I-5.9: Shear Modulus for $0 < z < 10$ m (KKL).

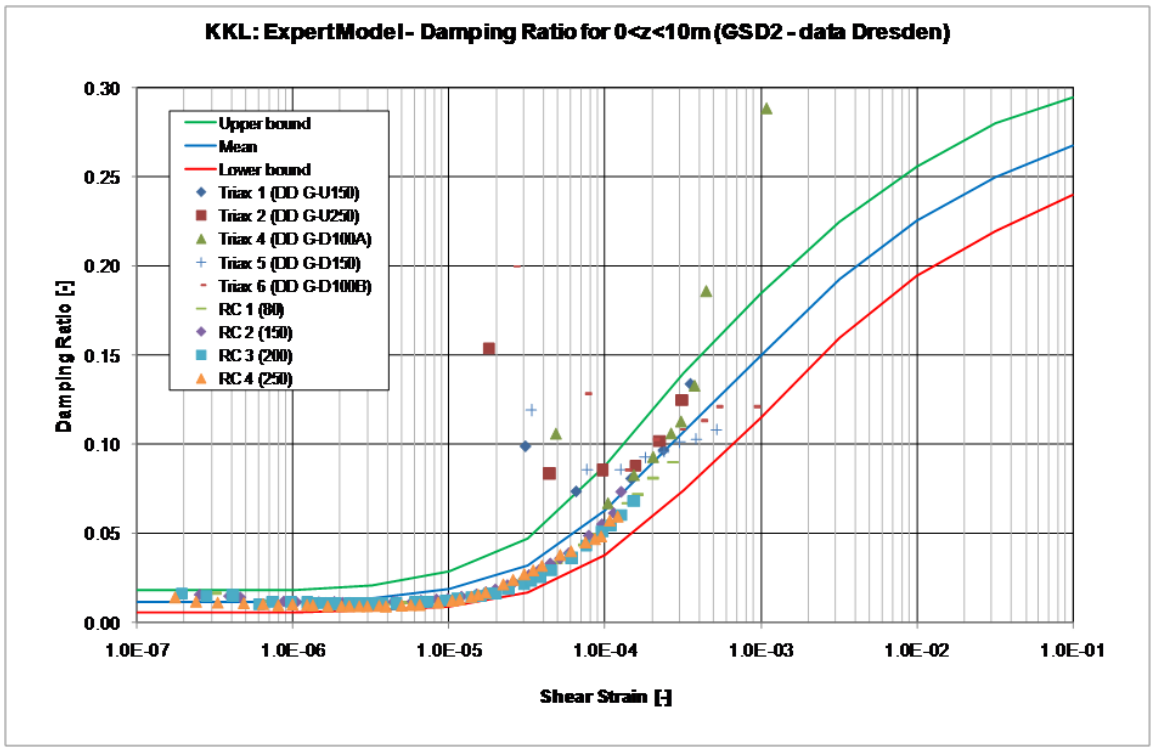

Figure I-5.10: Damping Ratio for $0 < z < 10$ m (KKL).

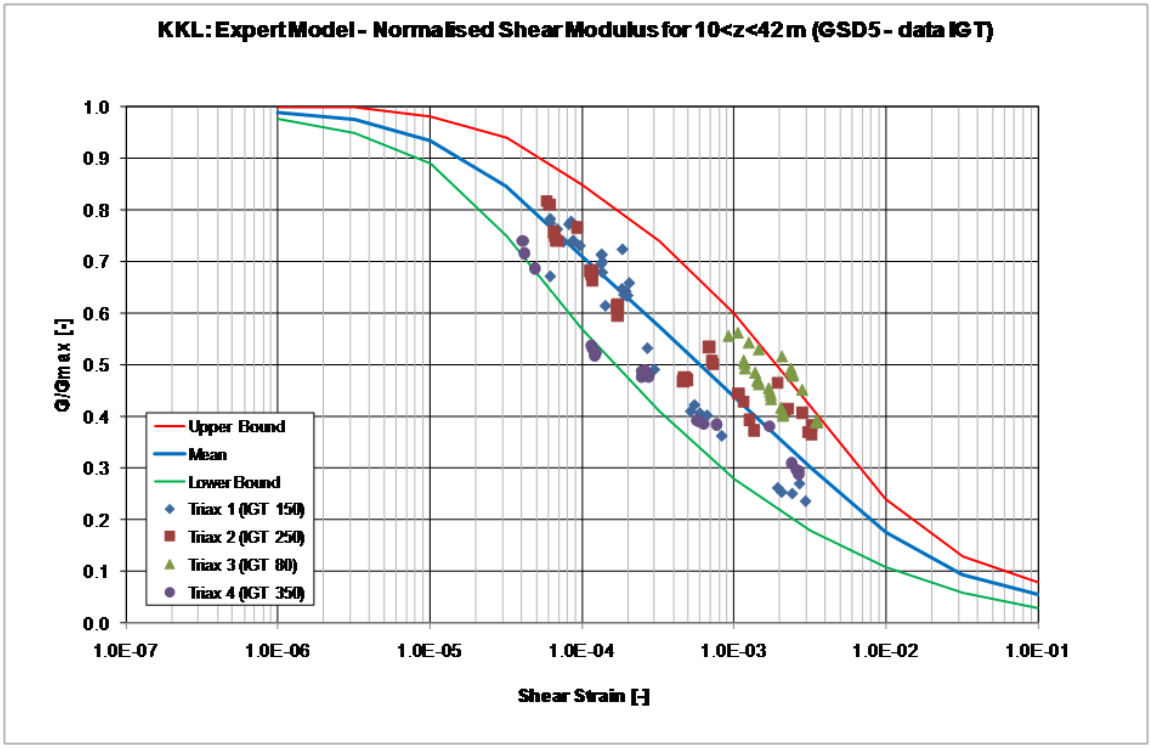

Figure I-5.11: Shear Modulus for $10 < z < 42$ m (KKL).

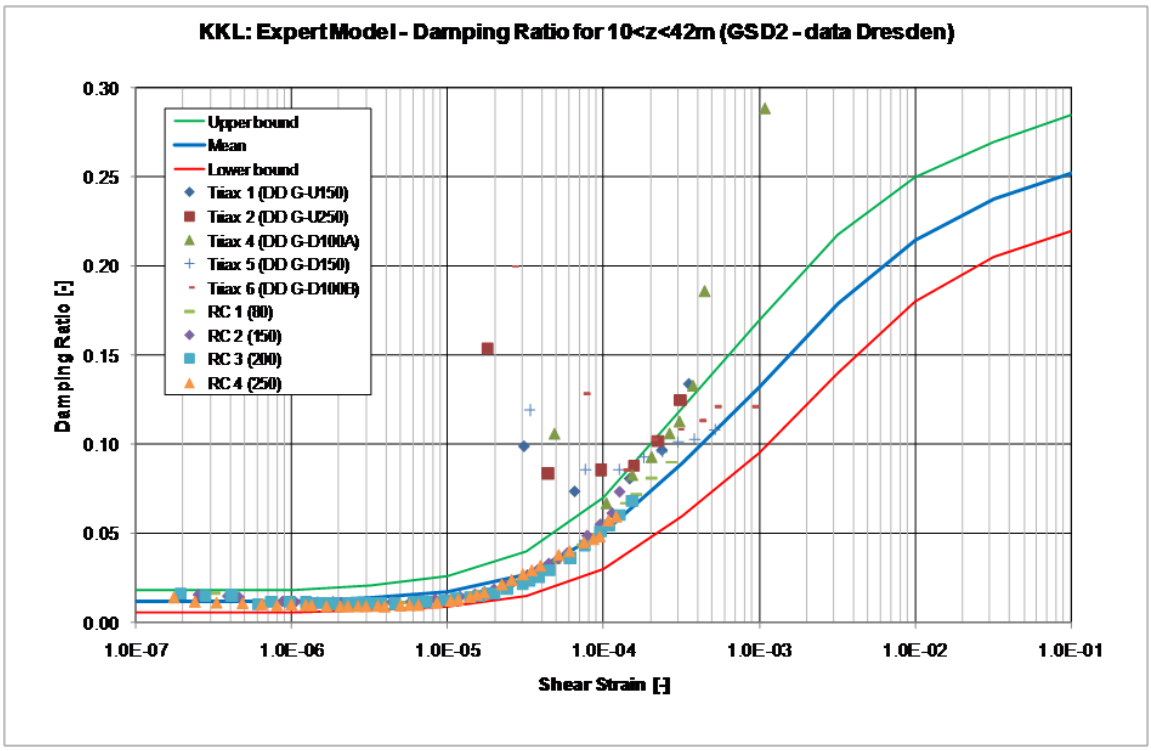

Figure I-5.12: Damping Ratio for $10 < z < 42$ m (KKL).

5.4 Supporting figures for Leibstadt

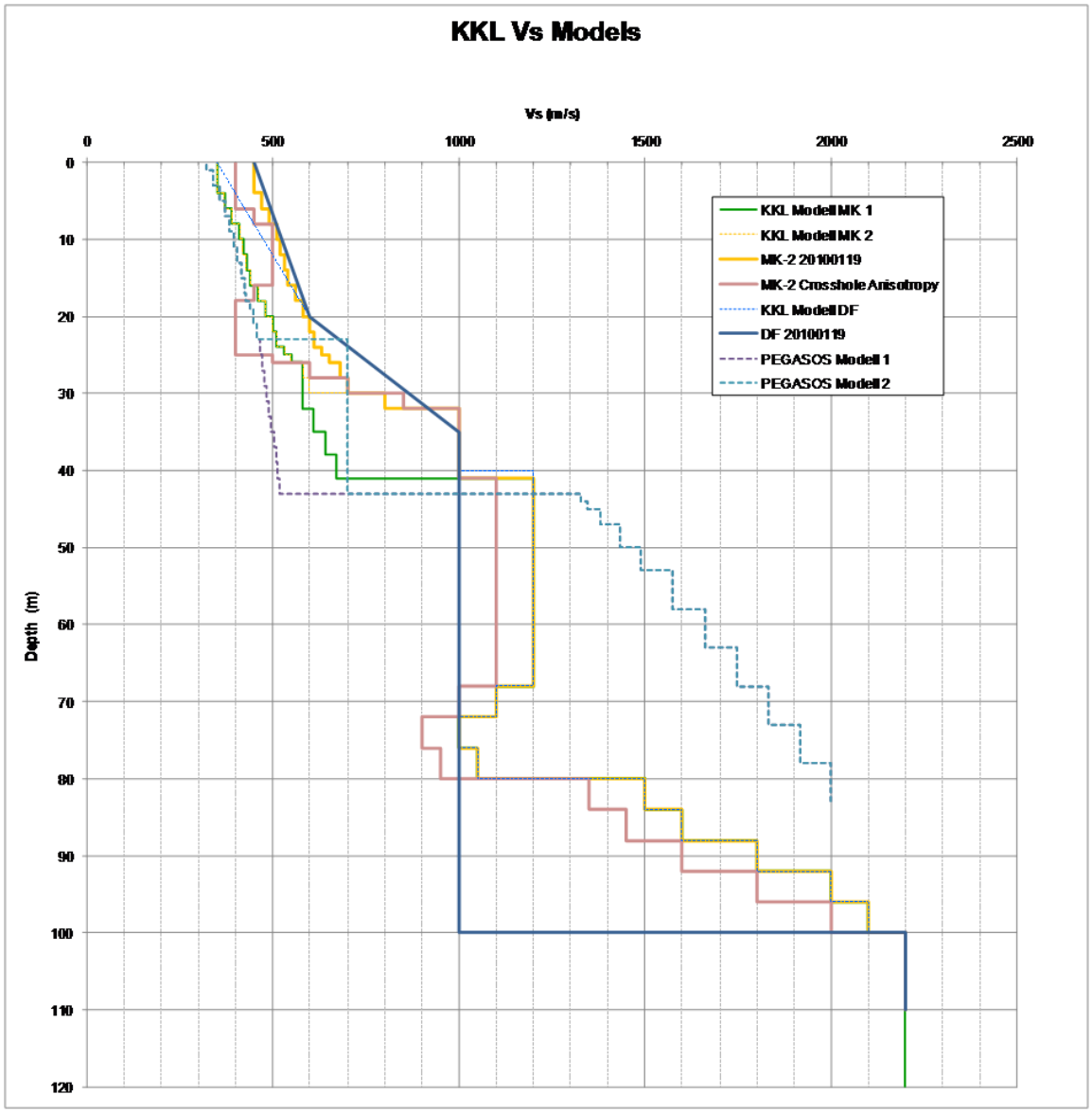

Figure I-5.13: V_S-profiles evaluated by the experts during previous meetings compared to the PEGASOS profiles (KKL).

Table I-5.1: Fundamental frequencies, Leibstadt site.

Profile	Frequency
P1 (MK-2 20100119)	3.40 Hz
P2 (MK-2 Crosshole Ani.)	2.92 Hz
P3 (DF 20100119)	2.27 Hz

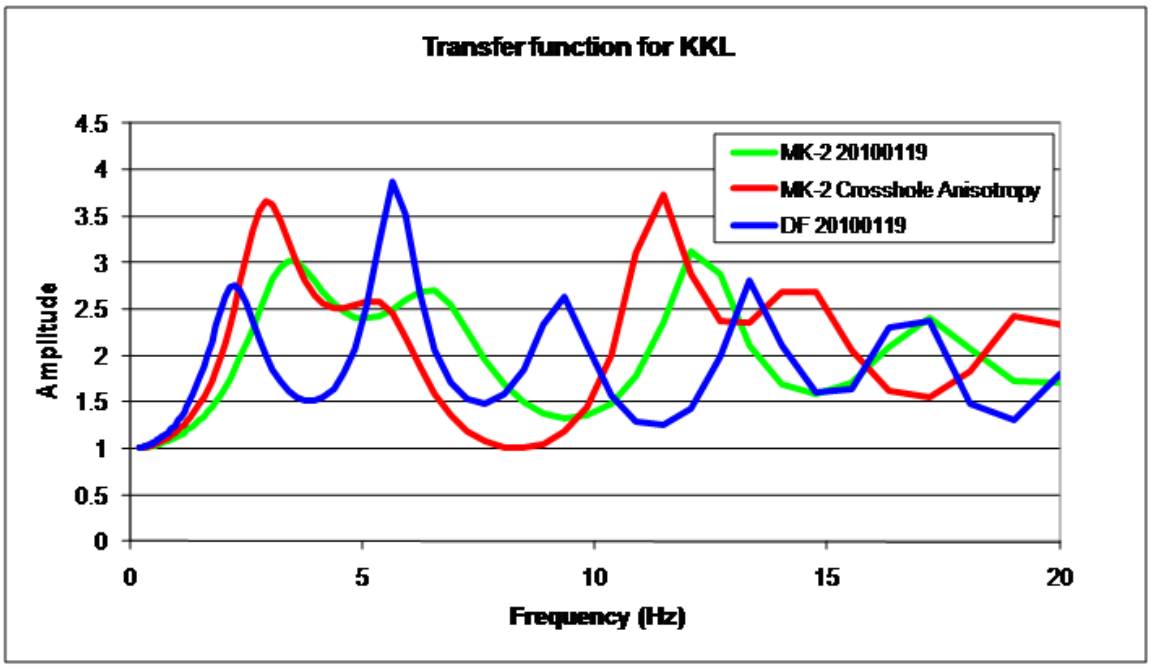

Figure I-5.14: Transfer functions for proposed soil profiles (KKL).

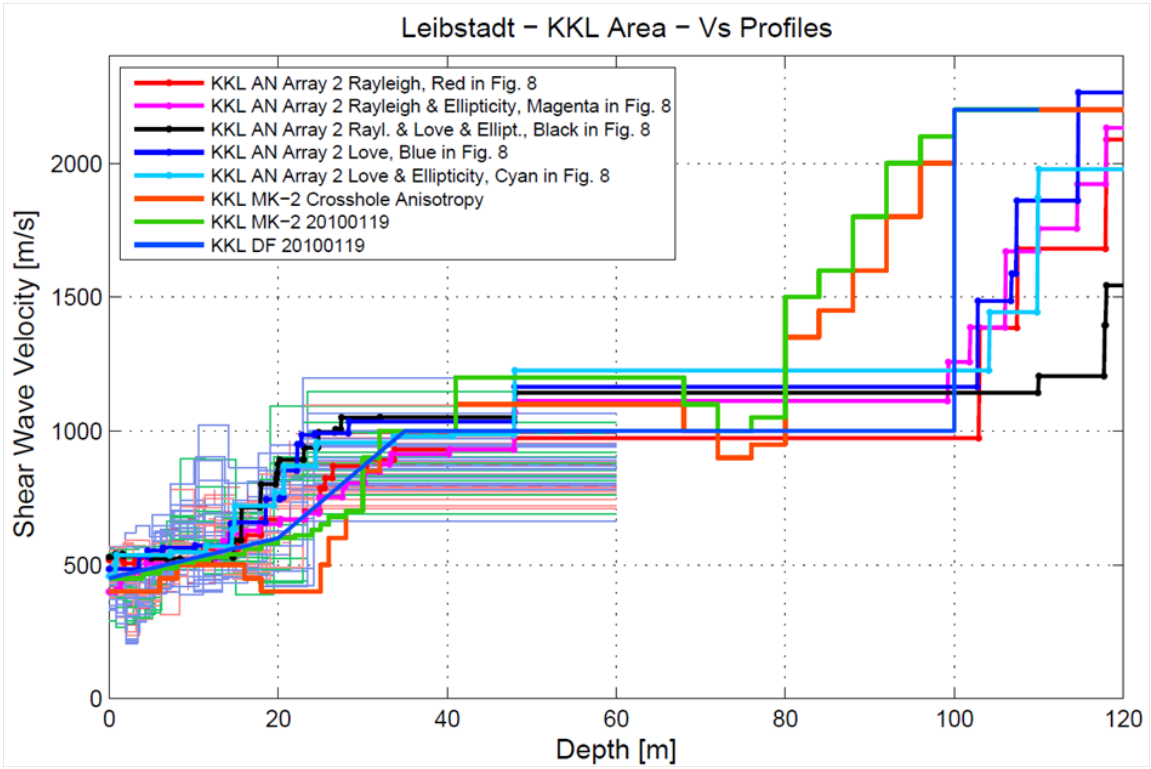

Figure I-5.15: V_S-Profiles (KKL).

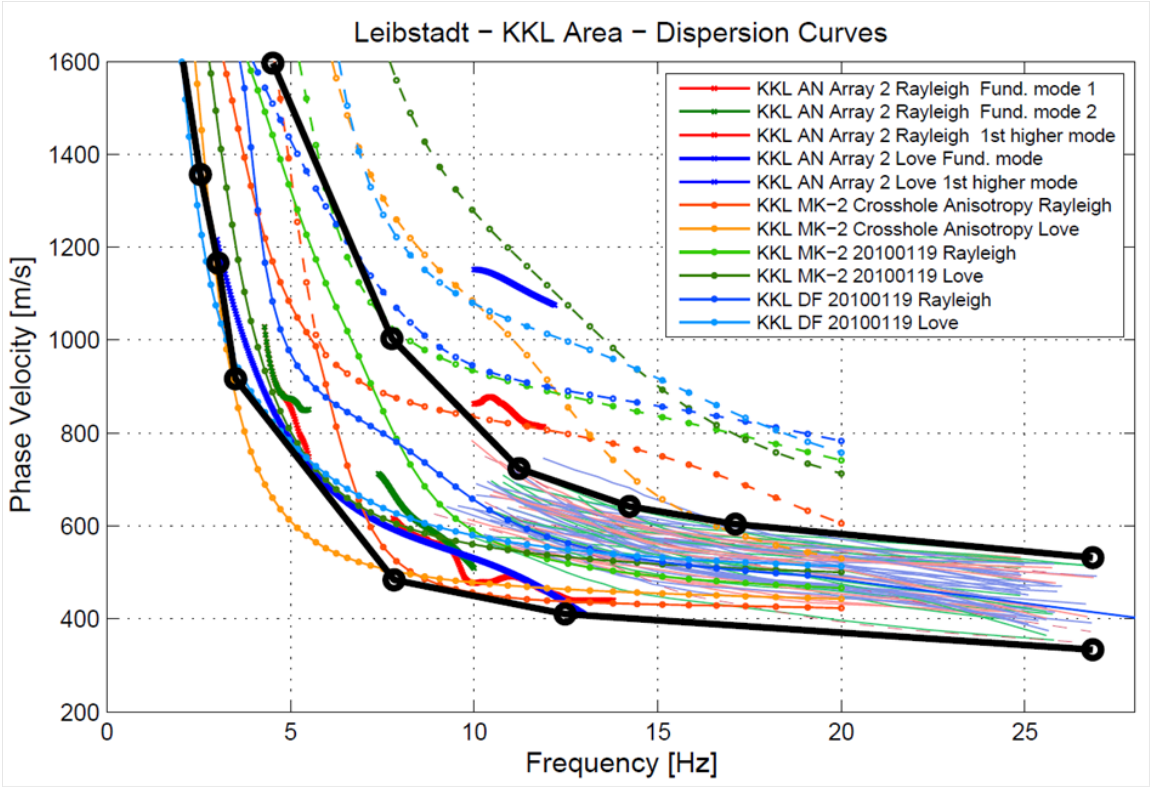

Figure I-5.16: Dispersion curves and bounds (KKL).

5.5 Comparison of PEGASOS vs. PRP Profiles and Material Models

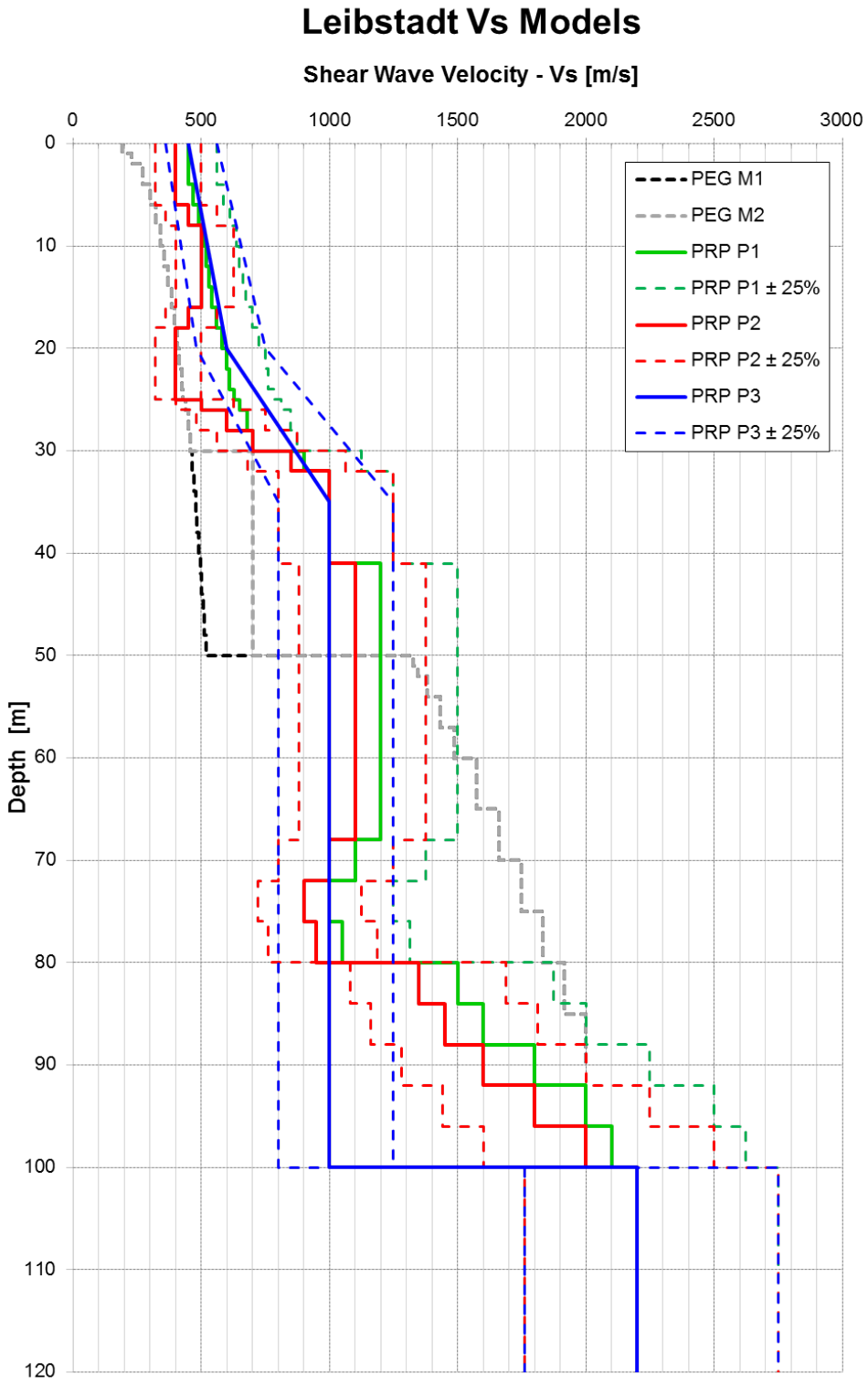

Figure I-5.17: Comparison of PEGASOS and PRP V_S-models for Leibstadt.

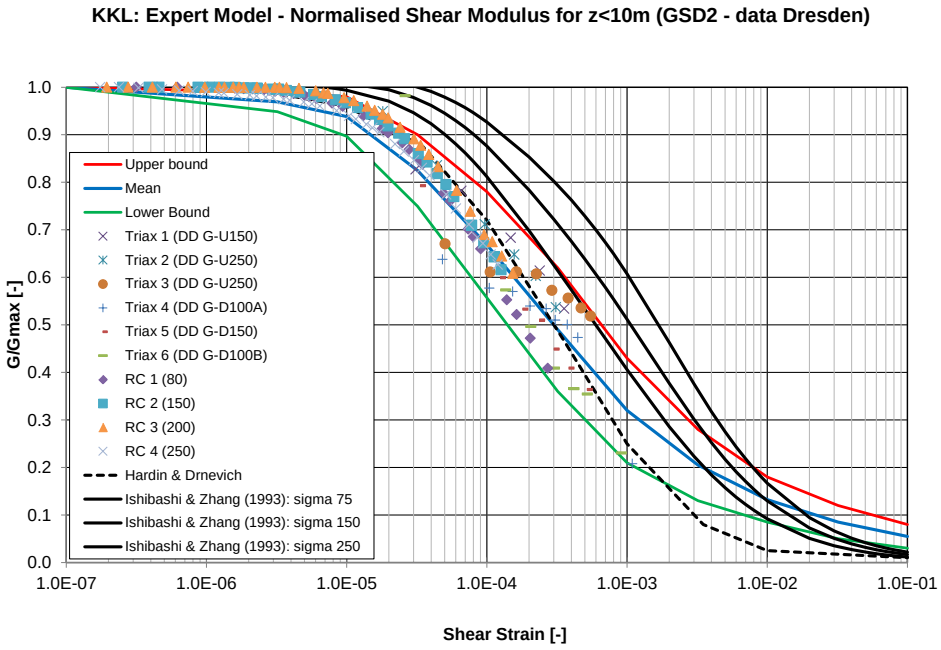

Figure I-5.18: Leibstadt - Shear modulus curves for gravel, $z < 10$ m.

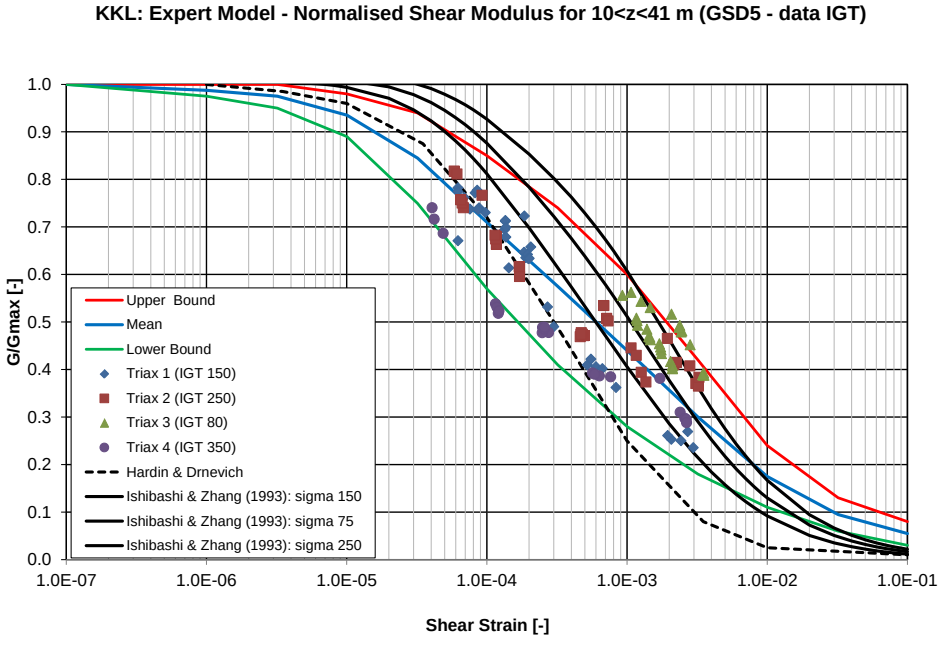

Figure I-5.19: Leibstadt - Shear modulus curves for gravel, $10 < z < 41$ m.

Chapter 6

Proposed Velocity Profiles for KKM Site

This chapter explains the rationale behind the suggestion of three additional velocity profiles for the Mühleberg site.

6.1 Initially Proposed Velocity Profile and Comments

The "composite" velocity profile proposed by AMEC is the result of a weighting of the different measurements and/or sources of information; The weights are different for the surface (gravel) layer, for which the largest weight is given to surface wave measurements (MASW and microtremor) and SPT values, and the underlying molasse for which borehole data (downhole and cross-hole) are given the predominant weights.

The corresponding velocity profile can thus be considered some kind of "average" profile. The corresponding dispersion curve falls indeed within the measured dispersion curves both at high and intermediate frequencies (Fig. I-6.2).

6.1.1 Alternative Velocity Profiles

The idea behind the selection of additional velocity profiles is to include most of the variability actually seen from the various in-situ measurements and/or their various interpretations by different teams, and which cannot be accounted for simply by considering the AMEC one plus or minus some percentage. During the SP3 meeting on 19. October 2009, it was decided to look for two additional profiles A1 and A2 (in addition to the AMEC one), with the following background ideas:

- Profile A1
  - Use MASW dispersion curve above 10 Hz.
  - Account for the fundamental frequency from H/V about 6 Hz (to be confirmed).
  - Expect higher soil velocity and weathered soil layer (the SPT values led to rather low shear-wave velocity values).

- Profile A2
  - Expect a velocity gradient in the molasse down to 50 to 60 m without a pronounced 6 Hz resonance.

A corresponding work was performed in early January 2010, which led to highly varying profiles because of a large variability within MASW results. It was thus decided to redo a similar work taking into account the dispersion curves at lower frequencies as derived from ambient vibration array measurements. In the following a summary of this additional work is provided. The surface wave dispersion curves obtained from MASW and array microtremor measurements do exhibit indeed a very significant variability over the site. The slowest MASW curves correspond to the westernmost measurements (line M2), while the fastest correspond to the easternmost one (EKKM, named as "M3 line" in the following): M1 line yield somewhat intermediate values. The two ambient vibration array measurements ("AMV" were performed close to the westernmost (M2) and easternmost (EKKM) MASW measurements. MASW and AMV dispersion curves are consistent at M2, and inconsistent at EKKM, while AMV measurements provide comparable DC – with low high frequency velocities – at the two sites: Plotting AMV and MASW dispersion curves on the same plot for EKKM (see attached pdf document) suggests that MASW curves to the east could possibly be interpreted as corresponding to the first higher Rayleigh mode.

As a consequence, in order to derive alternative velocity profiles, the SP3 experts proceeded as follows:

- All the measured dispersion curves from MASW and AMV were taken into account.
- Since no uncertainty was assigned to the MASW DC measurements, they were grouped in three sets corresponding to M1, M2 and M3 locations/lines (see Figure I-6.3), and the geometrical average and standard deviation were computed for each set.
- The different sets of DC curves (combining MASW and AMV measurements) were then inverted with the Geopsy software (which makes use of the neighborhood algorithm) with the following constraints:
  - The thickness of the surface (gravel) layer was forced to range between 8 and 10 m, as indicated by all in-situ borings and the resulting iso-thickness map
  - The velocity values within the gravel was forced:
    - to be larger than 180 m/s (a value which indeed was considered as very low by some experts),
    - to follow a linear increase with depth.
  - The velocity profile within the underlying Molasse was forced:
    - to include a weathered part on its top having a linear gradient over a thickness smaller than 50 m,
    - to reach a constant value at large depth, constrained to be within 1000 and 1200 m/s (values indicated by the borehole measurements, and corresponding to the deepest layer in AMEC profile),

    - not to exhibit any velocity jump between the bottom of the weathered part, and the top of the "non-weathered", constant velocity, deep Molasse.
- The fundamental frequency was constrained between 5 and 9 Hz.

Six sets of dispersion curves were inverted with these constraints (see Figure I-6.4):

- The combination of AMV at KKM site and MASW at M2 line (western part).
- The same ane the MASW curves at M1 line, considered as first higher mode of Rayleigh waves.
- AMV curves at EKKM site, considered as fundamental mode of Rayleigh waves for two distinct frequency ranges: 7 - 10 Hz and 15 - 20 Hz (the strange shape of the whole DC curve over the range 9.5 - 15 Hz was interpreted as related to mode jumps, an assumption which is consistent with the completely different values derived from MASW measurements at M3 line).
- The same and the MASW curves at M3 line, considered as first higher mode of Rayleigh waves.
- The MASW results at M1 line, considered as fundamental mode of Rayleigh wave.
- The MASW results at M3 line, considered as fundamental mode of Rayleigh wave.

The results of each of these inversions are displayed in the Figures I-6.5 to I-6.10, respectively, with a comparative summary in Figure I-6.11. In each case, the results consist in a family of velocity profiles, corresponding to different misfit values (the misfit is characterized by the squared difference between the average of measured DC value and the Rayleigh wave velocity of the considered velocity profile, normalized by the standard deviation of measurements, and summed over the whole frequency range(s) where measured DC are considered reliable). The misfit is simply color-coded, as shown in each figure, and the corresponding DC and ellipticity (H/V) curves are also displayed with the same color code.

Several common items can be concluded from these results:

- In every case, the "optimum" thickness is slightly larger than 8 m, in very good agreement with borehole data.
- The velocity values within the gravel layer are rather well constrained by the high frequency DC values. They however are very sensitive to the interpretation of MASW data.
    - They are rather low for the first four cases where AMV and MASW M2 curves are interpreted as fundamental mode of Rayleigh waves, and M1 and M3 MASW curves as first higher mode.
    - They are significantly higher for the last two cases where M1 and M3 MASW data are interpreted as fundamental mode of Rayleigh wave.
- The velocity profile within the Molasse in much less constrained. However, there is clear trend for a thicker and/or softer weathered part for the last two cases (eastern part, thickness around 35 - 40 m, velocity just beneath the gravel layer around 500 - 600 m/s. For the first 4 cases, the existence of a weathered part is not mandatory

to explain the data, and in any case, the velocity just beneath the gravel layer exceeds 700 m/s

For each case, the "optimum" profile, i.e. the one with the lowest misfit has been extracted: it should be considered only as representative of a family of acceptable profiles. The corresponding values are listed in Table I-6.1.

Table I-6.1: Representative models for each inversion case.

	Case	**1**	**2**	**3**	**4**	**5**	**6**
	Unit	**KKM-AMV**	**KKM- AMV**	**EKKM_AMV**	**EKKM_AMV**	**M1fund**	**M3fund**
	Unit	**+ M2fund**	**+ M2fund +M1first**	**(fund)**	**+ M3first**		
Gravel layer:							
	Thickness [m]	8.26	8.01	8.03	8.75	8.13	8.37
	Gradient	186 + 6.57 z	182 + 7.1 z	183 + 10.24 z	194 + 11.2 z	186 + 22.7 z	352 + 8.7 z
	Bottom velocity [m/s]	237	236	260	286	361	421
Molasse:							
	Thickness [m]	31	52	1	37	36	33
	Gradient	888 + 4.9 z	1034 + 0.7 z	754 + 36 z	768 + 6. z	389 + 15.2 z	352 + 19.6 z
	Top velocity [m/s]	929	1039	1043	821	513	516
	Bottom velocity [m/s]	1085	1076	1082	1052	1075	1178

Based on these results, the two following velocity profiles listed in Table I-6.2 are proposed, and displayed in Figures I-6.12 and I-6.13, respectively :

- M_DCmin : a low-velocity gravel over an only weakly weathered molasse
- M_DCmax : a high velocity gravel layer overlying a significantly weathered molasse

Table I-6.2: Proposed additional velocity models (February 2010).

	Profile	M_DCmin	M_DCmax
Gravel layer:	Thickness [m]	8	8
	Gradient	186 + 8 z	260 + 15 z
	Bottom velocity [m/s]	250	380
Upper Molasse:	Thickness [m]	30	35
	Gradient	910 + 5 z	369 + 17 z
	Top velocity [m/s]	950	505
	Bottom velocity [m/s]	1100	1100
Lower molasse:	**Velocity [m/s]**	1100	1100

6.1.2 Additional Fourth Model

The obtained DC for the DC_min model still correspond to slightly higher phase velocities than those observed with the ambient vibration array at KKM, as illustrated in Figure I-6.2. It was thus decided during the SP3 meeting of 5. March 2010, to look for a fourth model closer to the lower bound of western dispersion curves (KKM-AMV and M2). An preliminary inversion was performed "live" on 5. March from a "hand-digitized" DC curve close to the lower bound. The model parameterization was designed to allow weathered parts in the upper Molasse, with the possibility of different gradients (i;e. several layers in the upper Molasse). In order to derive a model which could be acceptable as a "best-estimate" one - and not simply as a lower bound, we thus decided to perform a new inversion, simply for the westernmost site corresponding to the slowest phase velocities, relaxing the constraints of no jump at the base of the weathered Molasse layer. The remaining constraints are the following:

- The thickness of the surface (gravel) layer was forced to range between 8 and 10 m, as indicated by all in-situ borings and the resulting iso-thickness map.
- The velocity values within the gravel was forced:
  - to be larger than 180 m/s (a value which indeed was considered as very low by some experts),
  - to follow a linear increase with depth.
- The velocity profile within the underlying Molasse was forced:
  - to include a weathered part on its top having a linear gradient over a thickness smaller than 50 m,
  - to reach a constant value at large depth, constrained to be within 1000 and 1200 m/s (values indicated by the borehole measurements, and corresponding to the deepest layer in AMEC profile).
- The fundamental frequency was constrained between 5 and 9 Hz.

With these constraints, a new model family was obtained, as illustrated in Figure I-6.14. From this, three tentative velocity profiles were tested for the fourth model, which are listed in Table I-6.3:

- The gravel layer is 8 to 10 m thick and its velocity is lower and exhibits a lower gradient – to match the M2 MASW results.
- The weathered molasse extends down to 32 m and has a linearly increasing velocity from 650 m/s to about 785 m/s at depth.

The corresponding dispersion profiles, dispersion curves and ellipticity are displayed in Figure I-6.15, and compared with the actual measurements on the westernmost area (KKM-AMV and M2). The "blue" model (M_P4_1) is still faster than the measurements and was therefore rejected. Yellow (M_P4_2) and red (M_P4_3) models are equivalent in the intermediate frequency range, but the "yellow" one is slightly faster at high frequencies. As a consequence,

Table I-6.3: Tentative velocity profiles for the fourth model.

	Profile	M_P4_1	M_P4_2	M_P4_3
Gravel layer:	Thickness [m]	8	10	**8.5**
	Gradient	200 + 5 z	200 + 5 z	**180 + 5 z**
	Bottom velocity [m/s]	240	250	**222.5**
Upper Molasse:	Thickness [m]	23.5	30	**35**
	Gradient	602 + 6 z	602 + 6 z	**602 + 6 z**
	Top velocity [m/s]	650	662	**653**
	Bottom velocity [m/s]	794	794	**794**
Lower molasse:	Velocity [m/s]	1100	1100	**1100**

the final model to be proposed as the fourth model is the "M_P4_3" model. An overall comparison of the four velocity models and the corresponding four dispersion curves is displayed in Figure I-6.16.

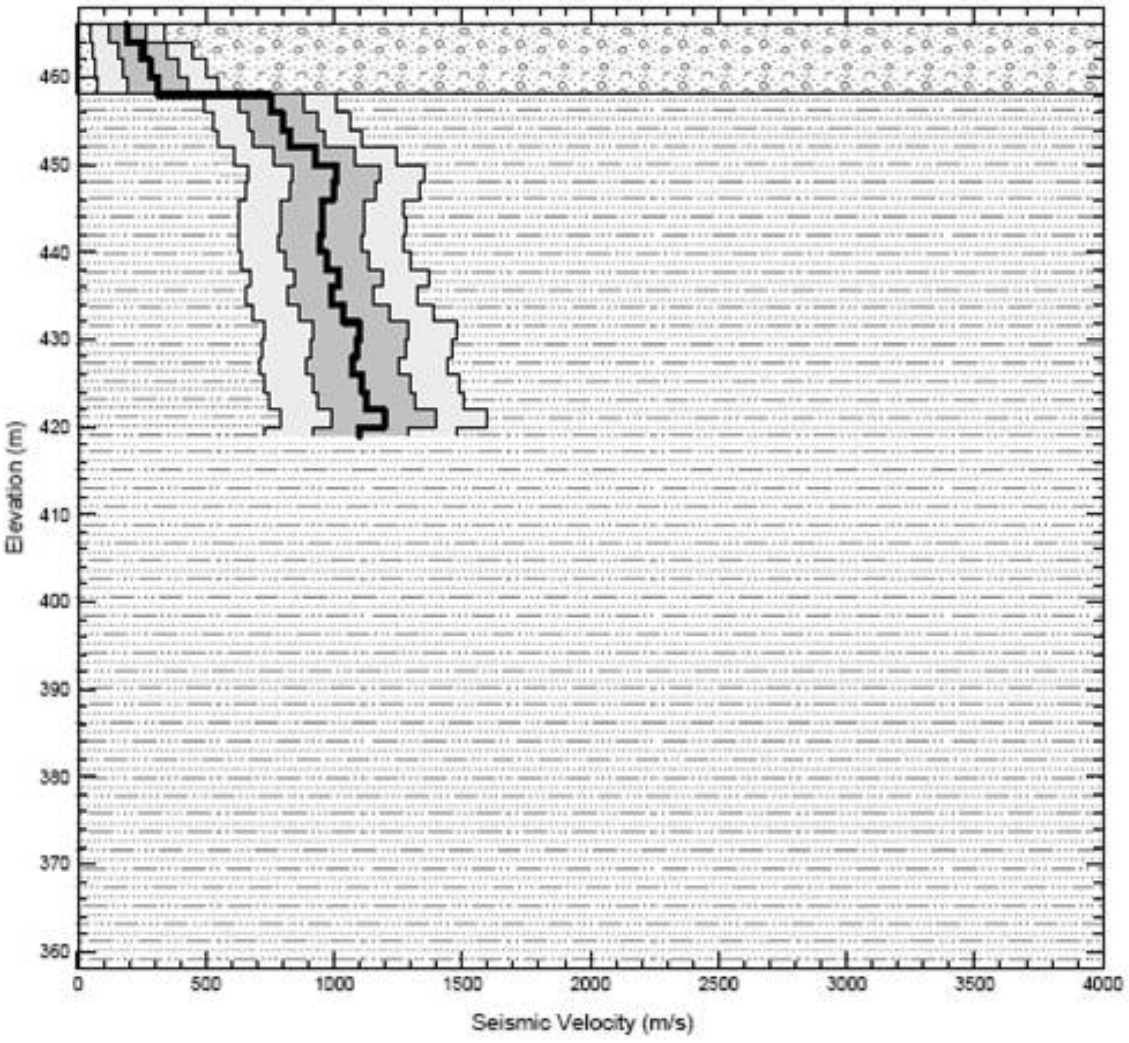

Figure I-6.1: AMEC velocity profile.

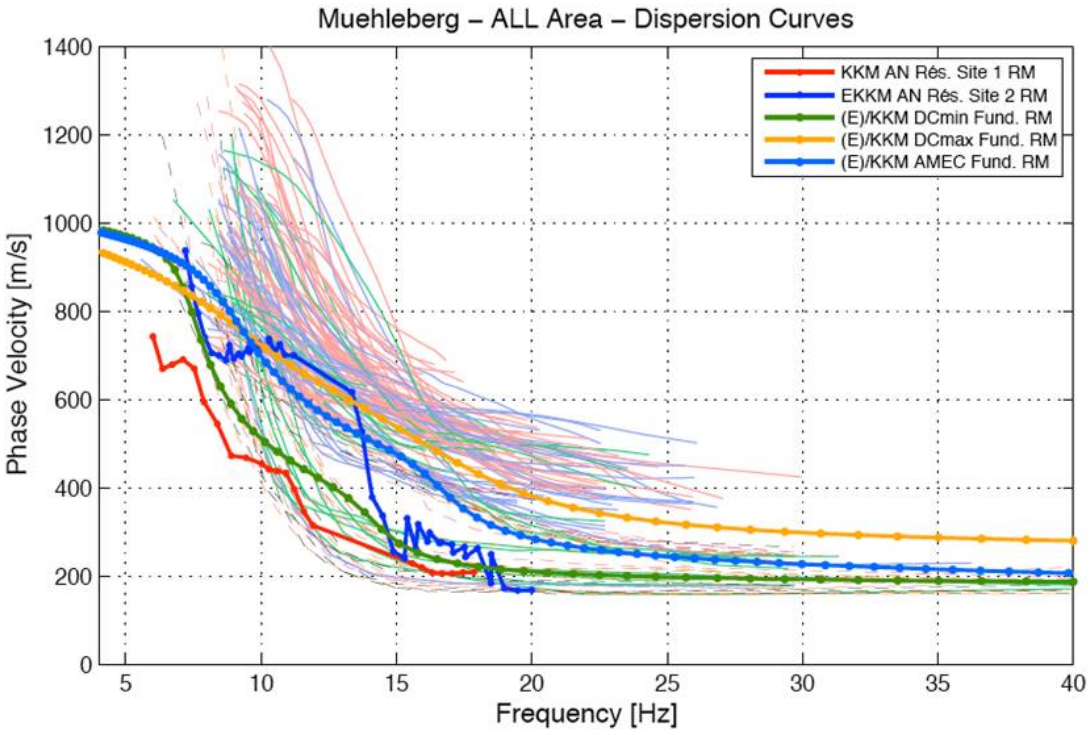

Figure I-6.2: Comparison of the dispersion corresponding to the AMEC velocity profile curve with measured ones (AMV and MASW) (From TP3-TN-1071 Soil_Models_Mühleberg V2.pdf).

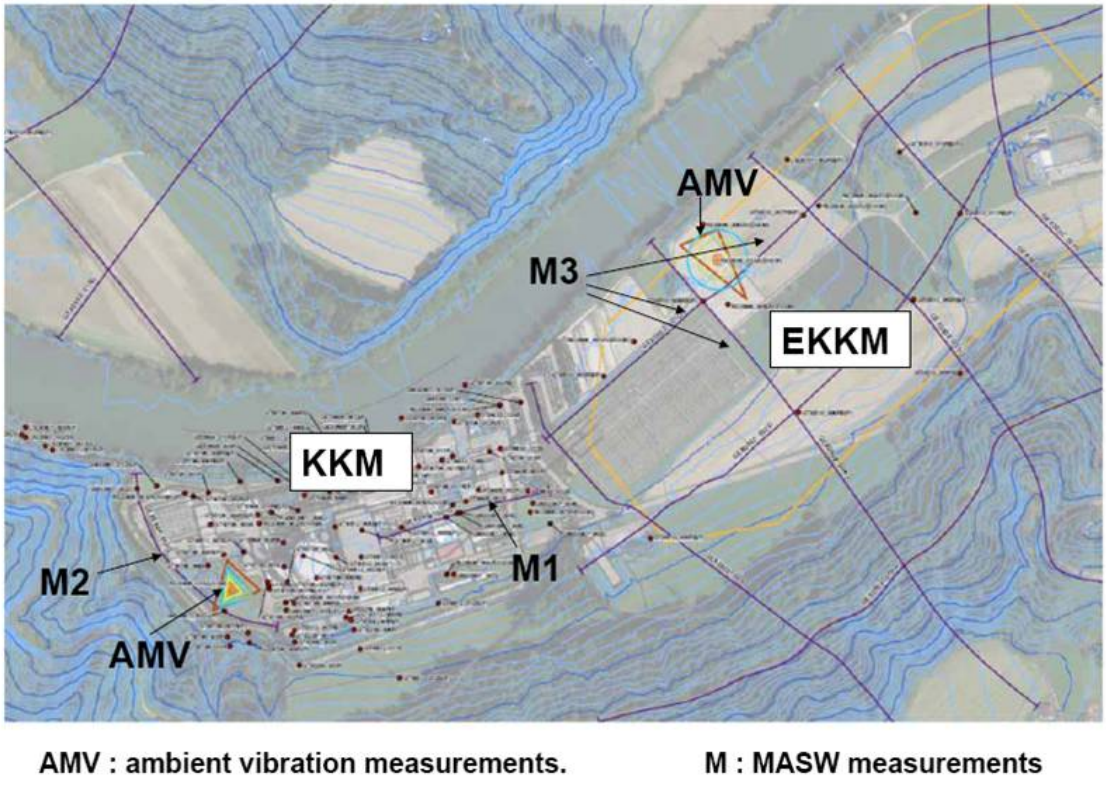

Figure I-6.3: Location of used AMV and MASW measurements.

Performed inversions

1. AMV_KKM + M2 (fund)
2. AMV_KKM + M2 (fund) + M1 (first)
3. AMV_EKKM
4. AMV_EKKM + M3 (first)
5. M1 (fund)
6. M3 (fund)

Constraints

- 1 linear gradient (180 < Vs < 1000 m/s)
- Interface between 8 and 10 m
- 1 linear gradient, Vs_bottom = Vs_½space
- ½ half space, (1000 < Vs < 1200 m/s)
- F0 between 5 and 9 Hz

Figure I-6.4: Overview of the performed constrained inversions.

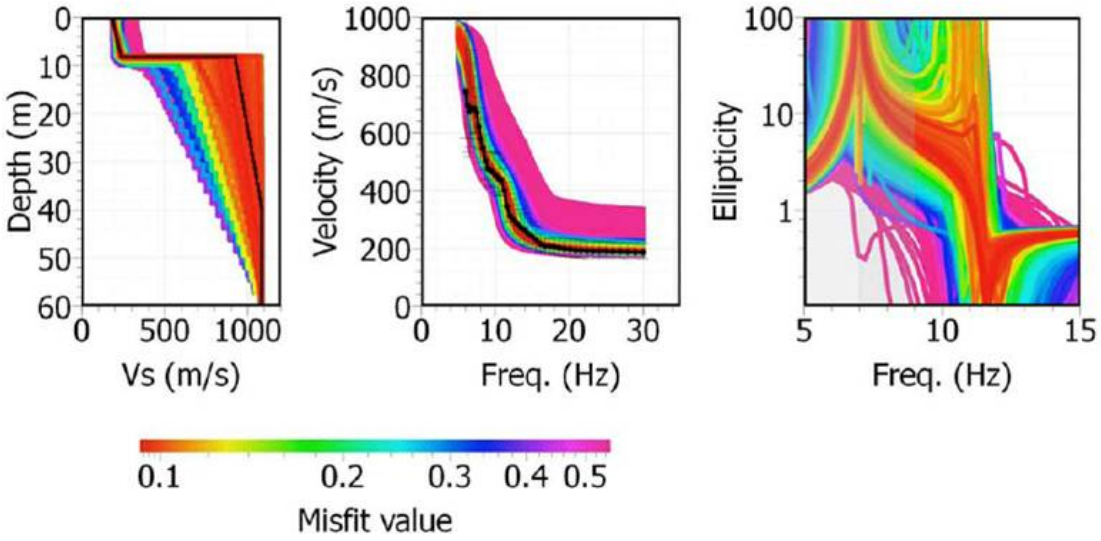

Figure I-6.5: Inversion results for the 1st case (AMV_KKM + M2fund). From left to right : S-wave velocity profiles, corresponding dispersion curves (fundamental mode) of Rayleigh waves and ellipticity curves. The color of curves corresponds to the misfit values according to the color code displayed on bottom. The black curve with vertical bars in the DC plot corresponds to the input data from ambient vibrations and MASW. The velocity profile considered in Table I-6.1 is the black one in the left plot.

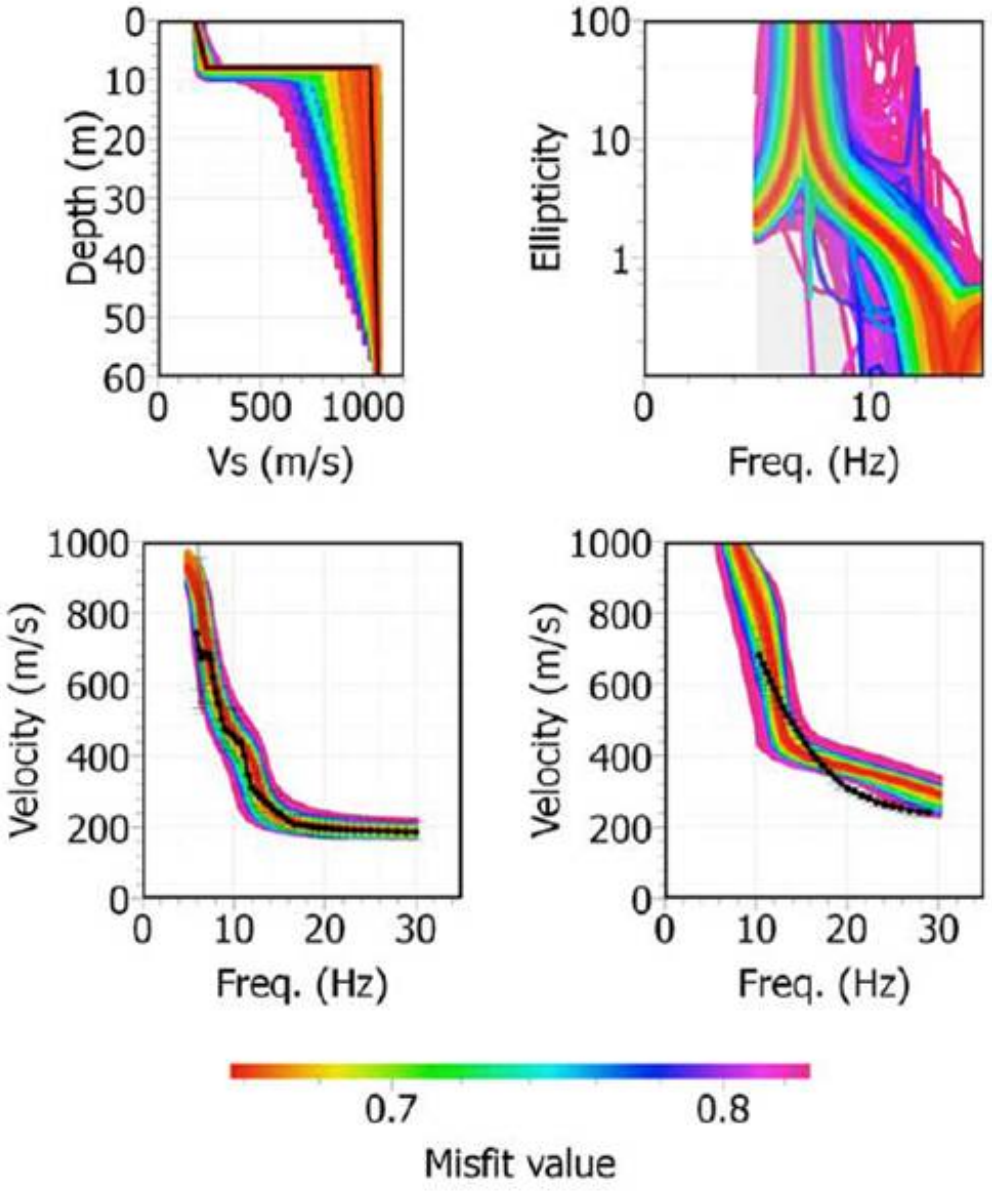

Figure I-6.6: Inversion results for the 2nd case (AMV_KKM + M2fund + M1first). Top left: S-wave velocity profiles; Top right: ellipticity curves; Bottom: dispersion curves for the fundamental (left) and first higher (right) modes of Rayleigh waves. See Figure I-6.5 caption for other explanations.

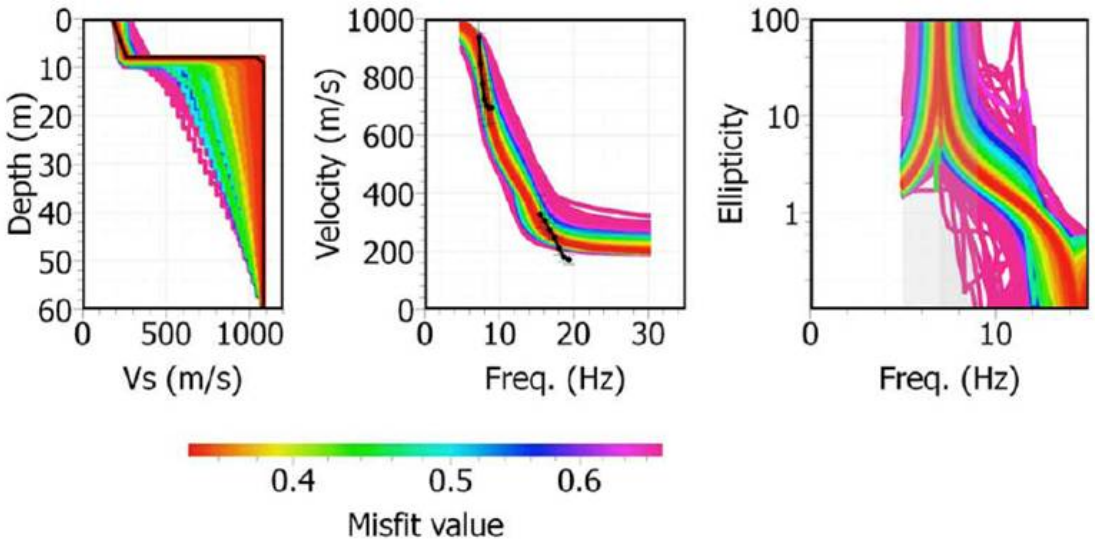

Figure I-6.7: Inversion results for the 3rd case (AMV_EKKM). From left to right: S-wave velocity profiles, corresponding dispersion curves (fundamental mode) of Rayleigh waves and ellipticity curves. See Figure I-6.5 caption for other explanations.

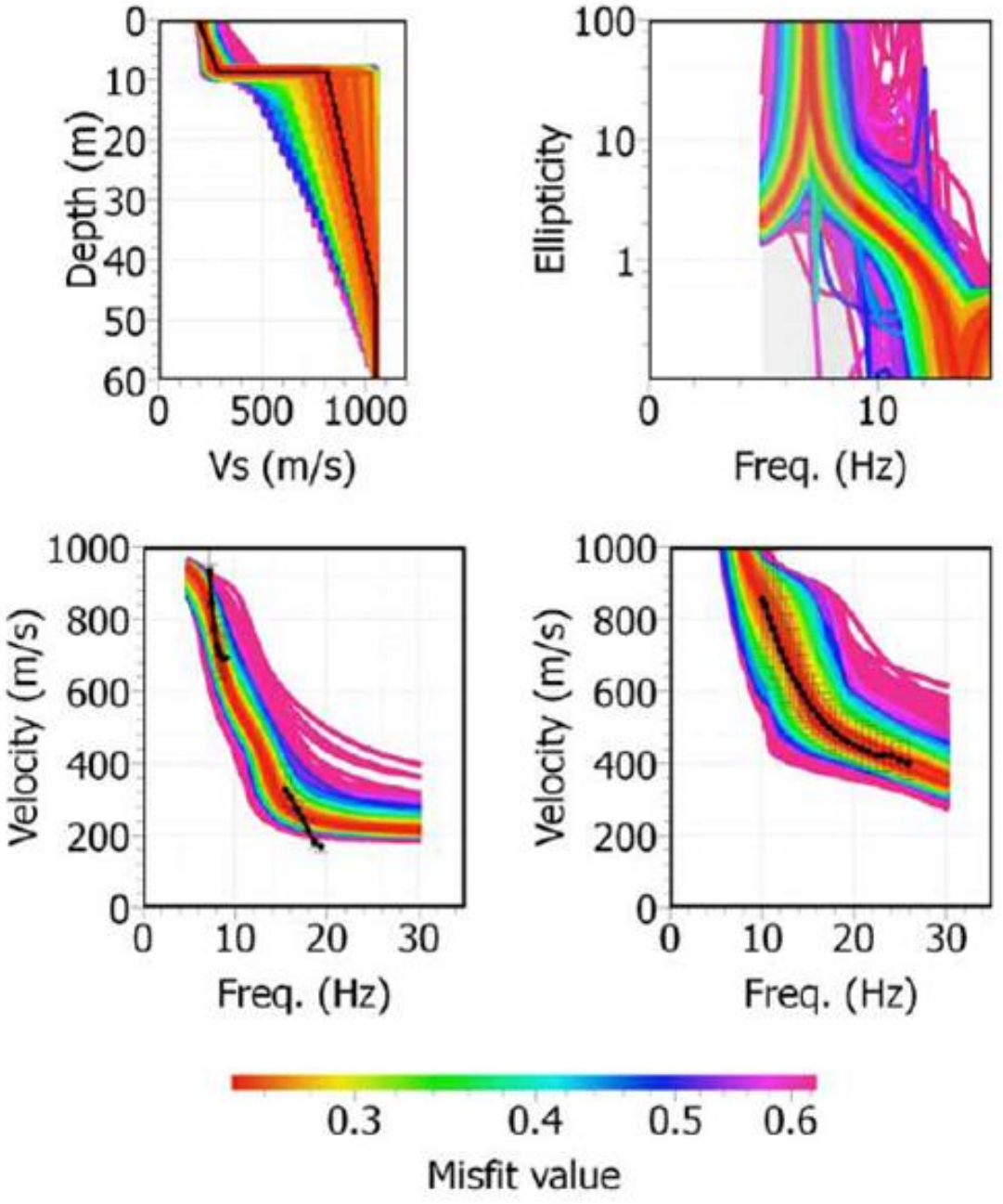

Figure I-6.8: Inversion results for the 4th case (AMV_EKKM + M3first). Top left: S-wave velocity profiles; Top right: ellipticity curves; Bottom: dispersion curves for the fundamental (left) and first higher (right) modes of Rayleigh waves. See Figure I-6.5 caption for other explanations.

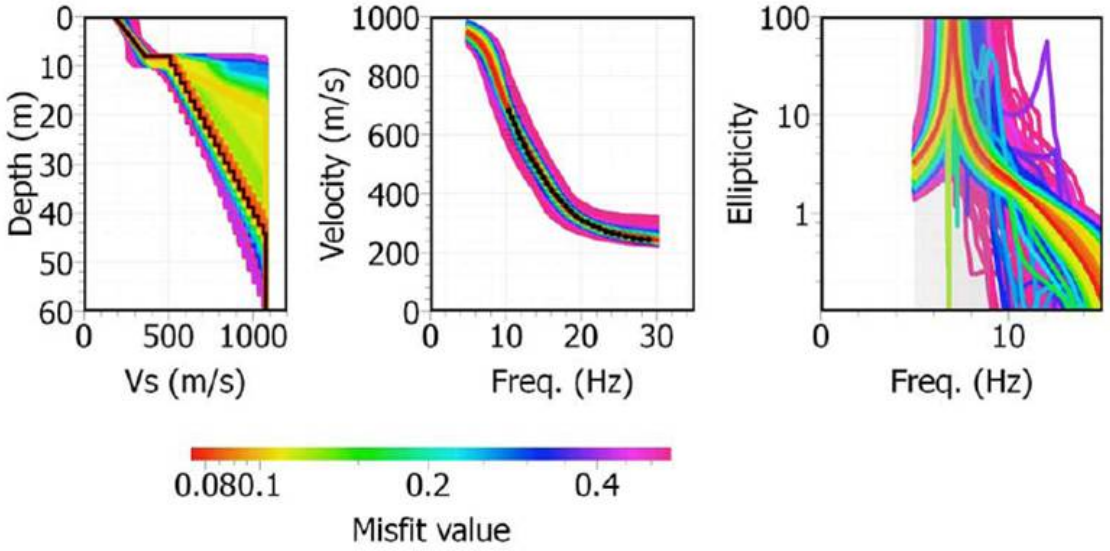

Figure I-6.9: Inversion results for the 5th case (MASW_M1fund). From left to right: S-wave velocity profiles, corresponding dispersion curves (fundamental mode) of Rayleigh waves and ellipticity curves. See Figure I-6.5 caption for other explanations.

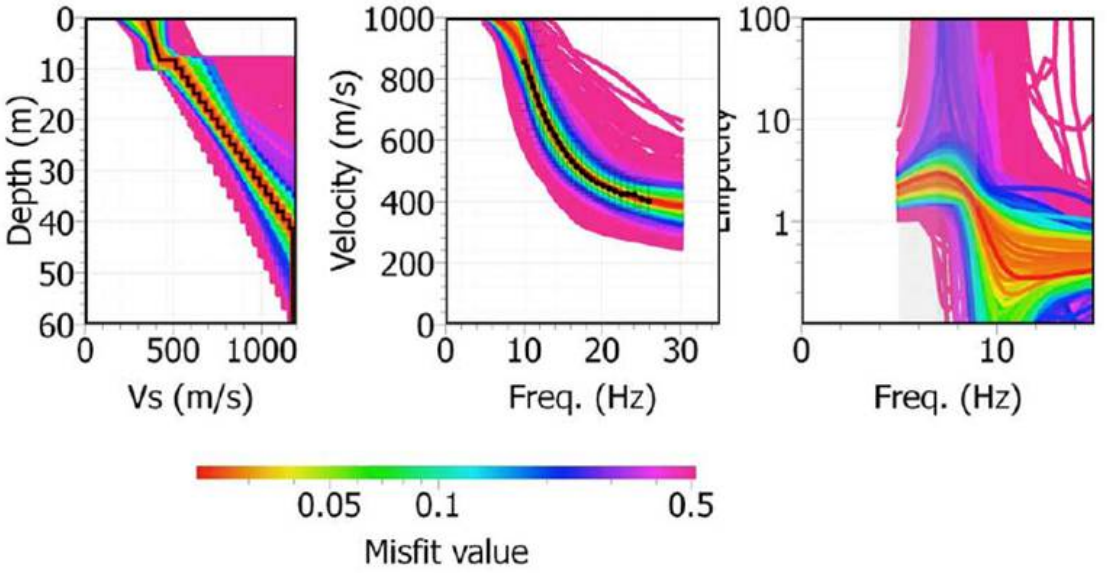

Figure I-6.10: Inversion results for the 6th case (MASW_M3fund). From left to right: S-wave velocity profiles, corresponding dispersion curves (fundamental mode) of Rayleigh waves and ellipticity curves. See Figure I-6.5 caption for other explanations.

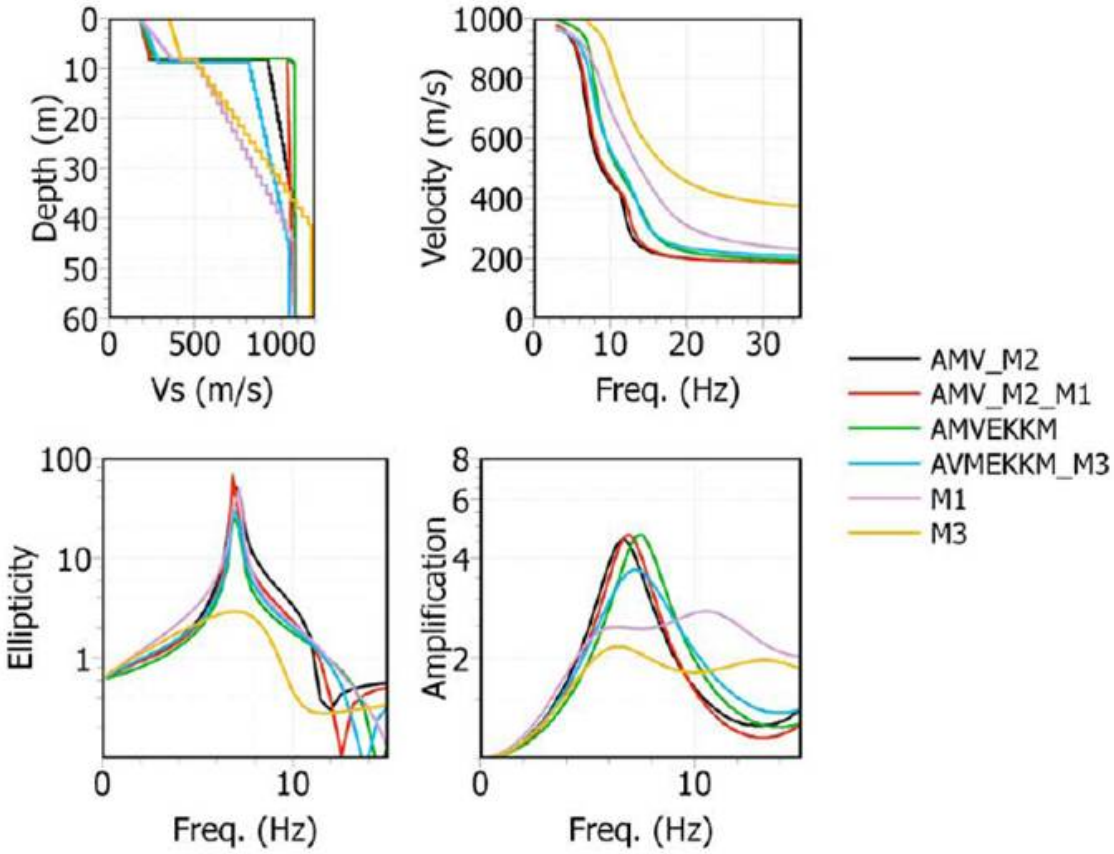

Figure I-6.11: Summary comparison for "best" inverted models in each of the six cases. Top left: velocity profiles; Top right: dispersion curves (fundamental mode of Rayleigh waves). Bottom left: elliptiicty curves for the fundamental mode of Rayleigh waves. Bottom right: Fourier transfer function for vertically incident plane S waves (with standard damping values).

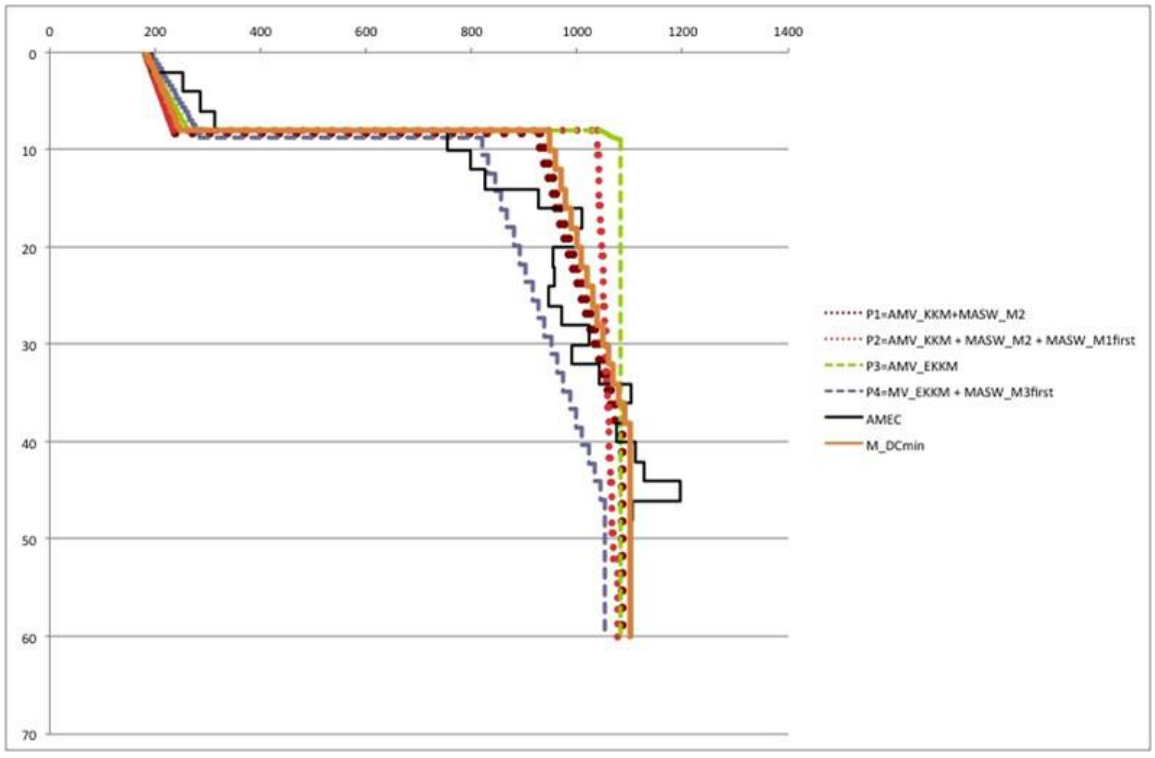

Figure I-6.12: Comparison between the proposed "M_DCmin" profile, the "best" profiles for cases 1 to 4, and the velocity profile proposed by AMEC . The corresponding DC are intermediate between the black and red curves, and on the blue and green curves on Figure I-6.11 (but closer however to the black and red).

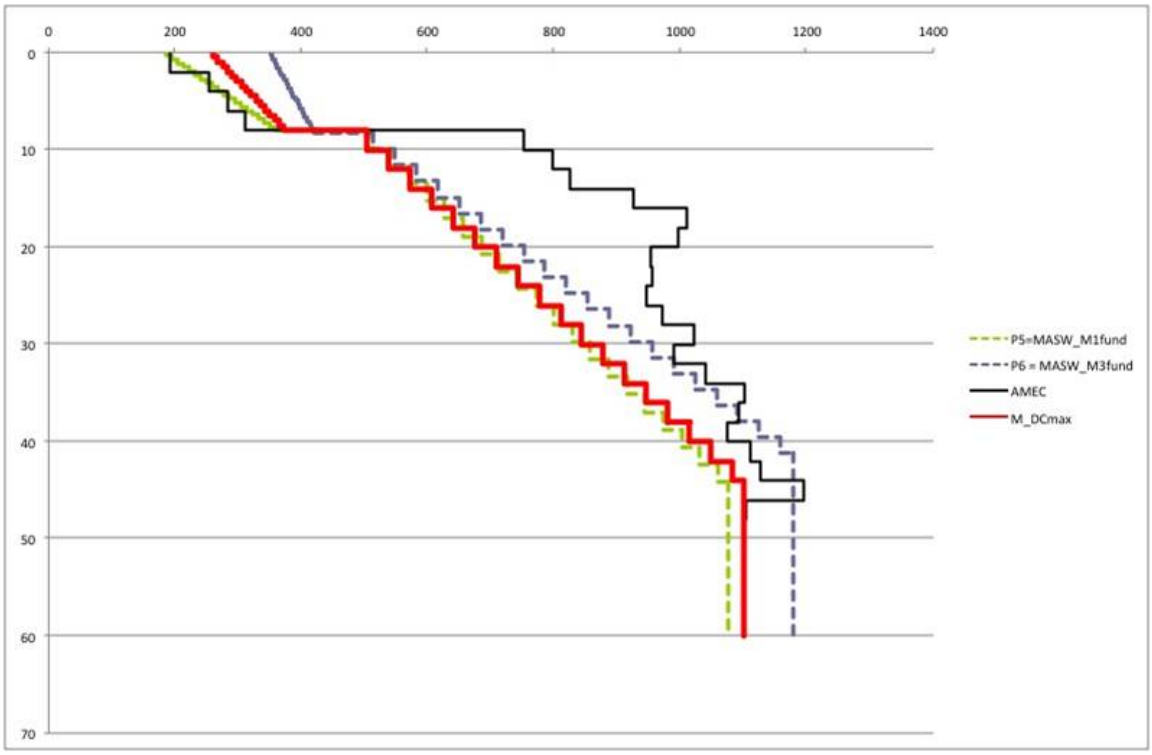

Figure I-6.13: Comparison between the proposed "M_DCmax" profile, the "best" profiles for cases 5 and 6, and the velocity profile proposed by AMEC. The corresponding DC are intermediate between the M1 (purple) and M3 (yellow) curves on Figure I-6.11, but closer however to the M1 one at low to intermediate frequency.

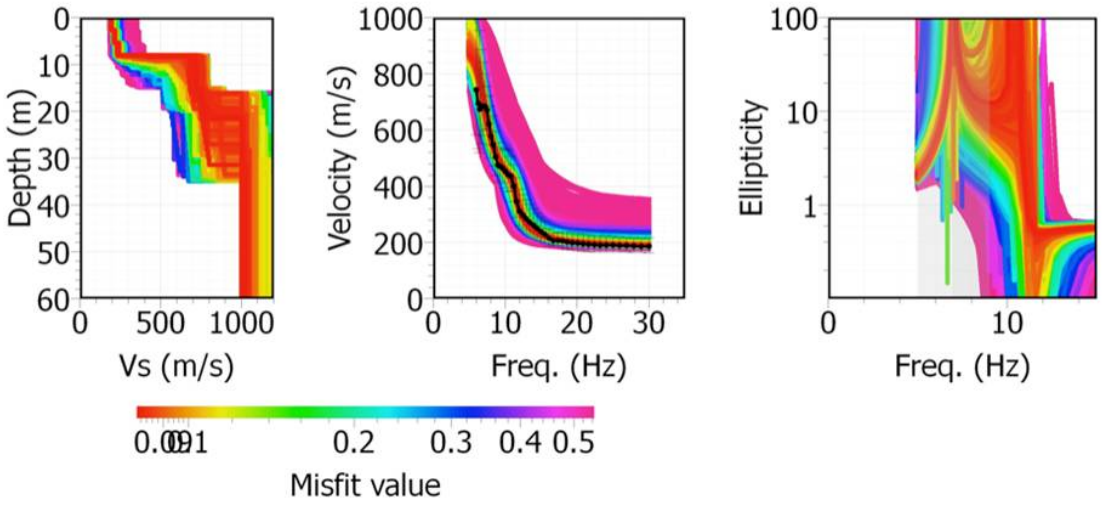

Figure I-6.14: New Inversion results for the 1st case (AMV_KKM + M2fund), relaxing the constraint of the absence of any velocity jump at the base of the weathered molasse layer. From left to right: S-wave velocity profiles, corresponding dispersion curves (fundamental mode) of Rayleigh waves and ellipticity curves. The colour of curves corresponds to the misfit values according to the color code displayed on bottom. The black curve with vertical bars in the DC plot corresponds to the input data from ambient vibrations and MASW. The velocity profile considered in Table I-6.1 is the black one in the left plot.

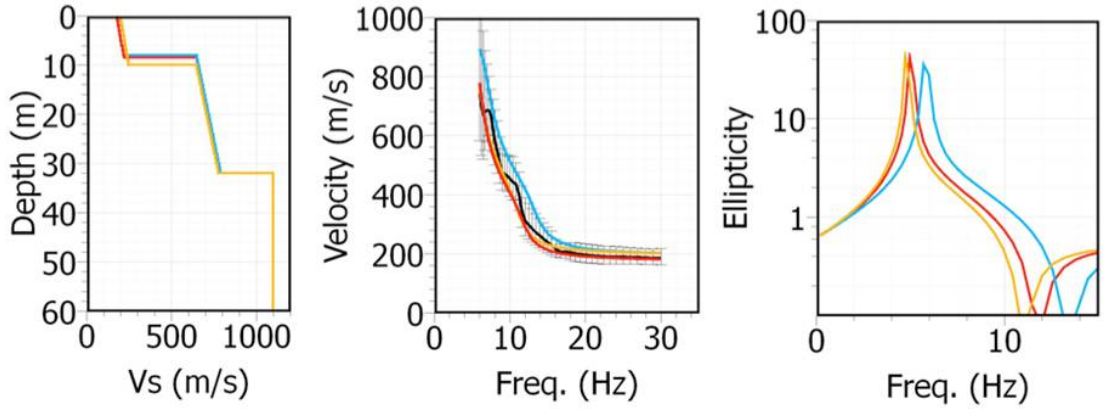

Figure I-6.15: Velocity profiles (left), dispersion curves (center - fundamental Rayleigh wave), and ellipticity curves (right) for the three tentative models M_P4_1 (blue), M_P4_2 (yellow) and M_P4_3 (red). The dispersion curves are compared with the KKM_AMV and M2 measurements (black line with bars representing the standard deviation).

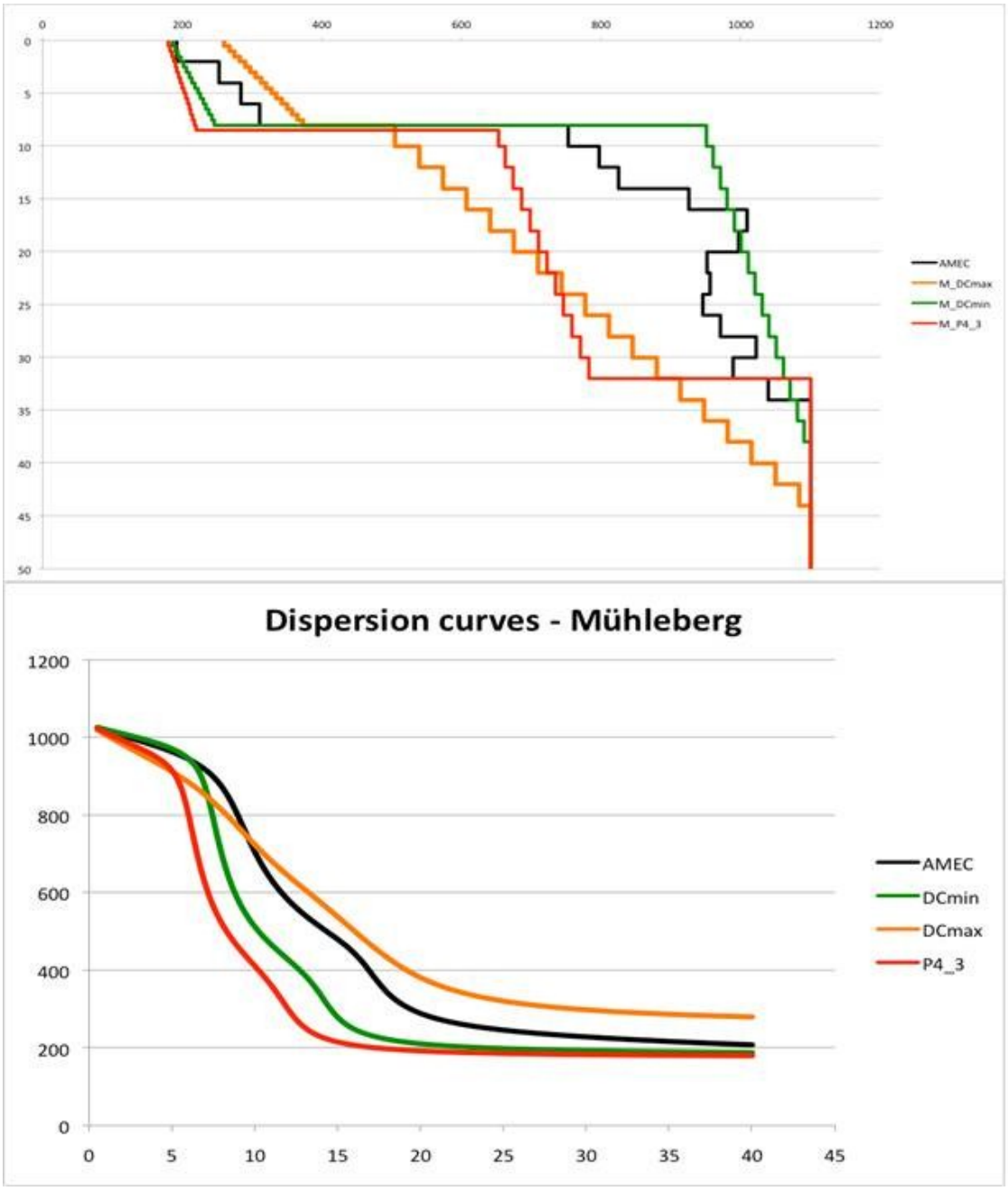

Figure I-6.16: Comparison between the four finally proposed models: AMEC, "M_DCmax", "M_DCmin" and "M_P4_3". Top: Velocity profiles. Bottom: Dispersion curves.

6.1.3 V_P-profile for Mühleberg

For Mühleberg the referenced model for the S-wave velocity profile is P1; the parameters take the values $\rho_S = 2.65$ t/m^3, $\rho = 2.2$ t/m^3 below the water table and $\rho_f = 1.0$ t/m^3, then $\varphi = 0.27$. The water bulk modulus was set equal to 1000 MPa in the soil layer. The final computed V_P is depicted in Figure I-6.17. Since no data are available for the site comparison with measured data is impossible.

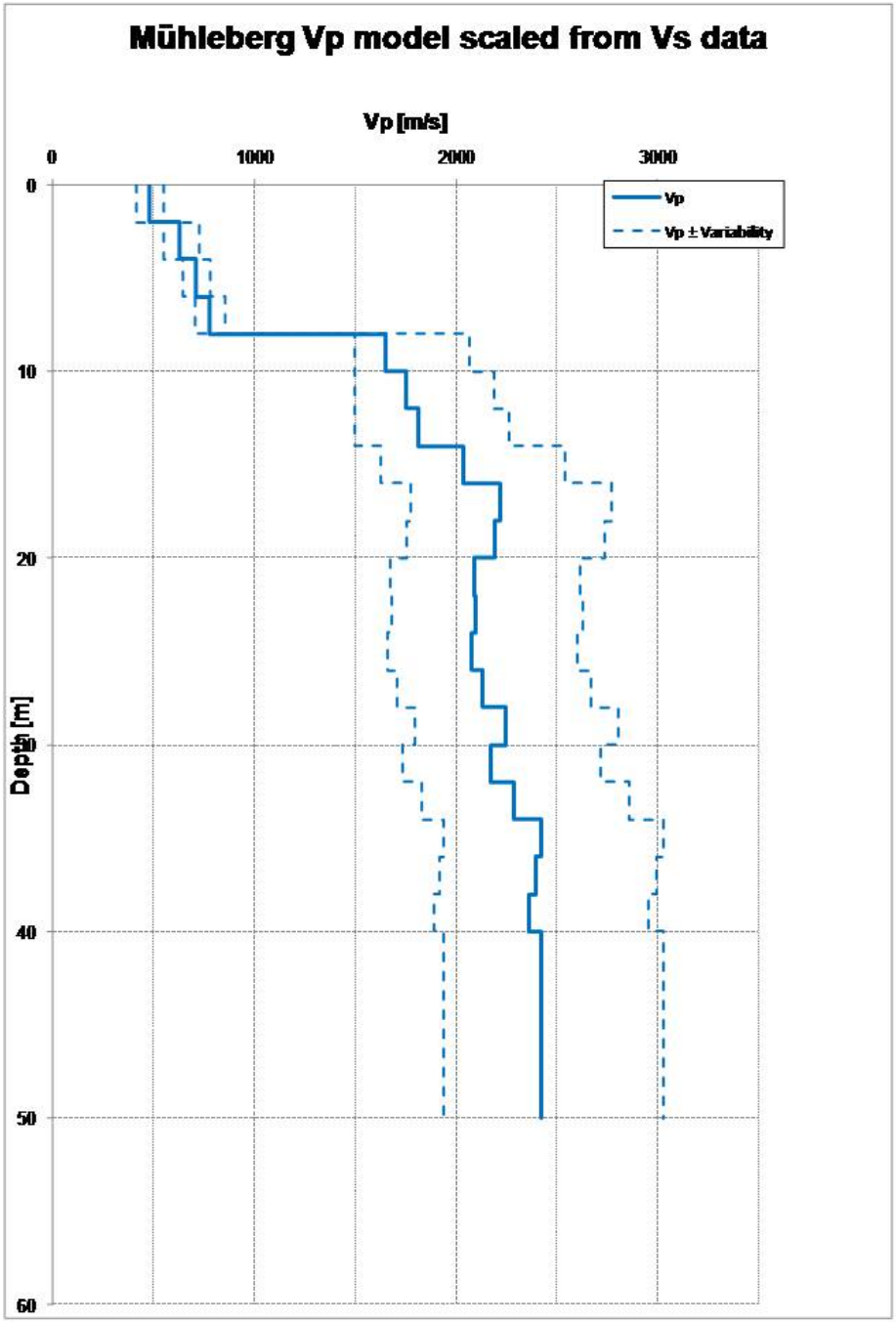

Figure I-6.17: Proposed V_P model for Mühleberg (KKM).

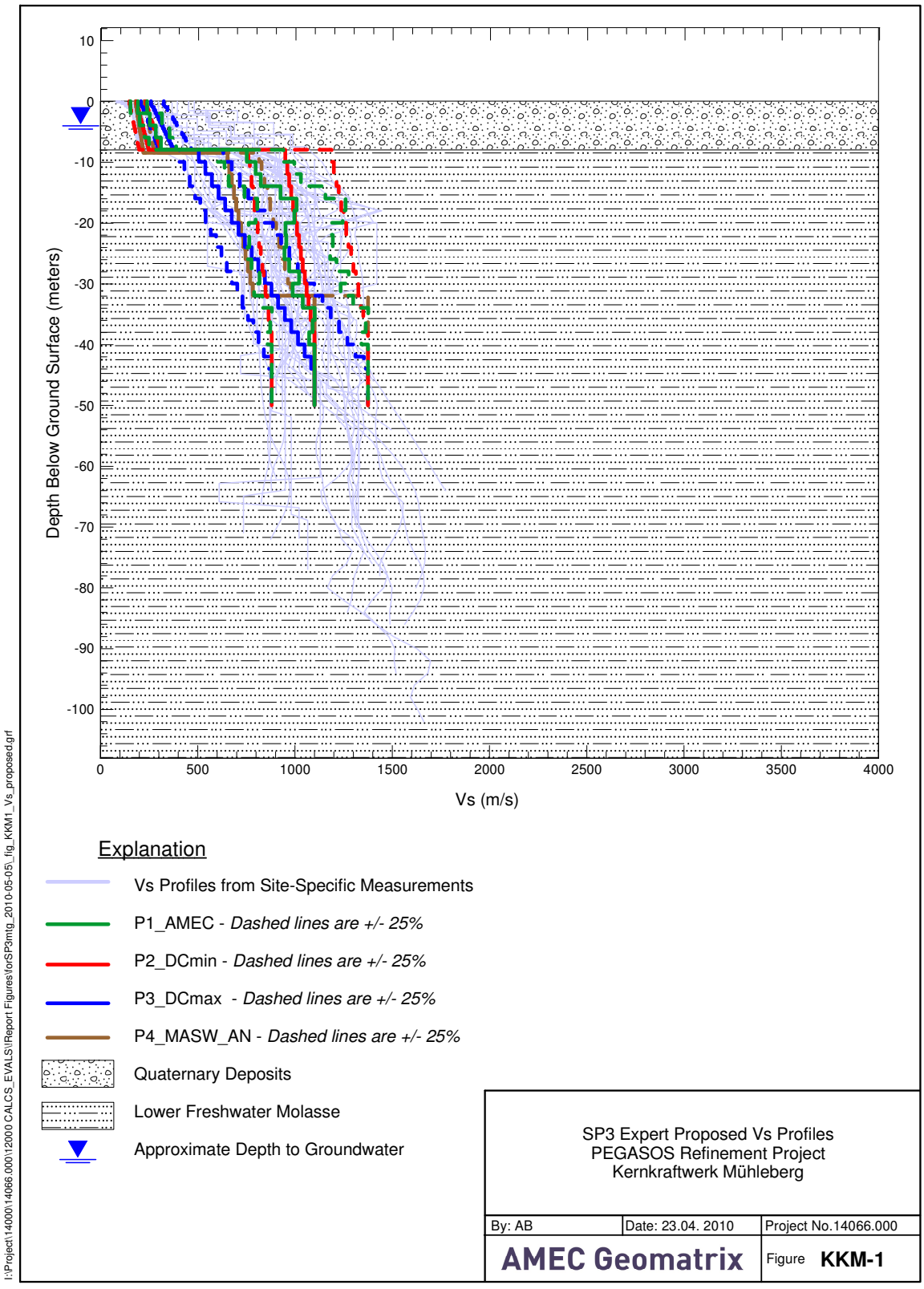

Figure I-6.18: V_S-profiles representative for the whole KKM area.

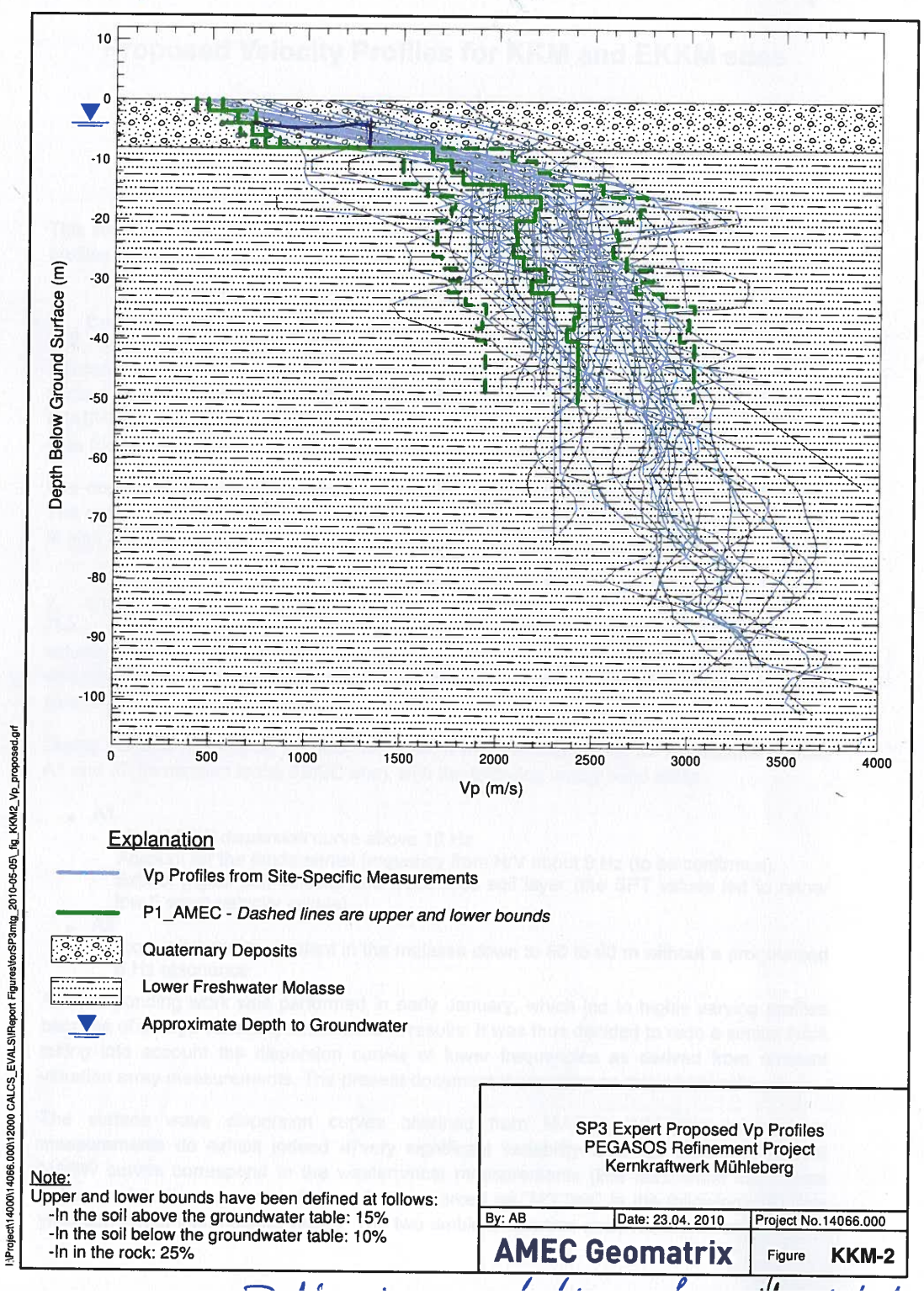

Figure I-6.19: V_P-profiles representative for the whole KKM area.

6.2 Material Models

6.2.1 General Comment

The selected models are based on first priority on tests results and on the results published by Rollins et al. [1998] and Menq [2003]. Menq's curve takes into account a dependence of G/G_{max} on the confining stress while Rollins' curve does not. Furthermore, Menq's curve corresponds to a weaker material compared to Rollins.

Accordingly, examination of the G/G_{max} curves shows that Menq's mean curve coincide with the lower bound of the tests data and Rollins mean to the upper bound. The mean curve is defined as the average between the lower bound and the upper bound curves.

As lower bound for the damping, Rollins mean damping curve was used, while Menq's mean curve was used for the upper bound. From the observations and from also theory, a stiffer material exhibits lower material damping and a softer material, higher material damping.

Those curves have been modified to a small extent to better fit the observed data.

6.2.2 Model for the Mühleberg Site

At the Mühleberg site, the laboratory test on the core samples could not be obtained and thus, the experts accounted for the lack of data by broadening the uncertainty. In the absence of specific data for this site, the experts decided to use the results obtained at Leibstadt as reference model. To reflect the additional uncertainty, the range between the lower bound curve and the upper bound curve for the reference model was increased. A comparison of the material model curves for Mühleberg and Gösgen is shown in the Figures I-6.27 and I-6.26. From these figures, one can see that the range between the lower and upper bound model of the material curves for Mühleberg is approximately twice as wide as for the Gösgen site, for which a lot new data could be retrieved.

6.2.3 EQL and RVT Computations

Estimates of the shear wave velocity and damping ratio in the Molasse:

For a harmonic wave at that predominant frequency in a homogeneous medium, the displacement pattern under the assumption of vertically propagating shear waves can be written:

$$d = d_1 \cos\left(\frac{2\pi z}{\lambda}\right), \tag{I-6.1}$$

where d_1 would be the displacement at the top of the layer and $\lambda = \frac{V_S}{f}$ the wave length. The shear strain is computed as:

$$\gamma = -\frac{2\pi d_1}{\lambda} \sin\left(\frac{2\pi z}{\lambda}\right) \leq \frac{2\pi d_1}{\lambda}. \tag{I-6.2}$$

The equivalent maximum shear strain is then:

$$\gamma_{eq} = 0.65\gamma = \frac{1.3\pi d_1}{\lambda}. \tag{I-6.3}$$

The time histories of motions provided by SP5 (see TP5-TB-1020), have been examined to estimate the ratio d_1/PGA and the predominant frequency of the input motion. These quantities are highly variable but the following approximations of the maximum equivalent shear strain can be calculated as a function of PGA in the Molasse ($V_S \approx 1000$ m/s):

Table I-6.4: Maximum equivalent shear strain as function of PGA.

PGA	γ_{eq}
0.05	0.4 E-4
0.1	0.1 E-4
0.2	1.6 E-4
0.4	3.2 E-4
0.75	6.0 E-4

Another approach is to used ratios for the quantities v/a and ad/v^2 where a, v, d are the peak ground acceleration, velocity and displacement. Such ratios have been proposed for rock sites by Johnson and M.L. [1978]. With their (median) values, admittedly based on few records, the calculations go as follows:

Table I-6.5: Alternative maximum equivalent shear strain as function of PGA.

	Magnitude 5.0			Magnitude 6.0			Magnitude 7.0		
v/a [m/s/g]	0.5			0.7			0.9		
ad/v^2	2.5			4.2			4.5		
PGA	v [cm/s]	d [cm]	γ_{eq}	v [m/s]	d [cm]	γ_{eq}	v [m/s]	d [cm]	γ_{eq}
0.05	2.5	0.3	9.9 E-05	3.5	1	1.2 E-04	4.5	1.8	1.2 E-04
0.1	5	0.6	2.0 E-04	7	2.1	2.3 E-04	9	3.6	2.5 E-04
0.2	10	1.3	4.0 E-04	14	4.1	4.7 E-04	18	7.3	5.0 E-04
0.4	20	2.5	7.9 E-04	28	8.2	9.3 E-04	36	14.6	9.9 E-04
0.75	37.5	4.7	1.5 E-03	52.5	15.4	1.8 E-03	67.5	27.3	1.9 E-03

The two groups of values are different but give the same order of magnitude. Based on the computed equivalent shear strain and the curves provided by AMEC for the Yucca Mountain tuff, and on similar curves for rocks, the following damping ratio and reduction factor to be applied to the elastic shear wave velocity can be proposed (Tab. I-6.6):

Table I-6.6: Damping ratio and reduction factor to be applied as function of PGA.

PGA	G/G_{max}	V_S/V_{Smax}	Damping ratio (%)
0.05	1	1	0.5
0.1	0.94	0.97	0.5
0.2	0.90	0.95	1.0
0.4	0.81	0.90	2.0
0.75	0.72	0.85	3.0

In the absence of specific data for the Molasse, the above estimates may be as good as guessing what could be the modulus reduction curve and damping curve. If seismologists have better estimates of the ratios v/a and ad/v^2 the calculations can easily be redone if necessary.

6.3 Supporting Figures for Mühleberg

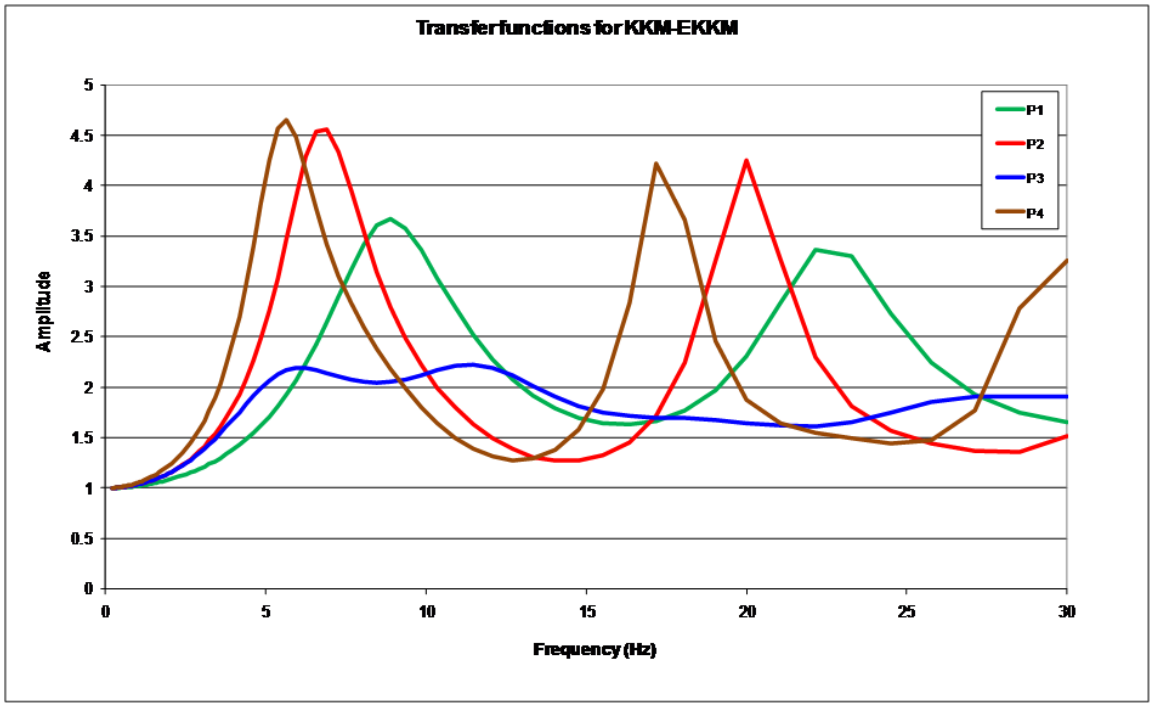

Figure I-6.20: Transfer functions for proposed soil profiles (KKM).

Table I-6.7: Fundamental frequencies, Mühleberg site.

Profile	Frequency
P1 (AMEC)	8.9 Hz
P2 (DCmin)	6.9 Hz
P3 (DCmax)	5.9 Hz
P4 (MASW-AN)	5.6 Hz

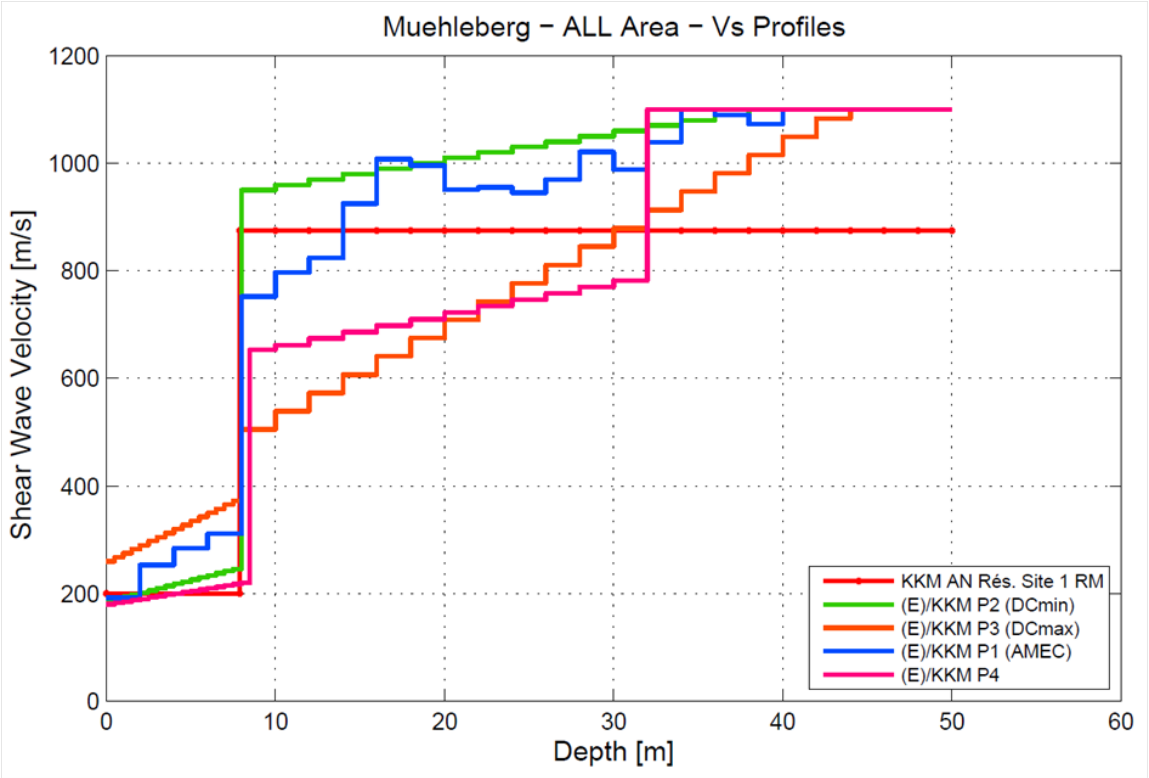

Figure I-6.21: V_S-Profiles (KKM).

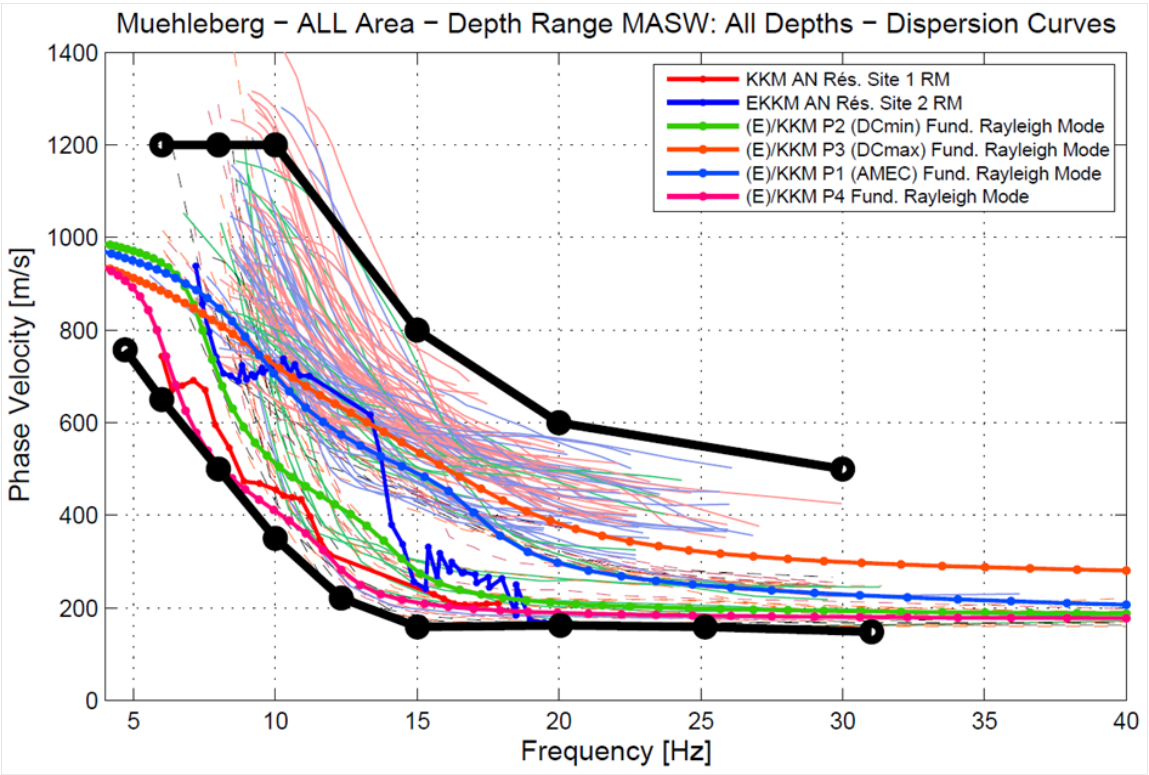

Figure I-6.22: Dispersion curves and bounds (KKM).

6.4 Comparison of PEGASOS vs. PRP Profiles and Material Models

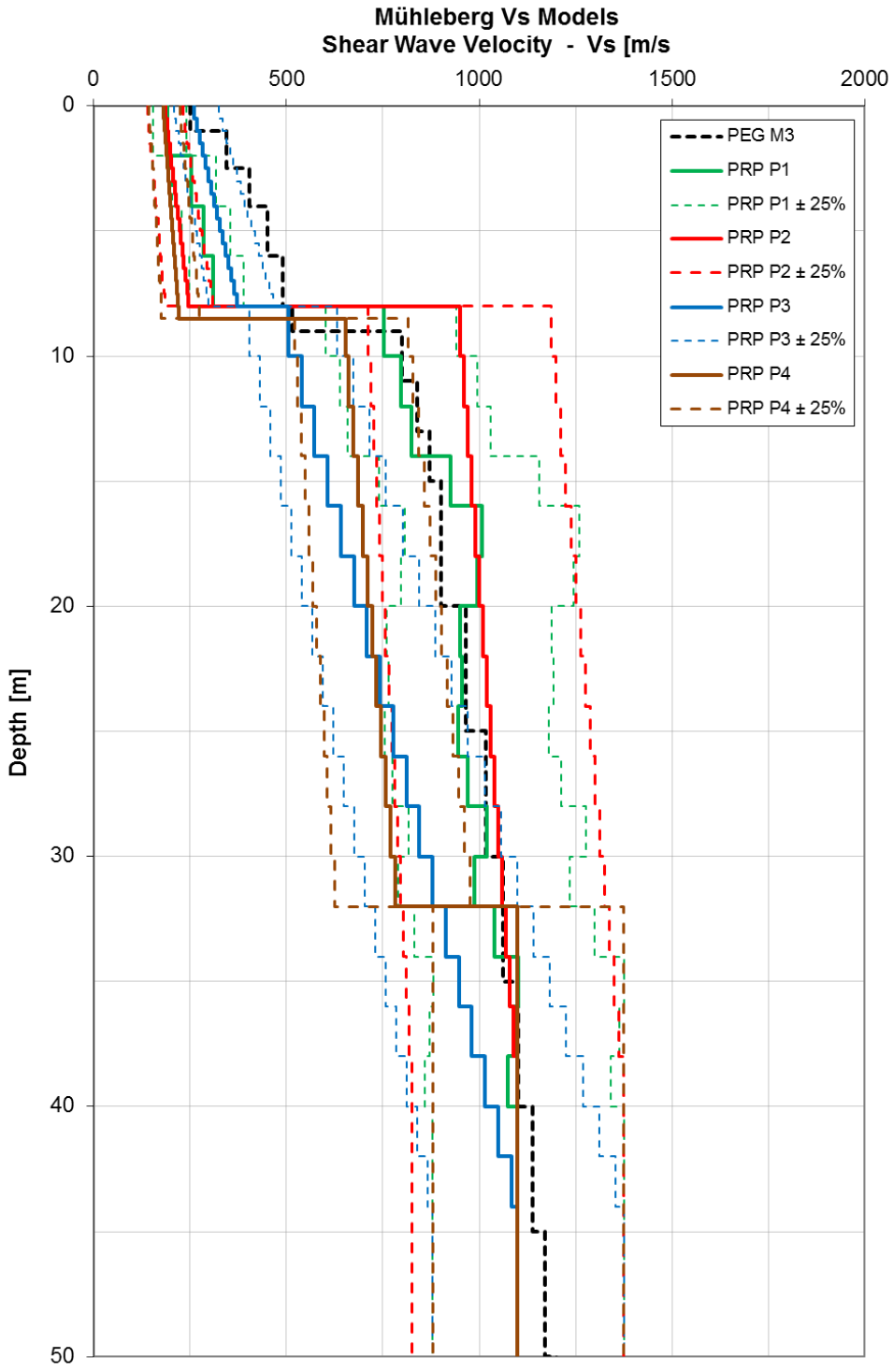

Figure I-6.23: Comparison of PEGASOS and PRP V_S-models for Mühleberg.

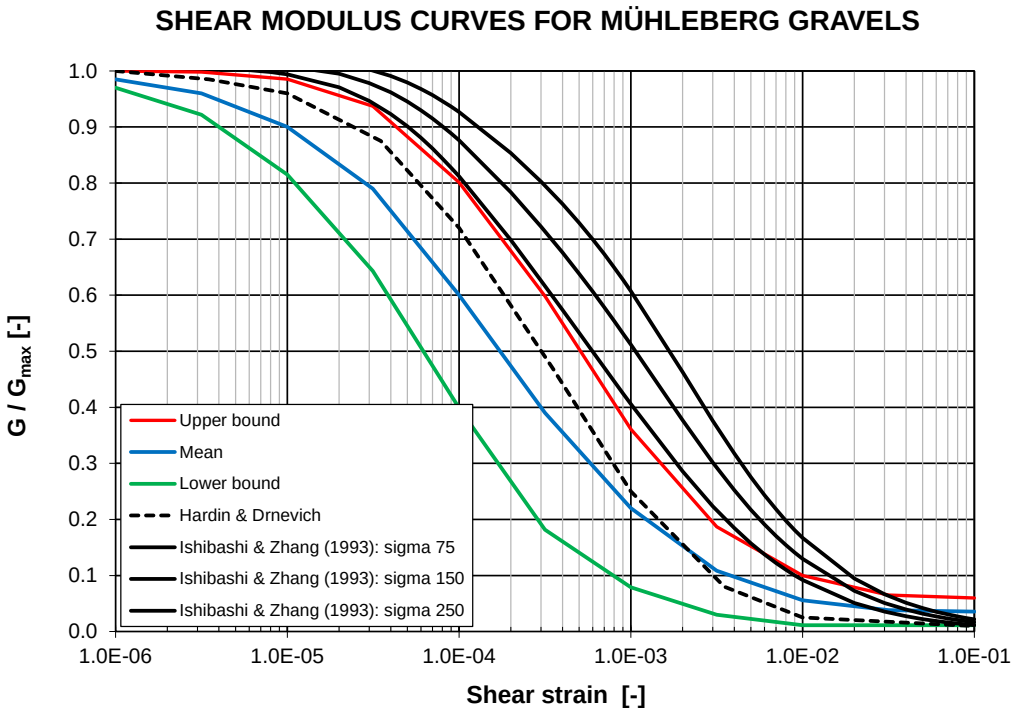

Figure I-6.24: Mühleberg - Shear modulus curves for gravel.

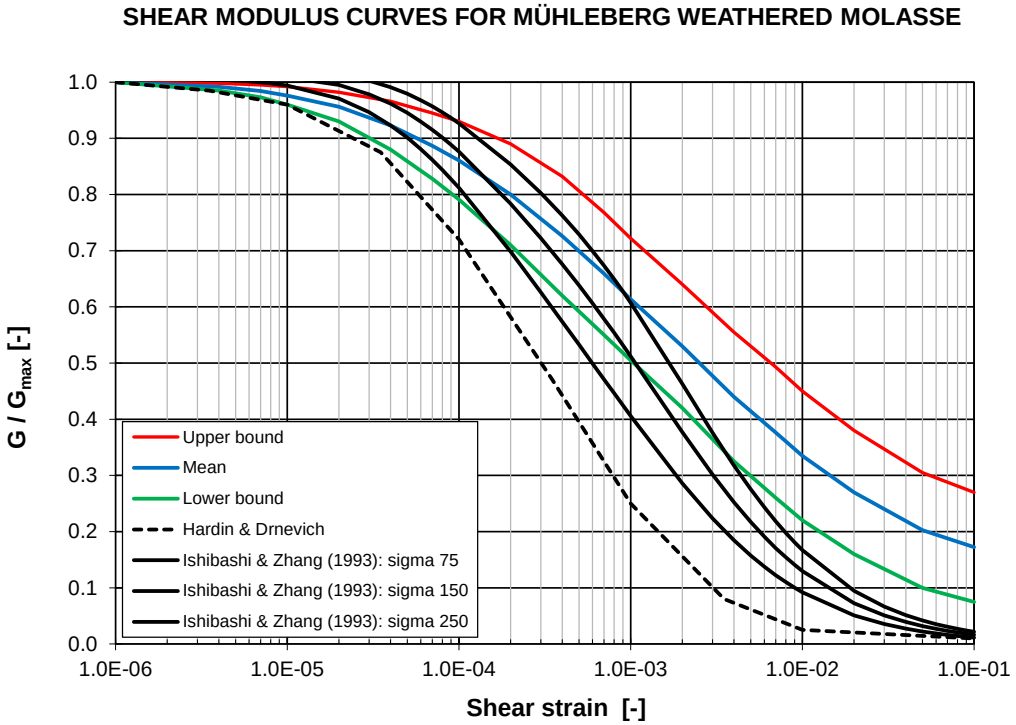

Figure I-6.25: Mühleberg - Shear modulus curves for weathered molasse.

6.5 Comparison of Material Models between KKM and KKG

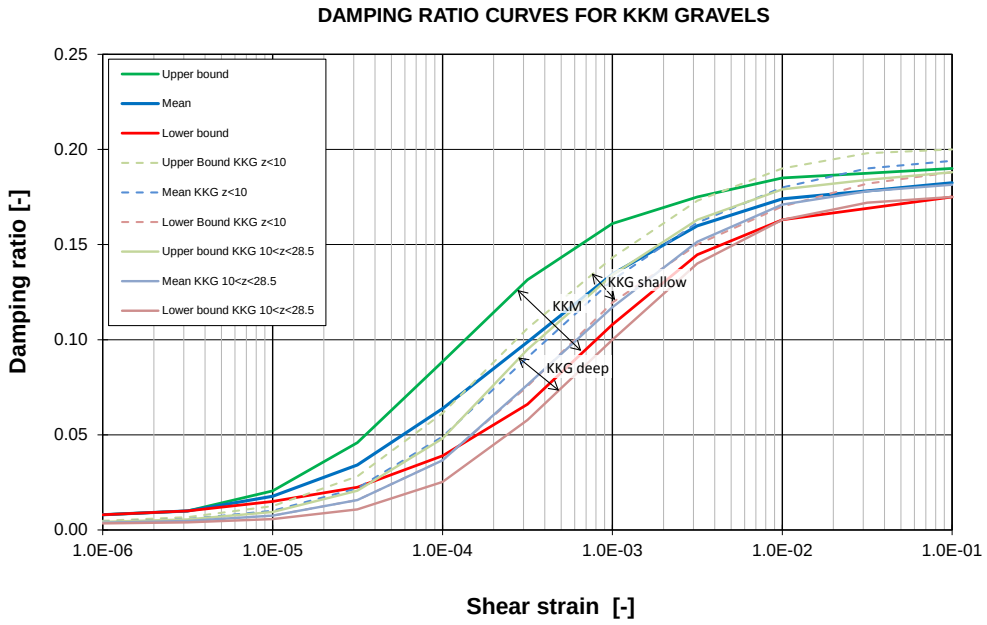

Figure I-6.26: Comparison of Shear modulus curves for Mühleberg and Gösgen. The solid lines represent the material model for KKM and the light and light dashed lines show the two models for KKG.

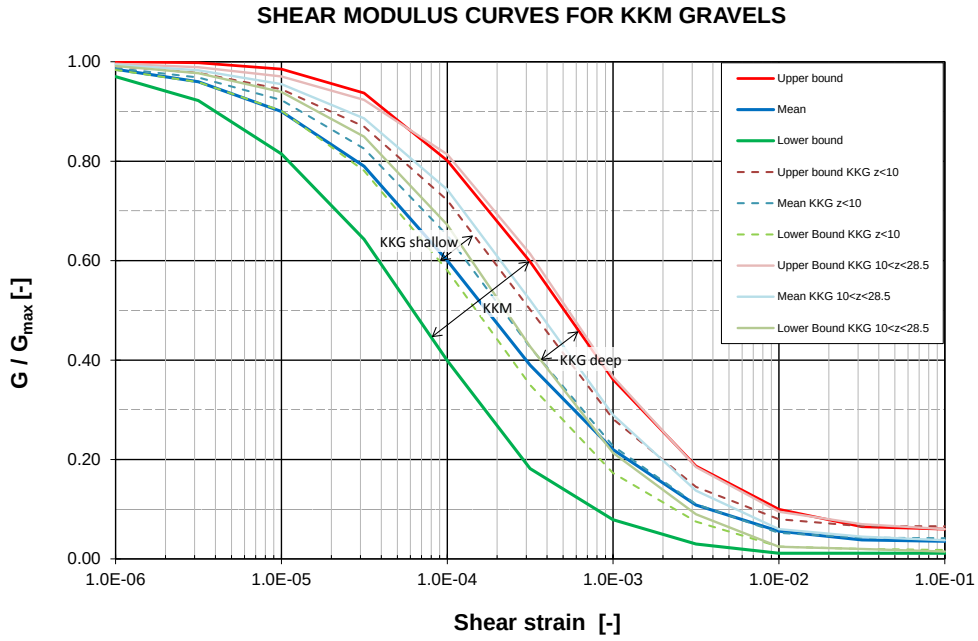

Figure I-6.27: Comparison of damping curves for Mühleberg and Gösgen. The solid lines represent the material model for KKM and the light and light dashed lines show the two models for KKG.

Chapter 7

Site Response Evaluations

Based on the proposed site-specific soil profiles and material properties, 1D site response computations were performed according to the technical specification in Renault and Abrahamson [2010] (PMT-TB-1014) and Renault [2013] (PMT-AN-1132). Three types of computations were performed:

- SHAKE type [Schnabel et al. 1972]
- RVT* (base case and with randomized profiles) [Vanmarcke 1972, 1975; Der Kiureghian 1980; Boore 1983]
- True non-linear

Table I-7.1 and I-7.2 provide an overview of all computations performed per site for each type [Renault 2011a]. All results from the different contractors were gathered by the project and compiled into a database [Hölker 2013a], which facilitated the comparison and uniform plotting of the results for the SP3 experts.

The different software codes used by the contractors are listed in Table I-7.3.

7.1 Input Motions Used for the Site Response Computations

The time histories to be used for the site response computations were defined by Bommer [2009] (TP5-TB-1020) and subsequently modified by Abrahamson [2010b] (TP5-SUP-1007) to match the SP3 requirements. The RVT input response spectra were developed by Abrahamson [2010a] (TP3-SUP-1009). The selection of records was conducted according to the following criteria: Three magnitude bins (with ±0.2 units around) $M_W = 5$, 6 and 7 earthquakes with distance range of 0–40 km. In total 10 horizontal-vertical component pairs for each magnitude level. Review the Fourier amplitude spectra and response spectra to check if the frequency content is appropriate and comparable to the spectra from the Swiss stochastic model and appropriate for the Swiss site conditions (κ and target shear-wave velocity at each site). The

*Random Vibration Theory

Table I-7.1: Global overview of amount of results for supporting computations for the horizontal and vertical component of ground motion with motion type and depth.

Site	Depth level	Horizontal			Vertical	
		EQL (SHAKE)	**RVT (base case + randomization)**	**True non-linear**	**EQL (SHAKE)**	**RVT (base case)**
Beznau	Surface ($z_1 = 0$ m)	1800, Outcrop	5088, Outcrop	151, Outcrop	90, Outcrop	9, Outcrop
	Elevation z_2 at depth -15 m	1800, Outcrop	5088, Outcrop	151, Within Layer	90, Outcrop	9, Outcrop
		1800, Within Layer			90, Within Layer	
Gösgen	Surface ($z_1 = 0$ m)	4320, Outcrop	4770, Outcrop	190, Outcrop	90, Outcrop	9, Outcrop
	Elevation z_2 at depth -9 m	4320, Outcrop	4770, Outcrop	190, Within Layer	90, Outcrop	9, Outcrop
		4320, Within Layer			90, Within Layer	
	Elevation z_3 at depth -15 m	4320, Outcrop	4770, Outcrop	190, Within Layer	90, Outcrop	9, Outcrop
		4320, Within Layer			90, Within Layer	
Leibstadt	Surface ($z_1 = 0$ m)	1350, Outcrop	3816, Outcrop	151, Outcrop	90, Outcrop	9, Outcrop
	Elevation z_2 at depth -10 m	1350, Outcrop	3816, Outcrop	151, Within Layer	90, Outcrop	9, Outcrop
		1350, Within Layer			90, Within Layer	
Mühleberg	Surface ($z_1 = 0$ m)	1800, Outcrop	5724, Outcrop	580, Outcrop	90, Outcrop	9, Outcrop
	Elevation z_2 at depth -7 m	1800, Outcrop	5724, Outcrop	580, Within Layer	90, Outcrop	9, Outcrop
		1800, Within Layer			90, Within Layer	
	Elevation z_3 at depth -14 m	1800, Outcrop	5724, Outcrop	580, Within Layer	90, Outcrop	9, Outcrop
		1800, Within Layer			90, Within Layer	
TOTAL		**44100**	**56922**	**3216**	**1710**	**108**

Table I-7.2: Overview of amount of runs for supporting computations for the horizontal and vertical component of ground motion at the ground surface (0m). Note: * Representing lower bound, mean, upper bound and are defined depth dependant. ** Non-linear cross check summarizes the required analysis for M6, PGA=0.05g with 1 time history (some contractors used all 10 time histories) and the analysis for M6, PGA=0.75g with 10 time histories by the second contractor.

Site	Data description	Amount of altern. profiles	Amount of mat. curves*	Horizontal				Vertical	
				EQL (SHAKE)	RVT (base case + randomization)	1-D true non-linear	1-D true non-linear (cross check)**	EQL (SHAKE)	RVT (base case)
Beznau	TP3-TN-1068 TP3-GTC-1012	4	3	1800	288+4800	140	11	90	9
Gösgen	TP3-TN-1070 TP3-GTC-1014	6	3	4320	270+4500	140	50	90	9
Leibstadt	TP3-TN-1067 TP3-GTC-1011	3	3	1350	216+3600	140	11	90	9
Mühleberg	TP3-TN-1071 TP3-GTC-1015	4	3	1800	324+5400	560	20	90	9
TOTAL				**10620**	**23214**	**1120**	**103**	**450**	**45**

Table I-7.3: Software codes used for the site response analyses.

Site	SHAKE	RVT	Non-Linear
KKG	SHAKE-AR by R. Attinger	APASHAKE by A. Asfura	Dynaflow (SUMDES for cross check)
KKB & KKL	SHAKE91 by. Idriss & Sun (1991)	RASCALS by W. Silva	SUMDES (Dynaflow for cross check)
KKM	SHAKE 10 modified version of SHAKE [Schnabel et al, 1972] by AMEC Geomatrix	STRATA by A. Kottke and E. Rathje	SUMDES (Dynaflow for cross check)

latter criterion indirectly covered the requirement to limit the records to NPP comparable V_{S30} ranges and site classes, respectively. The following databases were considered for the search by Bommer [2009]: NGA, European Strong-Motion, Alpine Strong-Motion, Swiss Strong-Motion and Canadian Strong-Motion database (the Japanese Strong-Motion database was considered, but not included in the final search).

7.1.1 Characteristics of Selected Time Histories

The basic characteristics of the records are presented in Tables I-7.4-I-7.6 for the three magnitude bins. The number given in the first column is the record identifier within the magnitude bin. The ID is the record identified in the source database, which is identified in the third column with self-explanatory codes. The final column identifies which of the two horizontal components has been selected (X, Y or Z). Shear-wave velocities, when known, are presented, otherwise the sites are simply noted to have been classified generically as "rock". In the case of the European data, this nominally implies V_{S30} in excess of 750 m/s. What can be seen from the Tables I-7.4-I-7.6 is that the magnitude and distance search criteria are well satisfied on the whole, with only one recording exceeding the distance limit of 40 km in the Mw 5 bin, three in the Mw 6 bin, and just two in the Mw 7 bin. Some earthquakes are represented by more than one record, but never more than four. Four recording stations each contribute two recordings (two in the same magnitude bin, the other two in different bins), but all other stations are represented by a single record only.

A particular comment may be warranted regarding record M_W6_05, the recording from St. André (Station no. 17) of the 1988 Saguenay earthquake in Quebec. The record was processed by the network operator in Canada with a filter cut-off at 0.67 Hz - see, for example, Boore and Atkinson [1992] - and is consequently very weak in terms of shaking at response periods of 1 second and greater (although it is also assumed that the filter was applied without removing a large part of the energy and that the cut-off was chosen to reflect the seemingly unusual nature of this record). Nevertheless, the SP5 and SP3 experts evaluated that this recording is be representative of certain types of stable continental earthquakes.

Based on the SP2 reevaluation of κ in 2013, a new set of input records was defined (see Renault [2013]; Gregor [2013], PMT-AN-1132, EXT-TN-1265 and TP3-WAF-1023) to be consistent with the high frequency content for the final κ values.

Table I-7.4: Characteristics of records selected for M_W 5 bin

No.	ID	DB	EQ Date	Mw	Station	Distance	Metric	V_S / Site	Comp.
1	59	EUR	07.05.1976	5.11	Tolmezzo	32.0 km	Rhyp	1021 m/s	X
2	465	EUR	30.03.1989	4.8	Toros	14.3 km	Rhyp	Rock	X
3	813	EUR	03.10.1997	5.17	Nocera U-B	10.0 km	Rhyp	Rock	Y
4	852	EUR	03.04.1998	5.11	Nocera U-B	12.5 km	Rhyp	Rock	Y
5	858	EUR	03.04.1998	5.11	Sellano	36.5 km	Rhyp	Rock	X
6	859	EUR	05.04.1998	4.84	Sellano	38.3 km	Rhyp	Rock	Y
7	878	EUR	04.01.1994	5.11	Adra (Almeria)	29.7 km	Rhyp	Rock	X
8	NAH7	CAN	25.07.1985	5.1	Nahanni-1	26 km	Rjb	Rock	X
9	12698	ALP	17.07.2001	4.89	Sole-01	41 km	Rhyp	3000 m/s	Y
10	12804	ALP	12.07.2004	5.2	Dreznica	8 km	Rhyp	851 m/s	Y

Table I-7.5: Characteristics of records selected for M_W 6 bin

No.	ID	DB	EQ Date	Mw	Station	Distance	Metric	V_S / Site	Comp.
1	242	EUR	19.09.1979	5.85	Cascia	5.7 km	Rhyp	Rock	Y
2	243	EUR	19.09.1979	5.85	San Vittorino	47.2 km	Rhyp	Rock	Y
3	246	EUR	19.09.1979	5.85	Arquata Tronto	22.4 km	Rhyp	Rock	Y
4	594	EUR	26.09.1997	5.89	Nocera Umbra	12.5 km	Rhyp	Rock	Y
5	SG10	CAN	25.11.1988	5.9	Andre	43 km	Rjb	Rock	X
6	455	NGA	24.04.1984	6.19	Gilroy #1	14.9 km	Rrup	1428 m/s	Y
7	537	NGA	07.08.1986	6.06	Poppet Flat	17.0 km	Rrup	685 m/s	X
8	663	NGA	10.01.1987	5.99	Mt Wilson	22.7 km	Rrup	822 m/s	Y
9	680	NGA	10.01.1987	5.99	CIT Kresge Lb	18.1 km	Rrup	969 m/s	X
10	3207	NGA	22.09.1999	6.2	TCU107	56.4 km	Rrup	474 m/s	X

Table I-7.6: Characteristics of records selected for M_W 7 bin

No.	ID	DB	EQ Date	Mw	Station	Distance	Metric	V_S / Site	Comp.
1	198	EUR	15.04.1979	6.84	Ulcinj Albatros	13 km	Rrup	1083 m/s	Y
2	200	EUR	15.04.1979	6.84	Herceg Novi	18 km	Rrup	875 m/s	Y
3	202	EUR	15.04.1979	6.84	Titograd GZ	57.3 km	Rhyp	Rock	Y
4	B329	CAN	23.12.1985	6.8	Nahanni-1	9 km	Rjb	Rock	Y
5	B331	CAN	23.12.1985	6.8	Nahanni-3	16 km	Rib	Rock	Y
6	126	NGA	17.05.1976	6.8	Karakyr	5.5 km	Rrup	660 m/s	Y
7	747	NGA	18.10.1989	6.93	Bear Valley #1	69.4 km	Rrup	597 m/s	X
8	763	NGA	18.10.1989	6.93	Gavilan Coll.	10.0 km	Rrup	730 m/s	X
9	765	NGA	18.10.1989	6.93	Gilroy #1	9.6 km	Rrup	1428 m/s	Y
10	809	NGA	18.10.1989	6.93	UCSC	18.5 km	Rrup	714 m/s	Y

Chapter 8

Evaluation of Maximum Ground Motions

8.1 Introduction

One of the tasks within SP3 was to define maximum ground motion models for soil. The SP3 experts have evaluated and documented the maximum ground motions at each NPP site in Pecker [2011] (TP3-TB-1074). Here only a brief summary of the simplified evaluations performed to estimate the maximum ground motions—essentially the peak ground acceleration—that could be anticipated at the ground surface of the five nuclear power plant sites (KKG, KKB, EKKB, KKL and KKM) is given, regardless of the amplitude of the rock motion. The reader is referred to the technical note for more details.

Basically three methodologies have been followed:

- Development of a theoretical model,
- Use of a theoretical approach published in the literature,
- Use of the nonlinear site response analysis carried out for the derivation of the amplification functions.

These methodologies have been previously applied during the PEGASOS project. However, improvements, which are indicated in the second section, have been implemented in the theoretical model and new non-linear analyses are available in PRP.

8.2 Theoretical Calculation

8.2.1 Wave Equation

The theoretical calculation is based on a simplified analytical solution for the site response which takes into account the frequency content of the input motion and the soil properties.

Let us consider a soil layer of finite thickness overlying a stiff bedrock, which for the purpose of this study will be considered as a rigid boundary.

We assume that the shear wave velocity varies with depth according to some power law of depth:

$$V(z) = V_s \left(\frac{z+d}{h+d}\right)^{\frac{p}{2}} \tag{I-8.1}$$

where h is the layer thickness and V_S the shear wave velocity at depth h. The parameter d is a new parameter that has been introduced with respect to the model used in PEGASOS to allow for a non-zero shear wave velocity at the ground surface.

From Equation I-8.1 the shear modulus is equal to:

$$G = \rho V^2(z) = \rho V_S^2 \left(\frac{z+d}{h+d}\right)^{p} \tag{I-8.2}$$

The wave equation for vertically propagating shear waves writes:

$$\frac{\partial \tau(z)}{\partial z} = \rho \frac{\partial^2 U(z,t)}{\partial t^2} \tag{I-8.3}$$

where $\tau(z)$§ is the shear stress and U the soil absolute displacement.

For a linear elastic material, the constitutive relationship is given by:

$$\tau(z) = G(z)\frac{\partial U(z,t)}{\partial z} = \rho V_S^2 \left(\frac{z+d}{h+d}\right)^{p} \frac{\partial U(z,t)}{\partial z} \tag{I-8.4}$$

It is convenient to make the following change of variables:

$$\zeta = \frac{z+d}{h+d}, \qquad H = h + d \tag{I-8.5}$$

and to introduce the relative displacement to the bedrock, u, and the bedrock displacement v_g.

Combining Equations I-8.3 to I-8.5, the wave equation in terms of displacements writes:

$$\frac{V_S^2}{H^2}\frac{\partial}{\partial \zeta}\left(\zeta^p \frac{\partial u}{\partial \zeta}\right) = \frac{\partial^2 u}{\partial t^2} + \ddot{v}_g(t) \tag{I-8.6}$$

The boundary conditions express that the relative displacement at the bedrock interface and the shear stress at the ground surface are equal to 0:

$$\zeta = d/H = \zeta_0, \qquad \tau(\zeta_0) = 0 \Rightarrow G(\zeta_0)\frac{\partial u}{\partial \zeta}|_{\zeta=\zeta_0} = 0 \tag{I-8.7}$$

with $\zeta = 1$ and $u(1,t) = 0$.

When the shear wave velocity is different from zero at the ground surface ($d > 0$), the first of the two boundary conditions reduces to:

$$\zeta = d/H = \zeta_0, \qquad \frac{\partial u}{\partial \zeta}|_{\zeta=\zeta_0} = 0 \tag{I-8.8}$$

When the shear wave velocity is equal to zero at the ground surface, the limit of the first boundary condition must be considered:

$$\zeta = 0, \qquad \tau(\zeta = 0) = 0 \Rightarrow \lim_{\zeta \to 0} G(\zeta)\frac{\partial u}{\partial \zeta} = 0 \tag{I-8.9}$$

Considering the homogeneous equation, without the forcing term $\dot{\vartheta}_g$, and using the technique of separation of variables $u(\zeta,t) = X(\zeta)y(t)$ Equation I-8.6 becomes:

$$\frac{V_S^2}{H^2}\frac{d}{d\zeta}\left(\zeta^p\frac{dX}{d\zeta}\right)y(t) = X(\zeta)\ddot{y}(t) \tag{I-8.10}$$

which can be written:

$$\frac{V_S^2}{H^2}\frac{\frac{d}{d\zeta}\left(\zeta^p\frac{dX}{d\zeta}\right)}{X(\zeta)} = \frac{\ddot{y}(t)}{y(t)} = cst = -\omega^2 \tag{I-8.11}$$

The first equation gives the mode shapes:

$$\frac{d}{d\zeta}\left(\zeta^2\frac{dX}{d\zeta}\right) + \frac{H^2}{V_S^2}\omega^2 X(\zeta) = 0 \tag{I-8.12}$$

with the boundary conditions:

$$\lim_{\zeta\to 0}\zeta^p X'(\zeta) = 0 \tag{I-8.13}$$

$X(1) = 0$

8.2.2 Modes Equation for the Ground Surface Acceleration

The solution to Equation I-8.12 has been obtained from Pecker [2005] and all the details are not repeated herein. The general solution is obtained as:

$$X(\zeta) = \zeta^{\frac{1-p}{2}}\left[AJ_v\left(\lambda\zeta^{\frac{2-p}{2}}\right) + BY_v\left(\lambda\zeta^{\frac{2-p}{2}}\right)\right] \tag{I-8.14}$$

where J_v and Y_v are Bessel's function of the first kind and second kind and $\lambda = \frac{2\omega H}{(2-p)V_S}$ The boundary conditions (I-8.13) together with the relationship (I-8.14) and the derivative of Equation I-8.14 [Pecker 2005] yield a system of two equations with two unknowns A and B. This system has a non-trivial solution if, and only if, its determinant is equal to zero. This condition provides the frequency equation, which possesses an infinite number of distinct real positive roots [Abramowitz and Stegun 1970]. To each of these roots is associated a mode shape X_m, which is normalized to 1.0 at the surface for convenience; the solution $u(\zeta,t)$ is expanded in terms of the mode shapes:

$$u(\zeta,t) = \sum_{m=1}^{\infty} X_m(\zeta)y_m(t) \tag{I-8.15}$$

Introducing the mode participation factor α_n:

$$\alpha_n = \frac{\int_{\zeta_0}^1 X_n(\zeta)d\zeta}{\int_{\zeta_0}^1 X_n^2(\zeta)d\zeta} \tag{I-8.16}$$

the maximum ground surface acceleration due to the contribution of N modes is expressed as:

$$\ddot{u}_max(z=0) = \left[\sum_{i=1}^{N}(\alpha_i S_a(\omega_i,\xi_i))^2\right]^{\frac{1}{2}} \tag{I-8.17}$$

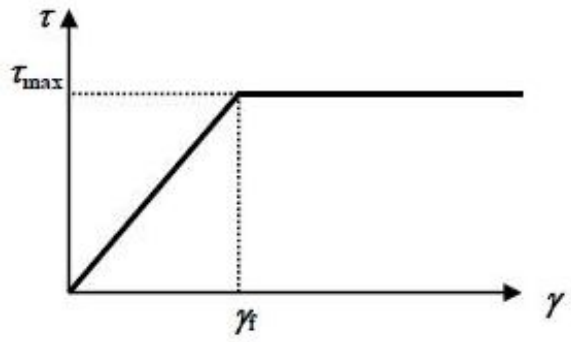

Figure I-8.1: Shear-stress-strain relationship.

where $S_a(\omega_i, \zeta_i)$ is the pseudo acceleration. Equation I-8.17 takes into account the fact that the mode shapes have been normalized to 1 at the ground surface ($X_i(\zeta_0) = 1$). The percentage of modal mass relative to the total mass of the soil column, which is an indicator of the number of modes N to retain, is:

$$m_n = \frac{1}{1-\zeta_0} \frac{\left[\int_{\zeta_0}^{1} X_n(\zeta) d\zeta\right]^2}{\int_{\zeta_0}^{1} X_n^2(\zeta) d\zeta} \tag{I-8.18}$$

The maximum shear strain at any depth within the profile is then expressed as:

$$\gamma_{max}(z) = \left[\sum_{i=1}^{N} \left(\frac{\partial u_i(z)}{\partial z}\right)^2\right]^{\frac{1}{2}} = \frac{1}{H}\left[\sum_{i=1}^{N} \left(\alpha_i \frac{S_a(\omega_i, \xi_i}{\omega_i^2} X_i'(\zeta)\right)^2\right]^{\frac{1}{2}} \tag{I-8.19}$$

With respect to the PEGASOS project the number of modes used in the analyses is no longer 3 but is controlled by Equation I-8.18 imposing a cumulative modal mass higher than 95%.

8.2.3 Determination of the Maximum Ground Surface Motion

We still assume, as in PEGASOS, a simplified elastic-perfectly plastic constitutive relationship for the soil layer; the shear stress–shear strain curve (Fig. I-8.1) is defined by two parameters:

- the shear strength τ_{max}
- the yield strain γ_f.

The shear modulus is then given by $G = \tau_{max}\gamma_f$.

As soon as, at any depth within the soil profile, the shear strain reaches γ_f, the maximum shear stress that can be transmitted is limited by τ_{max}; the ground surface acceleration cannot therefore exceed the value reached when $\gamma(z) = \gamma_f$

The procedure involves the following steps:

- Define the input motion at the rock interface by its pseudo acceleration response spectrum S_a^*.
- Compute the eigenfrequencies and mode participation factors

- Plot the shear strain (eq.I-8.19) versus depth together with the yield strain γ_f.
- Determine the depth z_0 and the minimum scaling factor μ for which $\gamma_f = \mu\gamma(z_0)$.
- Define $S_a = \mu\ S_a^*$ the maximum possible pseudo acceleration from which the maximum ground surface acceleration $\ddot{u}_{max}(z = 0)$ is determined (Equation (I-8.17)).

8.2.4 Determination of the Maximum Shear Strength and Yield Strain

As the procedure proposed above is rather crude and intends to estimate an upper bound for the maximum acceleration, which obviously will increase as the shear strength increases, the shear strength is expressed by the simplified conservative expression (which assumes that the at rest earth pressure coefficient is equal to 1.0):

$$\tau_{max} = \sigma'_v \tan\phi + c \tag{I-8.20}$$

Where σ_v is the vertical effective stress, ϕ is the soil friction angle and c its cohesion. As opposed to Pegasos, the yield strain is no longer constant but is also dependent on the effective stress. From the definition of the yield strain:

$$\gamma_f = \frac{\tau_{max}}{G} \tag{I-8.21}$$

It turns out that since τ_{max} is approximately proportional to σ_v and G to $\sqrt{\sigma'_v}$ that the yield strain is also proportional to $\sqrt{\sigma'_v}$. We write

$$\gamma_f = \gamma_{ref}\left(\frac{\sigma'_v}{\sigma_{ref}}\right)^{0,5} \tag{I-8.22}$$

For all sites the reference shear strain γ_{ref}, the reference stress σ_{ref}, and the cohesion have been taken equal to fixed values:

$$c = 35kPa, \qquad \sigma_{ref} = 100kPa, \qquad \gamma_{ref} = 2\% \tag{I-8.23}$$

The values for σ_{ref} and γ_{ref}, are typical of dense cohesionless materials and are confirmed by the cyclic triaxial tests conducted during the course of the project. Furthermore, the yield strain (Equation(I-8.22)) is not allowed to fall below 1%. A non-zero cohesion c was also measured in some tests; since we are looking for upper bounds it was decided to take it into account although it may look unusual for cohesionless soils. As a matter of fact it does not reflect a true cohesion but an apparent one due to the curve shaped of the Mohr-Coulomb failure envelope; this curved shape and apparent cohesion reflect the dilatancy of the very dense material. The friction angles entering Equation I-8.20 is site dependent; the retained values are based on the upper bound estimates of the subcontractor in charge of the non-linear site response analyses; they are summarized in Table I-8.1.

The variations with depth of the maximum shear stresses, yield strains and shear moduli, with the fit to Equation (I-8.2), are presented for each site in Figures I-8.2 to I-8.11.

8.2.5 Rock Response Spectrum

The input spectrum is taken as the mean response spectrum calculated over the ten time histories representing the magnitude 6 event (TP5-SUP-1007); this mean spectrum is computed for 20% damping and scaled to 10 m/s^2 (∼1 g). Since in the report we are concerned with large strains, close to soil failure, it is reasonable to assume that the soil damping ratio is at least equal to 20%. The individual response spectra and the mean taken into account in the analyses are represented in Figure I-8.12.

In the following the procedure will only be shown for the site Beznau. The results for the other sites can be found in Pecker [2011] (TP3-TB-1074).

8.2.6 Application to Beznau Site (KKB)

Results of the calculations for the first five modes are given in Table I-8.2. The natural frequencies range from 1.68 Hz to 14.5 Hz; the corresponding spectral accelerations for 20% damping (before scaling), S_a^*, are equal to 4.84 m/s^2 (first mode) and 15 m/s^2.

The strain profile computed with the previous data and equation (I-8.19) is plotted in Figure I-8.13 together with the yield strain; the yield strain is equal to the induced strain for: $\mu = 2.22$ and the critical depth is 2.25 m below the ground surface.

The maximum peak ground acceleration (Eq. I-8.17) is given by:

$$\boxed{\ddot{u}_{max} = 24.6 m/s^2} \tag{I-8.24}$$

8.3 Alternative Theoretical Model

8.3.1 Assumptions and Results

An alternative theoretical model has been proposed by Betbeder-Matibet [1993] to bound the maximum ground surface acceleration at the top of a soil layer overlying a rock formation. The method presents some similarity with the method developed in the previous paragraph and had already been used for PEGASOS. Its results have been revised in the present report to account for the revised soil characteristics. The model is based on the following assumptions:

- The shear modulus is constant with depth, which is equivalent to setting the parameter p in Equation I-8.2 equal to 0;
- the constitutive law for the soil is represented by the hyperbolic model, completely defined by the elastic shear modulus and the reference strain γ_r;
- the average soil column acceleration is limited by the available shear strength τ_{max} at the base of the profile divided by the mass of the soil column;
- the solution consists in relating the maximum surface acceleration to the average soil column acceleration; this is achieved by the computation of a fundamental "nonlinear" mode shape of the soil column.

The following equations are derived in Betbeder-Matibet [1993]:

$$\rho h A_m \leq \tau_{max} = \rho V_S^2 \gamma_r \tag{I-8.25}$$

where A_m is the average soil column acceleration, ρ the soil mass density, h the thickness of the soil column, V_S and γ_r the soil shear wave velocity and reference strain.

The reference shear strain is related to the elastic shear modulus, or wave velocity through:

$$\tau_{max} = \gamma_r \rho V_S^2 \tag{I-8.26}$$

It is then shown that the maximum ground surface acceleration is smaller than twice the average acceleration; consequently:

$$\ddot{u}_{max} \leq 2\frac{V_S^2 \gamma_r}{h} \tag{I-8.27}$$

The ground surface acceleration $\ddot{u}$is related to the rock acceleration $\ddot{u}_r$ by the following equation:

$$2\left(\frac{\ddot{u}_r}{\ddot{u}}\right)^2 = 0,25 + 2\left(\frac{\ddot{u}_r}{\ddot{u}_{max}}\right)^2 \tag{I-8.28}$$

From the above equation it appears that the maximum ground surface accelerations are attained for an infinite rock acceleration; 90% of the maximum ground surface acceleration is obtained for a rock acceleration equal to 73% of this maximum value. Finally, the ground surface acceleration becomes equal to the rock acceleration when the latter is equal to 94% of the maximum ground surface acceleration, which means that up to that value amplification is always predicted regardless of the soil characteristics and frequency content of the input motion.

8.3.2 Application to the Sites

The parameters entering the previous equations (I-8.25 to I-8.27) are summarized in Table I-8.3 for all five sites. With those parameters, the maximum computed ground surface accelerations are listed in the last column of the table.

The values computed above are smaller than those calculated in paragraph 2.0. The difference is as large as 40% for all sites except Leibstadt for which it is limited to 13%.This may possibly be attributed to the fact that Betbeder's solution assumes a constant shear modulus profile, which overestimates the natural frequency of the deposit; furthermore only the fundamental mode of vibration is considered and contribution of higher modes is neglected.

8.4 Amplification from Non-linear Site Response Analyses

The nonlinear site response analyses performed for the evaluation of the amplification factors can be used to tentatively assess the maximum ground surface accelerations. Numerous calculations covering a wide range of magnitudes, peak ground accelerations and soil properties have been carried out by the subcontractors. Those calculations are presented in references AMEC [2010c] (TP3-TB-1046), Pecker [2010] (TP3-TB-1055), Pelli [2010] (TP3-TB-1056) and their results embedded in the database and can be processed using the Matlab plotting tool Hölker [2013a]. Within the context of this report, which deals with the prediction of the maximum ground surface accelerations, the 85% fractile of the results and the upper bound soil

properties, which maximizes the soil strength, have been considered as upper bounds. Since most nonlinear calculations are not considered reliable above 30-40Hz by all subcontractors, the spectral accelerations at 30Hz are used as proxies for the peak ground accelerations; this assumption will probably slightly overestimate the true peak ground accelerations, which is not a real concern for the objective of the report.

Figures I-8.18 to I-8.22 present for each site the computed response spectra at the ground surface for the magnitude 6 event with an input rock acceleration of 2.5g and upper bound soil properties (upper graph in the figure); medians and fractiles are depicted in the figures. The bottom part of the figures represents the variations with input rock accelerations of the spectral accelerations at 30Hz for the upper bound soil properties and magnitude 6 events; only median (or mean) values are available. The bottom figures are depicted to check if a bound in the spectral acceleration has been attained for 2.5g input acceleration; when extrapolation beyond 2.5g is deemed necessary to define the upper value, the median extrapolated value is corrected to define the 85% fractile according to the top figures.

Examination of the figures show that except, may be, for KKB and KKM the two stiffer sites, little extrapolation is needed to define the maximum value. Based on those figures the maximum ground surface accelerations estimated from the nonlinear runs are listed in Table I-8.3. The maximum ground surface acceleration appears to be almost site independent, which could be explained by the fact that all sites have similar strength characteristics and that, according to the theoretical results of paragraph 2.0, the depth does not seem to play a major role since the maximum strength is mobilized in the top 10 meters. The major difference occurs for KKL and may be explained by the non homogeneous soil profile, with the cemented layer in depth, which drives away the theoretical model from the actual one.

8.5 Conclusions

The analyses carried out in this report are intended to define the maximum ground surface accelerations that could take place at the surface of any of the Swiss NPPs. Three different analyses have been implemented: two analytical models, one published in the literature and one specifically developed for this study; the third analysis is based on the results of the nonlinear site response analyses carried out independently.

From the results presented in this report and summarized in Table I-8.5, the following conclusions can be drawn:

- Betbeder's model seems, as compared to the other two methods, to underestimate the maximum ground surface accelerations that could develop on a given site.
- The alternative analytical model seems to yield better predictions for the maximum ground surface accelerations when compared to the nonlinear site responses analyses.
- The maximum ground surface acceleration does not seem to be very dependent on the site; this has been explained by the similarity between the strengths of the materials found at the five sites.

Based on those results proposals are made in Table I-8.5 for the possible maximum ground surface accelerations; for the reasons explained above they do not differ significantly from one

Table I-8.1: Parameters for maximum ground acceleration calculations.

Parameter	KKG	KKB	EKKB	KKL	KKM
V_S [m/s]	73	63	72	80	54
p	0.39	0.33	0.36	0.43	0.36
d [m]	5.2	3.2	4.0	4.0	12
h [m]	28.5	9.0	22.0	41.0	8.0
Water table depth [m]	6.5	6.0	6.0	26.0	4.0
f [°]	45	46.5	46.5	42	37.5
c [kPa]	35	35	35	35	35
e_{ref}	0.02	0.02	0.02	0.02	0.02
s_{ref} [MPa]	0.1	0.1	0.1	0.1	0.1

site to another and range from 0.25 g to 0.30 g. It is interesting to note that those values are not contradicted by observed ground accelerations, even for the last very strong earthquake in Japan on 11. March 2011 where maximum recorded accelerations reached 2.0 g to 3.0 g (Fig. I-8.23). However, these results must be taken with caution since the nature of the recording sites is unknown at this stage.

Table I-8.2: Frequencies and mode participation factors.

		KKG	KKB	EKKB	KKL	KKM
Mode 1	Frequency [Hz]	0.6	1.68	0.77	0.45	1.65
	Spectral acceleration [m/s^2]	1.27	4.84	1.74	0.81	4.74
	Mode participation factor	1.315	1.299	1.311	1.33	1.284
	Modal mass [%]	0.79	0.8	0.79	0.78	0.8
Mode 2	Frequency [Hz]	1.71	4.85	2.18	1.25	4.87
	Spectral acceleration [m/s^2]	4.95	15	6.8	3.31	15
	Mode participation factor	-0.493	-0.467	-0.488	-0.52	-0.442
	Modal mass [%]	0.1	0.1	0.1	0.1	0.1
Mode 3	Frequency [Hz]	2.83	8.06	3.61	2.07	8.11
	Spectral acceleration [m/s^2]	9.54	15	13.13	6.35	15
	Mode participation factor	0.302	0.283	0.298	0.322	0.266
	Modal mass [%]	0.04	0.03	0.04	0.04	0.03
Mode 4	Frequency [Hz]	3.95	11.27	5.05	2.88	11.35
	Spectral acceleration [m/s^2]	14.75	15	15	9.8	15
	Mode participation factor	-0.217	-0.203	-0.214	-0.232	-0.19
	Modal mass (%)	0.02	0.02	0.02	0.02	0.02
Mode 5	Frequency [Hz]	5.07	14.49	6.48	3.7	14.59
	Spectral acceleration [m/s^2]	15	15	15	13.57	15
	Mode participation factor	0.169	0.158	0.167	0.182	0.148
	Modal mass [%]	0.01	0.01	0.01	0.01	0.01

Table I-8.3: Soil parameters for Betbeder's model.

Site	Thickness [m]	Mass density [t/m^3]	Shear wave velocity [m/s]	Maximum shear stress [kPa]	Maximum ground surface acceleration [m/s^2]
KKG	28.5	2.2	500 - 550	430	13.7
KKB	9	2.2	350 - 400	200	20.2
EKKB	22	2.2	500 - 530	365	15.1
KKL	41	2.2	600 - 650	665	14.7
KKM	8	2.2	250 - 280	135	15.3

Table I-8.4: Maximum ground surface accelerations [g] from non-linear site response analyses.

	KKG	KKB	EKKB	KKL	KKM
Median	2.5	2.3	2.1	2.2	2.1
85% fractile	3	3	2.7	2.8	2.7

Table I-8.5: Summary of maximum ground surface accelerations [g].

	KKG	KKB	EKKB	KKL	KKM
Theoretical model	2	2.5	2.2	1.8	2.1
Betbeder's model	1.4	2	1.5	1.5	1.5
Non-linear site response analyses	2.5 - 3.0	2.3 - 3.0	2.1 - 2.7	2.2 - 2.8	2.1 - 2.7
Proposed range of values	2.5 – 3.0	2.5 – 3.0	2.2 – 2.7	2.3 – 2.8	2.1 – 2.6

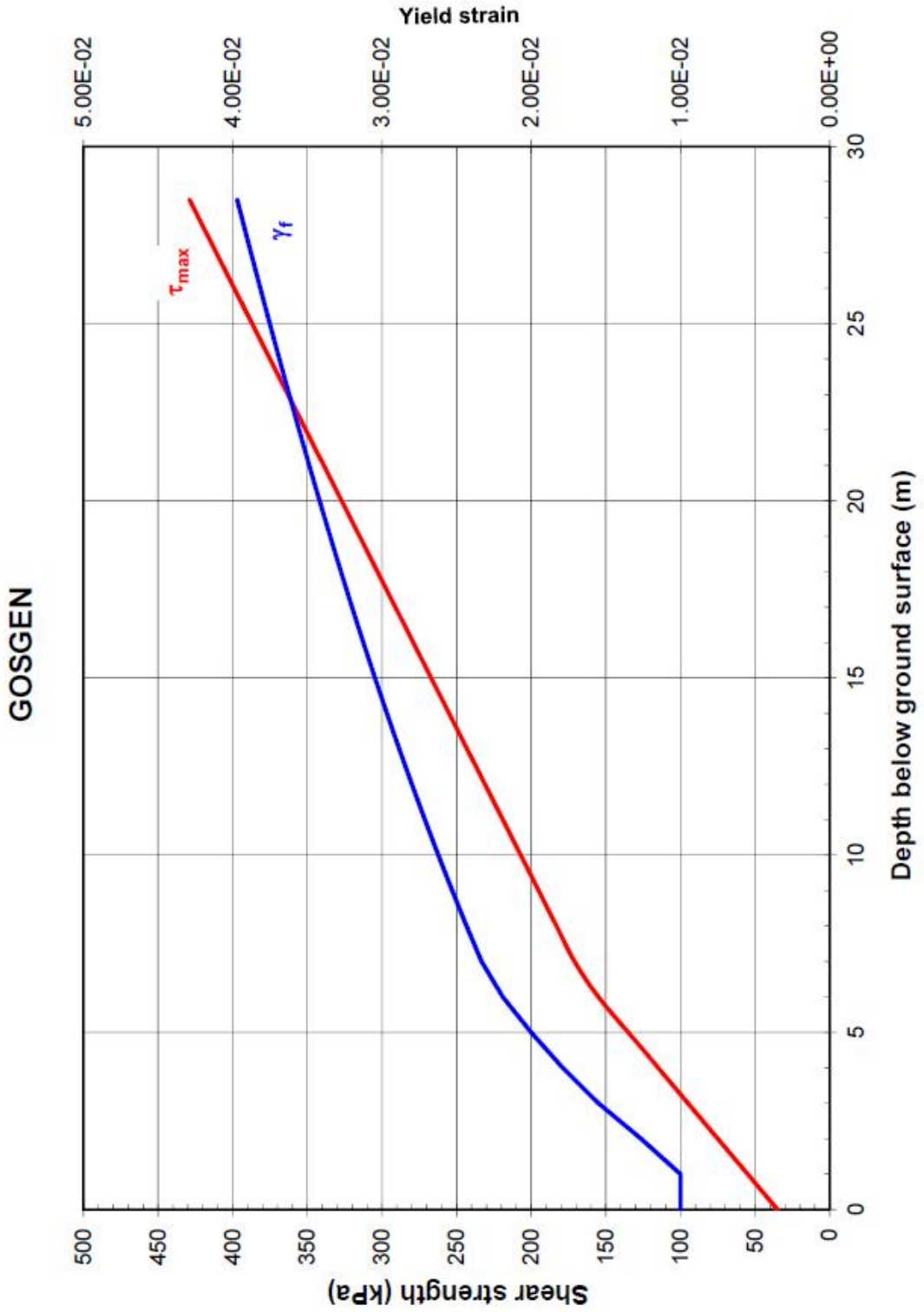

Figure I-8.2: KKG - Shear strength and yield strain versus depth.

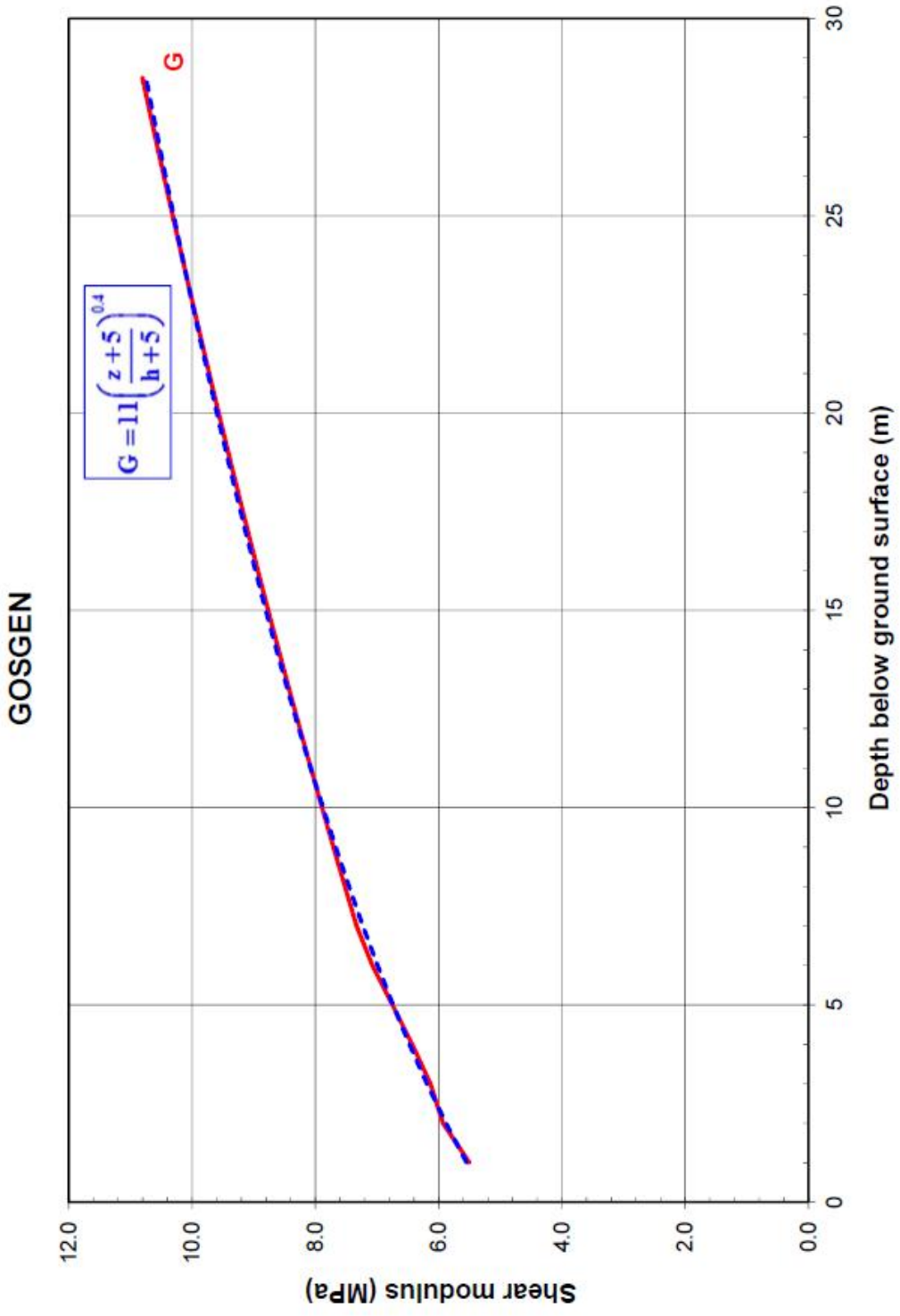

Figure I-8.3: KKG - Shear modulus versus depth.

Figure I-8.4: KKB - Shear strength and yield strain versus depth.

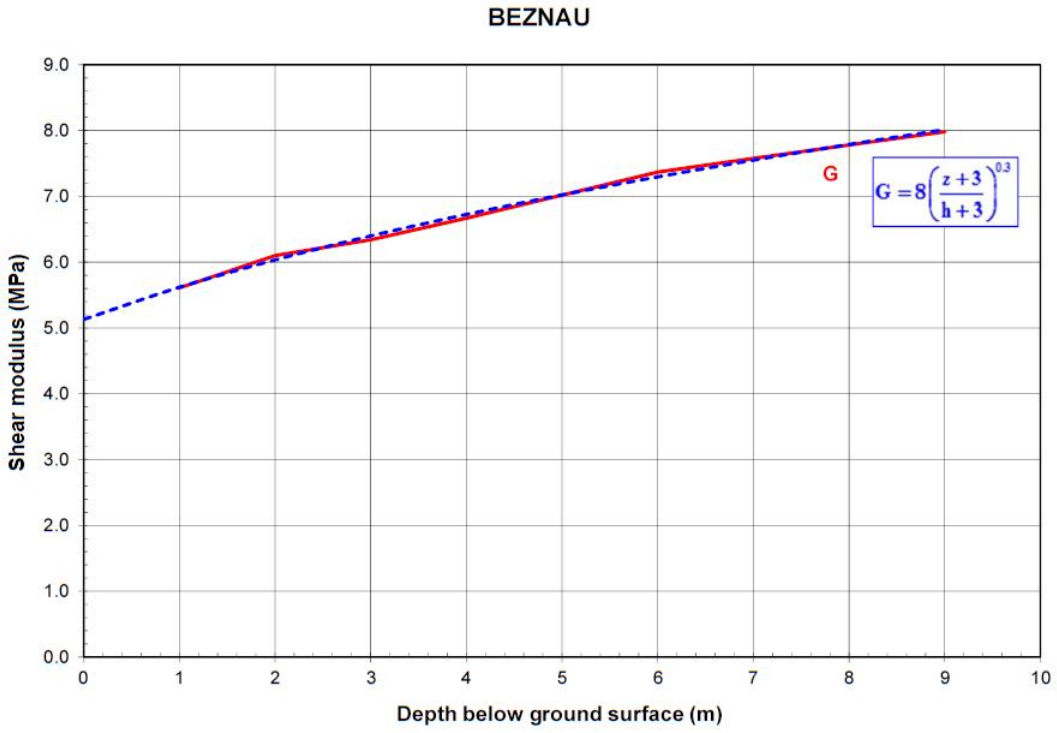

Figure I-8.5: KKB - Shear modulus versus depth.

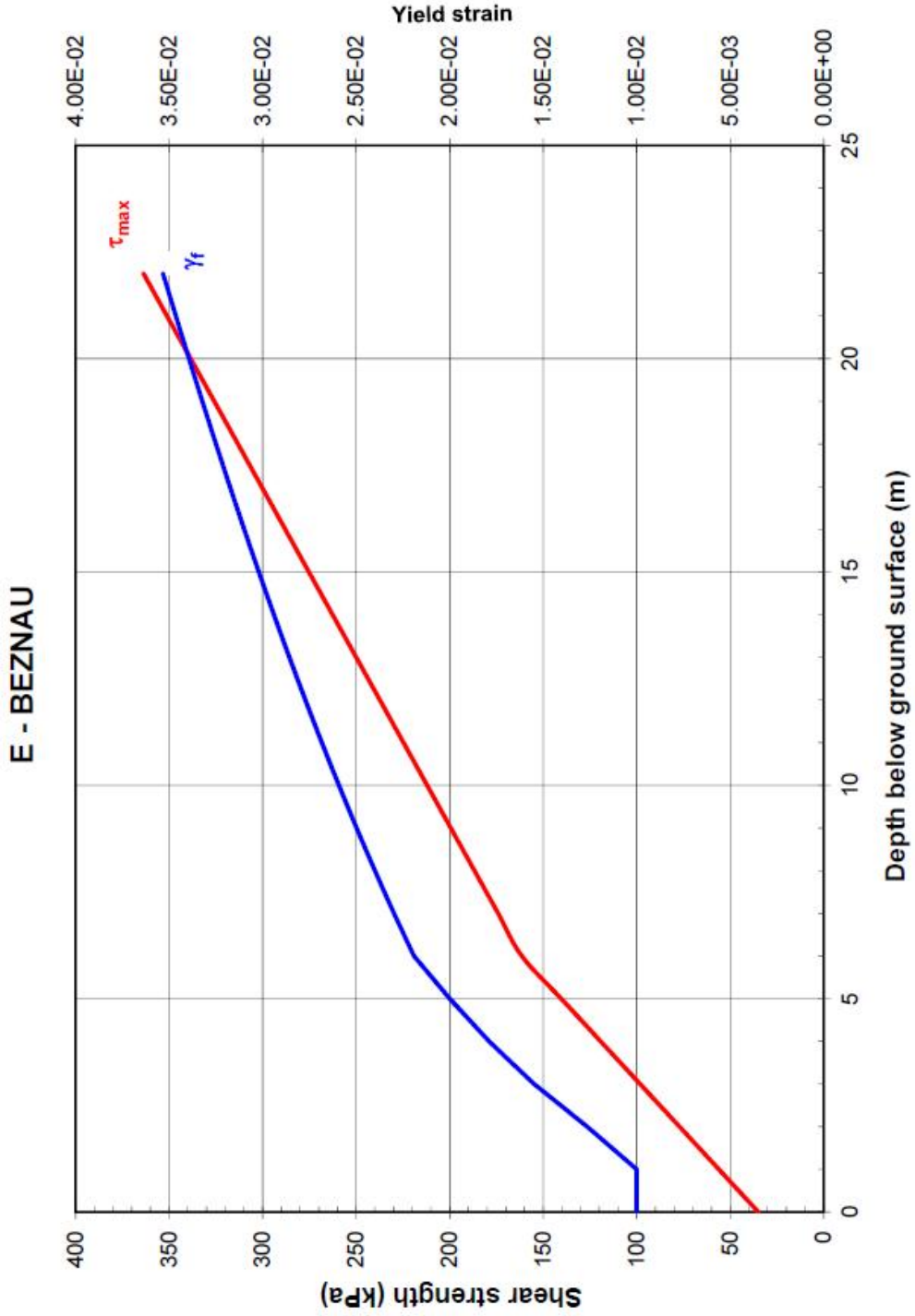

Figure I-8.6: EKKB - Shear strength and yield strain versus depth.

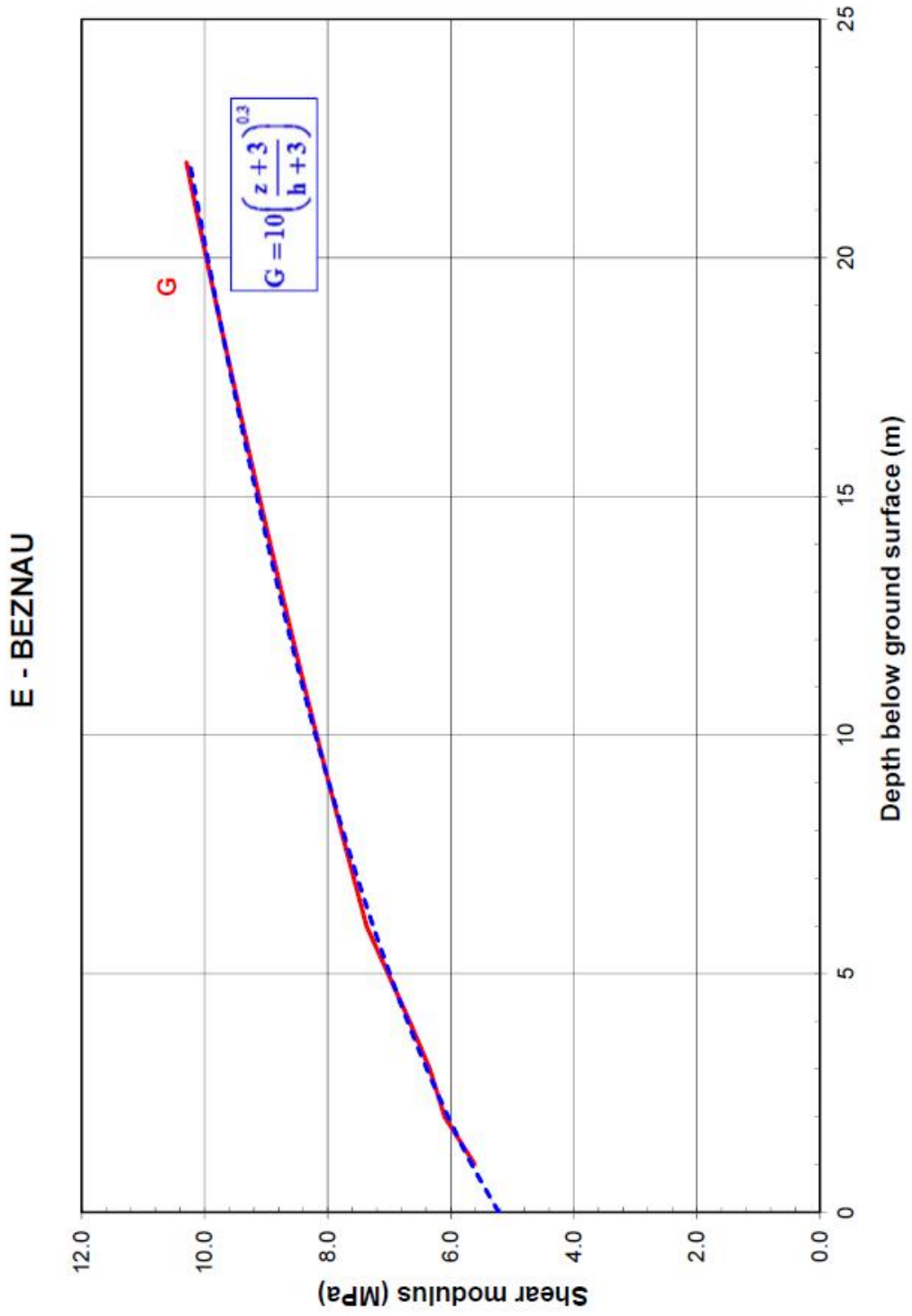

Figure I-8.7: EKKB - Shear modulus versus depth.

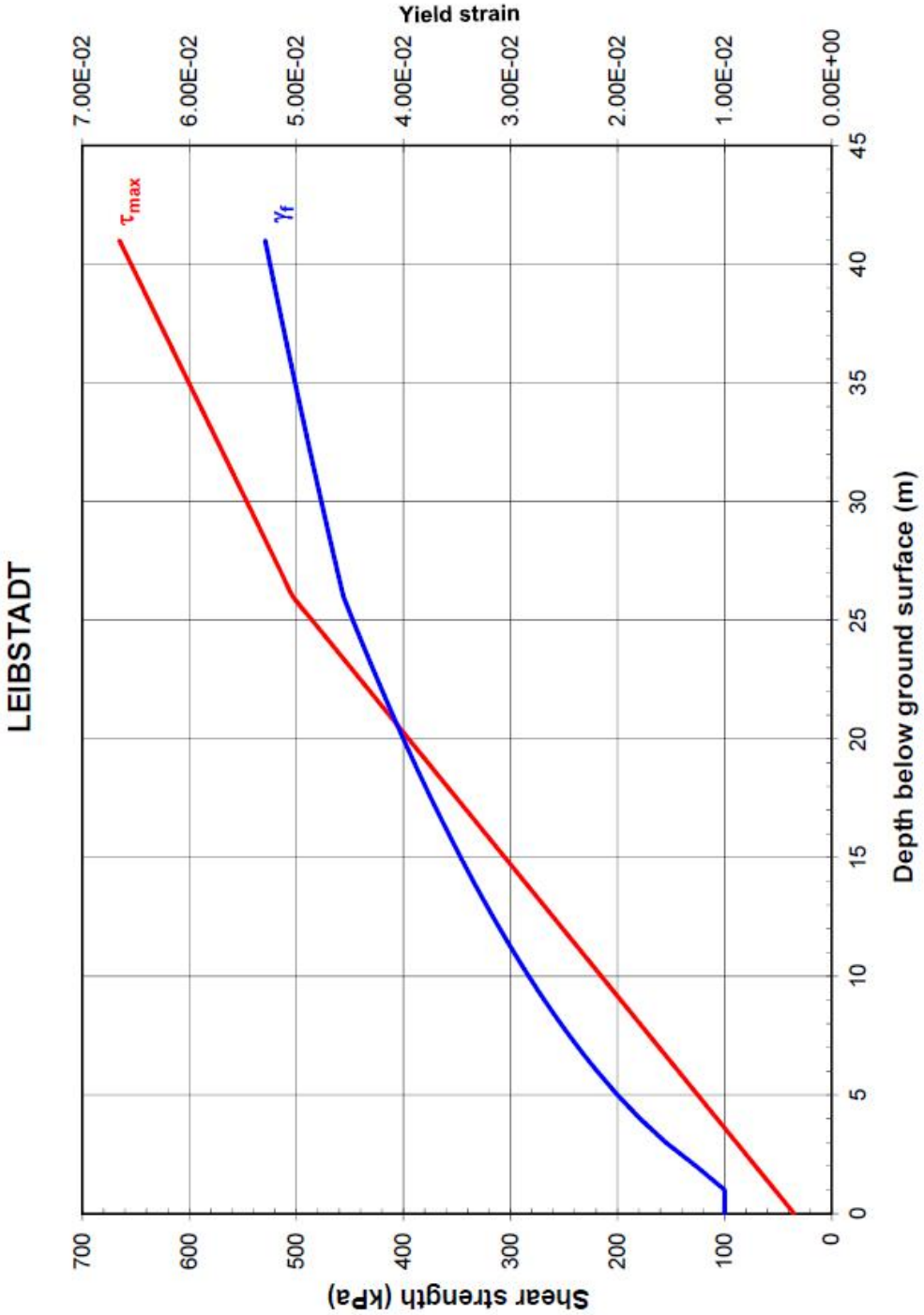

Figure I-8.8: KKL - Shear strength and yield strain versus depth.

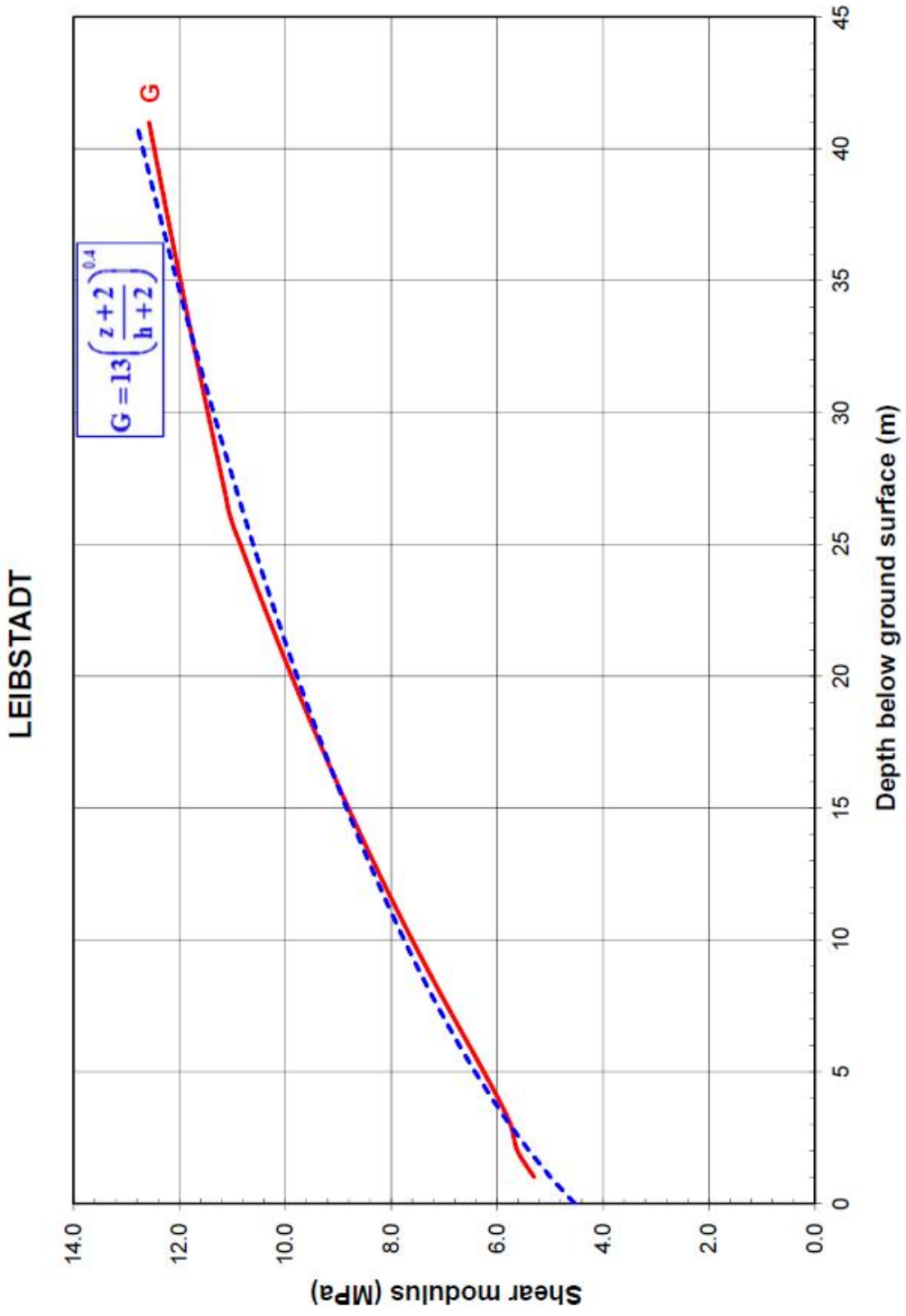

Figure I-8.9: KKL - Shear modulus versus depth.

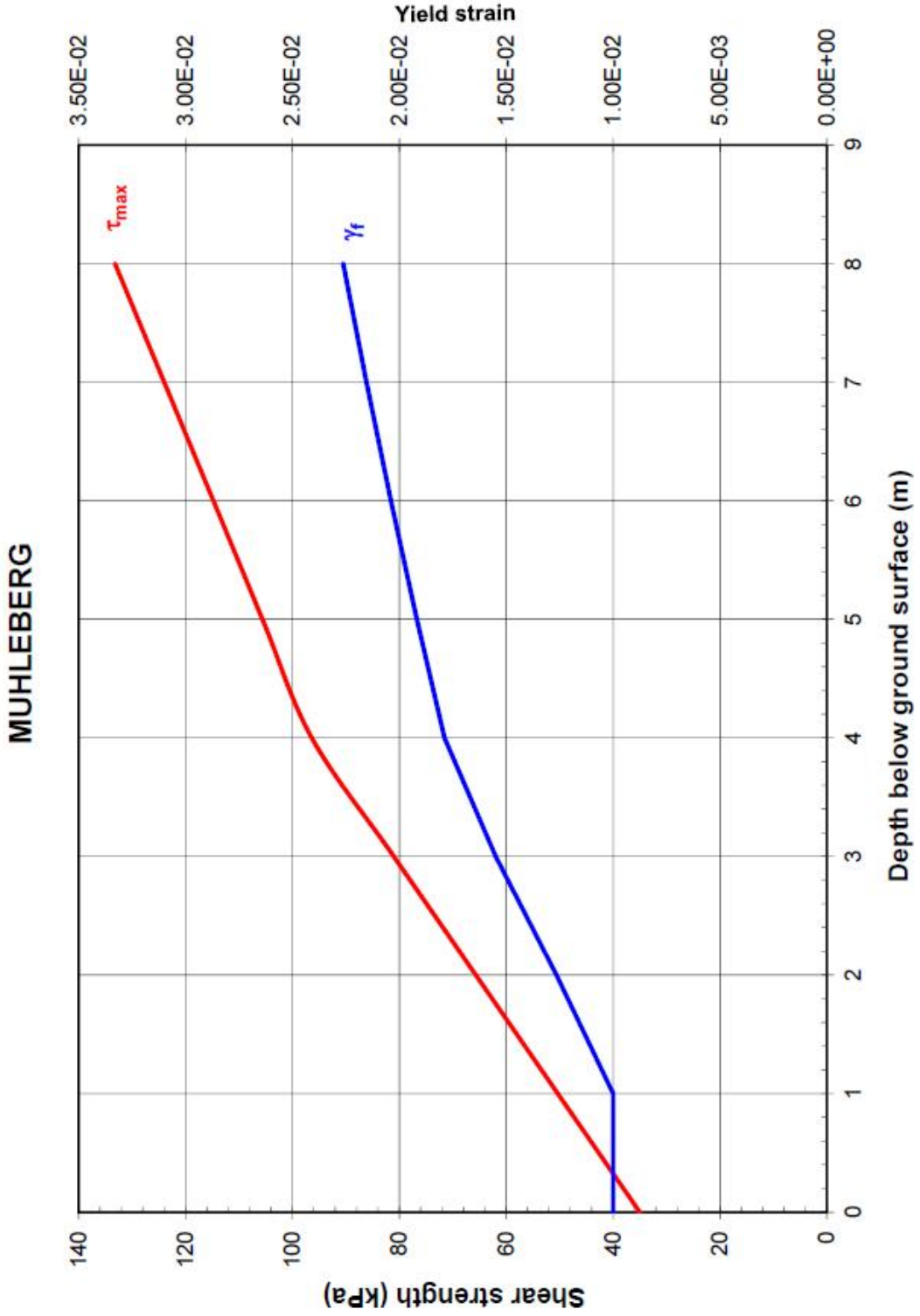

Figure I-8.10: KKM - Shear strength and yield strain versus depth.

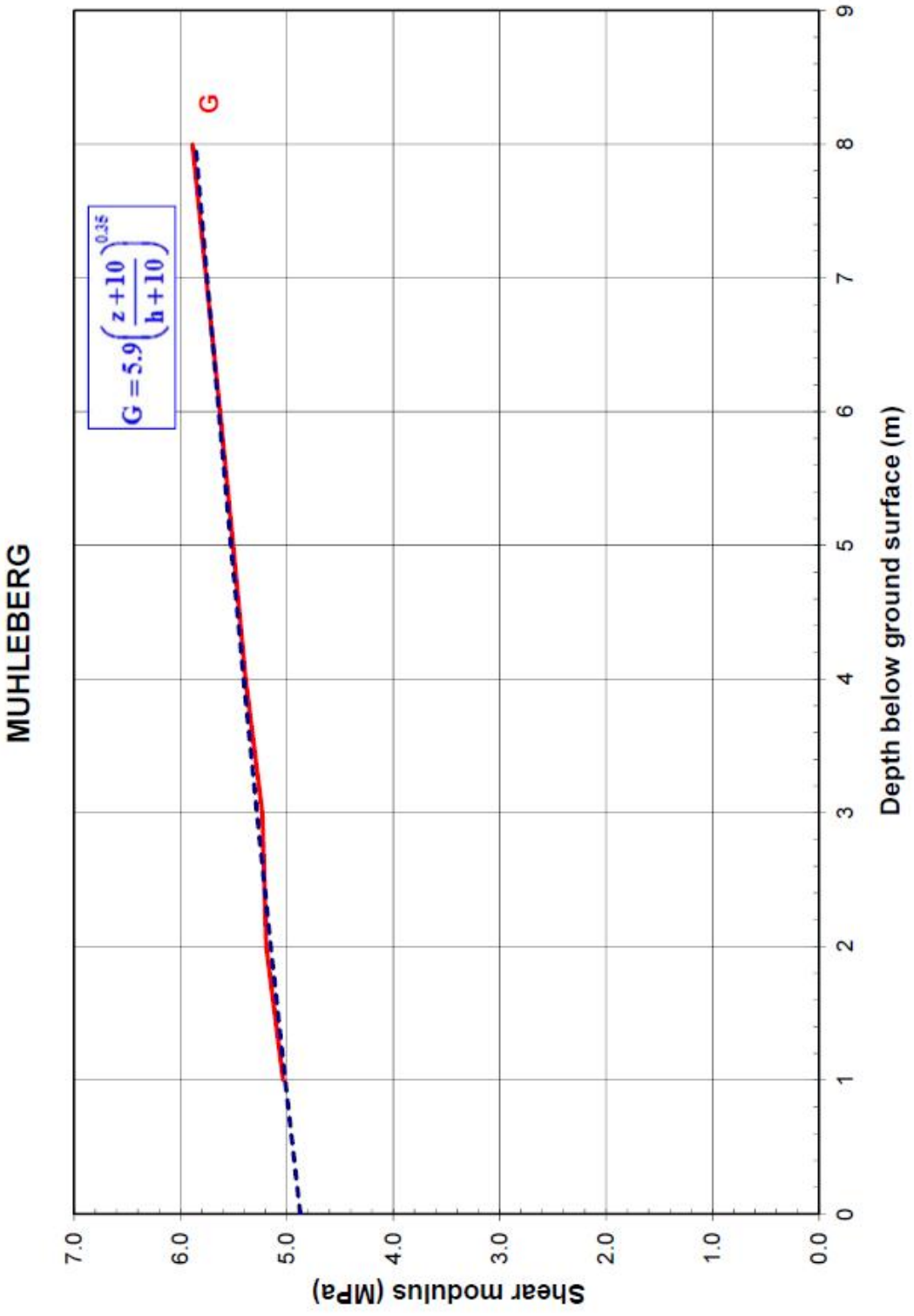

Figure I-8.11: KKM - Shear modulus versus depth.

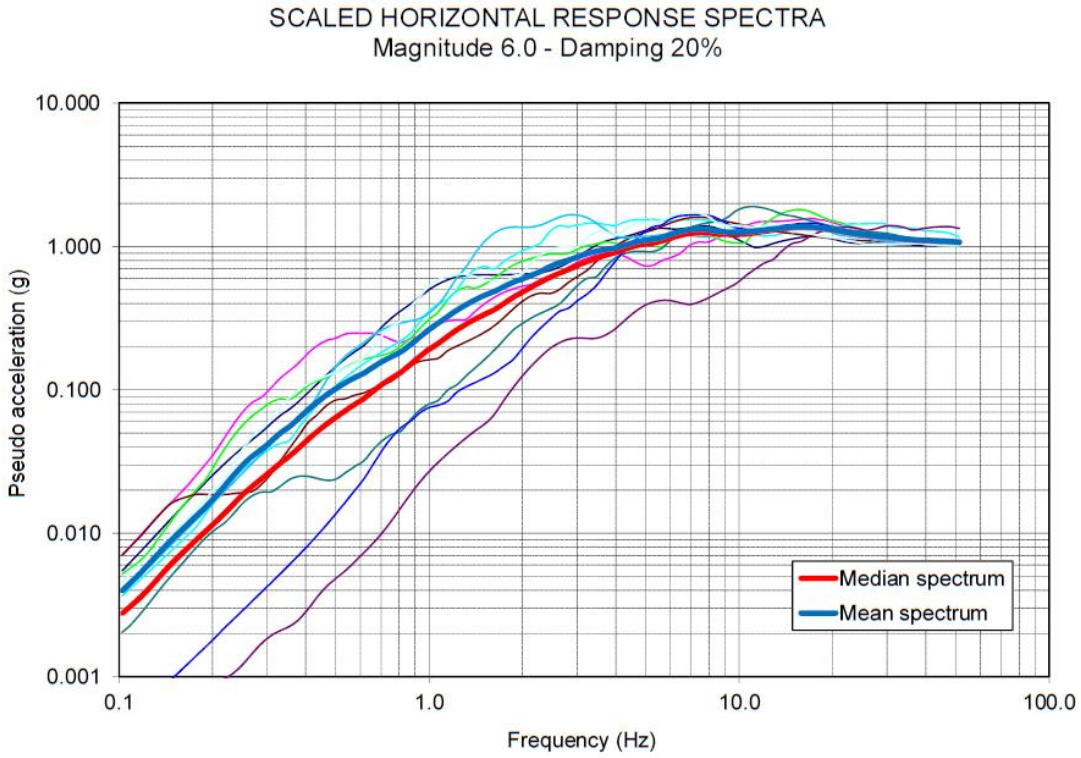

Figure I-8.12: Normalized rock spectrum.

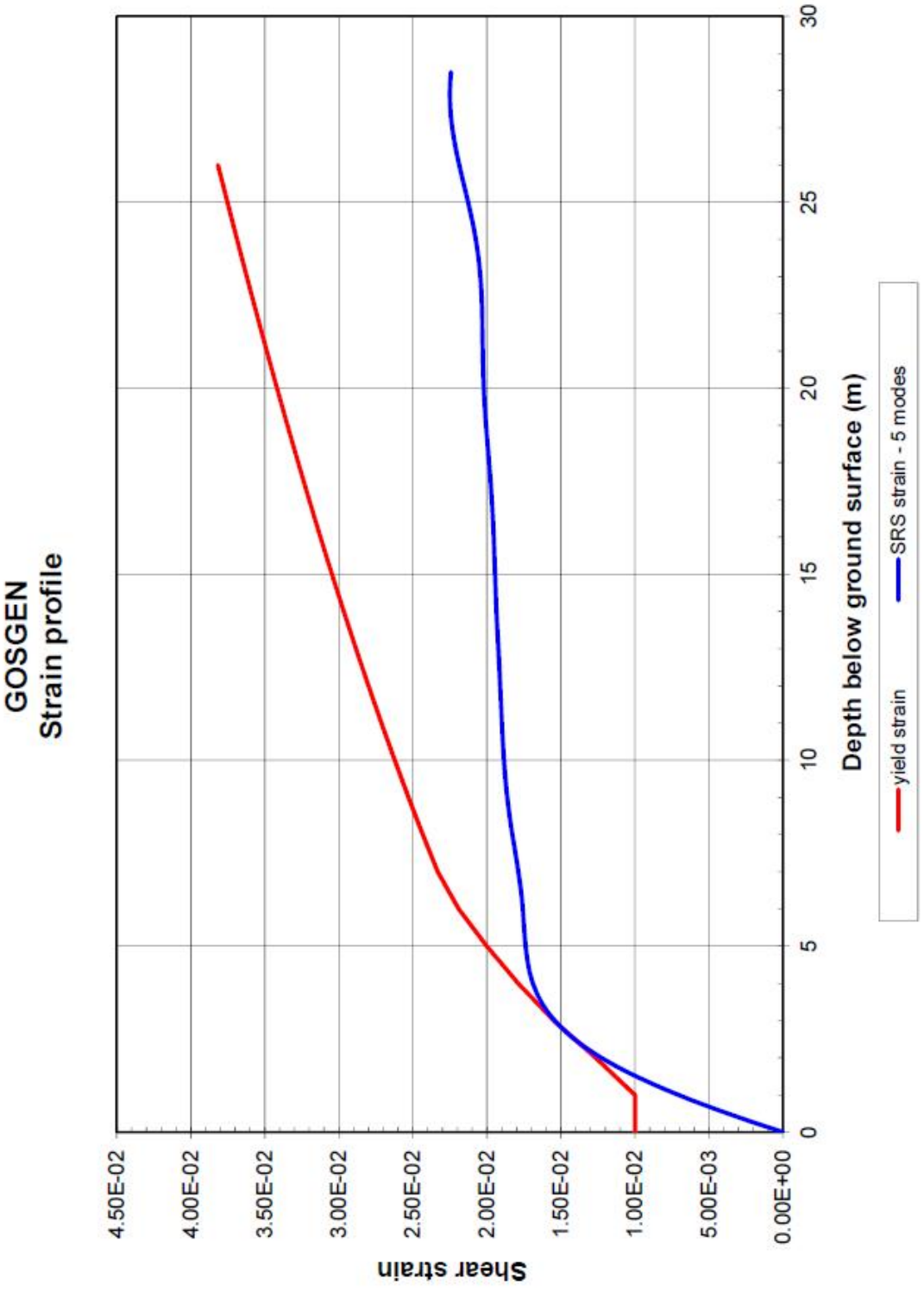

Figure I-8.13: KKG - Strain profile.

Figure I-8.14: KKB - Strain profile.

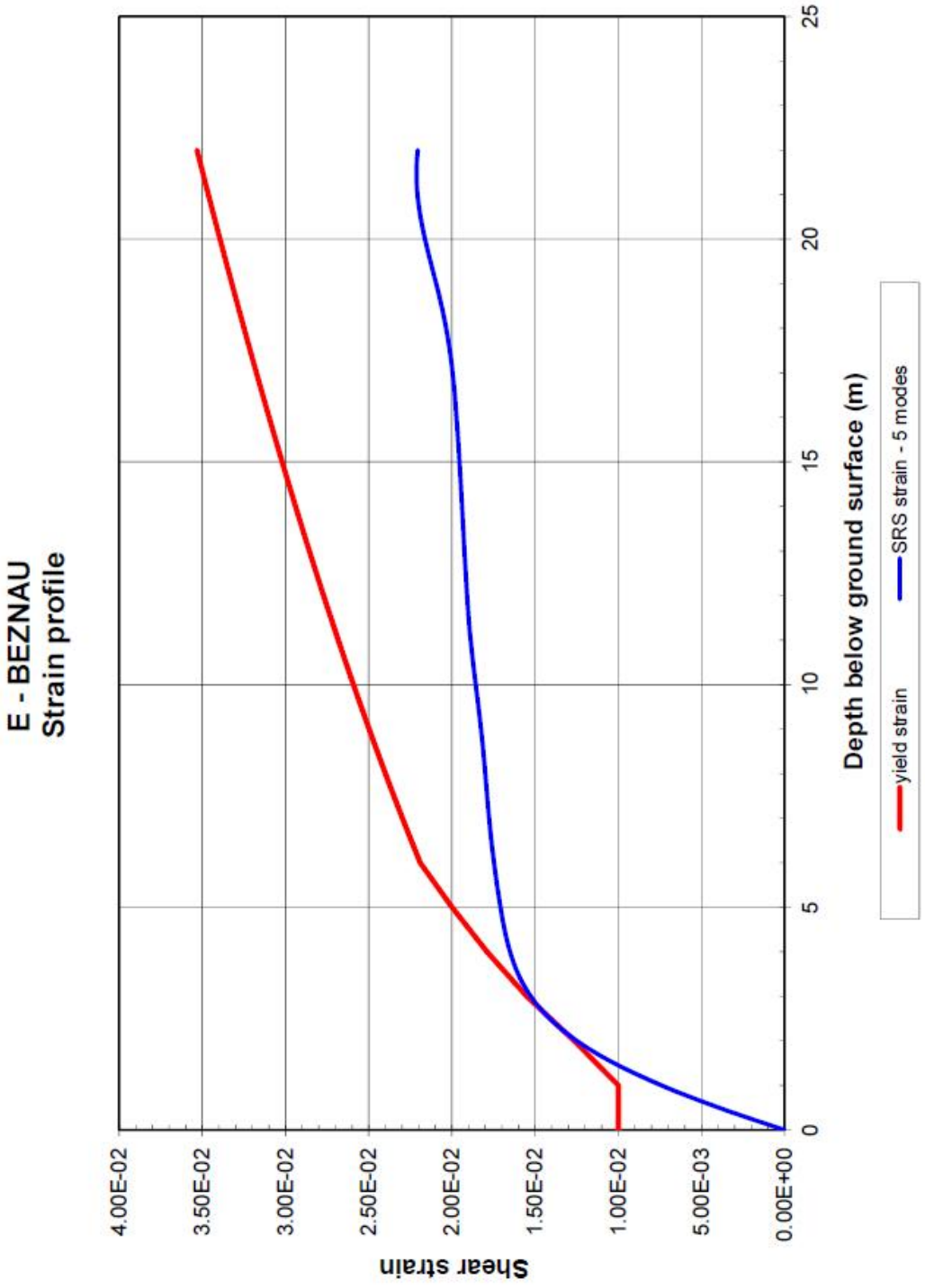

Figure I-8.15: EKKB - Strain profile.

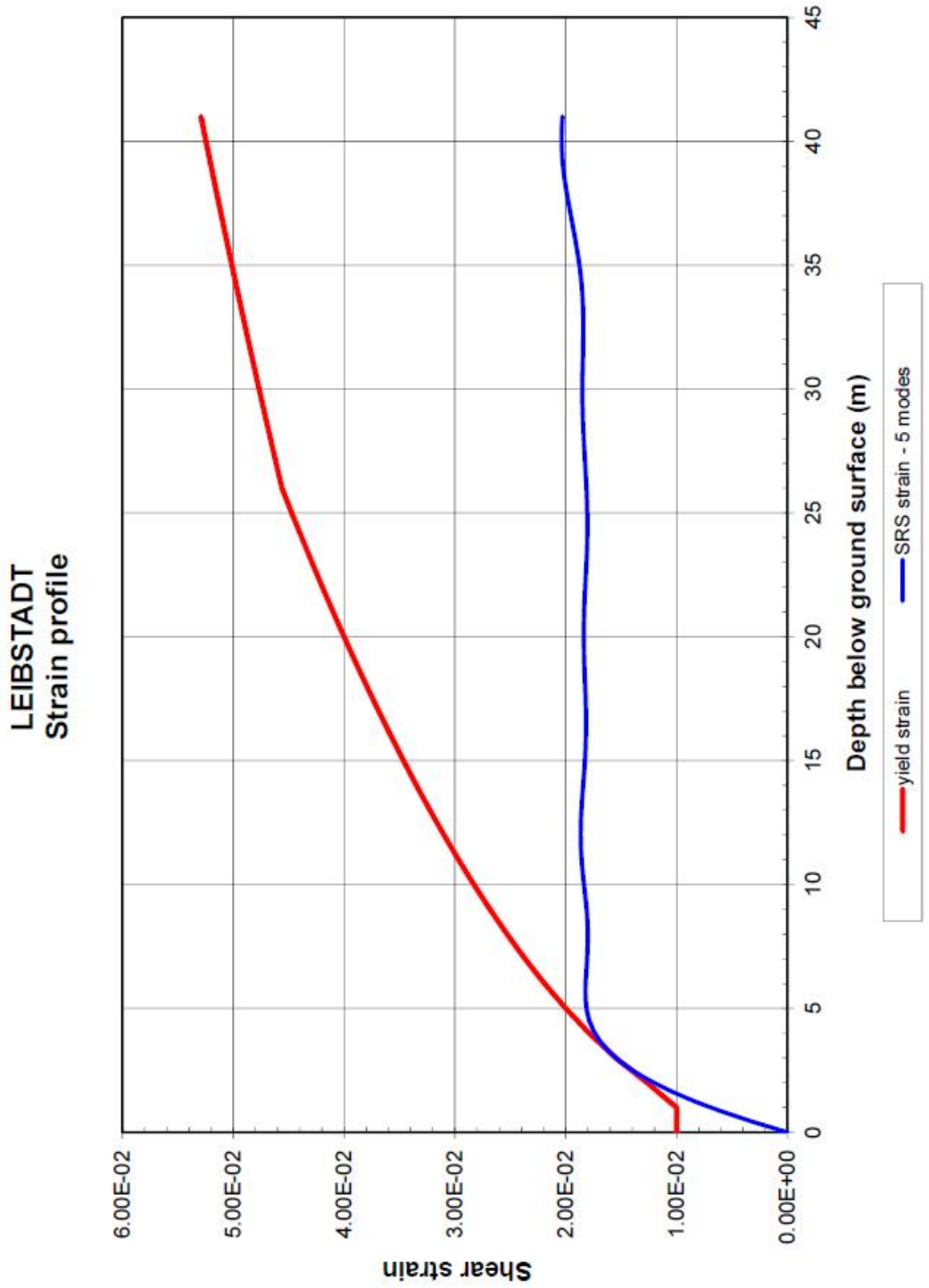

Figure I-8.16: KKL - Strain profile.

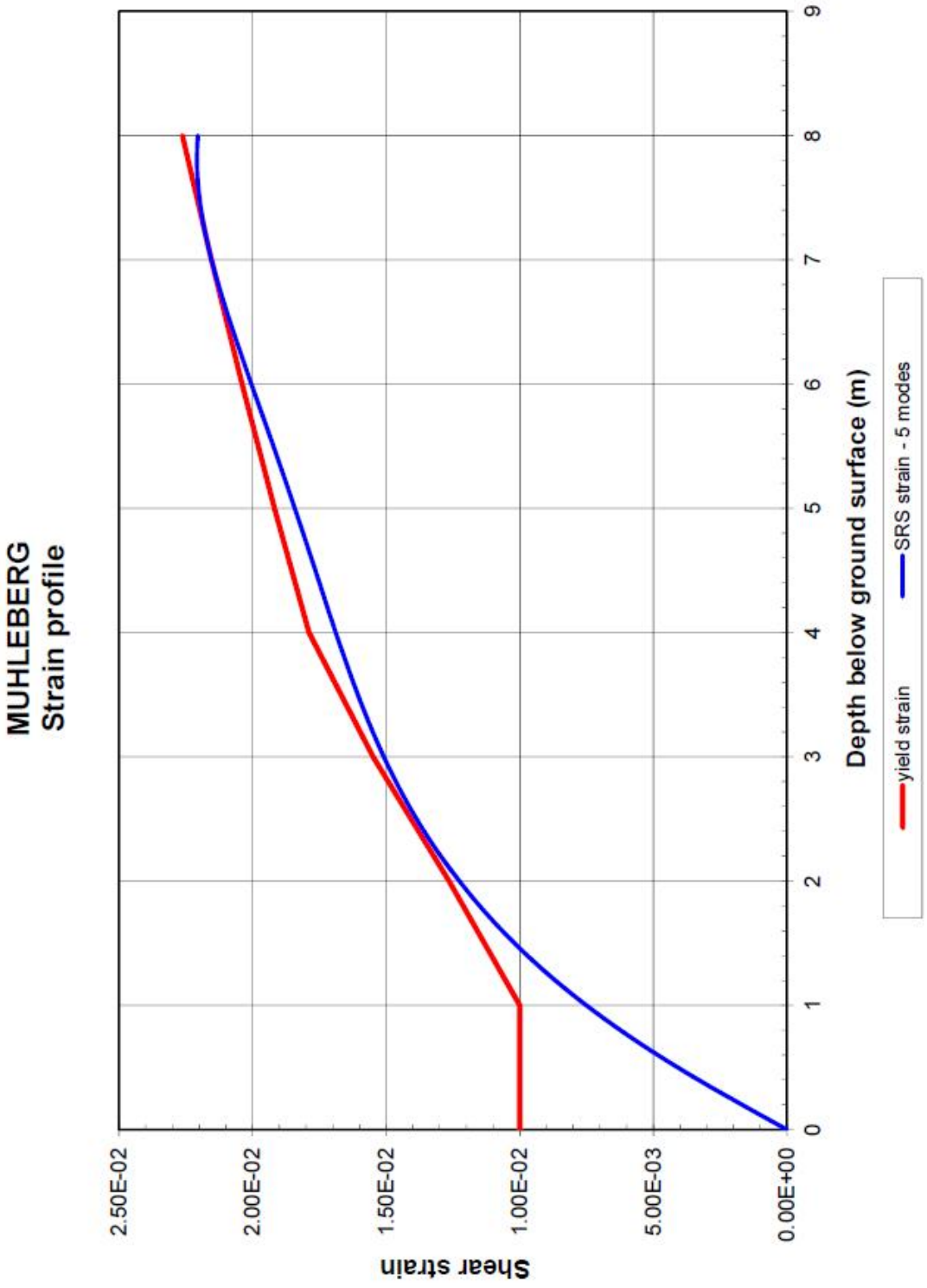

Figure I-8.17: KKM - Strain profile.

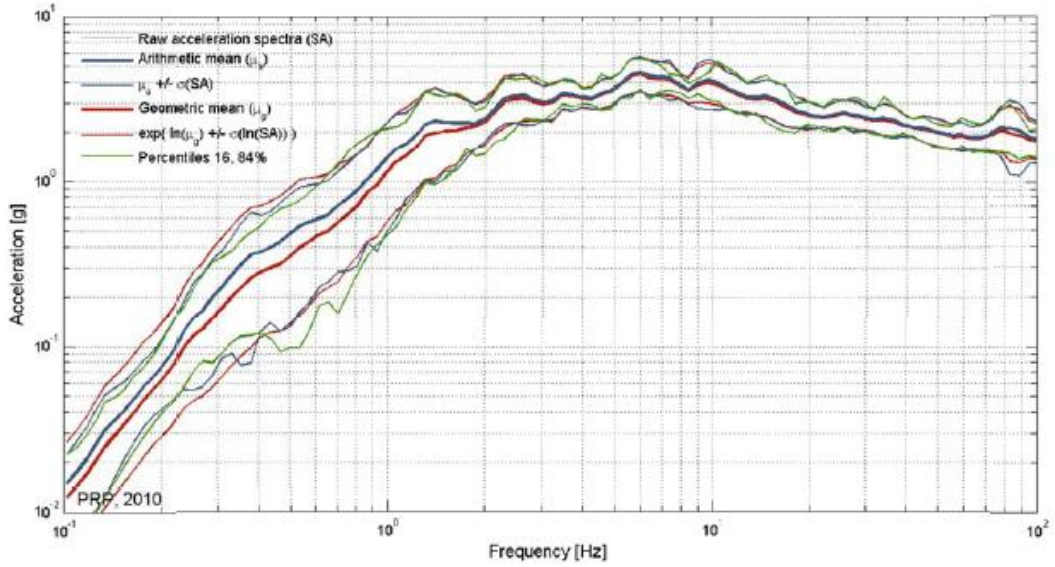

Goesgen, profile 6, material 3

Non linear 1
Magnitude 6, PGA 2.5g
Horizontal outcrop motion at surface

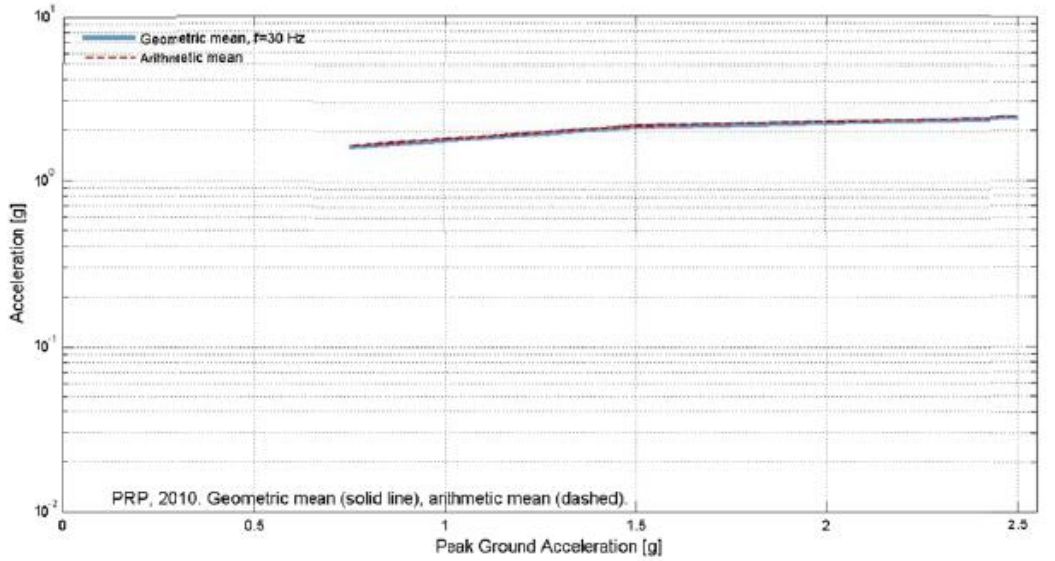

Goesgen, profile 6, material 3

Non linear 1
Magnitude 6, PGA <variable>
Horizontal outcrop motion at surface

Figure I-8.18: KKG - Ground surface response spectra for 2.5g; variation of spectral acceleration at 30Hz with pga.

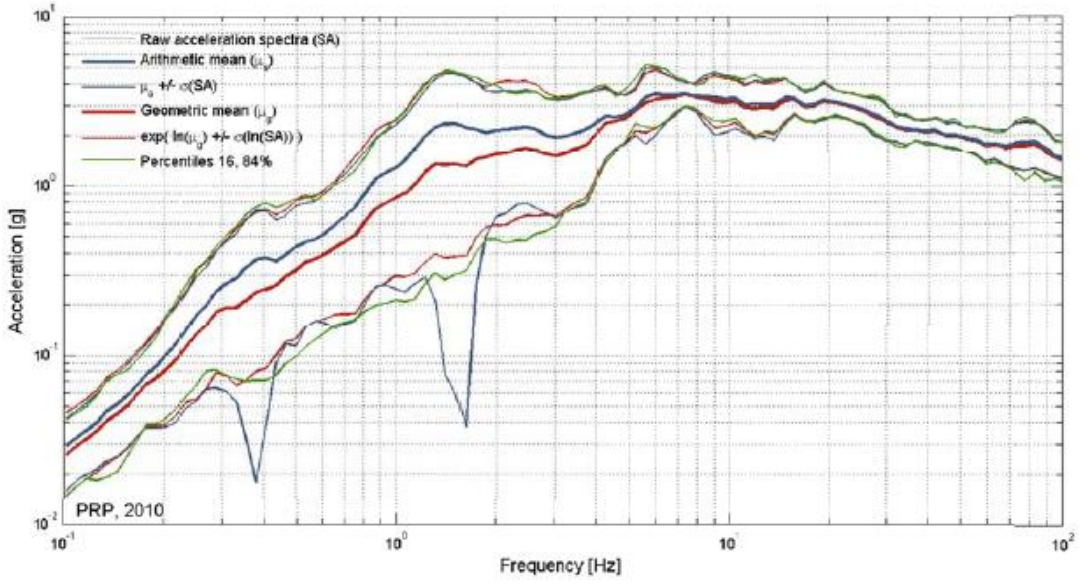

Beznau, profile 1, material 3

Non linear 1
Magnitude 6, PGA 2.5g
Horizontal outcrop motion at surface

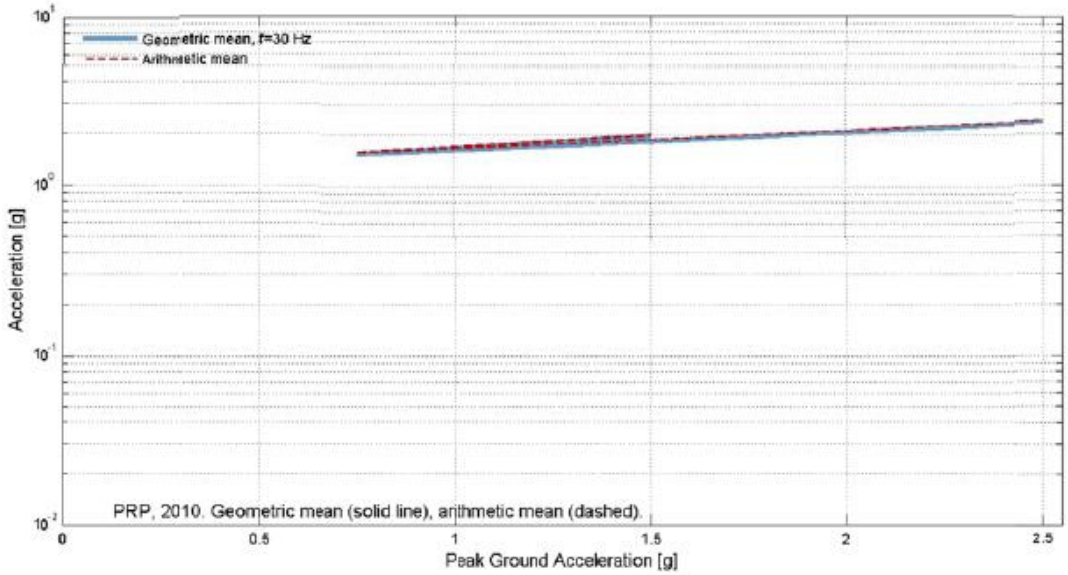

Beznau, profile 1, material 3

Non linear 1
Magnitude 6, PGA <variable>
Horizontal outcrop motion at surface

Figure I-8.19: KKB - Ground surface response spectra for 2.5 g; variation of spectral acceleration at 30 Hz with PGA.

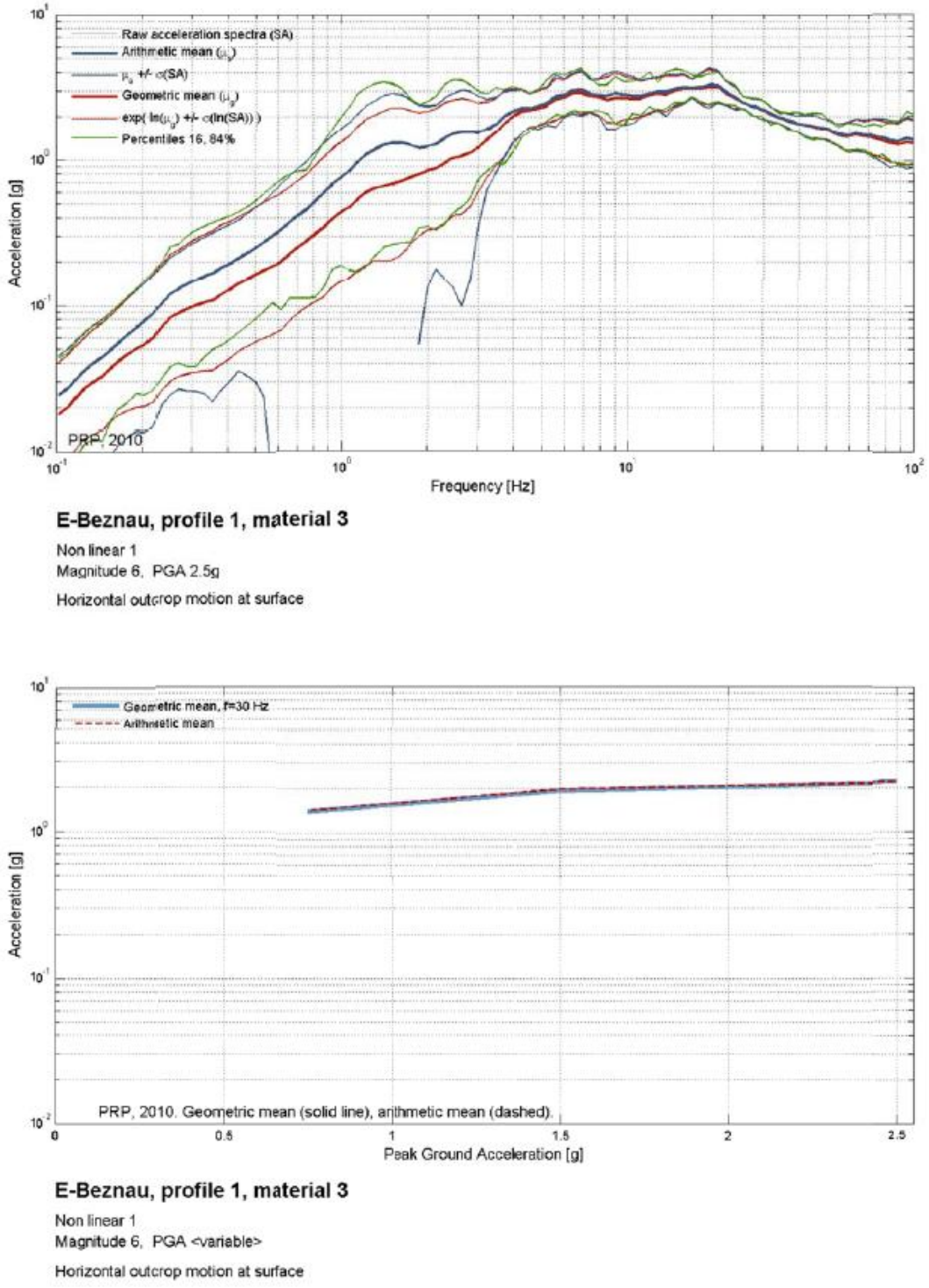

Figure I-8.20: EKKB - Ground surface response spectra for 2.5g; variation of spectral acceleration at 30Hz with pga.

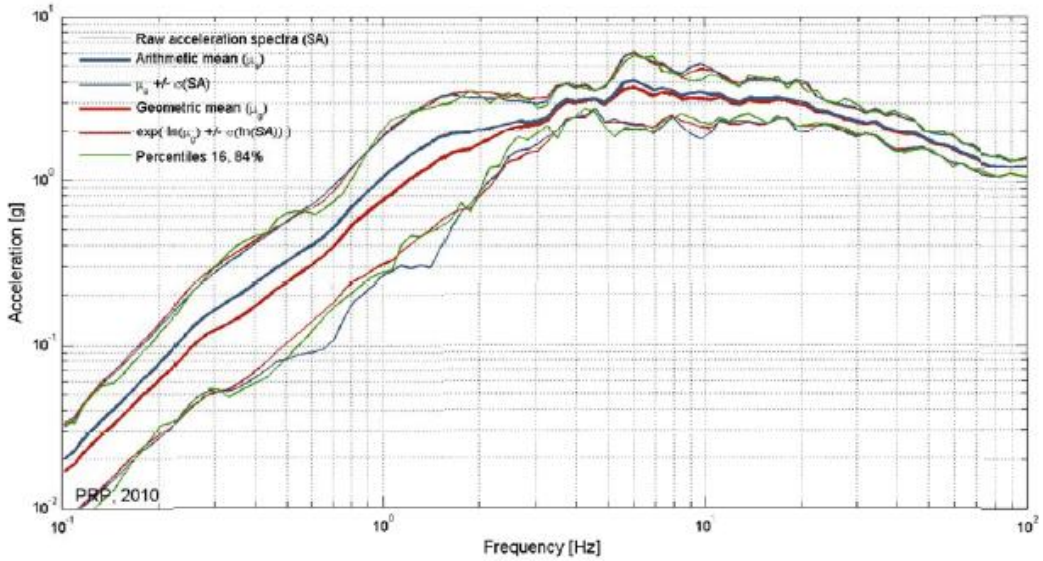

Leibstadt, profile 1, material 3

Non linear 1
Magnitude 6, PGA 2.5g

Horizontal outcrop motion at surface

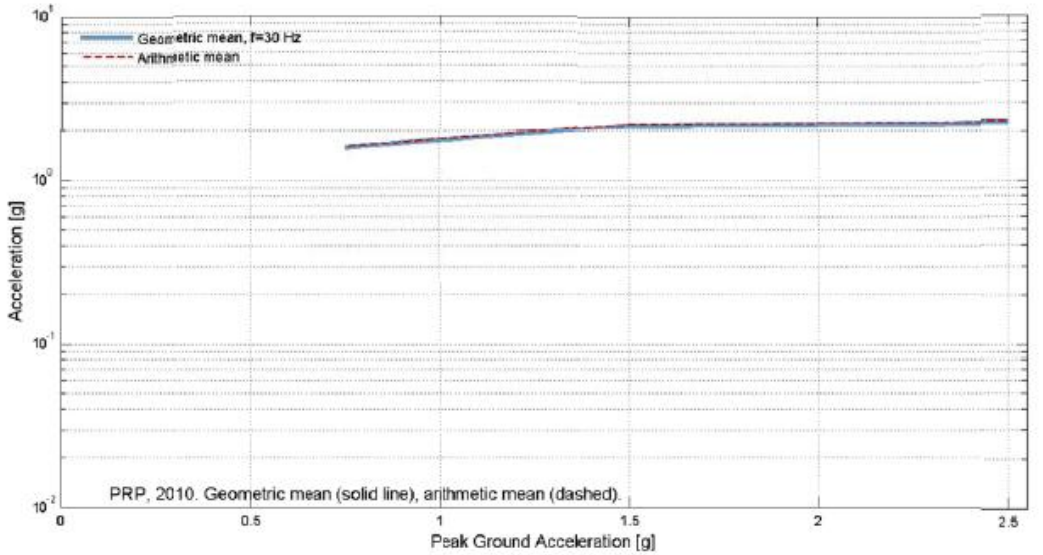

Leibstadt, profile 1, material 3

Non linear 1
Magnitude 6, PGA <variable>

Horizontal outcrop motion at surface

Figure I-8.21: KKL - Ground surface response spectra for 2.5g; variation of spectral acceleration at 30Hz with pga.

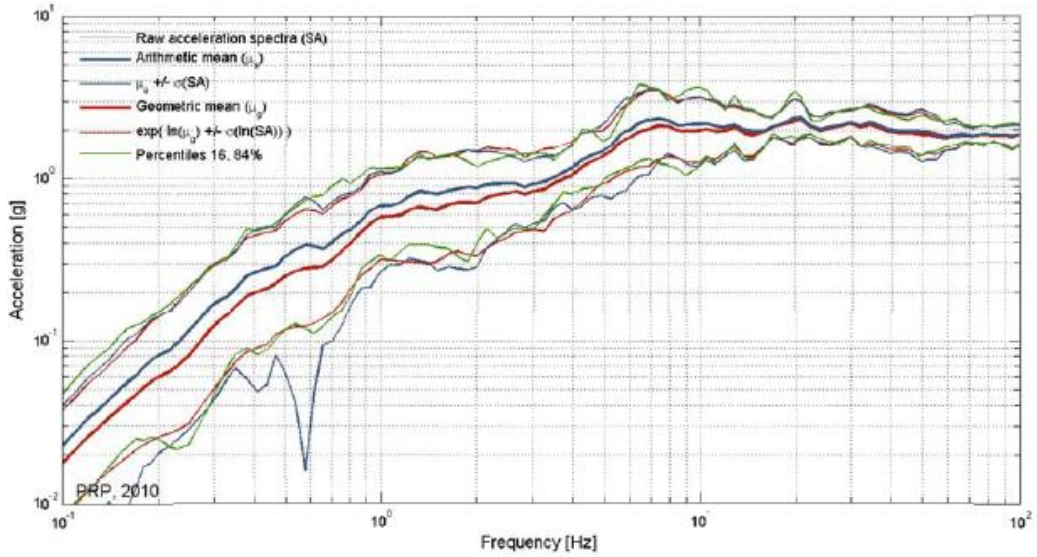

Muehleberg, profile 1, material 3

Non linear 1
Magnitude 6, PGA 2.5g
Horizontal outcrop motion at surface

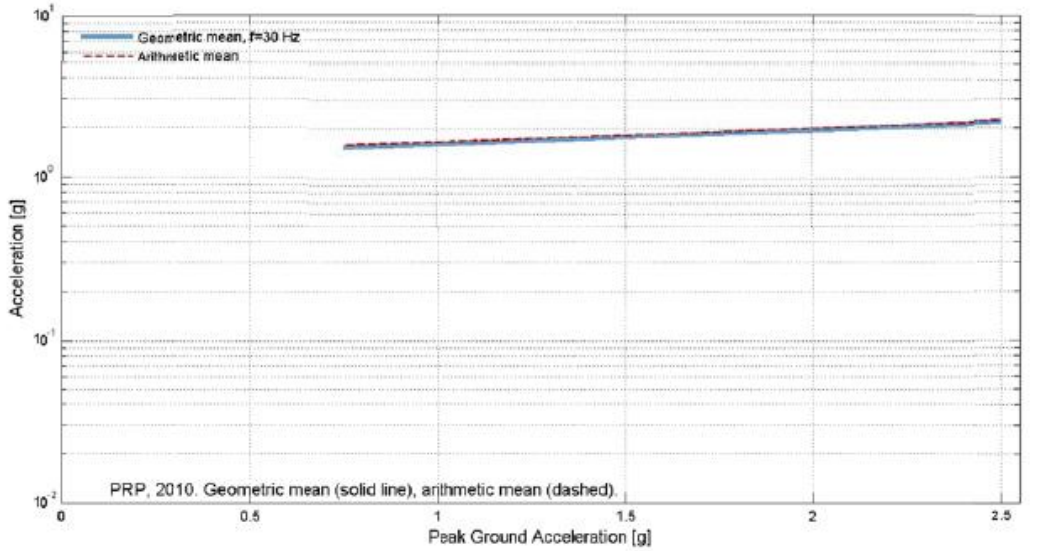

Muehleberg, profile 1, material 3

Non linear 1
Magnitude 6, PGA <variable>
Horizontal outcrop motion at surface

Figure I-8.22: KKM - Ground surface response spectra for 2.5g; variation of spectral acceleration at 30Hz with pga.

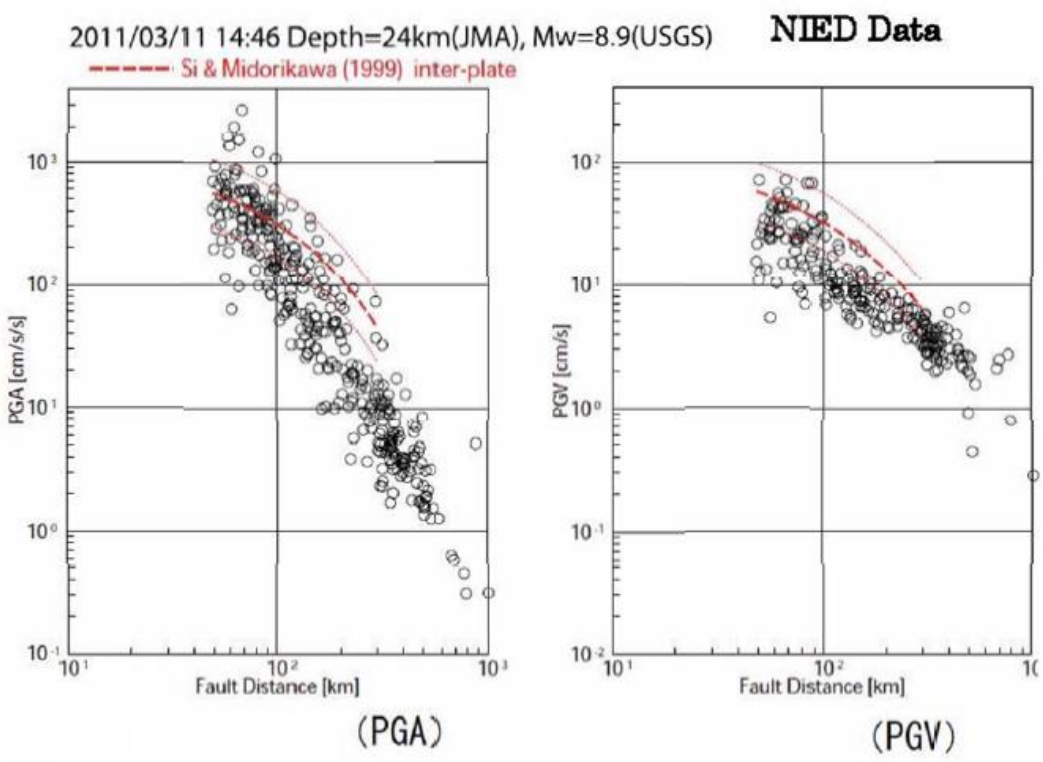

Attenuation of PGA (cm/s/s) of the horizontal component and PGV (cm/s); PGA is the measured value and PGV is the computed value converted for the hard foundation with the shear velocity of 600m/s. Data source: NIED

Figure I-8.23: Recorded accelerations during the March 11, 2011 earthquake in Japan.

Chapter 9

Liquefaction Evaluation

The possibility of liquefaction was investigated for all the NPP sites by [Pecker and Studer 2013] (EXT-TN-1270). This was done, on the one hand, by means of 1D non-linear soil amplification calculations with effective stresses and, on the other hand, with the aid of empirical relations, e.g. [Youd and Idriss 2001]. Additional comments provided by the SP3 experts at an earlier stage are summarized below.

9.1 Comment on Site Investigations for KKG & ATEL - Static and Dynamic Tests

(Comments on report No. 2008_01_003: "PEGASOS Refinement Project - Standortuntersuchungen für KKG & ATEL - Statische und dynamische Versuche, ZAF e.V., HTW Dresden")

Permeability at the Gösgen Site:

In the report is stated that no liquefaction occurred for silty sand (soil type no 2) in undrained cyclic triaxial tests.

Usually, the stress path for identification of liquefaction potential is chosen in a way that the deviator changes its algebraic sign. During the test, the stress path changes between triaxial compression and extension.

The measurements indicate that the test was purely performed in extension mode. The deviator did not change its algebraic sign assuming a constant effective confining pressure σ'_3 of 150 κPa.

Regarding the grain size distribution, it can be expected that the silty sand will liquefy. In case the relative density is very high, the cyclic stress ratio need to be chosen accordingly high. However, at least cyclic mobility behavior should be seen in the measurements, which is not visible in Figure I-9.1.

Suggested Additional Work:

Following additional work should be performed:

Test No.	Diameter d [mm]	Height h [mm]	Density ρ [g/cm^3]	Initial water content w_a [-]	Final water content w_e [-]	Confining pressure σ'_3 [kPa]	Pore water pressure [kPa]
7_0	150.0	285.0	1.963	0.1462	0.1842	150.0	400.0

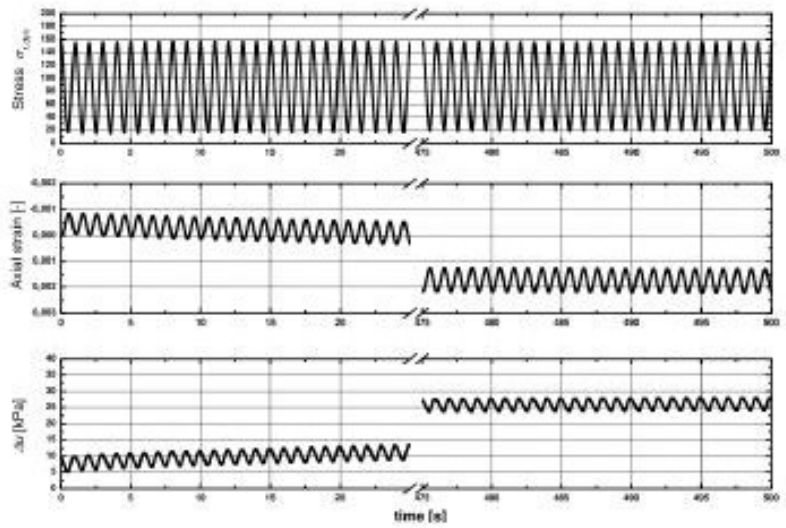

Figure I-9.1: Development of axial strain, the magnitude of applied cyclic stress, and the development of excess pore-water pressure plotted versus the time (soil type no. 2).

- Phase 1:
  - Checking of measurement data
  - Evaluation of relative density of soil samples investigated
  - Display diagram of stress path $q - p'$-plot
  - Display of $q - \varepsilon_q$-plot
  - Display of $p' - \varepsilon_1$-plot
  - Statement of the laboratory for the chosen stress path
- Phase 2:
  - repetition of undrained cyclical triaxial test with stress reversal
  - analysis of tests accordingly to phase 1

9.2 Amendment to Comment from 4 Nov. 2009 on Site Investigations for KKG & ATEL - Static and Dynamic Tests

(Related to the report No. 2008_01_003: PEGASOS Refinement Project - Standort-Untersuchungen für KKG & ATEL - Statische und dynamische Versuche, ZAF e.V., HTW Dresden)

A. Pecker and J. Studer discussed the topic of the cyclic tests performed in Dresden and came to the following conclusions:

1. Liquefaction potential will be assessed by SPT correlations. That is the best solution for insitu conditions.

2. Cyclic tests are needed for non linear calculations. Stiffness and damping parameters can be derived from results of the tests performed. Cyclic induced Pore water pressure increases can be derived from correlations to SPT values.

⇒ **Therefore, no repetition of tests is needed.**

It has to be mentioned again that A. Pecker and J. Studer consider liquefaction in the Alluvium not as a problem. The soil is dense and well compacted. In gravel under such conditions, the pore water increase is limited and a real liquefaction is not possible. In fine Materials (soil type 2) a certain pore water pressure increase will happen, but this material is located in lenses so the stability of the entire soil body is not affected and earthquake induced pore water increases will dissipate rapidly into the previous neighboring soil.

Part II

Assessments of Pierre-Yves Bard

Chapter 1

Evaluation Summary (EG3-ES-1014) of P.-Y. Bard

1.1 Introduction

The present document addresses the logic tree to be used for the assessment of site amplification factors and maximum ground motion for the horizontal component of ground motion, for the 5 NPP sites considered in this study, and the corresponding depths as indicated in the following table.

Table II-1.1: List of sites and depths for estimation of site-specific amplification factor.

Site		Depths		
Beznau	KKB	z1 = 0m	z2 = 15m	
E-Beznau	EKKB	z1 = 0m	z2 = 15m	
Gösgen	KKG	z1 = 0m	z2 = 9m	z3 = 15m
Leibstadt	KKL	z1 = 0m	z2 = 10m	
Mühleberg	KKM	z1 = 0m	z2 = 7m	z3 = 14m

Table II-1.2: List of V_{S30} values (m/s) for the various profiles of each site.

Site		P1	P2	P3	P4	P5	P6
Beznau	KKB	510	523	487	548		
E-Beznau	EKKB	489	548	468			
Gösgen	KKG	480	458	425	449	545	480
Leibstadt	KKL	545	457	580			
Mühleberg	KKM	537	506	508	411		

The travel-time average of S-wave velocity over the top 30M are indicated in Table II-1.1, II-1.2 for each of the various velocity profiles of each site. They are indicative of rather stiff sites, where no significant amplification would be expected according to usual standards. However, the presence at rather shallow depth of hard rock, with S-wave velocity values

much higher than the usual value of 800 m/s, results in non-negligible impedance contrasts responsible for wave trapping and subsequent resonant effects.

1.2 Median Amplification of Horizontal Ground Motion

1.2.1 Approach

The logic tree finally adopted for the probabilistic assessment of site-specific amplification factors within the PRP-SP3 project is deeply inspired from the logic tree developed for the PEGASOS project 8 years earlier. Several modifications were however introduced to account for the significantly enriched site information, for the larger number of numerical simulations performed for each site, and for the evolution of background knowledge and common understanding in about one decade. It is based mainly on a 'physical' interpretation of site effects, which are viewed as wave propagation effects influenced by the soil geometry (not only 1D, but also 2D and 3D), the wave type (SH, SV or P-waves the incident wavefield in the very near field of strong events might be also very different from plane waves), and the soil mechanical characteristics which, under strong shaking, are modified by non-linear behaviour. It takes into account a significant amount of epistemic uncertainty, especially at large strains.

1.2.2 Logic Tree Structure

The basic logic tree is described in Figure II-1.1. It includes the following branches

- Velocity profile
- Non-linear properties
- Computation approach (Linear [= combination of SHAKE and *RVTbasecase* for pga = 0.05g], SHAKE, RVT, Non-linear), including two distinct sub-branching:
  - the RVT approach includes a sub-branching to account for two different subsets: base case (actual velocity profile and material properties), and all other cases, taking into account the spatial heterogeneities in soil profile and material properties;
  - the existence of two sets of linear equivalent computations (RVT and SHAKE, with different input spectra and time histories) did not lead to additional sub-branching, but to a specific use of the each set of computations depending on the branch, in relation especially to the interpolation / extrapolation issues.
  - the NL approach is thought to be more and more uncertain as the PGA is increasing, so that a sub-branching is introduced to modify the NL results to reflect the increasing epistemic uncertainty;.
- 2D/3D-effects: the two branches are intended to account for epistemic uncertainties of the size of those effects

As in the PEGASOS logic tree, there is no sub-branching for the wave type and incidence characteristics, which are considered NOT to affect the median site amplification. This assumption is probably wrong from a purely physical viewpoint, as, for instance, surface amplification for incident SH or SV-waves is significantly affected by the incidence angle; however, considering the unavailability of this information in the previous logic tree (SP1 - SP2), it is considered as already incorporated in the aleatory variability of the incoming motion, and withdrawn from the site amplification logic tree to avoid any double counting. For the ground motions at depth, the same logic trees as for the surface motion were selected. Special issues that had to be addressed for the two additional depth levels included the following:

- Estimation of the proper NL (non-linear) amplification factors (i.e., for 'outcropping' motion) which were not readily available.
- Estimation of 2D/3D-effects at depth

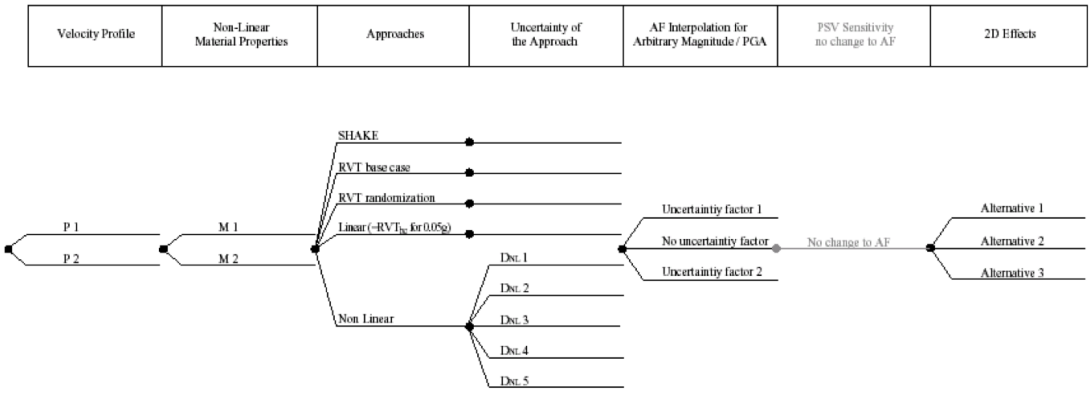

Figure II-1.1: Generic logic tree-structure for horizontal ground motion.

1.2.3 Model Evaluations Common to All Sites

Velocity Profiles

Compared to the PEGASOS project, a huge amount of new site information has been gathered with various kinds of geotechnical and geophysical investigation techniques. It is a pity however that the site amplification factor could not be constrained unambiguously by instrumental estimates through earthquake recordings. I am personally convinced that one of the best ways to constrain the epistemic uncertainty on low strain amplification at its lowest possible level would be to look for an appropriate balance between geophysical and geotechnical surveys on one side and seismological measurements with sensitive instruments recording local, regional and distant earthquakes on the other side. The used site investigation techniques included invasive drillings with borehole measurements in different frequency ranges leading to velocity profiles with varying resolution, and non-invasive, active, and passive measurements providing direct estimates of the surface wave dispersion curves at lower frequency ranges, and thus indirect control on the velocity profile. Each type of investigations has its own merits and shortcomings :

- **borehole measurements.** The main advantages are two : they offer a high resolution (especially sonic logging and cross-hole), and provide measurements for vertically propagating waves, similar to the real case of earthquake induced wavefield.

  Their two main shortcomings come

  a from their frequency range, which is much higher than the earthquake engineering frequency range (especially for sonic logging and cross-hole), so that they may ignore the effects of short and intermediate scale heterogeneities, leading to biased results (weathered and fractured material in particular), and

  b from the fact that provide point measurements which do not account for lateral variability.

- **Non-invasive measurements**. Their advantages and shortcomings are complementary of those of borehole measurements. To their detriment, they offer a very poor resolution of the velocity profile (they cannot identify thin layers), they often cannot constrain the deep bedrock velocity, and they provide measurements for horizontally propagating surface waves, constraining mainly the S-waves and only poorly the P-wave values. Inversely, they provide measurements in the right frequency range taking into proper account the effects of spatial heterogeneities, and they also provide "smoothed" measurements of the velocities over finite extents (typically tens to hundreds of meters)

While the present practice in the geotechnical earthquake engineering community is to rely more on borehole measurements, I consider both types should be given an equal weight. Therefore, my way to assign weights to the various profiles considered for each site has been to take into account three different, independent criteria :

- their proximity to the borehole measurements (in terms of velocity profiles),
- their proximity to non-invasive measurements (in terms of dispersion curves for Rayleigh waves and whenever possible Love waves),
- and their proximity to the measured site fundamental frequency as derived from H/V processing of microtremors.

Material Properties / Non-linear Curves

In the PEGASOS project, no (or only extremely few and old) site specific laboratory measurements were available: two widely used, but very different sets of non-linear degradation curves had thus been considered. For the present PRP project, new soil samples have been retrieved and analyzed (except for KKM), leading, for each site, to a set of three models, including a "best-estimate" model (BE or m2) and two bounding models considered as lower bound (LB or M1) and upper bound (UB or M3). A reasonable weight assignment should therefore consider a symmetric distribution (equal weight on LB and UB) with a larger weight on the central one (i.e., between 0.2 – 0.6 – 0.2, and 0.3 – 0.4 – 0.3).

This has been the starting point for each site, with a larger central value for sites with a larger number of soil samples and measurements. The next step has been to visually compare the available measured values with the proposed (LB, BE, UB) curves, and to modify their

respective weights accordingly, which may result in non-symmetric distributions. This exercise is somewhat subjective and made more difficult for sites including different soil units that can undergo significant Non-linearities with different NL curves.

Background for Weighting the Different Computational Approaches

Three different computational approaches have been considered for each site: two linear equivalent approaches (SHAKE and RVT), and the Non-linear (NL) simulations. The RVT computation types can be separated in two groups, the RVT "base case" (RVT_{bc}) and the randomized RVT (RVT_{ran}), for which the soil velocity profile is assumed to deviate "randomly" (with a prescribed distribution and some spatial correlation length however) from the "base case" profile, together with the non-linear degradation curves which are assumed to be fully correlated with the velocity deviations (a slower velocity being associated with a more non-linear material).

In addition, two sets of linear equivalent (i.e., SHAKE + RVT, 2010 and 2013) computations are available for each site, with different input spectra. While the 2010 computations involved significantly different input spectral shapes for SHAKE and RVT cases, respectively, with significantly higher frequency content for the RVT2010 computations leading to significantly different high-frequency responses, the 2013 computations used consistent spectral shapes between the two approaches, with improved consistency with the SP2 results as they take into account different κ values tuned to the bedrock velocity. Ideally, only the 2013 computations should be used; however, as the time histories and input spectra used for the 2013 SHAKE computations are significantly different from those used for the (2010) NL computations, it was necessary to keep the 2010 linear equivalent results for a number of intermediate interpolation/ extrapolation computations involving NL results (and for the assessment of changes in aleatory variability as well, 1.3).

All computations are not available for all cases, i.e., all combinations of (profile, material, PGA, magnitude). This results in the need for either interpolation from nearest cases, or specific consideration in the weight assignment: for instance, NL computations were performed only for one profile on each site, while RVT_{ran} computations were performed only around the "M2" material properties.

Considering the lower degree of verification and validation for LE and NL simulations compared to the low-strain (linear) case for which a much larger number of comparisons with weak motion data is available in the scientific literature, I decided to individualize in my logic tree the results obtained with the LE approach (SHAKE and RVT_{bc}) for the smallest PGA level (0.05g) and to use them, with appropriate weighting, also for higher PGA levels. These results are labelled in the following as "linear" (L) approach, because it is considered that strain levels remain very small. The "numerical approach" subtree thus includes five branches, corresponding the "L", "SHAKE", "RVT_{bc}", "RVT_{ran}" and "NL" computations. Their relative weighting depends primarily on the level of input motion for the weighting between linear (L), linear-equivalent (SHAKE, RVT_{bc}, RVT_{ran}) and the non-linear (NL) results. It also depends on the frequency for the relative weighting between the two kinds of linear equivalent methods: SHAKE and RVT. The first dependance is addressed in the next section, while the second one is addressed in the following one.

Dependence on Ground Motion Level: Controlled by the Strain Level

While the control parameter for the computations has been the input PGA level, the relevant parameter for the weighting of the three main approaches is considered to be the strain level in the soil column, and more particularly the ratio between the peak strain value and the "reference" strain γ_{50} for which the shear modulus is reduced to half its initial value. At very low strains, the NL approach is not necessary, and may even provide unsatisfactory results because of the poor accounting for the low strain visco-elastic damping: it should be assigned a zero or very small weight. Linear equivalent approaches are valid as long as the strain γ is not too far beyond the 'reference strain' γ_{50} for which the shear modulus is reduced to half its initial value, while at very large strains ($\gamma >> \gamma_{50}$), only the NL approach is – in principle – relevant. However, the parameters to be used in fully NL models are not 100% constrained by the available information for each site, and the associated results should thus be considered to bear a higher degree of epistemic uncertainty than the L or LE results. The relative weighting L / LE / NL is thus based on the strain levels rather than on PGA levels. These strains are computed with the *RVTbasecase* approach, because it is the approach for which most results have been obtained, and interpolation errors are thus limited. These strains are to be computed from the 2013 RVT_{bc} computations, as the corresponding input spectra are considered to be the most representative of the real situation for each of the 4 sites.

However, all the corresponding figures and tables shown in the present document (Table II-1.3 and Annex 1.10) are based on the old 2010 computations: they are simply indicative of the main trends, while the actual computations in the actually implemented model are based on the $RVT_{bc,2013}$ strain computations

The procedure is detailed below:

- At each depth, compute γ/γ_{50} from RVT base case computations.
- Evaluate the maximum ratio $(\gamma/\gamma_{50})_{max}$ over the whole soil thickness
- When $(\gamma/\gamma_{50})_{max} < 1$, consider only Linear, SHAKE and RVT results. Linear approach is assigned a weight of 20%, and linear-equivalent approaches a total weight of 80%. The relative weight between SHAKE [w_0 (SHAKE)] and RVT cases [w_0 (RVT)] is detailed below in Section 1.2.3

  Linear approach (RVT_{bc} + SHAKE 0.05 g): 0.20
  SHAKE approach : 0.80 . w_0(SHAKE)
  RVT approach: 0.80 . w_0(RVT)
  NL approach: w(NL) = 0.

- When $1 < (\gamma/\gamma_{50})_{max} < 10.0$, consider simultaneously the four approaches: Linear, SHAKE, RVT, Non-linear.

  Linear approach (RVT_{bc}+$SHAKE0.05g$) : $0.20*Red\_Lin[(\gamma/\gamma_{50})_{max}]$ $[decrease from 0.2\% to 0.]$
  SHAKE approach :$0.80.w_0(SHAKE).\ Red\_LE[(\gamma/\gamma_{50})_{max}]$
  RVT approach: $0.80.w_0(RVT).\ Red\_LE[(\gamma/\gamma_{50})_{max}]$
  NL approach:$w(NL) = 1. - 0.80 * Red\_LE\ [(\gamma/\gamma 50)max]-$
  $0.20 * Red\_Lin[(\gamma/\gamma_{50})_{max}]$

- When $(\gamma/\gamma_{50})_{max} > 10.0$, drop the linear approach, and keep only the SHAKE, RVT, and $Non-linear$ ones.

  Linear approach ($RVTbasecase$ 0.05 g): 0
  SHAKE approach : w_0(SHAKE) . 0.20
  RVT approach: w_0(RVT) . 0.20
  NL approach: $w(NL) = 0.80$

  with the function $Red\_LE(x)$ defined as follows:
  $Red\_LE(x) = 1 when x < 1$
  $Red\_LE(x) = 1–0.75 log(x) when 1 < x < 10.0$
  $Red\_LE(x) = 0.25 when x > 10.0$

  and the function $Red\_Lin(x)$ defined as follows:
  $Red\_Lin(x) = 1 when x < 1$
  $Red\_Lin(x) = 1 log(x) when 1 < x < 10.0$
  $Red\_Lin(x) = 0. when x > 10.0$

The minimum weight of 20% for the linear equivalent approach even at high strains is introduced as one of the means to indicate the large epistemic uncertainty for such large ground motion. These relative weights are illustrated on II-1.2 and II-1.3

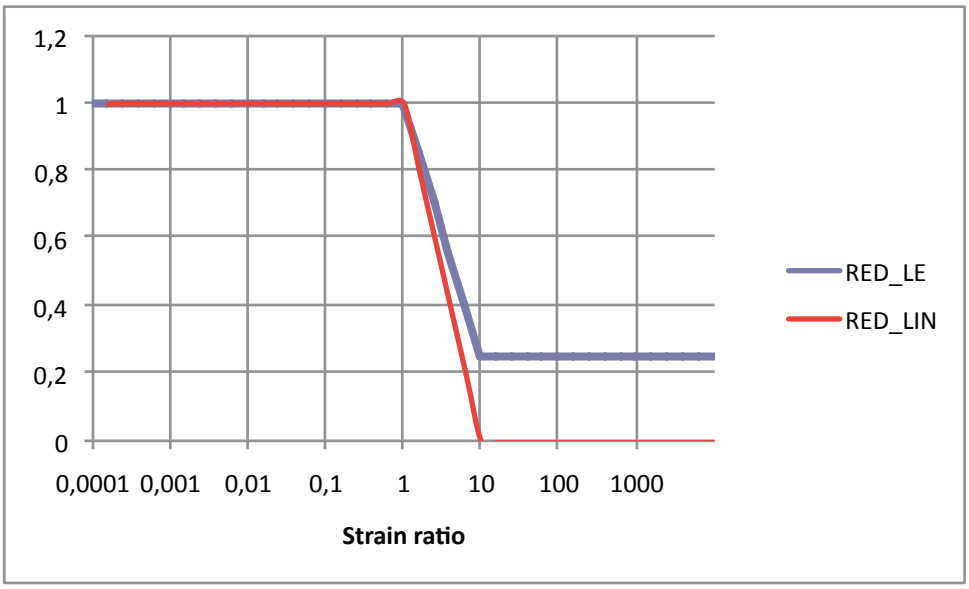

Figure II-1.2: Illustration of the strain dependence of functions Red_LE and Red_lin.

Important Notes:

- The Non-Linear results are available only for one single velocity profile, and mainly for the "best-estimate" material set . The idea of the relative weighting NL /LE is that, for each subbranch corresponding to a given velocity profile and material set, the NL results will be used with the relative weighting indicated above, and with the specific

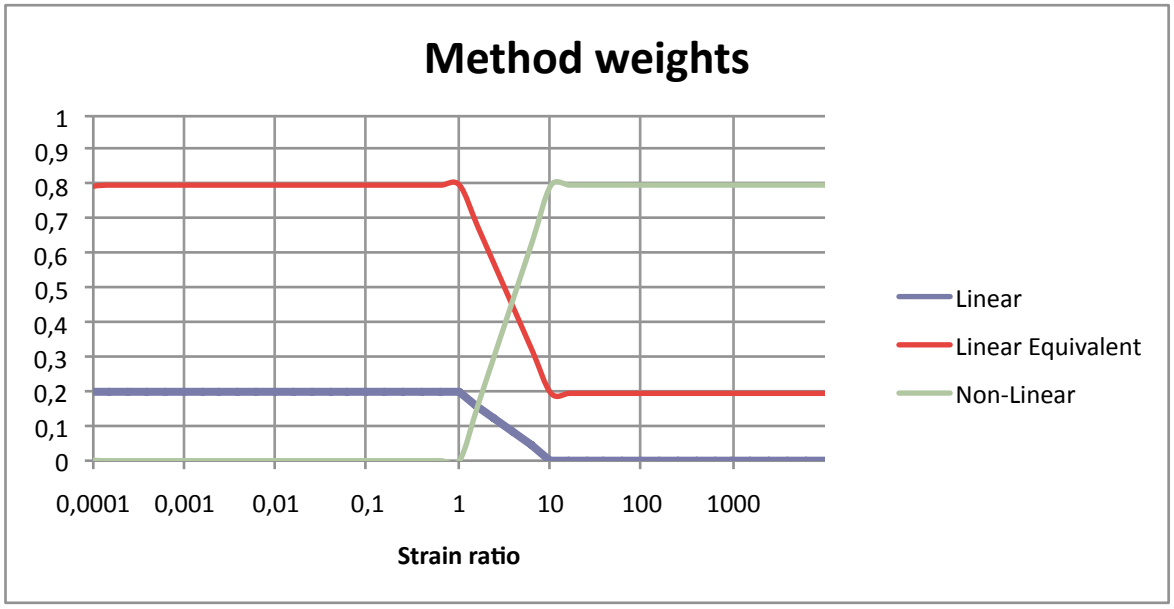

Figure II-1.3: Relative weights of the linear, linear equivalent and non-linear results as a function of RVT_{bc} strain ratio.

interpolation formula detailed below in 1.2.4. As a consequence, for any of the four sites, the NL results will be used several times, but with different weights (related with RVT_{bc} strain ratios obtained for each soil velocity profile – material set) and slightly different interpolated values.

- The RVT results for "randomized" soil properties (RVT_{ran}) are available "only" considering randomization around the best-estimate material properties (m2). As for the NL results, their results are therefore used in three different subbranches.

- There is no absolute minimum weight for SHAKE or RVT results taken separately, as their individual weighting depends on the frequency as explained below. Only their combined weighting is set at a minimum of 20% through the *Red_LE* function.

- The PGA values corresponding to the threshold values of 1 and 10 for the peak strain ratio as derived from the RVT_{bc} computations are listed in II-1.3 for each profile and material properties of each site. The way these values were obtained is displayed in more detail in Annex 1.10 . This table indicates that, except for KKL profiles 1 and 3, the NL results should be accounted for for PGA levels below 0.4g (all yellow cells), and are assigned their maximum weights (80%) for PGA values ranging from 0.8 g to up to 4 g : there is therefore a need to extrapolate the RVT_{bc} peak strain ratio values beyond 1.5 g for profiles P2 of EKKB, P5 of KKG and all KKG profiles (red cells). As indicated above, these values are only indicative as they are based on the 2010 computations, but the specific formulae detailed below in Section 1.2.3 are based on the 2013 RVT_{bc} strain values.

Table II-1.3: List of PGA values corresponding to the threshold values of RVT_{bc} peak strain ratios of 1 and 10, for all profiles of all sites and all material properties. The values in this table are based on the 2010 RVT_{bc} computations, and should be considered only as indicative.

	Material properties 1 (LB)		Material properties 2 (BE)		Material properties 3 (UB)	
Site & Profile	PGA ($\gamma_{max} = \gamma_{50}$)	PGA ($\gamma_{max} = 10.\gamma_{50}$)	PGA ($\gamma_{max} = \gamma_{50}$)	PGA ($\gamma_{max} = 10.\gamma_{50}$)	PGA ($\gamma_{max} = \gamma_{50}$)	PGA ($\gamma_{max} = 10.\gamma_{50}$)
KKB						
P1	0,12	0,4	0,16	0,75	0,2	1,17
P2	0,1	0,34	0,14	0,58	0,16	0,91
P3	0,13	0,41	0,18	0,78	0,22	1,31
P4	0,12	0,42	0,16	0,79	0,2	1,22
EKKB						
P1	0,12	0,44	0,16	0,8	0,2	1,25
P2	0,15	0,61	0,21	1,15	0,25	1,73
P3	0,11	0,45	0,14	0,7	0,16	0,93
KKG						
P1	0,17	0,86	0,18	1,09	0,19	1,32
P2	0,15	0,85	0,17	1,03	0,18	1,19
P3	0,13	0,72	0,14	0,89	0,15	1
P4	0,09	0,43	0,1	0,56	0,11	0,66
P5	0,2	1,13	0,22	1,46	0,24	1,7
KKL						
P1	0,35	2,36	0,42	3,23	0,47	4,18
P2	0,24	1,89	0,3	2,68	0,35	3,41
P3	0,35	2,17	0,43	3,25	0,5	4,35
KKM						
P1	0,08	0,27	0,11	0,54	0,14	0,79
P2	0,05	0,22	0,08	0,4	0,1	0,56
P3	0,1	0,35	0,15	0,71	0,2	1,16
P4	0,04	0,17	0,06	0,31	0,07	0,41

Relative Weighting Between SHAKE and RVT: Frequency Dependence

SHAKE and RVT approaches are based on similar concepts as to soil behaviour (linear equivalent), but implement it in different ways, which have advantages and disadvantages.

RVT frequency-dependent reliability

The computation of response spectra through the RVT approach is generally reliable at intermediate and high frequencies (large number of cycles), but it is NOT reliable in two cases:

- at low frequencies because of the approximation used for the peak values: the small number of cycles alters the relevancy of the random vibration theory.
- around the main resonant frequencies, as it was shown recently by Kottke and Rathje [2013] that RVT results exhibit a systematic overestimation of the amplification.

Therefore, I assign a frequency dependent weight, defined as follows:

- For $0 < f < f1$: w0(RVT,f) = 0 and w0 (SHA) = 1
- For $f1 < f < f2$: w0(RVT,f) = (log(f/f1)/(log(f2/f1)) $RWRVT_{MF}$ and w0(SHA) = 1 -w0(RVT)
- For $f > f2$: w0(RVT,f) = $RWRVT_{MF}$ and w0(SHA) = $1-RWRVT_{MF} = RWSHA_{MF}$

Soil profile variability

The RVT_{ran} approach considers variability in the soil layering and in the non-linear characteristics, while SHAKE does not. This is useful because such a variability is always present; it is, however, at least partially taken into account in the SHAKE approach with the different soil profiles and/or material properties for each site, especially in the PRP studies where extensive site investigations have been performed. In addition, soil heterogeneities in the RVT_{ran} approach induce three artefacts which may be troublesome:

- high frequency waves may be artificially damped away in relation with "kinematic" diffraction on such heterogeneities.
- they may result in unrealistic strain concentration in thin low velocity layers, which in turn result in artificial damping and decoupling.
- the implicit consideration of randomness in only one spatial direction (the vertical one) overemphasizes the effect of vertical variability.

However, this explicit accounting of the soil variability is of special interest for the KKL site, where the available geotechnical information indicates the presence of such small scale heterogeneities with an alternance of cemented and non-cemented gravel layers.

Input motion

The a priori good point of RVT approach is the accounting for phase variability, which is interesting for consideration of amplification factor in terms of ratio of response spectra (even though the random phase assumption is not realistic at all for actual earthquake recordings). This "advantage" of RVT is balanced however by the consideration of 10 different time histories for SHAKE computations.

Another "advantage" of RVT input motion is the "automatic" adaptation of the input signal characteristics -including duration - to the PGA level, which is much more satisfactory, from a physical viewpoint, than a crude amplitude scaling of actual accelerograms to the PGA level, over a range as large as 0.05 to 1.5 g.

On the other hand, a recently discovered (and rather amazing after so many years of extensive use in the US) drawback of the RVT approach a the systematic overestimation bias of the amplification factor around the main resonant frequencies [Kottke and Rathje 2013].

Finally, the last comment is related with the systematic differences in the input motion considered in RVT and SHAKE 2010 computations, with a richer high-frequency content for RVT. These differences resulted in significant differences in the corresponding amplification factors, especially for large intermediate and PGA values : the high frequency amplification was significantly smaller for the RVT approach, and this reduction was increasing with increasing PGA, degraded material properties ($m1 > m2 > m3$) and increasing bedrock velocities. (The latter point is linked with the lower κ value for lower bedrock V_{S30}).

These observations led to an intermediate model with a strong high-frequency dependence as detailed in the version 9 of my evaluation summary in order to adjust the high frequency amplification to the shape of the actual input spectra. This was implemented through the introduction of a [f3, f4] frequency range over which the relative weighting of RVT results is varies linearly from its intermediate frequency value RWT_{MF} to its high frequency value RWT_{HF}, while the SHAKE relative weighting receives the complementary weighting.

- For $f2 < f < f3$: w0(RVT) = $RWRVT_{MF}$ and w0(SHA) = $1 - RWRVT_{MF} = RWSHA_{MF}$
- For $f3 < f < f4$: w0(RVT) = $[log(f4/f)RWRVT_{MF}+log(f/f3)RWRVT_{HF}]/(log(f4/f3)$ and w0(SHA) = $1 - w0(RVT)$
- For $f4 < f$: w0(RVT) = $RWRVT_{HF} and w0(SHA) = 1 - RWRVT_{HF}RWSHA_{HF}$

However, with the new 2013 computations, these HF differences completely disappeared, and such a high frequency relative weighting is no longer useful. As all the initial models up to early 2013 had implemented this high-frequency modulation, I therefore proposed to keep the initial software with adapted f3, F4 and weight values :

- taking $f3 = f4 = 100$ Hz
- taking $RWRVT_{HF} = -RWRVT_{MF}$ and $RWTSHA_{HF} = RWSHA_{MF}$

Wrap-up: final weights for the linear equivalent results

Considering the above, the final implementation of the relative weighting between RVT and SHAKE results exhibits a frequency dependence characterized by one single transition frequency ranges [f1 - f2]. After careful examination of all the results, it has been found simpler, while scientifically acceptable, to adopt the same frequency values for the 5 sites. The main issue is the assessment of the intermediate frequency weights $RWRVT_{MF}$ and $RWSHA_{MF}$ above [f2]. They are determined for each site independently of the PGA as detailed in the next paragraph and in Table II-1.4.

The main decision concerns the relative weighting $RWRVT_{MF}$ in the intermediate to high frequency range (i.e., from [f2 to 100Hz]) between RVT and SHAKE results.

This frequency range includes the main resonant peaks where the RVT_{bc} approach has an overestimation bias. As a consequence, I decided to assign a slightly larger weight for SHAKE computations: the basic weights $RWRVT_{MF}$ and $RWSHA_{MF}$ are equal to 40% and 60% respectively.

There is one exception however for the Leibstadt site, for which the recognized spatial variability of the cementation status pushed me to assign a 50% weight to SHAKE and 50% to RVT.

The final decision addresses the relative weight between RVT_{bc} and RVT_{ran} computations. Considering the facts that

a the same RVT_{ran} results will be considered in the three material subbranches,

b the epistemic uncertainty linked with the spatial randomness of soil profiles is partially accounted for with the 3 to 5 (6) different profiles for each site, and

c the overestimation bias is affecting mainly the RVT_{bc} case, I decided to assign an only slightly larger weight to RVT_{bc} than to RVT_{ran} (basically around 3/5 - 2/5).

This information is summarized in Table II-1.4 and Figure II-1.4.

Table II-1.4: Parameters for the relativ weighting of linear methods.

Site	f1	f2	f3	f4	$RWSHA_{MF}$ (Relative weight, intermediate frequency range, SHAKE)	$RWRVT_{MF}$ (Relative weight, intermediate frequency range, RVT)	$RWRVT_{bcMF}$ (Relative weight, intermediate frequency range, RVT_{bc})	$RWRVT_{ranMF}$ (Relative weight, intermediate frequency range, RVT_{ran})
KKB					0.6	0.4	0.2333	0.167
EKKB					0.6	0.4	0.233	0.167
KKG	0.5	1	100	100	0.6	0.4	0.233	0.167
KKL					0.5	0.5	0.300	0.2
KKM					0.6	0.4	0.233	0.167

Figure II-1.4: Example relative weights for the three linear equivalent approaches for the KKB, EKKB, KKG and KKM sites (top) and the KKL site (bottom).

Definition of the "Linear" Results (L)

Considering the above mentioned discussion of the respective pros and cons of each linear equivalent technique, the linear result, corresponding to to the linear equivalent amplification factor obtained for PGA = 0.05g, should be a combination between the SHAKE and RVT case. In order to be consistent with the previous section, the same frequency-dependent weighting is to be applied to the 0.05g SHAKE, RVT_{bc} and RVT_{ran} results, as displayed in Figure II-1.4.

Non-linear Computations

A significant difference between EQL and NL simulations is that the latter require soil parameters that are not fully constrained by the available information, which results in numerical uncertainties. These epistemic uncertainties should increase with increasing PGA level.

Moreover, while there has been in the past decades or years a significant number of verification exercises comparing the results of different wave propagation codes in the viscoelastic domain, leading to encouraging results, only very few similar exercises have been attempted for fully Non-linear simulations ; the only one I know of, the E2VP one (Euroseistest Verification and Validation Exercise organized in Europe from 2008 to 2011) did not produce very satisfactory

results, and at least required many iterations for different codes to converge on acceptably similar results.

Finally, the comparison between actual strong motion data and numerical simulation in the Non-linear domain, has been performed only at a limited number of sites (most often involving liquefaction or pore pressure effects), and acceptable levels of match were usually obtained after iterations to tune the NL model parameters to the desired, known results.

As a conclusion, I consider that the a priori level of reliability is much smaller for NL simulation codes than for visco-elastic simulations. I thus introduced in my PEGASOS 1 model 5 sub-branches to specifically include the epistemic uncertainties in the NL approach. I consider the advances in NL modelling, their verification and validation, has not been obvious enough in the last decade, so that I could remove this sub-branching. However, considering these potential uncertainties, the NL computations schedule in PRP include a number of cross-checks between independent NL simulation codes and teams. These cross-checks led to variable agreement levels: although they were rather bad for one site (KKM), they were however in general better than I expected.

I thus kept the logic of my PEGASOS sub-branching, but I tuned the uncertainty factors on the observed discrepancies or agreement between the two independent NL computations. In the following I first detail the structure of the sub-branching, and then I explain how I reached the values for the corresponding "free" parameters.

Uncertainty sub-branching structure For the 5 branches on the NL subtree, the amplification factors computed with the NL approach are modified by multiplying them by an 'NL uncertainty' factor U_{NL}, which vanishes at low frequency (i.e., much below the site fundamental frequency), and which is defined as follows

$$U_{NL}(f, f_0, pga, D_{NL}) = 10[D_{NL} E(kf/f_0).Ua(pga)]$$
$$U_{NL}(f, f_0, pga, D_{NL}) = 10E(kf/f_0) \times D_{NL} \times U_a(pga)$$

Where

- f_0 is the low strain fundamental frequency of the site (given for each of the 5 sites).
- κ is a multiplying factor introduced to account for the decrease of fundamental frequency at large strains: $k = 1. + K_{max} * Ua$, with $Ua = [log(pga/pgaref)/log(2.5/pga_{ref})]$, and κ bounded by 1 ($'low' pga, i.e., pga < pga_{ref}$, a site-dependent value) and $(K_{max} + 1)$ for $pga > 2.5g$, where K_{max} is also a site dependent value.
- E is a generic function defined as
  - $E(x) = 0. for x < 0.5$
  - $E(x) = log(2x)/log(2) for 0.5 < x < 1.0$
  - $E(x) = 1 for 1.0 < x$
- D_{NL} quantifies the deviation from the results of the NL simulation. These deviations are assumed to have a lognormal distribution, and the five branches correspond to the 5%, 25%, 50%, 75% and 95% percentiles, i.e., roughly speaking to the median

plus or minus one or two standard deviations. The 5 branches have thus fixed weights corresponding to this fractile distribution, and the uncertainty is scaled by a specific factor, S_{NL} (corresponding to 1 standard deviation), which is to be estimated for each site (as detailed in the next section).

- $D_{NL} = 2S_{NL}$: weight : 5%
- $D_{NL} = S_{NL}$: weight : 20%
- $D_{NL} = 0$: weight : 50%
- $D_{NL} = -S_{NL}$: weight : 20%
- $D_{NL} = -2S_{NL}$: weight : 5%

Tuning for each site

This models requires the specification of 3 parameters for each site: $pga_{ref}, K_{max}, and S_{NL}$. pga_{ref} corresponds to the PGA at which NL effects start to be significant. It is considered here as the PGA level corresponding to a RVT_{bc} strain ratio reaching 1. According to II-1.3, and considering mainly P1 profile, it is set to 0.15 g for KKB and EKKB, 0.2 g for KKG, 0.4 g for KKL and 0.1 g for KKM.

K_{max} corresponds to the maximum shift of fundamental frequency at high PGA / strain. From the examination of the amplification factors, it is taken equal to 2 for KKB, EKKB, KKG and KKL, and increased to 3 for KKM.

S_{NL} characterizes the "reliability" of the NL numerical simulations. It is derived from the comparison of the results of the two independent numerical simulations, labelled here NL1 and NL2 (for KKM it is indeed the "NL5" computation), for the case (M=6, pga=0.75g, mat=m2/BE). In each case, the amplification factors obtained for each of the 9 considered time histories have been compared in the frequency domain : $R_{NL12}(f;i) = AF_{NL1}(f;THi, i = 1,9)/AF_{NL2}(f;THi, i = 1,9)$, and their variability has been quantified by computing the geometric mean and standard deviation of R_{NL12} for each frequency, and also analysing their average and maximal values in the frequency range [0.5 - 30 Hz]. This variability is displayed, for each NPP site, in Annex 1.11, and the corresponding statistics are summarized in II-1.5, where

- mean (NL1/NL2) is the average value of R_{NL12} (f;i) for all time histories and frequencies in the range [0.5 - 30 Hz]
- $\sigma(NL1/NL2)$ is the average geometric standard deviation of R_{NL12} (f;i) for all time histories and frequencies in the range [0.5 - 30 Hz]
- $sigma_{max}$ is the maximum geometric standard deviation of R_{NL12} (i) over the range [0.5 - 30 Hz] (i.e., obtained at one single frequency value)
- $(Mean - Max/Mean - Min)^0.5$ is another "measure" of the maximum deviation over the whole frequency range [0.5 - 30 Hz]: it is the square root of the ratio between the

average of the envelope of all R_{NL12} (f) ratios for all time histories and the average of the lower bound of the envelope of all R_{NL12} (f) ratios for all time histories

- $(Max/Min)^0.5$ is the square root of the maximum variability observed over the whole frequency range [0.5 - 30 Hz] for the 9 time histories.

Table II-1.5: Statistics on comparisons between NL1 and NL2 computations for each site.

	EKKB	KKB	KKG	KKL	KKM
mean (NL_1/NL_2)	0.9	1.02	0.96	1.02	0.58
sigma (NL_1/NL_2)	1.26	1.24	1.08	1.12	1.45
$sigma_{max}$	1.53	1.44	1.19	1.3	1.98
$(Mean - Max/Mean - Min)^{0.5}$	1.69	1.64	1.19	1.46	3.05
$(Max/Min)^{0.5}$	2.26	2	1.43	1.95	4.07

This table shows clearly that, according to these criteria, the most reliable result are obtained for KKG, then for KKL, then (KKB and EKKB), and the worst for KKM. The low value for KKL should however be pt in perspective since it corresponds to a PGA level which is very close to the onset of significant non-linearity: only small differences should therefore be expected.

It is not fully straightforward to translate these results in terms of values for S_{NL}. This is done, however, considering that the observed variability corresponds to the intermediate PGA level of 0.75g, i.e., S_{NL} should be compared to $log10(sigma)/Ua(0.75g)$. Considering the uncertainty in the estimate of pga_{ref}, and the strong underlying assumptions on this uncertainty model, the final S_{NL} proposed values are rounded to simple values. KKL uncertainty is set at the same level as KKB and EKKB, rather than paying too much attention to the raw value of $log10(sigma)/Ua(0.75g)$, while the S_{NL} value for KKM is increased considering also the large mean differences between the two computations (see II-1.5).

Table II-1.6: Summary of NL uncertainty parameters for the five sites.

Site	pga_{ref} Tuning	P_i-M_j	K_{max}	Ua (0.75g)	sigma (R_{NL}-12)	S_{NL}	S_{NL}, **final**
KKB	0.15	+ cf Table	2	0.57	1.26	0.17	**0.15**
EKKB	0.15	2.4	2	0.57	1.24	0.165	**0.15**
KKG	0.2	for	2	0.52	1.08	0.07	**0.075**
KKL	0.4	each	2	0.34	1.12	0.14	**0.15**
KKM	0.1	P_i-M_j	3	0.62	1.45	0.26	**0.3**

The supporting graphics are provided in Annex 1.11

Magnitude / PGA Dependence of Site Amplification: Interpolation of Available Results for Missing Computations

Direct results from RVT, SHAKE and NL computations are available only for discrete values of magnitudes and PGA. In addition, some of them (NL computations) have been computed only for a specific soil profile.

An interpolation scheme therefore needs to be designed in order to estimate the corresponding amplification factors for any value of the (M, PGA) couple.

As the wider set of available results corresponds, in most cases (except KKG), to RVT computations, the interpolation scheme is based on the RVT base case, which consists a kind of skeleton for the sets of results.

This decision was maintained despite the late (2013) discovery of the overestimation bias of the RVT_{bc} approach around the main resonant peaks: it is considered that the accounting for the ratios between SHAKE or NL results and RVT_{bc} results, together with the systematicity of this overestimation effect, warrants a satisfactory interpolation scheme.

Despite the apparent complexity of formulas, the interpolation is very simple, based on a piecewise one or two-dimensional linear interpolation on a log scale for PGA, and linear scale for magnitude.

RVT Case

Amplification factor

The objective is to estimate the amplification factor $AF_{RVT}(pga, M)$ corresponding to RVT approach for arbitrary values of PGA and M.

Let $M1 < m < M2$ be the two nearest magnitudes for which the RVT amplification factor is known, and let $A1 < pga < A2$ be the two nearest peak accelerations for which the RVT amplification factor is known,then the interpolation formula is:

$$AF_{RVT}(pga, M) = C11 * AF_{RVT}(A1, M1) + C21 * AF_{RVT}(A2, M1) + C12 * AF_{RVT}(A1, M2) + C22 * AF_{RVT}(A2, M2)$$

With

$$C11 = (M2 - M).(LA_2 - L_{pga})/[(M2 - M1).(LA_2 - LA_1)]$$
$$C12 = (M–M1).(LA_2 - L_{pga})/[(M2 - M1).(LA_2 - LA_1)]$$
$$C21 = (M2 - M).(L_{pga} - LA_1)/[(M2 - M1).(LA_2 - LA_1)]$$
$$C22 = (M–M1).(L_{pga} - LA_1)/[(M2 - M1).(LA_2 - LA_1)]$$

Where

$$Lpga = log(pga); LA1 = log(A1); LA2 = log(A2)$$

If there is no need for magnitude interpolation, these formula should be reduced to piecewise linear interpolation with respect to the log PGA values.

Strains $(\gamma/\gamma 50)max$

The weights between the various approaches are based on the estimation of the ratio $(\gamma/\gamma_{50})_{max}$ for the $RVTbasecase$ (see 1.2.3).

This ratio has thus to be estimated for any arbitrary value of (PGA, M). The proposed scheme is similar to the one proposed above for the amplification factor: Once having computed the coefficients C11, C12, C21 and C22 as indicated above, the coefficients should be used to interpolate $(\gamma/\gamma_{50})_{max}$ values, with the following formula:

$$(\gamma/\gamma_{50})_{max}(pga, M) = C11*(\gamma/\gamma_{50})_{max}(A1, M1)+C21*(\gamma/\gamma_{50})_{max}(A2, M1)+C12*(\gamma/\gamma_{50})_{max}(A1, M2)+ C22 * (\gamma/\gamma_{50})_{max}(A2, M2)$$

Important note : in the case where $(\gamma/\gamma_{50})_{max}, RVT_{bc}(1.5g, M)$ is still smaller than 10 (cf II-1.3), its value needs to be extrapolated at larger PGA in order to estimate the relative weights between L, LE and NL results. In such a situation, the linear trend between log $[(\gamma/\gamma 50)max, RVT_{bc}]$ and log(PGA) should be established from all the available values, i.e., from 0.05 to 1.5 g, and extrapolated until log $[(\gamma/\gamma_{50})_{max}, RVT_{bc}]$ reaches a value of 1 as shown in 1.10; beyond the corresponding PGA values, there is no need to compute the $(\gamma/\gamma_{50})_{max}, RVT_{bc}$ value, and the L, LE and NL weights should be set to 0, 0.2 and 0.8, respectively.

SHAKE Case

The SHAKE amplification factors AF_{SHA} are available, in general, for 5 acceleration levels (0.05, 0.1, 0.2, 0.4, 0.75 g) and for each velocity profile / material properties and each magnitude. For the KKG site however, they are also available for three additional PGA values: 1, 1.5 and 2.5 g. In this latter case, there is no need for using the present interpolation scheme for SHAKE results; conversely, symmetric formulas should be used to guide the interpolation of less numerous RVT_{bc} results. The objective is thus to estimate $AF_{SHA}(pga, m)$ for arbitrary values of PGA and M. The basis of the interpolation is the proximity between RVT base case (" RVT_{bc}") and SHAKE computations. The main issue is not so much the interpolation than the extrapolation to PGA values larger than 0.75g.

These interpolated and extrapolated SHAKE amplification factors are needed for both 2013 and 2010 computations, because of the need of 2010 SHAKE results for the interpolation of NL results (see Section 1.2.3 below). In both cases however, the scheme is guided by the 2013 RVT results, as they considered closer to the SHAKE 2010 and 2013 results than the RVT 2010 results.

Let $A1 < pga < A2$ be the two nearest peak accelerations for which the amplification factor is known with SHAKE computations and let $M1 < m < M2$ be the two nearest magnitudes for which the amplification factors are known,then the estimation formula for any soil column is:

$$AF_{SHAyear}(pga, M) = AF_{RVT_{bc2013}}(pga, M) * R_{SHAyear-RVT_{bc2013}}(pga, M)$$

where :

- $AF_{RVT_{bc2013}}(pga, M)$ is derived as described in 1.2.3 on the basis of 2013 computations
- $R_{SHAyear-RVT_{bc2013}}$ is the SHAKE (2010 or 2013) to RVT_{bc} (2013) ratio computed on the same profile, for the same magnitude and on the basis of the 2013 RVT computations.

Estimating the 'SHAKE to RVT_{bc}' ratio $R_{SHA-RVT_{bc}}$

Whatever the SHAKE computational year, $R_{SHAyear-RVT_{bc2013}}$ is noted in the following lines as $R_{SHA-RVT_{bc}}$ for simplicity, and is interpolated from the nearest (acceleration, magnitude) sets for which both computations are available for the same profile and material properties, in the same way as it was proposed in the previous section for the interpolation of the RVT results.

$R_{SHA}-RVT_{bc}(pga, M) = C11 * R_{SHA-RVT_{bc}}(A1, M1) + C21 * R_{SHA-RVT_{bc}}(A2, M1) + C12 * R_{SHA}-RVT_{bc}(A1, M2) + C22 * R_{SHA-RVT_{bc}}(A2, M2)$

With

$C11 = (M2 - M).(LA_2 - L_{pga})/[(M2 - M1).(LA_2 - LA_1)]$
$C12 = (M–M1).(LA_2 - L_{pga})/[(M2 - M1).(LA_2 - LA_1)]$
$C21 = (M2 - M).(L_{pga} - LA_1)/[(M2 - M1).(LA_2 - LA_1)]$
$C22 = (M–M1).(L_{pga} - LA_1)/[(M2 - M1).(LA_2 - LA_1)]$

Where
$L_{pga} = log(pga); LA1 = log(A1); LA2 = log(A2)$

Special case : $pga > 0.75g$
In such a case, simply use the $SHA-RVT_{bc}$ ratios obtained for $pga = 0.75g$:
$R_{SHA-RVT_{bc}}(pga, M) = R_{SHA-RVT_{bc}}(0.75g, M)$

Special case : $pga < 0.05g$
In such a case, simply use the $SHA-RVT_{bc}$ ratios obtained for $pga = 0.05g$:
$R_{SHA-RVT_{bc}}(pga < 0.05g, M) = R_{SHA-RVT_{bc}}(0.05g, M)$

Important note: In this section, it should be understood that these formulas should be applied for the same site profile and material properties. They are therefore not specifically indicated in the formulas, for sake of a lighter presentation and reading.

Non-linear Case

The non-linear amplification factors, $AF_{NL}(pga, M)$, are available only for a limited number of acceleration levels (0.4, 0.75, 1.5 g , + 0.05 for $M6 - M2$ and 2.5 g for M6-M3) and for one single set of velocity profile properties per site; apart from sensitivity studies for $pga = 0.75g$ and M6, only M2 (BE) material properties are considered. The objective is thus to estimate the NL amplification factor AF_{NL} for arbitrary values of PGA and M, and arbitrary profile.

Considering the significant differences in input motion between RVT_{bc} and NL cases, the interpolation scheme is based here primarily on the SHAKE 2010 computations corresponding to the same input time histories, with some correction factors however which also use the 2013 RVT_{bc} results since SHAKE results are not available at large PGA values.

General case $(0.4g \leq pga \leq 1.5g, 5 \leq m \leq 7)$

Let us consider the profile P_i and material properties M_j. The estimation of the non-linear amplification factor is derived as follows:

$$AF_{NL}(pga, M; Pi_Mj) = AF_{SHAKE2010}(pga, M, Pi\_Mj) * R_{NL-Shake_{|(pga,M,Pi\_Mj)}}$$

where :

• $AF_{SHAKE2010}(pga, M; Pi\_Mj)$ is the SHAKE amplification factor for the actual soil profile and material properties, derived as explained in the previous section for arbitrary PGA and m values from the 2010 SHAKE computations.

• $R_{NL_{|SHAKE}}(pga, M; Pi\_Mj)$ is the NL to SHAKE ratio, estimated from the nearest common (M,PGA) couples for the relevant soil profile. Its estimation is detailed in the following, and combines 2010 and 2013 computations

This NL_{SHAKE} ratio is indeed based on the value of this ratio for the reference profile and material properties (i.e., P1 - P6 for KKG - and M2/BE), and corrected for the changes in material properties and profile:

$$R_{NL_{|SHAKE}}(pga, M, Pi\_Mj) = R_{NL_{|SHAKE}}(pga, M, P1\_M2) * COR_{mat} * COR_{profile}$$

Where
• $R_{NL_{|SHAKE}}(pga, M, P1\_M2) = AF_{NL}(pga, M, P1\_M2)/AF_{SHAKE2010}(pga, M, P1\_M2)$
• $COR_{mat} = AF_{NL}(0.75g, 6, P1\_Mj)/AF_{NL}(0.75g, 6, P1\_M2) * COR_{pga}$
• $COR_{pga} = AF_{RVT_{bc2013}}(pga, M, Pi\_Mj)/AF_{RVT_{bc2013}}(0.75g, M, Pi\_Mj)$
• $COR_{profile} = AF_{RVT_{bc2013}}(pga, M, Pi\_Mj)/AF_{RVT_{bc2013}}(pga, M, P1\_Mj)$

The $AF_{NL}(pga, M, P1\_M2)$ and $AF_{SHAKE}(pga, M, P1\_M2)$ quantities, for arbitrary PGA and magnitude values, should be derived from the piecewise linear interpolation on log(PGA) values of 2010 computations, and the use of RVT_{bc2013} results, as described in the previous sections (1.2.3 and 1.2.3).

Particular case $(pga < 0.4g)$ **and** $(\gamma/\gamma_{50})_{max} > 1$ **(quite often. . .)**

There is need for low PGA interpolation; it could formally be achieved by piecewise linear interpolation using the NL computation for magnitude 6, but it is considered preferable to guide the interpolation using the information on strains, by considering two terms, one related to the PGA value, and the other one to the actual velocity profile and material properties:

$$R_{NL_{|SHAKE}}(pga, m, Pi\_Mj) = F_{pga} * Fprofile, mat$$

where

$$F_{pga} = D1 * R_{NL_{SHAKE}}(0.4g, 6, P1\_M2) + D2.R_{NL_{SHAKE}}(0.05g, 6, P1\_M2)$$

with

$D1 + D2 = 1$
$D1 = 0 if (\gamma/\gamma_r)_{max} < 1$
$D1 = log[(\gamma/\gamma_r)_{max}]/[log(\gamma/\gamma_r)_{max}, 0.4g]$ if $(\gamma/\gamma_r)_{max} > 1$

and $(\gamma/\gamma_r)_{max}$ is computed from the 2013 RVT_{bc} strain ratio at the PGA value under consideration, while $(\gamma/\gamma_r)_{max}, 0.4g$ is the value of $(\gamma/\gamma_r)_{max}$ obtained for the RVT base case at 0.4g PGA level and $magnitude6$, as computed in 2013.

$F_{profile}, mat = AF_{RVT_{bc}}(pga, M, Pi\_Mj)/AF_{RVT_{bc}}(pga, M, P1\_M2)$ (based on the 2013 computations)

1.2.4 Extrapolation for Large PGA and/or Magnitude Values

The input acceleration levels and/or corresponding magnitudes may exceed the maximum values considered for most of the computations, i.e., 1.5 g and 7, respectively. It is therefore necessary to define an extrapolation scheme. The procedures detailed below apply to amplification factors obtained with the Linear Equivalent (SHAKE, RVT) and Non Linear approaches. They obviously do not apply to the "linear approach" (mix of $RVTbasecase$ and SHAKE 0.05g) – in case it would be required with a non-zero weight at high acceleration levels -. The design of this extrapolation procedure has taken into account the SP2 information according which there is no need to estimate amplification factors for PGA levels exceeding 2.5g.

Large Input Acceleration Levels: Beyond 1.5 g up to 2.5g –and $M \leq 7$

Non-linear results, reference profile *(P1, P6 for Gösgen)*

For each site, there exists one NL computation for a 2.5 g PGA level; it is performed however only for UB material properties (M3) and magnitude 6.

The first step is to get an estimate of the NL results for other material properties and magnitudes

$$AF_{NL}(2.5g, 6; P1\_Mj) = AF_{NL}(2.5g, 6, P1\_M3) * AF_{NL}(1.5g, 6, P1\_Mj) / AF_{NL}(1.5g, 6, P1\_M3)$$

$$AF_{NL}(2.5g, m; P1\_Mj) = AF_{NL}(2.5g, 6, P1\_Mj) * AF_{NL}(1.5g, m, P1\_M2) / AF_{NL}(1.5g, 6, P1\_M2)$$

The second step is to get an estimate of the NL results for arbitrary PGA values (between 1.5g and 2.5g) from linear interpolation (on a log PGA axis) between the computed values at 1.5g and those so-estimated at 2.5g.

RVT results, all profiles and magnitudes

For the KKG site, this estimation should be based actually on the available 2013 SHAKE results, which can be interpolated at this PGA level since computations were performed up to 2.5g, and from the 2013 RVT / SHAKE ratios at 1.5g :

$$AF_{RVT_{bc}}(pga, M; Pi\_Mj) = AF_{SHA}(pga, M; Pi\_Mj) * AF_{RVT_{bc}}(1.5g, m; Pi\_Mj) / AF_{SHA}(1.5g, m; Pi\_Mj)$$

$$AF_{RVT_{ran}}(pga, M; Pi\_M2) = AF_{SHA}(pga, M; Pi\_M2) * AF_{RVT_{ran}}(1.5g, m; Pi\_M2) / AF_{SHA}(1.5g, m; Pi\_M2)$$

For the four other sites, the extrapolation uses the existing large PGA NL computation (and estimations, see the previous section) for the reference profile, and the $RVT2013_{NL}$ ratios at 1.5g, according to the following formulae:

$$AF_{RVT_{bc}}(pga > 1.5g, m; Pi\_Mj) = AF_{NL}(pga, M, P1\_Mj) * AF_{RVT_{bc}}(1.5g, M, Pi\_Mj) / AF_{NL}(1.5g, 6, P1\_Mj)$$

$$AF_{RVT_{ran}}(pga > 1.5g, m; Pi\_M2) = AF_{NL}(pga, M, P1\_M2) * AF_{RVT_{ran}}(1.5g, M, Pi\_M2) / AF_{NL}(1.5g, m, P1\_M2)$$

SHAKE results, all profiles and magnitudes

For KKG, the SHAKE results in this PGA range should be directly interpolated from the available SHAKE computations (maximum PGA value : 2.5g)(for both 2010 and 2013 computations, as needed). For other sites, the extrapolation should be performed in a way similar to the one described for RVT results, i.e., making use of the existing large PGA NL computation (and estimations, see previous section) for the reference profile, and the $SHAKE_{NL}$ ratios at 1.5g, according to the following formulae:

$AF_{SHAyear}(pga > 1.5g, M; Pi\_Mj) = AF_{NL}(pga, M, P1\_Mj) * AF_{SHAyear}(1.5g, m; Pi\_Mj)$
$/AF_{NL}(1.5g, 6; P1\_Mj)$

This formula can be applied to both 2010 and 2013 SHAKE computations, provided the same "year" results are used in the two terms of the equation.

Large Magnitudes (> 7)

For magnitudes > 7, simply use the amplification factors computed or estimated corresponding to Magnitude 7.

1.2.5 2D/ 3D-effects

The subsoil / surface topography structure always exhibit some amount of lateral variations. The few 2D-computations for the Leibstadt case indicate the possibility of significant geometrical effects due to nearby lateral heterogeneities, in relation – in that particular case - to the topography of the river terrace. A survey of the cross-sections for each NPP site shows the existence of such lateral heterogeneities, at variable distances from the NPP site, and with variable geometrical characteristics. In addition, NPP themselves, which are very stiff concrete structures, constitute heterogeneities that do radiate some energy back into the soil, which then propagate at least partly as surface waves. The physics of the wave diffraction makes this phenomenon sensitive to many parameters: wave type (plane / surface wave, P, SV, SH – in relation to source depth and mechanism), incidence characteristics (incidence, azimut). It seems impossible to account for all these effects in a "pseudodeterministic" way, especially when the consideration of the source (magnitude, distance, azimuth) and the site effects are completely decoupled. A simplified model has therefore been built to account for these geometrical effects. Its formulation is based on the interpretation of 2D/3D-effects as surface waves diffracted by the main lateral heterogeneities, and its quantitative parameters have been calibrated on the results obtained for the Leibstadt case. This model is described below; its parameters are heavily site dependent and are therefore detailed for each site in the relevant sections. Since some uncertainties exist in the estimates of these effects, a subbranching has been introduced with different parameter values, and different weights.

General formula:

The amplification factors derived with either approach should be multiplied by a 2D factor A_{2D} defined as:

$A_{2D}(f, \zeta) = 1 + C_{2D}(f, \zeta)$

with

$C_{2D}(f, \zeta) = A(f, f_0)B(f, \zeta)$

where

f is the frequency
f_0 is the fundamental frequency at the site under consideration
ζ is an average damping value in the surficial soils where surface waves diffracted on lateral heterogeneities are propagating.

Frequency dependence: A (f, f_0)
The Leibstadt computations (from D. Fäh and P.-Y. Bard), as well as the abundant scientific literature, indicate that 2D- and 3D- effects appear only above the site fundamental frequency, f_0. A (f, f_0) is therefore defined as a ramp function on a logarithmic frequency axis:

$$A(f, f_0) = A0(f/f_0)$$

with

$A0(x) = 0$ for $x \leq 0.7$
$A0(x) = -(log(x/0.7))/log(0.7)$ for $0.7 < x \leq 1$
$A0(x) = 1$ for $1 < x$

Geometrical / damping dependence : $B(f, \zeta)$

The diffracted waves are generated on the lateral heterogeneities, and then propagate to the site; their amplitude at the site will therefore depend both on the distance to the heterogeneities, and on the damping values. The proposed model therefore is:

$$B(f, \zeta) = C^0_{2D}.exp(-2\pi\zeta avfl/\beta m)$$

where

- C^0_{2D} represents, in some way, the amplitude of the diffracted waves (normalized to the incident wavefield) at their origin, i.e. on the heterogeneity; it is also, approximately, the largest possible 2D- effect at the site (corresponding to the low strain / very low damping case). This value is uncertain, and, for each site, different values are proposed with different weights.
- the last term exp $(-2\pi\zeta avfl/\beta m)$ represents the amplitude decay due to the propagation from the heterogeneity to the site:
- ζav is the average damping over the soil column: it is PGA dependent because of NL material degradation (see below).
- l is the distance of the NPP site to the closest lateral heterogeneity

- βm is the velocity of surface waves propagating in the surface layers (i.e., Rayleigh or Love waves). For stratified media with depth-dependent velocities, this velocity is frequency dependent (dispersion curve). The values considered for each site have been selected from the analysis of the measured dispersion curves at frequencies around and above the fundamental frequency f_0.

Estimating βm

- Linear case : The values $\beta_M 0$ considered for each site have been selected from the analysis of the measured dispersion curves at frequencies around and above the fundamental frequency f_0.

- Linear equivalent case (SHAKE and RVT) : Higher strains will induce a decrease of the soil shear-wave velocities, and therefore of the surface wave velocities $\beta_M 0$. This decrease is not uniform but varies with depth depending on the strain profile. Trying to take into account in an "exact" way would lead to a complex model inconsistent with the crudeness of this 2D/3D model. Therefore, an "average" decrease of β_M is considered based on an "average" strain level estimated from the peak strain ratio $(\gamma/\gamma_{50})_{max}$ as computed in the RVT_{bc} approach (2013 computations).
  - the "strain ratio" profiles exhibit a very high variability with site, profile, material properties and PGA value, with however a significant localization of peak strains close to large velocity contrasts. It is therefore considered that, for the present purpose, an "average, effective" strain ratio $(\gamma/\gamma_{50})_{eff}$ equal to one fifth of the peak strain ratio $(\gamma/\gamma_{50})_{max}$. This low value takes into consideration the depth dependence of the strain ratio, and the fact the peak strain is reached only once in the time history.
  - the resulting velocity decrease is then estimated as equal to $[1/(1+(\gamma/\gamma_{50})_{eff})]^{0.5}$.
  - the estimation formula is thus $\beta M = \beta_M 0.[1/(1+0.2(\gamma/\gamma_{50})_{max})]^{0.5}$.
  - Note : considering lower β_M values will result in decreasing the importance of 2D/3D effects

- Non-linear case : simply apply the β_M values from the linear equivalent approach

Estimating ζ_{av}

- Linear case : $\zeta_{av} = 0.0125$ (corresponds to a quality factor Q value of 40)

- Linear equivalent case (SHAKE and RVT) : Considering the strain ratio profiles,the damping increase linked with NL behavior is depth dependent. In order to be consistent with the estimation of the reduction of surface wave velocity β_M, an average damping is estimated from the "average, effective" strain ratio $(\gamma/\gamma 50)_{eff}$ through the formula $\zeta_{av} = 0.0125 + \zeta_{max}.(\gamma/\gamma_{50})_{eff}/[1. + (\gamma/\gamma_{50})_{eff}]$ The resulting formula is therefore : $\zeta_{av} \approx 0.0125 + 0.06.(\gamma/\gamma_{50})_{max}/[1. + 0.2(\gamma/\gamma_{50})_{max}]$

- Non-linear case : simply apply the ζ_{av} values from the linear equivalent approach

The Tables II-1.9, II-1.11, II-1.14, II-1.17 and II-1.20 presented in the next sections provide, for each NPP site, the values of f_0, C^0_{2D}, l, $\beta m0$ and h, as well as the corresponding weighting. Three sub-branches are introduced with different weights to account for the uncertainties in the parameter estimates (mainly indeed C^0_{2D}). One of the subbranches corresponds to $C^0_{2D} = 0$, as it is likely, that the input motion estimates prior to the site effect computations contain (at least partly) some unknown amount of 2D/3D-effects. The other values are based on the actual geological cross-sections at each site, and some subjective 'expert judgement', calibrated on the computed effects for Leibstadt. The parameter studies performed in that case also show the large sensitivity to damping values. From the Leibstadt 2D-computations, one may conceive that NL 1D-effects may have been overemphasized in the existing literature based on observed strong motion data simply because 2D/ 3D-effects become less and less important as damping increases.

2D/3D-effects at depth

For the motion at depth, the same surface wave interpretation will be kept: as the amplitude of ground motion is strongly depth-dependent for surface waves, the 2D/3D surface factors are modified by a depth-dependent factor C(z), except for the sites which are located beneath the sediment-basement interface responsible for the trapping of surface waves. The 1D-amplification factors derived with either approach should thus be multiplied by a 2D factor A_{2D} defined as:

$$A_{2D}(f, \zeta, z) = 1 + A(f, f_0)B(f, \zeta).C(z)$$

The C(z) factor is estimated with a very simple assumption, corresponding both to the depth dependence due to vertically incident S-waves, and to mode shapes around the fundamental frequencies:

$$C(z) = Max|cos(\omega z/c)|, 0.2 \approx Max|cos(2\pi f z/\beta_M)|, 0.2$$

Where βm is the average shear wave velocity already specified for these 2D-effects. The minimum value of 0.2 is introduced to avoid the vanishing at some frequencies, as it is considered that in real nature, the interferences at depth can never be totally destructive because of heterogeneities. Comparing the thicknesses h of the 'trapping layers' (see relevant section for surface motion) with the actual depth of the various sites, this formulation should therefore be applied to the two deep sites at Beznau ($h = 80m > z2 = 15m$), E-Beznau ($h = 60m > z2 = 15m$), Gösgen ($h = 28m > z3 = 15m$), and Leibstadt ($h = 30m > z2 = 10m$). However, this $2D$-overamplification term should NOT be applied to the two sites at depth ($z2 = 7m$ and $z3 = 14m$) at Mühleberg, for which the shallow gravel layer is only 8 m thick: for this particular case, there is no subbranching for 2D-effects (or, in other terms, 1 single branch with weight 100% for the value $C_{2D} = 0$).

1.2.6 Estimation of "Outcropping Motion" NL Amplification Factors at Depth

General Scheme

The available NL amplification factors are the AF_{NL} values at the surface (outcrop, noted as AF_{NL},surf) and at depth for within motion (noted as $AF_{NL,depth-within}$). Simultaneously, the Linear Equivalent amplification factors obtained with SHAKE computations (AF_{SHA}) are available both for within and outcropping motion. Therefore, the following ways were considered to estimate the requested values of $AF_{NL,depth-outcrop.}$ were considered:

- Option 1 : considering only outcropping motions
  $AF_{NL,depth-outcrop} = AF_{NL,surf}.AF_{SHA2010,depth-outcrop}/AF_{SHA2010,surf}$
  The correcting factor is here based on the assumption that the variations with depth are similar for NL and LE approaches, provided they are based on the same time histories (hence the use of 2010 SHAKE computations and estimates)
- Option 2 : considering only motions at depth
  $AF_{NL,depth-outcrop} = AF_{NL,depth-within}.AF_{SHA2010,depth-outcrop}/AF_{SHA2010,depth-within}$
  The correcting factor is here based on the assumption that the variations between outcropping and within motions are similar for NL and LE (SHAKE) approaches, provided they are based on the same time histories (hence again the use of 2010 SHAKE computations and estimates)

Each option has some advantages and drawbacks: **Option 1** leads to more stable estimates (no destructive interferences in outcropping motion), but it does not take into account the possible localization of deformation in NL computations. And vice-versa for **option 2**.

As a consequence, the estimations of $AF_{NL,depth-outcrop}$ are made with a sub-branching considering these two options, with weights $W1 = 40\%$ for option 1 and weight $W2 = 60\%$ for the second one. **Option 2** is slightly preferred because it takes into account only ground motion at depth, which should be better in case of strain localization at some depth)

Additional Details

The Non-Linear amplification factors AF_{NL} are available, at surface and depth, only for one velocity profile and limited sets of (PGA, material properties) per site. Therefore, the above formulae should be applied for all sets of (PGA,M,Pi_Mj) after interpolation of the available results. This should be done according to the following procedure :

a estimate the $AF_{NL,depth-within}$ for all sets of (PGA, magnitude, Profile, material properties) as described for $AF_{NL,surf}$ in sections 1.2.3 and 1.2.4

b estimate the $AF_{SHA,depth-outcrop}$ and $AF_{SHA,depth-within}$ for all sets of (PGA, magnitude, Profile, material properties) as described for $AF_{SHA,surf}$ in sections 1.2.3 and 1.2.4, using the 2010 SHAKE computations (and 2013 RVT computations when needed for interpolation / extrapolation).

c apply the within - outcrop conversion formulae

1.2.7 Beznau

Site-Specific Model Evaluations

Weighting of Velocity Profiles

The various velocity profiles have been all derived in order to match the available geophysical and geotechnical investigations. Their weighting of the velocity profiles has been derived according to the following "principles":

- each of them is a priori acceptable and is given a starting equal weight
- then the weights are modified according to the "proximity" to

  the measured velocity profiles from invasive investigations (cross-hole, down-hole or suspension logging),

  the measured dispersion curves resulting from non-invasive, surface wave measurements (active and passive)

  the measured fundamental frequency resulting from the H/V processing of microtremor measurements

Such a "proximity" can be investigated by comparing the profile or its attributes (dispersion curve, fundamental frequency) to the measured values. This comparison is summarized in II-1.7 on the basis of observations displayed in II-1.35, II-1.36 through II-1.37.

Table II-1.7: Summary of comparison between profile attributes and measurements for KKB site.

Profile	Borehole data: velocity profile	Non-invasive surveys: Dispersion curve	f_0	Final weights
P1	fair	good (10)	rather low	30%
P2	good at depth	good (5)	rather low	30%
P3	fair	Lower bound (26)	rather low	15%
P4	good at surface	Variable, good at high frequency (18)	rather low	25%

Some of the velocity profiles (II-1.35) were designed more specifically on the basis of borehole measurements, some other on the basis of non-invasive surveys. For KKB, the borehole information was predominant for profiles P2 (principally at large depth within the bedrock) and P4 (principally at shallow depth within the top gravel and top of opalinus clay).

A meaningful index of the agreement of dispersion curves is provided by the number of randomized velocity profiles (that were generated for the RVT computations) that had to be excluded because they exceeded the uncertainty bounds (lower or higher) set for the dispersion curves on the basis of measurements. These numbers are listed within parentheses in II-1.7: a large number indicates that the dispersion curve of the base profile is close to one of the two bounds at least at some frequency, as illustrated in II-1.36.

Similarly, the fundamental frequency of the base profile, and the distribution of fundamental frequencies for the selected randomized profiles, can be compared (II-1.37) with the uncertainty intervals set up for the site (2.0 - 3.3 Hz for KKB).

From this set of comparisons, the profile P3 turns out to be the one with the worst performance from its too-close proximity with the lower DC bound, while profiles P1 and P2 exhibit a rather satisfactory and comparable behavior, with a slight better BH rating for P2 and DC rating for P1. As a consequence, the initial equal weights of 25% were raised for profiles P1 and P2 (5% each), and decreased for P3 (10%). These weight modifications were however deliberately chosen not be too large because the 4 profiles had been carefully selected to match the uncertain and variable available data.

Note : in an ideal situation, there should be a fourth item in this comparison (which personally I would have rated very high), i.e. the comparison between instrumentally observed transfer functions and computed ones. The existing in-situ instrumentation has not however allowed, till now, to obtain such an instrumental amplification function.

Weighting of Material Properties

There are three sets of used NL properties : a "best -estimate" (M2) and two "extreme" cases supposed to bound the deviations from the average behavior (M1, lower bound, and M3, upper bound). The a priori weights for these three sets is symmetric, with emphasis on the central, bestestimate curves (see 1.2.3)

Data are available only for the gravel layers, and not for the Opalinus Clay. The weighting is thus based mainly on the gravel data. II-1.38 compares the actually measured degradation curves for the gravels, and the set of three curves used in the computations (lower bound - M1 -, bestestimate - M2 -, and upper-bound - M3 -). Shear modulus data group very close to the M3 curve at low strain, and mainly in between M2 and M3 curves at larger strains. Damping data also group close to the M3 curves at low strain, but largely exceed even the M1 curves at larger strains.

It is not easy to account for these apparent inconsistencies. However, considering the fact that at large strains, the largest weight is given to fully NL computations, for which the shear modulus degradation is only approximated, and the damping values could be extremely different from the lab tests, the weights have been assigned in view mainly of linear equivalent computations used at small and intermediate strains. Therefore, the weight distributions exhibits a strong bias towards the M3 set: up to 5 10^{-4} strain, the data are much closer to M3 than to M2; M1 is however taken into consideration (20%) because of some the rather high damping measurements even at small to intermediate strain.

Alternative 2D-parameters

According to the cross-sections initially provided by PROSEIS in the PEGASOS project, the subsoil structure is varying mainly along the EW direction for the very surface, but there also exist some variations at larger depth along the NS cross-section. From the cross-section NPP_B_CENTRE, the edge is located 250 m to the west. I anticipate an 'edge' effect in the shallow surficial layer; however, the velocity profiles show that there is not much impedance contrast at this interface, so that the profile may not be relevant. From the cross-section

Table II-1.8: Weighting the NL property sets for KKB and EKKB sites.

Measurements	Comments	M1= Lower bound	M2= Best estimate	M3= Upper bound
Good quality lab data for the gravles, old and highly questionalbe for opalinusclay	Lad tests provide shear modulus data close to the upper bound at small and intermediate strains	20%	35%	45%

NPP_B_NS, the edge is located 300 m to the north. I anticipate a significant 'edge' effect in the opalinuston unit.. This should clearly produce some effects around the fundamental frequency.

In addition, from all cross-sections, the surface layer thickness irregularities just below the NPP should induce some wave trapping. Therefore, the parameters for the additional 2D/3D-effects take into account the NS 2D variations in the deep structure, and are associated with the fundamental frequency $f_0 = 2.5Hz$, and the thick layers including opalinustone, with h=80 m. Since this unit has a limited NL behavior, I do not expect much NL reduction effect in this 2D amplification; it is, however, 'automatically' adjusted through the damping parameter ζ_{av}

Summary of Weights and Parameters for Beznau

1.2.8 E-Beznau

Site-specific Model Evaluations

Weighting of Velocity Profiles

As for KKB, the three selected velocity profiles are compared to the borehole measurements in II-1.39, to the measured dispersion curves in II-1.40, and to the measured fundamental frequency in II-1.41.

Profile P2 is the closest to CH measurements at large depth, but less central than P1 in terms of dispersion curve. Profile P3 exhibits relatively low velocities (compared to borehole measurements) in the deeper parts (10-20m) of the gravel layer, and its dispersion curve is close to the lower bound at high frequencies, but the corresonding fundamental frequency is in the center of the confidence interval. For these reasons, all three profiles are considered almost equally acceptable, with however a slightly larger weight for P1, because of its good performance on two out of the three "proximity items. The corresponding weights are summarized in II-1.10.

Weighting of Material Properties

The data and curves are the same as those used for KKB. R The weights are therefore the same, see 1.2.7 and Table II-1.8 for further details.

Table II-1.9: Summary of weights and computational parameters for the horizontal ground motion at KKB (Beznau) site.

Velocity profile				
P1 0.3	P2 0.3		P3 0.15	P4 0.25
Non-linear properties				
M1 0.2		M2 0.35		M3 0.45
Approaches				
Deformation range $(\gamma/\gamma_{50})_{max}$	RWF (SHAKE)	RWF (RVT)	Linear (0.05g)	Non-linear
< 1	0.48	0.32	0.2	0
$> 1 and < 10$	$0.48 * Red\_LE$ $[(\gamma/\gamma_{50})_{max}]$	$0.32 * Red\_LE$ $[(\gamma/\gamma_r)_{max}]$	$0,2 * Red\_LE$ $[(\gamma/\gamma_r)_{max}]$	Complement to 1 + sub-branching
> 10	0.12	0.08	0	0.8+sub-branching
Frequency dependent, dependent, weighting of EQL techniques (SHAKE, RVT_{bc}, RVT_{ran})				
frequency	$F < f1 =$ 0.5 Hz	$0.5Hz < f < f2$ =1Hz		$F > 1Hz$
SHAKE	1	Ramp,log(f)		0.6
RVT_{bc}	0	Ramp,log(f)		0.233
RVT_{ran}	0	Ramp,log(f)		0.167
RVT Subsets				
Base case 0.5825			Random model 0.4175	
NL Uncertainties				
S_{NL} Factor:0.15			$pga_{ref} = 0.15$	$K_{max} = 2$
Magnitude / PGA interpolation + extrapolations				
Linear	SHAKE		RVT	Non-linear
See formulas				
2D-effects: $A_{2D} = 1 + C_{2D}(f,\zeta) = 1 + C^0_{2D}.A_0(f/f_0).exp(-2\pi\zeta_{av} fl/\beta_M)$ $\beta_M = \beta_{m0}.[1/(1 + 0.2(\gamma/\gamma_{50})_{max})]^{0.5}, \zeta_{av} \approx 0.0125 + 0.06.(\gamma/\gamma_{50})_{max}/[1. + 0.2(\gamma/\gamma_{50})_{max}]$				
Fixed parameters	$f_0 = 2.5Hz$	$l = 300m$	$\beta m_0 = 800m/s$	$h = 80m$
Alternative choice for parameters and corresponding weights	$C^0_{2D} = 0.0$ weight 0.40		$C^0_{2D} = 0.2$ weight 0.40	$C^0_{2D} = 0.5$ weight 0.20

Table II-1.10: Summary of comparison between profile attributes and measurements for the EKKB site.

Profile	Borehole data: velocity profile	Non-invasive surveys: Dispersion curve	f_0	Final weights
P1	good	good (25)	rather high	40%
P2	good at depth	close to upper bound at intermediate frequency (58)	rather high	30%
P3	fair	Fair, close to lower bound at high frequency (26)	good	30%

2D-parameters

The parameters are taken the same as for KKB, except for the thickness of the "surface-wave trapping layer", which is reduced to 60m since it is considered to be consisting of the group gravle + Opalinus Clay.

1.2.9 E-Beznau - Summary of Weights and Parameters

Table II-1.11: Summary of weights and computational parameters for the horizontal ground motion at EKKB (E-Beznau) site.

Velocity profile				
P1 0.4		P2 0.3		P3 0.3
Non-linear properties				
M1 0.2		M2 0.35		M3 0.45
Approaches				
Deformation range $(\gamma/\gamma_{50})_{max}$	RWF (SHAKE)	RWF (RVT)	Linear (0.05g)	Non-linear
< 1	0.48	0.32	0.2	0
> 1 and < 10	$0.48 * Red\_LE$ $[(\gamma/\gamma_{50})_{max}]$	$0.32 * Red\_LE$ $[(\gamma/\gamma_r)_{max}]$	$0,2 * Red\_LIN$ $[(\gamma/\gamma_r)_{max}$	Complement to 1 sub-branching
> 10	0.1	0.1	0	$0.8 + sub - branching$
Frequency dependent, relativ weighting of EQL techniques (SHAKE, RVT_{bc},RVT_{ran})				
frequency	$F < f1 =$ 0.5Hz	$0.5Hz < f < 1Hz$		$f > 1Hz$
SHAKE	1	Ramp,log(f)		0.6
RVT_{bc}	0	Ramp,log(f)		0.233
RVT_{ran}	0	Ramp,log(f)		0.167
RVT Subsets				
Base case $0,233/0.4 = 0.5825$			Random model $0.167/0.4 = 0.4175$	
NL Uncertainties				
S_{NL} Factor:0.15		$pga_{ref} = 0.15$		$K_{max} = 2$
Magnitude/ PGA interpolation + extrapolations				
Linear	SHAKE	RVT	Non-linear	
See formulas				
2D-effects: $A_{2D} = 1 + C_{2D}(f,\zeta) = 1 + C^0_{2D}.A_0(f/f_0).exp(-2\pi\zeta_{av} fl/\beta_M)$ $\beta_M = \beta_{M0}.[1/(1 + 0.2(\gamma/\gamma_{50})_{max})]^{0.5}, \zeta_{av} \approx 0.0125 + 0.06.(\gamma/\gamma_{50})_{max}/[1. + 0.2(\gamma/\gamma_{50})_{max}]$				
Fixed parameters	$f_0 = 2.5Hz$	$l = 300m$	$m = 600m/s$	$h = 60m$
Alternative choice for parameters and corresponding weights		$C^0_{2D} = 0.0$ weight 0.40	$C^0_{2D} = 0.20$ weight 0.40	$C^0_{2D} = 0.50$ weight 0.20

1.2.10 Gösgen

Site-specific Model Evaluations

Weighting of Velocity Profiles

There are six velocity profiles for Gösgen. Three of them (P1 to P3) correspond to very deep velocity profiles, the other three (P4 to P6) to shallow profiles down to a bedrock considered as very hard (2500 m/s) and homogeneous below 30 m depth.

Their comparison to the available borehole data (CH, DH) and sonic-logs are displayed in II-1.42 for rather shallow depth (less than 100 m) and II-1.43 for large depth (down to about 600 m). Considering that in most cases the effects of deep bedrock are not specifically addressed, and that the deep velocity profiles are not known, I consider that such effects are basically taken into account in the empirical ground motion prediction equations, and probably contribute partly to the associated (aleatory) variability. Having a high weight on these deep profiles introduces a significant risk of some double counting of this variability, by some adding epistemic uncertainty to the aleatory variability built in the rock hazard estimate.I therefore decided to assign a twice larger global weight to shallow velocity profiles P4 to P6, compared to deep velocity profiles P1 to P3.

Deep velocity profiles:

Figures II-1.42 and II-1.43 show that profile P2 is supported only by down-hole data within top part of the bedrock (between 30 and 90 m depth), while profiles P1 and P3 are in better agreement with CH and sonic data in the same units. At larger depth, profile P3 is closer to the available measurements than the two other.

Dispersion curves (Figure II-1.44 left) are not constrained at low frequency ($f < 4Hz$). At intermediate frequencies (5-10 Hz), profile P1 is close to the average between lower and upper bounds, while profile P3 is the closest to the lower bound (while not far from one of the individual curves derived from array microtremor measurements). I did not pay too much attention to this information in my weighting, since the constrains correspond mainly to the shallow velocity structure.

The associated resonance frequencies, displayed in II-1.45, exhibit a relatively large scatter for profiles P1 and P2, which also exhibit a noticeable low frequency peak between 0.5 and 1 Hz, while they are distributed over a much more narrow range for P3: in the latter case, they are controlled by the gravel layer, while in the two former cases, the deep structure interacts significantly. Profiles P1 and P2 are thus the only ones that could be consistent with the observed (small amplitude) H/V peak below 1 Hz.

As a result, I assign the largest weight to profile P3 (20%), an intermediate weight (10%) to profile P1 because it is consistent with intermediate depth CH data and low frequency small peak, and the lowest weight (5%) to profile P2 because the down-hole data it is consistent with seem unrealistic at very shallow depth. However, there is one "mystery" with the Gösgen site : the very large velocity contrast between gravels and the underlying bedrock should in theory result in a much clearer peak around 5 Hz in the H/V curves. One possible explanation could be the strong contamination of microtremor measurements from industrial noise linked

with the on site activity.

Shallow velocity profiles

Profile P6 is the same as P1 down to 200 m, without the deeper velocity fluctuations, in particular the low velocity zone around 400 m depth. As the exact dispersion curves and frequency distribution for P6 were not available in the supporting documents, I used the those of P1, considering only the intermediate and high frequency parts related with the shallow velocity profile.

The cross-hole measurements provide rather consistent values within the gravel layer, and the best agreement if found for profile P6/P1 compared with P4 and P5. Downhole and sonic measurements provide generally higher S-wave values within the gravel, especially at intermediate depth. profiles P4 and P5 are therefore offering a slightly better agreement with them, and a lower agreement with CH data. Profile P4 has the largest velocity at the bottom of gravel layer, but the consistency with the observed frequency could be reached only with rather low velocity at the very surface, leading to a low Rayleigh wave velocity at high frequency (see Figure II-1.44 right).

The distribution of fundamental frequencies (II-1.45), which is satisfactory for all profiles, does not indicate to prefer one profile to the others.

As a consequence, the about 2/3 total weight for shallow profiles is distributed as follows: 30% for P6, 20% for P4, and 15% for P5 (a small priority was given to P4 compared to P5, because it allows to cover the whole range of DC values at high frequency : all other profiles, except P3, are closer to the upper bound)

Weighting of Material Properties

The proposed three sets of NL properties are very close to one another (much closer than for KKB-EKKB sites), because of the number, quality and homogeneity of lab data. Given this proximity between M1, M2 and M3, the initial symmetric weighting has been set to 25% (M1), 50% (M2), 25% (M3) in order to assign significant weight to "extreme" values.

Figure II-1.46 indicates that the at shallow depth ($z < 10m$), the measured shear modulus generally lies in between M2 and M3 model, while the damping values are generally even below M3 values. At larger depth, shear modulus measurements seem to be predominantly in between M1 and M2 (with some questions however on the low strain normalization), while daming values again are generally in between M2 and M3.

As a consequence, the weighting has been very slightly shifted towards M3, so that the finally assigned weights are 25% for M1, 45% for M2 (-5%), and 30% for M3 (+5%).

2D-parameters

According to the cross-sections initially provided by PROSEIS, the subsoil structure is varying mainly along the NS direction, and these variations are only very slight.

- The NS cross-section NPP_G_CENTRE exhibits a thinning of the surface layer down to about 10 m at 550 m north of the NPP site. There also exist some thickness irregularities under the NPP (but this is probably due to the larger density of borings).

Table II-1.12: Summary of comparison between profile attributes and measurements for KKG site.

Profile	Borehole data: velocity profile	Non-invasive surveys: Dispersion curve	f_0	Final weights
P1	OK for CH and sonic at intermediate depth lower values than available data at larger depth	good, close to the upper bound at high frequency (6)	good	10%
P2	Only DH at intermediate depth	good, close to the upper bound at high frequency (15)	good	5%
P3	Best for CH and sonic	Lower bound (13)	good	20%
P4	Slightly larger than CH, closer to (highly scattered) DH	Good at intermediate frequency, close to the lower bound at high frequency (18)	good	20%
P5	Slightly larger than CH, closer to (highly scattered) DH	close to the upper bound at intermediate and high frequency (26)	good	15%
P6	Good agreement with CH slightly smaller values than sonic and DH	? same as P1 (6)? close to lower bound at intermediate frequency, central at high frequency	good	30%

Table II-1.13: Weighting the NL property sets for KKG site.

Measurements	Comments	M1 = Lower bound	M2 = Best Estimate	M3 = Upper Bound
Good quality lab data for the gravels	Well constrained measurements slightly intermediate between the M2 and M3 models at shallow depth	25%	45%	30%

- From the cross-section NPP_G_EW, I do not anticipate significant effects since the thickness is rather regular, and the distance to the thinning section on the West is about 900 m: diffracted waves have time and distance to damp out, especially as they are high frequency ($f > 5Hz$) and short wavelength.

Therefore, there probably exist some 2D-effects, but much less pronounced than for Leibstadt (modelled) and Beznau (expected).

Summary of Weights and Parameters for Gösgen

Table II-1.14: Summary of weights and computational parameters for the horizontal ground motion at KKG (Gösgen) site.

Velocity profile					
P1 0.1	P2 0.05	P3 0.2	P4 0.2	P5 0.15	P6 0.3
Non-linear properties					
M1 0.25		M2 0.45		M3 0.3	
Approaches					
Deformation range $(\gamma/\gamma_{50})_{max}$	Linear (0.05g)	RWF(SHAKE)	RWF(RVT)	Non-linear	
< 1 > 1 and < 10 > 10	0.2 $02 * Red\_LIN$ $[(\gamma/\gamma_{50})_{max}$ 0	0.48 $0.48 * Red\_LE$ $[(\gamma/\gamma_{50})_{max}]$ 0.12	0.32 $0.32 * Red\_LE$ $[(\gamma/\gamma_{r})_{max}]$ 0.08	0 Complement to 1 +sub-branching 0.80 + subbranching	
Frequency dependent relative weighting of EQL techniques (SHAKE, RVT_{bc}, RVT_{ran})					
frequency	$F < f1 =$ 0.5Hz	$0.5 < f$ $1Hz$		$f > 1Hz$	
SHAKE	1	Ramp, log(f)		0.6	
RVT_{bc}	0	Ramp, log(f)		0.233	
RVT_{ran}	0	Ramp, log(f)		0.167	
RVT Subsets					
Base case			Random model		
0.233/0.40=0.5825			0.167/0.40=0.4175		
NL Uncertainties					
$S_{NL} = 0.075$		$pga_{ref} = 0.2$		$K_{max} = 2$	
Magnitude / PGA interpolation + extrapolations					
Linear		SHAKE	RVT	Non-linear	
See formulas					
2D-effects : $A_{2D} = 1 + C_{2D}(f, \zeta) = 1 + C^0_{2D}.A_0(f/f_0).exp(-2\pi\zeta_{av} fl/\beta_M)$ $\beta_M = \beta_{M0}.[1/(1 + 0.2(\gamma/\gamma_{50})_{max})]^{0.5}, \zeta_{av} \approx 0.0125 + 0.06.(\gamma/\gamma_{50})_{max}/[1. + 0.2(\gamma/\gamma_{50})_{max}]$					
Fixed parameters	$f_0 = 5.0Hz$	$l = 550m$	$\beta_m = 600m/s$	$h = 28m$	
Alternative choice for parameters and corresponding weights	$C^0_{2D} = 0.$ weight 0.70			$C^0_{2D} = 0.20$ weight 0.30	

1.2.11 Leibstadt

Site-specific Model Evaluations

Weighting of Velocity Profiles

There are three velocity profiles for Leibstadt. Their comparison with the available in-situ data are displayed in a similar way as for the previous sites in II-1.47 (cross-hole and down-hole), II-1.48 (dispersion curves) and II-1.49 (fundamental frequencies). Profiles P1 and P2 are very close to cross-hole data (old ones : 1973, 1975, for P1, most recent ones : 2009, for P2) while P3 was derived mainly from non-invasive, surface wave measurements and is not as close, especially at depth in the bedrock.

Therefore, the best agreement with measured dispersion curves is found for profile P3, while the less satisfactory is for profile P2 which is very close to the lower bound: it might indicate that the low velocity zone at intermediate depth in the gravel may be only local at the CH site, and not representative of the whole area.

Finally the distribution of fundamental frequencies exhibits a satisfactory match for all three profiles.

As a consequence, I consider all three profiles should be considered with relatively similar weights, with a slight "hitch" however for P2 as the low velocity zone is probably only local, and a slight preference for P1 compared to P3 as the former is probably closer to the relaity at depth in the bedrock (too simple profile for P3 because of lack of resolution of non-invasive techniques): the final weights are 40%, 25%, and 35%, for P1, P2 and P3, respectively.

Table II-1.15: Summary of comparison between profile attributes and measurements for KKL site.

Profile	Borehole data : velocity profile	Non-invasive surveys : Dispersion curve	f_0	Final weights
P1	Very good (CH 1973 at shallow depth anisotropy-corrected CH 2009 at larger depth)	good at high frequency close to the upper bound at low frequency (14)	good	40%
P2	Very good (CH 2009 at all depths)	Very close to the lower bound at intermediate and high frequency(19)	good	25%
P3	Good at shallow depth (gravel) simplified at larger depth	Very central very good (0)	good	35%

Weighting of Material Properties

The proposed three sets of NL properties include almost all measured data points, including damping values (Figure II-1.50); they account in a satisfactory way of the larger variability at depth (probably due to the variable cementation level). No asymmetry or bias can be seen and I therefore assign a symmetric weight distribution for M1 and M3. Considering the concentration of data close to the M2 curves - especially for damping values, I assign a

relatively high weight to M2. As a consequence, the final weights are 20% for M1, 60% for M2 , and 20% for M3.

Table II-1.16: Weighting the NL property sets for KKL site.

Measurements	Comments	M1 = Lower bound	M2 = Best Estimate	M3 = Upper Bound
Good quality lab data for the gravels	Well balanced data around M2	20%	60%	20%

2D-parameters

The two series of computations performed in the PEGASOS project (from D. Fäh and P.-Y. Bard) were consistent in exhibiting significant 2D effects, which are larger in case of waves coming from the N – NW (corresponding to forward diffraction on the river terrace). These computations could be approximately fitted with a C_{2D}^0 around 30%.

The maps and the various cross-sections ($NPP\_L\_CENTRE, NPP\_L\_EW, NPP\_L\_NW - SE$) all indicate close lateral variations linked with the river terrace:

- NS: the terrace is located 120 m to the north of the NPP site
- EW: the terrace is located 150 - 300 m to the west of the NPP (irregular topogr. to the west)
- NW-SE: the terrace is located about 100 m to the NW of the NPP site

In addition, the same terrace is bending, and is also present 350 m to the ENE of the NPP site. Considering such a structure, I anticipate some kind of 3D-effects. I therefore include a sub-branch with larger values for C_{2D}^0 parameter .

Summary of Weights and Parameters for Leibstadt

Table II-1.17: Summary of weights and computational parameters for the horizontal ground motion at KKL (Leibstadt) site.

Velocity profile				
P1 0.4		P2 0.25		P3 0.35
Non-linear properties				
M1 0.2		M2 0.6		M3 0.2
Approaches				
Deformation range $(\gamma/\gamma_{50})_{max}$	Linear (0.05g)	RWF(SHAKE)	RWF(RVT)	Non-linear
< 1	0.2	0.40	0.40	0
> 1 and < 10	$0.2 * Red\_LIN$ $[(\gamma/\gamma_{50})_{max}$	$0.40 * Red\_LE$ $[(\gamma/\gamma_r)_{max}]$	$0.40 * Red\_LE$ $[(\gamma/\gamma_r)_{max}]$	Complement to 1 +sub-branching
> 10	0	0.10	0.10	0.80+sub-branching
Frequency dependent relative weighting of EQL techniques (SHAKE, RVT_{bc}, RVT_{ran})				
frequency	$F < f1 =$ 0.5Hz	$F1 < f$ $< f2$		$f > 1Hz$
SHAKE	1	Ramp log(f)		0.50
RVT_{bc}	0	Ramp log(f)		0.30
RVT_{ran}	0	Ramp log(f)		0.20
RVT Subsets				
	Base case $0.3/0.50 = 0.60$			Random model $0.2/0.5 = 0.40$
NL Uncertainties				
$S_{NL} = 0.15$		$pga_{ref} = 0.4$		$K_{max} = 2$
Magnitude / PGA interpolation + extrapolations				
Linear	SHAKE	RVT		Non-linear
See formulas				
2D-effects : $A_{2D} = 1 + C_{2D}(f,\zeta) = 1 + C^0_{2D}.A_0(f/f_0).exp(-2\pi\zeta_{av} fl/\beta_M)$ $\beta_M = \beta_{M0}.[1/(1 + 0.2(\gamma/\gamma_{50})_{max})]^{0.5}, \zeta_{av} \approx 0.0125 + 0.06.(\gamma/\gamma_{50})_{max}/[1. + 0.2(\gamma/\gamma_{50})_{max}]$				
Fixed parameters		$f_0 = 3.0Hz$	$l = 100m$	$\beta_m = 600m/s$ $h = 30m$
Alternative choice for parameters and corresponding weights		$C^0_{2D} = 0.$ weight 0.30	$C^0_{2D} = 0.30$ weight 0.50	$C^0_{2D} = 0.60$ weight 0.20

1.2.12 Mühleberg

Site-specific Model Evaluations

Weighting of Velocity Profiles

There are four velocity profiles for KKM, and relatively few in-situ measurements (mainly down-hole and non-invasive surface wave measurements). Their comparison with the available in-situ data are displayed in Figure II-1.51 (molasse unit) and A3.18 (gravel layer) for the velocity profiles, Figure II-1.53 for the dispersion curves, and Figure II-1.54 for the fundamental frequencies.

P1 is the "best estimate" profile proposed by AMEC on the basis of a weighting of the different available results, and relies for about 50% on borehole data, for about 30% on surface wave data (active and passive), and for the remaining on P-wave velocity profile derived from refraction and tomography data and estimated Poisson's coefficient. P2, P3 and P4 were derived mainly from the non-invasive surface-wave measurements, which could be interpreted in different ways, depending on the identification of some curves as corresponding to the fundamental of first higher mode. P2 and P3 were proposed first as alternative models fitting respectively each of the two interpretations: P2 considers high velocity MASW values as associated with the first higher mode of Rayleigh waves, and has therefore low velocity values in the gravel, lying over an only weakly weathered molasse, while P3 keeps the fundamental mode interpretation for MASW curves and therefore assigns higher velocity for the gravel layer, which has to be compensated by a significantly weathered molasse.

The last profile, P4, was added in order to match one specific array microtremor measurement exhibiting very low velocities from intermediate to high frequencies: it thus includes both a gravel layer with very low velocity (around 200 m/s) and a 20 m thick, significantly weathered molasse layer.

It turns out that the variability of actual measurements is very large, and that almost all profiles are acceptable in some respects. The initial weights are therefore equally distributed (25% for each). However, profile P4 is very extreme with low velocities and offers only a poor agreement with most in-situ data from the gravel layers. Therefore, this is the profile I assign the lowest weight. On the contrary, P1 is the profile that was derived with the largest weight on the borehole data, while the three other were based only on dispersion curves, with only little consideration for borehole data. I therefore decided to assign the largest weight to profile P1, which is a kind of 'best estimate" profile. And the two profiles P2 and P3 are considered equally acceptable, with their unchanged initial values of 25%.

Weighting of Material Properties

There are no specific lab test measurements for neither the gravel layer nor the weathered molasse. The consequence is a rather wide set of models, and also an a priori an equal weight such as 33% - 34% - 33% leading to the largest possible epistemic uncertainty.

Figure II-1.55 compares the proposed three sets of NL properties with more classical NL curves, those used for the PEGASOS project (Hardin & Drnevich, Ishibashi & Zhang). This indicates that the three NL properties sets considered for the gravel layer correspond to highly NL material, which will result in a very pronounced decrease of amplification and

Table II-1.18: Summary of comparison between profile attributes and measurements for KKM site.

Profile	Borehole data : velocity profile	Non-invasive surveys : Dispersion curve	f_0	Final weights
P1	OK	Intermediate predominantly fundamental mode interpretation for MASW results cnsistent with	rather high	40%
P2	OK in the molasse rather low in the gravel	good close to the lower bound at high frequency(2)	good	25%
P3	OK in the gravel rather low in the molasse	Intermediate (fundamental mode interpretation) (0)	rather low (6 Hz)	25%
P4	Very low in gravels, and rather low also in the shallow molasse part	Very close to the lower bound at all frequencies (33)	very low (close to 5Hz)	10%

even deamplification starting at moderate ground motion levels. On the contrary, the curves considered for weathered molasse are only very weakly non-linear, so that the amplification and Non-linearity will predominantly concentrate in the shallow gravels.

As a consequence, I pay more attention to the NL comparison for gravels (Figure II-1.55 left), and I decided to significantly skew the weight distribution towards the M3 model: my final weights are 15% for M1 (-18%), 45% for M2 (+11%) and 40% (+7%) for M3.

Table II-1.19: Weighting the NL property sets for KKM site.

Measurements	Comments	M1 = Lower bound	M2 = Best Estimate	M3 = Upper Bound
None		15%	45%	40%

Alternative 2D-parameters

According to the cross-sections initially provided by PROSEIS, the topography and subsoil exhibit significant lateral variations since the NPP site is within a river valley having an EW "banana" shape". The most relevant cross-sections are those perpendicular to local valley axis, i.e., NPP_M_CENTRE (NS through the site), $M\_EAST(NNW - SSEeastoftheNPP)$ and $M\_WEST(NNE - SSWwestoftheNPP)$

- The NS cross-section NPP_M_CENTRE exhibit a valley type topography, filled with thin quaternary layers over a total distance of about 700 m and a maximum thickness of about 15 m. The NPP site is located 200 m north of the southern edge of this sedimentary filling.

- The 2 other cross-sections are similar, with however a smaller lateral extent for the surficial soil layer (450 m), and similar thicknesses (up to 15 m). Along these directions, the soil layer edges are located 150 to 250 m away from the NPP.

Therefore, there probably exist some 2D-effects, but less pronounced than for Leibstadt, and only at high frequency. I include a three-branch sub-tree with respective C_{2D}^0 coefficients and weights, respectively, of (0.0, 30%), (0.1, 60%), and (0.3, 10%)

Summary of Weights and Parameters

1.3 Aleatory Variability of Horizontal Ground Motion

1.3.1 Approach

General Comments

The aleatory variability logic tree I proposed for the PEGASOS project included several terms, resulting in non-negligible values and a significant increase of the final total ground motion aleatory variability. The different terms were the following :

- the variability associated to the effect of the input signal waveform (i.e., signal phase), which was captured from the variance of the amplification factor as a function of time history : $\sigma^2 TH, AF$
- the variability associated to the soil profile spatial "aleatory" variability, as estimated from the RVT calculations for randomised profiles : $\sigma^2 RVT_{ran}$
- the variability associated with the variability of incident wave field (wave type, incidence angle and azimuth) : $\sigma^2 0 PSV$
- and finally the variability $\sigma^2 2D$ associated with the sensitivity of 2D/3D-effects to incident wave field

$\sigma^2 site, H = \sigma^2 rock, H + \sigma^2 AF, H$

with

$\sigma^2 AF, H = \sigma^2 TH, AF(+\sigma^2 RVT) + \sigma^2 0, PSV + \sigma^2 2D$

Revisiting this analysis 8 years later, a period during which a large amount of additional literature has been published on this "hot" issue of aleatory variability, I consider that almost all these terms, while actually contributing to the aleatory variability at a given site, are already present in the aleatory variability term of the rock motion. No rock site actually corresponds to a homogeneous half-space, and thus includes at least some part of the variability linked with the response of horizontally stratified media, also including some part of lateral variability (surface topography effects for instance): it thus includes a component for each for these four terms

$\sigma^2 TH, AF, \sigma^2 RVT, \sigma^2 0, PSV$

Table II-1.20: Summary of weights and computational parameters for the horizontal ground motion at KKM (Mühleberg) site.

Velocity profile				
P1 0.4	P2 0.25		P3 0.25	P4 0.10
Non-linear properties				
M1 0.15		M2 0.45		M3 0.4
Approaches				
Deformation range $(\gamma/\gamma_{50})_{max}$	Linear (0.05g)	RWF(SHAKE)	RWF(RVT)	Non-linear
< 1	0.2	0.48	0.32	0
> 1 and < 10	0,2* Red_LIN $[(\gamma/\gamma_{50})_{max}$	0.48*Red_LE $[(\gamma/\gamma_r)_{max}]$	0.32*Red_LE $[(\gamma/\gamma_r)_{max}]$	Complement to 1 +sub-branching
> 10	0.0	0.12	0.08	0.80+sub-branching
Frequency dependent relative weighting of EQL techniques (SHAKE, RVT_{bc}, RVT_{ran})				
frequency	$F < f1 =$ 0.5Hz	$0.5 < f$ $< 1Hz$		$f > 1Hz$
SHAKE	1	Ramp log(f)		0.6
RVT_{bc}	0	Ramp log(f)		0.233
RVT_{ran}	0	Ramp log(f)		0.167
RVT Subsets				
Base case $0.233/0.40 = 0.5825$			Random model $0.167/0.40 = 0.4175$	
NL Uncertainties				
$S_{NL} = 0.30$		$pga_{ref} = 0.10$		$K_{max} = 3$
Magnitude / PGA interpolation + extrapolations				
Linear	SHAKE	RVT		Non-linear
See formulas				
2D-effects : $A_{2D} = 1 + C_{2D}(f,\zeta) = 1 + C^0_{2D}.A_0(f/f_0).exp(-2\pi\zeta_{av} fl/\beta_m)$ $\beta_m = \beta_{m0}.[1/(1 + 0.2(\gamma/\gamma_{50})_{max})]^{0.5}, \zeta_{av} \approx 0.0125 + 0.06.(\gamma/\gamma_{50})_{max}/[1. + 0.2(\gamma/\gamma_{50})_{max}]$				
Fixed parameters		$f_0 = 9.0Hz$	$l = 200m$	$\beta_m = 500m/s$ $h = 8m$
Alternative choice for parameters and corresponding weights		$C^0_{2D} = 0.$ weight 0.30	$C^0_{2D} = 0.10$ weight 0.60	$C^0_{2D} = 0.30$ weight 0.10

and $\sigma^2 2D$. In addition, as the σ term of GMPE's is generally estimated globally, taking into account simultaneously rock, stiff and soft sites, the resulting values are certainly "contaminated" by the specific aleatory variability parts of non-rock sites.

The only specific term that is not present in the rock aleatory variability $\sigma^2 rock, H$ is the one linked with the sensitivity of the Non-Linear response to the characteristics of the incident signal and wave-field, as rock response is assumed to be linear at least within the range of PGA levels considered here.

Therefore, I reduced my four-component estimate of the additional aleatory variability linked only to site response to only one component, $\sigma^2 NL$.

$$\sigma^2 soil = \sigma^2 rock + \sigma^2 TH, AF_{NL}$$

In addition to this "evolution" of my original PEGASOS model, another component has to be taken into account : the above formula is valid only if the two components,
$\sigma^2 rock$ and $\sigma^2 TH, AF_{NL}$,
are independent of each other. When it is not the case, this relationship should be corrected taking into account the cross correlation between the two components, i.e.,

$$\sigma^2 soil = \sigma^2 rock + \sigma^2 TH, AF_{NL} + 2Cor(AF_{NL}, S_{a,rock})$$

To estimate this correlation, one must thus also consider, within each set of 9-10 time histories, the evolution of AF_{NL} with the spectral ordinate value. This information is not directly available (but could rather easily be derived), the number of time histories may be however too small to derive valid relationships between AF_{NL} and $S_{a,rock}$; in addition, such a correlation would need to be derived, at each frequency, with the corresponding rock spectral value at the frequency of interest (since PGA has the same value for all time histories).

An alternative approach is to estimate directly σ^2 soil and to consider its evolution with the level of input ground motion in the NL case, compared to the linear case

$$\Delta\sigma^2 SA_{NL}(f) \approx \sigma^2 SA, soil - \sigma^2 SA, lin \approx \sigma^2 SA, soil - \sigma^2 rock$$

So, instead of computing directly the correlation, it is also possible to work on the increase (or decrease) of variability in the final spectral ordinate value SA_{NL}.

The first issues to address are thus to estimate these two terms "$\Delta\sigma^2 AF_{NL}$" and "$\Delta\sigma^2 SA_{NL}$", i.e., the changes in the variability of amplification factors and response spectra due to the NL response.

Model Construction

Comparing the Variability of AF_{NL} for Different Time Histories with the one of AF_{LIN} :

$$\Delta\sigma^2 AF_{NL} = \sigma^2 TH, AF_{NL} - \sigma^2 TH, AF_{LIN}$$

Considering the very small amount of actual recordings with unambiguously proved NL behavior, it is not easy to estimate this specific component $\sigma 2NL$. I attempted to get a site-specific estimate from the available computations, by comparing the variability of the

amplification factors derived from Non-Linear computations $[\sigma^2 TH, AF_{NL}(f, pga; P1\_Mj)]$ to the corresponding variability of linear computations.

$$\Delta\sigma^2 AF_{NL}(f) \approx \sigma^2 TH, AF_{NL}(f; pga, M; P1\_Mj) - \sigma^2 TH, AF_{SHAKE}(f; 0.05g, M; P1\_Mj)$$

Such an estimate is meaningful only if the time histories used for input in the linear and non-linear computations have the same dispersion characteristics: for the PRP case, this can be done only on the 2010 SHAKE and NL computations, since the 2013 computations involved only the linear equivalent approach, and with completely different, much less variable input spectra.

Since these computations are not available for neither all PGA nor all magnitude values, nor all material properties, and since also they might sometimes be negative, I tried to derive some simple relationships between these quantities and some explaining variables. Three explaining variables have been considered : the most physical one is the peak strain ratio as derived from the NL computations, the second and third are more tractable parameters that are available for almost all computations : the peak strain ratio $(\gamma/\gamma 50)max, RVT_{bc}$ derived from RVT_{bc}, and the PGA value.

In order to "stabilize" the results, the original $\sigma^2 TH, AF_{NL}(f)$ and $\sigma^2 TH, AF_{SHAKE}(f)$ have been smoothed in the frequency domain with a 10 sample wide, box shaped, running window.

This work was first performed globally on the 2010 computations, considering all available results for all surface sites altogether. As the correlation did not prove satisfactory for the two last variables, the regression analysis was repeated separately for each NPP site and each depth. The results are displayed in 1.13, Figures II-1.56, II-1.57,II-1.58, II-1.59, II-1.60 and II-1.61 for surface receivers, II-1.62 to II-1.63, II-1.64, II-1.65 and II-1.66 for depth z2, and II-1.67, II-1.68 and II-1.69 for depth z3.

They depict, as a function of frequency, the correlation between
$\Delta\sigma^2 AF_{NL}(f; pga, m; P1\_Mj)$
and $log(\gamma/\gamma_{50})max, \_NL(f; pga, m; P1\_Mj), \Delta\sigma^2 AF_{NL}(f; pga, m; P1\_Mj)$
and log $(\gamma/\gamma_{50})max, RVT_{bc}(f; pga, m; P1\_Mj)$,
and $\Delta\sigma^2 AF_{NL}(f; pga, m; P1\_Mj)$ and log(PGA). Several quantities are displayed:

- the correlation coefficient RAF(f) (three of them, for each considered explanatory variable)
- the variance of the $\Delta\sigma^2 AF_{NL}(f; pga, m; P1\_Mj)$ for all the PGA, magnitude and material properties available, as well as the variance reduction resulting form the derived prediction equations (directly linked to the corresponding correlation coefficient)
- the coefficients a (slope) and b (constant term) of these derived equations

$$\Delta\sigma^2 AF_{NL}(f; pga, m; P1\_Mj) = aAF(f).log(\gamma/\gamma 50)max, \_NL(f; pga, m; P1\_Mj) + \beta AF(f)$$

$$\Delta\sigma^2 AF_{NL}(f; pga, m; P1\_Mj) = aAF(f).log(pga) + bAF(f)$$

The correlation coefficients RAF(f), as well as the regression coefficients [e.g., aAF (f) and bAF(f)], are specific to each NPP site and each depth.

These results show that the "best" overall correlation is generally obtained with the NL peak strain ratio (except for the KKM case), while the correlations obtained with the RVT_{bc} peak strain ratio and PGA are generally comparable (slightly better with PGA for EKKB and KKM, slightly worse for KKG). These results also show that the "explanatory power" of the considered variable varies significantly with frequency, with a general trend to be rather small at low frequencies (no or limited variance reduction), significant at intermediate frequencies, and decreases at high frequencies (beyond 20 Hz).

The results of these analyses are listed, for each site and depth, in an attached excel file ("regression_pga_AV_SA+AF_z1z2z3.xlsx", sheets AF_KKx)

Comparing the Variability of SA_{NL} for Different Time Histories with the one of SA_{LIN} :

$\Delta\sigma^2 SA_{NL} = \sigma^2 TH, SA_{NL} - \sigma^2 TH, SA_{LIN}$

As indicated in 1.3.1, it is mandatory to check also whether the variability of the non-linear response spectra varies with PGA. A similar analysis to the one of the previous section was thus performed, considering the non-linear response spectra instead of the non-linear amplification factors, and comparing them with the variability of the linear response spectra (again instead of the linear amplification factors). As for the amplification factor, this is meaningful only if the input time histories exhibit the same dispersion characteristics for the linear and non-linear computations, which imposes to use the 2010 SHAKE and NL computations.

I thus computed the quantity :

$$\Delta\sigma^2 SA_{NL}(f) \approx \sigma^2 TH, SA_{NL}(f; pga, m; P1\_Mj) - \sigma^2 TH, SA_{SHAKE}(f; 0.05g, M; P1\_Mj)$$

and investigated its correlations with PGA and RVT_{bc} peak strain ratios $[(\gamma/\gamma 50)max, RVT_{bc}]$ for each site and depth: a positive value for the correlation RSA(f) would indicate an increase of ground motion variability due to NL behavior, while a negative one would indicate a decrease, in connection for instance with the saturation of ground motion under extreme input motion.

The results are displayed in Figures II-1.69 to II-1.81 and listed in an attached excel file ("regression_pga_AV_SA+AF_z1z2z3.xlsx", sheets SA_KKx) in exactly the same way as for the amplification factors. The most remarkable features of these results may be summarized as follows:

- there are two sites with clear negative correlations: KKG and KKL. For intermediate frequencies (typically 1 - 8 Hz), the aleatory variability of NL response spectra is reduced with respect to the linear case, at all depths (Figures II-1.72, II-1.73, II-1.77, II-1.78 and II-1.80). Outside these frequency range however, a reverse trend may exist.
- A similar, though less pronounced, trend may be detected at site EKKB surface, and KKB and EKKB z2 depths (Figures II-1.71, II-1.75 and II-1.76);
- all sites except KKM exhibit a (slight) trend to increased variability at low frequencies.

- concerning correlations with the various parameters, there is no systematic and clear differences between the performance of log(PGA) and $log(\gamma/\gamma_{50})max, RVT_{bc}$. Therefore, as for the $\Delta\sigma^2 AF_{NL}$ case, only correlations with PGA will be considered for the logic tree model.

$$\Delta\sigma^2 SA_{NL}(f; pga, m; P1\_Mj) = a_{SA}(f).log(pga) + b_{SA}(f)$$

The results of these analyses are listed, for each site and depth, in an attached excel file ("$regression\_pga\_AV\_SA + AF\_z1z2z3.xlsx$", $sheets SA_K Kx$).

A comparison of correlation coefficients obtained for $\Delta\sigma^2 AF_{NL}(f)$ and $\Delta\sigma^2 SA_{NL}(f)$ with PGA is depicted in Figures II-1.82 to II-1.86, for each site and depth, in order to better illustrate the correspondance between each kind of correlation, and to better understand the assignment of weights to each approach.

1.3.2 Logic Tree and Weight

My logic tree for the aleatory variability thus finally includes three branches :

- one with no change at all in the aleatory variability corresponding to rock motion
- the second one ("AF") corresponding to an increase of the aleatory variability, estimated from the increase of aleatory variability of the amplification factor, and assuming it is NOT correlated with the rock input motion :

  $\Delta\sigma^2 AF_{NL}(f; pga, m; P1\_Mj) = aAF(f).log(pga) + bAF(f)$
- the third one ("SA") corresponding to a variation of the aleatory variability as estimated directly from the aleatory variability of the resulting ground motion :

  $\Delta\sigma^2 SA_{NL}(f; pga, m; P1\_Mj) = aSA(f).log(pga) + bSA(f)$

As the second branch implies a strong uncorrelation assumption, I assign it a lower weight (actually twice less) than to the third branch.

It should be noted that the third branch may correspond either to a reduction of the aleatory variability (negative value for $\Delta\sigma^2 SA_{NL}$), or to an increase (positive value for $\Delta\sigma^2 SA_{NL}$), while the second branch only lads to an increase of the aleatory variability. In other terms, increase in the aleatory variability may occur in two circumstances:

- there exists a noticeable increase of both $\Delta\sigma^2 AF_{NL}$ and $\Delta\sigma^2 SA_{NL}$ with increasing PGA
- there exists a noticeable increase of $\Delta\sigma^2 AF_{NL}$ without any clear trend of $\Delta\sigma^2 SA_{NL}$ with increasing PGA

It is interesting to notice that there does not exist any case with noticeable increase $\Delta\sigma^2 SA_{NL}$ without any clear trends on $\Delta\sigma^2 AF_{NL}$, except at extreme frequencies (below 0.5 Hz or beyond 50 Hz) for KKB and KKL.

Conversely, decrease in the aleatory variability corresponds to only one case : there exists a noticeable decrease of $\Delta\sigma^2 SA_{NL}$ with increasing PGA. Interestingly enough, all such cases are associated with an increase of $\Delta\sigma^2 AF_{NL}$ with increasing PGA, which does correspond to the saturation of ground motion with increasing PGA.

The next and important step is to assign weight to each of these three branches ($W_0, W_{AF} and W_{SA}$, respectively). The issue is indeed to propose numbers for $W_{AF} and W_{SA}, since W_0 = 1-(W_{AF}+W_{SA})$.

Considering that the values I use for the increase or decrease of aleatory variability are derived from correlations (with log(PGA)), it seems logical to connect this reliability with the value of the associated correlation coefficient (as displayed in Figures II-1.82 to II-1.86). I thus decided to consider the present results ($for AF_{NL} or for SA_{NL}$), only when the corresponding correlation coefficient exceeds a "threshold" value of 0.4 (positive or negative). This value may look rather small; they are not inconsistent however, with the correlation values accepted for the tuning of some GMPE parameters; a correlation coefficient of 0.4 is associated with a variance reduction of 8%, which might be helpful at very long return periods.

A first level of information can be gained from an "automatic assignment" of partial, intermediate "influence factors", I_{AF} and I_{SA}, directly related to these threshold values:

- $I_{AF} = Max(0; R_{AF} - 0.4; -R_{AF} - 0.4)/2$
  (in fact, R_{AF} is always positive)
- $I_{SA} = sign(RSA).Max(0; R_{SA} - 0.4; -R_{SA} - 0.4)/2$

These influence factors are displayed in II-1.5. They emphasize the existence of negative SA correlations for KKG and KKL (at all depths). The negative correlations at KKB z2 and KKM z3 are somewhat misleading since the corresponding aleatory variability remain very small as the corresponding sites are in the "geotechnical bedrock" (opalinuston and molasse, respectively).

From this information, I decided to assign the following weights:

- when $R_{SA} \leq 0.4, W_{SA} = 0$
- when $R_{AF} \leq 0.4, W_{AF} = 0$
- when $R_{SA} < -0.4$,
  - $W_{AF} = 0.$
  - $W_{SA} = -(R_{SA} + 0.4)$
- otherwise
  - $W_{SA} = (R_{SA} - 0.4)$
  - $W_{AF} = (R_{AF} - 0.4)/2 * Min[1; (R_{SA} + 0.4)]$
  - (this last term is intended to lead to some smoothing of the W_{AF} value since it is automatically set to 0 when $R_{SA} < -0.4$: the AF branch gets its full weight when both R_{AF} and R_{SA} are larger than 0.4)

The weights automatically assigned with this procedure are displayed in Figure II-1.6.

Along the "AF" branch , the changes in aleatory variability should be computed with the "$\Delta\sigma^2_{AFNL}$" formulae from the PGA level.

Along the "SA" branch, the changes in aleatory variability should be computed from the PGA level with the "$\Delta\sigma^2_{SANL}$" formulae.

1.3.3 Practical Implementation

Regularising and Simplifying the Branches and Weights

The "raw" results displayed in Figure II-1.6 exhibit a rather complex behavior, with rapid changes as a function of frequency, implying a discrete number of "sequences" where a given branch should be taken into account over a continuous frequency range. This results in a somewhat uncomfortable feeling about the robustness of the approach. Therefore, in order to keep only the most prominent features, I decided to set up a few "common sense" rules as detailed below :

- dropping a whole sequence whenever the maximum weight over the full frequency range remains below 5%
- dropping a whole sequence whenever the maximum change in aleatory variability $\Delta\sigma^2$ (positive or negative) at 2.5g is smaller than 0.05.
- dropping a sequence whenever its full frequency width is smaller than 15% of the central frequency (i.e., 1.5 Hz at 10Hz,)

Applying these rules results in the results displayed in Figures II-1.7 to II-1.14, which are much simpler than the raw ones (Figures II-1.6 and II-1.15). Figure II-1.7 displays the frequency dependence of the final weights for each branch at each depth of each site. Figures II-1.8 and II-1.9 display the frequency dependence of the corresponding regression coefficients for the SA and AF branches, respectively, at each depth of each site. Figures II-1.10 to II-1.14 summarize the results for each site, also including the values of the aleatory variability changes (positive or negative) between 0.1g and 2.5g, for each depth of each site.

Issues Linked with Decreasing the AV

Principle

The proposed model implies to reduce the aleatory variability in some cases (intermediate frequencies, KKG and KKL): this is impossible with the standard implementation for computing the total aleatory variability combining SP1, SP2 and SP3.

I therefore propose the following way to include such a reduction in σ.

The aleatory variability considered here is the "single-station" $\sigma\phi^2_{SS}$ at surface. For a soft site, as reminded earlier in this section, the classical approach is to consider the different terms in the aleatory variability as independent, so that the final aleatory variability is simply the square root of the squared aleatory components, which is written simply as :

$\phi^2_{SS,soil} = \phi^2_{SS,rock} + \Delta\sigma^2 response$

In order to make possible a reduction of the aleatory variability, I propose to rewrite this equation :

$\phi^2_{SS,soil} = (\phi^2_{SS,rock} - C) + (\Delta\sigma^2 response + C)$

or $\phi^2_{SS,soil} = \phi^2_{SS,rock,mod} + (\Delta\sigma^2 response + C)$

with

$\phi^2_{SS,rock,mod} = (\phi^2_{SS,rock} - C)$

and C chosen so that the quantity $(\Delta\sigma^2 response + C)$ is always positive.

The corresponding rock input hazard should therefore be computed with a modified (reduced) aleatory variability.

This should be done for three sites : KKB, KKG and KKL. It is not needed for the two other (EKKB and KKM) where there are no reduction of the aleatory variability due to the NL response.

Choosing the "C" Value: "Simple" Option

As outlined in the previous sections and in Figures II-1.7 to II-1.14 (and the Annex A4), there are basically two main cases where $\Delta\sigma^2_{response}$ is negative (KKG and KKL, intermediate frequencies), and an additional one, not fully understood : the $z2$ site at KKB, which is within the opalinuston unit. The value of C is thus determined by looking at the maximum reduction due to a negative value of $\Delta\sigma^2_{response}$, which corresponds to KKL around 3 Hz, with a value of $\Delta\sigma^2_{SANL}$ (3 Hz; 2.5g) equal to about -0.25.

Therefore, I propose to take C = 0.3, and to replace all the formulae of section

$\Delta\sigma^2_{SANL}(f; pga, m; P1\_Mj) = a_{SA}(f).log(pga) + b_{SA}(f)$

by the modified formulae

$\Delta\sigma^2_{SANL}(f; pga, m; P1\_Mj) = a_{SA}(f).log(pga) + [b_{SA}(f) + C]$

which consists simply in adding C = 0.3 to the constant term.

Choosing the "C" Value: More Complex, "Optimized" Option

Another option, as the reduction is PGA and frequency dependent, could be to take a PGA and frequency-dependent dependent C term, in the form $C = y(f).log(pga) + z(f)$, where $y(f)$ and $z(f)$ would be taken as the envelope of the opposite all $a_{SA}(f)$ and $b_{SA}(f)$ terms over all sites and depths, i.e., over KKB (z2) , KKG and KKL.

Such an option would add some complexity, without changing the final result. But depending on the way this step will be implemented, it might be preferred. I thus provided in a special sheet of the attached excel file (named "Minimum SANL - Envelope") the corresponding values for $y(f)$ and $z(f)$: they are non-zero only in the frequency range [1.7 Hz - 14 Hz]. The corresponding variations of

$\Delta\sigma^2_{SANL}$ with PGA are provided in the same sheet.

Important Note for the Implementation of the Formulae Providing $\Delta\sigma^2_{SANL}(f,pga)$ and $\Delta\sigma^2 AFNL(f,pga)$:

The actual values of $\Delta\sigma^2_{SANL}(f,pga)$ and $\Delta\sigma^2_{AFNL}(f,pga)$ at low PGA values should be close to 0.

The linear regressions with $a(f)$ and $b(f)$ are only approximations, and may be wrong at very low PGA values. In order to avoid wrong values at low PGA, the formulae should be implemented in the following way :

- AF case : R_{AF} is always positive, so the formula should be
  - $\Delta\sigma^2_{AFNL}(f,pga) = Max\{0; a_{AF}(f).log(pga) + b_{AF}(f)\}$
- SA case : R_{SA} may be either negative or positive, so the formulae should be
  - if $R_{SA} < -0.4, \Delta\sigma^2_{SANL}(f,pga) = Min\{0; a_{SA}(f).log(pga) + b_{SA}(f)\}$
  - if $R_{SA} > 0.4, \Delta\sigma^2_{SANL}(f,pga) = Max\{0; a_{SA}(f).log(pga) + b_{SA}(f)\}$

Attached Excel File

The results of all these analyses are listed, for each site and depth, in an attached excel file ("$weights + coef\_aleatory\_final\_modmanuel\_seuil5\%.xlsx$"). This excel contains several sheets. The raw results as deriving from the analysis explained in sections 1.3.1 and 1.3.2, are provided in the sheets "KKX_AF"$and KKX\_SA$" describing the raw correlations for $\Delta\sigma^2_{AFNL}(f,pga)$ and $\Delta\sigma^2_{SANL}(f,pga)$, respectively (with the two or three depths required for each site in each sheet). This excel file also contains, for each site, two additional sheets labelled "$KKX\_final\_weights$"and"$KKX\_pga\_dependence$", providing the adjusted weights and the associated variability with PGA (respectively), according to the "rules" explained in Section 1.3.3. It also includes a graphic sheet with all the figures displayed in Figures II-1.7 to II-1.14.

1.4 Maximum Horizontal Ground Motions

Evaluating the maximum possible ground motion at a given site is not a simple task. As far as site effects are concerned, the only source of limitations in the ground motion lies in the maximum strains that a given soil can withstand, beyond which it fails. While such a failure is conceivable – and actually is a real phenomenon - for shearing stresses and strains – roughly corresponding to horizontal motion -, it is much less obvious for normal (compressive) stresses and strains – mainly corresponding to vertical motion in a first, rough approximation.

1.4.1 Evaluation of Proposed Models

There has been basically two different approaches proposed, updating what had already been done for the PEGASOS project

- estimating the maximum PGA from the maximum possible strains, and associating a normalized response spectrum ($document TP3-TB-1074\_SP3-MaxGM_3 3-08N2A-$

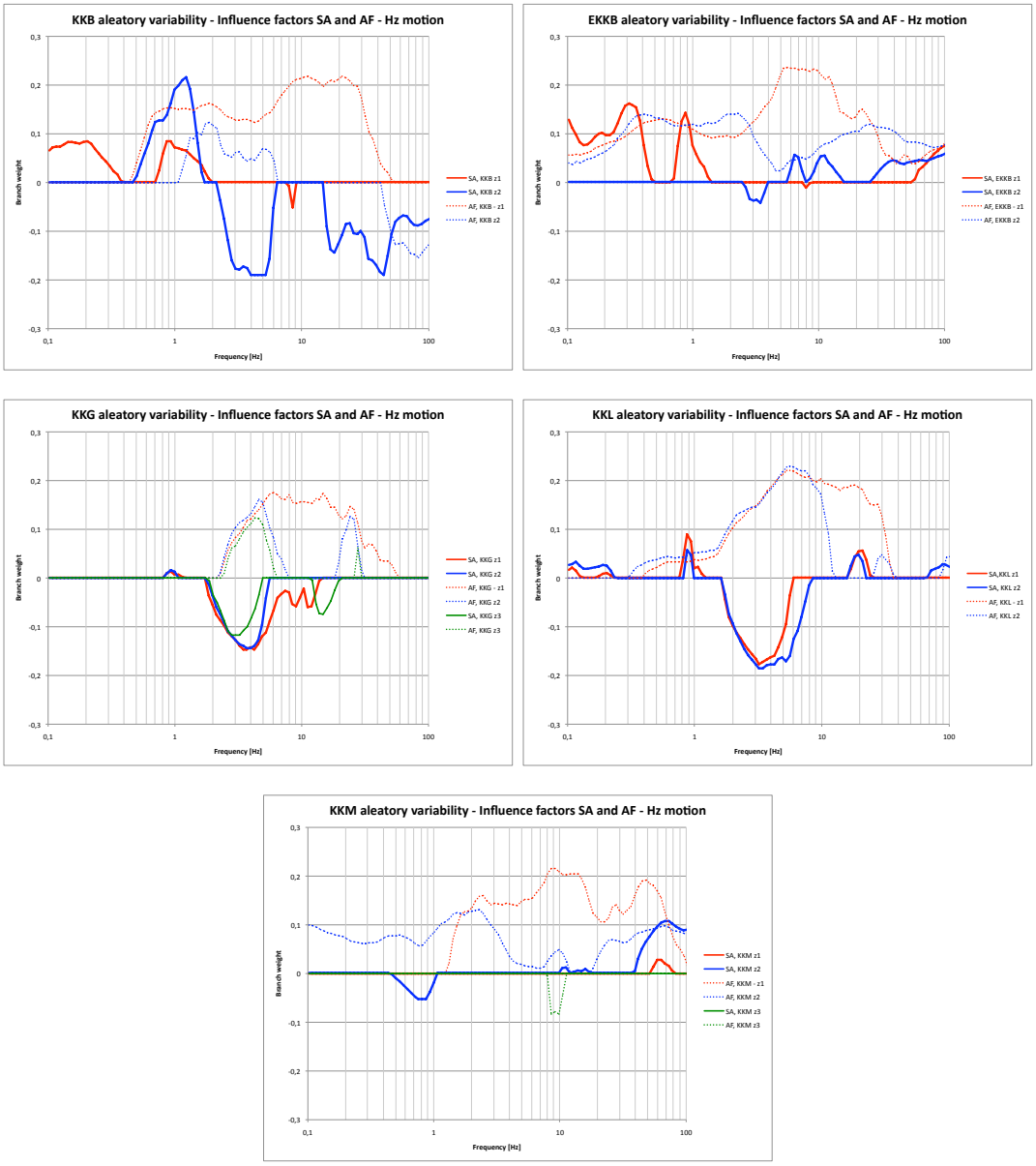

Figure II-1.5: "Influence factors" automatically derived from the analysis of correlations between the aleatory variability of amplification factors (AF, dotted lines) and response spectra (SA, solid lines) computed with the NL approach, according to the procedure described in the text, for each KK site (different cells) and depth (different colors). "Negative" influence factors are simply introduced to image the frequency bands where the correlation coefficients are negative; this occurs only for response spectra.

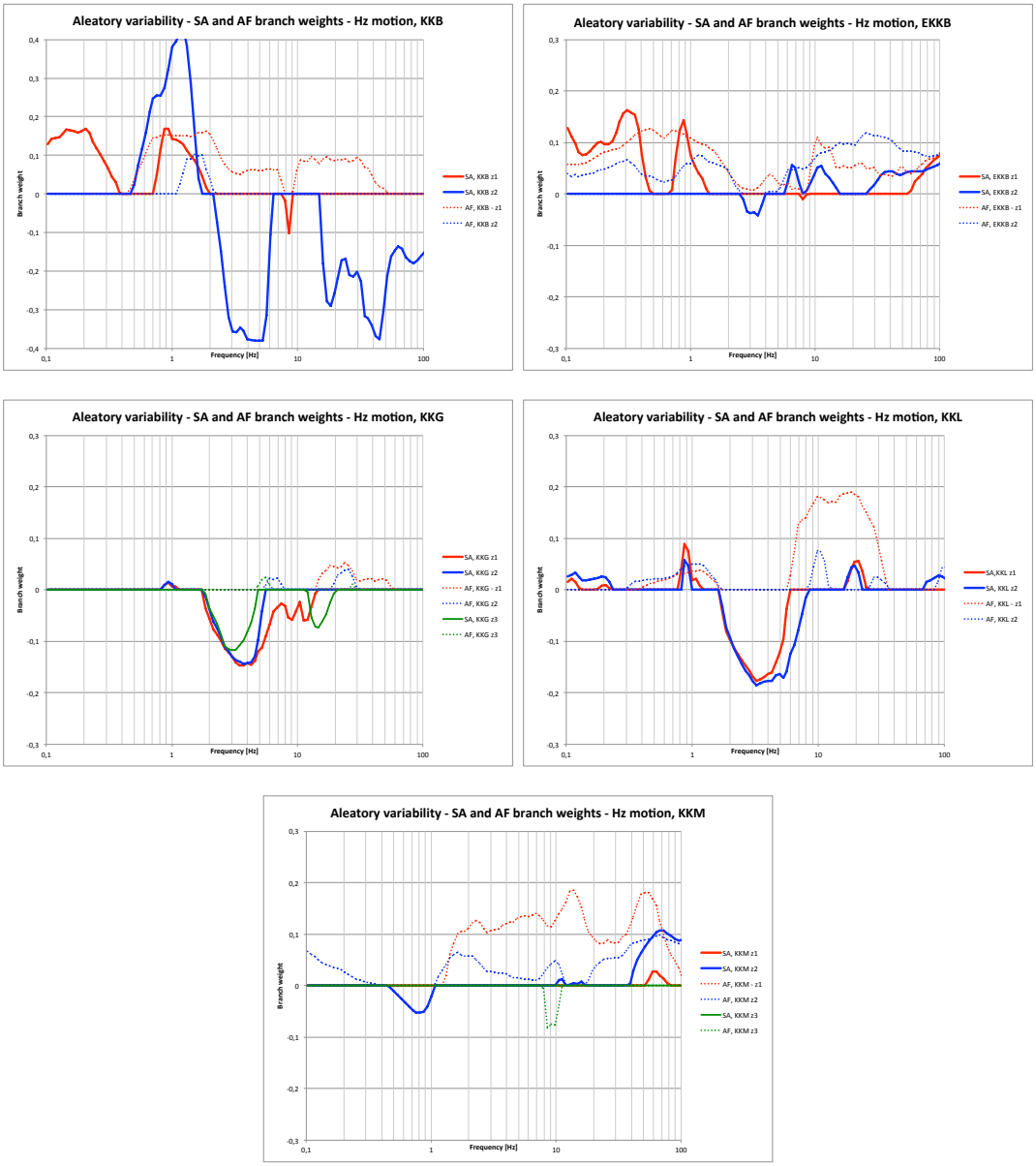

Figure II-1.6: Weights automatically derived from the analysis of correlations between the aleatory variability of amplification factors (AF, dotted lines) and response spectra (SA, solid lines) computed with the NL approach, according to the procedure described in the text (section 3.2), for each KK site (different cells) and depth (different colors). "Negative" weights are simply introduced to image the frequency bands where the correlation coefficients are negative; this occurs only for response spectra.

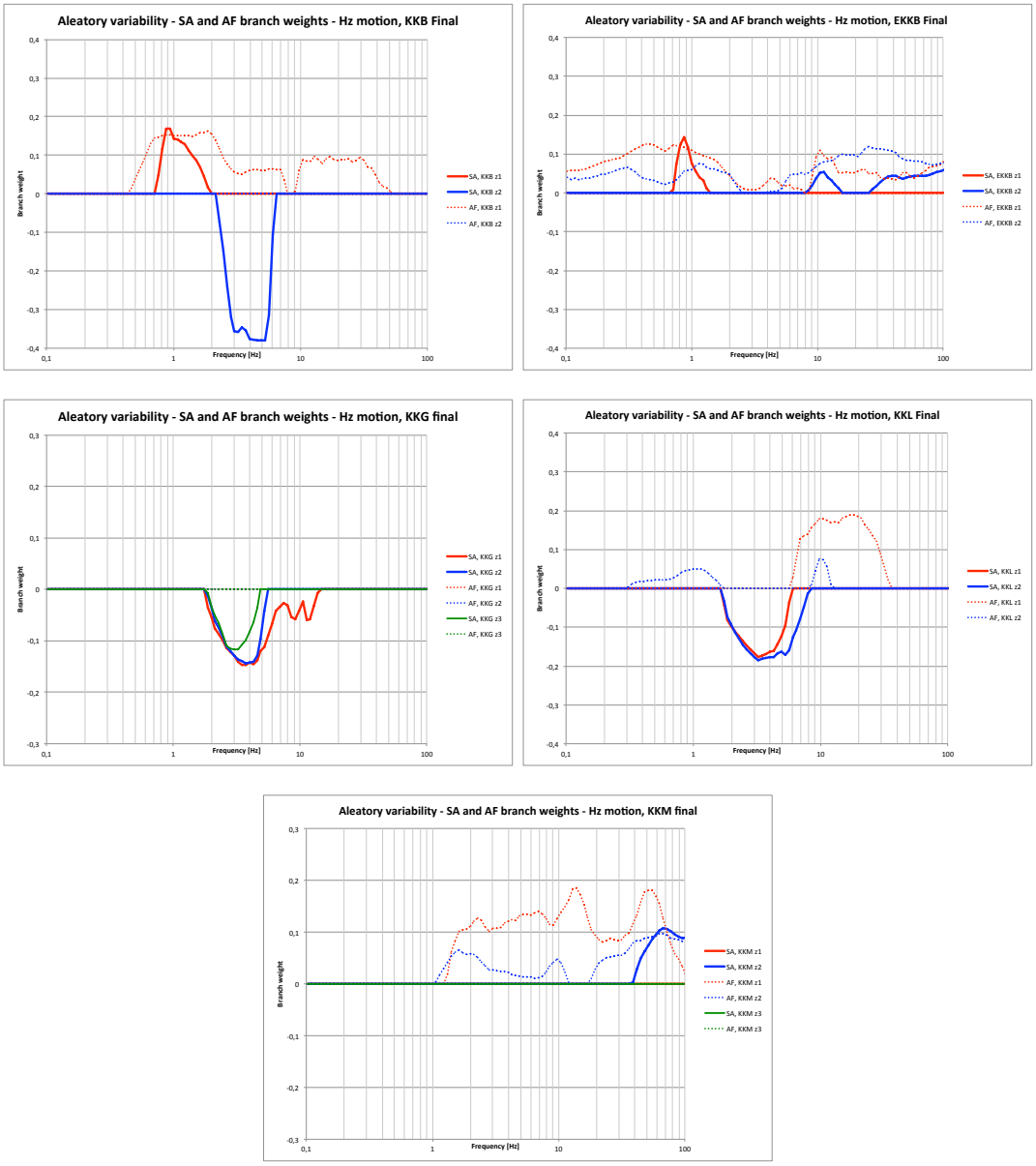

Figure II-1.7: Final weights for the AF and SA branches of the aleatory variability logic tree, after manual tuning taking into account the rules described in section 3.3 of the text. AF branch, dotted lines; SA branch, solid lines. Each cell corresponds to a different site, each color to a different depth). "Negative" weights are simply introduced to image the frequency bands where the correlation coefficients are negative; this occurs only for the SA branch.

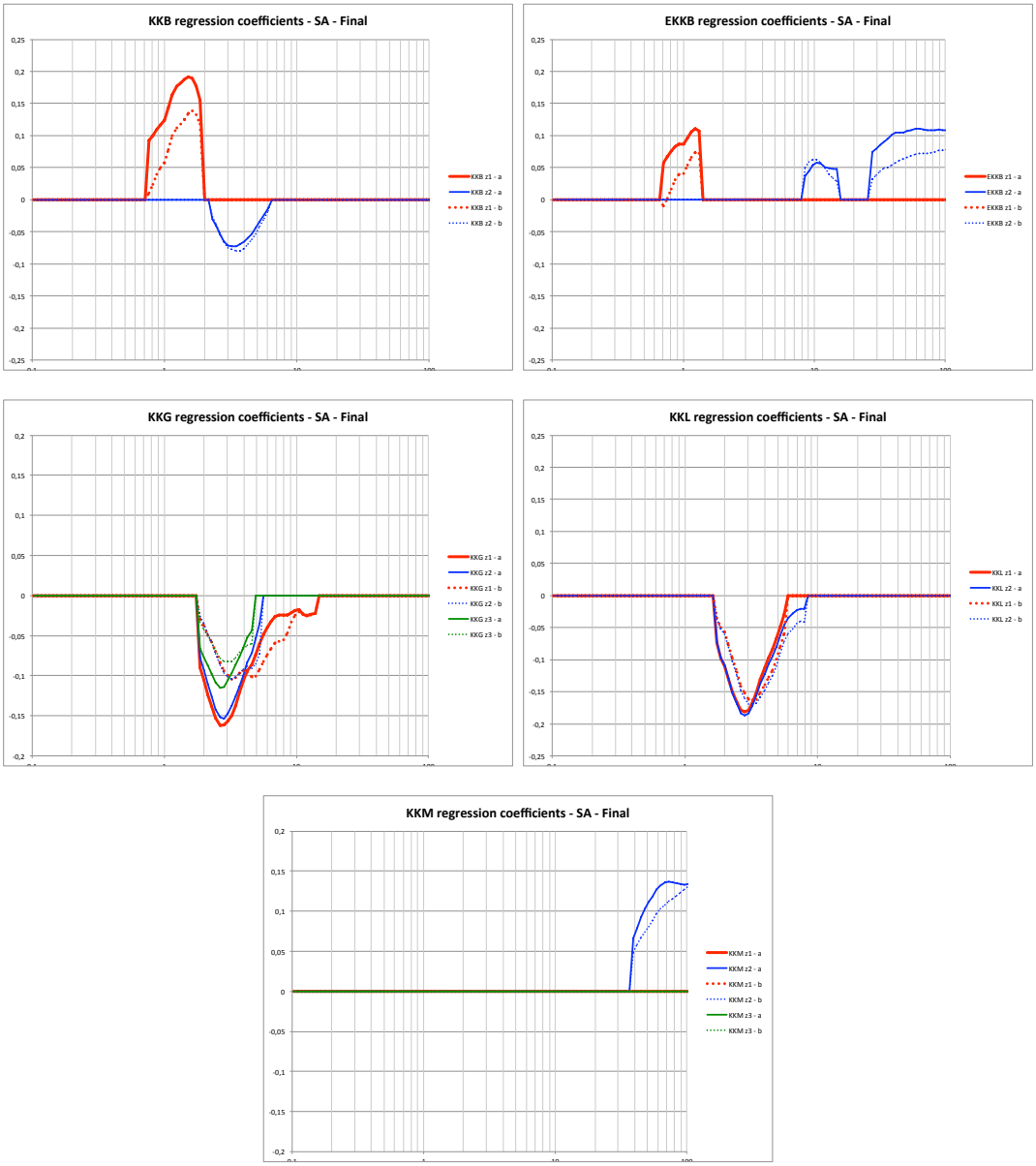

Figure II-1.8: Correlation coefficient a and b for the SA branch. Each cell corresponds to a different site, each color to a different depth (red = surface or z1, blue = z2, green = z3). Solid lines correspond to a coefficient, dotted lines to b coefficient in the relationship : $\Delta\sigma^2_{SANL}(f;pga) = a_{SA}(f).log(pga) + b_{SA}(f)$.

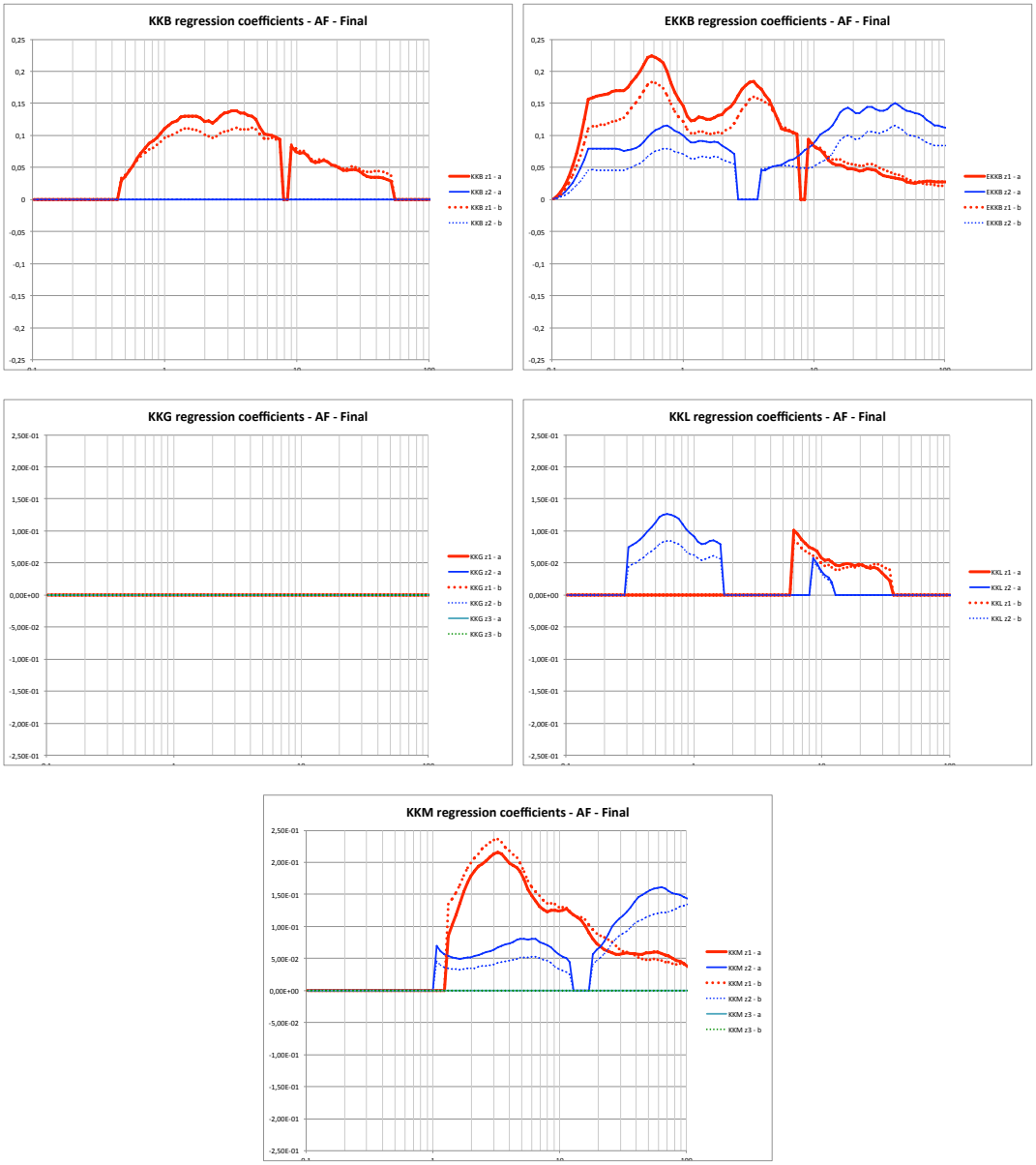

Figure II-1.9: Correlation coefficient a and b for the AF branch. Each cell corresponds to a different site, each color to a different depth (red = surface or z1, blue = z2, green = z3). Solid lines correspond to a coefficient, dotted lines to b coefficient in the relationship: $\Delta\sigma^2_{AFNL}(f; pga) = a_{AF}(f).log(pga) + b_{AF}(f)$.

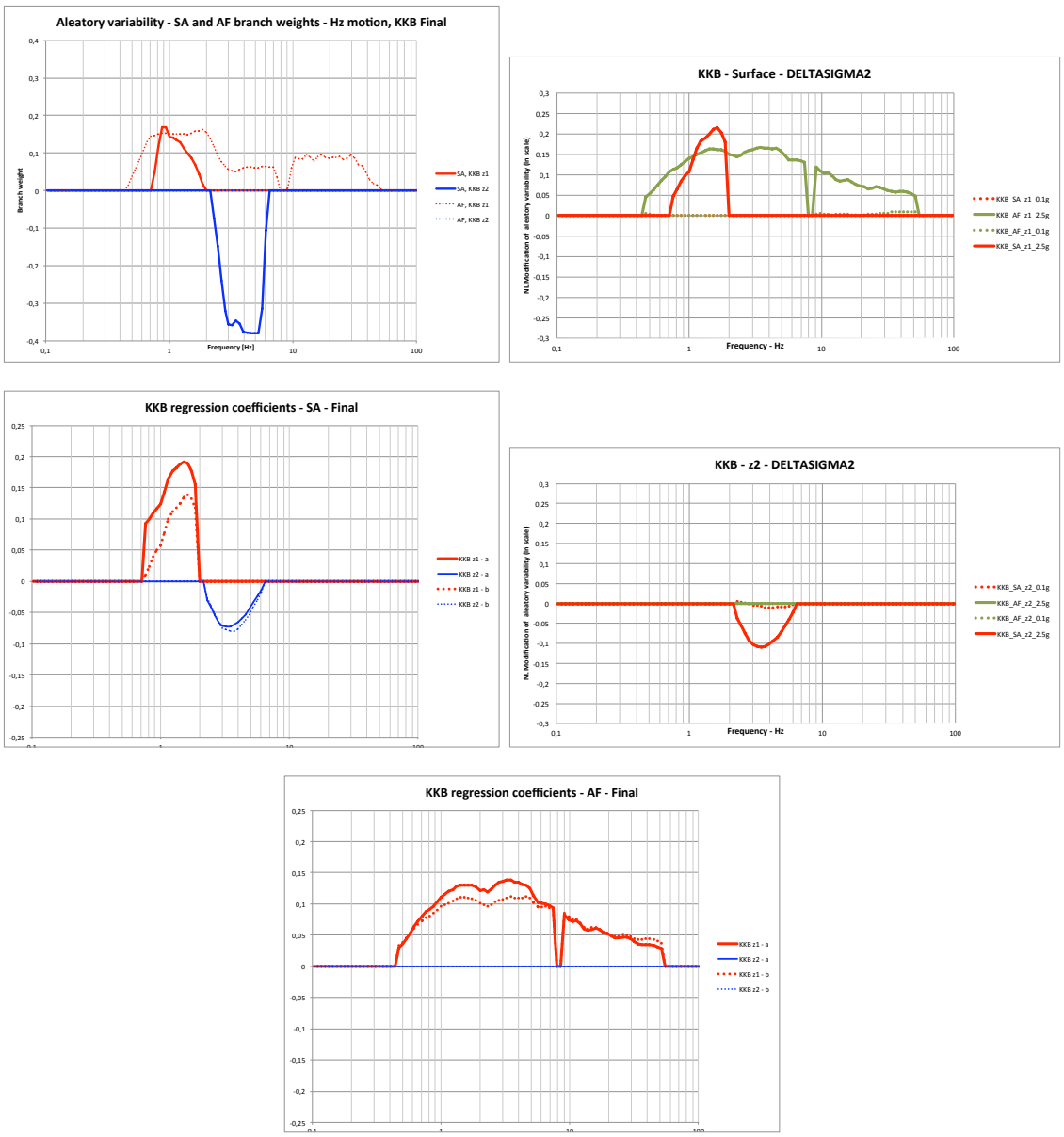

Figure II-1.10: Summary results for KKB. Top left: final weights: Middle left : regression coefficients for the SA branch; Bottom left: regression coefficient for the AF branch; in this left column each color corresponds to a different depth (red=surface, blue = z2). The right column displays the maximum changes (positive and negative) for the aleatory variability along the AF and SA branches between 0.1g (dotted line) and 2.5 g (solid line) for the SA (red) and AF (green) branches. Top frame = surface site, middle frame = z2 depth.

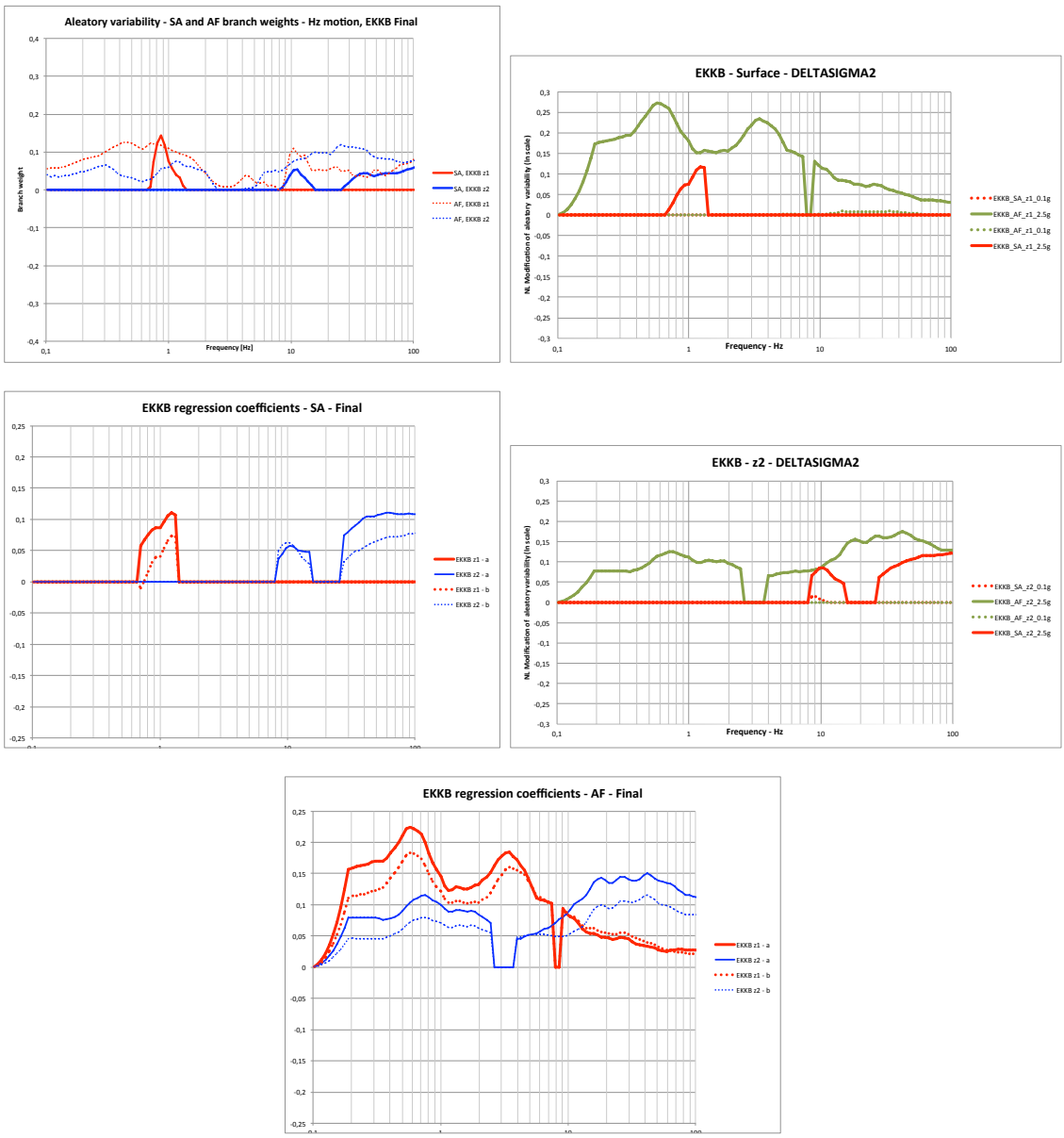

Figure II-1.11: Summary results for EKKB. Top left: final weights: Middle left : regression coefficients for the SA branch; Bottom left: regression coefficient for the AF branch; in this left column each color corresponds to a different depth (red=surface, blue = z2). The right column displays the maximum changes (positive and negative) for the aleatory variability along the AF and SA branches between 0.1g (dotted line) and 2.5 g (solid line) for the SA (red) and AF (green) branches. Top frame = surface site, middle frame = z2 depth.

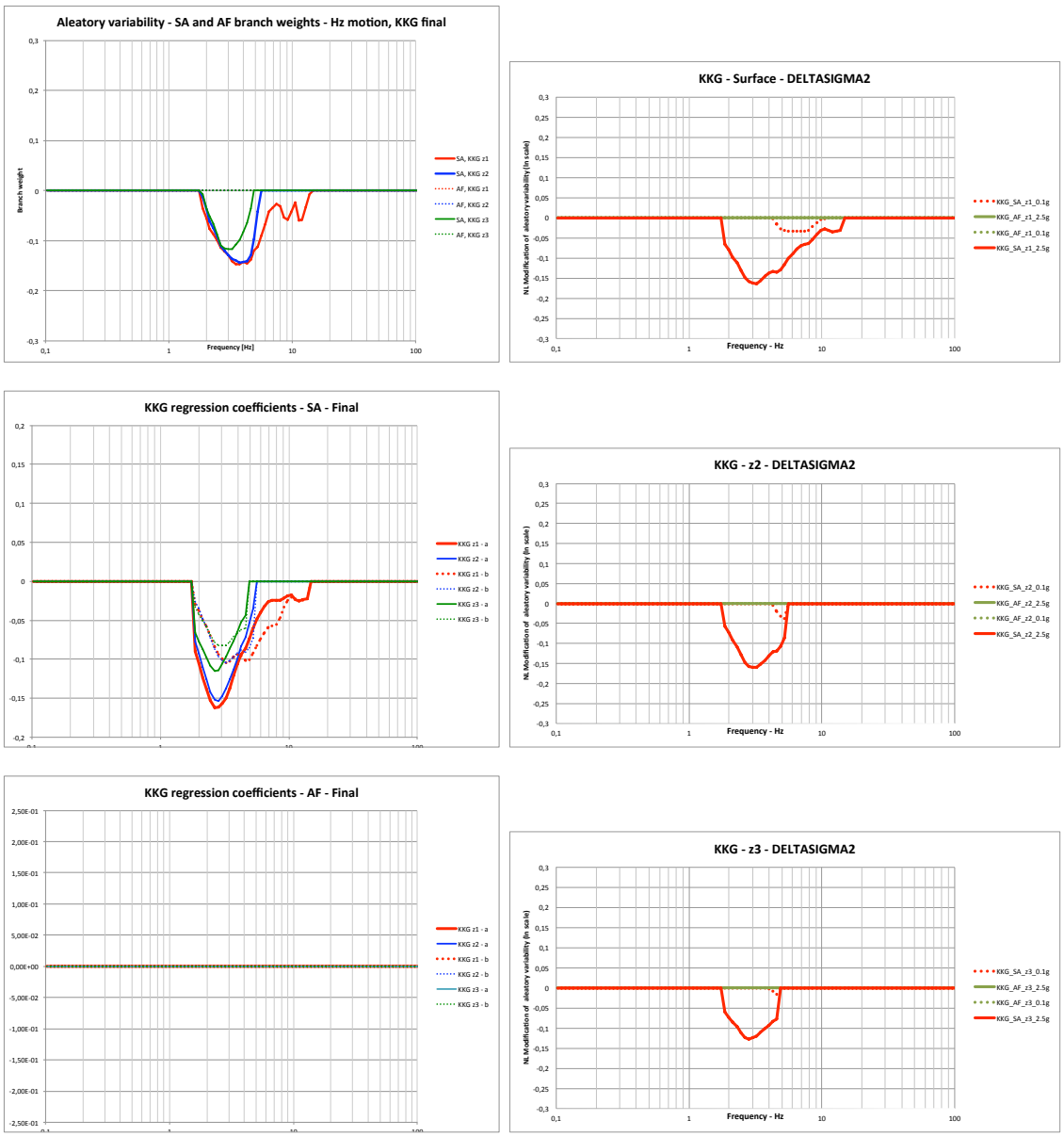

Figure II-1.12: Summary results for KKG. Top left: final weights: Middle left : regression coefficients for the SA branch; Bottom left: regression coefficient for the AF branch; in this left column each color corresponds to a different depth (red=surface, blue = z2). The right column displays the maximum changes (positive and negative) for the aleatory variability along the AF and SA branches between 0.1g (dotted line) and 2.5 g (solid line) for the SA (red) and AF (green) branches. Top frame = surface site, middle frame = z2 depth, bottom frame = z3 depth.

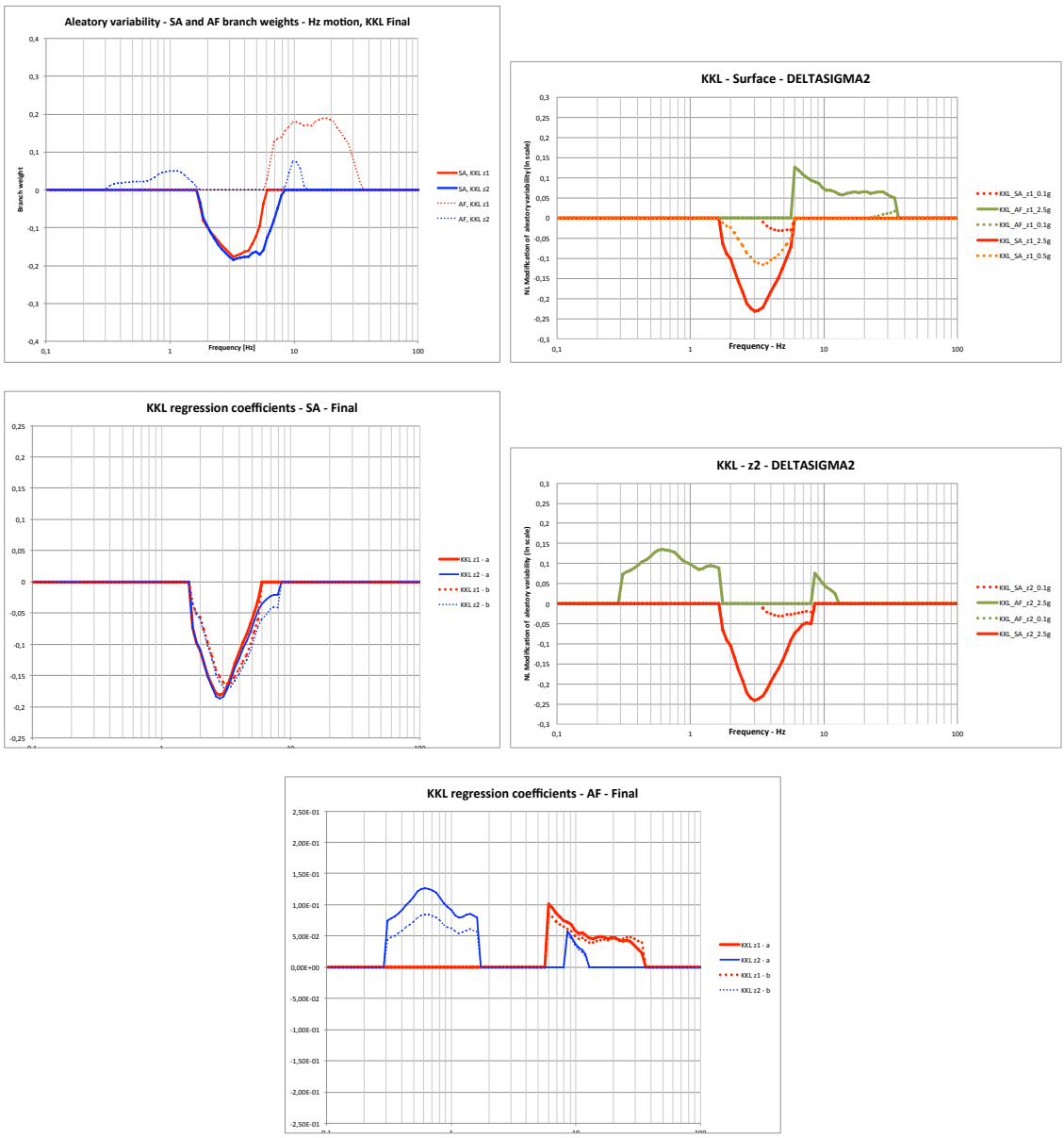

Figure II-1.13: Summary results for KKL. Top left: final weights: Middle left : regression coefficients for the SA branch; Bottom left: regression coefficient for the AF branch; in this left column each color corresponds to a different depth (red=surface, blue = z2). The right column displays the maximum changes (positive and negative) for the aleatory variability along the AF and SA branches between 0.1g (dotted line) and 2.5 g (solid line) for the SA (red) and AF (green) branches. Top frame = surface site, middle frame = z2 depth.

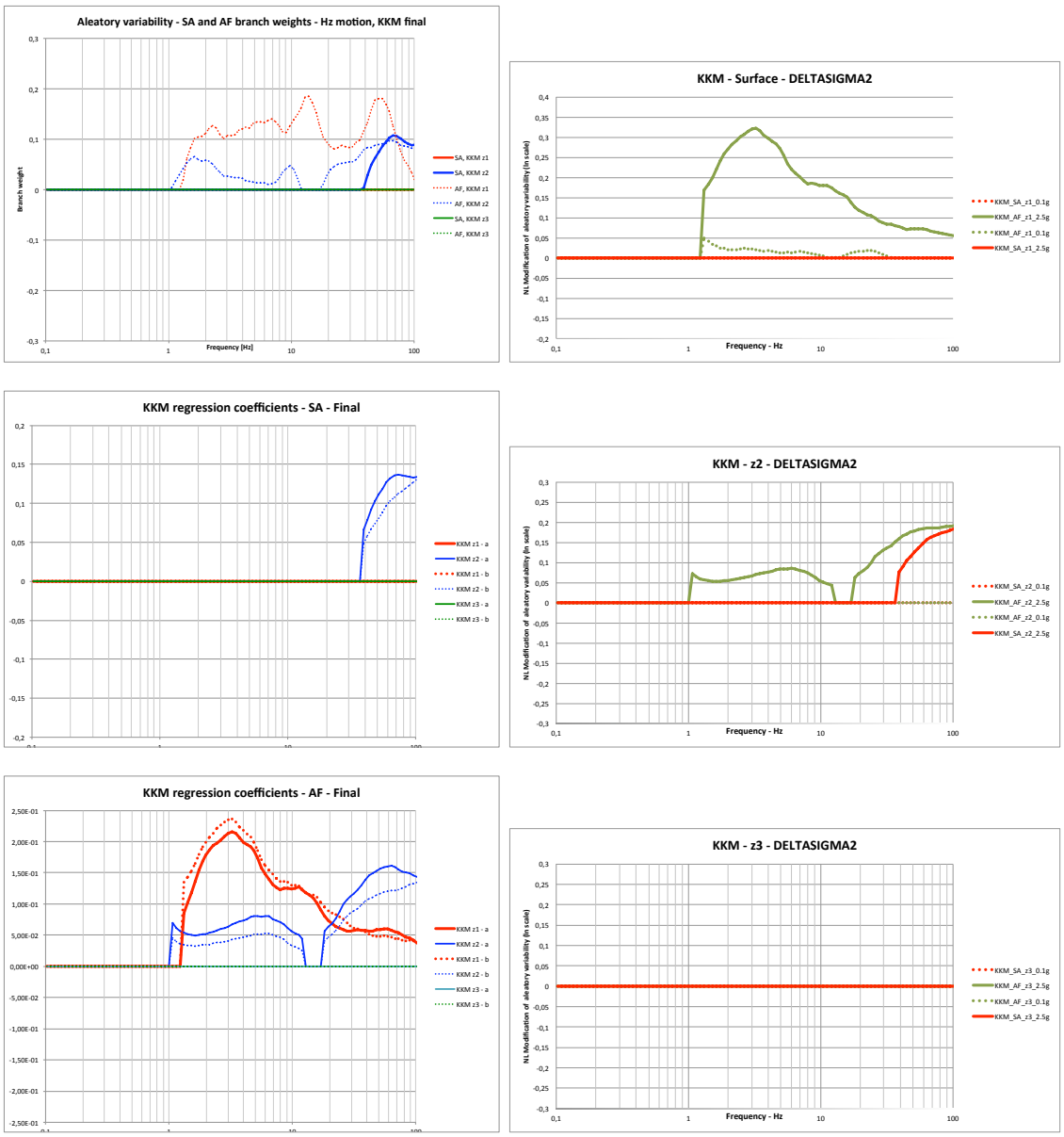

Figure II-1.14: Summary results for KKM. Top left: final weights: Middle left : regression coefficients for the SA branch; Bottom left: regression coefficient for the AF branch; in this left column each color corresponds to a different depth (red=surface, blue = z2). The right column displays the maximum changes (positive and negative) for the aleatory variability along the AF and SA branches between 0.1g (dotted line) and 2.5 g (solid line) for the SA (red) and AF (green) branches. Top frame = surface site, middle frame = z2 depth, bottom frame = z3 depth.

$Pecker25-03-2011$ "PEGASOS Refinement Project: Evaluation of maximum ground motions - Report n°2", March 2011, by A. Pecker).

- estimating the maximum spectral ordinate for each frequency/period, on the basis of observed maximum ground motion throughout the world (empirical approach, document EXT-TB-1067 Empirical MaxGM Report_Strasser, "Determination of empirical maximum ground motions for PEGASOS Refinement Project", by F. Strasser).

The following sections describe briefly my perception of the pros and con's of each approach, before proposing the corresponding logic tree.

Estimation of Maximum PGAs (TP3-TB-1074)

Basically, this approach is based on an estimate of the (depth dependent) shear strength, and an estimate of the yield shear strain. The first one is derived from cohesion and friction parameters of the soil, while the second one is estimated to be around 2% .

The subsequent estimate of the maximum acceleration comes from a modal representation of the soil response, with appropriately adjusted shear wave velocities and damping. It reduces the actual velocity profile to a simpler case, with one non-linear soil layer exhibiting a "smooth" velocity gradient. The soil damping is taken equal to 20% at large strain.

This approach is also compared with a simpler one (the "Betbeder-Matibet's one), and the series of NL computations for input motion scaled to 2.5g, the maximum ground surface accelerations being then associated with the 85% fractile of the the spectral ordinates at 30 Hz results (considered as a proxy to PGA because of the assumed lack f reliability of higher frequency spectral ordinates) . It thus provides several estimates of the maximum PGA possibly reached upon failure, which are summarized in Table II-1.21.

This approach provides maximum PGA estimates that seem "reasonable" (Table 5 p.20 of Pecker's document TP3-TB-1074_SP3); however, it relies on several assumptions that may not be correct

- at failure, the soil velocity profile follows a power law depth dependence, derived from the shear strength profile and the assumption of quasi constant strain over the whole profile. One may indeed prefer a totally different approach where the strain is localized at a given depth, with a very sharp reduction of elastic parameters at this very depth
- the shear strength under dynamic excitation is similar to the shear strength under static load. This may be correct, but I am not totally convinced. The range of "plausible" friction angles under dynamic loading may exceed the range of "plausible" friction angles under static loading
- the yield strain (2-3%) under dynamic excitation is similar to the yield strain under static load. Again, this may be correct but I am not fully convinced.
- at failure, the modal approach may still be used to estimate the peak strains and accelerations. I often heard many structural and geotechnical engineers totally reject such an assumption when applied to civil engineering concrete structures and soil geotechnical structures as well.

- even though the order the values resulting form ths approach compare fairly with the results of the NL modelling, there are differences, with results of numerical simulation that exceed the predicted maximum values

Conversely, the a priori advantages of this approach are that it is the only site specific one, and that it relies on a mechanical analysis that has some physical grounds.

As a result of these considerations, I do take into account this approach since it is the only one to provide an estimate having some physical / mechanical basis, but, as my confidence on the results of such an approach is limited, I add some sub-branching with different scaling factors to introduce a significant amount of epistemic uncertainty on the values issued by such an approach.

In order to apply this approach, I must assign a "base PGA" value rather than using the ranges proposed by A. Pecker. On the basis of these results, I took as base maximum PGA value the maximum of the estimates from the theoretical model and from the NL runs. These values are listed in the last row of Table II-1.21

Table II-1.21: Maximum PGA values (in g) derived from site specific mechanical analysis.

Site	KKB	EKKB	KKG	KKL	KKM
Theoretical model	2.5 (g)	2.2	2	1.8	2.1
Betbeder's model	2	1.5	1.4	1.5	1.5
Non-linear site response analyses	2.3 to 3.0	2.1 to 2.7	2.5 to 3.0	2.2 to 2.8	2.1 to 2.7
Proposed range of values (by A. Pecker, Table 5 TP3-TB-1074)	2.5 -3.0	2.2-2.7	2.5-3.0	2.3-2.8	2.1-2.6
Propositions, base PGA	2.5	2.2	2.5	2.2	2.1

Maximum Recorded Horizontal Motion (EXT-TB-1067)

This approach is purely empirical and simply looks at the maximum ground motion ever recorded for each frequency. The only link between this approach and site conditions is through the soil categorization in different site classes. I constitutes an update of the analysis performed by D. Fäh for the PEGASOS project, based on the gathering of a comprehensive dataset including more recent accelerograms of the last decade.

Clearly, such an approach can only provide some "qualitative" indication on a "lower bound" for such a maximum ground motion, since such "maximum" motions can only increase with the increasing number of instruments and seismic events. In addition, such an approach is clearly not site-specific, since sites are grouped in very gross site categories.

The results as compiled by F. Strasser and displayed through her plotting tool, do not point to any dependence on site class (maxima are very similar for site classes A-B (NEHRP) and C-D-E (NEHRP), and no clear dependence on distance up to several tens of kms.

This approach presents the advantage to be totally free of any underlying model, and may therefore reflect, in some way, the level of maximum ground motion that one may reasonably anticipate, irrespective of any other considerations on the regional seismic hazard and local site conditions. Since I am not convinced of some of the underlying assumptions of the Pecker's model, I trust a little bit more such a purely empirical approach; however, I will introduce some sub-branching to allow some larger values for the maximum ground motions, since future events can only raise the values compiled by F. Strasser.

In order to get some hints on the amount of scaling required by the limited period of observation, I investigated the evolution of the maximum values with time (irrespective of site conditions, distance and magnitude bins). The results are displayed in Figure II-1.15 for absolute values of PGA, PGV and spectral ordinates at various periods, and in Figure II-1.16 with a common relative scale based on the today's maximum values .

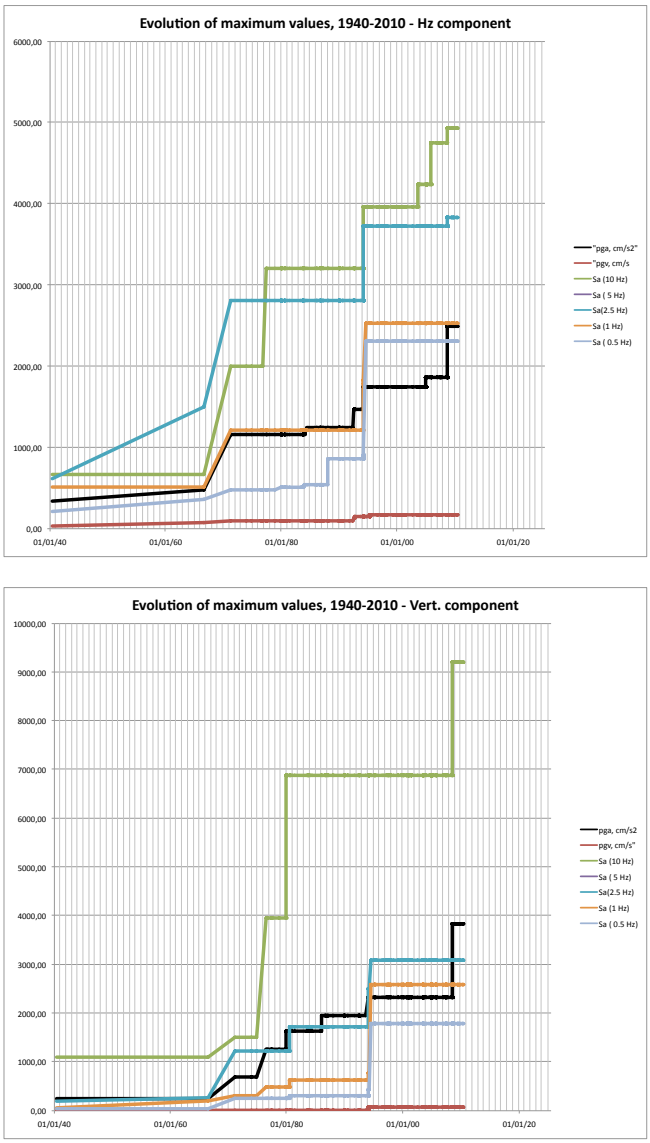

Figure II-1.15: Evolution of maximal values for PGA, PGV and different spectral ordinates as a function of time (1940-2010). Left: Horizontal component; Right: Vertical component.

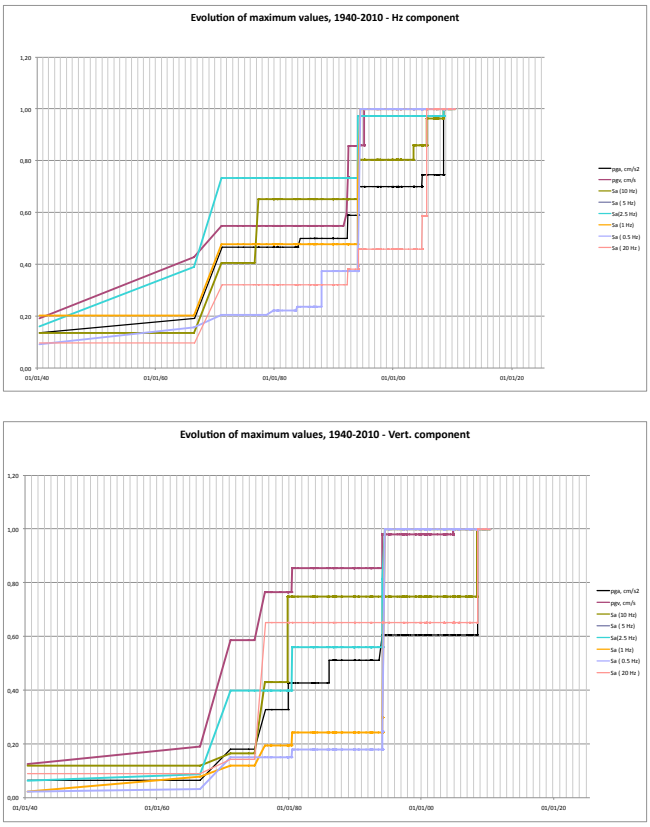

Figure II-1.16: Evolution of maximal values for PGA, PGV and different spectral ordinates as a function of time (1940-2010). In order to homogenize the scaling, each parameter has been scaled to its present maximum value. Left: Horizontal component; Right: Vertical component.

These plots indicate that significant increases have occurred over the last 15 years, especially at high frequencies (PGA, Sa (20 Hz) and Sa (10 Hz)): it is therefore legitimate to anticipate that today's maxima may increase by several tens of % over the next decades.

Moreover, I also displayed the data compiled by F. Strasser by grouping them in different magnitude bins and/or site conditions. Results are displayed in Figures II-1.17 (magnitude bins) and II-1.18 (site conditions). In each case, considering the relatively limited amount of such "extreme" data, I did not use sub-groups per magnitude and site bin, which would consist in a too small amount of data to be statistically representative.

The conclusions of these displays are that :

- (there exist very high values in the lowest magnitude bin for the vertical component, that look exactly like the high magnitude vertical component : some values may need to be checked)
- long period motions are presently higher for the two lowest magnitude bins
- there exist significant differences between the maxima for the magnitude 5.5 to 6.5 bin and the three other bins.

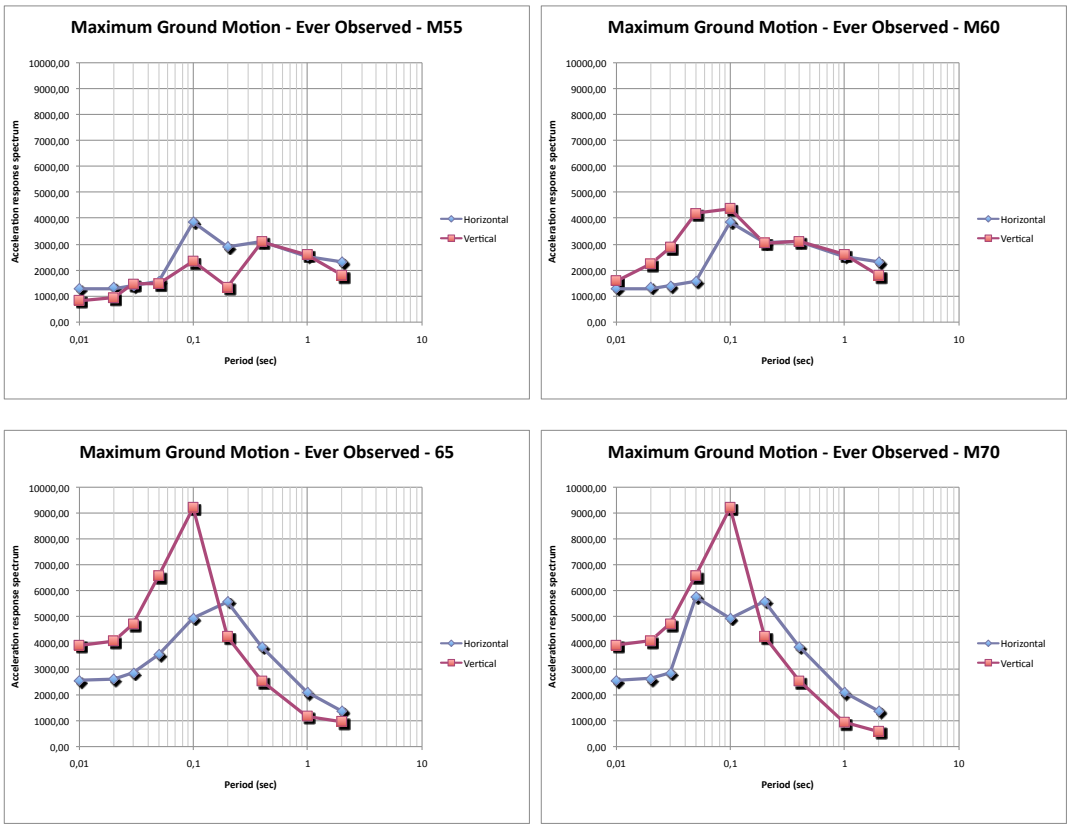

Figure II-1.17: Maximum spectra corresponding to different magnitude bins, for both horizontal motion (blue) and vertical motion (brown). All site conditions are considered together. Top left: $5 \leq M \leq 6$; Top right: $5.5 \leq M \leq 6.5$; Bottom left: $6 \leq M \leq 7$; Bottom right: $6.5 \leq M \leq 7.5$.

- rock spectra (NEHRP A+B) are significantly lower than stiff and soft soil spectra (NEHRP C+D+E), while highest spectra have been observed on stiff soils (NEHRP C). This may have a physical meaning but needs to be balanced by the fact that there much fewer data on rock sites (51 : 34 A + 17 B) than on sediments (129 C, 116 D and 5 E)

- these purely empirical PGA values are consistent with the theoretical values derived from a mechanical analysis

As the NPP sites are basically C-type sites, the conclusion is that we should consider the highest spectra: this is what I will do in my logic tree.

1.4.2 Logic Tree Structure

My logic tree starts with two main branches, one for Pecker's estimate of PGA, the other one for Strasser's estimate of maximum ground motion.

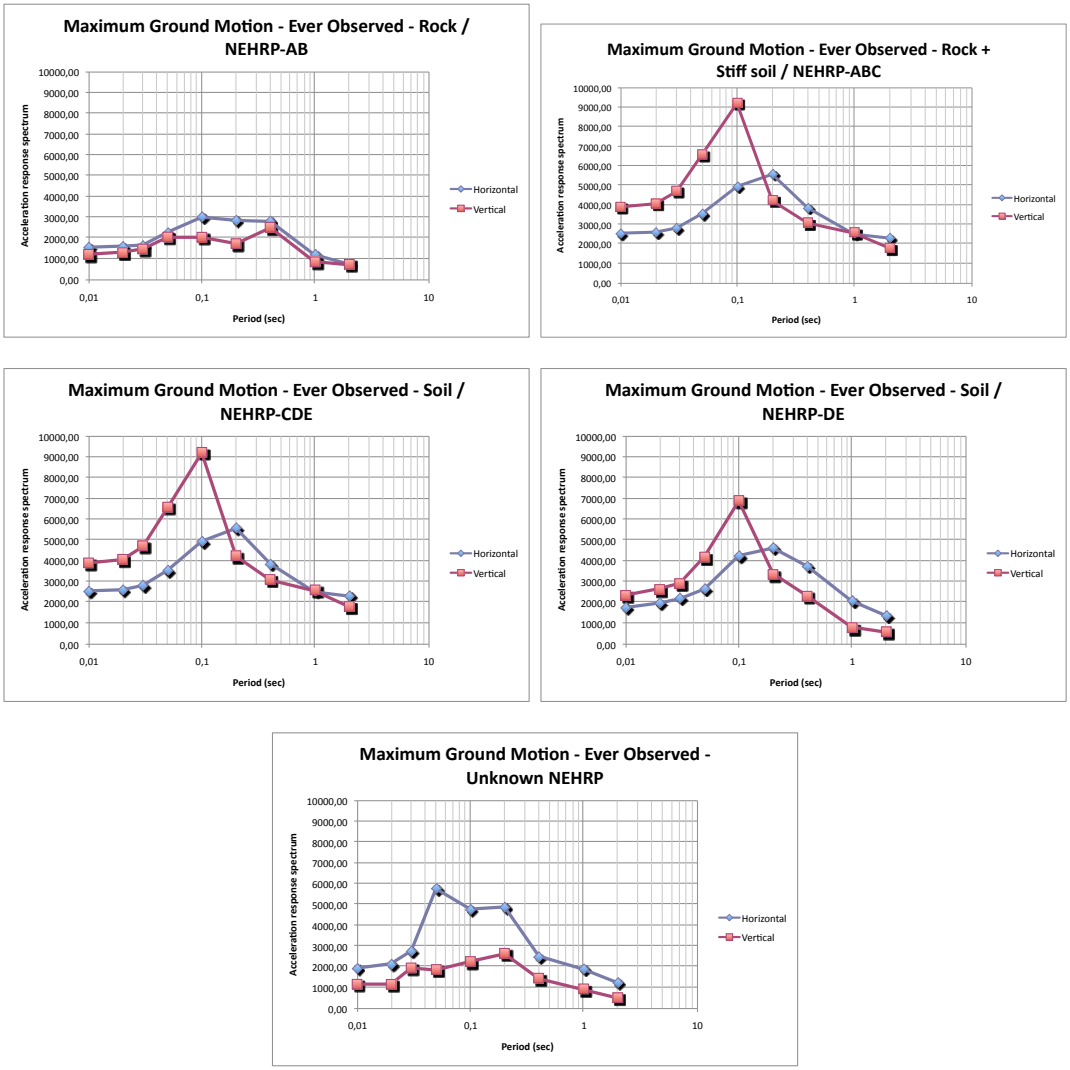

Figure II-1.18: Maximum spectra corresponding to different site conditions, for both horizontal motion (blue) and vertical motion (brown), and for all magnitude bins altogether. Top left : Rock, NEHRP A&B; Top right : Rock and Stiff, NEHRP A,B&C; Middle left : Sediments, NEHRP C,D&E ; Middle right : Sift sediments, NEHRP D&E; Bottom left: unknown site conditions.

1.4.3 Pecker's Approach Branch

Overall Weight

Considering the simplicity of the mechanical model with respect to the reality, I will assign to this approach a smaller weight, 1/3.

Uncertainty in PGA Values

I consider that the maximum PGA estimates given in Table II-1.21 following Pecker's document are highly uncertain. To represent this epistemic uncertainty, I therefore introduce a sub-branching with four branches with different scaling factors. The scaling values are designed to be consistent with the observed, purely empirical values, and their evolution with time, allowing changes (especially in the high frequency range) of several tens of % over one decade or less. I thus considered four values, the three first corresponding to a symmetric distribution around the unit value, and the last one being introduced to account for any "surprise" which can never be ruled out, as was repeatedly learnt over the past decades

Table II-1.22: Pecker's approach: Anchoring PGA values and associated weights for the five NPP sites.

Site		KKB	EKKB	KKG	KKL	KKM
Base PGA value (G)		2.5	2.2	2.5	2.2	2.1
Scaling factor	Weight					
0.8	20%	2	1.76	2	1.76	1.68
1	50%	2.5	2.2	2.5	2.2	2.1
1.25	20%	3.125	2.75	3.125	2.75	2.625
1.5	10%	3.75	3.3	3.75	3.3	3.15

Associated Spectra

Given the PGA, one must then associate an acceleration spectrum, anchored to such PGA values. Two approaches are possible:

- applying the normalized spectra derived from non-linear computations at 2.5 g for each site (i.e., taking the geometrical average of the response spectra computed with the NL model for the 9 different time hostories, and dividing it by the average spectral value at 100 Hz)

- applying the normalized spectra deduced from the existing strong motion records. The corresponding spectra are displayed in Figure II-1.19 (together with the listing of the average values), which was derived by taking the geometrical average of normalized spectral shape observed for all the "extreme" recordings selected in document EXT-TB-1067. This figure shows that the normalized shapes are very similar for M60 and M70 bins, and the listed values are the average of both normalized shapes.

I use both approaches with a slightly higher gain for the empirical spectra equal weights, considering that NL computations are derived only for one profile: 40% for the first one, 60% for the second one

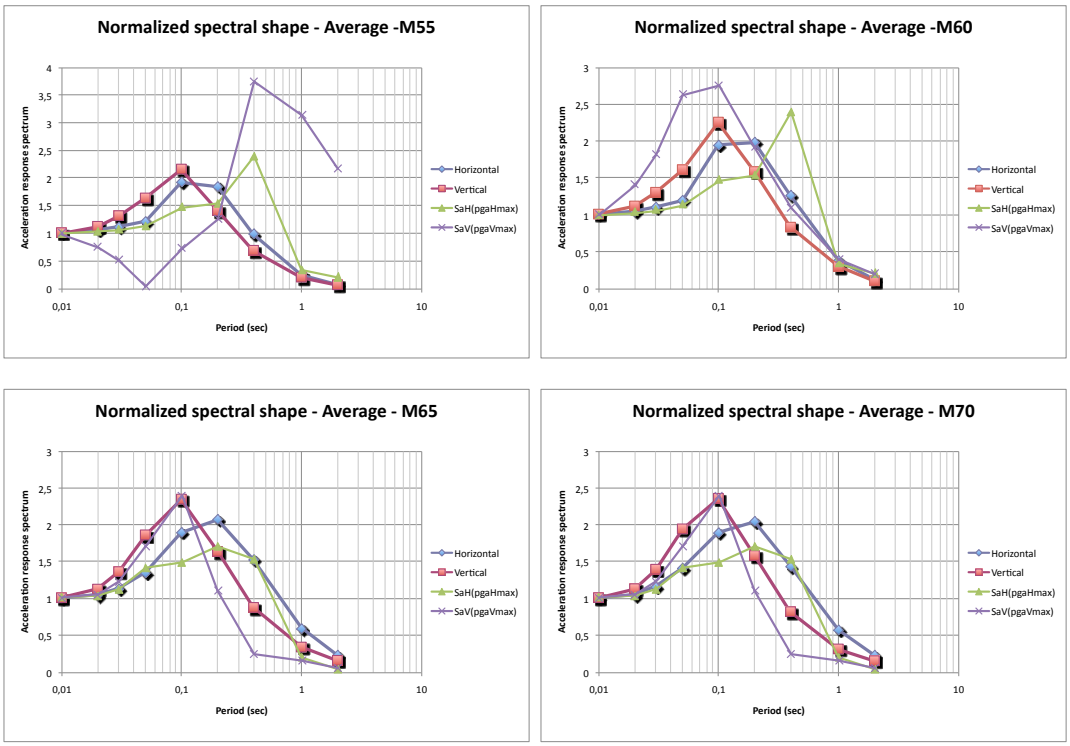

Figure II-1.19: Normalized spectra to be used in the "Peckers" theoretical approach.

Table II-1.23: Normalized spectra.

Period (s)	0.01	0.02	0.03	0.05	0.1	0.2	0.4	1	2
M55, H	1.01	1.06	1.12	1.21	1.93	1.85	0.99	0.26	0.08
M60, H	1.01	1.05	1.11	1.2	1.95	1.99	1.27	0.38	0.13
M65, H	1.01	1.05	1.13	1.35	1.9	2.08	1.53	0.59	0.23
M70, H	1.01	1.05	1.16	1.41	1.89	2.05	1.44	0.58	0.23
Normalized shape, H	**1**	**1.05**	**1.13**	**1.31**	**1.91**	**2.07**	**1.5**	**0.55**	**0.21**

1.4.4 Strasser's Purely Empirical Approach Branch

Overall Weight

This approach provides directly estimates over the whole spectrum, and it is based on present day observations without any theoretical considerations. This is the alternative approach to the Pecker's theoretical one, the complementary weight is therefore 2/3.

Magnitude Sub-branching

The analysis in Section 1.4.1 showed that the "maximum" spectra are significantly different for magnitude 6 and magnitude 7 bins. I will thus introduce a first sub-branching to account

for these two cases. The magnitude 6 branch should predominantly apply to all computations considering magnitudes lower than 6.5, while magnitude 7 branch should predominantly apply to all computations corresponding to magnitude 6.5 and above, with a ramp weight in between:

- $w_{(M6)} = 0.2 + 0.6(7 - M)$, bounded by $0.8(M < 6)$ and $0.2(M > 7)$
- $w_{(M7)} = 0.8 + 0.6(M - 7)$, bounded by $0.2(M < 6)$ and $0.8(M > 7)$

where M is the magnitude associated with the input spectrum. But this may not be easy to implement in the overall coding of PRP, as this requires to keep teack of the magnitude M corresponding to a incident spectrum. This needs some clarification with SP2 and SP5.

An alternative approach could be to assign weights to the M60 and M70 maximum spectra, independently of the site amplification computations. I indicate such a weight in Table 4.8, which is 60% for magitude 6 branch and 40% for magnitude 7 branch.

The spectra for each magnitude bin are displayed and listed in Figure II-1.20, which raise a surprising issue : the maximum horizontal ground motion is larger for the M6 bin than for the M7 bin at periods larger than 1 s. Morereover, the difference is larger than the considered scaling factors introduced to take into account the fact that such maximum ever recorded motion will increase in the future. Therefore, the M7 observed maxima were raised to the M6 maxima, as shown in Figure II-1.20.

Uncertainty Sub-branching

In order to account for the fact that the presently obtained maximum spectra are a lower-bound estimate of the "true" maximum spectra (if this has a meaning), I introduce a further sub-branching into three branches, where the spectral ordinate values are multiplied, respectively, by scaling factors 1.0, 1.2 and 1.4. The first branch implicitly considers the present day ever observed maximum spectral ordinates to be the true maxima: it has obviously little chances to be true, and it is attributed a limited weight. The two other scaling factor values, which can be only indicative, are derived from an analysis of the increase of the maximum values with time over the last decades: as displayed in Figure II-1.15 and II-1.16, the last two decades experienced increases of about 30% in average. Considering that the increase over the last two decades, and especially the last one, is also partly due to the much larger density of accelerometers in Japan and the occurrence of several magnitude 6 to 7 events inland, at close distance from recording stations: I do not anticipate jumps higher than a few tens of % in the next decades.

I assign slightly larger weights for the larger scaling factors for magnitude 6 bin, because of the smaller source size and the lower probability to have a station at very close distance from the energetic part of the rupture.

1.5 Maximum Ground Motion at Depth

For all sites at depth which are still within the sediments, I consider exactly the same ground motion than at the surface.

Table II-1.24: Summary of weights for the sub-branching corresponding to "Strasser's" empirical approach.

Magnitude, relative weight	Scaling factor and associated related weights 1	1.2	1.4
Magnitude 6 60%	30%	50%	20%
Magnitude 7 40%	45%	45%	10%

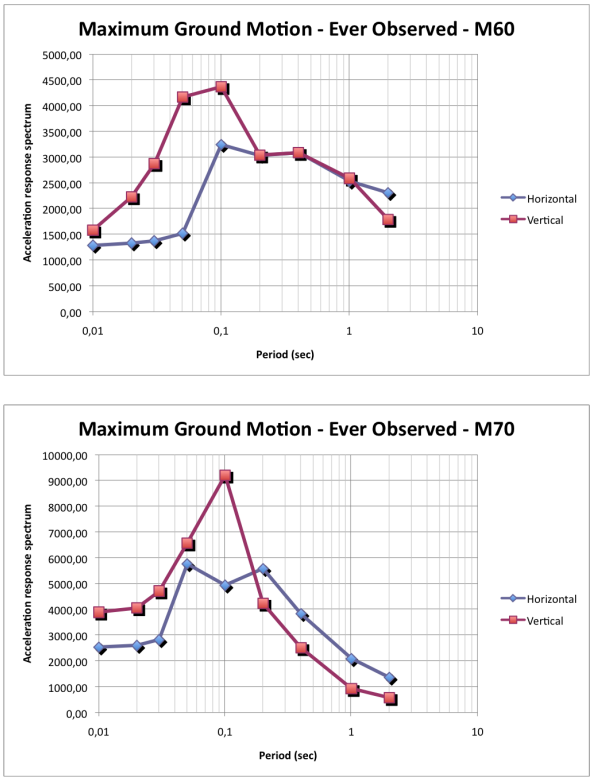

Figure II-1.20: Maximum spectra to be used in the "Strassers" empirical approach.

Table II-1.25: Maximum spectra.

Normalized shape, H	1	1.05	1.13	1.31	1.91	2.07	1.5	0.55	0.21
Period (s)	0.01	0.02	0.03	0.05	0.1	0.2	0.4	1	2
Sa values, M6 (m/s^2)	12.9	13.3	13.73	15.6	38.55	30.35	30.9	25.3	23.1
Sa values, M7 (m/s^2)	25	26	28	58	50	56	38	21	14
Corrected SA values, M7 (m/s^2)	**25**	**26**	**28**	**58**	**50**	**56**	**38**	**25.3**	**23.1**

For sites which are within the (soft) rock, i.e., KKMz3 and KKBz2, the branches using the Pecker's approach should be dropped, so that a full weight should be given to the empirical approach.

Another change for these two sites could be to use only "rock" maximum spectra (i.e., NEHRP A+B), but considering the large difference between A+B and C, this can be reliably done only if the sites selected for the extreme recordings do have actually measured velocities (i.e., not simply inferred from SPT values or other indirect measurements). I did not find explicit, unambiguous information on this issue in the EXT-TB-1067 report.

1.6 Median Amplification of Vertical Ground Motion

1.6.1 Approach

As in the PEGASOS project, I considered three main approaches to estimate the vertical ground motion:

- the first approach is simply to consider that site conditions do not affect the vertical ground motion: the amplification factor is equal to 1 for all frequencies. Such an approach is certainly wrong for an arbitrary site; however, as the four NPP sites all correspond to stiff soils, and as usual GMPE's certainly merge rock and stiff soil sites in the "rock site" category because of poor geotechnical information, such a simple approach is not to be totally ruled out.
- the second approach is to use the V/H ratios in combination with the estimated median horizontal ground motion to derive an estimation of the vertical ground motion: it may be done either with observed ratios from real strong motion data, or with theoretical ratios
- the third approach is to estimate the amplification factors with a 1D soil response analysis accounting for specific site properties. These results are available from SHAKE computations considering different PGA levels for one P wave velocity and damping profile (associated to the base profile P1).

The weight of the first approach depends mainly on the similarity of the considered site to a rock site.

The second approach (V/H) may be declined with several options. The first one, using purely empirical V/H GMPE, presents the advantage that it relies on real observations including the dependence of the V/H ratio with magnitude and distance, especially for large events. The drawback is the lack of physical interpretation, and the poor link with specific site conditions, except for the recent results from ETHZ on the basis of the quarter wavelength velocity. The second option is to use "theoretical" V/H ratios based on the recent results by Kawase and Sancez-Sesma (2011), showing that the average H/V ratio for earthquake signals should be proportional to the ratio between S-wave transfer function for horizontal motion and the P-wave transfer function for vertical motion.

In the third approach, the results depend on the computational parameters (velocity profiles, NL parameters, input signals), and might be affected by the incident wave-field type, and

possible 2D- or 3D-effects (in a similar way to what is considered for horizontal ground motion).

Its main advantage is to be site-specific, and its main drawback is related with the poor experience on the NL response at high PGA, together with the limited PGA range of available computations (0.1 ? 0.75 g). In this approach, the dependency of the V/H ratio on hypocentral distance is accounted for only through the differences in GMPEs used for horizontal and vertical motion, respectively, in the SP2part.

Note that both the second and third approaches make use of the SHAKE vertical motion results.

1.6.2 Logic Tree Structure

The structure of the logic tree is displayed on the Figure II-1.21 below, where are also indicated the weights as detailed in the next section.

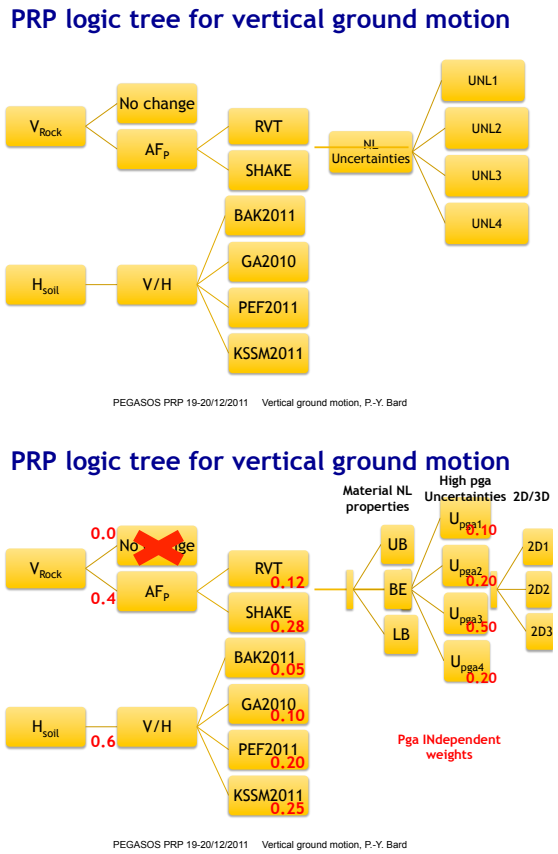

Figure II-1.21: Generic logic tree for the vertical ground motion. Top: without weights. Bottom: with generic weights.

1.7 Model Evaluations Common to All Sites

1.7.1 Relative Weighting Between the Three Main Approaches

'No change' branch

V_{S30} values as listed previously for surface sites (Table II-1.60) and later (Table II-1.32) do indicate that all sites - according to this limited criterion - are stiff sites in the usual GMPE terminology, with V_{S30} values between 400 and 600 m/s. There is no obvious reason to introduce a difference in the weighting of this approach for any of these sites according only to V_{S30} values. Considering also the depth to bedrock, it is possible to isolate Mühleberg with very thin quaternary deposits, but the corresponding bedrock is significantly softer than for all other sites.

Table II-1.26: NPP site V_{S30}.

NPP	V_{S30} [m/s]
Mühleberg	1100
Beznau	1800
Leibstadt	2200
Gösgen	2500

Therefore, the weight will be identical for the five sites for surface ground motion, but could change for ground motion at depth.

Relative Weighting Between the V/H and AF_P Approaches

For the PEGASOS project, I considered a PGA dependent relative weighting between approaches #2 and #3: the basic reason for this was the fact that approach #2 was not site-specific, while approach #3 was. I was thus assigning larger weight at approach #3 at low pga's, for which case I consider the computations as more reliable, and equal weight at large PGA, since approach #2 is based on actual strong motion recordings

A significant amount of work has been achieved on the V/H ratio over recent years, and there now exist site-specific components in some of the V/H approaches (PEF2011 and KSSM2011). I therefore decided for PRP to drop the PGA dependence of the relative weighting between approaches #2 and #3.

My initial plan was to systematically assign an about twice larger weight to approach #2, whatever the PGA. However, after the discussions during the December 2011 and May 2012 workshops, about the limitations of the V/H approach considering the absence of NL terms in most available GMPEs, and the strong NL effect arising from the horizontal amplification factors, I decided to revise this relative weighting and to assign approach #2 (V/H) only 1.5 times the weight assigned to approach #3 (EQL, AFV) Simultaneously, my weighting option is to assign a significantly larger weight to site-specific branches, to be consistent with the horizontal logic-tree where only site-specific approaches are considered..

I consider approach #3 to be much more relevant than approach #1, since, despite the relatively high V_{S30} value, there does exist a sedimentary cover which should significantly affect the vertical component as it does affect the horizontal motion. I have no reason to

introduce a difference between sites at this stage. Since despite the relatively high V_{S30} values, the site-specific analysis did lead to significant amplification, I decided to drop the "no-change" approach for surface sites

- weight $(nochange) = 0.0$
- **weight (V/H) = 0.6**
- **weight (EQL)= 0.4**

The 0 weight for the no-change approach is specific to the surface sites, it may be non-zero for sites at depth.

1.7.2 Details on the V/H Approach

The V/H ratio has been shown over recent years to be a powerful site descriptor (indeed with H/V rather V/H ratios...), and there exists a very rich literature on the link between H/V and site conditions, characterized in terms of fundamental frequency, dispersion curve and/or velocity profile. It is in particular worth to mention the latest theoretical developments (Sanchez-Sesma et al. [2011], Sánchez-Sesma et al. [2011]; Kawase et al. [2011]) using the diffuse wave - field theory to establish formal equations relating H/V to ratios of S and P wave transfer functions (when considering earthquake recordings) and ratios of colocalized Green's functions (when considering noise recordings). However, while these theoretical relationships are valid only for average ratios, empirical observations do evidence the sensitivity of the V/H ratio to other, non-site parameters : source-site distance, focal mechanism, and to a lesser degree magnitude.

Available Methods

There now exists several available GMPE type equations providing a direct estimate of the V/H ratio as a function of the magnitude, distance and site conditions : Campbell and Bozorgnia [2003] is one of the oldest available relations. I used it for the PEGASOS study because it was the only one available at that time; however, I drop it in the present PRP study, because it is derived from the combination of two separate GMPE's addressing individually the H and V components on the same dataset. I prefer more recent studies addressing directly the link between the V/H ratio and magnitude, distance and site conditions.

I will therefore consider here three more recent V/H GMPE's: Gülerce and Abrahamson [2011], Akkar et al. [2011], and Poggi et al. [2011]. These models are labeled in the following as GA10, BAK11 and PEF11, respectively. The two first GMPE's are very classical, with rather detailed descriptions of earthquake and distance, and an "elementary" site description in terms only of V_{S30} – continuous dependency for GA10, discrete site classes for BAK11 - , while the third one is much more site specific, using site profile descriptors (frequency dependent quarter wavelength velocities and impedance contrasts) while having an elementary earthquake and distance descriptor. There also exist two other options :

- the first one is a purely empirical one, associated with the latest results from ETHZ linking the V/H ratios corresponding to earthquake recordings to V/H ratios derived from ambient noise V/ H measurements.(Edwards et al. [2011a]).

- The second one is a purely theoretical one, associated with the latest findings on the H/V ratio. from the diffuse wave field theory (Sánchez-Sesma et al. [2008]; Kawase et al. [2011])

Personally, I am not convinced by the empirical correlations proposed by Edwards et al. [2011b], for various reasons. First, from a purely "technical" viewpoint, their correlations are based on very few data (only 26 sites), and Figure 1 exhibits a very poor apparent correlation coefficient between the ratio between $V/HeqandV/Hmicrotremor$, and the QWL velocity: the intrinsic variability of this RV/H ratio looks significantly larger than the (fuzzy) trend explained through the Quarter Wavelength velocity. In addition, this reference does not provide any indication on the reduction of variance (of this RV/H ratio) provided by the proposed linear regression for each dimensionless frequency (the "sigma" shown on bottom of their Figure 3 should have been compared with the total variability of the original RV/H) data. In addition, I doubt such a correlation could exist in general from a theoretical viewpoint. Indeed the recent H/V interpretations in terms of diffuse field theory (Sánchez-Sesma et al. [2008]; Sánchez-Sesma et al. [2011] , Sanchez-Sesma et al. [2011] Kawase et al. [2011]) related the earthquake H/V ratio to body waves, and microtremor ratios to a mixture of body and surface waves. In addition, older empirical investigations (Haghshenas et al. [2008]) were not so conclusive in $H/V_{eq} - H/V_{noise}$ correlations, except for the location of the fundamental frequency. I will thus drop this approach, despite its definitely interesting attribute to be site specific and based on simple, rather robust local measurements.

The last option offers the possibility to link directly an "average" V/H ratio to the ratio of the S- to the P-wave transfer function – modulated by the square of the S/P-wave velocity ratio β_R/a_R in the underlying half-space (Kawase et al. [2011], later referred to as KSSM11).

The original equation by Kawase et al. [2011] i.e.,

$$\frac{H(\theta,\omega)}{V(\theta,\omega)} = \sqrt{\frac{2\alpha_H}{\beta_H}} \times \frac{TF_1(\theta\omega)}{TF_3(\theta\omega)}$$

can be rewritten as :

$$\frac{V(f)}{H(f)} = \sqrt{\frac{\beta_R}{\alpha_R}} \times \frac{TF_P(f)}{TF_S(f)}$$

where TF1 and TFS denote the S-wave transfer function under vertically incident S-waves, while TF3 and TFP denote the P-wave transfer function (still under vertical incidence). The last formula takes into account the fact that Kawase et al. [2011] considered the total energy on the horizontal component, so that the factor $\sqrt{2}$ should be dropped when considering a single component. Finally, the last step is to approximate this Fourier spectral ratio by the ratio of amplification factors, so that the final equation writes as :

$$\frac{V(f)}{H(f)} \approx \sqrt{\frac{\beta_R}{\alpha_R}} \times \frac{AF_V(f)}{AF_H(f)}$$

where AFV and AFH are the amplification factors for vertical and horizontal components, respectively.

Weighting

The total weight of the V/H approach is thus 60% (for surface ground motion) The last approach is valid on average provided the diffuse wave-field assumption can be done. This is more likely to be acceptable for far events (and thus rather low PGA events), and less likely for nearby, shallow events that do control the hazard at high PGA and low probabilities. This latter approach should indeed, in principle, have a decreasing weight with increasing PGA.

My initial plan was therefore to introduce a PGA dependence for GA10, BAK11 and KSSM11 (while keeping a PGA independent, rather large weight to PEF11),as follows: their overall weight remains the same, but the the first two have increasing weights when PGA increases:

- $W(PEF11) = 0.20$, so that $W(GA10)+WA(BAK11)+W(KSSM11) = 0.6-0.2 = 0.4$
- $W(GA10) = 2W(BAK11) = 2/3(0.4–W(KSSM11))$
- $W(KSSM11) = 0.25–0.15(pga/0.75)$ with a minimum value of 0.10 at large PGA
- $W(GA10) = 0.10 + 0.10(pga/0.75)$
- $W(BAK11) = W(GA10)/2 = 0.05 + 0.05(pga/0.75)$

Nevertheless, considering the NL bias emphasized over the last workshops of December 2011 and May 2012 in the V/H approach using GMPEs, I finally decided (June 2012) to drop this PGA dependence, and to keep KSSM11 the same large weight whatever the PGA value: KSSM11 makes use of the actual site-specific responses, and automatically corrects for the large differences in the amount of NL behaviour on the horizontal and vertical components.

The final weighting between these different approaches takes into account their ability to account for the site-specific characteristics PGA dependence oft he transfer functions (non-linearities), the magnitude-distance dependence, and the existence of a background theory. As a result, the technique I assign the larger confidence is KSSM11 (0.25), then PFE11 (0.20), then GA10 (10), and BAK11 is given the lowest weight (0.05) despite the "European" specificity because of the very poor site characterization it takes into account.

Additional Indications for the V/H Approach: Implementation Issues

- Need for a deaggregation
  Most of the V/H approaches exhibit a distance dependence (GA10, BAK11, PEF11); therefore, for a given (M, pga) pair, the rock hazard should be deaggregated to get the corresponding (M, R) pairs with their respective weights. Then, for each (M,R) pair, the relevant V/H ratio can be estimated with the V/H formulae.

- Use of computed amplification factors AF_V and AF_H
  The fourth method makes use of the P- and S-wave amplification factors computed with the equivalent linear approach. These computations are available for a limited set of accelerations (0.1, 0.4 and 0.75 g), three different material properties, and two different computing methods : RVT base case and SHAKE. The corresponding AF_V/AF_H ratios should be computed as explained below :

- the 2013 computations are to be used

- in principle, the V/H ratio on rock depends on magnitude, distance (and focal mechanism). The usual case is that PGA values are different on the horizontal and vertical components of rock motion. Therefore, the AF_V/AF_H should be computed with different PGA levels on the vertical and horizontal components, with a pga_V value chosen as a function of pga_H, magnitude and deaggregated distance. Such an acceleration tuning, though possible, would be rather complex, while AF_V results exhibit only a slight dependency on pga_V, as illustrated on Figures II-1.87 (2010 computations) and II-1.88 (2013 computations). Therefore, for sake of simplicity, it is proposed to compute this ratio taking identical values for pga_V and pga_H on rock.

- RVT_{bc} / SHAKE : a careful look at the respective 2010 results from either method shows that the AF_V/AF_H ratios computed from RVT_{bc} reach rather large values at high frequencies (Figure II-1.89), significantly higher that what is predicted in the purely empirical V/H GMPE's, even when considering the scaling factor equal to the square root of S to P wave velocity in the base rock. Except for Mühleberg, it exceeds a value of 3 between 30 and 50 Hz. Therefore, I decided, for this part of the logic tree, to drop the RVT_{bc} results and to consider only the AF_V/AF_H ratios computed with the SHAKE approach. I kept the same decision after the 2013 computations, even though the SHAKE and RVT_{bc} computations are more similar (see Figure II-1.90), because of the systematic overestimation bias at resonant frequencies, and of the remaining discrepancies in some cases.

- The AF_V/AF_H amplification factors do exhibit a dependence on material properties (m1, m2, m3), even though it is significantly smaller for AF_V than for AF_H, as displayed on Figures II-1.91 and II-1.92 for the case $pga_v = 0.75g$. One solution could be to introduce a subbranching with the same relative, site-dependent weights as detailed in Tables II-1.9, II-1.11, II-1.14, II-1.17 and II-1.20. For sake of simplicity, I prefer to use only the weighted average derived as follows:

$$AF_{V/H}(f;pga) = w(M1).AF_{V/H}(f;pga,M1) + w(M2).AF_{V/H}(f;pga,M2)$$
$$+w(M3).AF_{V/H}(f;pga,M3) where AF_{V/H}(f;pga,M\_j) = AF_V(f;pga,Mi)/AF_H(f;pga,M\_j)$$

- Missing values in the frequency domain : interpolation / extrapolation

The values for V/H ratio are in some cases available only for a limited set of frequencies / periods that do not necessarily correspond to the values selected for the horizontal amplification factors. In such cases, some interpolation is thus needed: the recommended procedure is to estimate V/H for the two nearby periods / frequencies, and then use simple linear interpolation on the log values (log(V/H)).

The quarter wavelength technique proposed in PEF11 provides V/H values in the [0.5, 20 Hz] range, which is not totally sufficient. It needs in particular to be extended at high frequencies. It is proposed simply to use the values given for f = 20 Hz for all needed higher frequencies. If needed, values for frequencies below 0.5 Hz should extrapolated the same way.

1.7.3 Linear Equivalent Approach

SHAKE and RVT base case computations are available for the best estimate profile, magnitude 6, 3 acceleration levels (0.1, 0.4 and 0.75 g) and the 3 material properties. It is therefore needed

a) to assign the relative weighting between SHAKE and RVT_{bc} results

b) to detail the relative weighting for the different material properties

c) to detail the interpolation / extrapolation procedures

RVT$_{bc}$ / SHAKE

The RVT and SHAKE results are not exactly similar even for the 2013 computations. The 2010 differences were generally smaller than for the S-wave amplification factors, and restricted to the high frequency domain, as shown in Figures II-1.93 to II-1.100. The high frequency differences did not exhibit, however, the same behaviour as for the horizontal component: amplification factors are generally larger for RVT_{bc} than for SHAKE, while it was the opposite for AFH. The 2013 computations (Figures II-1.94,II-1.97, II-1.99 and II-1.100 still exhibit a slight overestimation bias around the resonant frequencies and some higher frequency differences, mainly for KKB and KKL (the two sites which have the lower P-wave fundamental frequencies). In parallel, the low frequency values of the amplification factor from AFV, SHAKE and AFV, RVT_{bc} are very close to 1: there is therefore no need to have a difference between both approaches at low frequencies. I thus adopted the same decision as for the horizontal ground motion concerning the frequency modulation of the relative weighting between RVT_{bc} and SHAKE, i.e. to fully drop the high frequency modulation. As there are no low frequency modulation, the RVT_{bc} / SHAKE relative weighting is fully frequency Independent for the vertical motion. Because of the RVT_{bc} flaw around peak frequencies recently discovered, I decided to assign a much larger weight to SHAKE computations than to RVT_{bc} computations : 70% - 30%.

The corresponding weights are listed in Table II-1.27 and in Figure II-1.22 below. the values are exactly the same for all sites, including for KKL : there is no reason to assign a slightly increased weight to the RVT computations for KKL, since the randomisation only takes into account the input motion, and not the profile.

Table II-1.27: Parameters for the relative weighting of linear equivalent methods for the vertical motion.

Site	Frequency dependence	$RWSHA_{AFV}$ (Relative weight, SHAKE)	$RWRVT_{AFV}$ (Relative weight, RVT_{bc})
KKB		0.7	0.3
EKKB		0.7	0.3
KKG	NONE	0.7	0.3
KKL		0.7	0.3
KKM		0.7	0.3

Relative Weighting for Different Material Properties

The origin of the non-linearities on the vertical component are exactly the same as those of the horizontal component, i.e., those related to the shear modulus degradation. As a consequence, they are accounted for in exactly the same way, i.e., with a sub-branching in three branches m1, m2 and m3, the weights of which are the same as those given in Tables II-1.9, II-1.11, II-1.14, II-1.17 and II-1.20. for each site

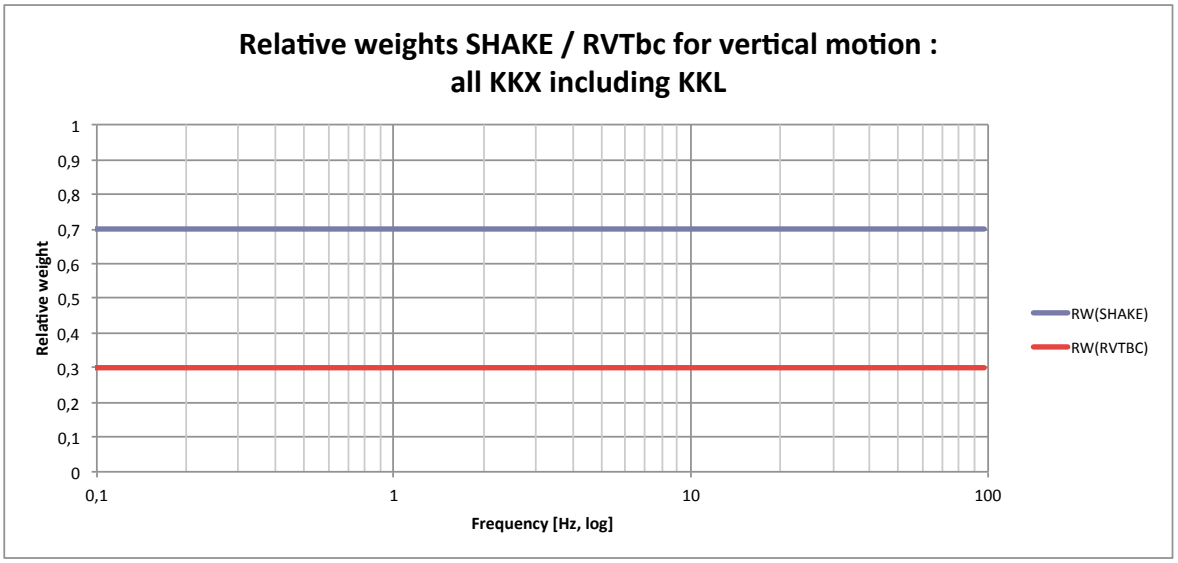

Figure II-1.22: Relative weighting between SHAKE and RVT_{bc} approaches for the vertical motion at KKB, EKKB, KKG KKL and KKM sites.

Interpolation for Arbitrary Values of PGA and M

SHAKE vertical amplification factors were computed only for magnitude 6 input signals, and for three PGA levels: 0.1, 0.4 and 0.75 g.

- Other magnitude values Since magnitude dependence is implicitly included in the V/H approach, and as we do not have any basis to guide the extrapolation of vertical amplification factors to other magnitudes, I prefer not to consider any magnitude dependence for this "SHAKE" approach branch.
- PGA interpolation The proposed interpolation follows the logarithmic interpolation scheme proposed for the horizontal amplification factor:

$AFv(pga) = B1 * AFV(A1, 6) + B2 * AFV(A2, 6)$
with
$B1 = (LA2 - L_{pga})/(LA2 - LA1)$
$B2 = (L_{pga} - LA1)/(LA2 - LA1)$
where
$L_{pga} = log(pga); LA1 = log(A1); LA2 = log(A2)$

A1 and A2 are the nearest PGA values for which the vertical amplification factors AFv are computed

Special case: Low PGA values ($< 0.1g$)
Simply consider the $0.1g\,value$: $AFv(pga < 0.1g, Mi) = AFv(0.1g, M = 6, Mi)$
Special case: High PGA values ($> 0.75g$)
Simply consider the 0.75 g result: $AFv(pga > 0.75g, Mi) = AFv(0.75g, M = 6, Mi)$

Uncertainties and Extrapolation for Large Values of PGA

This is a highly uncertain exercise: some strong motion recordings show that in some cases Non-linear effects result in increased vertical amplification (e.g. Port Island vertical array in Kobé, Kushiro records). This could not be ruled out for the sites under consideration (except may be Leibstadt where the water table is quite deep), as they include some water saturated, granular soils. In addition, the initial non-linear computations as a response to two-component signals (H + V) had to be abandoned because of numerical instabilities probably at least partly related to large vertical accelerations (exceeding 1 g at the surface).

Therefore, even though we consider here linear equivalent approaches, I introduce an "uncertainty factor" (which certainly includes a significant part of subjectivity), with the assumption, however, that NL effects affect vertical ground motion essentially beyond the fundamental vertical resonance frequency f_v. The main idea is to base the estimates on the results computed for the actual PGA value, by multiplying them by an "uncertainty" function UV_{pga} which is assigned different values along each subbranch

$$U_{V\,pga}(f, f_V, pga, D_{pga}) = 10[D_{pga}E(k_v f/f_v).Va(pga)]$$

Where

- f_V is the low strain, site dependent fundamental frequency for the vertical component site (given for each of the 5 sites in Table II-1.28, and which can be checked in Figures II-1.87 and II-1.91).
- k is a multiplying factor introduced to account for the (very slight) decrease of fundamental frequency at large strains: $kv = 1.+Va$, with $Va = [log(pga/pgaref)/log(2.5/pgaref)]$ - bounded by 0 and 1 -, and kv bounded by 1 ($'low'pga, i.e., pga < pgaref$) and 2 for $pga > 2.5g$.
- pga_{ref} is the reference PGA value beyond which the NL behavior is considered to start being significant. While I was initially considering to take it equal to 0.75 g to introduce this uncertainty only beyond 0.75g, I finally decided to introduce this subbranching beyond the same pga_{ref} values as for horizontal motion. This allows me to drop the subbranching considered in the PEGASOS study to cover the uncertainties due to the missing compûtations for the other velocity profiles (see next section).
- E is a generic function defined as

  $E(x) = 0$ for $x < 0.5$

  $E(x) = log(2x)/log(2)$ for $0.5 < x < 1.0$

  $E(x) = 1$ for $1.0 < x$

- D_{pga} quantifies the deviation from the EQL simulation for 0.75g. These deviations are assumed to be up or down by 50% with a 20% weight, and up by 100% with a 10% weight. There are therefore 4 branches have thus fixed weights corresponding to this fractile distribution.

$$D_{pga} = 0.30 : weight : 10\%$$
$$D_{pga} = 0.15 : weight : 20\%$$
$$D_{pga} = 0 : weight : 50\%$$
$$D_{pga} = -0.15 : weight : 20\%$$

[This extrapolation scheme is slightly biased towards higher values, because of the few observations exhibiting such higher amplification on vertical component when the horizontal component is reduced by NL effects.]

Table II-1.28: Parameters for the uncertainty factors on vertical component: Low strain fundamental frequencies for vertical motion and reference PGA.

Site	KKB	EKKB	KKG	KKL	KKM
f_v(Hz)	5.5	7.5	20	7.5	23
$pga_{ref}(g)$	0.15	0.15	0.2	0.4	0.15

Missing SHAKE Computations (Profiles P2-P6)

Vertical amplification factors have been computed only for the reference velocity profile P1. The question thus arises about the need (and the way) to estimate it for other velocity profiles. For the PEGASOS project, I had included a way to account for the profile variability based on the computed variability on the horizontal amplification factors. I could have reproduced the same procedure in the present PRP studies. However, I finally decided not to do so, for the following reasons :

- A significant part of the P-wave amplification factor is indeed controlled by the water table level, which is independent of the S-wave velocity profile. The expected profile to profile variability should therefore be significantly smaller for P-wave incidence than fr S-wave incidence

- At least part of the epistemic uncertainty linked with the various velocity profiles is accounted for through the various V/H models.

- There is a significant part of arbitrary "expert" judgement in introducing provisions for missing computations without any test case.

- I already introduced an uncertainty factor increasing with increasing PGA values (beyond pga_{ref}, see Section 1.7.3), which I consider to cover the effects of profile uncertainty.

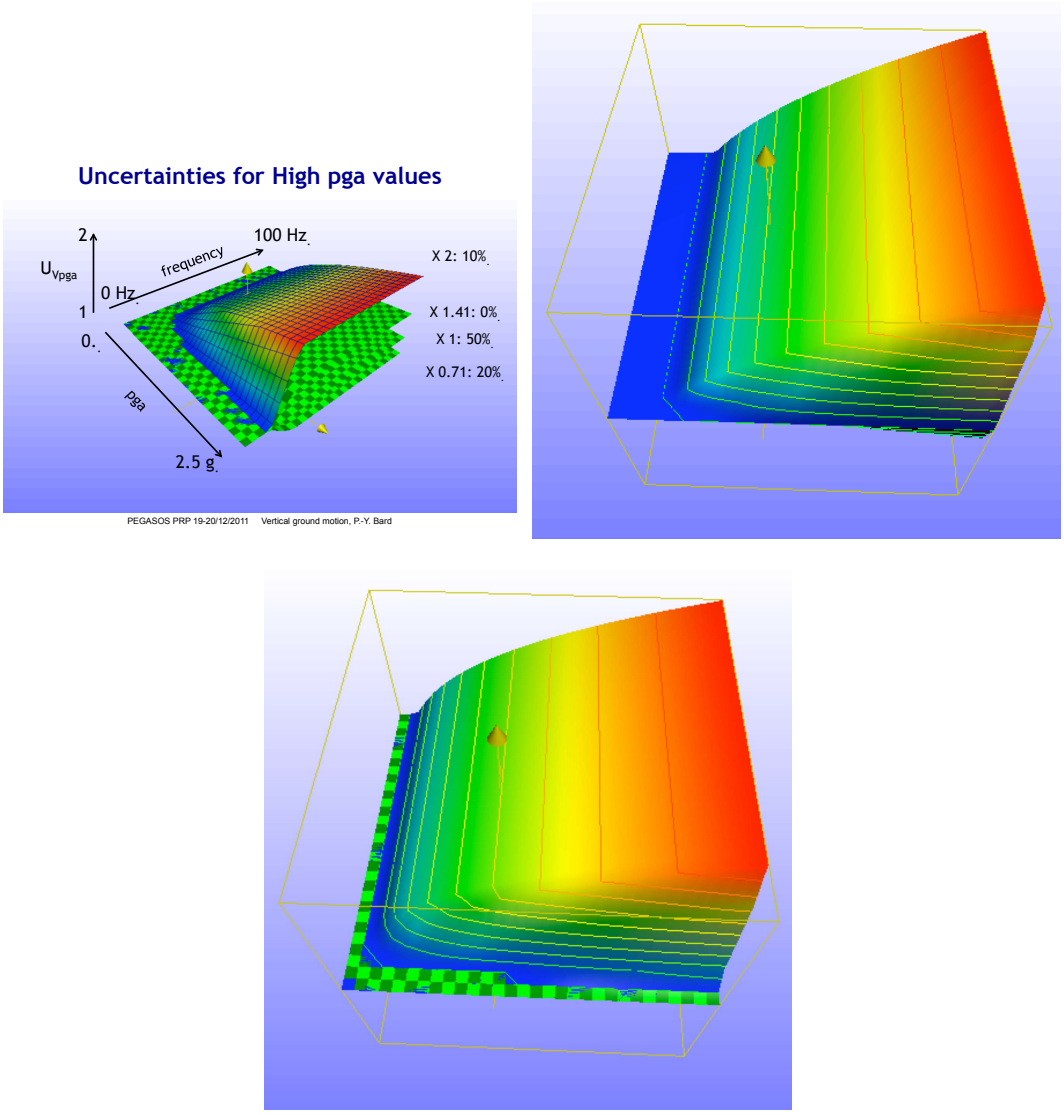

Figure II-1.23: Generic shape of the uncertainty factor as a function of frequency and PGA (top) and examples for sites KKL (bottom left) and KKM (bottom right).

2D/ 3D-effects

No specific computations has been performed to investigate the 2D or 3D-effects on vertical motion. However, observations in many sites, as well as computations on "canonical models" show that 2D/ 3D-effects generate Rayleigh waves that affect the vertical component at frequencies corresponding to the vertical component resonant frequency. Therefore, I also consider 2D/ 3D-effects on the vertical component, in a way very similar to what is done for the horizontal component, with effects shifted however to higher frequencies. The formula is the same as for the horizontal components, except for the fundamental frequency and the velocity; the damping term is not changed as it corresponds to Rayleigh waves, for which the S-wave characteristics (velocity and damping) are of primary importance. The approach is described below, but it should be first emphasized that the 2D/ 3D correction factor should be applied ONLY to the first branch ($V_{rock} * AF_V$) of the vertical motion logic tree, i.e., the EQL branch: this is because the V/H branch is based on the horizontal motion which already

takes into account the 2D/ 3D-effects on the horizontal motion.

General formula:

The amplification factors derived with the EQL computations (i.e., SHAKE and RVT_{bc}) should be multiplied by a 2D factor A_{2D}^{V} defined as:

$A_{2D}^{V}(f, \zeta av) = 1 + C_{V,2D}(f, \zeta_{av})$
with
$C_{V,2D}(f, \zeta_{av}) = A(f, fv)Bv(f, \zeta_{av})$
where
f is the frequency
f_v is the fundamental frequency for the vertical component at the site under consideration
ζ_{av} is an average damping value in the near-surface soils where surface waves diffracted on lateral heterogeneities are propagating.

Frequency dependence: A (f, f_v)
The results available in the scientific literature indicate that 2D- and 3D-effects appear only above the site fundamental frequency f_v.$A(f, f_v)$ is therefore defined as a ramp function on a logarithmic frequency axis:
$A(f, f_v) = A_0(f/f_v)$
with
$A_0(x) = 0$ for $x < 0.7$
$A_0(x) = -(log(x/0.7))/log(0.7)$ for $0.7 < x1$
$A_0(x) = 1$ for $1 < x$

Geometrical / damping dependence: $B(f, \zeta av)$

The diffracted waves are generated on the lateral heterogeneities, and then propagate to the site; their amplitude at the site will therefore depend both on the distance to the lateral heterogeneities, and on the damping values. The proposed model is therefore given by:
$B_V(f, \zeta av) = C_{2D}^{V}.exp(-2\pi\zeta avfl/C_R)$
where:

- C_{2D}^{V} represents, in some way, the amplitude of the diffracted waves (normalized to the incident wavefield) at their origin, i.e. on the heterogeneity; it is also, approximately, the largest possible 2D effect at the site (corresponding to the low strain / very low damping case). This value is uncertain, and, for each site, different values are proposed with different weights. These values are thought slightly smaller than the corresponding values for the horizontal component, because only Rayleigh waves are affecting vertical motion, while horizontal motion is affected by both Rayleigh and Love waves. One has however to keep in mind that these perturbations are also related to direct S-waves which carry more energy than P waves.

- the last term exp $(-2\pi\zeta avfl/\beta m)$ represents the amplitude decay due to the propagation from the heterogeneity to the site:
- ζav is the average damping over the soil column: it is PGA dependent because of NL material degradation (see below).
- l is the distance of the NPP site to the closest lateral heterogeneity
- cR still represents the velocity of surface waves propagating in the surface layers (i.e., Rayleigh waves). For stratified media with depth-dependent velocities, this velocity is frequency dependent as witnessed in dispersion curves. The values considered for each site have been selected from the analysis of the measured dispersion curves at frequencies around and above the fundamental frequency f_v. They are thus smaller than the ..m values considered for the horizontal component, which also results in a lower importance

Estimating C_R

- Base (linear) C_R0 values : The values C_R0 considered for each site have been selected from the analysis of the measured dispersion curves at frequencies around and above the fundamental frequency f_V.
- Final value taking into account the non-linearities Higher strains will induce a decrease of the soil shear-wave velocities, and therefore of the surface wave velocities C_R0. This decrease is not uniform but varies with depth depending on the strain profile. Trying to take into account in an "exact" way would lead to a complex model inconsistent with the crudeness of this 2D/3D model. Therefore, an "average" decrease of C_R0 is considered based on an "average" strain level estimated from the peak strain ratio $(\gamma/\gamma 50)$ max as computed in the RVT_{bc} approach for horizontal motion.

  the "strain ratio" profiles exhibit a very high variability with site, profile, material properties and PGA value, with however a significant localization of peak strains close to high velocity contrasts. It is therefore considered that, for the present purpose, an "average, effective" strain ratio $(\gamma/\gamma 50)eff$ equal to one fifth of the peak strain ratio $(\gamma/\gamma 50)max$. This low value takes into consideration the depth dependence of the strain ratio, and the fact the peak strain is reached only once in the time history.

  the resulting velocity decrease is then estimated as equal to $[1/(1+(\gamma/\gamma_{50})_{eff})]0.5$.

  the estimation formula is thus $cR = cR0.[1/(1+0.2(\gamma/\gamma_{50})_{max})]0.5$.

  Note : considering lower C_R0 values results in decreasing the importance of 2D/ 3D-effects

Estimating ζav

Considering the strain ratio profiles,the damping increase linked with NL behavior is depth dependent. In order to be consistent with the estimation of the reduction of surface wave velocity C_R0, an average damping is estimated from the "average, effective" strain ratio

$(\gamma/\gamma_{50})_{eff}$ through the formula

$$\zeta av = 0.0125 + \zeta max.(\gamma/\gamma_{50})_{eff}/[1. + (\gamma/\gamma_{50})_{eff}]$$

The resulting formula is therefore :

$$\zeta av \approx 0.0125 + 0.06.(\gamma/\gamma_{50})_{max}/[1. + 0.2(\gamma/\gamma_{50})_{max}]$$

The Tables presented in the next sections provide, for each NPP site, the values of f_v, C_{2D}^V , l, cR and h, as well as the corresponding weighting. Three sub-branches are introduced with different weights to account for the uncertainties in the parameter estimates (mainly indeed C_{2D}^V). One of the subbranch corresponds to $C_{2D}^V = 0$, as it is likely that the actual data on which are based at least partly the input motion estimates, do include some – unknown - amount of 2D/3D-effects. The other values are based on the actual geological cross-sections at each site, and some subjective "expert judgement".

1.7.4 At-depth Amplification Factors

Table II-1.29: List of V_S values (m/s) at the considered depth for the various profiles of each site, together with the V_{S30}(z) for the corresponding average velocities over the underlying 30 meters.

Site	Depth	parameter	P1	P2	P3	P4	P5	P6
KKB	z2=15m	V_S(z)	600	550	450	756		
		V_{S30}(z)	761	855	679	801		
EKKB	z2=15m	V_S(z)	551	551	450			
		V_{S30}(z)	730	789	661			
KKG	z2=9m	V_S(z)	413	391	360	392	462	413
		V_{S30}(z)	759	653	670	859	862	759
KKG	z3=15m	V_S(z)	507	445	437	541	560	507
		V_{S30}(z)	1041	843	929	1232	1184	1041
KKL	z2=10m	V_S(z)	520	500	525			
		V_{S30}(z)	680	571	722			
KKM	z2=7m	V_S(z)	311	242	365	215		
		V_{S30}(z)	883	919	685	677		
KKM	z3=14m	V_S(z)	925	980	607	686		
		V_{S30}(z)	1014	1046	819	846		

The same basic approaches as described above for the surface motion are considered for motion at depth; however, some changes are introduced in the relative weights, since empirical V/H ratios are not available for motion at depth (neither outcropping nor within). The following sections highlight these changes.

No-change Branch

Some of these "deep" sites have $V_{S30}(z)$ values beyond 800 m/s, corresponding to rock (KKG z3, KKM z3), while the other exhibit lower but quite stiff values. This could justify to consider the "nochange" branch with a non-zero weight.

However, considering that a) the V_{S30} value is taken into account in the V/H approach (second branch of the logic tree), and b) amplification on vertical motion may also arise because of velocity contrasts existing within the "geotechnical" bedrock - which is taken into account in the third "EQL" approach -, I finally decided to totally drop this no-change drop even for the deepest and harder sites: their response is actually accounted for implicitly with the other branches of the logic tree.

Changes in the V/H Branch

There are no available V/H branch for sites at depth. However, since we consider here "outcropping motion" at depth, we will assume, for the GA10, BAK11 and PEF11 branches, that a reasonable estimate of the V/H ratio can be obtained by considering the velocity profile just beneath the considered site, while the fourth V/H branch KSSM11 derived from H and V SHAKE amplification factors does take into account the actual depth effects (apart from the destructive interference between upgoing and downgoing waves). The latter sub-branch is thus given a larger weight than for surface motion (+ 15% compared to surface site), while

the GA10 and PEF11 sub-branches are give a lower weight (-5 and -10%, respectively). the weight of the fourth subbranch (BAK11) is however not reduced because it already has the smallest weight.

The GA10 and BAK11 branches should be applied in a similar way as for surface sites, but with the V_{S30} values corresponding to the average velocities in the underlying 30 meters (from z to z+30m): these values are indicated in Table II-1.29. The values corresponding to profile P1 should be used, since it is considered that the associated variability is already covered by the branch to branch variability. Similarly, the PEF11 branch should be used as for the surface motion, but simply based on modified QWL values, computed on the velocity profile starting from the considered depth.

Finally, the V/H EQL (SHAKE) computations should simply use the "outcropping" H and V motion computed with the P1 profile at the right depth, and multiplied by the same velocity ratio $(\beta R/\alpha R)1/2$.

"EQL" Branch

The sub-branches and their weights should be exactly the same as those described for the surface motion (sub-branching for SHAKE / RVT_{bc} approach, material properties, uncertainties increasing with increasing PGA, and 2D/3D-effects). There are however a few differences concerning :

the amount of uncertainties (i.e., D_{pga} values), which I considered as to be reduced with increasing stiffness.

the amplitude of 2D/3D-effects, which should be reduced or even vanish due to the decrease of Rayleigh wave amplitude with depth

- High PGA uncertainties I kept the same branching (4 branches) and the same weights, but I reduced the D_{pga} values with increasing stiffness and depth. The values are listed in Tables II-1.29 to II-1.32.
- 2D/3D-effects at depth

For the motion at depth, the same surface wave interpretation are kept: as the amplitude of ground motion is strongly depth-dependent for surface waves, the 2D/3D-surface factors are modified by a depth-dependent factor C(z), except for the sites which are located beneath the sedimentbasement interface responsible for the trapping of surface waves. It is thus proposed to apply the same correcting factor C(z) to the surface "overamplification" factor $A^V_{2D}(f, \zeta av, z)$

$$A^V_{2D}(f, \zeta av, z) = 1 + A(f, f_v)B_v(f, \zeta av).C_v(f, z)$$

The $C_v(f, z)$ factor cannot be estimated with a simple formula as for the horizontal motion; I propose to estimate it by assuming that the Rayleigh wave modal shape for vertical motion is close to the depth dependence of the 1D SHAKE amplification factor for P waves:

$$C_V(f,z) = AF_{V,SHAKE}(f,z;pga,M2)/AF_{V,SHAKE}(f,z=0;pga,M2)$$

(This formula implies a PGA dependence, and an interpolation and extrapolation scheme for missing PGA values: the same simple procedure as the one described in Section 1.7.3 should be used).

Comparing the thicknesses h of the 'trapping layers' (see relevant section for surface motion) with the actual depth of the various sites, this formulation should therefore be applied to the deep sites at Beznau ($h = 80m > z2 = 15m$), E-Beznau ($h = 60m > z2 = 15m$), Gösgen ($h = 28m > z3 = 15m$), and Leibstadt ($h = 30m > z2 = 10m$).

However, this 2D-overamplification term should NOT be applied to the two sites at depth ($z2 = 7 and z3 = 14m$) at Mühleberg, for which the shallow gravel layer is only 8 m thick: for this particular case, there is no subbranching for 2D-effects (or, in other terms, 1 single branch with weight 100% for the value $C_{2D} = 0$).

1.7.5 Beznau

Site-specific Model Evaluations

Modified Weights for at Depth Motion

The modifications at depth concern mainly two items :

- the relative weighting between the V/H sub-branches (as explained above in Section 1.7.4)
- the total amplitude of the uncertainty factors on the EQL approach branch : the total range is reduced from (0.71, 1.0, 1.41, 2.0) at surface to (0.83, 1.0, 1.20, 1.41) at depth. At a 15 m depth, the geology is not longer gravel but opalinus clay, which does exhibit however some Non-linear characteristics

Alternative 2D-parameters

The same weights as for the horizontal motion are to be applied. The C^v_{2D} coefficients are slightly reduced to take into account the fact that only Rayleigh waves contribute to the vertical motion. The velocities are changed because they are associated to Rayleigh waves which have a frequency dependent velocity: the values were derived from the measured dispersion curves around the fundamental frequency for vertical motion.

Summary of Weights and Computational Parameters for Vertical Motion at Beznau

Table II-1.30: KKB Beznau: Vertical ground motion Weights and parameters for the median site amplification factor.

Method and weights					
Depth	No change	V/H GA10	BAK11	PEF11	KSSM11	EQL SHAKE & RVT_{bc}
$z1 = 0m$	0	0.1	0.05	0.2	0.25	0.40 (see below)
$z2 = 15m$	0	0.05	0.05	0.2	0.3	0.40 (see below)
Velocity profile						
Irrelevant: only P1, with P1 V_{S30} values						
Non-linear properties (for the EQL and KSSM11 branches)						
M1			M2		M3	
0.2			0.35		0.45	
Bedrock velocity values for the V/H KSSM11 branch						
$\alpha_R = 4050m/s$				$\beta_R = 1800m/s$		
Frequency independent, relative weighting of EQL techniques (SHAKE, RVT_{bc})						
frequency				0-100Hz		
SHAKE				0.70		
RVT_{bc}				0.30		
Uncertainties and high $pga's$						
Formula: Scaling factor $U_{h_{pga}}(f, f_v, pga, D_{pga}) = 10\,[D_{pga} E(k_v f/f_v).V_a(pga)]$						
$E(x) = 0 for x < 0.5$ $E(x) = log(2x)/log(2) for 0.5 < x < 1.0$ $E(x) = 1 for 1.0 < x$				$k_v = 1. + V_a$		$V_a = [log(pga/pga_{ref})/$ $log(2.5/0.75)]$
Parameter values		$f_v = 5.5Hz$		$pga_{ref} = 0.15g$		
Relative weights and D_{pga} values						
Weight	0.2	0.5		0.2		0.1
z1	$D_{pga} = -0.15$	$D_{pga} = 0.$		$D_{pga} = +0.15$		$D_{pga} = +0.30$
z2	$D_{pga} = -0.08$	$D_{pga} = 0.$		$D_{pga} = +0.08$		$D_{pga} = +0.15$
$2D$ - effects: $A_{2D} = 1 + C_{v,2D}(f, \zeta) = 1 + C^v_{2D}.A_0(f/f_v).exp(-2\pi\zeta_{av} f l/C_r)$ $c_R = c_{R0}.[1/(1 + 0.2(\gamma/\gamma_{50})_{max})]^{0.5}, \zeta_{av} \approx 0.0125 + 0.06.(\gamma/\gamma_{50})_{max}/[1. + 0.2(\gamma/\gamma_{50})_{max}]$ γ from Shake horizontal motion (profile P1, material m^2)						
Fixed parameters		$f_v = 5.5Hz$ $l = 300m$		$c_{R0} = 700m/s$		$h = 80m$
Alternative choice for parameters and corresponding weights		$C^0_{2D} = 0.0$ weight 0.40		$C^0_{2D} = 0.15$ weight 0.40		$C^0_{2D} = 0.40$ weight 0.20

1.7.6 E-Beznau

Site-specific Model Evaluations

Modified Weights for at Depth Motion

The rationale and the values are the same as for KKB. The site at depth is still in gravel (and not in opalinus clay), but its velocity is comparable.

Alternative 2D-parameters

The same weights as for the horizontal motion are to be applied. The C^v_{2D} coefficients are slightly reduced to take into account the fact that only Rayleigh waves contribute to the vertical motion. The velocities are changed because they are associated to Rayleigh waves which have a frequency dependent velocity: the values were derived from the measured dispersion curves around the fundamental frequency for vertical motion.

Summary of Weights and Parameters for Vertical Motion at E-Beznau

Table II-1.31: EKKB E-Beznau: Vertical ground motion. Weights and parameters for the median site amplification factor.

Method and weights					
Depth	No change	V/H GA10	BAK11	PEF11	KSSM11	EQL SHAKE & RVT_{bc}
$z1 = 0m$	0	0.1	0.05	0.2	0.25	0.40 (see below)
$z2 = 15m$	0	0.05	0.05	0.2	0.30	0.40 (see below)
Velocity profile						
Irrelevant: only P1, with P1 V_{S30} values						
Non-linear properties (for the EQL and KSSM11 branches)						
M1			M2		M3	
0.2			0.35		0.45	
Bedrock velocity values for the V/H KSSM11 branch						
$\alpha_R = 4050m/s$				$\beta_R = 1800m/s$		
Frequency independent, relative weighting of EQL techniques (SHAKE, RVT_{bc})						
frequency			0.100Hz			
SHAKE			0.7			
RVT_{bc}			0.3			
Uncertainties and high $pga's$						
Formula: Scaling factor $U_{h_{pga}}(f, f_v, pga, D_{pga}) = 10^{[D_{PGA}{}^{E(k_v f/f_v).V_a(pga)}]}$						
$E(x) = 0 for x < 0.5$ $E(x) = log(2x)/log(2) for 0.5 < x < 1.0$ $E(x) = 1 for 1.0 < x$				$k_v = 1. + V_a$		$V_a = [log(pga/pga_{ref})/log(2.5/0.75)]$
Parameter values		$f_v = 7.5Hz$		$pga_{ref} = 0.15g$		
Relative weights and $D_{pga} values$						
Weight	0.2	0.5		0.2		0.1
$z1 = 0m$	$D_{pga} = -0.15$	$D_{pga} = 0.$		$D_{pga} = +0.15$		$D_{pga} = +0.30$
$z2 = 15m$	$D_{pga} = -0.08$	$D_{pga} = 0.$		$D_{pga} = +0.08$		$D_{pga} = +0.15$
$2D$ - effects: $A_{2D} = 1 + C_{v,2D}(f, \zeta) = 1 + C^v_{2D}.A_0(f/f_v).exp(-2\pi\zeta_{av} fl/C_R)$, $c_R = c_{R0}.[1/(1 + 0.2(\gamma/\gamma_{50})_{max}]^{0.5}, \zeta_{av} \approx 0.0125 + 0.06.(\gamma/\gamma_{50})_{max}/[1. + 0.2(\gamma/\gamma_{50})_{max}]$ γ from SHAKE horizontal motion (profile P1, material m^2)						
Fixed parameters		$f_v = 7.5Hz$ $l = 300m$		$c_{R0} = 600m/s$		$h = 60m$
Alternative choice for parameters and corresponding weights		$C^V_{2D} = 0.0$ weight 0.40		$C^V_{2D=0.15}$ weight 0.40		$C^v_{2D} = 0.4$ weight 0.20

1.7.7 Gösgen

Site-specific Model Evaluations

Modified Weights for at Depth Motion

There are 2 sites at depth, the largest depth (15 m) being the same as for KKB and EKKB. The uncertainty factors are thus the same as the deepest site, and have intermediate values at the intermediate depth (9 m): the total range is reduced from (0.71, 1.0, 1.41, 2.0) at surface to (0.79, 1.0, 1.26, 1.58) at 9m depth and (0.83, 1.0, 1.20, 1.41) at 15 m depth.

Alternative 2D-parameters

The same weights as for the horizontal motion are to be applied. The C^v_{2D} coefficients are slightly reduced to take into account the fact that only Rayleigh waves contribute to the vertical motion. The velocities are significantly reduced because they are associated to Rayleigh waves at a much larger frequency than for the horizontal component.

Summary of Weights and Parameters for Vertical Motion at Gösgen

Table II-1.32: KKG Gösgen: Vertical ground motion - Summary of weights and computational parameters for the median site amplification factor.

Method and weights					
Depth	No change	V/H GA10	BAK11	PEF11	KSSM11	EQL SHAKE & RVT_{bc}
$z1 = 0m$	0	0.1	0.05	0.2	0.25	0.40 (see below)
$z2 = 9m$	0	0.05	0.05	0.2	0.30	0.40 (see below)
$z3 = 15m$	0	0.05	0.05	0.2	0.30	0.40 (see below)
Velocity profile						
Irrelevant : only P1, with P1 V_{S30} values						
Non-linear properties (for the EQL and KSSM11 branches)						
M1			M2			M3
0.25			0.45			0.3
Bedrock velocity values for the V/H KSSM11 branch						
$\alpha_R = 4330m/s$				$\beta_R = 2500m/s$		
Frequency dependent, relative weighting of EQL techniques (SHAKE, RVT_{bc})						
frequency				0.100Hz		
SHAKE				0.7		
RVT_{bc}				0.3		
Uncertainties and high $pga's$						
$Formula : Scalingfactor U_{h_{pga}}(f, f_V, pga, D_{pga}) = 10^{[D_{pga} E(k_v f/f_v).V_a(pga)]}$						
$E(x) = 0 for x < 0.5$ $E(x) = log(2x)/log(2) for 0.5 < x < 1.0$ $E(x) = 1 for 1.0 < x$				$k_v = 1. + V_a$		$V_a = [log(pga/pga_{ref})/log(2.5/0.75)]$
Parameter values		$f_v = 20Hz$		$pga_{ref} = 0.20g$		
D_{pga} values and relative weights						
Weights	0.2	0.5		0.2		0.1
$z1 = 0m$	$D_{pga} = -0.15$	$D_{pga} = 0.$		$D_{pga} = +0.15$		$D_{pga} = +0.30$
$z2 = 9m$	$D_{pga} = -0.10$	$D_{pga} = 0.$		$D_{pga} = +0.10$		$D_{pga} = +0.20$
$z3 = 15m$	$D_{pga} = -0.08$	$D_{pga} = 0.$		$D_{pga} = +0.08$		$D_{pga} = +0.15$
$2D$ - effects : $A_{2D} = 1 + C_{V,2D}(f, \zeta) = 1 + C^V_{2D}.A_0(f/f_V).exp(-2\pi\zeta_{av} fl/c_R)$, $c_R = c_{R0}.[1/(1 + 0.2(\gamma/\gamma_{50})_{max})]^{0.5}, \zeta_{av} \approx 0.0125 + 0.06.(\gamma/\gamma_{50})_{max}/[1. + 0.2(\gamma/\gamma_{50})_{max}]$ $\gamma from SHAKE horizontal motion(profile P1, material m2)$						
Fixed parameters		$f_v = 20Hz$ $l = 550m$			$c_{R0} = 300m/s$ $h = 28m$	
Alternative choice for parameters and corresponding weights		$C^v_{2D} = 0.0$ weight 0.70			$C^v_{2D} = 0.15$ weight 0.30	

1.7.8 Leibstadt

Site-specific Model Evaluations

Modified Weights for at Depth Motion

There is one site at depth, its depth (10 m) being about the same as for the intermediate site at KKG. The uncertainty factors are thus the same as this intermediate site, especially as it is also in gravel): the total range is reduced from (0.71, 1.0, 1.41, 2.0) at surface to (0.79, 1.0, 1.26, 1.58) at 10 m depth.

Alternative 2D-parameters

The same weights as for the horizontal motion are to be applied. The C_{2D}^{v} coefficients are slightly reduced to take into account the fact that only Rayleigh waves contribute to the vertical motion. The velocities are not reduced because from the examination of Rayleigh wave dispersion curves around 7-8 Hz.

Summary of Weights and Computational Parameters for Vertical Motion at Leibstadt

Table II-1.33: KKL Leibstadt: Vertical ground motion. Weights and parameters for the median site amplification factor.

Method and weights					
Depth	No change	V/H GA10	BAK11	PEF11	KSSM11	EQL SHAKE & RVT_{bc}
$z1 = 0m$	0	0.1	0.05	0.2	0.25	0.40 (see below)
$z2 = 10m$	0	0.05	0.05	0.2	0.30	0.40 (see below)
Velocity profile						
Irrelevant : only P1, with P1 V_{S30} values						
Non-linear properties (for the EQL and KSSM11 branches)						
M1 0.2				M2 0.6		M3 0.2
Bedrock velocity values for the V/H KSSM11 branch						
$\alpha_R = 4840m/s$				$\beta_R = 2200m/s$		
Frequency independent, relative weighting of EQL techniques (SHAKE, RVT_{bc})						
frequency SHAKE RVT_{bc}				0.100Hz 0.70 0.30		
Uncertainties and high $pga's$						
Formula : Scaling factor $Uh_{pga}(f, f_V, pga, D_{pga}) = 10^{[D_{pga}E(k_v f/f_v).V_a(pga)]}$						
$E(x) = 0 for x < 0.5$ $E(x) = log(2x)/log(2) for 0.5 < x < 1.0$ $E(x) = 1 for 1.0 < x$				$k_v = 1. + V_a$		$V_a = [log(pga/pga_{ref})$ / log(2.5/0.75)]
Parameter values		$f_v = 7.5Hz$		$pga_{ref} = 0.40g$		
D_{pga} values and relative weights						
Weight $z1 = 0m$ $z2 = 10m$	0.2 $D_{pga} = -0.15$ $D_{pga} = -0.10$	0.5 $D_{pga} = 0.$ $D_{pga} = 0.$		0.2 $D_{pga} = +0.15$ $D_{pga} = +0.10$		0.1 $D_{pga} = +0.30$ $D_{pga} = +0.20$
$2D$ - effects : $A_{2D} = 1 + C_{V,2D}(f, \zeta) = 1 + C^V_{2D}.A_0(f/f_V).exp(-2\pi\zeta_{av} fl/c_R)$, $c_R = c_{R0}.[1/(1 + 0.2(\gamma/\gamma_{50})_{max})]^{0.5}, \zeta_{av} \approx 0.0125 + 0.06.(\gamma/\gamma_{50})_{max}/[1. + 0.2(\gamma/\gamma_{50})_{max}]$ $\gamma from SHAKE horizontal motion(profile P1, material m2)$						
Fixed parameters		$f_v = 7.5Hz$	$l = 100m$		$c_{R0} = 600m/s$	$h = 30m$
Alternative choice for parameters and corresponding weights			$C^V_{2D} = 0.0$ weight 0.30		$C^V_{2D} = 0.20$ weight 0.50	$C^V_{2D} = 0.40$ weight 0.20

1.7.9 Mühleberg

Site-specific Model Evaluations

Modified Weights for at Depth Motion

There are 2 sites at depth : the first one ($z2 = 7m$) is still in the gravel layer - very close to the underlying molasse, and the second one ($z3 = 14m$) is in the weathered molasse. Considering ost of the non-linear effects are associated with the gravel layer, I assign to z2 the same reduced uncertainty factors as for KKB and EKKB z2, and a slightly larger reduction at z3.

Alternative 2D-parameters

The same weights as for the horizontal motion are to be applied. The C^v_{2D} coefficients are slightly reduced to take into account the fact that only Rayleigh waves contribute to the vertical motion. The velocities are significantly reduced because they are associated to Rayleigh waves at a much larger frequency than for the horizontal component. The 2D/3D-subbranching should NOT be applied to the deep sites z2 and z3.

Summary of Weights and Computational Parameters for Vertical Motion at Mühleberg

1.8 Aleatory Variability on Vertical Ground Motion

For the horizontal motion, it was considered that only the non-linear behavior of soft soil could involve some additional aleatory variability in relation with the site response. As a consequence, since the non-linear behavior is much less pronounced for vertical motion, it is simply assumed that the site response does not imply any additional aleatory variability on the vertical motion.

1.9 Maximum Vertical Ground Motion

To the opposite of the logic tree for horizontal motion, only one main branch is considered for the the vertical motion, corresponding to the "Strasser's" purely empirical approach from maximum recorded vertical ground motion : there are no "theoretical upper bounds.

The same surprising issue as for horizontal ground motion is faced for the recorded maximum vertical ground motion : it is larger for the M6 bin than for the M7 bin at periods larger than 0.4 s. Morereover, the difference is much larger than the considered scaling factors introduced to take into account the fact that such maximum ever recorded motion will increase in the future. Therefore, the M7 observed maxima were raised to the M6 maxima, as shown in Figure II-1.24.

The weights for the scaling factor and the mix between M6 and M7 maxima is the same as for the horizontal component and is listed in Table II-1.35.

Table II-1.34: KKM Mühleberg: Vertical ground motion. Weights and parameters for the median site amplification factor.

Method and weights						
Depth	No change	V/H GA10	BAK11	PEF11	KSSM11	EQL SHAKE & RVT_{bc}
$z1 = 0m$	0	0.1	0.05	0.2	0.25	0.40 (see below)
$z2 = 7m$	0	0.05	0.05	0.2	0.30	0.40 (see below)
$z3 = 14m$	0	0.05	0.05	0.2	0.30	0.40 (see below)
Velocity profile						
Irrelevant : only P1, with P1 V_{S30} values						
Non-linear properties (for the EQL and KSSM11 branches)						
M1 0.15				M2 0.45		M3 0.4
Bedrock velocity values for the V/H KSSM11 branch						
$\alpha_R = 2420m/s$				$\beta_R = 1100m/s$		
Frequency independent, relative weighting of EQL techniques (SHAKE, RVT_{bc})						
frequency SHAKE RVT_{bc}				0.100Hz 0.70 0.30		
Uncertainties and high pga's						
$Formula : Scalingfactor U_{h_{pga}}(f, f_V, pga, D_{pga}) = 10^{[D_{pga} E(k_v f/f_v).V_a(pga)]}$						
$E(x) = 0 for x < 0.5$ $E(x) = log(2x)/log(2) for 0.5 < x < 1.0$ $E(x) = 1 for 1.0 < x$				$k_v = 1. + V_a$		$V_a = [log(pga/pga_{ref})]/$ $[log(2.5/0.75)]$
Parameter values		$f_v = 23Hz$		$pga_{ref} = 0.15g$		
D_{pga} values and relative weights						
Weight $z1 = 0m$ $z2 = 7m$ $z3 = 14m$	0.2 $D_{pga} = -0.15$ $D_{pga} = -0.08$ $D_{pga} = -0.05$	0.5 $D_{pga} = 0.$ $D_{pga} = 0.$ $D_{pga} = 0.$		0.2 $D_{pga} = +0.15$ $D_{pga} = +0.08$ $D_{pga} = +0.05$		0.1 $D_{pga} = +0.30$ $D_{pga} = +0.15$ $D_{pga} = +0.10$
2D-effects : $A_{2D} = 1 + C_{V,2D}(f, \zeta) = 1 + C^V_{2D}.A_0(f/f_V).exp(-2\pi\zeta_{av} fl/c_R)$, $c_R = c_{R0}.[1/(1 + 0.2(\gamma/\gamma_{50})_{max})]^{0.5}, \zeta_{av} \approx 0.0125 + 0.06.(\gamma/\gamma_{50})_{max}/[1. + 0.2(\gamma/\gamma_{50})_{max}]$ γ from SHAKE horizontal motion (profile P1, material M2)						
Fixed parameters		$f_v = 23Hz$	$l = 200m$	$c_{R0} = 200m/s$		$h = 8m$
Alternative choice for parameters and corresponding weights		$C^V_{2D} = 0.0$ weight 0.30		$C^V_{2D} = 0.07$ weight 0.60		$C^V_{2D} = 0.20$ weight 0.10

Table II-1.35: Summary of weights for the sub-branching corresponding to "Strassers" empirical approach.

Magnitude, relative weight		Scaling factor and associated related weights 1	1.2	1.4
magnitude 6	60%	30%	50%	20%
magnitude 7	40%	45%	45%	10%

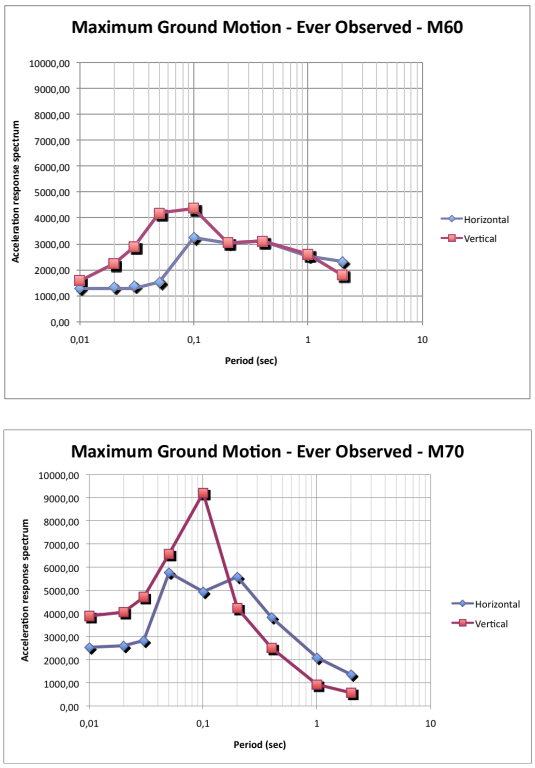

Figure II-1.24: Maximum spectra to be used in the "Strassers" empirical approach.

Table II-1.36: Maximum spectra to be used in the "Strassers" empirical approach

Period (s)	0.01	0.02	0.03	0.05	0.1	0.2	0.4	1	2
Sa values, M6 (m/s^2)	15.8	22.3	28.8	41.7	43.7	30.4	30.9	25.9	17.9
Sa values, M7 (m/s^2)	39	41	47	66	92	42	25	9.2	5.7
Corrected Sa values, M7 (m/s^2)	39	41	47	66	92	42	30.9	25.9	17.9

1.10 ANNEX A1: Supporting documents for the assessment of the threshold PGA values corresponding to the selected threshold values for RVT_{bc} strain ratio

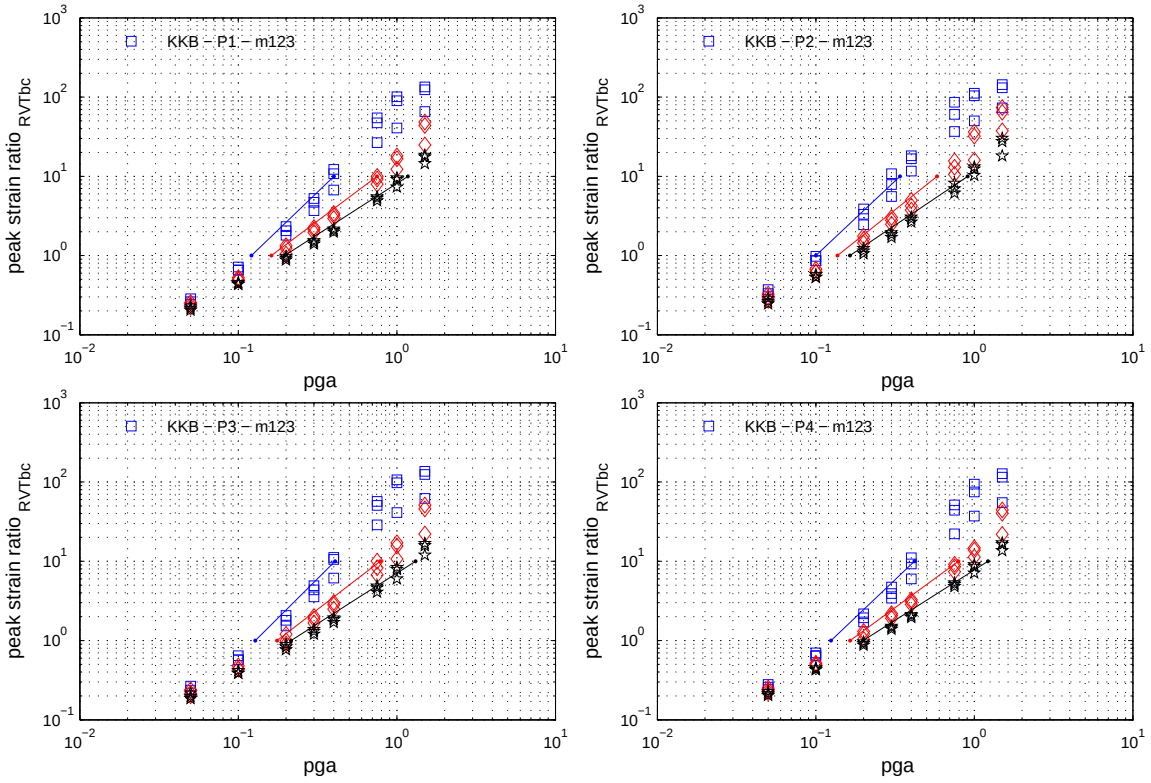

Figure II-1.25: KKB - Dependance of RVT_{bc} peak strain ratio as a function of PGA for the four considered velocity profiles (P1, top left; P2, top right; P3, bottom left; P4, bottom right), and the three material properties (M1, blue; M2, red; M3, black). Symbols correspond to existing computations; solid lines correspond to loglog correlations.

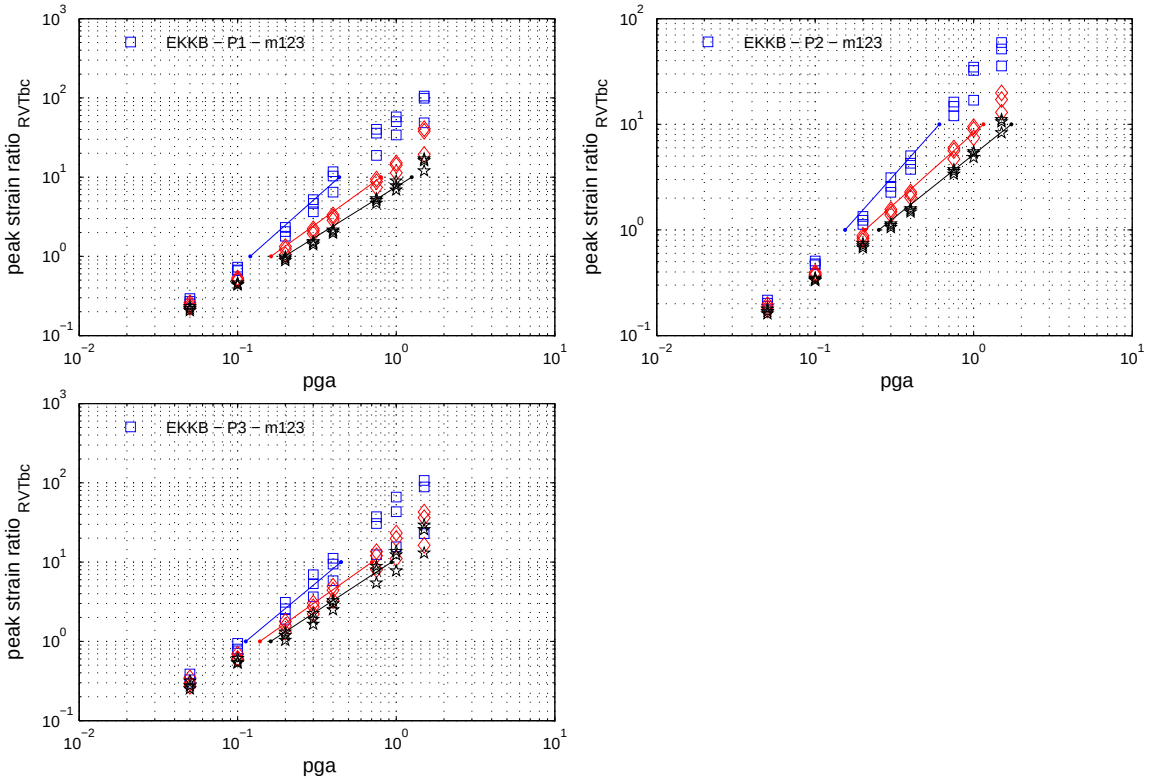

Figure II-1.26: EKKB - Dependance of RVT_{bc} peak strain ratio as a function of PGA for the three considered velocity profiles (P1, top left; P2, top right; P3, bottom left), and the three material properties (M1, blue; M2, red; M3, black). Symbols correspond to existing computations; solid lines correspond to log-log correlations.

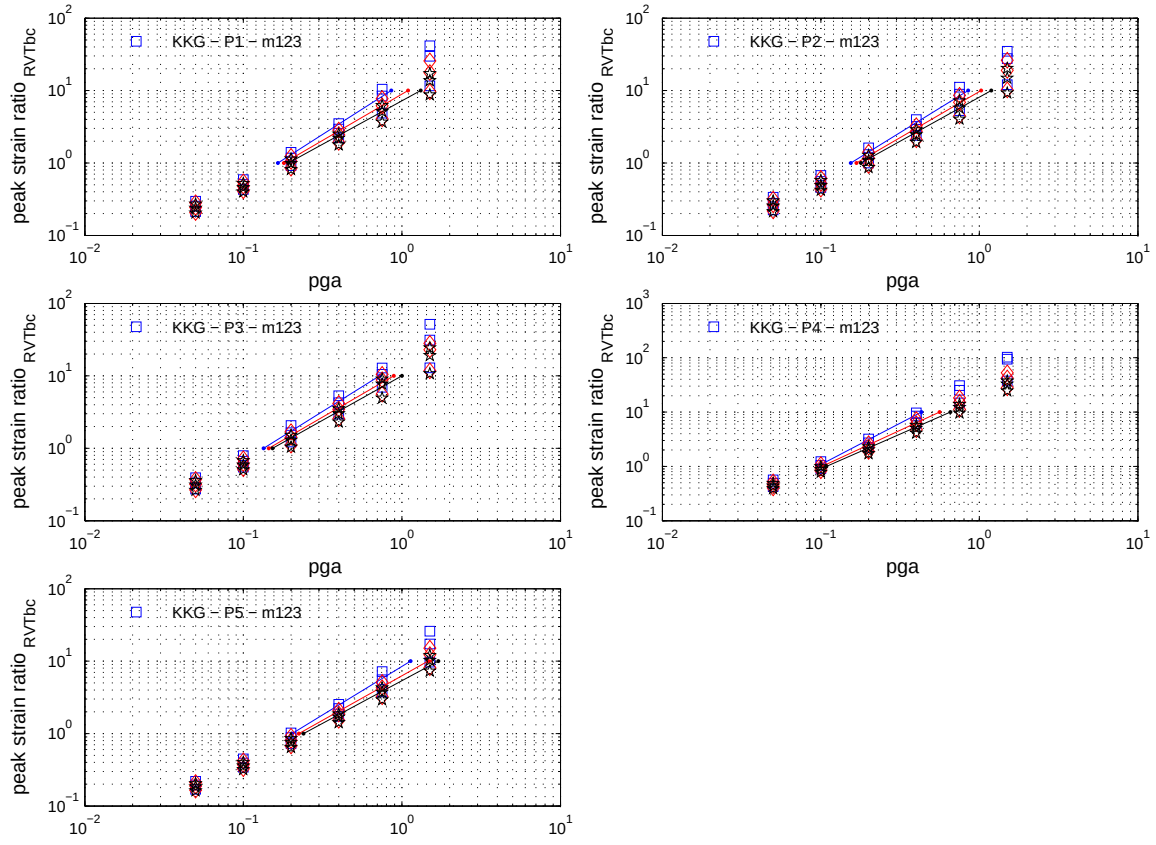

Figure II-1.27: KKG - Dependance of RVT_{bc} peak strain ratio as a function of PGA for the five considered velocity profiles (P1, top left; P2, top right; P3, middle left; P4, middle right; P5, bottom left), and the three material properties (M1, blue; M2, red; M3, black). Symbols correspond to existing computations; solid lines correspond to loglog correlations.

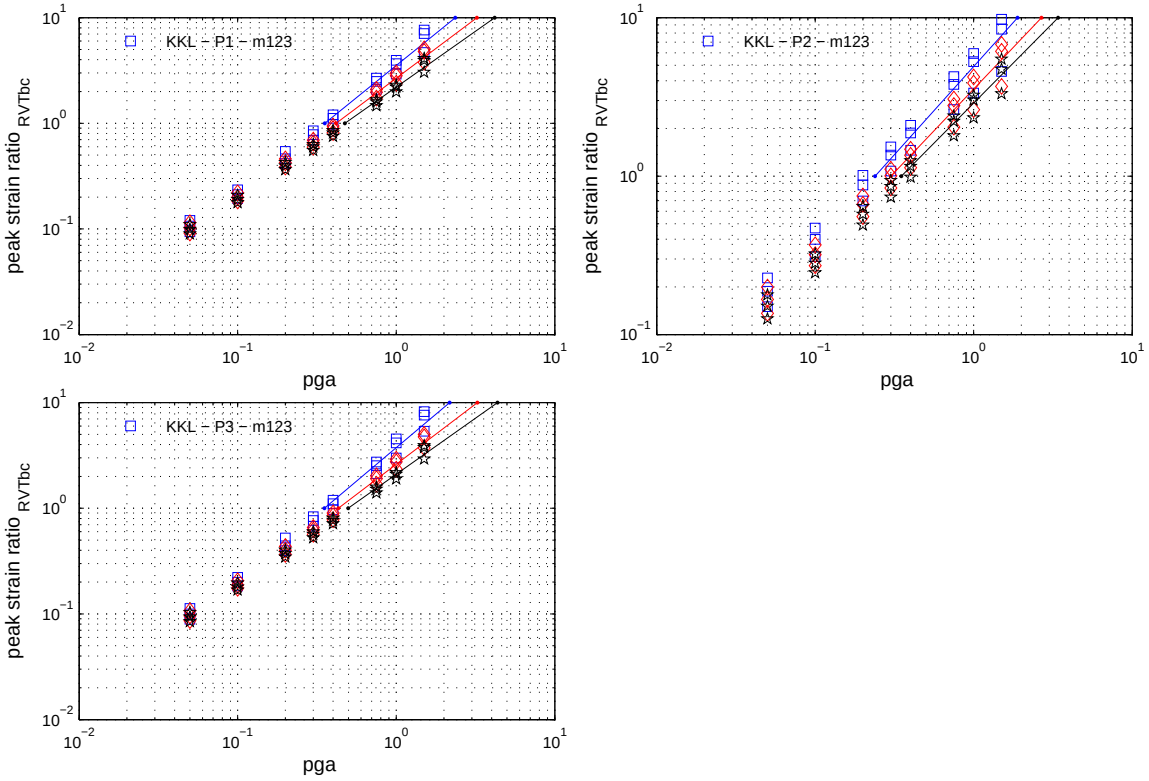

Figure II-1.28: KKL - Dependance of RVT_{bc} peak strain ratio as a function of PGA for the three considered velocity profiles (P1, top left; P2, top right; P3, bottom left), and the three material properties (M1, blue; M2, red; M3, black). Symbols correspond to existing computations; solid lines correspond to loglog correlations.

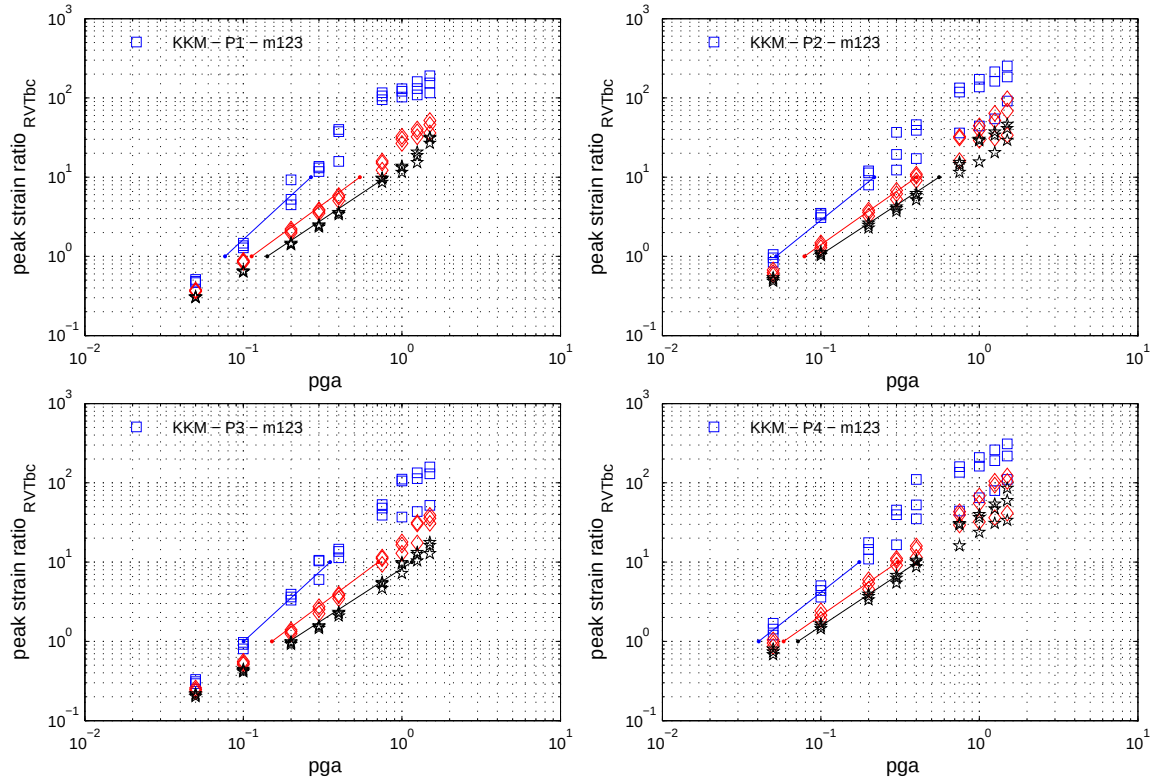

Figure II-1.29: KKM - Dependance of RVT_{bc} peak strain ratio as a function of PGA for the four considered velocity profiles (P1, top left; P2, top right; P3, bottom left; P4, bottom right), and the three material properties (M1, blue; M2, red; M3, black). Symbols correspond to existing computations; solid lines correspond to loglog correlations.

1.11 ANNEX A2 : Supporting documents for the quantification of uncertainty sub-branching for NL computations

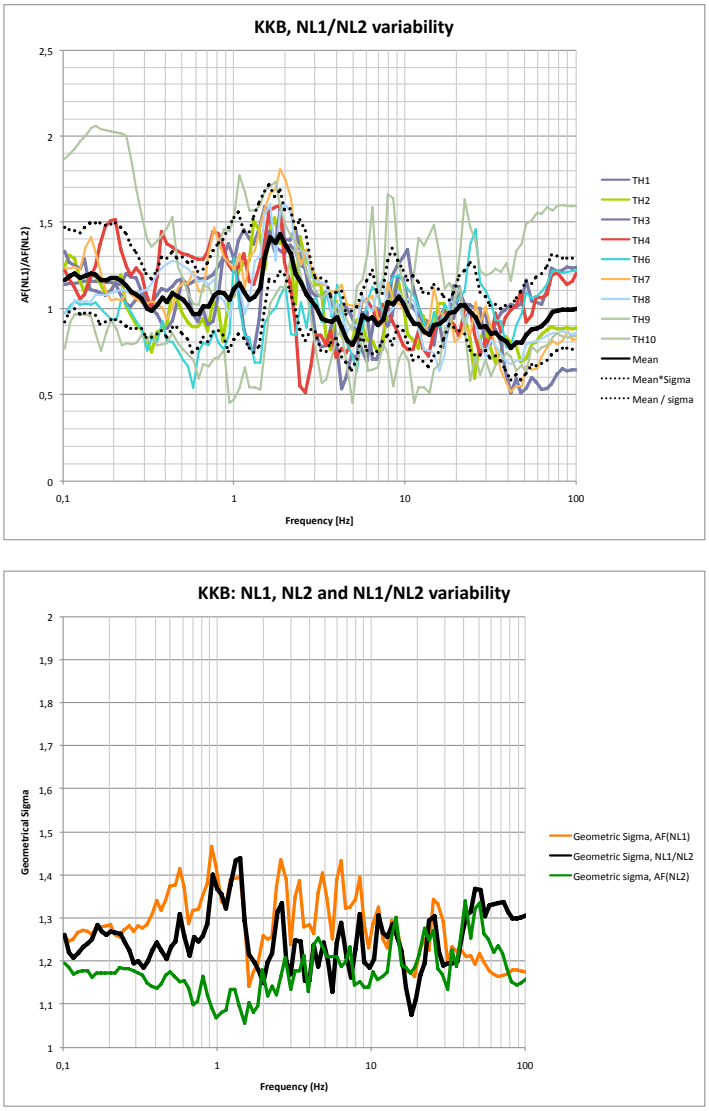

Figure II-1.30: KKB : Comparisons between NL1 and NL2 computations for M6, M2, 0.75g and the 9 time histories. Top: ratio between NL1 and NL2 amplification factors for each of the 9 time histories (color, slid lines) + geometric average (back, solid) and geometric plus/minus one standard deviation (black, dotted) Bottom: Geometric standard deviation for the ratio of NL1/NL2 amplification factors for the 9 time histories (black, solid line), compared with the standard deviations of the amplification factors derived for NL1 (solid, orange) and NL2 (solid, green).

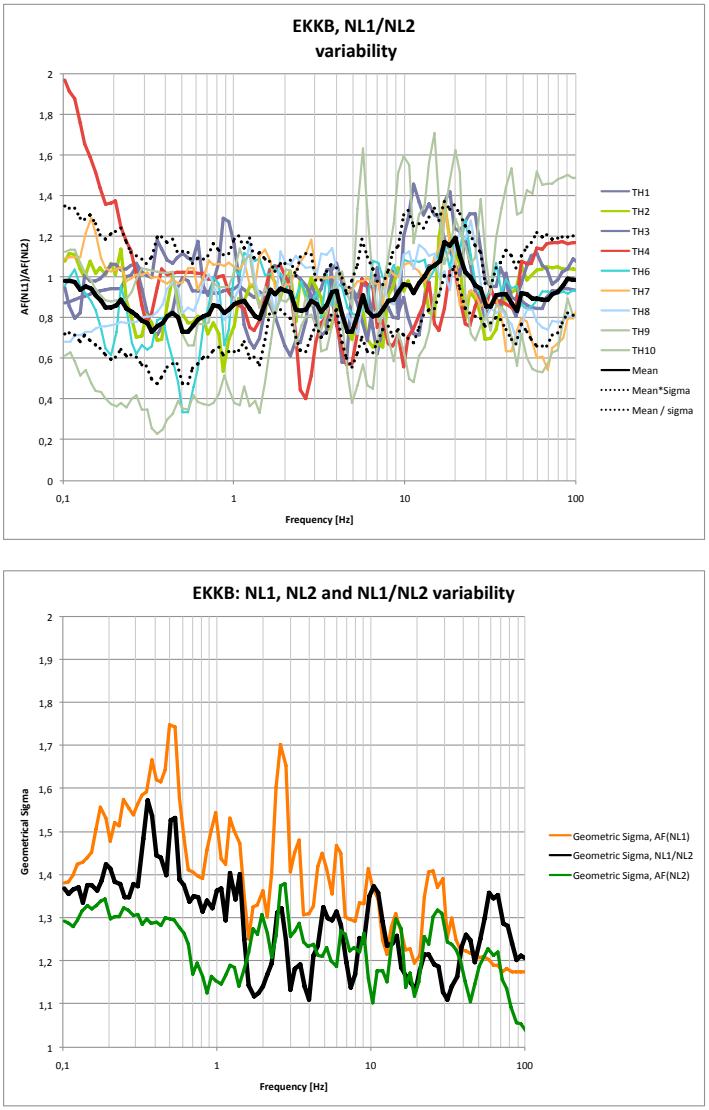

Figure II-1.31: EKKB : Comparisons between NL1 and NL2 computations for M6, M2, 0.75g and the 9 time histories. Top: ratio between NL1 and NL2 amplification factors for each of the 9 time histories (color, slid lines) + geometric average (back, solid) and geometric plus/minus one standard deviation (black, dotted) Bottom: Geometric standard deviation for the ratio of NL1/NL2 amplification factors for the 9 time histories (black, solid line), compared with the standard deviations of the amplification factors derived for NL1 (solid, orange) and NL2 (solid, green).

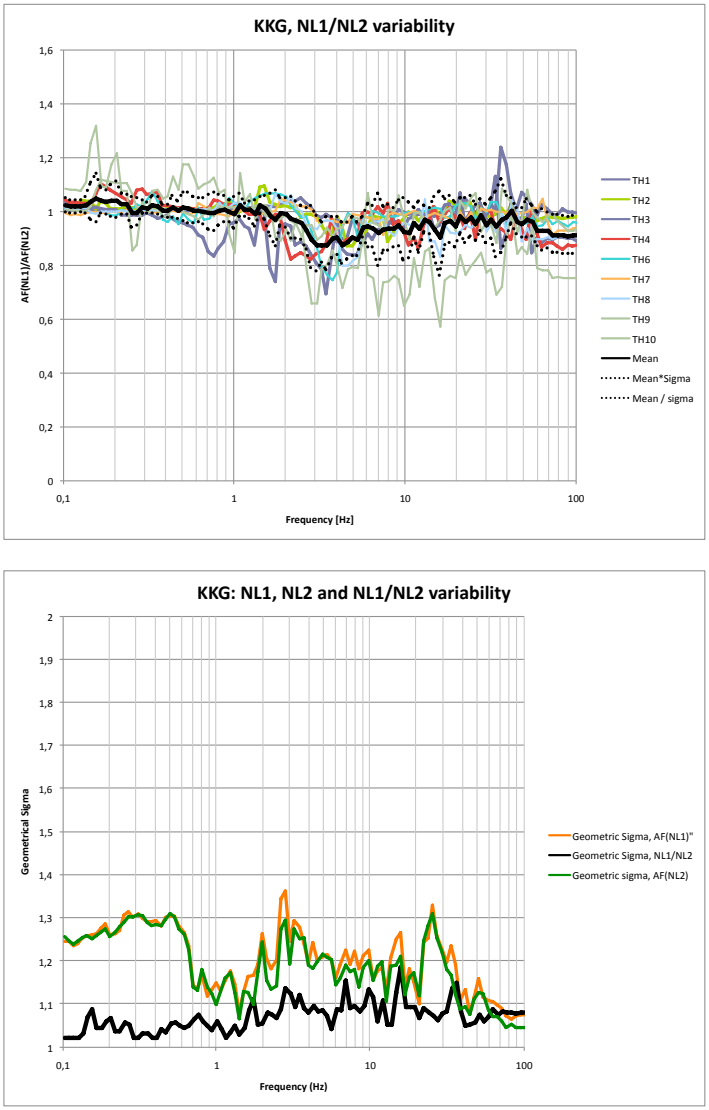

Figure II-1.32: KKG: Comparison between NL1 and NL2 computations for M6, M2, 0.75g and the 9 time histories. Top: ratio between NL1 and NL2 amplification factors for each of the 9 time histories (color, slid lines) + geometric average (back, solid) and geometric plus/minus one standard deviation (black, dotted) Bottom: Geometric standard deviation for the ratio of NL1/NL2 amplification factors for the 9 time histories (black, solid line), compared with the standard deviations of the amplification factors derived for NL1 (solid, orange) and NL2 (solid, green).

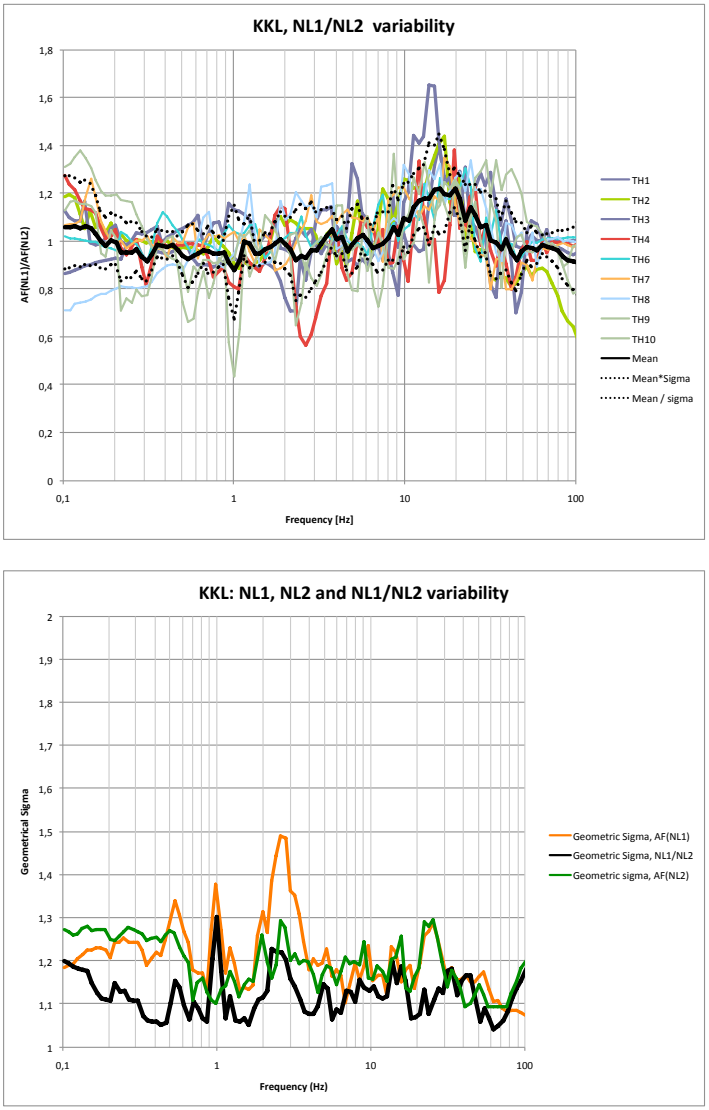

Figure II-1.33: KKL: Comparison between NL1 and NL2 computations for M6, M2, 0.75g and the 9 time histories. Top: ratio between NL1 and NL2 amplification factors for each of the 9 time histories (color, slid lines) + geometric average (back, solid) and geometric plus/minus one standard deviation (black, dotted) Bottom: Geometric standard deviation for the ratio of NL1/NL2 amplification factors for the 9 time histories (black, solid line), compared with the standard deviations of the amplification factors derived for NL1 (solid, orange) and NL2 (solid, green).

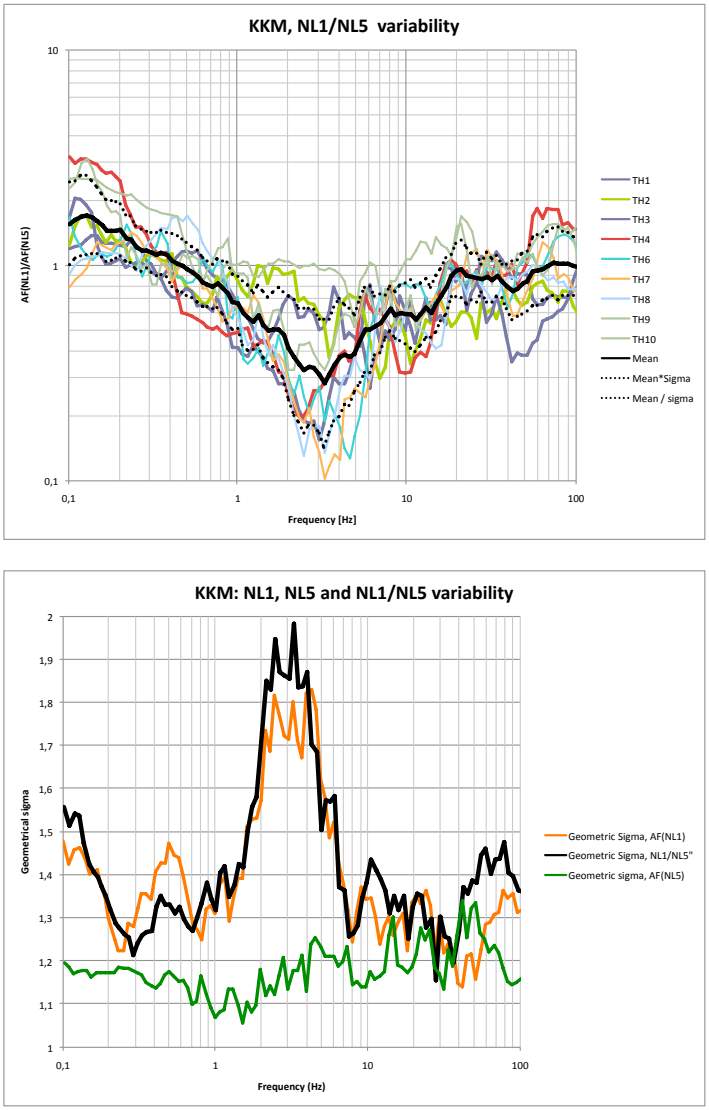

Figure II-1.34: KKM: Comparison between NL1 and NL2 computations for M6, M2, 0.75g and the 9 time histories. Top: ratio between NL1 and NL2 amplification factors for each of the 9 time histories (color, slid lines) + geometric average (back, solid) and geometric plus/minus one standard deviation (black, dotted) Bottom: Geometric standard deviation for the ratio of NL1/NL2 amplification factors for the 9 time histories (black, solid line), compared with the standard deviations of the amplification factors derived for NL1 (solid, orange) and NL2 (solid, green).

1.12 ANNEX A3 : Supporting documents for the assignment of weights for velocity profile and material properties for each site

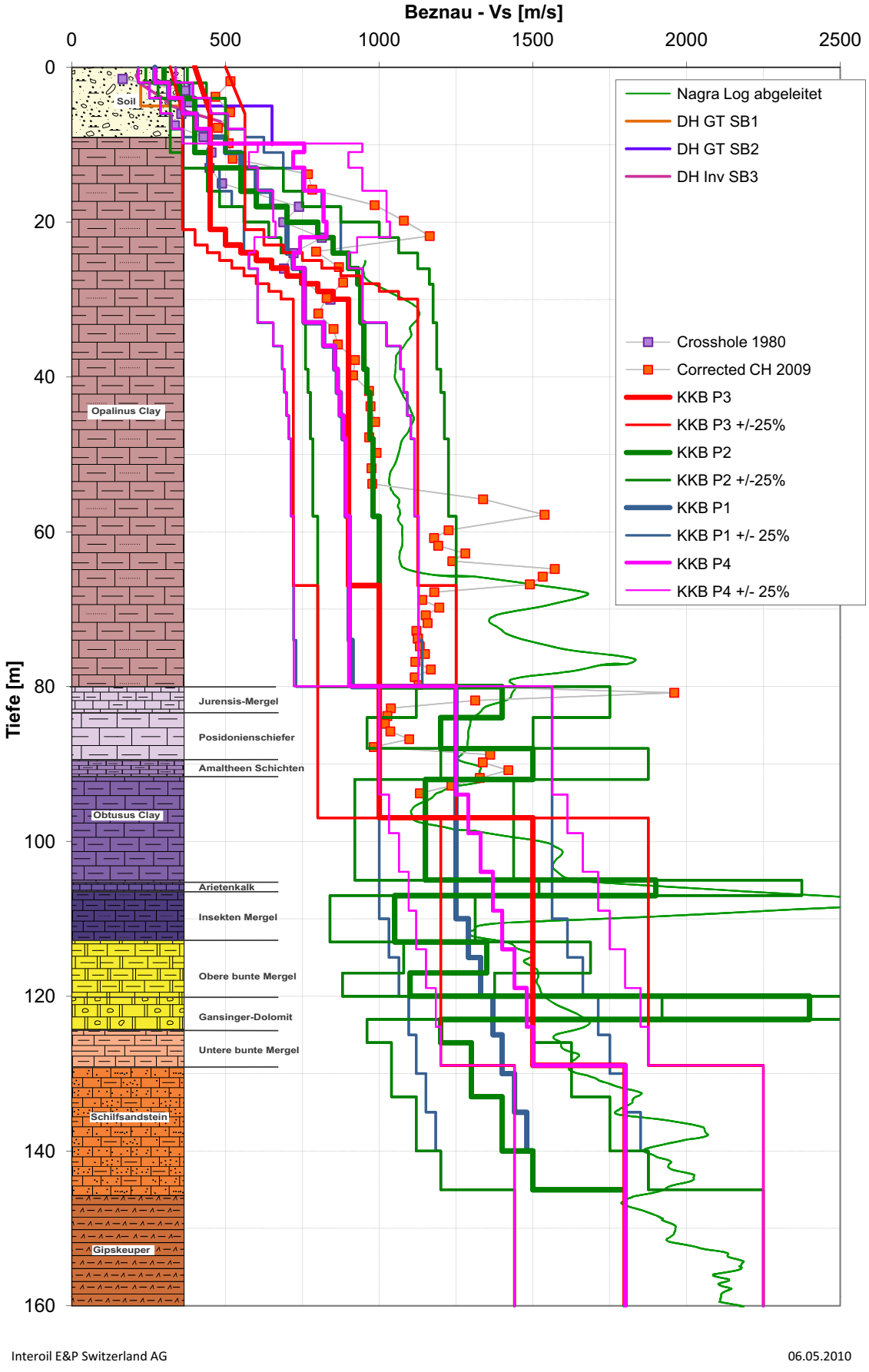

Figure II-1.35: KKB - Comparison of the four selected S-wave velocity profiles (P1 through P4) with the actual borehole measurements (CH and DH).

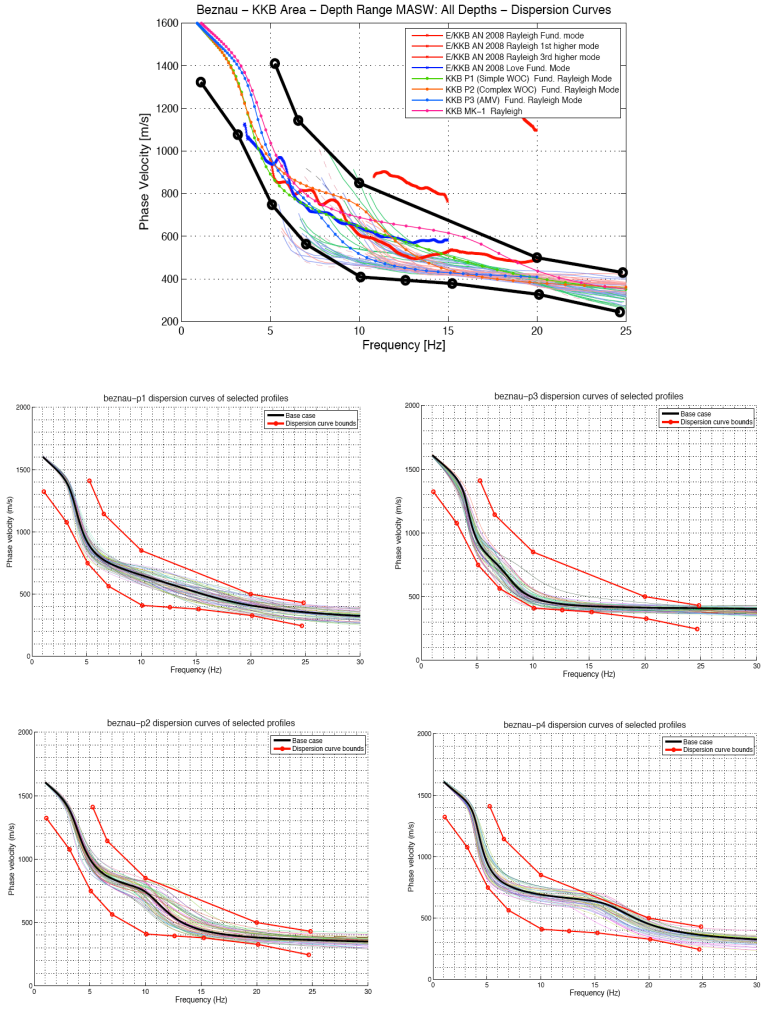

Figure II-1.36: KKB - Comparison of the dispersion curves of the 50 randomized profiles associated with the four selected velocity profiles (P1, middle left; P2, bottom left; P3, middle right; P4, bottom right) with the designed bounds for the fundamental Rayleigh mode. The top frame displays the dispersion curves actually measured with passive microtremor array techniques (thick lines) and with active MASW techniques (thin lines).

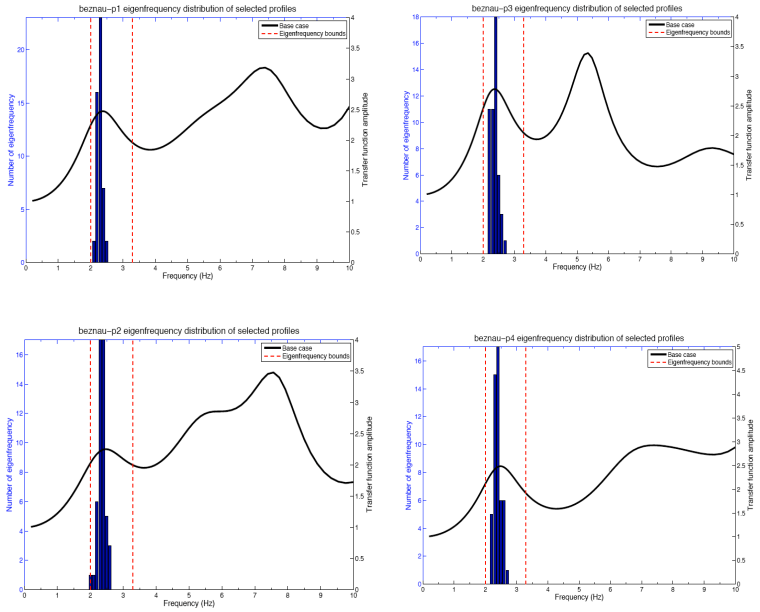

Figure II-1.37: KKB - Comparison of the distribution of fundamental frequencies of the 50 selected randomized profiles with the corresponding "uncertainty bounds" (vertical red dashed lines). (Top left : P1; bottom left : P2; top right: P3; bottom left : P4). The solid line represents the transfer function of each profile (respectively) for vertically incident S waves.

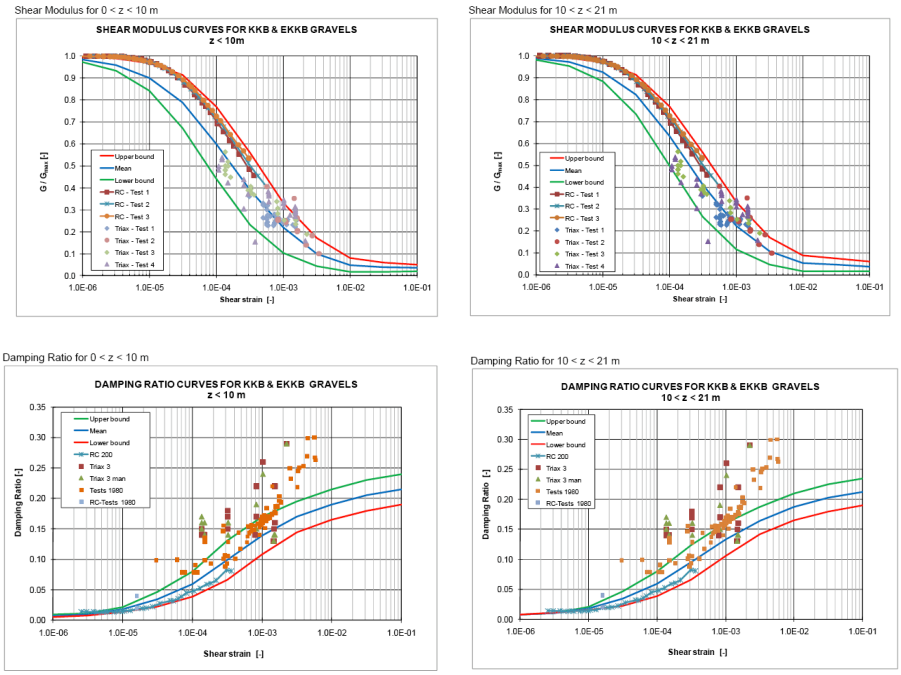

Figure II-1.38: KKB - Comparison of the selected NL curves (green: lower bound / blue: mean / red: upper bound) with the actually available data for KKB and EKKB. Top: shear modulus degradation as a function of strain / Bottom: damping increase as a function of strain. Left: shallow gravels ($z < 10m$) / Right: deep gravels (only for EKKB). There are no data for opalinuston.

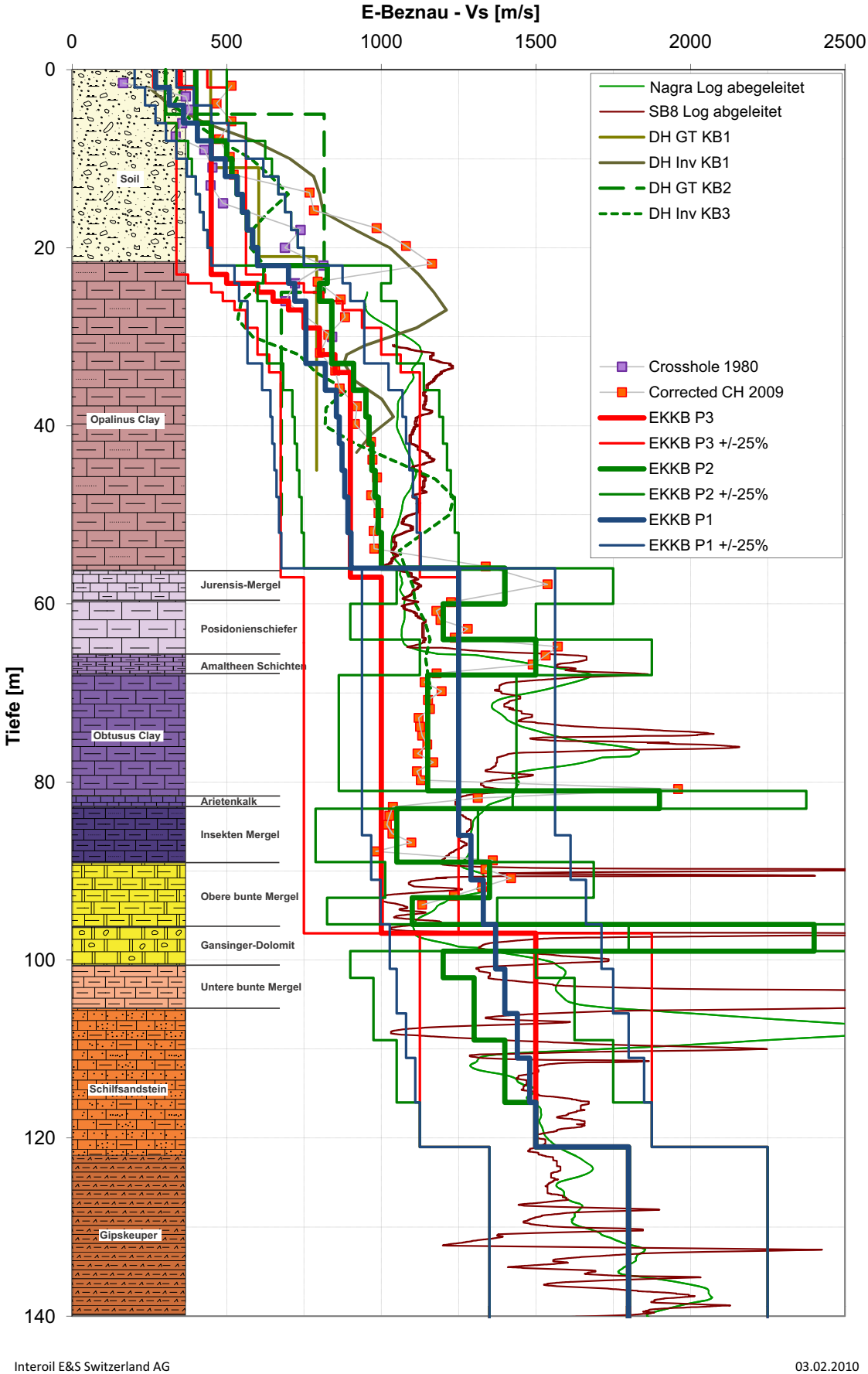

Figure II-1.39: KKB - Comparison of the three selected S-wave velocity profiles (P1 through P3) with the actual borehole measurements (CH and DH).

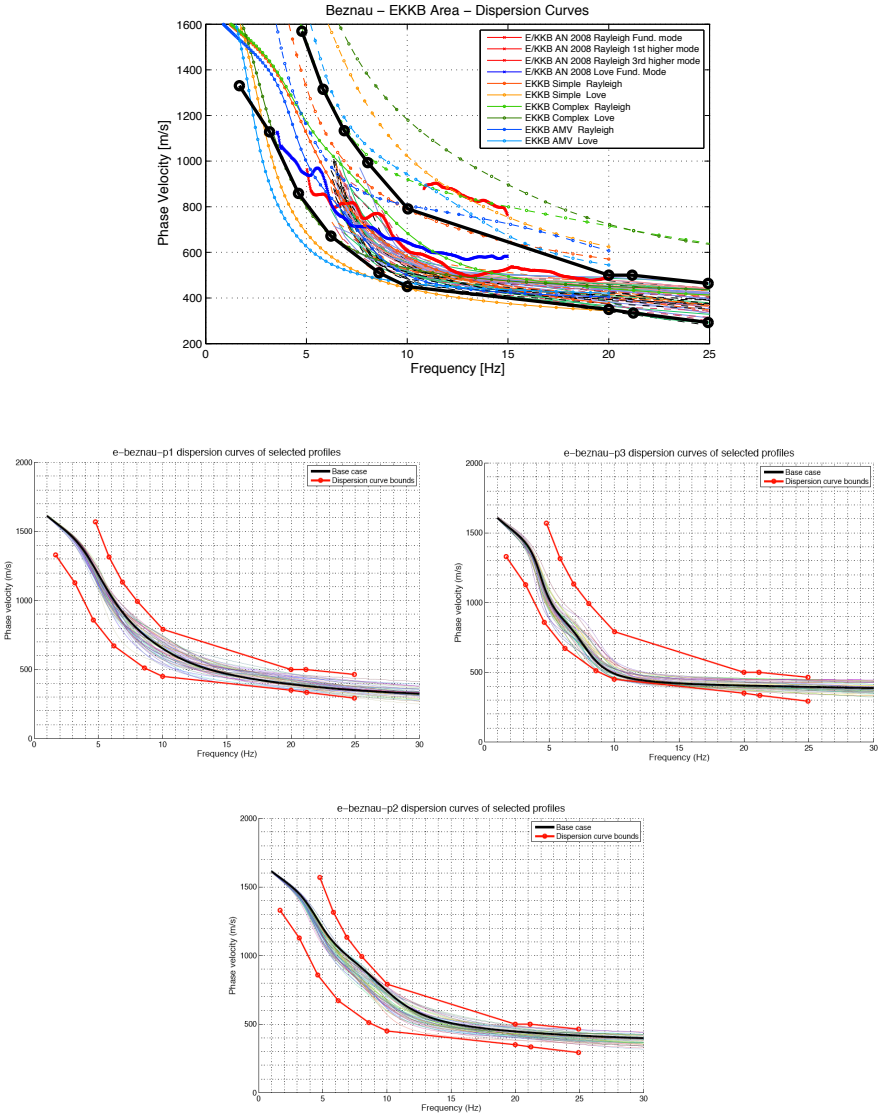

Figure II-1.40: EKKB - Comparison of the dispersion curves of the 50 randomized profiles associated with the three selected velocity profiles (P1, middle left; P2, bottom left; P3, middle right) with the designed bounds for the fundamental Rayleigh mode. The top frame displays the dispersion curves actually measured with passive microtremor array techniques (thick lines) and with active MASW techniques (thin lines).

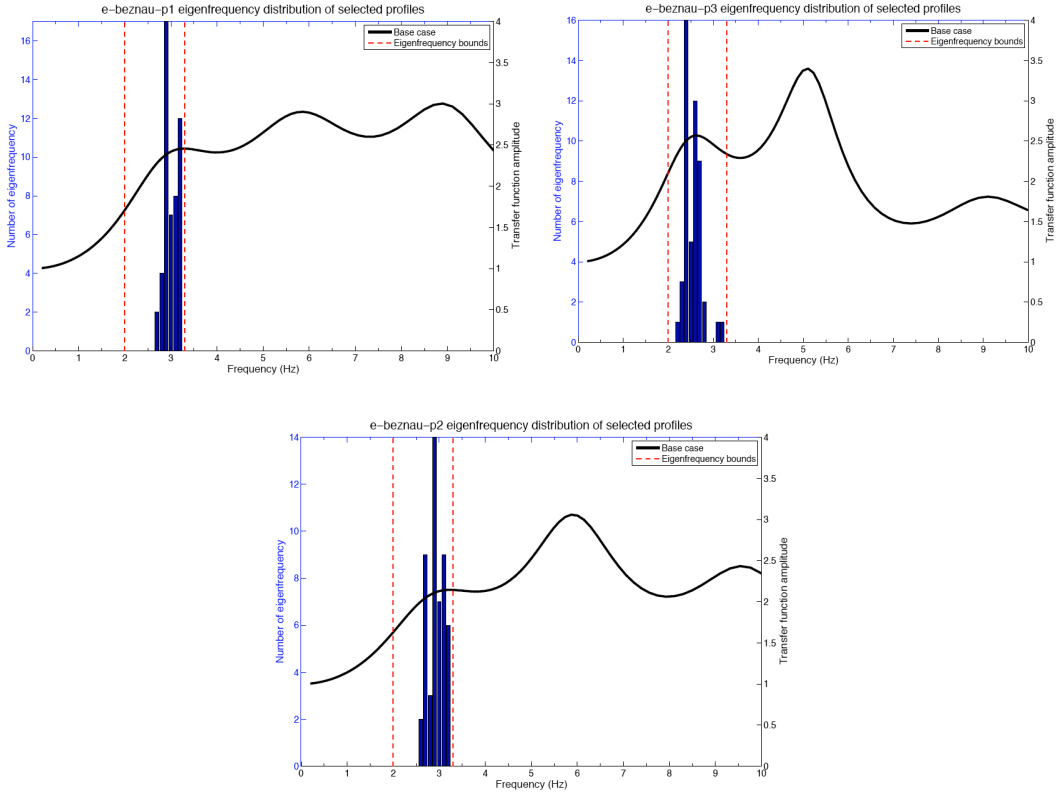

Figure II-1.41: EKKB - Comparison of the distribution of fundamental frequencies of the 50 selected randomized profiles with the corresponding "uncertainty bounds" (vertical red dashed lines) for the three velocity profiles P1-P3 (Top left : P1; bottom left : P2; top right: P3). The solid black line represents the transfer function of each profile (respectively) for vertically incident S-waves.

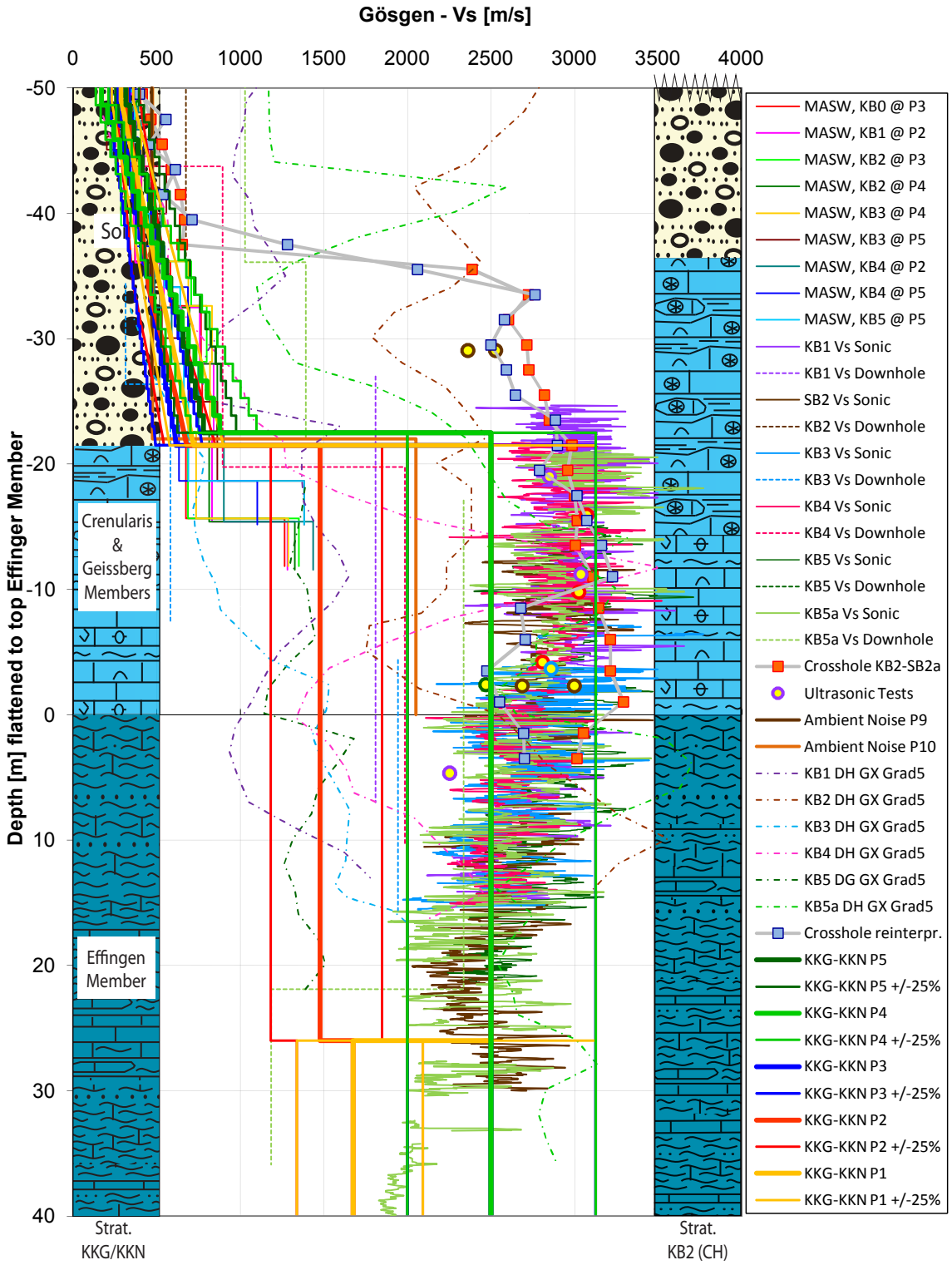

Figure II-1.42: KKG - Comparison at rather shallow depth (smaller than 100 m) of the six selected S-wave velocity profiles (P1 through P6, considering that P6 is identical to P1 down to 30m, with a constant 2.5 km/s velocity at larger depth) with the actual borehole measurements (CH and DH).

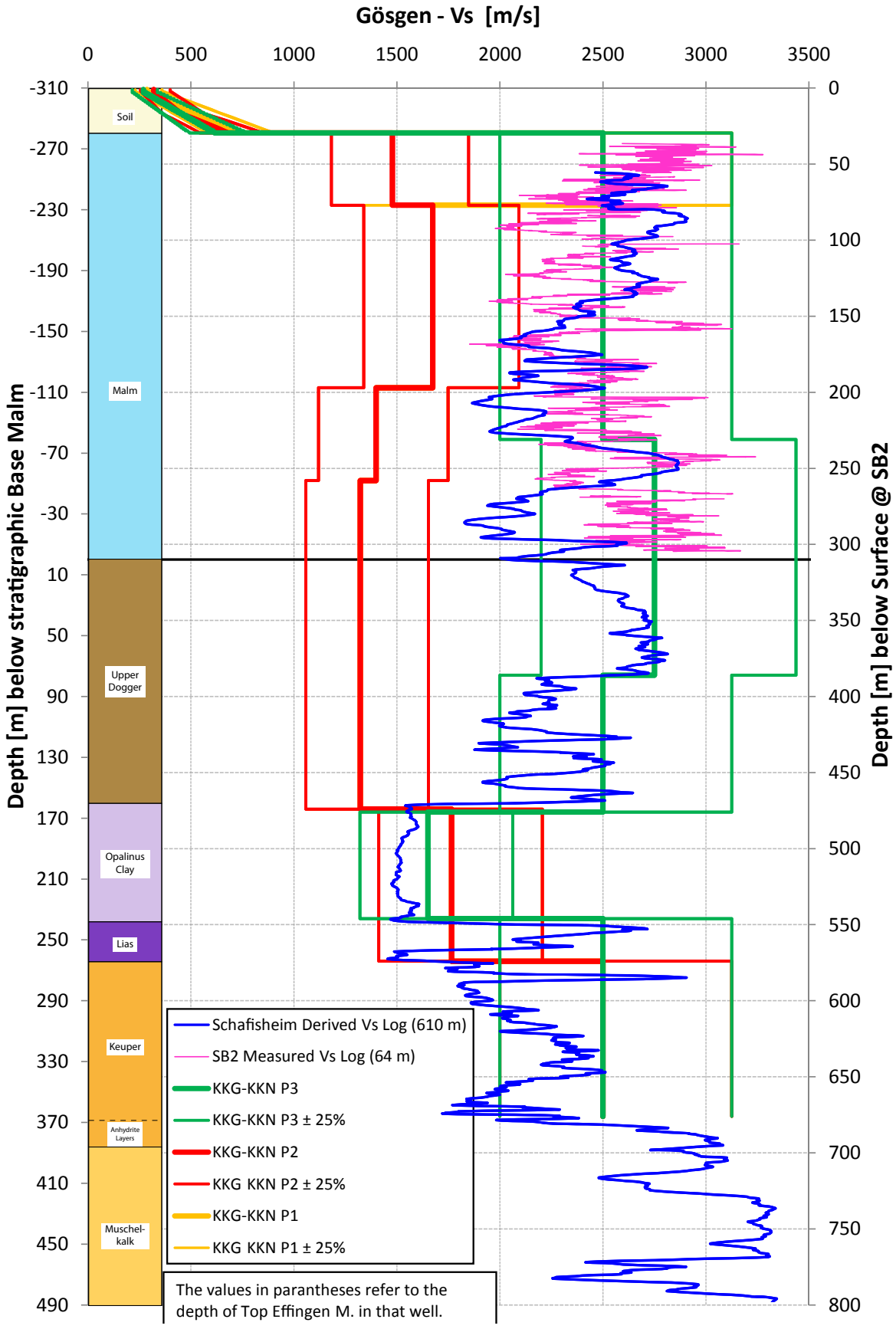

Figure II-1.43: KKG - Same as Figure A3.8 but for larger depth (down to 700 m).

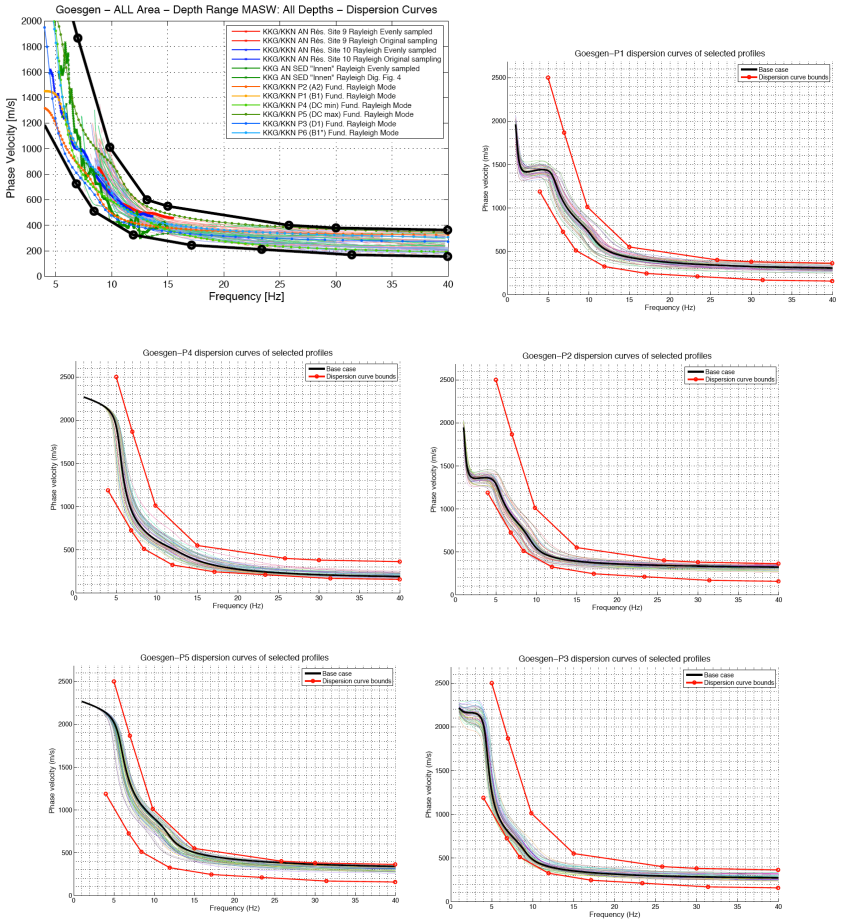

Figure II-1.44: KKG - Comparison of the dispersion curves of the 50 randomized profiles associated with five of the six selected velocity profiles (on the left : deep profiles P1 through P3; on the right, shallow profiles, P5 and P6) with the designed bounds for the fundamental Rayleigh mode. The top frame displays the dispersion curves actually measured with passive microtremor array techniques (thick lines) and with active MASW techniques (thin lines).

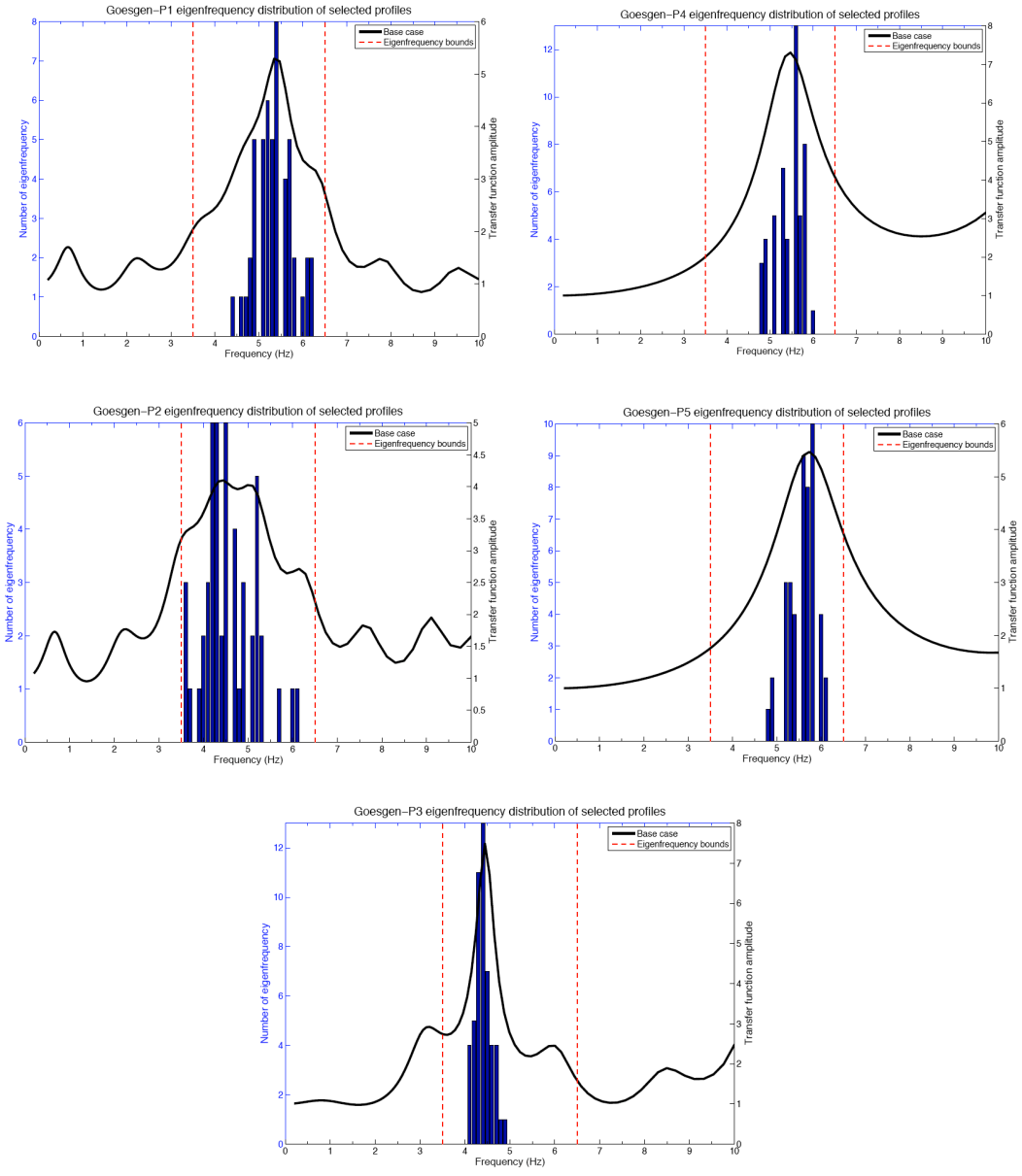

Figure II-1.45: KKG - Comparison of the distribution of fundamental frequencies of the 50 selected randomized profiles with the corresponding "uncertainty bounds" (vertical red dashed lines). (Left: deep profiles, P1 to P3 from top to bottom; Right: shallow profiles P4 and P5). The solid line represents the transfer function of each profile (respectively) for vertically incident S-waves.

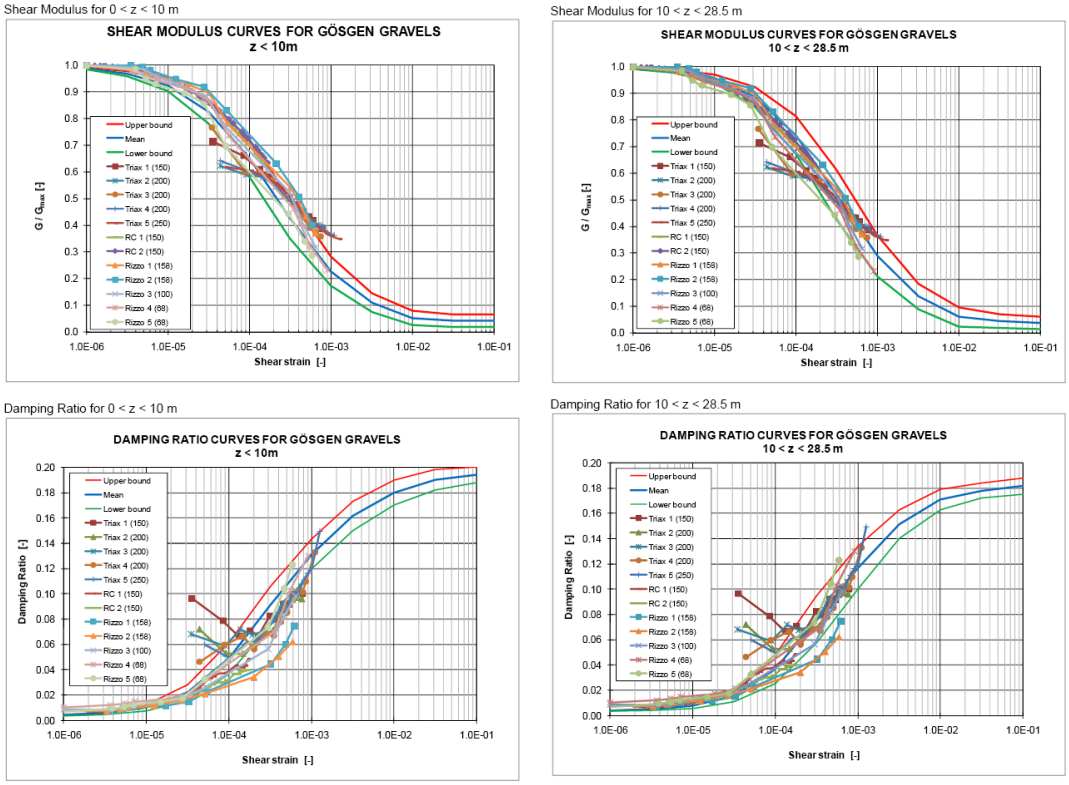

Figure II-1.46: KKG - Comparison of the selected NL curves (green: lower bound / blue: mean / red: upper bound) with the actually available data for KKG. Top: shear modulus degradation as a function of strain / Bottom: damping increase as a function of strain. Left: shallow gravels ($z < 10m$) / Right: deep gravels ($10m < z < 28.5m$).

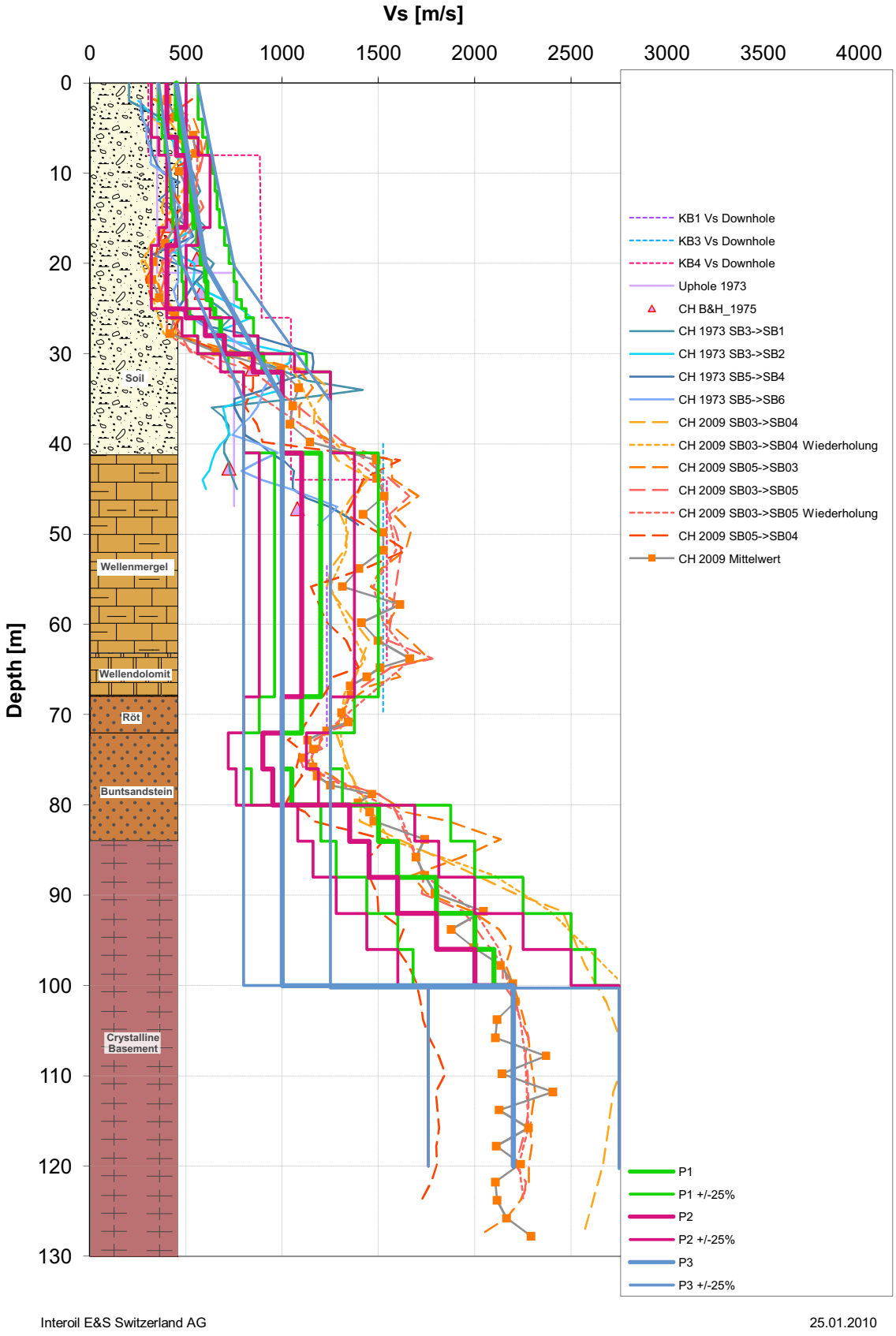

Figure II-1.47: KKL - Comparison of the three selected S-wave velocity profiles (P1 thourgh P3) with the actual borehole measurements (CH and DH).

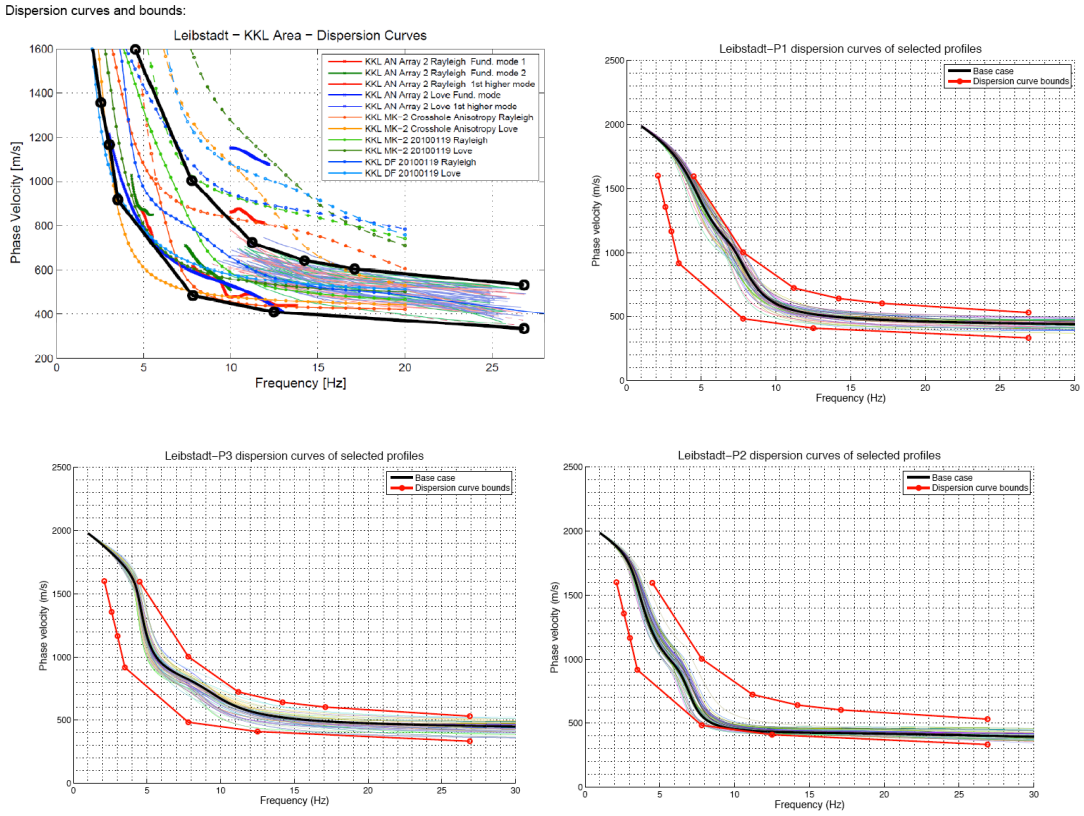

Figure II-1.48: KKL - Comparison of the dispersion curves of the 50 randomized profiles associated with the three selected velocity profiles (P1, middle left; P2, bottom left; P3, middle right) with the designed bounds for the fundamental Rayleigh mode. The top frame displays the dispersion curves actually measured with passive microtremor array techniques (thick lines) and with active MASW techniques (thin lines).

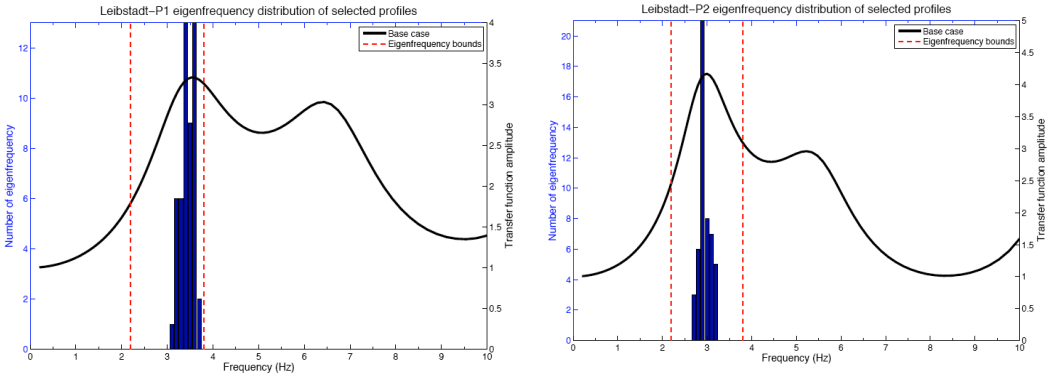

Figure II-1.49: KKL - Comparison of the distribution of fundamental frequencies of the 50 selected randomized profiles with the corresponding "uncertainty bounds" (vertical red dashed lines). (Top left: P1; bottom left: P2; (equivalent plot for P3 is unavailable)). The solid line represents the transfer function of each profile (respectively) for vertically incident S-waves. The right figure compares these S-wave transfer functions for the three profiles.

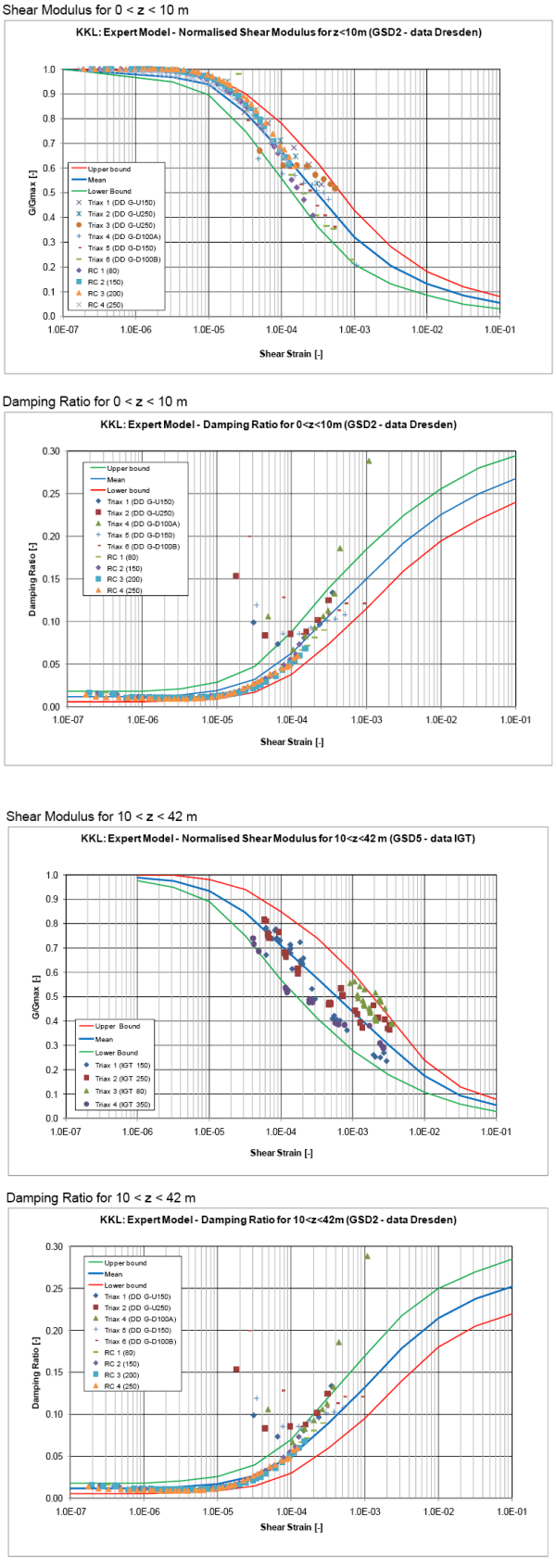

Figure II-1.50: KKL - Comparison of the selected NL curves (green : lower bound / blue: mean / red: upper bound) with the actually available data for KKB and EKKB. Top: shear modulus degradation as a function of strain / Bottom: damping increase as a function of strain. Left: shallow gravels ($z < 10m$) / Right: deep gravels ($10 < z < 42m$). There are no data for opalinuston.

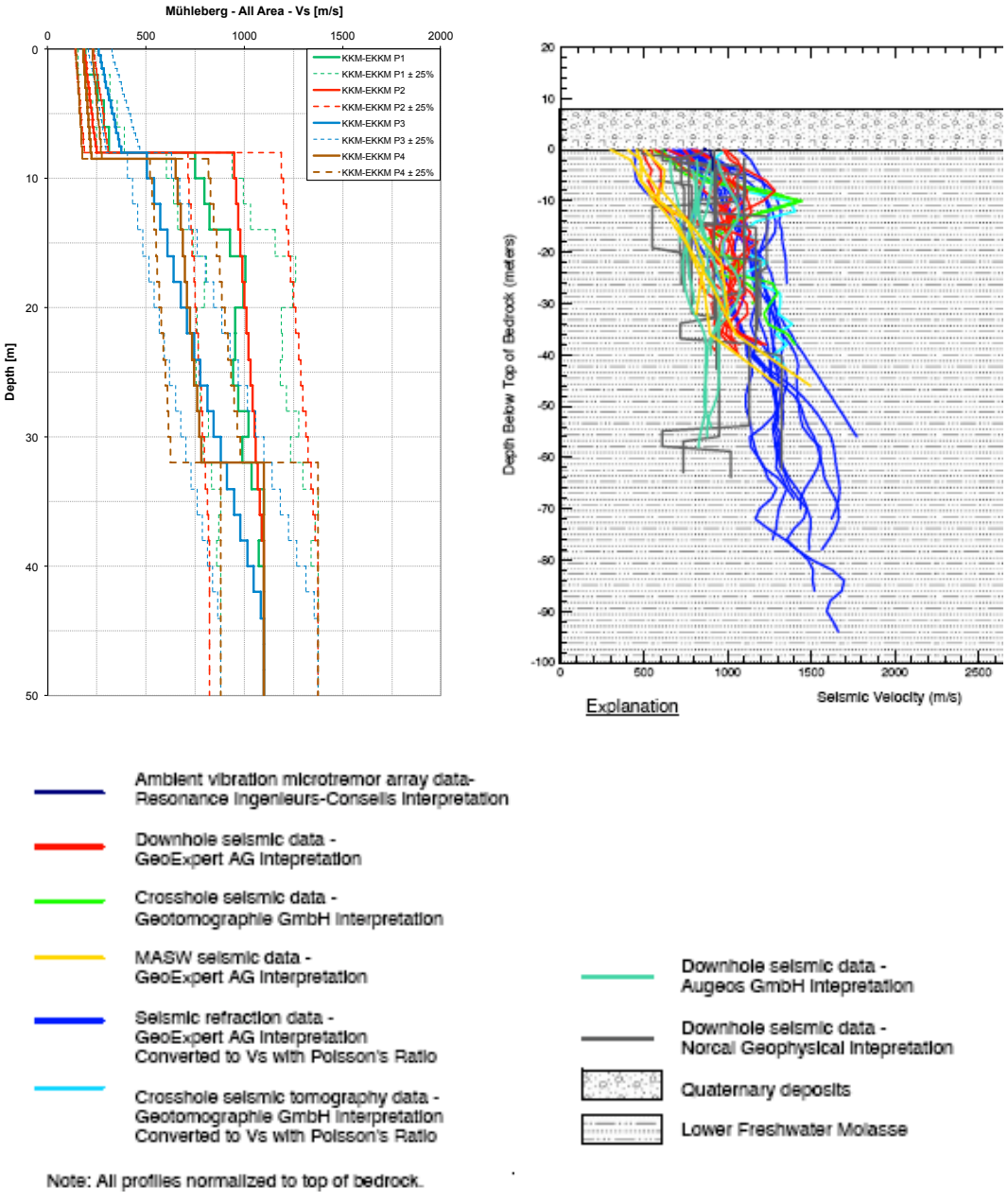

Figure II-1.51: KKM - Comparison of the four selected S-wave velocity profiles (P1 through P4) with the in-situ measurements in the underlying molasse unit.

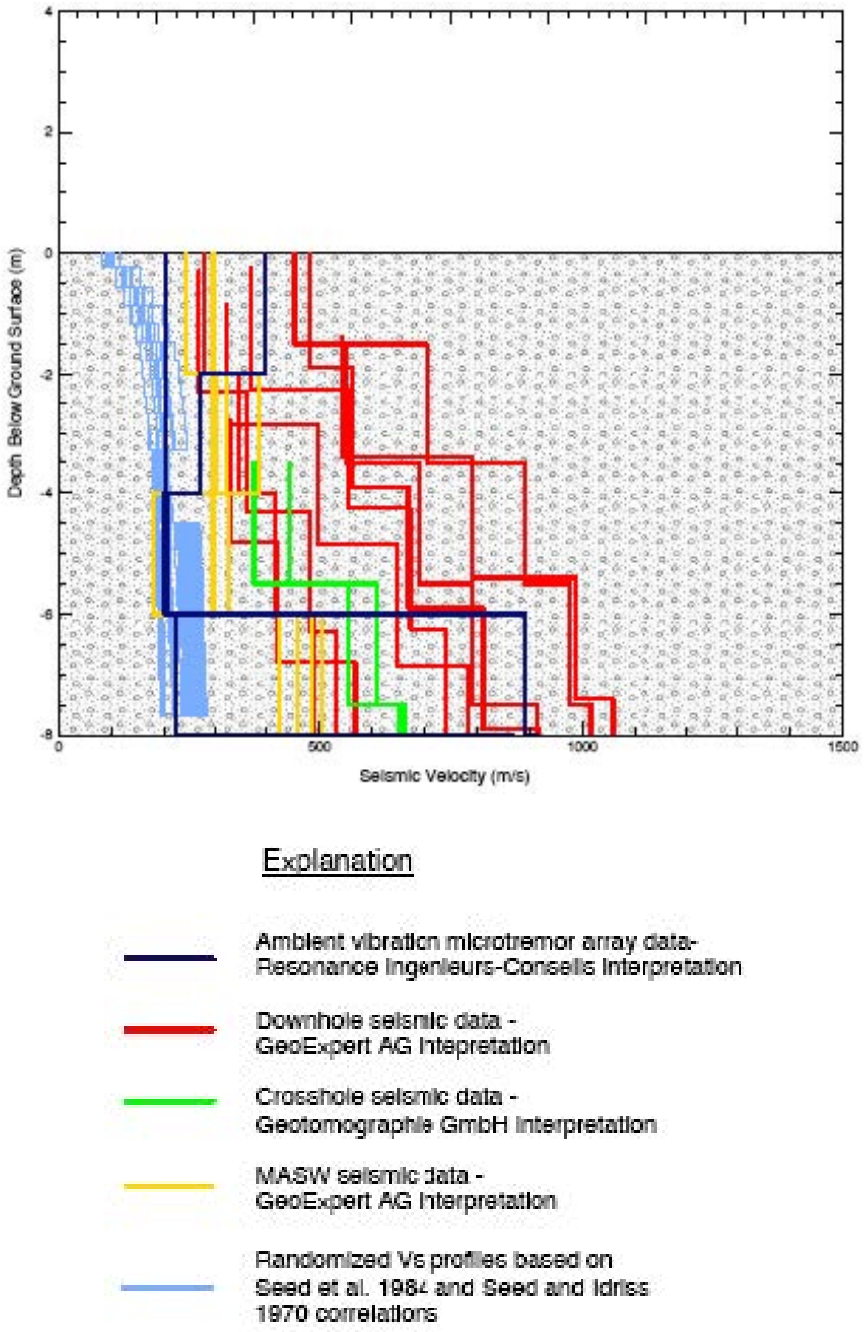

Figure II-1.52: KKM - Compilation of available in-situ measurements for the gravel layer at KKM site.

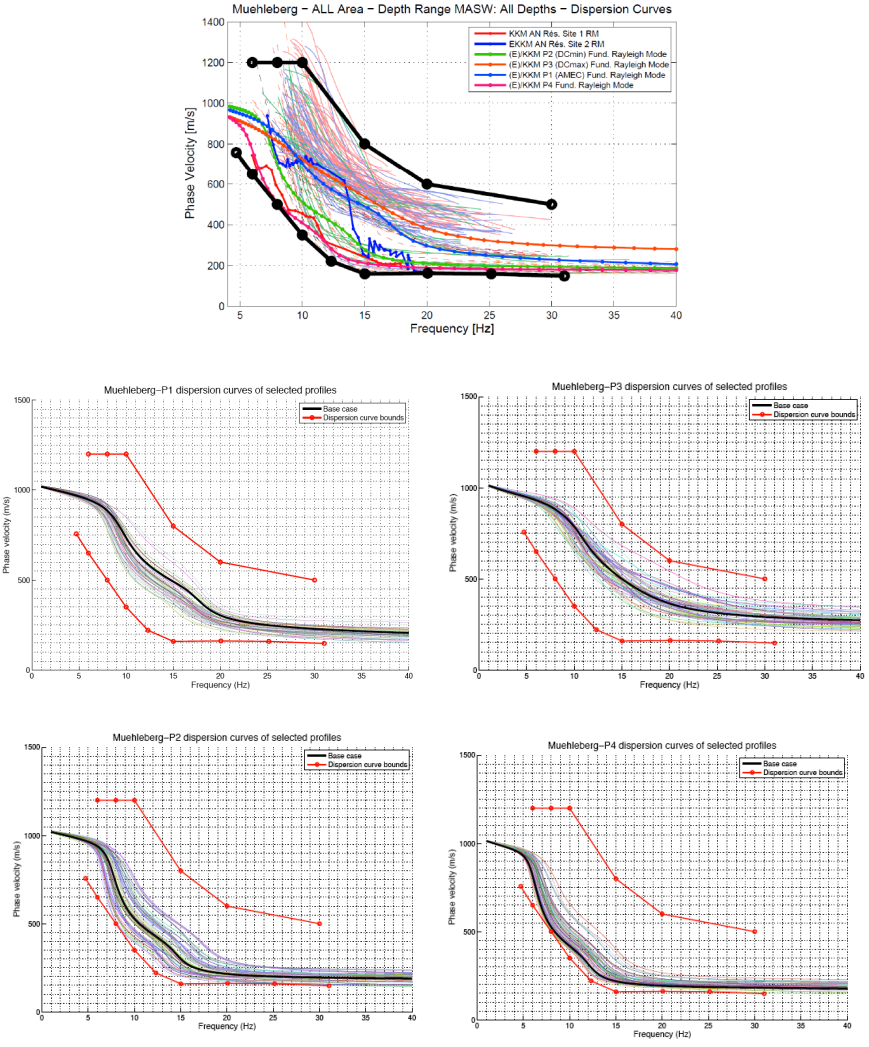

Figure II-1.53: KKM - Comparison of the dispersion curves of the 50 randomized profiles associated with the four selected velocity profiles (P1, middle left; P2, bottom left; P3, middle right; P4, bottom right) with the designed bounds for the fundamental Rayleigh mode. The top frame displays the dispersion curves actually measured with passive microtremor array techniques (thick lines) and with active MASW techniques (thin lines).

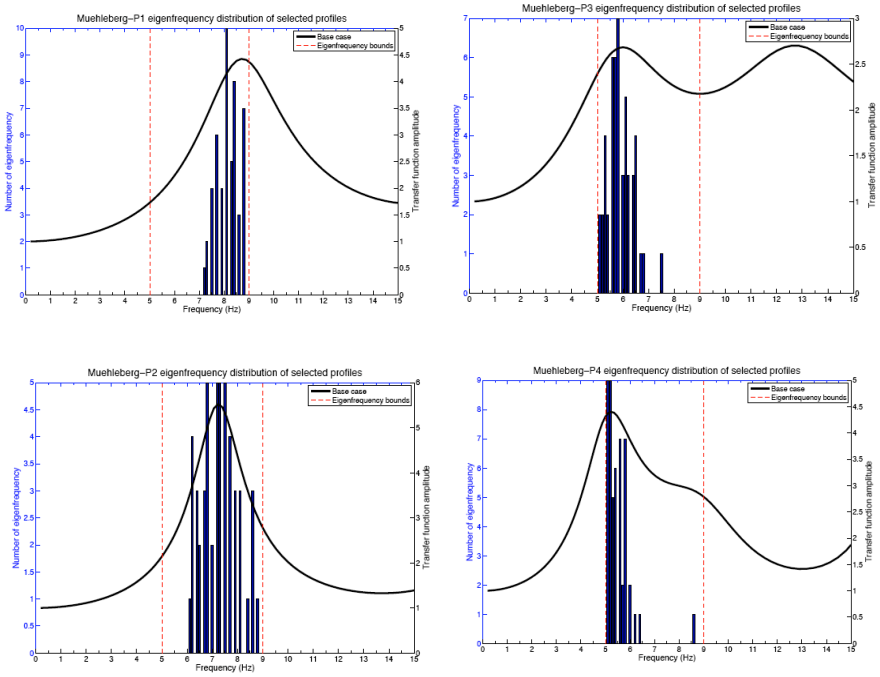

Figure II-1.54: KKM - Comparison of the distribution of fundamental frequencies of the 50 selected randomized profiles with the corresponding "uncertainty bounds" (vertical red dashed lines). (Top left: P1; bottom left: P2; top right: P3; bottom left: P4). The solid line represents the transfer function of each profile (respectively) for vertically incident S-waves.

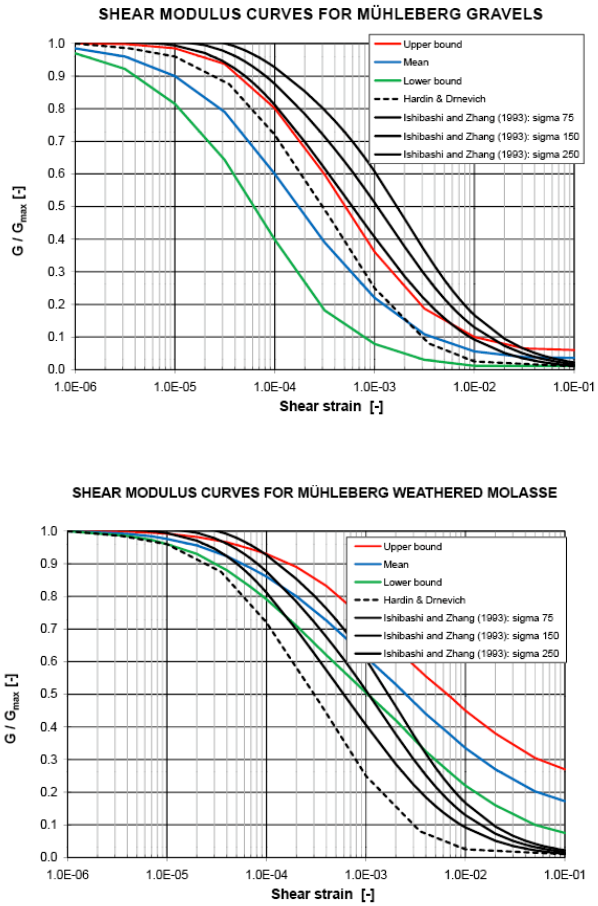

Figure II-1.55: KKM - Comparison of the selected NL curves (green : lower bound / blue : mean / red: upper bound) with other "classical" curves (Hardin Drnevich, Ishibashi & Zhang). Top: shear modulus degradation as a function of strain / Bottom: damping increase as a function of strain. Left: shallow gravels ($z < 10m$) / Right: molasse. There are no measured data for KKM site.

1.13 ANNEX A4 : Supporting documents for the quantification of aleatory variability due to non-linear site response

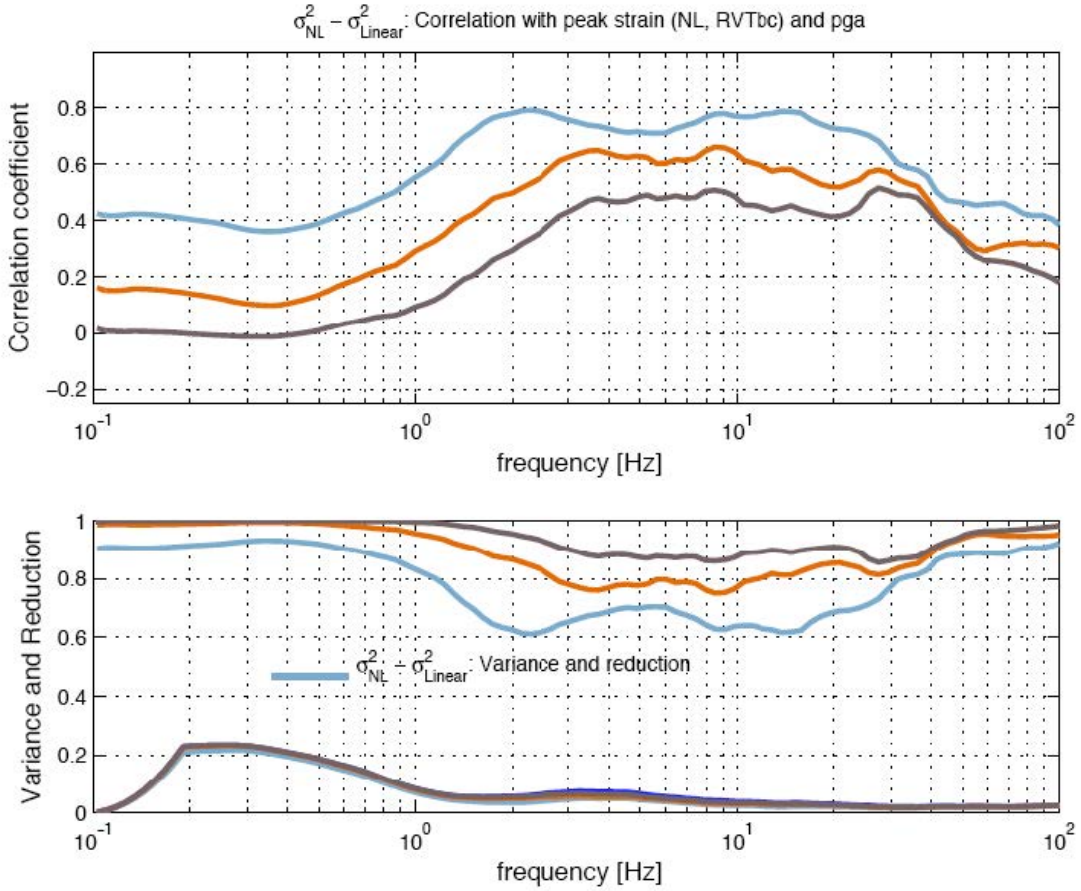

Figure II-1.56: Correlation between the increase of variability of NL amplification factors with respect to Linear amplification factors for the ground motion at surface, and various ground motion level indicators: peak strain ratio as derived from the NL computations (blue line), peak strain ratio as derived from the RVT_{bc} computations (orange line), and input PGA level (see text). Top: Correlation coefficient for each of the GM parameters, as a function of frequency from 0.1 to 100 Hz Bottom: Variance reduction derived from log linear regression analysis.

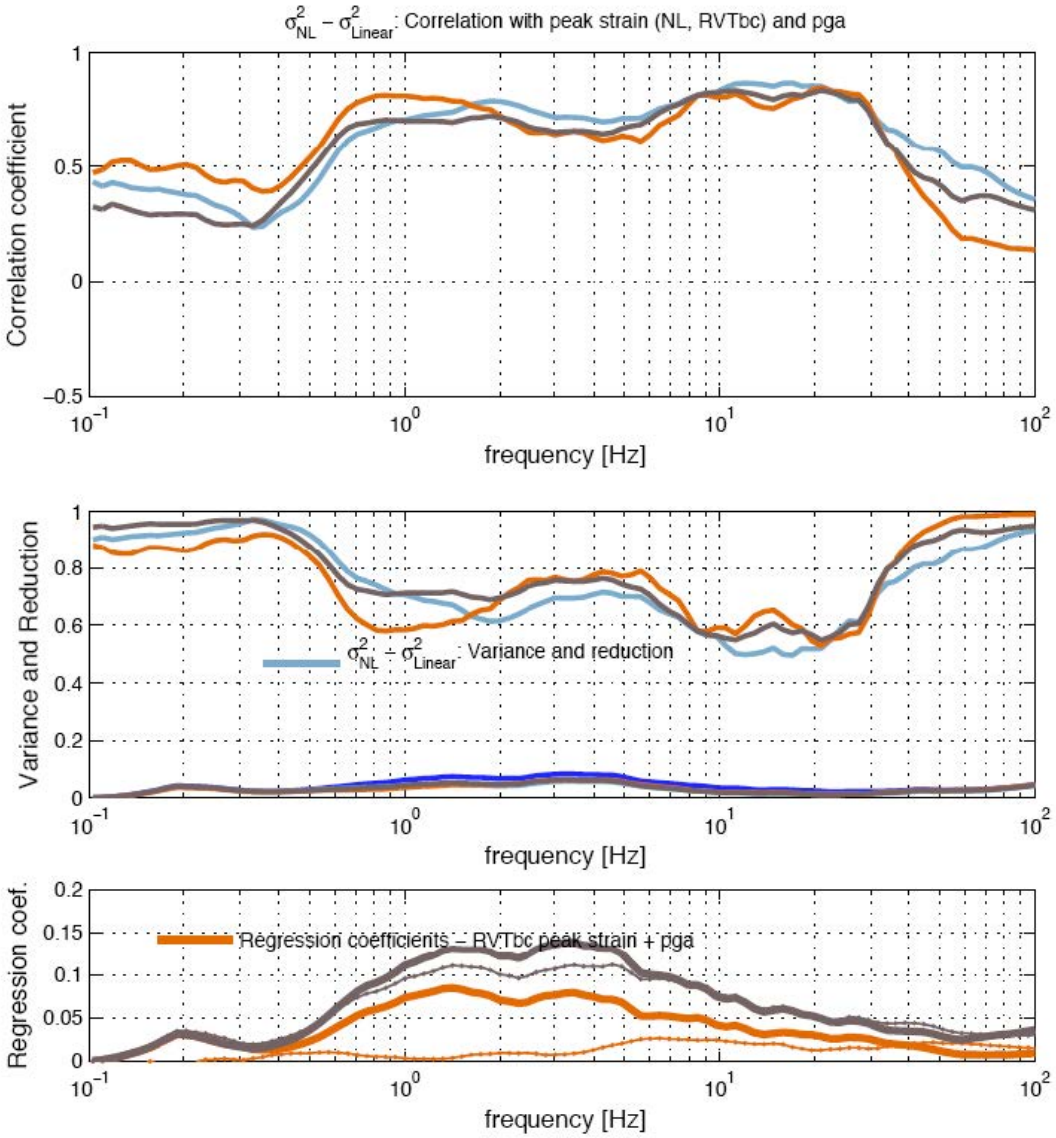

Figure II-1.57: KKB - Correlation between the increase of variability of NL amplification factors with respect to Linear amplification factors for the ground motion at surface, and various ground motion level indicators: peak strain ratio as derived from the NL computations (blue line), peak strain ratio as derived from the RVT_{bc} computations (orange line), and input PGA level (grey line). See text for further explanations. Top: Correlation coefficient for each of the GM parameters, as a function of frequency from 0.1 to 100 Hz Middle: Variance reduction derived from log linear regression analysis. Bottom: Regression coefficients (slope in thick line, constant term in thin line) for both RVT_{bc} peak strain ratio (orange) and PGA (grey).

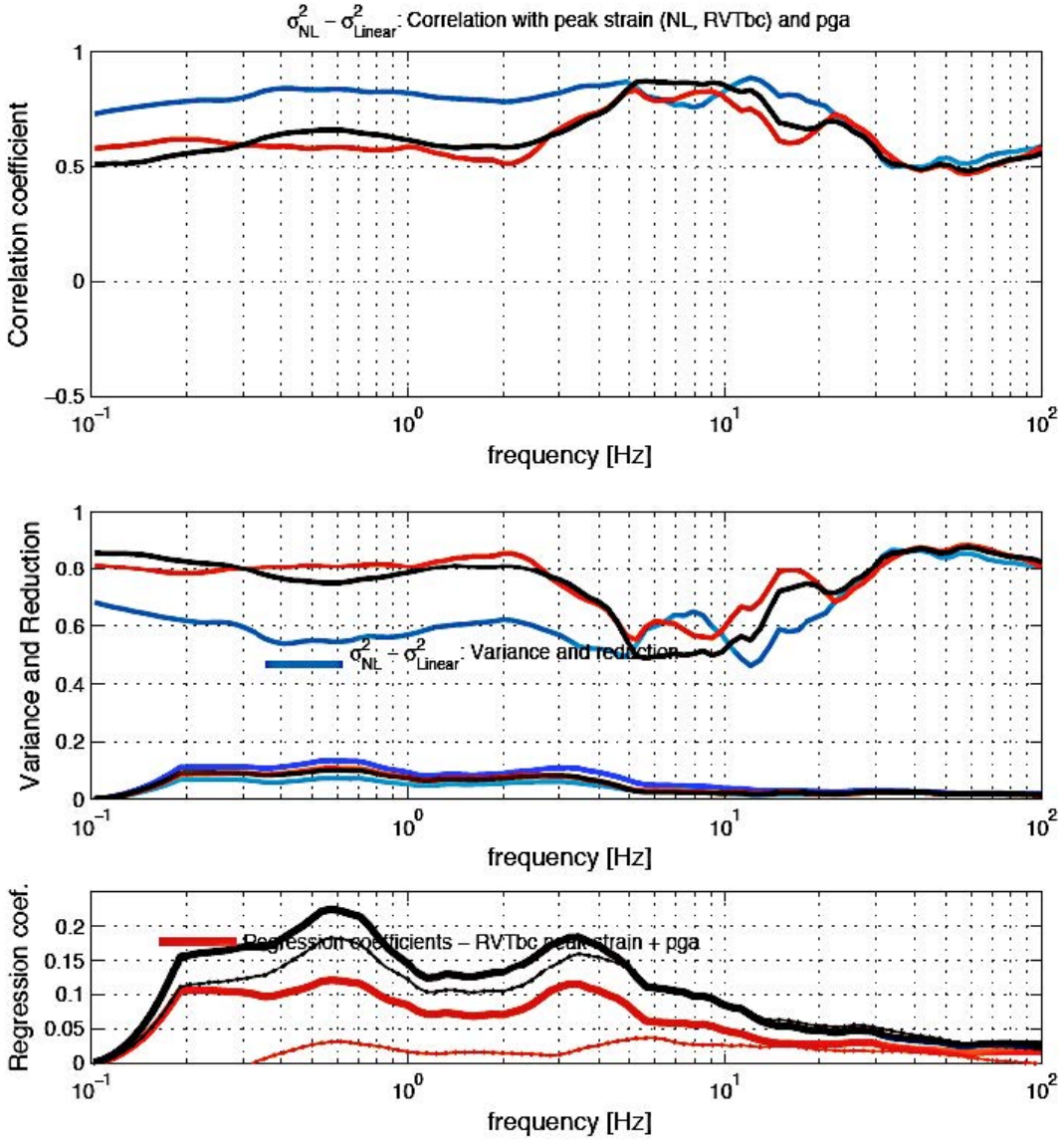

Figure II-1.58: EKKB - Correlation between the increase of variability of NL amplification factors with respect to Linear amplification factors for the ground motion at surface, and various ground motion level indicators : peak strain ratio as derived from the NL computations (blue line), peak strain ratio as derived from the RVT_{bc} computations (orange line), and input PGA level (grey line). See text for further explanations. Top: Correlation coefficient for each of the GM parameters, as a function of frequency from 0.1 to 100 Hz
Middle: Variance reduction derived from log linear regression analysis.
Bottom: Regression coefficients (slope in thick line, constant term in thin line) for both RVT_{bc} peak strain ratio (orange) and PGA (grey)
NL amplification factors with respect to Linear amplification factors
.

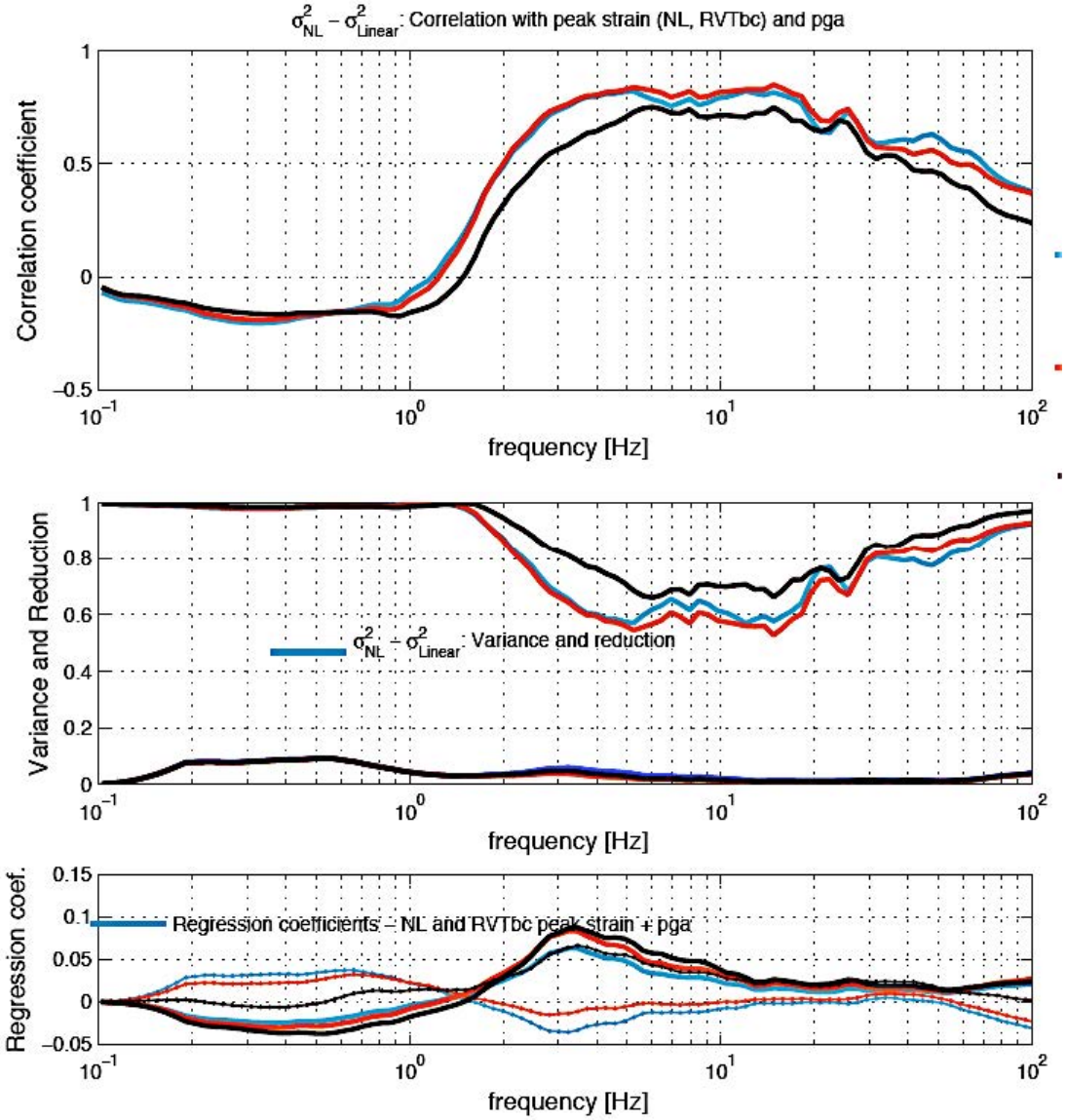

Figure II-1.59: KKG - Correlation between the increase of variability of NL amplification factors with respect to Linear amplification factors for the ground motion at surface, and various ground motion level indicators : peak strain ratio as derived from the NL computations (blue line), peak strain ratio as derived from the RVT_{bc} computations (orange line), and input PGA level (grey line). See text for further explanations. Top: Correlation coefficient for each of the GM parameters, as a function of frequency from 0.1 to 100 Hz
Middle: Variance reduction derived from log linear regression analysis.
Bottom: Regression coefficients (slope in thick line, constant term in thin line) for both RVT_{bc} peak strain ratio (orange) and PGA (grey).

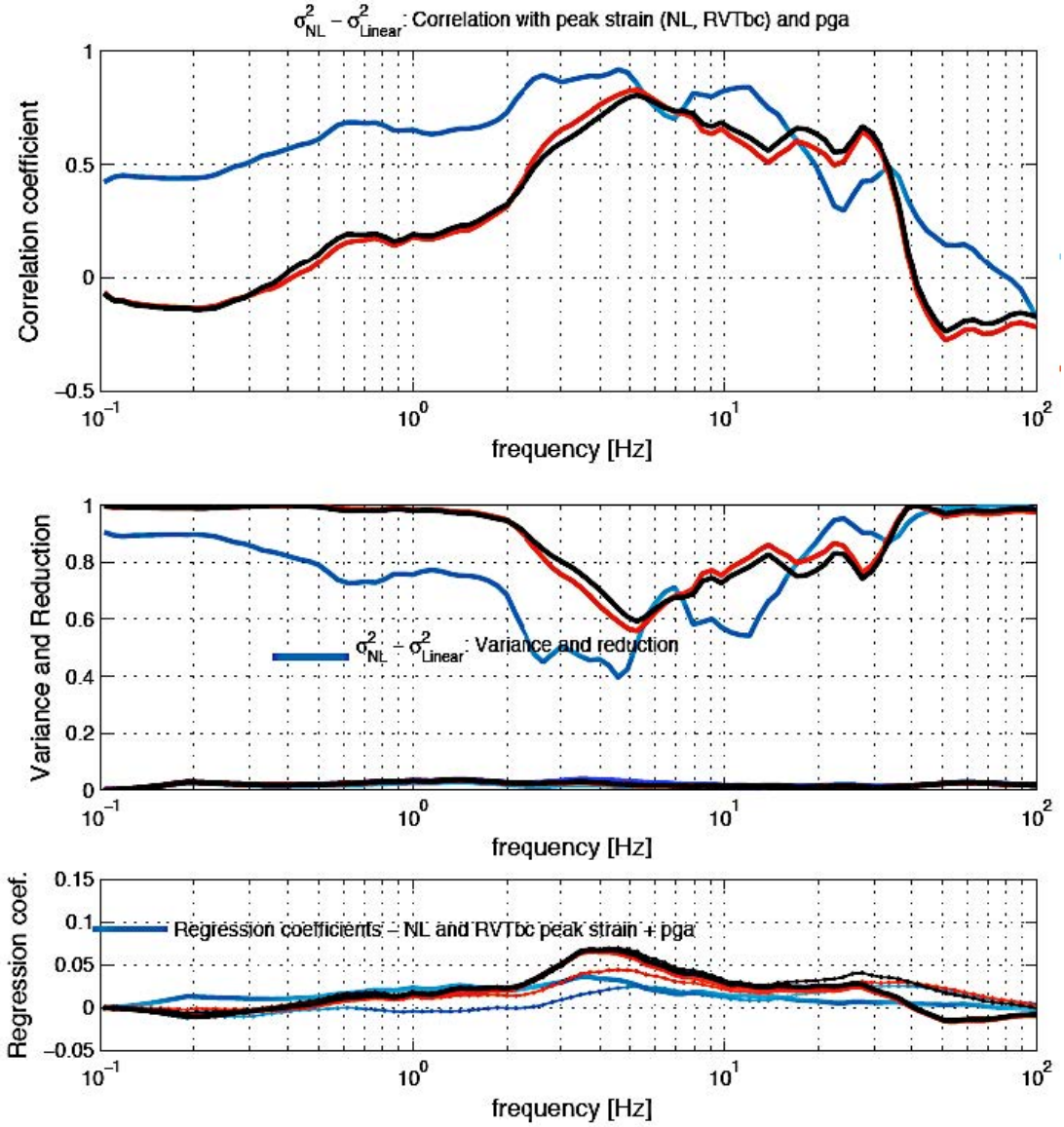

Figure II-1.60: KKL - Correlation between the increase of variability of NL amplification factors with respect to Linear amplification factors for the ground motion at surface, and various ground motion level indicators : peak strain ratio as derived from the NL computations (blue line), peak strain ratio as derived from the RVT_{bc} computations (orange line), and input PGA level (grey line). See text for further explanations. Top: Correlation coefficient for each of the GM parameters, as a function of frequency from 0.1 to 100 Hz
Middle: Variance reduction derived from log linear regression analysis.
Bottom: Regression coefficients (slope in thick line, constant term in thin line) for both RVT_{bc} peak strain ratio (orange) and PGA (grey).

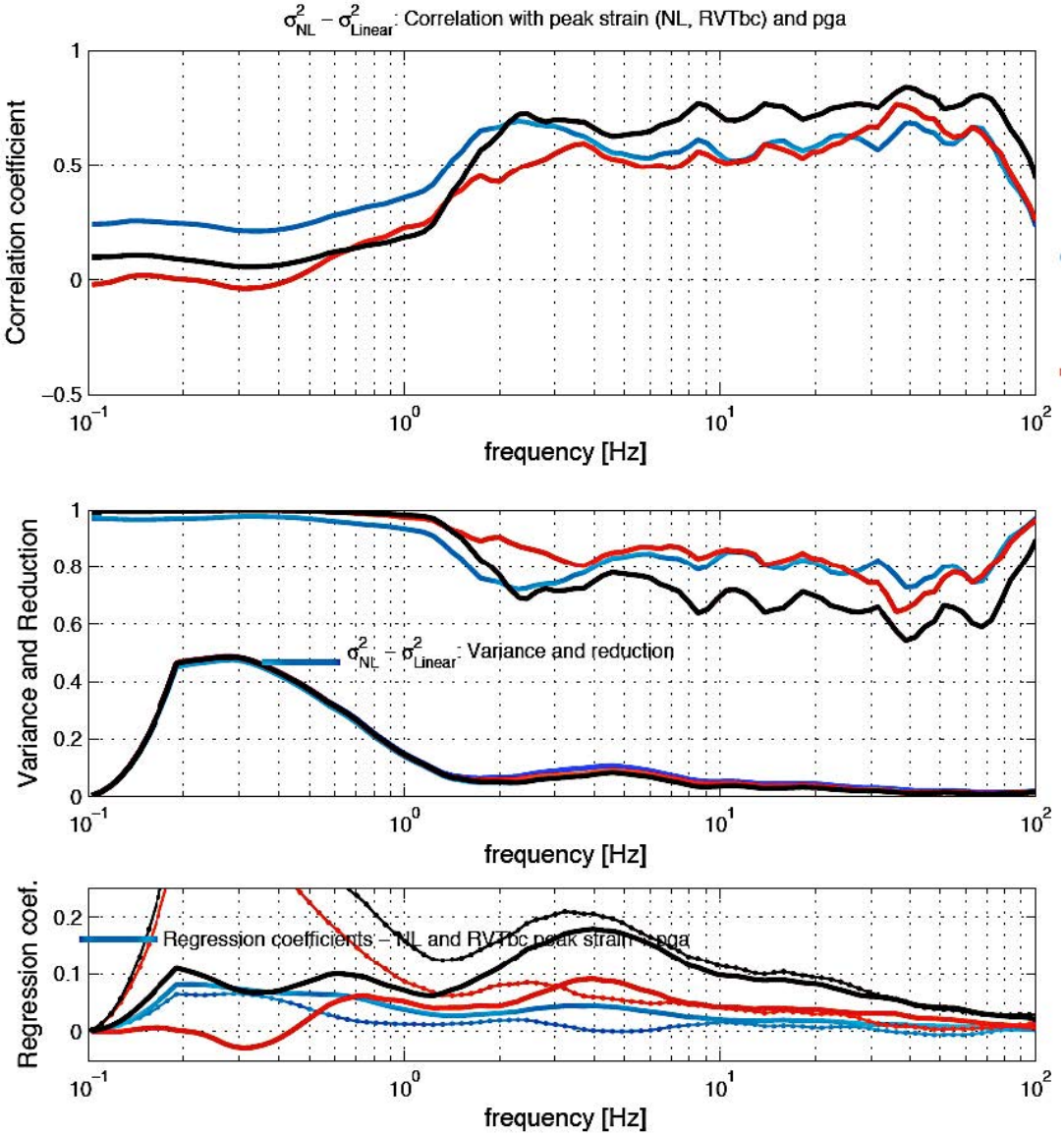

Figure II-1.61: KKM - Correlation between the increase of variability of NL amplification factors with respect to Linear amplification factors for the ground motion at surface, and various ground motion level indicators : peak strain ratio as derived from the NL computations (blue line), peak strain ratio as derived from the RVT_{bc} computations (orange line), and input PGA level (grey line). See text for further explanations. Top: Correlation coefficient for each of the GM parameters, as a function of frequency from 0.1 to 100 Hz
Middle: Variance reduction derived from log linear regression analysis.
Bottom: Regression coefficients (slope in thick line, constant term in thin line) for both RVT_{bc} peak strain ratio (orange) and PGA (grey).

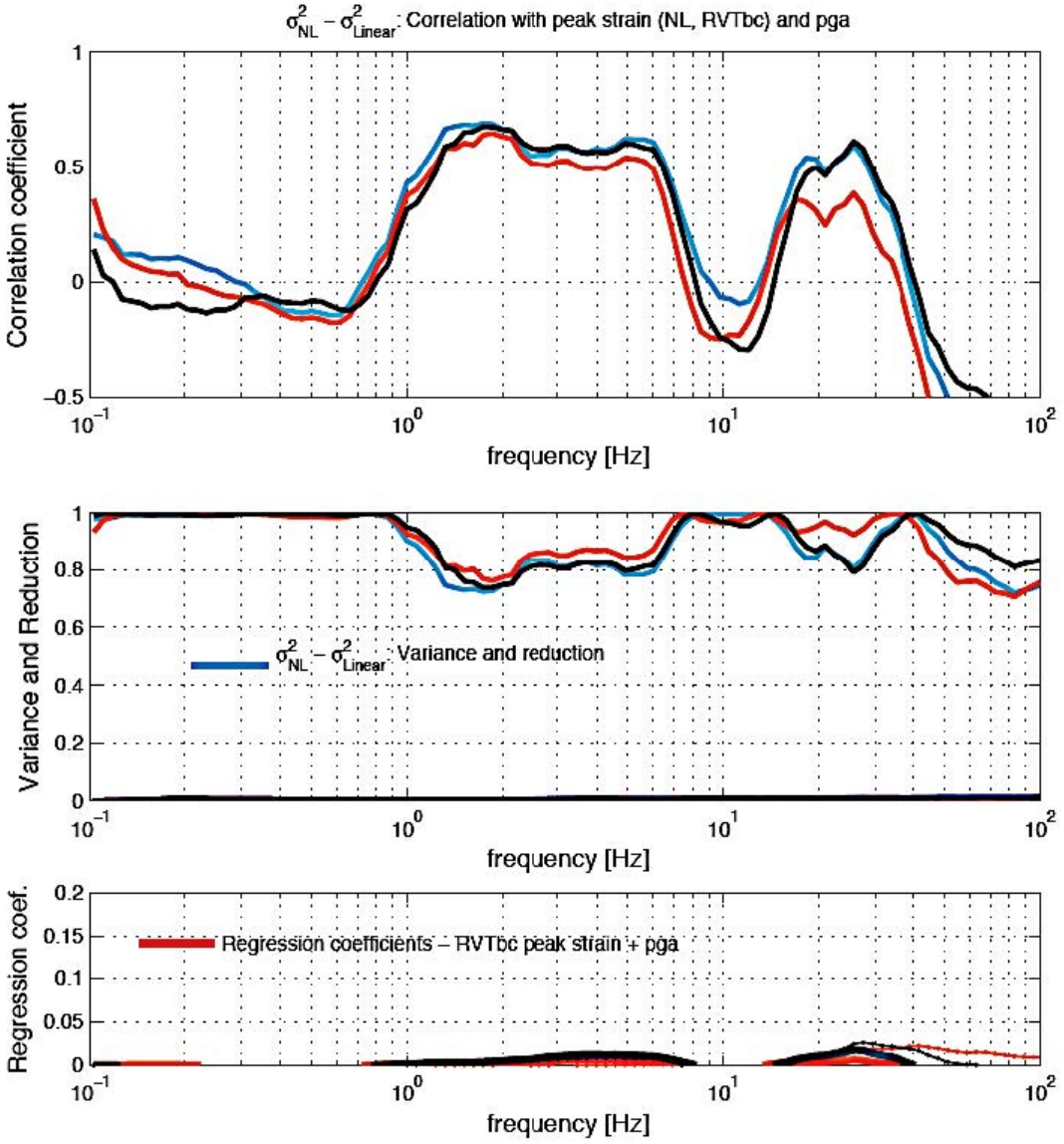

Figure II-1.62: KKB - Correlation between the increase of variability of NL amplification factors with respect to Linear amplification factors for the ground motion at depth z2, and various ground motion level indicators : peak strain ratio as derived from the NL computations (blue line), peak strain ratio as derived from the RVT_{bc} computations (orange line), and input PGA level (grey line). See text for further explanations. Top: Correlation coefficient for each of the GM parameters, as a function of frequency from 0.1 to 100 Hz
Middle: Variance reduction derived from log linear regression analysis.
Bottom: Regression coefficients (slope in thick line, constant term in thin line) for both RVT_{bc} peak strain ratio (orange) and PGA (grey).

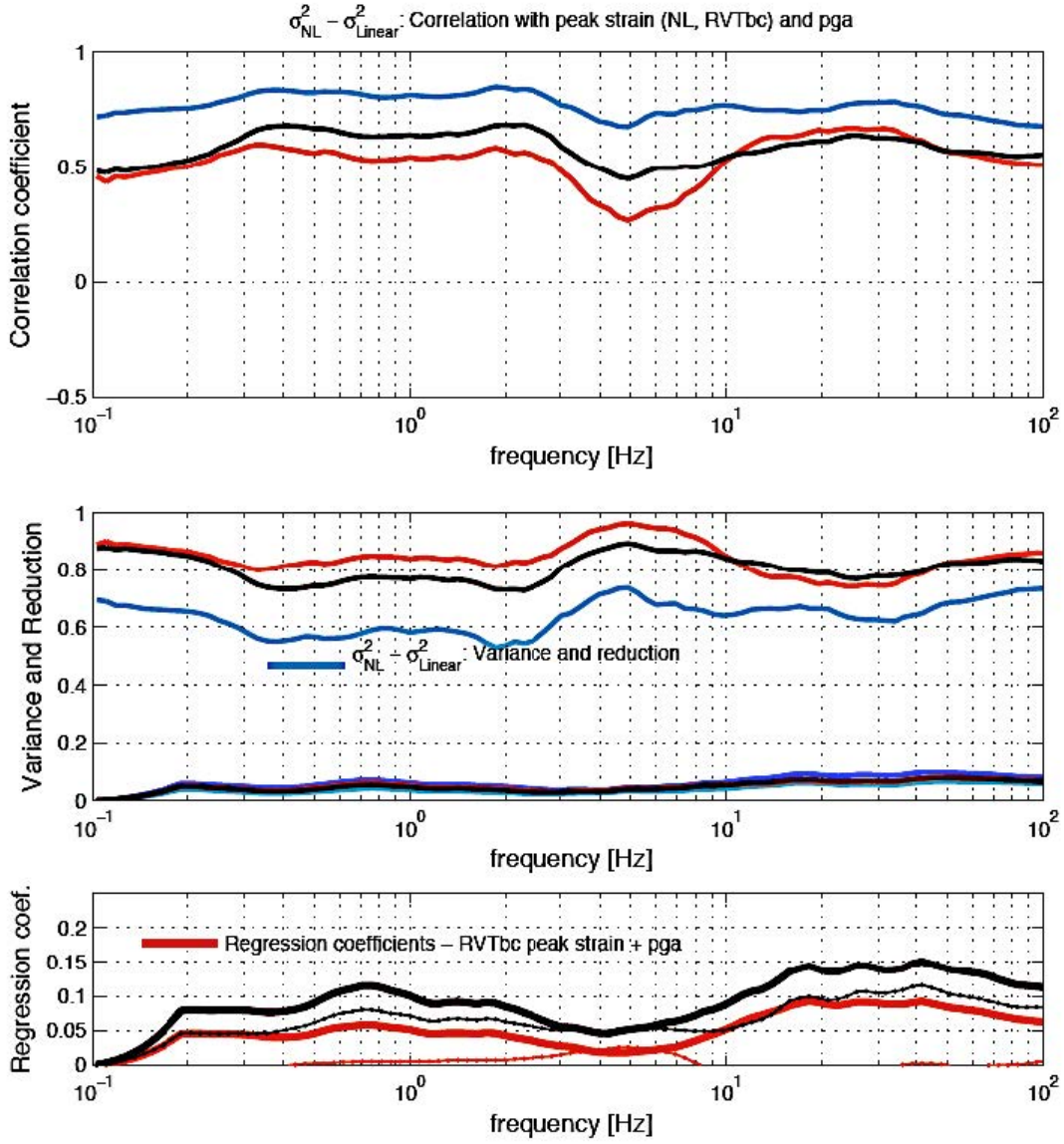

Figure II-1.63: EKKB - Correlation between the increase of variability of NL amplification factors with respect to Linear amplification factors for the ground motion at depth z2, and various ground motion level indicators : peak strain ratio as derived from the NL computations (blue line), peak strain ratio as derived from the RVT_{bc} computations (orange line), and input PGA level (grey line). See text for further explanations. Top: Correlation coefficient for each of the GM parameters, as a function of frequency from 0.1 to 100 Hz
Middle: Variance reduction derived from log linear regression analysis.
Bottom: Regression coefficients (slope in thick line, constant term in thin line) for both RVT_{bc} peak strain ratio (orange) and PGA (grey).

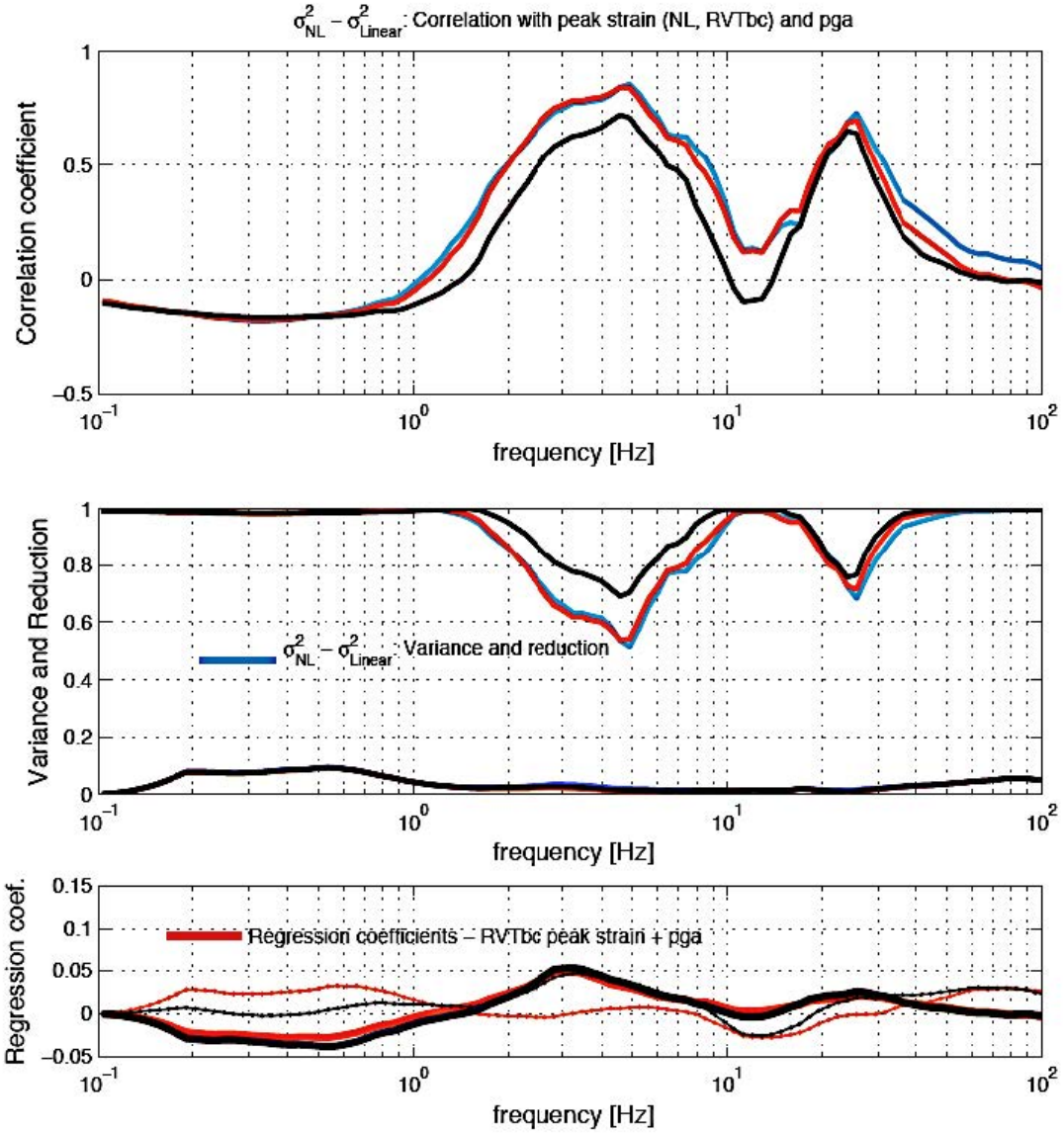

Figure II-1.64: KKG - Correlation between the increase of variability of NL amplification factors with respect to Linear amplification factors for the ground motion at depth z2, and various ground motion level indicators : peak strain ratio as derived from the NL computations (blue line), peak strain ratio as derived from the RVT_{bc} computations (orange line), and input PGA level (grey line). See text for further explanations. Top: Correlation coefficient for each of the GM parameters, as a function of frequency from 0.1 to 100 Hz
Middle: Variance reduction derived from log linear regression analysis.
Bottom: Regression coefficients (slope in thick line, constant term in thin line) for both RVT_{bc} peak strain ratio (orange) and PGA (grey).

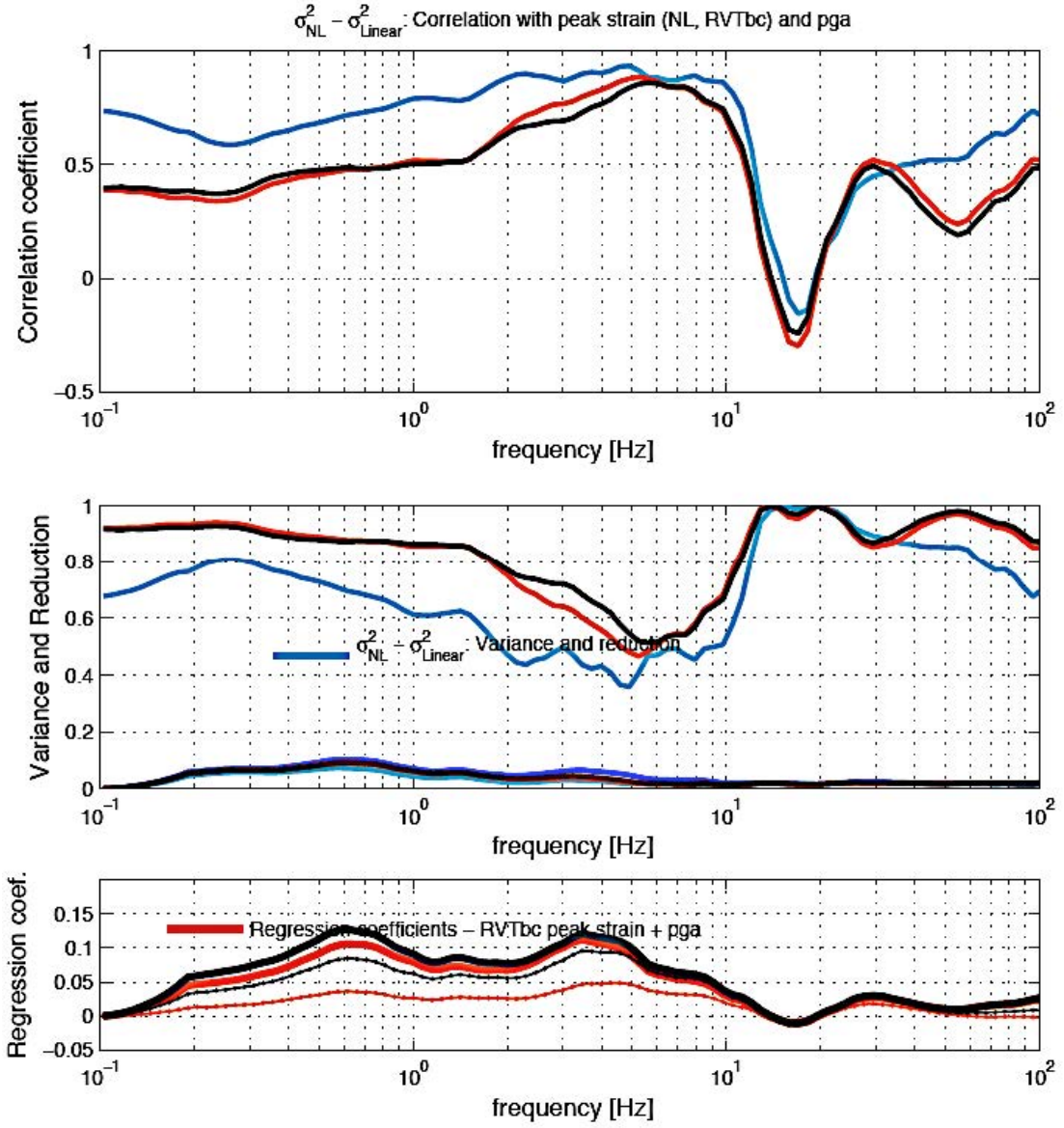

Figure II-1.65: KKL - Correlation between the increase of variability of NL amplification factors with respect to Linear amplification factors for the ground motion at depth z2, and various ground motion level indicators : peak strain ratio as derived from the NL computations (blue line), peak strain ratio as derived from the RVT_{bc} computations (orange line), and input PGA level (grey line). See text for further explanations. Top: Correlation coefficient for each of the GM parameters, as a function of frequency from 0.1 to 100 Hz
Middle: Variance reduction derived from log linear regression analysis.
Bottom: Regression coefficients (slope in thick line, constant term in thin line) for both RVT_{bc} peak strain ratio (orange) and PGA (grey).

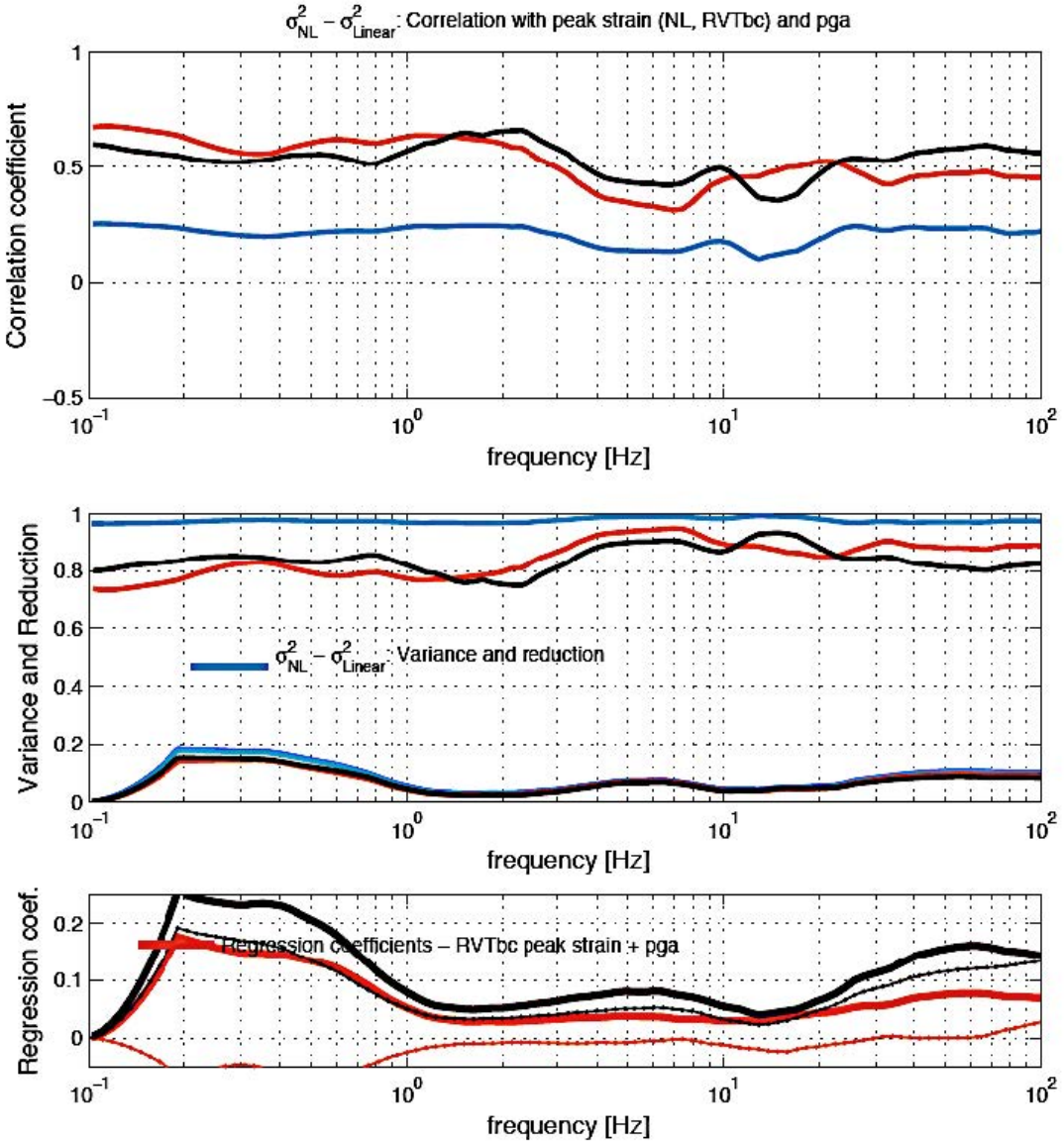

Figure II-1.66: KKM - Correlation between the increase of variability of NL amplification factors with respect to Linear amplification factors for the ground motion at depth z2, and various ground motion level indicators : peak strain ratio as derived from the NL computations (blue line), peak strain ratio as derived from the RVT_{bc} computations (orange line), and input PGA level (grey line). See text for further explanations. Top: Correlation coefficient for each of the GM parameters, as a function of frequency from 0.1 to 100 Hz
Middle: Variance reduction derived from log linear regression analysis.
Bottom: Regression coefficients (slope in thick line, constant term in thin line) for both RVT_{bc} peak strain ratio (orange) and PGA (grey).

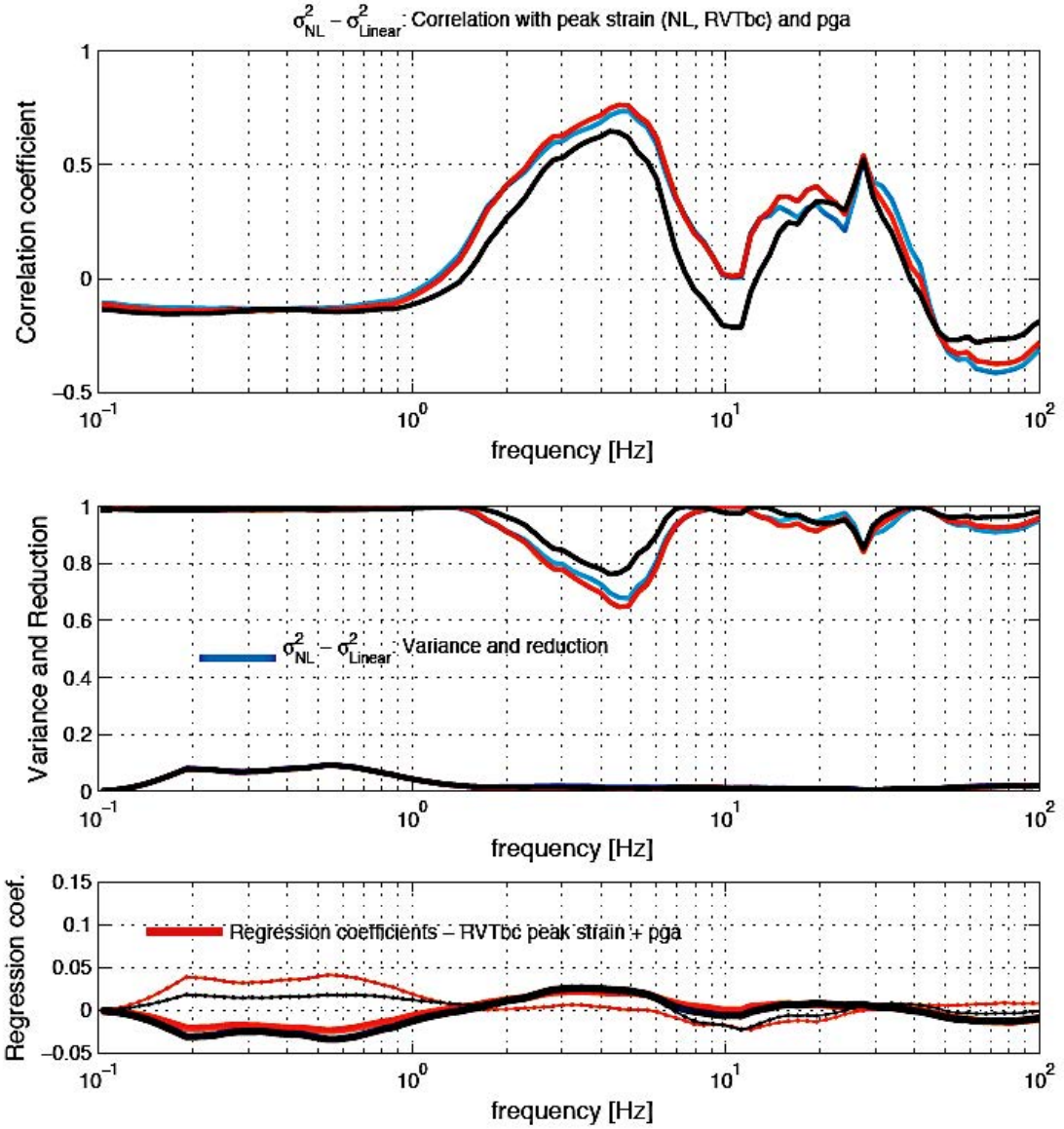

Figure II-1.67: KKG - Correlation between the increase of variability of NL amplification factors with respect to Linear amplification factors for the ground motion at depth z3, and various ground motion level indicators : peak strain ratio as derived from the NL computations (blue line), peak strain ratio as derived from the RVT_{bc} computations (orange line), and input PGA level (grey line). See text for further explanations. Top: Correlation coefficient for each of the GM parameters, as a function of frequency from 0.1 to 100 Hz
Middle: Variance reduction derived from log linear regression analysis.
Bottom: Regression coefficients (slope in thick line, constant term in thin line) for both RVT_{bc} peak strain ratio (orange) and PGA (grey).

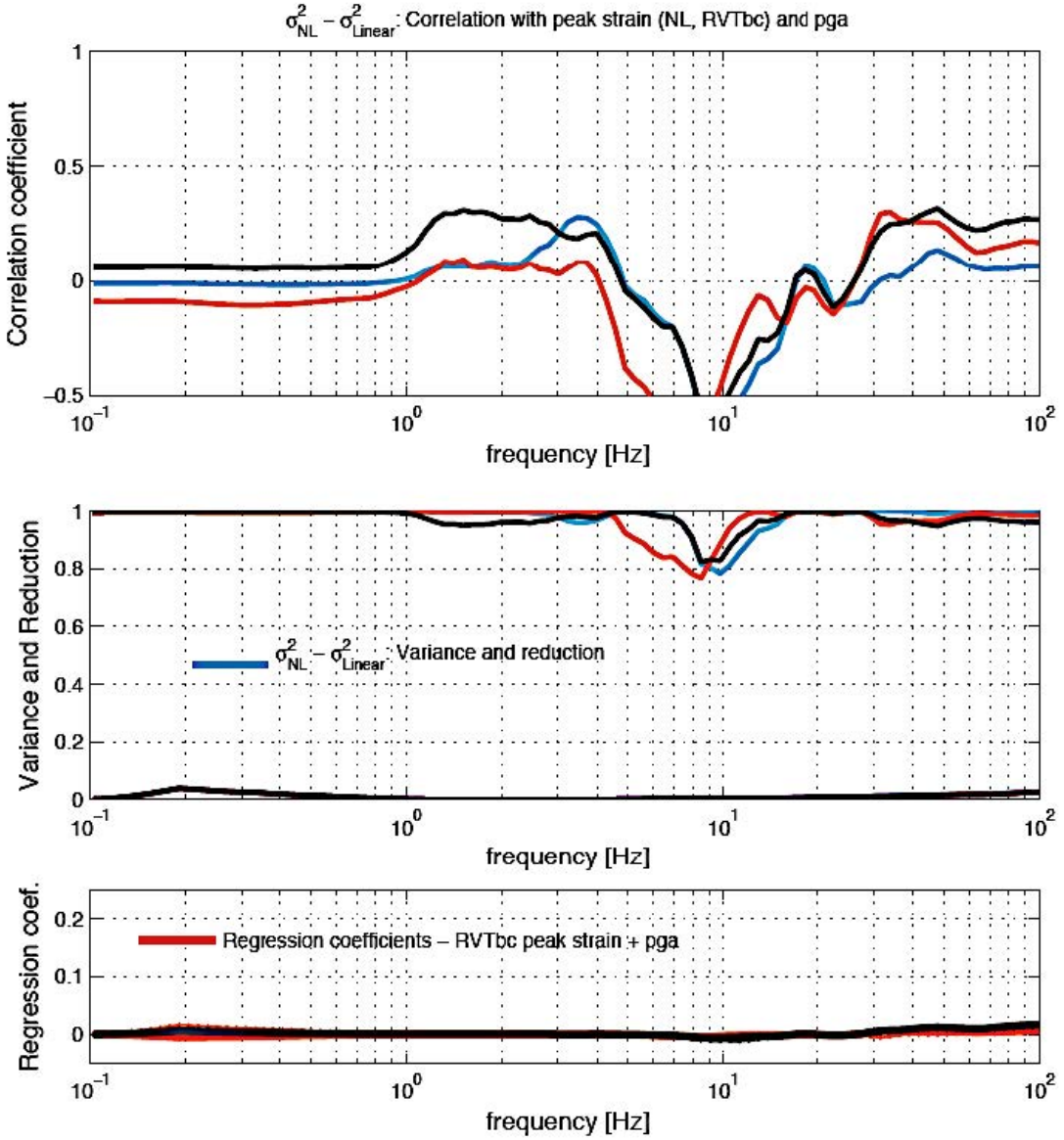

Figure II-1.68: KKM - Correlation between the increase of variability of NL amplification factors with respect to Linear amplification factors for the ground motion at depth z3, and various ground motion level indicators : peak strain ratio as derived from the NL computations (blue line), peak strain ratio as derived from the RVT_{bc} computations (orange line), and input PGA level (grey line). See text for further explanations. Top: Correlation coefficient for each of the GM parameters, as a function of frequency from 0.1 to 100 Hz
Middle: Variance reduction derived from log linear regression analysis.
Bottom: Regression coefficients (slope in thick line, constant term in thin line) for both RVT_{bc} peak strain ratio (orange) and PGA (grey).

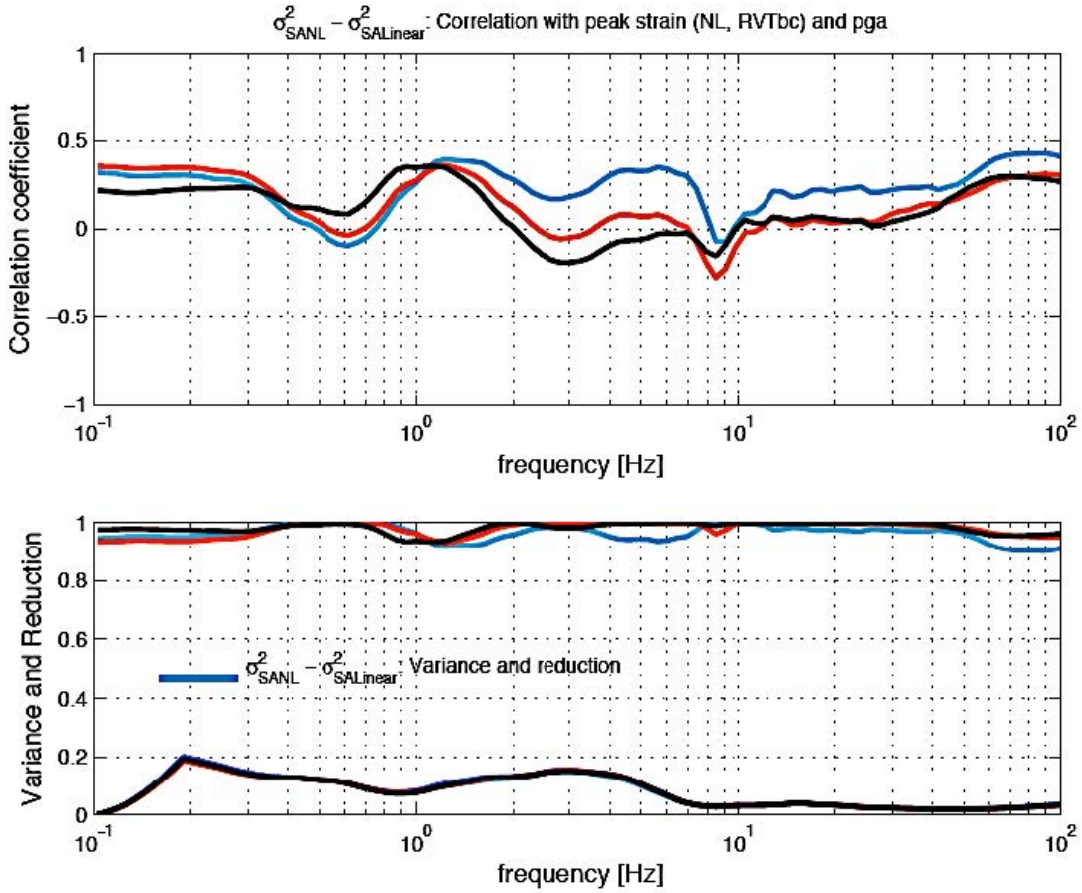

Figure II-1.69: Correlation between the increase (or decrease) of variability of NL response spectra with respect to Linear response spectra, and various ground motion level indicators : peak strain ratio as derived from the NL computations (blue line), peak strain ratio as derived from the RVT_{bc} computations (orange line), and input PGA level (see text). Top: Correlation coefficient for each of the GM parameters, as a function of frequency from 0.1 to 100 Hz
Bottom: Variance reduction derived from log linear regression analysis.

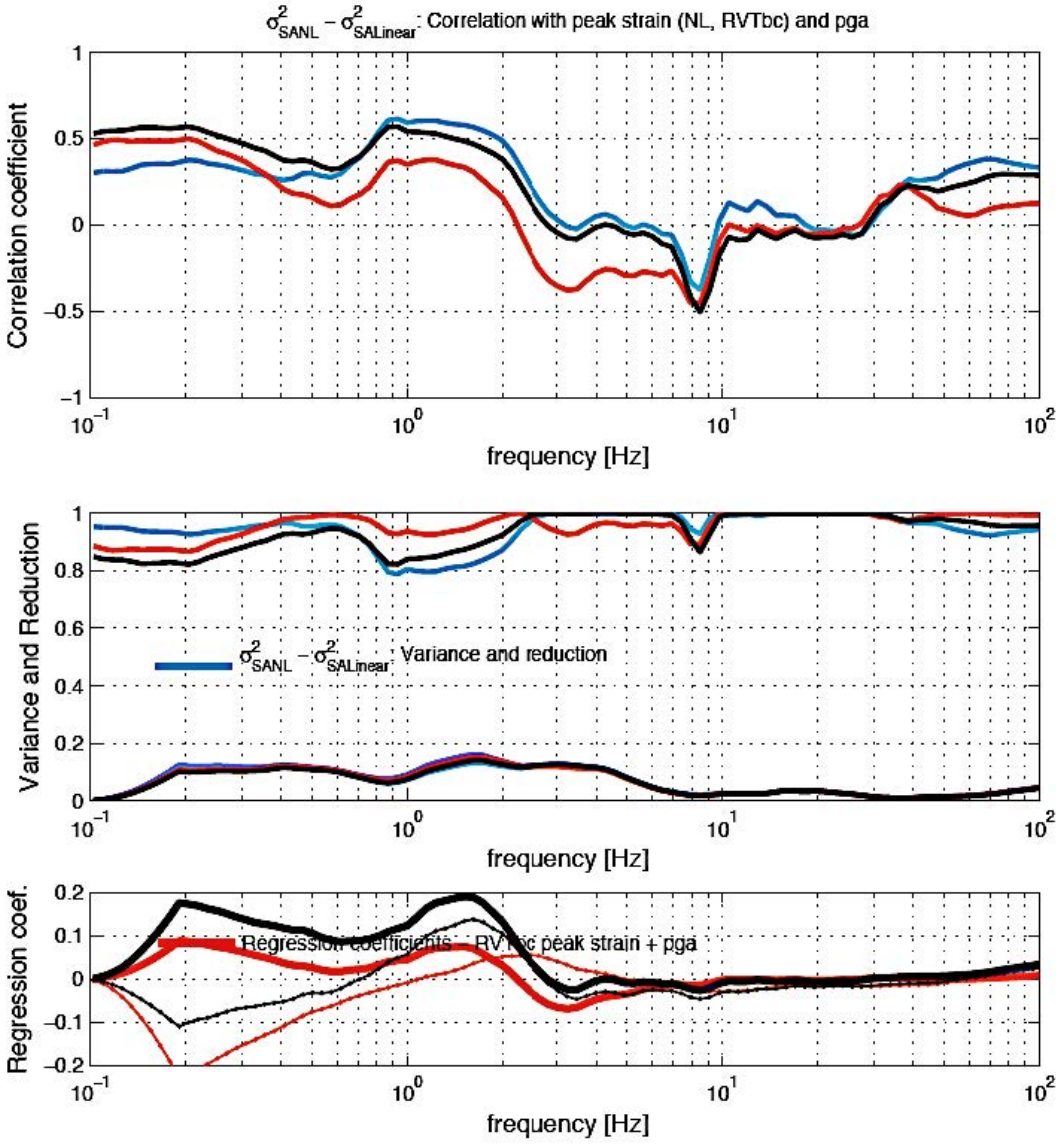

Figure II-1.70: KKB - Correlation between the increase (or decrease) of variability of NL response spectra with respect to Linear response spectra, and various ground motion level indicators : peak strain ratio as derived from the NL computations (blue line), peak strain ratio as derived from the RVT_{bc} computations (orange line), and input PGA level (grey line). See text for further explanations. Top: Correlation coefficient for each of the GM parameters, as a function of frequency from 0.1 to 100 Hz
Middle: Variance reduction derived from log linear regression analysis.
Bottom: Regression coefficients (slope in thick line, constant term in thin line) for both RVT_{bc} peak strain ratio (orange) and PGA (grey).

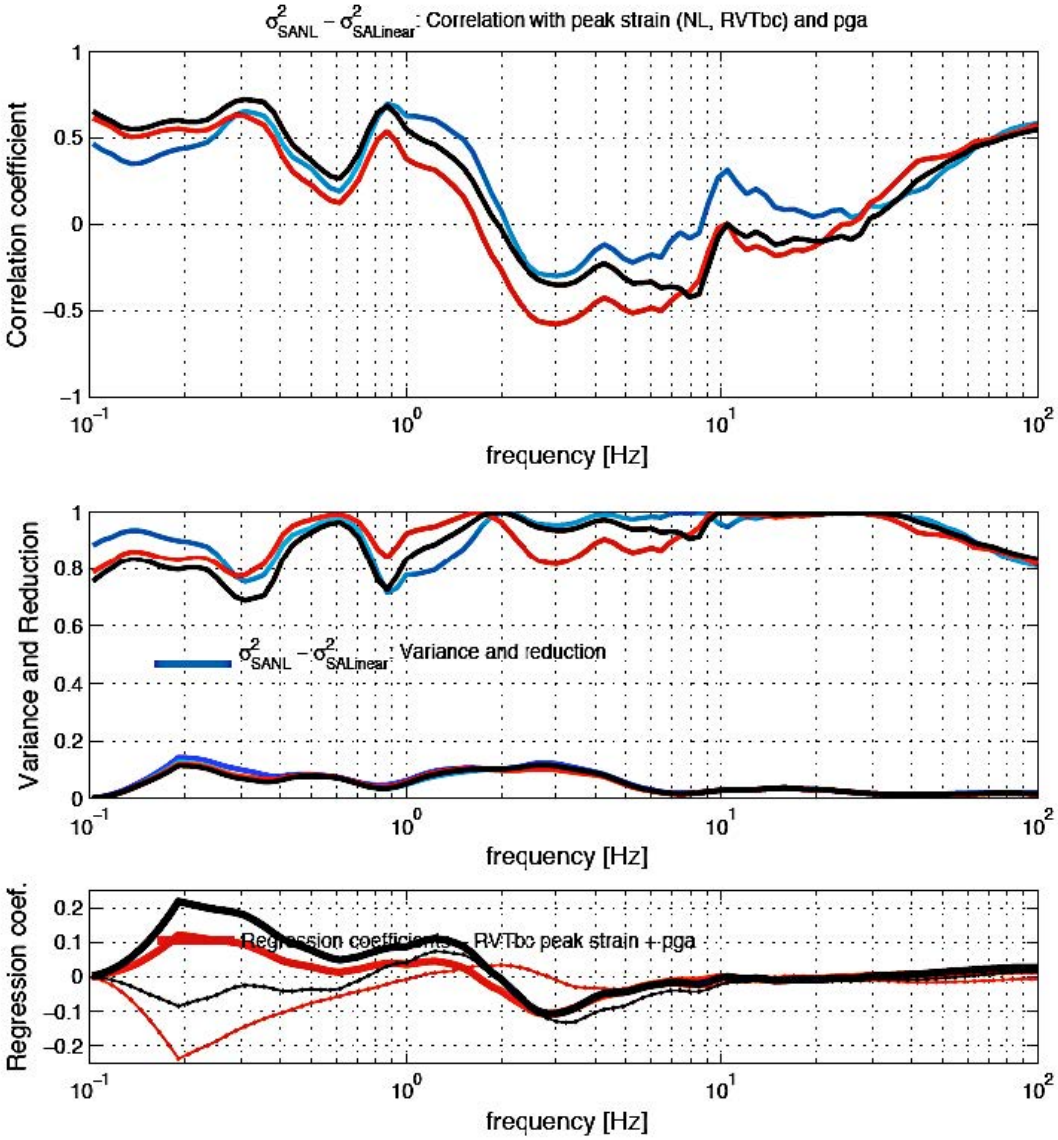

Figure II-1.71: EKKB - Correlation between the increase (or decrease) of variability of NL response spectra with respect to Linear response spectra, and various ground motion level indicators : peak strain ratio as derived from the NL computations (blue line), peak strain ratio as derived from the RVT_{bc} computations (orange line), and input PGA level (grey line). See text for further explanations. Top: Correlation coefficient for each of the GM parameters, as a function of frequency from 0.1 to 100 Hz
Middle: Variance reduction derived from log linear regression analysis.
Bottom: Regression coefficients (slope in thick line, constant term in thin line) for both RVT_{bc} peak strain ratio (orange) and PGA (grey).

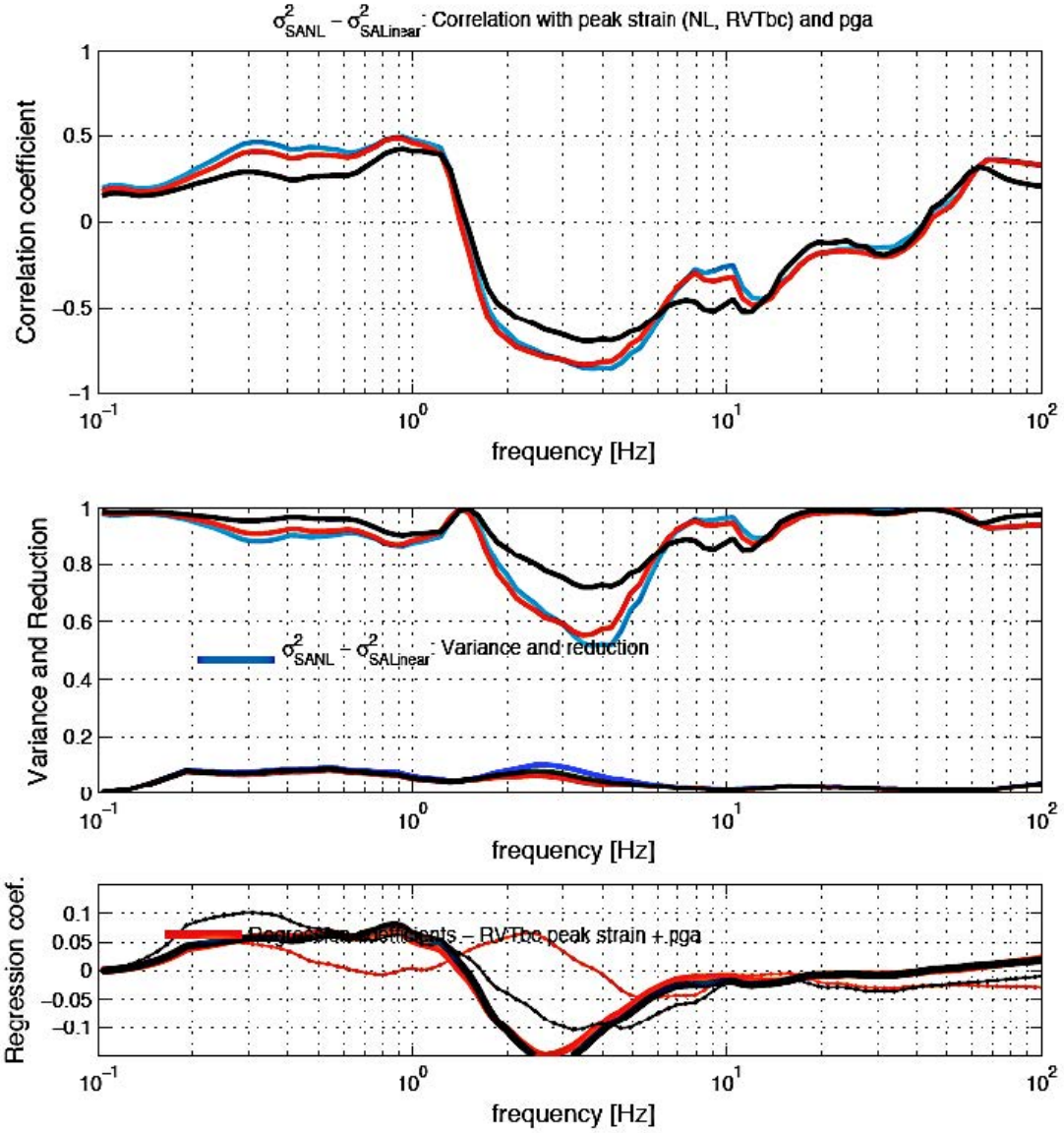

Figure II-1.72: KKG - Correlation between the increase(or decrease) of variability of NL response spectra with respect to Linear response spectra, and various ground motion level indicators : peak strain ratio as derived from the NL computations (blue line), peak strain ratio as derived from the RVT_{bc} computations (orange line), and input PGA level (grey line). See text for further explanations. Top: Correlation coefficient for each of the GM parameters, as a function of frequency from 0.1 to 100 Hz
Middle: Variance reduction derived from log linear regression analysis.
Bottom: Regression coefficients (slope in thick line, constant term in thin line) for both RVT_{bc} peak strain ratio (orange) and PGA (grey).

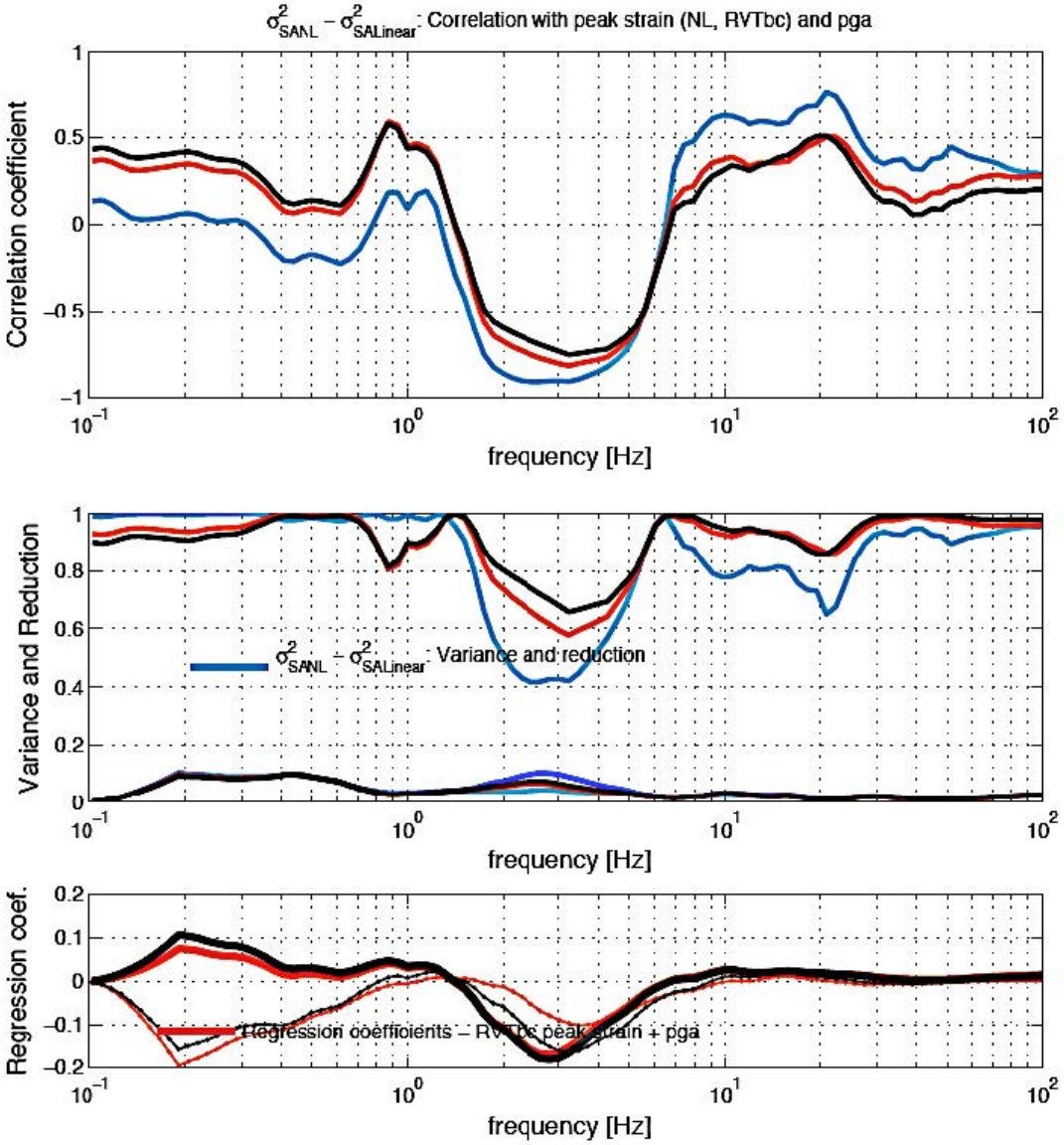

Figure II-1.73: KKL - Correlation between the increase(or decrease) of variability of NL response spectra with respect to Linear response spectra, and various ground motion level indicators : peak strain ratio as derived from the NL computations (blue line), peak strain ratio as derived from the RVT_{bc} computations (orange line), and input PGA level (grey line). See text for further explanations. Top: Correlation coefficient for each of the GM parameters, as a function of frequency from 0.1 to 100 Hz
Middle: Variance reduction derived from log linear regression analysis.
Bottom: Regression coefficients (slope in thick line, constant term in thin line) for both RVT_{bc} peak strain ratio (orange) and PGA (grey).

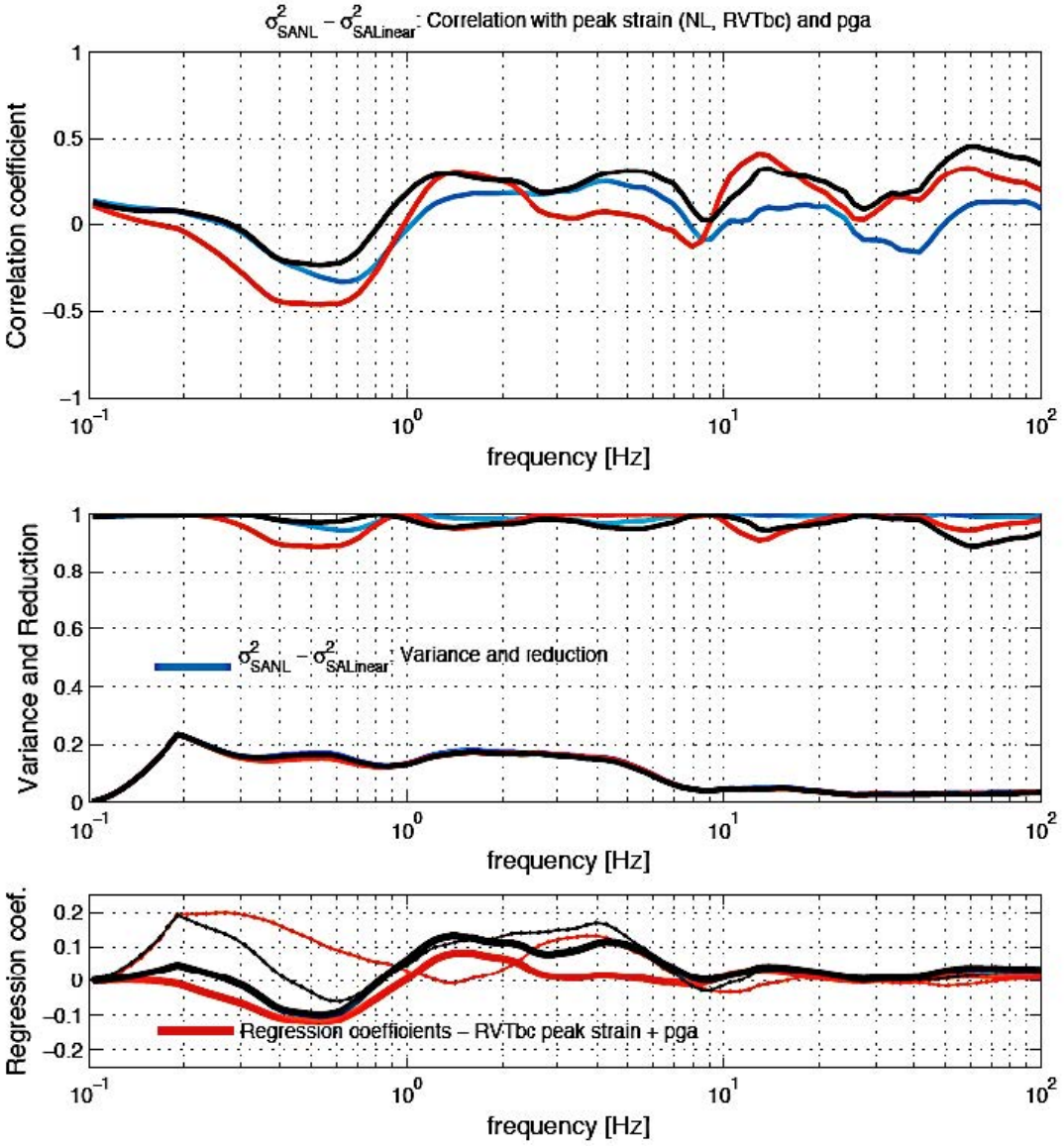

Figure II-1.74: KKM - Correlation between the increase(or decrease) of variability of NL response spectra with respect to Linear response spectra, and various ground motion level indicators : peak strain ratio as derived from the NL computations (blue line), peak strain ratio as derived from the RVT_{bc} computations (orange line), and input PGA level (grey line). See text for further explanations. Top: Correlation coefficient for each of the GM parameters, as a function of frequency from 0.1 to 100 Hz
Middle: Variance reduction derived from log linear regression analysis.
Bottom: Regression coefficients (slope in thick line, constant term in thin line) for both RVT_{bc} peak strain ratio (orange) and PGA (grey).

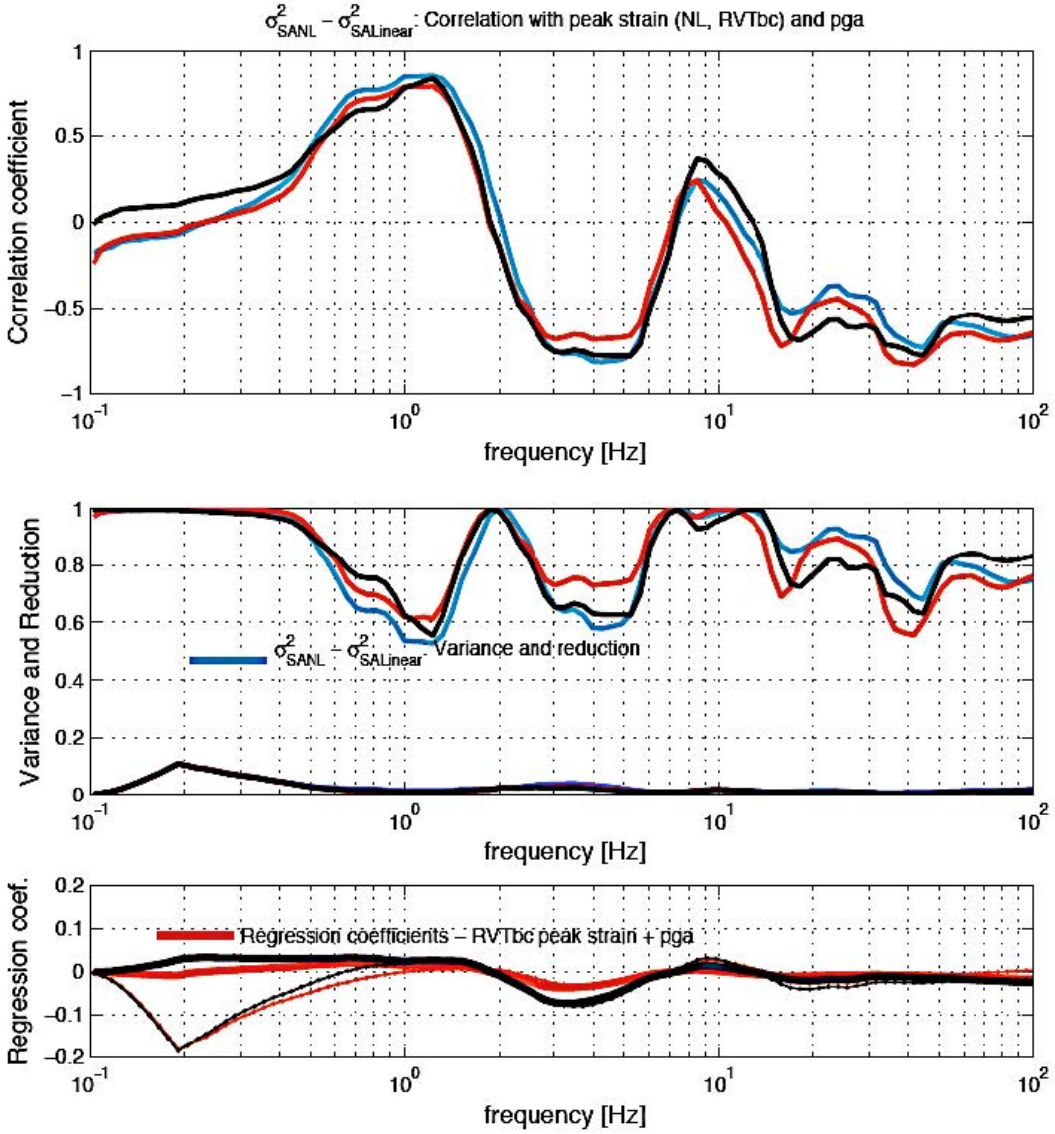

Figure II-1.75: KKB - Correlation between the increase (or decrease) of variability of NL response spectra with respect to Linear response spectra for the ground motion at depth z2, and various ground motion level indicators : peak strain ratio as derived from the NL computations (blue line), peak strain ratio as derived from the RVT_{bc} computations (orange line), and input PGA level (grey line). See text for further explanations. Top: Correlation coefficient for each of the GM parameters, as a function of frequency from 0.1 to 100 Hz
Middle: Variance reduction derived from log linear regression analysis.
Bottom: Regression coefficients (slope in thick line, constant term in thin line) for both RVT_{bc} peak strain ratio (orange) and PGA (grey).

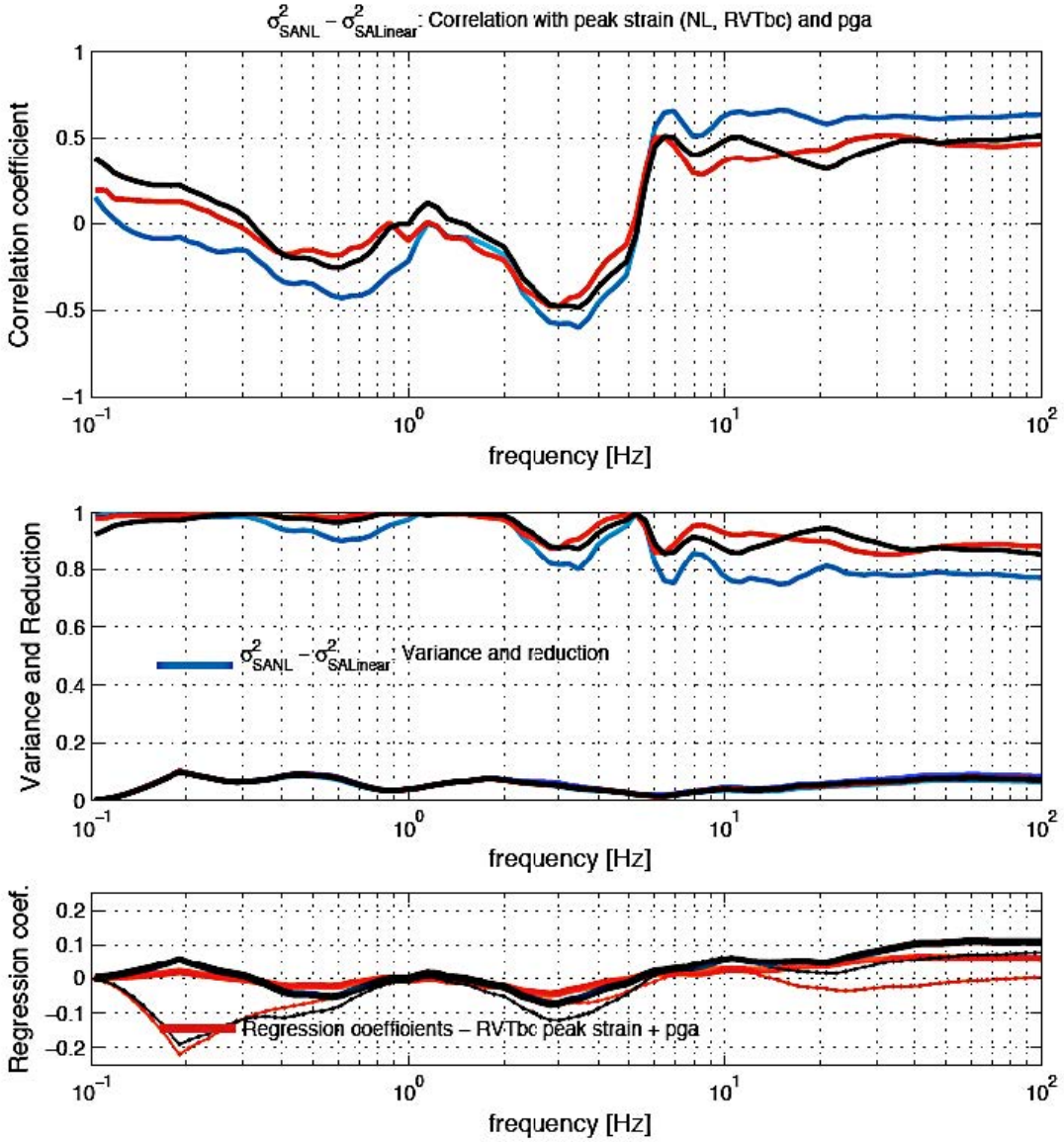

Figure II-1.76: EKKB - Correlation between the increase (or decrease) of variability of NL response spectra with respect to Linear response spectra for the ground motion at depth z2, and various ground motion level indicators : peak strain ratio as derived from the NL computations (blue line), peak strain ratio as derived from the RVT_{bc} computations (orange line), and input PGA level (grey line). See text for further explanations. Top: Correlation coefficient for each of the GM parameters, as a function of frequency from 0.1 to 100 Hz
Middle: Variance reduction derived from log linear regression analysis.
Bottom: Regression coefficients (slope in thick line, constant term in thin line) for both RVT_{bc} peak strain ratio (orange) and PGA (grey).

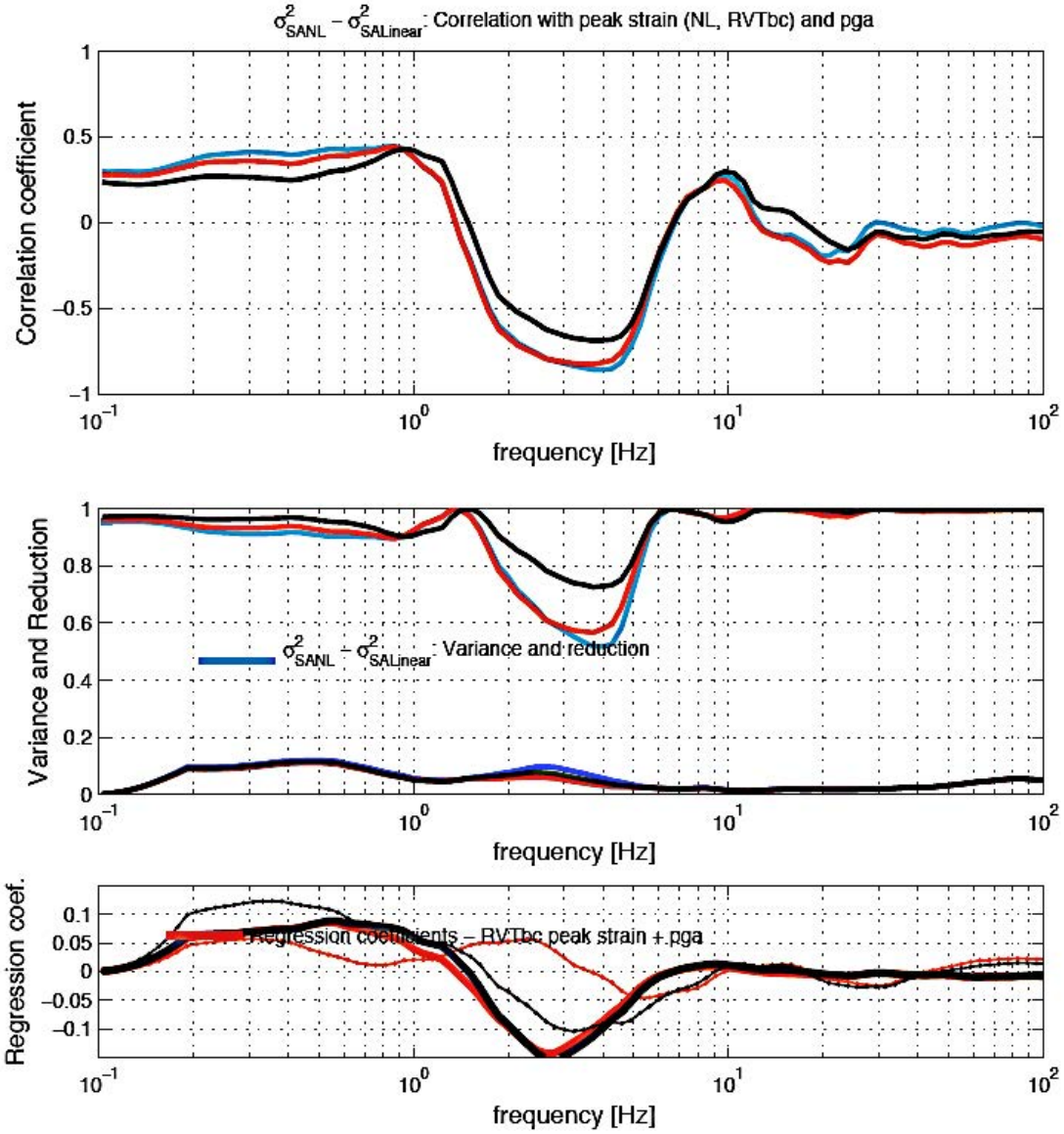

Figure II-1.77: KKG - Correlation between the increase (or decrease) of variability of NL response spectra with respect to Linear response spectra for the ground motion at depth z2, and various ground motion level indicators : peak strain ratio as derived from the NL computations (blue line), peak strain ratio as derived from the RVT_{bc} computations (orange line), and input PGA level (grey line). See text for further explanations. Top: Correlation coefficient for each of the GM parameters, as a function of frequency from 0.1 to 100 Hz
Middle: Variance reduction derived from log linear regression analysis.
Bottom: Regression coefficients (slope in thick line, constant term in thin line) for both RVT_{bc} peak strain ratio (orange) and PGA (grey).

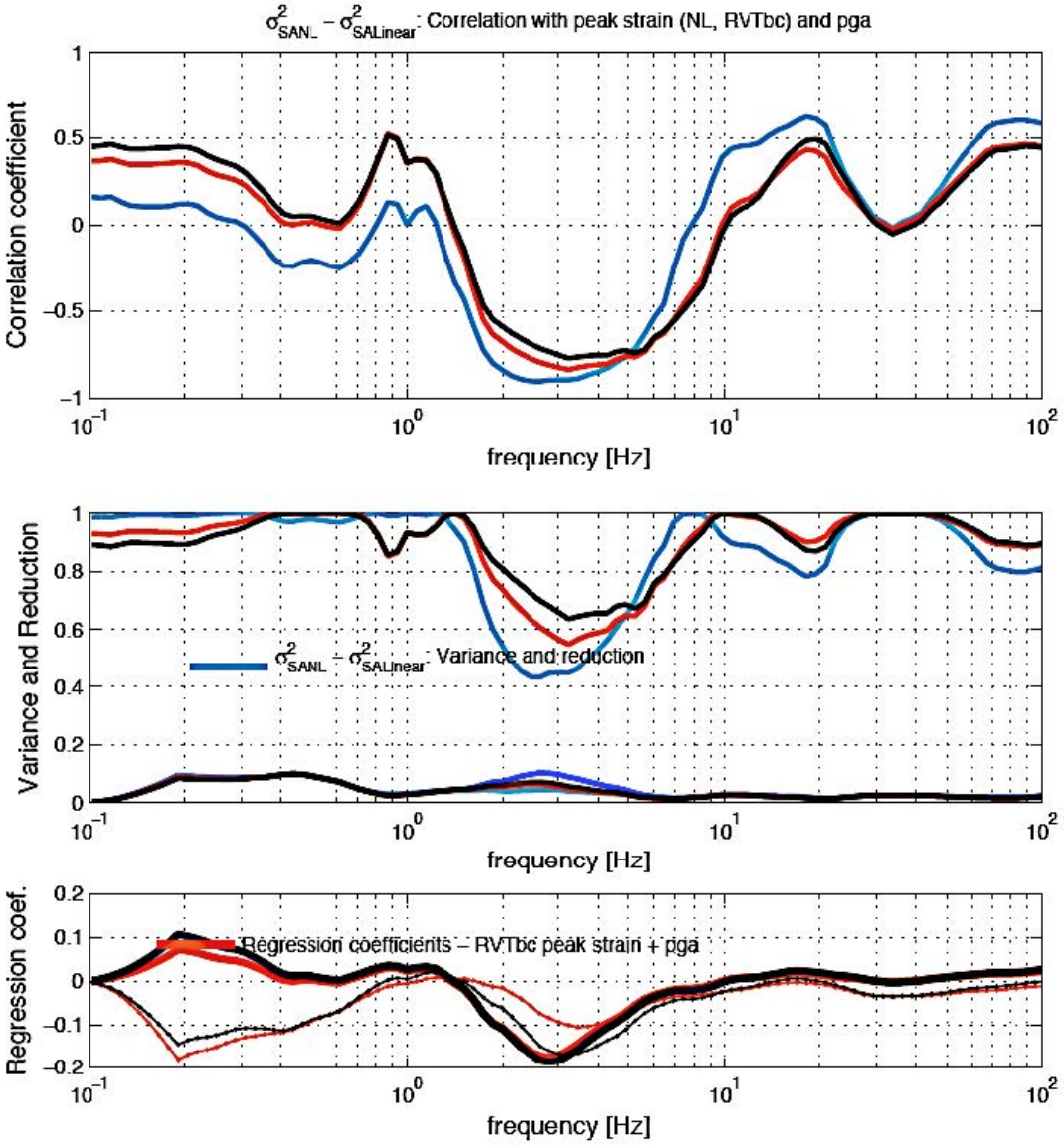

Figure II-1.78: KKL - Correlation between the increase (or decrease) of variability of NL response spectra with respect to Linear response spectra for the ground motion at depth z2, and various ground motion level indicators : peak strain ratio as derived from the NL computations (blue line), peak strain ratio as derived from the RVT_{bc} computations (orange line), and input PGA level (grey line). See text for further explanations. Top: Correlation coefficient for each of the GM parameters, as a function of frequency from 0.1 to 100 Hz
Middle: Variance reduction derived from log linear regression analysis.
Bottom: Regression coefficients (slope in thick line, constant term in thin line) for both RVT_{bc} peak strain ratio (orange) and PGA (grey).

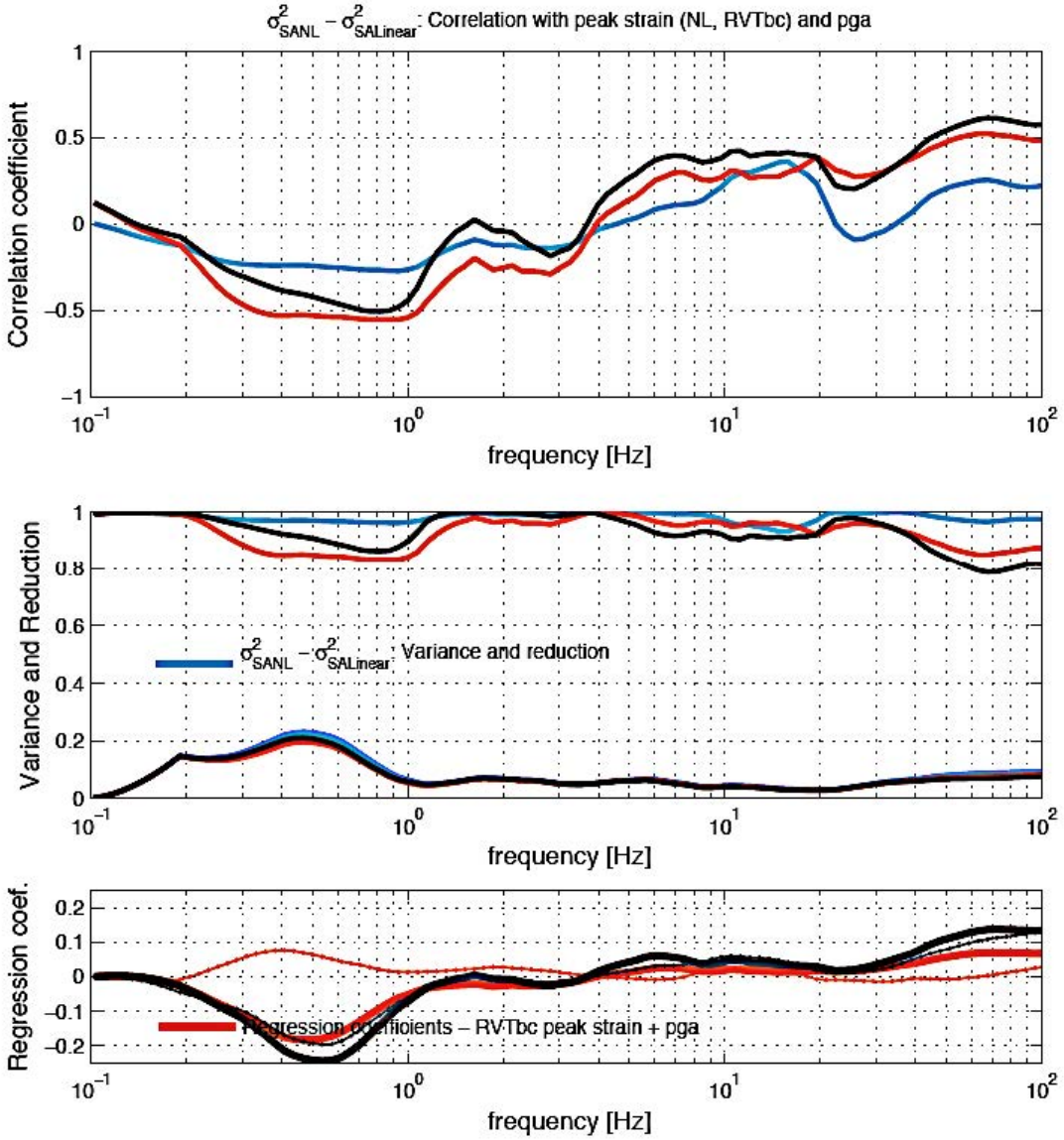

Figure II-1.79: KKM - Correlation between the increase (or decrease) of variability of NL response spectra with respect to Linear response spectra for the ground motion at depth z2, and various ground motion level indicators : peak strain ratio as derived from the NL computations (blue line), peak strain ratio as derived from the RVT_{bc} computations (orange line), and input PGA level (grey line). See text for further explanations. Top: Correlation coefficient for each of the GM parameters, as a function of frequency from 0.1 to 100 Hz
Middle: Variance reduction derived from log linear regression analysis.
Bottom: Regression coefficients (slope in thick line, constant term in thin line) for both RVT_{bc} peak strain ratio (orange) and PGA (grey).

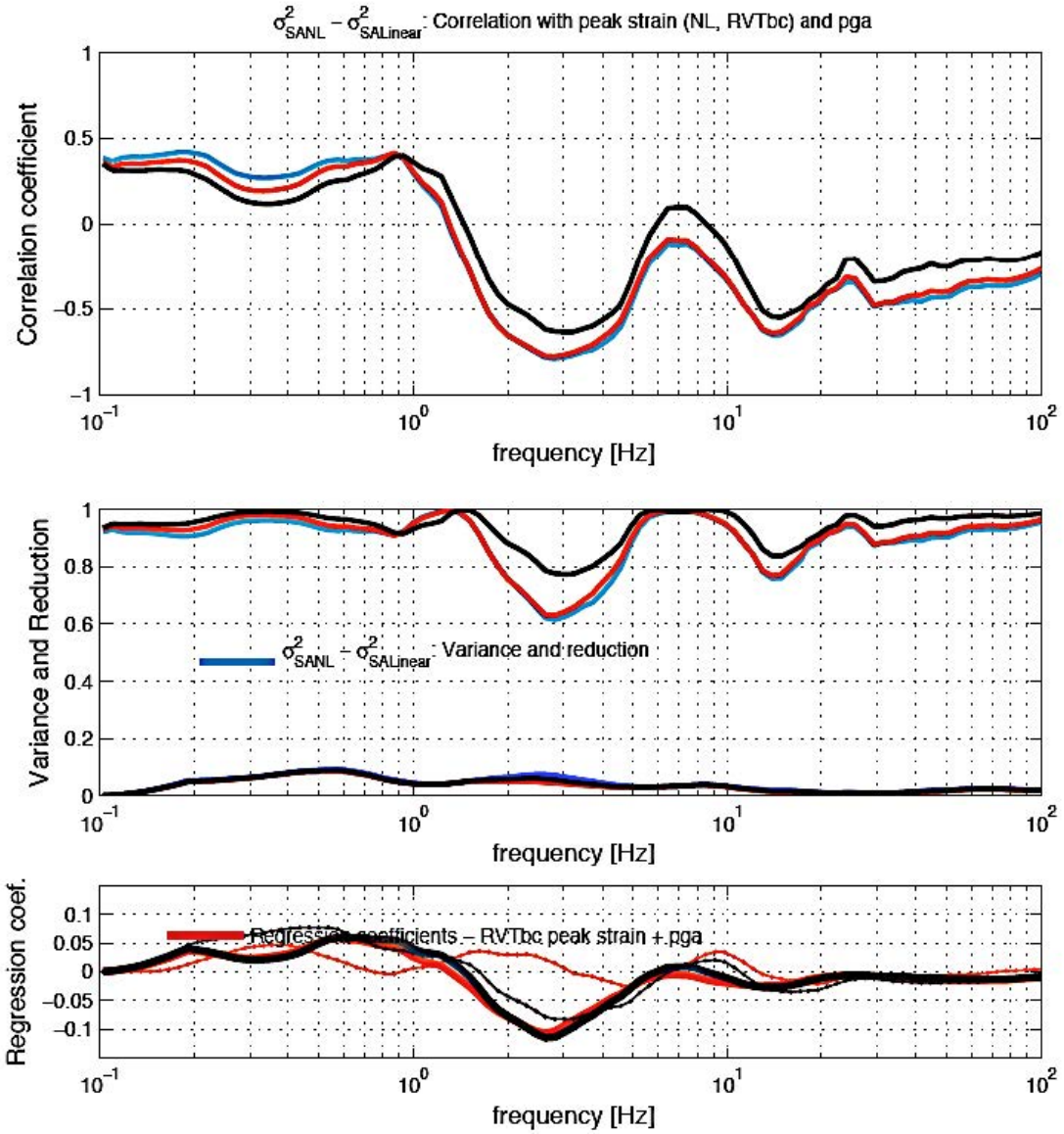

Figure II-1.80: KKG - Correlation between the increase (or decrease) of variability of NL response spectra with respect to Linear response spectra for the ground motion at depth z3, and various ground motion level indicators : peak strain ratio as derived from the NL computations (blue line), peak strain ratio as derived from the RVT_{bc} computations (orange line), and input PGA level (grey line). See text for further explanations. Top: Correlation coefficient for each of the GM parameters, as a function of frequency from 0.1 to 100 Hz
Middle: Variance reduction derived from log linear regression analysis.
Bottom: Regression coefficients (slope in thick line, constant term in thin line) for both RVT_{bc} peak strain ratio (orange) and PGA (grey).

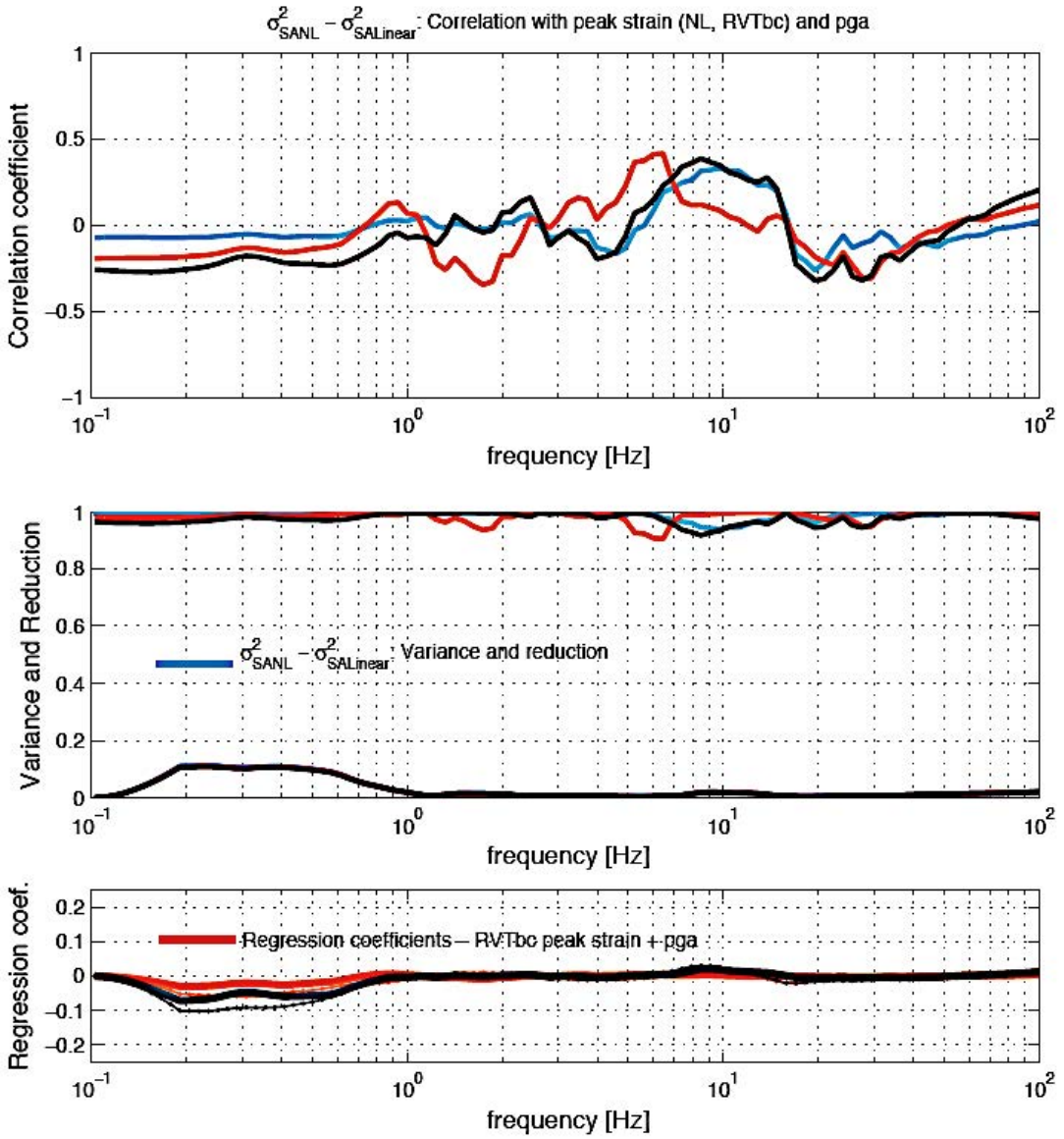

Figure II-1.81: KKM - Correlation between the increase (or decrease) of variability of NL response spectra with respect to Linear response spectra for the ground motion at depth z3, and various ground motion level indicators : peak strain ratio as derived from the NL computations (blue line), peak strain ratio as derived from the RVT_{bc} computations (orange line), and input PGA level (grey line). See text for further explanations. Top: Correlation coefficient for each of the GM parameters, as a function of frequency from 0.1 to 100 Hz
Middle: Variance reduction derived from log linear regression analysis.
Bottom: Regression coefficients (slope in thick line, constant term in thin line) for both RVT_{bc} peak strain ratio (orange) and PGA (grey).

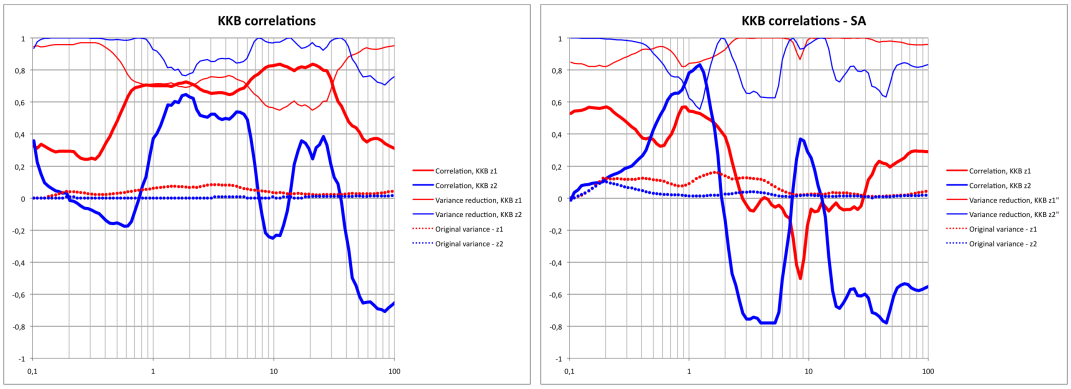

Figure II-1.82: KKB - Overview of the correlations between PGA level and the variability of NL amplification factors (top), and the variability of NL response spectra (bottom) for the two different depths (surface, z1, in red ; and depth z2 = 15 m, in blue).

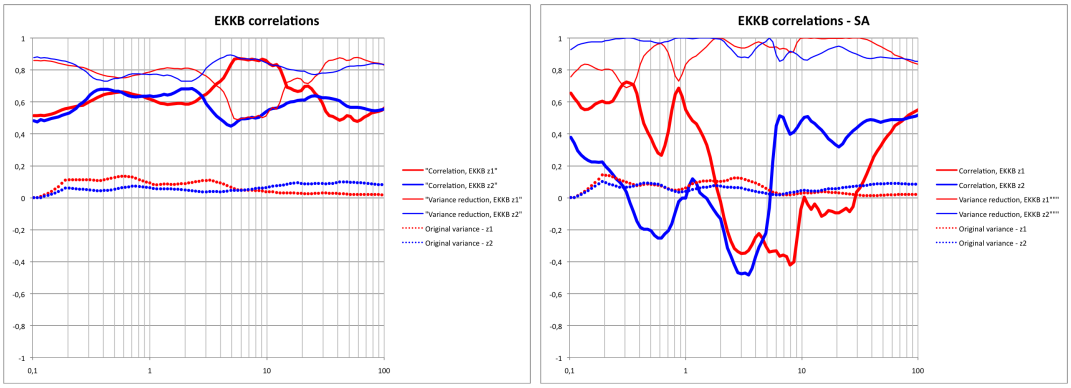

Figure II-1.83: EKKB - Overview of the correlations between PGA level and the variability of NL amplification factors (top), and the variability of NL response spectra (bottom) for the two different depths (surface, z1, in red ; and depth z2 = 15 m, in blue).

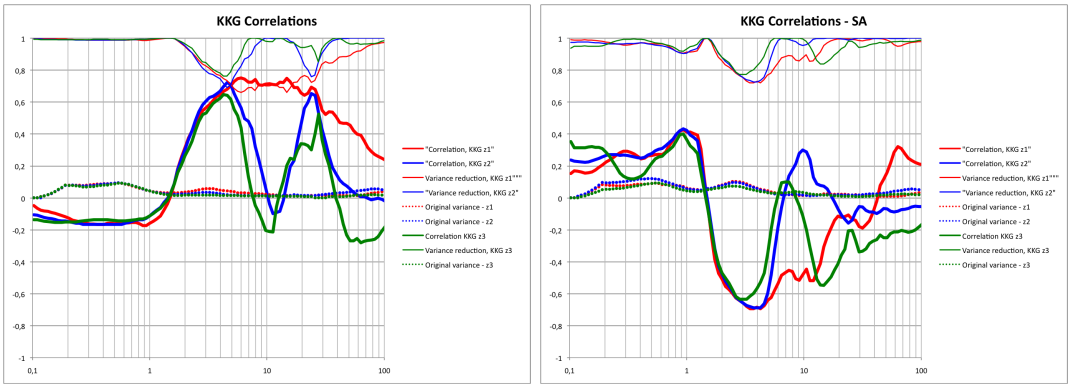

Figure II-1.84: KKG - Overview of the correlations between PGA level and the variability of NL amplification factors (top), and the variability of NL response spectra (bottom) for the two different depths (surface, z1, in red ; depth z2 = 9 m, in blue; depth z3 = 15 m, in green).

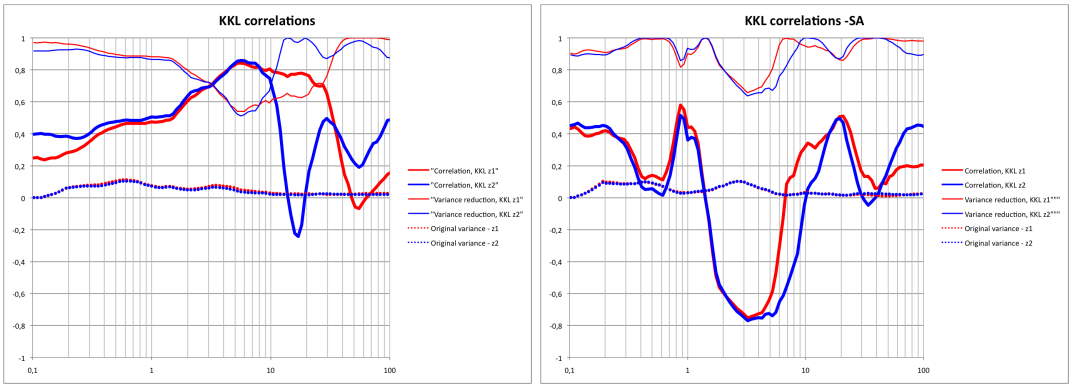

Figure II-1.85: KKL - Overview of the correlations between PGA level and the variability of NL amplification factors (top), and the variability of NL response spectra (bottom) for the two different depths (surface, z1, in red ; and depth z2 = 10 m, in blue).

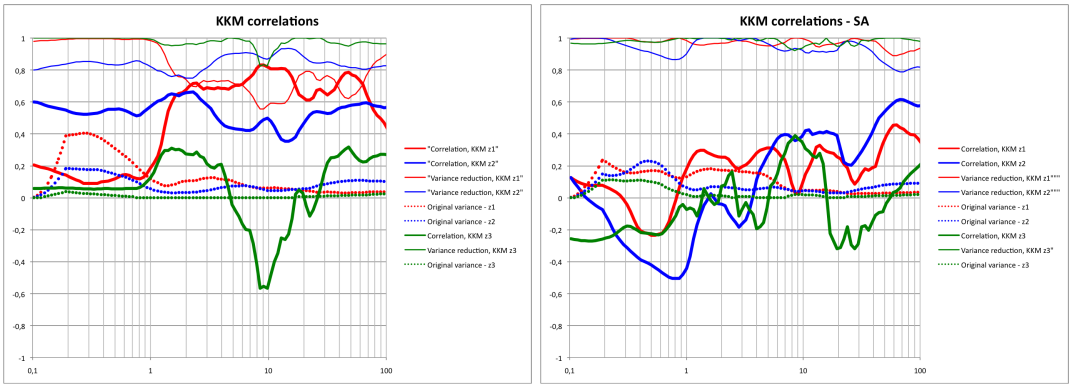

Figure II-1.86: KKM - Overview of the correlations between PGA level and the variability of NL amplification factors (top), and the variability of NL response spectra (bottom) for the two different depths (surface, z1, in red ; depth z2 = 7 m, in blue and depth z3 = 14 m, in green).

1.14 ANNEX A5 : Supporting documents for logic tree model of median amplification on vertical ground motion

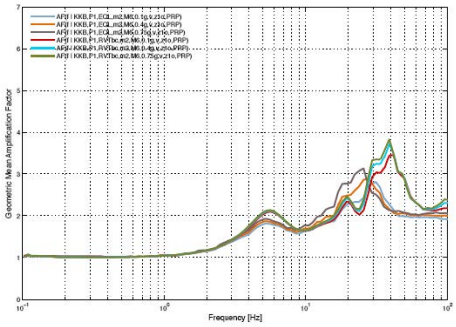

(a) KKB

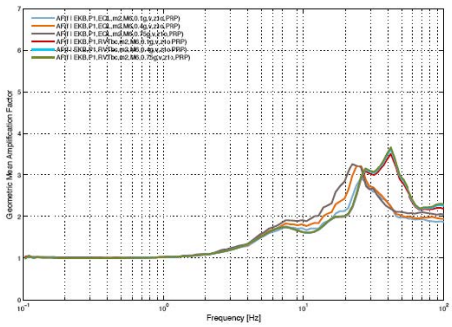

(b) EKKB

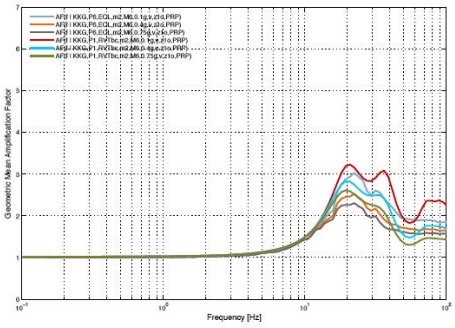

(c) KKG

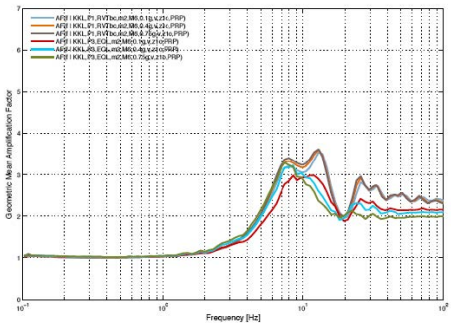

(d) KKL

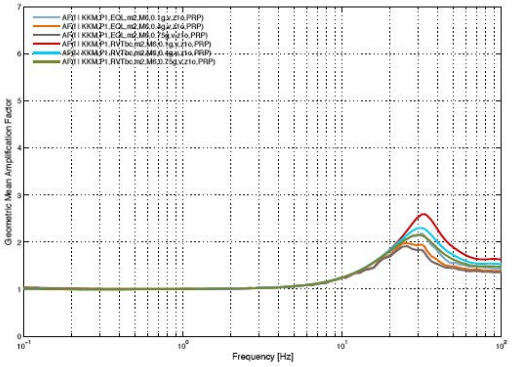

(e) KKM

Figure II-1.87: Dependence of the vertical amplification factor on vertical component as a function of pga_V for the 2010 computations.
In each case, the different curves display the amplification factor computed with SHAKE and RVT_{bc} approaches for 0.1, 0.4 and 0.75 g, and for the BE material properties (M2). In each case, the color code for the different curves is the following: light blue-grey: SHAKE, 0.1g; orange: SHAKE, 0.4g; grey: SHAKE, 0.75g; red: RVT_{bc}, 0.1g; blue: RVT_{bc}, 0.4g; green: RVT_{bc}, 0.75g.

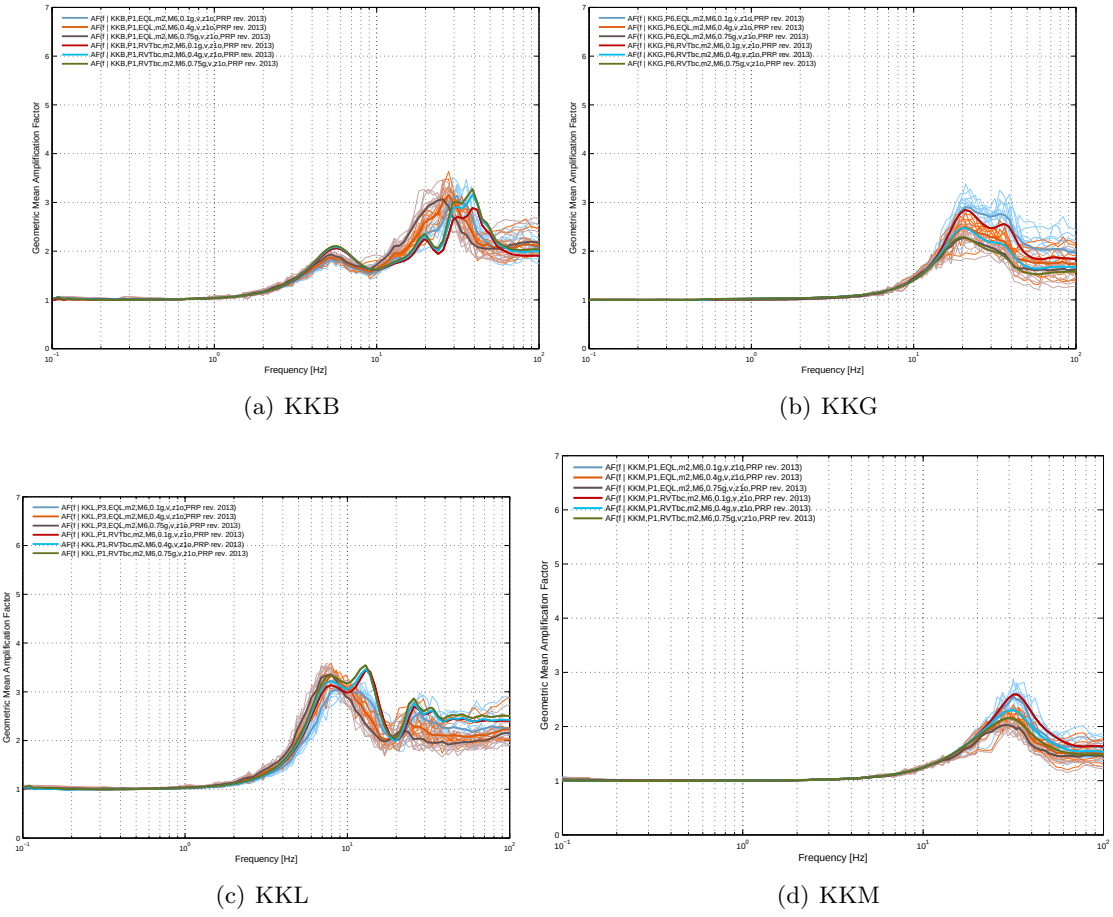

(a) KKB (b) KKG

(c) KKL (d) KKM

Figure II-1.88: Dependence of the vertical amplification factor on vertical component as a function of pga_V for the 2013 computations.
In each case, the different curves display the amplification factor computed with SHAKE and RVT_{bc} approaches for 0.1, 0.4 and 0.75 g, and for the BE material properties (M2). In each case, the color code for the different curves is the following: light blue-grey: SHAKE, 0.1g; orange: SHAKE, 0.4g; grey: SHAKE, 0.75g; red: RVT_{bc}, 0.1g; blue: RVT_{bc}, 0.4g; green: RVT_{bc}, 0.75g.

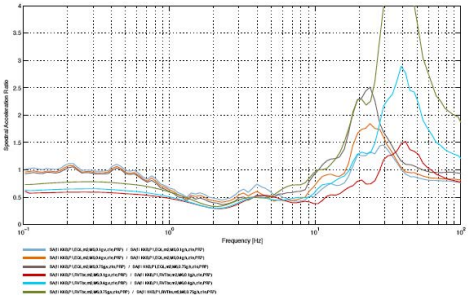

(a) KKB

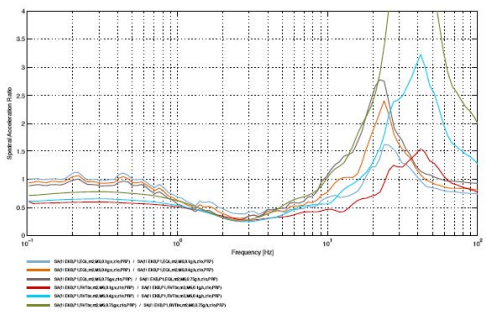

(b) EKKB

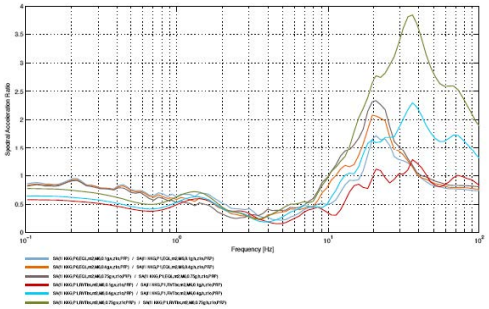

(c) KKG

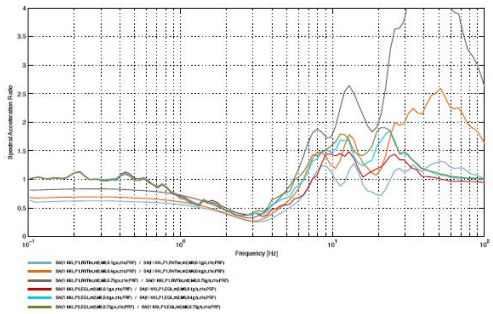

(d) KKL

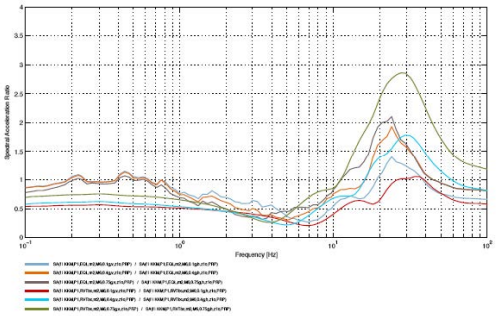

(e) KKM

Figure II-1.89: Variability of the computed AF_V/AF_H as a function of the approach (SHAKE or RVT_{bc}) and pga_V (0.1, 0.4, 0.75g) for the 2010 computations.
In each case, the color code for the different curves is the following: light blue-grey: SHAKE, 0.1g; orange: SHAKE, 0.4g; grey: SHAKE, 0.75g; red: RVT_{bc}, 0.1g; blue: RVT_{bc}, 0.4g; green: RVT_{bc}, 0.75g. All computations correspond to the BE material properties (M2).

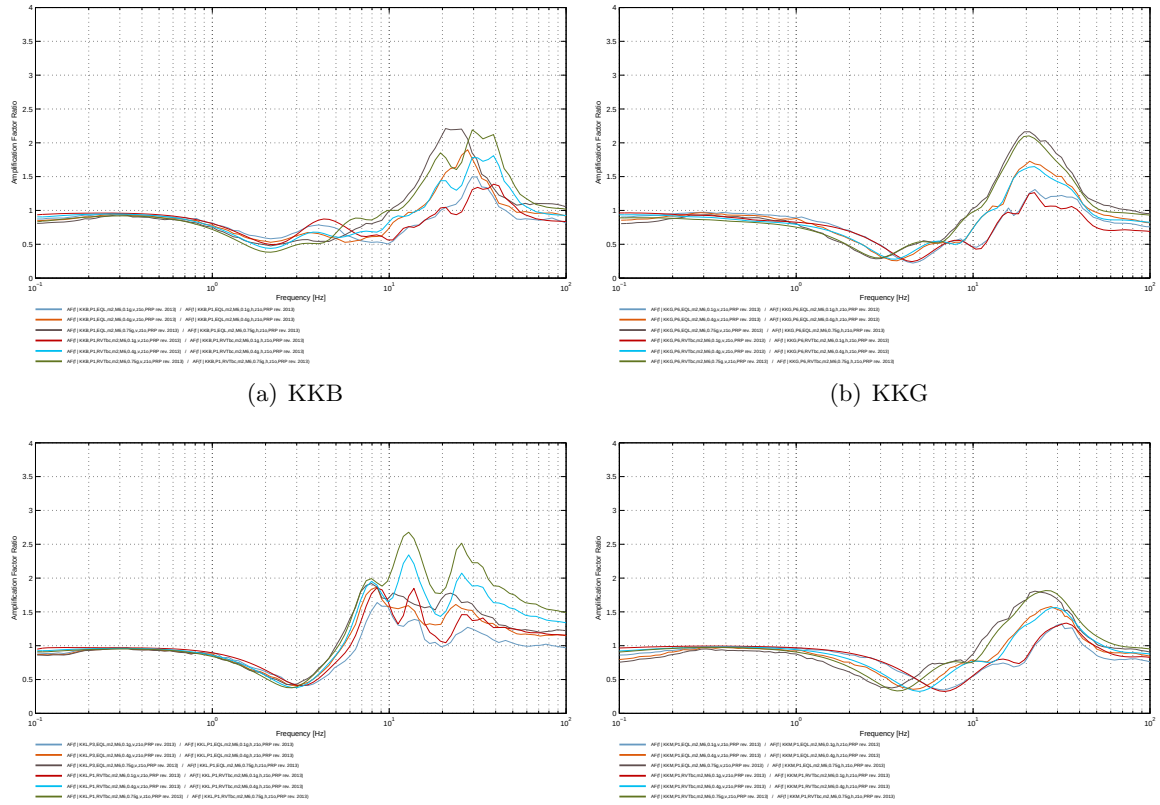

(a) KKB (b) KKG

(c) KKL (d) KKM

Figure II-1.90: Variability of the computed AF_V/AF_H as a function of the approach (SHAKE or RVT_{bc}) and pga_V (0.1, 0.4, 0.75g) for the 2013 computations.
In each case, the color code for the different curves is the following: light blue-grey: SHAKE, 0.1g; orange: SHAKE, 0.4g; grey: SHAKE, 0.75g; red: RVT_{bc}, 0.1g; blue: RVT_{bc}, 0.4g; green: RVT_{bc}, 0.75g. All computations correspond to the BE material properties (M2).

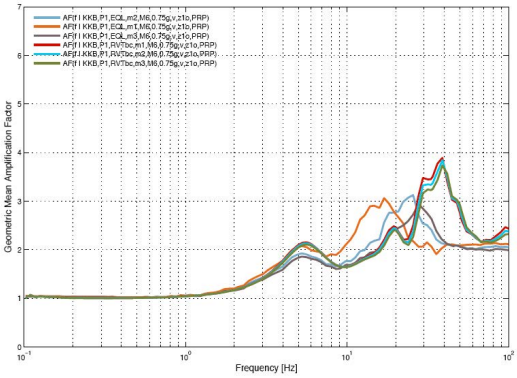

(a) KKB

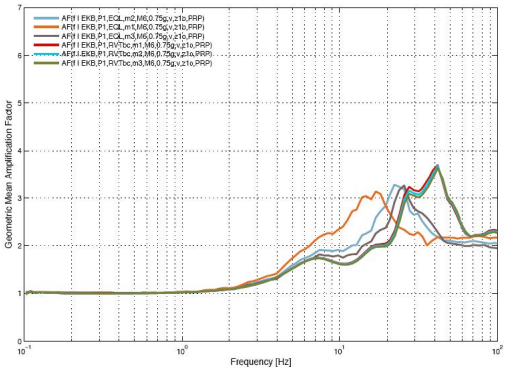

(b) EKKB

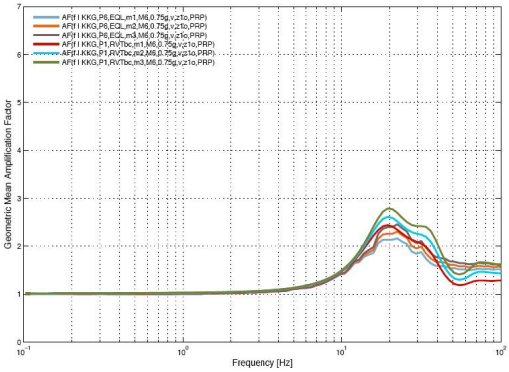

(c) KKG

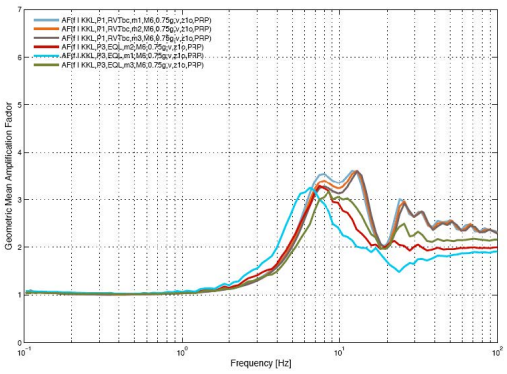

(d) KKL

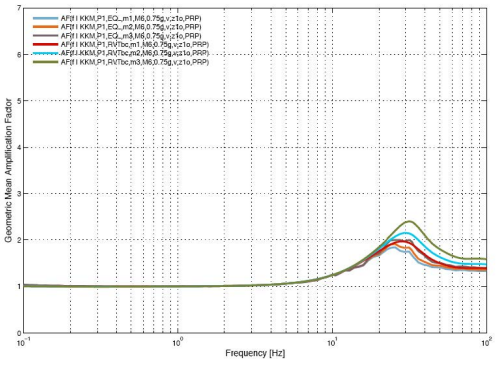

(e) KKM

Figure II-1.91: Variability of the computed AFV amplification factors as a function of the approach (SHAKE or RVT_{bc}) and material properties (M1, M2, M3) for the largest acceleration case (0.75g) and for the 2010 computations.
In each case, the color code for the different curves is the following: light blue-grey: SHAKE, M1 (except for KKB and EKKB : M2); orange: SHAKE, M2 (except for KKB and EKKB: M1); grey: SHAKE, M3; red: RVT_{bc}, M1; blue: RVT_{bc}, M2; green: RVT_{bc}, M. All computations correspond to a peak incident vertical acceleration of 0.75g.

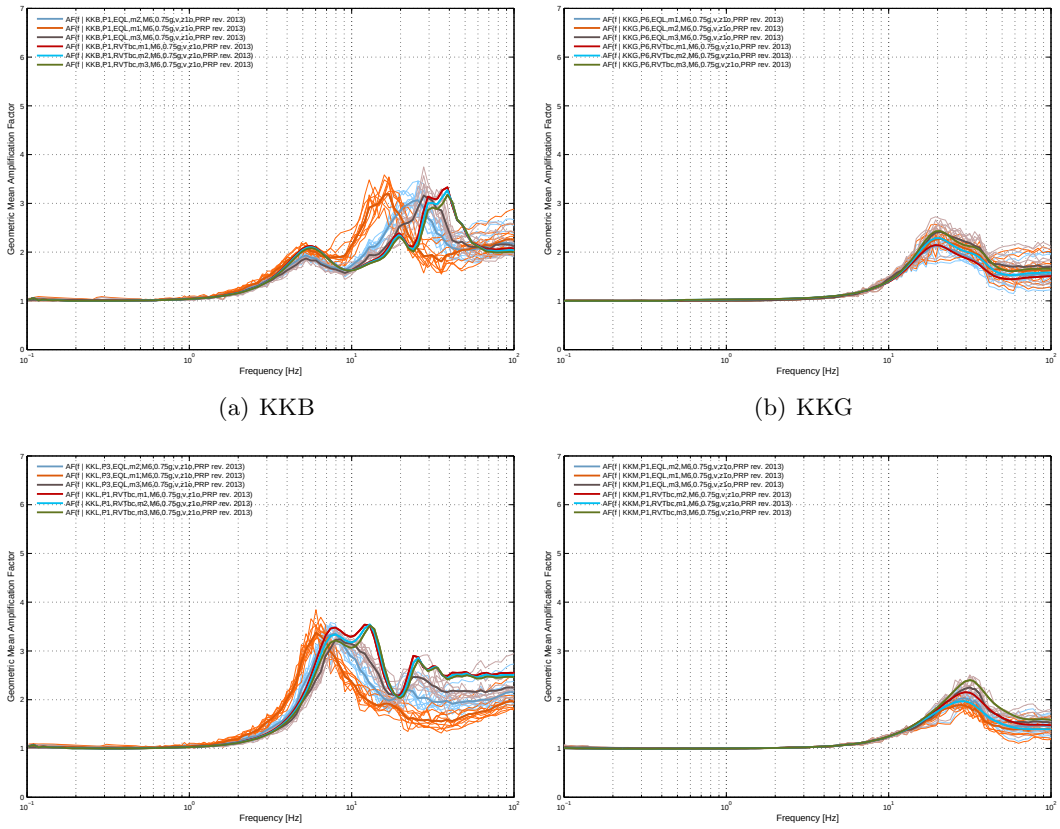

(a) KKB (b) KKG

(c) KKL (d) KKM

Figure II-1.92: Variability of the computed AFV amplification factors as a function of the approach (SHAKE or RVT_{bc}) and material properties (M1, M2, M3) for the largest acceleration case (0.75g) and for the 2013 computations.
In each case, the color code for the different curves is the following: light blue-grey: SHAKE, M1 (except for KKB and EKKB : M2); orange: SHAKE, M2 (except for KKB and EKKB: M1); grey: SHAKE, M3; red: RVT_{bc}, M1; blue: RVT_{bc}, M2; green: RVT_{bc}, M. All computations correspond to a peak incident vertical acceleration of 0.75g.

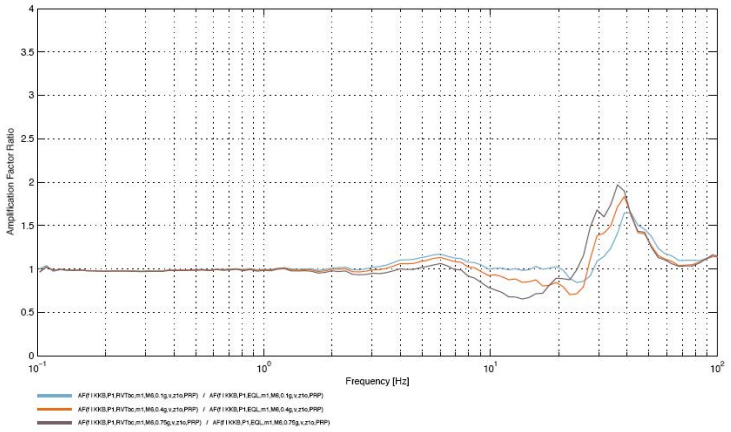

(a) M1 (Lower Bound) case

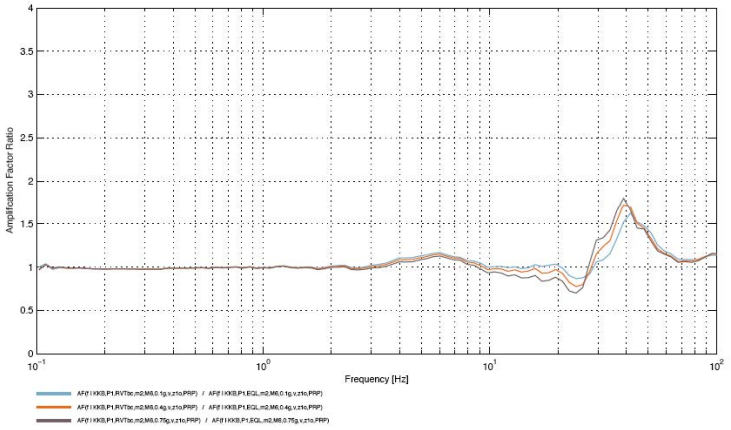

(b) M2 (Best-Estimate)

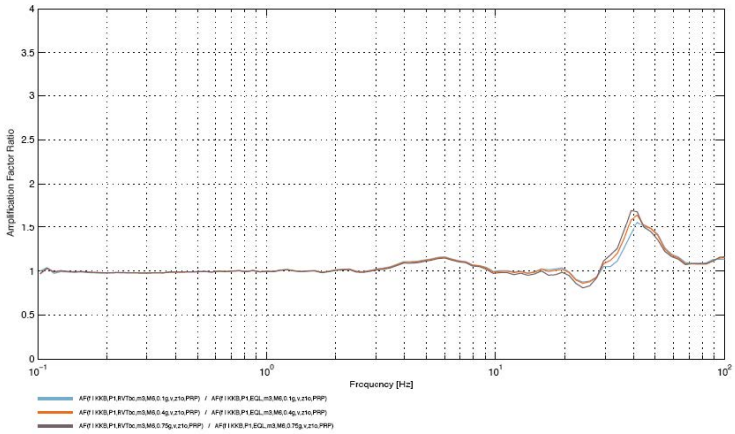

(c) M3 (Upper Bound)

Figure II-1.93: Variability of the ratio between the AFV amplification factors computed with RVT_{bc} and SHAKE approaches for KKB site, for all acceleration levels and various material properties, in the case of 2010 computations.
In each case, the color code for the different curves is the following: light bluegrey: 0.10g, ; orange: 0.4g; grey: 0.75g.

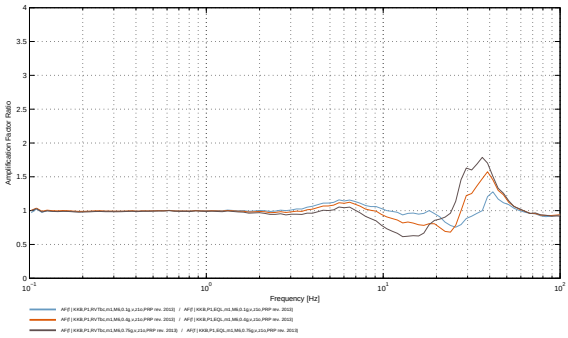

(a) M1 (Lower Bound) case

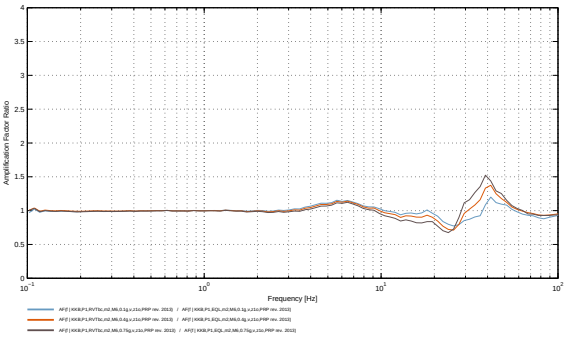

(b) M2 (Best-Estimate)

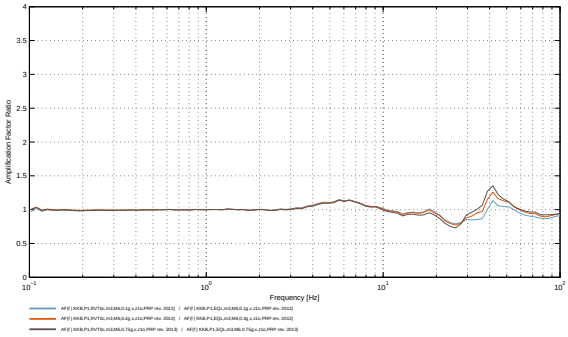

(c) M3 (Upper Bound)

Figure II-1.94: Variability of the ratio between the AFV amplification factors computed with RVT_{bc} and SHAKE approaches for KKB site, for all acceleration levels and various material properties, in the case of 2013 computations.
In each case, the color code for the different curves is the following: light bluegrey: 0.10g, ; orange: 0.4g; grey: 0.75g.

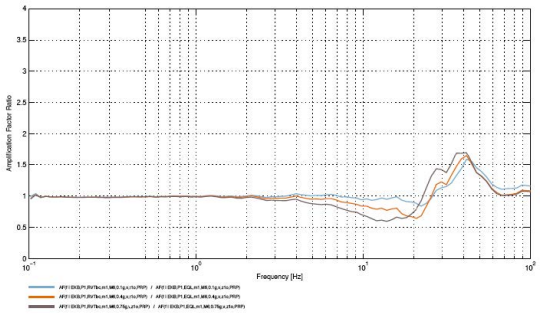

(a) M1 (Lower Bound) case

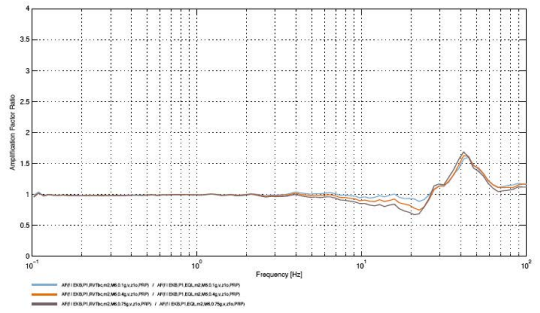

(b) M2 (Best-Estimate)

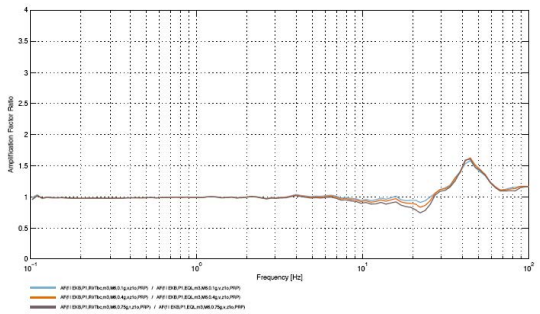

(c) M3 (Upper Bound)

Figure II-1.95: Variability of the ratio between the AFV amplification factors computed with RVT_{bc} and SHAKE approaches for EKKB site, for all acceleration levels and various material properties, in the case of 2010 computations (the only available for the EKKB site). In each case, the color code for the different curves is the following : light bluegrey: 0.10g, ; orange: 0.4g; grey: 0.75g.

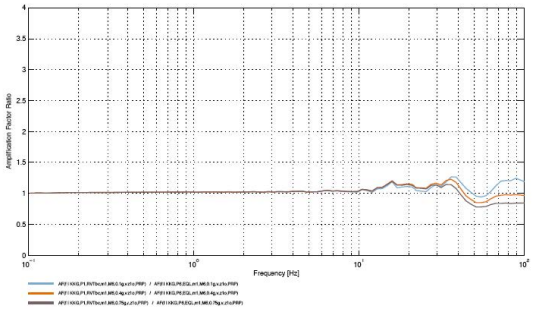

(a) M1 (Lower Bound) case

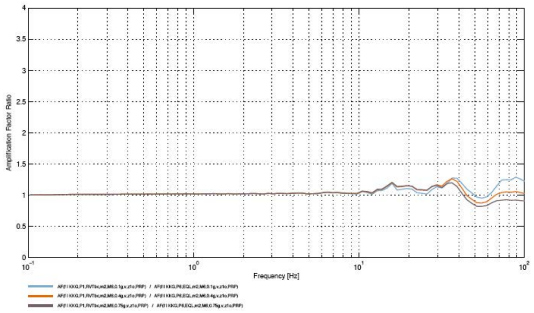

(b) M2 (Best-Estimate)

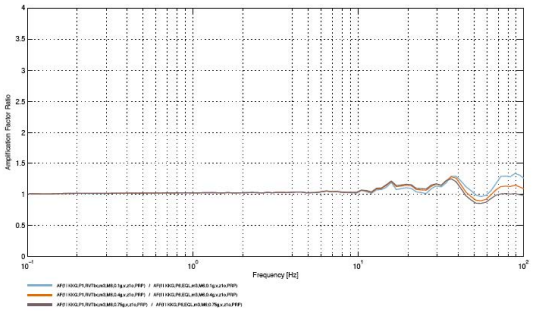

(c) M3 (Upper Bound)

Figure II-1.96: Variability of the ratio between the AFV amplification factors computed with RVT_{bc} and SHAKE approaches for KKG site, for all acceleration levels and various material properties, in the case of 2010 computations.
In each case, the color code for the different curves is the following: light bluegrey: 0.10g, ; orange: 0.4g; grey: 0.75g.

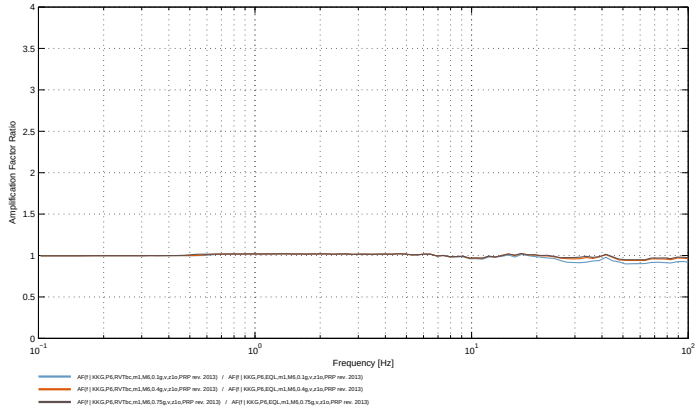

(a) M1 (Lower Bound) case

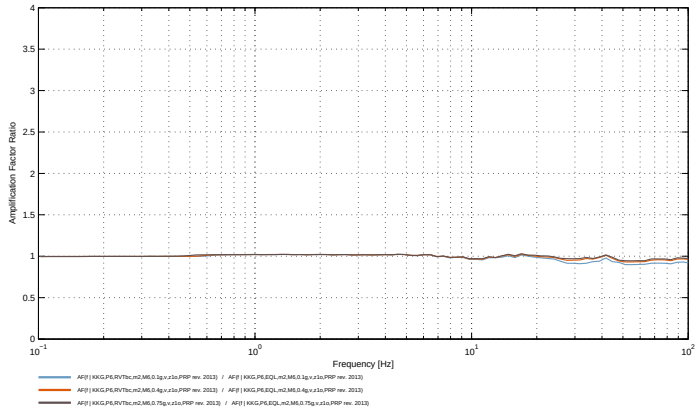

(b) M2 (Best-Estimate)

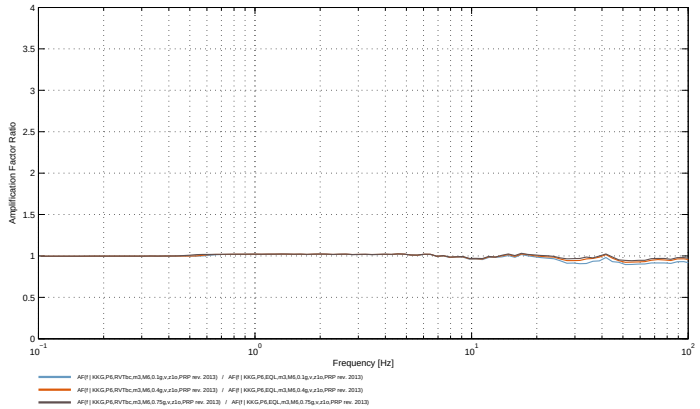

(c) M3 (Upper Bound)

Figure II-1.97: Variability of the ratio between the AFV amplification factors computed with RVT_{bc} and SHAKE approaches for KKG site, for all acceleration levels and various material properties, in the case of 2013 computations.
In each case, the color code for the different curves is the following: light bluegrey: 0.10g, ; orange: 0.4g; grey: 0.75g.

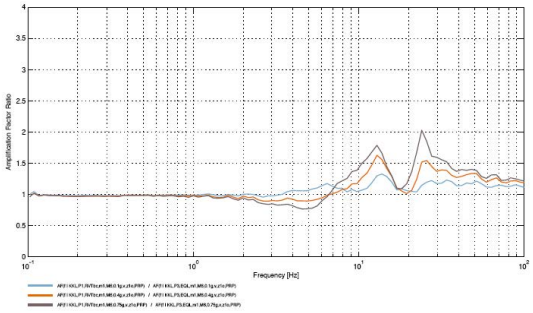

(a) M1 (Lower Bound) case

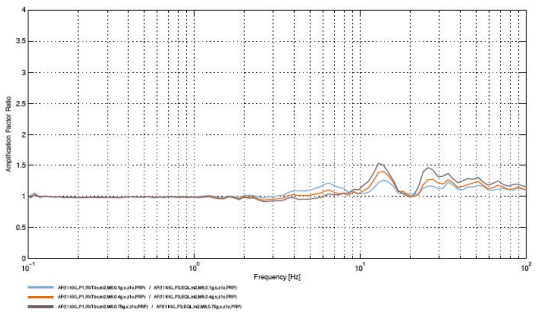

(b) M2 (Best-Estimate)

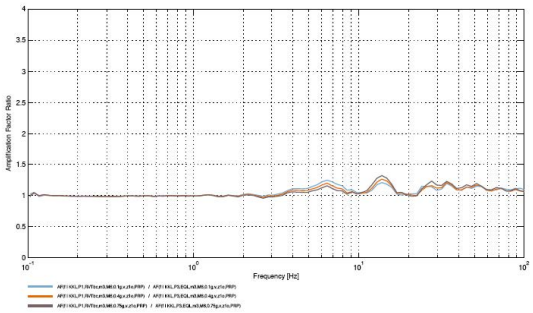

(c) M3 (Upper Bound)

Figure II-1.98: Variability of the ratio between the AFV amplification factors computed with RVT_{bc} and SHAKE approaches for KKL site, for all acceleration levels and various material properties, in the case of 2010 computations.
In each case, the color code for the different curves is the following: light bluegrey: 0.10g, ; orange: 0.4g; grey: 0.75g.

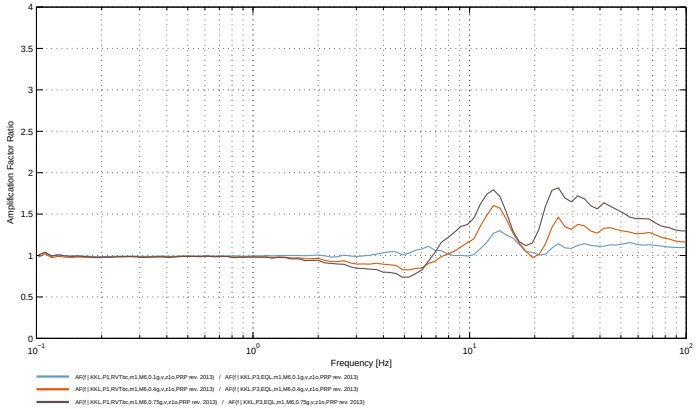

(a) M1 (Lower Bound) case

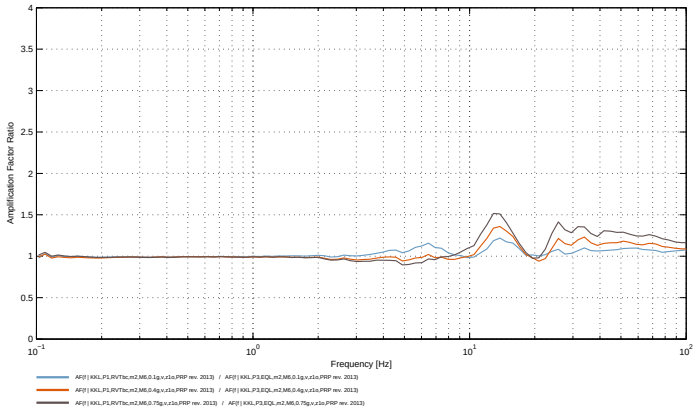

(b) M2 (Best-Estimate)

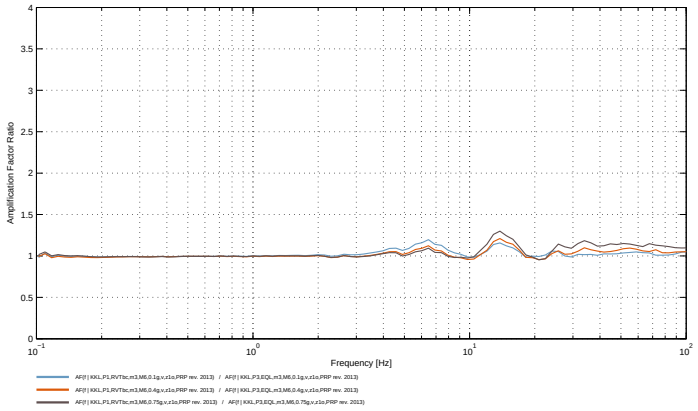

(c) M3 (Upper Bound)

Figure II-1.99: Variability of the ratio between the AFV amplification factors computed with RVT_{bc} and SHAKE approaches for KKL site, for all acceleration levels and various material properties, in the case of 2013 computations.
In each case, the color code for the different curves is the following: light bluegrey: 0.10g, ; orange: 0.4g; grey: 0.75g.

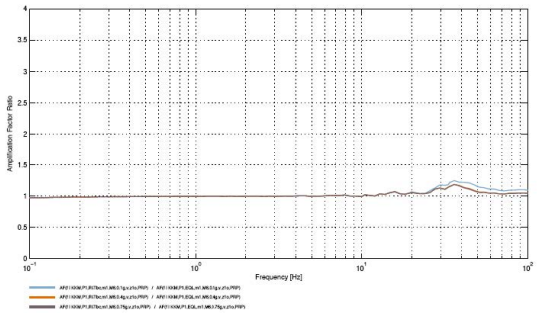

(a) M1 (Lower Bound) case

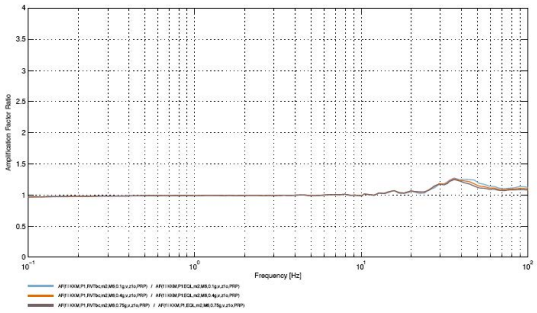

(b) M2 (Best-Estimate)

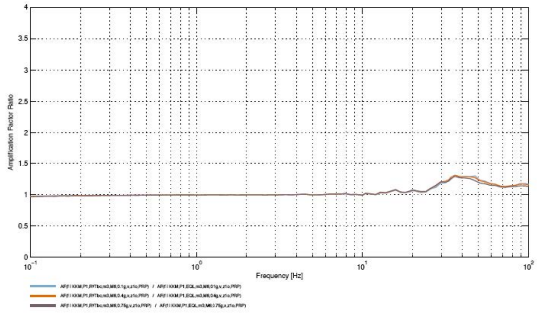

(c) M3 (Upper Bound)

Figure II-1.100: Variability of the ratio between the AFV amplification factors computed with RVT_{bc} and SHAKE approaches for KKM site, for all acceleration levels and various material properties, in the case of 2010 computations.
In each case, the color code for the different curves is the following: light bluegrey: 0.10g, ; orange: 0.4g; grey: 0.75g.

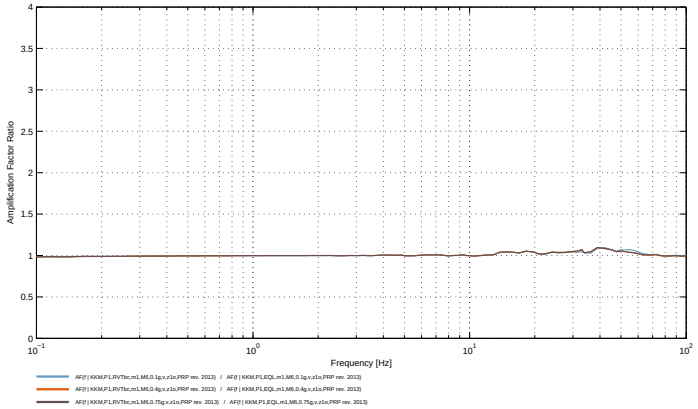

(a) M1 (Lower Bound) case

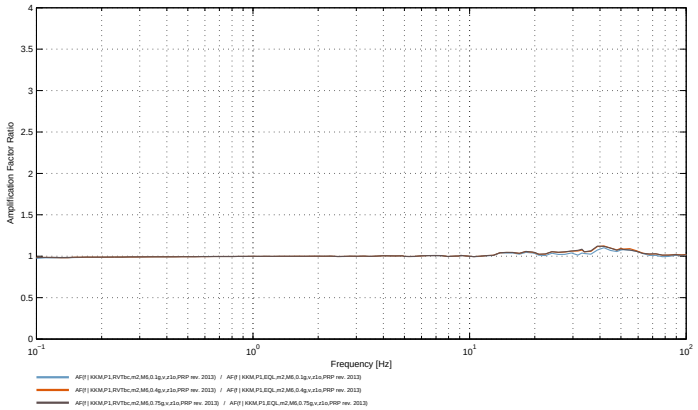

(b) M2 (Best-Estimate)

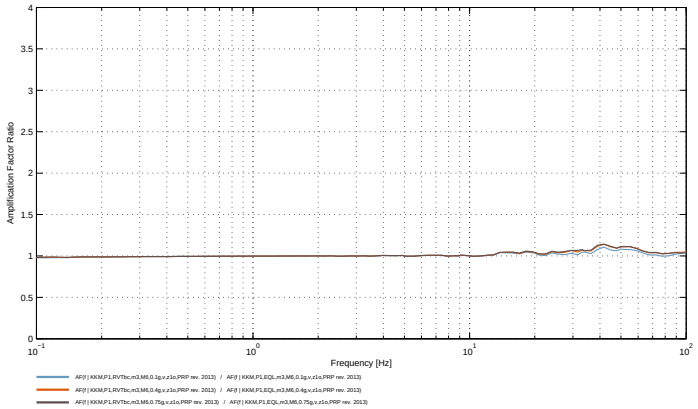

(c) M3 (Upper Bound)

Figure II-1.101: Variability of the ratio between the AFV amplification factors computed with RVT_{bc} and SHAKE approaches for KKM site, for all acceleration levels and various material properties, in the case of 2013 computations.
In each case, the color code for the different curves is the following: light bluegrey: 0.10g, ; orange: 0.4g; grey: 0.75g.

Chapter 2

Hazard Input Document for P.-Y. Bard (EG3-HID-1005)

Written by the PMT, SP4 and TFI

2.1 Introduction

This Hazard Input Document (HID) describes the implementation, evaluation and results of Pierre-Yves Bard's geotechnical assessment of sites effects (the "model" or "SP3 model") at the NPP sites Beznau, Gösgen, Leibstadt and Mühleberg, delivered on 20.08.2013. The purpose of this document is to provide a technical description of the model as implemented. The results of model evaluation are compiled into a so-called SIF (Soil hazard Input File), which, among the rock hazard results, is input to the soil hazard evaluations. This HID addresses technical and procedural aspects. It does not provide a rational discussion of the models or the results.

2.2 Model Description

The geotechnical assessment by Pierre-Yves Bard is described in part II, Chapter 1 (EG3-ES-1014). The models concern six quantities:

- Amplification of horizontal ground motion,
- Aleatory variability of horizontal motion amplification,
- Maximum horizontal ground motion,
- Amplification of vertical ground motion and V/H scaling,
- Aleatory variability of vertical motion amplification and V/H scaling factors, and
- Maximum vertical ground motion,

which are all developed as functions of spectral frequency, which consider the up-going wavefield ("outcrop motion") and which depend on site, target depth, PGA and magnitude. All models are formulated as logic trees, yielding epistemic uncertainty. These logic tree models are described in the following.

2.2.1 Amplification of Horizontal Ground Motion

The logic tree model for amplification of horizontal ground motion features six levels of branching (Fig. II-2.1), among which epistemic uncertainty is developed.

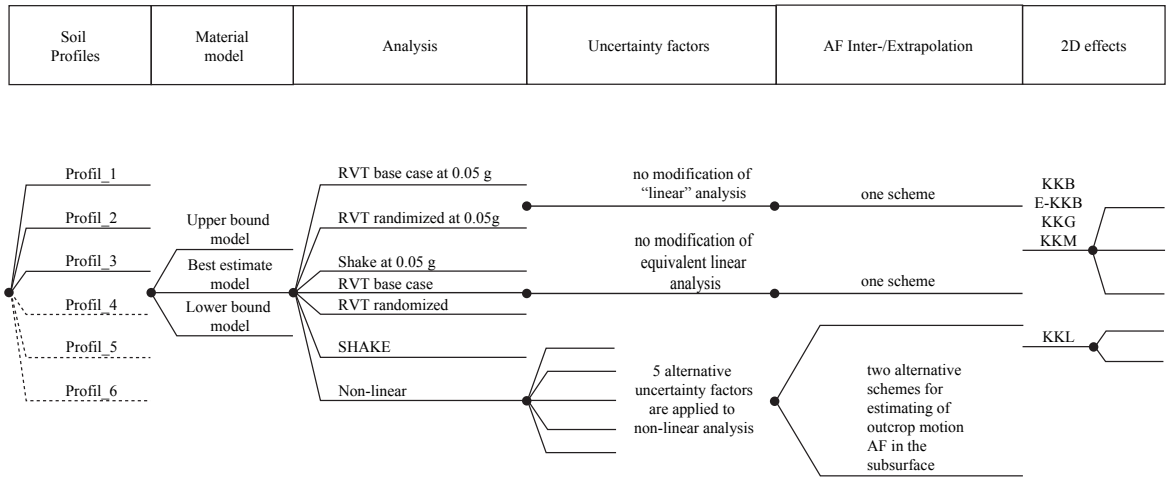

Figure II-2.1: Horizontal ground motion logic tree for P.-Y. Bard

Level 1

develops soil profile alternatives. The soil profiles are described in Renault [2010a, b, c, d, e] [TP3-TN-1068...1071] and in the report Part I. The assigned weights are given in Table II-2.1. They dependent on the NPP site and are frequency-invariant. They are implemented in the *sp3b_Profile* routine of Hölker [2012] (TP4-HSW-1002).

Table II-2.1: Weights of soil profiles in level 1 of the logic tree model for amplification of horizontal ground motion.

Soil profile	P1	P2	P3	P4	P5	P6
Beznau	0.30	0.30	0.15	0.25	-/-	-/-
Gösgen	0.10	0.050	0.20	0.20	0.15	0.30
Leibstadt	0.40	0.25	0.35	-/-	-/-	-/-
Mühleberg	0.40	0.25	0.25	0.10	-/-	-/-

Level 2

develops the material and shear modulus models. Generally a "lower bound", "best estimate" and "upper bound" model have been defined in TP3-TN-1068...1071. The weights assigned to the material models are given in Table II-2.2. These weights depend on NPP site are frequency-invariant and are implemented in *sp3b_Material*.

Table II-2.2: Weights of material models in level 2 of the logic tree model for amplification of horizontal ground motion.

Material model	Lower bound	Best estimate	Upper bound
Beznau	0.20	0.35	0.45
Gösgen	0.25	0.45	0.30
Leibstadt	0.20	0.60	0.20
Mühleberg	0.15	0.45	0.40

Level 3

develops the alternative amplification functions given due to different computational approaches (referred to as site response analyses or SRA methods). Conceptually a "linear", a "linear-equivalent" and a "non-linear" approach is considered. Practically those are represented by seven alternative SRA being considered:

- SHAKE for PGA=0.05 g representing the "linear" approach;
- RVT base case (RVT_{bc}) for PGA=0.05 g representing the "linear" approach;
- RVT randomized (RVTr) for PGA=0.05 g representing the "linear" approach;
- SHAKE for the PGA level at hand, "linear-equivalent" approach;
- RVT_{bc} for the PGA level at hand, "linear-equivalent" approach;
- RVT_r for the PGA level at hand, "linear-equivalent" approach;
- Non-linear SRA for the PGA level at hand.

These alternatives and their weights are implemented in *sp3b_Method*. The weights depend on spectral frequency and on a strain ratio γ_{max}/γ_{50}, which by itself is specific to site, magnitude, PGA, and soil profile. This strain ratio is defined as

$$\gamma_{max}/\gamma_{50} = max\left[max\{\gamma(z)_{layer\,1}\}/\gamma_{50,layer1}, \ldots, \quad max\{\gamma(z)_{layer\,n}\}/\gamma_{50,layer\,n}\right] \quad \text{(II-2.1)}$$

where $\gamma(z)$ is the maximum shear strain per soil layer derived from the RVT_{bc} SRA for the best estimate material model; and where γ_{50} is the shear strain corresponding to $G/G_{max} = 0.5$ of the shear modulus reduction curve corresponding to the soil layer at hand. At PGA levels for which no SRA is available the ratio γ_{max}/γ_{50} is linearly interpolated from available analyses on a log(PGA) scale.

The weights (W) assigned to the 7 alternative SRAs are defined per spectral frequency f by equations as follow:

$$W_{SHAKE(0.05g)} = W_{SHAKE} \cdot W_{LIN} \tag{II-2.2a}$$
$$W_{RVT_{bc}(0.05g)} = W_{bc}(1 - W_{SHAKE})W_{LIN} \tag{II-2.2b}$$
$$W_{RVT_{r}(0.05g)} = (1 - W_{bc})(1 - W_{SHAKE})W_{LIN} \tag{II-2.2c}$$
$$W_{SHAKE(PGA)} = W_{SHAKE} \cdot W_{EQL} \tag{II-2.2d}$$
$$W_{RVT_{bc}(PGA)} = W_{bc}(1 - W_{SHAKE})W_{EQL} \tag{II-2.2e}$$
$$W_{RVT_{r}(PGA)} = (1 - W_{bc})(1 - W_{SHAKE})W_{EQL} \tag{II-2.2f}$$
$$W_{NL} = 1 - (W_{EQL} + W_{LIN}) \tag{II-2.2g}$$

where

$$W_{SHAKE}(f) = \begin{cases} 1, & f < 0.5Hz \\ -1.661\log(f) + 0.5, & 0.5 < f < 1 \quad \text{at Leibstadt} \\ 0.5, & f > 1 \quad \text{at Leibstadt} \\ -1.3288\log(f) + 0.6, & 0.5 < f < 1 \quad \text{at other sites} \\ 0.6, & f > 1 \quad \text{at other sites} \end{cases} \tag{II-2.2h}$$

$$W_{EQL}(\gamma_{max}/\gamma_{50}) = 0.8 \begin{cases} 1, & \gamma_{max}/\gamma_{50} < 1 \\ 1 - 0.75\log(\gamma_{max}/\gamma_{50}), & 1 < \gamma_{max}/\gamma_{50} < 10 \\ 0.25, & \gamma_{max}/\gamma_{50} > 10 \end{cases} \tag{II-2.2i}$$

$$W_{LIN}(\gamma_{max}/\gamma_{50}) = 0.2 \begin{cases} 1, & \gamma_{max}/\gamma_{50} < 1 \\ 1 - \log(\gamma_{max}/\gamma_{50}), & 1 < \gamma_{max}/\gamma_{50} < 10 \\ 0, & \gamma_{max}/\gamma_{50} > 10 \end{cases} \tag{II-2.2j}$$

$$W_{bc} = \begin{cases} 0.60, & \text{at Leibstadt site} \\ 0.5825, & \text{at other sites} \end{cases} \tag{II-2.2k}$$

Level 4

develops uncertainty factors, which are applicable only to the amplification functions based on NL SRA. No sub-branching occurs for branches based on SHAKE or RVT SRA. Five sets of frequency-dependent uncertainty factors are defined resulting in five branches. Uncertainty factors $U(f)$ are defined in Equations II-2.3a to II-2.3d and Table II-2.3, where f is spectral frequency [Hz], where f_0 is the soil-profile-specific fundamental frequency, and where site-specific parameters and weights are given in Table II-2.3. These uncertainty factors and their weights are implemented in *sp3b_NL_Uncert*.

$$U(f) = 10^{(E(f)\,D\,Ua(PGA))} \tag{II-2.3a}$$

$$E(f) = \begin{cases} 0 & (kf/f_0) < 0.5 \\ \log(2kf/f_0) & 0.5 < (kf/f_0) < 1.0 \\ 1 & (kf/f_0) > 1.0 \end{cases} \quad \text{(II-2.3b)}$$

$$k = 1 + k_{max} U_a \quad \text{(II-2.3c)}$$

$$U_a(PGA) = \begin{cases} 0 & \log(PGA/PGA_{ref})/\log(2.5/PGA_{ref}) < 0 \\ \log(PGA/PGA_{ref})/\log(2.5/PGA_{ref}) & 0 < \log(\cdots)/\log(\cdots) < 1 \\ 1 & \log(\cdots)/\log(\cdots) > 1 \end{cases} \quad \text{(II-2.3d)}$$

Table II-2.3: Site-specific parameters and weights underlying the computation of scaling factors applicable to amplification functions based on NL SRA to account for modeling uncertainty.

	PGA_{ref}	k_{max}	D	weights
Beznau	0.15	2	0.15 · {2, 1, 0, -1, -2}	0.05, 0.2, 0.5, 0.2, 0.05
Gösgen	0.2	2	0.075 · {2, 1, 0, -1, -2}	0.05, 0.2, 0.5, 0.2, 0.05
Leibstadt	0.4	2	0.15 · {2, 1, 0, -1, -2}	0.05, 0.2, 0.5, 0.2, 0.05
Mühleberg	0.1	3	0.30 · {2, 1, 0, -1, -2}	0.05, 0.2, 0.5, 0.2, 0.05

Level 5

is a placeholder, which reflects the interpolation of amplifications functions for intermediate PGA levels and the estimation of amplifications functions for non-evaluated SRA parameter sets. In general no sub-branching occurs in level 5, except for branches based on NL SRA if a sub-surface target is considered. In this case a twofold sub-branching applies, which reflects two alternative estimates of outcrop-motion from within-motion analyses.

The inter-/extrapolation procedures themselves are addressed in a separate section below.

Level 6 develops three alternative scaling functions, $C_{2D}(f)$, applicable to amplification functions in order to capture 2D and 3D effects. These scaling functions are defined by Equations II-2.4a to II-2.4f, where f is spectral frequency [Hz], z is the target layer depth [m] and where the site-specific parameters and weights are summarized in Table II-2.4. The scaling functions and weights are implemented in *sp3b_2d effects*.

$$C_{2D}(f) = A(f) \quad B(f) \quad C(f) \quad \text{(II-2.4a)}$$

$$A(f) = \begin{cases} 0 & f/f_0 < 0.7 \\ -\log(f/(0.7f_0))/\log(0.7) & 0.7 < f/f_0 < 1.0 \\ 1 & f/f_0 > 1.0 \end{cases} \quad \text{(II-2.4b)}$$

$$B(f) = C_0 \exp(-2.0\pi\zeta f L/(va)) \tag{II-2.4c}$$

$$C(f) = \begin{cases} 1 & z = 0 \\ \max[0.2, |\cos(2.0\pi f z/(va))|] & z > 0 \end{cases} \tag{II-2.4d}$$

$$\zeta = \begin{cases} 0.0125 & \text{"linear" cases} \\ 0.0125 + 0.06\,(\gamma_{max}/\gamma_{50})/(1 + 0.2\,\gamma_{max}/\gamma_{50}) & \text{EQL and NL cases} \end{cases} \tag{II-2.4e}$$

$$a = \sqrt{\frac{1}{1 + 0.2\gamma_{max}/\gamma_{50}}} \tag{II-2.4f}$$

Table II-2.4: Site-specific parameters underlying the computation of scaling factors applicable to all amplification functions to account for 2D and 3D effects, which are not considered by the 1D SRA modeling approaches.

	f_0	L	v	C_0	weights
Beznau	2.5	300	800	0.0, 0.2, 0.5	0.4, 0.4, 0.2
Gösgen	5	550	600	0.0, 0.2	0.7, 0.3
Leibstadt	3	100	600	0.0, 0.3, 0.6	0.3, 0.5, 0.2
Mühleberg	9	200	500	0.0, 0.1. 0.3	0.3, 0.6, 0.1

2.2.2 Aleatory Variability of Horizontal Motion Amplification

The site-specific change in aleatory variability of horizontal ground motion, $\sigma_h(f)$, is quantified by a one level logic tree developing three alternative scenarios:

$$\sigma_1(f) = \sqrt{\max[0.0, a_{AF}(f)\log(PGA) + b_{AF}(f)]} \qquad W_1 = W_{AF}(f) \tag{II-2.5a}$$

$$\sigma_2(f) = \sqrt{\max[0.0, a_{SA}(f)\log(PGA) + b_{SA}(f)]} \qquad W_2 = W_{SA}(f) \tag{II-2.5b}$$

$$\sigma_3(f) = 0 \qquad W_3 = 1 - (W_1 + W_2) \tag{II-2.5c}$$

where the coefficients a_{AF}, b_{AF}, a_{SA} and b_{SA} and the weights W_{AF} and W_{SA} are functions of spectral frequency, which are provided as electronic attachment to the evaluation summary EG3-ES-1014 (see part II, chapters 1.10 to 1.14).

This uncertainty $\sigma_h(f)$ is considered a site-effect-specific variability, which is additional to the variability already included in the rock hazard. For certain frequency/PGA/site combinations P.-Y. Bard considers an overall variability reduction (reduction from rock to soil hazard), which he expresses by means of negative-valued terms $(a\log(\text{PGA}) + b)$ in Equation II-2.5b. The TFI decided, that the variability reduction should be neglected for the implementation. Zero site-effect-specific aleatory variability is assumed in such cases.

2.2.3 Maximum Horizontal Ground Motion

The logic tree for maximum horizontal ground motion (Figure II-2.2) features 3 levels of branching.

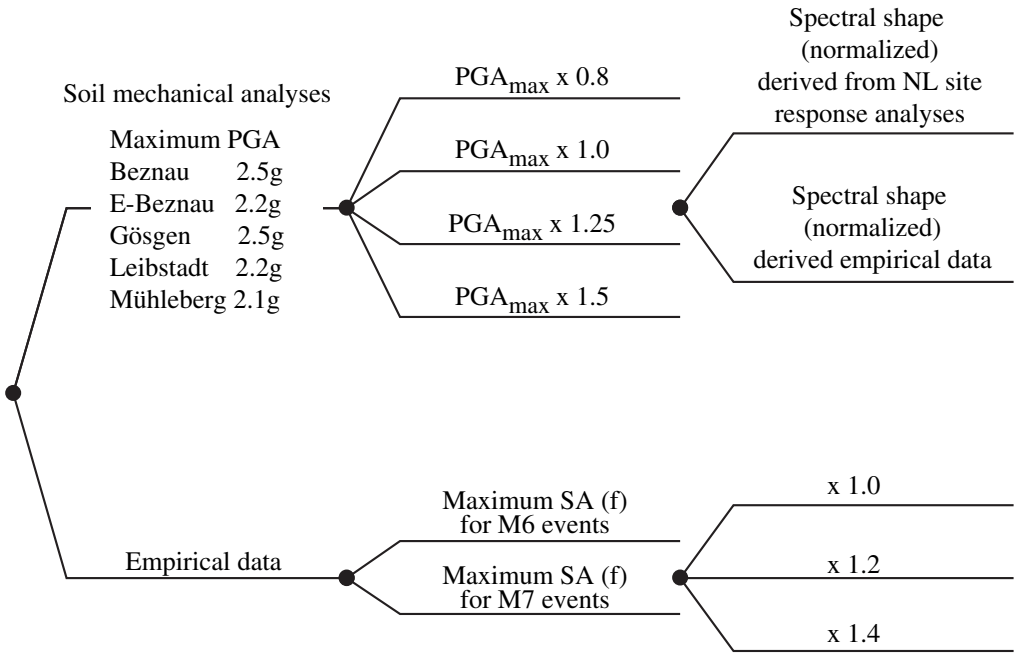

Figure II-2.2: Logic tree model, which develops maximum acceleration spectra for horizontal ground motion.

Level 1

splits the model between modeled maximum ground motion and observed (empirical) maximum ground motion. The first branch is referred to as the "soil mechanical" approach. It is based on modeled maximum PGA values [Pecker 2011] (TP3-TB-1074). It is assigned a weight of 0.333 except for subsurface targets at Beznau and Mühleberg in which case the weight is zero. The second branch is referred to as the "empirical" approach. Maximum ground motion spectra are derived from a waveform database [Strasser 2012]. Its weight is complementary to that of the soil mechanical approach.

Level 2

develops the maximum ground motion spectra. On the soil mechanical branch two alternative spectral shapes (S1 and S2) are multiplied with the maximum PGA value. S1 is the PGA-normalized acceleration spectrum resulting from the site-specific NL SRA for 2.5 g and profile 1 (or profile 6 at Gösgen). In case of sub-surface targets this shape is scaled to correct from outcrop to within motion. S2 is given in Table II-2.5. On the empirical branch two smoothed composite spectra for $M6$ and $M7$ respectively are developed. These spectra (S3 and S4) are specified in Table II-2.5.

Level 3

develops alternative scaling factors, which are applied to the spectra to account for epistemic uncertainty. Scaling factors and corresponding weights depend on the first level of branching and reflected in Figure II-2.2.

Table II-2.5: Spectral shape (S2) and spectral acceleration (S3 and S4) utilized in the maximum horizontal ground motion model. (*The values for 0.1 Hz were extrapolated by SP4 based on the "nearest neighbor".)

Frequency [Hz]	0.1*	0.5	1	2.5	5	10	20	33	50	100
S2 [-]	0.21	0.21	0.55	1.5	2.07	1.91	1.31	1.13	1.05	1
S3 [g]	2.36	2.36	2.58	3.15	3.09	3.93	1.59	1.4	1.36	1.32
S4 [g]	2.36	2.36	2.58	3.87	5.71	5.1	5.91	2.85	2.65	2.55

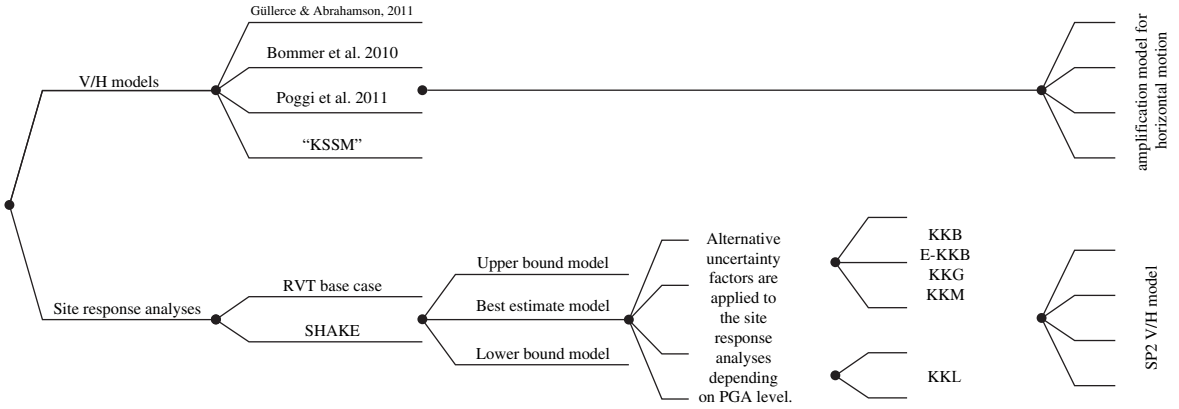

Figure II-2.3: Logic tree model, which develops V/H scaling factors and site-specific amplification factors.

2.2.4 V/H Scaling and Amplification of Vertical Ground motion

The logic tree model of site effects of vertical motion (Figure II-2.3) is a composite model, which separates at

Level 1

into two main branches: One branch considers V/H ratios defined by the SP3 expert and the logic tree model for amplification of horizontal ground motion. 60% weight is assigned to this branch. The other main branch (40% weight) develops amplification functions for vertical ground motion and is expanded by the V/H model by the SP2 experts.

Level 2 on the SP3 V/H branch

develops alternative V/H scaling functions. These V/H scaling functions are provided by empirical GMPEs except the Kawase et al. [2011] approach, which derives a V/H scaling function from the site response analyses. The V/H scaling functions are implemented in routines as follow: Gülerce and Abrahamson [2011] in *sp3c_vhGA10*; Bommer et al.

[2011] in *sp3c_vhABK10*; Poggi et al. [2011] in *sp3c_vhPEF11* and Kawase et al. [2011] in *sp3b_vhKSSM11*. Weights of the V/H scaling functions are given in Table II-2.6.

Level 3

and following levels **on the SP3 V/H branch** reflect to the logic tree model for amplification of horizontal ground motion.

Level 3 on the vertical motion SRA branch

develops alternative analysis methods, which are RVT base case (weight 30%) and SHAKE (weight 70%).

Level 3 on the vertical motion SRA branch

develops the three material models. Weights and implementation are identical to the horizontal motion case (Table II-2.2).

Table II-2.6: Weights assigned to the V/H scaling functions defined by SP3 (not to be confused with the SP2 V/H model, which is included into the model).

Any site	Gülerce and Abrahamson, 2011	Bommer et al., 2011	Poggi et al., 2011	Kawase et al., 2011
Surface	0.1667	0.0833	0.3333	0.4167
Embedded layers	0.0833	0.0833	0.3333	0.5000

Level 4 on the vertical motion SRA branch

develops alternative scaling factors, which are applicable to the amplifications functions in order to capture modeling uncertainty. The scaling function, $U(f)$ with f representing spectral frequency, is defined by Equations II-2.3a, II-2.3b, II-2.3d and II-2.6. The site- and target-layer-specific parameters and weights are given in Table II-2.7.

$$\kappa = \begin{cases} 1 & PGA < PGA_{ref} \\ 1 + U_a & PGA_{ref} < PGA < 2.5 \\ 2 & PGA > 2.5 \end{cases} \tag{II-2.6}$$

where U_a refers to Equation II-2.3d. These uncertainty factors (scaling functions) are implemented in *sp3b_UncertFac_vertical*.

Level 5 on the vertical motion SRA branch

develops alternative scaling functions applicable to amplification functions in order to capture 2D and 3D effects. The definition of the scaling functions is identical to the horizontal motion case as defined in Equations II-2.4a to II-2.4f. The site-specific parameters and weights are given in Table II-2.8. The scaling functions and weights are implemented in *sp3b_2d effects*.

Table II-2.7: Site-specific parameters and weights required for the computation of vertical motion modeling uncertainty factors.

		PGA_{ref} [g]	f_0 [Hz]	D	weights
Beznau	surface	0.15	5.5	-0.15, 0.0, 0.15, 0.30	0.2, 0.5, 0.2, 0.1
	z2			-0.08, 0.0, 0.08, 0.15	...
Gösgen	surface	0.2	20	-0.15, 0.0, 0.15, 0.30	
	z2			-0.10, 0.0, 0.10, 0.20	
Leibstadt	surface	0.4	7.5	-0.15, 0.0, 0.15, 0.30	
	z2			-0.10, 0.0, 0.10, 0.20	
Mühleberg	surface	0.15	23	-0.15, 0.0, 0.15, 0.30	
	z2			-0.08, 0.0, 0.08, 0.15	
	z3			-0.05, 0.0, 0.05, 0.10	

Table II-2.8: Site-specific parameter and weights underlying the computation of scaling factors applicable to vertical motion amplification factors to account for 2D and 3D effects.

	f_0 [Hz]	L [m]	v [m/s]	C_0	weights
Beznau	5.5	80	700	0.0, 0.15, 0.4	0.4, 0.4, 0.2
Gösgen	20	28	300	0.0, 0.15	0.7, 0.3
Leibstadt	7.5	30	600	0.0, 0.2, 0.4	0.3, 0.5, 0.2
Mühleberg	23	8	200	0.0, 0.07, 0.2	0.3, 0.6, 0.1

Level 6 and following levels on the vertical motion SRA branch

reproduce the V/H model by the SP2 experts. The SP2 V/H model is implemented as a table of V/H ratios provided within SP4. The V/H ratios depend on the site, the spectral frequency, magnitude and PGA (or annual probability of exceedance, respectively). Within the SP3mod software this table and the weights assigned by the SP2 experts to the GMPEs are stored in the environment variable *sp3db.sp2VH*.

2.2.5 Maximum Vertical Ground Motion

The logic tree for maximum vertical ground motion has the same structure as the "empirical data" model subset for horizontal motion (Fig. II-2.2). Two alternative composite spectra, which represent $M6$ and $M7$ events, are considered. These spectra (S5 and S6) are given in Table II-2.9. The weights and applicable scaling factors are identical to the horizontal motion case, i.e. are reflected by the numbers given in Figure II-2.2.

Table II-2.9: Spectral accelerations (S5 and S6) utilized in the maximum vertical ground motion model. (*The values for 0.1 Hz were extrapolated by SP4 based on the "nearest neighbor".)

Frequency [Hz]	0.1*	0.5	1	2.5	5	10	20	33	50	100
S5 [g]	1.83	1.83	2.64	3.15	3.09	4.45	4.25	2.94	2.27	1.61
S6 [g]	1.83	1.83	2.64	3.15	4.28	9.38	6.73	4.79	4.18	3.98

2.2.6 Inter- and Extrapolation of Amplification Functions

Amplifications functions are derived from 1D site response analyses (SRA), whereby different computational approaches (RVT, SHAKE, NL) are utilized. Primarily amplification is implemented as function of spectral frequency (referred to as "amplification function" is the following). The results of all SRAs were resampled to 60 spectral frequencies (Table II-2.10). The full parameter space of the site- and component-specific amplification functions spans spectral frequency, PGA, magnitude, material model, V_S-profile, target depth and motion type [PMT-TB-1014].

For evaluation of the SP3 model and processing of the results into SIFs the amplification functions need to be inter-/extrapolated for arbitrary PGA levels within the range 0.05 to 2.5 g. Depending on the computational approach, amplification functions for non-computed parameter sets need to be estimated from existing parameter sets. Inter-/extrapolation of amplification functions for arbitrary magnitudes within the range 4 to 8 is required in principle, but the soil hazard software covers this utilizing linear interpolation. Within this HID amplification functions are considered only for the discrete magnitude 5, 6 and 7.

RVT

Base case and randomized amplification functions for horizontal motion are available for all parameter sets (except Gösgen profile 6 discussed below). Hence they require only inter- and extrapolation of amplification functions for desired PGA. Within the PGA range 0.05 to 1.5 g linear interpolation of amplification on a log(PGA) dependence is performed per spectral frequency. For PGA levels above 1.5 g extrapolation factors are defined per spectral frequency, which scale the RVT amplification function for 1.5 g. The extrapolation factors are based on SHAKE amplification functions in case of Gösgen site or NL amplification functions for other sites. They are defined as ratio, where the denominator is the SHAKE or NL amplification function for 1.5 g and where the numerator is the SHAKE or NL amplification function for the desired PGA level. This numerator amplification function is interpolated from the respective 1.5 g and 2.5 g amplification functions using linear interpolation of amplification in log(PGA) space. In case of Gösgen profile 6 the RVT amplification function is estimated by scaling the amplification function for profile 1, where the scaling function are ratios of the PGA-closest SHAKE amplification function for profile 6 in the numerator and the PGA-closest SHAKE amplification function for profile 1 in the denominator. Inter-/extrapolation of RVT amplification functions for horizontal motion is implemented in *sp3b_interpAF_RVT*.

SHAKE

Amplification functions for horizontal motion are available for all parameter sets. Therefore only inter- and extrapolation of amplification functions for the desired PGA is required. For Gösgen site SHAKE amplification functions cover the full PGA range of 0.05 g to 2.5 g. These amplification functions are interpolated for the desired PGA level using linear interpolation on log(PGA) scale. For the other sites SHAKE amplification functions for arbitrary PGA are derived from scaling the RVT (base case) amplification function for desired PGA by SHAKE/RVT ratios. The SHAKE/RVT ratios (per spectral frequency) are based on the SRA effectively available in the database and they are linearly interpolated for desired PGA on log(PGA) scale. For desired PGA larger than 1.5 g the SHAKE/RVT ratio at 1.5 g is utilized.

Inter/extrapolation of SHAKE amplification functions for horizontal motion is implemented in *sp3b_interpAF_SHAKE*.

Non-linear

NL amplification functions for horizontal motion are available only for some parameter sets. Therefore inter-/extrapolation for desired PGA is required and a scheme for estimating NL amplification functions at parameter sets, for which no NL SRA are available, is required. The concept is to obtain the SHAKE amplification function (AF_{SHAKE}) for anticipated the PGA level and parameter set and to scale it by a correction functions ($C_{NLSHAKE}$ and C_{WO}) to estimate the anticipated NL amplification function (AF_{NL})

$$AF_{NL} = AF_{SHAKE} \cdot C_{NLSHAKE} \cdot C_{WO}. \tag{II-2.7}$$

The correction $C_{NLSHAKE}$ is a function of spectral frequency, is implemented in *sp3b_ratNLSHA* and is defined as

$$C_{NLSHAKE} = C_{Mat} \cdot C_{PGA} \cdot C_{Profile} \cdot AF_{NL,P1,m2}/AF_{SHAKE,P1,m2}, \tag{II-2.8}$$

where

- $C_{Mat} = AF_{NL}$ (anticipated material) / AF_{NL} (best est. mat.) for the primary profile, $M6$, PGA=0.75 g,
- $C_{PGA} =$ $AF_{RVT_{bc}}$ (anticipated PGA) / $AF_{RVT_{bc}}$ (PGA=0.75 g) for the anticipated parameter set,
- $C_{Profile} =$ $AF_{RVT_{bc}}$ (anticipated profile) / $AF_{RVT_{bc}}$ (primary profile) for the anticipated parameter set,
- $AF_{NL,P1,m2} =$ the NL amplification for the primary profile, best estimate material model interpolated for the anticipated PGA level,
- $AF_{SHAKE,P1,m2} =$ the SHAKE amplification for the primary profile, best estimate material model interpolated for the anticipated PGA level; note that here the SRA results of 2010 are used.

The correction C_{WO} attempts to scale the amplification function from "within" motion to "outcrop" motion type. For surface targets this scaling is not applicable, i.e. C_{WO} takes a value of 1. For sub-surface targets two alternative C_{WO} scaling functions are defined resulting in a twofold sub-branching. For details of the C_{WO} scaling functions the reader is referred to Section 1.2.6 of part II, chapter 1 [EG3-ES-1014].

Equations II-2.7 and II-2.8 and C_{WO}-related sub-branching is implemented in *sp3b_interpAF_NL*.

The amplification function $AF_{NL,P1,m2}$ for desired PGA within the range of 0.4 g to 1.5 g is obtained by linear interpolation on log(PGA) scale of the existing NL SRA. For PGA levels larger than 1.5 g the NL amplification function is estimated on the basis of ratios from the NL SRA_s for 1.5 g and 2.5 g available for the upper bound material model. For further technical details of this step the reader is referred to Section 1.2.4 of part II, Chapter 1 [EG3-ES-1014]. This procedure is implemented in *sp3b_interpAF_NLp1m2*.

RVT base case and SHAKE for Vertical Motion

Amplification functions for **vertical motion** are required only for parameter sets available in the SRA database. For PGA levels within the range 0.1 g to 0.75 g amplification factors are linearly interpolated on a log(PGA) scale per spectral frequency using the existing analyses for 0.1, 0.4 and 0.75 g. For PGA levels below 0.1 g or above 0.7 g the PGA-nearest amplification function is adopted. Inter-/extrapolation of RVT and SHAKE amplification functions for vertical motion is implemented in *sp3b_interpAF_vertical*.

2.3 Model Implementation and Review History

The development of the models by the SP3 expert and its implementation by SP4 were carried out contemporary when partial model descriptions became available. P.-Y. Bard's model was implemented on the basis of evaluation summary EG3-ES-1014 (see part II, Chapter 1), version 4 of 4. July 2011, version 7 of 18. October 2011, version 8 of 24. March 2012 and version 9 of 14. August 2012; and workshop presentations on 17. March 2011 [TP3-RF-1350], 6. July 2011 [TP3-RF-1383] and 19. December 2011 [TP3-RF-1433]; and e-mail communications of 26. and 27. April 2013. The model implementation has been adjusted to the revised evaluation summary version 9 of 14. August 2012 and version 10 of 20. August 2013.

The models are implemented by means of four programs addressing aspects as follow:

- *HM_SP3_Bard*
  - Amplification of horizontal ground motion;
  - Aleatory variability of horizontal motion amplification.
- *MaxHM_SP3_Bard*
  - Maximum horizontal ground motion.
- *VM_SP3_Bard*
  - Amplification of vertical ground motion;
  - V/H scaling factors;
  - Aleatory variability of vertical motion amplification (if defined by SP3) and V/H scaling.
- *MaxVM_SP3_Bard*
  - Maximum vertical ground motion.

These programs are part of the "SP3mod" software Hölker [2012] (TP4-HSW-1002), which is designed as MATLAB toolbox with an associated database holding the site response analyses and described in Hölker [2013b] (TP4-TN-1197). MATLAB releases 2011a to 2012b have been utilized for development and model evaluation.

P.-Y. Bard reviewed the implementation (MATLAB code) of the models in meetings held on 10. May 2011, 5. July 2011 and 3. September 2012. S. Thomassin provided an external review of the implementation of the horizontal motion models in August 2012 and of the vertical motion models in January 2013.

2.4 Model Evaluation

All models have been evaluated per site (Beznau, Gösgen, Leibstadt and Mühleberg) and target layer (surface and one or two sub-surface layers) as defined in table 1 of Renault [2011a] (PMT-TN-1139) or section 4.2 of Renault and Abrahamson [2010] (PMT-TB-1014), respectively. The parameter space is spanned by magnitude, peak ground acceleration (PGA) and spectral frequency, which are discretized as detailed in Table II-2.10.

The model for E-Beznau site has been last evaluated in December 2012 and became obsolete with the revised SHAKE and RVT analyses of April 2013. Final model evaluations for Beznau, Gösgen, Leibstadt and Mühleberg were performed in September 2013.

Table II-2.10: Discretization of the parameter space of the SP3 models

Parameter	Discretization
Magnitude	5, 6, 7
PGA [g]	0.05, 0.1, 0.15, 0.2, 0.25, 0.3, 0.4, 0.5, 0.6, 0.75, 1.0, 1.25, 1.5, 1.75, 2.0, 2.25, 2.5
Freq. [Hz]	0.2, 0.3, 0.4, 0.5, 0.8, 0.9, 1, 1.1, 1.2, 1.3, 1.5, 1.8, 2, 2.2, 2.3, 2.5, 2.7, 2.9, 3, 3.1, 3.2, 3.4, 3.5, 4, 4.4, 4.5, 5, 5.3, 5.4, 5.5, 5.6, 5.7, 5.75, 5.9, 6, 6.9, 7, 8, 8.9, 9, 10, 11, 12, 13, 14, 15, 17, 20, 22, 25, 30, 33, 40, 45, 50, 60, 70, 80, 90, 100

2.5 Processing of Model Results into SIFs (SP3-to-SP4 interface)

The logic tree models for amplification and aleatory variability yield a set of amplification and aleatory variability functions and associated weights. For amplification (or equivalently aleatory variability) these results may be described as

$$AF_i(f, PGA, M) \quad \text{and} \quad W_i(f, PGA, M) \quad \text{for } i = 1, 2, \ldots, n \tag{II-2.9}$$

where i is the indexing of logic tree branches, f is spectral frequency, PGA is peak ground acceleration, M is magnitude, AF is amplification and W is the associated weight.

Two modifications are applied to the data representation when the results are processed into a SIF: The n logic tree branches are summarized into 17 fractiles (Tab. II-2.11) taking into account the weights of the branches. The parameter space dimension PGA is scaled to spectral accelerations (SA), where the relation between SA, PGA and frequency is given by the spectra used as input motions for the site response analyses. Given these two modifications the amplification (and equivalently aleatory variability) results are represented in the SIF by

$$AF_j(f, SA, M) \tag{II-2.10}$$

where j is the index of the discrete fractiles defined in Table II-2.11.

The logic tree models for maximum ground motion yield maximum spectral acceleration values on soil, $maxSA_i(f)$, and associated weights $W_i(f)$, where i is the indexing of logic tree branches and f is spectral frequency. Concerning the SIF these results are summarized into 17 discrete fractiles, if the number of logic tree branches exceeds 17.

Otherwise the native $maxSA$ spectra and associated weights are transcribed to the SIF.

The aim of summarizing the model results to 17 fractiles is to reduce the number of combinations required in soil hazard evaluation, which is motivated by maintaining acceptable computing time. The 17 fractiles are associated with fixed weights as given in Table II-2.11. These weights are derived from bin width, where the fractiles are bin centers and where the bin bounds are the mean values of neighboring fractiles or 0 or 1, respectively.

The site effect model for vertical motion features two components:

(a) Amplification factors, which conceptually are to be applied to vertical motion rock hazard, and

(b) V/H scaling factors, which are to be combined with the horizontal motion amplification factors and to be applied to horizontal motion rock hazard.

For SIF processing of the vertical motion model additionally the V/H scaling models by the SP2 experts are imported and are applied to component (a). This way both model components describe V/H scaling and amplification and can be processed into a single SIF, which is applicable to the horizontal motion rock hazard.

The details of the SP3-to-SP4 interface processing are described in Hölker [2013b] (TP4-TB-1197).

Table II-2.11: Discrete fractiles and associated weights utilized to summarize the logic tree model results.

Percentiles	0.13, 0.62, 2.28, 5, 10, 20, 30, 40, 50, 60, 70, 80, 90, 95, 97.72, 99.38, 99.87
Weights	0.00375, 0.01075, 0.0219, 0.0386, 0.075, 0.10, 0.10, 0.10, 0.10, 0.10, 0.10, 0.10, 0.075, 0.0386, 0.0219, 0.01075, 0.00375

2.6 Results: SIFs (Soil Input Files or SiteMod Files)

The raw logic tree model results (intermediate model results) and the SIF-processed model results are saved into so-called "SiteMod" data structures in MATLAB format. A "SiteMod" data structure contains the SIF required by the soil hazard software and it additionally contains the unprocessed logic tree model results for the parameter space described in Table II-2.10. The details and internal format of the "SiteMod" data structure are described in Hölker [2013b] (TP4-TN-1197). Furthermore each "SiteMod" data file contains a descriptive self-documentation. The model result files associated with this HID are:

- SiteMod.Beznau.Bard.z1h.FullModel.mat
- SiteMod.Beznau.Bard.z1v.FullModel.mat
- SiteMod.Beznau.Bard.z2h.FullModel.mat
- SiteMod.Beznau.Bard.z2v.FullModel.mat

- SiteMod.Goesgen.Bard.z1h.FullModel.mat
- SiteMod.Goesgen.Bard.z1v.FullModel.mat
- SiteMod.Goesgen.Bard.z2h.FullModel.mat
- SiteMod.Goesgen.Bard.z2v.FullModel.mat

- SiteMod.Leibstadt.Bard.z1h.FullModel.mat
- SiteMod.Leibstadt.Bard.z1v.FullModel.mat
- SiteMod.Leibstadt.Bard.z2h.FullModel.mat
- SiteMod.Leibstadt.Bard.z2v.FullModel.mat

- SiteMod.Muehleberg.Bard.z1h.FullModel.mat
- SiteMod.Muehleberg.Bard.z1v.FullModel.mat
- SiteMod.Muehleberg.Bard.z2h.FullModel.mat
- SiteMod.Muehleberg.Bard.z2v.FullModel.mat
- SiteMod.Muehleberg.Bard.z3h.FullModel.mat
- SiteMod.Muehleberg.Bard.z3v.FullModel.mat

The token "z1h" indicates target layer and wavefield component, where "z1" is surface, "z2" is the upper embedded layer and "z3" is the lower embedded layer (as per table 1 PMT-TN-1139) and where "h" is horizontal motion and "v" is vertical motion.

The token "FullModel" indicates that the file contains a full SP3 model. Other files, which contain model subsets only exist and have been created for parameter sensitivity analyses.

All SIFs (SiteMod files) are applicable to horizontal motion rock hazard results !

The SIFs for horizontal motion contain amplification models only while the SIFs for vertical motion contain combined amplification and V/H scaling models.

2.6.1 SIF Figures

The model results, i.e. the content of the "FullModel" SIFs listed in the previous section, have been systematically visualized by means of seven figures types:

- XY graph showing amplification versus PGA for selected spectral frequencies;
- An image display showing median amplification versus PGA and frequency;
- XY graph showing amplification versus SA on rock for a set of spectral frequencies;
- An image display showing the ratio of the 80% over the 20% fractile of amplification versus PGA and spectral frequency;
- XY graph showing maximum acceleration on soil versus spectral frequency;
- An image display showing median aleatory variability versus PGA and frequency (for horizontal motion only);

- An image display showing mean aleatory variability versus PGA and frequency (for horizontal motion only);

which are attached to this HID as an electronic appendix containing PNG and EPS files. Examples of these figures are discussed in Hölker [2013b] (TP4-TN-1197).

Chapter 3

Appendix to EG3-HID-1005 for P.-Y. Bard

A direct link to files for the final SP3 hazard feedback is given here:

Horizontal Motion Amplification Functions and Maximum Ground Motion

- Ratio of the 80% over the 20% fractile of amplification versus PGA and spectral frequency:
  Open external file: FigSIF.Bard.HM.AMPFp80p20-PGA-FREQ.
- Amplification versus PGA for selected spectral frequencies:
  Open external file: FigSIF.Bard.HM.AMPF-PGA.
- Amplification versus SA on rock for a set of spectral frequencies:
  Open external file: FigSIF.Bard.HM.AMPF-SA.
- Mean amplification versus PGA and frequency:
  Open external file: FigSIF.Bard.HM.MeanAMPF-PGA-FREQ.
- Median amplification versus PGA and frequency:
  Open external file: FigSIF.Bard.HM.MedAMPF-PGA-FREQ.
- Maximum acceleration on soil versus spectral frequency:
  Open external file: FigSIF.Bard.HM.MaxGM.

Horizontal Motion Aleatory Variability

- Median aleatory variability versus PGA for a set of spectral frequencies:
  Open external file: FigSIF.Bard.HM.AVAR-PGA.

- Median aleatory variability versus PGA and frequency:
  Open external file: FigSIF.Bard.HM.AVAR-PGA-FREQ.
- Aleatory Variability versus SA for a set of spectral frequencies:
  Open external file: FigSIF.Bard.HM.AVAR-SA.

Horizontal Motion Amplification Functions and Maximum Ground Motion

- Ratio of the 80% over the 20% fractile of amplification versus PGA and spectral frequency:
  Open external file: FigSIF.Bard.VM.AMPFp80p20-PGA-FREQ.
- Amplification versus PGA for selected spectral frequencies:
  Open external file: FigSIF.Bard.VM.AMPF-PGA.
- Amplification versus SA on rock for a set of spectral frequencies:
  Open external file: FigSIF.Bard.VM.AMPF-SA.
- Mean amplification versus PGA and frequency:
  Open external file: FigSIF.Bard.VM.MeanAMPF-PGA-FREQ.
- Median amplification versus PGA and frequency:
  Open external file: FigSIF.Bard.VM.MedAMPF-PGA-FREQ.
- Maximum acceleration on soil versus spectral frequency:
  Open external file: FigSIF.Bard.VM.MaxGM.

Chapter 4

QA-Certificate EG3-QC-1064

QA Certificate	PEGASOS REFINEMENT PROJECT
EG3-QC-1064	

Hazard Input Document (HID)

Expert group:	**EG3**	***HID designation:***	**EG3-HID-1005**
Expert:	P.-Y. Bard	***Expert Model (EXM)***	EG3-EXM-1005

HID parameterisation of Expert Model:

TFI:	N. A. Abrahamson	***Hazard Input Specialist of TFI-team:***	A. Hölker

HID based on Elicitation Documents: ☒ EG3-ES-1014

HID based on Exp. Assessments (EXA): ☒ EG3-EXA-1033

Remarks on the HID model parameterisation in terms of hazard computation input:

The undersigned Hazard Input Specialist confirms that this HID includes all required (subproject specific) input information for hazard computations. No further interpretations of this input will be required and no simplifications except Algorithmic Pinching according to paragraph 2.9 of the QA-Guidelines will be applied to convert this HID into hazard software Input Files.

Signature:

HID acceptance by the Expert / Expert Group:

Date of HID review by the Expert / Expert group: 02.12.2013

HID accepted: ☒ ***HID not accepted:*** ☐

Reasons for non-acceptance of HID / Recommendations:

None, except the regret that the reduction of sigma in some cases with strong non-linearities cannot be implemented.

The undersigned Expert(s) accept(s) the parameterisation proposed in this HID as a faithful and adequate representation of his/their Expert Model. He/they confirm(s) that this HID is free of errors and agree(s) to its use as hazard computation input.

Signature Expert 1 / Expert:

Signature Expert 2:

Signature Expert 3:

Part III

Assessments of Donat Fäh

Chapter 1

Evaluation Summary (EG3-ES-1015) of D. Fäh

1.1 Introduction

This evaluation summary describes a possible way to estimate the amplification of seismic waves during strong earthquakes at the four existing and three originally planned NPP sites in Switzerland. This includes an evaluation of the aleatory variability, and of the maximum possible ground motion. The amplification function is different at the sites, and depends on the ground motion level, the magnitude, and the characteristics and geometry of the soft sediment cover. Epistemic uncertainty is introduced in order to account for the uncertainties of the model parameters and the modeling techniques. This document is based on the assessment during the PEGASOS project with specific changes in the logic tree structure due to new data, and due to changes in the procedure, mainly related to interface issues between SP2 and SP3.

1.2 Median Amplification of Horizontal Ground Motion

1.2.1 Approach

This part describes the general concept to estimate amplification at a specific site with the logic tree approach. Compared to PEGASOS, PRP performed extensive measurements of shear wave velocities, shear moduli and damping curves as a function of strain for the soils at the NPP sites. This work was carried out by the NPPs according to the project specifications defined in PMT-TB-1010 [Renault et al. 2008]. This additional data and the better description of material properties is the main reason for specific changes in the logic tree originally proposed. The scheme is based on four levels of ground motion, and the possible physical models that approximate the behaviour of the soils at that ground motion level. At a certain level the site can behave in different ways. This is treated with different branches in the logic tree. The level of epistemic uncertainty increases with an increase in shaking. The ground motion levels and the related physical models are as follows:

Level 1: The physical model is based on the equivalent linear theory.

Level 2: Non-linear behaviour or equivalent linear models are used.

Level 3: Mostly non-linear behaviour of the soil is expected.

Level 4: The soil column is expected to fail.

For example at level 1.2.1, the site response can be either non-linear or described by an equivalent-linear model with different degrees of non-linear behaviour. The SP3 experts defined the models for the one-dimensional site response analyses to be carried out, such that soil amplification can be calculated at the locations of the Swiss nuclear power plants. The intention of the SP3 experts was to keep the number of models as low as possible in order to reduce the computational effort for the site-response calculations. The specifications on 1D site response calculations for NPP sites are defined in report PMT-TB-1014 [Renault and Abrahamson 2010]. The specifications cover three methodologies for the site response analyses: equivalent linear frequency domain analysis using program SHAKE, equivalent linear Random Vibration analysis (RVT) and full non-linear time domain analysis (NL). RVT is used for randomized soil profiles whereas SHAKE and non-linear runs are not using any soil randomization procedure. Computations are available for a broad range of ground motion parameters with Random Vibration Theory (RVT using different software), SHAKE and truly non-linear methods (using software Sumdes and Dynaflow). All computations are listed in report PMT-TN-1139 [Renault 2011a]. The starting point in the logic tree are the results obtained from these one-dimensional modeling techniques. All other effects are treated with correction factors.

Computations with SHAKE and RVT have been performed in 2010 and repeated in 2013, due to changes in the site-specific kappa models for the rock conditions at depth assessed by SP2 experts.

All these one-dimensional computations have some advantages (+) and disadvantages (-). They are summarized in the following list:

1. In equivalent-linear RVT approach to develop amplification factors, the motion is propagated from the source to the site using the single- or double-corner source model. In PRP the single-corner source model and attenuation properties of the Swiss stochastic model [Edwards et al. 2010] is used to generate the input ground motion by varying source distance and stress-drop (Comment by N. Abrahamson "Development of Spectra for RVT Calculations" July, 29, 2010). Generally ground motion at long periods is overpredicted with a single corner source model. The point source stochastic parameters for each site are given in PMT-TN-1084 to compute the amplification functions in 2010. The duration model to be used for each site to be associated with the response spectra is specified in TP2-TN-1097. This site specific definition of input motions was using the findings for the rock properties at the sites of Swiss NPPs proposed in 2010. Specifically the kappa values were low when compared with the final assessment of the SP2 experts in 2013. In order to model high PGA values, a high stress-drop was needed in RVT computations, which results in a high input ground-motion over a broad frequency band and long duration. Due to the low kappa values selected to generate the input motion,

the resulting amplification function at high frequencies above 10Hz were much smaller than those obtained with SHAKE. In 2013 all computations were repeated assuming a kappa value between 0.025 for KKM and 0.020 for KKG (Report PMT-AN-1132). These values were derived by fitting the uniform hazard spectra for different return periods. The resulting kappa values however seem to be high when compared with the estimates of the SP2 expert, resulting in the possible problem that the amplification function at high frequency might be overestimated in the 2013 computations. Still the amplification functions above 10Hz obtained by RVT are generally slightly smaller than those obtained by SHAKE, and a higher weight is given to the RVT results for higher frequencies.

RVT is always used without soil randomisation, because the randomisation leads to a reduction in the amplification factor due to the averaging of results from different velocity structures. Randomization corresponds to an averaging over models, and therefore, results cannot directly be compared to SHAKE and non-linear runs. For this reason, amplifications from specified profiles (base cases, and selected profiles from the set of randomized profiles) are only used. Different software is used by the different contractors. While Software STRATA (site Mühleberg) and RASCALS (sites Beznau and Leibstadt) utilize standard results from random-vibration theory, the results from APASHAKE (site Gösgen) applies a different formulation for the peak-to-RMS factor that is simliar to the one applied by Dr. Walter J. Silva during the PEGASOS project, together with a correction factor accounting for 'additional' non-linear behaviour. According to W. Silva this additional correction factor compensates for the tendency of equivalent-linear results to over-predict the amplitude of resonances when compared to non-linear modelling (see also Rathje and Ozbey, 2006). This factor is not applied in PRP because it corresponds to an adjustment for non-linear behaviour that is taken care of in the proposed logic trees. The factor depends on the velocity profile, and is only important for large velocity contrasts between bedrock and sediments, and for resonance frequencies above 3 Hz (Kottke and Rathje, 2013). While the factors are higher at the fundamental frequency of resonance they are lower at the troughs. Since different amplification functions for different profiles and different degrees of non-linear behaviour are averaged when applying the logic tree, amplification and deamplification at least partially compensate. For APASHAKE (contractor Asfura) the amplification factors are generally lower around fo than obtained with the other methods, and therefore these results would need to be adjusted. Tests however showed that such correction is depending on magnitude, distance and input ground motion, and therefore, a correction is not straight forward. It has to remain an open issue which of the proposed peak-to-RMS factors provides more realistic ground motion estimates, but the differences from the randomization of the soil profiles are larger than the discussed effects. The advantages and disadvantages of RVT can be summarized as follows:

+ RVT is using a Swiss specific attenuation model and source model, and the rock properties (V_S, κ) at each NPP site to define ground motion in rock.
+ Result corresponds to a large number of SHAKE runs.
- RVT uses stationary random signals, which is not correct at low frequency and might be slightly too high at the fundamental frequency of resonance and too low at the troughs of the amplification function.

- RVT with single-corner point source approximation generally over-predicts ground motion at low frequencies ($< 2Hz$).

2. SHAKE is used for different scaled seismograms as input. The selected records are documented in TP5-TB-1020 for the results in 2010, and in PMT-AN-1132 for the results in 2013. The problem in selecting recorded waveforms was to find records for the requested magnitude-distance range and for unweathered rock sites, for which the shear-wave velocity is close to the reference rock velocity of the specific NPP sites. High-frequency content in the selected waveforms is small, probably due the damping in the unwanted weathered layers. No adjustment of the records was performed to enhance the high-frequency range of the waveforms in 2010. Amplification factors for response spectra at high frequency resulting from SHAKE runs are therefore high, because they are strongly influenced by the amplification at lower frequencies around 10Hz. Such amplification factors should be given lower weight when applied to GMPEs proposed by SP2, since the GMPEs are adjusted to the site specific vs30 and kappa values. In 2013 all computations were repeated assuming a kappa value between 0.025 for KKM and 0.020 for KKG (Report PMT-AN-1132). Since the kappa values are rather high, the amplification functions at high frequency for SHAKE were only slightly reduced relative to the computations in 2010.

   The advantages and disadvantages of SHAKE can be summarized as follows:

   ± No source model is needed (No source effects included).
   + "Realistic" time signals are used that are based on observation.
   - The ground motion level of the input is high because the entire spectrum is scaled as documented in TP5-TB-1020.
   - Input motions might be affected by site effects, and the high-frequency content of the ground motion is low.
   - There is only a limited number of input time-series, and average results might be affected by unwanted effects in particular waveforms.

3. Non-linear computations were performed only once in 2010 with two constitutives models (programs: SUMDES and DYNAFLOW) and were not repeated in 2013 with the new input motions. All non-linear computation used undrained conditions leading to fast pore pressure build-up in water-saturated soils. Contractors needed to estimate a large number of material parameters, which was one of the main reasons for differences in results between contractors. This different parameter selection introduced epistemic uncertainty, that is accounted for in the logic tree. Originally it was planned to use combined input ground motion on the horizontal and vertical component. This however led to problems in cases during which vertical acceleration reached values larger than 1g. Because this state could not be realistically modelled, it was decided to only use input of horizontal ground motion. This decision excludes a certain type of non-linear soil behaviour. Problems occurred in the layers close to the surface in which effective stress is almost zero. Significant spikes that are considered to be numerical where produced in these layers (in the upper 2 m) for a number of computations, before the excess of

pore water pressure. Since results are very sensitive to the parameter selection, these spikes were prominent mostly for one contractor (A. Pecker). One contractor (F. Pelli) applied viscous damping to prevent these problems. Dissipation of pore pressure in the upper layers would also help, but was not applied. In the first series of computations, for some input motions liquefaction occurred at magnitude 5 that should not happen in real circumstances. A test performed by A. Pecker showed that when using the waveforms originally applied during PEGASOS, these spikes and unwanted liquefaction did not occur, which is an indicator that the ground motion level of the input motion used in PRP is significantly higher than the ones used in PEGASOS (see report on input spectra). Later adjustments by A. Pecker (PRP report TP3-TN-1174) improved the instabilities in the non-linear computations that appeared when tensile stresses developed close to the ground surface during shaking. These instabilities caused the development of high frequency peaks in the computed motions at the ground surface. Non-linear site response can also be opposite to the general expectations (from equivalent linear modeling) that amplification is increasing with increasing ground motion. Such behaviour was observed for some computations, and was also observed for particular sites in the KiK-net dataset (e.g. site IWTH25 with a thick layer of fill material). The advantages and disadvantages of the non-linear runs can be summarized as follows:

+ results are valid for high strain levels

- The ground motion level of the input is high because the entire spectrum is scaled as documented in TP5-TB-1020.
- Some parameters used in the modeling are unknown, and had to be estimated by the contractors. The parameters were probably adjusted stepwise, due to the interaction of contractors.
- There is small high frequency content in the input ground motion and amplification factors can only be used up to a certain frequency (about 20-30 Hz).
- Input motion might be affected by site effects.

Based on an evaluation of the advantages and disadvantages, RVT from the 2013 computations has been selected as the basic method to treat equivalent linear models at low ground motion levels. The RVT input ground motion seems to be more adequate at intermediate frequencies (about 2.0-10Hz, see examples in report EXT-TN-1130). A correction term introduced in the logic tree takes into account the differences between RVT and SHAKE results. For these SHAKE /RVT ratios the 2013 computations are used. The most important differences in SHAKE and RVT are the frequency content of the rock input ground motion in the 2010 computations. RVT input motion is very rich at frequencies larger than 10 Hz due to the low kappa values used. This affects the amplification functions above 10Hz, resulting in very small values. Therefore the RVT computations from 2010 are not used anymore. In order to account for the differences in modelling non-linear behaviour SHAKE/non-linear factors and non-linear/RVT factors are introduced in the logic tree. For the SHAKE/non-linear factors the 2010 computations are used, for both SHAKE and non-linear computations, because the input ground is the same in both methods. For non-linear/RVT factors, the RVT results from 2013 are used, because the frequency content of input motions are more similar to the input motion used for the non-linear computations.

The magnitude dependence of the amplification factor is taken into account stepwise for given magnitude ranges. Three ranges are selected M = 5 - 6, M = 6 - 7, M = 7 - 8. Most computations performed to estimate site amplifications are applying a high input ground-motion for the given magnitude.

The equivalent linear model is considered to be not valid anymore when a strong reduction of the average shear-wave velocity, V_S, of the soils is observed [Travasarou 2002](PEGASOS report TP3-TN-0212, Part 2). Elasto-plastic behaviour should limit the V_S reduction. Table III-1.1 is giving a qualitative summary for the RVT computations performed during the PEGASOS project where a strong V_S reduction is observed. Then we have to change to ground motion level 1.2.1. In level1.2.1, non-linear behaviour becomes important, and this is treated for each NPP site. The results obtained for Leibstadt during PEGASOS are mostly caused by a soil profile that includes a cemented layer, that however was not confirmed during the site investigations during PRP. This basically will lead to changes in the general soil behaviour at site Leibstadt. There are no observed data from sites with similar geology at the NPP sites for which non-linear soil behaviour was identified (e.g. the sites of the KiK-net stations outlined in report EXT-TB-1072). However most of the data are for PGA values below 0.3 g, and therefore below the range in which significant non-linear soil response is expected.

Table III-1.1: Ground motion level at which RVT shows a strong V_S reduction. This table summarizes the assessment during the PEGASOS project . b: Beznau; g: Gösgen; l: Leibstadt; m: Mühleberg.

PGA range in g	Magnitude 5	Magnitude 6	Magnitude 7
– 0.05			
0.05 – 0.1			
0.1 – 0.2			
0.2 – 0.4		l	ll
0.4 – 0.8		gllllll	gllllll
0.8 – (1.6)	ggllllllmm	bbbgggllllllllllmm	bbbbbgggllllllllllm

When the strain reaches 0.5 - 1%, the modeling with an equivalent-linear model becomes unrealistic and we have to move to level item:Level 3. In order to estimate this limit, maximum strain has been considered in PEGASOS (III-1.2) and is assessed in III-1.3 for the soil profiles defined during PRP. During PEGASOS maximum strain were available for SHAKE runs [Travasarou 2002] (TP3-TN-0212, Part 7) and RVT computations. Maximum strains obtained with SHAKE were always larger than in the RVT runs by a factor of about 2. Table III-1.2 summarizes the maximum strains obtained from the SHAKE runs [Travasarou 2002] (TP3-TN-0212, Part 7) for ground motion PGA level 0.4 and 0.75 g for the soil profiles defined in PEGASOS.

For the computations performed during PRP in 2010 the strains reached with SHAKE are in general also significantly larger than for RVT, which could be explained by the high ground motion level of the input ground motions or the specific waveforms used in SHAKE. Single peaks in the waveforms might lead to temporary high strains, leading to high velocity reduction in specific layers, and additional increase in strain. This is a specific issue of equivalent linear modelling that might not simulate real soil behaviour.

The mean maximum strains obtained from the different profiles averaged over randomized RVT runs, at the different ground motion levels are given in Table III-1.3 for all sites. Sites Beznau and Gösgen reach similar strains. The strains reached at Leibstadt are lowest, whereas at Mühleberg site the strains in the soil layers reach very high values also at low ground motion levels. A general issue for site Mühleberg is that no laboratory test were performed with soil samples from the site. That's why non-linear computations at Mühleberg site are the most problematic and the most unreliable.

Alternatively as proposed by Pecker the ratio γ/γ_{50} could be used to define the validity range of equivalent linear models, so that when τ_{max} is reached, equivalent linear results (RVT , SHAKE) should not be used (Email communication by A: Pecker: Mai 4, 2011). This happens approximately for the condition $10 < \gamma/\gamma_{50}$. This estimate of τ_{max} was performed by Pecker, and it corresponds to an upper bound for equivalent linear models because pore-pressure built-up is not considered in RVT and SHAKE computations. The PGA level at which τ_{max} is reached is for Gösgen is 0.6g-0.7 g, Beznau 0.5-0.75 g, E-Beznau 0.35-0.7 g, Leibstadt 0.3 g, and Mühleberg 0.17-45 g. For Mühleberg, the lower values are probably a lower bound mostly due to the fact that high strains are observed within a thin layer in the soft sediments, which is not consistently observed in the entire area. For Leibstadt the maximum strains are reached at larger depth (around 20 m) as opposed to the other sites where they are reached in the top 5 m. The G/G_{max} curve for Leibstadt in depth are intended to reflect some cementation of the gravel layers and therefore the decrease of G/G_{max} with shear strain is slower than for the other sites. Since on the other hand the strength characteristics are not so high (e.g. friction angle that is too low even if the values are based on measurements) and probably do not reflect the strong supposed cementation, it turns out that the maximum strength in non-linear computations is reached at small strain levels induced by small pga's. The problem arises from the fact that the strength parameters and the G/G_{max} curve are less consistent with each other than for the other sites, and therefore the assessment is less reliable. In conclusion we can assume that the limit of reliable results for equivalent linear modelling is similar to the other sites in the range 0.4-0.7 g.

In what concerns level 1.2.1, [Pecker 2002] PEGASOS Report TP3-TN-0205 evaluated the maximum shear strain as a function of depth with a non-linear model, for an extreme case with input motion of PGA = 1.5 g at site Gösgen. Maximum shear strain at site Gösgen is 4%, mean values are at about 0.5%. In the non-linear computations with SUMDES [Pelli 2002](TP3-TB-0048) for Gösgen, one input motion produced complete failure of the soil column. This is level 1.2.1 ground motion with very large displacements, where the modelling results do not give the correct answer. Similar assessment will be discussed in a special report that will be prepared at a later stage of the PRP project. A general discussion is given in the chapter on maximum ground motion where this transition to level 1.2.1 is discussed in more detail.

Table III-1.2: Maximum strains in% obtained from the SHAKE runs [Travasarou 2002] (TP3-TN-0212, Part 7) for ground motion level 0.4 and 0.75 g.

Site	Model 1	Model 2	Model 3	Model 4
Beznau	0.1–0.5 / 0.1–1.3	0.1–0.3 / 0.1–1.3	0.1–0.3 / 0.2–1.1	
Gösgen	0.1 / 0.1–0.25	0.1–0.2 / 0.1–2.0		
Leibstadt	0.1 / 0.1–0.4	0.1–0.8 / 0.1–2.0	0.1 / 0.1–0.3	0.1–0.9 / 0.1–2.5
Mühleberg	0.02 / 0.02–0.06	0.02 / 0.02–0.12		

Table III-1.3: Mean maximum strains in % obtained from the all randomized runs for the soil profiles defined in PRP at the sites for different ground motion levels. Only the mean material property is used for this assessment. The color indicates the ground motion level introduced in Section 1.2.1.

KKB PGA range in g	Magnitude 5	Magnitude 6	Magitude 7
0.3	0.02-0.04	0.04-0.06	0.04-0.06
0.4	0.05-0.08	0.06-0.10	0.07-0.15
0.75	0.10-0.25	0.20-0.35	0.20-0.40
1	0.20-0.35	0.40-0.60	0.50-0.70
1.5	0.30-0.50	0.80-1.00	1.00-1.50

EKKB PGA range in g	Magnitude 5	Magnitude 6	Magitude 7
0.3	0.03-0.06	0.03-0.08	0.04-0.10
0.4	0.04-0.10	0.06-0.15	0.06-0.15
0.75	0.10-0.20	0.15-0.35	0.20-0.45
1	0.20-0.30	0.30-0.60	0.30-0.70
1.5	0.30-0.40	0.50-0.90	0.60-1.00

KKL PGA range in g	Magnitude 5	Magnitude 6	Magitude 7
0.3	0.02-0.04	0.02-0.06	0.03-0.07
0.4	0.04-0.07	0.03-0.08	0.03-0.09
0.75	0.06-0.10	0.07-0.15	0.08-0.15
1	0.08-0.15	0.10-0.20	0.10-0.25
1.5	0.10-0.20	0.20-0.35	0.20-0.40

KKG/KKN PGA range in g	Magnitude 5	Magnitude 6	Magitude 7
0.3	-	-	-
0.4	0.04-0.10	0.05-0.20	0.06-0.15
0.75	0.09-0.20	0.15-0.30	0.15-0.35
1	-	-	-
1.5	0.20-0.50	0.40-0.80	0.50-1.00

KKM/EKKM PGA range in g	Magnitude 5	Magnitude 6	Magitude 7
0.3	0.06-0.20	0.07-0.25	0.08-0.30
0.4	0.08-0.20	0.10-0.35	0.15-0.40
0.75	0.20-0.50	0.30-0.75	0.40-0.80
1	0.30-0.60	0.50-1.00	0.60-1.50
1.5	0.40-0.80	0.80-1.50	1.00-2.00

1.2.2 Logic Tree Structure

This section describes the general logic tree, which is applicable to all sites, and discusses its organization. The example for NPP site Beznau is used to explain the different branches of the tree. The logic tree is given in Figure III-1.1. The pair PGA / Magnitude (as discretized in III-1.2 and III-1.3) is the parameter to decide in which Ground Motion Level to start the logic tree. This is different for the NPP sites, and is given in the chapter of the respective site. The discussion provided in Section 1.2.1 provides the base for the decision. RVT input in SP3 soil response and GMPEs proposed by SP2 are intended to be adjusted to the site specific V_{S30} and κ values which relates the spectral acceleration SA at a specific frequency to the PGA value of the ground motion level. No additional complexity of the logic tree is therefore proposed. The ground motion levels and physical model for the different NPP sites are as follows:

Level 1: BASE: RVT without soil randomization (low strain) for all sites. For a given PGA, the next lower existing ground motion level of the RVT run is selected.

Level 2: BASE: non-linear (at 0.4 and 0.75 g), and RVT without soil randomization (0.2g, 0.3g, 0.4g)

Level 3: BASE: non-linear (at 0.4, 0.75, and 1.5 g). The equivalent-linear model (at 0.4, 0.75, and 1.0g) is also included, but might not be valid anymore for some profiles, and is therefore given a low weight.

Level 4: failure of the soil column; Mühleberg is expected to be the first sites to do so.

Computed amplification factors from RVT and non-linear methods are used in the branch. All other effects are treated with correction factors in the following branches. The soil profiles, the different branches and correction factors are discussed in the next chapters. The validity of this evaluation is limited to frequencies above 0.45 Hz.

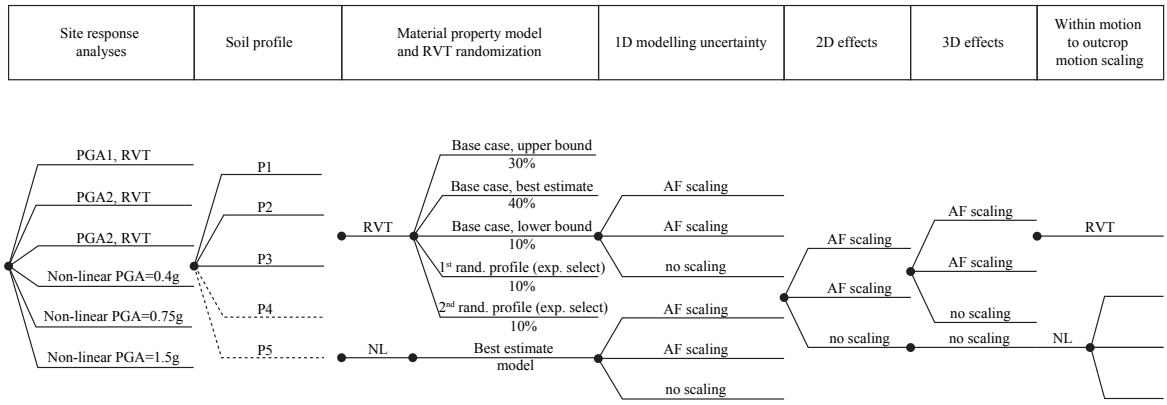

Figure III-1.1: Logic tree for NPP site Beznau, used to estimate the median ampl. of the horizontal ground motion.

1.2.3 Model Evaluations

The PEGASOS Project was conducted according to the "Senior Seismic Hazard Analysis Committee" (SSHAC) level 4. The general structure of the PEGASOS Refinement Project

(PRP) is based on the PEGASOS project. It was initially started with the intention of performing SSHAC Level 3 analyses. During the project, in 2009, it was decided to change the SSHAC Level to 4. In a SSHAC Level 4 analyses, the experts in all subprojects are requested to cover the Center, Body and Range of possible models as given/defined by the technically informed community. This section describes first the soil profiles and then the corrections applied to the amplifications in the logic tree that are common to all sites. The correction factors are in most cases functions of frequency. Some are site dependent, others not.

Soil Profile and Material Properties

The geotechnical and geophysical investigations at the nuclear power plant (NPP) sites form the basis for the definition of the soil/rock profiles for the site-response calculations. The investigations required at each site are specified in Appendix B of the project plan (PMT-TB-1010). For all sites, extensive documentation was prepared by the power plant owners and their contractors. Various models are proposed in the reports, taking into consideration the geological and geotechnical data, along with the geophysical and laboratory measurements. The structural models derived by SP3 from this material for the site-response calculation are valid for the geological structures in the approximate neighborhood of security-relevant structures like the reactor building or the emergency building. However, it is generally not possible to perform seismic measurements in their direct vicinity (except for the originally planned NPPs). The evaluation of the relevant sites has consequently to be obtained by inter- or extrapolation, taking into account all measurements at possibly similar structures in the direct vicinity. The result are a number of different possible structural models.

The SP3 experts extended the model space in order to cover the Center, Body and Range of possible models for the site-response calculation. This assessment included all geophysical measurements, even if in some cases the uncertainties of the measurements were high (e.g., for some downhole measurements). Measurements were excluded in cases where the area was outside the area of interest (e.g., for some MASW results at site Beznau) or when dispersion curves were highly questionable. The SP3 experts took into account high-frequency measures of wave velocity (sonic, cross-hole) and low frequency measures (e.g., surface wave methods), in addition to the effect of anisotropy as identified at some sites, and borehole information.

The centre, body and range issue led to an increase in the number of soil/rock models originally proposed by NPP experts. The defined models need to be within the bounds specified for the measured fundamental frequency of resonance, f_0, and for the observed dispersion curves of the Rayleigh wave fundamental mode. The f_0 is defined from the range of measured values from H/V spectral ratios, plus an additional uncertainty in the upper and lower frequency band. The fundamental frequencies of resonance of the proposed models were tested using 1D soil response analysis. The range of dispersion curves allowed is defined by a validation process of the dispersion curves obtained from ambient vibration array measurements and MASW. Also in this case the permitted range is slightly increased by the SP3 experts.

Parameters defining the non-linear behaviour are based on first priority on test results and on the experimental data published by Rollins et al. [1998] and Menq [2003]. Menq's curves take into account a dependence of G/G_{max} on the confining stress while Rollins' curves do not. Furthermore, Menq's curve corresponds to a weaker material compared to Rollins. Accordingly, examination of the G/G_{max} curves shows that Menq's mean curve coincide with

the lower bound of the tests data and Rollins mean to the upper bound. The mean curve is defined as the average between the lower bound and the upper bound curves. For damping, Rollins mean damping curve was used for the lower bound, while Menq's mean curve was used for the upper bound. From the observations and also from theory, a stiffer material exhibits lower material damping and a softer material, higher material damping. Those curves had been modified to a small extent to better fit the observed data. A problem from laboratory testing was that measured G/G_{max} curves and damping are uncorrelated, which contradicts the model assumption. Errors in laboratory testing have the effect of generally producing lower G/G_{max} curves, and therefore pushing the values to lower bounds. For these reasons less weight is given to the lower bound material properties, and weights are mainly distributed between the best-estimate curves and the upper bound.

The SP3 experts defined the models for the one-dimensional site response analyses to be carried out, such that soil amplification can be calculated at the locations of the Swiss Nuclear Power Plants. The intention of the SP3 experts was to keep the number of models as low as possible in order to reduce the computational effort for the site-response calculations.

RVT uses soil randomization in order to cover possible models with layering not resolved by the proposed models and covering the range of possible models. The soil randomization allows for variations of up to 25% on the V_S-profile, assuming log-normal distribution in each soil layer, whereas the 25% correspond to 2 standard deviations. The resulting V_S-profiles however were checked to be within the bounds specified for the fundamental frequency of resonance f_0 and the dispersion curve of the Rayleigh wave fundamental mode defined for each site. If the realizations are outside the specified bounds, alternative realizations were searched. In total, 50 feasible realizations have been provided for each original base profile (TP3-SUP-1088_V_S-profiles_selected_for_RVT.zip). From these 50 profiles 2 profiles were added to each base case in order to better define the range of possible models.

In the following weights to different models are assigned. The equivalent-linear models (modulus and damping curves) are weighted as follows for the RVT runs:

Base case, upper bound non-linear material properties with weight: 0.3

Base case, best estimate non-linear material properties with weight: 0.4

Base case, lower bound non-linear material properties with weight: 0.1

For each base profile (best estimate material) , 2 additional models from the randomization process are included, that are characterized by features of observed dispersion curves not covered by the base case. Each of the randomized profiles with weight: 0.1

For the different NPP sites, soil profiles (base cases) are weighted according to the following summary. The reason in case of an unequal weighting is provided as well.

Non-linear computation are only performed for the best estimate profile. The cases for the upper and lower material properties are used for the definition of the corrections factors. The specifc weights given to the non-linear runs are provided in the logic tree of each NPP.

- Leibstadt site (KKL)

The models (profiles) are defined in report [Renault 2010c] TP3-TN-1067. The selection of soil profiles are based on the report of project SOBE-BEL KKL (Reference Documents for site Leibstadt to PRPSP3/WS2), the experts feedback on KKL site investigation results TP3-TN-1054, and the additional data requested and provided in TP3-GTC-1010 Additional-Site-Invest-Data_KKL.zip, as well as the quality-checked dispersion curves from MASW and ambient vibration array analysis. Eigenfrequency bounds for f_0 are in the range 2.2 - 3.8 Hz. In PEGASOS, one soil profile at KKL site included a cemented layer, that however was not confirmed with the site investigations performed in PRP.

The velocity profiles proposed by the NPP experts gave a predominant weight to borehole data. In addition there was a trend for too low velocity values at very shallow depth. The amount of anisotropy in the bedrock below 41 m depth was found slightly larger than accounted for in the original velocity profiles of the NPP experts. The 3 velocity profiles proposed by the SP3 experts try to assign a balanced weight to all sources of information, i.e., both surface wave and body wave techniques.

Model P1 (MK-2-20100119) is a "hybrid" one taking into account surface wave (ambient vibrations and MASW) and body wave (cross-hole, downhole) measurements. The basic idea was to use cross-hole data in the bedrock (i.e., from top Wellenmergel at 41 m depth, which cannot be sampled with much details with surface wave techniques), and to use surface wave data for the gravel layer.

Model P2 (MK2-Crosshole-Anisotropy) is the most complex one and is based mainly on the cross-hole data, with some corrections. The very shallow velocity (top 4 m) has been assigned a 400m/s value as derived from MASW dispersion curves that have high frequency (15-25 Hz) Rayleigh wave velocities larger than this value. The correction for anisotropy of cross-hole data has been slightly increased with respect the ratios given in the TB-213-KG09003 for Wellenmergel, Wellendolomit and Buntsandstein units (according to anisotropy values reported in the document "KKL_Ratios_Anisotropy_100104.pdf").

Model P3 (DF-20100119) is the simplest one and is based on the inversion of the dispersion curves obtained from ambient vibration measurements. The original model proposal by SED has been slightly modified (slight velocity increase) at shallow depth to match the high-frequency dispersion curves derived from MASW measurements, and to match the fundamental frequency as well.

The weights to the soil profiles are given in the following Table III-1.4. P1 and P3 have equal weight. P2 has slightly lower weights because the dispersion curve is very close to the lower bound, and the profile is mainly based on high-frequency measures of wave velocity.

- Beznau site (KKB)

The models are defined in report [Renault 2010a] TP3-TN-1068. The models take into account all the information released in the report of project SOBE-BEL KKB and EKKB (Reference

Table III-1.4: Selected profiles for Leibstadt site, with the fundamental frequency of resonance of the profile and the weights used in the logic tree.

Leibstadt KKL	Base case or Nr. of the added profile from randomization	f_0 [Hz]	Weight	Comment
P1	Base case	3.4		Hybrid
(MK-2-20100119)	Profile 20	3.6	0.4	
	Profile 37	3.3		
P2	Base case	2.9		Mainly from cross-hole data
(MK2-Crosshole-Anisotropy)	Profile 26	3.1	0.2	(High frequency measurement)
	Profile 65	3.1		
P3	Base case	2.3		Mainly from ambient vibrations
(DF-20100119)	Profile 11	2.5	0.4	
	Profile 32	2.8		

Documents for site Beznau to PRPSP3/WS2), the file TP3-GTC-1009_Additional-Site-Invest-Data_KKB-EKKB, in particular the documents TN-290.05-3-Profile_NOK_postWS.pdf and Beznau_DC_V_S_comparisons, the experts feedback on KKB site investigation results "TFIRF-1149 Abrahamson_Summary_KKB-KKL", as well as the quality-checked dispersion curves from MASW and ambient vibration array analysis. Eigenfrequency bounds for f_0 are in the range 2.0 - 3.3 Hz.

The profiles first proposal by the NPP experts (KKB213D0016_Rev.0) included a reduction of the impedance contrast at the base of Opalinus Clay (higher velocities in Opalinus Clay, and lower in top Lias) compared to the previous PEGASOS velocity profiles. The proposed models were based primarily on cross-hole data, with correction factors to account for anisotropy, especially in the Opalinus Clay. The SP3 experts proposed slight modifications and assigned a balanced weight to all sources of information, i.e., both surface wave and body wave techniques. This was done by adapting the model MK1 and MK2 proposed by NPP experts, and by proposing a third model based primarily on measured dispersion curves especially for the shallow and intermediate depth ranges of the structure. The adaptations were driven by the observation that the corresponding Rayleigh wave velocities were too fast at intermediate to high frequencies in the model MK1 and MK2. This was adjusted by the introduction of some weathering at the top of the Opalinus Clay.

Model P1 (simple WOC; WOC = Weathered Opalinus Clay)is the modified MK2 model. The bedrock in P1 does not take into account the short wavelength vertical heterogeneities associated with thin layering. In the top 15 m of Opalinus Clay the velocity has been reduced between 9 and 24 m depth, removing any low velocity zones in the Opalinus Clay. The dispersion curves for P1 are consistent both with the ambient vibration dispersion curves at intermediate frequencies (because of the weathered top Opalinus Clay) and the high frequency low MASW velocities (low surface velocities in gravel).

Model P2 (complex WOC) is the modified MK1 model, with a complex velocity profile in the Lias units, following the cross-hole data. The modifications consist in reducing

the velocity down to a depth of 26 m, i.e., in the gravel layer (9m thick) and in the upper part of Opalinus Clay. With this modification the disperison curve of P2 is better matching measured dispersion curves at intermediate (ambient vibration measurements) and high (MASW) frequencies.

Model P3 (AMV) is essentially derived from the inversion of dispersion curves, which do not allow the resolution of thin layers. The base model was the model proposed by SED on the basis of array recordings of ambient vibrations, with some extrapolation at large depth on the basis of borehole data, and some reduction of velocities in the upper part of Opalinus Clay to better fit the MASW results.

Model P4 is the originally proposed MK2 model that assumes no weathered layer of Opalinus Clay. Above 10 Hz, the resulting dispersion curves are close to the upper bound defined by the SP3 experts. Such values were basically not observed with MASW.

The weights to the soil profiles are given in the following table. P1, P2 and P3 have equal weight. P4 is given the same weight because it is the only model for unweathered opalinus clay. The issue related to the measured dispersion curves remains problematic.

- Beznau site (EKKB)

The models (profiles) are defined in report [Renault 2010e], [Renault 2010b] TP3-TN-1069. The models proposed for EKKB were adapted from the KKB models taking into account the larger thickness of gravel layer, the slightly smaller depth of the top Lias, and the slightly smaller depth of the reference homogeneous bedrock (Top Gipskeuper). Eigenfrequency bounds for f_0 are in the range 2.0 - 3.3 Hz.

Model P1 (simple WOC; WOC = Weathered Opalinus Clay). The only change with respect to the KKB corresponding profiles are the depth range 9-22 m with gravel instead of Opalinus Clay with an almost linear gradient from 450m/s to 600m/s, and the changes in the depth of the Opalinus Clay to Lias interface, and the gradient has been moved upward by 8 m to match the Top Gipskeuper depth of 121 m instead of 129 m.

Model P2 (complex WOC). The changes with respect to the KKB profile are very similar to those performed for the model P1. However, the base model was the EKKB unmodified MK2 model proposed by the NPP experts. The velocity profile within the Opalinus Clay is slightly different.

Model P3 (AMV). The changes with respect to the KKB profile P3 are slightly lower velocities in the top 6 m of the gravel layer, a much thinner weathered part at the top of Opalinus Clay, a thickness change of the two homogeneous layers below Opalinus Clay and above Gipskeuper.

The weights to the soil profiles are given in the following table. Profiles P1 and P3 have equal weight, slightly higher than that for profile P2, because their dispersion curves slightly better compare with the observations. There is however no good match of none of the profiles with the observed Love wave dispersion curve.

Table III-1.5: Selected profiles for Beznau site KKB, with the fundamental frequency of resonance of the profile and the weights used in the logic tree.

Beznau KKB	Base case or Nr. of the added profile from randomization	f_0 [Hz]	Weight	Comment
P1 (simple WOC)	Base case	2.3	0.25	consistent both with the ambient vibration dispersion curves at intermediate frequencies and the high frequency low MASW velocities
(Weathered Opalinus Clay)	Profile 44	2.2		
	Profile 57	2.2		
P2 (complex WOC)	Base case	2.5	0.25	matching measured dispersion curves at intermediate ambient vibration measurements and high frequencies MASW results
	Profile 22	2.4		
	Profile 55	2.6		
P3 (AMV)	Base case	2.5	0.25	From inversion of dispersion curves, which do not allow the resolution of thin layers
(based on ambient vibration)	Profile 25	2.4		
	Profile 45	2.4		
P4 (originally proposed MK2)	Base case	2.5	0.25	Only model with no weathering of Opalinus Clay, however in disagreement with MASW results
	Profile 39	2.4		
	Profile 50	2.6		

- Gösgen site (KKG and KKN)

The models (profiles) are defined in report [Renault 2010c] TP3-TN-1070. All profiles are representative of the whole area of the KKG/KKN site as proposed by NPP experts in their original report.

The selection of soil profiles are based on report IO09-TA0618_Main_Report_June2009.pdf, the additional data requested and provided by SP3 experts in TP3-GTC-1008 Additional-Site-Invest-Data_KKG-KKN_Dez-2009.zip, the assessment in report TP3-TN-1062 Pecker_Velocity Profile_AP_Rev B.pdf, the alternative rock profiles proposed in report TP3-TN-1061 Fäh_DescriptionSummary_KKG_rock.pdf and the quality-checked dispersion curves from MASW and ambient vibration array analysis. Eigenfrequency bounds for f_0 are in the range 3.5 - 6.5 Hz. The density for the sediment layers above the ground water table is

Table III-1.6: Selected profiles for Beznau site EKKB, with the fundamental frequency of resonance of the profile and the weights used in the logic tree.

Beznau EKKB	Base case or Nr. of the added profile from randomization	f_0 [Hz]	Weight	Comment
P1 (simple WOC)	Base case	3.1	0.35	Dispersion curve slightly better compare with the observations
(Weatherer Opalinus Clay)	Profile 60	3.2		
	Profile 71	3.1		
P2 (complex WOC)	Base case	3.2	0.3	Different velocities in Opalinus Clay
	Profile 41	3.1		
	Profile 88	3		
P3 (AMV)	Base case	2.5	0.35	Dispersion curve slightly better compare with the observations
(based on ambient vibration)	Profile 62	2.4		
	Profile 63	2.5		

2.0 g/cm3 and for the layers below the ground water table 2.2 g/cm3.

In order to account for the uncertainties in the measured S-wave velocities in rock, several models for the rock are proposed that explain some of the observed features. No model explains all observations. For this reason several rock profiles need to be defined so that the range of possible rock models is covered. The models that explain the observed H/V peak at about 0.6Hz and the dispersion curves from ambient-vibration observations are models P1 and P2, which are characterized by a velocity inversion at greater depth. Model P2 takes into account the low average S-waves in rock obtained from downhole measurements at different borehole sites, whereas P1 considers the measurements from cross-hole and sonic logs in the uppermost rock layer. Both models consider an average soil-velocity profile with a total thickness of 28.5 meters. The rock reference velocity is defined as 2500m/s, which is reached at a depth of 558m for P1 and P2.

Additional models with high S-wave rock velocity are included (models P3, P4 and P5), as originally proposed by NPP experts. These rock models were derived mostly from cross-hole measurements and the sonic logs. Model P3 is based on measurements performed by NAGRA in the Swiss Foreland. In the soil layer an average soil-velocity profile is taken with a total thickness of 27.5 meters. The rock reference velocity of 2500m/s is reached at a depth of 530m. Models P4(DCmin) and P5(DCmax) are selected to cover the range of measured velocities in the soil layer, as defined by the measured dispersion curves. The rock layer is chosen assuming a constant velocity in the uppermost layer that corresponds to the rock reference velocity of 2500m/s and is reached at a depth of 27.5 m. For the non-linear calculation only one of the velocity models is chosen which corresponds to the best estimate of the proposed soil profiles. The SP3 experts agreed on the soil profile proposed in model P1. Because non-linear computations are restricted in model size and can hardly treat models of a depth of 500-600m, a new model was defined (model P6(B1*)) that combines the soil profile from model P1 with

the constant-velocity rock model as in models P4(Dcmin) and P5(DCmax). Profile P6 used for the non-linear computations is considered to be the same as profile P1. The weights to the soil profiles are the same for site KKG and KKN. They are given in the following table, by balancing between softer and harder rock on the one side, and models that explain the H/V peak at 0.6Hz and others that do not.

Table III-1.7: Selected profiles for Gösgen site, with the fundamental frequency of resonance of the profile and the weights used in the logic tree.

Gösgen KKG and KKN	Base case or Nr. of the added profile from randomization	f_0 [Hz]	Weight	Comment
P1 (B1)	Base case	5.3	0.2	Explains H/V peak at 0.6Hz From cross-hole and sonic logs
	Profile 13	6		
	Profile 36	4.8		
P2 (A2)	Base case	5.4	0.4	Explains H/V peak at 0.6Hz From down-hole data
	Profile 22	4.3		
	Profile 55	4.2		
P3 (D1 modified)	Base case	4.4	0.2	
	Profile 31	4.4		
	Profile 35	4.8		
P4 (DCmin)	Base case	5.4	0.1	Soil layers explaining the lower dispersion curves
	Profile 18	5		
	Profile 25	5.9		
P5 (DCmax)	Base case	5.7	0.1	Soil layers explaining the higher dispersion curves
	Profile 24	5.9		
	Profile 33	5.9		

- Mühleberg site (KKM and EKKM)

The models (profiles) are defined in report TP3-TN-1071. All profiles are representative of the whole area of the KKM/EKKM site. The derivation of the profiles proposed by the SP3 experts is summarized in report KKM_Profile_Proposal_Final.pdf. Four velocity profiles are proposed. Eigenfrequency bounds for f_0 are in the range 5 - 9 Hz.

Model P1 (AMEC) is the "composite" velocity profile proposed by AMEC. It is the result of a weighting of the different measurements and/or sources of information. The weights are different for the surface gravel layer, for which the largest weight is given to surface wave measurements (MASW and ambient vibrations) and SPT values, and the underlying molasse for which borehole data (downhole and cross-hole) are given the predominant weights. The corresponding velocity profile can thus be considered some kind of "average" profile. The dispersion curve of profile P1 falls within the measured dispersion curves both at high and intermediate frequencies.

The idea behind the selection of velocity profiles P2 and P3 is to include most of the variability seen from the various in-situ measurements and/or their various interpretations by different teams. Model P2 (Dcmin) includes a low-velocity gravel over an only weakly weathered molasse, model P3 (DCmax) describes a high velocity gravel layer overlying a significantly weathered molasse. The obtained disperison curves for the P2 model still correspond to slightly higher phase velocities than those observed with the ambient vibration array. It was thus decided a fourth model P4 closer to the lower bound of the dispersion curves measured in the western part of the investigation area.

The weights to the soil profiles are the same for site KKM and EKKM. They are given in the following table. Models P1, P2, P3 and P4 are weighted equally due to the variability of the rock (weathered and unweathered) in the area of interest. This spatial variability of the weathered rock is very high and cannot be mapped in detail.

Table III-1.8: Selected profiles for Mühleberg site, with the fundamental frequency of resonance of the profile and the weights used in the logic tree.

Mühleberg KKM and EKKM	Base case or Nr. of the added profile from randomization	f_0 [Hz]	Weight	Comment
P1 (AMEC)	Base case	8.9	0.25	"Composite" velocity profile
	Profile 22	7.2		
	Profile 67	7.7		
P2 (DCmin)	Base case	6.9	0.25	Low-velocity gravel over an only weakly weathered molasse
	Profile 22	7.2		
	Profile 26	6.3		
P3 (DCmax)	Base case	5.9	0.25	High velocity gravel layer overlying a significantly weathered molasse
	Profile 3	5.1		
	Profile 40	5.9		
P4 (MASW-AN)	Base case	5.6	0.25	Close to the lower bound of the dispersion curves
	Profile 66	6.3		
	Profile 83	5.3		

Factor for the 1D Modeling Uncertainty

A numerical modelling technique is always based on a physical model and some assumptions, and therefore has limits for the applicability. The factor for the 1D modelling uncertainty accounts for the differences that can result when different numerical modelling techniques are applied. Different frequency bands with different levels of uncertainty are distinguished:

$0.45Hz < f < f_0/2$: At low frequencies, amplification should not go to 1, because peseudo spectral acceleration (PSA) is computed from spectral displacement SD), and amplifica-

tion in displacement is not 1. Amplification factors obtained from RVT go to one at low frequency, and are therefore less reliable than SHAKE results. RVT does not provide fully satisfactory results at low frequency.

$f_0/2 < f < 15Hz$: Frequency range around the fundamental mode of resonance and higher.

$15Hz < f$: In the high-frequency range, the effect of the high frequency content in input ground motion is most important.

The fundamental frequency of resonance f_0 was determined from the H/V ambient vibration measurements at the NPP sites and is different for each profile (Beznau site: f_0 between 2.0 -3.3 Hz; Gösgen site: f_0 between 3.5-6.5 Hz; Leibstadt site: f_0 between 2.2-3.8 Hz; Mühleberg site: f_0 between 5.0-9.0 Hz). All models have a fundamental frequency of resonance given in Tables III-1.4 to III-1.8 that are in the range defined by SP3 for the corresponding site. In the following the f_0 values correspond to the values of the linear case, as provided in the tables.

RVT is using a Swiss specific attenuation and source model, and the specific rock properties (V_S, κ) for each NPP site to define input ground motion in rock. For RVT the 2013 computation are used due to the updated SP2 estimates for kappa. Ratios between SHAKE and RVT (base case without soils randomization), non-linear and RVT (base case without soils randomization), and SHAKE and non-linear are used to estimate the 1D modelling uncertainty. This has been performed using the computations at specific ground motion levels for all magnitudes. Because rock properties (V_{S30}, κ) are different at each NPP site, these correction factors need to be computed for each site separately. For the correction term introduced in the logic tree to account for the differences between RVT and SHAKE results, the 2013 computations are used. For the SHAKE/non-linear factors the 2010 computations are used, for both, SHAKE and non-linear computations, because the input ground is the same in both methods. For the non-linear/RVT factors, the RVT results from 2013 are used, because the frequency content of input motions are more similar to the input motion used for the non-linear computations. In addition a correction factor is applied for the non-linear branches that account for the missing runs in the non-linear computations for the different profiles (SHAKE(Profile Px)/SHAKE(Profile P1 or P6)). For the factors, the 2013 computations are taken.

First the correction factors as a function of frequency at ground motion Level 1 is assessed. SHAKE/RVT is obtained from the computations at 0.05 g, 0.1 g and 0.2 g for all common runs at one site (e.g. for Leibstadt and Mühleberg: number of profiles * 3 material properties * 3 pga levels * 3 magnitude levels). For Beznau distiction is made between KKB and EKKB. In order to compute the geometric mean of the correction factors, the factors obtained from one profile are first normalized to the profiles' f_0, and then averaged at each f/f0 value over all profiles. The correction factors SHAKE/RVT (geometric mean) are given in Figure III-1.2 for the five sites separetaly, together with the single curves for each common run and profile. The frequency axis is normalized to f_0. The non-linear/RVT factor is computed from the common runs at 0.05g and 0.4g (4 runs for Gösgen, Leibstadt and Mühleberg (NL1), 4 runs for Beznau KKB and for EKKB). The correction factors (geometric mean) are given in Figure III-1.4 for the five sites, together with the single factors for each common run. The frequency axis is normalized to f_0 for each profile.

The base for the selection of weights of the branches in the logic tree are the advantages and disadvantages of the computational methods, the problems of RVT at low frequencies and

the level of non-linear behavior as discussed in Section 1.2.1. Differences between RVT and SHAKE are specifically important at low and high frequencies. RVT computations are given a lower weight at low frequencies as discussed before.

The weights in Level 1 are as follows:

- Level 1: SHAKE/RVT at 0.05, 0.1, 0.2 g and non-linear/RVT at 0.05 g and 0.4g

Logic tree for the frequency range	$0.45Hz < f < f_0/2$:
0.65	SHAKE/RVT factor
0.3	1.0
0.05	non-linear/RVT factor
Logic tree for the frequency range	$f_0/2 < f < 15Hz$:
0.3	SHAKE/RVT factor
0.65	1.0
0.05	non-linear/RVT factor
Logic tree for the frequency range	$15Hz < f$:
0.2	SHAKE/RVT factor
0.75	1.0
0.05	non-linear/RVT factor

The SHAKE/RVT correction factor for Level 2 is derived from the results at 0.4 and 0.75g for all common cases, and is shown in Figure III-1.3. The SHAKE/non-linear factor is computed from the runs at 0.05g and 0.4g (4 runs for Gösgen, Leibstadt and Mühleberg (NL1), 4 runs for Beznau KKB and for E-KKB). The correction factors (geometric mean) are given in Figure III-1.5 for the five sites separetely, together with the single factors for each run. The frequency axis is normalized to f_0 for each profile.

In addition a correction factor is applied for the non-linear branches that account for the missing runs in the non-linear computations for the different profiles (SHAKE(Profile Px)/SHAKE(Profile P1 or P6)). The geometric mean is taken for all profiles Px (x: profile number) and material properties, and the runs at 0.4g and 0.75g (see Figure III-1.6).

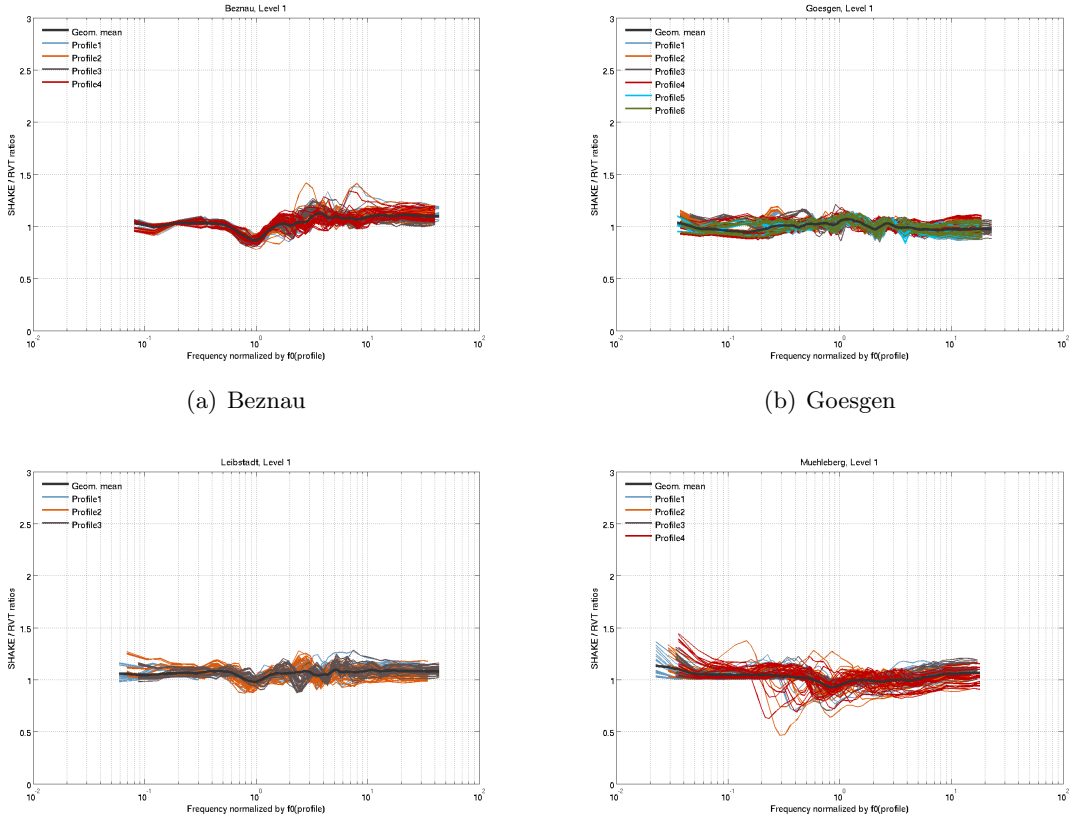

(a) Beznau

(b) Goesgen

(c) Leibstadt

(d) Muehleberg

Figure III-1.2: Correction factors SHAKE/RVT for Level 1(geometric mean) for the four sites a) Beznau KKB, b) Gösgen, c) Leibstadt and d) Mühleberg, together with the factors for each common run and profile (colors are for the different profiles). The frequency axis is normalized to f_0, the fundamental frequency of resonance of each profile.

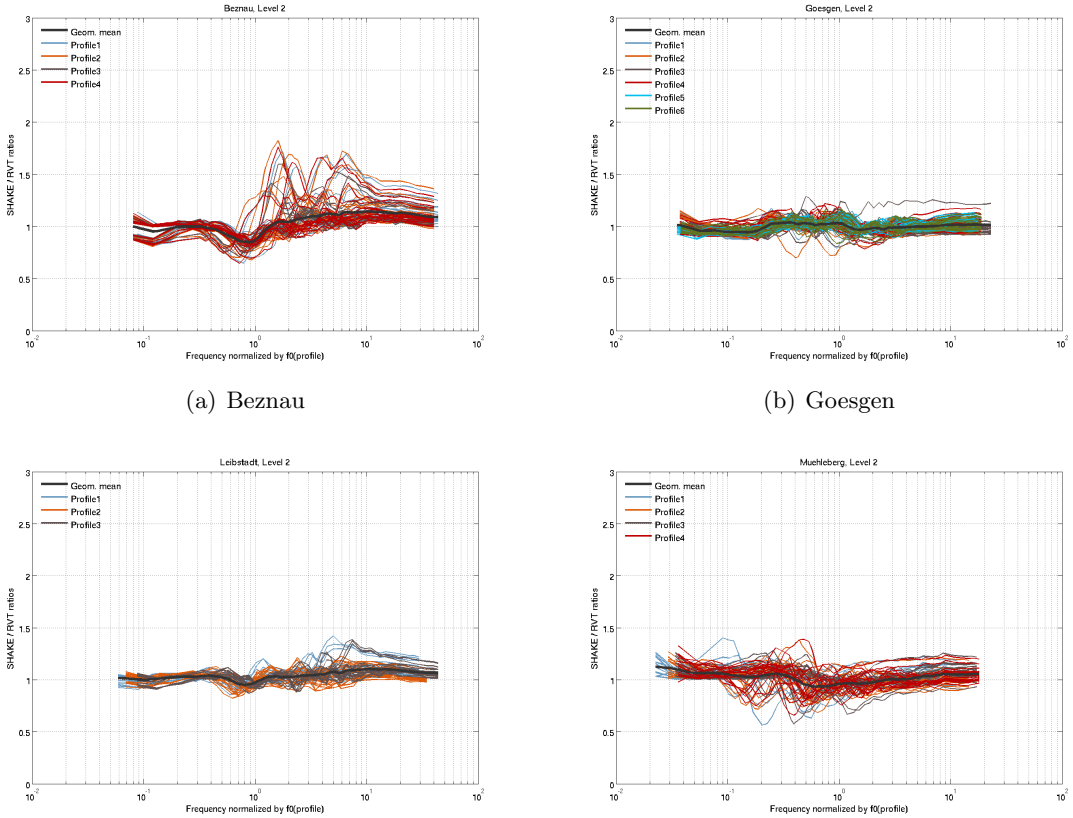

(a) Beznau

(b) Goesgen

(c) Leibstadt

(d) Muehleberg

Figure III-1.3: Correction factors SHAKE/RVT for Level 2 (geometric mean) for the four sites a) Beznau KKB, b) Gösgen, c) Leibstadt and d) Mühleberg, together with the factors for each common run and profile (colors are for the different profiles). The frequency axis is normalized to f_0, the fundamental frequency of resonance of each profile.

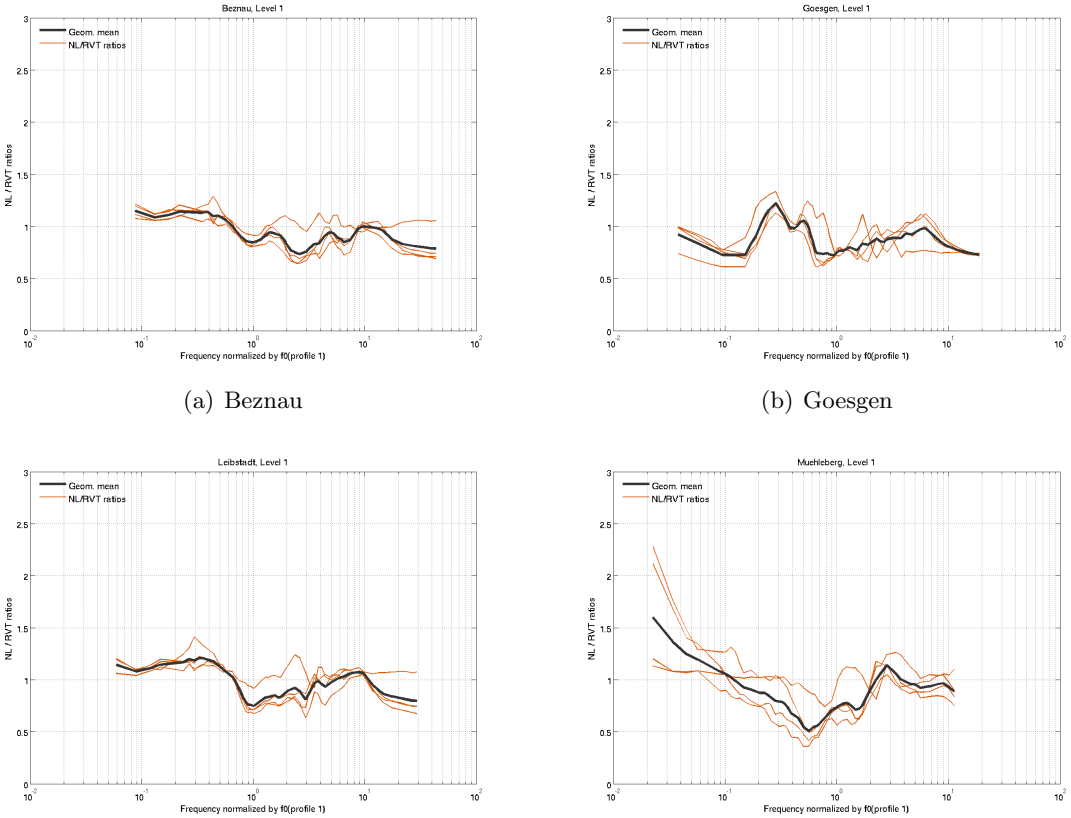

(a) Beznau

(b) Goesgen

(c) Leibstadt

(d) Muehleberg

Figure III-1.4: Correction factors non-linear/RVT (geometric mean) for the four sites a) Beznau KKB, b) Gösgen, c) Leibstadt and d) Mühleberg, together with the factors for each common run. The frequency axis is normalized to f_0, the fundamental frequency of resonance of each profile.

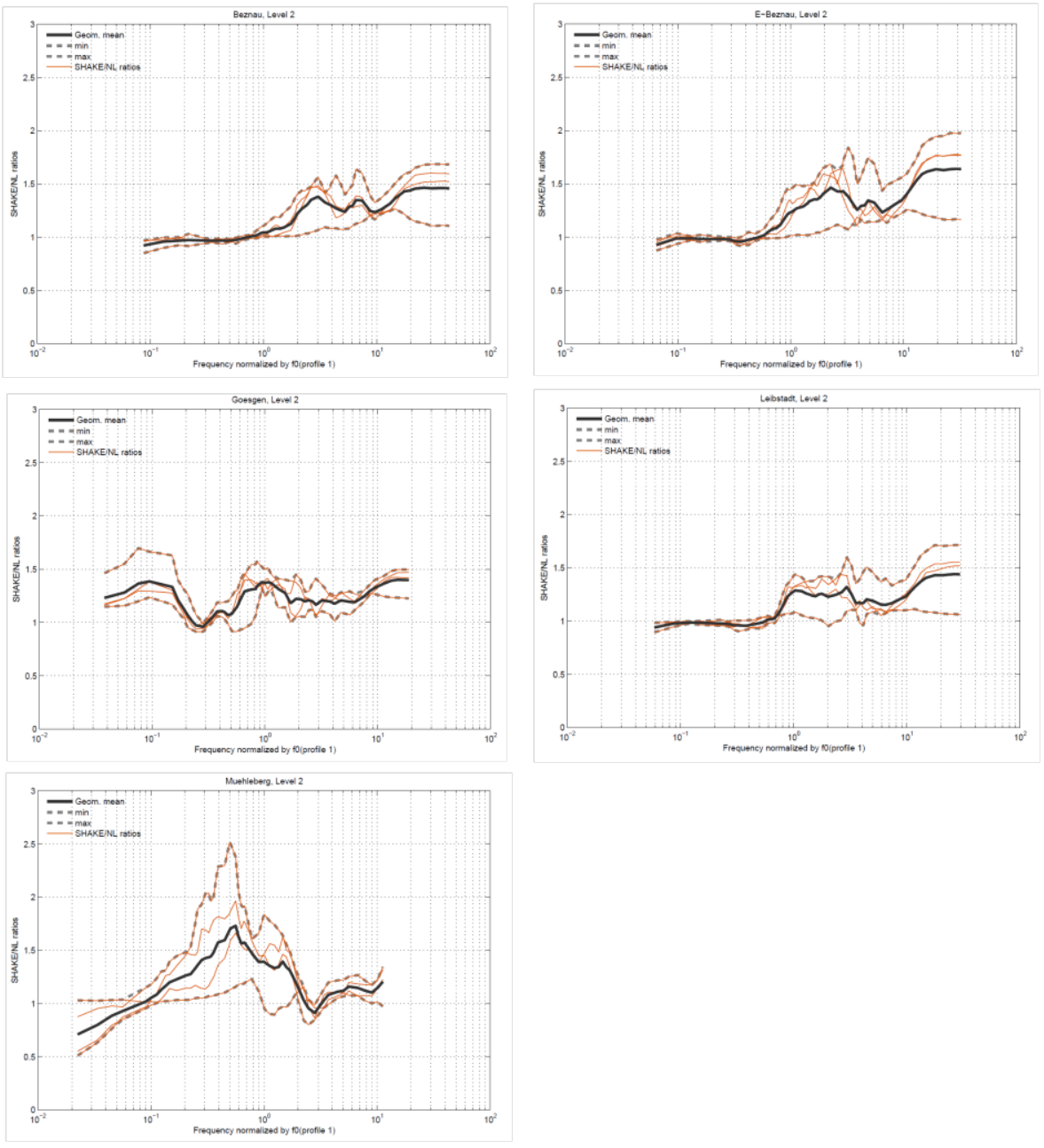

Figure III-1.5: Correction factors SHAKE/non-linear (geometic mean) for the five sites a) Beznau KKB, b) Beznau E-KKB c) Gösgen, d) Leibstadt and e) Mühleberg, together with the factor obtained for each common run. The frequency axis is normalized to f_0, the fundamental frequency of resonance of the profile.

The weights of the branches in the logic tree in Level 2 are as follows:

- Level 2: SHAKE/RVT at 0.4g and 0.75g; non-linear/RVT at 0.05g and 0.4 g is the same as in Level 1, and SHAKE/non-linear at 0.05g and 0.4g.

Logic tree for the frequency range	$0.45Hz < f < f_0/2$:
0.6	SHAKE/RVT factor
0.3	1.0
0.1	non-linear/RVT factor
Logic tree for the frequency range	$f_0/2 < f < 15Hz$:
0.2	SHAKE/RVT factor
0.7	1.0
0.1	non-linear/RVT factor
Logic tree for the frequency range	$15Hz < f$:
0.1	SHAKE/RVT factor
0.8	1.0
0.1	non-linear/RVT factor
Non-linear Branch	
0.5	1.0
0.2	SHAKE/non-linear factor
0.3	SHAKE(profile Px)/SHAKE(Profile P1 or P6)

In Level 3, two new types of factors are included for the non-linear branches when compared to Level 2. The first type corresponds to the maximum, geometric mean and minimum factor obtained from all ratios SHAKE/non-linear for 0.4 g and 0.75 g for all common cases. The correction factors are given in Figure III-1.7 for the five sites Beznau KKB, Beznau EKKB, Gösgen, Leibstadt and Mühleberg, together with the single factors of each commen run. The frequency axis is normalized to f_0. The second type of factors is an uncertainty estimate between the two constitutive models used in non-linear modeling for the profiles used in cross-check analysis at a particular site. The non-linear runs for Mühleberg site are not used because high strains and strong non-linear behaviour are mainly observed within a thin layer in the soft sediments, which is not consistently observed in the entire area. The same frequency dependent factor is used for all sites. The main contractor for Leibstadt and Beznau is F. Pelli (Contractor 2), for Gösgen A. Pecker (Contactor 1). AMEC is the main contractor for Mühleberg (Contractor 3). Ratios non-linear(other contractor)/non-linear(Contractor 1) are given in Figure III-1.8. These ratios are applied to sites Gösgen. For Leibstadt, Beznau, E-Beznau and Mühleberg the inverse of the minimum and maximum ratios needs to be applied in the logic tree, as A. Pecker (Contractor 1) was the contractor performing the cross-check analyses.

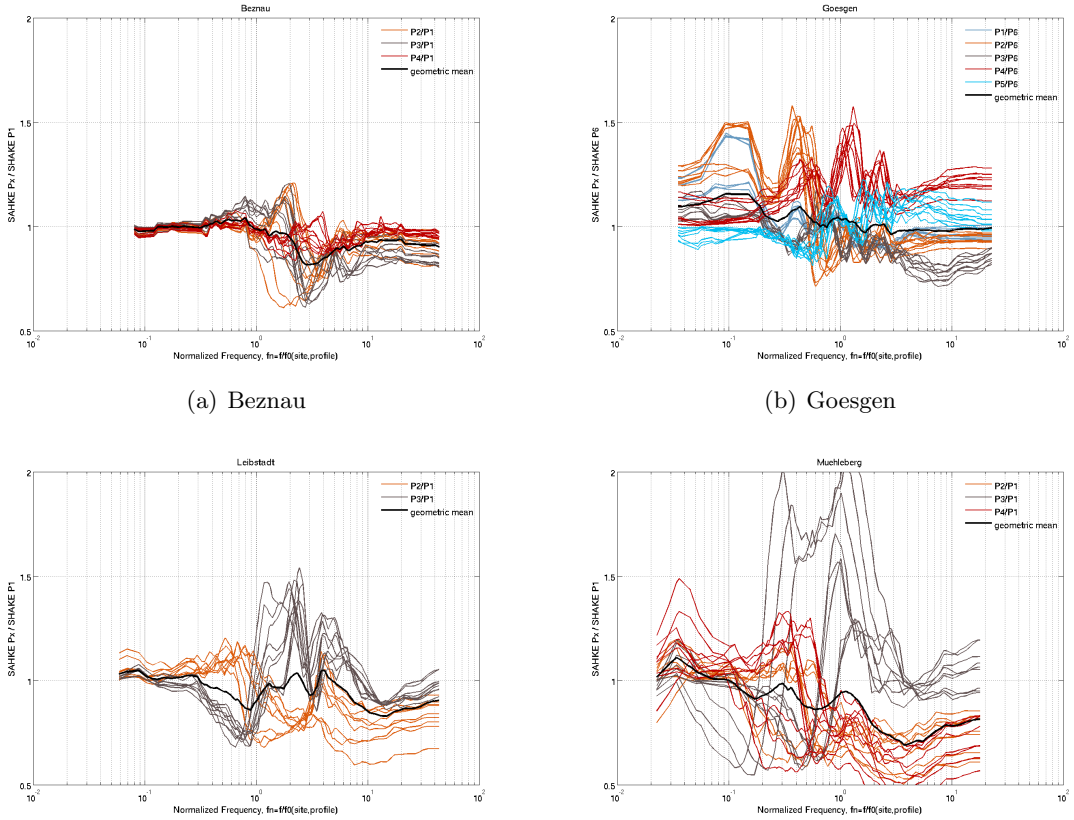

(a) Beznau

(b) Goesgen

(c) Leibstadt

(d) Muehleberg

Figure III-1.6: Correction factors SHAKE(profile Px)/SHAKE(Profile P1 or P6) (geometic mean over all common models) for the four sites a) Beznau KKB, b) Gösgen, c) Leibstadt and d) Mühleberg, together with the factor obtained for each common run. The frequency axis is normalized to f_0, the fundamental frequency of resonance of the profile.

The weights of the branches in the logic tree in Level 3 are as follows:

- Level 3: SHAKE/RVT at 0.4g and 0.75 g as in Level 2; non-linear/RVT at 0.05g and 0.4 g is the same as in Level 1, maximum and minimum SHAKE/non-linear factor for 0.4 g and 0.75 g, and maximum and minimum ratio for the constitutive non-linear models.

LT for the frequency range	$0.45Hz < f < f_0/2$:
0.6	SHAKE/RVT factor
0.3	1.0
0.1	non-linear/RVT factor
LT for the frequency range	$f_0/2 < f < 15Hz$:
0.2	SHAKE/RVT factor
0.7	1.0
0.1	non-linear/RVT factor
LT for the frequency range	$15Hz < f$:
0.1	$SHAKE/RVT$ factor
0.8	1.0
0.1	non-linear/RVT factor
Non-linear Branches:	
0.3	1.0
0.2	SHAKE(profile Px)/SHAKE(Profile P1 or P6)
0.1	Maximum Ratio (SHAKE/non-linear at 0.4g and 0.75g)
0.1	Geometric Mean (SHAKE/non-linear at 0.4g and 0.75g)
0.1	Minimum Ratio (SHAKE/non-linear at 0.4g and 0.75g)
0.1	Maximum Ratio (non-linear(additional_constitutive_model)/non-linear)
0.1	Minimum Ratio (non-linear(additional_constitutive_model)/non-linear)

Factor for Correction of Non-vertical Incidence

In general, the incidence of seismic waves is non-vertical. This is due to the fact that the sources are located at a certain distance from the site and different wave types exist with different incidence angles. RVT, SHAKE and all non-linear computations are restricted to the vertical incidence of SH waves. During the PEGASOS project all amplification factors referred to the same rock condition (average V_S of 2000m/s), and a factor was applied in the PEGASOS project that accounted for the problem of non-vertical incidence at the particular NPP site.

Non-vertical incidence is now included in SP2 ground motion model because a site-specific rock reference is used for each NPP. All branches accounting for non-vertical incidence are therefore removed for the logic tree used in PRP

Existence of 2D-effects and Application of a General Correction Factor

Two dimensional amplification effects may play an important role and are treated in this section. We distinguish between two cases, in the first case 2D-effects are assumed to occur

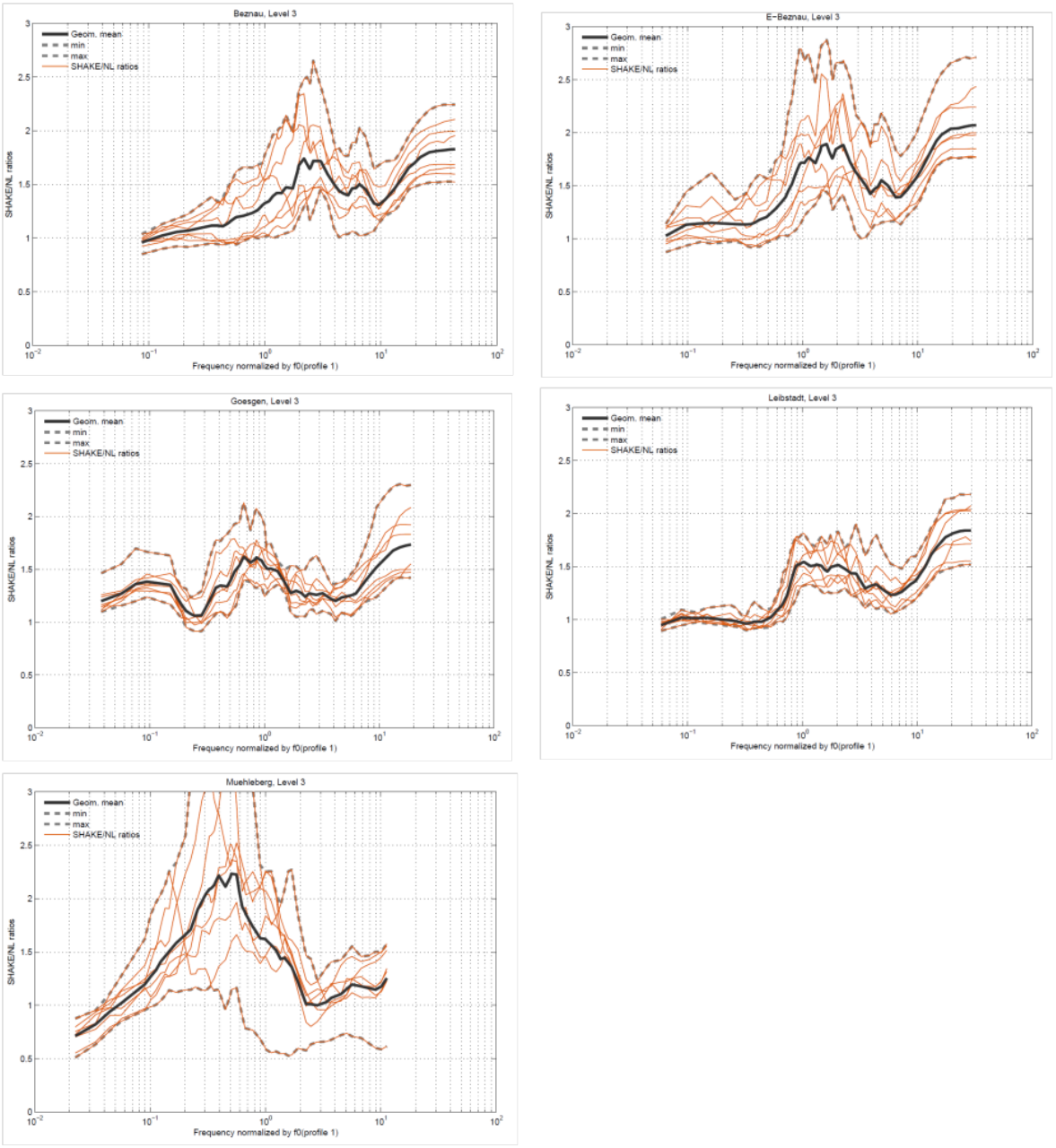

Figure III-1.7: Maximum, geometric mean and minimum SHAKE/non-linear factor for the five sites a) Beznau KKB, b) Beznau E-KKB c) Gösgen, d) Leibstadt and e) Mühleberg, together with all factors for 0.4 g and 0.75 g. The frequency axis is normalized to f_0, the fundamental frequency of resonance.

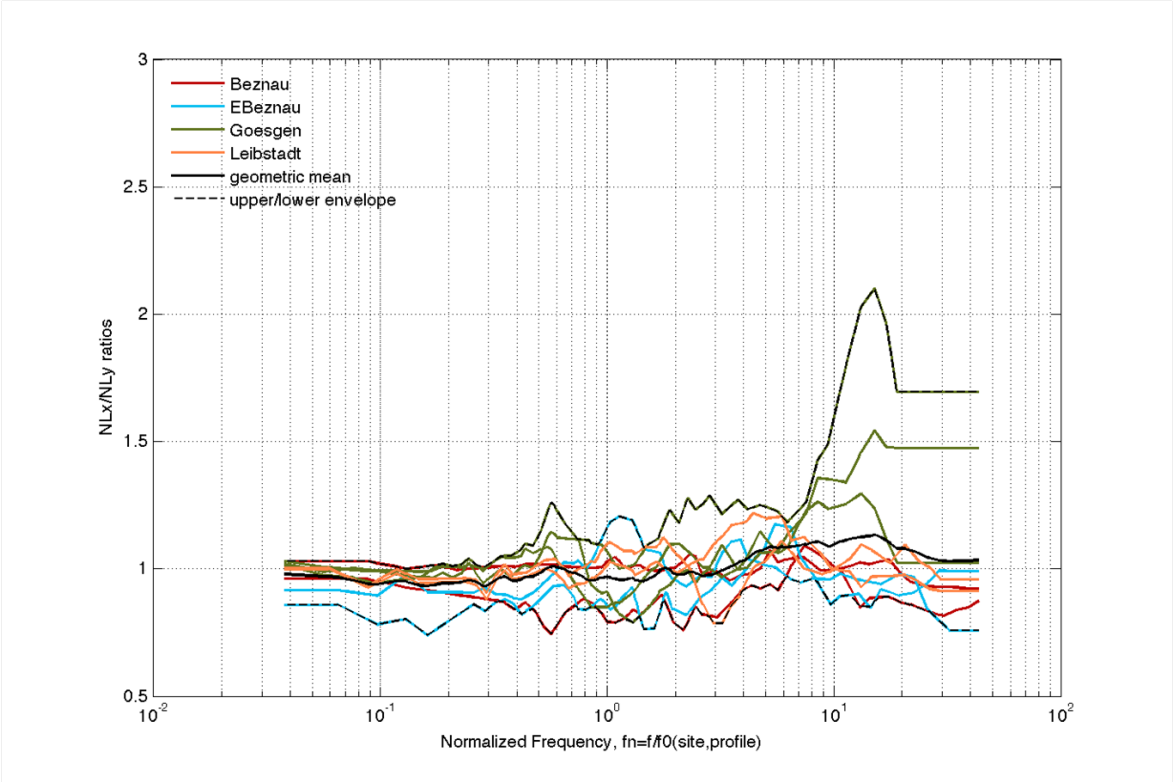

Figure III-1.8: Maximum and minimum ratios non-linear(other contractor)/non-linear(contractor 1) derived from results for the four sites Beznau KKB, Beznau E-KKB, Gösgen, and Leibstadt, together with the factor obtained for each common run at al depth levels. The frequency axis is normalized to f_0, the fundamental frequency of resonance.

(j = 1), and in the second case 2D-effects are excluded (j = 2). During project PEGASOS, two-dimensional computations were performed only for site Leibstadt, and such computations were not extended for PRP. In these computations we distinguished between distant sources ($> 20km$) that are either shallow or deep [Fäh 2002b] (TP3-TN-0168), and sources that are close or located below the site [Bard 2002a] (TP3-TN-0186). For the distant sources we moreover distinguished between sources to the north and sources to the south, because the computed amplification levels are different for the two cases. During PRP no additional work was performed to estimate 2D-effects. For this reasons we apply the same procedure to account for 2D-effects, however adjusting the weights for each site based on the new data from site investigations, and simplifying the procedure as outlined below. The factors for distant sources were originally computed from the ratios between the 2D SH-wave computations [Fäh 2002b] (TP3-TN-0168) and the modal summation results (SH component in report [Fäh 2002a] TP3-TN-0167). During PEGASOS the following notation was introduced:

- PND = 0.4 probability of the earthquake located to the north and deep (ND)
- PNS = 0.1 probability of the earthquake located to the north and shallow (NS)
- PSD = 0.4 probability of the earthquake located to the south and deep (SD)
- PSS = 0.1 probability of the earthquake located to the south and shallow (SS)
- FND = 2-D factor for earthquakes located to the north and deep (ND)

- FNS = 2-D factor for earthquakes located to the north and shallow (NS)
- FSD = 2-D factor for earthquakes located to the south and deep (SD)
- FSS = 2-D factor for earthquakes located to the south and shallow (SS)

The factor as function of frequency for the four cases was simplified as follows:

- 2-D factor for earthquakes located to the north and deep (ND)

$f < f_0/2 : F_{ND} = 1.0$
$f_0/2 < f < fo$: ramp from $F_{ND} = 1.0 to F_{ND} = 1.3$
$f_0 < f < 4f_0 : F_{ND} = 1.3$
$4f_0 < f < 6f_0$: ramp from $F_{ND} = 1.3 to F_{ND} = 1.0$
$6f_0 < f : F_{ND} = 1.0$

- 2-D factor for earthquakes located to the north and shallow (NS)

$f < f_0/2 : FNS = 1.0$
$f_0/2 < f < f_0$: ramp from $FNS = 1.0 to FNS = 1.7$
$f_0 < f < 4f_0 : FNS = 1.7$
$4f_0 < f < 6f_0$: ramp from $FNS = 1.7 to FNS = 1.0$
$6f_0 < f : FNS = 1.0$

- 2-D factor for earthquakes located to the south and deep (SD)

$f < f_0/2 : FSD = 1.0$
$f_0/2 < f < f_0$: ramp from $FSD = 1.0 to FSD = 1.2$
$f_0 < f < 4f_0 : FSD = 1.2$
$4f_0 < f < 6f_0$: ramp from $FSD = 1.2 to FSD = 1.0$
$6f_0 < f : FSD = 1.0$

- 2-D factor for earthquakes located to the south and shallow (SS)

$f < f_0/2 : FSS = 1.0$
$f_0/2 < f < f_0$: ramp from $FSS = 1.0 to FSS = 0.9$
$f_0 < f < 4f_0 : FSS = 0.9$
$4f_0 < f < 6f_0$: ramp from $FSS = 0.9 to FSS = 1.0$
$6f_0 < f : FSS = 1.0$

where f_0 is fundamental frequency of resonance, as defined in paragraph 1.2.3. These factors are valid for all shaking levels. The probabilities PND, PNS, PSD, and PSS for sources to be shallow or deep, and the location to the north or south are unknown and they are estimated to be 0.4, 0.1, 0.4, and 0.1.

The factors for close sources were computed from the ratios between the 2D and 1D computations [Bard 2002a] (TP3-TN-0186) for vertically incident SH waves. The cases for -30°, 0°, +30° incidence and for the low strain level are included. The correction factor as a function of frequency is simplified as follows:

- F2D_close: correction factor for 2D-effects from a close source

$f < f_0/2 : F_{2D\_close} = 1.0$
$f_0/2 < f < f_0$: ramp from $F_{2D\_close} = 1.0 to F_{2D\_close} = 1.25$
$f_0 < f < 4f_0 : F_{2D\_close} = 1.25$
$4f_0 < f < 6f_0$: ramp from $F_{2D\_close} = 1.25 to F_{2D\_close} = 1.0$
$6f_0 < f : F_{2D\_close} = 1.0$

For Gösgen, Beznau and Mühleberg no computations have been performed in order to estimate 2D-effects. The results from site Leibstadt are applied to these sites. Possible 2D-effects cannot be excluded for Beznau, Gösgen and Mühleberg. The expressions "north" and "south" in these cases do not express geographical directions but refer only to the different cases in the Leibstadt-site computations. The functions are adapted to the different sites by selection of the appropriate fundamental frequency of resonance f_0 defined in paragraph 1.2.3. The probability for 2D-effects is controlled by the branches j = 1 (2D-effects) and j = 2 (no 2D-effects). The probabilities for the different NPP sites are estimated and given in Table III-1.9. The basis for the different probabilities of 2D-effects at the different sites are the topographical features, the subsurface geometry, as well as the spatial variablity in measured velocity profiles and H/V ratios in the area of the NPP. The more pronounced the 2D geometry and variability is, the higher is the probability for 2D wave propagation effects.

Table III-1.9: Estimated probabilities for 2D-effects at the different NPP sites.

	j = 1 (2D-effects)	j = 2 (no 2D-effects)
Beznau	0.2	0.8
Gösgen	0.2	0.8
Leibstadt	0.7	0.3
Mühleberg	0.2	0.8

Hazard computations are performed in two steps: source and attenuation are treated together in the first step, and site effects are treated separately in the second step. The probability that a source of a certain magnitude is distant (Pdist) or close (Pclose) depends on the results of the hazard de-aggregation in the first step.

The probabilities were estimated based on the deaggreation performed during PEGASOS, and on the expert discussion during the SP1 workshops. The weights are provided in Table III-1.10 for the two distance ranges. The probabilities in Table III-1.10 are only used for testing the logic tree. In the final hazard computations the magnitude and distance information is brought along the hazard computation, and the corresponding branches can be assigned without estimating the probabilities P_{dist} and P_{close}.

The magnitude 5 earthquakes contribute more to the hazard for close distances. Because correction for non-vertical incidence is removed in PRP, we can approximate the combination

Table III-1.10: Probabilities for close (P_{close}) and distant sources (P_{dist}) , used only for testing purpose. This table mimics the deaggregation of the hazard.

	Magnitude 5 – 6	Magnitude 6 – 7	Magnitude 7 – 8
Source closer than 20 km or below the site	0.8	0.5	0.2
Source distance $> 20km$	0.2	0.5	0.8

of corrections to one mean correction factor Fcorrj for 2D-effects, depending on the magnitude level.

$$F_{corr}{}^{j} = P_{dist} * F_{2D\_dist}{}^{j} + P_{close} * F_{2D\_close}{}^{j}$$

where

a P_{dist} = probability that earthquake is distant
P_{close} = probability that earthquake is close

c $F_{2D\_dist}{}^{j}$ = correction factor for 2D-effects from a distant source
$F_{2D\_dist}{}^{1} = P_{ND} * F_{ND} + P_{NS} * F_{NS} + P_{SD} * F_{SD} + P_{SS} * F_{SS}$ for 2D-effects = yes
$F_{2D\_dist}{}^{2} = 1$ for 2D-effects = no

where:

P_{ND} = probability of the earthquake located to the north and deep (ND)
P_{NS} = probability of the earthquake located to the north and shallow (NS)
P_{SD} = probability of the earthquake located to the south and deep (SD)
P_{SS} = probability of the earthquake located to the south and shallow (SS)
F_{ND} = 2-D factor for earthquakes located to the north and deep (ND)
F_{NS} = 2-D factor for earthquakes located to the north and shallow (NS)
F_{SD} = 2-D factor for earthquakes located to the south and deep (SD)
F_{SS} = 2-D factor for earthquakes located to the south and shallow (SS)

d $F_{2D\_close}{}^{1}$ = correction factor for 2D-effects from a close source
$F_{2D\_close}{}^{2} = 1$ for 2D-effects = no

During the PEGASOS project the correction factors $F_{corr}{}^{j}$ was taken magnitude dependent and was applied for all ground motion levels. Compared to the PEGASOS project the correction factor for non-vertical incidence is now removed, which simplifies the correction expression. Moreover, the whole treatment is moved from the aleatory part to a specific branch in the logic tree. Figure III-1.9 shows the correction factors for distant sources ($F_{2D\_dist}{}^{1}$) and close sources ($F_{2D\_close}{}^{1}$) for different magnitudes. It is evident that the differences are not significant to justify a complex logic tree structure related to the 2D-effects. For this reasons

we simplify the branch for 2D-effects in the logic tree as follows, independent on magnitude, but still model, respectively f_0 specific:

2D-effects YES	weight in Table III-1.9	$F_{2D\_close}{}^1$
2D-effects NO	weight in Table III-1.9	Factor is 1.0

The impact of azimuthal dependence of 2D-effects on aleatory variability is discussed further on. The correction factor is applied to all ground motion levels.

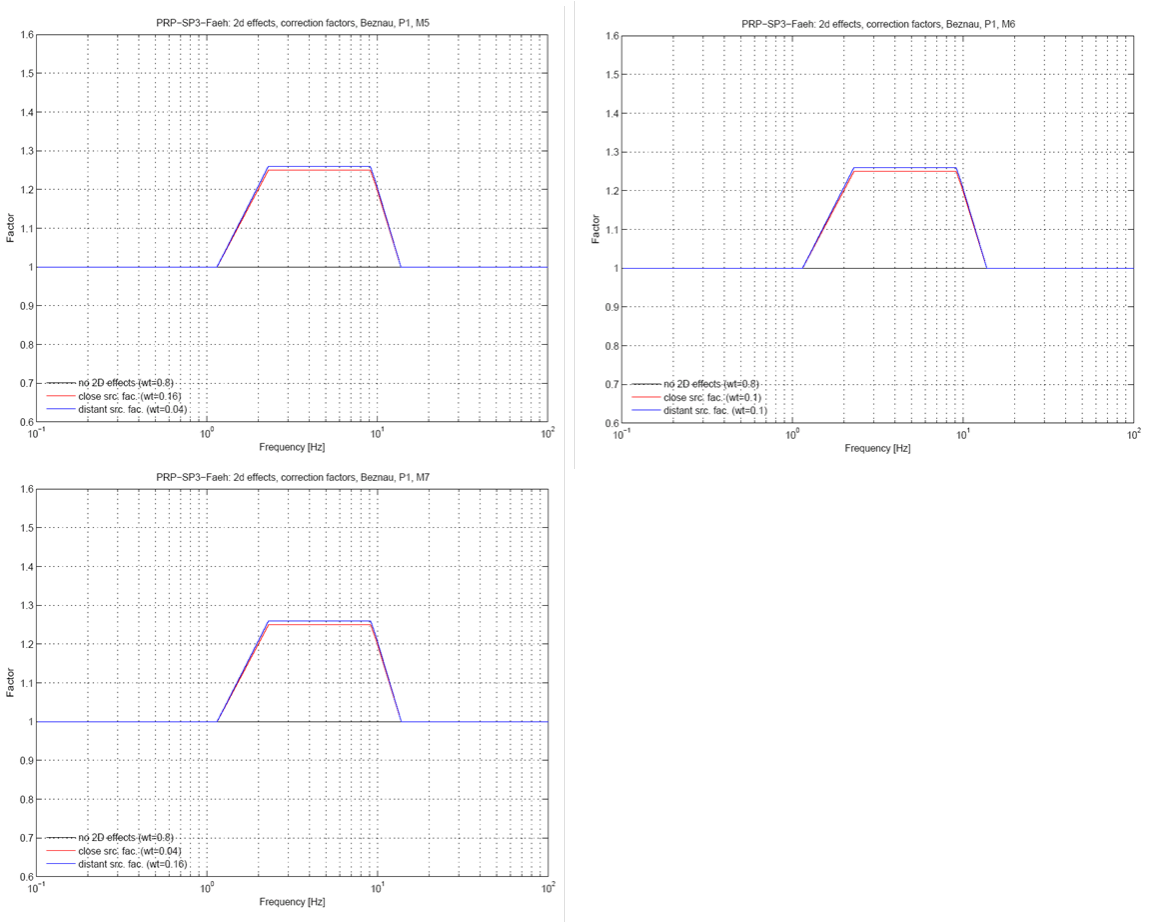

Figure III-1.9: Correction factors for 2D-effects for distant sources ($F_{2D_{dist}}{}^1$) and close sources ($F_{2D\_close}{}^1$) at different of magnitude levels. The example is given for site Beznau KKB.

Existence and Correction Factor for 3D-effects

Constructive interference of waves may occur in structures with a 3D geometry that permits the 3D focusing of seismic waves. This is taken into considerations only for the branches "2D-effects-YES" (j=1). For these sites the geometry of the soft sediment could cause 3D resonance effects. No 3D computations have been performed for the NPP sites, and the correction factors and probabilities are estimated. The basis for the different weights of 3D-effects at the different sites is the topographical feature, the subsurface geometry and the variability of measured velocity profiles and H/V spectral ratios. The more pronounced the 3D geometry is, the higher is the weight for 3D wave propagation effects. The correction

factors originally proposed in PEGASOS were based on the consideration of a geometrical superposition of two propagating waves, as follows:

2D-effects YES	weight	3D YES	0.2	Factor 1
			0.8	Factor 2
2D-effects YES	weight	3D NO	Factor is 1.0	

The factors 1 1.2.3 and 2 1.2.3 as function of frequency were again simplified by a similar function as introduced in paragraph 1.2.3:

Definition of Factor 1 :

$f < f_0/2$: Factor 1 = 1.0
$f_0/2 < f < f_0$: ramp from Factor 1 = 1.0 to Factor 1 = 1.4
$f_0 < f < 4f_0$: Factor 1 = 1.4
$4f_0 < f < 6f_0$: ramp from Factor 1 = 1.4 to Factor 1 = 1.0
$6f_0 < f$: Factor 1 = 1.0

Definition of Factor 2:

$f < f_0/2$: Factor 2 = 1.0
$f_0/2 < f < f_0$: ramp from Factor 2 = 1.0 to Factor 2 = 1.2
$f_0 < f < 4f_0$: Factor 2 = 1.2
$4f_0 < f < 6f_0$: ramp from Factor 2 = 1.2 to Factor 2 = 1.0
$6f_0 < f$: Factor 2 = 1.0

As was proposed for 2D-effects, the two factors can be combined in one combined factor. The resulting combined factor is shown in Figure III-1.10, and the weight are defined as follows:

Logic tree for Leibstadt:

2D-effects YES	0.3	3D YES	0.2	Factor 1
			0.8	Factor 2
2D-effects YES	0.7	3D NO	Factor is 1.0	

Logic tree for Beznau, Mühleberg and Gösgen:

2D-effects YES	0.1	3D YES	0.2	Factor 1
			0.8	Factor 2
2D-effects YES	0.9	3D NO	Factor is 1.0	

The impact of 3D-effects on aleatory variability is discussed further on. The combined factor is taken magnitude independent and is applied to all ground motion levels.

Correction for Parametric Uncertainty

During PEGASOS these branches accounted for the uncertainties of the soil parameters. Extensive measurements were performed at each NPP site, and different velocity profiles are

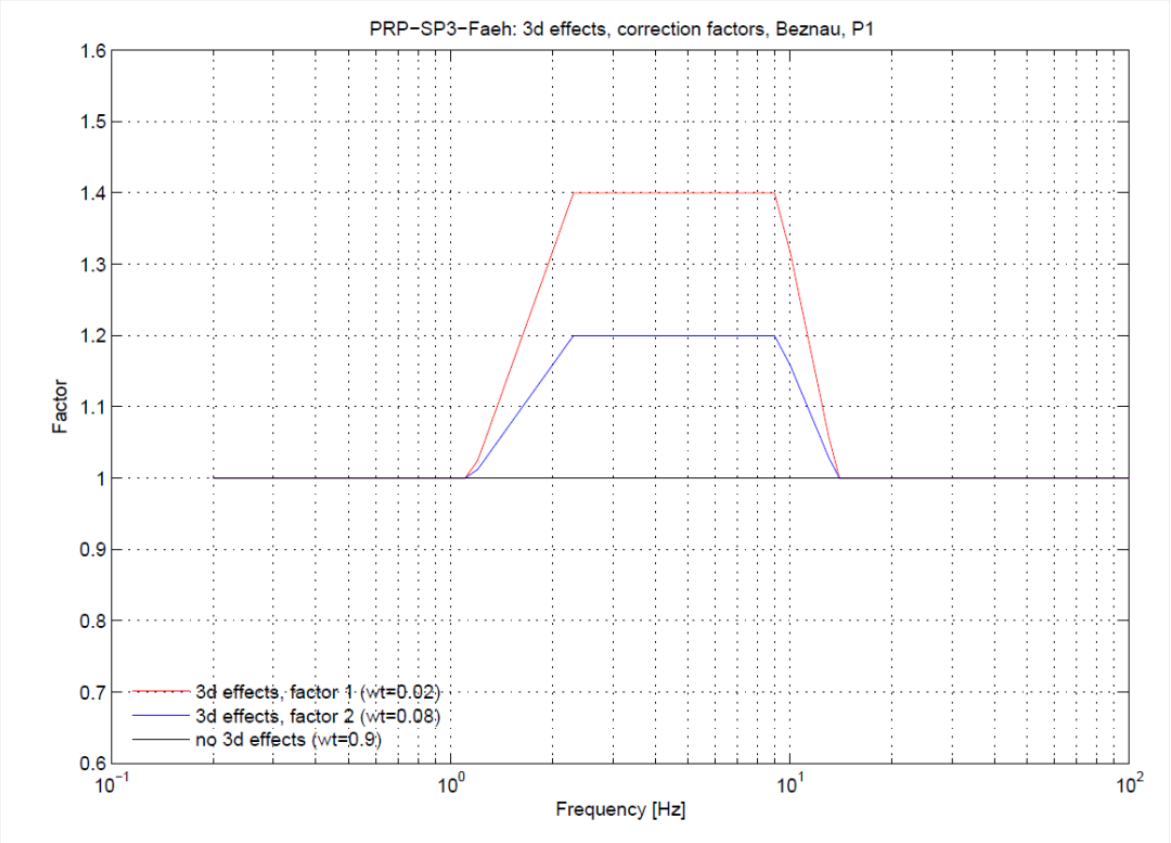

Figure III-1.10: Correction factors 3D-effects for site Beznau KKB.

now used in PRP that account for these uncertainties. These branches are therefore deleted for the logic tree used in PRP

1.2.4 Beznau

Logic Tree for Beznau, KKB and EKKB

The logic tree for site Beznau with the weights and branches is given in Figure III-1.1.

Site-specific Model Evaluations

The ground motion levels for Beznau (KKB and EKKB) are defined in Table III-1.11. The discussion is provided in Section 1.2.1. The PGA-range in the first column is for the reference ground motion on reference bedrock with S-wave velocity of 1800m/s at the surface. For the non-linear branches only the runs for the preferred material properties are used. There is only a weak dependence on magnitude, and therefore magnitude class 5-6 or lower uses results from magnitude 5, magnitude 6-7 class uses results from magnitude 6, and magnitude 7-8 class or higher uses results from magnitude 7.

The ground motion levels, physical model and weights in the logic tree for site Beznau are as follows:

Table III-1.11: Definitions of the level of ground motion for site Beznau.

PGA range in g	Magnitude 5 – 6	Magnitude 6 – 7	Magitude 7 – 8
– 0.05	Level 1	Level 1	Level 1
0.05 – 0.1	Level 1	Level 1	Level 1
0.1 – 0.3	Level 1	Level 1	Level 1
0.3 – 0.5	Level 1	Level 2a	Level 2a
0.5 – 0.8	Level 2a	Level 2b	Level 2b
0.8 – 1.5	Level 2b	Level 3a	Level 3a
1.5 –	Level 2b	Level 3b	Level 3b
Failure of soil column			Level 4

Weight:

- Level 1

  1.0 For a given PGA/Magnitude, the next lower ground motion level of the RVT run is selected (RVT without soil randomization). For the PGA range 0.3-0.5g (magnitude 5-6), the computation at 0.3g is selected.

- Level 2a

  0.2 RVT without soil randomization at 0.2 g and the given magnitude.

  0.5 RVT without soil randomization at 0.3 g and the given magnitude.

  0.1 RVT without soil randomization at 0.4 g and the given magnitude.

  0.2 Non-linear at 0.4g. In the high frequency range extrapolated. Extrapolation above 30 Hz from the mean in the range [10 Hz, 30 Hz].

  0.0 Non-linear at 0.75g. In the high frequency range extrapolated. Extrapolation above 30 Hz from the mean in the range [10 Hz, 30 Hz].

- Level 2b

  0.1 RVT without soil randomization at 0.2 g and the given magnitude.

  0.1 RVT without soil randomization at 0.3 g and the given magnitude.

  0.2 RVT without soil randomization at 0.4 g and the given magnitude.

  0.4 Non-linear at 0.4 g. In the high frequency range extrapolated. Extrapolation above 30 Hz from the mean in the range [10 Hz, 30 Hz].

  0.2 Non-linear at 0.75g. In the high frequency range extrapolated. Extrapolation above 30 Hz from the mean in the range [10 Hz, 30 Hz].

- Level 3a

  0.2 Non-linear at 0.4 g. In the high frequency range extrapolated. Extrapolation above 30 Hz from the mean in the range [10 Hz, 30 Hz].

0.4 Non-linear at 0.75g. In the high frequency range extrapolated. Extrapolation above 30 Hz from the mean in the range [10 Hz, 30 Hz].

0.1 Non-linear at 1.50g. In the high frequency range extrapolated. Extrapolation above 30 Hz from the mean in the range [10 Hz, 30 Hz].

0.1 RVT without soil randomization at 0.4 g and the given magnitude.

0.1 RVT without soil randomization at 0.75 g and the given magnitude.

0.1 RVT without soil randomization at 1.00 g and the given magnitude.

- Level 3b

0.1 Non-linear at 0.4 g. In the high frequency range extrapolated. Extrapolation above 30 Hz from the mean in the range [10 Hz, 30 Hz].

0.2 Non-linear at 0.75g. In the high frequency range extrapolated. Extrapolation above 30 Hz from the mean in the range [10 Hz, 30 Hz].

0.4 Non-linear at 1.50g. In the high frequency range extrapolated. Extrapolation above 30 Hz from the mean in the range [10 Hz, 30 Hz].

0.1 RVT without soil randomization at 0.4 g and the given magnitude.

0.1 RVT without soil randomization at 0.75 g and the given magnitude.

0.1 RVT without soil randomization at 1.00 g and the given magnitude.

The basis for the selection of weights of the branches in the logic tree is the advantages and disadvantages of the computational methods and the level of non-linear behavior as discussed in Section 1.2.1.

1.2.5 Gösgen

Logic Tree for Gösgen

The logic tree for site Gösgen has the same generic structure as shown in III-1.1.

Site-specific Model Evaluations

The ground motion levels for Gösgen are defined in Table III-1.12. The discussion is provided in Section 1.2.1. The PGA-range in the first column is for the reference ground motion on bedrock with S-wave velocity of 2500m/s at the surface. For the non-linear branches only the runs for the preferred material properties are used. The ground motion levels, physical model and weights in the logic tree for site Gösgen are the same as for Beznau and are as follows.

In 2010 not all requested RVT runs were performed for site Gösgen. (missing runs 0.3g and 1.0g) and epistemic uncertainty was increased, while in 2013 all runs were performed and the site Gösgen is treated the same way as the other sites.

Weight:

- Level 1

Table III-1.12: Definitions of the level of ground motion for site Gösgen.

PGA range in g	Magnitude 5 – 6	Magnitude 6 – 7	Magitude 7 – 8
– 0.05	Level 1	Level 1	Level 1
0.05 – 0.1	Level 1	Level 1	Level 1
0.1 – 0.3	Level 1	Level 1	Level 1
0.3 – 0.5	Level 1	Level 2a	Level 2a
0.5 – 0.8	Level 2a	Level 2b	Level 2b
0.8 – 1.5	Level 2b	Level 3a	Level 3a
1.5 –	Level 2b	Level 3b	Level 3b
Failure of soil column			Level 4

1.0 For a given PGA/Magnitude, the next lower ground motion level of the RVT run is selected (RVT without soil randomization). For the PGA range 0.3-0.5g (magnitude 5-6), the computation at 0.2g is selected, because the computation at 0.3g is not existing.

- Level 2a

  0.2 RVT without soil randomization at 0.2 g and the given magnitude.

  0.5 RVT without soil randomization at 0.3 g not existing

  0.1 RVT without soil randomization at 0.4 g and the given magnitude.

  0.2 Non-linear at 0.4g. In the high frequency range extrapolated. Extrapolation above 30 Hz from the mean in the range [10 Hz, 30 Hz].

  0.0 Non-linear at 0.75g. In the high frequency range extrapolated. Extrapolation above 30 Hz from the mean in the range [10 Hz, 30 Hz].

- Level 2b

  0.1 RVT without soil randomization at 0.2 g and the given magnitude.

  0.1 RVT without soil randomization at 0.3 g not existing

  0.2 RVT without soil randomization at 0.4 g and the given magnitude.

  0.4 Non-linear at 0.4 g. In the high frequency range extrapolated. Extrapolation above 30 Hz from the mean in the range [10 Hz, 30 Hz].

  0.2 Non-linear at 0.75g. In the high frequency range extrapolated. Extrapolation above 30 Hz from the mean in the range [10 Hz, 30 Hz].

- Level 3a

  0.2 Non-linear at 0.4 g. In the high frequency range extrapolated. Extrapolation above 30 Hz from the mean in the range [10 Hz, 30 Hz].

  0.4 Non-linear at 0.75g. In the high frequency range extrapolated. Extrapolation above 30 Hz from the mean in the range [10 Hz, 30 Hz].

0.1 Non-linear at 1.50g. In the high frequency range extrapolated. Extrapolation above 30 Hz from the mean in the range [10 Hz, 30 Hz].

0.1 RVT without soil randomization at 0.4 g and the given magnitude.

0.1 RVT without soil randomization at 0.75 g and the given magnitude.

0.1 not exiting RVT without soil randomization at 1.00 g and the given magnitude.

- Level 3b

0.1 Non-linear at 0.4 g. In the high frequency range extrapolated. Extrapolation above 30 Hz from the mean in the range [10 Hz, 30 Hz].

0.2 Non-linear at 0.75g. In the high frequency range extrapolated. Extrapolation above 30 Hz from the mean in the range [10 Hz, 30 Hz].

0.4 Non-linear at 1.50g. In the high frequency range extrapolated. Extrapolation above 30 Hz from the mean in the range [10 Hz, 30 Hz].

0.1 RVT without soil randomization at 0.4 g and the given magnitude.

0.1 RVT without soil randomization at 0.75 g and the given magnitude.

0.1 not exiting RVT without soil randomization at 1.00 g and the given magnitude.

1.2.6 Leibstadt

Logic Tree for Leibstadt

The logic tree for site Leibstadt has the same generic structure as shown in III-1.1.

Site-specific Model Evaluations

The ground motion levels for Leibstadt are defined in Table III-1.13. The discussion is provided in Section 1.2.1. The PGA-range in the first column is for the reference ground motion on bedrock with S-wave velocity of 2200m/s at the surface. For the non-linear branches only the runs for the preferred material properties are used. According to Table III-1.3 the strains that are reached in the soils when using equivalent linear modelling are smaller than for the sites Beznau and Gösgen. This contradicts to the results from non-linear computation where the maximum strains are reached at rather low ground motion levels and at larger depth (around 20m) as opposed to the other sites. The G/G_{max} curve for Leibstadt in depth are intended to reflect some cementation of the gravel layers and therefore the decrease of G/G_{max} with shear strain is slower than for the other sites. Since on the other hand the strength characteristics are not so high (e.g. friction angle that is too low even if the values are based on measurements) and do not reflect the strong supposed cementation, it turns out that the maximum strength in non-linear computations is reached at small strain levels induced by small pga's. The problem arises from the fact that the strength parameters and the G/G_{max} curve are less consistent with each other than for the other sites, and therefore the assessment is less reliable. In conclusion we can assume that the limit of reliable results for equivalent linear modelling is similar to the other sites in the range 0.4-0.7g. The weights are slightly increased for RVT computations at the particular ground motion levels to account for the resulting low strains in the equivalent linear runs.

Table III-1.13: Definitions of the level of ground motion for site Leibstadt

PGA range in g	Magnitude 5 – 6	Magnitude 6 – 7	Magitude 7 – 8
– 0.05	Level 1	Level 1	Level 1
0.05 – 0.1	Level 1	Level 1	Level 1
0.1 – 0.3	Level 1	Level 1	Level 1
0.3 – 0.5	Level 1	Level 2a	Level 2a
0.5 – 0.8	Level 2a	Level 2b	Level 2b
0.8 – 1.5	Level 2b	Level 3a	Level 3a
1.5 –	Level 2b	Level 3b	Level 3b
Failure of soil column			Level 4

The ground motion levels, physical model and weights in the logic tree for site Leibstadt are as follows:

Weight:

- Level 1

  1.0 For a given PGA/Magnitude, the next lower ground motion level of the RVT run is selected (RVT without soil randomization). For the PGA range 0.3-0.5g (magnitude 5-6), the computation at 0.3g is selected.

- Level 2a

  0.4 RVT without soil randomization at 0.2 g and the given magnitude.

  0.4 RVT without soil randomization at 0.3 g and the given magnitude.

  0.1 RVT without soil randomization at 0.4 g and the given magnitude.

  0.1 Non-linear at 0.4g. In the high frequency range extrapolated. Extrapolation above 30 Hz from the mean in the range [10 Hz, 30 Hz].

  0.0 Non-linear at 0.75g. In the high frequency range extrapolated. Extrapolation above 30 Hz from the mean in the range [10 Hz, 30 Hz].

- Level 2b

  0.1 RVT without soil randomization at 0.2 g and the given magnitude.

  0.1 RVT without soil randomization at 0.3 g and the given magnitude.

  0.2 RVT without soil randomization at 0.4 g and the given magnitude.

  0.4 Non-linear at 0.4 g. In the high frequency range extrapolated. Extrapolation above 30 Hz from the mean in the range [10 Hz, 30 Hz].

  0.2 Non-linear at 0.75g. In the high frequency range extrapolated. Extrapolation above 30 Hz from the mean in the range [10 Hz, 30 Hz].

- Level 3a

  0.2 Non-linear at 0.4 g. In the high frequency range extrapolated. Extrapolation above 30 Hz from the mean in the range [10 Hz, 30 Hz].

  0.3 Non-linear at 0.75g. In the high frequency range extrapolated. Extrapolation above 30 Hz from the mean in the range [10 Hz, 30 Hz].

  0.1 Non-linear at 1.50g. In the high frequency range extrapolated. Extrapolation above 30 Hz from the mean in the range [10 Hz, 30 Hz].

  0.1 RVT without soil randomization at 0.4 g and the given magnitude.

  0.2 RVT without soil randomization at 0.75 g and the given magnitude.

  0.1 RVT without soil randomization at 1.00 g and the given magnitude.

- Level 3b

  0.1 Non-linear at 0.4 g. In the high frequency range extrapolated. Extrapolation above 30 Hz from the mean in the range [10 Hz, 30 Hz].

  0.2 Non-linear at 0.75g. In the high frequency range extrapolated. Extrapolation above 30 Hz from the mean in the range [10 Hz, 30 Hz].

  0.3 Non-linear at 1.50g. In the high frequency range extrapolated. Extrapolation above 30 Hz from the mean in the range [10 Hz, 30 Hz].

  0.1 RVT without soil randomization at 0.4 g and the given magnitude

  0.2 RVT without soil randomization at 0.75 g and the given magnitude.

  0.1 RVT without soil randomization at 1.00 g and the given magnitude.

—-

1.2.7 Mühleberg

Logic Tree for Mühleberg

The logic tree for site Mühleberg has the same generic structure as shown in III-1.1.

Site-specific Model Evaluations

The ground motion levels for Mühleberg are defined in Table III-1.14. The discussion is provided in Section 1.2.1. The PGA-range in the first column is for the reference ground motion on bedrock with S-wave velocity of 1100m/s at the surface. For the non-linear branches only the runs for the preferred material properties are used. This model is characterized by a thin layer that shows very strong non-linear behaviour at low ground motion level. Because this layer is not characteristic for the entire area, higher weights are given to the RVT runs than for the other NPP sites. Because high strains (see Table III-1.3) are mainly observed within a thin layer in the soft sediments, which is not consistently observed in the entire area, no change in the levels is done when referred to sites Beznau and Gösgen. Moreover only limited laboratory investigations on non-linear soil behaviour has been performed, resulting

Table III-1.14: Definitions of the level of ground motion for site Mühleberg.

PGA range in g	Magnitude 5 – 6	Magnitude 6 – 7	Magitude 7 – 8
– 0.05	Level 1	Level 1	Level 1
0.05 – 0.1	Level 1	Level 1	Level 1
0.1 – 0.3	Level 1	Level 1	Level 1
0.3 – 0.5	Level 1	Level 2a	Level 2a
0.5 – 0.8	Level 2a	Level 2b	Level 2b
0.8 – 1.5	Level 2b	Level 3a	Level 3a
1.5 –	Level 2b	Level 3b	Level 3b
Failure of soil column			Level 4

in very uncertain parameters decribing non-linear soil behaviour. Therefore the weights for the non-linear runs are reduced.

The ground motion levels, physical model and weights in the logic tree for site Mühleberg are as follows:

Weight:

- Level 1

  1.0 For a given PGA/Magnitude, the next lower ground motion level of the RVT run is selected (RVT without soil randomization). For the PGA range 0.3-0.5g (magnitude 5-6), the computation at 0.3g is selected.

- Level 2a

  0.2 RVT without soil randomization at 0.2 g and the given magnitude.

  0.5 RVT without soil randomization at 0.3 g and the given magnitude.

  0.1 RVT without soil randomization at 0.4 g and the given magnitude.

  0.2 Non-linear at 0.4g. In the high frequency range extrapolated. Extrapolation above 30 Hz from the mean in the range [10 Hz, 30 Hz].

  0.0 Non-linear at 0.75g. In the high frequency range extrapolated. Extrapolation above 30 Hz from the mean in the range [10 Hz, 30 Hz].

- Level 2b

  0.1 RVT without soil randomization at 0.2 g and the given magnitude.

  0.2 RVT without soil randomization at 0.3 g and the given magnitude.

  0.2 RVT without soil randomization at 0.4 g and the given magnitude.

  0.3 Non-linear at 0.4 g. In the high frequency range extrapolated. Extrapolation above 30 Hz from the mean in the range [10 Hz, 30 Hz].

0.2 Non-linear at 0.75g. In the high frequency range extrapolated. Extrapolation above 30 Hz from the mean in the range [10 Hz, 30 Hz].

- Level 3a

  0.2 Non-linear at 0.4 g. In the high frequency range extrapolated. Extrapolation above 30 Hz from the mean in the range [10 Hz, 30 Hz].

  0.3 Non-linear at 0.75g. In the high frequency range extrapolated. Extrapolation above 30 Hz from the mean in the range [10 Hz, 30 Hz].

  0.1 Non-linear at 1.50g. In the high frequency range extrapolated. Extrapolation above 30 Hz from the mean in the range [10 Hz, 30 Hz].

  0.1 RVT without soil randomization at 0.4 g and the given magnitude.

  0.2 RVT without soil randomization at 0.75 g and the given magnitude.

  0.1 RVT without soil randomization at 1.00 g and the given magnitude.

- Level 3b

  0.1 Non-linear at 0.4 g. In the high frequency range extrapolated. Extrapolation above 30 Hz from the mean in the range [10 Hz, 30 Hz].

  0.2 Non-linear at 0.75g. In the high frequency range extrapolated. Extrapolation above 30 Hz from the mean in the range [10 Hz, 30 Hz].

  0.3 Non-linear at 1.50g. In the high frequency range extrapolated. Extrapolation above 30 Hz from the mean in the range [10 Hz, 30 Hz].

  0.1 RVT without soil randomization at 0.4 g and the given magnitude.

  0.2 RVT without soil randomization at 0.75 g and the given magnitude.

  0.1 RVT without soil randomization at 1.00 g and the given magnitude.

1.3 Median Amplification of Vertical Ground Motion

1.3.1 Approach

Very few computations have been performed to estimate the amplification on the vertical component. The cases for which computations were performed in PRP are all based on the idea that amplification on the vertical component is only due to amplification of P waves. This is certainly incorrect because non-vertically propagating S waves (both for the PSV case) and Rayleigh waves can contribute significantly to the ground motion on the vertical component also at high ground motion levels. The resulting uncertainty caused by the lack of reliable computations is accounted for by an increased epistemic uncertainty.

Three main branches of the logic tree are proposed to estimate the amplification for the vertical component of motion: A) a branch based on empirical relations for V/H spectral ratios and on the results for the median amplification of the horizontal motion, B) a branch based on the computations performed for the vertical component with RVT assuming vertically propagating P-waves (2013 results), and C) and a branch based on the vertical ground motion

estimate (no amplification on the vertical component is assumed). Branch B) and C) are applied to the estimate of the vertical hazard proposed by myself in the SP2 expert group, by using V/H spectral ratios for rock condition. For case B), one V_ρ-profile was derived for each site by taking the best estimate model and applying a V_ρ/V_S velocity factor of 2.5 in the sediment layer and $\sqrt{3}$ in the rock. The constraint of the water table restricts V_ρ such that the velocity needs to be larger than 1600m/s. More details are found in the the corresponding summary reports for each site.

1.3.2 Logic Tree Structure

This section describes the general logic tree, which is applicable to all sites. The logic tree is given in Figure III-1.11, and depends on the magnitude, the distance, and the ground motion level. Lower weight is given to concepts B and C, because SP2 ground motion includes not only P-wave ground motion but also S-wave energy. Moreover SP2 ground motion might be affected by shallow resonance effects in the used V/H ratios for rock (Edwards and Fäh, SED report SED/PRP/R/033/20111223). More weight is given to Concept A because it is based on observed data. However only few data exist with the clear signature for non-linear soil response at sites that are similar to the NPP sites.

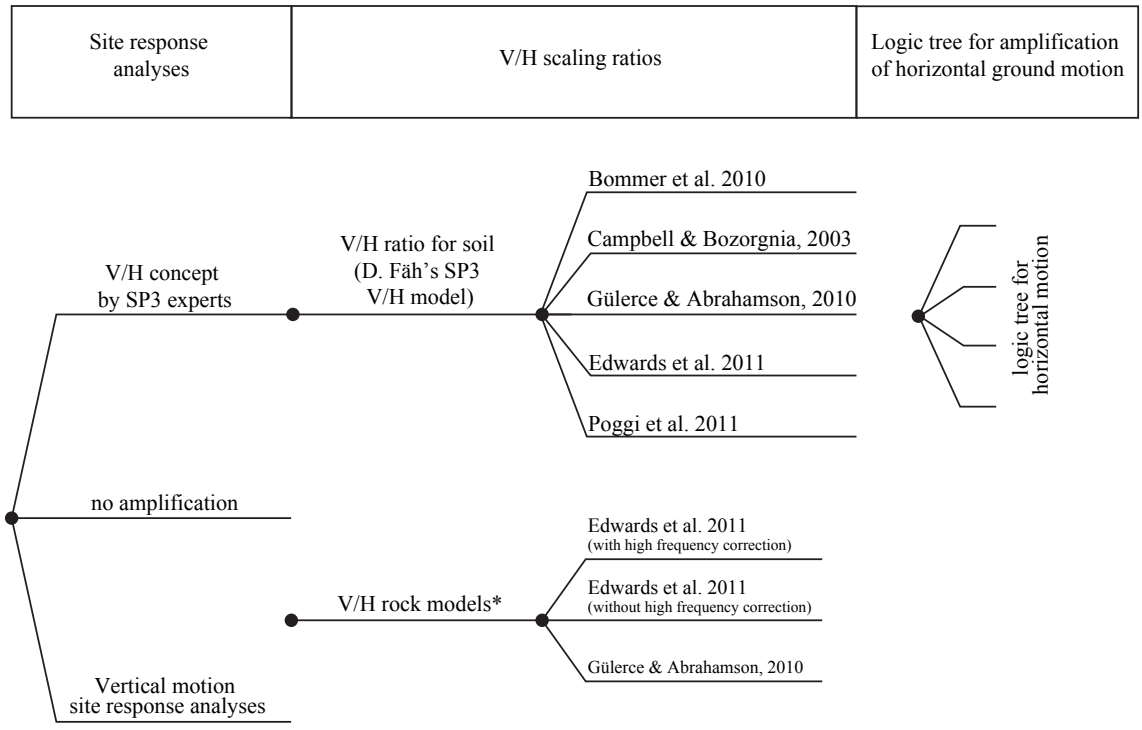

Figure III-1.11: Logic tree used to estimate the median amplification of the vertical ground motion

Distant source	Ground Motion Level 1&2	1.0	Concept A
		0.0	Concept C
	Ground Motion Level 3	0.8	Concept A
		0.2	Concept C
Close source	Ground Motion Level 1&2	1.0	Concept A
		0.0	Concept B
		0.0	Concept C
	Ground Motion Level 3	0.7	Concept A
		0.1	Concept B
		0.2	Concept C

These branches and factors are discussed in the next chapter. Close sources are the sources closer than 20 km or below the site. The magnitude and distance information is brought along the hazard computation. The validity of the assessment for the vertical component is also limited to frequencies above 0.45 Hz. This logic tree is applied entirely to the horizontal motion rock hazard results. The vertical rock hazard corresponds to my SP2 model developed using V/H spectral ratios for rock.

Concept "A" Based on Empirical V/H Ratios

Global empirical V/H concepts are proposed by Gülerce and Abrahamson [2011], Bommer et al. [2011], and Campbell and Bozorgnia [2003]. The methods are outlined in report TP2-TB-1061 [Bommer and Akkar 2010]. The Campbell and Bozorgnia [2003] relation needed some assumptions for the implementation that are not yet documented. V/H reported in NUREG 6728 [McGuire et al. 2001] are related to code-type spectra and are therefore not used. The V/H ratio is a function of the source distance and in some relations of magnitude and PGA level. The V/H ratios in these relatios have a distinct peak at large frequencies in the near-source region. The high-amplitude, high-frequency vertical ground motion that are observed in near-source seismograms might be related ot S-to-P conversion within the transition zone between the underlying bedrock and overlying softer sediments or by direct P-waves. The model by Gülerce and Abrahamson include non-linear soil behaviour that is based on modeling, however confined to the available observational data. The different methods provide similar results for V/H in the linear range of material behaviour. The shape of the V/H curve in the different empirical models is given by the bulk of the data used to derive the relation, with the V/H trough at the average f_0 in the dataset (2 Hz for Gülerce and Abrahamson and Akkar et al. relations, 1.5 Hz for Campell and Bozorgnia relation) and the V/H peak at around 15 Hz at 2-3 times f_0. It is therefore a feature that is not corresponding to the $f_0's$ measured at the NPPs, especially for sites Gösgen and Mühleberg. The available meta-data in the database used in Gülerce and Abrahamsom is judged to be of higher quality then other relations: The Gülerce and Abrahamson model is therefore used in the logic tree with a high weight but only at low ground motion level. Campbell and Bozorgnia [2003] and Bommer et al. [2011] relations are included in the logic tree with a smaller weight at low ground motion level.

Two new concepts based on observed V/H are proposed in SED report SED/PRP/R/031/20110702 (PRP reoport TP3-TB-1084). These concepts are site-specific and are based on observed V/H ratios from earthquake recordings combined with measured velocity profiles and in one method also with ambient vibration recordings. Both methods make use of the velocity

profiles proposed by SP3 experts for the NPP sites, and V/H ratios are therefore site-specific. The first method (Method 1) is based on observed V/H ratios from earthquakes recorded at the KiK-net sites, using the quarter-wavelength representation of the velocity profiles. A predictive equation to obtain the vertical to horizontal ratio (V/H) of ground-motion for sediment sites has been established accounting for resonance phenomena at soft sediment sites. A parameter is directly derived from the quarter-wavelength velocity and represents the frequency dependent seismic impedance contrast at the site. At high frequencies above 30 Hz the value at 30 Hz is taken. The second method (Method 2) is based on observed ambient vibration V/H ratios and V/H ratios from earthquake recordings at the stations of the Swiss seismic network. Ambient vibration data for Japanese sites were not available, limiting the generality of the second method. At NPP sites ambient vibration measurements are used to estimate V/H of earthquake recordings. At frequencies where the V/H is not available for method 2, the values from method 1 are taken. Specifically, V/H ratios from method 2 are not available at low frequencies (TP3-TB-1084: <0.8 Hz for Beznau and Leibstadt; <1.05 Hz for Goesgen and Muehelebrg) and are replaced V/H ratios from method 1. Global empirical V/H ratios and site-specific V/H concepts are equaly weighted. The Gülerce and Abrahamson [2011] model is based on data mainly in the magnitude range 5.0 to 7.5, with a good distance coverage, PGA values mostly below 0.2 g and V_{S30} of sites below about 900m/s. For the higher ground motion levels non-linear behaviour might be expected, and more weight might be given to the method proposed by Gülerce and Abrahamson, because the method accounts for non-linear soil behaviour, at least theoretically. However, this non-linear behaviour is only applied to the horizontal component, even if it is evident that the vertical component contains S-wave energy (This also depends which part of the seismogram defines the PSA in a given frequency band). In the range of non-linear soil behaviour, this assumption leads to very high V/H ratios for frequencies above 10 Hz, in the range of the extrapolation of the method. It seems that this feature can so far not be confirmed by observation as shown in Figures III-1.12(a); III-1.12(b) and III-1.13 in the KNet and KiK-net data.

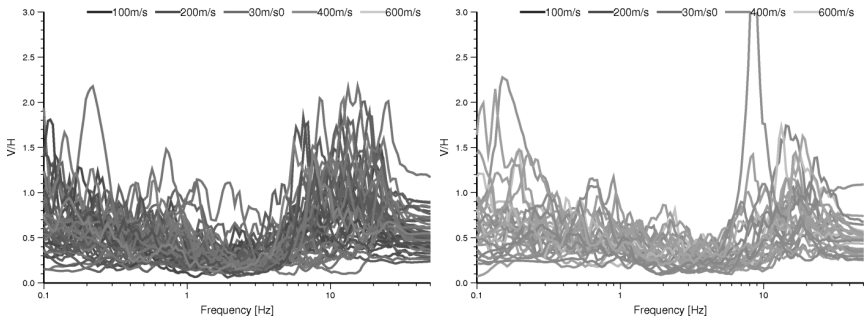

(a) A 200 and 400 m/s (b) B 400 to 600 m/s

Figure III-1.12: V/H ratios for data selected from KNet for which recorded accelerations on at least one component exceeded 5ms-2 , with V_{S30} between a) and b). 5% damped pseudo-spectral acceleration was computed for each component. V/H ratios were then computed for the PSA spectra using the geometrical mean of the horizontal components.

If we assume that PSA on the vertical and horizontal components are due to the S-wave arrivals, then we can assume that non-linear soil response should act in a similar manner on the vertical and horizontal components, and that V/H ratios derived from the linear range

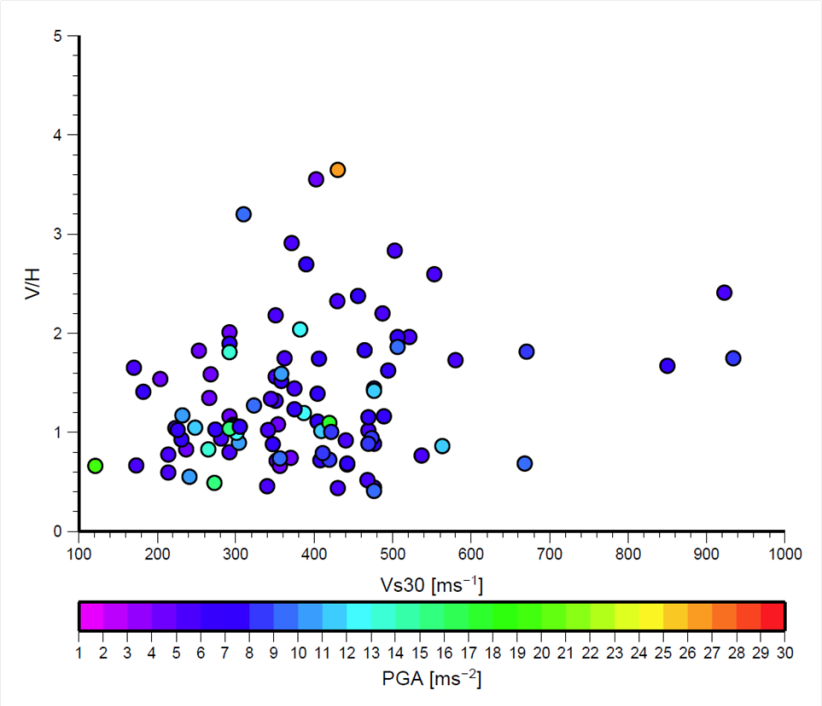

Figure III-1.13: Peak of the V/H spectra (for $f > 8Hz$) versus V_{S30} at KNet and KiK-net sites. Symbol colour indicates PGA of the larger horizontal component.

of the soil response can be extrapolated into the non-linear range. All models depend on distance and frequency, most also depend on magnitude and PGA. This requires the definition of the mean distance for given magnitude that is brought along the hazard computation. SED method 1 and 2 are site-dependent and profile dependent.

Ground Motion Level 1	1.0	Concept A	0.3	Gülerce&Ambrahamson (2010)
			0.1	Bommer et al. (2011)
			0.1	Campell and Bozorgnia (2003)
			0.4	SED Method 1 based on KiK-net data
			0.1	SED Method 2 based on Swiss data
Ground Motion Level 2	1.0	Concept A	0.10	Gülerce&Ambrahamson (2010)
			0.20	Bommer et al. (2011)
			0.20	Campell and Bozorgnia (2003)
			0.45	SED Method 1 based on KiK-net data
			0.05	SED Method 2 based on Swiss data
Ground Motion Level 3	0.8	Concept A	0.00	Gülerce&Ambrahamson (2010)
			0.25	Bommer et al. (2011)
			0.25	Campell and Bozorgia (2003)
			0.50	SED Method 1 based on KiK-net data
			0.0	SED Method 2 based on Swiss data

Concept "B" Based on the Computations for the Vertical Component

It is assumed that the vertical component is amplified due the amplification of vertical incident P-waves, assuming a source below the site, or simply that amplification in PSA is defined by the P-wave arrivals. RVT computations from 2013 are selected in order to be compatible with the logic tree for the horizontal component. The average amplification of the available runs at 0.4g and at 0.75g, computed for each site separately, is used. The vertical rock hazard corresponds to my SP2 model developed using V/H spectral ratios for rock, so that this logic tree branch is applied entirely to the horizontal motion rock hazard results.

Concept "C" Based on the SP2 Vertical Ground Motion Estimate

By assuming that the vertical component of motion is not affected by site-effects, we can take the ground motion estimate for the vertical component obtained from SP2. We might justify such assumption because soil terms in GMPEs on the vertical component are generally smaller than on the horizontal. The vertical rock hazard corresponds to my SP2 model developed using V/H spectral ratios for rock, so that this logic tree branch is applied entirely to the horizontal motion rock hazard results.

1.4 Aleatory Variability of Horizontal Ground Motion

1.4.1 Approach

According to Al Atik et al. [2010], when a partial non-ergodic assumption that only removes the systematic site-specific effects is applied to the ground motion on soil (single-site scenario), the site-to-site variability ϕ_{S2S} is an epistemic uncertainty. This uncertainty is estimated by SP2 from a large number of observation from seismic stations worldwide, including different soil conditions with different V_S profiles. Due to the large variety of site conditions the site-to-site variability ϕ_{S2S} proposed by SP2 has to be much larger than the epistemic uncertainty obtained with the proposed logic tree for each NPP site at low ground motion level. The difference tells us something about our informedness related to the local structure at the NPP sites. With the partial non-ergodic assumption, the aleatory variability of the single-site scenario, ϕ_{SS}, can be written as:

$$\sigma_{SS} = \sqrt{\phi_{Amp}^2 + \phi_{P2P}^2 + \phi_0^2 + \tau_{L2L}^2 + \tau_0^2} \quad \text{(III-1.1)}$$

$$\sigma_{SS} = \sqrt{\phi_{SS}^2 + \tau^2} \quad \text{(III-1.2)}$$

The aleatory variability considered in this chapter is this single station sigma σ_{SS}. The term ϕ_{Amp} represents variability in the site amplification. The term τ_{L2L} is the standard deviation of the location-to-location residual. The path-to-path residual represents the average shift of the observed site-specific region-specific ground motion from the mean site-specific model prediction and has a standard deviation of ϕ_{P2P}. The term τ_0 is the standard deviation of between-events residual for an earthquake remaining after removing the earthquake location-specific effects, and the term ϕ_0 is the standard deviation of unexplained path and radiation pattern effects.

The term to be assessed is ϕ_{Amp} that is much smaller then the combined other uncertainties. The site conditions at the NPPs are not special in terms of site amplification, and therefore, it is expected that the aleatory variability σ_{SS} is covered by the proposed SP2 model from worldwide data. Due to the large number of different stations used, the SP2 model for σ_{SS} also covers some 2D and 3D-effects, and no uncertainty is also added for these effects.

The SP2 model for σ_{SS} is based on observations with site response that is mostly in the linear regime, and it has to be evaluated if ϕ_{Amp} needs to be increased for non-linear soil behaviour. The single-station sigma report [Rodriguez-Marek and Cotton 2011] (TP2-TB-1058) shows a reduction with increasing magnitude. The ground motions in the dataset are mostly below 0.2g, and this decrease can therefore not be assigned conclusively to non-linear soil behaviour.

On the one hand, non-linear calculations show higher variability driven by specific properties of the different input time-histories. The soil behaviour is more or less non-linear depending on properties of the input motion, and the higher variability of the amplification seems to be correlated with the input motion, wheres the variability of the resulting ground motion seems to get lower with increasing ground motion level. Only a limited number of input ground motion were used, and it is difficult to assess if time series include particular properties related to site-effects at the recording sites or other particularities of the site. When increasing the PGA level, non-linear behaviour should decrease the variability once τ_{max} is reached. This is also observed for some cases in particular frequency bands and would decrease aleatory variability. On the other hand, non-linear computations get less reliable the more PGA is increased. The epistemic uncertainty in the proposed logic tree is increased with increasing input ground motion, assuming also a wide range of possible non-linear behaviour, and "simulating" an increased variability of soil behaviour. Adding additional aleatory uncertainty therefore includes the risk for counting the same effect twice. For these reasons no additional aleatory variability for non-linear behaviour is included in the proposed model. As a consequence all uncertainty in the proposed logic tree for horizontal ground motion is placed in increased epistemic uncertainty by assuming very different non-linear soil behaviour at high ground motion levels. In the logic tree proposed during the PEGASOS project the aleatory variability included the variability of the mean correction factor for non-vertical incidence and 2D-effects. Non-vertical incidence is now included in the SP2 model because a site-specific rock reference is used for each NPP. 2D and 3D-effects are accounted for explicitly in the proposed PRP logic tree.

1.5 Aleatory Variability of Vertical Ground Motion

1.6 Approach

For the vertical component empirically derived aleatory variability is generally higher than for the horizontal. The aleatory variability is taken from the estimate of SP2, and no additional aleatory variability is added. However if SP2 selects a different aleatory variability for the horizontal and vertical component, then this has the be corrected in the way that the aleatory variability needs to be increased for all branches based on V/H ratios that are applied to the horizontal ground motion. This correction could be done based on the sigma of the used V/H ratios. This however would require the treatment of correlation between the horizontal and vertical component, an information that is not available. For this reason, simply the difference

of the two sigmas used by SP2 is added, but only for the branch with concept A:

$$\sqrt{\sigma_V^2 - \sigma_H^2}$$

1.7 Maximum Ground Motions

This part provides an estimate of the possible maximum ground motion for the horizontal and vertical component. As a base the assessment performed during PEGASOS is used, which was based on the recommendations by Pecker et al. [2003](TP3-TN-0354) and the maximum observed ground motions [Ripperger and Fäh 2003] (TP3-TN-0359). Since theoretical and numerical results have a high uncertainty caused by the lack of experience and observations, the assumed epistemic uncertainty is very high. In the following the assessment during PEGASOS is evaluated, using the new findings proposed by Pecker [2011] (TP3-TB-1074) and the collection of maximum observed ground motion data [Strasser and Zulu 2010] (EXT-TB-1067 and related database and Matlab tool).

1.7.1 Horizontal Component

During PEGASOS the maximum peak ground accelerations (PGA) were estimated by Pecker et al. [2003] (PEGASOS report TP3-TN-0354) as follows: for Beznau 20m/s^2, for Gösgen 15m/s^2, for Leibstadt 15m/s^2, and for Mühleberg 16m/s^2. No estimate of the maximum spectral acceleration as a function of frequency was provided. The spectral shapes were derived from the maximum observed ground motion summarized in Ripperger and Fäh [2003] PEGASOS report TP3-TN-0359. This is illustrated in Figure III-1.14. Two possible shapes of the spectra were taken into account for the horizontal component, as is shown in Figure III-1.15. The factors are given in Table III-1.15. The high plateau value derived from the observed maximum ground motions (see Figure III-1.14) accounted for small-frequency-band peaks in possible response spectra. A common shape was proposed for all NPP sites, because at high ground motion levels non-linear effects will cause energy transfer between different frequencies, which makes the behaviour unpredictable. PGA values higher than those proposed by Pecker et al. [2003] are not excluded, and some of the non-linear computations performed during PEGASOS also supported this assumption. This choice also accounted for additional effects such as 2D/3D-effects, when the failure introduces a solid-liquid interface that is able to trap S-wave energy. For this reason the logic tree also included a branch with maximum PGA values that are twice the values proposed by Pecker et al. [2003]. For PRP A.Pecker reviewed his assessment by using an improved method ([Pecker 2005]) as well as Bethbeder's model and the results from the non-linear runs at 2.5g input ground motion. This resulted in increased maximum PGA values at the sites as summarized in Table III-1.16 [Pecker 2011]. The highest values are obtained from the non-linear runs. However PGA values were determined at 30Hz due to unreliable results in non-linear computations for frequencies above 30Hz. The maximum PGA values are therefore overestimating the real PGA. Pecker argued that no significant difference can be observed between the sites, and due to the uncertainty of his assessment a site specific maximum ground motion is not justified. Taking into account all the facts the maximum PGA is estimated 25m/s^2 for all sites.

Table III-1.15: Factors applied to the PGA values in order to compute the maximum spectral acceleration for the horizontal component at a given frequency. Factor 1 defines a flatter spectrum than Factor 2.

Frequency [Hz]	Factor 1	Factor 2
0.45	1.5	2
1	2	3
2.5	2.5	4
5	2.5	4
10	2	3
20	1.5	2
50	1	1
100	1	1

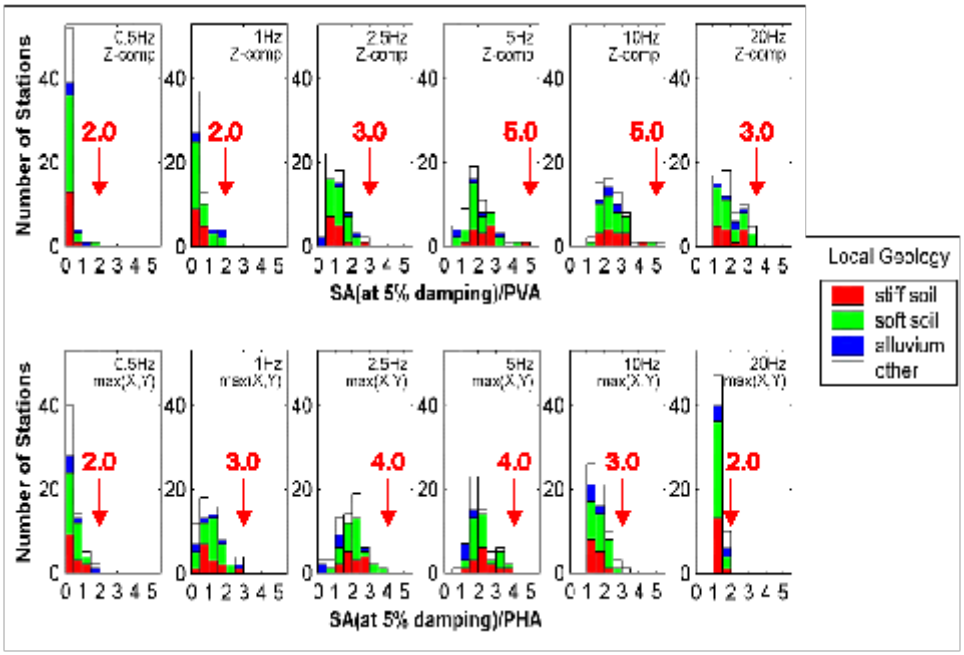

Figure III-1.14: Derivation of the spectral shapes for maximum ground motion from the maximum observed ground motion summarized ([Ripperger and Fäh 2003] PEGASOS TP3-TN-0359).

Table III-1.16: Summary of maximum surface acceleration (PGA values in g) taken from Pecker [2011] (TP3-TB-1074), considering analytical models and numerical simulations.

	KKG	KKB	EKKB	KKL	KKM
Theoretical model	2	2.5	2.2	1.8	2.1
Betbeder's model	1.4	2	1.5	1.5	1.5
Non-linear site response analyses	2.5 to 3.0	2.3 to 3.0	2.1 to 2.7	2.2 to 2.8	2.1 to 2.7
Proposed range of values	2.5 - 3.0	2.5 - 3.0	2.2 - 2.7	2.3 - 2.8	2.1 - 2.6

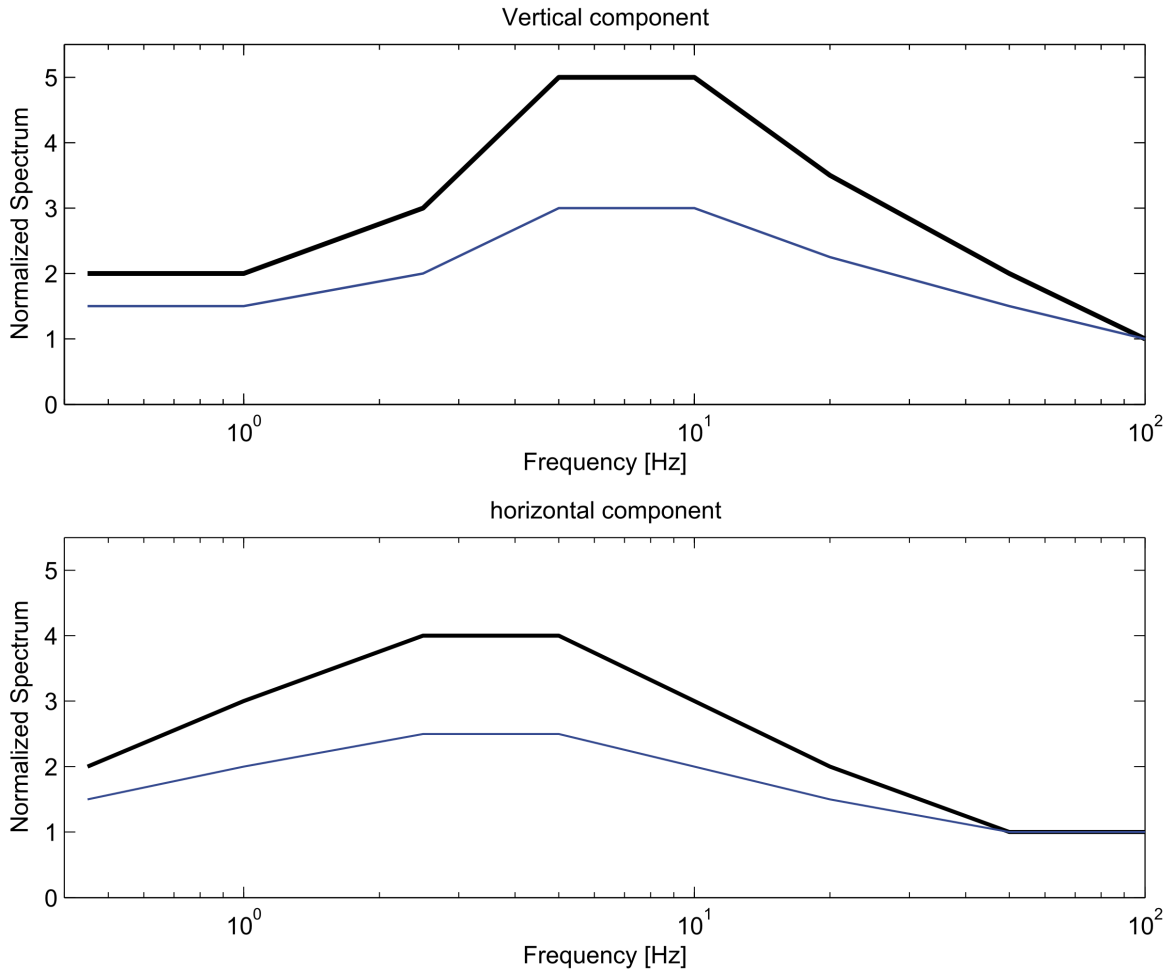

Figure III-1.15: Shapes of the spectra for maximum ground motions for the horizontal and vertical component, normalized to PGA. It is noticed that the plateau of the spectrum for the vertical component is higher than for the horizontal, and shifted in the frequency range to higher frequencies.

Logic Tree Structure

The logic tree used for all sites with the weights and branches is given in Figure III-1.16. Four alternative spectra for maximum horizontal ground motion are proposed, each associated with a certain weight. These spectra are based on the two alternative synthetic spectra, which were derived during PEGASOS from observed spectra in [Ripperger and Fäh 2003] TP3-TN-0359. Since observations most probably will not cover all possible values, we have to expect higher values than shown in Figure III-1.17. This is accounted for by two PGA levels in the logic tree. The scaling is one or two times the maximum PGA value of 25 m/s^2 for each site, which was estimated based on PRP report TP3-TB-1074. The weights are provided in Figure III-1.16. Multiplying the lower PGA with a plateau value 2.0-2.5 for the frequency range 2.5-10 Hz (about Factor 1 in Table III-1.15), results in spectral accelerations in the range 50 and 60m/s^2 reached for some non-linear runs. Higher weight is therefore given to the estimate of PGA of 25 m/s^2 and Factor 2. This PGA values are preferred over the factor of 2 increased values because they are based on the computed soil strengths. The spectral shape of the lowest maximum ground motion in Figure III-1.15 corresponds approximately the maximum observed ground motions shown in Figures III-1.17 and III-1.18. For the higher PGA value, the flat spectrum is preferred. In order to smooth the influence of the 4 upper bound models, each of the four spectra is subdivided into 5 separate spectra which range from 50% to 100%.

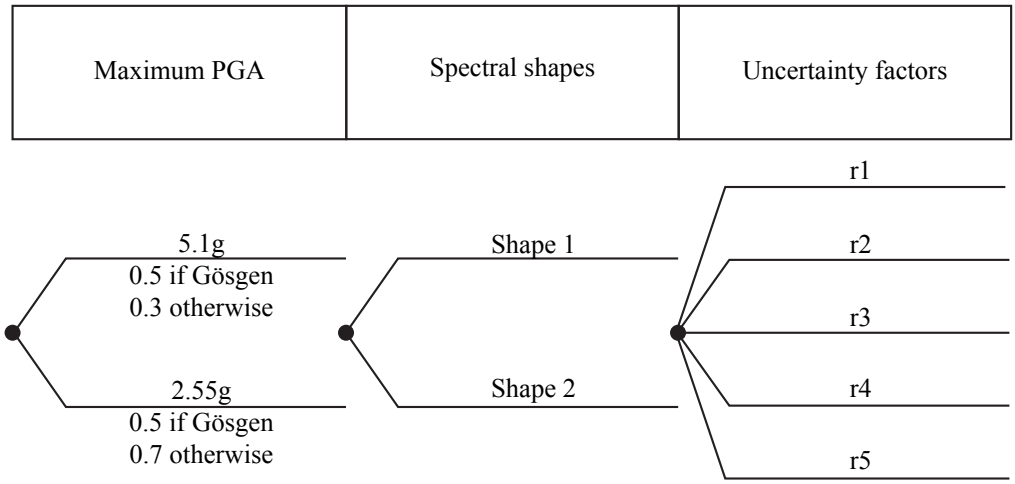

Figure III-1.16: Frequency dependent logic tree used to estimate the maximum spectral acceleration for the horizontal component.

1.7.2 Vertical Component

No computations are available for estimating the maximum ground motion on the vertical component. Therefore, the logic tree structure for the maximum vertical ground motion is proposed to be similar to the one for the horizontal component. The maximum peak ground accelerations (PGA) are taken from Section 1.7.1 (derived from PRP report TP3-TB-1074) and are assumed to be also valid estimates for the vertical component, assuming similar S-wave energy on the vertical component. The spectral shapes are derived from the maximum observed ground motion summarized in the PEGASOS report [Ripperger and Fäh 2003] (TP3-TN-0359) for the vertical component (Figure III-1.15). Two possible shapes of the spectra are taken into account (Table III-1.17). Factors are applied to the PGA values in

0.7	MAX(PGA) = 1.0 * 25m/s^2				
		0.3	Factor 1	applied to obtain the	max spectral acceleration
			0.1	Resulting spectral acceleration	is 80% of the max
			0.15	Resulting spectral acceleration	is 85% of the max
			0.2	Resulting spectral acceleration	is 90% of the max
			0.25	Resulting spectral acceleration	is 95% of the max
			0.3	Resulting spectral acceleration	is 100% of the max
		0.7	Factor 2	applied to obtain the	max spectral acceleration
			0.1	Resulting spectral acceleration	is 80% of the max
			0.15	Resulting spectral acceleration	is 85% of the max
			0.2	Resulting spectral acceleration	is 90% of the max
			0.25	Resulting spectral acceleration	is 95% of the max
			0.3	Resulting spectral acceleration	is 100% of the max
0.3	MAX(PGA) = 2.0 * 25m/s^2				
		0.8	Factor 1	applied to obtain the	max spectral acceleration
			0.2	Resulting spectral acceleration	is 60% of the max
			0.2	Resulting spectral acceleration	is 70% of the max
			0.2	Resulting spectral acceleration	is 80% of the max
			0.2	Resulting spectral acceleration	is 90% of the max
			0.2	Resulting spectral acceleration	is 100% of the max
		0.2	Factor2	applied to obtain the	max spectral acceleration
			0.2	Resulting spectral acceleration	is 60% of the max
			0.2	Resulting spectral acceleration	is 70% of the max
			0.2	Resulting spectral acceleration	is 80% of the max
			0.2	Resulting spectral acceleration	is 90% of the max
			0.2	Resulting spectral acceleration	is 100% of the max

order to compute the maximum spectral acceleration for the vertical component at a given frequency. For intermediate frequencies, linear interpolation is proposed. The amplification factors are the same for all sites.

Logic Tree Structure

The logic tree for the vertical component for all sites with the weights and branches is the same as in Figure III-1.16. The basis for the weights is similar to the horizontal component, and explained in Section 1.7.1. The weights for the highest ground motion level is increased, due to the fact that P-wave energy still can pass a liquefied layer. Neither observational data nor non-linear computation exist to constrain this assessment. Moreover the phenomenon of cyclic mobility theoretically allows very high acceleration on the vertical component.

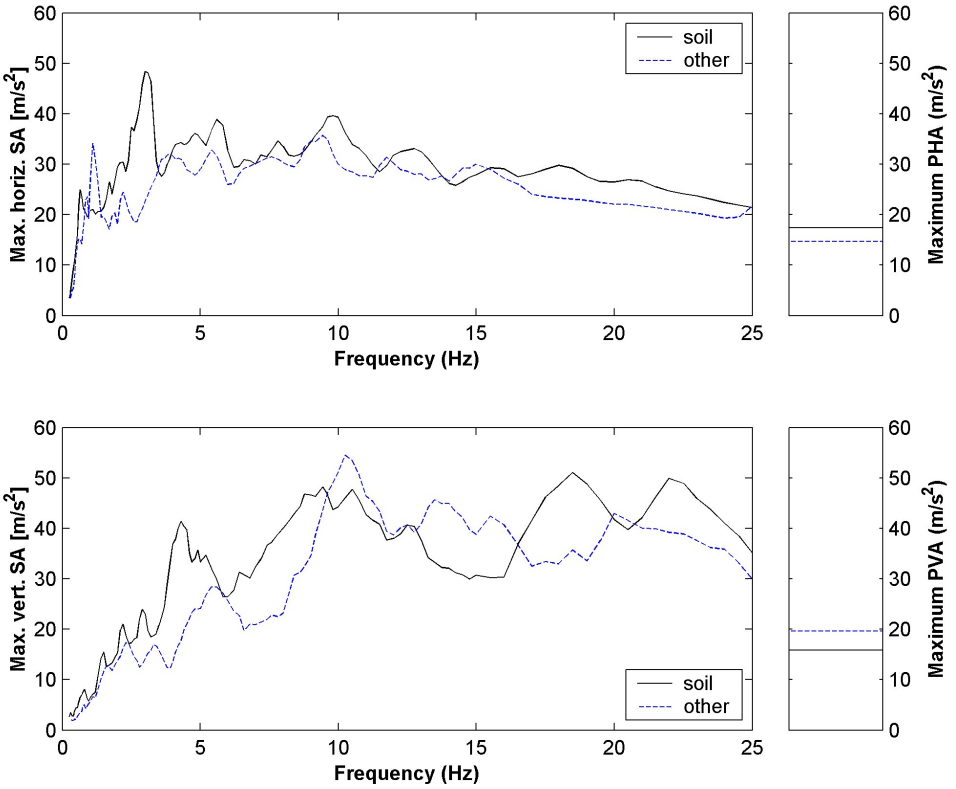

Figure III-1.17: Maximum spectral acceleration and maximum peak acceleration of all the records (from PEGASOS report TP3-TN-0359). Top: Maximum horizontal SA and maximum peak horizontal acceleration (PHA). Bottom: Maximum vertical SA and maximum peak vertical acceleration (PVA). Solid black line: local geology is "stiff soil", "soft soil" or "alluvium". Dashed blue line: local geology is "rock", "very soft soil" or unknown.

Table III-1.17: Factors applied to the PGA values in order to derive the spectral shape of the maximum spectral acceleration for the vertical component at a given frequency.

Frequency [Hz]	Factor 3	Factor 4
0.45	1.5	2
1	1.5	2
2.5	2	3
5	3	5
10	3	5
20	2.25	3.5
50	1.5	2
100	1	1

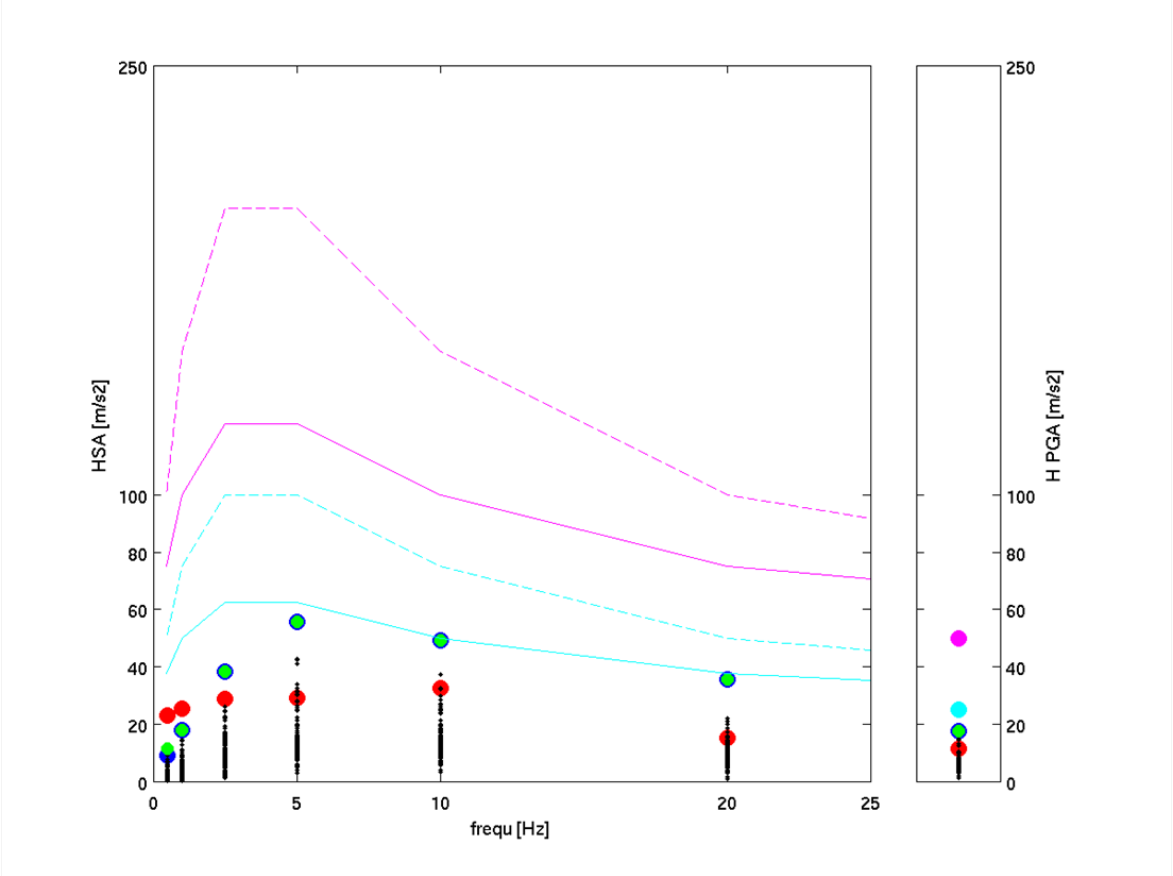

Figure III-1.18: Maximum horizontal spectral acceleration and maximum horizontal peak acceleration of all the records from the collection of maximum observed ground motion data [Strasser and Zulu 2010] (PRP report EXT-TB-1067 and related database and matlab tool) for soil class C (that results in the highes values) together with the spectra used estimate the maximum spectral acceleration. Large red dots are the maxima observed for Mw=5-6, blue circles for Mw=6-7 and green dots for Mw=6.5-7.5.

1.8 Amplification for Outcropping Motion at Intermediate Depth Levels 2 and 3

The project specified that the amplification has to be estimated for outcropping motion. The difficulty is that the concept of outcropping motion (only up-going waves) does not exist in nature and has nothing to do with real ground motion observed at elevation 2 and 3.

The amplification factors are provided for the computations with SHAKE and RVT. It is, however, not possible to directly relate the non-linear ground motion at depth with the outcropping motion. There is also no direct relation to scale the non-linear result with the computations using SHAKE and RVT.

Surface wave propagation and 2D or 3D-effects cannot be handled by the concept of outcropping motion. However, such effects will also contribute to the wavefield at depth. For this reason, such effects will be included also in the intermediate depth levels in the same manner as for the surface.

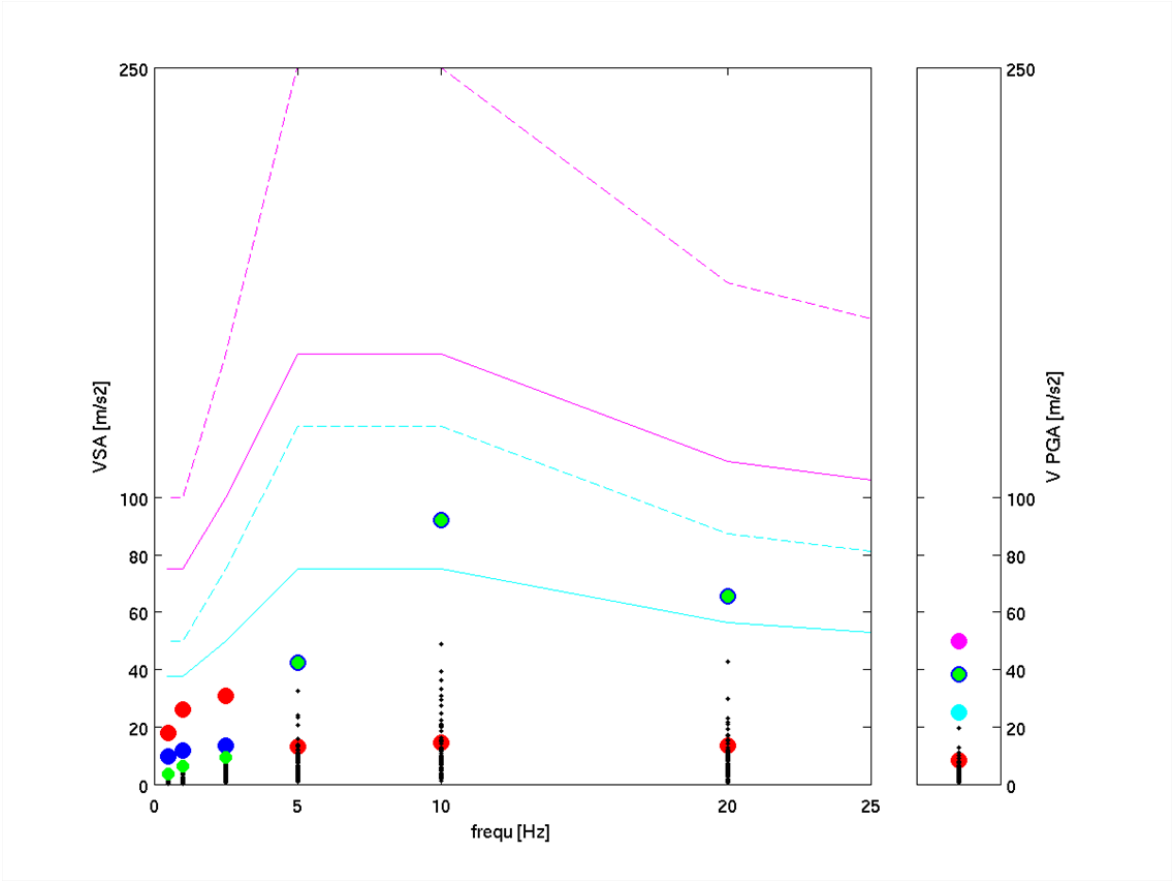

Figure III-1.19: The same as Fig6-5A but for the maximum vertical spectral acceleration and maximum vertical peak acceleration.

1.8.1 Median Amplification for the Horizontal Component

The logic trees proposed for the surface are also applied to the intermediate depth levels with a series of changes. For the RVT branches, the outcropping motion amplification is taken at the respective depth levels. The results obtained in 2013 are used. The non-linear runs provide the "within layer" ground motion at depth and not the outcropping ground motion. Therefore, the non-linear-case amplification factors have to be corrected with the available information. Two types of ratios of motion at depth were proposed during PEGASOS and used to scale the ground motions from the non-linear runs. Therefore two procedures a) and b) were originally considered for the correction of the non-linear amplification factors:

1. a) We can expect comparable results between RVT or SHAKE and the non-linear calculation at low level of shaking, if the ratio between incident wave and total wave-field is assumed to be the same for the different modeling schemes. We can compute the following ratios (at PGA of 0.4 g, site-specific (one model) and at each elevation level separately):

RAT1 = (amplification RVT)/(amplification non-linear)
RAT2 = (amplification SHAKE)/(amplification non-linear)

0.3	MAX(PGA) = 1.0 * 25m/s^2				
		0.3	Factor 3	applied to obtain the	max spectral acceleration
			0.1	Resulting spectral acceleration	is 80% of the max
			0.15	Resulting spectral acceleration	is 85% of the max
			0.2	Resulting spectral acceleration	is 90% of the max
			0.25	Resulting spectral acceleration	is 95% of the max
			0.3	Resulting spectral acceleration	is 100% of the max
		0.7	Factor 4	applied to obtain the	max spectral acceleration
			0.1	Resulting spectral acceleration	is 80% of the max
			0.15	Resulting spectral acceleration	is 85% of the max
			0.2	Resulting spectral acceleration	is 90% of the max
			0.25	Resulting spectral acceleration	is 95% of the max
			0.3	Resulting spectral acceleration	is 100% of the max
0.7	MAX(PGA) = 2.0 * 25m/s^2				
		0.8	Factor 3	applied to obtain the	max spectral acceleration
			0.2	Resulting spectral acceleration	is 60% of the max
			0.2	Resulting spectral acceleration	is 70% of the max
			0.2	Resulting spectral acceleration	is 80% of the max
			0.2	Resulting spectral acceleration	is 90% of the max
			0.2	Resulting spectral acceleration	is 100% of the max
		0.2	Factor 4	applied to obtain the	max spectral acceleration
			0.2	Resulting spectral acceleration	is 60% of the max
			0.2	Resulting spectral acceleration	is 70% of the max
			0.2	Resulting spectral acceleration	is 80% of the max
			0.2	Resulting spectral acceleration	is 90% of the max
			0.2	Resulting spectral acceleration	is 100% of the max

The ratios are a function of frequency, with the following definitions:

amplification RVT: for the outcropping motion in the base case, results obtained in 2013
amplification SHAKE: for the outcropping motion, results obtained in 2010
amplification non-linear: for the ground motion, results obtained in 2010

With this ratio the non-linear amplification factors could be corrected so that it approximates the amplification for outcropping motion. The ratios RAT1 and RAT2 are given in Figures III-1.20 and Figures III-1.21. It is evident that the amplification factors for outcropping motion are larger at high frequencies than the amplification factors for ground motion, due to the intrinsic attenuation of the waves in the surface part of the soft sediments.

1. b)For the SHAKE computations the amplification factors for ground motion and outcropping motion are available. With their ratio, we can correct the non-linear amplification factors:

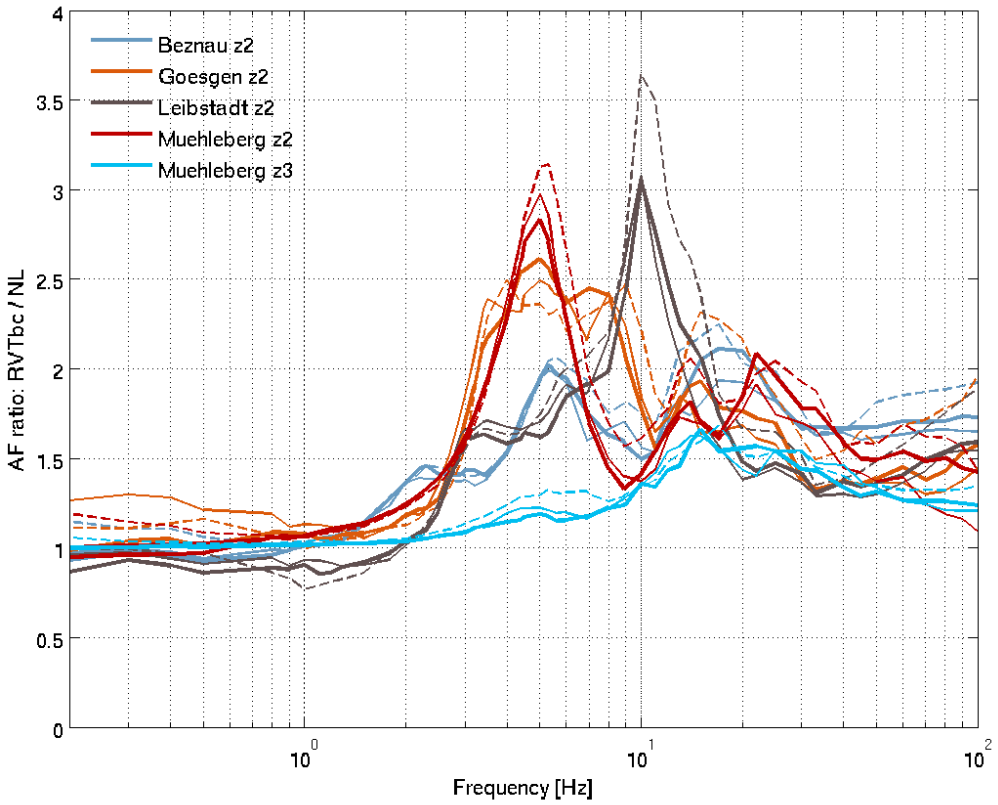

Figure III-1.20: Correction factors RAT1 for outcroping motion in the non-linear runs. Ratio between amplification for outcropping motion obtained with the RVT base case and amplification for ground motion obtained with the non-linear run are shown for the four sites Beznau KKB, Gösgen, Leibstadt and Mühleberg_z2. PGA level is always 0.4 g. The examples are at depth level 2 for all sites. M5: dashed thin line, M6: solid thick line, M7: solid thin line. And at depth level 3 for site Mühleberg_z3

RAT3= (SHAKE outcropping motion)/(SHAKE ground motion)

RAT3 is computed for all models at one site, using the SHAKE results from 2013, each PGA level and at the corresponding depth level (Figures III-1.22 and III-1.23). In order to compute the geometric mean of the correction factors for one site, the factors obtained from one profile are first normalized to the profiles' f_0, and then averaged at each f/f0 value over all profiles. If no SHAKE computations exist at a certain PGA level, the ratio from the closest PGA level is selected, e.g. for the correction of non-linear runs at 1.5g, RAT3 values from SHAKE at 0.75g is used.

For the non-linear branches in the logic trees, the within ground-motion amplification factor at depth is taken and could be multiplied by the factors RAT1, RAT2 and RAT3, defined above. For the ratio RAT1, there is the risk for double counting computations using RVT, and therefore this ratio is not used. The same is true for RAT2 because the difference between SHAKE and non-linear computations has been accounted for in the section on modelling uncertainty. Only term RAT3 is therefore applied, because this term does not include corrections due to different modeling techniques. The weights to the branches are as

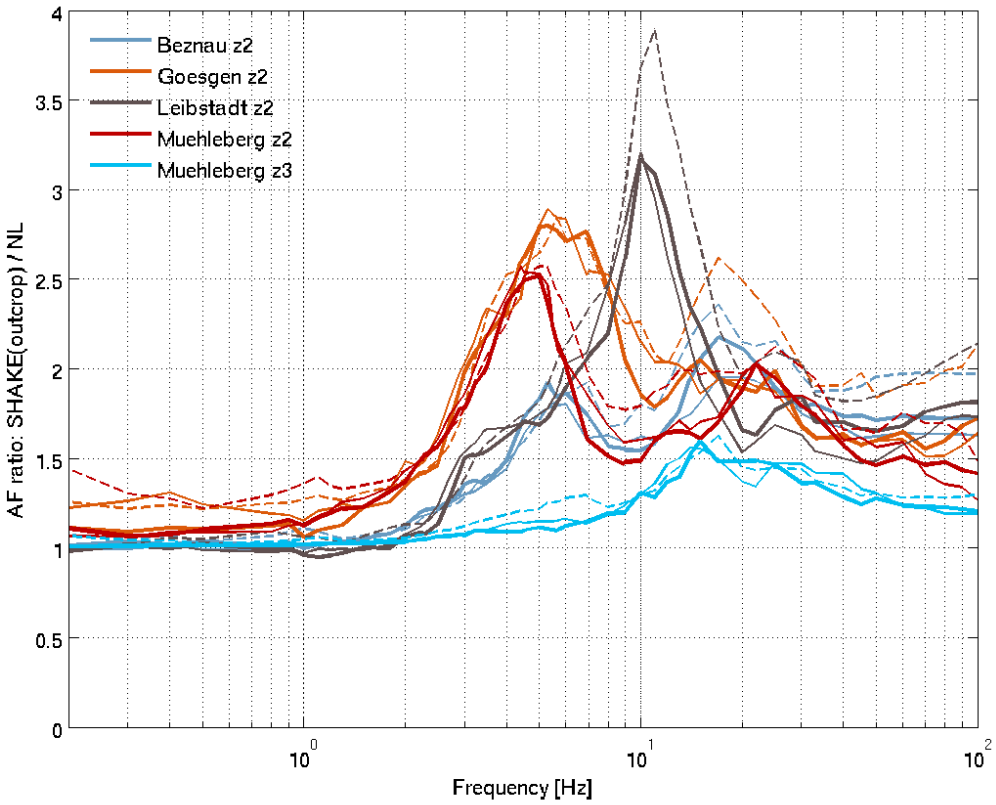

Figure III-1.21: Correction factors RAT2 for outcroping motion in the non-linear runs. Ratio between amplification for outcropping motion obtained with SHAKE and amplification for ground motion obtained with the non-linear run are shown for the four sites Beznau KKB, Gösgen, Leibstadt and Mühleberg_z2 and Mühleberg_z3. PGA level is always 0.4 g. The examples are at depth level 2 for all sites. M5: dashed thin line, M6: solid thick line, M7: solid thin line. And at depth level 3 for site Mühleberg_z3

follows:

0.0	apply factor	RAT1	
0.0	apply factor	RAT2	
0.2	apply factor	RAT3	(geometric mean - 1 sigma)
0.6	apply factor	RAT3	(geometric mean)
0.2	apply factor	RAT3	(geometric mean + 1 sigma)

This introduces epistemic uncertainty related to the lack of the outcropping motion in the non-linear case. The wave propagation effects other than vertically incident SH wave (2D-effects, inclined wave effects, PSV case) were only computed for the surface. Since there are no specific computations performed concerning these wave propagation effects, no change to the scheme for the surface is proposed.

1.8.2 Median Amplification for the Vertical Component

For the vertical component we keep the same procedure as for the surface, including some modifications for the concept A and B. For concept A, we use the same procedure as for the surface layer. The estimate for the amplification on the vertical component is obtained

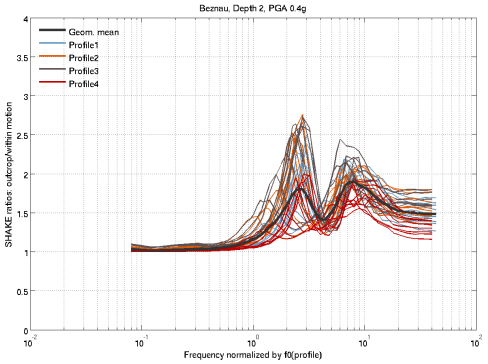

(a) Beznau

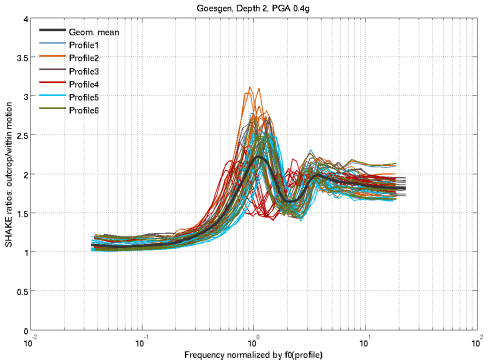

(b) Goesgen

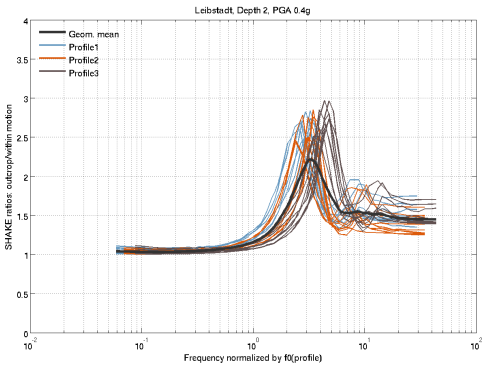

(c) Leibstadt

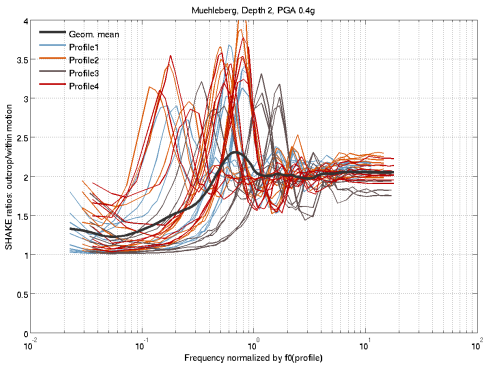

(d) Muehleberg

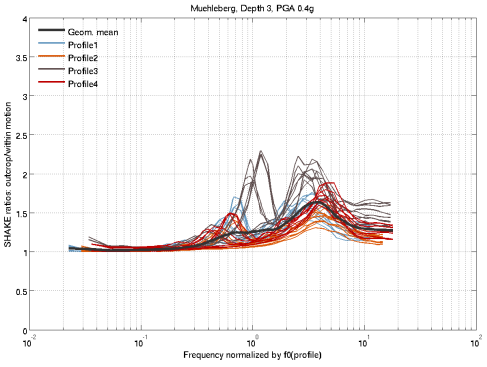

(e) Level 3

Figure III-1.22: Correction factors RAT3 (geometric mean) for outcroping motion in the non-linear runs, normalized to f_0, at PGA level of 0.4 g. Ratio between amplification for outcropping motion obtained with SHAKE and amplification for within ground motion obtained also with SHAKE are shown for the four sites a) Beznau KKB, b) Gösgen, c) Leibstadt and d) Mühleberg_z2. Also shown are the ratios for all the profiles, given in different colour. The examples are at depth level 2 for all sites and at depth level 3 for site Mühleberg.

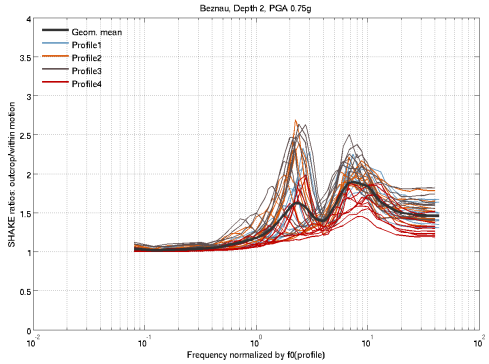

(a) Beznau

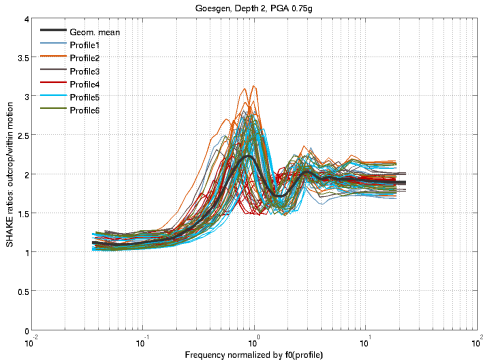

(b) Goesgen

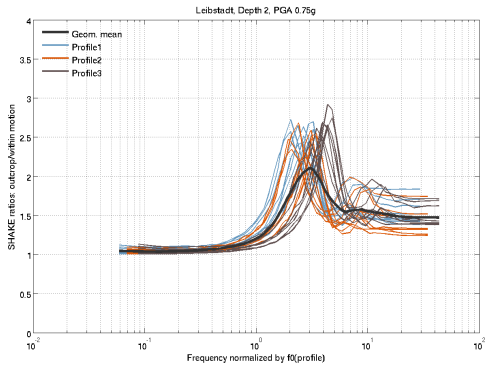

(c) Leibstadt

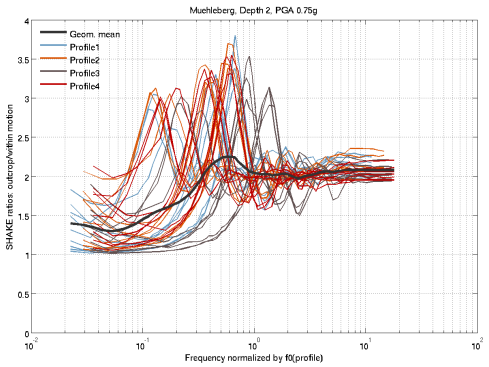

(d) Muehleberg

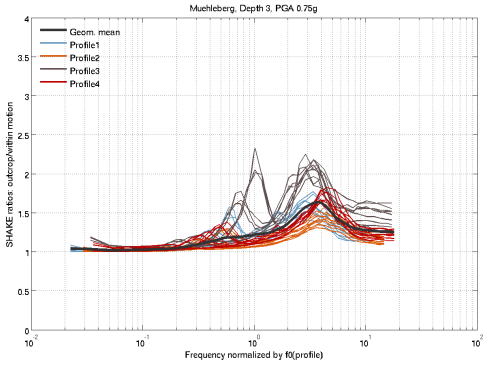

(e) Level 3

Figure III-1.23: Correction factors RAT3 (geometric mean) for outcroping motion in the non-linear runs, normalized to f_0, at PGA level of 0.75 g. Ratio between amplification for outcropping motion obtained with SHAKE and amplification for within ground motion obtained also with SHAKE are shown for the four sites a) Beznau KKB, b)Gösgen, c) Leibstadt and d) Mühleberg_z2. Also shown are the ratios for all the profiles, given in different colour. The examples are at depth level 2 for all sites and at depth level 3 for site Mühleberg.

from the estimate of the horizontal component using different V/H spectral ratios. This however needs an adjustment of the V_{S30} for the global empirical V/H concepts (Gülerce and Abrahamson [2011], Bommer et al. [2011] and Campbell and Bozorgnia [2003]), as well as of the quarter-wave length velocity as function of frequency for SED method 1, starting in both cases from the respective intermediate level downwards. Since no V/H ambient vibration measurements are available at depth, the V/H values of SED method 2 are substituted by the one's of method 1. For concept B (RVT branches), the computations in 2013 for outcropping motion at the different elevation levels are used instead of the ground motion at surface.

1.8.3 Aleatory Variability

Aleatory variability of the ground motion amplification at depth is computed in the same way as for the surface level, assuming that aleatory variability of outcropping amplification factors are equal to the aleatory variability of the ground motion amplification at surface.

1.8.4 Maximum Ground Motion

For the layers at depth the same procedure is applied as for the surface level. The same four spectral shapes are used. With high probability, the failure occurs in the upper 5 meters of the sediments. Failure introduces a reflecting solid liquid interface. Maximum ground motion is therefore expected to be larger at depth than at surface. This can be seen from the non-linear runs in some of the computations (Pecker's presentation "Maximum ground motion at depth" of October 20, 2003). The expected higher values at depth will be accounted for by giving different weights to the four possible spectra. The weights are provided in Table III-1.18 for the horizontal ground motion and Table III-1.19 for the vertical ground motion. The weights for the high-PGA spectra were increased compared to the surface level because the layers that may be liquefied are above the intermediate depth levels 2 and 3.

Table III-1.18: Maximum ground motion weights for horizontal component.

0.5	MAX(PGA) = 1.0 * 25m/s^2				
		0.3	Factor 1	applied to obtain the	max spectral acceleration
			0.1	Resulting spectral acceleration	is 80% of the max
			0.15	Resulting spectral acceleration	is 85% of the max
			0.2	Resulting spectral acceleration	is 90% of the max
			0.25	Resulting spectral acceleration	is 95% of the max
			0.3	Resulting spectral acceleration	is 100% of the max
		0.7	Factor 2	applied to obtain the	max spectral acceleration
			0.1	Resulting spectral acceleration	is 80% of the max
			0.15	Resulting spectral acceleration	is 85% of the max
			0.2	Resulting spectral acceleration	is 90% of the max
			0.25	Resulting spectral acceleration	is 95% of the max
			0.3	Resulting spectral acceleration	is 100% of the max
0.5	MAX(PGA) =2.0 * 25m/s^2				
		0.8	Factor 1	applied to obtain the	max spectral acceleration
			0.2	Resulting spectral acceleration	is 60% of the max
			0.2	Resulting spectral acceleration	is 70% of the max
			0.2	Resulting spectral acceleration	is 80% of the max
			0.2	Resulting spectral acceleration	is 90% of the max
			0.2	Resulting spectral acceleration	is 100% of the max
		0.2	Factor2	applied to obtain the	max spectral acceleration
			0.2	Resulting spectral acceleration	is 60% of the max
			0.2	Resulting spectral acceleration	is 70% of the max
			0.2	Resulting spectral acceleration	is 80% of the max
			0.2	Resulting spectral acceleration	is 90% of the max
			0.2	Resulting spectral acceleration	is 100% of the max

Table III-1.19: Maximum ground motion weights for vertical component.

0.2	MAX(PGA) = 1.0 * 25 m/s^2				
		0.3	Factor 3	applied to obtain the	max spectral acceleration
			0.1	Resulting spectral acceleration	is 80% of the max
			0.15	Resulting spectral acceleration	is 85% of the max
			0.2	Resulting spectral acceleration	is 90% of the max
			0.25	Resulting spectral acceleration	is 95% of the max
			0.3	Resulting spectral acceleration	is 100% of the max
		0.7	Factor 4	applied to obtain the	max spectral acceleration
			0.1	Resulting spectral acceleration	is 80% of the max
			0.15	Resulting spectral acceleration	is 85% of the max
			0.2	Resulting spectral acceleration	is 90% of the max
			0.25	Resulting spectral acceleration	is 95% of the max
			0.3	Resulting spectral acceleration	is 100% of the max
0.8	MAX(PGA) =2.0 * 25 m/s^2				
		0.8	Factor 3	applied to obtain the	max spectral acceleration
			0.2	Resulting spectral acceleration	is 60% of the max
			0.2	Resulting spectral acceleration	is 70% of the max
			0.2	Resulting spectral acceleration	is 80% of the max
			0.2	Resulting spectral acceleration	is 90% of the max
			0.2	Resulting spectral acceleration	is 100% of the max
		0.2	Factor 4	applied to obtain the	max spectral acceleration
			0.2	Resulting spectral acceleration	is 60% of the max
			0.2	Resulting spectral acceleration	is 70% of the max
			0.2	Resulting spectral acceleration	is 80% of the max
			0.2	Resulting spectral acceleration	is 90% of the max
			0.2	Resulting spectral acceleration	is 100% of the max

Chapter 2

Hazard Input Document for D. Fäh (EG3-HID-1006)

Written by the PMT, SP4 and TFI

2.1 Introduction

This Hazard Input Document (HID) describes the implementation, evaluation and results of Donat Fäh's geotechnical assessment of sites effects (the "model" or "SP3 model") at the NPP sites Beznau, Gösgen, Leibstadt and Mühleberg, deliverd on 26.04.2013. The purpose of this document is to provide a technical description of the model as implemented. The results of model evaluation are compiled into a so-called SIF (Soil hazard Input File), which, among the rock hazard results, is input to the soil hazard evaluations. This HID addresses technical and procedural aspects. It does not provide a rational discussion of the models or the results.

2.2 Model Description

The geotechnical assessment by Donat Fäh is described in part III, Chapter 1 (EG3-ES-1015). The models concern six quantities:

- Amplification of horizontal ground motion,
- Aleatory variability of horizontal motion amplification,
- Maximum horizontal ground motion (truncation model),
- Amplification of vertical ground motion and V/H scaling,
- Aleatory variability of vertical motion amplification and V/H scaling factors, and
- Maximum vertical ground motion (truncation model),

which are developed as functions of spectral frequency, which consider the up-going wavefield ("outcrop motion") and which depend on site, target depth, magnitude and PGA. The models are formulated as logic trees, yielding epistemic uncertainty. These logic tree models are described in the following.

2.2.1 Amplification of Horizontal Ground Motion

The logic tree model for amplification of horizontal ground motion has seven levels of branching (Fig. III-2.1), among which epistemic uncertainty is developed.

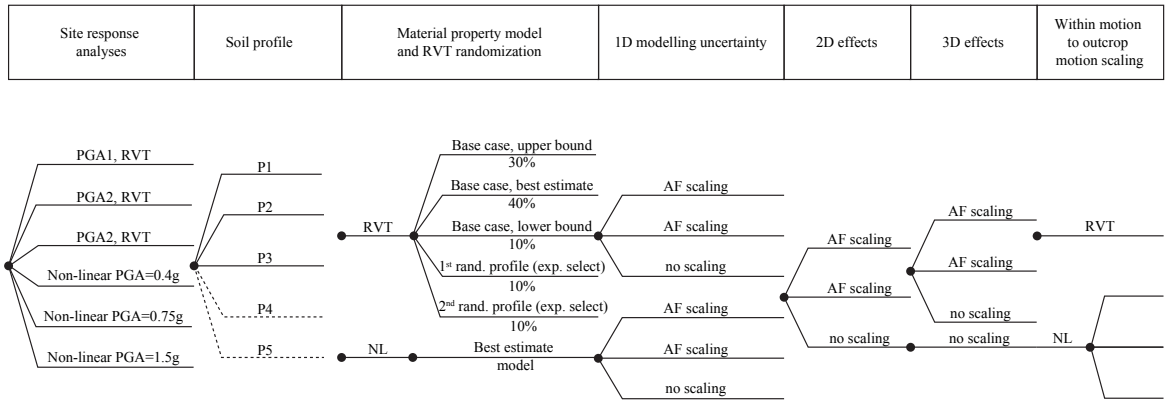

Figure III-2.1: Logic tree model, which develops amplification functions applicable to horizontal ground motion.

Level 1

In level 1 a set of site response analyses is defined. The set depends on the "ground motion level", which is a proxy-quantity to magnitude and PGA. The definition of ground motion levels and the selection of site response analyses and associated weights are summarized in Table III-2.1. Ground motion levels are implemented in *sp3f_level* and the definition of site response analyses and weights to be used are implemented in *sp3f_SRAdef* of the *SP3mod* software TP4-HSW-1002 [Hölker 2012].

Level 2

expands the alternative soil (V_S) profiles. This sub-branching is applicable only for branches based on RVT analyses. The soil profiles are described in Renault [2010a, b, c, d, e] [TP3-TN-1068...1071] and in the report Part I. The assigned weights are given in Table III-2.2. No sub-branching occurs on branches based on the NL analyses, because only the primary profile (P1 for Beznau, Leibstadt and Mühleberg sites and P6 for Gösgen site) is used. The weights are implemented in *sp3f_PROFILEdef*.

Level 3

expands the material models depending on the site response analysis underlying the logic tree branch at hand. "Material model" in the context of D. Fäh's model is a combination of the shear modulus reduction models [TP3-TN-1068...1071] and the V_S-profile randomizations in

Table III-2.1: Columns 1-3: Definition of discrete ground motion levels depending on magnitude and PGA. Columns 4-10: Definition of sets of site response analyses (SRA) and associated weights applicable within the ground motion levels. The alternative SRAs within a set per ground motion level results in logic tree branching, where the weights depend on the NPP site. The SRAs to be used are explicitly defined by method, magnitude and PGA (columns 4, 5 and 6). No interpolation of amplification functions for intermediate PGA levels is therefore required.

Ground motion level	Mag. range	PGA range [g]	SRA Method	SRA Mag.	SRA Avail. PGA [g]	Weights KKB	KKG	KKL	KKM
1	4-6	PGA < 0.5	RVT	(*)	No sub-branching.				
	6-8	PGA < 0.3			Use of the RVT analysis for the largest PGA (available in the database), which is smaller than the anticipated PGA. Exception: If M<6 and 0.4≤PGA≤0.5 use the 0.3g RVT analysis.				
2	4-6	0.5≤PGA<0.8	RVT	(*)	0.2	0.2	0.2	0.4	0.2
	6-8	0.3≤PGA<0.5	RVT		0.3	0.5	0.5	0.4	0.5
			RVT		0.4	0.1	0.1	0.1	0.1
			NL		0.4	0.2	0.2	0.1	0.2
2.5	4-6	PGA≥0.8	RVT	(*)	0.2	0.1	0.1	0.1	0.1
	6-8	0.5≤PGA<0.8	RVT		0.3	0.1	0.1	0.1	0.2
			RVT		0.4	0.2	0.2	0.2	0.2
			NL		0.4	0.4	0.4	0.4	0.3
			NL		0.75	0.2	0.2	0.2	0.2
3	6-8	0.8≤PGA<1.5	NL	(*)	0.4	0.2	0.2	0.2	0.2
			NL		0.75	0.4	0.4	0.3	0.3
			NL		1.5	0.1	0.1	0.1	0.1
			RVT		0.4	0.1	0.1	0.1	0.1
			RVT		0.75	0.1	0.1	0.2	0.2
			RVT		1.0	0.1	0.1	0.1	0.1
3.5	6-8	PGA≥1.5	NL	(*)	0.4	0.1	0.1	0.1	0.1
			NL		0.75	0.2	0.2	0.2	0.2
			NL		1.5	0.4	0.4	0.3	0.3
			RVT		0.4	0.1	0.1	0.1	0.1
			RVT		0.75	0.1	0.1	0.2	0.2
			RVT		1.0	0.1	0.1	0.1	0.1

(*) SRA magnitudes depend on the magnitude range associated with the applicable ground motion level. Magnitude 5 analyses are used for the magnitude range 4 to 6, magnitude 6 analyses are used for the magnitude range 6 to 7 and magnitude 7 analyses are used for the magnitude range 7 to 8.

Table III-2.2: Weights of soil profiles in level 2 of the logic tree model for amplification of horizontal ground motion. These weight are applicable only to branches based on RVT analyses.

Soil profile	P1 or P6	P2	P3	P4	P5
Beznau	0.25	0.25	0.25	0.25	-/-
Gösgen	0.20	0.40	0.20	0.10	0.10
Leibstadt	0.40	0.20	0.40	-/-	-/-
Mühleberg	0.25	0.25	0.25	0.25	-/-

RVT [TP3-SUP-1008]. A five-fold sub-branching is implemented on logic tree branches based on RVT in level 1. This sub-branching considers the RVT base case analyses for the three shear modulus reduction models "lower bound", "best estimate" and "upper bound" and additionally two RVT analyses for the best estimate shear modulus reduction model based on two selected randomized V_S-profiles. D. Fäh's selection of the two randomized V_S-profiles per site and the underlying base case V_S-profile is reprinted in Table III-2.3. The weights assigned to the five branches are 10% for the lower bound, 40% for the best estimate, 30% for upper bound shear modulus reduction model and 10% each for the two V_S-profile randomizations. No sub-branching is implemented on branches based on NL analysis in level 1. In such case only the NL amplification functions based on the best estimate material model are used. The weights assigned in level 3 are implemented in *sp3f_MATERIALdef*.

Level 4

implements a branching to account for modeling uncertainty. Three to seven sets of alternative modeling uncertainty factors are defined depending on the analysis method (RVT or NL) underlying the considered branch. These factors are function of spectral frequency. They scale the amplification function resulting in multiple scaled versions of the considered amplification function, which yield sub-branching and hence develop epistemic uncertainty.

Modeling uncertainty factors applicable to RVT branches are: (a) SHAKE/RVT ratios, (b) "ones", i.e. no modification and (c) NL/RVT ratios. The associated weights depend on the ground motion level and spectral frequency (see Table III-2.4).

The SHAKE/RVT ratios are obtained by:

- Gathering the SHAKE and RVT base case amplification functions for all soil profiles, for PGAs 0.05 g, 0.1 g and 0.2 g, if the ground motion level is 1, or for PGAs 0.4 g and 0.75 g, if the ground motion level is 2 or 3, for all soil models and magnitudes 5, 6 and 7;
- Normalizing the spectral frequencies by the fundamental frequency, which is specific to the considered $V_S - profile$.
- Resampling the amplification functions to the set of unique normalized spectral frequencies;
- Computing the geometric mean SHAKE/RVT ratio per frequency from the amplification factors by the analyses;

- Scaling the normalized frequencies by the fundamental frequency of the considered V_S-profile.

The NL/RVT ratios are obtained by the same approach, but the considered PGA levels are 0.05 g and 0.4 g for all ground motion levels. Frequency normalization and resampling is not required, because only one V_S-profile is considered.

The modeling uncertainty factors applicable to RVT amplification functions and the associated weights are implemented in *sp3f_UncertFac1d_lin* and subroutines *sp3f_ratio_shake_rvt and sp3f_ratio_nl_rvt*.

The modeling uncertainty factors applicable to NL branches and the associated weights are described in Table III-2.5. They are implemented in *sp3f_UncertFac1d_nl, sp3f_ratio_shake_nl, sp3f_ratio_NLxNLy* and *sp3f_shakePxP1_fac*.

Table III-2.3: Indices of the two V_S-profile randomizations, which are used per site and per base case V_S-profile in level 3 of the logic tree for amplification of horizontal ground motion. Index 1 is the V_S-profile randomization index used in the RVT results [TP3-TB-1049]. Index 2 is the V_S-profile randomization index used in the definition/selection of the profile randomizations [TP3-SUP-1008]. f_0 is the fundamental frequency corresponding to the randomized V_S-profiles.

V_S-profile		P1		P2		P3		P4		P5	
Beznau	Index 1	37	48	22	50	14	28	30	38	-/-	-/-
	Index 2	44	57	22	55	25	45	39	50	-/-	-/-
	f_0 [Hz]	2.2	2.2	2.4	2.6	2.4	2.4	2.4	2.6	-/-	-/-
Gösgen	Index 1	11	33	20	42	26	30	11	16	19	24
	Index 2	13	36	22	55	31	35	18	25	24	33
	f_0 [Hz]	6	4.8	4.3	4.2	4.4	4.8	5	5.9	5.9	5.9
Leibstadt	Index 1	15	29	18	47	11	32	-/-	-/-	-/-	-/-
	Index 2	20	37	26	65	11	32	-/-	-/-	-/-	-/-
	f_0 [Hz]	3.6	3.3	3.1	3.1	2.5	2.8	-/-	-/-	-/-	-/-
Mühleberg	Index 1	13	42	20	24	3	36	36	45	-/-	-/-
	Index 2	22	67	22	26	3	40	66	83	-/-	-/-
	f_0 [Hz]	7.2	7.7	7.2	6.3	5.1	5.9	6.3	5.3	-/-	-/-

Level 5

develops a two-fold sub-branching to account for 2D effects. The scenarios are: Either 2D effects have no impact on the amplification function or 2D effects modify the amplification function. The latter is modeled by means of spectral scaling factors. The weights assigned to the two scenarios depend on the site (Tab. III-2.6). The spectral scaling factors depend on the source-to-site distance. They are defined in Table III-2.7. Both are implemented in *sp3f_2dEffectFactors*.

The source-to-site distance used in this context is derived from the deaggregation of the rock hazard results. The deaggregation provides Joyner-Boore distances per magnitude, PGA and spectral frequency. Given the magnitudes and PGA levels for which the SP3 models

Table III-2.4: Weights assigned to modeling uncertainty factors applicable to RVT amplification functions. f0 is the fundamental frequency associated with the $V_S - profile$ underlying the RVT analysis.

Ground motion level	Factors	Spectral frequency bands $f < f_0/2$	$f_0/2 \leq f < 15$ Hz	15 Hz $\leq$ f
1	A. SHAKE/RVT	0.65	0.3	0.2
	B. Ones	0.3	0.65	0.75
	C. NL/RVT	0.05	0.05	0.05
2 or 3	A. SHAKE/RVT	0.6	0.2	0.1
	B. Ones	0.3	0.7	0.8
	C. NL/RVT	0.1	0.1	0.1

are evaluated (Tab. III-2.15) the arithmetic mean Joyner-Boore distance over the discrete spectral frequencies as per Table III-2.15 is adopted as source-to-site distance.

Level 6

develops a three-fold sub-branching to account for 3D effects. This sub-branching is applicable only in cases when the amplification function was modified due to consideration of 2D effects. Three scenarios are: No modification of the amplification function and modification of the amplification function by scaling factors A or B, respectively. The weights of these scenarios are given in Table III-2.6. The spectral scaling factors A and B are given in Table III-2.8. Both are implemented in *sp3f_3dEffectFactors*.

Level 7

implements an optional three-fold sub-branching, which provides differently scaled NL amplification functions adjusted from "within motion" (up- and down-going wavefield) to the anticipated "outcrop motion" (upgoing wavefield only). This scaling and sub-branching is applicable only in case of embedded target layers and branches based on NL analyses. The alternative scaling functions and associated weights are given in Table III-2.9.

Table III-2.5: Modeling uncertainty factors and associated weights applicable to NL amplification functions.

Modelling uncertainty factors		Weights depending on ground motion level	
		$2 \leq$ GML < 3	$3 \leq$ GML
No scaling	Constantly ones.	0.5	0.3
SHAKE Px/P1	Geometric mean spectral ratios of SHAKE amplification functions for PGAs 0.4 g and 0.75 g, surface targets, all magnitudes, all material models and all V_S-profiles (except the primary V_S-profile) over the parameter-corresponding SHAKE amplification function for the primary V_S-profile. The geometric mean ratios are computed on f_0-normalized frequency nodes. The SHAKE Px/P1 ratios are implemented in the routines *sp3f_shakePxP1_fac* and *sp3f_ratio_shake_shake.*	0.3	0.2
SHAKE/NL mean	Geometric mean spectral ratios of SHAKE amplification functions over NL amplification functions for the primary profile, for all magnitudes, all material models and two PGA levels, which are 0.05 g and 0.4 g, if the ground motion level is less than 3, or 0.4 g and 0.75 g, if the ground motion level is 3 or above. These ratios are implemented in *sp3f_ratio_shake_nl.*	0.2	0.1
SHAKE/NL upper envelope	Upper envelope of above described SHAKE/NL ratios. These ratios are implemented in *sp3f_ratio_shake_nl.*	0	0.1
SHAKE/NL lower envelope	Lower envelope of above described SHAKE/NL ratios. These ratios are implemented in *sp3f_ratio_shake_nl.*	0	0.1
NLx/NLy upper envelope	Upper envelope of the spectral ratios of the NL-SRA amplification functions by AMEC or Pelli (depending on the site) over the NL-SRA amplification functions by Pecker, where all pairs of NL SRAs are considered, which are available for magnitude 6, PGA 0.75 g, the best estimate material model, all target layers at all sites. The envelope is computed from f_0-normalized spectral ratios and scaled to the site-specific fundamental frequency. These ratios are implemented in *sp3f_ratio_NLxNLy.*	0	0.1
NLx/NLy lower envelope	Lower envelope of above described *NLx/NLy* ratios. These ratios are implemented in *sp3f_ratio_NLxNLy.*	0	0.1

Table III-2.6: Weights assigned to the alternative scenarios concerning the impact of 2D and 3D effects to the amplification functions. Modification of an amplification function due to 3D effects is applicable only, if 2D effects were considered to change the amplification function.

	Beznau	Gösgen	Leibstadt	Mühleberg
2D effects change the amplification function	0.20	0.20	0.70	0.20
2D effects have no impact on the amplif. function	0.80	0.80	0.30	0.80
3D effects, spectral scaling factors A	0.02	0.02	0.06	0.02
3D effects, spectral scaling factors B	0.08	0.08	0.24	0.08
3D effects have no impact on the amplif. function	0.90	0.90	0.70	0.90

Table III-2.7: Spectral scaling factors applicable to amplifications functions in order to account for 2D effects, which were not considered in the 1D site response analyses. These scaling factors depend on the source-to-site distance (which is derived from deaggregation of the rock hazard results) and are interpolated linearly on a log-frequency scale for the spectral frequencies defined in Table III-2.15. f_0 is the fundamental frequency specific to the site and V_S-profile [PMT-TB-1014] or the randomized profile (Tab. III-2.3).

Frequency [Hz]	0.1	$f_0/2$	f_0	4 f_0	6 f_0	100
Scaling factors for distances <20km	1	1	1.25	1.25	1	1
Scaling factors for distances >20km	1	1	1.26	1.26	1	1

Table III-2.8: Spectral scaling factors applicable to amplifications functions in order to account for 3D effects in addition to 2D effects. The factors are interpolated linearly on a log-frequency scale for the spectral frequencies defined in Table III-2.15. f_0 is the fundamental frequency specific to the site and V_S-profile [PMT-TB-1014] or the randomized profile (Tab. III-2.3).

Frequency [Hz]	0.1	$f_0/2$	f_0	$4f_0$	$6f_0$	100
Scaling factors A	1	1	1.4	1.4	1	1
Scaling factors B	1	1	1.2	1.2	1	1

Table III-2.9: Scaling factors and weights applicable to NL branches in case of embedded layers to scale amplification functions from within motion to outcrop motion and account for associated uncertainty.
$R_i(f_n)$ represents set of spectral ratios of amplification factors associated with f_0-normalized frequencies, f_n, where index i reflects analyses for all magnitudes, V_S-profiles and material models at a given site, target layer and PGA level; and where R are ratios of amplification factors by SHAKE analyses for outcrop motion over within motion. With f_0 as fundamental frequency, which is specific to the site and V_S-profile.

Spectral scaling factors	Spectral frequency	Weight
μ geom($R(f_n)$) $-\sigma(R(f_n)$)	$f_n \cdot f_0$	0.20
μ geom($R(f_n)$)	$f_n \cdot f_0$	0.60
μ geom($R(f_n)$) $+\sigma(R(f_n)$)	$f_n \cdot f_0$	0.20

2.2.2 Aleatory Variability of Horizontal and Vertical Motion

Aleatory variability in SP3 is conceptually defined as variability, which is additional to the variability already included in the rock hazard results. For horizontal and vertical motion this additional variability is considered zero.

2.2.3 V/H Scaling and Amplification of Vertical Ground Motion

The logic tree model of site effects of vertical motion (see Figure III-2.2) is a composite model, which separates at

Level 1

three main branches (concepts): The first concept is to scale horizontal ground motion on soil by V/H ratios defined by the SP3 expert. The second concept is to scale vertical ground motion on rock to vertical motion on soil based on RVT analyses. The third concept is that vertical ground motion on rock and soil are identical (no amplification). The weights of these concepts depend on the magnitude, PGA level and the source-to-site distance. They are implemented in *sp3f_vm_concept* and are specified in Table III-2.10.

Table III-2.10: Concepts and associated weights for modeling vertical motion site effects.

Source-to-site distance [km]	Ground motion level depending on magnitude and PGA according to Table III-2.1			
	< 3	≥ 3		
< 20	V/H	V/H	RVT	no AF
	100%	70%	10%	20%
≥ 20	V/H	V/H	RVT	no AF
	100%	80%	0	20%

Level 2 on V/H branches

replicates the entire amplification model for horizontal ground motion.

Level 3 on V/H branches

develops alternative V/H scaling functions based on empirical GMPEs. The considered GMPEs and the associated weights are specified in Table III-2.11. The V/H ratios depend on up to 6 parameters: PGA, magnitude, spectral frequency, a source-to-site distance, V_{S30}, and fault style. PGA, magnitude and frequency are parameter space dimensions for which SP3 models are evaluated (Tab. III-2.15). The source-to-site distance is itself a function of PGA, magnitude and spectral frequency and is obtained from the deaggregation of the rock hazard results. V_{S30} velocities are specific to the soil profile used in the amplification model for horizontal motion, which is implemented upstream and summarized as level 2 in Figure III-2.2. Concerning fault style the weighted mean V/H ratios over the fault styles are used, where weights and fault styles are obtained from the deaggregation of the rock hazard results.

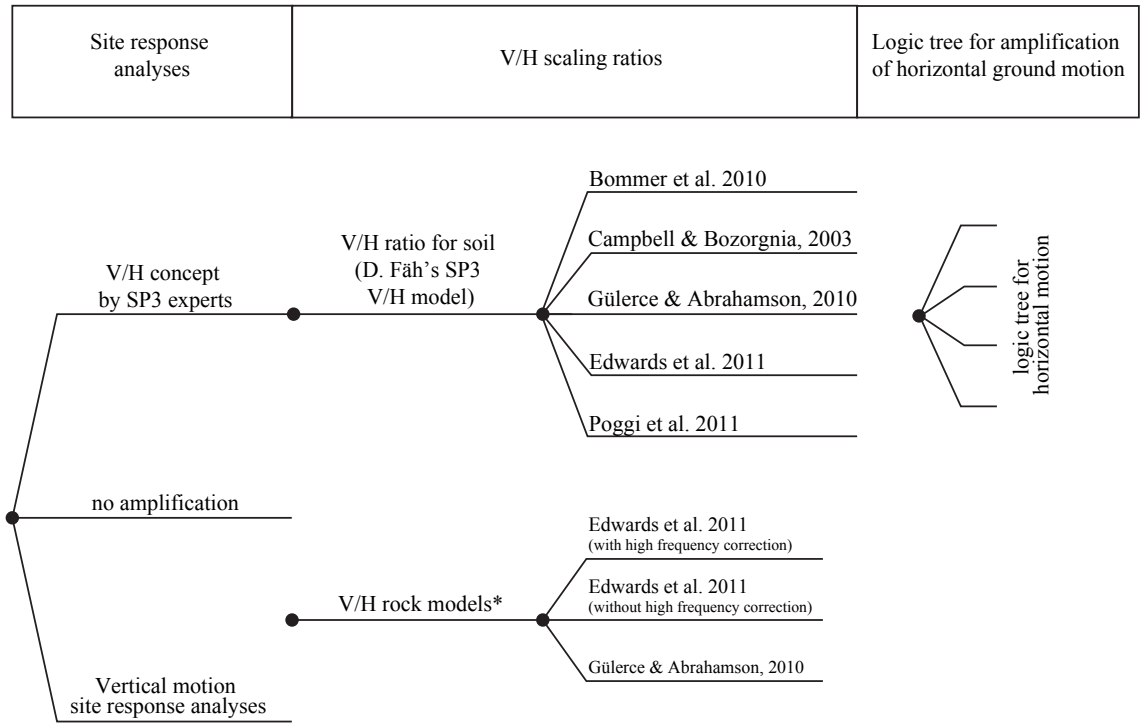

Figure III-2.2: Logic tree model, which develops V/H scaling factors and site-specific amplification factors.

Level 2 on the "no amplification" and RVT branch

does not develop sub-branching, because only a single amplification function is defined. In case of "no amplification" that amplification function takes value 1 constantly. In case of RVT the arithmetic mean amplification per spectral frequency is computed from the RVT analysis results for magnitude 6, PGA 0.4 g and 0.75 g, lower bound, best estimate and upper bound soil models.

Level 3 on the "no amplification" and RVT branch

replicates the entire SP2 V/H model. Using the entire SP2 V/H instead of only D. Fäh's SP2 V/H model (as per EG3-ES-1015) was required by the TFI. The SP2 V/H model is implemented as a table of V/H ratios provided within SP4. The V/H ratios depend on the site, the spectral frequency, magnitude and PGA. Within the *SP3mod* software this table and the weights assigned by the SP2 experts to the GMPEs are stored in the environment variable *sp3db.sp2VH*.

2.2.4 Inter- and Extrapolation of Amplification Functions

D. Fäh's assessment does not require interpolation of amplification functions for intermediate PGA levels or estimation of amplification functions for non-evaluated parameter sets. This is, because he uses the concept of discrete ground motion levels for which he explicitly defines, which site response analyses out of the database are to be used.

Table III-2.11: GMPEs and associated weights utilized for modeling V/H scaling factors applicable to horizontal ground motion on soil.

V/H model	Ground motion level depending on magnitude and PGA according to Table III-2.1		
	< 2	$2 \cdots 3$	≥ 3
Gülerce and Abrahamson [2011] (EXT-RF-1337)[1]	0.30	0.10	0
Bommer et al. [2011] (EXT-RF-1336)[1]	0.10	0.20	0.25
Campbell et al. [2003] (EXT-RF-1338)[1]	0.10	0.20	0.25
Poggi et al. [2011] (TP3-TB-1084) part 1[2]	0.40	0.45	0.50
Edwards et al. [2011b] (TP3-TB-1084) part 2[3]	0.10	0.05	0

[1] The V/H ratios are evaluated for the fault styles "normal", "strike-slip" and "reverse" and the weighted mean of the V/H ratios is computed per spectral frequency using weights obtained from the deaggregation of the rock hazard results.
[2] V/H ratios at spectral frequencies above 30 Hz are replaced by the value at 30 Hz.
[3] V/H ratios by the Edwards et al. [2011b] model are replaced by V/H ratios by the Poggi et al. [2011] model at low frequencies. Threshold frequencies are 0.8 Hz for the Beznau and Leibstadt sites and 1.05 Hz for the Gösgen and Mühleberg sites.

2.2.5 Maximum Horizontal and Vertical Ground Motion (Truncation Models)

The logic tree model of maximum horizontal and vertical ground motion (Fig. III-2.3) develops alternative maximum ground motion spectra by means of three levels of branching. These spectra are used as truncation models and are defined as

$$SA_{max}(f) = PGA_{max}\, X(f)\, R \tag{III-2.1}$$

where PGA_{max} is a maximum PGA_{value} on soil, $X(f)$ is a PGA-normalized spectral shape and R is a scaling factor (or "reduction factor" according to the terminology in EG3-ES-1015).

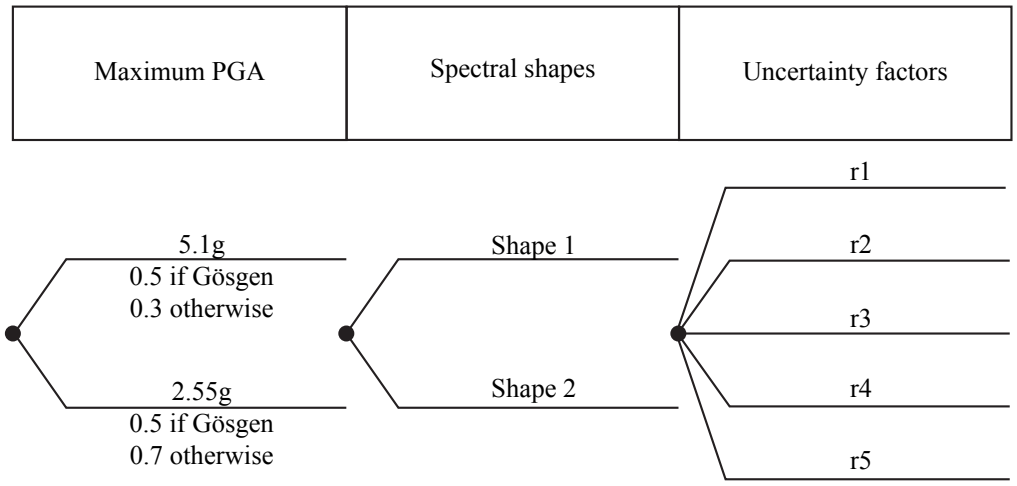

Figure III-2.3: Horizontal and vertical maximum ground motion logic tree for D. Fäh. The maximum PGA is defined as 50 m/s^2 and 25 m/s^2.

Level 1

develops two alternative maximum PGA values on soil. They are defined as 5.1 g (=50 m/s^2 / 9.81) and 2.55 g (=25 m/s^2 / 9.81). The associated weights depend on the target layer depth and are given in Table III-2.12.

Table III-2.12: Weights of alternative maximum PGA_{soil} values.

	Horizontal motion		Vertical motion	
	PGA$_{max}$=25 m/s^2	PGA$_{max}$=50 m/s^2	PGA$_{max}$=25 m/s^2	PGA$_{max}$=50 m/s^2
Surface	0.70	0.30	0.30	0.70
Embedded layers	0.50	0.50	0.20	0.80

Level 2

implements a twofold branching, providing two alternative spectral shapes. These spectral shapes and their associated weights, which depend on the PGA$_{max}$ value and the wavefield component, are given in Table III-2.13.

Table III-2.13: Spectral shapes and associated weights utilized in modeling maximum ground motion truncation spectra.

		Weight if PGA$_{max}$		Spectral Frequency [Hz]								
Motion	Shape	25 m/s^2	50 m/s^2	0.1	0.45	1	2.5	5	10	20	50	100
Horizontal	1	0.30	0.80	1.5	1.5	2	2.5	2.5	2	1.5	1	1
	2	0.70	0.20	2	2	3	4	4	3	2	1	1
Vertical	1	0.30	0.80	1.5	1.5	1.5	2	3	3	2.25	1.5	1
	2	0.7	0.2	2	2	2	3	5	5	3.5	2	1

Level 3

expands 5 alternative reduction factors, which scale the maximum ground motion spectra. These factors and the associate weights depend on the spectral shape defined in level 2 and are identical for vertical and horizontal ground motions. They are specified in Table III-2.14.

Table III-2.14: Scaling (reduction) factors applicable to maximum ground motion spectra. The factors depend on the spectral shape (see Table III-2.13). The associated weights are given in brackets.

	Reduction factors and weights				
Shape 1	0.8 (10%)	0.85 (15%)	0.90 (20%)	0.95 (25%)	1.0 (30%)
Shape 2	0.6 (20%)	0.7 (20%)	0.8 (20%)	0.9 (20%)	1.0 (20%)

2.3 Model Implementation and Review History

The development of the models by the SP3 expert and its implementation by SP4 were carried out contemporary when partial model descriptions became available. D. Fäh's model was implemented on the basis of the evaluation summary EG3-ES-1015 (see part III, Chapter 1), version 26 of 23. April 2012 and version 30 of 26. April 2013, on presentations by D. Fäh at the SP3 workshops on 17. March 2011 (TP3-RF-1351), 6. July 2011 (TP3-RF-1384) and 19. December 2011 (TP3-RF-1434) and on explanations provided in three meetings held on 14. July 2011, 20. April and 23. April 2012.

The models are implemented by means of four programs addressing aspects as follow:

- *HM_SP3_Faeh*
  - Amplification of horizontal ground motion;
  - Aleatory variability of horizontal motion amplification.
- *MaxHM_SP3_Faeh*
  - Maximum horizontal ground motion.
- *VM_SP3_Faeh*
  - Amplification of vertical ground motion;
  - V/H scaling factors;
  - Aleatory variability of vertical motion amplification and V/H scaling.
- *MaxVM_SP3_Faeh*
  - Maximum vertical ground motion.

These programs are part of the "SP3mod" software Hölker [2012] (TP4-HSW-1002), which is designed as MATLAB toolbox with an associated database holding the site response analyses and described in Hölker [2013b] (TP4-TN-1197). MATLAB releases 2011a to 2012b have been utilized for development and model evaluation.

The implementation (MATLAB code) of the models was presented to and discussed with D. Fäh in above listed three meetings. S. Thomassin provided an external review of the implementation of the horizontal motion models in August 2012 and of the vertical motion models in January 2013.

2.4 Model Evaluation

All models have been evaluated per site (Beznau, Gösgen, Leibstadt and Mühleberg) and target layer (surface and one or two subsurface layers) as defined in table 1 of Renault [2011a] (PMT-TN-1139) or section 4.2 of Renault and Abrahamson [2010] (PMT-TB-1014), respectively. The parameter space is spanned by magnitude, peak ground acceleration (PGA) and spectral frequency, which are discretized as detailed in Table III-2.15.

The model evaluations for magnitudes 5 and 6 have been replicated, assigned magnitudes 5.9 and 6.9 and added to the set of results. This is done, because in D. Fäh's model magnitude is considered like a step function, but the SHZ does linear interpolation of amplification depending on magnitude. Using the auxiliary magnitude nodes 5.9 and 6.9 the concept of discrete ground motion bins is preserved. Linear interpolation of AF(M) within the magnitude intervals 5.9 to 6 and 6.9 to 7 is kept to avoid discontinuities in the amplification model.

The model for E-Beznau site has been last evaluated in December 2012 and became obsolete with the revised SHAKE and RVT analyses of April 2013. Final model evaluations for Beznau, Gösgen, Leibstadt and Mühleberg were performed in May 2013.

Table III-2.15: Discretization of the parameter space of the SP3 models

Parameter	Discretization
Magnitude	5, 6, 7 and 5.9, 6.9 (replicated results of the $M5$ and $M6$ model evaluations)
PGA [g]	0.05, 0.1, 0.15, 0.2, 0.25, 0.3, 0.4, 0.5, 0.6, 0.75, 1.0, 1.25, 1.5, 1.75, 2.0, 2.25, 2.5
Freq. [Hz]	0.2, 0.3, 0.4, 0.5, 0.8, 0.9, 1, 1.1, 1.2, 1.3, 1.5, 1.8, 2, 2.2, 2.3, 2.5, 2.7, 2.9, 3, 3.1, 3.2, 3.4, 3.5, 4, 4.4, 4.5, 5, 5.3, 5.4, 5.5, 5.6, 5.7, 5.75, 5.9, 6, 6.9, 7, 8, 8.9, 9, 10, 11, 12, 13, 14, 15, 17, 20, 22, 25, 30, 33, 40, 45, 50, 60, 70, 80, 90, 100

2.5 Processing of Model Results into SIFs (SP3-to-SP4 Interface)

The logic tree models for amplification and aleatory variability yield a set of amplification and aleatory variability functions and associated weights. For amplification (or equivalently aleatory variability) these results may be described as

$$AF_i(f, PGA, M) \quad \text{and} \quad W_i(f, PGA, M) \quad \text{for } i = 1, 2, \ldots, n \tag{III-2.2}$$

where i is the indexing of logic tree branches, f is spectral frequency, PGA is peak ground acceleration, M is magnitude, AF is amplification and W is the associated weight.

Two modifications are applied to the data representation when the results are processed into a SIF: The n logic tree branches are summarized into 17 fractiles (Tab. III-2.16) taking into account the weights of the branches. The parameter space dimension PGA is scaled to spectral accelerations (SA), where the relation between SA, PGA and frequency is given by the spectra used as input motions for the site response analyses. Given these two modifications the amplification (and equivalently aleatory variability) results are represented in the SIF by

$$AF_j(f, SA, M) \tag{III-2.3}$$

where j is the index of the discrete fractiles defined in Table III-2.16.

The logic tree models for maximum ground motion yield maximum spectral acceleration values on soil, $maxSA_i(f)$, and associated weights $W_i(f)$, where i is the indexing of logic tree branches and f is spectral frequency. Concerning the SIF these results are summarized into

17 discrete fractiles, if the number of logic tree branches exceeds 17. Otherwise the native $maxSA$ spectra and associated weights are transcribed to the SIF.

The aim of summarizing the model results to 17 fractiles is to reduce the number of combinations required in soil hazard evaluation, which is motivated by maintaining acceptable computing time. The 17 fractiles are associated with fixed weights as given in Table III-2.16. These weights are derived from bin width, where the fractiles are bin centers and where the bin bounds are the mean values of neighboring fractiles or 0 or 1, respectively.

The site effect model for vertical motion features two components:

(a) Amplification factors, which conceptually are to be applied to vertical motion rock hazard, and

(b) V/H scaling factors, which are to be combined with the horizontal motion amplification factors and to be applied to horizontal motion rock hazard. For SIF processing of the vertical motion model additionally the V/H scaling models by the SP2 experts are imported and are applied to component (a).

This way both model components describe V/H scaling and amplification and can be processed into a single SIF, which is applicable to the horizontal motion rock hazard.

The details of the SP3-to-SP4 interface processing are described in Hölker [2013b] (TP4-TN-1197).

Table III-2.16: Discrete fractiles and associated weights utilized to summarize the logic tree model results.

Percentiles	0.13, 0.62, 2.28, 5, 10, 20, 30, 40, 50, 60, 70, 80, 90, 95, 97.72, 99.38, 99.87
Weights	0.00375, 0.01075, 0.0219, 0.0386, 0.075, 0.10, 0.10, 0.10, 0.10, 0.10, 0.10, 0.10, 0.075, 0.0386, 0.0219, 0.01075, 0.00375

2.6 Results: SIFs (Soil Input Files or SiteMod Files)

The raw logic tree model results (intermediate model results) and the SIF-processed model results are saved into so-called "SiteMod" data structures in MATLAB format. A "SiteMod" data structure contains the SIF required by the soil hazard software and it additionally contains the unprocessed logic tree model results for the parameter space described in Table III-2.15. The details and internal format of the "SiteMod" data structure are described in Hölker [2013b] (TP4-TN-1197). Furthermore each "SiteMod" data file contains a descriptive self-documentation. The model result files associated with this HID are:

- SiteMod.Beznau.Faeh.z1h.FullModel.mat
- SiteMod.Beznau.Faeh.z1v.FullModel.mat
- SiteMod.Beznau.Faeh.z2h.FullModel.mat
- SiteMod.Beznau.Faeh.z2v.FullModel.mat

- SiteMod.Goesgen.Faeh.z1h.FullModel.mat
- SiteMod.Goesgen.Faeh.z1v.FullModel.mat
- SiteMod.Goesgen.Faeh.z2h.FullModel.mat
- SiteMod.Goesgen.Faeh.z2v.FullModel.mat

- SiteMod.Leibstadt.Faeh.z1h.FullModel.mat
- SiteMod.Leibstadt.Faeh.z1v.FullModel.mat
- SiteMod.Leibstadt.Faeh.z2h.FullModel.mat
- SiteMod.Leibstadt.Faeh.z2v.FullModel.mat

- SiteMod.Muehleberg.Faeh.z1h.FullModel.mat
- SiteMod.Muehleberg.Faeh.z1v.FullModel.mat
- SiteMod.Muehleberg.Faeh.z2h.FullModel.mat
- SiteMod.Muehleberg.Faeh.z2v.FullModel.mat
- SiteMod.Muehleberg.Faeh.z3h.FullModel.mat
- SiteMod.Muehleberg.Faeh.z3v.FullModel.mat

The token "z1h" indicates target layer and wavefield component, where "z1" is surface, "z2" is the upper embedded layer and "z3" is the lower embedded layer (as per table 1 of PMT-TN-1139) and where "h" is horizontal motion and "v" is vertical motion.

The token "FullModel" indicates that the file contains a full SP3 model. Other files, which contain model subsets only exist and have been created for parameter sensitivity analyses.

All SIFs (SiteMod files) are applicable to horizontal motion rock hazard results ! The SIFs for horizontal motion contain amplification models only while the SIFs for vertical motion contain combined amplification and V/H scaling models.

2.6.1 SIF Figures

The model results, i.e. the content of the "FullModel" SIFs listed in the previous section, have been systematically visualized by means of seven figures types:

- XY graph showing amplification versus PGA for selected spectral frequencies;
- An image display showing median amplification versus PGA and frequency;
- XY graph showing amplification versus SA on rock for a set of spectral frequencies;
- An image display showing the ratio of the 80% over the 20% fractile of amplification versus PGA and spectral frequency;
- XY graph showing maximum acceleration on soil versus spectral frequency;
- An image display showing median aleatory variability versus PGA and frequency (for horizontal motion only);

- An image display showing mean aleatory variability versus PGA and frequency (for horizontal motion only).

which are attached to this HID as an electronic appendix containing PNG and EPS files. Examples of these figures are discussed in Hölker [2013b] (TP4-TN-1197).

Chapter 3

Appendix to EG3-HID-1006 for D. Fäh

A direct link to files for the final SP3 hazard feedback is given here:

Horizontal Motion Amplification Functions and Maximum Ground Motion

- Ratio of the 80% over the 20% fractile of amplification versus PGA and spectral frequency:
  Open external file: FigSIF.Faeh.HM.AMPFp80p20-PGA-FREQ.
- Amplification versus PGA for selected spectral frequencies:
  Open external file: FigSIF.Faeh.HM.AMPF-PGA.
- Amplification versus SA on rock for a set of spectral frequencies:
  Open external file: FigSIF.Faeh.HM.AMPF-SA.
- Mean amplification versus PGA and frequency:
  Open external file: FigSIF.Faeh.HM.MeanAMPF-PGA-FREQ.
- Median amplification versus PGA and frequency:
  Open external file: FigSIF.Faeh.HM.MedAMPF-PGA-FREQ.
- Maximum acceleration on soil versus spectral frequency:
  Open external file: FigSIF.Faeh.HM.MaxGM.

Horizontal Motion Aleatory Variability

- Median aleatory variability versus PGA for a set of spectral frequencies:
  Open external file: FigSIF.Faeh.HM.AVAR-PGA.
- Median aleatory variability versus PGA and frequency:
  Open external file: FigSIF.Faeh.HM.AVAR-PGA-FREQ.

- Aleatory Variability versus SA for a set of spectral frequencies:
  Open external file: FigSIF.Faeh.HM.AVAR-SA.

Horizontal Motion Amplification Functions and Maximum Ground Motion

- Ratio of the 80% over the 20% fractile of amplification versus PGA and spectral frequency:
  Open external file: FigSIF.Faeh.VM.AMPFp80p20-PGA-FREQ.
- Amplification versus PGA for selected spectral frequencies:
  Open external file: FigSIF.Faeh.VM.AMPF-PGA.
- Amplification versus SA on rock for a set of spectral frequencies:
  Open external file: FigSIF.Faeh.VM.AMPF-SA.
- Mean amplification versus PGA and frequency:
  Open external file: FigSIF.Faeh.VM.MeanAMPF-PGA-FREQ.
- Median amplification versus PGA and frequency:
  Open external file: FigSIF.Faeh.VM.MedAMPF-PGA-FREQ.
- Maximum acceleration on soil versus spectral frequency:
  Open external file: FigSIF.Faeh.VM.MaxGM.

Chapter 4

QA-Certificate EG3-QC-1065

QA Certificate

EG3-QC-1065

PEGASOS REFINEMENT PROJECT

Hazard Input Document (HID)

Expert group: EG3 ***HID designation:*** **EG3-HID-1006**

Expert: D. Fäh ***Expert Model (EXM)*** EG3-EXM-1006

HID parameterisation of Expert Model:

TFI: N. A. Abrahamson ***Hazard Input Specialist of TFI-team:*** A. Hölker

HID based on Elicitation Documents: ☒ EG3-ES-1015

HID based on Exp. Assessments (EXA): ☒ EG3-EXA-1034 to EG3-EXA-1037

Remarks on the HID model parameterisation in terms of hazard computation input:

The undersigned Hazard Input Specialist confirms that this HID includes all required (subproject specific) input information for hazard computations. No further interpretations of this input will be required and no simplifications except Algorithmic Pinching according to paragraph 2.9 of the QA-Guidelines will be applied to convert this HID into hazard software Input Files.

Signature:

HID acceptance by the Expert / Expert Group:

Date of HID review by the Expert / Expert group: 02.12.2013

HID accepted: ☒ ***HID not accepted:*** ☐

Reasons for non-acceptance of HID / Recommendations:

The undersigned Expert(s) accept(s) the parameterisation proposed in this HID as a faithful and adequate representation of his/their Expert Model. He/they confirm(s) that this HID is free of errors and agree(s) to its use as hazard computation input.

Signature Expert 1 / Expert:

Signature Expert 2:

Signature Expert 3:

Part IV

Assessments of Alain Pecker

Chapter 1

Evaluation Summary (EG3-ES-1016) of A. Pecker

1.1 Introduction

This evaluation summary is resulting from the evaluations and discussions performed throughout the PRP, providing the underlying reasoning for the selection of final models and weights. During this evaluation process, different sets of data, models, and methods proposed by the technical community and that are relevant to the hazard analysis have been considered. The integration of the available information into the proposed models and weights are furthermore aimed so as to represent the centre, body, and range of a technically defensible interpretation.

It presents the evaluation of the site response characterization at the location of the 5 Swiss Nuclear Power Plants. This evaluation is given in terms of frequency dependent amplification factors which, applied to the bedrock response spectrum, yields the ground surface response spectrum. The amplification factors are provided for the vertical motion and for the horizontal ground motion.

According to the project requirements these amplification factors are estimated following several approaches which, based on our evaluation of their reliability and fit for purpose, have been assigned different weights in a logic tree structure. In addition to the median estimate of the amplification factors, the aleatory variability is also provided attempting to prevent double counting with the evaluation made by SP2.

Finally, since the rock hazard model coming from the work of Experts groups 1 and 2 may lead to strong earthquake scenarios with very high rock accelerations, the maximum motion that any of the studied soil sites can transmit to the ground surface has been evaluated based on the ultimate shear resistance capacity of the soil strata.

All the evaluations presented in this report are based on the results of the calculations and studies carried out by various entities within the framework of the PEGASOS Refinement Project (PRP), whom reports were made available to us. It must be noted that, although the results presented in the numerous reports look reliable, no in depth check of the results have been performed by us. In addition to the previous analyses, those carried out within

the framework of the former PEGASOS Project (PP) are also taken into account when they provide relevant information that has not been either reassessed or superseded.

1.2 Median Amplification of Horizontal Ground Motion

1.2.1 Approach

The available data for the evaluation of the amplification factors consists of:

- 1D RVT runs
- 1D SHAKE runs
- Parametric studies to study the influence of P-SV waves (former PEGASOS Project)
- 2D runs at one site (former PEGASOS Project)
- Non-linear analysis

An evaluation of the results is required to assign a degree of confidence to each of the methods. This has been done on the basis of currently admitted practice, past experience and robustness of the different methods as briefly explained below. More details are given for each site in the relevant paragraphs.

Basically, for the 1D amplification studies, the dominant factor used to assign different weights to the different models is the induced shear strain. It is known that equivalent linear analyses are only valid up to a certain level of ground shaking. When the input level becomes too high, answers from SHAKE cease to be reliable because non-linear behavior can no longer be approximated by equivalent linear model and, in addition, damping is overestimated especially for the medium to high frequency range [Mohammadioun and Pecker 1984; Martin 1975; Assimaki et al. 2000]. The usually accepted domain of validity of the equivalent linear approximation is for strains smaller than 0.1 % to 0.5 %. Beyond that fact, the shape of the G/G_{max} curves may have a profound influence on the results and governs their validity. They cannot be chosen independently of the soil type, soil resistance and state of stresses. It was therefore checked that the strength mobilized (or equivalently the induced stress) within the soil profile did not exceed the available resistance; when this situation happens, the calculations are no longer considered reliable. For all those situations where the strain goes beyond a given threshold, the non-linear calculations were deemed more appropriate to define the amplification factors. In the logic tree these thresholds in terms of induced shear strain have been converted to thresholds in peak ground acceleration to relate them to input parameters.

With regards to the other alternatives offered by the various calculations, 2D calculations were only used when specific results were available because no reliable scientifically based methods are available to estimate its impact in the absence of specific calculations. All other alternatives were considered as part of the aleatory variability but they are considered to be already accounted for in SP2; for instance, P-SV calculations are considered part of the aleatory variability because the calculations presented in the database already incorporate a

degree of aleatory variability due to the location of the source, depth of the focus, etc, all effects considered by SP2.

Most of the variability is attributed to variability in the input motion, reflected in all the runs (SHAKE, RVT, non-linear); additional variability coming from the other factors was considered less significant; in particular randomization of the soil profiles in the RVT runs was thought to be unrealistic based on the study by Assimaki et al. [2003]. However, considering the way SP2 derived the input motions, it is again considered that full variability is already accounted for in SP2, at least for linear or equivalent linear analyses. Aleatory variability due to input motions is only included for the non-linear analyses if it is relevant, i.e. when the calculated variability in the non-linear runs exceeds the variability in the equivalent linear analyses.

1.2.2 Logic Tree Structure

The general structure of the logic tree common to all sites is shown in Figure IV-1.1: Generic logic tree for mean horizontal motion for the horizontal ground motion.

The first branches relate to the site data: velocity profiles and material characteristics; the next branch is based on the PGA values, but as explained above is actually related to the induced shear strain. The next branches differentiate for frequencies "around" the fundamental frequency of the soil profile ($f1 < f < f2$) where RVT results are less reliable Kottke and Rathje [2013] and frequencies above or below it. In the low frequency range ($f < f1$) the RVT runs are not as accurate as the other methods; in the medium frequency range ($f2 < f < f3$) the RVT and SHAKE spectra are similar and therefore they are assigned the same weight. Finally above f_3, typically of the order of 30-50Hz, none of the methods is really accurate. Basically the logic tree stops at the end of these branches except for Leibstadt where alternatives are considered for the 2D amplifications based on the available amplification studies.

It must be noted that the *pgas* and frequency branches represent conditional branches rather than alternative branches

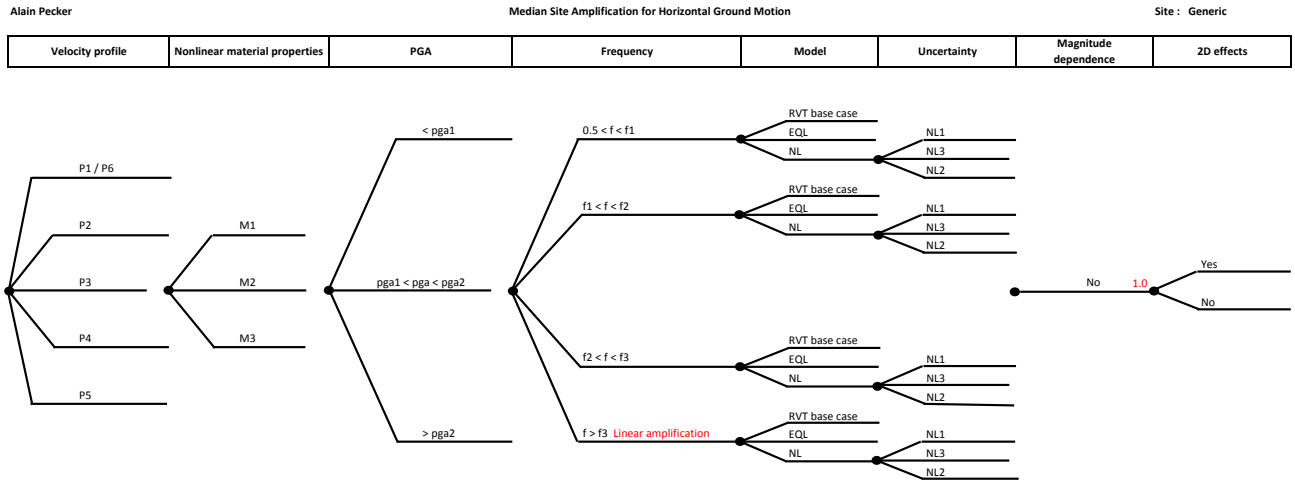

	0.5 < f < f1			f1 < f < f2			f2 < f < f3			f3 < f < 100		
	EQL	RVT	NL	EQL	RVT	NL	EQL	RVT	NL	EQL	RVT	NL
pga < pga1	x1_1	x1_2	x1_3	x2_1	x2_2	x2_3	x3_1	x3_2	x3_3	x4_1	x4_2	x4_3
pga1 < pga < pga2	y1_1	y1_2	y1_3	y2_1	y2_2	y2_3	y3_1	y3_2	y3_3	y4_1	y4_2	y4_3
pga2 < pga	z1_1	z1_2	z1_3	z2_1	z2_2	z2_3	z3_1	z3_2	z3_3	z4_1	z4_2	z4_3

$$\sum_{j=1,3} x_{i\_j} = 1.0 \quad \sum_{j=1,3} y_{i\_j} = 1.0 \quad \sum_{j=1,3} z_{i\_j} = 1.0$$

NL1 : main contractor
NL2 : cross check analyses
NL3 : sensitivity studies (Mühleberg only)

$$AMP(f > f_3) = AMP(f_3)$$

Figure IV-1.1: Generic logic tree for mean horizontal motion.

1.2.3 Model Evaluations Common to All Sites

Definition of Threshold Strains

As explained previously the main parameter to discriminate between methods (linear, equivalent linear, non-linear) is the maximum strain reached during the earthquake. Basically, three threshold levels are defined; these threshold levels are conveniently defined as fractions or multiples of γ 50, the strain corresponding to a reduction of 50% of the shear modulus. Strains below the first threshold level correspond to small strains, typically less than 10^{-4} or $\gamma/\gamma_{50} < 1$, for which all methods are equally reliable. The second threshold level corresponds to moderate strains up to which RVT and SHAKE analyses may still be valid. This threshold strain is determined on the basis of our experience, on the examination of the G/G_{max} curves provided as input data and on the comparison of stress-strain curves derived from the G/G_{max} curves and from the non-linear constitutive models. The last two aspects are detailed below. The shape of the G/G_{max} curves may have a profound influence on the results and governs their validity. The G/G_{max} versus curve is another way to present the shear stress - shear strain curve $\tau = f(\gamma)$. Therefore it cannot be chosen independently of the soil type, soil resistance and state of stresses. In the SHAKE and RVT analyses, three material models have been used corresponding to best estimate curves, lower bound and upper bound ones. They partially account for the state of stresses since different curves are provided for different vertical effective overburden but none of them fully reflects the soil resistance or the soil type. In order to assess the validity of those models, for each site and each material model, the curves G/G_{max} have been rearranged in the following way: The shear stress at any depth is:

$$\tau = G\gamma \tag{IV-1.1}$$

which may be written as:

$$\tau = \frac{G}{G_{max}} G_{max}\gamma < \tau_{max} \tag{IV-1.2}$$

At any depth under the assumption of vertically propagating shear waves, which is the assumption made in the SHAKE or RVT runs, the maximum shear stress, τ_{max}, is expressed as a function of the vertical effective stress σ'_v, the coefficient of at rest earth pressure K_0, the soil friction angle ϕ' and the cohesion C:

$$\tau_{max} = \left(\left[\frac{(1+K_0)}{2} \sigma'_v sin\phi' + Ccos\phi' \right]^2 - \left[\frac{(1-K_0)}{2} \sigma'_v \right]^2 \right)^{1/2} \tag{IV-1.3}$$

Equation (2.2) can also be written:

$$\frac{\tau}{\tau_{max}} = \frac{G}{G_{max}} \frac{G_{max}}{\tau_{max}} \gamma_{50} \frac{\gamma}{\gamma_{50}} \leq 1 \tag{IV-1.4}$$

Using the curves G/G_{max} provided for each model, τ/τ_{max} can be drawn as a function of γ/γ_{50}. As soon as τ/τ_{max} exceed 1.0 the model is deemed no longer valid, which sets another threshold γ/γ_{50} on the shear strain, or equivalently on PGA. Typically this second threshold corresponds to $\gamma/\gamma_{50} = 5\ to\ 10$. Another estimate of this second threshold is also obtained from a comparison of the shear stress-shear strain curve (equation 2.1) established from the G/G_{max} curve and the one obtained from numerical simulations carried out with the non-linear constitutive models. The threshold strain is defined as the strain at which both curves tend to deviate significantly. The estimate of the threshold strains is based on the best estimate soil properties.

Definition of Frequency Ranges

Comparing the results of RVT runs without randomization to SHAKE results, it appears that the RVT runs look accurate in predicting the resonant frequency of the profile although they overpredict the amplification. A possible explanation indicating that SHAKE amplifications are more accurate at the resonant frequency of the profile than RVT ones is discussed in Kottke and Rathje [2013]. Away from the peak the agreement is poor between both types of analysis, especially for the low magnitudes. When the magnitude increases the agreement becomes better. Consequently, in a frequency band $[f_1, f_2]$ centered around the peak, typically 0.8 Hz to 8 - 10 Hz, SHAKE analyses are assigned larger than RVT.

In the low frequency range ($0.5Hz < f < f1$), the RVT runs invariably indicate an amplification close to 1.0 which is not correct. In that frequency range the amplification should be equal to the ratio of the ground surface displacement divided by the rock displacement. A typical value would be in the range 1.2 to 1.5 depending on the profile stiffness, which is correctly predicted by the SHAKE runs.

Above f_2 and up to a frequency f_3 , with the recent implementation of $V_S - \kappa$ corrections, the shape of the shapes of RVT and SHAKE spectra are both representative of the Swiss seismic conditions with the same frequency content. Therefore, both methods are given the same weight. The new RVT or SHAKE rock spectra (PRP 2013) are compatible but they differ from the previous ones (PRP 2010). Nevertheless, the median spectra computed from the previous time histories (chosen before $V_S - \kappa$ corrections) and from the new ones are close to each other. Since only SHAKE and RVT analyses have been rerun the amplification functions referred to in this evaluation summary are those calculated from the new analyses for RVT and SHAKE, (PRP 2013). For the non-linear analyses, the old results, which are deemed representative in view of the previous comments, are those obtained with the old time histories (PRP 2010).

Finally, although we were instructed to provide amplification functions up to 100Hz, the calculations are not deemed reliable above a given frequency, f_3, of the order of 30-50Hz. Equivalent linear analyses are known to overdamp high frequencies because the strain compatible characteristics are computed based on the induced strains, which are governed by the low frequency response; the high frequency component of strains are much smaller. The accuracy of the non-linear runs in the high frequency range depends on the mesh size, integration algorithm, which may introduce numerical damping, modeling of damping for linear elastic materials (Rayleigh damping), etc... All contractors have been asked to estimate the highest frequency that they consider reliable in the non-linear runs and they all indicated 30 to 50 Hz

[PMT and Renault 2010] (PRP- PMT-TN-1126). The upper frequency threshold, f_3, in our logic tree is based on this estimate. Above f_3 the amplification is assumed to be constant and equal to the amplification calculated at frequency f_3:

$$AMP(f > f_3) = AMP(f_3)\frac{S_{a\_input}(f)}{S_{a\_input}(f_3)} \tag{IV-1.5}$$

where $S_{a_{input}}$ is the spectral acceleration of the input time history. An example of the different frequency ranges is depicted in the following Figure IV-1.2.

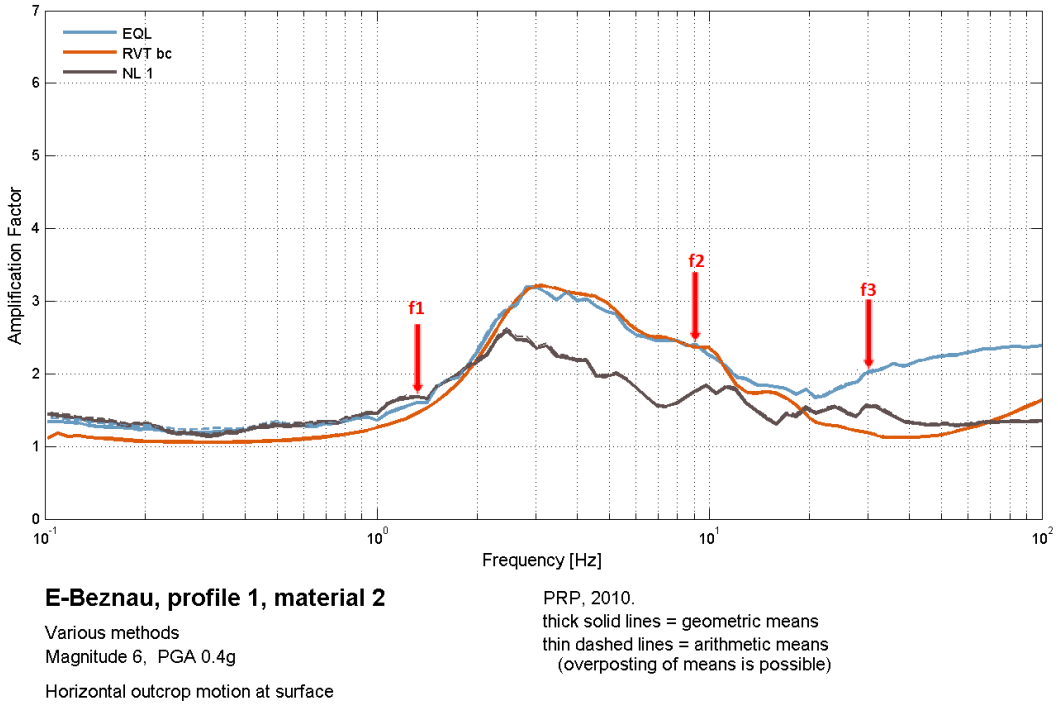

Figure IV-1.2: Illustration of frequency thresholds.

Magnitude Dependence of Amplification Functions

No magnitude dependence of the amplification function is introduced in the logic tree. There are several reasons for that choice:

a None of the new generation of Ground Motion Prediction Equations (GMPE), based on statistical evaluation of records, includes a specific magnitude dependent term in the site amplification function [Power et al. 2008; Cauzzi and Faccioli 2008]. Since several independent parameters were introduced in that component of the GMPEs, it is reasonable to consider that the absence of a magnitude dependent correction is due to the lack of clear evidence in the data.

b Plots of amplification functions do not show any significant magnitude dependence in the frequency range of interest [0.5, f_3], except may be between 0.5Hz and 1Hz for

magnitude 5 and EQL and NL calculations; RVT base case calculations do not show any magnitude dependence, but it has been pointed out that they are not reliable in that frequency range. The calculations that may show some magnitude dependence of the amplification function are those related to RVT randomized calculations (not used in our logic tree) and EQL calculations at high PGA, which are, anyhow, assigned a low weight in the logic tree.

Several examples are given below illustrating the low dependence of the amplification function on the magnitude whatever the analysis type and PGA amplitude.

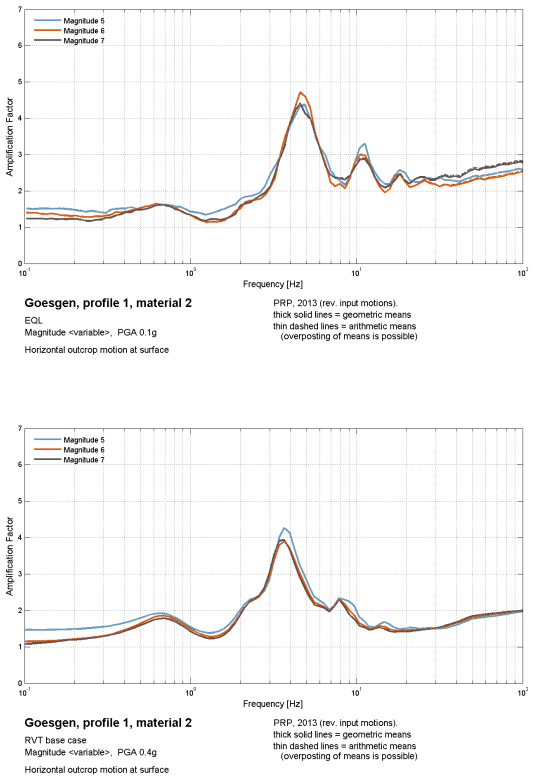

Figure IV-1.3: Illustration of magnitude dependence of amplification functions.

As a conclusion, I do not consider any magnitude dependence for the amplification. The amplification shall be computed as the arithmetic mean of the amplifications for the three magnitudes when results at other magnitudes than 6 are available; otherwise only the results for magnitude 6 are taken into account.

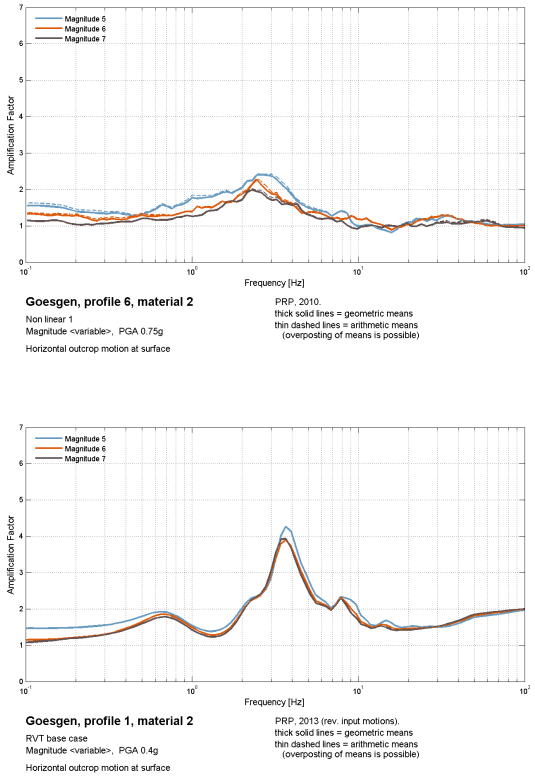

Figure IV-1.4: Illustration of magnitude dependence of amplification functions.

Interpolation for Missing Runs

Interpolation on the amplification functions may be needed because all methods, PGA levels or soil profiles have not been run. Interpolation (extrapolation) schemes defined below refer to the magnitude 6 calculations. Within one set of calculations (e.g. EQL, RVT or NL runs) and for a given soil profile and material type, interpolation on the amplification function is carried out for each frequency using a piecewise cubic interpolation, with Log(PGA) as the independent variable. If extrapolation beyond the latest calculated PGA is needed (EQL runs beyond 0.75g for instance), the extrapolation is based on the $RVT_{basecase}$results:

$$EQL(pga) = \frac{EQL(0.75g)}{RVT_{bc}(0.75g)} RVT_{bc}(pga) \tag{IV-1.6}$$

Above 1.5g no RVT runs are available and the amplification function calculated for 1.5g is kept unchanged for higher $pgas$. Below 0.1g no runs are available and the amplification function calculated for 0.1g is kept unchanged for lower $pgas$. Since for high $pgas$ EQL runs are given a small weight, the impact of the extrapolation scheme on the overall median amplification function is small. However, for Gösgen no extrapolation is needed and the results from SHAKE can be used directly for interpolation. For the missing NL runs, with the same profile but different material types (LB, UB), the ratio of the amplification function of NL(LB or UB) to NL(BE) is calculated for 0.75g and applied to NL(BE) at the requested PGA. This is justified by the small impact of the material type on the amplification function as illustrated by the following Figure IV-1.5: the ratio of the amplification functions for two different materials, but for the same profile, is indeed close to 1.

For the missing NL runs with a different profile P_x, but with the same material, the amplification is calculated according to the following scheme:

- For frequencies less than f_2 : calculate the ratio $R = AMP_{NL}/AMP_{EQL}$
- For frequencies larger than f_2 : calculate the ratio $R = AMP_{NL}/AMP_{RVT\_base\,case}$
- Apply the ratio R to the corresponding EQL (for $f < f2$) or RVT_base case (for $f > f2$) amplification functions calculated for profile P_x to get the amplification function AMP_{NL} for P_x.

$$AMP_{NL}(P_x, f < f_2) = AMP_{NL}(P_1, f < f_2) \frac{AMP_{EQL}(P_x, f < f_2)}{AMP_{EQL}(P_1, < f_2)} \tag{IV-1.7}$$

$$AMP_{NL}(P_x, f > f_2) = AMP_{NL}(P_1, f > f_2) \frac{AMP_{RVT\_bc}(P_x, f > f_2)}{AMP_{RVT\_bc}(P_1, > f_2)} \tag{IV-1.8}$$

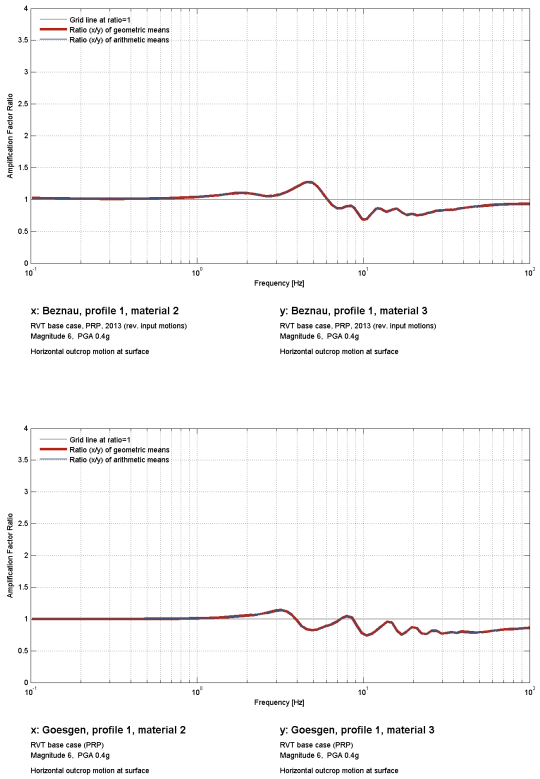

Figure IV-1.5: Influence of material type on the shape of the amplification function.

Non-linear Calculations

The epistemic uncertainty in the Non-linear calculations is treated by developing three (or four for Mühleberg) branches in the logic tree; the main branch, with the largest weight, is assigned to the main contractor calculations; the other two branches are derived from the results of the cross check analyses performed by a different contractor. This epistemic uncertainty reflects the fact that the amount of soil data required for the calibration of the various constitutive models was not exhaustive and therefore that each contractor has to make decisions based on his own experience. As cross check analyses are only performed for one case, it is suggested, once the database of NL_1 runs has been completed following the previously detailed procedures, to "compute" the NL_2 amplification functions as:

$$NL_2(pga, mat) = \frac{NL_2(0.75g, BE)}{NL_1(0.75g, BE)} NL_1(pga, mat) \tag{IV-1.9}$$

Effect of Inclined Waves

In the framework of the original PEGASOS Project P-SV waves analyses have been carried out for three sites: Beznau, Gösgen and Leibstadt. The studies by Fäh took into account random factors such as fault distance, depth, strike angle, dip, duration [Renault 2010d] (PEGASOS TP3-TN-0167). The variation exhibited by the results seems to be covered by the other studies. Since these studies include parametric studies on random variables, they are

more useful to estimate the aleatory contribution to the results. In addition, results obtained by Bard [Bard 2002b] (PEGASOS TP3-RF-0310) are in agreement with those by Fäh.

2D-effects

This effect has been studied for Leibstadt by both Bard and Fäh in the framework of the original PEGASOS Project. The study by Fäh cannot be used: the amplification is said to be calculated from the rock motion, which is obtained by replacing the soil layers by rock in the model. My understanding is that the topographic effect is included in the calculation of the rock motion and results are therefore not directly comparable to those of the 1D runs.

The study by Bard does not show a significant effect of the 2D topography. Since the Leibstadt site has been chosen as the site being the most likely to evidence 2D topographic effect, it can be concluded that this effect has indeed a minor impact on the results. Variations covered by the other parametric studies largely encompass the 2D-effect: the amplification due to 2D-effect is less than 20 % for moderate shaking level. For Leibstadt, the amplification calculated for magnitude 6, pga=0.4g, around the fundamental frequency of the deposit is of the order of 3.0; considering variations in the soil profile and material characteristics broadens the amplification from 2.8 to 4.8, a seventy percent variation, much larger than the 20% attributed to 2D-effect.

3D-effects

No calculations have been performed to assess the 3D-effect. However, based on the small impact of the 2D topography for Leibstadt, which is believed to be the site where the strongest topographic effect should be noticed, the effect of 3D topography is neglected. In addition, I am not aware of well-established standard to estimate a priori this effect.

1.2.4 Beznau

Logic Tree for Beznau

The Logic Tree for Beznau is represented in Figure IV-1.6.

Site-specific Model Evaluations

Alternative Velocity Profiles

The weights assigned to each velocity profile are based on the following considerations: Four velocity profiles are considered, P1 to P4. The first two are based on cross hole measurements. The third one results from the inversion of the dispersion curves (ambient vibration measurements); there is no resolution of the thin layers and the gradient in the Opalinus Clay is not really substantiated by the other measurements; it is nevertheless assigned a small weight because back calculations of the plant settlements after construction with this profile are acceptable. Profile P4 is based on profile MK2 proposed by the contractor with a slight reduction in the Opalinus Clay and a simpler profile beneath; it fits the fundamental frequency of the site.

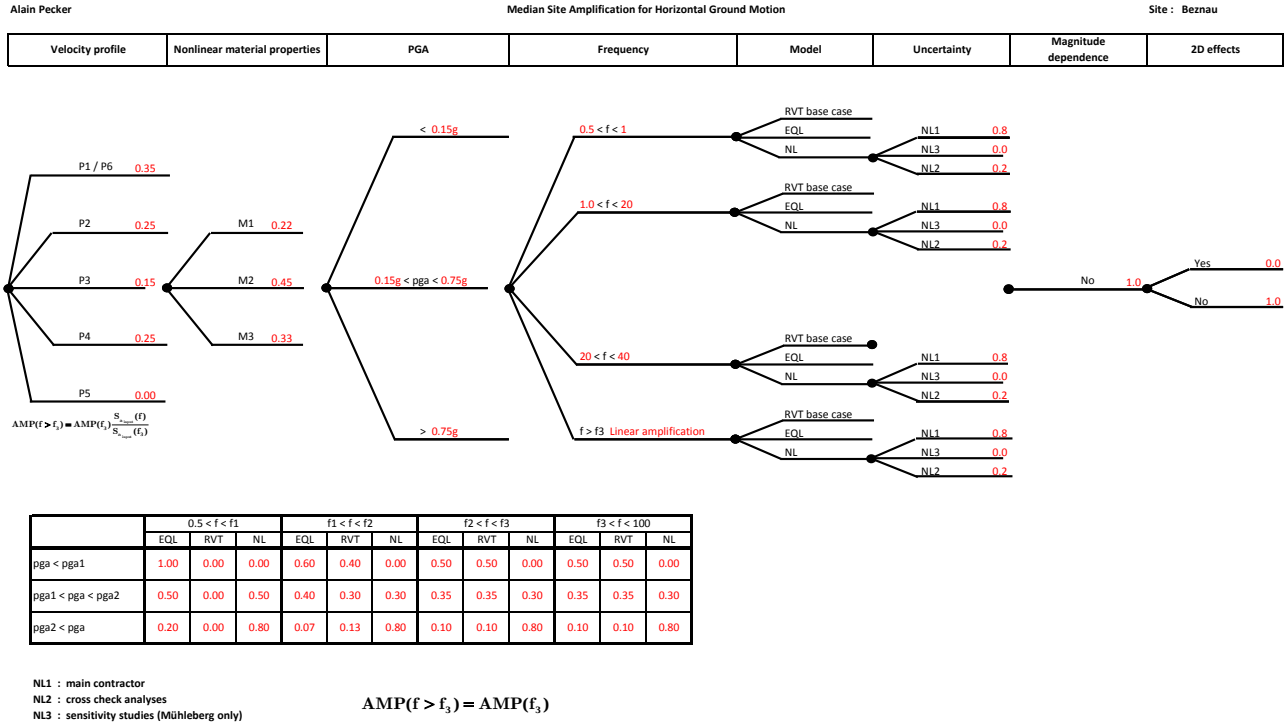

	0.5 < f < f1			f1 < f < f2			f2 < f < f3			f3 < f < 100		
	EQL	RVT	NL	EQL	RVT	NL	EQL	RVT	NL	EQL	RVT	NL
pga < pga1	1.00	0.00	0.00	0.60	0.40	0.00	0.50	0.50	0.00	0.50	0.50	0.00
pga1 < pga < pga2	0.50	0.00	0.50	0.40	0.30	0.30	0.35	0.35	0.30	0.35	0.35	0.30
pga2 < pga	0.20	0.00	0.80	0.07	0.13	0.80	0.10	0.10	0.80	0.10	0.10	0.80

NL1 : main contractor
NL2 : cross check analyses
NL3 : sensitivity studies (Mühleberg only)

$\mathbf{AMP(f > f_3) = AMP(f_3)}$

Figure IV-1.6: Logic tree for Beznau.

Alternative Non-linear Properties

The material curves for best estimate, lower bound and upper bound characteristics have been established on the basis of existing laboratory data and of published experimental data for similar materials. For G/G_{max} the proposed curves bracket all the data points, which is not necessarily representative of the actual behaviour. In fact, laboratory measurements may be subject to testing errors, remolding of samples, transformation uncertainties (calculation of G from measurement of E) which tend to increase the scatter as recognized by Set et al. [2011]. For instance, it is shown in this paper that uncertainties in the yield strength may affect the G/G_{max} curves; this uncertainty is already accounted for in the non-linear models and should not be counted twice. Consequently, the weights assigned to each of the three material models (BE, UB and LB) is chosen after examination of the laboratory data and expert judgment. The range of most probable values is defined from those data and does necessarily span the whole range proposed for the calculations. This range, for the case of Beznau is represented by the dotted lines in Figure IV-1.7.

These two curves are defined according to:

$$(\frac{G}{G_{max}})_u = (\frac{G}{G_{max}})_{mean} + \alpha \left[(\frac{G}{G_{max}})_{UB} - (\frac{G}{G_{max}})_{mean} \right] \tag{IV-1.10}$$

$$(\frac{G}{G_{max}})_1 = (\frac{G}{G_{max}})_{mean} + \beta \left[(\frac{G}{G_{max}})_{LB} - (\frac{G}{G_{max}})_{mean} \right] \tag{IV-1.11}$$

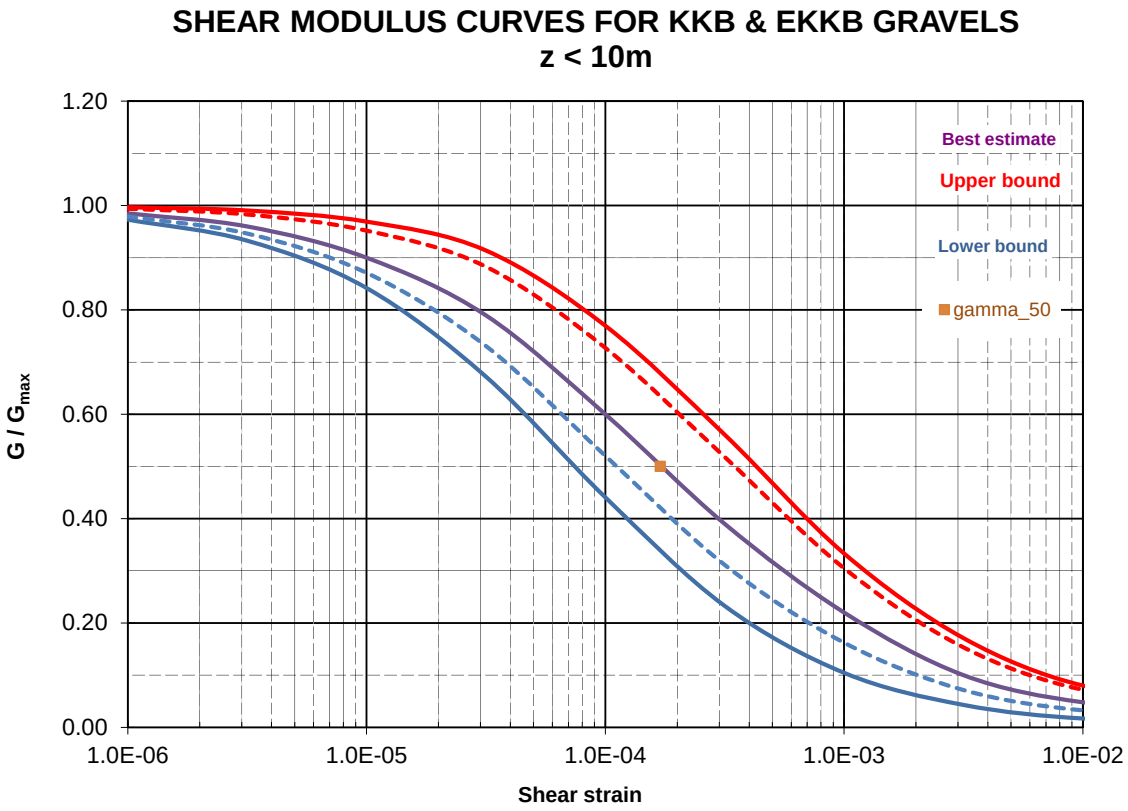

Figure IV-1.7: Definition of the range of most probable curves (dotted lines).

Then, if p, q_1, q_2 represent the weights assigned to the mean curve, to the LB curve and to the UB curve, it is assumed that

$$q_2 = \alpha p, q_1 = \beta p \tag{IV-1.12}$$

In that way, $\alpha = 0$ means that the data above the mean curve are not reflecting true uncertainties, but are caused by testing errors, and consequently the UB curve is assigned zero weight. On the contrary if $\alpha = 1$ the full range between the mean and the UB curve is deemed possible; both curves are given the same weight. The same applies for the LB curve, replacing α by β . Once α and β are chosen the weights given to the mean curve (p), the LB curve (q_1) and the UB curve (q_2) are computed as:

$$p = \frac{1}{1+\alpha+\beta}, q_1 = \frac{\beta}{1+\alpha+\beta}, q_2 = \frac{\alpha}{1+\alpha+\beta} \tag{IV-1.13}$$

For Beznau the values are $\alpha = 0.75$ and $\beta = 0.50$.

Threshold Strains

As shown in Figure IV-1.7, γ_{50} is equal to 1.7 10^{-4}.

The top 9 M consist of gravels and sandy gravel in a medium dense to dense state; the water table is at 6.0 M depth. Following the procedure described in Section 1.2.3 and based on the

strength properties chosen by each contractor the maximum shear stress at any depth z is calculated with $c = 20kPa$, $\phi = 44.5°$ and $K_0 = 0.7$. Plots of the normalized shear stress versus the normalized shear strain are shown in Figure IV-1.8 for three representative depths in the top 9m.

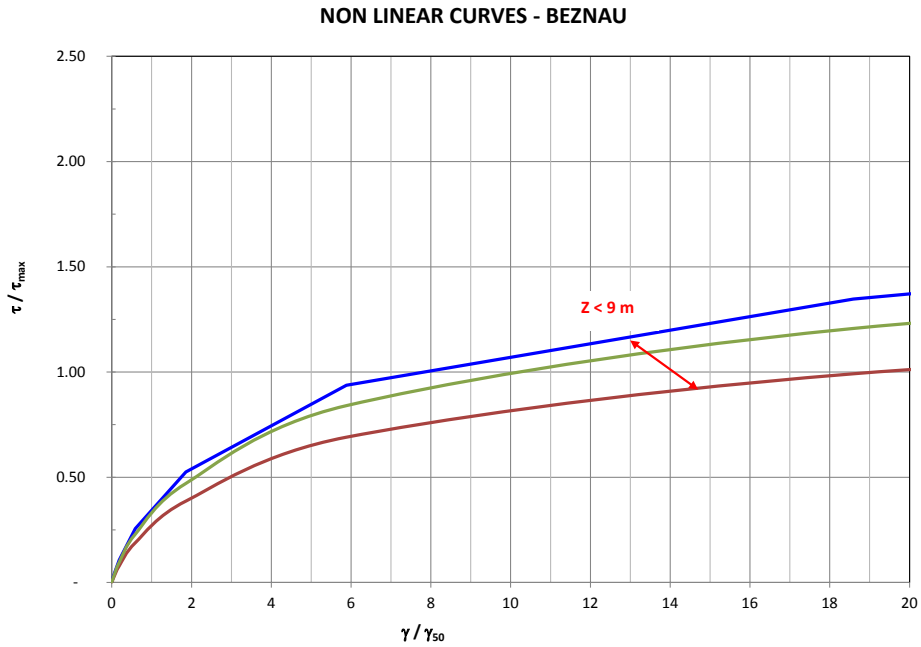

Figure IV-1.8: Normalized shear stress vs normalized shear strain.

The comparison of the $G/G_{max}(mean)$ curve and of the same curve obtained through calibration of the non-linear constitutive model is shown in Figure IV-1.9.

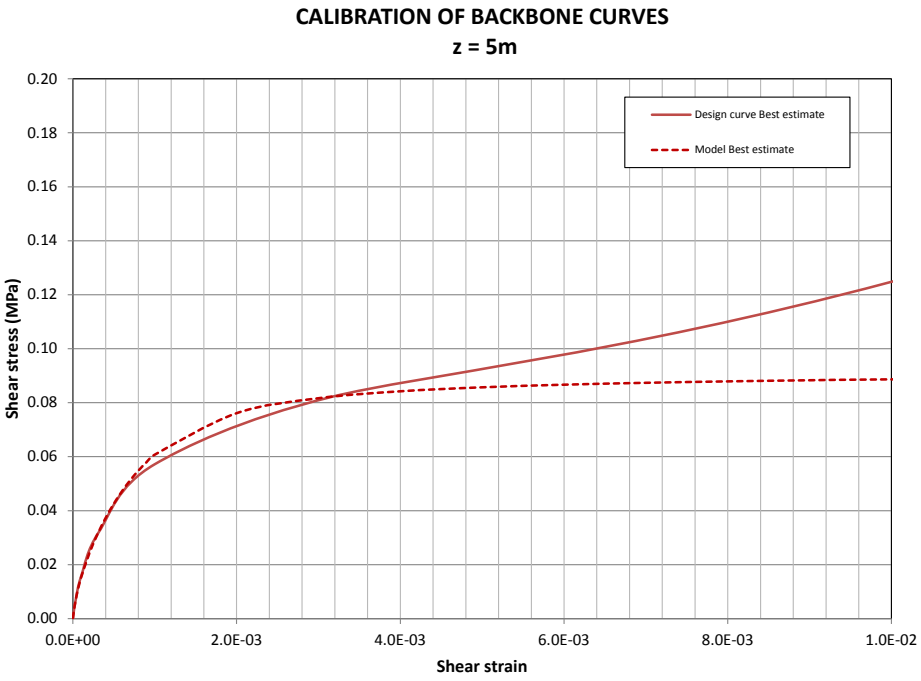

Figure IV-1.9: Non-linear curves from EQL (solid line) and NL (dotted line) calculations.

Both curves are rather consistent and clear show that for strains larger than approximately 2.5 10^{-3} the EQL curves are no longer valid; consequently the second threshold strain was set at $\gamma/\gamma_{50} = 15$. This threshold strain has to be converted in PGA as shown in Figure IV-1.10.

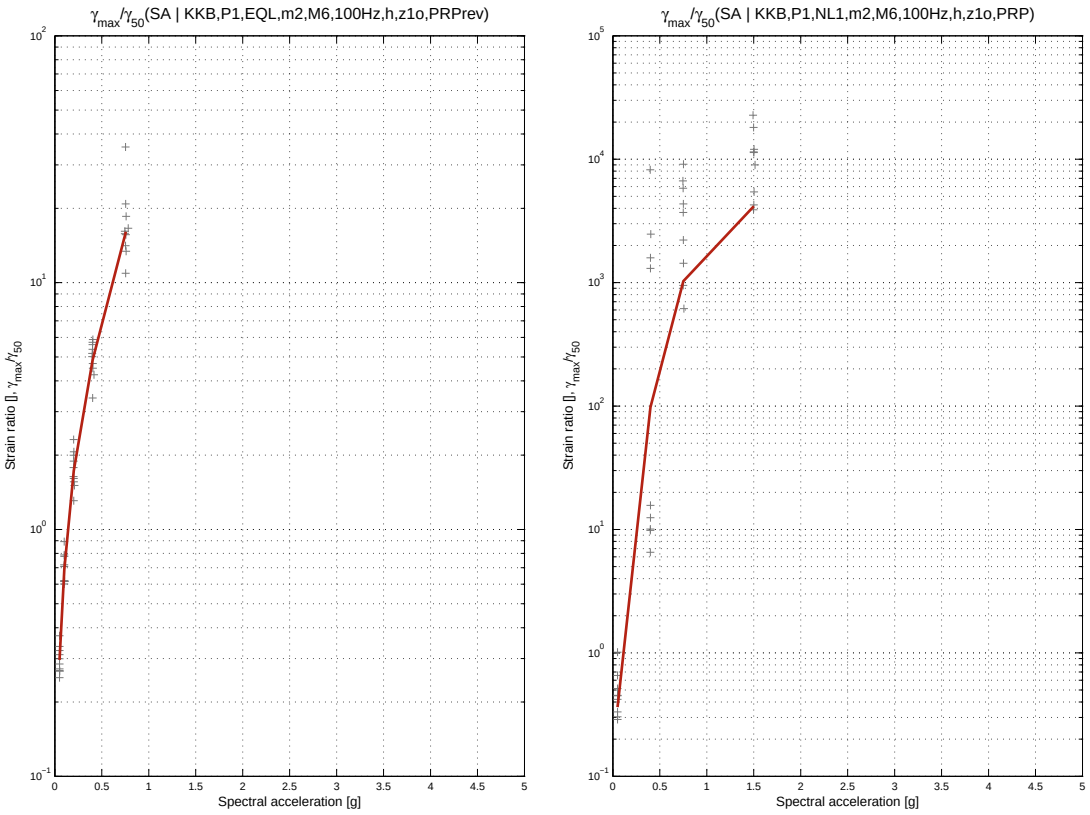

Figure IV-1.10: Relationship between normalized strain and PGA (EQL & NL runs).

Figure IV-1.10 shows that $\gamma/\gamma_{50} = 1$ is reached for a PGA included between 0.10g and 0.13g and $\gamma/\gamma_{50} = 15$ for PGA of the order of 0.50g to 0.75g The EQL runs are therefore valid up to a peak ground acceleration of 0.75 g (strains smaller than 0.2 - 0.25 %). However, a small weight has still been given to the EQL runs above PGA=0.75g in order not to entirely rely on one set of calculations.

Frequency Ranges

The first frequency f_1 is defined as half the frequency, f_{0min}, of the lowest peak identified in the amplification functions for magnitude 6 and all $pgas$; frequency f_2 corresponds to twice the frequency, f_{0max}, of the highest peak identified in the amplification functions for magnitude 6 and all $pgas$. The runs considered for the identification of f_1 and f_2 are either the EQL runs or the NL ones. The procedure is illustrated below in Figure IV-1.11.

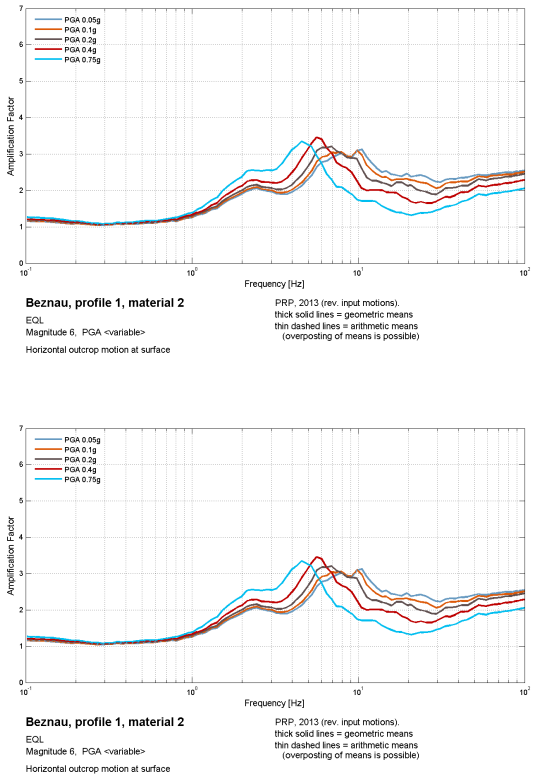

Figure IV-1.11: Amplification functions for all $pgas$: left EQL runs; right NL runs.

Based on those curves f_{0min} varies between 4Hz (EQL runs) and 2Hz (NL runs); hence, $f_i = 1Hz$. The upper range is defines by $f_{0max} = 10Hz$, hence $f_2 = 20Hz$. Finally f_3 is taken equal to 40Hz.

Final Weights

The final weights for the branches of the logic tree are provided in Figure IV-1.6 below the logic tree.

1.2.5 E-Beznau

The Logic Tree for E-Beznau is represented in Figure IV-1.12.

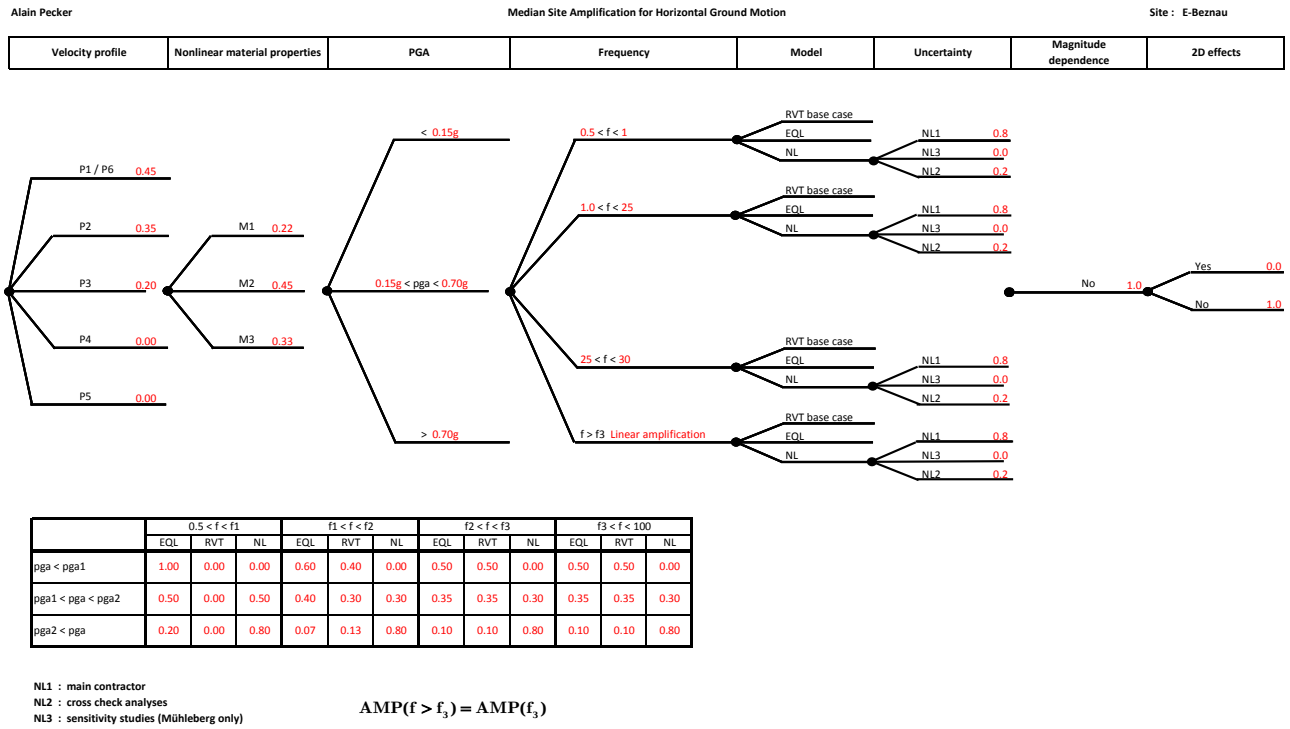

	0.5 < f < f1			f1 < f < f2			f2 < f < f3			f3 < f < 100		
	EQL	RVT	NL	EQL	RVT	NL	EQL	RVT	NL	EQL	RVT	NL
pga < pga1	1.00	0.00	0.00	0.60	0.40	0.00	0.50	0.50	0.00	0.50	0.50	0.00
pga1 < pga < pga2	0.50	0.00	0.50	0.40	0.30	0.30	0.35	0.35	0.30	0.35	0.35	0.30
pga2 < pga	0.20	0.00	0.80	0.07	0.13	0.80	0.10	0.10	0.80	0.10	0.10	0.80

Figure IV-1.12: Logic tree for E-Beznau.

Site-specific Model Evaluations

Alternative Velocity Profiles

Three velocity profiles are considered, P1 to P3. The velocity profiles are directly adapted from the KKB profiles with due accounting for the changes in the thickness of gravel and Opalinus Clay layers and the total depth over the Gipskeuper formation. Consequently, the same philosophy as for KKB applies in the definition of the weights. Profiles P1 and P2 directly issued from direct measurements (cross hole) are assigned the largest weights; profile P3 based on ambient vibration measurement is assigned the lowest one. The respective weights between all three profiles are similar to those defined for KKB.

Alternative Non-linear Properties

The same approach as for KKB is followed. The range of most probable G/G_{max} curves, based on examination of the soil data is shown in Figure IV-1.7 for the top 10M of gravels and in Figure IV-1.13 for the layers beneath 10M. Those curves were obtained with the same value of α and β as for Beznau, i.e. 0.75 and 0.5. Therefore the weights given at each branch of the logic tree is the same.

Threshold Strains

As shown in Figure IV-1.7 and Figure IV-1.14, γ_{50} is equal to 1.7 10^{-4} for the top 10M and to 2 10^{-4} below. Figure IV-1.14 presents the normalized shear stress versus normalized shear strain for layers above 10M (similar to Figure IV-1.7) and for the deeper layers. For the computations of the vertical effective stress, the water table is at 6M depth.

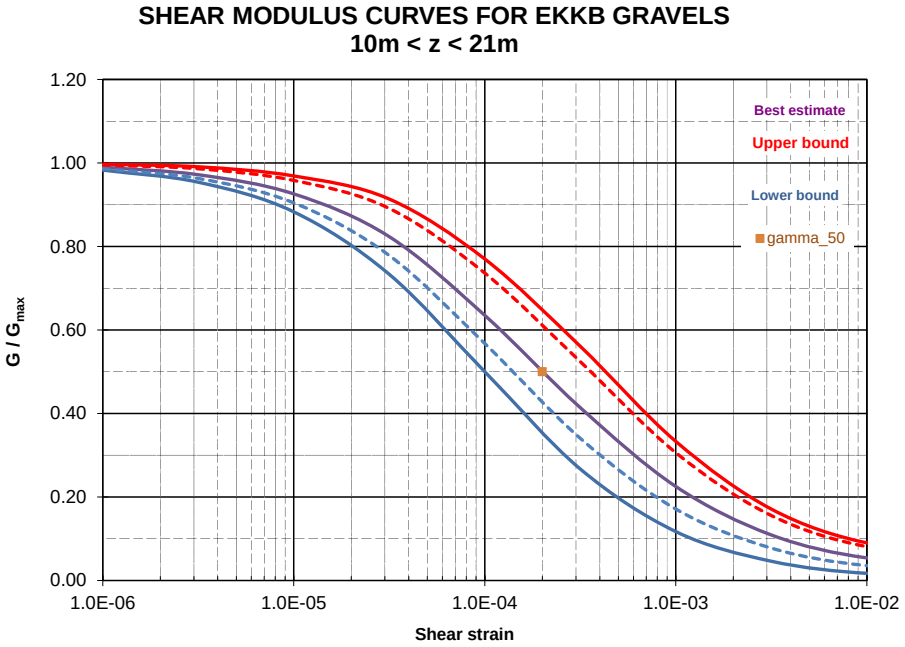

Figure IV-1.13: Definition of the range of most probable curves (dotted lines).

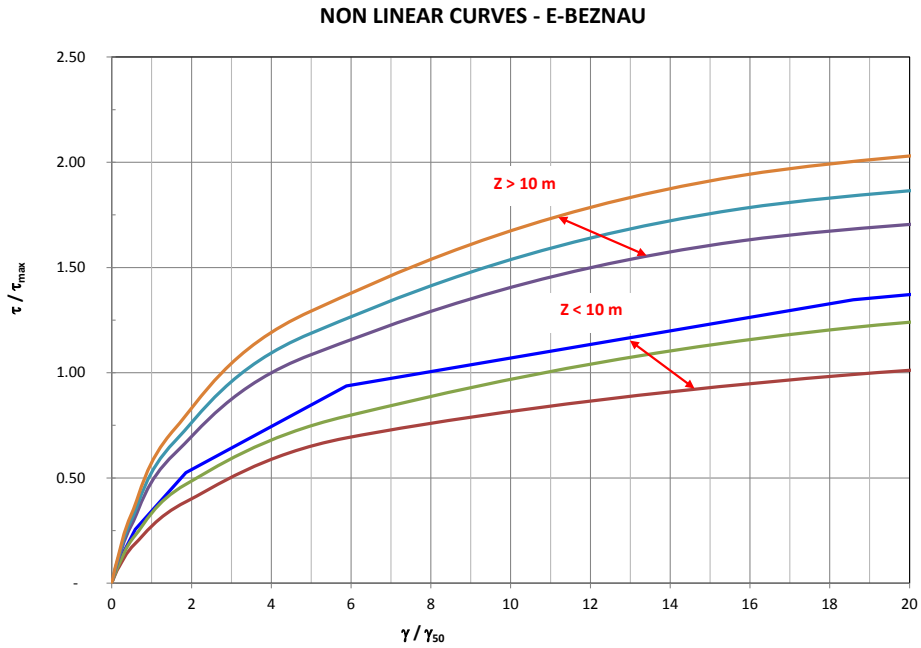

Figure IV-1.14: Normalized shear stress vs normalized shear strain.

Depending on the depth of the layers the range of validity of the curves varies significantly: for shallow layers it corresponds to γ/γ_{50} equal to 15 and for deep layers to γ/γ_{50} to 3. However examination of the variation of maximum shear strain with depth, one example of which is depicted in Figure IV-1.15, clearly shows that the maximum strain is reached in the top 10 Meters.

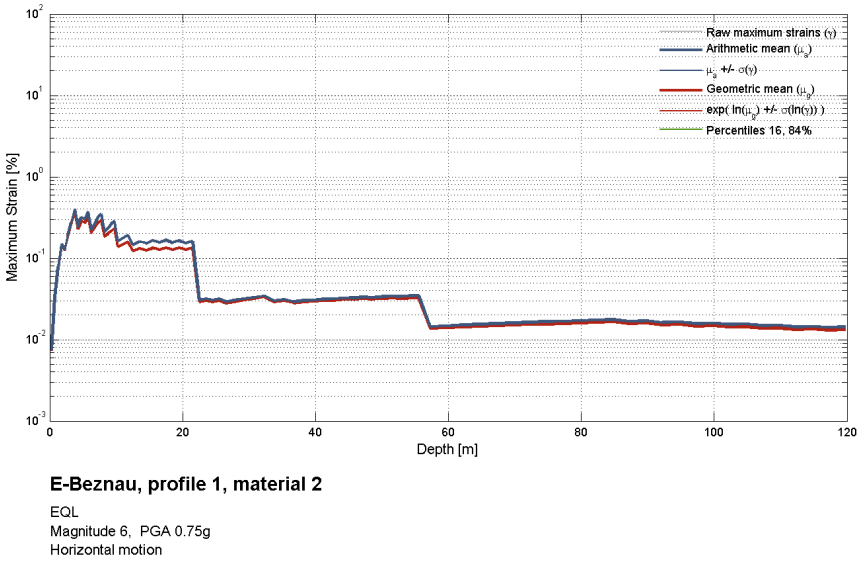

Figure IV-1.15: Variation of maximum shear strain with depth.

Therefore, the soil column response will be governed for large *pgas* by the behavior of the surficial deposits and the second threshold strain is corresponds to γ/γ_{50} equal to 15. Once converted in terms of PGA, following the approach developed in paragraph 1.2.5, the *pgas* thresholds are 0.15g and 0.70g.

Frequency Ranges

The same approach as for Beznau is followed from which it results that $f_{0min} = 2$ to 3Hz and $f_{0max} = 12.5Hz$. The frequency range $[f_1, f_2]$ spans from the minimum value to twice the maximum one. The maximum frequency f_3 is taken equal to 30Hz.

Final Weights

The final weights for the branches of the logic tree are provided in Figure IV-1.12 below the logic tree.

1.2.6 Gösgen

Logic Tree for Gösgen

Figure IV-1.16 shows the Logic Tree for Gösgen.

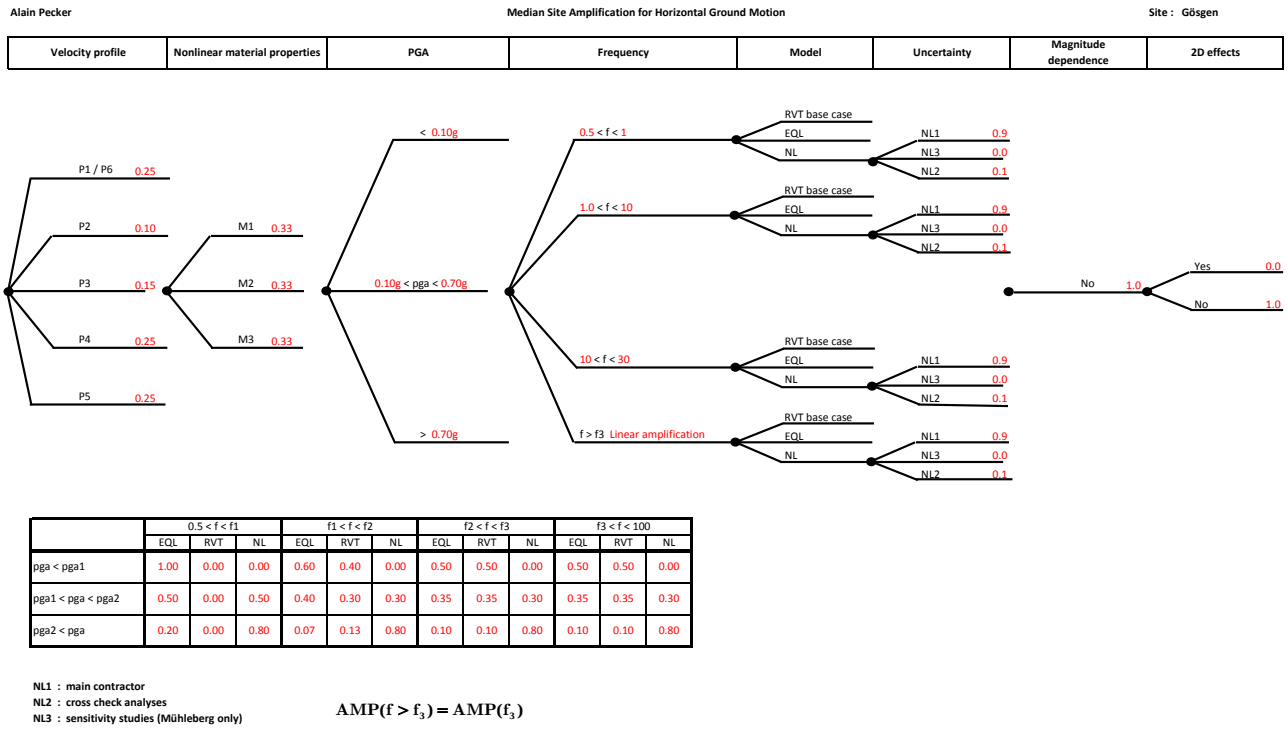

	0.5 < f < f1			f1 < f < f2			f2 < f < f3			f3 < f < 100		
	EQL	RVT	NL	EQL	RVT	NL	EQL	RVT	NL	EQL	RVT	NL
pga < pga1	1.00	0.00	0.00	0.60	0.40	0.00	0.50	0.50	0.00	0.50	0.50	0.00
pga1 < pga < pga2	0.50	0.00	0.50	0.40	0.30	0.30	0.35	0.35	0.30	0.35	0.35	0.30
pga2 < pga	0.20	0.00	0.80	0.07	0.13	0.80	0.10	0.10	0.80	0.10	0.10	0.80

NL1 : main contractor
NL2 : cross check analyses
NL3 : sensitivity studies (Mühleberg only)

$AMP(f > f_3) = AMP(f_3)$

Figure IV-1.16: Logic tree for Gösgen.

Site-specific Model Evaluations

Alternative Velocity Profiles

Six shear wave velocity profiles are considered, labeled P1 to P6. As a matter of fact P1 and P6 are similar and only differ by the fact that for non-linear analyses the depth of the soil profile is reduced; they are consequently merged in a single profile. Therefore P1 and P6 are considered as a unique profile. Profiles P3 to P4 are based on direct shear wave velocity measurements (cross hole and sonic tests). P3 is a more regional profile than a site specific one; it therefore assigned a somewhat lower weight. Profile P2 is based on downhole measurements and yields low V_S values; it is intended to reflect the frequency 0.6Hz that appears in the H/V ratios. However, profile P1, based on V_S inversion, does also account for that frequency. Based on these considerations it was decided to assign equal weights to profiles P1/P6, P4 and P5, which differ only by the shear wave velocities in the alluvia but are equally plausible; a somewhat lower weight is assigned to P3, because we doubt that the velocity inversion exhibited at 500m depth could be reliably assessed from indirect measurements, and the lowest one to P2 because the V_S values appear too small in view of the ground description.

Alternative Non-linear Properties

Down to 28.5m the profile is composed of sands and gravels in a medium dense state; the friction angle is taken equal to 45°and the cohesion to 20kPa. The water table is at 6.5m depth. The most probable range of G/G_{max} curves for this site coincides with the bounds provided in the specifications. Therefore $\alpha = 1$ and $\beta = 1$. All branches of the logic tree are assigned the same weight.

Threshold Strains

Figure IV-1.17 presents the normalized shear stress versus normalized shear strain for layers above 10m and for the deeper layers. For the computations of the vertical effective stress, the water table is at 6.5m depth; the strength properties are c=20kPa and $\phi = 45°$ and the at rest earth pressure coefficient $K_0 = 0.7$.

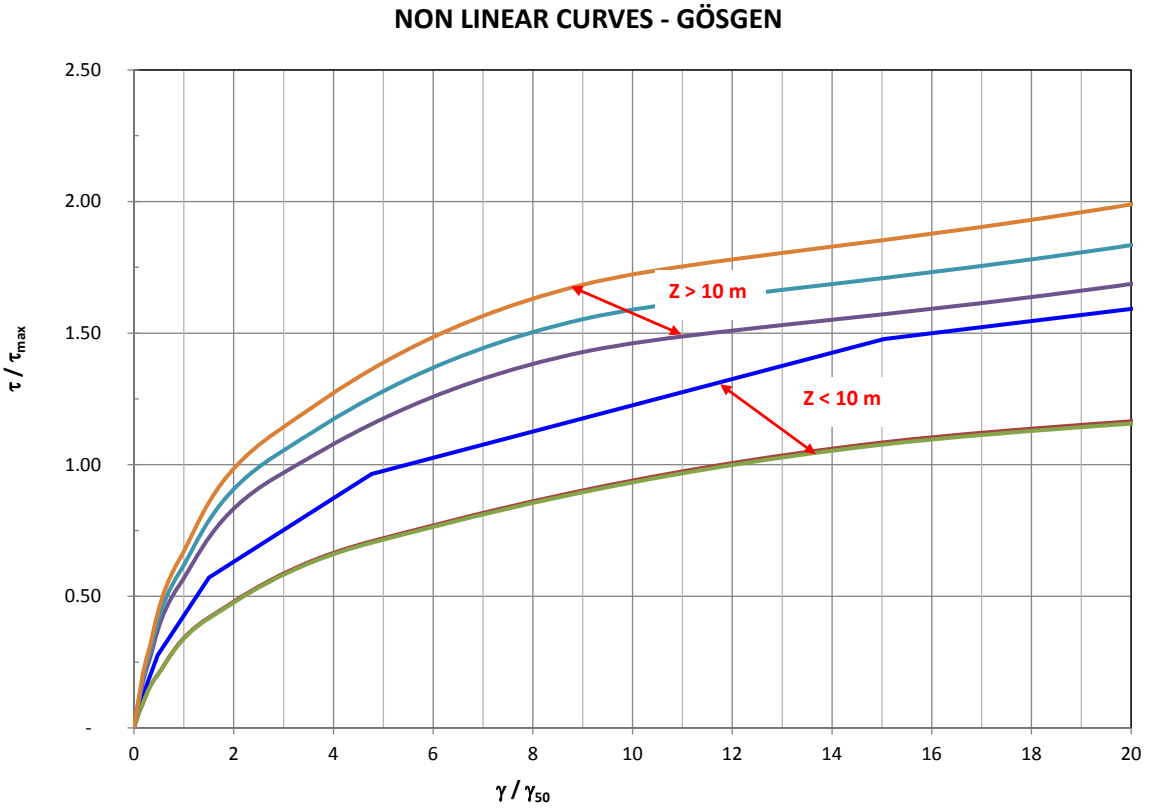

Figure IV-1.17: Normalized shear stress vs normalized shear strain.

Depending on the depth of the layers the range of validity of the curves varies significantly: for shallow layers it corresponds to γ/γ_{50} equal to 12 and for deep layers to γ/γ_{50} equal to 3. However examination of the variation of maximum shear strain with depth shows that the maximum strain is reached in the top 10meters, around 8m depth.

Comparison of the non-linear curves established for the calibration of the constitutive model with those provided in the specification (Figure IV-1.18) shows that, combined with the results shown in Figure IV-1.17, γ/γ_{50} is in the range 12 to 16. In terms of PGA, following the approach presented in paragraph 1.2.4, the thresholds are converted to 0.10g and 0.70g.

Frequency Ranges

The same approach as for Beznau is followed from which it results that $f_{0min} = 2Hz$ and $f_{0max} = 5Hz$. The frequency range $[f_1, f_2]$ spans from half the minimum value to twice the maximum one. The maximum frequency f_3 is taken equal to 30Hz.

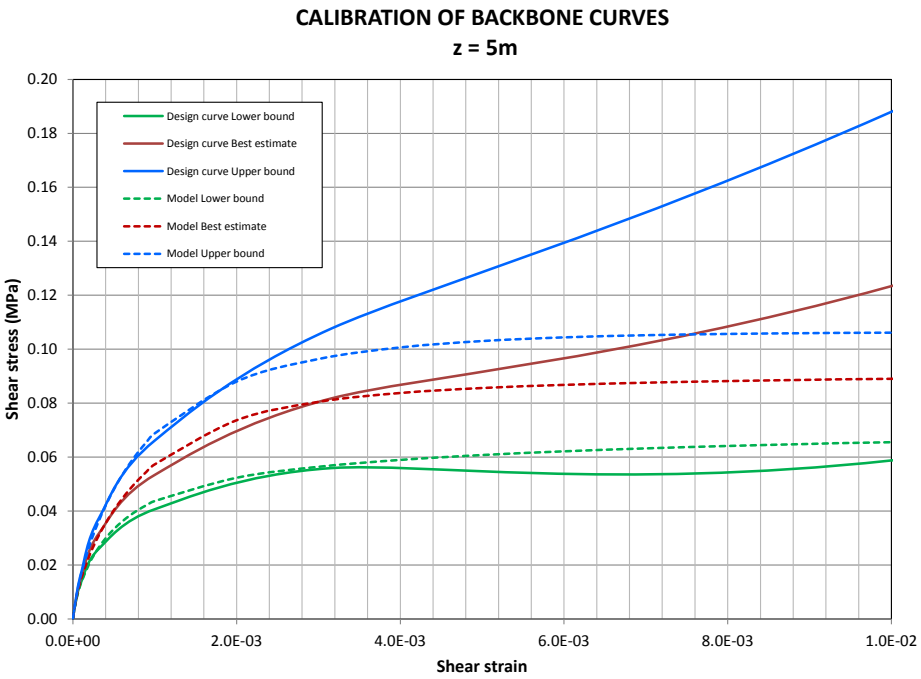

Figure IV-1.18: Non-linear curves from EQL (solid line) and NL (dotted line) calculations.

Final Weights

The final weights for the branches of the logic tree are provided in Figure IV-1.16 below the logic tree.

1.2.7 Leibstadt

Logic Tree for Leibstadt

The Logic Tree for Leibstadt is shown in Figure IV-1.19.

Site-specific Model Evaluations

Alternative Velocity Profiles

Three profiles are considered; all profiles rely on the cross hole data for the rock units. Profile P1 takes into account surface wave measurements (ambient vibration, MASW) for the definition of the velocity profile in the gravel layers; it therefore combines the largest number of data. Profile P2 is the most complex one; the velocity in the shallow gravel layer is decreased to 400m/s, and the effect of anisotropy in the cross hole data is accounted for. Profile P3 is the simplest one and based on the inversion of the dispersion curves obtained from ambient vibration measurements. Profiles P1 and P2 are considered the most reliable and are assigned equal weights; profile P3, which is not based on direct measurements in the gravel layers, is considered over simplistic and is given a smaller weight.

Alternative Non-linear Properties

The same approach as for KKB is followed. The range of most probable G/G_{max} curves, based on examination of the soil data is shown in Figure IV-1.20 for the top 10m of gravels

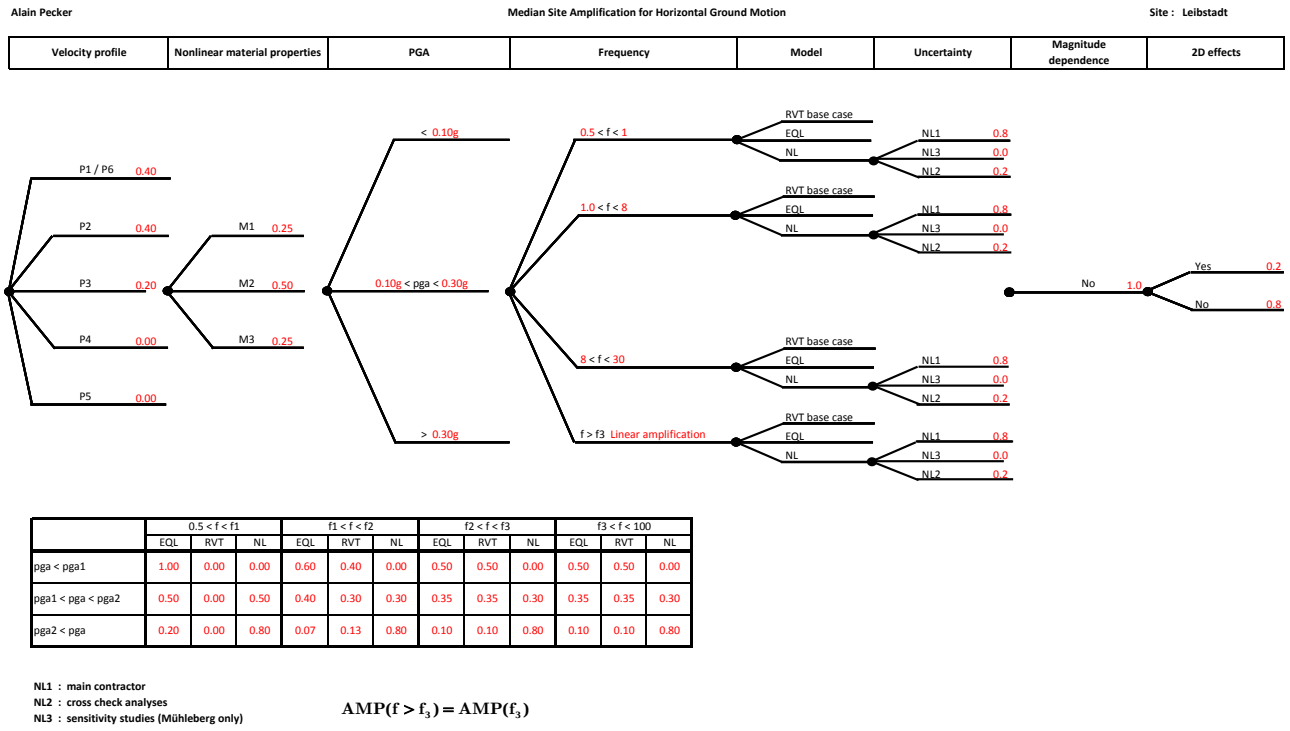

	0.5 < f < f1			f1 < f < f2			f2 < f < f3			f3 < f < 100		
	EQL	RVT	NL	EQL	RVT	NL	EQL	RVT	NL	EQL	RVT	NL
pga < pga1	1.00	0.00	0.00	0.60	0.40	0.00	0.50	0.50	0.00	0.50	0.50	0.00
pga1 < pga < pga2	0.50	0.00	0.50	0.40	0.30	0.30	0.35	0.35	0.30	0.35	0.35	0.30
pga2 < pga	0.20	0.00	0.80	0.07	0.13	0.80	0.10	0.10	0.80	0.10	0.10	0.80

Figure IV-1.19: Logic tree for Leibstadt.

and for the layers beneath 10m. Those curves were obtained with $\alpha = \beta = 0.5$. Therefore the weight of the best estimate curve is equal to 0.5 and the weights of the two bound curves are the same and equal to 0.25.

Threshold Strains

Figure IV-1.21 presents the normalized shear stress versus normalized shear strain for layers above 10m and for the deeper layers. For the computations of the vertical effective stress, the water table is at 26m depth; the strength properties are c=25kPa and $\phi = 38.5°$ and the at rest earth pressure coefficient $K_0 = 0.45$.

Like for E-Beznau or Gösgen, depending on the depth of the layers the range of validity of the curves vary significantly: for shallow layers it corresponds to γ/γ_{50} equal to 2 and for deep layers to γ/γ_{50} equal to 0.7. However examination of the variation of maximum shear strains with depth shows that the maximum strain is reached around 20m depth (Figure IV-1.22).

Comparison of the non-linear curves established for the calibration of the constitutive model with those provided in the specification (Figure IV-1.23) shows that, combined with the results shown in Figure IV-1.21, γ/γ_{50} is in the range 0.7 to 0.9.

Sensitivity analyses have been conducted by increasing the friction angle to 43°, the cohesion to 50kPa and the at rest earth pressure coefficient to 0.7 to reflect the presence of the cemented layer at depth. The effect of these changes is to slightly increase γ/γ_{50} derived from the G/G_{max} curves up to 1.0; no additional calibration of the non-linear constitutive model has been redone and therefore the value 0.7 to 0.9 remains the same for this approach. As the second threshold strain corresponds to $\gamma/\gamma_{50} = 1.0$, it means that the first threshold strain should be less than 1.0, as opposed to the other sites. Based on the examination of Figures

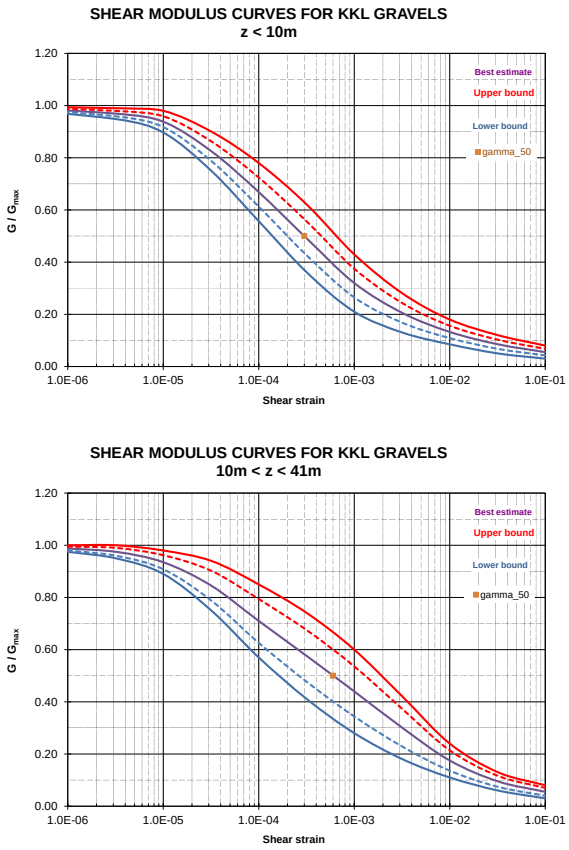

Figure IV-1.20: Definition of the range of most probable curves (dotted lines).

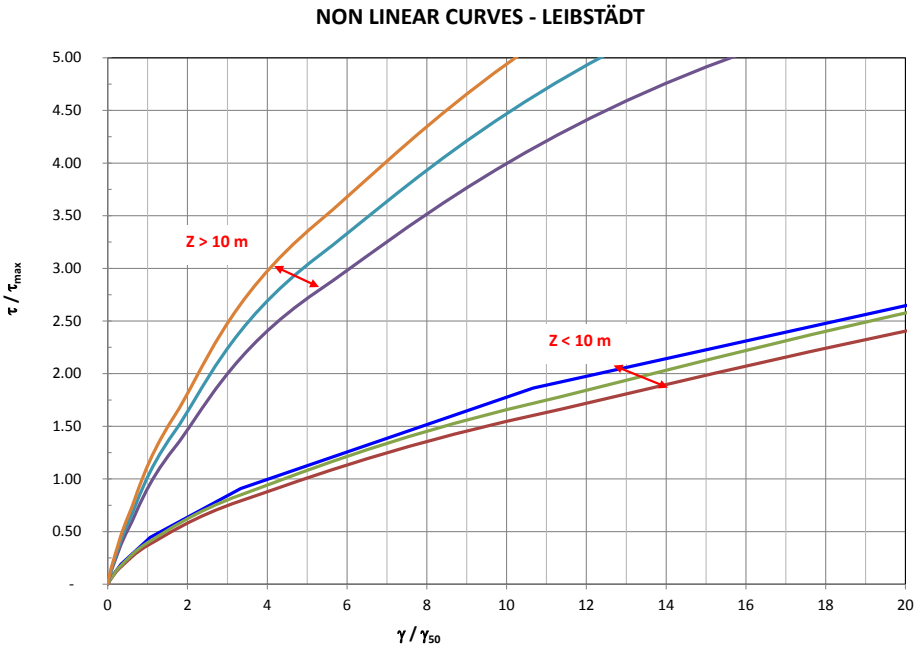

Figure IV-1.21: Normalized shear stress vs normalized shear strain.

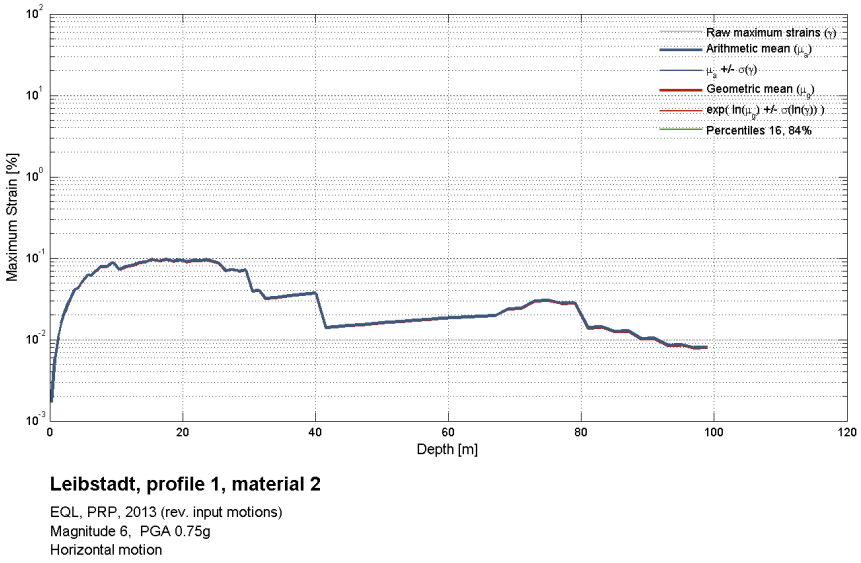

Figure IV-1.22: Maximum shear strain vs depth.

IV-1.20 and IV-1.23, a value of to γ/γ_{50} equal to 0.2 has been retained, corresponding to $G/G_{max} = 0.7$ In terms of PGA, following the approach presented in paragraph 1.2.4, the two thresholds are eaqual to 0.10g and 0.30g.

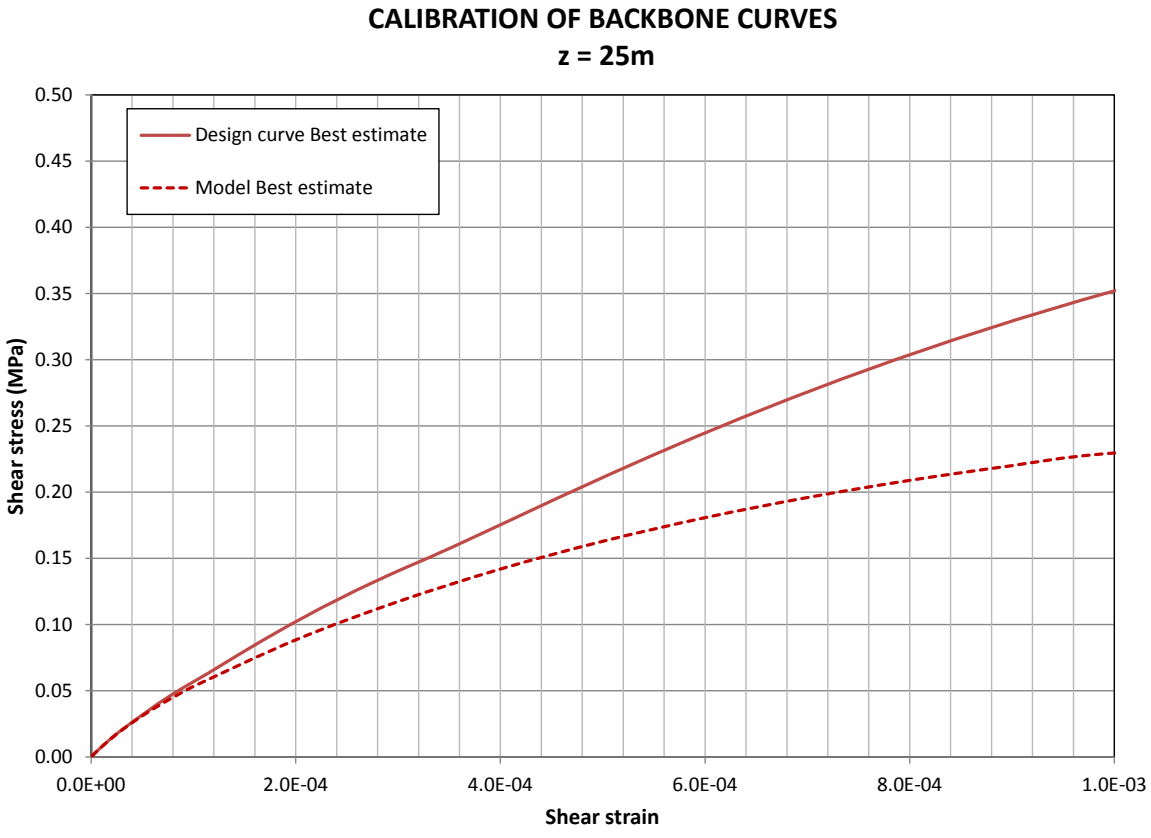

Figure IV-1.23: Non-linear curves from EQL (solid line) and NL (dotted line) calculations.

Frequency Ranges

The same approach as for the other sites is followed from which it results that $f_{0min} = 2Hz$ and $f_{0max} = 4Hz$. The frequency range $[f_1, f_2]$ spans from half the minimum value to twice the maximum one. The maximum frequency f_3 is taken equal to 30Hz.

2D Amplification

For that site the amplification shall be computed as the mean of the amplifications computed at receivers 10 to 19 in Bard [2002a] (TP3-TN-0186). Only the curves corresponding to the high strain case with vertical incidence need to be considered. Figure IV-1.24 extracted from this document gives the ratio of the amplification factor of 2D to 1D calculations. This figure shows that the amplification is significant only close to the resonant frequency f_0 of the layer and is limited to 20%. Somewhat higher amplification, and also deamplification, can be noticed for specific receivers but we will not consider this effect that may arise from the constructive or destructive interference of waves at precise locations of the receivers with respect to the source location. This is an aleatory type of variability, which will not be considered, because already dealt with by SP2.

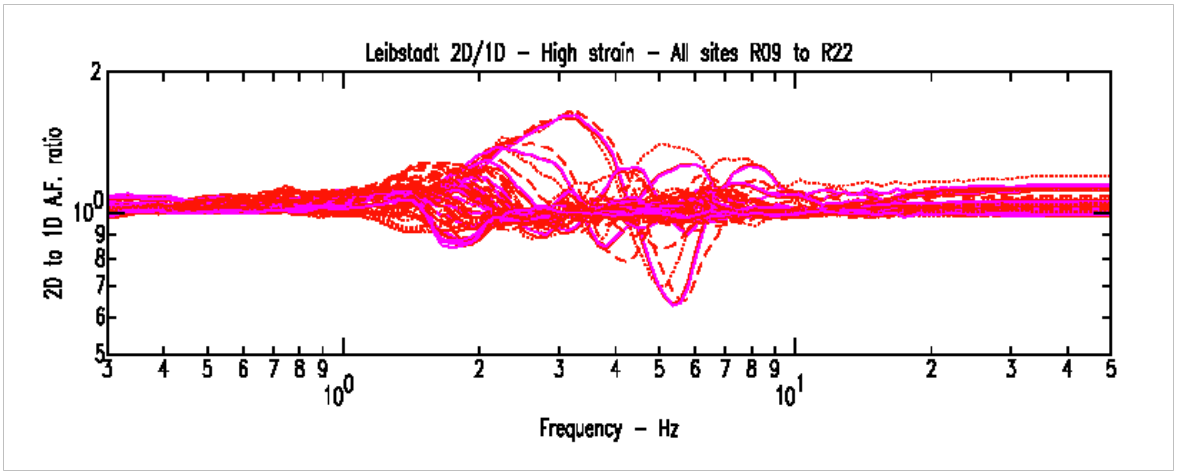

Figure IV-1.24: Ratios of 2D to 1D amplification for the high strain case.

To account for the "average" 2D amplification, we recommend to use the following correction factor C to be applied to the 1D amplification:

f < 0.5 f0	C = 1
0.5 f0 < f < 0.7 f0	C = 1 + (f/f0-0.5)
0.7 f0 < f < f0/0.7	C = 1.2
f0/07< f < 2 f0	C = 1.2-0.35 (f/f0-1/0.7)
f > 2 f0	C = 1

As noticed in paragraph 1.2.7 the resonant frequency of the layer varies between $f_{0min} = 2Hz$ and $f_{0max} = 4Hz$; we recommend to take $f_0 = 3Hz$ for the calculations of the 2D amplification correction factor.

Final Weights

The final weights for the branches of the logic tree are provided in Figure IV-1.19 below the logic tree.

1.2.8 Mühleberg

Logic Tree for Mühleberg

Figure IV-1.25 shows the Logic Tree for Mühleberg.

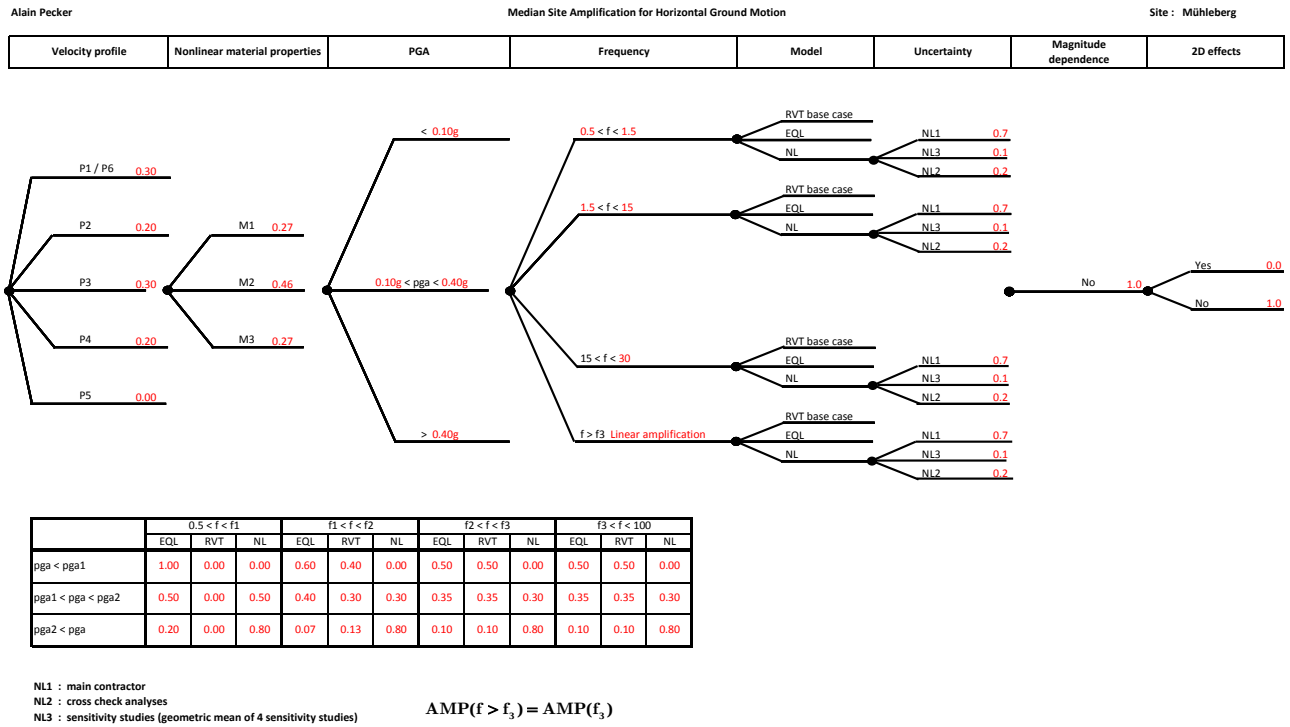

	0.5 < f < f1			f1 < f < f2			f2 < f < f3			f3 < f < 100		
	EQL	RVT	NL	EQL	RVT	NL	EQL	RVT	NL	EQL	RVT	NL
pga < pga1	1.00	0.00	0.00	0.60	0.40	0.00	0.50	0.50	0.00	0.50	0.50	0.00
pga1 < pga < pga2	0.50	0.00	0.50	0.40	0.30	0.30	0.35	0.35	0.30	0.35	0.35	0.30
pga2 < pga	0.20	0.00	0.80	0.07	0.13	0.80	0.10	0.10	0.80	0.10	0.10	0.80

NL1 : main contractor
NL2 : cross check analyses
NL3 : sensitivity studies (geometric mean of 4 sensitivity studies)

$AMP(f > f_3) = AMP(f_3)$

Figure IV-1.25: Logic tree for Mühleberg.

Site-specific Model Evaluations

Alternative Velocity Profiles

Four profiles, P1 to P4, have been defined. Profile P1 was originally proposed by the contractor and is based on a weighting of the different measurements and source of information. The alternative velocity profiles P2 to P4 were developed mainly to fit the dispersion curves from MASW and microtremor measurements. Profiles P2 and P3 differ from velocity gradient in the gravel layer and the presence of a significantly weathered part in the underlying molasse. Profiles P3 with the larger velocities in the gravel seems more realistic and will be given thesame weight as profile P1. The two other profiles exhibit a rather low velocity in the gravel material, which looks to us rather unusual, and consequently will be given a somewhat lower weight.

Alternative Non-linear Properties

The same approach as for the other sites is followed. The range of most probable G/G_{max} curves is based on our experience because no specific measurements are available for this site. In order to account for the large uncertainty that exists the curves shown in Figure IV-1.26 were obtained with $\alpha = \beta = 0.6$. Therefore the weight of the best estimate curve is equal to 0.46 and the weights of the two bound curves are the same and equal to 0.27.

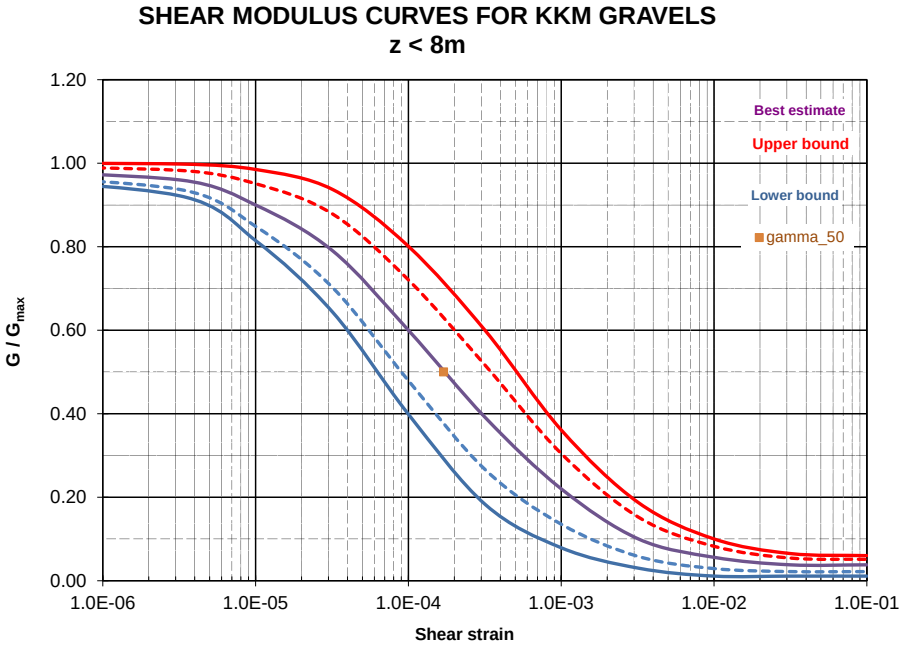

Figure IV-1.26: Definition of the range of most probable curves (dotted lines).

Threshold Strains

Figure IV-1.27 presents the normalized shear stress versus normalized shear strain for the gravel layers. For the computations of the vertical effective stress, the water table is at 4m depth; the strength properties are c=20kPa and $\phi = 37.5°$ and the at rest earth pressure coefficient $K_0 = 0.7$.

Comparison of the non-linear curves established for the calibration of the constitutive model with those provided in the specification (Figure IV-1.28) shows that, combined with the results shown in Figure IV-1.26, γ/γ_{50} is in the range 11 to 12. In terms of PGA, following the approach presented in paragraph 1.2.4, the threshold values are equal to 0.10g and 0.40g.

Frequency Ranges

The same approach as for the other sites is followed from which it results that $f_{0min} = 3.5Hz$ and $f_{0max} = 8Hz$. The frequency range $[f_1, f_2]$ spans from half the minimum value to twice the maximum one. The maximum frequency f_3 is taken equal to 30Hz.

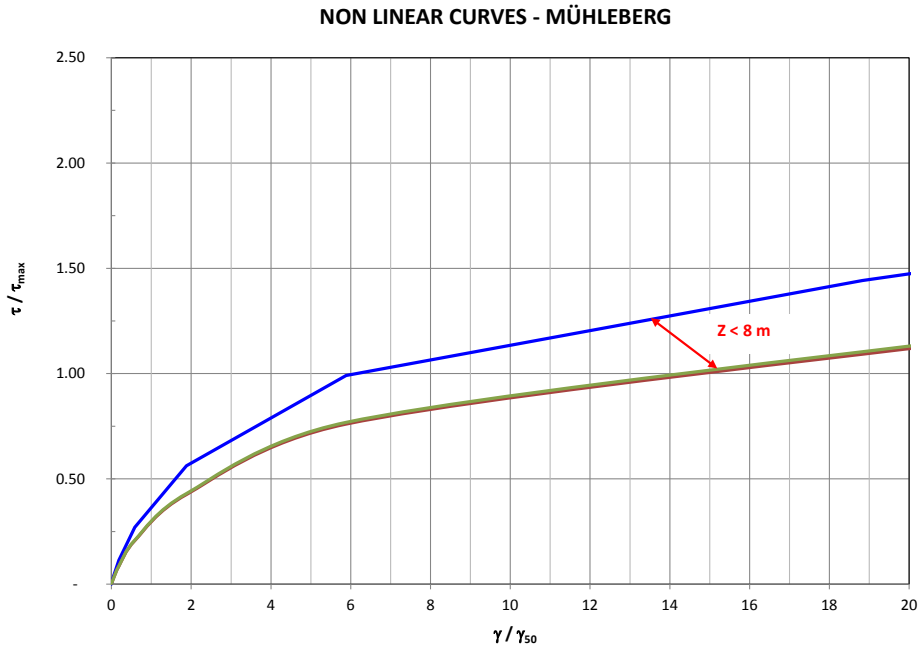

Figure IV-1.27: Normalized shear stress vs normalized shear strain.

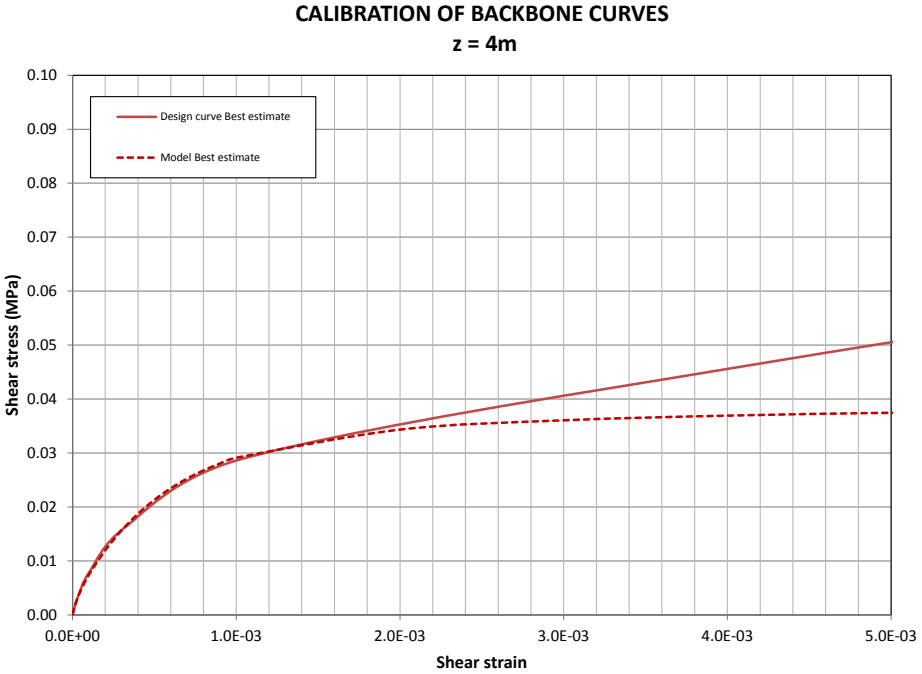

Figure IV-1.28: Non-linear curves from EQL (solid line) and NL (dotted line) calculations.

Final Weights

The final weights for the branches of the logic tree are provided in Figure IV-1.25 below the logic tree.

1.3 Median Amplification of Vertical Ground Motion

1.3.1 Approach

The logic tree for the vertical motions considers alternatives based on the no amplification choice, amplifications computed from SHAKE and RVT_{bc} runs and empirical models based on the H/V ratio.

1.3.2 Logic Tree Structure

For the mean amplification of the vertical ground motion the rationale for assigning the weights is based on the physics of the phenomenon. In saturated soils the P waves travel through the water; the bulk modulus of the soil skeleton may be slightly affected by the induced shear strain but the overall bulk modulus, which is the sum of the soil skeleton bulk modulus and of the water bulk modulus, will be almost unaffected; furthermore, the P-wave velocity is large and consequently the natural frequency of the soil column is high. In a dry soil, the propagation of P waves is controlled by the skeleton properties:

$$\rho V_p^2 = K + \frac{4}{3}G \tag{IV-1.14}$$

Those properties are influenced by the shear strain but the bulk modulus K to a lesser extent than the shear modulus G. This P-wave velocity is smaller than in a saturated layer and consequently the natural frequency of vibration of the soil column is smaller.

Therefore, amplifications will depend on the natural frequency of the soil column and will be much less dependent on the pga input amplitude than for the horizontal motion (governed by the S-wave velocity); below that frequency almost no amplification of P-waves will take place and a no amplification branch is introduced in the logic tree. Nevertheless, it is recognized that vertical motion is not induced only by vertical propagation of P-waves, but also by P-SV waves; this is reflected in the logic tree by introduction of a branch based on experimental V/H ratios, which inherently contain the contributions of all wave types. The third branch in the logic tree is based on numerical 1-D amplifications obtained with equivalent linear calculations.

Above the natural frequency defined above, amplification can be calculated either from the EQL or RVT_{bc} runs, or from statistical correlations of the V/H ratios. Amongst the statistical correlations that were made available to us, only one depends on the level of input motion [Gülerce and Abrahamson 2011]. All other correlations, aside from the NUREG correlation that is not considered in our evaluation, (i.e. Bommer et al. [2011], Campbell and Bozorgnia [2003], Edwards et al. [2011b]), do not exhibit such dependence. According to the previous statements regarding the relative dependence of the S and P-wave velocities on the induced strain, it would seem that an increase in the input motion will be reflected by an almost

similar increase in the vertical amplification, while the increase in the horizontal motion will be smaller due to the soil non-linearities; consequently the V/H ratio should depend on the amplitude of the input motion. Accordingly, more weight is attributed to the Gülerce and Abrahamson [2011] correlation than to others.

1.3.3 Model Evaluations Common to All Sites

For all sites the logic tree (see generic logic tree in Figure IV-1.29) starts with two branches related to the natural frequency of the soil column. The frequency threshold is not exactly the fundamental frequency of the profile but some fraction (approximately one half) of it since below that frequency almost no amplification will be assumed. The natural frequency is read off the amplification functions calculated in the RVT base case and SHAKE analyses, for all material models and amplitudes of the input motion (0.1g, 0.4g and 0.75g); in fact, it turns out that the frequency is only slightly dependent on the input motion amplitude, confirming that the vertical motion is not really affected by the non-linearities. The branches that are conditional on PGAs are introduced to discriminate between the weights attributed to the V/H branches: document TFI-TN-1235 clearly shows that amplification estimated from the V/H ratios and the non-linear amplifications are not fully consistent with calculations at least for high PGAs. From the results presented in this document a typical value for the PGA threshold is 0.1-0.2g. As explained before V/H branches have been introduced because they contain information on the amplification arising from wave fields (P-SV) that are not considered in the calculations and are therefore maintained albeit this limitation; however, based on the previous comment very low weight has been assigned to V/H branches for large PGAs and, as a matter of fact, zero weight has been assigned to V/H correlations that do not account for non-linear effects (all correlations but Gülerce-Abrahamson one).

After these two branches, three branches are introduced depending on the calculation method of the amplification:

- a no amplification branch for which the weight depends on the stiffness of the soil profile and it capability to develop a non-linear behavior. For stiffer sites, a higher weight will be attributed to that branch. In addition more weight is attributed to the no amplification branch for frequencies below the natural frequency of the soil column;
- one branch, with two sub-branches for which amplification is computed either from the EQL or from the RVT_{bc} calculations; for frequencies smaller than f_1 each of the sub-branch is given the same relative weight than for the horizontal motion although in the very low frequency range RVT is not deemed fully reliable; however, a small weight being given to the calculations for low frequencies, the impact on the results will be negligible; for frequencies larger than f_1, and for the same reasons as for the horizontal motion, equal weight is given to the RVT and SHAKE calculations. Unlike for the horizontal motion, it is not deemed necessary to introduce another frequency band to discriminate between RVT and SHAKE runs because, for vertical motions, there is no fundamental difference between both methods since no iterations are performed on the soil properties and the frequency is larger than f_2 defined for horizontal motions;
- a branch for the V/H ratios, with two sub-branches: one for the Gülerce and Abrahamson [2011] correlation with the highest weight between both, and one that corresponds to the

geometric mean of all other correlations. As explained for large PGAs those branches are assigned a low weight for Gülerce-Abrahamson correlation and zero weight for the others.

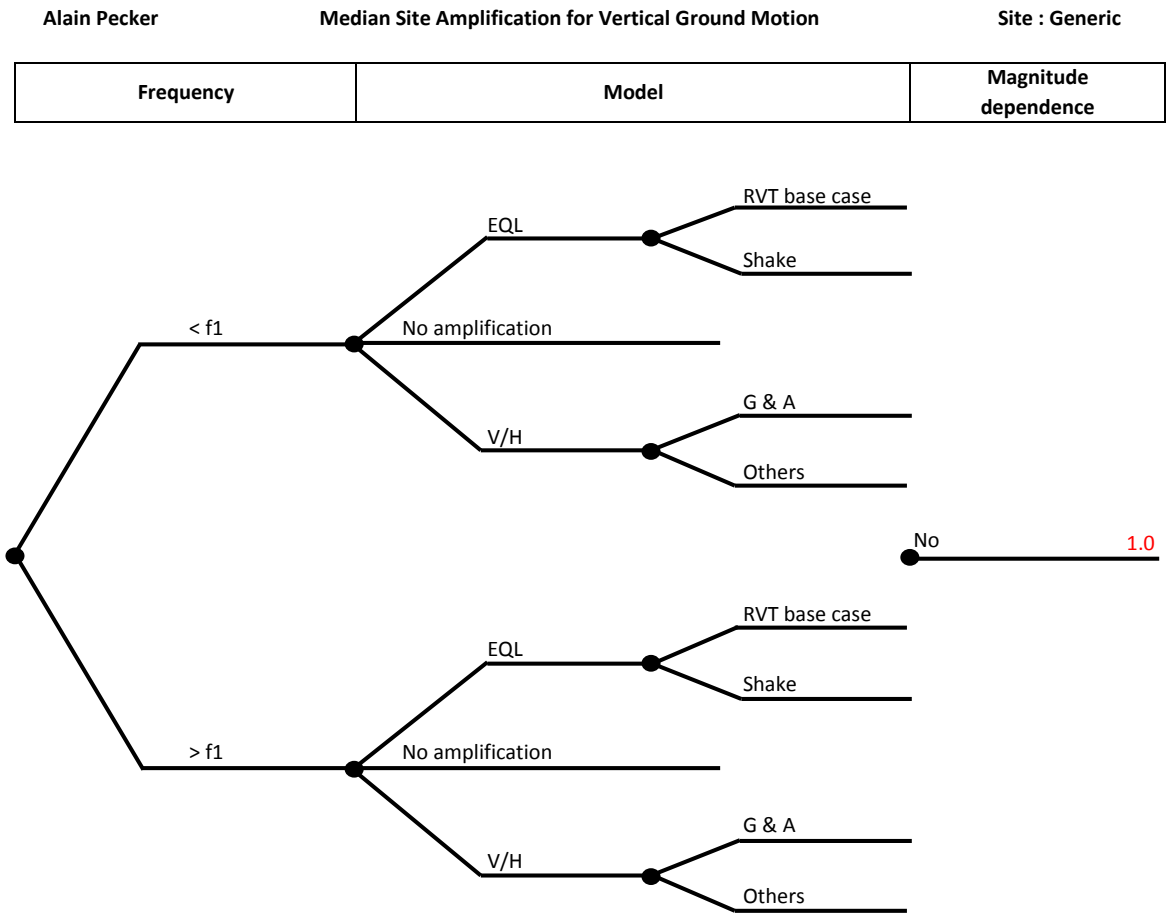

Figure IV-1.29: Generic logic tree for median vertical motion.

As for the horizontal motion, no magnitude dependence is considered in the logic tree. Unlike for the horizontal motion, there is no conditional branch based on the PGA amplitude because, as explained above, the soil properties are weakly dependent on this amplitude; consequently the weights in the logic tree do not depend on PGA. The amplification function based on site response analyses (RVT or SHAKE) shall be computed, for a given PGA input, as the arithmetic mean of the amplifications for the three materials.

For the V/H ratios, in order to be consistent with the previous approach used for results based on numerical calculations, the amplifications should be computed as the arithmetic mean of amplifications for magnitudes 5, 6 and 7 and the relevant distances (retrieved from deaggregation of the seismic hazard). For a given site, the average shear wave velocity, V_{S30}, is computed as the arithmetic mean over all profiles.

1.3.4 Interpolation for Missing Runs

Interpolation on the amplification functions may be needed because all PGA levels have not been run. Interpolation (extrapolation) schemes are defined as follows:

Within one set of calculations (e.g. EQL or RVT runs) and the mean of the three material types, interpolation on the amplification function is carried out for each frequency using a piecewise linear interpolation, with Log(PGA) as the independent variable. If extrapolation beyond the latest calculated PGA is needed (beyond 0.75g), the amplification function calculated for 0.75g is kept unchanged for higher *pgas*. The same applies to *pgas* smaller than 0.1g: no extrapolation is performed below 0.1g and the amplification is the one calculated at 0.1g

1.3.5 Beznau

Logic Tree for Beznau

The Logic Tree with median site amplification for the vertical motions for Beznau is shown in Figure IV-1.30.

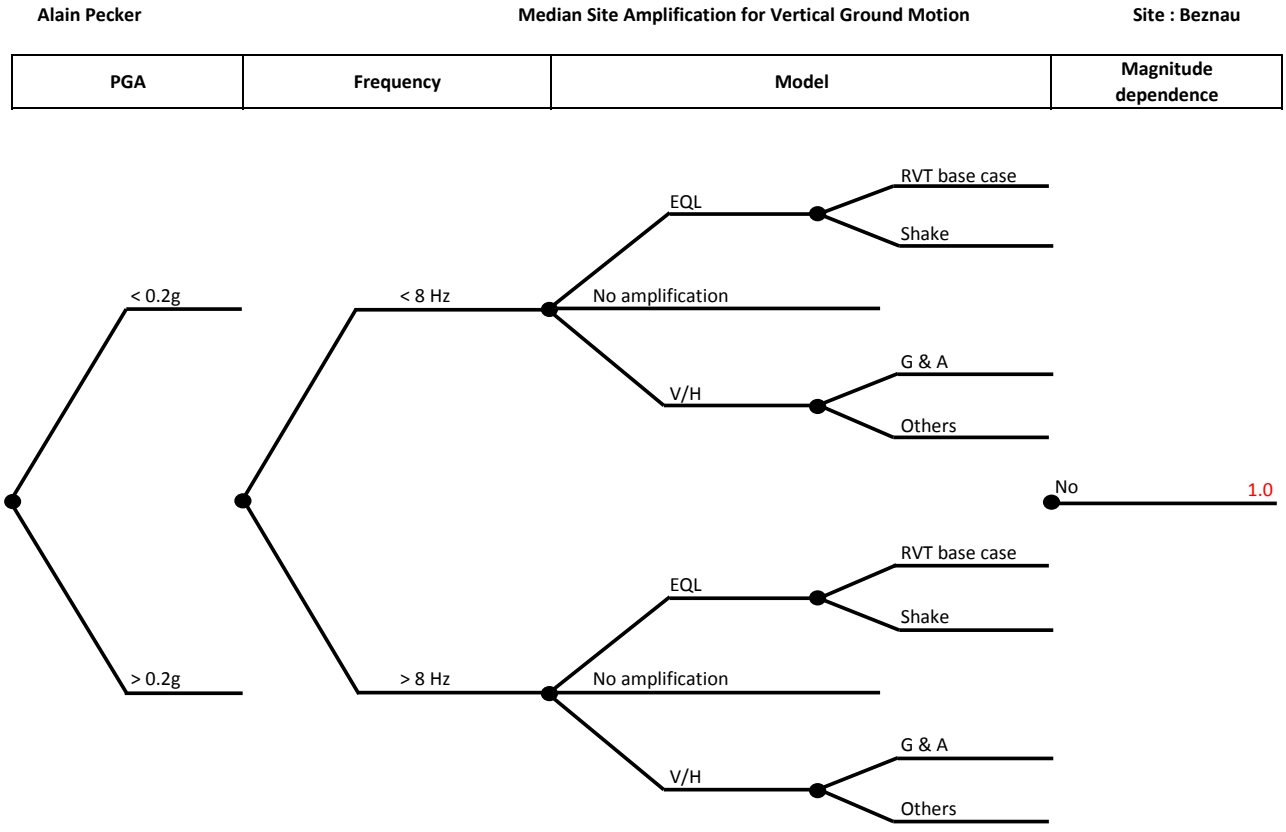

	f < f1					f1 < f				
	EQL		No amp	V/H		EQL		No amp	V/H	
	Shake	RVT		G & A	Others	Shake	RVT		G & A	Others
pga < pga1	0.2	0.1	0.2	0.4	0.1	0.25	0.25	0	0.4	0.1
pga1 < pga	0.4	0.3	0.2	0.1	0	0.45	0.45	0	0.1	0

Figure IV-1.30: Logic Tree for median site amplification for vertical ground motion - Beznau.

Site-specific Model Evaluations

The water table at Beznau is at 6.0 m below the ground surface. Because the site should develop significant non-linearities under horizontal excitation, the weight attributed to the no amplification assumption is limited. FigureIV-1.31 presents the variation of the vertical amplification for all available runs (SHAKE, RVT_{bc} , pga =0.1, 0.4 and 0.75g and all three materials). Examination of the figure shows that the natural frequency of the soil column is in the range 15 to 40Hz; therefore the frequency threshold f_1 is set equal to 8Hz.

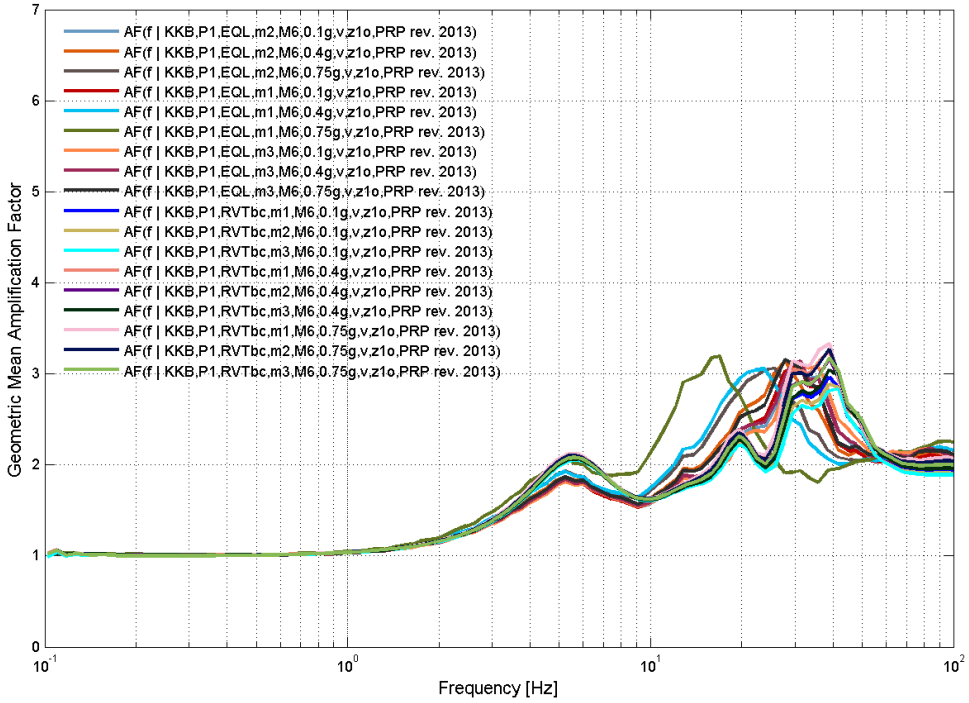

Figure IV-1.31: Vertical amplification from calculations - Beznau.

1.3.6 E-Beznau

Logic Tree for E-Beznau

The Logic Tree with median site amplification for the vertical motions for E-Beznau is shown in Figure IV-1.32.

Site-specific Model Evaluations

The water table at E-Beznau is at 6.0 m below the ground surface. Like for Beznau the site should develop significant non-linearities under horizontal excitation, the weight attributed to the no amplification assumption is limited. Figure IV-1.33 presents the variation of the vertical amplification for all available runs (SHAKE, RVT_{bc} , pga =0.1, 0.4 and 0.75g and all three materials). Examination of the figure shows that the natural frequency of the soil column is in the range 20 to 40Hz; therefore the frequency threshold f_1 is set equal to 10Hz.

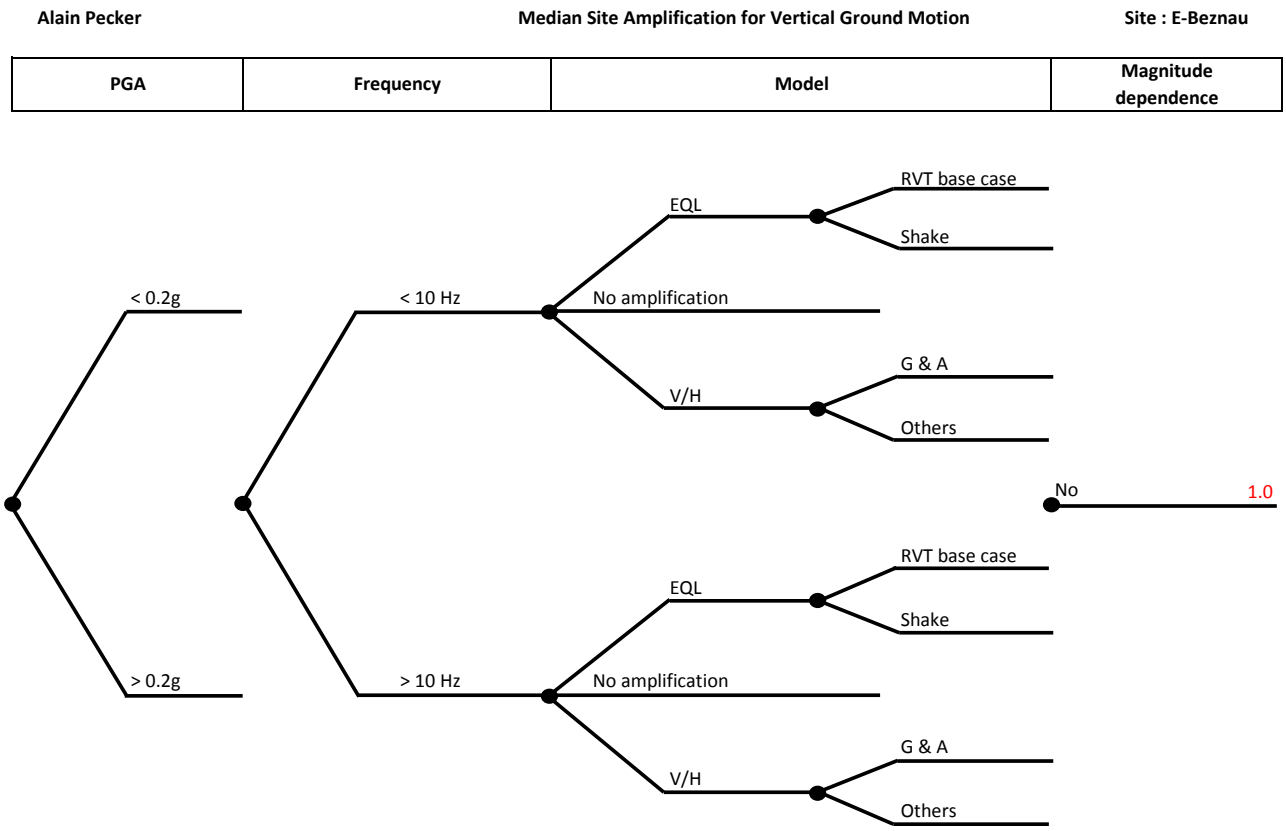

	f < f1					f1 < f				
	EQL		No amp	V/H		EQL		No amp	V/H	
	Shake	RVT		G & A	Others	Shake	RVT		G & A	Others
pga < pga1	0.2	0.1	0.2	0.4	0.1	0.25	0.25	0	0.4	0.1
pga1 < pga	0.4	0.3	0.2	0.1	0	0.45	0.45	0	0.1	0

Figure IV-1.32: Logic Tree for median site amplification for vertical ground motion - E-Beznau.

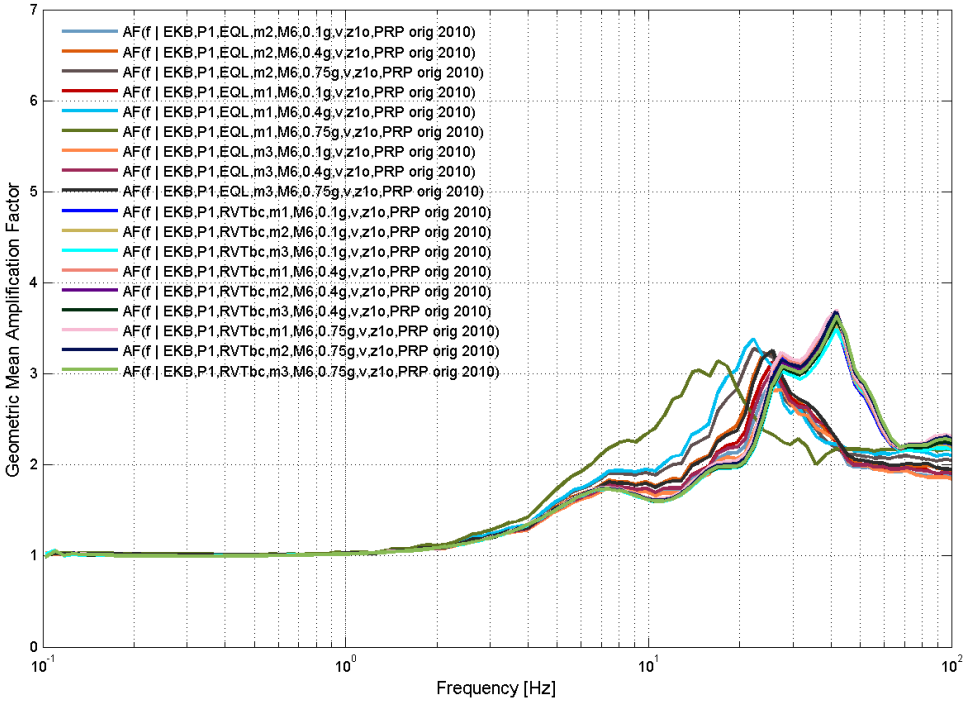

Figure IV-1.33: Vertical amplification from calculations - E-Beznau.

1.3.7 Gösgen

Logic Tree for Gösgen

Figure IV-1.34 shows the Logic Tree with median site amplification for vertical motions for Gösgen.

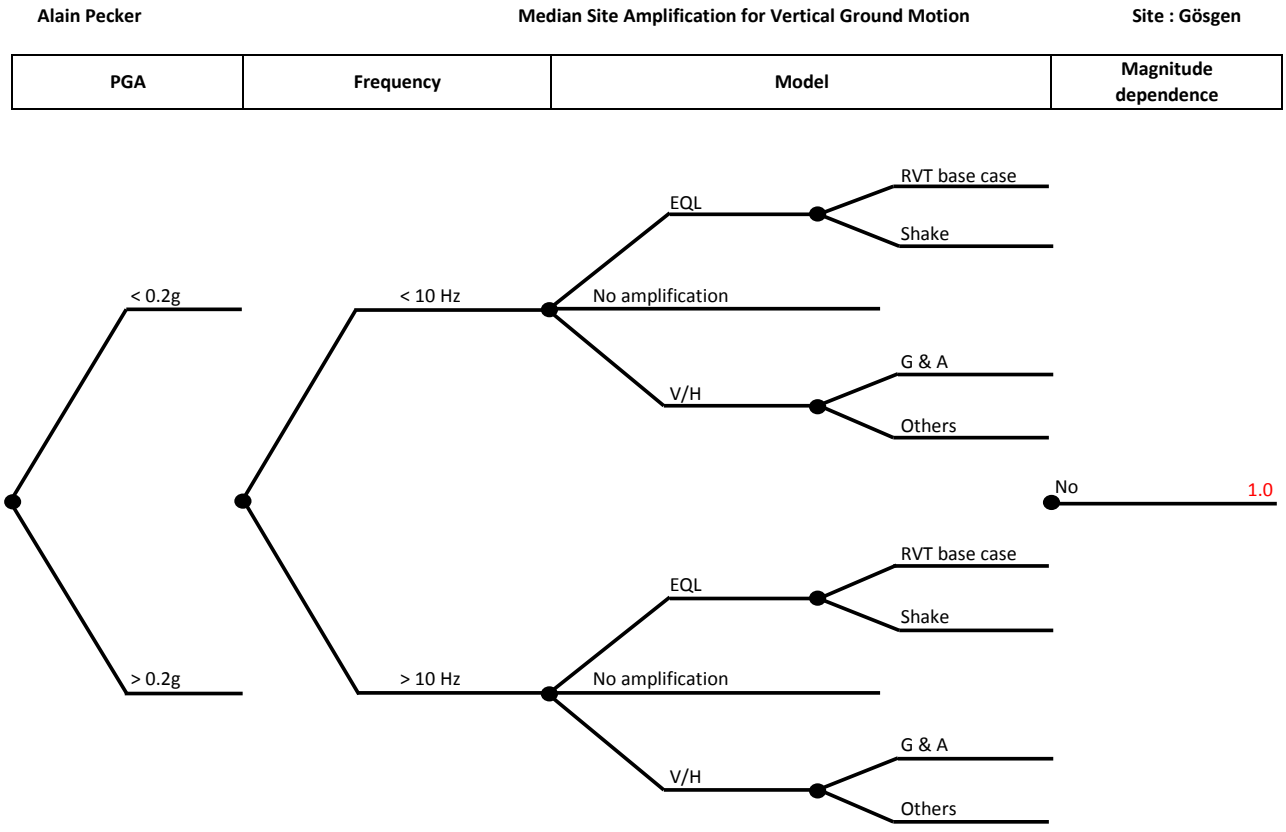

	f < f1					f1 < f				
	EQL		No amp	V/H		EQL		No amp	V/H	
	Shake	RVT		G & A	Others	Shake	RVT		G & A	Others
pga < pga1	0.15	0.05	0.3	0.4	0.1	0.25	0.25	0	0.4	0.1
pga1 < pga	0.35	0.25	0.3	0.1	0	0.45	0.45	0	0.1	0

Figure IV-1.34: Logic Tree for median site amplification for vertical ground motion - Gösgen.

Site-specific Model Evaluations

The site is very similar to E-Beznau with a water table depth of 6.5m. However, due to the high impedance contrast at the soil-rock interface, the amplification is less spread between frequencies. Therefore, for frequencies smaller than f_1 less amplification is expected and the no-amplification branch is given more weight. Figure IV-1.35 presents the variation of the vertical amplification for all available runs (SHAKE, RVT_{bc} , pga =0.1, 0.4 and 0.75g and all three materials). Examination of the figure shows that the natural frequency of the soil column is in the range 20 to 40Hz; therefore the frequency threshold f_1 is set equal to 10Hz.

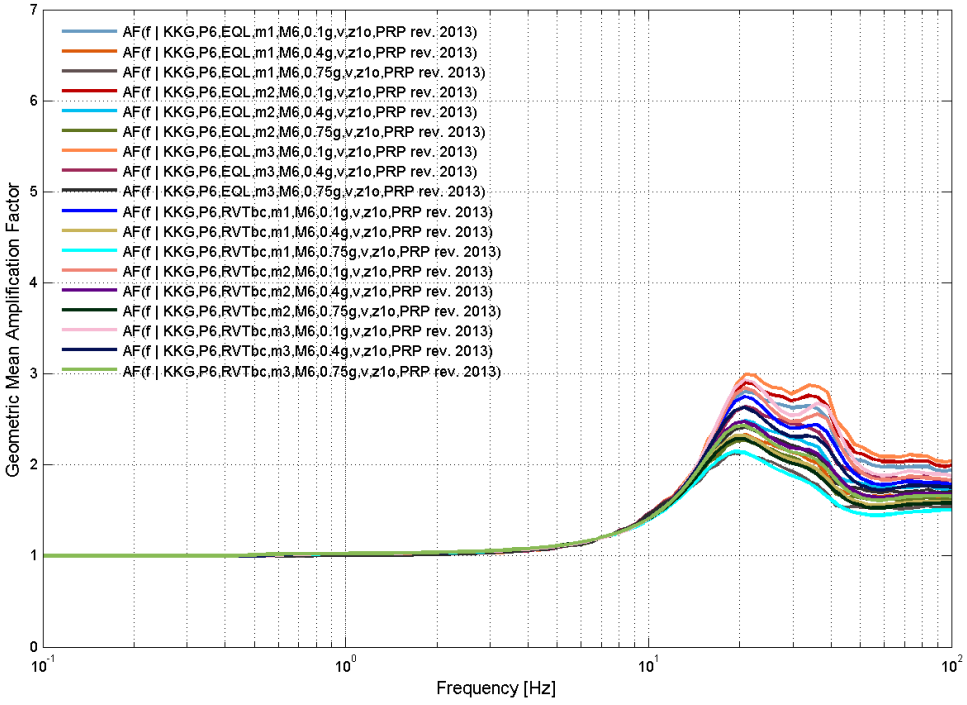

Figure IV-1.35: Vertical amplification from calculations - Gösgen.

1.3.8 Leibstadt

Logic Tree for Leibstadt

Figure IV-1.36 shows the Logic Tree with median site amplification for vertical ground motion for Leibstadt.

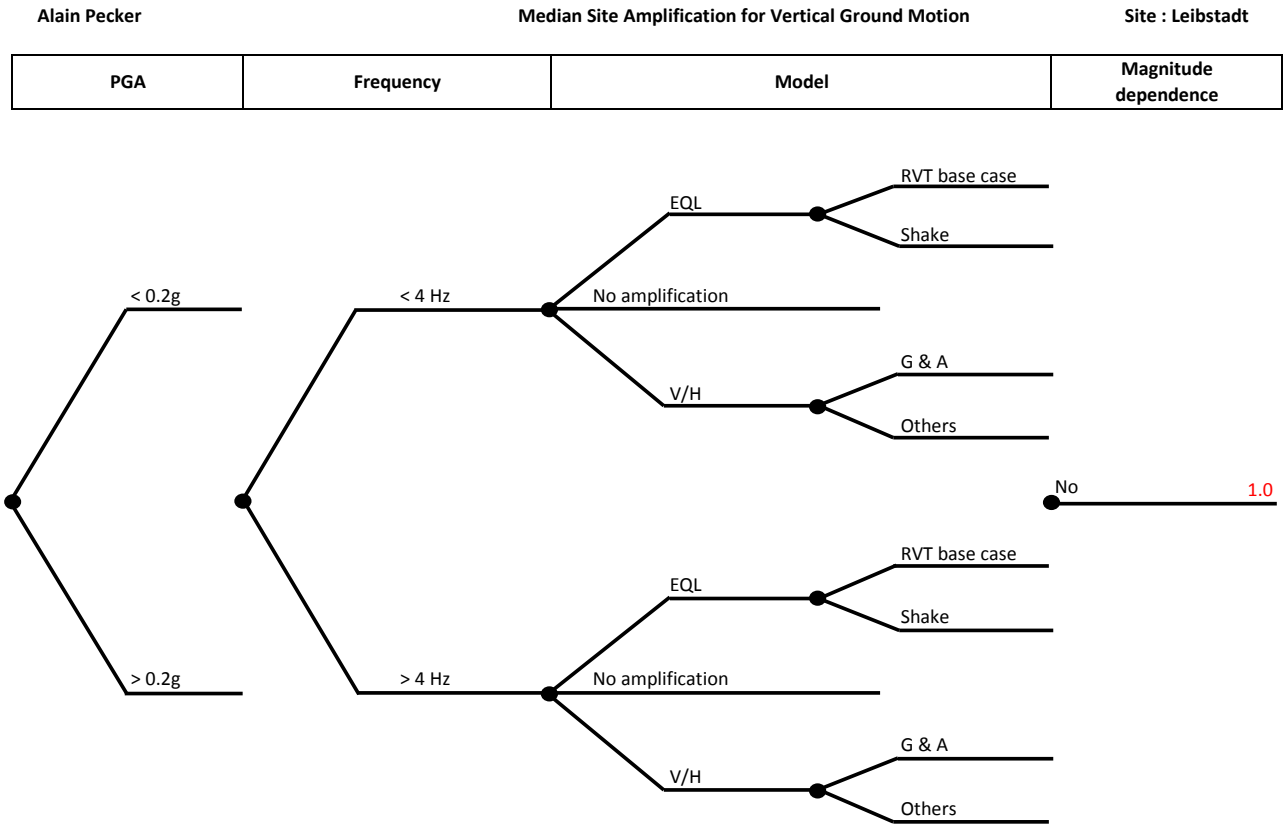

	f < f1					f1 < f				
	EQL		No amp	V/H		EQL		No amp	V/H	
	Shake	RVT		G & A	Others	Shake	RVT		G & A	Others
pga < pga1	0.25	0.15	0.1	0.4	0.1	0.25	0.25	0	0.4	0.1
pga1 < pga	0.5	0.3	0.1	0.1	0	0.45	0.45	0	0.1	0

Figure IV-1.36: Logic Tree for median site amplification for vertical ground motion - Leibstadt.

Site-specific Model Evaluations

For this site the water table is deep at 25.5 m below the ground surface and natural frequencies of the soil column are therefore smaller. In addition, the soil profile consists of medium dense sand in which strong non-linear behavior is expected. Therefore, the no amplification branch is given a reduced weight with respect to the other sites.

Figure IV-1.37 presents the variation of the vertical amplification for all available runs (SHAKE, RVT_{bc} , pga =0.1, 0.4 and 0.75g and all three materials). Examination of the figure shows that the natural frequency of the soil column is in the range 8 to 15Hz; therefore the frequency threshold f_1 is set equal to 4Hz.

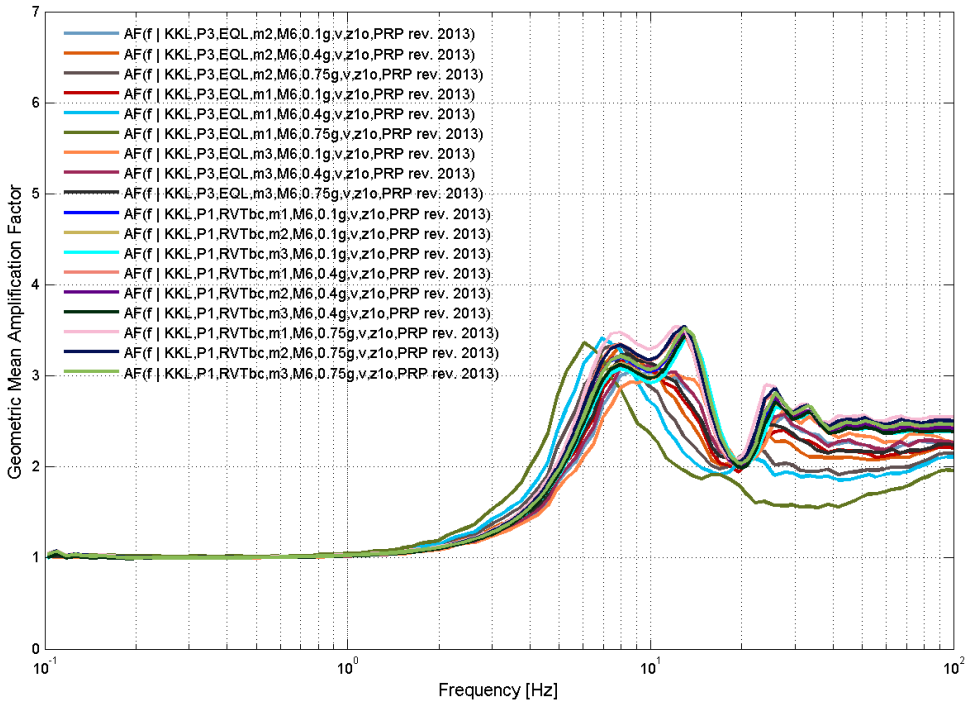

Figure IV-1.37: Vertical amplification from calculations - Leibstadt.

1.3.9 Mühleberg

Logic Tree for Mühleberg

Figure IV-1.38 shows the Logic Tree with median site amplification for vertical ground motion for Mühleberg.

Site-specific Model Evaluations

The Mühleberg site is the stiffer site for which non-linear soil behavior should be limited. Therefore the no amplification branch is given a significant weight, like for Gösgen. Figure IV-1.39 presents the variation of the vertical amplification for all available runs (SHAKE, RVT_{bc} , pga =0.1, 0.4 and 0.75g and all three materials). Examination of the figure shows that the natural frequency of the soil column is around 30Hz; therefore the frequency threshold f_1 is set equal to 15Hz.

1.4 Aleatory Variability of Horizontal Ground Motion

1.4.1 Approach

The aleatory variability is assumed to arise from the variability in the input motions (reflected in the SHAKE, RVT and NL runs), from the variability in the soil profile across the site associated with the random location of the earthquake (reflected in the RVT randomized calculations), from the variability observed in the P-SV runs arising from different incidence angles and from that observed, when available, in the 2D runs and linked to the position of

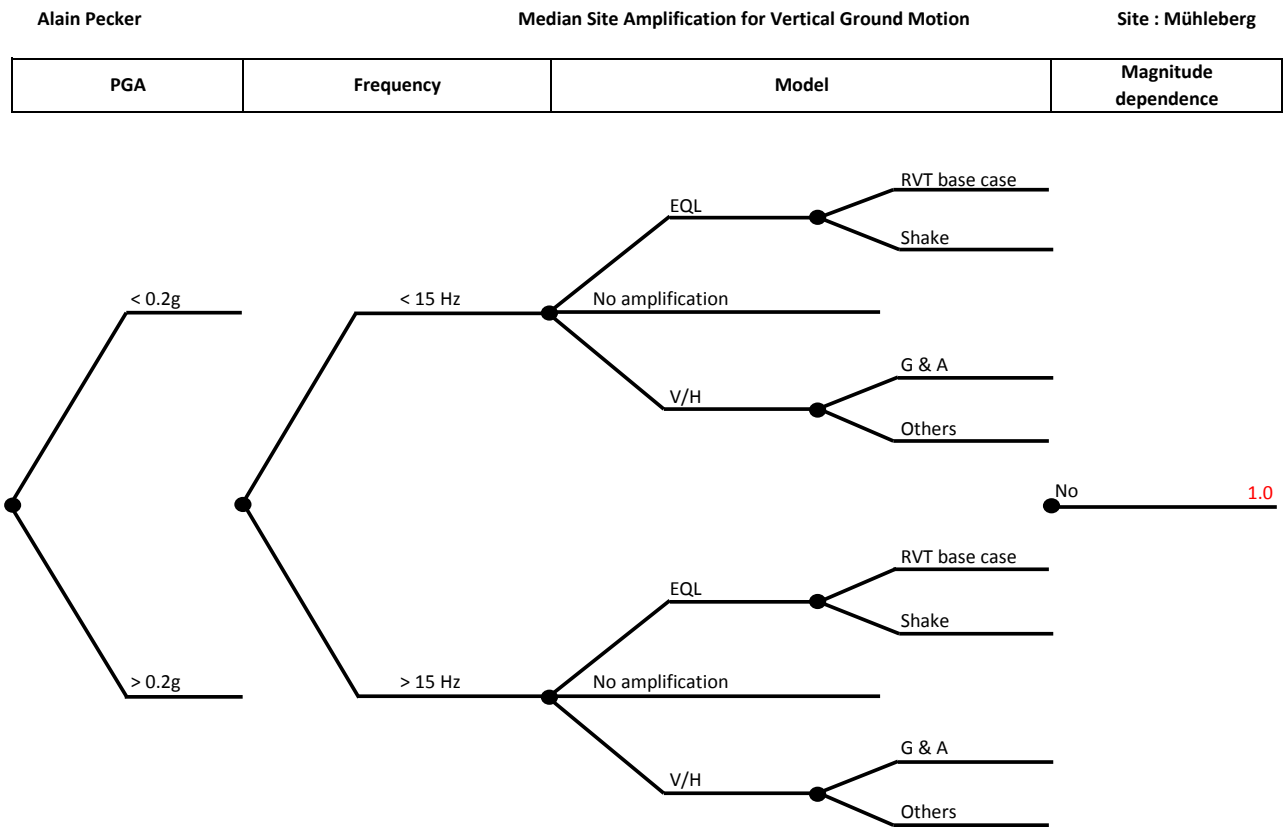

	f < f1					f1 < f				
	EQL		No amp	V/H		EQL		No amp	V/H	
	Shake	RVT		G & A	Others	Shake	RVT		G & A	Others
pga < pga1	0.15	0.05	0.3	0.4	0.1	0.25	0.25	0	0.4	0.1
pga1 < pga	0.35	0.25	0.3	0.1	0	0.45	0.45	0	0.1	0

Figure IV-1.38: Logic Tree with median site amplification for vertical ground motion - Mühleberg.

the receivers. The discussions held during the SP3 workshops and document TP2-TB-1081 [Abrahamson 2012] made clear that all these factors are already accounted for by SP2 at least assuming a linear behavior for the soil medium and an average soil condition. Therefore, in order to avoid double counting, the only component that possibly needs to be considered is the variability associated with the non-linear soil behavior.

1.4.2 Variability due to Non-linear Soil Behavior

It is known that non-linear calculations may be sensitive to small details in the input motions, small changes in the input parameters of the constitutive model, etc... It may therefore be argued that the variability in the ground surface response may be increased with respect to the variability obtained assuming quasi linear behavior due to these factors. If this is the case, the standard deviation of the amplification function obtained in the non-linear runs should be larger than the standard deviation obtained in the EQL runs.

This aspect has been investigated by plotting the standard deviation of the spectral acceler-

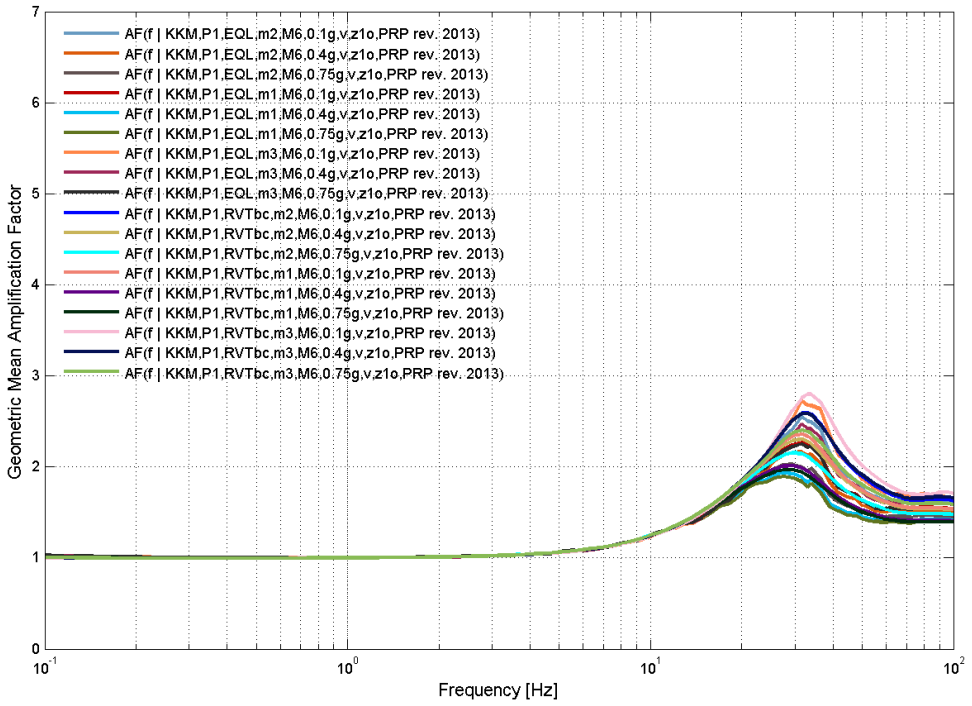

Figure IV-1.39: Vertical amplification from calculations - Mühleberg.

ations at very low PGA levels where linear elastic behavior governs the response and at a high PGA (1.5g) available in non-linear runs. Opposite to what has been done in the report, results are here plotted only for the PRP 2010 analyses, which make use of the same time histories for non-linear and equivalent linear calculations. That procedure allows a one to one comparison between non-linear calculations and equivalent linear calculations without introducing additional differences. The results are shown in Figures IV-1.40, IV-1.41, IV-1.42, IV-1.43 and IV-1.44.

On the one hand, examination of the preceding figures shows that no definite conclusions can be drawn: sometimes the EQL calculations exhibit more variability than the NL ones (Beznau), sometimes the standard deviation is of the same order in both sets (KKG), and finally sometimes the standard deviation of the NL runs is larger, in a restricted frequency band centered around the fundamental frequency of the site, than in the EQL runs (KKM). We did not find any clear reason to explain the differences in behavior among the five sites. On the other hand, physical reasons should indicate that the variability would decrease for high input motions, for which the soil behaves more non-linear; this is because the response is more and more controlled by strength properties that are less subject to epistemic uncertainty than the moduli.

As a consequence, since non-linear runs (except for KKM in a restricted frequency band) and physical reasons indicate that variability should be less or equal to the variability obtained in linear runs, our logic tree does not include any aleatory variability. The aleatory variability for vertical ground motion should be added at the end of our logic tree and taken equal to the rock aleatory variability provided by SP2.

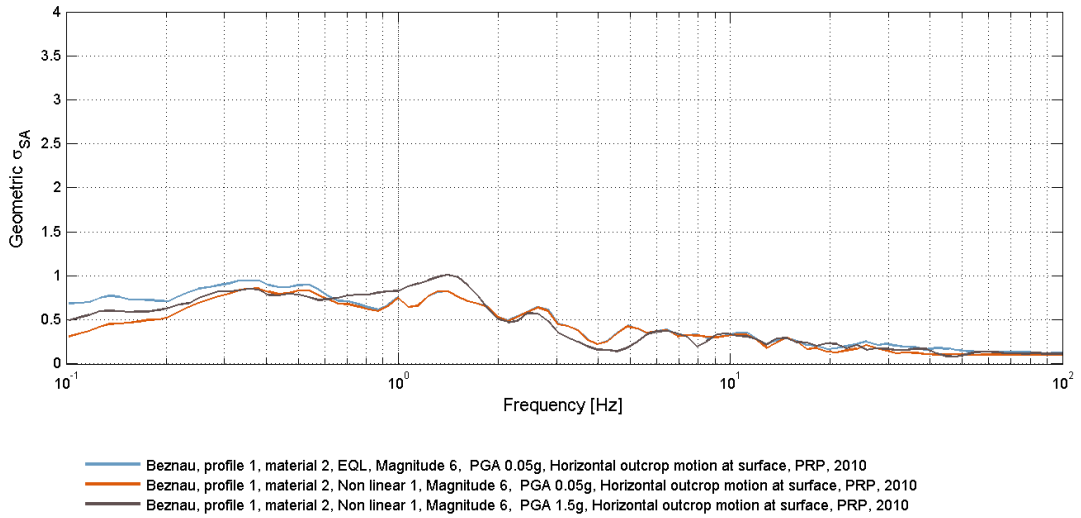

Figure IV-1.40: Beznau - Comparison of standard deviation in EQL (0.05g) and NL runs (1.5g).

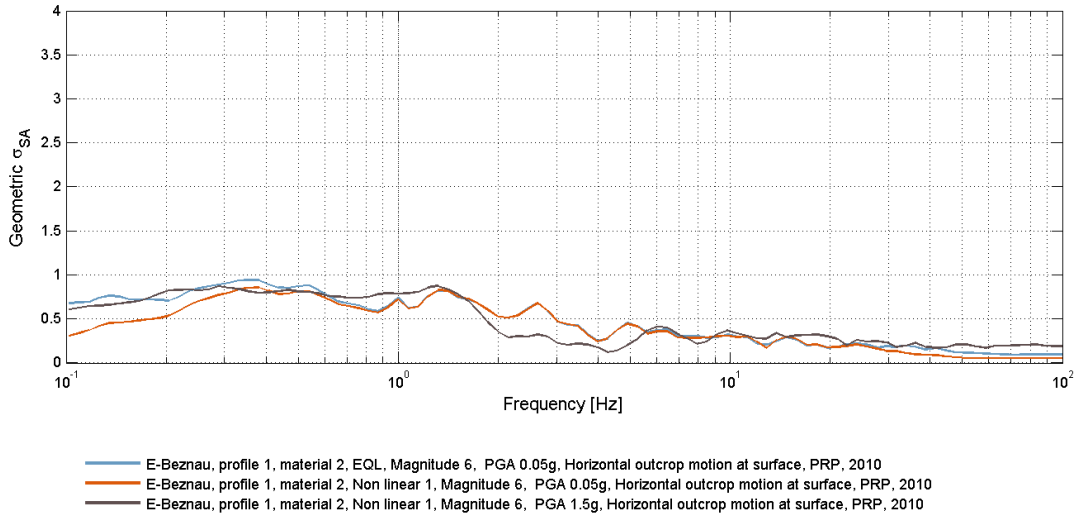

Figure IV-1.41: E-Beznau - Comparison of standard deviation in EQL (0.05g) and NL runs (1.5g).

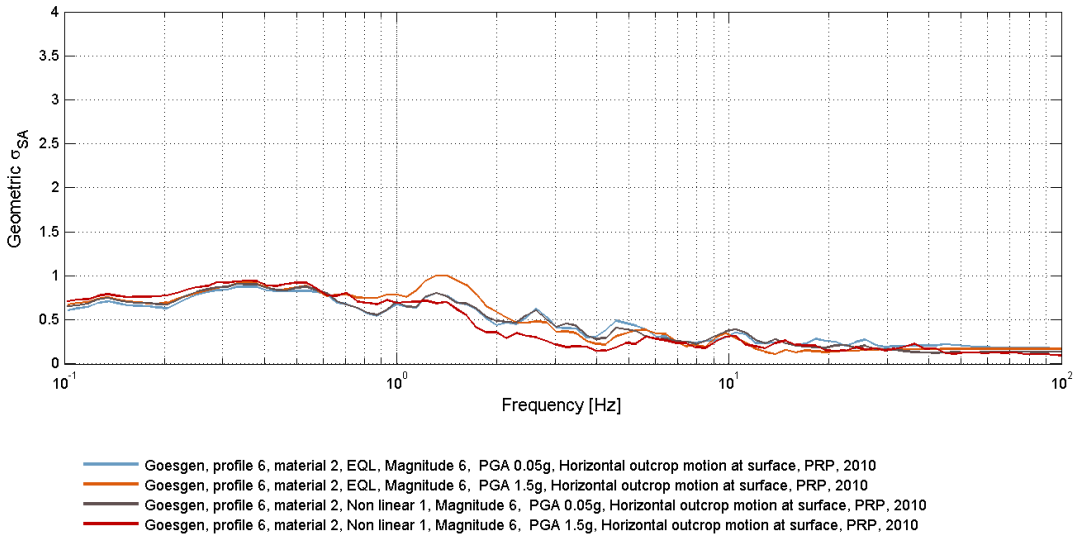

Figure IV-1.42: Gösgen - Comparison of standard deviation in EQL (0.05g) and NL runs (1.5g).

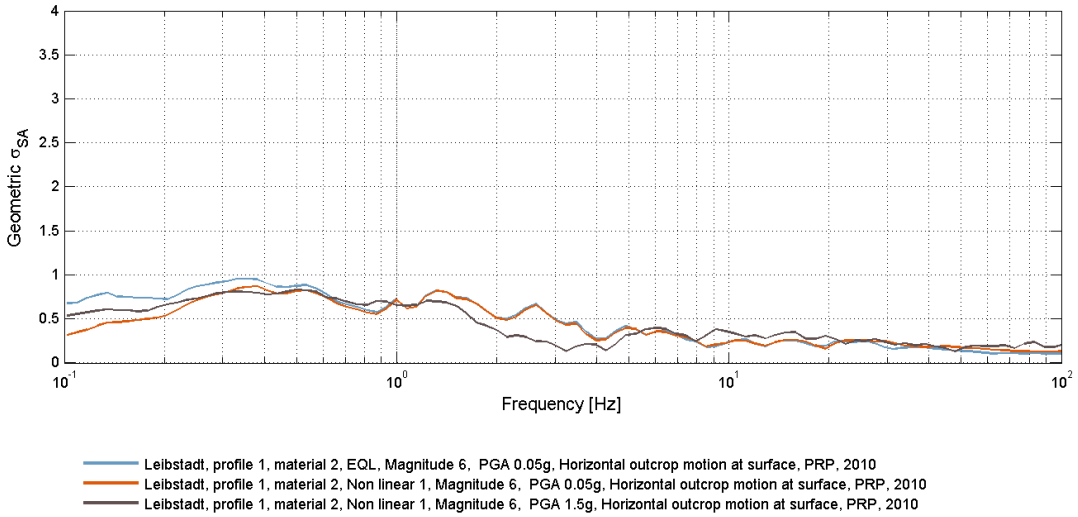

Figure IV-1.43: Leibstadt - Comparison of standard deviation in EQL (0.05g) and NL runs (1.5g).

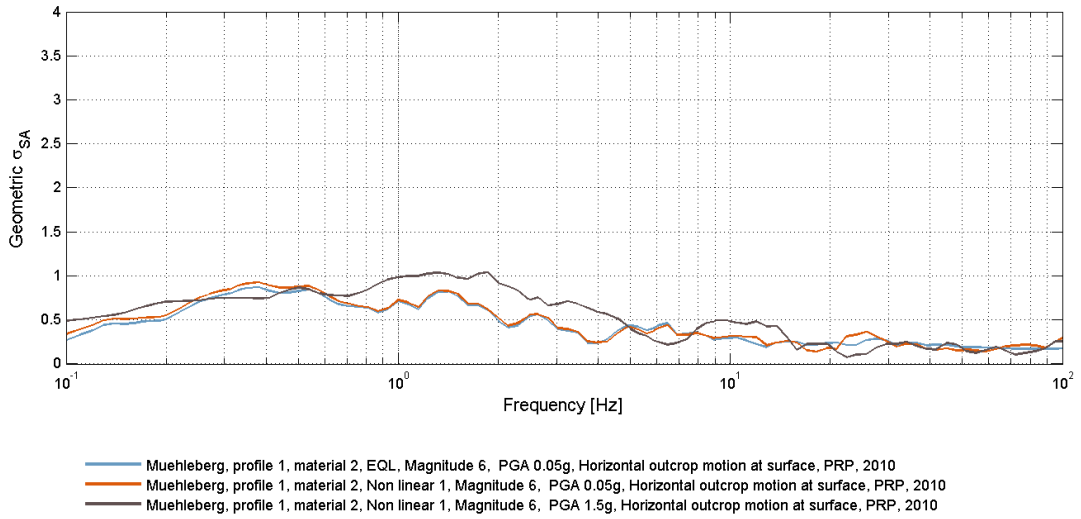

Figure IV-1.44: Mühleberg Comparison of standard deviation in EQL (0.05g) and NL runs (1.5g).

1.5 Aleatory Variability of Vertical Ground Motion

The same approach as for the aleatory variability related to the horizontal motion is followed. The aleatory variability is assumed to arise from the variability in the input motions (reflected in the SHAKE, RVT runs), from the variability in the soil profile across the site associated with the random location of the earthquake, from the variability observed in the P-SV runs arising from different incidence angles. As detailed for the horizontal motion, all these factors are already accounted for by SP2. The only component that possibly needs to be considered is the variability associated with the non-linear soil behavior; however, the impact of non-linearity is small on the vertical response of the soil column because most sites are under water and therefore the P-wave velocity is more controlled by the velocity in water than by the soil characteristics; in addition, P-wave velocity in water is not a significant variable parameter, except may be when full saturation of the soil is not achieved. The only site for which the previous statement may not be totally true is Leibstadt with a deep water table. However it has been pointed out that the aleatory variability in the horizontal non-linear runs was smaller than in the elastic runs, especially for that specific site (see Figure IV-1.43). As a consequence, physical reasons indicating that variability should be less than the variability observed in horizontal motions, which is already either accounted for by SP2, our logic tree does not include any aleatory variability. Therefore the aleatory variability for vertical ground motion should be added at the end of our logic tree and taken equal to the rock aleatory variability provided by SP2.

1.6 Maximum Ground Motions

1.6.1 Horizontal Component

There does not exist a well-established method to estimate the maximum ground motion that a soil profile can transmit to the ground surface. However, it is recognized and well admitted that the soil cannot transmit arbitrarily large motion due to its limited shear resistance capacity. This maximum motion can be estimated from numerical analyses as those carried out for the five NPP sites with increasing input motions, from theoretical models based on an assumed soil constitutive behavior and from experimental evidences gathered during actual earthquakes. All these approaches are taken into account in the foregoing evaluation.

Maximum Peak Ground Acceleration

Evaluation of the maximum peak acceleration at the ground surface has been performed in GDS, 2011. All three methods listed above have been used and compared together. The results have been summarized in table 5 from this report, which is reproduced as Table IV-1.1 below.

Table IV-1.1: Summary of maximum ground surface accelerations (m/s^2).

	KKG	KKB	EKKB	KKL	KKM
Pecker's model	2	2.5	2.2	1.8	2.1
Betbeder's model	1.4	2	1.5	1.5	1.5
Non-linear site response analyses	2.5 - 3.0	2.3 - 3.0	2.1 - 2.7	2.2 - 2.8	2.1 - 2.7
Proposed range of values	2.5 – 3.0	2.5 – 3.0	2.2 – 2.7	2.3 – 2.8	2.1 – 2.6

Two theoretical models are available for the evaluation of the maximum PGA; the first one [Pecker 2011] has been developed specifically for this study and the second one [Betbeder-Matibet 1993] is published in the literature. The applications of both models to the five NPP sites are given in Table IV-1.1.

Non-linear analyses have been carried out with the upper bound soil properties up to 2.5g input PGA at the rock outcrop. Extrapolation of the curves giving the ground surface acceleration as a function of the input (rock outcrop) acceleration yields to the maximum values listed in Table IV-1.1. Apart from Leibstadt, the calculated values are in very good agreement with the numerical analyses. The poorer agreement for Leibstadt has been explained in the aforementioned report; the presence of a cemented layer towards the base of the soil column is not easily handled by the theoretical model.

The observed motions during actual earthquakes have been reviewed with the plotting tool developed for PRP and accompanying the report "Determination of empirical maximum ground motions for PEGASOS Refinement Project" prepared by Strasser and Zulu [2010] (report 2010-0177). We focused on the NEHRP soil class C ($366m/s < V_{s30} < 762m/s$) which reflects the soil category of the five NPP's. The results are presented in Figure IV-1.45 ,

Examination of Figures IV-1.45 shows that the maximum recorded acceleration does not exceed 2-2.5g. However it must be kept in mind that the data represents the maximum

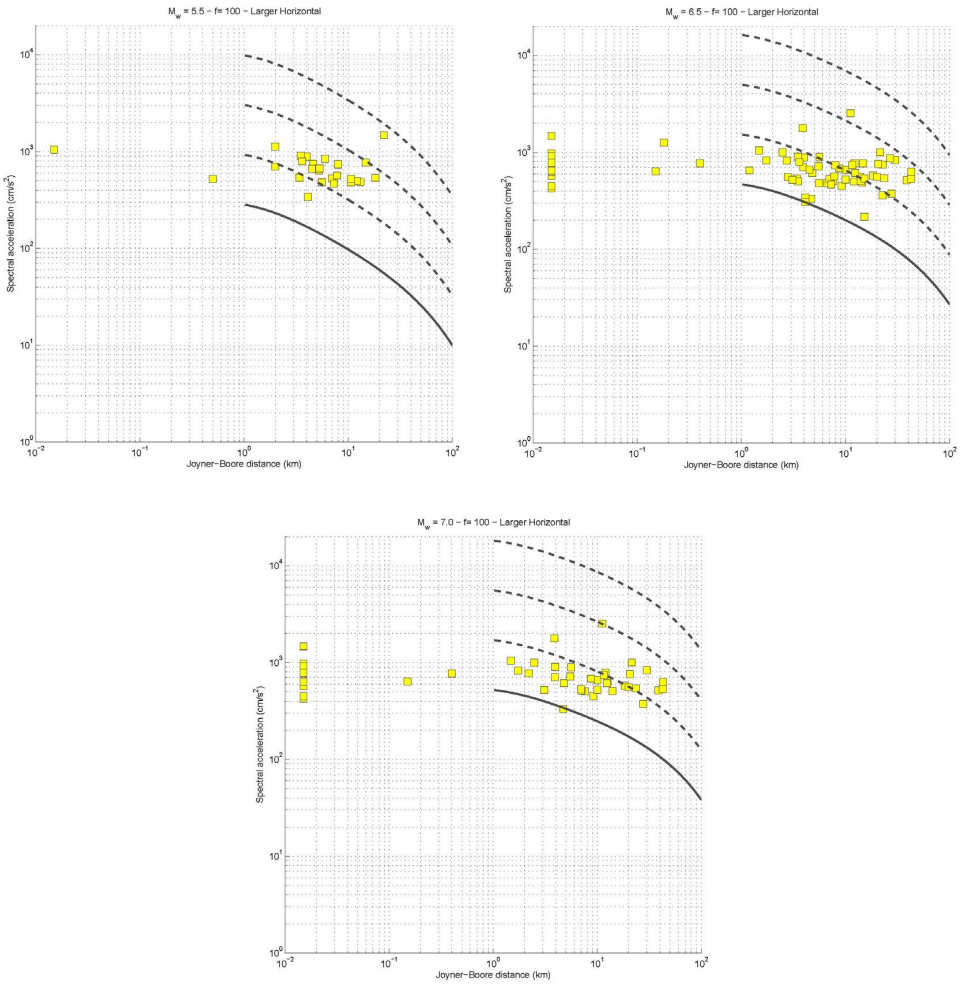

Figure IV-1.45: Maximum recorded ground surface acceleration for NEHRP class C soil.

recorded motion on a given site but not necessarily the maximum ground motion that the site can sustain. It can, however, be noted that the results are not in contradiction with those obtained by the other approaches. Furthermore, the results do not exhibit any magnitude dependence.

Response Spectra

The spectral shapes, which are site dependent, are originally based on the median response spectrum at the ground surface calculated in the non-linear runs with the upper bound properties and an input rock outcrop of 2.5g. One such example of these response spectra is shown in Figure IV-1.46. The simplified spectrum is initially defined to envelop the geometric mean (red curve) with few linear segments. In addition, it was checked that runs with smaller PGA on rock do not induce larger spectral accelerations in some frequency ranges. When that situation occurs, the spectral shape for the maximum ground motion takes those runs into consideration to define an envelope. For illustration purpose, Figure IV-1.47 presents, for EKKB, the spectral shapes for all runs in the database (except the RVT randomized runs) and the spectral shape finally chosen.

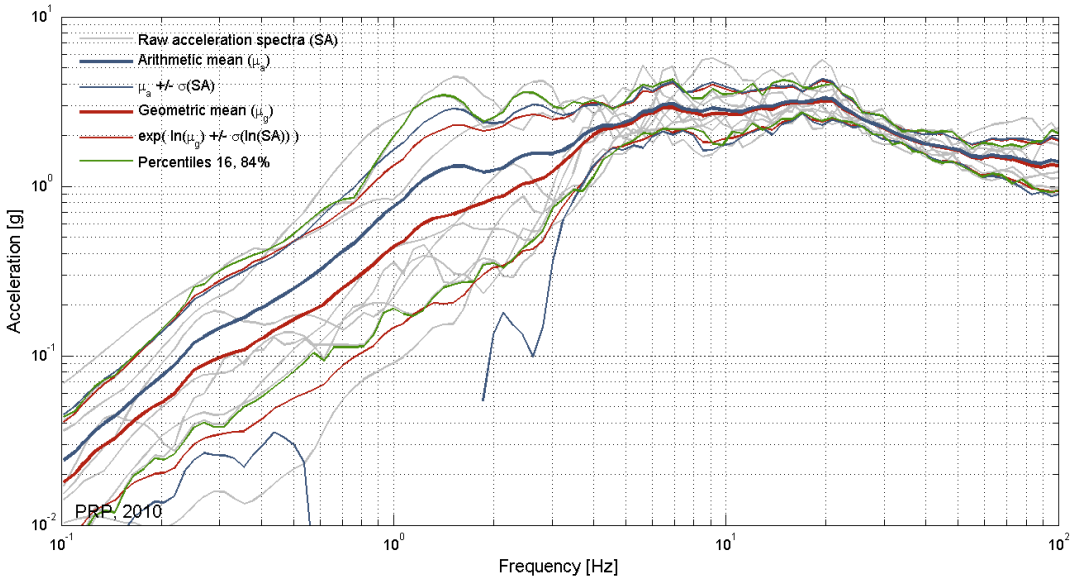

E-Beznau, profile 1, material 3

Non linear 1
Magnitude 6, PGA 2.5g

Horizontal outcrop motion at surface

Figure IV-1.46: Non-linear response spectra at 2.5g rock outcrop.

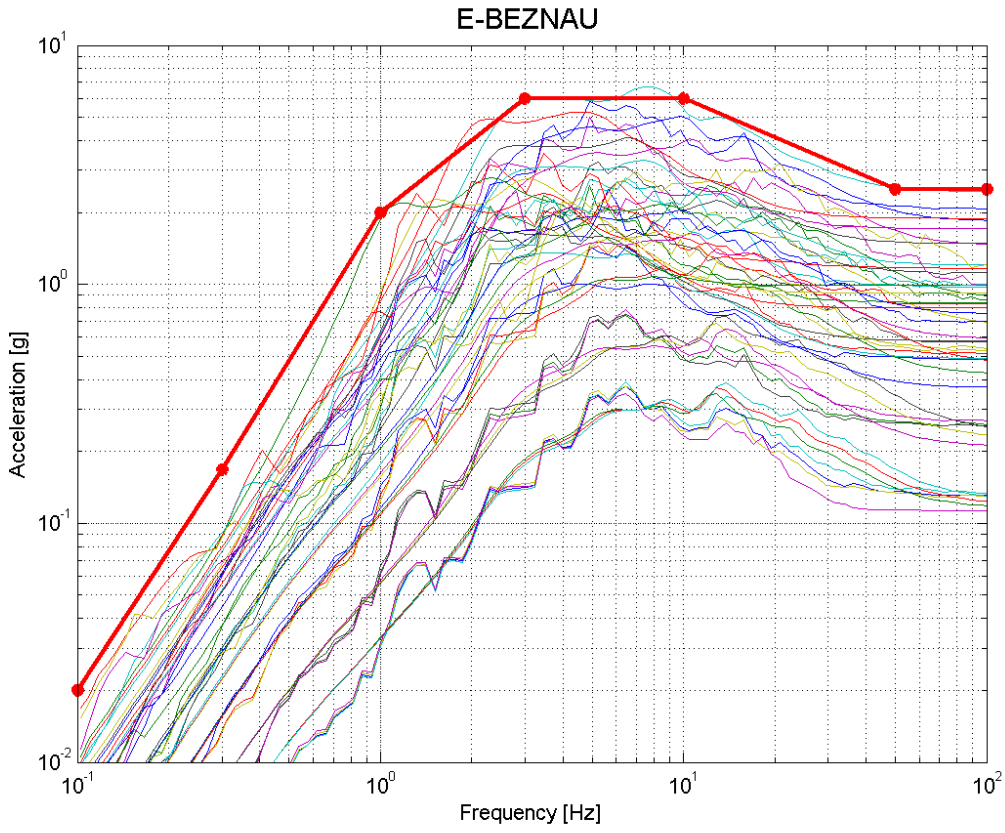

Figure IV-1.47: Response spectra for all calculations.

The spectral shapes calculated for each site are presented in Figure IV-1.49 and the numerical values at the control periods given in Table IV-1.48 .

Leibstadt		Gosgen		Beznau		E-Beznau		Muhleberg	
Frequency (Hz)	Amplification	Frequency (Hz)	Amplification	Frequency (Hz)	Amplification	Frequency (Hz)	Amplification	Frequency (Hz)	Amplification
0.1	0.007	0.1	0.006	0.1	0.016	0.1	0.008	0.1	0.010
0.3	0.050	0.3	0.100	0.3	0.100	0.3	0.067	0.3	0.085
1.5	0.800	1.0	1.250	1.3	1.080	1.0	0.800	1.0	0.850
3.0	2.300	2.0	2.500	3.0	2.500	3.0	2.400	3.5	2.500
12.0	2.300	6.0	2.500	15.0	2.500	10.0	2.400	10.0	2.500
50.0	1.000	50.0	1.000	50.0	1.000	50.0	1.000	40.0	1.000
100.0	1.000	100.0	1.000	100.0	1.000	100	1.000	100.0	1.000

Figure IV-1.48: Table: Normalized spectral shapes of the NPP sites.

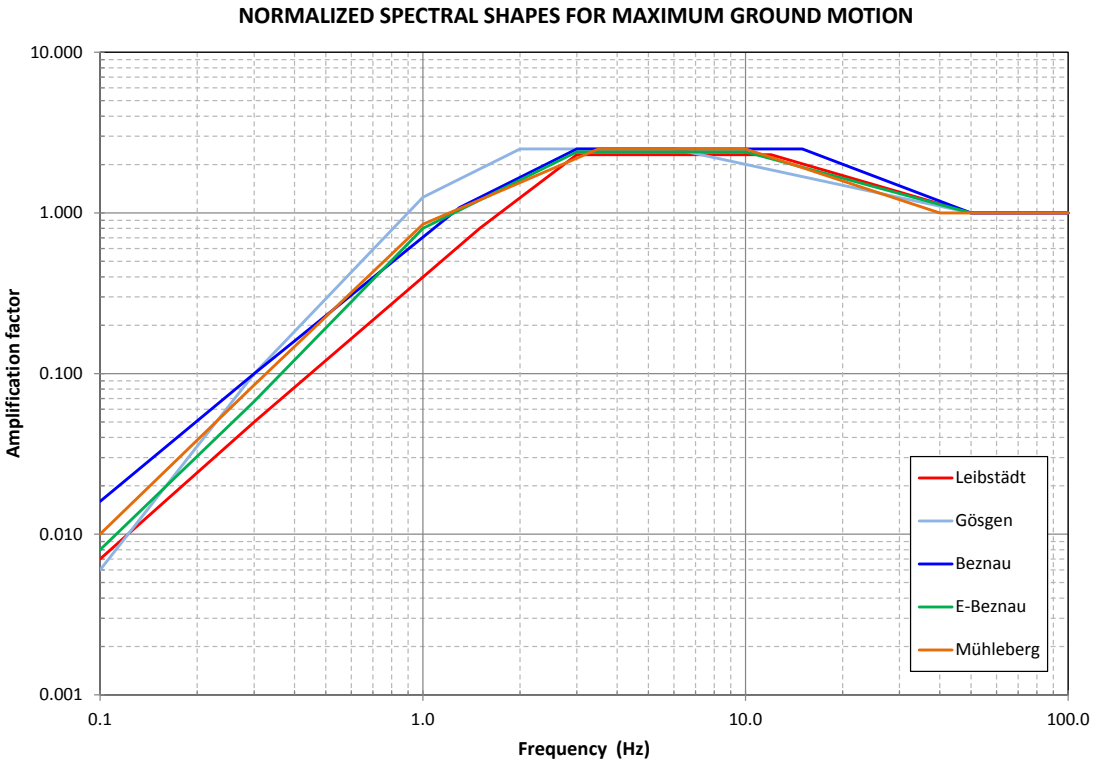

Figure IV-1.49: Normalized spectral shapes for maximum ground motions.

The spectral accelerations are then defined by scaling the spectral accelerations with PGA read from the envelop spectrum.

Logic Tree Structure

The logic tree for the maximum horizontal ground surface motion is given in Figure IV-1.50.

Each of the approaches listed above corresponds to a different branch of the logic tree. Depending on the degree of confidence in the approaches, different weights are assigned for the branches. The logic tree applies to the determination of the peak ground surface acceleration. Once this value is determined, the normalized spectral shape defined in Table IV-1.48 is anchored to the PGA.

In order to reflect the uncertainty in the determination of the soil resistance, to each of the three main branches of the logic tree, three sub-branches are added: the main sub-branch corresponds to the maximum PGA listed in the table of Figure IV-1.50; the two additional sub-branches correspond to maximum peak ground accelerations equal to 0.9 and 1.2 times the previous values. Since Betbeder's model consistently underpredicts the maximum ground surface acceleration, even with respect to observations, a zero weight has been assigned. A somewhat larger weight has been given to the numerical calculations with respect to the analytical ones, because the numerical models are more accurate and flexible to represent the true behavior of the soil; analytical models inherently contain simplified modeling assumptions.

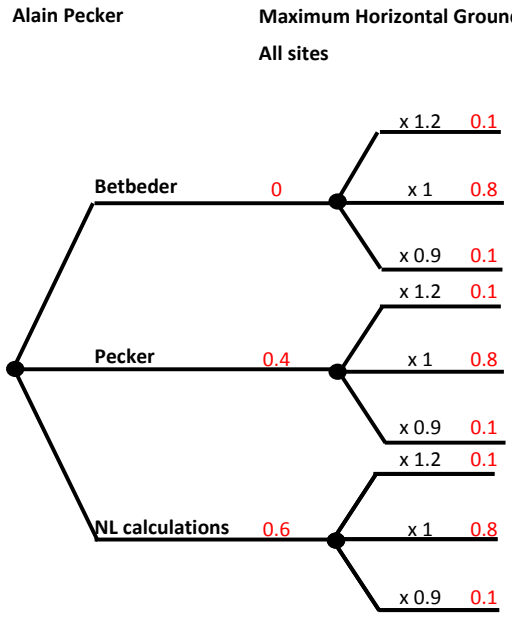

Maximum accelerations in g

	KKG	KKB	EKKB	KKL	KKM
Betbeder	1.4	2.0	1.5	1.5	1.5
Pecker	2.0	2.5	2.2	1.8	2.1
NL calculations	2.8	2.8	2.5	2.6	2.4

Figure IV-1.50: Logic tree for maximum horizontal ground motion.

1.6.2 Vertical Component

For the horizontal motion, there is a physical background for limiting the maximum surface motion. The vertical motion is associated mainly with P waves traveling through the soil deposit. Granular soils do not exhibit a failure condition, which would limit the transmitted stresses, for stress paths corresponding to uniaxial compression-tension; this is especially obvious when the soil is saturated because the P wave travels through the fluid. Therefore, there is no reason for limiting the maximum vertical ground surface motion.

1.7 Ground Motion at Depth

It is requested that the ground motions be computed at different depths at each site for the reactor building depth and for Mühleberg also for the Turbine building depth. These depths are listed in Table IV-1.2. The two values at Gösgen correspond to the depths of the reactor

building on both sites KKG and EKKG, which have been considered as a unique site for the site response calculations.

Table IV-1.2: Building depths for the NPP sites.

	Beznau	E-Beznau	Gösgen	Leibstadt	Mülheberg
Depth z_2	-15 m	-15m	-9 m	-10 m	-7 m
Depth z_3	-	-	-15 m	-	-14 m

1.7.1 Median Amplification of Horizontal Ground Motion

The derivation of the logic tree for the ground motions at depth follows the same line of reasoning as for the ground surface motion, therefore preserving the structure of the logic trees. Nevertheless some adaptations are required to account for the missing information. That information relates to the outcropping motions in the non-linear analyses.

The branches of the logic trees remain the same with the same weights. Although the maximum strain may occur above the elevation of interest, the same PGA thresholds are kept to be consistent with the definition of outcrop motions in SHAKE, which are also influenced by the reflected downgoing waves.

For the RVT and SHAKE runs the amplification factors of the surface motions are just replaced by the amplification factors of the outcrop motions at depth; these amplification factors are readily available from the numerical simulations.

For the non-linear analyses, only the amplification factors for the surface motion and the within motion at depth are available. To estimate what would be the outcrop amplification factors from the non-linear runs, two options are possible:

Method 1: use the ratio X_1 of the outcrop motion to the surface motion from the SHAKE (or RVT) runs, and apply the same ratio to the non-linear surface motions;

Method 2: use the ratio X_2 of the outcrop motion to the within motion from the SHAKE (or RVT) runs, and apply the same ratio to the non-linear within motions.

Both options have been tested on a theoretical example for vertically propagating shear waves. Let us consider a two layer system and let us assume that we want to extract the outcrop motion at the layer interface. The following notations are used:

- h = top layer thickness
- A = amplitude of the upgoing wave in the top layer, equal to the amplitude of the downgoing wave to satisfy the free surface condition
- A_2 = amplitude of the upgoing wave in the bottom layer
- A_2' = amplitude of the downgoing wave in the bottom layer

- q = impedance ratio between both layers

$$q = \frac{\rho_1 V_{S1}}{\rho_2 V_{S2}} \tag{IV-1.15}$$

- β = damping ratio of top layer

Then (Pecker, 2010):

$$X_1 = \frac{outcrop}{surface} = \frac{A_2}{A} = \frac{1}{2}\left[(1+q)e^{-\frac{i\omega h}{(1+i\beta)V_{s1}}} + (1-q)e^{+\frac{i\omega h}{(1+i\beta)V_{s1}}}\right] \tag{IV-1.16}$$

$$X_2 = \frac{outcrop}{within} = \frac{A_2}{A_2 + A_2'} = \frac{1}{2}\left[\frac{(1+q)e^{-\frac{i\omega h}{(1+i\beta)V_{s1}}} + (1-q)e^{+\frac{i\omega h}{(1+i\beta)V_{s1}}}}{e^{-\frac{i\omega h}{(1+i\beta)V_{s1}}} + e^{+\frac{i\omega h}{(1+i\beta)V_{s1}}}}\right] \tag{IV-1.17}$$

An example of the variation of both quantities versus $\omega h/V_{S1}$ is depicted in Figure IV-1.51 for an impedance ratio of 0.8 and a damping ratio of 10

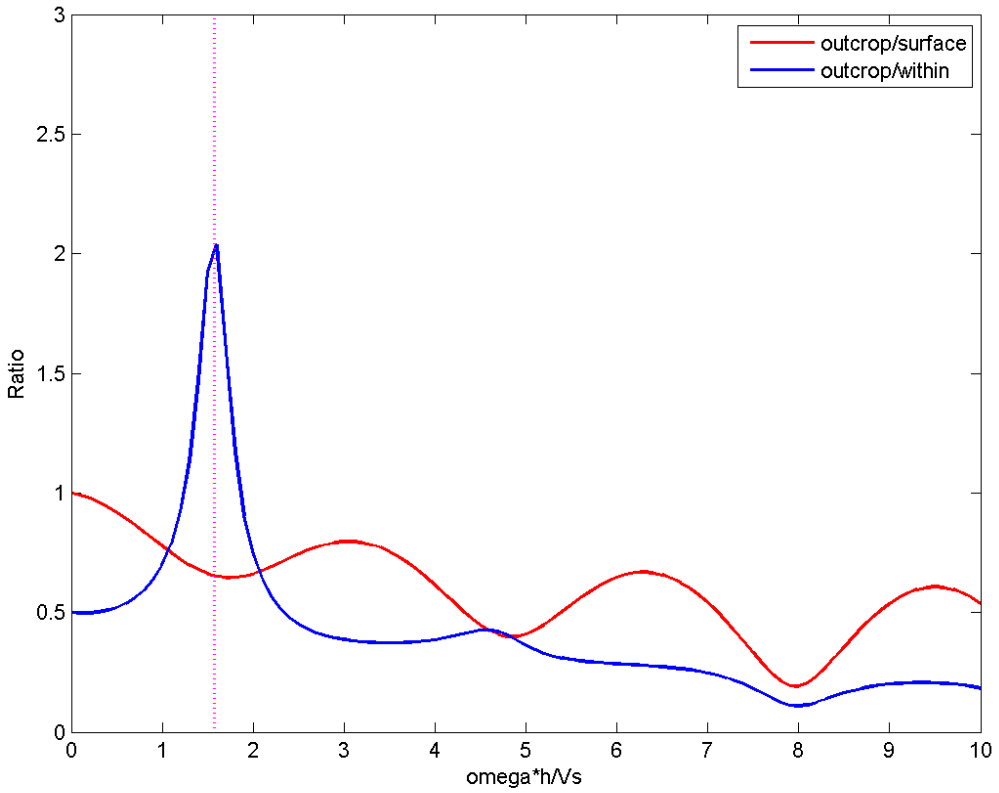

Figure IV-1.51: Variation of X_1 and X_2 vs dimensionless frequency.

It is obvious that method 2 yields very rapid changes in the ratio as the dimensionless frequency approaches the resonant frequency of layer 1; that dimensionless resonant frequency $(\pi/2)$ is directly related to the shear wave velocity of the top layer which, in turn, depends

on the calculation method. When calculating X_1 and X_2 as described above, the result is function of the strain compatible shear wave velocity calculated at the end of the iterations in SHAKE (or RVT). If X_1 and X_2 are now applied to the results of the non-linear runs, there is no reason for VS1 in the non-linear runs to be exactly equal to this value. For illustration purposes, let us assume that the shear wave velocity in the non-linear runs is 5% smaller than in the SHAKE (or RVT) runs: $V_{S1}^{*} = 0.95 V_{S1}$. From the previous Equations IV-1.16, IV-1.17 it immediately follows that:

- Exact outcrop motion in non-linear runs:

$$A_2^* = A^* \frac{1}{2}\left[(1+q^*)e^{-\frac{i\omega h}{(1+i\beta)V_{S1}^*}} + (1-q^*)e^{+\frac{i\omega h}{(1+i\beta)V_{S1}^*}}\right] \tag{IV-1.18}$$

- Calculated from method 1:

$$A_2^* = X_1 A^* \tag{IV-1.19}$$

- Calculated from method 2:

$$A_2^* = X_2 A^* \left[e^{-\frac{i\omega h}{(1+i\beta)V_{S1}^*}} + e^{+\frac{i\omega h}{(1+i\beta)V_{S1}^*}}\right] \tag{IV-1.20}$$

Obviously when $V_{S1}^* = V_{S1}$ all three methods give the same answer.

The ratios A_2^*/A^* calculated from Equations IV-1.18, IV-1.19 and IV-1.20 have been plotted in Figure IV-1.52 for $q = 0.8$,$\beta = 0.1$ and $V_{S1}^* = 0.95V_{S1}$.

Examination of Figure IV-1.52 immediately shows, which could be anticipated from Figure IV-1.51, that method 1 is a better approximation of the exact solution, especially close to the resonant frequency of the top layer.

Therefore it is recommended, for the non-linear analyses, to use the ratios outcrop/surface derived from the SHAKE analyses and to apply them to the amplification factors computed at the ground surface in the non-linear analyses.

Along the same lines as for the surface motion, the interpolation procedure for the missing runs will be the same.

Since all cases are computed for the RVT runs, no interpolation is needed for those runs to compute the ratios outcrop/surface. Since no magnitude dependence is assumed in our model, these ratios should be taken equal to the arithmetic mean of the ratios for the three magnitudes.

For the only site for which 2D-effects are incorporated in the median amplification (Leibstadt), the same amplification factors as for the surface motions are used; this is based on the fact that the amplification is created by the cliff geometry, the dimension of which is much larger than the buildings depths.

1.7.2 Median Amplification of Vertical Ground Motion

The logic tree for the mean vertical motion is kept unchanged, except for the amplification factors which are the outcrop amplification factors. For the V/H ratios, the statistical correlations should be used with for $V_{S,30}$ the value computed below the depth of interest.

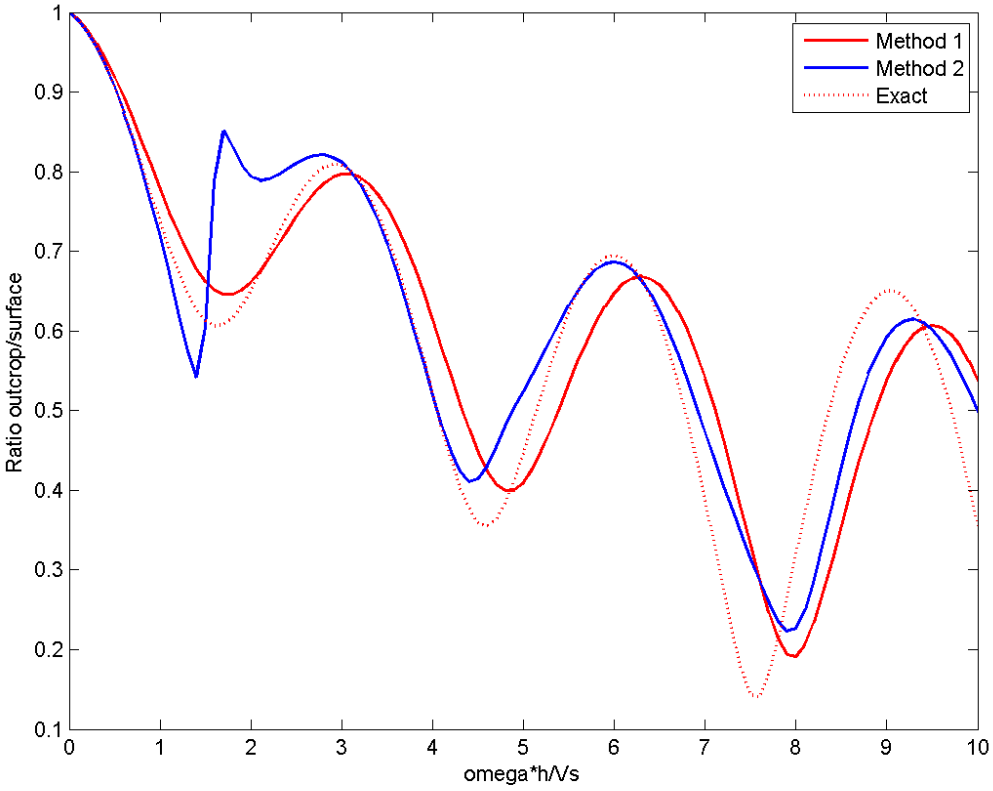

Figure IV-1.52: Comparison of methods 1 and 2 to the exact solution.

1.7.3 Aleatory Variability of Horizontal Ground Motion

As for the ground surface amplification, no aleatory variability is considered for the motions at depth.

1.7.4 Aleatory Variability of Vertical Ground Motion

As for the ground surface amplification, no aleatory variability is considered for the motions at depth.

1.7.5 Maximum Horizontal Ground Motion

The maximum ground motions at depths have been computed in document "Maximum ground motions-Sensitivity studies and ground motions at depth" [Pecker] (TP3-TN-0403). Two different approaches have been used: a theoretical model and the non linear finite element site response analyses. Both evaluations refer to within ground motions. It has been noted in the previously mentioned document that the evaluations derived from the theoretical model certainly overestimate the attenuation with depth especially for depths located close to the bedrock interface. From those evaluations it appears that the attenuation in the peak ground acceleration should range from factors of 1.0 to 2.0. The lower attenuation factor is applicable to the shallow depth, whereas the larger one is applicable to the deeper depth. Given the fact that these attenuation factors are based on within-motions, they have to be amplified to

go from the within-motion to the outcrop-motion. Figures IV-1.34 and IV-1.35, from that document, show that this amplification factor could be in the range of 1.2 (for shallow depths) to 1.7 (for deeper depths). Multiplying both factors would give a net multiplication factor of 0.8 (1.7/2.0) to 1.2 (1.2/1.0) to be applied to the maximum ground surface motion. Since the depths of interest are rather close to the ground surface, a large reduction in the maximum ground surface motion does not seem appropriate; this is clearly evidenced by the SHAKE runs, at high rock acceleration, where the ratios outcrop/surface are in the range 0.8 to 1.2. Therefore it is proposed to use the maximum ground surface motion as a base case and to add, at the end of the logic tree for maximum ground motions, 3 branches with weights 80 %, 10 % and 10 %. These branches are respectively associated with multiplication factors of 1.0, 0.8 and 1.2 applied to the base case.

The response spectra for the maximum outcropping ground motions have the same normalized shapes as for the surface motions and are anchored at the appropriate PGA.

1.7.6 Maximum Vertical Ground Motion

No maximum bound is put on the vertical motion, like for the surface motion.

Chapter 2

Hazard Input Document for A. Pecker (EG3-HID-1007)

Written by the PMT, SP4 and TFI

2.1 Introduction

This Hazard Input Document (HID) describes the implementation, evaluation and results of Alain Pecker's geotechnical assessment of sites effects (the "model" or "SP3 model") at the NPP sites Beznau, Gösgen, Leibstadt and Mühleberg, delivered on 01.07.2013. The purpose of this document is to provide a technical description of the model as implemented. The results of model evaluation are compiled into a so-called SIF (Soil hazard Input File), which, among the rock hazard results, is input to the soil hazard evaluations. This HID addresses technical and procedural aspects. It does not provide a rational discussion of the models or the results.

2.2 Model Description

The geotechnical assessment by Alain Pecker is described in part III, Chapter 1 (EG3-ES-1016). The models concern six quantities:

- Amplification of horizontal ground motion,
- Aleatory variability of horizontal motion amplification,
- Maximum horizontal ground motion (truncation model),
- Amplification of vertical ground motion and V/H scaling,
- Aleatory variability of vertical motion amplification and V/H scaling factors, and
- Maximum vertical ground motion (truncation model),

which are developed as functions of spectral frequency, which consider the up-going wavefield ("outcrop motion") and which depend on site, target depth, and PGA. In contrast to the models by the other SP3 experts, the models by Alain Pecker are invariant of magnitude. The models are formulated as logic trees, yielding epistemic uncertainty. These logic tree models are described in the following.

2.2.1 Amplification of Horizontal Ground Motion

The logic tree model for amplification of horizontal ground motion has five levels of branching (Fig. IV-2.1), among which epistemic uncertainty is developed.

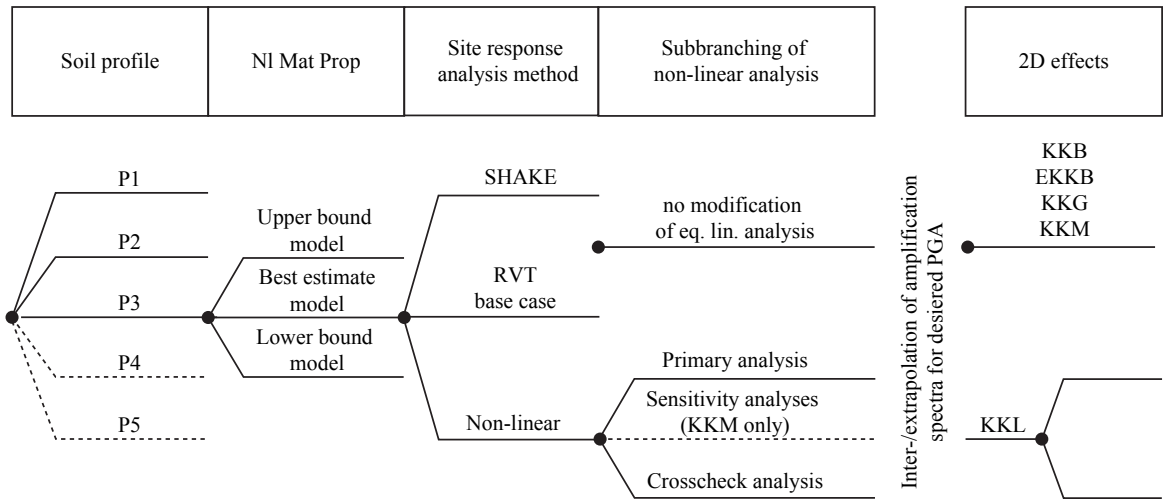

Figure IV-2.1: Logic tree model, which develops amplification functions applicable to horizontal ground motion.

Level 1

develops soil profile alternatives. The soil profiles are described in Renault [2010a, b, c, d, e] [TP3-TN-1068...1071] and in the report Part I. The assigned weights are given in Table IV-2.1. They dependent on the NPP site and are invariant of spectral frequency. Profiles 1 and 6 at Gösgen site are considered identical and are used equivalently. The weights are implemented in the *sp3p_Profile* routine of Hölker [2012] (TP4-HSW-1002).

Table IV-2.1: Weights of soil profiles in level 1 of the logic tree model for amplification of horizontal ground motion.

Soil profile	P1 or P6	P2	P3	P4	P5
Beznau	0.35	0.25	0.15	0.25	-/-
Gösgen	0.25	0.10	0.15	0.25	0.25
Leibstadt	0.40	0.40	0.20	-/-	-/-
Mühleberg	0.30	0.20	0.30	0.20	-/-

Level 2

develops the material and shear modulus models. Generally a "lower bound", "best estimate" and "upper bound" model have been defined in TP3-TN-1068...1071. The weights assigned to the material models are given in Table IV-2.2. These weights are specific to the NPP site, are independent of spectral frequency and are implemented in *sp3p_Material*.

Table IV-2.2: Weights of material models in level 2 of the logic tree model for amplification of horizontal ground motion.

Material model	Lower bound	Best estimate	Upper bound
Beznau	0.22	0.45	0.33
Gösgen	0.333	0.334	0.333
Leibstadt	0.25	0.50	0.25
Mühleberg	0.27	0.46	0.27

Level 3

defines alternative amplification functions based on the different computational approaches to the site response analyses (SRA). The considered approaches are SHAKE, RVT base case and NL (non-linear). The RVT analyses based on the randomized V_S-profiles are not considered. The associated weights (Tab. IV-2.3) depend on PGA level and spectral frequency with PGA ranges and frequency bands being specific to the NPP sites (Tab. IV-2.4). The weights are implemented in *sp3p_Method_horizontal*.

Table IV-2.3: Weights depending on spectral frequency and PGA level assigned to results of computational site response analysis methods. The site-specific PGA ranges and spectral frequency bands are given in Table IV-2.4.

Freq. band	1			2			3		
PGA range	SHAKE	RVT	NL	SHAKE	RVT	NL	SHAKE	RVT	NL
A	1.00	0	0	0.60	0.40	0	0.50	0.50	0
B	0.50	0	0.50	0.40	0.30	0.30	0.35	0.35	0.30
C	0.20	0	0.80	0.07	0.13	0.80	0.10	0.10	0.80

Table IV-2.4: Site-specific PGA ranges and spectral frequency bands underlying the definition of weights assigned to the SRA methods in Table IV-2.3.

	PGA ranges [g]			Spectral frequency bands [Hz]		
	A	B	C	1	2	3
Beznau	0 . . . 0.15	0.15 . . . 0.75	0.75 . . . 2.5	0.1 . . . 1.0	1.0 . . . 20	20 . . . 100
Gösgen	0 . . . 0.1	0.1 . . . 0.7	0.7 . . . 2.5	0.1 . . . 1.0	1.0 . . . 10	10 . . . 100
Leibstadt	0 . . . 0.1	0.1 . . . 0.3	0.3 . . . 2.5	0.1 . . . 1.0	1.0 . . . 8	8 . . . 100
Mühleberg	0 . . . 0.1	0.1 . . . 0.4	0.4 . . . 2.5	0.1 . . . 1.5	1.5 . . . 15	15 . . . 100

Level 4

implements a branching to account for modeling uncertainty of the NL method. Therefore this branching is applicable only to NL branches, i.e. no sub-branching occurs on branches using SHAKE or RVT SRA. As alternative to the primary NL analysis the results of the NL crosscheck and sensitivity analyses are used. Analysis results and associated weights are:

Beznau,Leibstadt:	Primary NL by Pelli 80%,	crosscheck NL by Pecker 20%
Gösgen:	Primary NL by Pecker 90%,	crosscheck NL by AMEC 10%
Mühleberg:	Primary NL by AMEC 70%,	crosscheck NL by Pecker 20%,
	and 3 NL sensitivity analyses by AMEC each 3.3%.	

These weights are implemented in *sp3p_Method_NLsub*.

Level 5

develops a two-fold sub-branching to account for possible 2D effects at Leibstadt site. The first branch (80% weight) assumes that 2D effects have no effect on the amplification function. On the second branch (20% weight) spectral scaling factors, $S(f)$ in Equation IV-2.1, are developed, which are applicable to the amplification function. No sub-branching is implemented at other sites. 2D effects are implemented in *sp3p_2dEffects*.

$$S(f) = \begin{cases} 1 & f < f_0/2 \\ 0.5 + f/f_0 & f_0/2 < f < 0.7 f_0 \\ 1.2 & 0.7 f_0 < f < f_0/0.7 \\ 1.2 - 0.35\,(f/f_0 - 1/0.7) & f_0/0.7 < f < 2 f_0 \\ 1 & f > 2 f_0 \end{cases} \tag{IV-2.1}$$

where f is spectral frequency and f_0 is the site- and V_S-profile-specific fundamental frequency.

2.2.2 Aleatory Variability of Horizontal and Vertical Motion

Aleatory variability in SP3 is conceptually defined as variability, which is additional to the variability already included in the rock hazard results. For horizontal and vertical motion this additional variability is considered zero.

2.2.3 Maximum Horizontal Ground Motion

The logic tree model of maximum horizontal ground motion (Fig. IV-2.2) develops alternative maximum ground motion spectra by means of two levels of branching. These spectra are used as truncation model and are defined as

$$SA_{max}(f) = PGA_{max}\, U\, X(f) \tag{IV-2.2}$$

where PGA_{max} is a maximum PGA value on soil, U is an uncertainty factor and $X(f)$ is a PGA-normalized spectral shape.

Level 1

develops two alternative maximum PGA values on soil (PGA_{max} in Equation IV-2.2). Both are based on modeling. No empirical data are utilized. The first alternative (weight 40%) uses

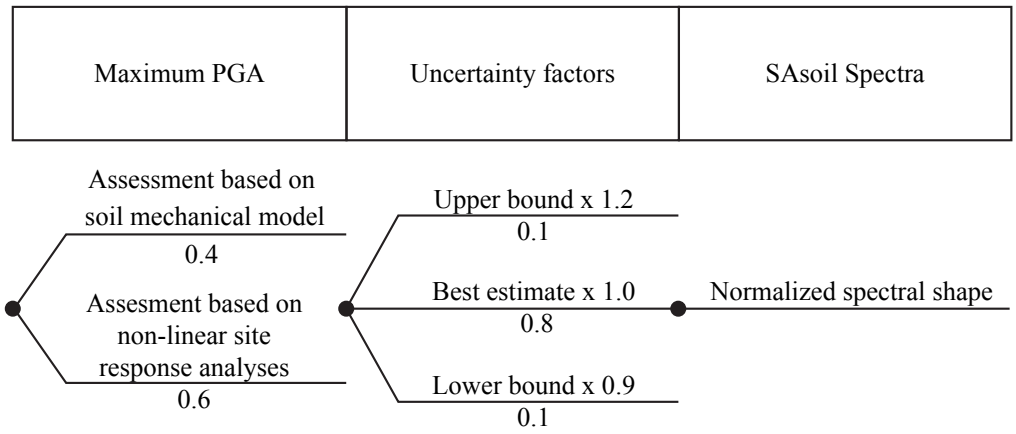

Figure IV-2.2: Logic tree model, which develops maximum acceleration spectra for horizontal ground motion.

a maximum PGA value derived from a soil mechanical model [Pecker 2011] (TP3-TB-1074). Maximum PGA values are: Beznau 2.5 g, Gösgen 2.0 g, Leibstadt 1.8 g and Mühleberg 2.1 g. The second alternative (weight 60%) uses a maximum PGA value derived from the non-linear site response analyses. Maximum PGA values are: Beznau 2.8 g, Gösgen 2.8 g, Leibstadt 2.6 g and Mühleberg 2.4 g.

Level 2

implements a 3-fold branching, which develops an uncertainty factor (U in Equation IV-2.2). The uncertainty factors are 1.2, 1.0 and 0.9 (independently of spectral frequency) and associated weights are 10%, 80% and 10%.

Level 3

as per Figure IV-2.2 does add further uncertainty, but provides one spectral shape, $X(f)$ in Equation IV-2.2. This shape is given per NPP site (Tab. IV-2.5) and is normalized so that the value at 100 Hz (PGA) equals 1. It is linearly interpolated on $\log(f)$ and $\log(X)$ scales for frequencies not given in Table IV-2.5.

Table IV-2.5: Spectral shapes per NPP site utilized in maximum ground motion (truncation) modeling.

Frequency [Hz]	0.1	0.3	1.3	3	15	50	100
Beznau	0.016	0.1	0.108	2.5	2.5	1	1
Gösgen	0.006	0.1	1.25	2.5	2.5	1	1
Leibstadt	0.007	0.05	0.8	2.3	2.3	1	1
Mühleberg	0.01	0.085	0.85	2.5	2.5	1	1

2.2.4 V/H Scaling and Amplification of Vertical Ground Motion

The logic tree model of site effects of vertical motion (Figure IV-2.3) is a composite model, which separates at

Level 1

three main branches: The first branch is based on V/H ratios defined by the SP3 expert. The second branch assumes, that vertical motion on rock equals vertical motion on soil, i.e. amplification is 1. The third branch develops amplification functions for vertical ground motion. The weights assigned to these branches depend on the site, PGA level and spectral frequency (Tsb. IV-2.6) and are implemented in *sp3p_Approach_vertical*. The first branch (V/H ratios) is expanded by the logic tree model for amplification of horizontal ground motion, while the V/H model by the SP2 experts expands the second and third branch.

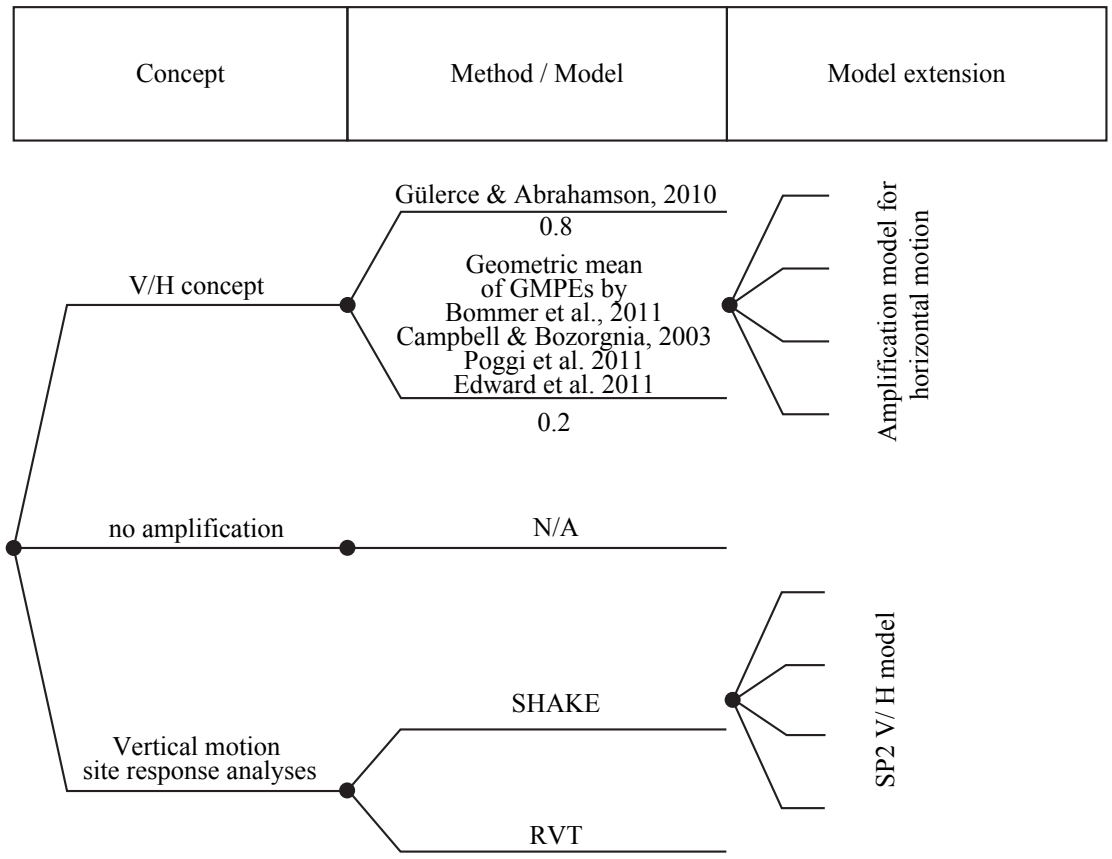

Figure IV-2.3: Logic tree model, which develops V/H scaling factors and site-specific amplification factors.

Level 2 on the SP3 V/H branch

develops alternative V/H scaling functions. Two options are considered: The model by Gülerce and Abrahamson [2011] is assigned a weight of 80%. The geometric mean of the models by Bommer et al. [2011], Campbell and Bozorgnia [2003], Poggi2012b (TP3-TB-1084, method 1) and Edwards et al. [2011b] (TP3-TB-1084, method 2) is assigned a weight of 20%. V/H ratios are evaluated per spectral frequency for magnitudes 5, 6 and 7 and the arithmetic mean V/H ratio is used. The frequency-, magnitude-, and PGA-, and site-specific source-to-site distances as defined by SP1 are used for V/H evaluation.

Table IV-2.6: Weights assigned to the approach of modeling vertical motion site effects. Approaches are "V/H" scaling ratios defined by the SP3 expert, "nAF" no amplification assuming that vertical motion on rock and soil are identical, and "EQL" representing vertical motion site response analyses.

PGA		Less or equal 0.2 g						Greater than 0.2 g					
Frequency f_1 [Hz]		f $\leq f_1$			f $> f_1$			f $\leq f_1$			f $> f_1$		
Approach		V/H	nAF	EQL	V/H	nAF	EQL	V/H	nAF	EQL	V/H	nAF	EQL
Beznau	8	0.5	0.2	0.3	0.5	0	0.5	0.1	0.2	0.7	0.1	0	0.9
Gösgen	10	0.5	0.3	0.2	0.5	0	0.5	0.1	0.3	0.6	0.1	0	0.9
Leibstadt	4	0.5	0.1	0.4	0.5	0	0.5	0.1	0.1	0.8	0.1	0	0.9
Mühleberg	15	0.5	0.3	0.2	0.5	0	0.5	0.1	0.3	0.6	0.1	0	0.9

Table IV-2.7: Weights assigned to the vertical motion site response analysis methods SHAKE and RVT.

PGA		Less or equal 0.2g				Greater than 0.2g			
Frequency f_1 [Hz]		f $\leq f_1$		f $> f_1$		f $\leq f_1$		f $> f_1$	
Method		SHAKE	RVT	SHAKE	RVT	SHAKE	RVT	SHAKE	RVT
Beznau	8	0.67	0.33	0.5	0.5	0.57	0.43	0.5	0.5
Gösgen	10	0.75	0.25	0.5	0.5	0.58	0.42	0.5	0.5
Leibstadt	4	0.625	0.375	0.5	0.5	0.625	0.375	0.5	0.5
Mühleberg	15	0.75	0.25	0.5	0.5	0.58	0.42	0.5	0.5

Level 3

and following levels **on the SP3 V/H branch** reflect to the logic tree model for amplification of horizontal ground motion.

Level 2 on the vertical motion SRA branch

develops alternative site response analysis methods, which are RVT base case and SHAKE. The weights depend on the site, PGA level and spectral frequency as per Table IV-2.7 and are implemented in *sp3p_Method_vertical*.

Level 3

and following levels **on the vertical motion SRA branch** and the no amplification branch reproduce the V/H model by the SP2 experts. The SP2 V/H model is implemented as a table of V/H ratios provided within SP4. The V/H ratios depend on the site, the spectral frequency, magnitude and PGA (or annual probability of exceedance, respectively). Within the *SP3mod* software this table and the weights assigned by the SP2 experts to the GMPEs are stored in the environment variable *sp3db.sp2VH*.

2.2.5 Maximum Vertical Ground Motion

No limitation of vertical motion maximum ground motion due to soil properties is assumed. Therefore the maximum ground motion truncation model is implemented as an infinity-valued

single spectrum.

2.2.6 Inter- and Extrapolation of Amplification Functions

Amplifications functions are derived from 1D site response analyses (SRA), whereby different computational approaches (RVT, SHAKE, NL) are utilized. Primarily amplification is implemented as function of spectral frequency (referred to as "amplification function" is the following). The results of all SRAs were resampled to 60 spectral frequencies (Tab. IV-2.8). The full parameter space of the site- and component-specific amplification functions spans spectral frequency, PGA, magnitude, material model, V_S-profile, target depth and motion type.

For evaluation of the SP3 model and processing of the results into SIFs the amplification functions need to be inter/extrapolated for arbitrary PGA levels within the range 0.05 to 2.5 g. Depending on the computational approach, amplification functions for non-computed parameter sets need to be estimated from existing parameter sets. In A. Pecker's model site-effects are generally considered to be invariant of magnitude. For any magnitude the arithmetic mean of the amplification functions resulting form the magnitude 5, 6 and 7 analyses are used.

RVT

amplification functions for **horizontal motion and vertical motion** are available for all required parameter sets (note, that A. Pecker considers profiles 1 and 5 at Gösgen as equivalent). Within the PGA range 0.05 to 1.5 g (horizontal motion) or the PGA range 0.1 to 0.75 g (vertical motion) amplification is interpolated per spectral frequency on a log(PGA) scale using a shape-preserving piecewise cubic interpolation provided as "pchip interpolation" within MATLAB. For PGA levels above 1.5 g (0.75 g for vertical motion) the amplification function by the PGA-nearest RVT analysis is adopted (i.e. nearest neighbor extrapolation is used). Only RVT base case analyses are used. In case of vertical motion the amplification functions for the lower bound, best estimate and upper bound material models are averaged (arithmetic mean), because the vertical motion model does not feature sub-branching for the material models. Inter-/extrapolation of the RVT base case amplification functions is implemented in *sp3p_interpAF_RVTbc*.

SHAKE

amplification functions for **horizontal motion and vertical motion** are available for all required parameter sets but are limited to the PGA range of 0.05 to 0.75 g except for Gösgen (where SHAKE analyses are available for PGA levels up to 2.5 g). Within the range of PGA levels for which SHAKE analyses are available, amplification is interpolated per spectral frequency using piecewise cubic interpolation on log(PGA) scale. In case of PGA-extrapolation nearest neighbor extrapolation is used for vertical motion and for horizontal motion the PGA-nearest available amplification function is scaled by spectral ratios of RVT base case amplification functions, where the nominator holds the RVT amplification function for desired PGA and the denominator holds the RVT amplification function for the PGA level corresponding to that of the PGA-nearest available SHAKE amplification function.

Inter/extrapolation of SHAKE amplification functions for horizontal motion are implemented in *sp3p_interpAF_SHAKE*.

Non-linear

NL amplification functions for **horizontal motion** are available only for some parameter sets. Therefore inter/extrapolation for desired PGA and a scheme for estimating NL amplification functions at parameter sets, for which no NL SRA are available, are required. This is implemented by applying spectral scaling factors to a reference amplification function (Equations IV-2.3a-IV-2.3f).

The reference amplification function, AF_{ref}(f), is interpolated for the anticipated PGA level. It reflects the average amplification at the surface resulting from the primary NL analyses for magnitude 5, 6 and 7, the best estimate material model and the primary V_s-profile. AF/PGA interpolation is a shape-preserving piecewise cubic interpolation on log(PGA) scale. In order to extent AF/PGA interpolation from 1.5 to 2.5 g the 2.5 g amplification function for the best estimate material model is estimated from that of the upper bound material model (for details please refer to chapter 1.

The spectral scaling (correction or transfer) factors are applied to AF_{ref}(f) to obtain an estimated amplification function for the desired method (primary or crosscheck NL), the desired material model and V_s-profile and outcrop motion at embedded layers.

$$AF(f) = AF_{ref}(f)\, C_m(f)\, C_P(f)\, C_{NL}(f)\, C_Z(f) \tag{IV-2.3a}$$

$$C_M(f|PGA, m, Z) = \frac{AF_{NL1}\,(f|P=1, m, nPGA, Z=1)}{AF_{NL1}\,(f|P=1, m=be, nPGA, Z=1)} \tag{IV-2.3b}$$

$$\text{with } nPGA = [0.75 \text{ or } 1.5] \text{ using the nearest neighbor to PGA}$$

$$C_P(f=\{f \le f_1\}|P, m, PGA) = \frac{AF_{SHAKE}\,(f|P, m, PGA, Z=1)}{AF_{SHAKE}\,(f|P=1, m, PGA, Z=1)} \tag{IV-2.3c}$$

$$C_P(f=\{f > f_1\}|P, m, PGA) = \frac{AF_{RVT}\,(f|P, m, PGA, Z=1)}{AF_{RVT}\,(f|P=1, m, PGA, Z=1)} \tag{IV-2.3d}$$

$$C_{NL}(f|Z) = \frac{AF_{NLx}\,(f|P=1, m=be, M=6, Z)}{AF_{NL1}\,(f|P=1, m=be, M=6, Z)} \tag{IV-2.3e}$$

$$C_Z(f|P, m, PGA, Z) = \frac{AF_{RVT}\,(f|P, m, PGA, Z)}{AF_{RVT}\,(f|P, m, PGA, Z=1)} \tag{IV-2.3f}$$

where f is spectral frequency, f_1 is a site-specific frequency given in Table IV-2.7, m is the material model (lower bound, best estimate, upper bound), M is magnitude, PGA is peak ground acceleration, P is the V_S-profile, NL refers to the set of NL results ($NL1$ are results by the primary contractor, NLx are cross-check or sensitivity results), Z refers to the target layer ($Z = 1$ is the surface and $Z > 1$ are embedded layers).

The amplification functions AF_{NL}, AF_{SHAKE} and AF_{RVT} in Equations IV-2.3b, IV-2.3c, IV-2.3d and IV-2.3f are generally averaged over magnitudes 5, 6 and 7.

2.3 Model Implementation and Review History

The development of the models by the SP3 expert and its implementation by SP4 were carried out contemporary when partial model descriptions became available. A. Pecker's model was

implemented on the basis of the evaluation summary EG3-ES-1016 (see part IV, Chapter 1), version 8 of 29. August 2012, an email communication of 26. April 2013 concerning the revised site response analyses and presentations by A. Pecker at the SP3 workshops on 17. March 2011 [TP3-RF-1352], 7. July 2011 [TP3-RF-1385] and 20. December 2011 [TP3-RF-1438]. The model implementation has been cross-checked with the revised evaluation summary version 9 of 1. July 2013.

The models are implemented by means of four programs addressing aspects as follow:

- *HM_SP3_Pecker*
  - Amplification of horizontal ground motion;
  - Aleatory variability of horizontal motion amplification.
- *MaxHM_SP3_Pecker*
  - Maximum horizontal ground motion.
- *VM_SP3_Pecker*
  - Amplification of vertical ground motion;
  - V/H scaling factors;
  - Aleatory variability of vertical motion amplification and V/H scaling.
- *MaxVM_SP3_Pecker*
  - Maximum vertical ground motion.

These programs are part of the "SP3mod" software Hölker [2012] (TP4-HSW-1002), which is designed as MATLAB toolbox with an associated database holding the site response analyses and described in Hölker [2013b] (TP4-TN-1197). MATLAB releases 2011a to 2012b have been utilized for development and model evaluation.

Alain Pecker reviewed the implementation (MATLAB code) of the models in meetings held on 25. July 2011 and 17. February 2012. S. Thomassin provided an external review of the implementation of the horizontal motion models in August 2012 and of the vertical motion models in January 2013.

2.4 Model Evaluation

All models have been evaluated per site (Beznau, Gösgen, Leibstadt and Mühleberg) and target layer (surface and one or two subsurface layers) as defined in table 1 of Renault [2011a] (PMT-TN-1139) or section 4.2 of Renault and Abrahamson [2010] (PMT-TB-1014), respectively. The parameter space is spanned by magnitude, peak ground acceleration (PGA) and spectral frequency, which are discretized as detailed in Table IV-2.8. A. Pecker's model is invariant of magnitude, but magnitude is a parameter dimension in the soil hazard evaluations. Therefore the model results are assigned three times to nominally magnitude 5, 6 and 7.

The model for E-Beznau site has been last evaluated in December 2012 and became obsolete with the revised SHAKE and RVT analyses of April 2013. Final model evaluations for Beznau, Gösgen, Leibstadt and Mühleberg were performed in May 2013.

Table IV-2.8: Discretization of the parameter space of the SP3 models

Parameter	Discretization
Magnitude	5, 6, 7 and 5.9, 6.9 (however, A. Pecker's model is invariant of magnitude)
PGA [g]	0.05, 0.1, 0.15, 0.2, 0.25, 0.3, 0.4, 0.5, 0.6, 0.75, 1.0, 1.25, 1.5, 1.75, 2.0, 2.25, 2.5
Freq. [Hz]	0.2, 0.3, 0.4, 0.5, 0.8, 0.9, 1, 1.1, 1.2, 1.3, 1.5, 1.8, 2, 2.2, 2.3, 2.5, 2.7, 2.9, 3, 3.1, 3.2, 3.4, 3.5, 4, 4.4, 4.5, 5, 5.3, 5.4, 5.5, 5.6, 5.7, 5.75, 5.9, 6, 6.9, 7, 8, 8.9, 9, 10, 11, 12, 13, 14, 15, 17, 20, 22, 25, 30, 33, 40, 45, 50, 60, 70, 80, 90, 100

2.5 Processing of Model Results into SIFs (SP3-to-SP4 Interface)

The logic tree models for amplification and aleatory variability yield a set of amplification and aleatory variability functions and associated weights. For amplification (or equivalently aleatory variability) these results may be described as

$$AF_i(f, PGA, M) \quad \text{and} \quad W_i(f, PGA, M) \quad \text{for } i = 1, 2, \ldots, n \tag{IV-2.4}$$

where i is the indexing of logic tree branches, f is spectral frequency, PGA is peak ground acceleration, M is magnitude, AF is amplification and W is the associated weight.

Two modifications are applied to the data representation when the results are processed into a SIF: The n logic tree branches are summarized into 17 fractiles (Tab. IV-2.9) taking into account the weights of the branches. The parameter space dimension PGA is scaled to spectral accelerations (SA), where the relation between SA, PGA and frequency is given by the spectra used as input motions for the site response analyses. Given these two modifications the amplification (and equivalently aleatory variability) results are represented in the SIF by

$$AF_j(f, SA, M) \tag{IV-2.5}$$

where j is the index of the discrete fractiles defined in Table IV-2.9.

The logic tree models for maximum ground motion yield maximum spectral acceleration values on soil, $maxSA_i(f)$, and associated weights $W_i(f)$, where i is the indexing of logic tree branches and f is spectral frequency. Concerning the SIF these results are summarized into 17 discrete fractiles, if the number of logic tree branches exceeds 17. Otherwise the native $maxSA$ spectra and associated weights are transcribed to the SIF.

The aim of summarizing the model results to 17 fractiles is to reduce the number of combinations required in soil hazard evaluation, which is motivated by maintaining acceptable computing time. The 17 fractiles are associated with fixed weights as given in Table IV-2.9.

These weights are derived from bin width, where the fractiles are bin centers and where the bin bounds are the mean values of neighboring fractiles or 0 or 1, respectively.

The site effect model for vertical motion features two components:

(a) Amplification factors, which conceptually are to be applied to vertical motion rock hazard, and

Table IV-2.9: Discrete fractiles and associated weights utilized to summarize the logic tree model results.

Percentiles:	0.13, 0.62, 2.28, 5, 10, 20, 30, 40, 50, 60, 70, 80, 90, 95, 97.72, 99.38, 99.87
Weights:	0.00375, 0.01075, 0.0219, 0.0386, 0.075, 0.10, 0.10, 0.10, 0.10, 0.10, 0.10, 0.10, 0.075, 0.0386, 0.0219, 0.01075, 0.00375

(b) V/H scaling factors, which are to be combined with the horizontal motion amplification factors and to be applied to horizontal motion rock hazard.

For SIF processing of the vertical motion model additionally the V/H scaling models by the SP2 experts are imported and are applied to component (a). This way both model components describe V/H scaling and amplification and can be processed into a single SIF, which is applicable to the horizontal motion rock hazard.

The details of the SP3-to-SP4 interface processing are described in Hölker [2013b] (TP4-TN-1197).

2.6 Results: SIFs (Soil Input Files or SiteMod Files)

The raw logic tree model results (intermediate model results) and the SIF-processed model results are saved into so-called "SiteMod" data structures in MATLAB format. A "SiteMod" data structure contains the SIF required by the soil hazard software and it additionally contains the unprocessed logic tree model results for the parameter space described in Table IV-2.8. The details and internal format of the "SiteMod" data structure are described in Hölker [2013b] (TP4-TN-1197). Furthermore each "SiteMod" data file contains a descriptive self-documentation. The model result files associated with this HID are:

- SiteMod.Beznau.Pecker.z1h.FullModel.mat
- SiteMod.Beznau.Pecker.z1v.FullModel.mat
- SiteMod.Beznau.Pecker.z2h.FullModel.mat
- SiteMod.Beznau.Pecker.z2v.FullModel.mat

- SiteMod.Goesgen.Pecker.z1h.FullModel.mat
- SiteMod.Goesgen.Pecker.z1v.FullModel.mat
- SiteMod.Goesgen.Pecker.z2h.FullModel.mat
- SiteMod.Goesgen.Pecker.z2v.FullModel.mat

- SiteMod.Leibstadt.Pecker.z1h.FullModel.mat
- SiteMod.Leibstadt.Pecker.z1v.FullModel.mat
- SiteMod.Leibstadt.Pecker.z2h.FullModel.mat
- SiteMod.Leibstadt.Pecker.z2v.FullModel.mat

- SiteMod.Muehleberg.Pecker.z1h.FullModel.mat
- SiteMod.Muehleberg.Pecker.z1v.FullModel.mat
- SiteMod.Muehleberg.Pecker.z2h.FullModel.mat
- SiteMod.Muehleberg.Pecker.z2v.FullModel.mat
- SiteMod.Muehleberg.Pecker.z3h.FullModel.mat
- SiteMod.Muehleberg.Pecker.z3v.FullModel.mat

The token "z1h" indicates target layer and wavefield component, where "z1" is surface, "z2" is the upper embedded layer and "z3" is the lower embedded layer (as per table 1 of PMT-TN-1139) and where "h" is horizontal motion and "v" is vertical motion.

The token "FullModel" indicates that the file contains a full SP3 model. Other files, which contain model subsets only exist and have been created for parameter sensitivity analyses.

All SIFs (SiteMod files) are applicable to horizontal motion rock hazard results !

The SIFs for horizontal motion contain amplification models only while the SIFs for vertical motion contain combined amplification and V/H scaling models.

2.6.1 SIF Figures

The model results, i.e. the content of the "FullModel" SIFs listed in the previous section, have been systematically visualized by means of seven figures types:

- XY graph showing amplification versus PGA for selected spectral frequencies;
- An image display showing median amplification versus PGA and frequency;
- XY graph showing amplification versus SA on rock for a set of spectral frequencies;
- An image display showing the ratio of the 80% over the 20% fractile of amplification versus PGA and spectral frequency;
- XY graph showing maximum acceleration on soil versus spectral frequency;
- An image display showing median aleatory variability versus PGA and frequency (for horizontal motion only);
- An image display showing mean aleatory variability versus PGA and frequency (for horizontal motion only).

which are attached to this HID as an electronic appendix containing PNG and EPS files. Examples of these figures are discussed in Hölker [2013b] (TP4-TN-1197).

Chapter 3

Appendix to EG3-HID-1007 for A. Pecker

A direct link to files for the final SP3 hazard feedback is given here:

Horizontal Motion Amplification Functions and Maximum Ground Motion

- Ratio of the 80% over the 20% fractile of amplification versus PGA and spectral frequency:
  Open external file: FigSIF.Pecker.HM.AMPFp80p20-PGA-FREQ.
- Amplification versus PGA for selected spectral frequencies:
  Open external file: FigSIF.Pecker.HM.AMPF-PGA.
- Amplification versus SA on rock for a set of spectral frequencies:
  Open external file: FigSIF.Pecker.HM.AMPF-SA.
- Mean amplification versus PGA and frequency:
  Open external file: FigSIF.Pecker.HM.MeanAMPF-PGA-FREQ.
- Median amplification versus PGA and frequency:
  Open external file: FigSIF.Pecker.HM.MedAMPF-PGA-FREQ.
- Maximum acceleration on soil versus spectral frequency:
  Open external file: FigSIF.Pecker.HM.MaxGM.

Horizontal Motion Aleatory Variability

- Median aleatory variability versus PGA for a set of spectral frequencies:
  Open external file: FigSIF.Pecker.HM.AVAR-PGA.

- Median aleatory variability versus PGA and frequency:
  Open external file: FigSIF.Pecker.HM.AVAR-PGA-FREQ.
- Aleatory Variability versus SA for a set of spectral frequencies:
  Open external file: FigSIF.Pecker.HM.AVAR-SA.

Horizontal Motion Amplification Functions and Maximum Ground Motion

- Ratio of the 80% over the 20% fractile of amplification versus PGA and spectral frequency:
  Open external file: FigSIF.Pecker.VM.AMPFp80p20-PGA-FREQ.
- Amplification versus PGA for selected spectral frequencies:
  Open external file: FigSIF.Pecker.VM.AMPF-PGA.
- Amplification versus SA on rock for a set of spectral frequencies:
  Open external file: FigSIF.Pecker.VM.AMPF-SA.
- Mean amplification versus PGA and frequency:
  Open external file: FigSIF.Pecker.VM.MeanAMPF-PGA-FREQ.
- Median amplification versus PGA and frequency:
  Open external file: FigSIF.Pecker.VM.MedAMPF-PGA-FREQ.
- Maximum acceleration on soil versus spectral frequency:
  Open external file: FigSIF.Pecker.VM.MaxGM.

Chapter 4

QA-Certificate EG3-QC-1066

QA Certificate

EG3-QC-1066

PEGASOS REFINEMENT PROJECT

Hazard Input Document (HID)

Expert group: EG3 ***HID designation:*** **EG3-HID-1007**

Expert: A. Pecker ***Expert Model (EXM)*** EG3-EXM-1007

HID parameterisation of Expert Model:

TFI: N. A. Abrahamson ***Hazard Input Specialist of TFI-team:*** A. Hölker

HID based on Elicitation Documents: ☒ EG3-ES-1016

HID based on Exp. Assessments (EXA): ☒ EG3-EXA-1038 to EG3-EXA-1039

Remarks on the HID model parameterisation in terms of hazard computation input:

The undersigned Hazard Input Specialist confirms that this HID includes all required (subproject specific) input information for hazard computations. No further interpretations of this input will be required and no simplifications except Algorithmic Pinching according to paragraph 2.9 of the QA-Guidelines will be applied to convert this HID into hazard software Input Files.

Signature:

HID acceptance by the Expert / Expert Group:

Date of HID review by the Expert / Expert group: 02.12.2013

HID accepted: ☒ ***HID not accepted:*** ☐

Reasons for non-acceptance of HID / Recommendations:

The undersigned Expert(s) accept(s) the parameterisation proposed in this HID as a faithful and adequate representation of his/their Expert Model. He/they confirm(s) that this HID is free of errors and agree(s) to its use as hazard computation input.

Signature Expert 1 / Expert:

Signature Expert 2:

Signature Expert 3:

Part V

Assessments of Jost A. Studer

Chapter 1

Evaluation Summary (EG3-ES-1017) of J. Studer

1.1 Introduction

This document is based on all documents and comments from Workshops 1 to 6 of SP3 and several web-meetings. It contains horizontal and vertical motion for surface as well as mean and minimum elevation at each site. It is consistent with the document EG3-HID-1008. Due to procedure requirements of the PSHA motions, at all elevations (surface, mean, minimum) have to be outcrop motions.

Note: The final text version was slightly edited by the TFI after the decease of J. Studer in order to reflect the late stage changes in the project.

1.2 Median Amplification of Horizontal Ground Motion

1.2.1 Approach

The logic tree structure was constructed according to the following criteria:

- Take into account all results of performed calculations if physically appropriate.
- Assume a smooth transition from small to high input acceleration levels so that interpolation is always possible. Extrapolation will be discussed in the individual chapters.
- Assume there are no bifurcations in the physical behavior.
- As a principle, always chose the simplest rule for interpolation (linear or nearly linear interpolation). This principle should contribute to the simplicity and clarity of the model.
- All steps have been visualized to check if the intermediate results behave as expected.
- All velocity profiles and all magnitudes have been used. If some data were missing, data from similar calculation were used (see individual chapters) if available and physically

reasonable. Otherwise, only the existing results were incorporated in the logic tree and the aleatory variability was increased.

1.2.2 Logic Tree Structure

In principle, for all soil elevations the logic tree has the same structure. Derivations are indicated in the corresponding chapters. The general structure of the model logic tree for the median horizontal site amplification is shown in Figure V-1.1. The weights for the branches and correction rules depend on individual site characteristics.

Rationale: Depending on the strain level, different calculation procedures have to be taken into account according to their validity ranges. E.g., in the lower strain levels, methods are based on (modified) linear equivalent calculations, whereas in the higher strain levels only true non-linear calculations are taken into account. In the intermediate range, an interpolation procedure will be applied.

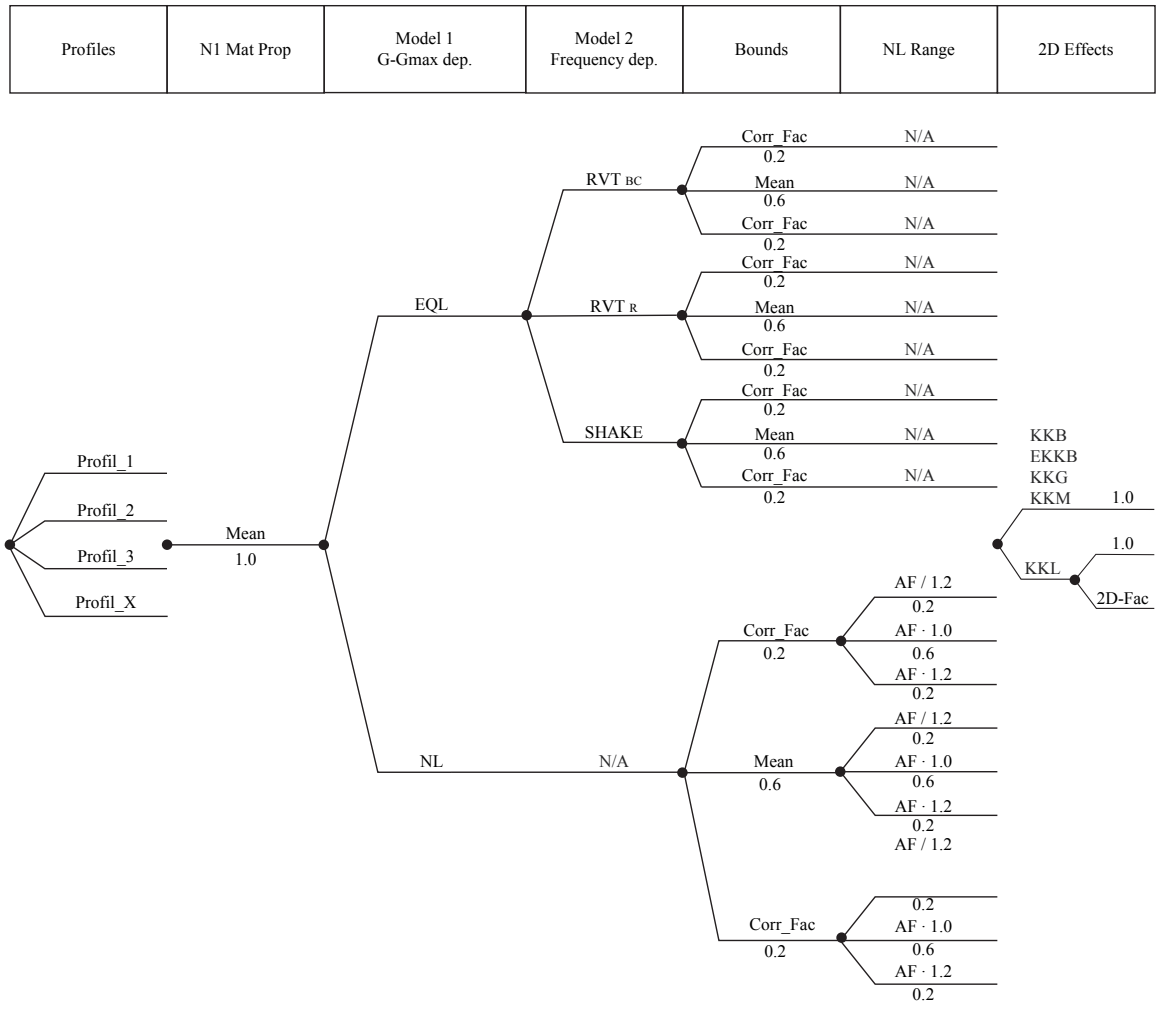

Figure V-1.1: Structure of model logic tree for median horizontal site amplification (with Corr_Fac $= \pm 1.6\sigma(RVT_R)$).

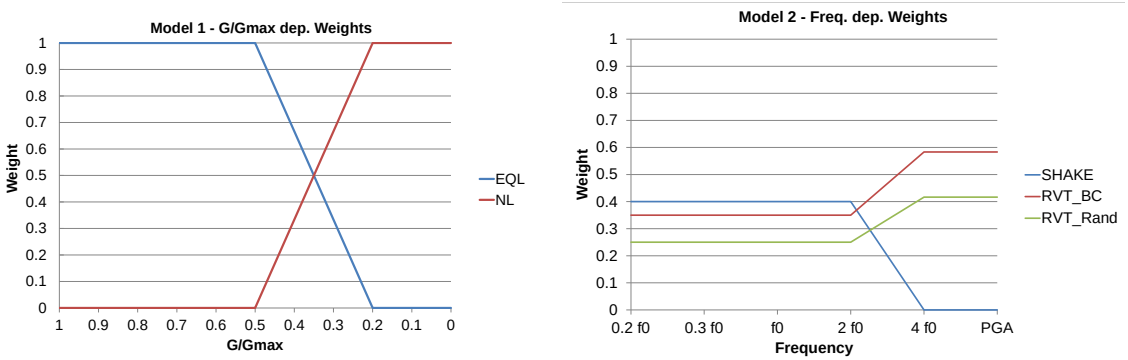

(a) Model 1 EQL vs. NL

(b) Model 2

Figure V-1.2: Weights of Model 1 (G/G_{max}) and Model 2 (Frequency dependant).

1.2.3 Model Evaluations Common to All Sites

The description follows the elements in the logic tree.

Maximum Input Ground Motion

This chapter is valid for all elevations. The selection of the appropriate procedure to calculate the amplification depends on the strain level in each element. In the low strain level, SHAKE, RVT_{bc} (base case) and RVT_R (randomized case) will be used. In the high strain range true Non-Linear (TNL or NL) procedures are applied. In the intermediate range a floating weighting procedure is used for all procedures to provide a smoother transition. The weighting rule may differ from site to site and in each site from profile to profile.

Rationale: The strain produced is dependent from the material properties in each profile.

General Set Up of the Logic Tree

Based on the original amplification results derived by the different methods, these results are "modified" in several steps and the modified amplification functions will be given weights according to the strain level. As representative strain level, the strain level derived from RVT_{bc} of the best V_S-profile and median material properties will be used.

Rational: EQL-Methods are only valid for low and median strain levels. TNL are valid in all strain levels but amplification data are only available for PGA levels larger/equal 0.4g. Therefore TNL PGA lower 0.4 are not taken into account in the low strain levels range. Strain levels are derived by RVT_{bc} best profile median material properties.

Velocity Profiles

All profiles are used. The weighting of each profile depends on the methods used in the investigations phase; a weak priority will be given to profiles which are dominantly derived by direct methods like cross-hole, in-hole or up- and down-hole methods. See individual chapter for each site.

Rational: The profiles are derived by several methods - direct V_S measurements (cross-hole etc.) and indirect measurements like MASW. Based on experience direct V_S measurements

provides the best correlation with the geological layering, whereas, e.g. dispersion curves, leads also to solutions which do not necessarily correspond to the detailed geology.

Non-linear Material Properties

In the beginning only mean values are used. Later the amplification functions are "modified" taking into account bounding results from RVT calculations (based on one standard deviation).

Method: SHAKE vs. RVT

Surface Motion: This section is valid for all elevations. For RVT and SHAKE, the calculated motions are in all elevations outcropping motions and can be used directly.

Common to both methods:

- 1-D vertical shear wave propagations
- Linear equivalent soil properties model

Advantages: Easy to understand and to use. Extensive experience available.

Disadvantages: Only one wave type (S-wave and only vertically traveling). In reality, all wave types and all incident angles exist. Linear equivalent soil model is only valid in the small and medium shear strain range. Results of both methods in the larger strain range are questionable.

Differences:

SHAKE: Individual time histories and appropriate selection of soil profile.

Advantages: Specific soil conditions and time histories can be modeled.

Disadvantages: Compared to RVT, only a limited number of time histories can be used. A soil profile randomization is not possible.

RVT: Randomization of time histories and soil profiles for a large number of cases is practical. For all acceleration levels, amplification results are available.

Advantages: For all acceleration levels amplification results are available. Statistical values are easily obtained.

Disadvantages: Also unrealistic, unnatural soil profiles and time histories will be considered if not strict boundary conditions are introduced. Therefore, eigenfrequencies of the profile have to fulfill certain given ranges. This restriction was introduced in the RVT calculations.

General weights: The weights of RVT and SHAKE versus the true non-linear (NL) computations depend on the G/G_{max} ratio (see Figure V-1.2(a)). The relative weights of RVT and SHAKE are a function of the frequency and defined in the Table V-1.1, and illustrated in Figure V-1.2(b).

Table V-1.1: Relative weights of SHAKE and RVT depending on the frequency f_0.

	$\leq 2f_0$	$2f_0 < x < 4f_0$	$\geq 4f_0$
SHAKE	0.40	Linear interpolation	0.05
RVT_{bc}	0.35	Linear interpolation	0.55
RVT_R	0.25	Linear interpolation	0.40

Table V-1.2: Relative weights of NL and EQL (SHAKE & RVT).

	$\geq 0.5G/G_{max}$	in between	$\leq 0.2G/G_{max}$
EQL	1	Linear interpolation	0
NL	0	Linear interpolation	1

Rationale: SHAKE and RVT have a similar theoretical background. But there are only limited time histories with SHAKE runs. With RVT, soil profiles also can be randomized, giving information about the aleatory randomness. The PEGASOS Refinement study aims at statistical data to estimate uncertainties. Therefore, RVT is given a higher weight.
Addition: After revision of the site amplifications in 2012 with consistent spectral shapes as input between SHAKE and RVT the relative weight between SHAKE and RVT is not well justified anymore. As this doesn't affect very much the results, the TFI decided to leave the tabulated weights of J. Studer as originally provided.

Reliability in the high and low frequency range:

The different methods provide in the low and in the high frequency range results which are partly questionable. In the low frequency range Bard [2003] (TP3-TN-0340) showed that low SHAKE provides reliable results. To take this into account, a "frequency correction procedure" was introduced (compare Figure V-1.2(a) and V-1.2(b)).

Mean and Minimum Elevation: All are outcrop motions and can be used directly.

Method: True Non-linear Calculations

Surface Motion: The results of the true non-linear calculations are outcropping motions, and can be used directly.

Mean and Minimum Elevations: Only within-motions have been calculated. To process further they have to be transferred to outcropping motions. Two methods are used, based on results from the SHAKE calculations, both with a weight of 50%:

$$NL_{outcropping,atdepth} = NL_{within,atdepth} \frac{SHAKE_{outcropping,atdepth}}{SHAKE_{within,atdepth}} \quad \text{(V-1.1)}$$

The SHAKE ratio is taken for the input ground motion level of 0.75 g and a magnitude of 6. In case of different profiles or materials, the average over all materials and profiles is taken (Beznau: average over all profiles, Leibstadt: average over 2 profiles and 2 materials, Gösgen

and Mühleberg: average over 2 materials).

$$NL_{outcropping,atdepth} = NL_{outcropping,atsurface} \frac{SHAKE_{outcropping,atdepth}}{SHAKE_{outcropping,atsurface}} \quad \text{(V-1.2)}$$

The SHAKE ratio is taken for the input ground motion level of 0.75 g and a magnitude of 6.

Rationale: For the true non-linear calculations, results only for within motions exist. In a wave field with different frequencies, outcrop motions cannot be derived directly from the within motions. The results from SHAKE calculations are taken to modify the true non-linear within motions to outcrop motions. Two ratios are taken, both with the same weight. There are no physical reasons to give different weights to the two ratios.

For the non-linear calculations not all PGA and magnitude combinations are available. For the magnitude case where extrapolation was necessary, the best-estimate (BE) case for 2.5g was estimated by scaling the 1.5g best-estimate results with the ratio of the upper bound case for 2.5g and 1.5g. Scaling the result with a real ratio from calculation results turned out to be more stable than simple linear extrapolation of the available values.

Magnitude Dependence of Site Amplification

This section is valid for all elevations. The logic tree is directly calculated with magnitudes 5, 6, and 7. Therefore no magnitude dependence correction function has to be taken into account.

Bound for Additional Epistemic Uncertainty

As only the mean non-linear material properties are used as basis for the logic tree, an additional level was introduced in order to indirectly capture this neglected epistemic uncertainty. Those bounds are based on consideration of the $/pm1.6/sigma$ of the RVT_R analyses, applied also to the RVT_{bc}, SHAKE and NL branches. The corresponding weights are given as 0.2/0.6/0.2.

Sub-branching in the True Non-linear Calculation

Compared to EQL calculation only few TNL calculations exist. To expand the epistemic uncertainty, a sub-branching for TNL was introduced (multiplied by a factor of 1.2 and divided by a factor of 1.2).

Rational: The sub-branching and the factor of 1.2 is a reasonable solution to increase the epistemic uncertainty. The sub-branching is considered to represent the $\pm 1.6\sigma$ and thus, is weighted accordingly with 0.2/0.6/0.2.

Effect of Inclined Waves

This section is valid for all elevations. Inclined waves are not taken into account directly, but considered through the aleatory variability.

Correction for 2D-effects

This correction is discussed in the Leibstadt site chapter. For all other sites, no 2-D corrections are taken into account.

1.2.4 Assessment of Missing Values

SHAKE Missing values:

- Interpolation: linear
- Extrapolation to 2.5g (or 1.25g at Beznau):

$$amp_{SHAKE_{n+1}} = \frac{amp_{RVT_{n+1}}}{amp_{RVT_n}} \times amp_{SHAKE_n} \tag{V-1.3}$$

- PGA 1.5g and 2.5g not needed at Beznau; PGA 1.0g, 1.25g, 1.5g and 2.5g not used at Mühleberg; PGA 1.5g and 2.5g are available at Gösgen

Rational: Linear interpolation simplest rule. Extrapolation ratios derived by a different method is a rational approach.

RVT Missing values:

- Interpolation: linear
- Extrapolation for 2.5g :

$$amp_{RVT_{2.5}} = \frac{amp_{TNL_{2.5,UB,M6}}}{amp_{TNL_{1.5,UB,M6}}} \times amp_{RVT_{1.5}} \tag{V-1.4}$$

- PGA 2.5g not needed at Beznau and Mühleberg; Gösgen is a special case and described in the application below.

Rational: Linear interpolation simplest rule, 2.5g is not used (in this strain level, TNL model is applied).

TNL Missing values (with NL1):

- M=6, BE
  - Interpolation: linear
  - Extrapolation to 2.5g:

$$amp_{TNL_{2.5,BE}} = \frac{amp_{TNL_{2.5,UB}}}{amp_{TNL_{1.5,UB}}} \times amp_{TNL_{1.5,BE}} \tag{V-1.5}$$

- M=5, BE
  - Interpolation: linear
  - Extrapolation to 2.5g:

$$amp_{TNL_{2.5,BE,M5}} = \frac{amp_{TNL_{2.5,UB,M6}}}{amp_{TNL_{1.5,UB,M6}}} \times amp_{TNL_{1.5,BE,M5}} \tag{V-1.6}$$

  - Extrapolation for 0.05 to 0.3g (not needed for Mühleberg):

$$amp_{TNL_{n,BE,M5}} = \frac{amp_{TNL_{n,BE,M6}}}{amp_{TNL_{n+1,BE,M6}}} \times amp_{TNL_{n+1,BE,M5}} \tag{V-1.7}$$

- M=7, BE
  - Interpolation: linear
  - Extrapolation to 2.5g:

$$amp_{TNL_{2.5,BE,M7}} = \frac{amp_{TNL_{2.5,UB,M6}}}{amp_{TNL_{1.5,UB,M6}}} \times amp_{TNL_{1.5,BE,M7}} \tag{V-1.8}$$

  - Extrapolation for 0.05 to 0.3g (not needed for Mühleberg):

$$amp_{TNL_{n,BE,M7}} = \frac{amp_{TNL_{n,BE,M6}}}{amp_{TNL_{n+1,BE,M6}}} \times amp_{TNL_{n+1,BE,M7}} \tag{V-1.9}$$

Note: The cross-check analyses NL2 (for Gösgen and Mühleberg also NL3 and NL4; NL5 for Mühleberg was not considered) are not used directly. Nevertheless, they are used to inform the evaluation of the additional range to be aplied on the NL-branches.

Rational: Compared with EQL calculations only few TNL calculations exist. Take NL2 into account to increase the epistemic uncertainty.

Application to site specific profiles SHAKE and RVT:

- Beznau: The same procedure is applied to the profiles 1 to 4.
- E-Beznau: The same procedure is applied to the profiles 1 to 3.
- Gösgen: The preferred profile is P6. The same procedure is applied to the profiles 1 to 6. *Reasoning: P1 and P6 are very similar. The difference is that P1 extend deeper into the rock compared to P6.*
  Assumption for RVT extrapolation for 2.5g:

$$\frac{amp_{RVT_{P1}}}{amp_{RVT_{P6}}} = \frac{amp_{SHAKE_{P1}}}{amp_{SHAKE_{P6}}} \tag{V-1.10}$$

  Leading to:

$$amp_{RVT_{n+1}} = \frac{amp_{SHAKE_{n+1}}}{amp_{SHAKE_{n}}} \times amp_{RVT_{n}} \tag{V-1.11}$$

- Leibstadt: The same procedure is applied to the profiles 1 to 3.
- Mühleberg: The same procedure is applied to the profiles 1 to 4.

TNL for other profiles:

- Beznau: No TNL values exist. RVT values exist for all PGA and M. TNL values for profile P1, BE exist for all PGA and M.
- E-Beznau: Same as for Beznau.

- Gösgen: No TNL values exist. SHAKE values exist for all PGA and M. TNL values P6, BE exist for all PGA and M.
- Leibstadt: No TNL values exist. RVT values exist for all PGA and M. TNL values P1, BE exist for all PGA and M.
- Mühleberg: No TNL values exist. RVT values exist for all PGA and M. TNL values P1, BE exist for all PGA and M.

Assumption (with P4 where a fourth profile is available):

$$\frac{amp_{TNL_{n,BE/UB/LB,P2/P3/P4}}}{amp_{TNL_{n,BE/UB/LB,P1}}} = \frac{amp_{RVT_{n,BE/UB/LB,P2/P3/P4}}}{amp_{RVT_{n,BE/UB/LB,P1}}} \tag{V-1.12}$$

and for Gösgen:

$$\frac{amp_{TNL_{n,BE/UB/LB,P1/P2/P3/P4/P5}}}{amp_{TNL_{n,BE/UB/LB,P6}}} = \frac{amp_{SHAKE_{n,BE/UB/LB,P1/P2/P3/P4/P5}}}{amp_{SHAKE_{n,BE/UB/LB,P6}}} \tag{V-1.13}$$

1.2.5 Beznau Horizontal

Overview of performed Calculations

Table V-1.3 shows the performed calculations.

Method	Profile	Material	Magnitude 5									Magnitude 6									Magnitude 7								
			0.05g	0.10g	0.20g	0.30g	0.40g	0.75g	1.00g	1.25g	1.50g	0.05g	0.10g	0.20g	0.30g	0.40g	0.75g	1.00g	1.25g	1.50g	2.50g	0.05g	0.10g	0.20g	0.30g	0.40g	0.75g	1.00g	1.25g	1.50g
EQL	P1	LB	10	10	10		10	10				9	9	9		9	9					10	10	10		10	10			
EQL	P1	BE	10	10	10		10	10				9	9	9		9	9					10	10	10		10	10			
EQL	P1	UB	10	10	10		10	10				9	9	9		9	9					10	10	10		10	10			
EQL	P2	LB	10	10	10		10	10				9	9	9		9	9					10	10	10		10	10			
EQL	P2	BE	10	10	10		10	10				9	9	9		9	9					10	10	10		10	10			
EQL	P2	UB	10	10	10		10	10				9	9	9		9	9					10	10	10		10	10			
EQL	P3	LB	10	10	10		10	10				9	9	9		9	9					10	10	10		10	10			
EQL	P3	BE	10	10	10		10	10				9	9	9		9	9					10	10	10		10	10			
EQL	P3	UB	10	10	10		10	10				9	9	9		9	9					10	10	10		10	10			
EQL	P4	LB	10	10	10		10	10				9	9	9		9	9					10	10	10		10	10			
EQL	P4	BE	10	10	10		10	10				9	9	9		9	9					10	10	10		10	10			
EQL	P4	UB	10	10	10		10	10				9	9	9		9	9					10	10	10		10	10			
RVTbc	P1	LB	1	1	1	1	1	1	1		1	1	1	1	1	1	1	1		1		1	1	1	1	1	1	1		1
RVTbc	P1	BE	1	1	1	1	1	1	1		1	1	1	1	1	1	1	1		1		1	1	1	1	1	1	1		1
RVTbc	P1	UB	1	1	1	1	1	1	1		1	1	1	1	1	1	1	1		1		1	1	1	1	1	1	1		1
RVTrand	P1	BE	50	50	50	50	50	50	50		50	50	50	50	50	50	50	50		50		50	50	50	50	50	50	50		50
RVTbc	P2	LB	1	1	1	1	1	1	1		1	1	1	1	1	1	1	1		1		1	1	1	1	1	1	1		1
RVTbc	P2	BE	1	1	1	1	1	1	1		1	1	1	1	1	1	1	1		1		1	1	1	1	1	1	1		1
RVTbc	P2	UB	1	1	1	1	1	1	1		1	1	1	1	1	1	1	1		1		1	1	1	1	1	1	1		1
RVTrand	P2	BE	50	50	50	50	50	50	50		50	50	50	50	50	50	50	50		50		50	50	50	50	50	50	50		50
RVTbc	P3	LB	1	1	1	1	1	1	1		1	1	1	1	1	1	1	1		1		1	1	1	1	1	1	1		1
RVTbc	P3	BE	1	1	1	1	1	1	1		1	1	1	1	1	1	1	1		1		1	1	1	1	1	1	1		1
RVTbc	P3	UB	1	1	1	1	1	1	1		1	1	1	1	1	1	1	1		1		1	1	1	1	1	1	1		1
RVTrand	P3	BE	50	50	50	50	50	50	50		50	50	50	50	50	50	50	50		50		50	50	50	50	50	50	50		50
RVTbc	P4	LB	1	1	1	1	1	1	1		1	1	1	1	1	1	1	1		1		1	1	1	1	1	1	1		1
RVTbc	P4	BE	1	1	1	1	1	1	1		1	1	1	1	1	1	1	1		1		1	1	1	1	1	1	1		1
RVTbc	P4	UB	1	1	1	1	1	1	1		1	1	1	1	1	1	1	1		1		1	1	1	1	1	1	1		1
RVTrand	P4	BE	50	50	50	50	50	50	50		50	50	50	50	50	50	50	50		50		50	50	50	50	50	50	50		50
NL1	P1	LB															9			9										
NL1	P1	BE					10	10			10	9				9	9			9						10	10			10
NL1	P1	UB															9			9	9									
NL2	P1	BE															9													

Figure V-1.3: Overview of calculations performed for Beznau.

V_S-profiles

Figure V-1.4 shows the soil investigation data and the evaluated soil profiles, Figure V-1.5 shows the finally used V_S-Profiles.

Table V-1.3: Weights for the profiles.

Profile	Weights	Rational
P 1	0.40	Represents best the data (direct measurements)
P 2	0.25	In the weathered opalinus clay more details are taken into account
P 3	0.10	Based mainly on ambient vibrations
P 4	0.25	Represents the data well

Strains

Figure V-1.6 shows the strain produced by the different methods in the different profiles.

Logic Tree for Beznau

The logic tree in Figure V-1.1 is valid for all elevations. The weights are given in Figures V-1.2(a) and V-1.2(b). No 2-D effects taken into account.

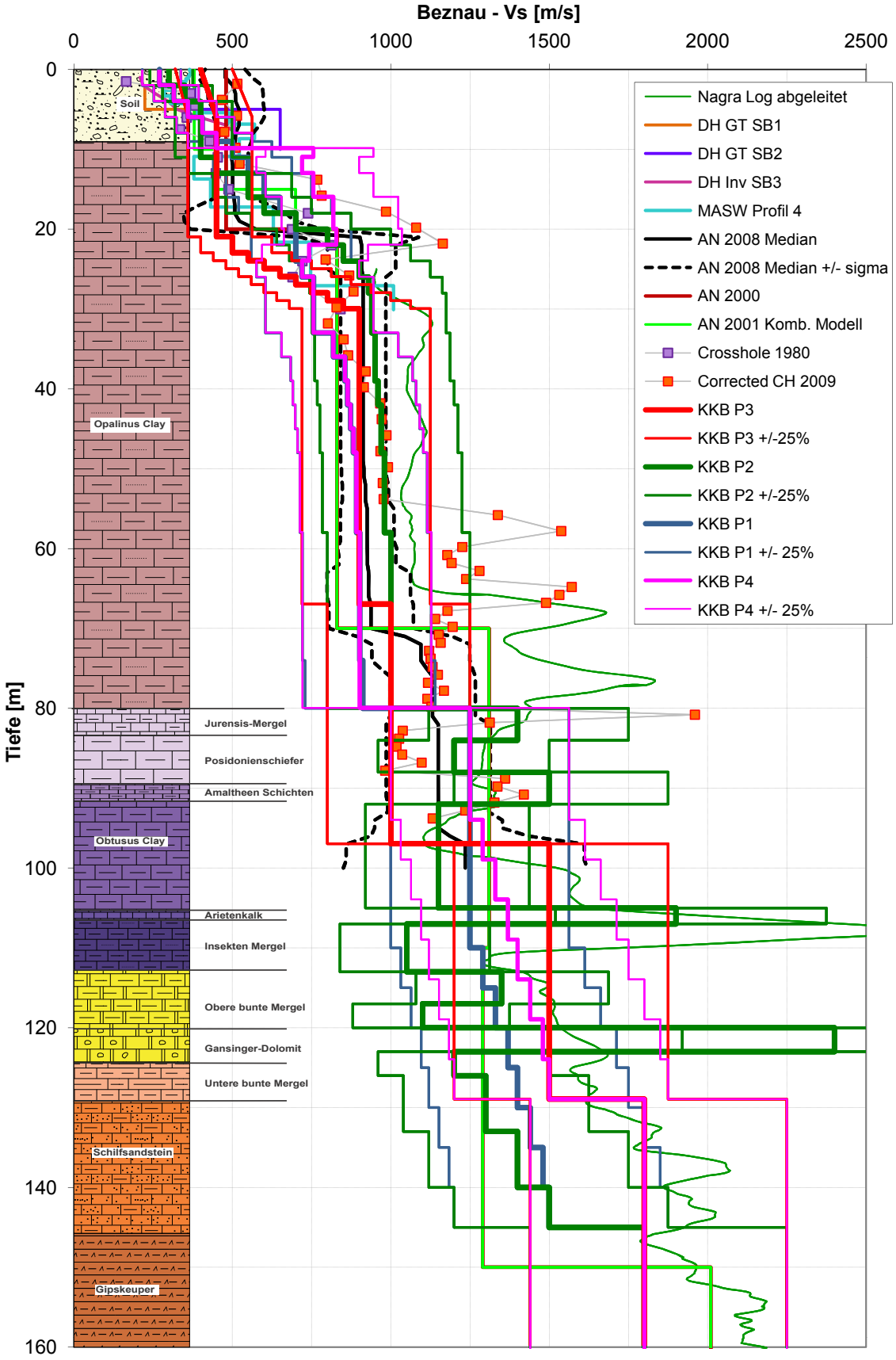

Figure V-1.4: Geological profile, V_S-results and V_S-profiles of Beznau.

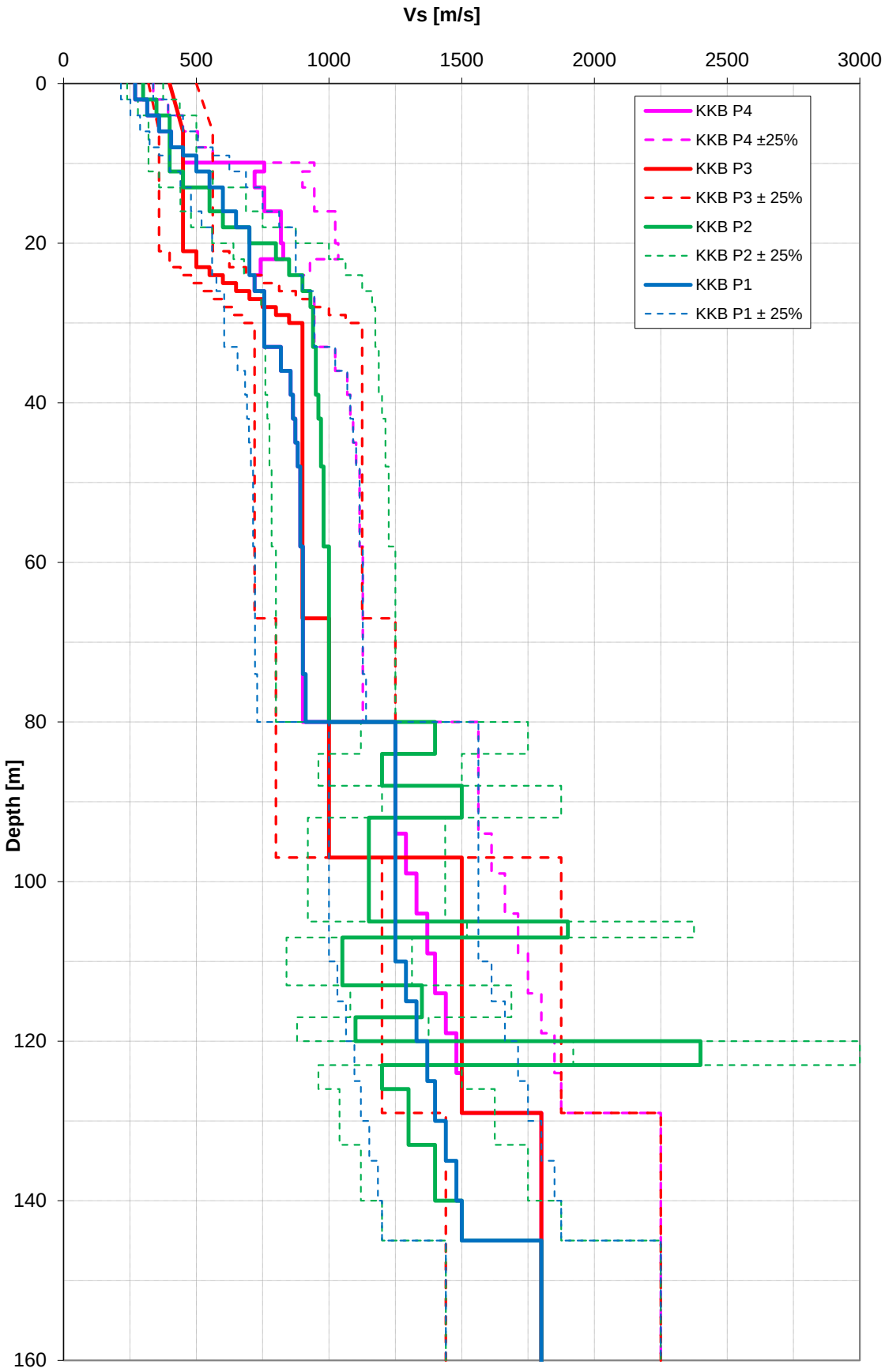

Figure V-1.5: Beznau V_S-profiles.

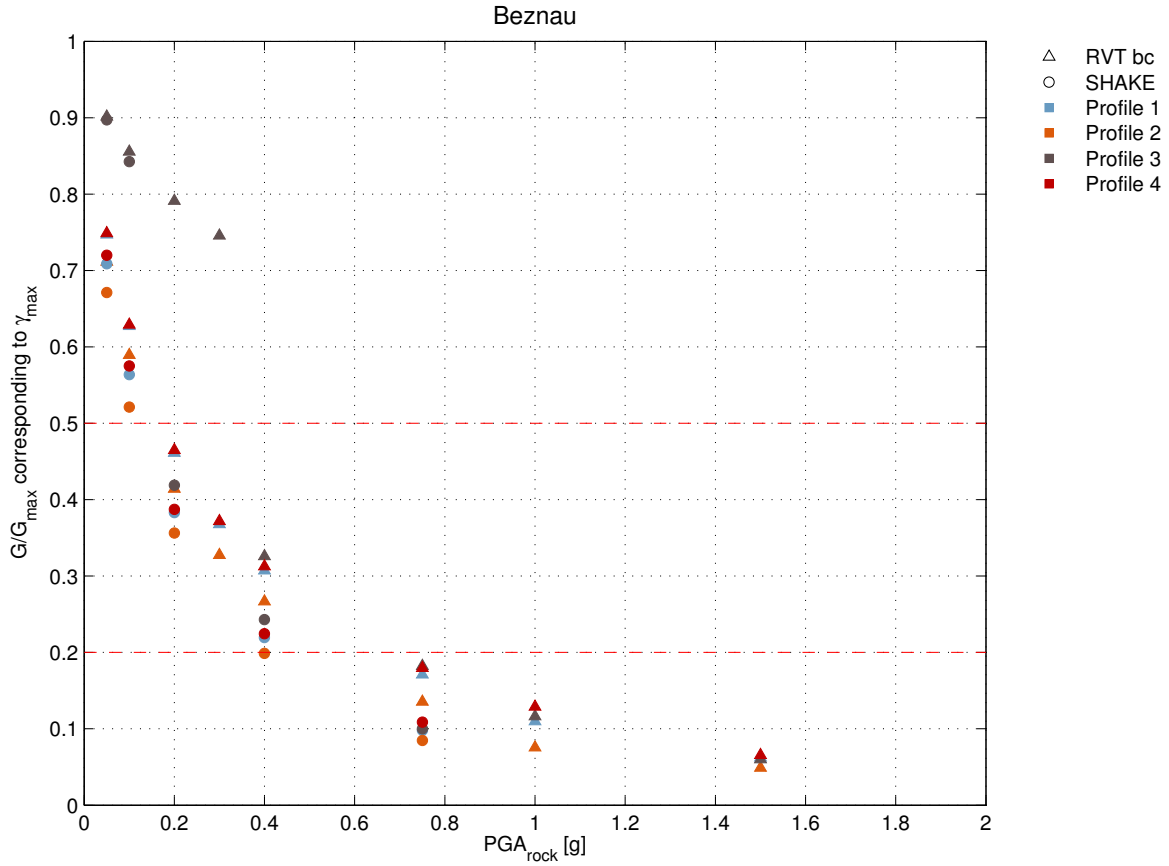

Figure V-1.6: Strains for Beznau profiles. Note: The color legend shows more profiles than available for the site.

1.2.6 E-Beznau Horizontal

Performed Calculations and Acquisition of Missing Values

This section is valid for all elevations.

Method	Profile	Material	Magnitude 5									Magnitude 6										Magnitude 7								
			0.05g	0.10g	0.20g	0.30g	0.40g	0.75g	1.00g	1.25g	1.50g	0.05g	0.10g	0.20g	0.30g	0.40g	0.75g	1.00g	1.25g	1.50g	2.50g	0.05g	0.10g	0.20g	0.30g	0.40g	0.75g	1.00g	1.25g	1.50g
EQL	P1	LB	10	10	10		10	10				9	9	9		9	9					10	10	10		10	10			
EQL	P1	BE	10	10	10		10	10				9	9	9		9	9					10	10	10		10	10			
EQL	P1	UB	10	10	10		10	10				9	9	9		9	9					10	10	10		10	10			
EQL	P2	LB	10	10	10		10	10				9	9	9		9	9					10	10	10		10	10			
EQL	P2	BE	10	10	10		10	10				9	9	9		9	9					10	10	10		10	10			
EQL	P2	UB	10	10	10		10	10				9	9	9		9	9					10	10	10		10	10			
EQL	P3	LB	10	10	10		10	10				9	9	9		9	9					10	10	10		10	10			
EQL	P3	BE	10	10	10		10	10				9	9	9		9	9					10	10	10		10	10			
EQL	P3	UB	10	10	10		10	10				9	9	9		9	9					10	10	10		10	10			
RVTbc	P1	LB	1	1	1	1	1	1	1		1	1	1	1	1	1	1	1		1		1	1	1	1	1	1	1		1
RVTbc	P1	BE	1	1	1	1	1	1	1		1	1	1	1	1	1	1	1		1		1	1	1	1	1	1	1		1
RVTbc	P1	UB	1	1	1	1	1	1	1		1	1	1	1	1	1	1	1		1		1	1	1	1	1	1	1		1
RVTrand	P1	BE	50	50	50	50	50	50	50		50	50	50	50	50	50	50	50		50		50	50	50	50	50	50	50		50
RVTbc	P2	LB	1	1	1	1	1	1	1		1	1	1	1	1	1	1	1		1		1	1	1	1	1	1	1		1
RVTbc	P2	BE	1	1	1	1	1	1	1		1	1	1	1	1	1	1	1		1		1	1	1	1	1	1	1		1
RVTbc	P2	UB	1	1	1	1	1	1	1		1	1	1	1	1	1	1	1		1		1	1	1	1	1	1	1		1
RVTrand	P2	BE	50	50	50	50	50	50	50		50	50	50	50	50	50	50	50		50		50	50	50	50	50	50	50		50
RVTbc	P3	LB	1	1	1	1	1	1	1		1	1	1	1	1	1	1	1		1		1	1	1	1	1	1	1		1
RVTbc	P3	BE	1	1	1	1	1	1	1		1	1	1	1	1	1	1	1		1		1	1	1	1	1	1	1		1
RVTbc	P3	UB	1	1	1	1	1	1	1		1	1	1	1	1	1	1	1		1		1	1	1	1	1	1	1		1
RVTrand	P3	BE	50	50	50	50	50	50	50		50	50	50	50	50	50	50	50		50		50	50	50	50	50	50	50		50
NL1	P1	LB															9			9										
NL1	P1	BE					10	10			10	9				9	9			9						10	10			10
NL1	P1	UB															9			9	9									
NL2	P1	BE															9													

Figure V-1.7: Overview of calculations performed for E-Beznau.

V_S-profiles

Table V-1.4: Weights for the profiles.

Profile	Weights	Rational
P 1	0.4	Best representation of measured data,
P 2	0.35	More details in the opalinus clay are taken into account
P 3	0.25	Based mainly on ambient vibrations

Strains

Figure V-1.10 shows the strain produced by the different methods in the different profiles.

Logic Tree for E-Beznau

The logic tree in Figure V-1.1 is valid for all elevations. The weights are given in Figures V-1.2(a) and V-1.2(b). No 2-D effects taken into account.

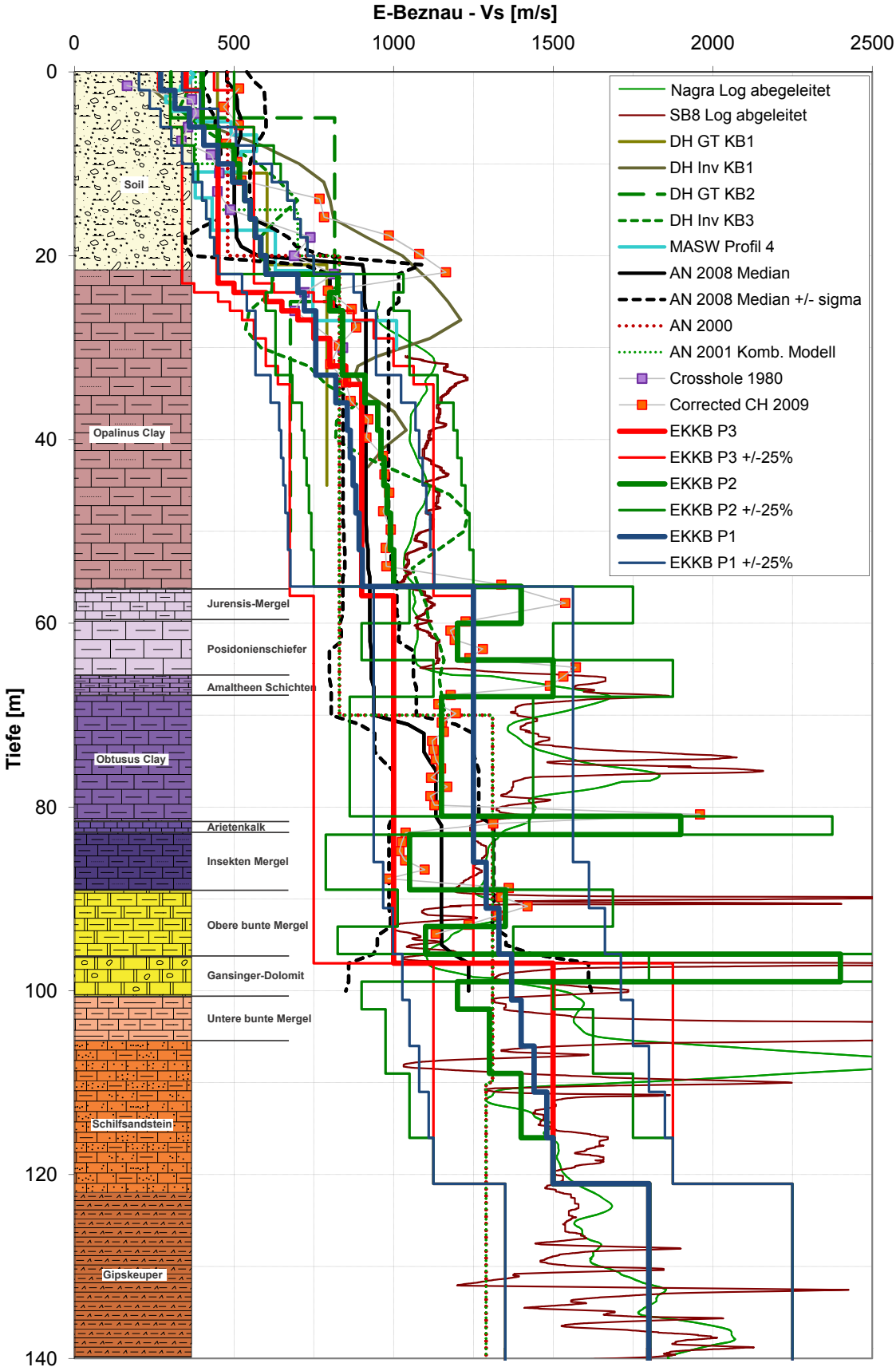

Figure V-1.8: Geological profile, V_S-results and V_S-profiles of E-Beznau.

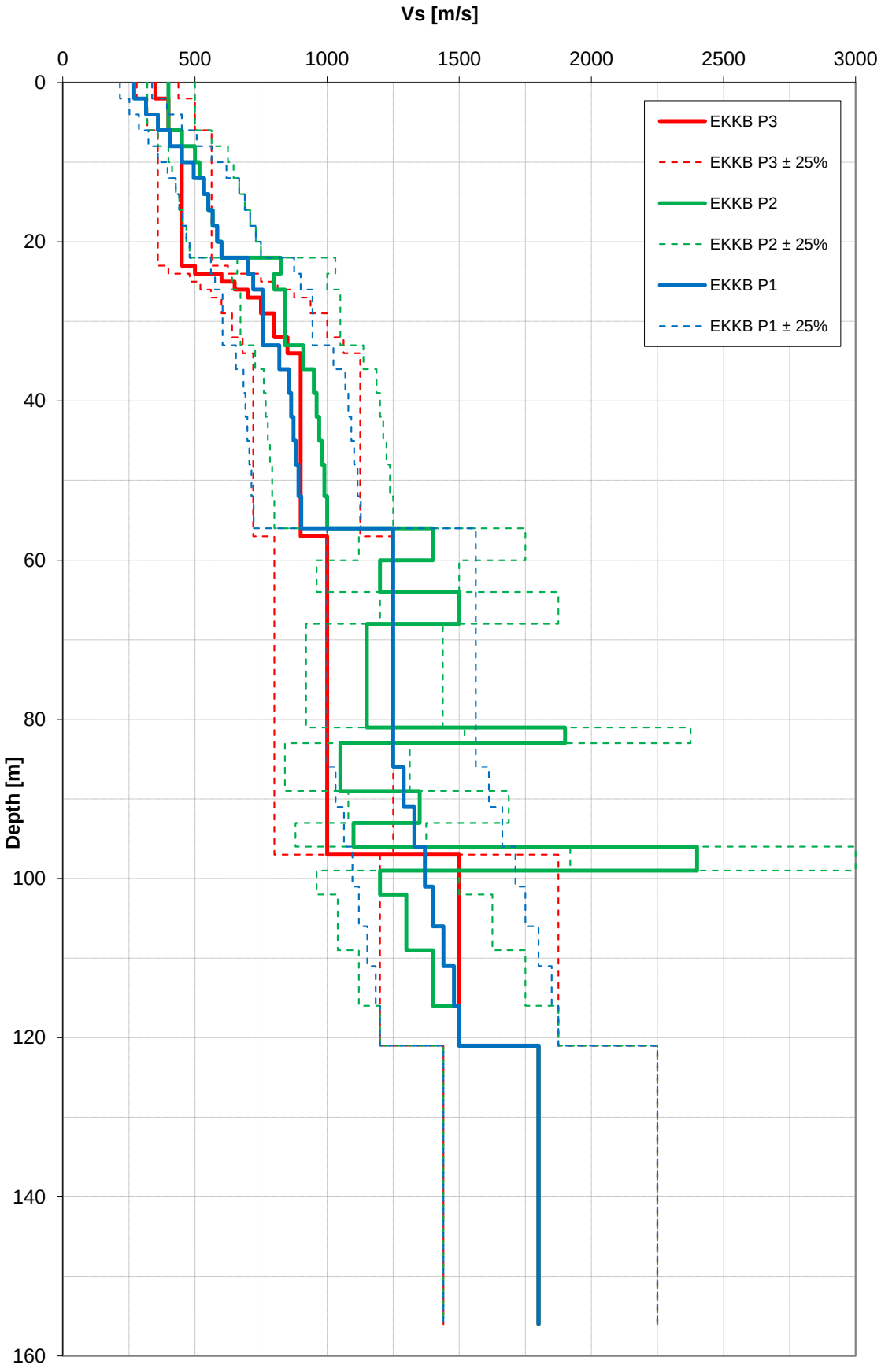

Figure V-1.9: E-Beznau V_S-profiles.

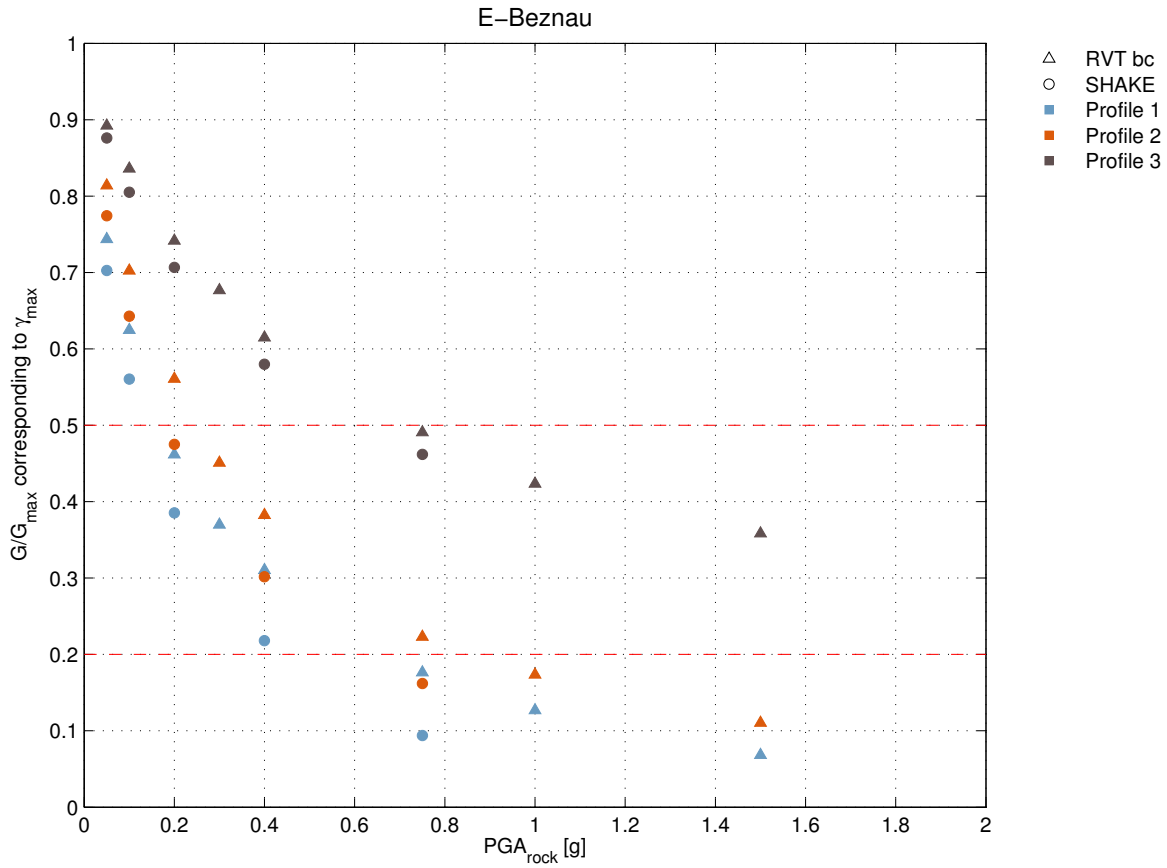

Figure V-1.10: Strains for E-Beznau profiles. Note: The color legend shows more profiles than available for the site.

1.2.7 Gösgen Horizontal

Performed Calculations and Acquisition of Missing Values

Method	Profile	Material	Magnitude 5										Magnitude 6										Magnitude 7									
			0.05g	0.10g	0.20g	0.30g	0.40g	0.75g	1.00g	1.25g	1.50g	2.50g	0.05g	0.10g	0.20g	0.30g	0.40g	0.75g	1.00g	1.25g	1.50g	2.50g	0.05g	0.10g	0.20g	0.30g	0.40g	0.75g	1.00g	1.25g	1.50g	2.50g
EQL	P1	LB	10	10	10		10	10	10		10	10	9	9	9		9	9	9		9	9	10	10	10		10	10	10		10	10
EQL	P1	BE	10	10	10		10	10	10		10	10	9	9	9		9	9	9		9	9	10	10	10		10	10	10		10	10
EQL	P1	UB	10	10	10		10	10	10		10	10	9	9	9		9	9	9		9	9	10	10	10		10	10	10		10	10
EQL	P2	LB	10	10	10		10	10	10		10	10	9	9	9		9	9	9		9	9	10	10	10		10	10	10		10	10
EQL	P2	BE	10	10	10		10	10	10		10	10	9	9	9		9	9	9		9	9	10	10	10		10	10	10		10	10
EQL	P2	UB	10	10	10		10	10	10		10	10	9	9	9		9	9	9		9	9	10	10	10		10	10	10		10	10
EQL	P3	LB	10	10	10		10	10	10		10	10	9	9	9		9	9	9		9	9	10	10	10		10	10	10		10	10
EQL	P3	BE	10	10	10		10	10	10		10	10	9	9	9		9	9	9		9	9	10	10	10		10	10	10		10	10
EQL	P3	UB	10	10	10		10	10	10		10	10	9	9	9		9	9	9		9	9	10	10	10		10	10	10		10	10
EQL	P4	LB	10	10	10		10	10	10		10	10	9	9	9		9	9	9		9	9	10	10	10		10	10	10		10	10
EQL	P4	BE	10	10	10		10	10	10		10	10	9	9	9		9	9	9		9	9	10	10	10		10	10	10		10	10
EQL	P4	UB	10	10	10		10	10	10		10	10	9	9	9		9	9	9		9	9	10	10	10		10	10	10		10	10
EQL	P5	LB	10	10	10		10	10	10		10	10	9	9	9		9	9	9		9	9	10	10	10		10	10	10		10	10
EQL	P5	BE	10	10	10		10	10	10		10	10	9	9	9		9	9	9		9	9	10	10	10		10	10	10		10	10
EQL	P5	UB	10	10	10		10	10	10		10	10	9	9	9		9	9	9		9	9	10	10	10		10	10	10		10	10
EQL	P6	LB	10	10	10		10	10	10		10	10	9	9	9		9	9	9		9	9	10	10	10		10	10	10		10	10
EQL	P6	BE	10	10	10		10	10	10		10	10	9	9	9		9	9	9		9	9	10	10	10		10	10	10		10	10
EQL	P6	UB	10	10	10		10	10	10		10	10	9	9	9		9	9	9		9	9	10	10	10		10	10	10		10	10
RVTbc	P1	LB	1	1	1	0	1	1	0		1		1	1	1	0	1	1	0		1		1	1	1	0	1	1	0		1	
RVTbc	P1	BE	1	1	1	0	1	1	0		1		1	1	1	0	1	1	0		1		1	1	1	0	1	1	0		1	
RVTbc	P1	UB	1	1	1	0	1	1	0		1		1	1	1	0	1	1	0		1		1	1	1	0	1	1	0		1	
RVTrand	P1	BE	50	50	50	0	50	50	0		50		50	50	50	0	50	50	0		50		50	50	50	0	50	50	0		50	
RVTbc	P2	LB	1	1	1	0	1	1	0		1		1	1	1	0	1	1	0		1		1	1	1	0	1	1	0		1	
RVTbc	P2	BE	1	1	1	0	1	1	0		1		1	1	1	0	1	1	0		1		1	1	1	0	1	1	0		1	
RVTbc	P2	UB	1	1	1	0	1	1	0		1		1	1	1	0	1	1	0		1		1	1	1	0	1	1	0		1	
RVTrand	P2	BE	50	50	50	0	50	50	0		50		50	50	50	0	50	50	0		50		50	50	50	0	50	50	0		50	
RVTbc	P3	LB	1	1	1	0	1	1	0		1		1	1	1	0	1	1	0		1		1	1	1	0	1	1	0		1	
RVTbc	P3	BE	1	1	1	0	1	1	0		1		1	1	1	0	1	1	0		1		1	1	1	0	1	1	0		1	
RVTbc	P3	UB	1	1	1	0	1	1	0		1		1	1	1	0	1	1	0		1		1	1	1	0	1	1	0		1	
RVTrand	P3	BE	50	50	50	0	50	50	0		50		50	50	50	0	50	50	0		50		50	50	50	0	50	50	0		50	
RVTbc	P4	LB	1	1	1	0	1	1	0		1		1	1	1	0	1	1	0		1		1	1	1	0	1	1	0		1	
RVTbc	P4	BE	1	1	1	0	1	1	0		1		1	1	1	0	1	1	0		1		1	1	1	0	1	1	0		1	
RVTbc	P4	UB	1	1	1	0	1	1	0		1		1	1	1	0	1	1	0		1		1	1	1	0	1	1	0		1	
RVTrand	P4	BE	50	50	50	0	50	50	0		50		50	50	50	0	50	50	0		50		50	50	50	0	50	50	0		50	
RVTbc	P5	LB	1	1	1	0	1	1	0		1		1	1	1	0	1	1	0		1		1	1	1	0	1	1	0		1	
RVTbc	P5	BE	1	1	1	0	1	1	0		1		1	1	1	0	1	1	0		1		1	1	1	0	1	1	0		1	
RVTbc	P5	UB	1	1	1	0	1	1	0		1		1	1	1	0	1	1	0		1		1	1	1	0	1	1	0		1	
RVTrand	P5	BE	50	50	50	0	50	50	0		50		50	50	50	0	50	50	0		50		50	50	50	0	50	50	0		50	
RVT	P6																															
NL1	P6	LB																9			9											
NL1	P6	BE					10	10			10		9				9	9			9						10	10			10	
NL1	P6	UB																9			9	9										
NL2	P6	BE																9														
NL3	P6	BE											9																			
NL4	P6	BE											9					9														

Note: For Gösgen the case NL4 is corresponding to the case "NL2" (= cross check by another contractor) at the other sites.
NL2 is the "2 Phase" and NL3 is the "Elastic" sensitivity computation of Géodynamique et Structures

Figure V-1.11: Overview of calculations performed for Gösgen.

V_S-profiles

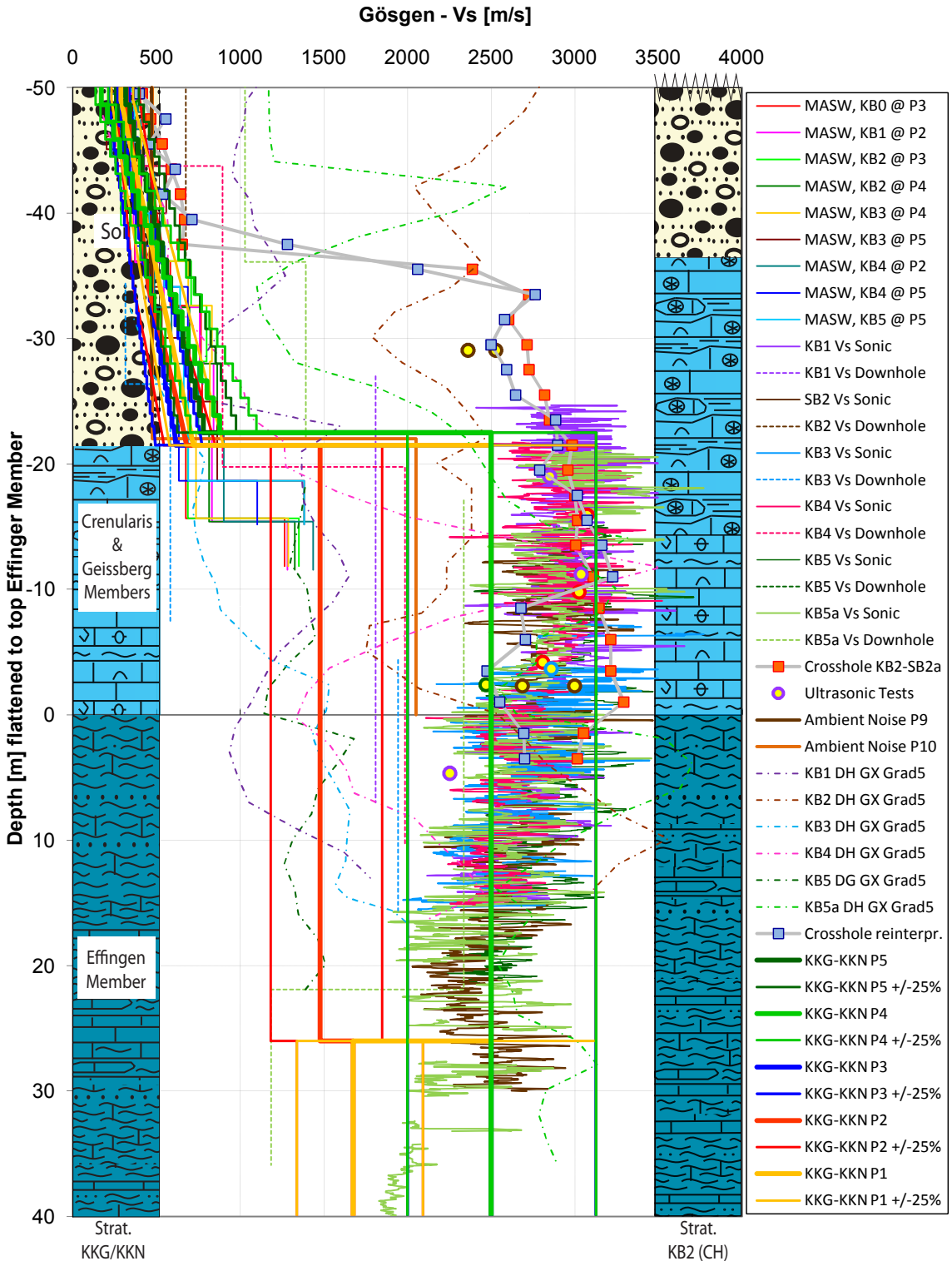

Figure V-1.12: Geological profile, V_S-results and V_S-profiles of Gösgen (lower profiles).

Strains

Figure V-1.16 shows the strain produced by the different methods in the different profiles.

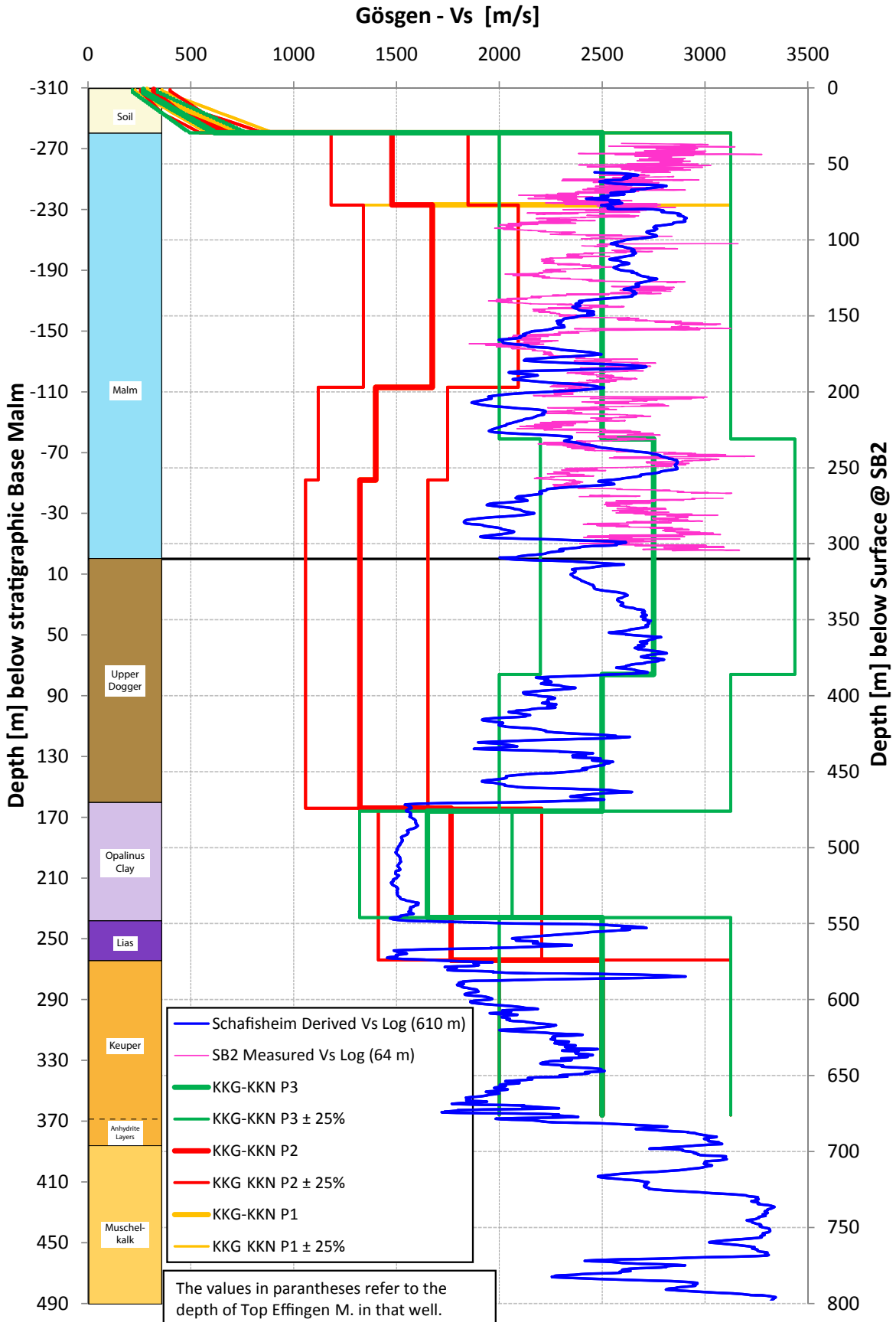

Figure V-1.13: Geological profile, V_S-results and V_S-profiles of Gösgen (deeper profiles).

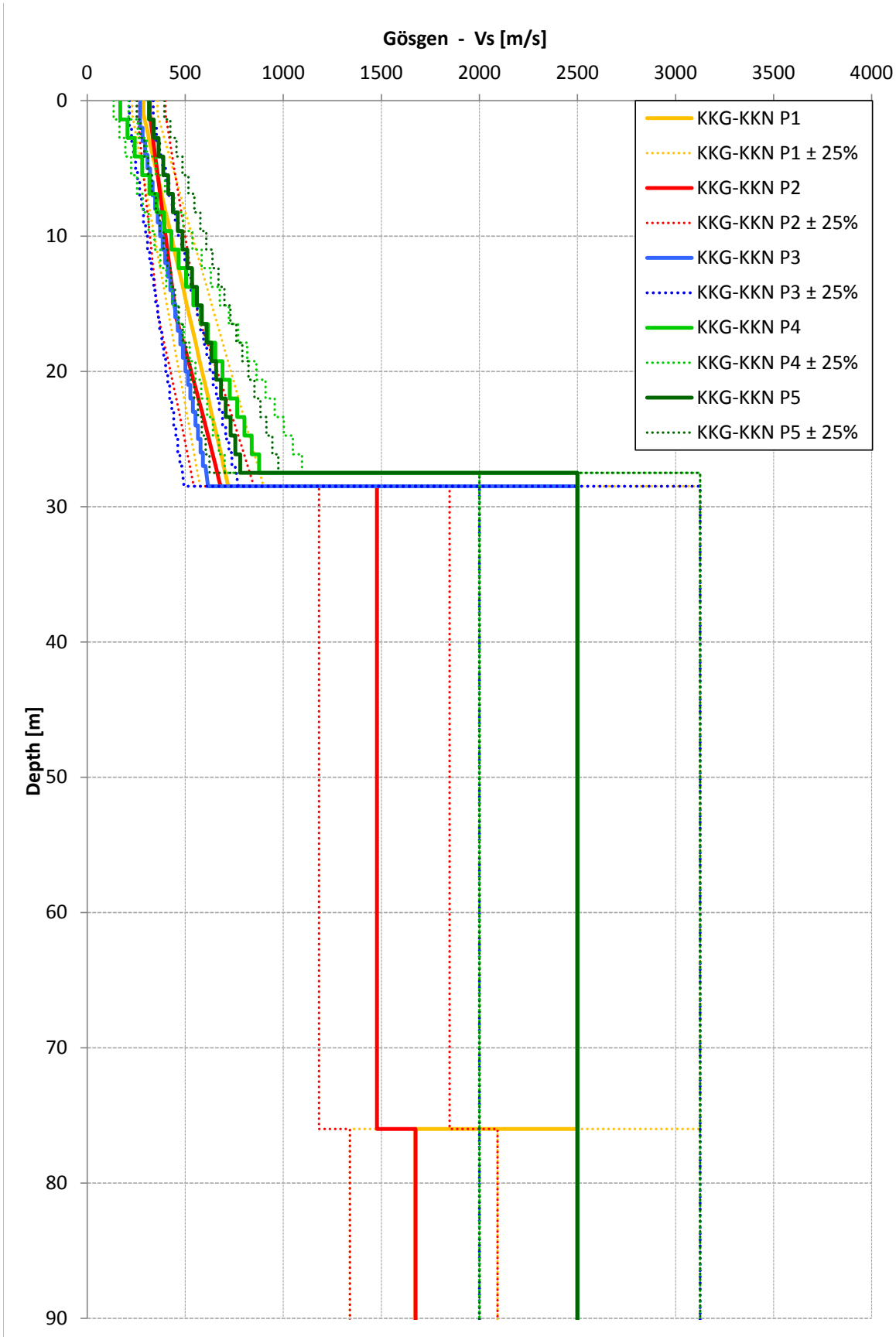

Figure V-1.14: V_S-profiles of Gösgen (shallower profiles).

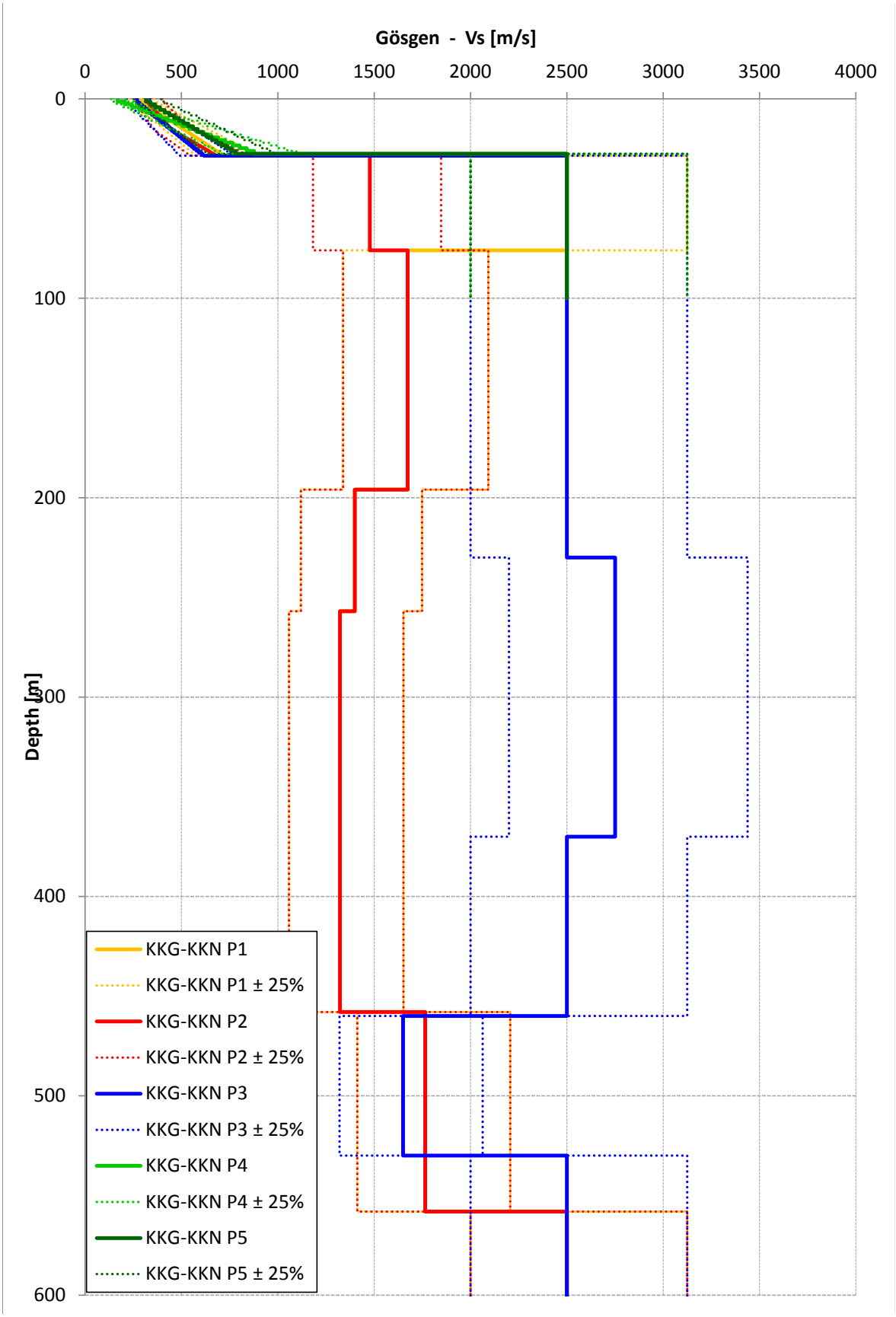

Figure V-1.15: V_S-profiles of Gösgen (deeper profiles).

Table V-1.5: Weights for the profiles.

Profile	Weights	Rational
P 1	0.2	As group the shallow (P4-P6) and deep (P1-P3)
P 2	0.2	profiles have the same weight (50%).
P 3	0.1	P3 gets lower weight, as its origin is an off-site profile
P 4	0.2	P1 is considered as best profile, it represents the measured data best.
P 5	0.2	P1 and P6 are in the upper part equal therefore their weights
P 6	0.1	are adjusted to be combined 0.30.

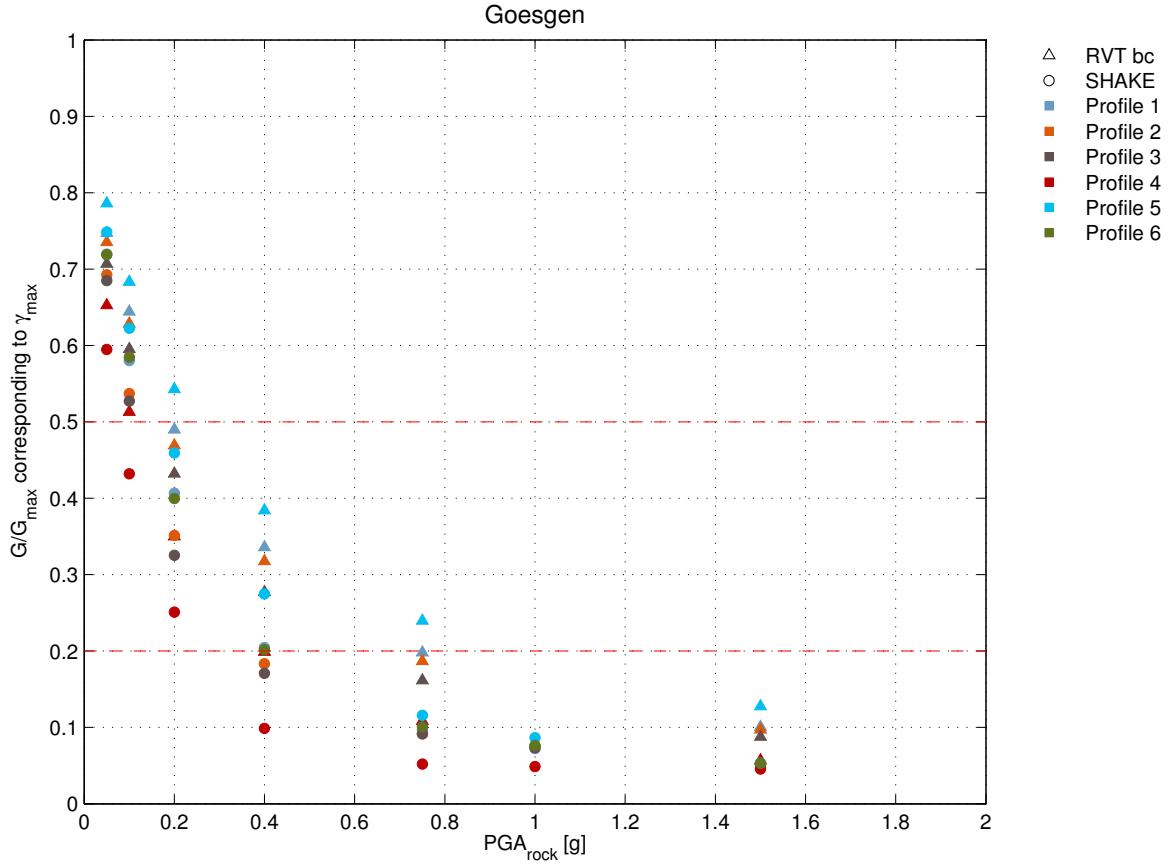

Figure V-1.16: Strains for Gösgen profiles.

Logic Tree for Gösgen

The logic tree in Figure V-1.1 is valid for all elevations. The weights are given in Figures V-1.2(a) and V-1.2(b). No 2-D effects taken into account.

1.2.8 Leibstadt Horizontal

Performed Calculations and Acquisition of Missing Values

Method	Profile	Material	Magnitude 5									Magnitude 6										Magnitude 7									
			0.05g	0.10g	0.20g	0.30g	0.40g	0.75g	1.00g	1.25g	1.50g	0.05g	0.10g	0.20g	0.30g	0.40g	0.75g	1.00g	1.25g	1.50g	2.50g	0.05g	0.10g	0.20g	0.30g	0.40g	0.75g	1.00g	1.25g	1.50g
EQL	P1	LB	10	10	10		10	10				9	9	9		9	9					10	10	10		10	10			
EQL	P1	BE	10	10	10		10	10				9	9	9		9	9					10	10	10		10	10			
EQL	P1	UB	10	10	10		10	10				9	9	9		9	9					10	10	10		10	10			
EQL	P2	LB	10	10	10		10	10				9	9	9		9	9					10	10	10		10	10			
EQL	P2	BE	10	10	10		10	10				9	9	9		9	9					10	10	10		10	10			
EQL	P2	UB	10	10	10		10	10				9	9	9		9	9					10	10	10		10	10			
EQL	P3	LB	10	10	10		10	10				9	9	9		9	9					10	10	10		10	10			
EQL	P3	BE	10	10	10		10	10				9	9	9		9	9					10	10	10		10	10			
EQL	P3	UB	10	10	10		10	10				9	9	9		9	9					10	10	10		10	10			
RVTbc	P1	LB	1	1	1	1	1	1	1		1	1	1	1	1	1	1	1		1		1	1	1	1	1	1	1		1
RVTbc	P1	BE	1	1	1	1	1	1	1		1	1	1	1	1	1	1	1		1		1	1	1	1	1	1	1		1
RVTbc	P1	UB	1	1	1	1	1	1	1		1	1	1	1	1	1	1	1		1		1	1	1	1	1	1	1		1
RVTrand	P1	BE	50	50	50	50	50	50	50		50	50	50	50	50	50	50	50		50		50	50	50	50	50	50	50		50
RVTbc	P2	LB	1	1	1	1	1	1	1		1	1	1	1	1	1	1	1		1		1	1	1	1	1	1	1		1
RVTbc	P2	BE	1	1	1	1	1	1	1		1	1	1	1	1	1	1	1		1		1	1	1	1	1	1	1		1
RVTbc	P2	UB	1	1	1	1	1	1	1		1	1	1	1	1	1	1	1		1		1	1	1	1	1	1	1		1
RVTrand	P2	BE	50	50	50	50	50	50	50		50	50	50	50	50	50	50	50		50		50	50	50	50	50	50	50		50
RVTbc	P3	LB	1	1	1	1	1	1	1		1	1	1	1	1	1	1	1		1		1	1	1	1	1	1	1		1
RVTbc	P3	BE	1	1	1	1	1	1	1		1	1	1	1	1	1	1	1		1		1	1	1	1	1	1	1		1
RVTbc	P3	UB	1	1	1	1	1	1	1		1	1	1	1	1	1	1	1		1		1	1	1	1	1	1	1		1
RVTrand	P3	BE	50	50	50	50	50	50	50		50	50	50	50	50	50	50	50		50		50	50	50	50	50	50	50		50
NL1	P1	LB															9			9										
NL1	P1	BE					10	10			10	9				9	9			9						10	10			10
NL1	P1	UB															9			9	9									
NL2	P1	BE															9													

Figure V-1.17: Overview of calculations performed for Leibstadt.

Fig. 2 15:

Table V-1.6: Weights for the profiles.

Profile	Weights	Rational
P 1	0.4	All 3 profiles with similar weight,
P 2	0.3	profile 1 is best representation.
P 3	0.3	

Strains

Figure V-1.20 shows the strain produced by the different methods in the different profiles.

Logic Tree for Leibstadt

The logic tree in Figure V-1.1 is valid for all elevations. The weights are given in Figures V-1.2(a) and V-1.2(b). 2-D effects are taken into account. The original PEGASOS evaluation summary provides a more detailed justification for using the 2D effects at the Leibstadt site.

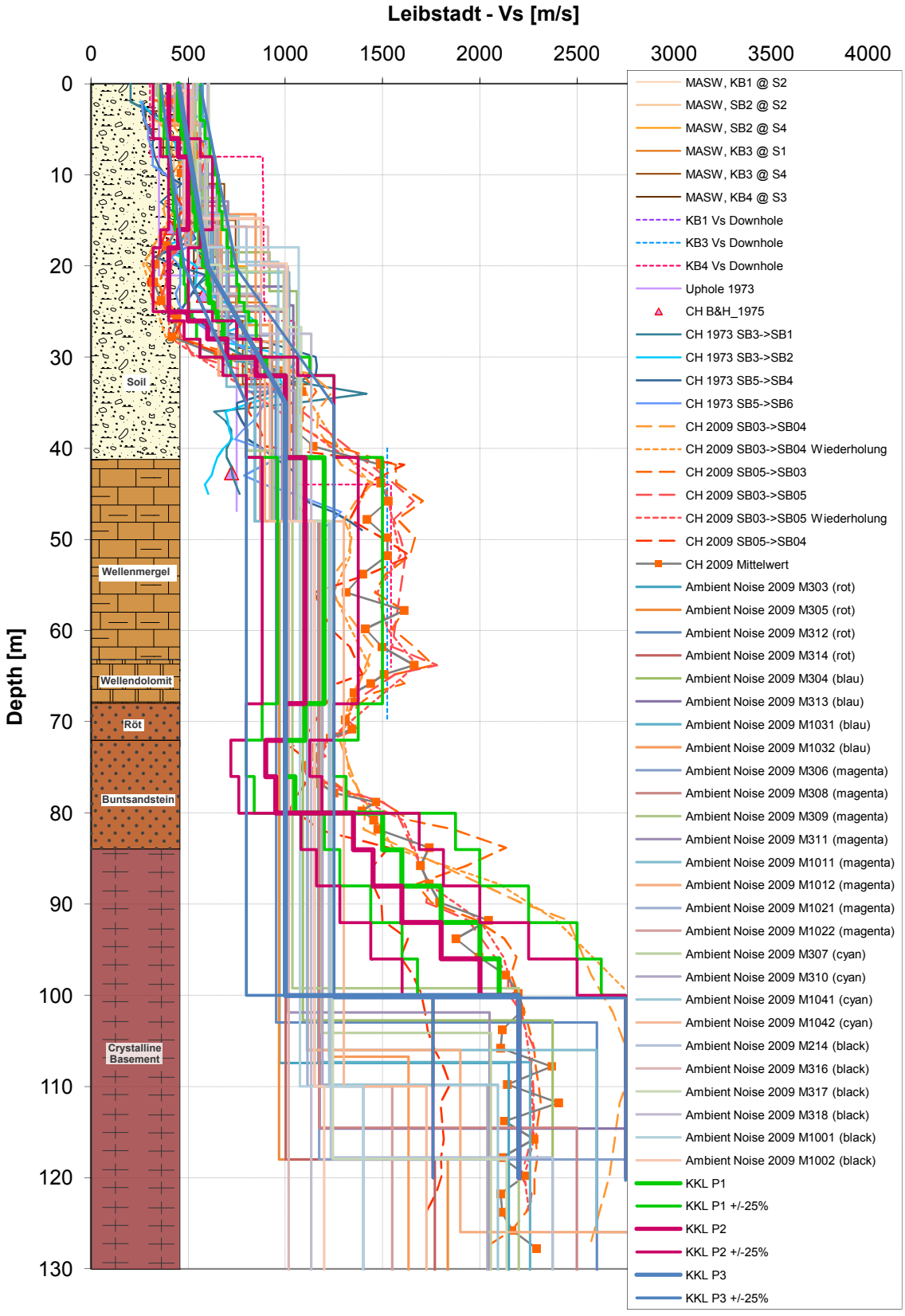

Figure V-1.18: Geological profile, V_S-results and V_S-profiles of Leibstadt.

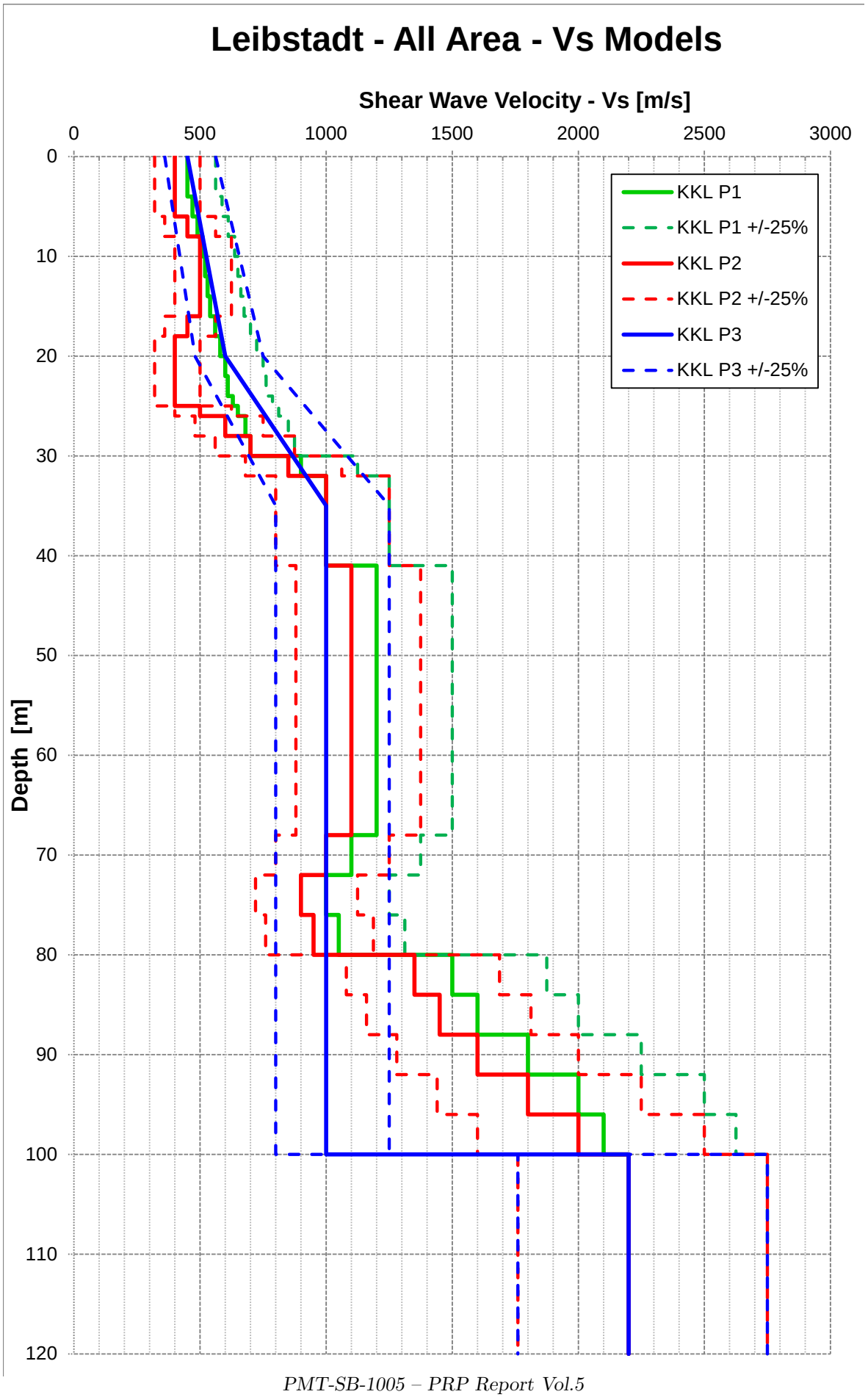

PMT-SB-1005 – PRP Report Vol.5

Figure V-1.19: V_S-profiles of Leibstadt.

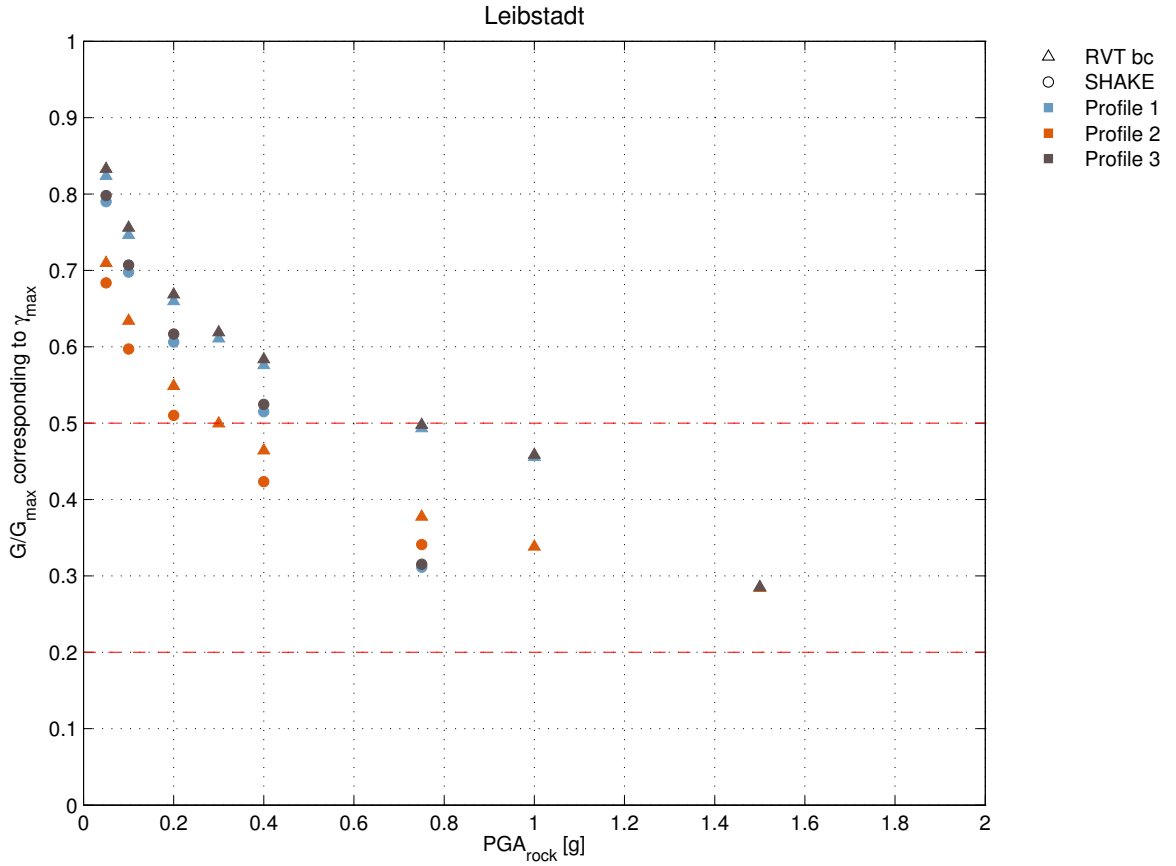

Figure V-1.20: Strains for Leibstadt profiles. Note: The color legend shows more profiles than available for the site.

Use of Results from 2-D Sensitivity Runs

Weights: 2D correction yes: 70%, 2D correction no: 30%

Rationale: Topographic situation suggests significant 2D effects at this site (Leibstadt NPP is located on a terrace).

The correction curves are derived from Bard [2002a] TP3-TN-0186. These curves describe the ratio between results from 2D and 1D calculation. Only measurements at the locations 10 to 19 are considered, since the relevant structures are situated within these locations.

Original curves from Bard [2002a] (TP3-TN-0186) (Low strain: 0.1 g, high strain curve: 0.4 g.) are represented in Figures V-1.21, V-1.22. The upper and lower envelopes including geometric and arithmetic mean values of these curves are shown in Figures V-1.23 , V-1.24.

- 2D correction rule:
  - PGA = 0.1 g: Take corresponding geometric mean from Figure V-1.23 for low strain
  - PGA = 0.4 g: Take corresponding geometric mean from Figure V-1.24 for high strain
  - Between 0.1 and 0.4 g: linear interpolation of the values.

– Above 0.4 g: take same values as for 0.4 g.

Rationale: The amplification effects of the 2D calculations from Bard (2002) show, that instead of one peak there are two peaks corresponding to the two fundamental periods located around 2.5 - 3.5 Hz and 6 - 8 Hz for the low strain range and 1 and 3 - 4 Hz for the high strain range. The 2D amplification is about 20 - 50% higher in the frequency range from 2.5 - 8 Hz and in average 20 - 25%. The geometric mean is selected to avoid too high weightings of extreme values. Calculations from Fäh [2002b] (TP3-TN-0240) are very similar. For my model, I rely on the 2D amplification factors from Bard.

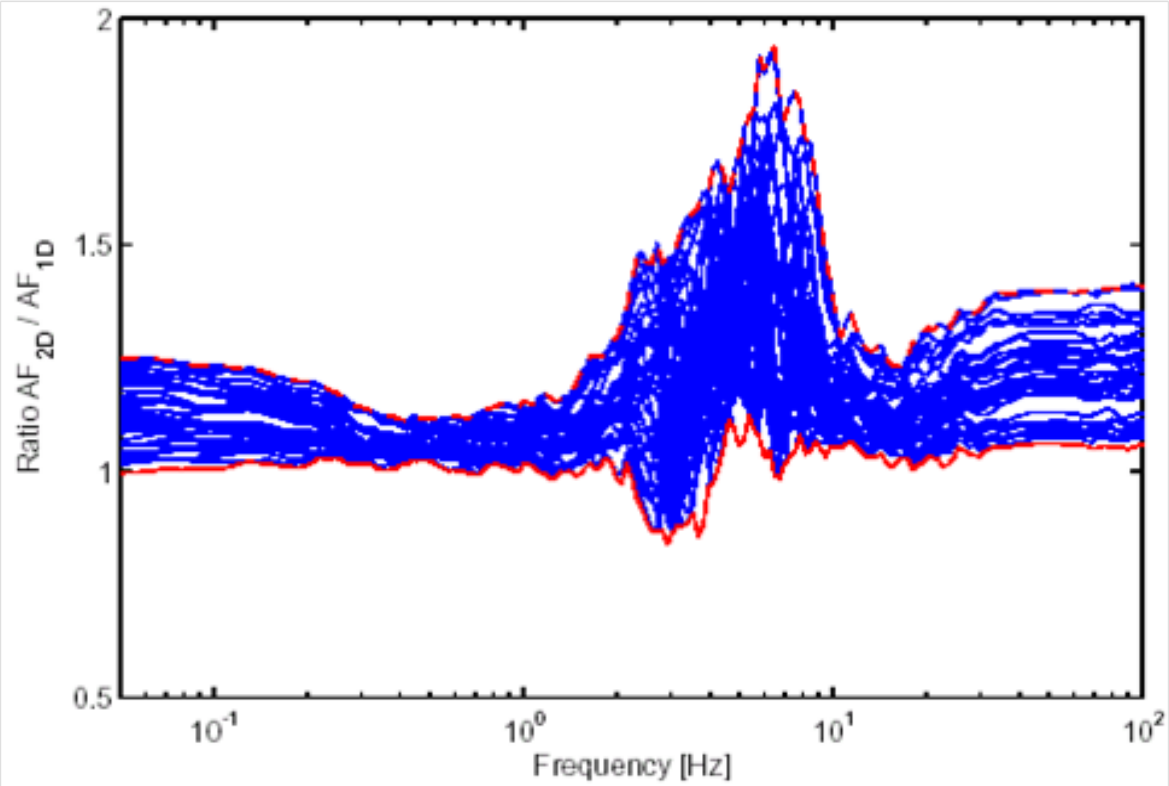

Figure V-1.21: Ratio 2D / 1D for low strain (0.1 g).

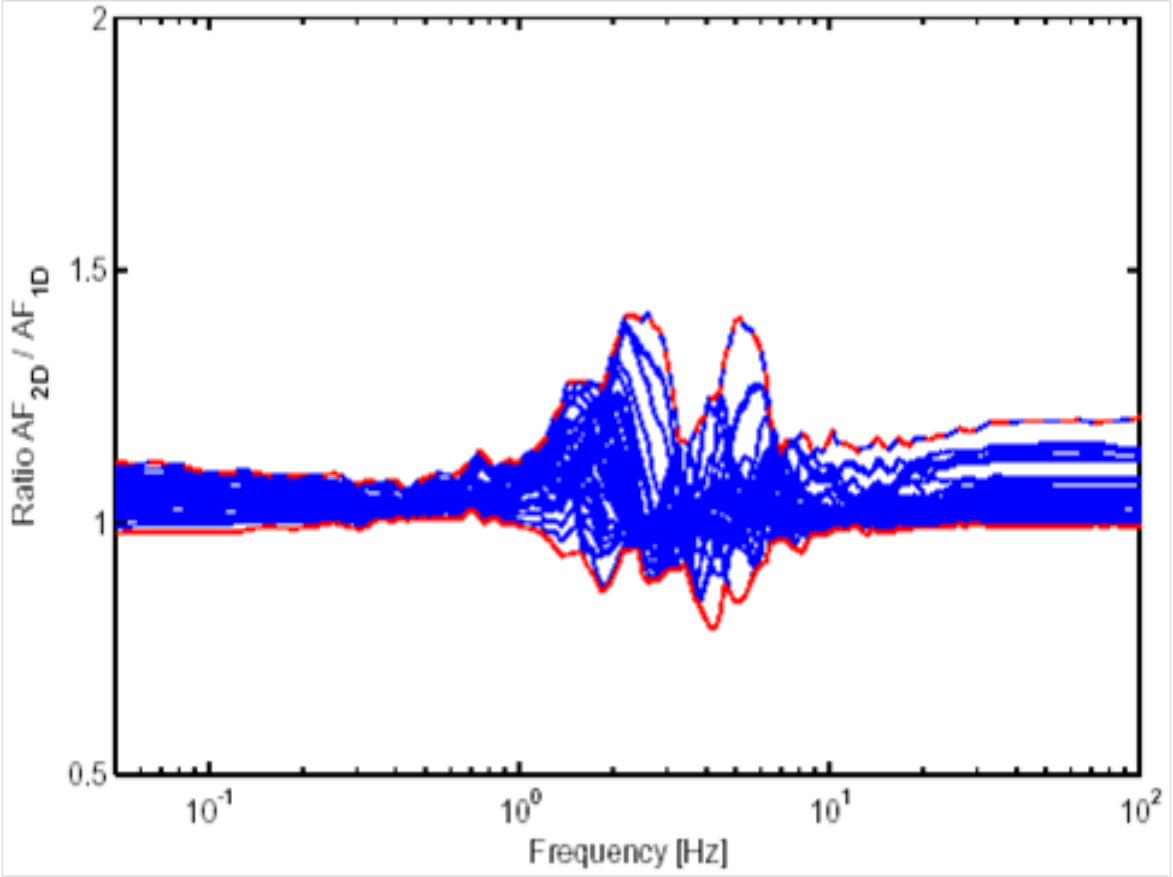

Figure V-1.22: Ratio 2D / 1D for high strain (0.4 g).

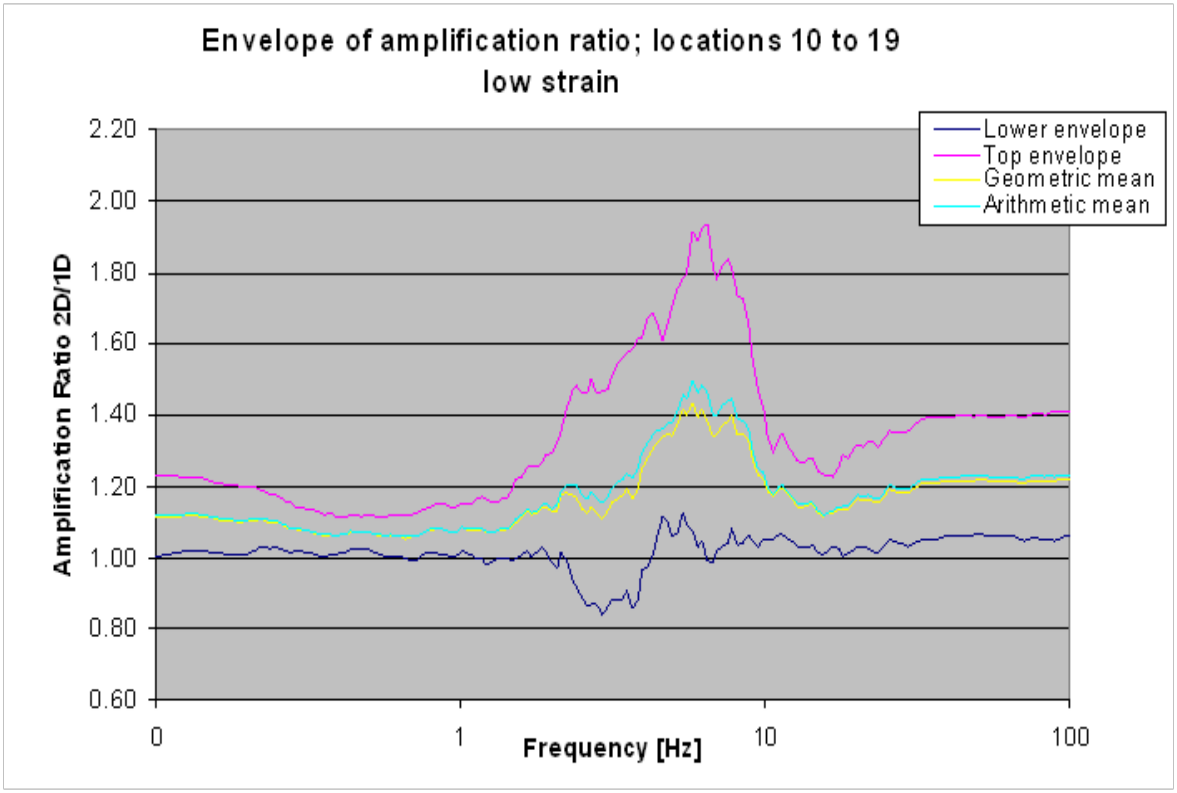

Figure V-1.23: Envelope of ratios 2D / 1D for low strain (0.1g), incl. mean.

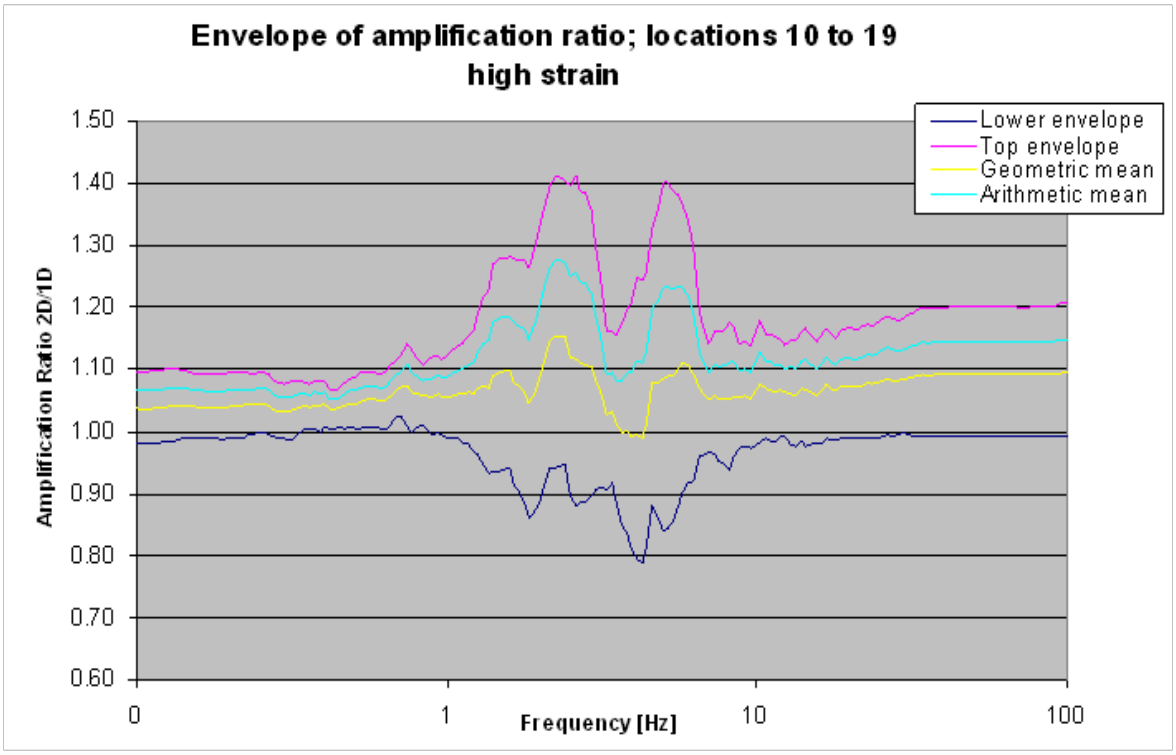

Figure V-1.24: Envelope of ratios 2D / 1D for high strain (0.4g), incl. mean.

1.2.9 Mühleberg Horizontal

Performed Calculations and Acquisition of Missing Values

Method	Profile	Material	Magnitude 5									Magnitude 6									Magnitude 7								
			0.05g	0.10g	0.20g	0.30g	0.40g	0.75g	1.00g	1.25g	1.50g	0.05g	0.10g	0.20g	0.30g	0.40g	0.75g	1.00g	1.25g	1.50g	2.50g	0.05g	0.10g	0.20g	0.30g	0.40g	0.75g	1.00g	1.25g	1.50g
EQL	P1	LB	10	10	10		10	10				9	9	9		9	9					10	10	10		10	10			
EQL	P1	BE	10	10	10		10	10				9	9	9		9	9					10	10	10		10	10			
EQL	P1	UB	10	10	10		10	10				9	9	9		9	9					10	10	10		10	10			
EQL	P2	LB	10	10	10		10	10				9	9	9		9	9					10	10	10		10	10			
EQL	P2	BE	10	10	10		10	10				9	9	9		9	9					10	10	10		10	10			
EQL	P2	UB	10	10	10		10	10				9	9	9		9	9					10	10	10		10	10			
EQL	P3	LB	10	10	10		10	10				9	9	9		9	9					10	10	10		10	10			
EQL	P3	BE	10	10	10		10	10				9	9	9		9	9					10	10	10		10	10			
EQL	P3	UB	10	10	10		10	10				9	9	9		9	9					10	10	10		10	10			
EQL	P4	LB	10	10	10		10	10				9	9	9		9	9					10	10	10		10	10			
EQL	P4	BE	10	10	10		10	10				9	9	9		9	9					10	10	10		10	10			
EQL	P4	UB	10	10	10		10	10				9	9	9		9	9					10	10	10		10	10			
RVTbc	P1	LB	1	1	1	1	1	1	1	1	1	1	1	1	1	1	1	1	1	1		1	1	1	1	1	1	1	1	1
RVTbc	P1	BE	1	1	1	1	1	1	1	1	1	1	1	1	1	1	1	1	1	1		1	1	1	1	1	1	1	1	1
RVTbc	P1	UB	1	1	1	1	1	1	1	1	1	1	1	1	1	1	1	1	1	1		1	1	1	1	1	1	1	1	1
RVTrand	P1	BE	50	50	50	50	50	50	50	50	50	50	50	50	50	50	50	50	50	50		50	50	50	50	50	50	50	50	50
RVTbc	P2	LB	1	1	1	1	1	1	1	1	1	1	1	1	1	1	1	1	1	1		1	1	1	1	1	1	1	1	1
RVTbc	P2	BE	1	1	1	1	1	1	1	1	1	1	1	1	1	1	1	1	1	1		1	1	1	1	1	1	1	1	1
RVTbc	P2	UB	1	1	1	1	1	1	1	1	1	1	1	1	1	1	1	1	1	1		1	1	1	1	1	1	1	1	1
RVTrand	P2	BE	50	50	50	50	50	50	50	50	50	50	50	50	50	50	50	50	50	50		50	50	50	50	50	50	50	50	50
RVTbc	P3	LB	1	1	1	1	1	1	1	1	1	1	1	1	1	1	1	1	1	1		1	1	1	1	1	1	1	1	1
RVTbc	P3	BE	1	1	1	1	1	1	1	1	1	1	1	1	1	1	1	1	1	1		1	1	1	1	1	1	1	1	1
RVTbc	P3	UB	1	1	1	1	1	1	1	1	1	1	1	1	1	1	1	1	1	1		1	1	1	1	1	1	1	1	1
RVTrand	P3	BE	50	50	50	50	50	50	50	50	50	50	50	50	50	50	50	50	50	50		50	50	50	50	50	50	50	50	50
RVTbc	P4	LB	1	1	1	1	1	1	1	1	1	1	1	1	1	1	1	1	1	1		1	1	1	1	1	1	1	1	1
RVTbc	P4	BE	1	1	1	1	1	1	1	1	1	1	1	1	1	1	1	1	1	1		1	1	1	1	1	1	1	1	1
RVTbc	P4	UB	1	1	1	1	1	1	1	1	1	1	1	1	1	1	1	1	1	1		1	1	1	1	1	1	1	1	1
RVTrand	P4	BE	50	50	50	50	50	50	50	50	50	50	50	50	50	50	50	50	50	50		50	50	50	50	50	50	50	50	50
NL1	P1	LB															9			9										
NL1	P1	BE					10	10			10	9				9	9			9						10	10			10
NL1	P1	UB															9			9	9									
NL2	P1	LB															9			9										
NL2	P1	BE					10	10			10	9				9	9			9						10	10			10
NL2	P1	UB															9			9	9									
NL3	P1	LB															9			9										
NL3	P1	BE					10	10			10	9				9	9			9						10	10			10
NL3	P1	UB															9			9	9									
NL4	P1	LB															9			9										
NL4	P1	BE					10	10			10	9				9	9			9						10	10			10
NL4	P1	UB															9			9	9									
NL5	P1	BE															9													

Note: For Mühleberg the case NL5 is corresponding to the case "NL2" (= cross check by another contractor) at the other sites.
NL2 is a sensitivity study where void ratios of all soils are increased by 20% from the base case NL1
NL3 is a sensitivity study where void ratios of all soils are decreased by 20% from the base case NL1
NL4 is a sensitivity study where the parameter hp, which governs the evolution of shear strains from increase in mean effective pressure, is increased from 35 to 45

Figure V-1.25: Overview of calculations performed for Mühleberg.

V_S-profiles

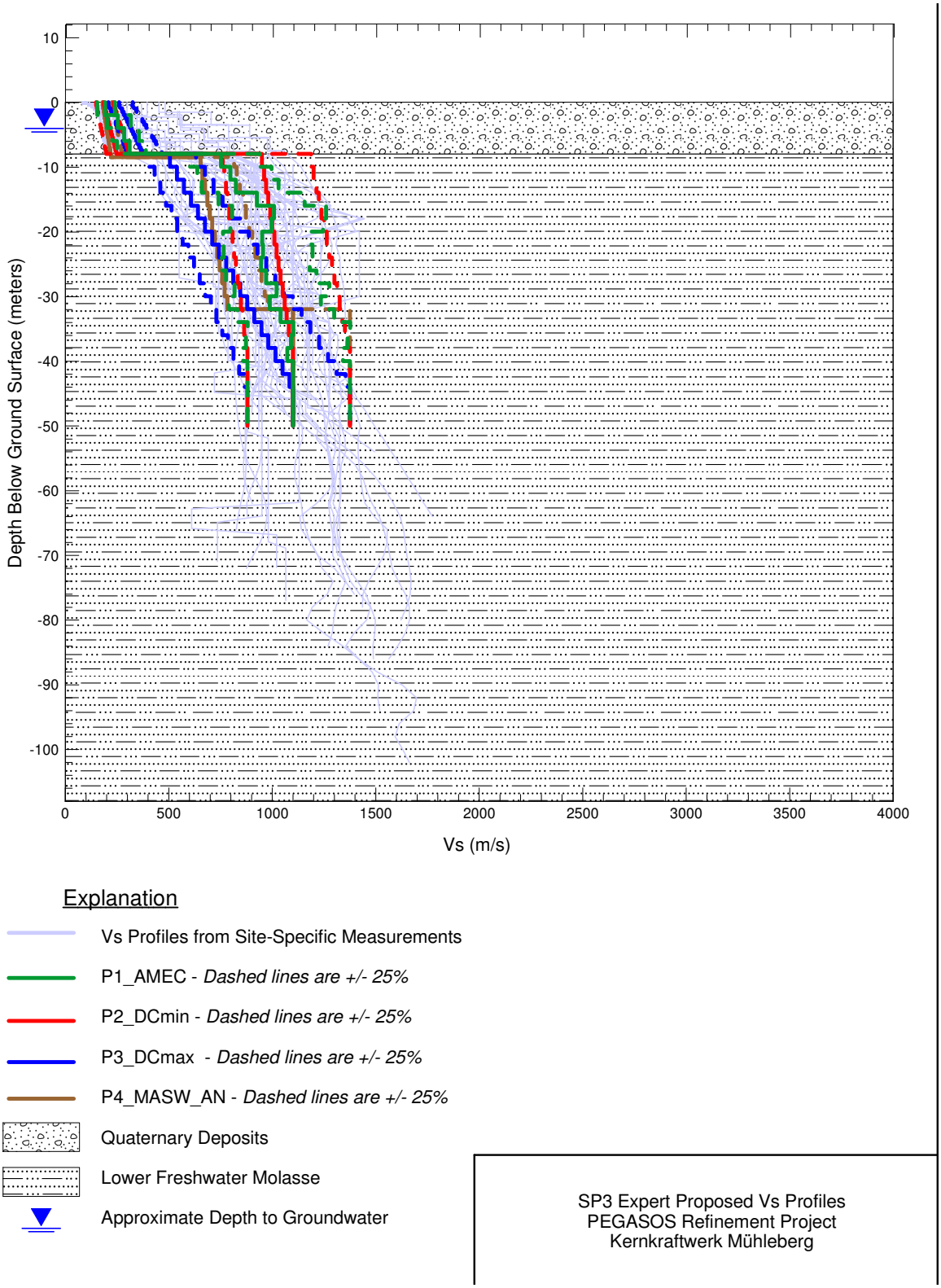

Figure V-1.26: Geological profile, V_S-results and V_S-profiles of Mühleberg.

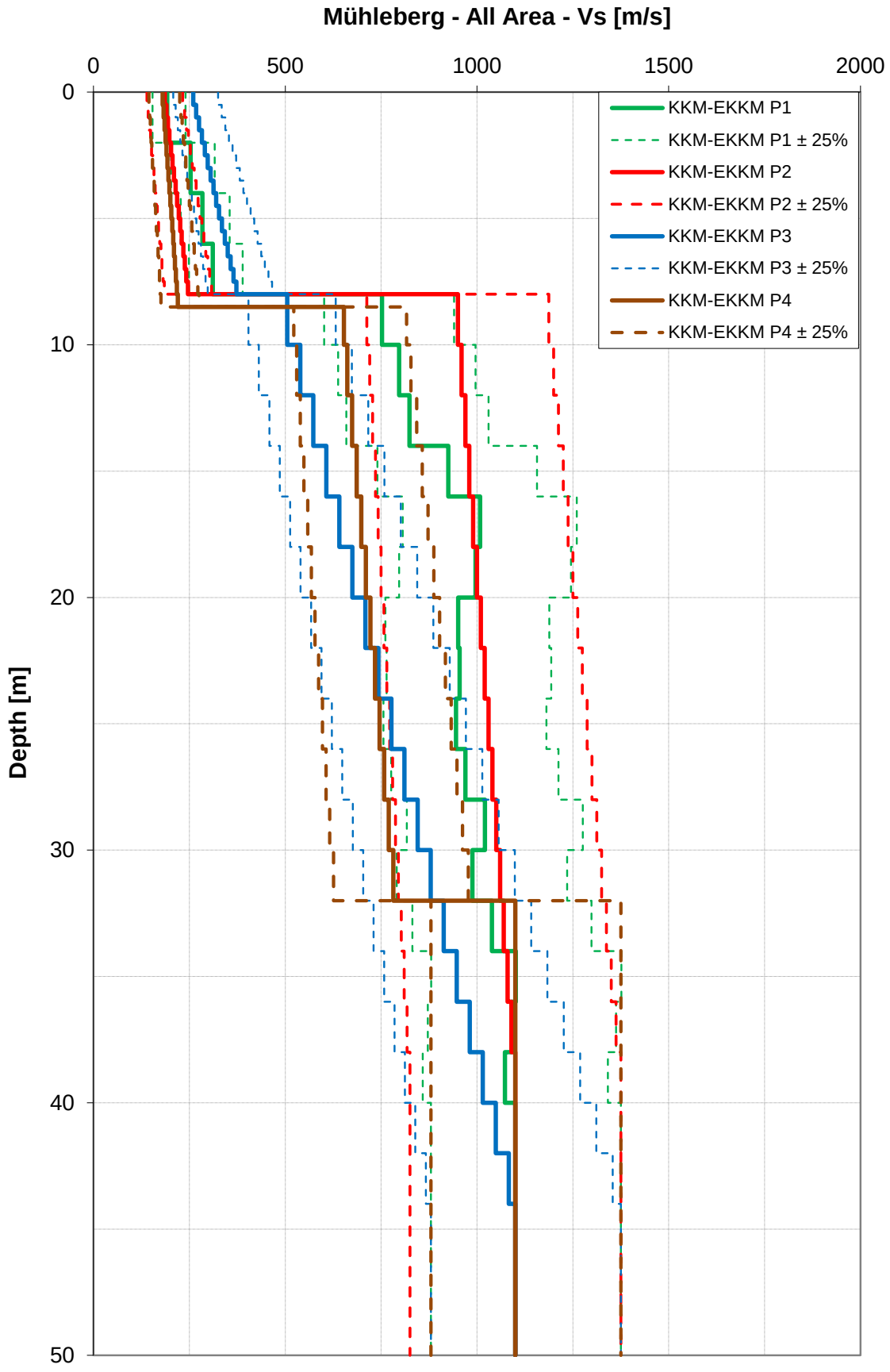

Figure V-1.27: V_S-profiles of Mühleberg.

Table V-1.7: Weights for the profiles.

Profile	Weights	Rational
P 1	0.3	All profiles with similar weights.
P 2	0.2	They cover the range of available data.
P 3	0.3	Profiles P2 and P4 are based on interpretations
P 4	0.2	performed based on lower bound dispersion curves.

Strains

Figure V-1.28 shows the strain produced by the different methods in the different profiles.

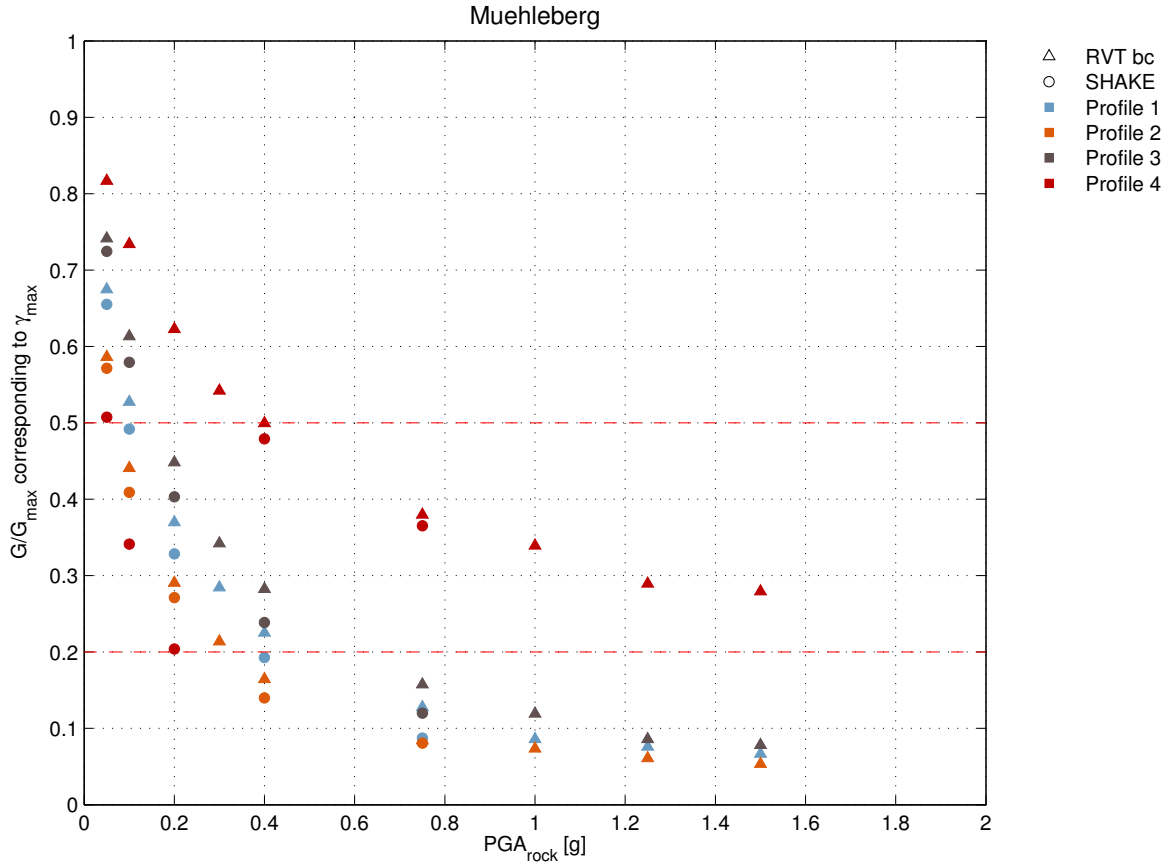

Figure V-1.28: Strains for Mühleberg profiles. Note: The color legend shows more profiles than available for the site.

Logic Tree for Mühleberg

The logic tree in Figure V-1.1 is valid for all elevations. The weights are given in Figures V-1.2(a) and V-1.2(b). No 2-D effects taken into account.

1.3 Median Amplification of Vertical Ground Motion

1.3.1 Approach

The logic tree for median amplification of vertical ground motion is constructed with the same general criteria used for median amplification of horizontal ground motion, see Section 1.2.1. There is a significant different due to the fact that the ground water has a stronger influence on the P-wave than on the S-wave.

1.3.2 Logic Tree Structure

The general structure of the model logic tree for the median vertical site amplification is shown in Figure V-1.29. The weights and correction rules depend on individual site characteristics. In principle for all elevations, the logic tree has the same structure. Derivations are indicated in the corresponding chapters. The branch starts with the input motion.

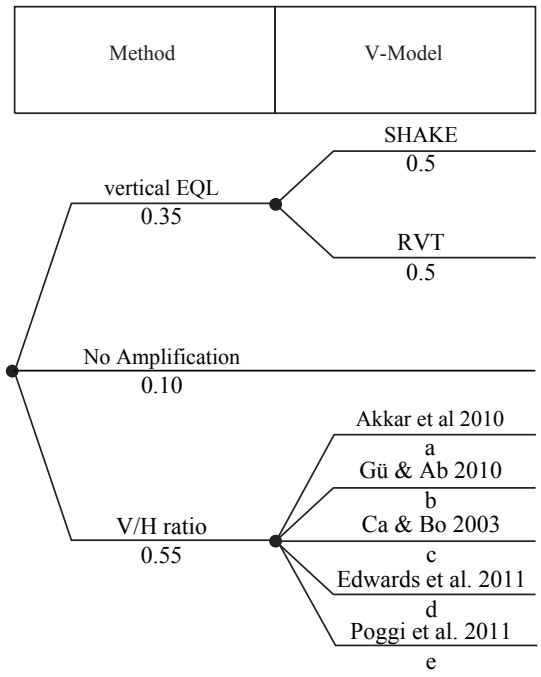

Figure V-1.29: Structure of model logic tree for median vertical site amplification.

1.3.3 Model Evaluations Common to All Sites

Different Methods for Computing the Vertical Site Response

This chapter is valid for all elevations. Exceptions are described in the individual sites. The following alternative methods will be used to define median vertical site amplification.

- Methods and weights: Vertical P-wave (EQL 35%: SHAKE 50%, RVT 50%)
- V/H ratio from SP2: 10%
- V/H ratio for soil: 55%

Rationale:
Important for the vertical ground motion is the location of the ground water table. At Beznau, Gösgen and Mühleberg, the ground water table is only few meters below the surface. At Leibstadt, it lies on a depth of about 30 m. In the alluvium layers below the ground water table, we will have P-wave velocities that are partly governed by the P-wave velocity of the water (1450 m/s). Therefore, only in the non-saturated part some degradation of the P-wave exists due to the strain level.

EQL is given a medium weight:

- *They are done on actual shear wave profiles and represent actual soil conditions best, but a limited number of calculations are available.*
- *SHAKE and RVT calculations are given the same weight. They are similar methods.*

V/H Ratios from SP2 (no amplification) have a low weight: They reflects the actual site condition only in a limited way (input level)

V/H Ratios have the largest weight. They are based on an extensive dataset.

Magnitude Dependence

Calculation results only for magnitude 6 exist. I assume no magnitude dependence.

Rationale: Due to the fact that in all sites large part of the profile is below the ground water table, for the area below the ground water table, the degradation of the vertical propagating P-waves will be smaller compared to the vertical propagating S-waves. Therefore, it can be expected that the magnitude dependence for the P-wave case will be smaller compared to the SH case.

Interpolation and Extrapolation to 1.5 g

Interpolation: Linear

Extrapolation to 1.5g is constant from the nearest neighbor (see Figure V-1.30).

Rational: The difference in amplification (Delta AF) contains the influence of degradation of the bulk-modulus and the increase of damping due to the higher PGA

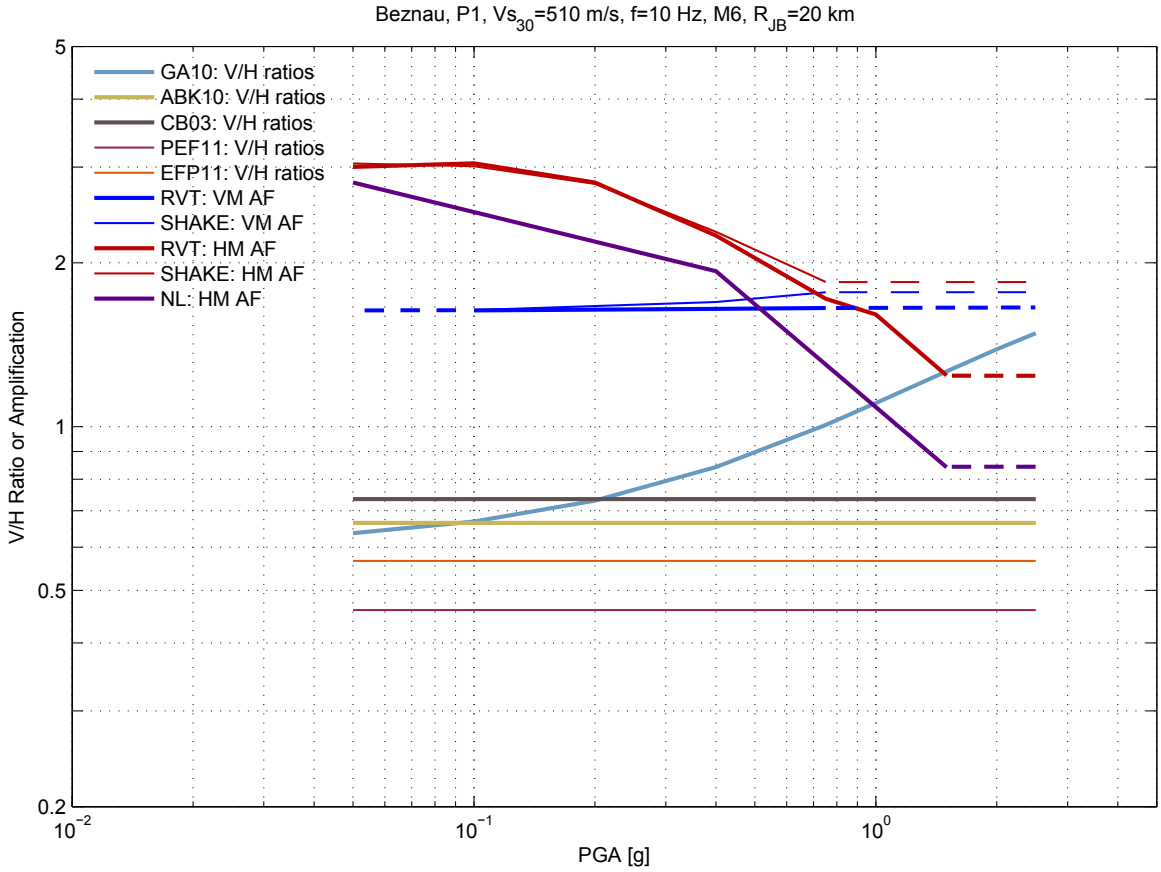

Figure V-1.30: Example for extrapolation to 1.5 g for the vertical ground motion. Here for Beznau, based on plots provided by A. Hölker on 13.03.2012 (see also Abrahamson and Hölker [2012])

Additional values:

PGA larger 1.5g: take value from 1.5 g (constant)
PGA lower 0.1g: take value from 0.2 g (constant)

2D-Effects

For the vertical component no 2D effects are assumed. They will be taken into account in the aleatory variability.

Rationale: Due to the topographic situation at all sites (except Leibstadt), no significant 2D effects for horizontal motion are expected. The same is true for vertical motion. In the case of Leibstadt, it is reasonable to assume that the 2D effects for the vertical ground motion will be smaller compared to the horizontal motion. Therefore, no 2D effects are taken into account for Leibstadt site.

V/H ratio from SP2 (No Amplification)

The V/H ratio calculated from SP2 is applied directly to the corresponding horizontal ground motion of Chapter 1.2, to get the amplification for vertical ground motion. The horizontal and vertical ground motions from SP2 are a function of frequency, magnitude and distance.

The needed frequencies and magnitudes can be adopted as given by the results of SP2, with the corresponding interpolation (defined in SP2) where necessary. Practically, the SP2 V/H ratios are to be applied subsequently to the site amplification logic tree.

V/H Ratios Equations

The characteristics of the different V/H ratios can be summarized as follows:

a) Bommer et al. [2011]
Ratios are based on strong motions accelerograms from Europe and the Middle East. They depend on M, style of faulting, distance and site classes (soft, stiff, rock). Good agreement with western US data.

b) Gülerce and Abrahamson [2010]
They are based on PEER_NGA database (world wide dataset, primarily US) and are consistent with GMPE of Abrahamson and Silva. Function on M, distance and accounts for differences in non linear site effects (V_{S30}).

c) Campbell and Bozorgnia [2003]
They are based on world wide database (1957 to 1995) from shallow crustal regions. M, style of faulting, distance and 4 site categories (firm soil, very firm soil, soft rock, firm rock).

d) Fäh et al. [2011] (TP3,TB-1084, Edwards et al., Part 2):
Data set from Switzerland (strong motion stations) and from Japan (KiK-Net), Quarter-length methodology.

e) Fäh et al. [2011] (TP3,TB-1084, Poggi et al., Part 1)
Data from KiK-Net $V_{S30} < 800$m/s. Ratios depend on M, distance, V_{S30}.

Default Weights (partially modified for individual sites and layers, as indicated in the sections below):

Ratios which are based on Swiss, European and middle east datasets have higher weights as well V_{S30} site classes.

Table V-1.8: Weights for the V/H models.

Model	Weight	Rational
a	0.15	Based on European and Middle East dataset; only 3 site classes
b	0.20	Based on world wide dataset but has V_{S30}
c	0.15	Based on world wide dataset but has only 4 site classes
d	0.05	Model for sites with deep hard rock
e	0.45	Soil model developed for Swiss NPP sites

Mühleberg and Beznau median and minimal depth have somewhat different weights, see individual sites. At those sites the hard rock is deeper compared to the other sites where the rock layer is shallow.

1.3.4 Beznau Vertical

Performed Calculations

Table V-1.31 shows the performed calculations.

Method	Profile	Material	Magnitude 6								
			Shaking level of horizontal component								
			0.05g	0.10g	0.20g	0.30g	0.40g	0.75g	1.00g	1.25g	1.50g
EQL	P1	LB		9			9	9			
EQL	P1	BE		9			9	9			
EQL	P1	UB		9			9	9			
RVTbc	P1	LB		1			1	1			
RVTbc	P1	BE		1			1	1			
RVTbc	P1	UB		1			1	1			

Figure V-1.31: Overview of vertical calculations performed for Beznau.

V_P-profile

Figure V-1.32 shows the soil investigation data and the evaluated compression wave soil profile.

Strains

Figure V-1.33 shows the strain produced by the different methods in the different profiles.

Logic Tree for Beznau

The logic tree corresponds to the general tree in Table V-1.31.

Site-specific Model Evaluations

Vertical component of profiles 2, 3 and 4: These profiles are not used.

Rationale: There exist no anchor values to be used

Minimum depth: The minimum depth is a soft rock site. Therefore, the weight of the models d) and e) are modified.

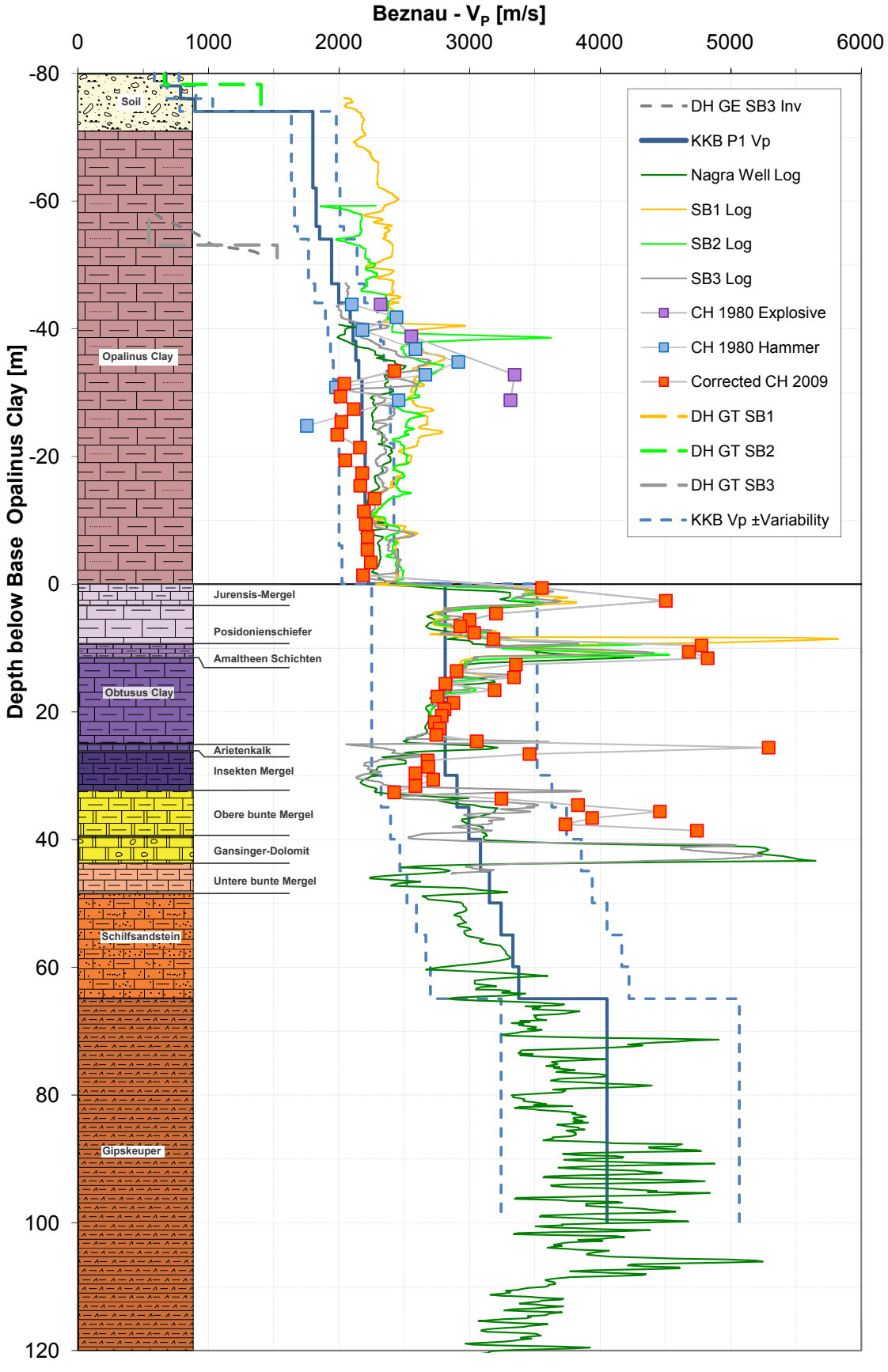

Figure V-1.32: V_P-profile at Beznau site including measurements and model.

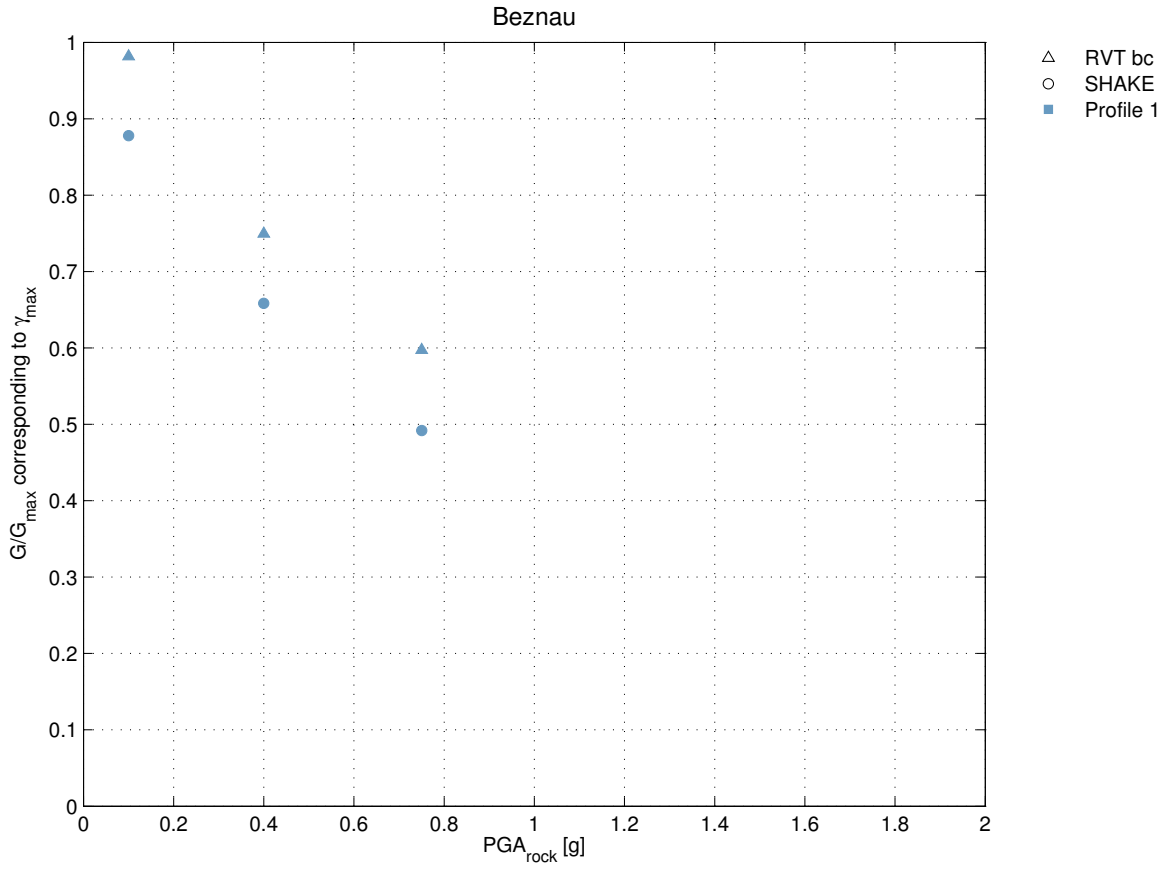

Figure V-1.33: V_P-strains at Beznau site. Note: Only profile P1 was used for the vertical computations, but the color legend shows more profiles than available for the site.

Table V-1.9: Modified weights for the V/H models at depth for Beznau.

Model	Weight	Rational
a	0.15	
b	0.2	
c	0.15	
d	0.3	Minimum depth is a soft rock site
e	0.2	Minimum depth is a soft rock site

1.3.5 E-Beznau Vertical

Performed Calculations

Table V-1.34 shows the performed calculations.

Method	Profile	Material	Magnitude 6								
			Shaking level of horizontal component								
			0.05g	0.10g	0.20g	0.30g	0.40g	0.75g	1.00g	1.25g	1.50g
EQL	P1	LB		9			9	9			
EQL	P1	BE		9			9	9			
EQL	P1	UB		9			9	9			
RVTbc	P1	LB		1			1	1			
RVTbc	P1	BE		1			1	1			
RVTbc	P1	UB		1			1	1			

Figure V-1.34: Overview of vertical calculations performed for E-Beznau.

V_P-profile

Figure V-1.35 shows the soil investigation data and the evaluated compression wave soil profile.

Strains

Figure V-1.36 shows the strain produced by the different methods in the different profiles.

Site-specific Model Evaluations

Vertical component of profiles 2 and 3: These profiles are not used.

Rationale: There exist no anchor values to be used

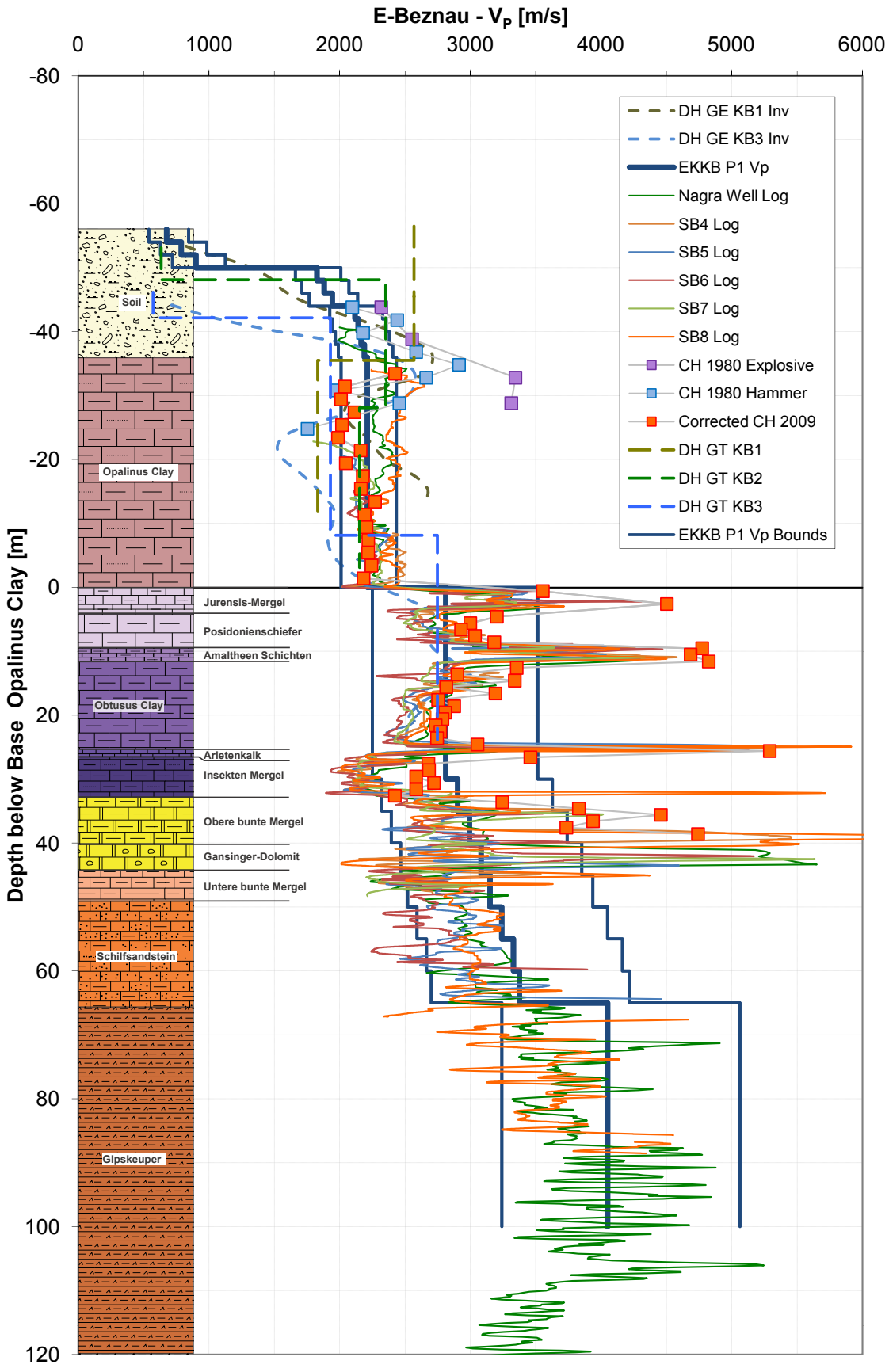

Figure V-1.35: V_P-profile at E-Beznau site including measurements and model.

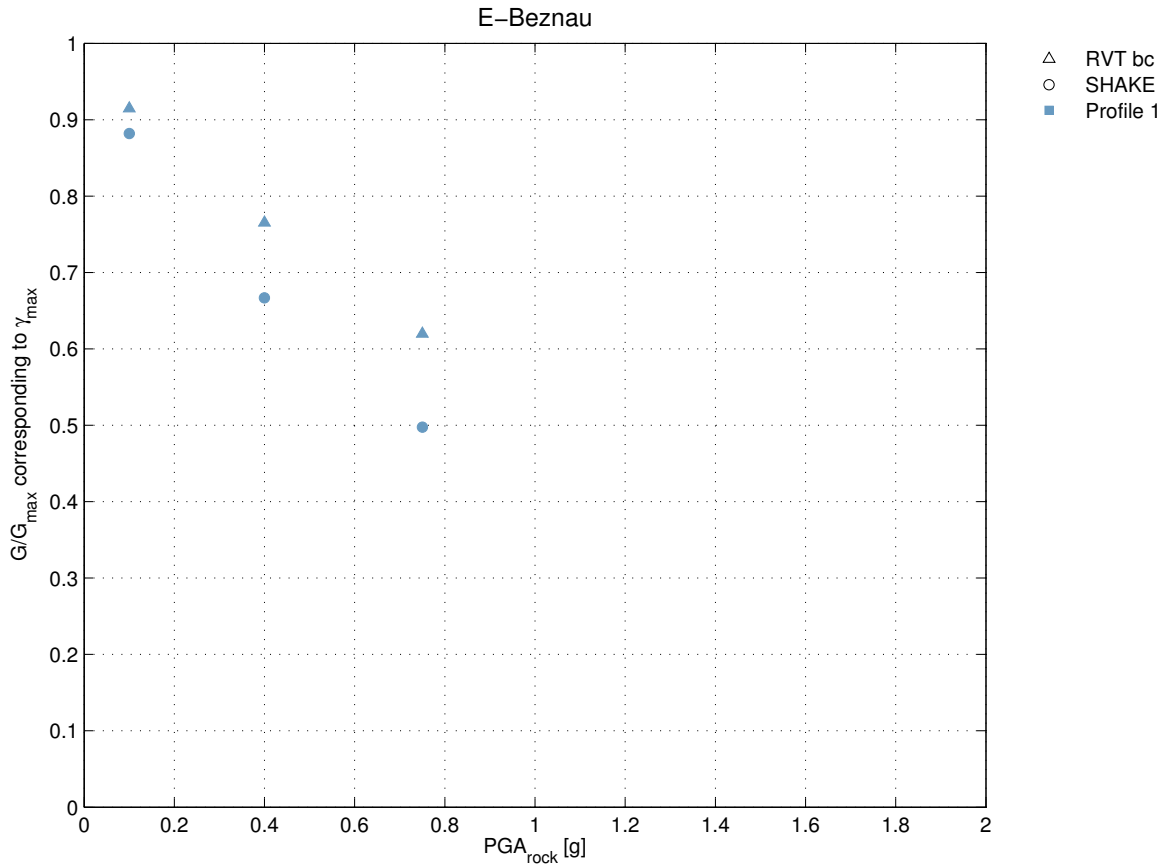

Figure V-1.36: V_P-strains at E-Beznau site. Note: Only profile P1 was used for the vertical computations, but the color legend shows more profiles than available for the site.

1.3.6 Gösgen Vertical

Performed Calculations

Table V-1.37 shows the performed calculations.

Method	Profile	Material	Magnitude 6								
			Shaking level of horizontal component								
			0.05g	0.10g	0.20g	0.30g	0.40g	0.75g	1.00g	1.25g	1.50g
EQL	P6	LB		9			9	9			
EQL	P6	BE		9			9	9			
EQL	P6	UB		9			9	9			
RVTbc	P1	LB		1			1	1			
RVTbc	P1	BE		1			1	1			
RVTbc	P1	UB		1			1	1			

Figure V-1.37: Overview of vertical calculations performed for Gösgen.

V_P-profile

Figure V-1.38 shows the soil investigation data and the evaluated compression wave soil profile.

Strains

Figure V-1.39 shows the strain produced by the different methods in the different profiles.

Logic Tree for Gösgen

The logic tree corresponds to the general tree in Table V-1.31.

Site-specific Model Evaluations

Vertical component for profile 2 and 3: These profiles are not used.

Rationale: There exist no anchor values to be used

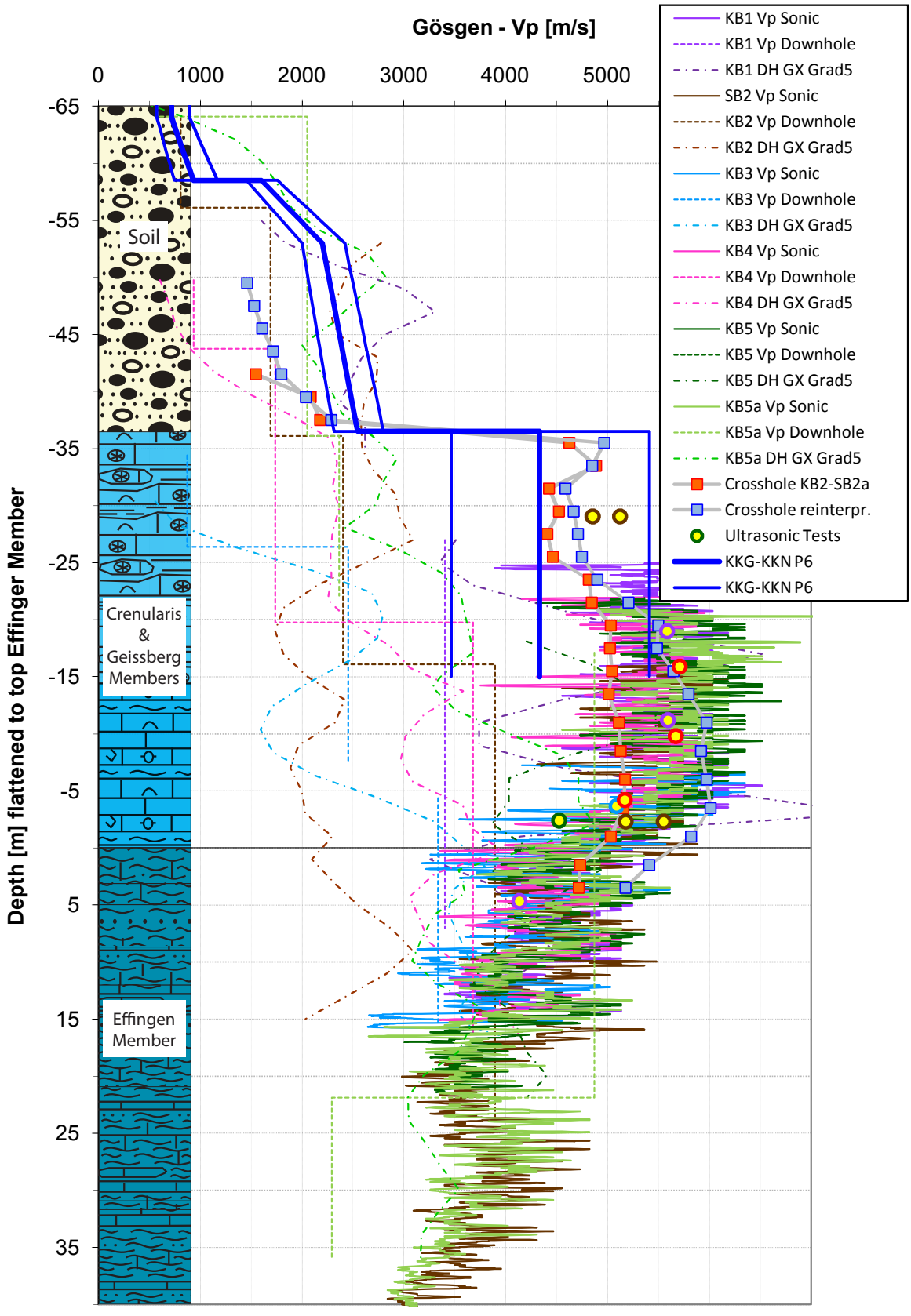

Figure V-1.38: V_P-profile at Gösgen site including measurements and model.

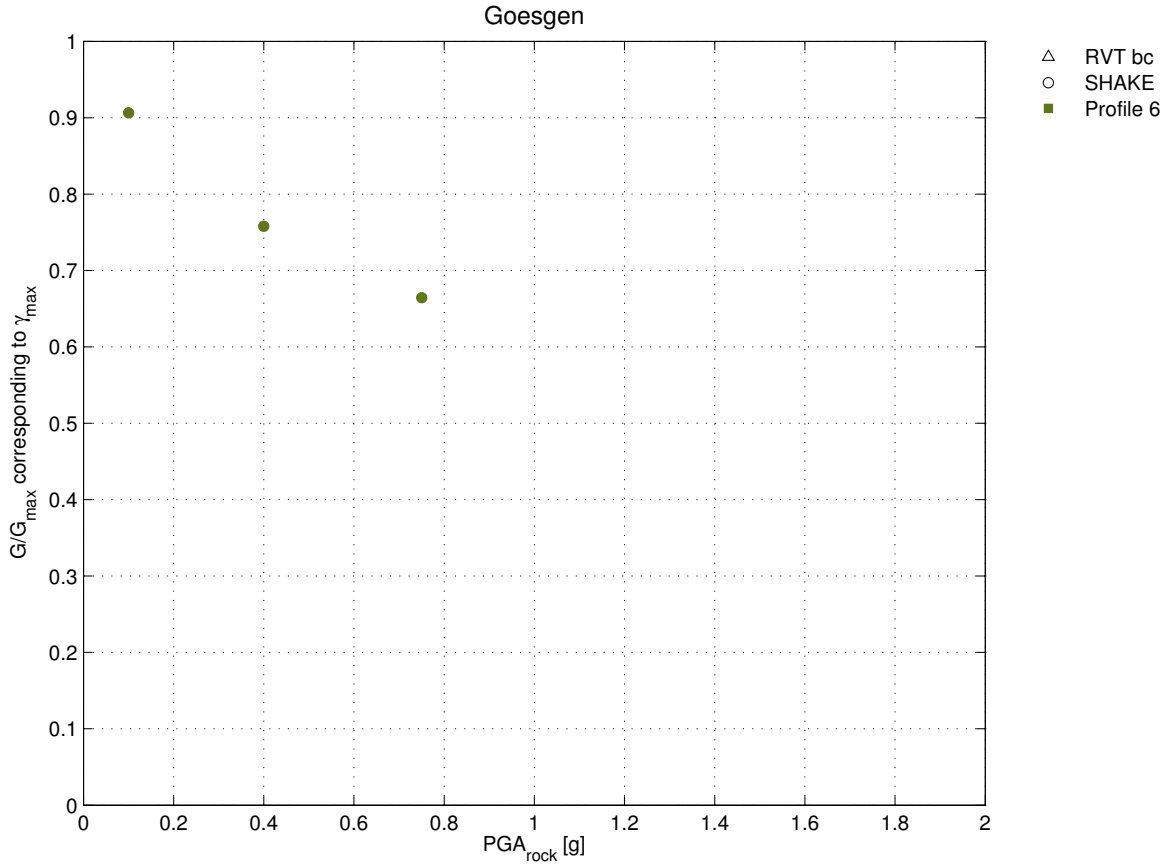

Figure V-1.39: V_P-strains at Gösgen site. Note: Only profile P6 was used for the vertical computations, but the color legend shows more profiles than available for the site.

1.3.7 Leibstadt Vertical

Performed Calculations

Table V-1.40 shows the performed calculations.

Method	Profile	Material	Magnitude 6								
			Shaking level of horizontal component								
			0.05g	0.10g	0.20g	0.30g	0.40g	0.75g	1.00g	1.25g	1.50g
EQL	P3	LB		9			9	9			
EQL	P3	BE		9			9	9			
EQL	P3	UB		9			9	9			
RVTbc	P1	LB		1			1	1			
RVTbc	P1	BE		1			1	1			
RVTbc	P1	UB		1			1	1			

Figure V-1.40: Overview of vertical calculations performed for Leibstadt.

V_P-profile

Figure V-1.41 shows the soil investigation data and the evaluated compression wave soil profile.

Strains

Figure V-1.42 shows the strain produced by the different methods in the different profiles.

Logic Tree for Leibstadt

The logic tree corresponds to the general tree in Table V-1.31.

Site-specific Model Evaluations

Vertical component for profile 2 and 3: These profiles are not used.

Rationale: There exist no anchor values to be used

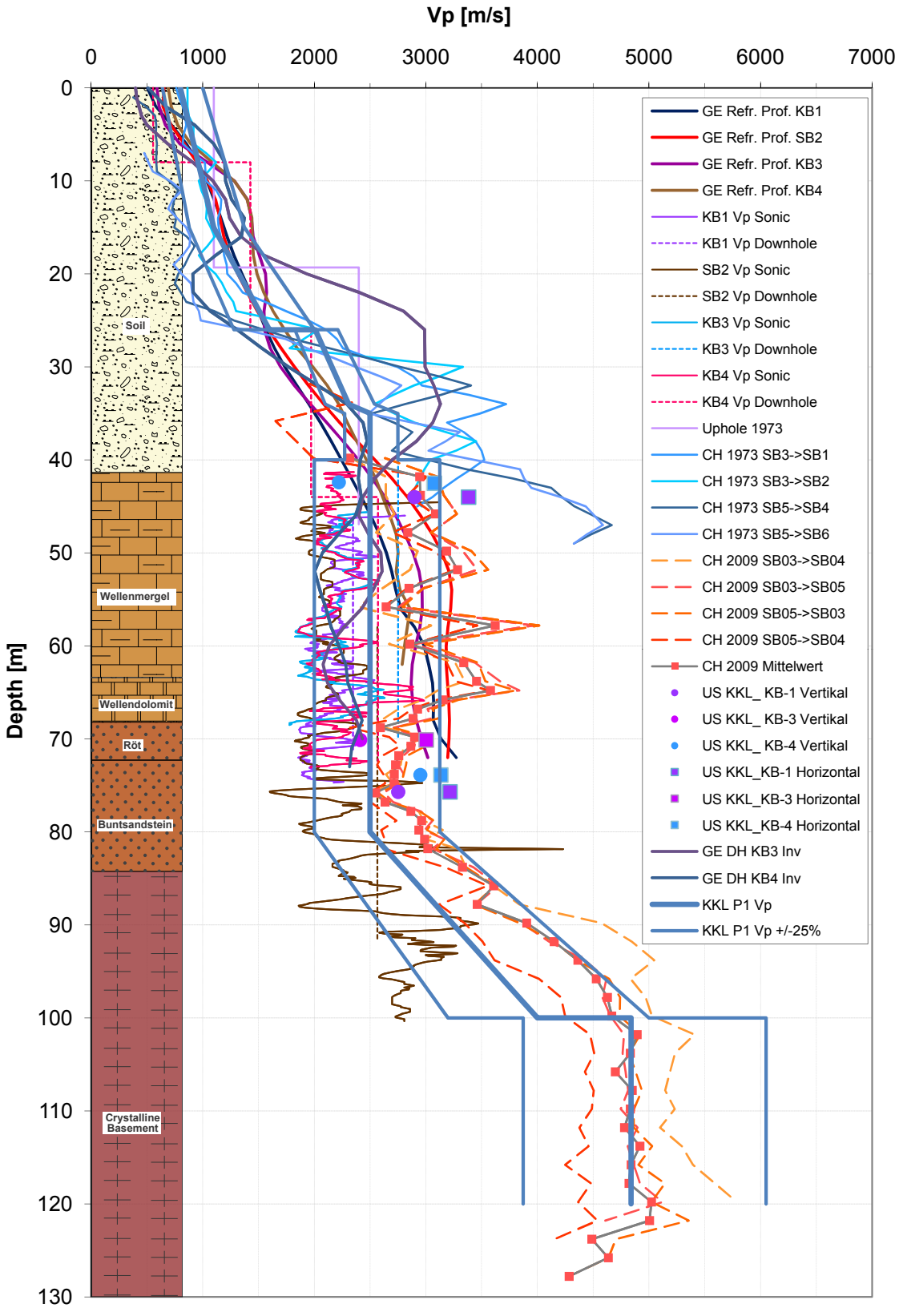

Figure V-1.41: V_P-profile at Leibstadt site including measurements and model.

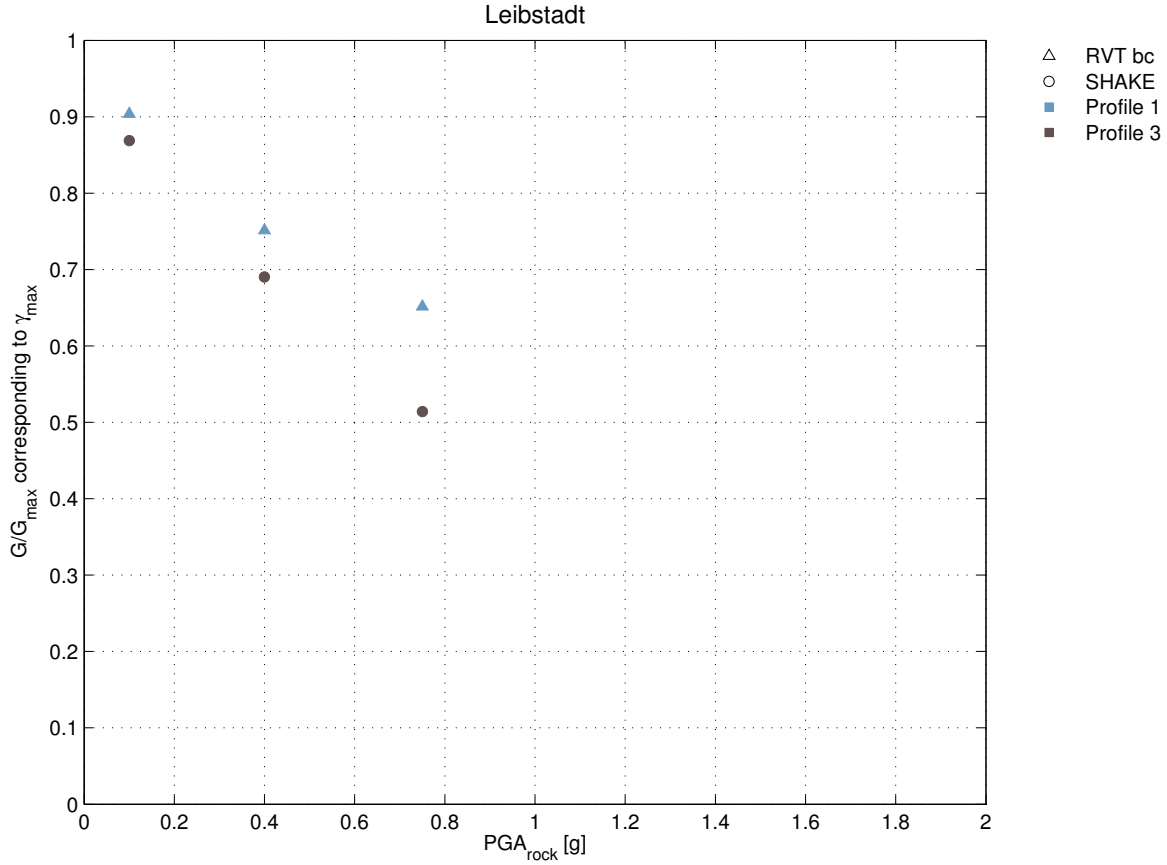

Figure V-1.42: V_P-strains at Leibstadt site. Note: Profile P1 was used for the vertical RVT computations and profile P3 for SHAKE, but the color legend shows more profiles than available for the site.

1.3.8 Mühleberg Vertical

Performed Calculations

Table V-1.43 shows the performed calculations.

Method	Profile	Material	Magnitude 6								
			Shaking level of horizontal component								
			0.05g	0.10g	0.20g	0.30g	0.40g	0.75g	1.00g	1.25g	1.50g
EQL	P1	LB		9			9	9			
EQL	P1	BE		9			9	9			
EQL	P1	UB		9			9	9			
RVTbc	P1	LB		1			1	1			
RVTbc	P1	BE		1			1	1			
RVTbc	P1	UB		1			1	1			

Figure V-1.43: Overview of calculations performed for Mühleberg.

V_P-profile

Figure V-1.44 shows the soil investigation data and the evaluated compression wave soil profile.

Strains

Figure V-1.45 shows the strain produced by the different methods in the different profiles.

Logic Tree for Mühleberg

The logic tree corresponds to the general tree in Table V-1.31.

Site-specific Model Evaluations

Vertical component for profile 2, 3 and 4: These profiles are not used.

Rationale: There exist no anchor values to be used

Minimum depth: The minimum depth is a soft rock site. Therefore, the weight of the models d) and e) are modified.

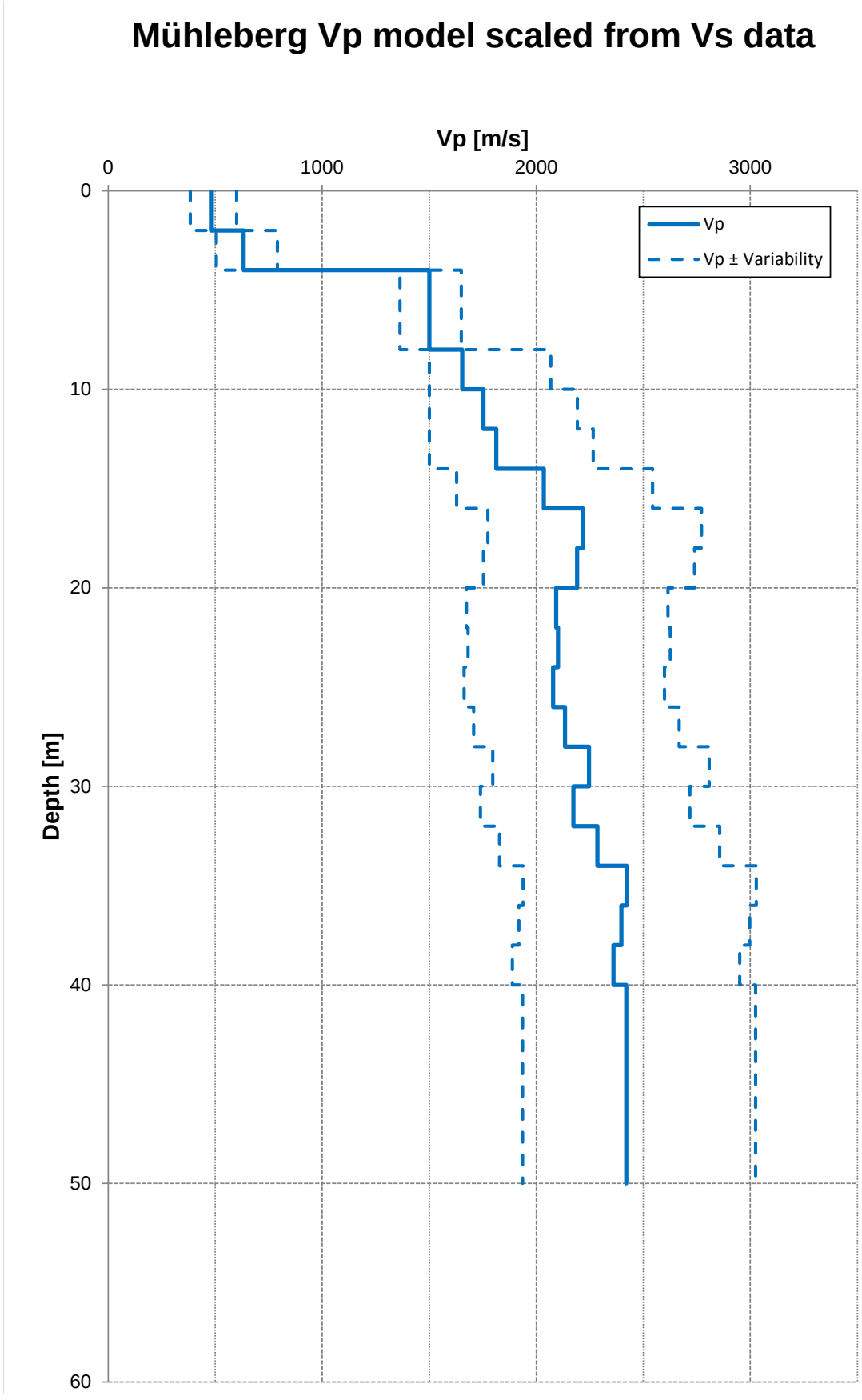

Figure V-1.44: V_P-profile for Mühleberg site scales from V_S data.

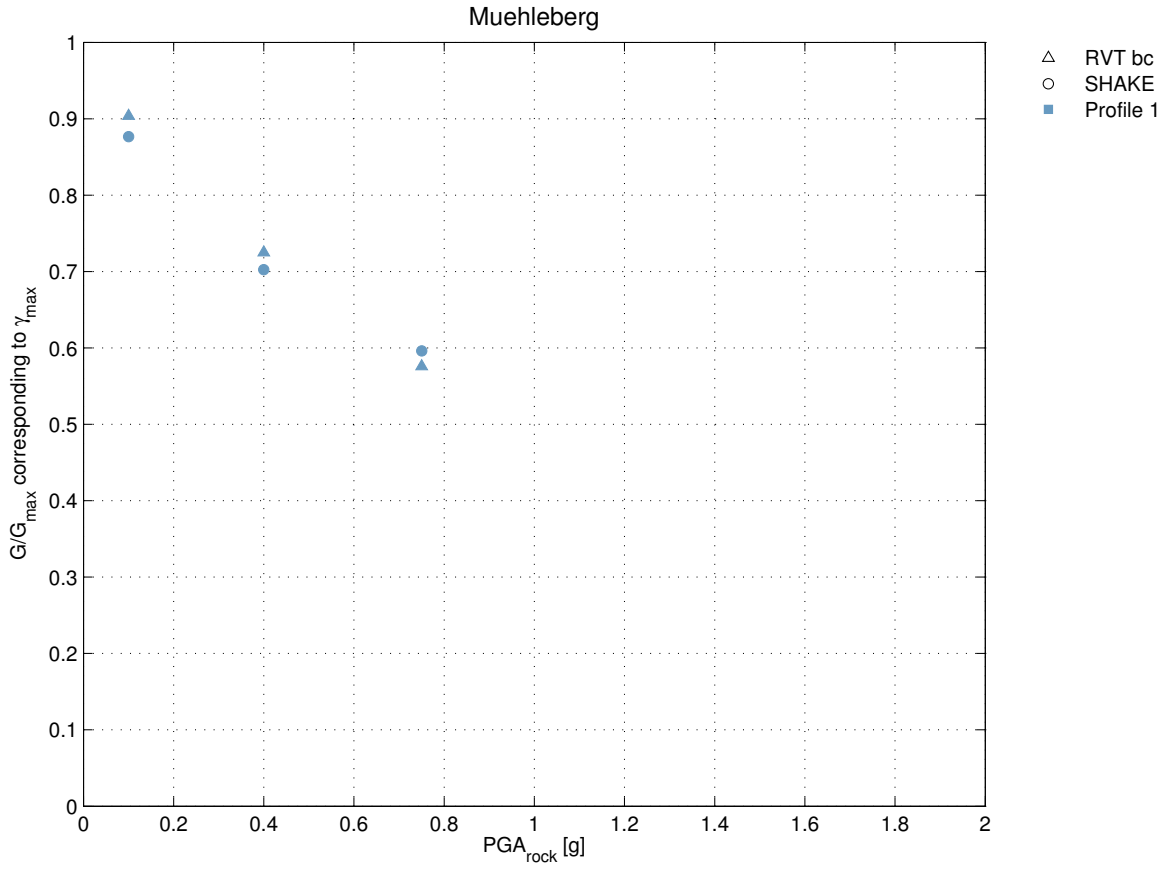

Figure V-1.45: V_P-strains at Mühleberg site. Note: Only profile P1 was used for the vertical computations, but the color legend shows more profiles than available for the site.

Table V-1.10: Modified weights for the V/H models at depth for Mühleberg.

Model	Weight	Rational
a	0.15	
b	0.20	
c	0.15	
d	0.30	Minimum depth is a soft rock site
e	0.20	Minimum depth is a soft rock site

1.4 Aleatory Variability of Ground Motion

The procedure below is valid for all elevations.

1.4.1 Approach

The aleatory variability represents the variability of.

- The spatial variability of the site conditions
- The variability of the time histories

SP2 removed the aleatory variability due to the variability in the median site-to-site amplification. The SP2 aleatory variability includes the variability in the amplification due to different input time histories (the site amplification variability about the median site amplification. SP3 needs to evaluate if this part of the aleatory variability from SP2 captures the site-specific variability from SP3 input motions. In particular, there may be increased aleatory variability to high input rock ground motion levels due to non-linear effects. Figures V-1.46 and V-1.46 compare the SP2 and SP3 terms for the amplification variability for each site. Figure V-1.48 shows the amount of aleatory variability that is added to the SP2 variability to capture the site-specific effects.

Figure V-1.46 shows the comparison for small PGA (surface). The figure indicates that the aleatory variability is within the SP2 variability and therefore can be neglected.

Figure V-1.47(a) shows the comparison for high PGA (surface), and the aleatory variability for Leibstadt and Mühleberg cannot be neglected there. Figure V-1.47(b) shows the variability for the sub-surface elevations for high PGA.

Figure V-1.48 shows the additional aleatory variability or high PGA values (≥ 0.4 g) to be added. For the horizontal ground motion at PGA < 0.4 g and the vertical ground motion (at all PGA) the additional variability is zero. Figure V-1.47(a) shows the corresponding comparison of the SP2 variability which was used to evaluate the additional variability per site where the sigma of the non-linear runs were above the SP2ΦAMP.

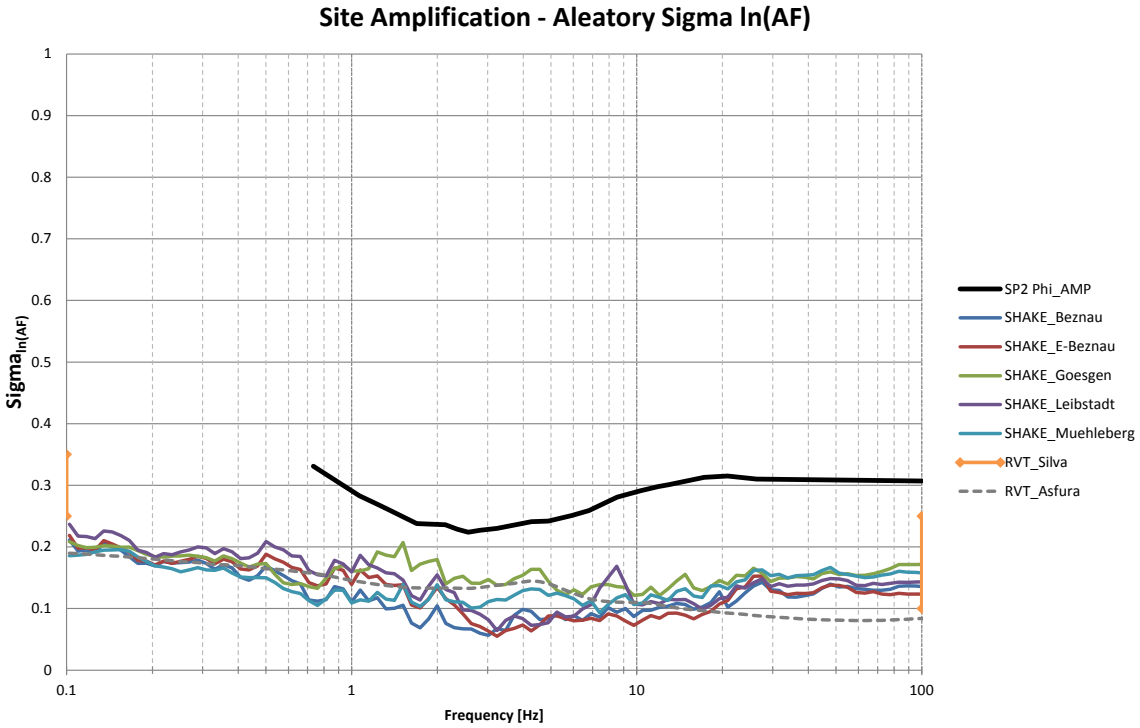

SP2ΦAMP: Rodriguez-Marek et al. (2011), Analysis of Single-Station Standard Deviation Using the KiK-net Data. BSSA, Vol.101, No.3, pp. 1242-1258, Table 9 and Figure 17.

SHAKE: PRP-SP3, mean $\sigma(\ln(\mathrm{AF}_{SHAKE}))$ for all profiles, all magnitudes, PGA$\leq$0.2g, mean material, surface.

RVT: Data file EXT-SUP-1031, mean $\sigma(\ln(\mathrm{AF}_{RVT}))$ due to random phase angels, for the Gösgen site, profiles P1-P5, all magnitudes, PGA$\leq$0.2g, mean material, surface.

Figure V-1.46: Site amplification - aleatory σ ln(AF), low PGA, surface, from TP3-RF-1346 and Renault [2011b] (TP3-TN-1195).

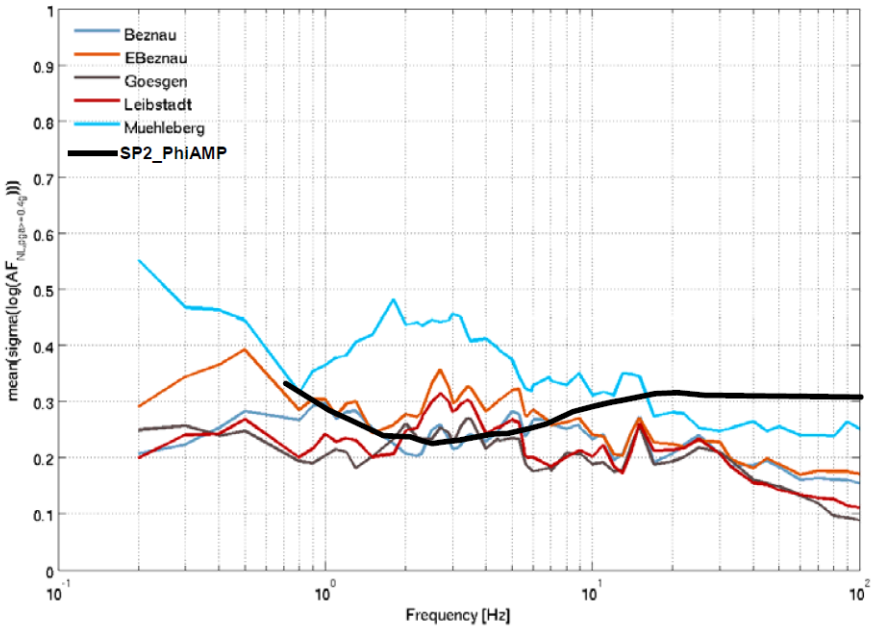

(a) Surface

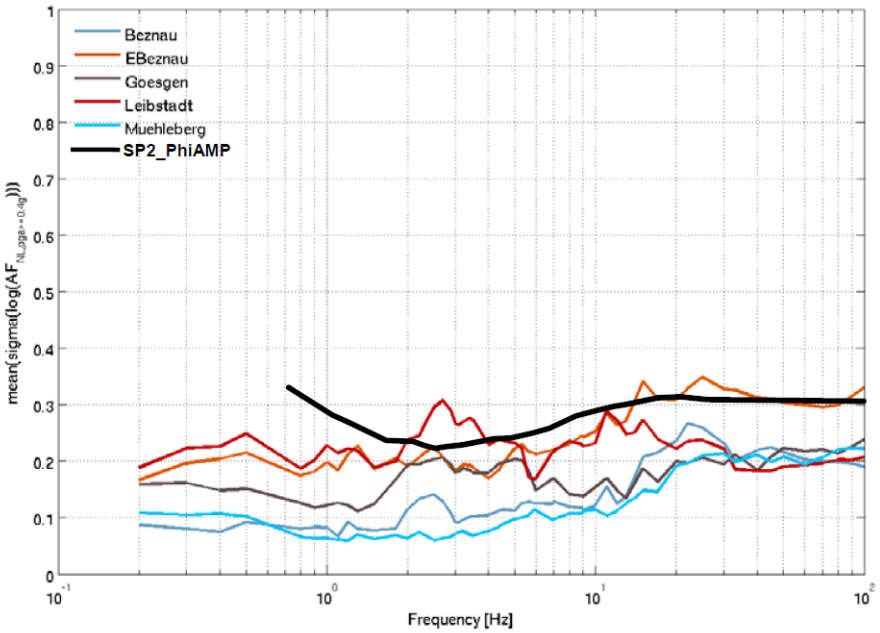

(b) Sub-surface

SP2ΦAMP: Rodriguez-Marek et al. (2011), Analysis of Single-Station Standard Deviation Using the KiK-net Data. BSSA, Vol.101, No.3, pp. 1242-1258, Table 9 and Figure 17.

NL: PRP-SP3, mean $\sigma(\ln(\mathrm{AF}_{NL}))$ of the NL1 computations for all profiles, all magnitudes, PGA≥0.4g, mean material.

Figure V-1.47: Aleatory variability for high PGA (≥ 0.4 g), based on the site specific non-linear results. Note: For the sub-surface, the red peak exceeding the black line at about 2.5 Hz corresponds to Leibstadt.

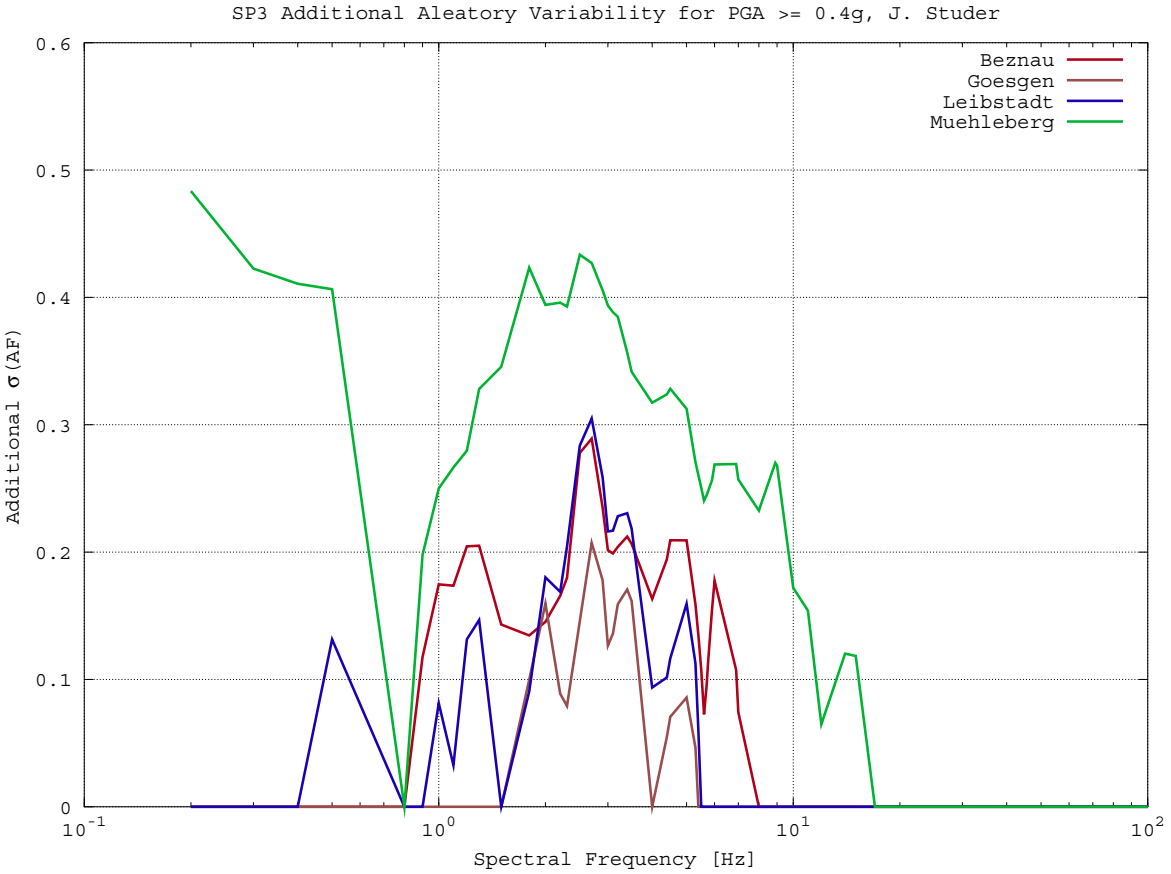

Figure V-1.48: Additional aleatory variability for high PGA ($\geq$ 0.4 g), based on the site specific non-linear results.

1.4.2 Aleatory Variability of the Horizontal Ground Motion

The aleatory variability will be assessed by the following formula: $\sqrt{\sigma^2_{site} - \sigma^2_{SP2}}$

Low PGA Level

For all sites and surface levels, the aleatory variability is contained in the SP2 values. Therefore no additional aleatory variability for SP3 has to be taken into account.

High PGA Level ($\geq 0.4g$)

Surface For the individual sites take as additional aleatory variability the envelope of the individual site curve in Figure V-1.47(a). And subtract the variability from SP2 with the above formula.

Subsurface For the individual sites take as additional aleatory variability the envelope of the individual site curve in Figure V-1.47(b) and subtract the variability from SP2 with the above formula. (For Beznau, E-Beznau, Gösgen, Mühleberg no additional aleatory variability has to be added.)

1.4.3 Aleatory Variability of the Vertical Ground Motion

To assess the vertical aleatory variability, the same procedure is used. Figures V-1.49 and V-1.50 compare the vertical variability to the horizontal variability (as shown in Figure V-1.47(a)). As can be seen, the vertical variability is much smaller than the horizontal and thus, it is assumed that it can be neglected.

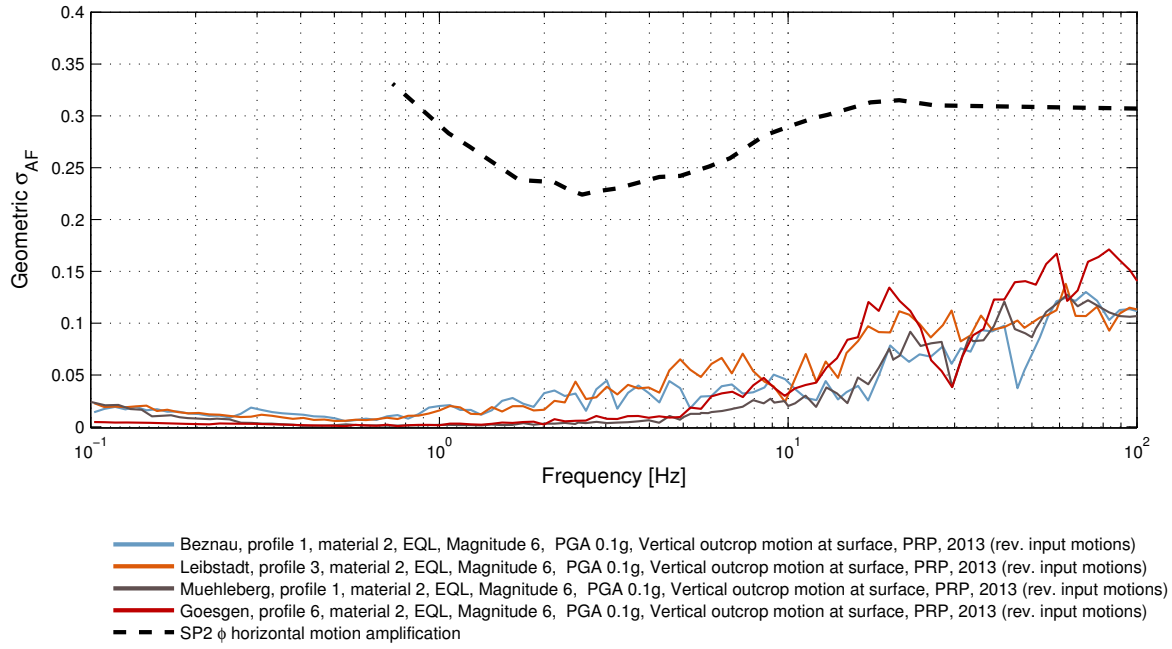

Figure V-1.49: Vertical aleatory variability small PGA compared to the horizontal.

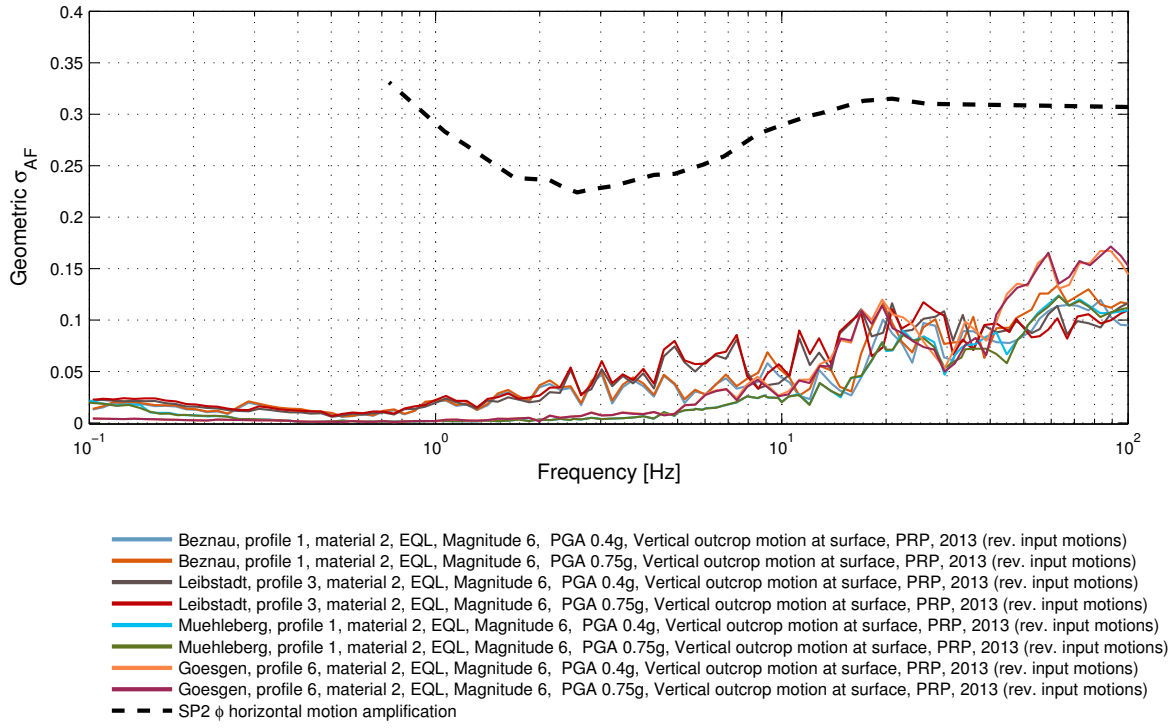

Figure V-1.50: Vertical aleatory variability SP3 high PGA ($\geq 0.4g$) compared to the horizontal.

Low PGA Level

For all sites, surface level the aleatory variability is contained in the SP2 values. Therefore no additional aleatory variability for SP3 has to be taken into account.

High PGA Level (equal/larger 0.4 g)

Surface The aleatory variability is also set to zero.

Subsurface The aleatory variability is also set to zero.

1.5 Maximum Ground Motions

The description of the model follows the individual branches.

1.5.1 General Concept for Horizontal Motion

Methods and General Rule

The maximum ground motion that can be transmitted depends on the soil strength. In principle, the same methodology is used for all elevations. Only weights and initial values reflect the individual elevations. Two branches are used to calculate the maximum ground motion. They are based on:

- Soil Mechanics Model
- Non-linear Calculations

For the assessment, the following data are available:

- Soil mechanic model: Pecker [2011] (TP3-TB-1074, see also TP3-RF-1319)
- Non-linear Calculations
- Observed data: Strasser and Zulu [2010] (EXT-TB-1067)

Approach

The same characteristics as for the Horizontal Median ground motion are used. Additionally, characteristic values for the shear strength, ϕ have been taken. To account for uncertainties of the material properties in the failure range, a ratio of $\pm$ 20% is taken. This ratio will account for the uncertainties of the shear strength (internal friction); this leads to a range of ϕ for the individual soil layers of about 37°to 48°. This uncertainty is considered as a 2 σ value. Therefore, the weights are taken in general 80% for the representative value and 10% for the upper and lower ranges.

Site Characterisations

- Beznau
  Characteristics of soil profile:
  - 9 m Gravel / Sand
  - 4 m weathered Opalinus Clay
  - $\Longrightarrow$ total 13 m top layer
  - Ground water table -3.0 m from surface.
    Depth of elevations: Mean elevation 6 m, minimum elevation 15 m.

- E-Beznau
  Characteristics of soil profile:
  - 22m Gravel / Sand
  - 4 m weathered Opalinus lay
  - Total 26 m top layer
  - Ground water table -3.0 m from surface.
    Depth of elevations: Mean elevation 6 m, minimum elevation 15 m.

- Gösgen
  Characteristics of soil profile:
  - 26 m Gravel / Sand
  - 4 m weathered Bedrock
  - $\Longrightarrow$ total 30 m top layer
  - Ground water table -5.0 m from surface.
    Depth of elevations: Mean elevation 5 m, minimum elevation 9 m.

- Leibstadt
  Characteristics of soil profile:
  - 50 m Gravel / Sand
  - 4 m weathered Bedrock
  - $\Longrightarrow$ total 54 m top layer
  - Ground water table -25.5 m from surface.
    Depth of elevations: Mean elevation 6 m, minimum elevation 10 m.

- Mühleberg
  Characteristics of soil profile:
  - 11 m Gravel / Sand
  - 4 m weathered Bedrock
  - $\Longrightarrow$ total 15 m top layer
  - Ground water table -4 m from surface.
    Depth of elevations: Mean elevation 7 m, minimum elevation 14 m.

General Evaluation of Proponent Models

Soil mechanic model: The model developed by Pecker is based on wave equation and shear strength of granular soil. It has the following assumptions:

- The increase of shear wave velocity originally is a power function of depth
- Material properties: Elasto-perfectly plastic, failure strength depends on confining pressure
- Unit weight: constant
- Mode shape: First three modes

The calculations have been performed for each site individually, and with the best fit for the actual shear wave velocities and strength profiles. In the frequency range of earthquakes, the soil properties depend primarily on the shear strain and only to a smaller extent on the loading velocities. In the failure strain range, use of static material properties is a good approach. This model works with classical soil mechanics assumptions; its validity is therefore proven in daily design practice, where we have extensive experience for the behavior of soils in the failure range. The material parameters of the individual sites are taken into account, which means the model is site specific. Pecker's model is taken with a weight (in general) of 40%.

Non-linear Calculations: These calculations use different up-to-date computer programs. The calculations are site specific. From experience in daily design work, a non-linear site response analysis depends on a large number of parameters, which are difficult to evaluate. The influence of the individual parameters is often not very clear, and results from different non-linear programs can differ. In PRP calculations have been verified by the use of different programs and different experienced personnel The result are not equal but consistent. There for I have changed my mind since PEGASOS and I give a weight of 60%.

Method Betbeder: It is based on the following assumptions:

- Only the fundamental mode is taken into consideration
- The shear modulus is constant with depth
- The constitutive rule for the soil is represented by the hyperbolic model
- The average soil column acceleration is limited by the available shear strength at the base of the profile divided by the mass of the soil column
- The solution consists in relating the maximum surface acceleration to the average soil column acceleration

This method is very simple and gives low values, which are considered not to be representative. In stiff soils, the higher frequencies have a significant influence. Therefore, Betbeder's model is not taken into account: weight 0%.

Observed data: This data provides lower bound values. The site characteristic of the observed data are not known in detail, therefore those data are not site specific. For the horizontal motion, those results are not taken into account. The results for PGA are in the order of the values derived from the soil mechanics model and have been used to adjust the soil mechanics model. Therefore, this data is not taken further into account.

1.5.2 Logic Tree and Weights for Horizontal Motion

The following logic tree in Figure V-1.51 is generally valid for all elevations.

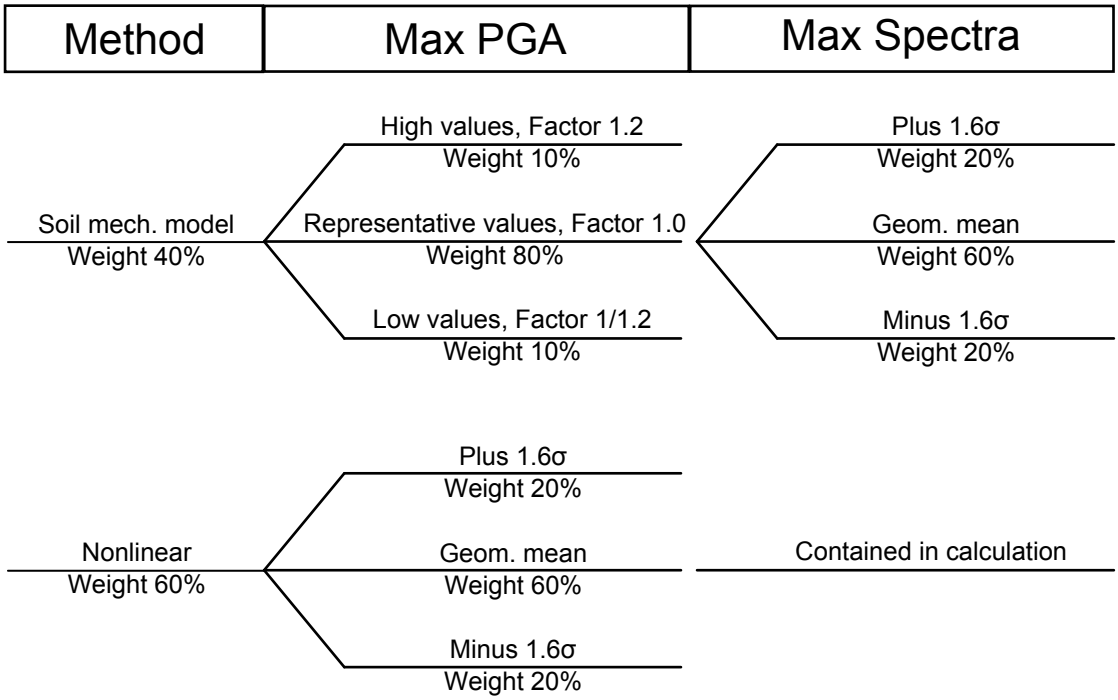

Figure V-1.51: Logic tree for horizontal motion.

Exceptions:

- Beznau, minimum elevation: Non-linear branch has weight 100%
- Mühleberg, minimum elevation: Elevation is located in rock; therefore no cut-off values for the alluvium are applicable.

Soil Mechanics Model Branch

Maximum PGA Surface

Based on the individual results of the calculations performed in Pecker [2011], taking into account the results from the soil mechanics model and the field observation, the following maximum peak ground accelerations (outcrop motions) are proposed for the individual sites at surface:

Table V-1.11: outcrop motions

Beznau:	$\ddot{u}_{max} = 2.5$g
E-Beznau:	$\ddot{u}_{max} = 2.2$g
Gösgen:	$\ddot{u}_{max} = 2.0$g
Leibstadt:	$\ddot{u}_{max} = 1.7$g
Mühleberg:	$\ddot{u}_{max} = 2.1$g

Maximum PGA, at Mean and Minimum Elevation

No results for maximum PGA ant mean and minimum elevation from the soil mechanics model exist. Results from TNL calculations are only within motions. They can be transferred to outcropping motions by the following formulas (each rule with a weight of 50%, whereby for the corresponding SHAKE values, the average between 30 Hz and 100 Hz is taken. The SHAKE ratio is taken for the input ground motion level of 0.75 g and a Magnitude of 6. In case of different profiles or materials, the average over all materials and profiles is taken.

$$PGA\_max_{outcropping,atdepth} = PGA\_max_{within,atdepth} \frac{SHAKE_{outcropping,atdepth}}{SHAKE_{within,atdepth}} \quad \text{(V-1.14)}$$

$$PGA\_max_{outcropping,atdepth} = PGA\_max_{within,atsurface} \frac{SHAKE_{outcropping,atdepth}}{SHAKE_{outcropping,atsurface}} \quad \text{(V-1.15)}$$

Take the mean value with a weight of 80%, the higher and lower value with a weight of each 10%, see Figure V-1.51.

Maximum PGA, at Minimum Elevation

- Beznau:
  The minimum elevation is located in rock. It can be assumed that the "rock layer" has a higher strength than the alluvium. Therefore, the soil mechanics branch is not taken into account, weight of 0%. Non-linear branch (see paragraph 1.5.2) is taken with weight 100%.

- E-Beznau:
  Both elevations are within the soil layer; therefore the logic tree Figure V-1.51 can be directly applied.

- Gösgen, Leibstadt:
  Both elevations are within the soil layer; therefore the logic tree Figure V-1.51 can be directly applied.

- Mühleberg:
  The minimum elevation is located in rock. It can be assumed that the "rock layer" has a higher strength than the alluvium. No cut off value based on the soil mechanics model is taken into consideration at minimum elevation.

Spectral Shape for Sites Different Elevations

Surface: Figure V-1.52 shows the normalized spectral shapes for the surface motion. They can be directly applied.

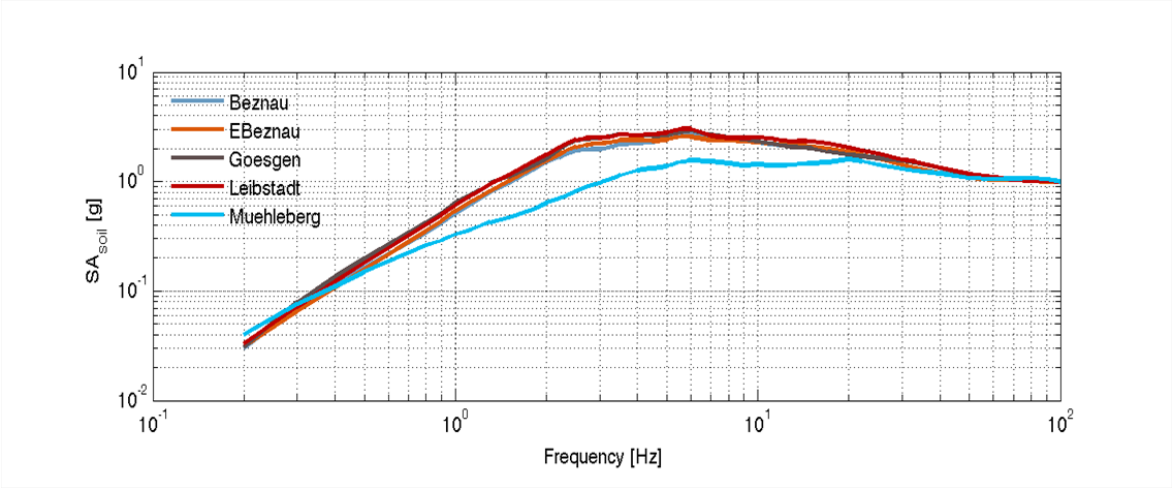

Figure V-1.52: Shapes of maximum ground motion, surface (normalized at PGA).

Mean and Minimum Elevation Figure V-1.53 shows the normalized spectra for the different sites for within motions. They have to be transferred to outcropping motions by the following formulas (each rule with a weight of 50%, whereby for the corresponding SHAKE values, the average between 30 Hz and 100 Hz is taken. The SHAKE ratio is taken for the input ground motion level of 0.75 g and a Magnitude of 6. In case of different profiles or materials, the average over all materials and profiles is taken):

$$PGA\_max_{outcropping,atdepth} = PGA\_max_{within,atdepth} \frac{SHAKE_{outcropping,atdepth}}{SHAKE_{within,atdepth}} \quad \text{(V-1.16)}$$

$$PGA\_max_{outcropping,atdepth} = PGA\_max_{within,atsurface} \frac{SHAKE_{outcropping,atdepth}}{SHAKE_{outcropping,atsurface}} \quad \text{(V-1.17)}$$

The resulting maximum ground motion spectral accelerations for each site as function of frequency are displayed as part of the HID appendix (EG3-HID-1008-Studer.SIF_Figures130503 FigSIF.Studer.HM.MaxGM.PNG.zip and FigSIF.Studer.VM.MaxGM.PNG.zip). Figure V-1.54(a) shows as an example the maximum ground motion values at Beznau for the surface.

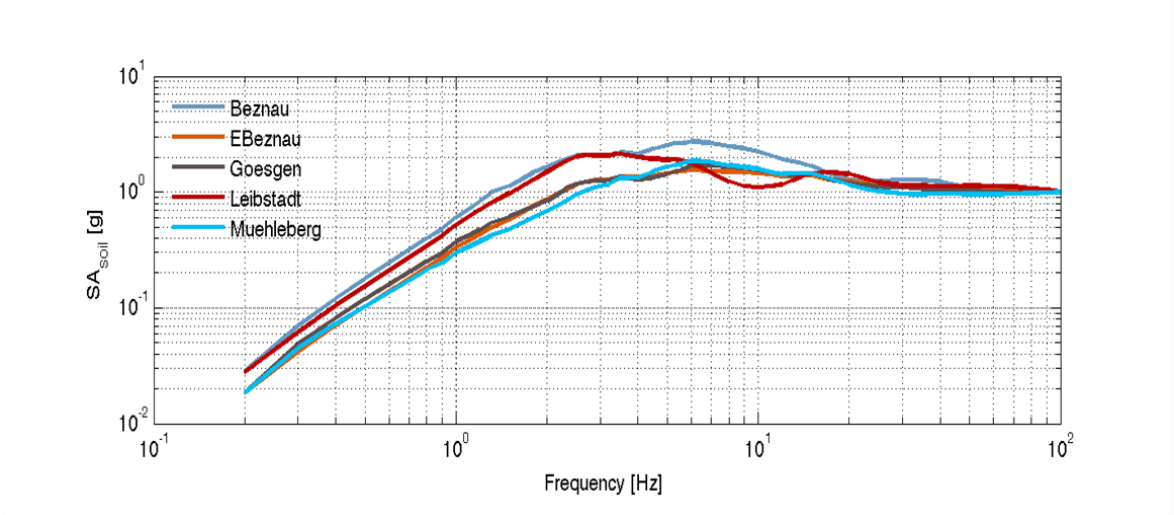

Figure V-1.53: Shapes of maximum ground motion, subsurface (normalized at PGA).

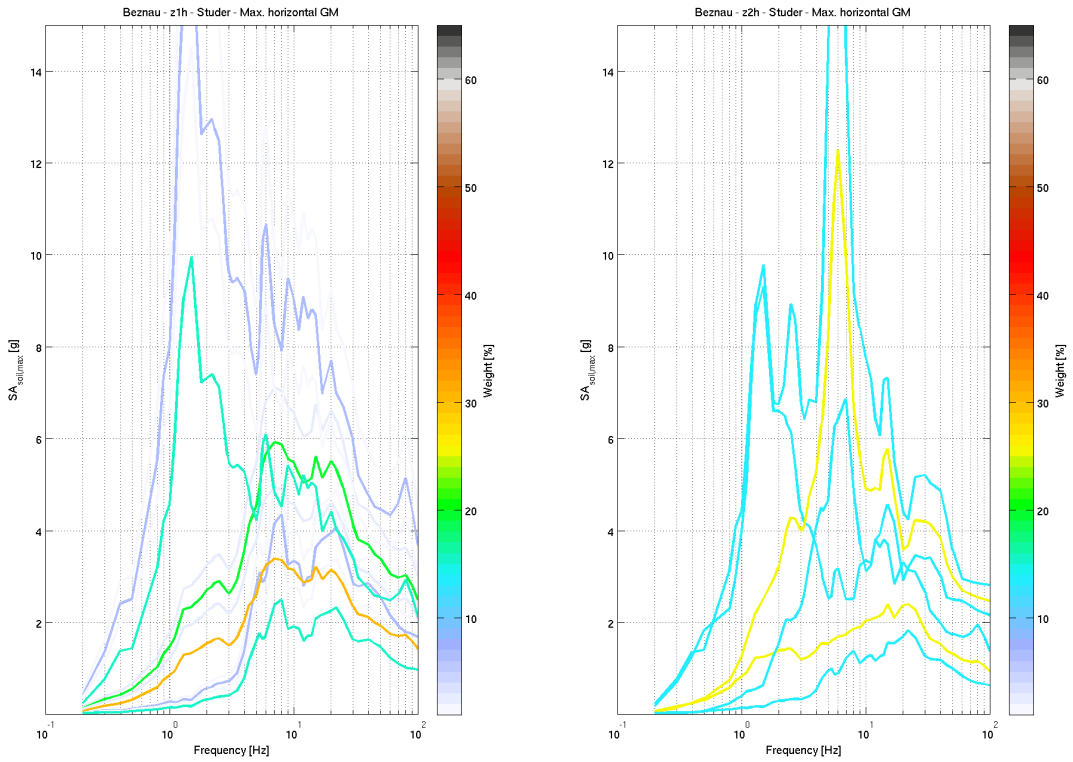

(a) Max GM at surface

(b) Max GM at sub-surface

Figure V-1.54: Example of maximum ground motions at surface and sub-surface for Beznau.

Non-linear Branch

Beznau, E-Beznau Gösgen and Mühleberg

This section is valid for all elevations, with the corresponding values at the elevation considered. Exception: For Beznau and Mühleberg minimum elevation, the non-linear branch takes 100% weight.

Surface motion can be taken directly.

Mean and minimum elevations are within motions and need to be transferred to outcropping motions with the formulas (each rule with a weight of 50%):

$$AF_{outcropping,atdepth} = AF_{within,atdepth} \frac{SHAKE_{outcropping,atdepth}}{SHAKE_{within,atdepth}} \quad \text{(V-1.18)}$$

$$AF_{outcropping,atdepth} = AF_{within,atsurface} \frac{SHAKE_{outcropping,atdepth}}{SHAKE_{outcropping,atsurface}} \quad \text{(V-1.19)}$$

for the corresponding frequency, and where AF is the spectral amplification. The SHAKE ratio is taken for the input ground motion level of 0.75 g and a Magnitude of 6. In case of different profiles or materials, the average over all materials and profiles is taken.

Leibstadt

This chapter is valid for all elevations, with the corresponding values at the elevation considered. Surface motion can be taken directly.

Mean and minimum elevations are within motions and need to be transferred to outcropping motions with the formulas (each rule with a weight of 50%):

$$AF_{outcropping,atdepth} = AF_{within,atdepth} \frac{SHAKE_{outcropping,atdepth}}{SHAKE_{within,atdepth}} \quad \text{(V-1.20)}$$

$$AF_{outcropping,atdepth} = AF_{within,atsurface} \frac{SHAKE_{outcropping,atdepth}}{SHAKE_{outcropping,atsurface}} \quad \text{(V-1.21)}$$

for the corresponding frequency, and where AF is the spectral amplification. The SHAKE ratio is taken for the input ground motion level of 0.75 g and a Magnitude of 6. In case of different profiles or materials, the average over all materials and profiles is taken.

1.5.3 General Concept for Vertical Motion

The strength of a soil element under normal loads is significant larger than under shear loading and the material also behaves stiffer. The strength under normal loading is governed by the grain strength. Therefore it is reasonable to assume an "unbounded" material strength compared to the material strength under shear loading. Therefore the maximal ground motion for vertical motion is taken as "unbounded".

Rational for Vertical Aleatory Variability:

The aleatory variability for the vertical component is set to zero.

Maximum Ground Motion for Vertical Motion:

- Unlimited for Beznau, Gösgen, Mühleberg.
- For Leibstadt: Special case as ground water table is very low. Three branches:
  - Unlimited (50%)
  - Spectrum as defined in Ripperger and Fäh [2003] (TP3-TN-0359) (25%)
  - 1.4 · Spectrum as defined in Ripperger and Fäh [2003] (TP3-TN-0359) (25%)

Chapter 2

Hazard Input Document for J. Studer (EG3-HID-1008)

Written by the PMT, SP4 and TFI

2.1 Introduction

This Hazard Input Document (HID) describes the implementation, evaluation and results of Jost Studer's geotechnical assessment of sites effects (the "model" or "SP3 model") at the NPP sites Beznau, Gösgen, Leibstadt and Mühleberg, delivered on 02.04.2012. The purpose of this document is to provide a technical description of the model as implemented. The results of model evaluation are compiled into a so-called SIF (Soil hazard Input File), which, among the rock hazard results, is input to the soil hazard evaluations. This HID addresses technical and procedural aspects. It does not provide a rational discussion of the models or the results.

2.2 Model Description

The geotechnical assessment by Jost Studer is described in part IV, Chapter 1 (EG3-ES-1017). The models concern six quantities:

- Amplification of horizontal ground motion,
- Aleatory variability of horizontal motion amplification,
- Maximum horizontal ground motion,
- Amplification of vertical ground motion and V/H scaling,
- Aleatory variability of vertical motion amplification and V/H scaling factors, and
- Maximum vertical ground motion,

which are all developed as functions of spectral frequency, which consider the up-going wavefield ("outcrop motion") and which depend on site, target depth, PGA and magnitude. The models are formulated as logic trees, yielding epistemic uncertainty. These logic tree models are described in the following.

2.2.1 Amplification of Horizontal Ground Motion

The logic tree model for amplification of horizontal ground motion considers six levels (Fig. V-2.1), among which epistemic uncertainty is developed.

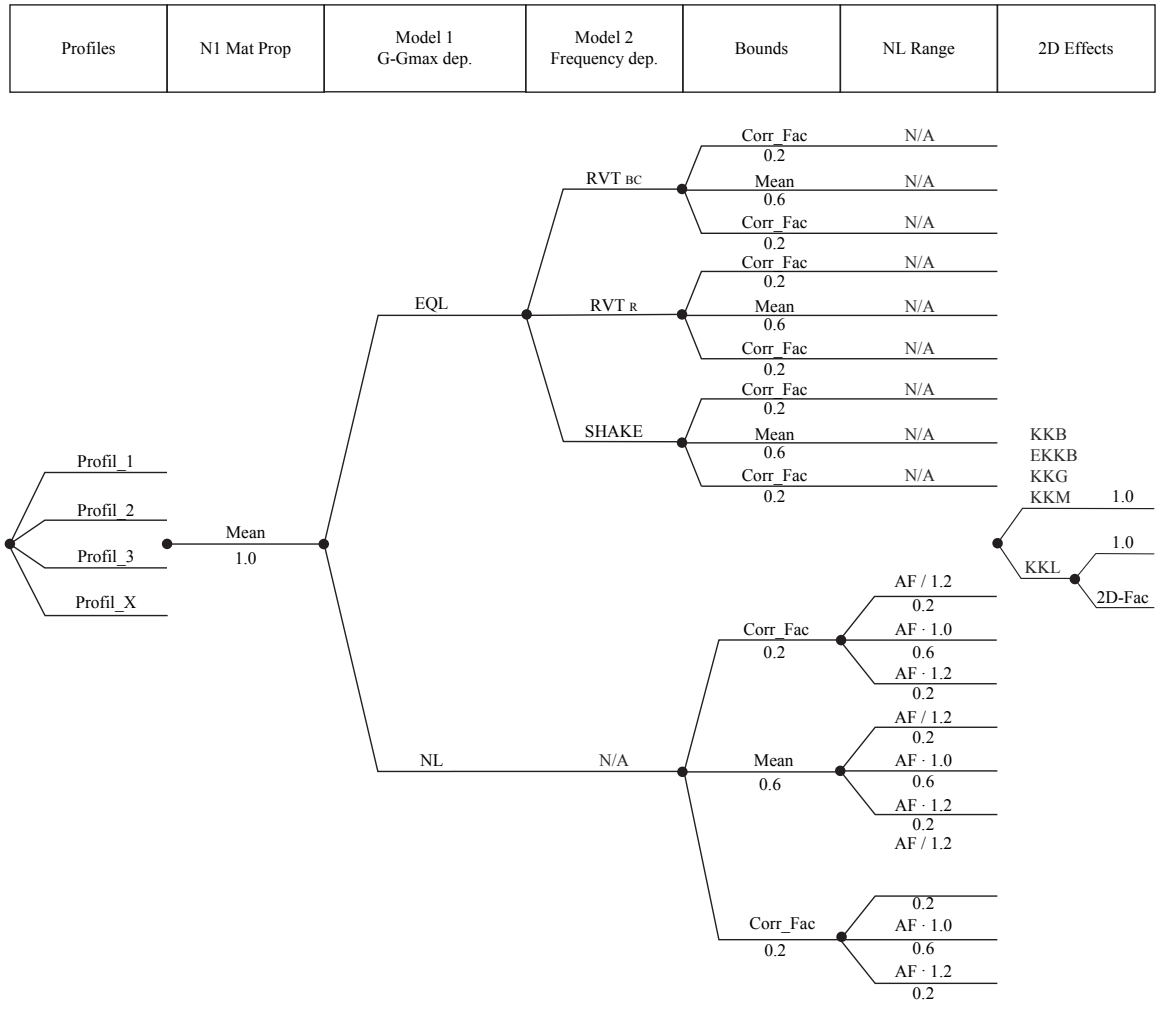

Figure V-2.1: Logic tree model, which develops amplification functions applicable to horizontal ground motion, by five (effective) or six (conceptual) levels of branching.

Level 1

develops soil profile alternatives. The soil profiles are described in Renault [2010a, b, c, d, e] [TP3-TN-1068...1071] and in the report Part I. The assigned weights are given in Table V-2.1. They dependent on the NPP site and are frequency-invariant. They are implemented in the *sp3s_Profile* routine of TP4-HSW-1002 [Hölker 2012].

Table V-2.1: Weights of soil profiles in level 1 of the logic tree model for amplification of horizontal ground motion.

Soil profile	P1	P2	P3	P4	P5	P6
Beznau	0.40	0.25	0.10	0.25	-/-	-/-
Gösgen	0.20	0.20	0.10	0.20	0.20	0.10
Leibstadt	0.40	0.30	0.30	-/-	-/-	-/-
Mühleberg	0.30	0.20	0.30	0.20	-/-	-/-

Level 2

conceptually would develop the material and shear modulus models. A "lower bound", "best estimate" and "upper bound" model have been defined in TP3-TN-1068 to 1071, but J. Studer decided to utilize only analyses based on the best estimate material model. No branching occurs on level 2 of the logic tree.

Level 3

develops alternative amplification functions based on the different computational approaches to the site response analyses (SRA). The considered approaches are SHAKE, RVT and non-linear. RVT is separated into analyses based on the "base case" V_S-profile and analyses based on the randomized V_S-profiles. For embedded layers two alternative scaling functions are applied to amplification functions based on the non-linear approach in order to correct from "within" motion at depth to "outcrop" motion. This yields in four levels of branching for surface targets or five levels of branching for embedded layer targets.

The weights assigned to the computational approaches are function of spectral frequency and a ratio $G/Gmax$. The weights are defined in Equations V-2.2a, V-2.2b, V-2.2c and V-2.2d, which utilize a linear ramp function defined in Equation V-2.1.

$$R(x, x1, x2) = \begin{cases} 0 & x < x1 \\ (x - x1)/(x2 - x1) & x1 < x < x2 \\ 1 & x > x2 \end{cases} \tag{V-2.1}$$

$$W_{NL} = 1 - R(G/Gmax, 0.2, 0.5) \tag{V-2.2a}$$

$$W_{SHAKE} = W_{NL} + 0.35R(f, 2f_0, 4f_0) - 0.4 \tag{V-2.2b}$$

$$W_{RVTbc} = W_{NL} - 0.2R(f, 2f_0, 4f_0) - 0.35 \tag{V-2.2c}$$

$$W_{RVTr} = W_{NL} - 0.15R(f, 2f_0, 4f_0) - 0.25 \tag{V-2.2d}$$

where f is spectral frequency [Hz] and f_0 is the site- and profile-specific fundamental frequency. The ratio G/G_{max} is derived from the shear modulus reduction curves [TP3-TN-1068...1071], which are functions of strain and which are specific to the soil layer. The applicable strain value is the maximum strain observed below target depth on the strain/depth profile resulting from the RVT base case analysis for the magnitude- and PGA-specific case at hand. The depth of the maximum strain pick determines the applicable shear modulus reduction curve. Figure V-2.2 exemplarily shows weights for a Beznau case.

Weights and branching is implemented in *sp3s_Method*. Maximum strain picking and determination of the ratio G/G_{max} is implemented in *sp3s_G/Gmax*.

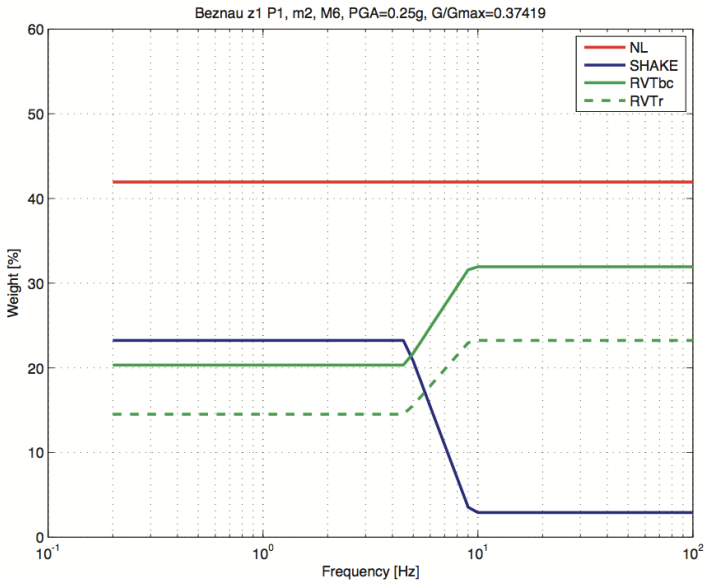

Figure V-2.2: Weights assigned per spectral frequency to the computational SRA approaches according to Equations V-2.2a to V-2.2d. The figure gives an example for Beznau, surface, profile 1, best estimate material model assuming a magnitude 6 event with a PGA of 0.25 g. The RVT base case analysis for this case suggests a maximum shear strain of 0.0041% at 5.5 m depth, which locates within the uppermost soil layer (gravels). Given this strain and the applicable G/G_{max} curve a G/G_{max} value of 0.374 is determined on which basis the weights of the non-linear (NL) versus the EQL (SHAKE, RVT) approaches is based.

Level 4

implements an amplification function envelope. This is archived by a 3-fold sub-branching defining a median (BE), upper (UB) and lower bound (LB) amplification function. The envelope is computed per spectral frequency as per Equations V-2.3a, V-2.3b, V-2.3c. The associated weights are 20% for the upper and lower bound and 60% for the median.

$$AF_{UB} = \exp[\text{mean}(\log(AF_{SRA\,method\,at\,hand})) + 1.6\sigma\,(\log(AF_{RVT\,rand}))] \quad \text{(V-2.3a)}$$

$$AF_{BE} = \exp[\text{mean}(\log(AF_{SRA\,method\,at\,hand}))] \quad \text{(V-2.3b)}$$

$$AF_{LB} = \exp[\text{mean}(\log(AF_{SRA\,method\,at\,hand})) - 1.6\sigma\,(\log(AF_{RVT\,rand}))] \quad \text{(V-2.3c)}$$

Level 5

develops scaling factors applicable to non-linear SRA branches in order to capture modeling uncertainty of the non-linear method. Three scaling factors 1.2 (weight 20%), 1.0 (weight 60%) and 1/1.2 (weight 20%) are defined resulting in a 3-fold sub-branching. This sub-branching is not applicable to branches based on RVT or SHAKE analyses.

Level 6

develops a two-fold sub-branching to account for possible 2D effects at Leibstadt site. The first option (30% weight) is, that 2D effects do not modify the amplification function. The second option (70% weight) is a modification of the amplification function by spectral scaling factors. In case of other sites than Leibstadt no sub-branching is applicable, i.e. only option 1 applies.

The spectral scaling factors are defined for PGA levels of 0.1 g and 0.4 g (Tab. V-2.2). They are based on analyses in Bard [2002a] (TP3-TN-0186). The values effectively used for implementation are the geometric mean values digitized from Figures V-1.23 and V-1.24 in EG3-ES-1017 (see Part V), which were linearly interpolated on log(frequency) scale. For cases of PGA<0.1 g or PGA>0.4 g the PGA-nearest factors are used. Weights and scaling factors are implemented in *sp3s_2d Effects*.

Table V-2.2: Spectral scaling factors (S) applicable to amplification function for Leibstadt site to account for 2D effects assuming a low PGA case (0.1 g) and a high PGA case (0.4 g). The scaling factors were digitized from the geometric mean values in Figures V-1.23 and V-1.24 in EG3-ES-1017.

Freq. [Hz]	0.2	0.4	0.8	1.3	2.2	3	5.8	7	8	10	15	33	50	100
$S_{PGA0.1g}$	1.1	1.06	1.08	1.07	1.18	1.12	1.42	1.35	1.37	1.22	1.13	1.21	1.22	1.21
Freq. [Hz]	0.2	0.3	0.8	1	1.5	1.8	2.2	3	4	5	6	7	40	100
$S_{PGA0.4g}$	1.04	1.03	1.06	1.05	1.09	1.06	1.15	1.09	1.01	1.08	1.11	1.05	1.09	1.09

2.2.2 Aleatory Variability of Horizontal and Vertical Motion

Aleatory variability in SP3 is conceptually defined as variability, which is additional to the variability already included in the rock hazard results. For vertical motion it is zero. For horizontal motion the default value is zero, too, but if PGA is equal to 0.4 g or larger and if the considered target is the surface (or at Leibstadt site also the embedded target) aleatory variability is defined per spectral frequency as per Equations V-2.4a and V-2.4b.

$$\sigma_{SP3} = \begin{cases} 0 & \Delta\sigma^2 < 0 \\ \sqrt{(\Delta\sigma^2)} & \Delta\sigma^2 > 0 \end{cases} \tag{V-2.4a}$$

$$\Delta\sigma^2 = \text{mean}[\sigma_{NL}(M, \text{PGA, material})]^2 - \sigma_{rock}^2 \tag{V-2.4b}$$

with M=5,6,7; PGA=0.4, 0.75, 1, 1.5, 2.5; material={lower bound, best estimate, upper bound} and
where σ_{NL} is the standard deviation of amplification from the non-linear SRA and where σ_{rock} is a standard deviation for rock sites published by Rodriguez-Marek et al. [2011]. σ_{rock} is reproduced in Table V-2.3. It is considered to be representative of the aleatory variability included in the rock hazard.

This model provides only a single aleatory variability function. Therefore the aleatory variability assessment has no epistemic uncertainty, i.e. no branching of the logic tree model is developed.

Table V-2.3: Spectral standard deviation for rock sites reported in Rodriguez-Marek and Cotton [2011].

Freq. [Hz]	0.7	1	1.2	1.3	1.7	2.1	2.3	2.6	2.8	3.2	4.3
σ_{rock}	0.331	0.283	0.27	0.261	0.238	0.236	0.229	0.224	0.227	0.23	0.241
Freq. [Hz]	4.9	5.9	6.8	8.6	10.3	12	13	17	21	26	100
σ_{rock}	0.242	0.251	0.259	0.281	0.291	0.298	0.301	0.313	0.315	0.31	0.307

2.2.3 Maximum Horizontal Ground Motion

The logic tree model of maximum horizontal ground motion (Fig. V-2.3) develops alternative maximum ground motion spectra by means of four levels of branching. The spectra are defined as:

$$SA_{max}(f) = PGA_{max}\, U\, \exp\left(\log(SA_n(f)) + 1.6\sigma(f)\right) \tag{V-2.5}$$

where PGA_{max} is a maximum PGA value, U is an uncertainty factor, $SA_n(f)$ is a normalized spectral shape and $\sigma(f)$ is an uncertainty being function of spectral frequency.

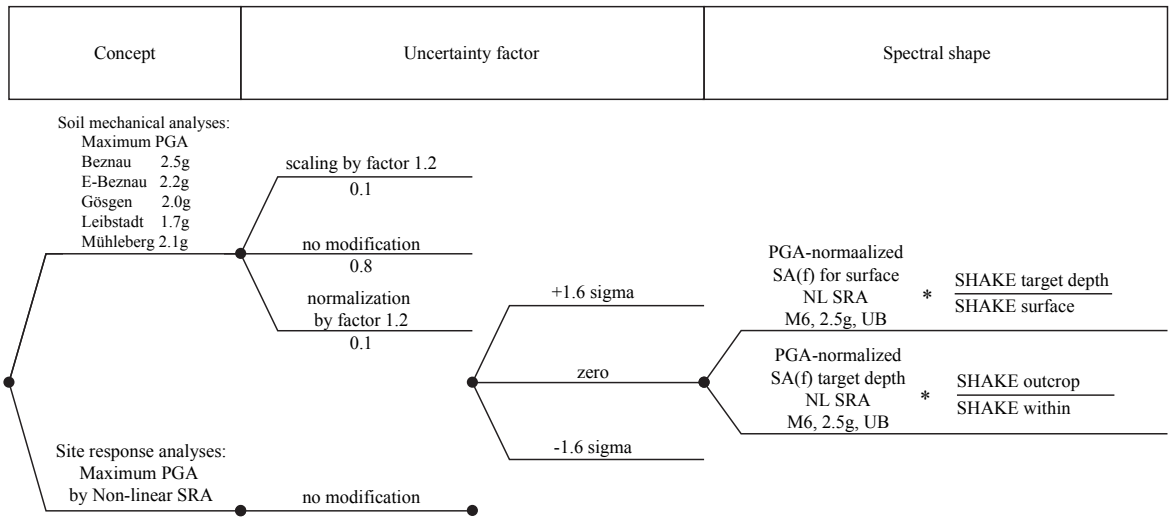

Figure V-2.3: Logic tree model, which develops maximum acceleration spectra for horizontal ground motion.

The maximum horizontal ground motion model described is applicable for all sites except the -14 m target at Mühleberg site. In the later case one maximum ground motion (truncation) is defined as "infinite", because the target substratum (unweathered Molasse) is assumed not to fail (liquefy).

Level 1

develops two alternative maximum PGA values on soil (PGA_{max} in Equation V-2.5). Both are based on modeling. No empirical data are utilized. Maximum PGA is either based on the soil mechanical model by [Pecker 2011] (TP3-TB-1074) (figure 3) or it is based on the magnitude 6 non-linear SRA for PGA_{rock} of 2.5 g. The concept based on the soil mechanical model is

assigned a weight of 40% (100% in case of Mühleberg site) for surface targets and 0% for the embedded targets. The concept based on the non-linear SRA is assigned complementary weight.

Level 2

implements a 3-fold branching, which develops an uncertainty factor (U in Equation V-2.5). This branching is effective only in case of the soil mechanical model. The uncertainty factors are 1.2, 1.0 and 1/1.2 and associated weights are 10%, 80% and 10%.

Level 3

develops an envelope around the "median" maximum ground motion. This is implemented by means of three branches: No modification of the "median" occurs on one branch; while on the other two branches a frequency-dependent uncertainty is added or subtracted, respectively. This uncertainty, $\sigma(f)$ in Equation V-2.5, is 1.6× the standard deviation of the log spectral accelerations resulting from the magnitude 6 non-linear SRA for PGA_{rock} of 2.5 g. The weights being assigned to the three branches are 20%, 60%, 20%, if on a branch based on the soil mechanical concept, or 25%, 50%, 25%, if on a branch based on the NL site response analysis.

Level 4

develops the spectral shape, $SA_n(f)$ in Equation V-2.5. For surface targets one shape (yielding no logic tree branching) is developed. This shape is the PGA-normalized acceleration spectrum resulting from the upper-bound material model, magnitude 6 non-linear SRA targeting at the surface and assuming 2.5 g PGA_{rock}. For subsurface targets two alternative shapes are developed (yielding a two-fold branching of the logic tree). Weights are 50% each. The first spectral shape is based on the PGA-normalized acceleration spectrum for the surface (as above) scaled by the ratio of the RVT acceleration spectra for 0.75 g with the spectrum for target depth and outcrop motion in the nominator and the spectrum for surface in the denominator. The second spectral shape is the PGA-normalized acceleration spectrum of the magnitude 6 non-linear SRA for PGA_{rock} of 2.5 g for the considered depth scaled by the ratio of RVT-based "outcrop motion" acceleration spectrum for 0.75 g at depth over the "within motion" corresponding spectrum.

2.2.4 V/H Scaling and Amplification of Vertical Ground Motion

The logic tree model of site effects of vertical motion (Fig. V-2.4) is a composite model, which separates at

Level 1

into three main branches: The first branch (35% weight) considers V/H ratios defined by the SP3 expert. It will be extended by the logic tree model for amplification of horizontal ground motion. The second branch (10% weight) assumes that vertical motion on rock equals vertical motion on soil, i.e. amplification is 1. This branch is expanded by the SP2 V/H model, because the vertical motion SIFs are applicable to horizontal motion rock hazard. The

third branch (55% weight) develops amplification functions for vertical motion and is then expanded by the V/H model by the SP2 experts.

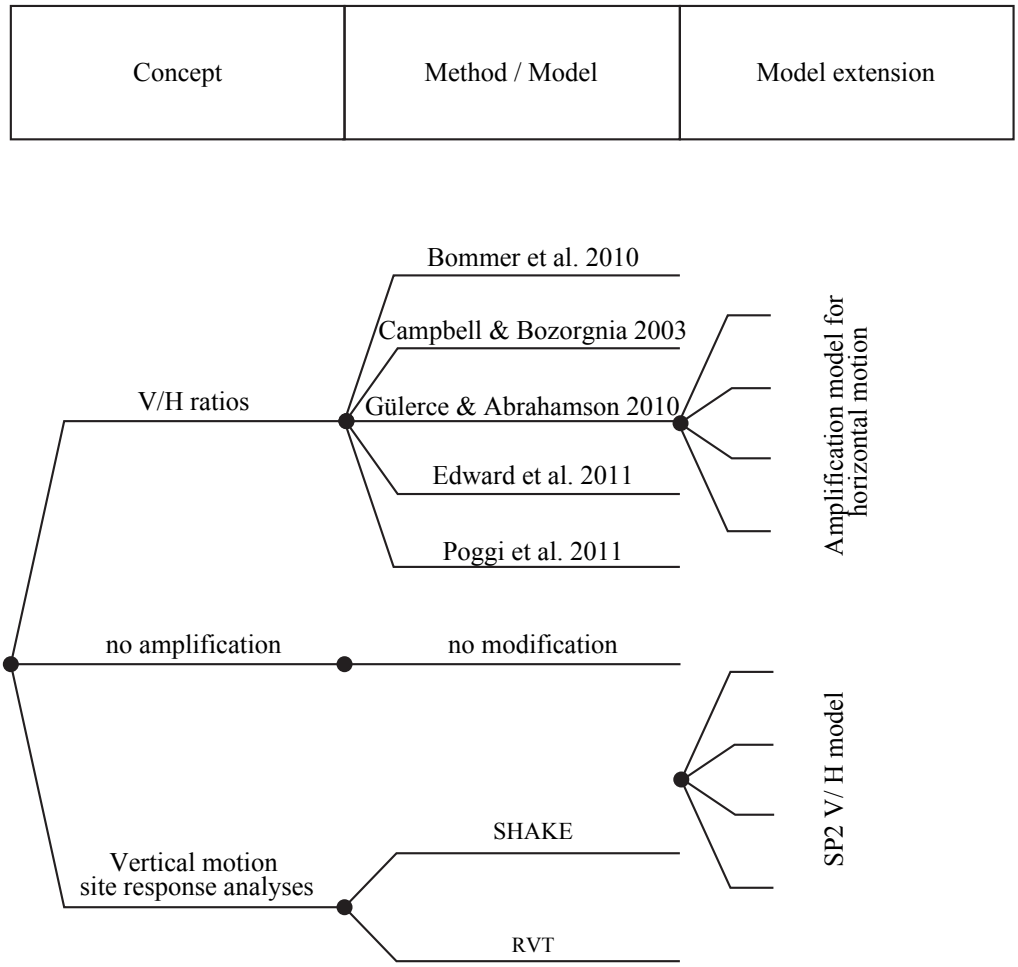

Figure V-2.4: Logic tree model, which develops V/H scaling factors and site-specific amplification factors.

Level 2

on the SP3 V/H branch develops alternative V/H scaling functions. These V/H scaling functions are provided by empirical GMPEs as per Table V-2.4.

Level 3

and following levels on the SP3 V/H branch reflect to the logic tree model for amplification of horizontal ground motion.

Level 2 on the vertical motion SRA branch

develops alternative analysis methods, which are RVT base case (weight 50%) and SHAKE (weight 50%). Only the best estimate material model is considered.

Level 3

and following levels **on the vertical motion SRA branch** reproduce the V/H model by the SP2 experts. The SP2 V/H model is implemented as a table of V/H ratios provided within SP4. The V/H ratios depend on the site, the spectral frequency, magnitude and PGA (or annual probability of exceedance, respectively). Within the SP3mod software this table and the weights assigned by the SP2 experts to the GMPEs are stored in the environment variable *sp3db.sp2VH*.

Table V-2.4: GMPEs utilized for modeling V/H scaling factors and associated weights defined by J. Studer.

V/H model	Default weight	Weight for Beznau, subsurface and Mühleberg -14 m
Gülerce and Abrahamson [2011]	0.20	0.20
Bommer et al. [2011]	0.15	0.15
Campbell et al. [2003]	0.15	0.15
Edwards et al. [2011b]	0.05	0.30
Poggi et al. [2011]	0.45	0.20

2.2.5 Maximum Vertical Ground Motion

For Beznau, Gösgen and Mühleberg sites it is assumed that maximum vertical ground motion is not limited by soil properties. Infinity-valued maximum ground motion truncation spectra are implemented for these sites. In case of Leibstadt site three scenarios as per Table V-2.5 are considered.

Table V-2.5: Maximum ground motion (truncation) spectra and weights for vertical motion applicable at Leibstadt site. Spectra SA_1 and SA_2 are derived from Ripperger and Fäh [2003] (TP3-TN-0359).

Weight	Freq. [Hz]	0.3	0.8	1.5	2.19	4.31	9.43	18.5	22	22.3	25	100
0.25	$SA_{max,1}$	0.366	0.81	1.532	2.103	4.18	4.878	5.182	5.057	5.031	3.613	1.631
0.25	$SA_{max,2}$	0.512	1.134	2.144	2.944	5.851	6.829	7.254	7.08	7.043	5.058	2.283
0.50	$SA_{max,3}$	infinite										

2.2.6 Inter- and Extrapolation of Amplification Functions

Amplifications functions are derived from 1D site response analyses (SRA), whereby different computational approaches (RVT, SHAKE, NL) are utilized. Primarily amplification is implemented as function of spectral frequency (referred to as "amplification function" is the following). The results of all SRAs were resampled to 60 spectral frequencies (Tab. V-2.6). The full parameter space of the site- and component-specific amplification functions spans spectral frequency, PGA, magnitude, material model, V_s-profile, target depth and motion type.

For evaluation of the SP3 model and processing of the results into SIFs the amplification functions need to be inter-/extrapolated for arbitrary PGA levels within the range 0.05 to 2.5 g. Depending on the computational approach, amplification functions for non-computed parameter sets need to be estimated from existing parameter sets. Inter-/extrapolation of amplification functions for arbitrary magnitudes within the range 4 to 8 is required in principle, but the soil hazard software covers this utilizing linear interpolation. Within the scope of this HID amplification functions are considered only for the discrete magnitude 5, 6 and 7.

RVT

amplification functions for **horizontal motion** (base case and randomized) and **vertical motion** (base case only) are available for all required parameter sets except Gösgen profile 6. Within the PGA range 0.05 to 1.5 g (horizontal motion) or the PGA range 0.1 to 0.75 g (vertical motion) amplification is interpolated linearly on a log(PGA) scale per spectral frequency. For PGA levels above 1.5 g (0.75 g for vertical motion) the amplification function by the PGA-nearest RVT analysis is adopted (i.e. nearest neighbor extrapolation). In case of Gösgen profile 6 the RVT amplification function is estimated by scaling the amplification function for profile 1, where the scaling function are ratios of the PGA-closest SHAKE amplification function for profile 6 in the numerator and the PGA-closest SHAKE amplification function for profile 1 in the denominator. Inter-/extrapolation of RVT amplification functions are implemented in $sp3s\_interp_{AF}\_RVT_{bc} and in sp3s\_interp_{AF}\_RVT_r$.

SHAKE

amplification functions for **horizontal motion and vertical motion** are available for all required parameter sets but are limited to the PGA range of 0.05 to 0.75 g except for Gösgen (where SHAKE analyses are available for PGA levels up to 2.5 g). Within the range of PGA levels for which SHAKE analyses are available, amplification is interpolated linearly on a log(PGA) scale per spectral frequency. In case of PGA-extrapolation the PGA-nearest available amplification function is scaled by a ratio of RVT base case amplification functions, where the nominator holds the RVT amplification function for desired PGA and the denominator holds the RVT amplification function for the PGA level corresponding to that of the PGA-nearest available SHAKE amplification function. Inter-/extrapolation of SHAKE amplification functions for horizontal motion are implemented in *sp3s_interp_AF_SHAKE*

Non-linear (NL)

amplification functions for **horizontal motion** are available only for some parameter sets. Therefore inter-/extrapolation for desired PGA is required and a scheme for estimating NL amplification functions at parameter sets, for which no NL SRA are available, is required. The approach is to first interpolate the NL amplification function for the primary profile (P6 at Gösgen, P1 at other sites) and the best estimate material for the anticipated PGA. Then scaling factors are applied per spectral frequency, which implement a correction from the primary to the anticipated profile and from the best estimate material model to the anticipated model.

$$AF_{NL}\left(f,P,m,M,PGA\right) = AF_{NL}\left(f|P=1,m=be,M,PGA\right) R_P(f)\, R_m\left(f|PGA\right) \quad \text{(V-2.6a)}$$

where f is spectral frequency, P is the soil profile, m is the material model, M is magnitude and PGA is peak ground acceleration on rock.

Within the PGA range of 0.05 to 1.5 g the amplification function $AF_{NL}\left(f|P=1,m=be,M,PGA\right)$ is PGA-interpolated from SRA available in the database. In order to extent this interpolation to PGA of 2.5 g, the NL amplification function for PGA=2.5 g is estimated by

$$AF_{NL}\left(f|m=be,2.5\,g,\ldots\right) = AF_{NL}\left(f|m=be,1.5\,g\right) AF_{NL}\left(f|m=ub,2.5\,g\right)/AF_{NL}\left(f|m=ub,1.5\,g\right) \quad \text{(V-2.6b)}$$

The spectral scaling ratios R_P in Equation V-2.6a are implemented as

$$R_P(f) = AF_{RVT_{bc}}\left(f|P\right)/AF_{RVT_{bc}}(f|P=1) \quad \text{(V-2.6c)}$$

using PGA-interpolation of RVT AF as described above. The spectral scaling ratios $R_m\left(f|PGA\right)$ in Equation V-2.6a are implemented, but are effectively not used, because only the best estimate material model is considered as per level 2 of the logic tree.

2.3 Model Implementation and Review History

The development of the models by the SP3 expert and its implementation by SP4 were carried out contemporary when partial model descriptions became available. J. Studer's model was implemented on the basis of draft versions of the evaluation summary EG3-ES-1017 (see part

V, Chapter 1), version 21 of 2. February 2012; on presentations by J. Studer at the SP3 workshops on 17. March 2011 [TP3-RF-1353], 7. July 2011 [TP3-RF-1386] and 20. December 2011 [TP3-RF-1439]; and on meetings held on 30. May 2011, 4. July 2011, 2. September 2011, 26. October 2011, 29. November 2011, 20. January 2012 and 2. April 2012.

No model modifications were undertaken subsequent to J. Studer's death except that the revised SHAKE and RVT analyses of 2013 are used. The TFI requested a test assessing the sensitivity of the model results to a modification of the relative weights of RVT and SHAKE similar as other experts did, and based on this decided to keep weights as originally defined by J. Studer.

The models are implemented by means of four programs addressing aspects as follow:

- *HM_SP3_Studer*
  - Amplification of horizontal ground motion;
  - Aleatory variability of horizontal motion amplification.
- *MaxHM_SP3_Studer*
  - Maximum horizontal ground motion.
- *VM_SP3_Studer*
  - Amplification of vertical ground motion;
  - V/H scaling factors;
  - Aleatory variability of vertical motion amplification and V/H scaling.
- *Max_VM_SP3_Studer*
  - Maximum vertical ground motion.

These programs are part of the "SP3mod" software Hölker [2012] (TP4-HSW-1002), which is designed as MATLAB toolbox with an associated database holding the site response analyses and described in Hölker [2013b] (TP4-TN-1197). MATLAB releases 2011a to 2012b have been utilized for development and model evaluation.

The implementation (MATLAB code) of the models was presented and discussed with J. Studer in above listed meetings. S. Thomassin provided an external review of the implementation of the horizontal motion models in August 2012 and of the vertical motion models in January 2013.

2.4 Model Evaluation

All models have been evaluated per site (Beznau, Gösgen, Leibstadt and Mühleberg) and target layer (surface and one or two subsurface layers) as defined in table 1 of Renault [2011a] (PMT-TN-1139) or section 4.2 of Renault and Abrahamson [2010] (PMT-TB-1014), respectively. The parameter space is spanned by magnitude, peak ground acceleration (PGA) and spectral frequency, which are discretized as detailed in Table V-2.6.

The model for E-Beznau site has been last evaluated in December 2012 and became obsolete with the revised SHAKE and RVT analyses of April 2013. Final model evaluations for Beznau, Gösgen, Leibstadt and Mühleberg were performed in May 2013.

Table V-2.6: Discretization of the parameter space of the SP3 models

Parameter	Discretization
Magnitude	5, 6, 7
PGA [g]	0.05, 0.1, 0.15, 0.2, 0.25, 0.3, 0.4, 0.5, 0.6, 0.75, 1.0, 1.25, 1.5, 1.75, 2.0, 2.25, 2.5
Freq. [Hz]	0.2, 0.3, 0.4, 0.5, 0.8, 0.9, 1, 1.1, 1.2, 1.3, 1.5, 1.8, 2, 2.2, 2.3, 2.5, 2.7, 2.9, 3, 3.1, 3.2, 3.4, 3.5, 4, 4.4, 4.5, 5, 5.3, 5.4, 5.5, 5.6, 5.7, 5.75, 5.9, 6, 6.9, 7, 8, 8.9, 9, 10, 11, 12, 13, 14, 15, 17, 20, 22, 25, 30, 33, 40, 45, 50, 60, 70, 80, 90, 100

2.5 Processing of Model Results into SIFs (SP3-to-SP4 Interface)

The logic tree models for amplification and aleatory variability yield a set of amplification and aleatory variability functions and associated weights. For amplification (or equivalently aleatory variability) these results may be described as

$$AF_i(f, PGA, M) \quad \text{and} \quad W_i(f, PGA, M) \quad \text{for } i = 1, 2, \ldots, n \tag{V-2.7}$$

where i is the indexing of logic tree branches, f is spectral frequency, PGA is peak ground acceleration, M is magnitude, AF is amplification and W is the associated weight.

Two modifications are applied to the data representation when the results are processed into a SIF: The n logic tree branches are summarized into 17 fractiles (Table V-2.7) taking into account the weights of the branches. The parameter space dimension PGA is scaled to spectral accelerations (SA), where the relation between SA, PGA and f is given by the spectra used as input motions for the site response analyses. Given these two modifications the amplification (and equivalently aleatory variability) results are represented in the SIF by

$$AF_j(f, SA, M) \tag{V-2.8}$$

where j is the index of the discrete fractiles defined in Table V-2.7.

Table V-2.7: Discrete fractiles and associated weights utilized to summarize the logic tree model results.

Percentiles:	0.13, 0.62, 2.28, 5, 10, 20, 30, 40, 50, 60, 70, 80, 90, 95, 97.72, 99.38, 99.87
Weights:	0.00375, 0.01075, 0.0219, 0.0386, 0.075, 0.10, 0.10, 0.10, 0.10, 0.10, 0.10, 0.10, 0.075, 0.0386, 0.0219, 0.01075, 0.00375

The logic tree models for maximum ground motion yield maximum spectral acceleration values on soil, $maxSA_i(f)$, and associated weights $W_i(f)$, where i is the indexing of logic tree branches and f is spectral frequency. Concerning the SIF these results are summarized into

17 discrete fractiles, if the number of logic tree branches exceeds 17. Otherwise the native $maxSA$ spectra and associated weights are transcribed to the SIF.

The aim of summarizing the model results to 17 fractiles is to reduce the number of combinations required in soil hazard evaluation, which is motivated by maintaining acceptable computing time. The 17 fractiles are associated with fixed weights as given in Table V-2.7. These weights are derived from bin width, where the fractiles are bin centers and where the bin bounds are the mean values of neighboring fractiles or 0 or 1, respectively.

The sit effect model for vertical motion features two components:

(a) Amplification factors, which conceptually are to be applied to vertical motion rock hazard, and

(b) V/H scaling factors, which are to be combined with the horizontal motion amplification factors and to be applied to horizontal motion rock hazard.

For SIF processing of the vertical motion model additionally the V/H scaling models by the SP2 experts are imported and are applied to component (a). This way both model components describe V/H scaling and amplification and can be processed into a single SIF, which is applicable to the horizontal motion rock hazard.

The details of the SP3-to-SP4 interface processing are described in Hölker [2013b] (TP4-TN-1197).

2.6 Results: SIFs (Soil Input Files or SiteMod Files)

The raw logic tree model results (intermediate model results) and the SIF-processed model results are saved into so-called "SiteMod" data structures in MATLAB format. A "SiteMod" data structure contains the SIF required by the soil hazard software and it additionally contains the unprocessed logic tree model results for the parameter space described in Table V-2.6. The details and internal format of the "SiteMod" data structure are described in Hölker [2013b] (TP4-TN-1197). Furthermore each "SiteMod" data file contains a descriptive self-documentation. The model result files associated with this HID are:

- SiteMod.Beznau.Studer.z1h.FullModel.mat
- SiteMod.Beznau.Studer.z1v.FullModel.mat
- SiteMod.Beznau.Studer.z2h.FullModel.mat
- SiteMod.Beznau.Studer.z2v.FullModel.mat
- SiteMod.Goesgen.Studer.z1h.FullModel.mat
- SiteMod.Goesgen.Studer.z1v.FullModel.mat
- SiteMod.Goesgen.Studer.z2h.FullModel.mat
- SiteMod.Goesgen.Studer.z2v.FullModel.mat
- SiteMod.Leibstadt.Studer.z1h.FullModel.mat
- SiteMod.Leibstadt.Studer.z1v.FullModel.mat

- SiteMod.Leibstadt.Studer.z2h.FullModel.mat
- SiteMod.Leibstadt.Studer.z2v.FullModel.mat
- SiteMod.Muehleberg.Studer.z1h.FullModel.mat
- SiteMod.Muehleberg.Studer.z1v.FullModel.mat
- SiteMod.Muehleberg.Studer.z2h.FullModel.mat
- SiteMod.Muehleberg.Studer.z2v.FullModel.mat
- SiteMod.Muehleberg.Studer.z3h.FullModel.mat
- SiteMod.Muehleberg.Studer.z3v.FullModel.mat

The token "z1h" indicates target layer and wavefield component, where "z1" is surface, "z2" is the upper embedded layer and "z3" is the lower embedded layer (as per table 1 of PMT-TN-1139) and where "h" is horizontal motion and "v" is vertical motion.

The token "FullModel" indicates that the file contains a full SP3 model. Other files, which contain model subsets only exist and have been created for parameter sensitivity analyses.

All SIFs (SiteMod files) are applicable to horizontal motion rock hazard results !

The SIFs for horizontal motion contain amplification models only while the SIFs for vertical motion contain combined amplification and V/H scaling models.

2.6.1 SIF Figures

The model results, i.e. the content of the "FullModel" SIFs listed in the previous section, have been systematically visualized by means of seven figures types:

- XY graph showing amplification versus PGA for selected spectral frequencies;
- An image display showing median amplification versus PGA and frequency;
- XY graph showing amplification versus SA on rock for a set of spectral frequencies;
- An image display showing the ratio of the 80% over the 20% fractile of amplification versus PGA and spectral frequency;
- XY graph showing maximum acceleration on soil versus spectral frequency;
- An image display showing median aleatory variability versus PGA and frequency (for horizontal motion only)
- An image display showing mean aleatory variability versus PGA and frequency (for horizontal motion only)

which are attached to this HID as an electronic appendix containing PNG and EPS files. Examples of these figures are discussed in Hölker [2013b] (TP4-TN-1197).

Chapter 3

Appendix to EG3-HID-1008 for J.A. Studer

A direct link to files for the final SP3 hazard feedback is given here:

Horizontal Motion Amplification Functions and Maximum Ground Motion

- Ratio of the 80% over the 20% fractile of amplification versus PGA and spectral frequency:
  Open external file: FigSIF.Studer.HM.AMPFp80p20-PGA-FREQ.
- Amplification versus PGA for selected spectral frequencies:
  Open external file: FigSIF.Studer.HM.AMPF-PGA.
- Amplification versus SA on rock for a set of spectral frequencies:
  Open external file: FigSIF.Studer.HM.AMPF-SA.
- Mean amplification versus PGA and frequency:
  Open external file: FigSIF.Studer.HM.MeanAMPF-PGA-FREQ.
- Median amplification versus PGA and frequency:
  Open external file: FigSIF.Studer.HM.MedAMPF-PGA-FREQ.
- Maximum acceleration on soil versus spectral frequency:
  Open external file: FigSIF.Studer.HM.MaxGM.

Horizontal Motion Aleatory Variability

- Median aleatory variability versus PGA for a set of spectral frequencies:
  Open external file: FigSIF.Studer.HM.AVAR-PGA.

- Median aleatory variability versus PGA and frequency:
  Open external file: FigSIF.Studer.HM.AVAR-PGA-FREQ.
- Aleatory Variability versus SA for a set of spectral frequencies:
  Open external file: FigSIF.Studer.HM.AVAR-SA.

Horizontal Motion Amplification Functions and Maximum Ground Motion

- Ratio of the 80% over the 20% fractile of amplification versus PGA and spectral frequency:
  Open external file: FigSIF.Studer.VM.AMPFp80p20-PGA-FREQ.
- Amplification versus PGA for selected spectral frequencies:
  Open external file: FigSIF.Studer.VM.AMPF-PGA.
- Amplification versus SA on rock for a set of spectral frequencies:
  Open external file: FigSIF.Studer.VM.AMPF-SA.
- Mean amplification versus PGA and frequency:
  Open external file: FigSIF.Studer.VM.MeanAMPF-PGA-FREQ.
- Median amplification versus PGA and frequency:
  Open external file: FigSIF.Studer.VM.MedAMPF-PGA-FREQ.
- Maximum acceleration on soil versus spectral frequency:
  Open external file: FigSIF.Studer.VM.MaxGM.

Chapter 4

QA-Certificate EG3-QC-1067

QA Certificate	PEGASOS REFINEMENT PROJECT
EG3-QC-1067	

Hazard Input Document (HID)

Expert group: EG3 ***HID designation:*** **EG3-HID-1008**

Expert: J. Studer ***Expert Model (EXM)*** EG3-EXM-1008

HID parameterisation of Expert Model:

TFI: N. A. Abrahamson ***Hazard Input Specialist of TFI-team:*** A. Hölker

HID based on Elicitation Documents: ☒ EG3-ES-1017

HID based on Exp. Assessments (EXA): ☒ EG3-EXA-1040 to EG3-EXA-1041

Remarks on the HID model parameterisation in terms of hazard computation input:

The undersigned Hazard Input Specialist confirms that this HID includes all required (subproject specific) input information for hazard computations. No further interpretations of this input will be required and no simplifications except Algorithmic Pinching according to paragraph 2.9 of the QA-Guidelines will be applied to convert this HID into hazard software Input Files.

Signature:

HID acceptance by the Expert / Expert Group:

Date of HID review by the Expert / Expert group: 02.12.2013

HID accepted: ☒ ***HID not accepted:*** ☐

Reasons for non-acceptance of HID / Recommendations:

The HID was signed by the TFI after the death of J. Studer. The original evaluation summary and SP3 models of J. Studer were maintained and carefully reviewed by the TFI.

The undersigned Expert(s) accept(s) the parameterisation proposed in this HID as a faithful and adequate representation of his/their Expert Model. He/they confirm(s) that this HID is free of errors and agree(s) to its use as hazard computation input.

Signature Expert 1 / Expert:

Signature Expert 2:

Signature Expert 3:

Bibliography

Abrahamson 2012 Abrahamson, N.: Master Ground Motion Logic Tree / prepared for PRP - PEGASOS Refinement Project. 2012 (TP2-TB-1081). – Technical Report. SP2 [cited at p. 506]

Abrahamson 2010a Abrahamson, N. A.: Development of Spectra for RVT Calculations / prepared for the PRP - PEGASOS Refinement Project. 2010 (TP3-SUP-1009). – Technical Report [cited at p. 133]

Abrahamson 2010b Abrahamson, N. A.: Time histories for the SP3 site response calculation / prepared for the PRP - PEGASOS Refinement Project. 2010 (TP5-SUP-1007). – Technical Report. Version 3.2 [cited at p. 133]

Abrahamson and Hölker 2012 Abrahamson, N.A. ; Hölker, A.: Evaluation of the nonlinearities in the candidate V/H models for SP3 in order to address the expert request for additional plots at the WS6/SP3 / prepared for PRP - PEGASOS Refinement Project. 2012 (TFI-TN-1235). – Technical Note [cited at p. 581, 654]

Abramowitz and Stegun 1970 Abramowitz, M. ; Stegun, I.A.: *Handbook of mathematical functions*. Vol. 9th Edition. Dover Publications Inc., 1970 [cited at p. 141]

Akkar et al. 2011 Akkar, S. ; Kale, O. ; Yenier, E. ; Bommer, J.J.: The high-frequency limit of usable response spectral ordinates from filtered amnalogue and digital strong-motion accelerograms. In: *Eartquake Engeneeing and Structural Dynamics* 40 (2011). http://dx.doi.org/10.1002/eqe.1095. – SHARE. – DOI 10.1002/eqe.1095 [cited at p. 252]

Al Atik et al. 2010 Al Atik, L. ; Abrahamson, N. ; Bommer, J.J. ; Scherbaum, F. ; Cotton, F. ; Kühn, N.: The Variability of Ground-Motion Prediction Models and Its Components. In: *Seismological Research Letters* 81 (2010), October, No. 5, p. 794–801. http://dx.doi.org/10.1785/gssrl.81.5.794. – DOI 10.1785/gssrl.81.5.794 [cited at p. 422]

AMEC 2009a AMEC: Additional data for the KKM/EKKM sites according to SP3 Experts requests on WS2a/SP3 (22.10.2009) / AMC Geomatrix Inc. 2009 (TP3-GTC-1007). – Geotechnical Database and Reports [cited at p. 5]

AMEC 2009b AMEC: Site investigations for KKM (& EKKM) / AMEC Geomatrix Inc. 2009 (TP3-GTC-1002). – Geotechnical Database and Reports [cited at p. 5]

AMEC 2010a AMEC: EQL & RVT Computation Results for KKM / AMEC Geomatrix Inc. 2010 (TP3-SUP-1012). – Supporting Computations Database [cited at p. 6]

AMEC 2010b AMEC: NL Computation Results for KKM / AMEC Geomatrix Inc. 2010 (TP3-SUP-1014). – Supporting Computations Database [cited at p. 6]

AMEC 2010c AMEC: Nonlinear Site Response Analysis Mühleberg Nuclear Power Plant - Volume 4 / AMEC Geomatrix Inc., prepared for PRP - PEGASOS Refinement Project. 2101 Webster Street, 12th Floor, Oakland, California 94612, USA, Decenber 11 2010 (TP3-TB-1046). – Technical Report. Part of TP3-SUP-1014 [cited at p. 145]

AMEC 2013 AMEC: KKM site response re-evaluation 2013 / AMEC Geomatrix Inc. 2013 (TP3-SUP-1086). – Supporting Computations Database [cited at p. 6]

Assimaki et al. 2000 Assimaki, D. ; Kausel, E. ; Whittle, A.: Model for dynamic shear modulus and damping for granular soils. In: *Journal of Geotechnical and Geoenvironmental Engineering* 126 (2000), No. 10, p. 859–869.. – SP3 [cited at p. 466]

Assimaki et al. 2003 Assimaki, D. ; Pecker, A. ; Popescu, R. ; Prévost, J.H.: Effects of spatial variability of soil properties on surface ground motion. In: *Journal of Earthquake Engineering* 7 (2003), No. Special issue 1, p. 1–44. – SP3 [cited at p. 467]

AXPO 2010a AXPO: Additional site investigation data for KKB/EKKB according to SP3 Experts requests during WS2b/SP3 (19.11.2009) / AXPO AG and Interoil. 2010 (TP3-GTC-1009). – Geotechnical Database and Reports [cited at p. 5]

AXPO 2010b AXPO: Additional site investigation data for KKL according to SP3 Experts requests during WS2b/SP3 (19.11.2009) / AXPO AG and Interoil. 2010 (TP3-GTC-1010). – Geotechnical Database and Reports [cited at p. 5]

AXPO 2010c AXPO: EQL & RVT Computation Results for KKB, EKKB & KKL / AXPO AG. 2010 (TP3-SUP-1013). – Supporting Computations Database [cited at p. 6]

AXPO 2010d AXPO: NL Computation Results for KKB, EKKB & KKL / AXPO AG. 2010 (TP3-SUP-1016). – Supporting Computations Database [cited at p. 6]

AXPO 2013 AXPO: KKB & KKL site response re-evaluation 2013 / AXPO AG. 2013 (TP3-SUP-1090). – Supporting Computations Database [cited at p. 6]

Bard 2002a Bard, P.-Y.: 2D SH computations for the Leibstadt nuclear power plant site Amplification factors in the low and high strain cases. / prepared for PRP - PEGASOS Refinement Project. 2002 (TP3-TN-0186). – Technical Note. SP3 [cited at p. 403, 405, 491, 571, 617]

Bard 2003 Bard, P.-Y.: A short note on the reliability of SHAKE amplification factors at low frequencies / LGIT/LCPC, perpared for the PEGASOS project. 2003 (TP3-TN-0340). – Technical Note [cited at p. 547]

Bard 2002b Bard, P.Y.: Variability of 1D-response for the 4 NPP sites under plane, oblique, SH, SV and P incidence. / prepared for PRP - PEGASOS Refinement Project. 2002 (TP3-RF-0310). – Technical Report. SP3 [cited at p. 476]

Betbeder-Matibet 1993 Betbeder-Matibet, J.: Calcul de l'effet de site pour une couche de sol. Troisième Colloque National de Génie Parasismique,. In: *Saint-Rémy-lès-Chevreuse* 1 (1993), March, No. DS1-DS10. – SP3 [cited at p. 144, 511]

Bommer et al. 2011 Bommer, J. J. ; Akkar, S. ; Kale, O.: A Model for Vertical-to-Horizontal Response Spectral Ratios for Europe and the Middle East. In: *Bulletin of the Seismological Society of America* 101 (2011), No. 4, p. 1783–1806. http://dx.doi.org/10.1785/0120100285. – EXT-RF-1336. – DOI 10.1785/0120100285 [cited at p. 358, 419, 437, 451, 495, 528, 582, 621]

Bommer 2009 Bommer, J.J.: Selected Accelerograms for Site Response Analyses (SP3) - Reviewed and approved by SP5 Experts / Imperial College Consultants Ltd, prepared for PRP - Pegasos Refinement Project. 2009 (TP5-TB-1020, Ver.2.1). – Technical Report. Ver. 2.1, SP3 + SP5 [cited at p. 133]

Bommer and Akkar 2010 Bommer, J.J. ; Akkar, S.: Models for the V/H (vertical to horizontal) Ratios of Spectral Response Ordinates and their Associated Variability / Imperial College Consultants Ltd., prepared for PRP - PEGASOS Refinement Project. 2010 (TP2-TB-1061). – Technical Report. SP2 [cited at p. 419]

Boore 1983 Boore, D. M.: Stochastic simulation of high-frequency ground motions based on seismological models of the radiated spectra. In: *Bulletin of the Seismological Society of America* 73 (1983), December, No. 6, p. 1865–1894 [cited at p. 133]

Boore and Atkinson 1992 Boore, D. M. ; Atkinson, G. A.: Source Spectra for the 1988 Saguenay, Quebec, Earthquakes. In: *Bulletin of the Seismological Society of America* 82 (1992), No. 2, p. 683–719 [cited at p. 137]

Campbell and Bozorgnia 2003 Campbell, K.W. ; Bozorgnia, Y.: Updated Near-Source Ground Motion (Attenuation) Relations for the Horizontal and Vertical Components of Peak Ground Acceleration and Acceleration Response Spectra. In: *Bulletin of the Seismological Society of America* 93 (2003), No. 1, p. 314–331 [cited at p. 252, 419, 437, 495, 528, 582]

Campbell et al. 2003 Campbell, R. ; Hardy, G. ; Ravindra, M.: Trial Plant Review of an American Nuclear Society External Event Probabilistic Risk Assessment Standard / EPRI. 300 Commerce Drive, Suite 200, Irvine, CA 92602, September 2003 (1009074). – EPRI report [cited at p. 451, 621]

Cauzzi and Faccioli 2008 Cauzzi, C. ; Faccioli, E.: Broadband (0.05 to 20 s) prediction of displacement response spectra based on worldwide digital records. In: *Journal of Seismology* 12 (2008), p. 453–475. http://dx.doi.org/10.1007/s10950-008-9098-y. – TP2-RF-1114. – DOI 10.1007/s10950–008–9098–y [cited at p. 471]

Der Kiureghian 1980 Der Kiureghian, A.: Structural response to stationary excitation. In: *Journal of the Engineering Mechanics Division ASCE* 106 (1980), No. 6, p. 1195–1213 [cited at p. 133]

Dobry et al. 1976 Dobry, R. ; Oweis, I. ; Urzua, A.: Simpliefied procedures for estimating the fundamental period of a soil profile. In: *Bull. Seismmol. Soc. Am.* 66 (1976), p. 1293–1321 [cited at p. 46]

Edwards et al. 2010 Edwards, B. ; Fäh, D. ; Allmann, B. ; Poggi, V.: Stochastic Ground Motion Model for Switzerland / SED, prepared for PRP - PEGASOS Refinement Project. 2010 (TP2-TB-1024). – Technical Report. SP2 [cited at p. 376]

Edwards et al. 2011a Edwards, B. ; Fäh, D. ; Giardini, D.: Attenuation of seismic shear wave energy in Switzerland. In: *Geophysical Journal International* 185 (2011), February, 11, No. 2, p. 967–984. http://dx.doi.org/10.1111/j.1365-246X.2011.04987.x. – SP2. – DOI 10.1111/j.1365–246X.2011.04987.x [cited at p. 252]

Edwards et al. 2011b Edwards, B. ; Fäh, D. ; Poggi, V.: Characterizing the vertical to horizontal ratio of ground-motion at soft sediment sites derived from recorded ambient vibrations / SED, prepared for PRP - PEGASOS Refinement Project. 2011 (TP3-TB-1084). – Technical Report [cited at p. 253, 451, 495, 528, 621]

Fäh 2002a Fäh, D.: Spectral Amplification for SH- and PSV waves at sites Beznau, Gösgen and Leibstadt / prepared for PRP - PEGASOS Refinement Project. 2002 (TP3-TN-0167). – Technical Note. SP3 [cited at p. 403]

Fäh 2002b Fäh, D.: Two-dimensional meodelling of SH-wave amplification at site Leibstadt (Rev. 1) / Swiss Seismological Service, ETH Zürich, prepared for the Pegasos Project. 2002 (TP3-TN-0168 (TP3-TN-0240)). – Techical Note. SP3 [cited at p. 403, 572]

Fäh et al. 2011 Fäh, D. ; Poggi, V. ; Edwards, B.: V/H of 5% Damped Response Spectra for NPP sediment sites / SED, prepared for PRP - PEGASOS Refinement Project. 2011 (TP3-TB-1084). – Technical Report. SP3 [cited at p. 582]

Gülerce and Abrahamson 2010 Gülerce, Z. ; Abrahamson, N. A.: Vector-Valued Probabilistic Seismic Hazard Assessment for the Effects of Vertical Ground Motions on the Seismic Response of Highway Bridges. In: *Earthquake Spectra, Earthquake Engineering Research Institute* 26 (2010), November, No. 4, p. 999–1016. http://dx.doi.org/DOI:10.1193/1.3464548. – DOI DOI: 10.1193/1.3464548 [cited at p. 582]

Gülerce and Abrahamson 2011 Gülerce, Z. ; Abrahamson, N.N.: Site-Specific Design Spectra for Vertical Ground Motion. In: *Earthquake Spectra* 27 (2011), January, 13, No. 4, p. 1023–1047. http://dx.doi.org/http://dx.doi.org/10.1193/1.3651317. – SP3 + SP2. – DOI http://dx.doi.org/10.1193/1.3651317 [cited at p. 252, 358, 419, 420, 437, 451, 495, 496, 528, 621]

Graizer 2011 Graizer, V.: Effects of Surface Geology on Seismic Motion: Treasure Island Geotechnical array - case study for site response analysis. In: *University of California Santa Barbara* (2011), August 23-26. – 4th IASPEI / IAEE International Symposium [cited at p. 6]

Gregor 2013 Gregor, N.: Development of Spectrum Compatible Acceleration Time Histories for the PEGASOS Refinement Project, re-evaluation in 2013 / prepared for the PRP - PEGASOS Refinement Project. 2013 (EXT-TN-1265). – Technical Report [cited at p. 137]

Haghshenas et al. 2008 Haghshenas, E. ; P.-Y., Bard ; N., Theodulidis ; SESAME WP04 Team (Atakan K., Cara F., Cornou C., Cultrera G., Di Giulio G., Dimitriu, P. , Fäh, D. , de Franco, R . , Marcellini, A., Pagani, M. , Rovelli, A. , Savvaidis, A. , Tento, A. , Vidal, S. AND Zacharopoulos, S.) : Empirical evaluation of microtremor H/V spectral ratio. In: *Bulletin of Earthquake Engineering* 6 (2008), p. 75–108. http://dx.doi.org/10.1007/s10518-007-9058-x. – DOI 10.1007/s10518–007–9058–x [cited at p. 253]

Hölker 2012 Hölker, A.: *SP3mod Toolbox (MATLAB) - Implementation of Geotechnical Assessments by SP3 Experts (software and data base).* Kirchenaeckerstr. 4, D-79798 Jestetten, November 5 2012. – TP4-HSW-1003, Ver. 13 [cited at p. 352, 363, 442, 453, 524, 532, 614, 624]

Hölker 2013a Hölker, A.: *Database and Plotting Tool for 1D Site Response Analyses for NPP Sites.* July 1 2013. – RDZ-ASW-1003 [cited at p. 6, 133, 145]

Hölker 2013b Hölker, A.: *SP3mod Toolbox (MATLAB) - Documentation for Implementation of Geotechnical Assessments by SP3 Experts (TP4-HSW-1002).* Kirchenaeckerstr. 4, D-79798 Jestetten: Geophysical Technologies & Consulting GmbH, February 7 2013. – TP4-TN-1197 [cited at p. 363, 365, 367, 453, 455, 457, 532, 534, 535, 624, 626, 627]

IAEA 2004 IAEA: Geotechnical Aspects of Site Evaluation and Foundations for Nuclear Power Plants - No. NS-G-3.6 / IAEA. 2004. – IAEA Safety Standards Series [cited at p. 3]

Interoil 2009a Interoil: Additional data for the KKG site according to SP3 Experts requests on WS2a/SP3 (22.10.2009) / Interoil E&P Switzerland AG. 2009 (TP3-GTC-1006). – Geotechnical Database and Reports [cited at p. 5]

Interoil 2009b INTEROIL: Extension of additional data for the KKG site according to SP3 Experts requests on WS2a/SP3 / Interoil E&P Switzerland AG. 2009 (TP3-GTC-1008). – Geotechnical Database and Reports [cited at p. 5, 64]

Interoil 2009c INTEROIL: Site investigations for KKG&ATEL (KKN) / Interoil. 2009 (TP3-GTC-1001). – Geotechnical Database and Reports [cited at p. 5, 49, 50, 64]

Johnson and M.L. 1978 JOHNSON, J.A. ; M.L., Traubenik: Magnitude dependent near-source ground motion spectra. In: *Earthquake Engineering and Soil Dynamics* Proc. of the ASCE Geotech. Eng. Div., Specialty Conf., Pasadena (1978), p. 530–539 [cited at p. 126]

Kawase et al. 2011 KAWASE, H. ; SÁNCHEZ-SESMA, F.J. ; MATSUSHIMA, S.: The Optimal Use of Horizontal-to-Vertical Spectral Ratios of Earthquake Motions for Velocity Inversions Based on Diffuse-Field Theory for Plane Waves. In: *Bulletin of the Seismological Society of America* 101 (2011), October, No. 5, p. 2001–2014. http://dx.doi.org/doi:10.1785/0120100263. – DOI doi: 10.1785/0120100263 [cited at p. 252, 253, 358]

KKG 2010 KKG: NL Computation Results for KKG/KKN / KKG. 2010 (TP3-SUP-1015). – Supporting Computations Database [cited at p. 6]

KKG 2013 KKG: KKG site response re-evaluation 2013 / KKG AG. 2013 (TP3-SUP-1091). – Supporting Computations Database [cited at p. 6]

KKG-KKN 2010 KKG-KKN: EQL & RVT Computation Results for KKG & KKN / KKG-KKN. 2010 (TP3-SUP-1011). – Supporting Computations Database [cited at p. 6]

Kottke and Rathje 2013 KOTTKE, A.P. ; RATHJE, E.M.: Comparison of Time Series and Random Vibration Theory Site Response Methods. In: *Bulletin of the Seismollogical Society of America* 103 (2013), June, No. 3, p. 2111–2127. http://dx.doi.org/10.1785/0120120254. – DOI 10.1785/0120120254 [cited at p. 6, 185, 186, 467, 470]

Martin 1975 MARTIN, P.P.: *Non linear methods for dynamic analyses of ground response.*, University of California, Berkeley, PhD thesis, 1975 [cited at p. 466]

McGuire et al. 2001 MCGUIRE, R. K. ; SILVA, W.J. ; COSTANTINO, C.J.: *Technical Basis for Revision of Regulatory Guidance on Design Ground Motions: Hazard- and Risk-consistent Ground Motion Spectra Guidelines.* U.S. Nuclear Regulatory Commission, Office of Nuclear Regulatory Research, Washington, DC 20555-0001, 2001 [cited at p. 419]

Menq 2003 MENQ, F.-Y.: *Dynamic Properties of Sandy and Gravelly Soils*, The University of Texas at Austin, PhD Thesis, 2003 [cited at p. 24, 45, 54, 72, 97, 125, 384]

Mohammadioun and Pecker 1984 MOHAMMADIOUN, B. ; PECKER, A.: Low frequency transfer of seismic energy by superficial soil deposits and soft rocks. In: *Earthquake Engineering and Structural Dynamics* 12 (1984), p. 537–564. – SP3 [cited at p. 466]

NAGRA 1992 NAGRA: Sondierbohrung Schafisheim - Untersuchungsbericht. Textband / NAGRA, Nationale Genossenschaft für die Lagerung Radioaktiver Abfälle. Baden, 1992 (88-11). – Technischer Bericht. 183 pages [cited at p. 50]

NAGRA 2001 NAGRA: Sondierbohrung Benken - Untersuchungsbericht. Textband / NAGRA, Nationale Genossenschaft für die Lagerung Radioaktiver Abfälle. Hardstrasse 73, CH-5430 Wettingen, August 2001 (00-01). – Technischer Bericht. ISSN 1015-2636, 288 pages [cited at p. 64]

NOK 2009a NOK: Site investigations for KKB & EKKB / NOK. 2009 (TP3-GTC-1003). – Geotechnical Database and Reports [cited at p. 5]

NOK 2009b NOK: Site investigations for KKL / NOK. 2009 (TP3-GTC-1004). – Geotechnical Database and Reports [cited at p. 5]

Pecker Pecker, A.: Maximum Ground Motions-Sensivity Studies and Motions at Depth / prepared for PRP - PEGASOS Refinement Project (TP3-TN-0403). – Technical Note. SP3 [cited at p. 520]

Pecker 2002 Pecker, A.: Gösgen Nuclear Power Plant Site, True Nonlinear Site Response Analysis / prepared for PRP - PEGASOS Refinement Project. 2002 (TP3-TN-0205). – Technical Note. SP3 [cited at p. 381]

Pecker 2005 Pecker, A.: Maximum Ground Surface Motion in Probabilistic Seismic Hazard Analyses. In: *Journal of Earthquake Engineering* 9 (2005), No. Special Issue 1 Number 4, p. 187–211 1–25. – Imperial College Press [cited at p. 141, 424]

Pecker 2010 Pecker, A.: Gösgen Nuclear Power Plant Site (KKG - KKN), Non-linear Site Response Analyses / Géodynamique et Structure, prepared for PRP - PEGASOS Refinement Project. 2010 (TP3-TB-1055). – Technical Report. Part of TP3-SUP-1015 [cited at p. 145]

Pecker 2011 Pecker, A.: Evaluation of Maximum Ground Motions / Géodynamique et Structure, prepared for PRP - PEGASOS Refinement Project. 2011 (TP3-TB-1074, Rev A). – Technical Report. SP3 [cited at p. 139, 144, 357, 424, 425, 511, 527, 604, 607, 618]

Pecker et al. 2003 Pecker, A. ; Koller, M. ; Studer, J.: Evaluation of Maximum Ground Motions / prepared for PEGASOS Project. 2003 (TP3-TN-0354). – Technical Report. SP3 [cited at p. 424]

Pecker and Studer 2013 Pecker, A. ; Studer, J.: Liquefaction Assessment at the Nuclear Power Plant Sites / Géodynamique et Structures, prepared for PRP - PEGASOS Refinement Project. Bagneux, France, March, 13 2013 (EXT-TN-1270). – Technical Report [cited at p. 171]

Pelli 2002 Pelli, F.: Nonlinear Site Response Analyses for Beznau, Gösgen , Leibstadt / prepared for PRP - PEGASOS Refinement Project. 2002 (TP3-TB-0048). – Technical Report. SP3 [cited at p. 381]

Pelli 2010 Pelli, F.: Nonlinear Site Response Analyses for Beznau (KKB, EKKB) and Leibstadt (KKL) - Analyses (Mean-UB-LB parameter values), Rev. 1.1 / GEODECO, prepared for PRP - PEGASOS Refinement Project. Via Aurelia 24, 16031 Bogliasco (Genova), Italy, December 30 2010 (TP3-TB-1056). – Technical Report. Part of TP3-SUP-1016 [cited at p. 145]

PMT and Renault 2010 PMT ; Renault, P.: Overview of non linear parameters used by all contractors for all NPP sites / swissnuclear, prepared for PRP - PEGASOS Refinement Project. 2010 (TP3-TN-1123). – Technical Note. SP3 [cited at p. 471]

Poggi et al. 2011 Poggi, V. ; Edwards, B. ; Fäh, D.: Derivation of a Reference Shear-Wave Velocity Model from Empirical Site Amplification. In: *Bulletin of the Seismological Society of America* 101 (2011), February, No. 1, p. 258–274. http://dx.doi.org/10.1785/0120100060. – DOI 10.1785/0120100060 [cited at p. 252, 358, 451, 621]

Power et al. 2008 Power, M. ; Chiou, B. ; Abrahamson, N. ; Bozorgnia, Y. ; Shantz, T. ; Roblee, C.: An Overview of the NGA Project. In: *Earthquake Spectra* 24 (2008), February, No. 1, p. 3–21. http://dx.doi.org/10.1193/1.2894833. – DOI 10.1193/1.2894833 [cited at p. 471]

Renault 2010a Renault, P.: Soil model for the Beznau site (KKB) / swissnuclear, prepared for PRP - PEGASOS Refinement Project. 2010 (TP3-TN-1068, V. 4). – Technical Note. SP3 [cited at p. 352, 386, 442, 524, 614]

Renault 2010b Renault, P.: Soil model for the E-Beznau site (EKKB) / swissnuclear, prepared for PRP - PEGASOS Refinement Project. 2010 (TP3-TN-1069, V.4). – Technical Note. SP3 [cited at p. 352, 388, 442, 524, 614]

Renault 2010c Renault, P.: Soil model for the Gösgen site (KKG and KKN) / swissnuclear, prepared for PRP - PEGASOS Refinement Project. 2010 (TP3-TN-1070, V.4). – Technical Note. SP3 [cited at p. 352, 386, 389, 442, 524, 614]

Renault 2010d Renault, P.: Soil model for the Leibstadt site (KKL) / swissnuclear, prepared for PRP - PEGASOS Refinement Project. 2010 (TP3-TN-1067, V4). – Technical Note. SP3 [cited at p. 352, 442, 475, 524, 614]

Renault 2010e Renault, P.: Soil model for the Mühleberg site (KKM and EKKM) / swissnuclear, prepared for PRP - PEGASOS Refinement Project. 2010 (TP3-TN-1069, V.4). – Technical Note. SP3 [cited at p. 352, 388, 442, 524, 614]

Renault 2011a Renault, P.: Overview of site response computations / swissnuclear, prepared for PRP - PEGASOS Refinement Project. 2011 (PMT-TN-1139, Ver. 3.1). – Technical Note. SP3 [cited at p. 133, 364, 376, 453, 532, 624]

Renault 2011b Renault, P.: Updated comparison of SP2-SP3 sigma components / swissnuclear, prepared for PRP - PEGASOS Refinement Project. 2011 (TP3-TN-1195). – Technical Note for SP3 [cited at p. 599]

Renault 2013 Renault, P.: Amendment to PMT-TB-1014 "Specification on 1D site response calculations for NPP sites" for re-evaluation in 2013 / swissnuclear, prepared for PRP - PEGASOS Refinement Project. 2013 (PMT-AN-1132). – Administrative Note. Ver. 4 [cited at p. 133, 137]

Renault and Abrahamson 2010 Renault, P. ; Abrahamson, N.: Specification on 1D site response calculations for NPP sites. / swissnuclear, prepared for PRP - PEGASOS Refinement Project. 2010 (PMT-TB-1014, Ver.4.5). – Technical Report. SP3 [cited at p. 6, 7, 46, 133, 364, 376, 453, 532, 624]

Renault et al. 2008 Renault, P. ; Heuberger, S. ; Abrahamson, N.: Specification for geotechnical and geophysical investigations at NPP sites / swissnuclear, prepared for PRP - PEGASOS Refinement Project. 2008 (PMT-TB-1010, Ver.3). – Technial Report. SP3 [cited at p. 3, 5, 375]

Ripperger and Fäh 2003 Ripperger, J ; Fäh, D.: Maximum Recorded Horizontal and Vertical Ground Motions / SED, prepared for PRP - PEGASOS Refinement Project. 2003 (TP3-TN-0359). – Technical Note. SP3 [cited at p. 424, 425, 427, 612, 622, 660]

Rodriguez-Marek and Cotton 2011 Rodriguez-Marek, A. ; Cotton, F.: Final Report: Single Station Sigma Project / prepared for PRP - PEGASOS Refinement Project. 2011 (EXT-TB-1058). – Technical Report. SP2 (Ver.7.1, 29 July) [cited at p. 423, 618, 660]

Rodriguez-Marek et al. 2011 Rodriguez-Marek, A. ; Montalva, G. A. ; Cotton, F. ; Bonilla, F.: Analysis of Single-Station standard deviation using the KiK-net Data. In: *Bulletin of the Seismological Society of America* 101 (2011), June, No. 3, p. 1242–1258. http://dx.doi.org/10.1785/0120100252. – DOI 10.1785/0120100252 [cited at p. 617]

Rollins et al. 1998 Rollins, K.M. ; Evans, M.D. ; Diehl, N.B.: Shear modulus and damping relationships fror gravels. In: *J. Geoenvironmental Eng. ASCE* 124 (1998), No. 5, p. 396–405 [cited at p. 24, 45, 54, 55, 72, 97, 125, 384]

Sanchez-Sesma et al. 2011 Sanchez-Sesma, F.J. ; Rodrýguez, M. ; Iturraran-Viveros, U. ; Luzon, F. ; Campillo, M. ; Margerin, L. ; Garcýa-Jerez, A. ; Suarez, M. ; Santoyo, M. A. ; Rodrýguez-Castellanos, A.: A theory for microtremor H/V spectral ratio: application for a layered medium. In: *Geophysical Journal International* 186 (2011), April, p. 221–225. http://dx.doi.org/doi:10.1111/j.1365-246X.2011.05064.x. – DOI doi: 10.1111/j.1365–246X.2011.05064.x [cited at p. 252, 253]

Schnabel et al. 1972 Schnabel, B. ; Lysmer, J. ; Seed, H.B.: *SHAKE - A computer program for earthquake response analysis of horizontally layered sites.* College of Engineering, University of California, Berkeley: Earthquake Engineering Research Center, December 1972. – Report No. EERC 72-12 [cited at p. 133]

Set et al. 2011 Set, K. ; Unutmaz, B. ; Cetin, K.O. ; Koprivica, S. ; Jeremic, B.: Soil uncertainty and its influence on simulated G/Gmax and damping behavior. In: *Journal of Geotechnical and Geoenvironmental Engineering* 137 (2011), No. 3, p. 218–226 [cited at p. 477]

Sánchez-Sesma et al. 2008 Sánchez-Sesma, F.J. ; Pérez-Ruiz, J.A. ; Campillo, M. ; Rodríguez-Castellanos, A.: Diffuse fields in dynamic elasticity. In: *Wave Motion* 45 (2008), p. 641–654 [cited at p. 253]

Sánchez-Sesma et al. 2011 Sánchez-Sesma, F.J. ; Weaver, R.L. ; Kawase, H. ; Matsushima, S. ; Luzón, F. ; Campillo, M.: Energy Partitions among Elastic Waves for Dynamic Surface Loads in a Semi-Infinite Solid. In: *Bulletin of the Seismological Society of America* Vol. 101 (2011), August, No. No. 4, p. pp. 1704–1709. http://dx.doi.org/doi:10.1785/0120100196. – DOI doi: 10.1785/0120100196 [cited at p. 252, 253]

Strasser 2012 Strasser, F.O.: *Maximum Ground Motions Database.* perpared for PRP - PEGASOS Refinement Project, January 1 2012. – EXT-WAF-1012, Version 9 [cited at p. 357]

Strasser and Zulu 2010 Strasser, F.O. ; Zulu, S.: Determination of empirical Maximum Ground Motions for PRP / CGS, prepared for PRP - PEGASOS Refinement Project. 2010 (EXT-TB-1067 CGS Report Number: 2010 - 0177). – Technical Report. SP2 + SP3 [cited at p. 424, 430, 511, 604]

swissnuclear 2011 swissnuclear: PEGASOS Refinement Project plan, V. 4.2 / swissnuclear, prepared for PRP - PEGASOS Refinement Project. 4600 Olten, Switzerland, April 7 2011 (PMT-TB-1012). – Technical Report. 44 pp. and 2 Appendices [cited at p. 3, 5]

Travasarou 2002 Travasarou, T.: Visualisation and Comparison of RVT and Shake Results / prepared for PRP - PEGASOS Refinement Project. 2002 (TP3-TN-0212). – Technical Note. SP3 [cited at p. 380, 381]

Vanmarcke 1972 Vanmarcke, E.H.: Properties of Spectral Moments with Applications to Random Vibration. In: *Journal of the Engineeing Mechanics Division Proceedings of the American Society of Civil Engineers* (1972), April, p. 425–446 [cited at p. 133]

Vanmarcke 1975 Vanmarcke, E.H.: On the distribution of the first-passage time for normal stationary random processes. In: *Journal of Applied Mechanics* 42 (1975), No. 1, p. 215–220 [cited at p. 133]

Youd and Idriss 2001 Youd, T.L. ; Idriss, I. M.: Liquefaction resistance of soils: Summary report from the 1996 NCEER/NSF Workshop on evaluation of liquefaction resistance of soils. In: *Journal of Geotechnical and Geoenvironmental Engineering, ASCE,* 127 (2001), p. 817–833. – TP3-TN-0359 SP3 [cited at p. 171]

Appendices

Appendix A

Hazard Feedback for SP3

The development and finalization of the HIDs were preceded by provision of hazard feedback plots for each SP3 expert. The different feedback plots are attached as electronic supplement to this report.

List of Figures

List of Tables